R-05-08

Preliminary site description

Simpevarp subarea – version 1.2

Svensk Kärnbränslehantering AB

April 2005

Svensk Kärnbränslehantering AB
Swedish Nuclear Fuel
and Waste Management Co
Box 5864
SE-102 40 Stockholm Sweden
Tel 08-459 84 00
+46 8 459 84 00
Fax 08-661 57 19
+46 8 661 57 19

ISSN 1402-3091
SKB Rapport R-05-08

Preliminary site description

Simpevarp subarea – version 1.2

Svensk Kärnbränslehantering AB

April 2005

Preface

The Swedish Nuclear Fuel and Waste Management Company (SKB) is undertaking site characterisation at two different locations, the Forsmark and Simpevarp areas, with the objective of siting a geological repository for spent nuclear fuel. An integrated component in the characterisation work is the development of a site descriptive model that constitutes a description of the site and its regional setting, covering the current state of the geosphere and the biosphere as well as those ongoing natural processes that affect their long-term evolution.

The Simpevarp candidate area consists of two subareas, named the Laxemar subarea and the Simpevarp subarea, that were prioritised for further investigations. The present report documents the site descriptive modelling activities (version 1.2) for the Simpevarp subarea. The overall objectives of the version 1.2 site descriptive modelling are to produce and document an integrated description of the site and its regional environments based on the site-specific data available from the initial site investigations and to give recommendations on continued investigations. The modelling work is based on primary data, i.e. quality-assured, geoscientific and ecological field data available in the SKB databases SICADA and GIS, available April 1, 2004.

The work has been conducted by a project group and associated discipline-specific working groups. The members of the project group represent the disciplines of geology, rock mechanics, thermal properties, hydrogeology, hydrogeochemistry, transport properties and surface ecosystems (including overburden, surface hydrogeochemistry and hydrology). In addition, some group members have specific qualifications of importance in this type of project e.g. expertise in RVS (Rock Visualisation System) modelling, GIS-modelling and in statistical data analysis.

The overall strategy to achieve a site description is to develop discipline-specific models by interpretation and analyses of the primary data. The different discipline-specific models are then integrated into a site description. Methodologies for developing the discipline-specific models are documented in methodology reports or strategy reports. A forum for technical coordination between the sites/projects sees to that the methodology is applied as intended and developed if necessary. The forum consists of specialists in each field as well as the project leaders of both modelling projects.

The following individuals and expert groups contributed to the project and/or to the report:

- Anders Winberg – project leader and editor,
- Karl-Erik Almén, Henrik Ask, Roy Stanfors – investigation data,
- Carl-Henric Wahlgren, Jan Hermanson, Philip Curtis, Ola Forssberg, Paul La Pointe, Eva-Lena Tullborg – geology,
- Eva Hakami, Flavio Lanaro, Isabelle Olofsson, Anders Fredriksson – rock mechanics,
- Jan Sundberg and co-workers – thermal properties,
- Ingvar Rhén, Sven Follin, Lee Hartley and the members of the HydroNET Group – hydrogeology,
- Marcus Laaksoharju and the members of the HAG group – hydrogeochemistry,
- Sten Berglund, Johan Byegård and co-workers – transport properties,
- Tobias Lindborg and the members of the SurfaceNET group – surface ecosystems (including overburden),
- Johan Andersson – confidence assessment,
- Fredrik Hartz and Anders Lindblom – production of maps and figures.

The report has been reviewed by the following members of SKB's international Site Investigation Expert Review Group (SIERG): Per-Eric Ahlström (Chairman); Jordi Bruno (Enviros, Spain); John Hudson (Rock Engineering Consultants, UK); Ivars Neretnieks (Royal Institute of Technology,

Sweden); Lars Söderberg (SKB); Mike Thorne (Mike Thorne and Associates Ltd, UK); Gunnar Gustafson (Chalmers University); Roland Pusch (GeoDevelopment AB). The group provided many valuable comments and suggestions for this work and also for future work. The latter group is not to be held responsible for any remaining shortcomings of the report. Additional review comments on the geological models were also provided by Raymond Munier (SKB).

Anders Ström
Site Investigations – Analysis

Summary

The objectives of the version 1.2 site descriptive modelling (SDM) of the Simpevarp subarea are to: produce and document an integrated description of the site and its regional environments based on the site-specific data available from the initial site investigations and to give recommendations on continued investigations on a continuous basis. The modelling work is based on primary data available at the time of the data freeze for Simpevarp 1.2, April 1, 2004.

The local scale model area (24 km^2) for the Simpevarp 1.2 modelling encompasses both the Simpevarp and Laxemar subareas. The local model area is located in the centre of a regional scale model area (273 km^2).

The surface data is in terms of geology essentially equitable to those used for SDM Simpevarp 1.1 and consequently large uncertainties still remain for the Laxemar subarea. The borehole data available for Simpevarp 1.2 are foremost related to the Simpevarp subarea where there are four new cored boreholes (KSH01A/B, KSH02, KSH03A/B and KAV04), new complementary data from two existing boreholes, KAV01 and KLX02, and three percussion boreholes positioned on the Simpevarp peninsula (HSH01–HSH03).

Model results

Surface ecosystem models in terms of pools and fluxes of carbon have been developed for the terrestrial (e.g. plants and animals) and limnic (e.g. algae and fish) systems using the Lake Frisksjön drainage area. Furthermore, a first marine ecosystem model has been developed for the Basin Borholmsfjärden.

The parts of the Simpevarp subarea located above sea level are largely outlined by the Simpevarp peninsula and the Hålö and Ävrö islands. The investigated area features a relatively flat topography (c. 0.4% topographical gradient), which largely reflects the surface of the underlying bedrock surface, and is also characterised by a high degree of bedrock exposures (38%). Till is the dominant Quaternary deposit which covers about 35% of the subarea.

Three principal lithological domains have been defined in the subarea, an A domain that is dominated by the Ävrö granite and which dominates on the island of Ävrö, Hålö and the northern parts of the peninsula, a domain B that is dominated by the fine-grained dioritoid and dominates the Simpevarp peninsula, a C domain that is characterised by a mixture of of Ävrö granite and quartz monzodiorite on the cape of the peninsula. A fourth domain is made up a few scattered domains of diorite to gabbro.

The ore potential in the area is considered negligible, with a real potential only for quarrying of building- and ornamental stone associated with the Götemar and Uthammar granite intrusions to the north and south of the investigated area, respectively.

In total, 22 deformation zones with high confidence of occurrence have been interpreted in the local scale model area. The understanding of the interpreted deformation zones of the Simpevarp subarea is considered adequate to make a preliminary assessment of available storage volumes for a deep repository. The two most important and volume-delineating deformation zones are ZSMNE012A, which trends north of the islands of Hålö and Ävrö, dipping towards the southeast under the Simpevarp peninsula, and ZSMNE024A which strikes northeast along the coast of the Ävrö island and the Simpevarp peninsula. The remaining uncertainty in the developed deformation zone model is primarily related to the interpreted “possible” zones (of low or intermediate confidence of occurrence), for the most part located in the neighbouring Laxemar subarea and throughout the regional scale model volume.

High rock stresses do not appear to be a major concern for the Simpevarp subarea. The current stress model indicates two stress domains, one with lower stresses in the Simpevarp subarea, east of deformation zone ZSMNE012A, compared with the area west thereof (including the Laxemar subarea) which shows comparatively higher stress levels. The magnitude of the maximum principal

stress (σ_1) at 500 m in the Simpevarp subarea is estimated at 10–22 MPa. This situation, supported by numerical stress modelling, is attributed to unloading of a wedge-formed rock volume underneath the Simpevarp peninsula and Hålö and Ävrö islands, as delineated by the intersecting deformation zones. Quantification of mechanical properties of the naturally fractured rock mass and rock associated with interpreted deformation zones is supported by new laboratory data on intact rock samples, underpinned by empirical and theoretical relationships.

The analysis of the thermal conductivity has developed considerably since Simpevarp 1.1. Our current understanding is that the thermal conductivity in the Simpevarp subarea is generally low. In terms of interpreted mean values for the identified lithological domains, the thermal conductivity varies within a relatively narrow interval (2.6–2.8 W/(m·K)). A methodology for upscaling of thermal conductivity data from core scale has also been developed. At the canister scale (L=2 m) the standard deviations span between 0.20 and 0.28.

The hydraulic properties of the Hydraulic Rock Domains are described in terms of a network of discrete fractures (DFN) with a geometrical description taken from the geological DFN model. A fracture transmissivity distribution is superimposed, and calibrated against existing hydraulic borehole data. The working hypothesis employed is that the hydraulic DFN model couples transmissivity (T) and size (L) through an inferred power-law relationship ($T=aL^b$), up to the size of the local minor deformation zones (L < 1,000 m).

All together 13 of the interpreted deformation zones have been tested hydraulically in boreholes. The range of interpreted transmissivity of these tested intercepts range from 10^{-8} to about 4×10^{-4} m^2/s. Different alternative hydraulic DFN models have been used to simulate effective values of hydraulic conductivity at different scales. The results of the generation of block hydraulic conductivities show that 20 m blocks on the average are less permeable than 10^{-8} m/s. Local groundwater flow regimes are assumed to develop at the Laxemar and Simpevarp subareas and are considered to extend down to depths of around 600–1,000 m, depending on local topography. In the Simpevarp subarea, close to the Baltic Sea coastline, where topographical variation is limited, depth penetration of local groundwater flow cells will be less marked. In contrast, the Laxemar subarea is characterised by higher topography, resulting in a much more profound groundwater circulation that appears to extend to approximately 1,000 m depth in the vicinity of borehole KLX02. Numerical modelling shows that groundwater flow is controlled by topography and the geometry of the system of modelled deformation zones. The modelling also identifies the Simpevarp subarea as an area of groundwater discharge (upward directed flow) at repository depth.

Three groundwater types have been identified in the Simpevarp subarea; the Type A (dilute and mainly of Na-HCO3) is found at shallow depths (< 100 m), Type B (brackish, mainly Na-Ca-Cl) at shallow to intermediate depths (150–300 m), Type C (saline (6,000–20,000 mg/l Cl, 25–30 g/L TDS), mainly Na-Ca-Cl) at intermediate to deep levels (> 300 m). The marked differences in the groundwater flow regimes (in terms of depth penetration of local flow cells) between the Laxemar and Simpevarp subareas are reflected in differences in measured groundwater chemistry. Furthermore, our current understanding is that the hydrochemical stability critera as set up by SKB are met, as inferred from groundwater sampling.

Applications of the hydraulic DFN models, and block hydraulic conductivites derived there from, show that all hydraulic DFN models defined for Simpevarp 1.2 can be made to match measured hydrogeochemical in situ data if the flow porosity is increased. Transient simulation of present day salinity distribution, on the basis of inferred transient boundary conditions (shore-line displacement due to isostatic land uplift and variable salinity of the water of the Baltic Sea), show results compatible with measured geochemical signatures in selected reference boreholes. The results further suggest that Littorina water, indicated by the characterisation, may be present near the coast and below the Baltic Sea.

The current retardation model provides a parameterisation for fresh intact (unaltered) and altered varieties of the rock types and modelled lithological domains in the subarea. Suggested porosities for intact fresh rock (in terms mean values in vol-%) on lithological domain level vary from 0.17 (Fine-grained dioritoid) to 0.40 (Ävrögranit). Suggested formation factors for intact fresh (reflecting diffusion characteristics, mean values) on lithological domain level vary from about 1.0×10^{-4} (Fine-grained dioritoid) to 2.9×10^{-4} (Ävrö granite).

Uncertainties

Important modelling steps have been taken in Simpevarp 1.2 and the main uncertainties are identified, in some cases quantified, or explored as model alternatives. Notwithstanding, some uncertainties still remain unquantified at this stage, and alternative hypotheses are retained only as hypotheses. Additional data, collected in the Simpevarp subarea following the Simpevarp 1.2 data freeze, may allow additional quantification, and may help further reduce the observed uncertainties.

For the geological model various possible alternative descriptions are inherent in uncertainties related to geometry (size/extent in lateral and vertical directions, dip and termination), uncertainties in characteristics/properties and confidence of existence of modelled lithological domains and deformations zones. No analysis of possible alternatives has however been pursued explicitly in the current modelling. This applies also to the possible existence of subhorizontal deformation zones. It should however be noted that only limited indications of subhorizontal deformation zones exist in the Simpevarp subarea. Similarly, no major subhorizontal deformation zones have been identified in the boreholes and underground openings of the Äspö Hard Rock Laboratory.

Alternatives for the geological DFN model have been developed based on alternative size models for the identified fracture sets. In hydrogeology, alternative hydraulic DFN models (with alternative assumptions regarding the correlation between fracture size and transmissivity) have been developed, and subsequently propagated in estimating block hydraulic conductivities and in the assignment of material properties to continuum regional scale hydrogeological flow models.

For the other disciplines, other alternative models (hypotheses) are possible, but have not been elaborated in model version Simpevarp 1.2.

Possible interactions between disciplines, and the interactions considered for version Simpevarp 1.2 are discussed. It is obvious that changes to the lithological model have a strong impact on most disciplines (e.g. rock mechanics, thermal and transport properties). The deformation zone model in particular influences the hydrogeological and rock mechanics models. Likewise, there is a strong interdependence between hydrogeology and hydrogeochemistry, primarily through the description of mixing, proposed as being mainly responsible for the evolution of the groundwater chemistry, including the distribution of salinity, over time. The hydrogeochemical model in turn is to a limited degree dependent on the chemical composition of the bedrock and the fracture minerals. There is also the coupling between geology (mineralogy), hydrogeochemistry and the transport model, for the sorption characteristics of the rock. Other aspects on the transport model stem from rock stress effects, both in virgin rock (affecting in situ measurements to establish the formation factor along boreholes) and in drill core rock samples (effects of unloading of rock stresses on laboratory results), on the magnitude and anisotropy of diffusion properties, possibly associated with any existing fabric (foliation) of the bedrock. However, what still remains to be better established and quantified are the interactions between the surface system and the bedrock system. This applies primarily to the turnover of water and chemical mass balances.

Conclusions

The Simpevarp 1.2 site descriptive model is found to be in general agreement with current understanding of the past evolution. This applies e.g. to the composition of present groundwater in relation to the bedrock lithology and fracture mineralogy. Furthermore, the hydrogeological modelling of groundwater chemical evolution arrives at reasonable present day groundwater compositions when compared with borehole data. No major surprises have been noted in the Simpevarp 1.2 modelling. In summary, more quantitative data have been produced for Simpevarp 1.2 compared with Simpevarp 1.1. Some alternatives have been explored and even propagated in the analysis, but uncertainty remains, particularly in the Laxemar subarea and the regional scale model volume. The modelling for Simpevarp 1.2 is furthermore characterised by a stronger element of interaction between disciplines.

Sammanfattning

Målen med version 1.2 av den platsspecifika modelleringen (SDM) av delområde Simpevarp är att: ta fram och dokumentera en integrerad beskrivning av platsen och dess regionala omgivning baserad på platsspecifika data som tagits fram inom ramen av de pågående platsundersökningarna i Oskarshamn och att kontinuerligt avge rekommendationer vad avser pågående undersökningar. Modellarbetet är baserat på primärdata som fanns vid datafrystillfället för Simpevarp 1.2 den 1 april, 2004.

Det lokala modellområdet (24 km^2) för Simpevarp 1.2 modelleringen innefattar både delområde Simpevarp och delområde Laxemar. Det lokala modellområdet är centrerat i det regionala modellområdet (273 km^2).

Utnyttjade geologiska ytdata överensstämmer i stort med de som utnyttjats för SDM Simpevarp 1.1 och följaktligen kvarstår stora osäkerheter kopplade till delområde Laxemar. Primärdata från borrhål för Simpevarp 1.2 kommer huvudsakligen från delområde Simpevarp där det finns fyra kärnborrhål (KSH01A/B, KSH02, KSH03A/B samt KAV04), nya kompletterande data från två existerande borrhål, KAV01 och KLX02, samt tre hammarborrhål (HLX01–HLX03) placerade på Simpevarpshalvön.

Modellresultat

Ytekologiska modeller i termer av reservoarer för, och flöden av kol har utvecklats för terresta (t.ex. växter och djur) och liminiska (t.ex. alger och fiskar) system med utgångspunkt från data från Frisksjöns avrinningsområde. Vidare har en första marin ekologisk modell utvecklats för Borholmsfjärden.

De delar av delområde Simpevarp som ligger ovan havsnivån avgränsas översiktligt av Simpevarpshalvön och öarna Hålö och Ävrö. Det undersökta området karakteriseras av en relativt flack topografi (c. 0.4 % topografisk gradient), som till stor del återger formen på den underliggande bergytan. Området är också karakteriserat av en hög andel berg i dagen (38 %). Den vanligaste kvartära avdelningen är morän som täcker ungefär 35 % av delområdet.

Tre huvudsakliga litologiska domäner har definierats i delområdet, en domän A som domineras av Ävrögranit och som återfinns på Ävrö, Hålö och de norra delarna av Simpevarpshalvön, en domän B som domineras av den finkorniga dioritoiden och är det dominerande inslaget på halvön, en domän C på halvöns östra udde, som karakteriseras av en blandning av Ävrögranit och kvartsmonzodiorit. En fjärde domän utgörs av ett fåtal spridda domäner bestående av diorit och gabbro.

Malmpotentialen i området bedöms som negligerbar med en reell potential endast för brytning av byggnadssten och prydnadssten associerad med Götemar- och Uthammargraniterna i norr respektive söder.

I det lokala modellområdet har totalt 22 deformationer med hög konfidensgrad i existens tolkats. Förståelsen av tolkade deformationszoner i delområde Simpevarp bedöms som tillräckligt för att göra en preliminär bedömning av tillgängliga förvarsvolymer för ett djupförvar. De två mest betydelsefulla och volymsavgränsande deformationszonerna är ZSMNE012A, som är belägen norr om Hålö och Ävrö, och stupar in under Simpevarpshalvön, och ZSMNE024A som stryker i nordostlig riktning längs Ävrös och Simpevarpshalvöns kuster. Den kvarstående osäkerheten i den framtagna deformationszonsmodellen är huvudsakligen kopplad till ”troliga” deformationszoner (med låg eller medium konfidensgrad kopplad till existens). De senare är till största del belägna i det närliggande delområde Laxemar och genomgående i det regionala modellområdet.

Höga bergspänningar verkar inte utgöra ett problem för delområde Simpevarp. Den aktuella spänningsmodellen indikerar två spänningsdomäner, en med mindre spänningsnivåer i delområde Simpevarp (öster om deformationszon ZSM012A), jämfört med situationen i området väster därom (inklusive delområde Laxemar) som uppvisar jämförelsevis högre spänningsnivåer. Storleken på den största huvudspänningen (i medeltal) på 500 m djup i delområde Simpevarp uppskattas till

10–22 MPa. Denna situation, understödd av numerisk modellering, tillskrivs avlastning av en kilformad bergvolym under Simpevarpshalvön och öarna Hålö och Ävrö, som avgränsas av i huvudsak två lutande, och skärande deformationszoner. Kvantifiering av den naturligt sprickiga bergmassans mekaniska egenskaper samt för berg associerat med tolkade deformationszoner understöds av nya laboratoriedata på intakta bergprover, understödda av empiriska och teoretiska samband.

Analysen av termisk ledningsförmåga har utvecklats markant sedan SDM Simpevarp 1.1. Vår nuvarande förståelse är att den termiska ledningsförmågan i delområde Simpevarp generellt är låg. I termer av tolkade medelvärden för de tolkade litologiska domänerna varierar den termiska ledningsförmågan i ett relativt smalt intervall (2.6–2.8 W/(m·K)). En metodologi för uppskalning av termiska data erhållna på decimeterskala (borrkärna) har utvecklats. På kanisterskala (L=2 m) har kopplade skattats i ett intervall 0.2 till 0.28.

De hydrauliska egenskaperna hos tolkade hydrauliska bergdomäner beskrivs utgående från ett diskret spricknätverk (DFN) med den geometrisk beskrivning som erhålls från den geologiska DFN-beskrivningen. DFN-modellen tillskrivs en fördelning av spricktransmissiviteter, som sedan kalibreras mot existerande resultat från hydrauliska tester i borrhål. En arbetshypotes är att den hydrauliska DFN-modellen kopplar transmissivitet (T) och storlek på konduktiva sprickor/strukturer (L) med hjälp av en potensfunktion (på formen $T=aL^b$), upp till en storlek motsvarande mindre deformationszoner (L < 1 000 m).

Totalt 13 av de tolkade deformationszonerna har testats hydrauliskt i borrhål. Variations-bredden i tolkad transmissivitet från dessa borrhålsintercept varierar från 10^{-8} till 4×10^{-4} m^2/s. Olika alternativa hydrauliska DFN-modeller har utnyttjats för att simulera effektiva blockmedelvärden av hydraulisk konduktivitet på olika skalor. Resultatet av beräkningen av blockmedelvärden visar att 20 m block i medeltal är mindre konduktiva än 10^{-8} m/s. Lokala grundvattenflödesregimer antas utvecklas i de två delområdena, och bedöms ha en vertikal utsträckning till cirka 600–1 000 m djup, beroende på lokal topografi. I delområde Simpevarp, nära Östersjöns kustlinje, och där den topografiska variationen är begränsad, är den vertikala utsträckningen av lokala flödesceller mer begränsad. Detta står i kontrast till delområde Laxemar, med en högre topografi, som resulterar i en mer markerad grundvattencirkulation som verkar ha en utsträckning till cirka 1 000 m djup i närheten av borrhål KLX02. Numerisk flödesmodellering visar att grundvattenflöde bestäms av topografi och geometrin hos det system av modellerade deformationszoner. Modelleringen identifierar delområde Simpevarp som ett område karakteriserat av uppåtriktat grundvattenflöde (utströmningsområde) på förvarsdjup.

Tre huvudsakliga grundvattenytyper har identifierats i delområde Simpevarp: Typ A (utspätt och av Na-HCO3 karaktär) som återfinns på ytliga djup (< 100 m); Typ B (bräckt, huvudsakligen av Na-Ca-Cl karaktär) som återfinns på ytliga till intermediära djup (150–300 m); Typ C (salt (6 000–20 000 mg/l Cl, 25–30 g/L TDS), huvudsakligen Na-Ca-Cl) på intermediära till stora djup (> 300 m). De markerade skillnaderna i grundvattenflödesregimer (i termer av penetration av lokala flödesceller) mellan delområde Simpevarp och Laxemar återspeglas i mätt vattenkemi. Därutöver visar vår nuvarande kunskap att mätta parametrar i grundvattenprover svarar upp på de hydrokemiska stabilitetskriteria som definierats av SKB.

Tillämpning av hydrauliska DFN-modeller och blockegenskaper deriverade på basis av dessa, visar att alla hydrauliska DFN-modeller som definierats för Simpevarp 1.2 kan användas för att rekonstruera mätta hydrokemiska parametrar i borrhål, om flödesporositeten i modellerna ökas. Transienta beräkningar av aktuell fördelning av salt, med hänsyn taget till transienta randvillkor (strandlinjeförskjutning på grund av isostatisk landhöjning och variabel salthalt i tidigare motsvarigheter till dagens Östersjön), visare resultat som är kompatibla med mätta geokemiska signaturer i utvalda referensborrhål. Resultaten visar dessutom att Littorinavatten, som också påvisats i platsundersökningarna, bör kunna återfinnas nära kusten och under Östersjön.

Den aktuella retardationsmodellen redovisar en parameterisering för intakt (ej omvandlad) och omvandlade varianter av de bergarter och modellerade litologiska domäner i delområdet. Föreslagna porositeter för intakt berg (i termer av medelvärden i volymsprocent) på domännivå varierar från 0.17 (finkorning dioritoid) till 0.40 (Ävrögranit). Föreslagna formationsfaktorer (motsvarande diffusionsegenskaper, i termer av medelvärden) för intakt berg på litologisk domännivå varierar från 1.0×10^{-4} (finkorning dioritoid) till 2.9×10^{-4} (Ävrögranit).

Osäkerheter

Som redovisats ovan har viktiga modelleringssteg tagits under Simpevarp 1.2. De huvudsakliga osäkerheterna är identifierade, i vissa fall kvantifierade, eller belysta i form av alternativa modeller. Trots allt så är vissa osäkerheter i detta skede inte kvantifierade och alternativa hypoteser behålls just som hypoteser, utan att behandlas explicit i modellanalyserna. Ytterligare data, som samlats in i delområde Simpevarp efter datafrysen för Simpevarp 1.2 kan möjliggöra ytterligare kvantifiering, och kan användas till att reducera observerade osäkerheter ytterligare.

För de geologiska modellerna så är olika alternativa beskrivningar möjliga givet osäkerheter i geometri (storlek/utsträckning lateralt och vertikalt, stupning och avslutning (bl.a. mot andra zoner)), osäkerheter i karaktär och egenskaper och konfidensgrad hos modellerade litologiska domäner och deformationszoner. Ingen analys av möjliga alternativa modeller har dock genomförts som en del av den aktuella modellversionen. Detta gäller också möjlig förekomst av subhorisontella zoner. Det bör påtalas att endast begränsade indikationer av möjliga subhorisontella deformationszoner finns i delområde Simpevarp. På motsvarande sätt har inga större subhorisontella zoner identifierats i borrhål och underjordsanläggningar på Äspö.

Alternativa geologiska DFN-modeller har utarbetats på basis av alternativa storleksmodeller för de identifierade sprickseten. I hydrogeologi har alternativa hydrauliska DFN-modeller (med alternativa antaganden om korrelationen mellan sprickstorlek och transmissivitet) tagits fram, som sedan har propagerats i beräkning av blockkonduktiviteter och i tillskrivning av egenskaper till upprättade regionala flödesmodeller.

För övriga ämnesområden är andra alternativa modeller (hypoteser) möjliga, men har inte bearbetats vidare inom ramen för modellversion Simpevarp 1.2.

Möjliga interaktioner mellan ämnesområden, och de faktiska interaktioner som beaktats för version Simpevarp 1.2 diskuteras. Det är uppenbart att förändringar i den litologiska modellen har ett stort genomslag på de flesta ämnesområdesmodellerna (t.ex. bergmekanik, termiska egenskaper och transportegenskaper). Deformationszonsmodellen påverkar i synnerhet de bergmekaniska och hydrogeologiska modellerna. På motsvarande sätt existerar ett stort inslag av ömsesidigt beroende mellan hydrogeologi och hydrogeokemi, främst genom beskrivningen av blandningsprocesser, som föreslås som huvudsakligen ansvarig för utvecklingen av grundvattenkemin, inklusive fördelning av salt, över tiden. Den hydrogeokemiska modellen är vidare i begränsad omfattning beroende av den kemiska sammansättningen hos berggrunden och sprickmineral. Dessutom finns också kopplingen mellan geologi (mineralogi), hydrogeokemi och transportmodellen, för beskrivningen av bergets sorptionsegenskaper. Andra aspekter rörande den framtagna transportmodellen är kopplade till bergspänningseffekter, både i bergmassan (som kan påverka in situ-mätningar för bestämning av formationsfaktor längs borrhål) och i laboratorium (effekter av spänningsavlastning), på bestämning av storlek och anisotropi hos bergets diffusionsegenskaper, delvis påverkat av bergets inneboende textur och foliation. Vad som dock återstår att etablera och bättre kvantifiera är samspelen mellan ”ytsystemet” och ”bergsystemet”. Detta gäller i första hand omsättning av vatten och kemiska massbalanser.

Slutsatser

Modellversion Simpevarp 1.2 med tillhörande beskrivning är i generell samklang och konsistens med nuvarande kunskap om områdets tidigare utveckling. Detta gäller t.ex. aktuell grundvatt ensammansättning ställt mot berggrundsgeologi och aktuella sprickmineral. Vidare så ger den hydrogeologiska modelleringen av grundvattnets kemiska utveckling rimliga aktuella kemier vid jämförelse med tillgängliga analysresultat från provtagning i borrhål. Inga stora överraskningar har noterats under modelleringen för modellversion Simpevarp 1.2. Mer kvantitativa data producerats for Simpevarp 1.2 jämfört med Simpevarp 1.1. Några alternativa modeller/hypoteser har undersökts, och även propagerats i analysen, men osäkerheter består, framförallt i delområde Laxemar och i den regionala modellvolymen. Vidare karakteriseras modelleringen för Simpevarp 1.2 av ett större inslag av interaktion mellan de ämnesvisa modellerna.

Contents

1 Introduction

1.1 Background

The Swedish Nuclear Fuel and Waste Management Company (SKB) is undertaking site characterisation at two different locations, the Forsmark and Simpevarp areas, with the objective of siting a geological repository for spent nuclear fuel. The characterisation work is divided into an initial site investigation phase and a complete site investigation phase, /SKB, 2001a/. The results of the initial investigation phase will be used as a basis for deciding on a subsequent complete investigation phase. The results of the complete site investigations will form the basis for selection of a repository site and the license application to construct a repository at that site. During the subsequent Construction and Detailed Investigation Phase additional (detailed) investigations will be performed.

An integrated component in the characterisation work is the development of a site descriptive model that constitutes a description of the site and its regional setting, covering the current state of the geosphere and the biosphere as well as those ongoing natural processes that affect their long-term evolution. The site description includes two main components:

- a written synthesis of each site summarising the current state of knowledge as well as describing ongoing natural processes which affect its long-term evolution, and
- a site descriptive model (made up of discipline-specific models), in which the collected information is interpreted and presented in a form which can be used in numerical models for rock engineering, environmental impact and long-term safety assessments.

More about the general principles for site descriptive modelling and its role in the site investigation programme can be found in the general execution programme for the site investigations /SKB, 2001a/. Figure 1-1 shows a graphical attempt to put the site-descriptive modelling into its context with mutual interdependencies with the various clients, the Site Investigations on the one hand, and Repository Engineering (Design) and Safety Assessment on the other. Based on Site-Descriptive Model (SDM) version 1.2, Repository Engineering produces layout D1 which jointly with SDM version Simpevarp 1.2 form the basis for the PSE (Preliminary Safety Evaluation) on the Simpevarp subarea. The Safety Report SR-Can is based on SDM version 1.2 for Forsmark and the Laxemar subarea. Another important recipient of the SDM is Environmental Impact Assessment, (the latter entity not illustrated in Figure 1-1) .

Central in the modelling work is the geological model which provides the geometrical context in terms of the characteristics, location, geometry and extent of deformation zones[1] and the rock mass units between the zones. Using the geological and geometrical description as a basis, descriptive models for other scientific disciplines (hydrogeology, hydrogeochemistry, rock mechanics, thermal properties and transport properties) are developed /SKB, 2000b/. In addition, a description is provided of the surface ecological system which includes the interface between the geosphere and the biosphere, as well as being the domain in which the radiological impacts of any releases of radionuclides from the repository are assessed.

Great care is taken to arrive at a general consistency in the description of the various models. In addition, a comprehensive assessment of uncertainty is undertaken and possible needs for alternative models are identified /Andersson, 2003/. First attempts along this path in the actual site descriptive modelling have been taken with the version 1.1 models of the Forsmark /SKB, 2004a/ and the Simpevarp subarea /SKB, 2004b/.

[1] The term *deformation zone* is used to designate an essentially 2-dimensional structure (sub-planar structure with a small thickness relative to its lateral extent) along which deformation has been concentrated /Munier et al. 2003/. See also Chapter 5 for use in this modelling.

Figure 1-1. *Site Descriptive Modelling (SDM) and its main product in a context. Illustrated is also the exchange of information (deliveries and feedback) between the main technical activities which provide data to the site modelling, or which makes use of the site modelling and the associated description.*

Models are developed at a regional scale (hundreds of square kilometres) and on a local scale (tens of square kilometres). The model on the regional scale serves to provide boundary conditions and a geological and hydrological context for the local scale models. Unlike the Forsmark area, two models are developed in the Simpevarp area, one for the Simpevarp subarea and one for the Laxemar subarea, cf. Section 1.3 and Figure 1-1. Descriptive model versions are produced at specified times that are adapted to the needs of the primary users, i.e. repository design and safety assessment. These specified times define a "data freeze" which defines the database that provides input to the model version in question. The results of the descriptive modelling also serve to produce feedback to, and set the priorities for the ongoing site characterisation.

1.2 Objectives and scope

The main overall objectives of the site modelling project are to develop and present a preliminary site description of the Simpevarp area based on field data collected during the initial site investigation. Furthermore, to give recommendations on continued field investigations based on results and experiences gained during the work with the development of site descriptive model versions.

The Simpevarp candidate area was originally about 50 km^2 in size. Early 2003 SKB identified two subareas, named the Laxemar subarea and the Simpevarp subarea, that were prioritised for further investigations /SKB, 2003b/, see Figure 1-2. As investigation activities proceeded with different speed at the two subareas it was decided to produce separate modelling reports for the two subareas.

The basis for both the interim version (model version Simpevarp 1.1 /SKB, 2004b/) and the preliminary site description (model version Simpevarp 1.2 (this report) and the subsequent Laxemar 1.2 site-descriptive model) are quality-assured, geoscientific and ecological field data from the Simpevarp area available in the SKB databases SICADA and GIS at the pre-defined dates. These dates for "data freeze" are April 1st 2004 for the preliminary site description of the Simpevarp subarea (model version Simpevarp 1.2) and November 1st 2004 for the Laxemar subarea (model version Laxemar 1.2). All new information that became available up to these dates has been used to re-evaluate the pre-existing knowledge built into the version 0 and version 1.1 of the site description, respectively, in order to re-asses the validity of the previous model version.

The specific objectives of the current version (version 1.2) of the preliminary site description for the Simpevarp subarea (this report) are to:

- produce and document an integrated description of the site and its regional environments based on the site-specific data available from the initial site investigations;
  - analyse the primary data available in data package Simpevarp 1.2,
  - build a three-dimensional site descriptive model,
  - perform an overall confidence assessment including systematic treatment of uncertainties and evaluation of alternative interpretations,
  - develop, document and evaluate alternative models in a systematic way,
  - perform modelling activities in close interaction with safety analysis and repository engineering,
  - highlight and, when the available data allow, answer all current site specific geoscientific and ecological key issues for understanding the site.
- perform the safety related geosphere and biosphere analyses as specified as Site Modelling in the planning document for the Preliminary Safety Evaluation (PSE) /SKB, 2002a/;
- give recommendations on continued investigations in the final document as well as on a continuous basis.

The current report constitutes the second (version 1.2 of the) preliminary site description for the Simpevarp subarea. As in all site investigations, there are still substantial uncertainties in the developed descriptive model. Not all of these uncertainties are crucial to the overall function and safety of a conceived repository. The concluding chapters discuss the relative importance of the various uncertainties identified, and also outline future work required to minimise or eliminate the important uncertainties.

1.3 Setting

The Simpevarp area is located in the province of Småland (County of Kalmar), within the municipality of Oskarshamn, and immediately adjacent to the Oskarshamn nuclear power plant (OI–OIII) and the Central interim storage facility for spent fuel (Clab), cf. Figure 1-2 and Figure 2-1. The Simpevarp area (including the Simpevarp and Laxemar subareas) is located close to the shoreline of the Baltic Sea. The easternmost part (Simpevarp subarea) includes the Simpevarp peninsula (which hosts the power plants and the interim storage facility for spent fuel (Clab), cf. Figure 2-1) and the islands Hålö and Ävrö. The island of Äspö, under which the Äspö Hard Rock Laboratory (Äspö HRL) is developed, is located some two kilometres north of the Simpevarp peninsula. The areal size of the Simevarp subarea is approximately 6.6 km^2, whereas the Laxemar subarea covers some 12.5 km^2. A detailed description of underlying primary data for the site-descriptive model, including geographical information and definition of modelling areas is provided in Chapter 2.

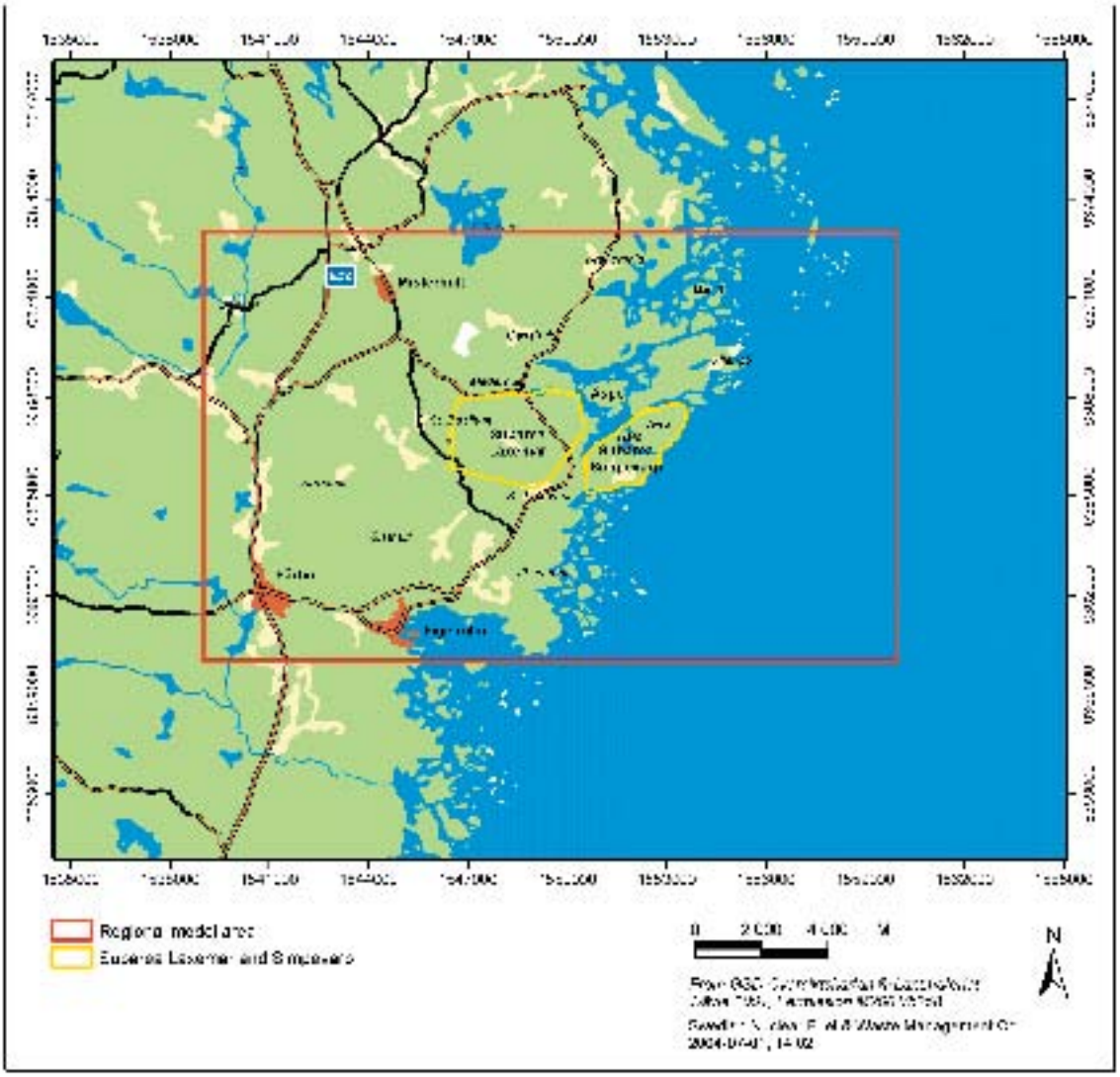

Figure 1-2. *Overview of the Simpevarp area and identification of the Simpevarp and Laxemar subareas.*

1.4 Methodology and organisation of work

1.4.1 Methodology

The project is multi-disciplinary in that it covers all potential properties of the site that are of importance for the overall understanding of the site, for the design of the deep repository, for safety assessment and for the environmental impact assessment. The overall strategy to achieve this (illustrated in Figure 1-3) is to develop discipline-specific models by interpretation and analyses of the quality-assured primary data stored in the two SKB databases, SICADA and GIS. The different discipline-specific models are then integrated into a unified site description. Old existing data from the construction of the power plants, the Clab facility and the Äspö Hard Rock Laboratory (Äspö HRL) are also incorporated in the analysis, see below.

The site descriptive modelling comprises the iterative steps of primary data evaluation, of descriptive and quantitative modelling in 3D, and of overall confidence evaluation. A strategy for achieving sufficient integration between disciplines in producing site descriptive models is documented in a separate strategy document for integrated evaluation /Andersson, 2003/, but has been developed further during the work with model versions 1.1 for Forsmark and Simpevarp. An account of the application of this integration strategy in the current modelling is accounted for in Chapter 12.

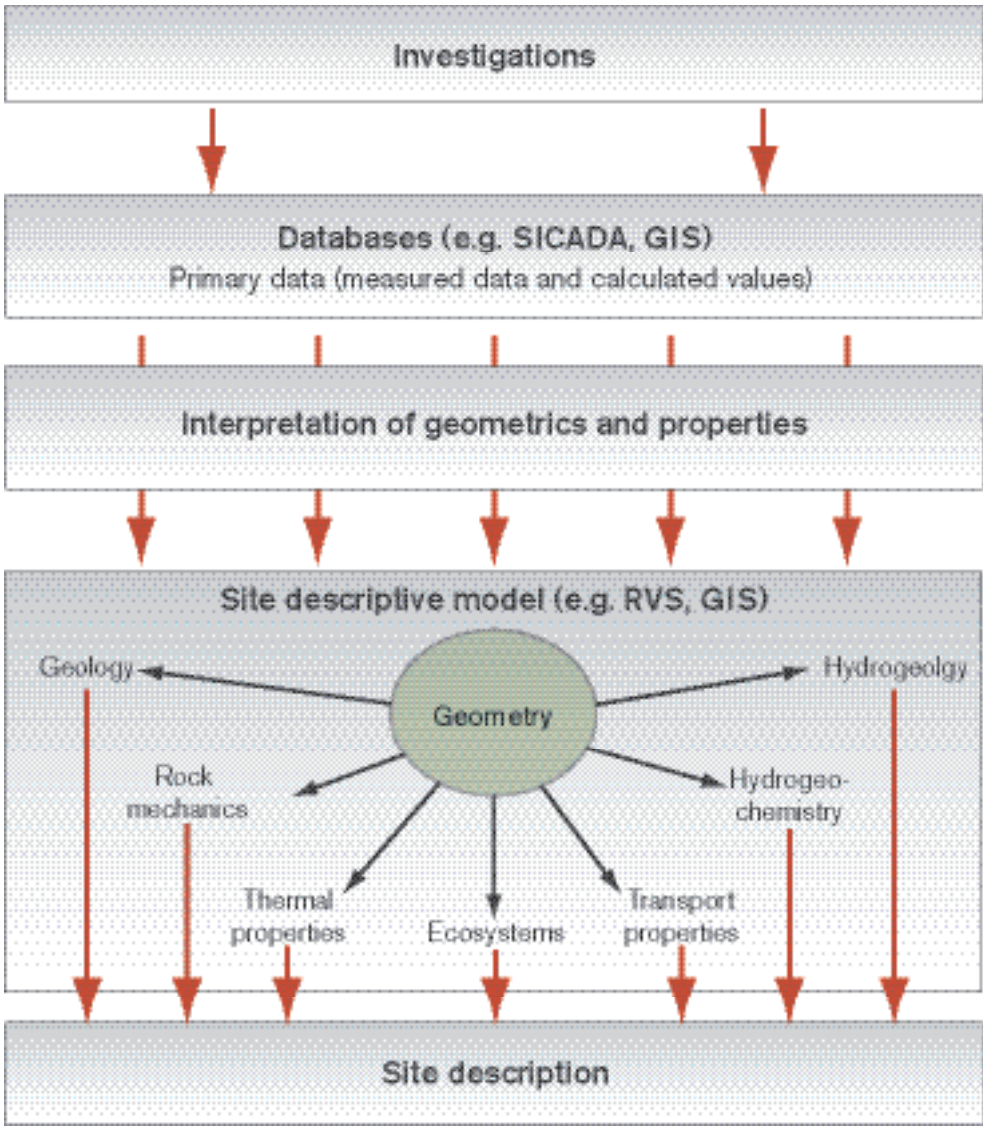

Figure 1-3. *From site investigations to site description. Primary data from site investigations are collected in databases. Data are interpreted and presented in a site descriptive model, which consists of a description of the geometry of different units in the model and the corresponding properties of the site /from SKB, 2002a/.*

Data are first evaluated within each discipline and then the evaluations are cross-checked between the disciplines. Three-dimensional modelling, with the purpose of estimating the distribution of parameter values in space, as well as their uncertainties, follows. The geometrical framework for modelling is taken from the geological model, and is subsequently used by the rock mechanics, thermal and hydrogeological modelling etc. (see Figure 1-4). The three-dimensional description should present the parameters with their spatial variability over a relevant and specified scale, with the uncertainty included in this description. If required, different alternative descriptions should be provided.

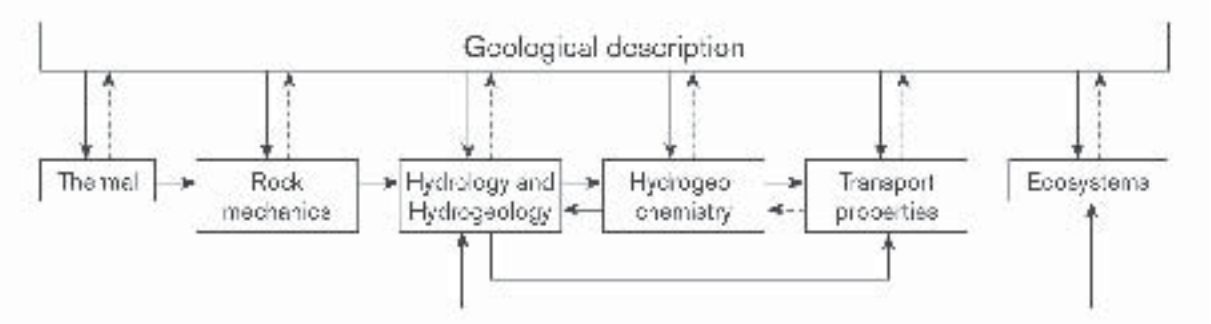

Figure 1-4. *Interrelations and feedback loops between the different disciplines in site descriptive modelling where geology provides the geometrical framework /from Andersson, 2003/.*

Methodologies for developing site descriptive models are based on experiences from earlier SKB projects, e.g. the Äspö HRL and the Laxemar modelling test projects. Before the underground laboratory at Äspö was built, forecasts of the geosphere properties and conditions at depth were made based on pre-investigations carried out around the Äspö island. Comparisons of these forecasts with observations and measurements in tunnels and boreholes underground and evaluation of the results showed that it is possible to reliably describe geological properties and conditions with the aid of analyses and modelling /Rhén et al. 1997a,b; Stanfors et al. 1997/. The Laxemar modelling test project /Andersson et al. 2002a/ was set up with the intention to explore the adequacy of the available methodology for site descriptive modelling based on surface and borehole data and to identify potential needs for developments and improvements in methodology. The project was a methodology test using available data from the Laxemar area. Subsequently, as previously mentioned, full application of the developed methodologies has been undertaken in the version 1.1 descriptive modelling of the Forsmark /SKB, 2004a/ and Simpevarp /SKB, 2004b/ areas.

The current methodologies for developing the discipline-specific models are documented in methodology reports or strategy reports. In the present work, the guidelines given in those reports have been followed to the extent possible with the data and information available at the time for data freeze for model version Simpevarp 1.2. How the work was carried out is described further in Chapters 4 through 11. For more detailed information on the methodologies the reader is referred to the methodology reports. These are:

- Geological Site Descriptive Modelling /Munier et al. 2003; Munier, 2004/.
- Rock Mechanical Site Descriptive Modelling /Andersson et al. 2002b/.
- Thermal Site Descriptive Modelling /Sundberg, 2003a/.
- Hydrogeological Site Descriptive Modelling /Rhén et al. 2003/.
- Hydrogeochemical Site Descriptive Modelling /Smellie et al. 2002/.
- Transport Properties Site Descriptive Modelling /Berglund and Selroos, 2003/.
- Ecosystem Descriptive Modelling /Löfgren and Lindborg, 2003/.

According to /Andersson, 2003/, the overall confidence evaluation should be based on the results of the individual discipline modelling and involve the different modelling teams. The confidence is assessed by carrying out checks concerning e.g. the status and use of primary data, uncertainties in derived models, and various consistency checks such as between models and with previous model versions. This strategy has been followed when assessing the overall confidence in model version Simepvarp 1.2. The core members of the project and the activity leaders from the Simpevarp site investigation group together accomplished protocols addressing uncertainties and biases in primary data, uncertainty in models and potential for alternative interpretations, consistency at interfaces between disciplines, consistency with understanding of past evolution and consistency with previous model versions. The results are described in Chapter 12.

1.4.2 Organisation of work

The work has been conducted by a project group and associated discipline-specific working groups, or persons engaged by members of the project group. The members of the project group represent the disciplines of geology, rock mechanics, thermal properties, hydrogeology, hydrogeochemistry, transport properties and surface ecosystems (including overburden, surface hydrogeochemistry and hydrology). In addition, some group members have specific qualifications of importance in this type of project e.g. expertise in RVS (Rock Visualisation System) modelling, GIS-modelling and in statistical data analysis.

Each discipline representative in the project group was given the responsibility for the assessment and evaluation of primary data and for the modelling work concerning his/her specific discipline. This task was then done either by the representatives themselves, or together with other experts or groups of experts outside the project group. In this context the discipline-specific groups set up by SKB play an important role. These are essentially run by the person responsible for the given discipline and are used for carrying out site modelling tasks, and for providing technical links between the site organisation, the site modelling team and the principal clients (Repository Engineering, Safety Assessment and Environmental Impact Assessment). Table 1-1 identifies the NET-groups actively involved in the site modelling work. Supporting reports have been produced for some of the discipline-specific work carried out within the framework of model version Simpevarp 1.2. References to these supporting reports are given at the appropriate places in subsequent chapters of this report.

The project group has met at regular intervals to discuss the progress and integration of the work and specific questions that have emerged during the modelling work. In addition, the project group has had a workshop addressing uncertainties, integration of and interaction between disciplines and overall confidence in the analysis made and models produced. The information exchange between the modelling project and the site investigation team is an important component of the project, which is facilitated by the fact that some of the project members are also engaged as experts in the site investigation team. In addition, the investigation leader of the site investigations at Simpevarp has participated in most of the modelling project meetings.

Table 1-1. Discipline-related analysis groups active in the site modelling work and their mandates/objectives.

Dicipline	NET-Group	Mandate
Geology	GeoNET	Constitute the group for execution of the geological modelling as specified by the geological part of the site modelling projects promote and to promote technical exchange of experiences and coordination between the two modelling projects and the site organisations.
Rock Mechanics and Thermal Properties	MekNET	Coordination of modelling tasks for rock mechanics and thermal properties at both sites. Resource for development and maintenance of method descriptions.
Hydrogeology	HydroNET	Execution of the hydrogeological modelling, constitute a forum for all modellers within hydrogeology (needs of site modelling and safety assessment and design), promote technical exchange of experiences
Hydrogeochemistry	HAG	To model the groundwater data from the sites and assure that the data quality is sufficient. Produce site descriptive hydrogeochemical models. Integrate the description with other disciplines and make recommendations for further site investigations
Surface system	SurfaceNET	To model and describe the surface system by description by subdiscipline (biotic and abiotic), model the properties in a distributed way (maps and 3D), model the processes interdisciplinary (space and time), describe the different ecosystems (conceptually and site specific), describe and model the flow of matter in the landscape, define and connect the biosphere objects, produce site descriptions to support environmental impact assessment (EIA).

1.4.3 Important changes compared to Simpevarp 1.1 work

Simpevarp 1.1 suffered from a planned delay of the geological model in order to make use of a new lineament analysis. This planned delay implied that the hydrogeological modelling for Simpevarp 1.1 was based on the version 0 regional structural model. The availability of a full geological model for Simpevarp 1.2 allows for a full hydrogeological modelling sequence as reported in Chapter 8. Overall, the proper sequencing of modelling activities, with availability of a comprehensive geological model has provided a much better opportunity for integration of results of individual disciplines and confidence building.

Important changes to the overall modelling strategies include development of an updated appendix /Munier, 2004/ to the strategy document for Geology /Munier et al. 2003/ which details and clarifies the foreseen products expected from the geological Discrete Feature Network (DFN) modelling.

An additional change in premises is related to redistribution of work on transport parameterisation between the site-descriptive modelling and Safety Assessment to the effect that flow-related transport parameters are handled by Safety Assessment and are not presented as part of the bedrock transport properties modelling herein. The hydrogeological site-descriptive modelling may still use flow-related transport parameters for their analysis, but the results are in this case used/presented in a context of site-understanding, rather than as measures of solute transport.

Compared with the structure of the version 1.1 reports, the version 1.2 reports have been changed to the effect that all major disciplines now are covered by individual chapters that encompass the full chain going from primary data screening, exploratory analysis to 3D modelling and assessment of uncertainties. This report is a first trial of this new approach to presentation, cf. Section 1.5.

1.5 This report

This report presents the preliminary site description for the Simpevarp subarea. For reasons explained in Section 2.8 the local model volume also includes the Laxemar subarea. However, new data for updating of previous model versions – at the time of the data freeze – essentially only existed for the Simpevarp subarea. Hence, uncertainties for the Laxemar subarea are significantly higher than those for the Simpevarp subarea.

This report follows an updated structure for descriptive modelling reports for the initial investigation phase which differs significantly from that applied to the version 1.1 reports for Forsmark and Simpevarp. Chapter 2 summarises available primary data and provide an overview of their usage. Chapter 3 provides an account of the development of the geosphere and the surface systems in an evolutionary perspective. Chapters 4 through 10 in sequence provide accounts of the modelling of surface ecology, geology, rock mechanics, thermal properties, hydrogeology, hydrogeochemistry and transport properties, respectively. Each chapter includes the discipline-based accounts of evaluation of the primary data, three-dimensional modelling and discussion of identified uncertainties associated with the developed models. Chapter 11 encapsulates the resulting descriptive model of the Simpevarp subarea in a condensed form. Chapter 12 discusses overall consistency between the various disciplines and identifies the interactions between disciplines, and finally outlines possible alternative interpretations in light of observed uncertainties. Chapter 13 provides the overall conclusions of the work performed and i.a. discusses implications for the continued site investigation work and the future modelling process.

2 Available data and other prerequisites for the modelling

The database used for the site-descriptive modelling is evolving, successively adding more data, as more boreholes are completed. Each defined model version is associated with a "data freeze" defined at a discrete point in time. This chapter sets out to define the database used for the Simpevarp 1.2 modelling, and other associated premises and prerequisites for the modelling work. The account given here is provided primarily for future reference and for traceability. Specific data are not provided, nor discussed. References are however given to the appropriate data sources. Details of the data are to be found in other reports in the SKB P-series[1] of reports relating to the Site Investigation. Discussions on specific data and how they have been used can be found Chapters 4 through 10. Chapter 12 discusses what data were available, but not used, and explains why those data were not used.

2.1 Overview

Investigations have been in process at the Simpevarp subarea from about March 2002. The data freeze for the Simpevarp 1.1 model version was set at July 1, 2003. The position in relation to the availability of important geological data at that time is described in /SKB, 2004b/. The data freeze for version Simpevarp 1.2 was set at April 1, 2004. At that time the stature of geological database was significantly improved and the associated modelling had been undertaken. However, although the lineament data and analysis was essentially complete and fully covered the whole regional scale modelling area, one important component – the lithological mapping of the Laxemar subarea and regional surroundings – was yet to be completed and delivered. In fact, access to the Laxemar area was not granted until December 2003. Apart from the geological component, the database at April 1, 2004 comprised additional elements of surface and borehole investigations. The latter component comprised data from three new cored boreholes, complementary data from two old cored boreholes, and data from three percussion-drilled boreholes. The surface investigation data included work primarily focused on the Simpevarp subarea (investigations of outcrop solid geology and the overburden (Quaternary deposits)). Review of old geological data from the construction of the nuclear power plants and the Clab facility) had not been carried out to the extent originally proposed. The database for the site-descriptive modelling for Simpevarp 1.2 consequently comprises:

- Primary data used in Simpevarp model versions 0 /SKB, 2002b/ and 1.1 /SKB, 2004b/.
- Data previously not considered (i.e. the new primary data obtained from the second stage of the initial site investigations and, partially, data arising from review of old geological information).

2.1.1 Primary data collected before the start of the site investigation

The major data sources for the version 0 model of the Simpevarp area, developed before the beginning of the site investigations in the Simpevarp area, were:

- Information from the feasibility study /SKB, 2000a/.
- Selected sources of "old data".
- Additional data collected and compiled during the preparatory work for the site investigations, especially relating to the discipline "Surface Ecosystems".

[1] The P-series report the results of the ongoing site investigations at Oskarshamn (Simpevarp and Laxemar subareas) and Forsmark. These reports are available on the SKB web page together with reports in the SKB R- and TR-series (www.skb.se).

The version 0 descriptive model of the Simpevarp area /SKB, 2002b/ was based on data available before the beginning of the site investigations, for the most part not collected for reasons directly related to deep disposal of spent nuclear fuel. An important component of the work was the compilation of a data inventory, in which the location and scope of all potential sources of relevant data were detailed and evaluated with respect to potential usefulness in future descriptive modelling. This included a general description of existing geographically based data, most of which are stored in the SKB GIS, a survey of data already stored in the SICADA database, and an inventory of other sources of data, whose information content had not yet been assessed and/or input into SICADA or the SKB GIS.

Data sources relevant to the site descriptive modelling of the Simpevarp area which remained to be evaluated/converted/inserted into existing official databases included data related to the construction of the Simpevarp nuclear power plants (OI–OIII) and associated tunnels and storage caverns. They also included data related to the interim storage facility for spent nuclear fuel (Clab), and data related to the siting, pre-investigation, predictive modelling, construction and operative phases of the Äspö Hard Rock Laboratory (Äspö HRL). In addition, other data sources related e.g. to earlier site investigations at Bussvik, Laxemar, Kråkemåla, Simpevarp and Ävrö were only partially included in SICADA at the time of the version 0 modelling

It is emphasised that comprehensive detailed revisiting, analysis and inclusion of the data mentioned above in the various modelling steps was not possible for version Simpevarp 1.1, and not even for version Simpevarp 1.2. However, the need for such activities is recognised as a complement to future work on site investigation in the event such re-analysis and re-interpretation will add substantially to the understanding of the investigated site.

2.1.2 Investigations performed and data colleted during the site investigations up until the data freeze for Simpevarp 1.2

The site investigations that began in March 2002 have comprised the following major components:

1) Establishment of a coordinate system including fixed points and defined grid corner points distributed across the Simpevarp area.
2) Surface investigations.
3) Drilling, including investigations during drilling.
4) Borehole investigations performed following completion of each individual borehole.

Below, those investigations that provided data for the Simpevarp 1.2 data freeze are identified and outlined.

The surface investigations undertaken in the Simpevarp subarea comprised the following:

- Airborne photography (performed in 2001).
- Airborne and surface geophysical investigations.
- Lithological mapping of the rock surface.
- Mapping of structural characteristics.
- Mapping of Quaternary deposits and soils.
- Marine geological investigations.
- Water level measurements, hydraulic tests and hydrogeochemical sampling in boreholes completet in the overburden (se listing below).
- Hydrogeochemical sampling of surface waters.
- Various surface ecological inventory compilations and investigations.

The drilling activities during this time have comprised:

- Four approximately 1,000 m deep cored boreholes (KSH01A, KSH02, KSH03A and KAV04) and two 100 m cored boreholes (KSH01B and KSH03B) in the immediate vicinity of two of the deep holes cf. Figure 2-1. To this should also be added borehole KLX04 drilled in the Laxemar subarea (from which only limited investigation data are available, e.g. stress measurements).
- Three percussion drilled boreholes (HSH01, HSH02 and HSH03) with lengths ranging up to 200 m and reaching depths of 185–200 m.
- Weight sounding at 23 sites and soil/rock drilling of 19 boreholes (machine augering to rock surface for total depth of overburden). The latter includes four boreholes drilled for environmental monitoring in conjunction with drill sites on the Simpevarp peninsula. Furthermore, manual augering of 17 boreholes, in conjunction with mapping of the overburden. Details of these boreholes and their spatial distribution are provided in /SKB, 2005/.

The borehole investigations following the drilling of the boreholes in bedrock can broadly be divided into the following:

- Logging of the bedrock parts of the core-drilled and percussion-drilled boreholes using; BIPS colour TV-camera, borehole radar with a directional antenna and a conventional suite of geophysical logs (employing electric, magnetic and radioactive methods).
- Detailed mapping of the core-drilled boreholes using the drill core and BIPS-images (so-called Boremap-mapping) and geophysical logging data from the borehole.
- Rock stress measurements using the overcoring or the hydrofracturing techniques.
- Mapping of percussion-drilled boreholes in solid rock using BIPS images – no drill core exists, the mapping is here supported by samples of drill cuttings and geophysical logging data.
- Hydraulic measurements in bedrock parts of core-drilled boreholes and percussion-drilled boreholes, and in soil boreholes (full depth).
- Sampling of rock and fractures for determination of density, porosity, susceptibility, mineralogy, geochemistry, diffusivity, sorption properties, rock strength and thermal properties.
- Groundwater sampling in the bedrock parts of core-drilled boreholes, percussion-drilled boreholes, and in soil boreholes.

All data are stored in the SKB databases SICADA and SKB GIS. The basic primary data are also described in the SKB P-series of reports, cf. tables in Section 2.7 cataloguing data used by the individual disciplines.

2.2 Previous model versions

2.2.1 Version 0

The version 0 model of the Simpevarp area /SKB, 2002/ constitutes the point of departure for all future versions of descriptive models in the Simpevarp area. The database on which is it based is equivalent to the data available at the onset of the site investigation, which essentially is identical to the data compiled for the Oskarshamn feasibility study, /SKB, 2000a/. This database is mainly 2D (surface data) with the exception of data from the Äspö HRL, and is general and regional, rather than site-specific. Consequently, the version 0 model was developed at a regional scale. The principal components of the reporting are;

- An overview of the contents of the available data bases at the time (SICADA and GIS) and, more importantly, an inventory and assessment of relevant data in other “external” databases.
- A systematic overview of data needs and data availability for developing a site descriptive model for the Surface Eco systems (biosphere).
- A more detailed treatment of the existing data base and construction of descriptive model version 0 of the geosphere at the regional scale.

The geoscientific disciplines represented in the descriptive modelling are Geology, Rock mechanics, Hydrogeology and Hydrogeochemistry. Within each discipline identified uncertainties and alternative models are discussed with variable levels of detail.

2.2.2 Models developed as part of Äspö HRL and Ävrö work

Models preceding the version 0 model of the Simpevarp area included models developed on the basis of characterisation data produced for the siting and construction of the Äspö HRL. In this process, descriptive models have been developed for the Äspö island and its immediate environs /Rhén et al. 1997/. As part of the operational phase of the Äspö HRL, descriptive models, including conceptual models of fractures and fracture systems have been developed as part of the TRUE Programme /Winberg et al. 2000; Andersson et al. 2002c/, the Fracture Classification and Characterisation Project (FCC) /Mazurek et al. 1997; Bossart et al. 2001/, Äspö Task Force work /Dershowitz et al. 2003/ and the Prototype Repository Project /Rhén and Forsmark, 2001/. More recently, an effort has been made within the so-called GEOMOD project to revisit the 1997 site-scale descriptive models of Äspö, also attempting to incorporate the new information from the experimental work undertaken during the operational phase on a larger scale /e.g. Berglund et al. 2003/.

In preparation for the SKB site investigation programme, the Rock Visualization System (RVS) was tested out using information from the island of Ävrö /Markström et al. 2001/. A series of models of deformation zones and lithology was developed, incorporating successively more information starting from using surface information only, adding surface geophysics (reflection seismics), and finally incorporating data from existing core-drilled and percussion-drilled boreholes. Important feedbacks to the modelling process using RVS were also provided.

2.2.3 Laxemar test application

A more full-fledged test of the developed methodology for site descriptive modelling was made on the Laxemar area /Andersson et al. 2002b/. The intent was to explore whether the available methodology for site descriptive modelling using surface and borehole data was adequate, and further to identify needs for new developments and improvements. With limitations in scope – thermal properties and transport properties and surface ecology were not included – a descriptive model more or less equivalent to a version 1.2 descriptive model on a local scale was developed. The underlying data consisted of various types of surface data and data from two deep core-drilled boreholes. Controls of internal consistency and processing of the primary data for use in 3D modelling were undertaken.

In order to promote cross-discipline interpretation and check for consistency, the evaluation/modelling was performed individually for each discipline followed by cross-checking. The resulting hydrogeological description comprised hydraulic properties for defined geometrical units and pressure and flow boundary conditions applicable to present day conditions. The hydrogeochemical evaluation which i.a. included assessments of origin, turnover times and lateral/vertical distribution of groundwater included consistency checks with the hydrogeological model, which enhanced the confidence in the overall model. The hydrogeochemical model also included a conceptual model of the post-glacial development of the geochemical system. The rock mechanics description comprised the virgin rock stress field and the distribution of deformation and strength properties of the intact rock, fractures and deformation zones, and the fractured rock mass. In conclusion, despite its limited scope, the resulting description can be viewed as an illustration of the type of product that will emerge at the end of the initial site investigation stage. This indicated that the type of descriptive modelling outlined in the general execution programme is achievable. Hence, the Laxemar test application served as a preliminary and provisional model for the ongoing site-descriptive modelling in the Forsmark and Simpevarp areas.

2.2.4 Simpevarp 1.1

For the Simepvarp version 1.1 modelling the surface-based data sets were, in a relative sense, extensive compared with data sets from deep boreholes, were the information largely was limited to information from one new c. 1,000 m deep cored borehole (KSH01A) and two old cored boreholes (KLX01 and KLX02, in the Laxemar subarea).

Discipline-specific models were developed for the selected regional and local model volumes and these models were subsequently integrated into a unified site description. The procedures and guidelines given in strategy reports by discipline were followed to the extent possible, given the data and information available at the time of data freeze.

Compared with version 0 there were considerable additional features in the version Simpevarp 1.1, especially in the geological description and in the description of the near surface. The developed geological models of lithology and deformation zones were based on borehole information and surface data of much higher resolution. The lithology model included four interpreted rock domains and the deformation zone model included 14 zones of interpreted high confidence (of existence). A discrete fracture network (DFN) model was developed, including attempts to assess fracturing imposed by interpreted deformation zones. The rock mechanics strength model was based on information from the Äspö Hard Rock Laboratory and an empirical mechanical classification of data from KSH01A and data from outcrops. A first model of thermal properties of the rock was developed largely based on data from the Äspö HRL, and projections based on density and mineral content.

As a consequence of the planned delay in parts of the geological model for Simpevarp 1.1, the hydrogeological description was based solely on the version 0 regional structural model. Hydrogeological simulations of the groundwater evolution since the last glaciation were compared with the developed hydrogeochemical conceptual model. The conceptual model of the development of post-glacial hydrogeochemistry was updated. A first model of the transport properties of the rock was presented, although still rather immature, due to lack of site-specific data in support of the model. There was information regarding the distribution of Quaternary deposits, and some information about the stratigraphy of the till.

There was much uncertainty in the version Simpevarp 1.1 site descriptive model. However, the main uncertainties were regarded as being identified, some of which quantified and others left as input to alternative hypotheses. However, since a main reason for uncertainty in Simpevarp 1.1 was lack of data and poor data density, and as many more data were expected in future data freezes, it was not judged meaningful to carry the uncertainty quantification or the generation of alternative models too far.

2.3 Geographical data

The Simpevarp area, cf. Figure 1-2, is located close to the shoreline of the Baltic Sea and the investigated area extends out into the sea. The eastern-most land masses in the area include the Simpevarp peninsula, the Ävrö and Hålö islands and associated smaller islets. The western limit is located immediately west of the main highway (Route E22) that runs essentially north-south. The geographical data available for the Simpevarp version 0 site descriptive model are presented in /SKB, 2002, Section 2.1/. This report includes the applicable coordinate system, available maps (general map, topographic map, cadastral index map), digital orthophotography and elevation data.

The applicable coordinate system used for spatial coordinates for the version Simpevarp 1.2 modelling are:

- X/Y (N/E): The national 2.5 gon V 0:–15, RT90 system (“RAK”).
- Z (elevation): The national RH 70 levelling system /Wiklund, 2002/.

2.4 Surface investigations

Because of late access to Laxemar subarea, surface investigations were primarily constrained to the Simpevarp subarea (including the islands of Ävrö and Hålö), cf. Figure 2-3. An exception was Surface Ecology for which the collected data primarily are related to the regional scale model area. The investigations covered the following disciplines:

1. Bedrock geology.
2. Quaternary geology.

3. Geophysics.
4. Meteorology, hydrology and hydrogeology.
5. Hydrogeochemistry (boreholes in overburden and surface waters).
6. Surface ecology.

In the following, the investigations that have provided data for the data freeze Simpevarp 1.2 are summarised according to discipline. Bedrock geology and geophysical information are treated as one group, given their close interrelation.

2.4.1 Bedrock geology and geophysics

Bedrock mapping of the Simpevarp subarea started early in 2003 and continued until late in the year. As a consequence, the data freeze for the version Simpevarp 1.1 bedrock geological map and the integrated lineament interpretation was postponed to Dec 1, 2003. The bedrock mapping of the neighbouring Laxemar subarea and regional environs was initiated in the spring of 2004 and processing of the mapping continued till late fall 2004. As a consequence, the lithological and geophysical basis for the lithological modelling and lineament is essentially unchanged for version Simpevarp 1.2. The following data were available at the time of data freeze Simpevarp 1.2 (April 1, 2004):

- Geological outcrop database from SGU (Geological Survey of Sweden) field work.
- Bedrock map.
- Data from petrochemical and geochemical analyses made on surface samples collected from outcrops.
- Fracture mapping of outcrops (Scanline, Bedrock map).
- Detailed fracture mapping of selected outcrops (N=4) (area mapping).
- Ground-surface geophysical measurements.
- Interpretation of topographic data on land (from airborne photography).
- Interpretation of airborne geophysical data (Magnetic, EM, VLF, gamma-ray spectrometric data, evaluated depth of overburden).
- Lineament map over the Simpevarp area (Simpevarp and Laxemar subareas and regional surroundings).

2.4.2 Overburden

Overburden here refers to all surficial deposits irrespective of their origin. Mapping of Quaternary deposits in the Simpevarp subarea was initiated early in 2003 and was concluded in early fall of the same year.

Surface data

The surface data available for data freeze Simpevarp 1.2 comprised:

- Field data from mapping of Quaternary deposits.
- Map of Quaternary deposits of the (terrestrial parts of the) Simpevarp subarea.

Stratigraphical data

- Results from 19 machine-augered boreholes to establish total depth of overburden.
- Results from 17 manually augered boreholes.
- Results from 23 weigth-soundings.

2.4.3 Meteorology, hydrology and hydrogeology

- Meteorological data from a new station established on Äspö.
- Delineation and description of catchment areas, water courses and lakes.
- Manual “simple” discharge measurements in water courses.
- Manual and automatic water level measurements in cased machine-augered boreholes.
- Hydraulic tests (slug tests) in cased machine-augered boreholes completed in overburden (In total 13, 11 in the Simpevarp subarea and 2 in the Laxemar subarea), cf. Figure 2-2.

2.4.4 Hydrology and surface water hydrogeochemsitry

The hydrogeochemical surface investigations included in data freeze Simpevarp 1.2 comprised:

- Hydrogeochemical sampling in cased machine-augered boreholes. Representative sample only from one borehole cf. Figure 2-2.
- Sampling and analyses of precipitation.
- Sampling and analyses of surface waters.

2.4.5 Surface ecology

The surface investigations made exclusively as part of the surface ecological programme, and producing data for data freeze Simpevarp 1.2 comprised:

Terrestrial (biotic)

- Bird population survey.
- Mammal population survey.
- Vegetation mapping.

Surface waters (biotic)

- Compilation of information existing in 2002.
- Benthic fauna in sediments.
- Interpretation of dominant species.
- Macrophyte communities.

2.5 Borehole investigations

Compared to Simpevarp 1.1, which only included data from two new cored borehole and old data from two existing cored boreholes, Simpevarp 1.2 is based on a total of 5 new cored boreholes plus old and new complementary information from three old cored boreholes.

The borehole investigations generating new data for the Simpevarp 1.2 data freeze were performed in the following cored and percussion-drilled boreholes, cf. Figure 2-1:

- Cored boreholes: KSH01A/B, KSH02, KSH03A/B, KAV01, KAV04, KLX02 and KLX04 (rock stress data only).
- Percussion-drilled boreholes: HSH01, HSH02 and HSH03.

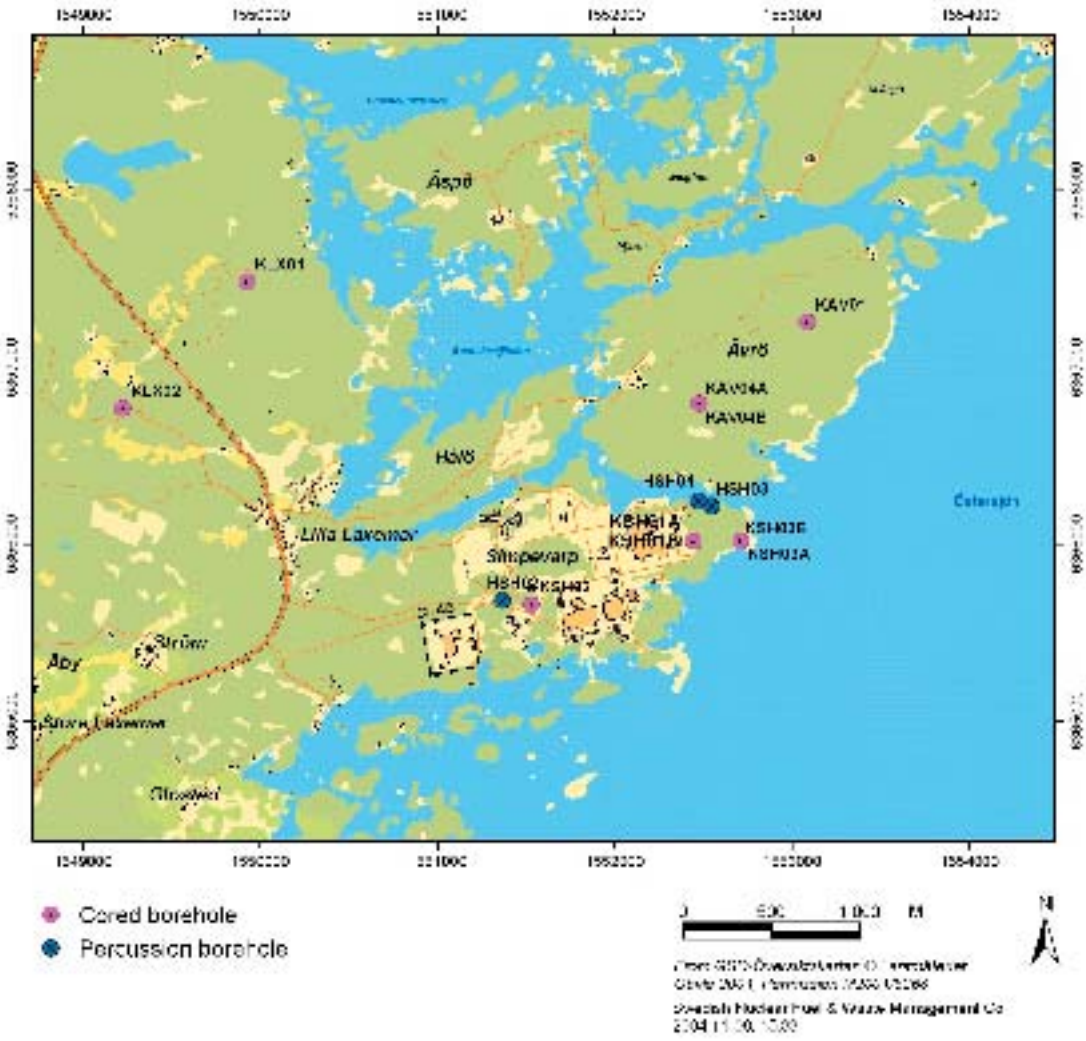

Figure 2-1. *Overview map of new core-drilled and percussion-drilled boreholes in the Simpevarp subarea.*

The investigations performed in the boreholes can be divided into three distinct groups:

- Measurements conducted during the drilling processes (either on a continuous basis or at discrete depth intervals in the borehole).
- Measurements conducted once the new borehole was completed (usually various types of continuous logs).
- Complementary measurements in old cored boreholes (KAV01 and KLX02) in order to elevate the stature of investigation to a level corresponding with the new cored boreholes.

Each of the three borehole types (cored, percussion, soil) were, in various ways, and to variable degrees, associated with the three groups of investigation modes outlined above. The investigation methods associated with the three modes are presented in Sections 2.5.1 through 2.5.3, respectively, followed by a comment on the borehole data included in the data freeze for Simpevarp 1.2.

To the new complementary data collected in old boreholes were also added selected old data and information from existing exploration boreholes, principally from the cored boreholes KLX01 located in the Laxemar subarea and boreholes from the Äspö HRL.

Detailed information about the types of boreholes completed in the overburden and their spatial distribution is provided in /SKB, 2005/.

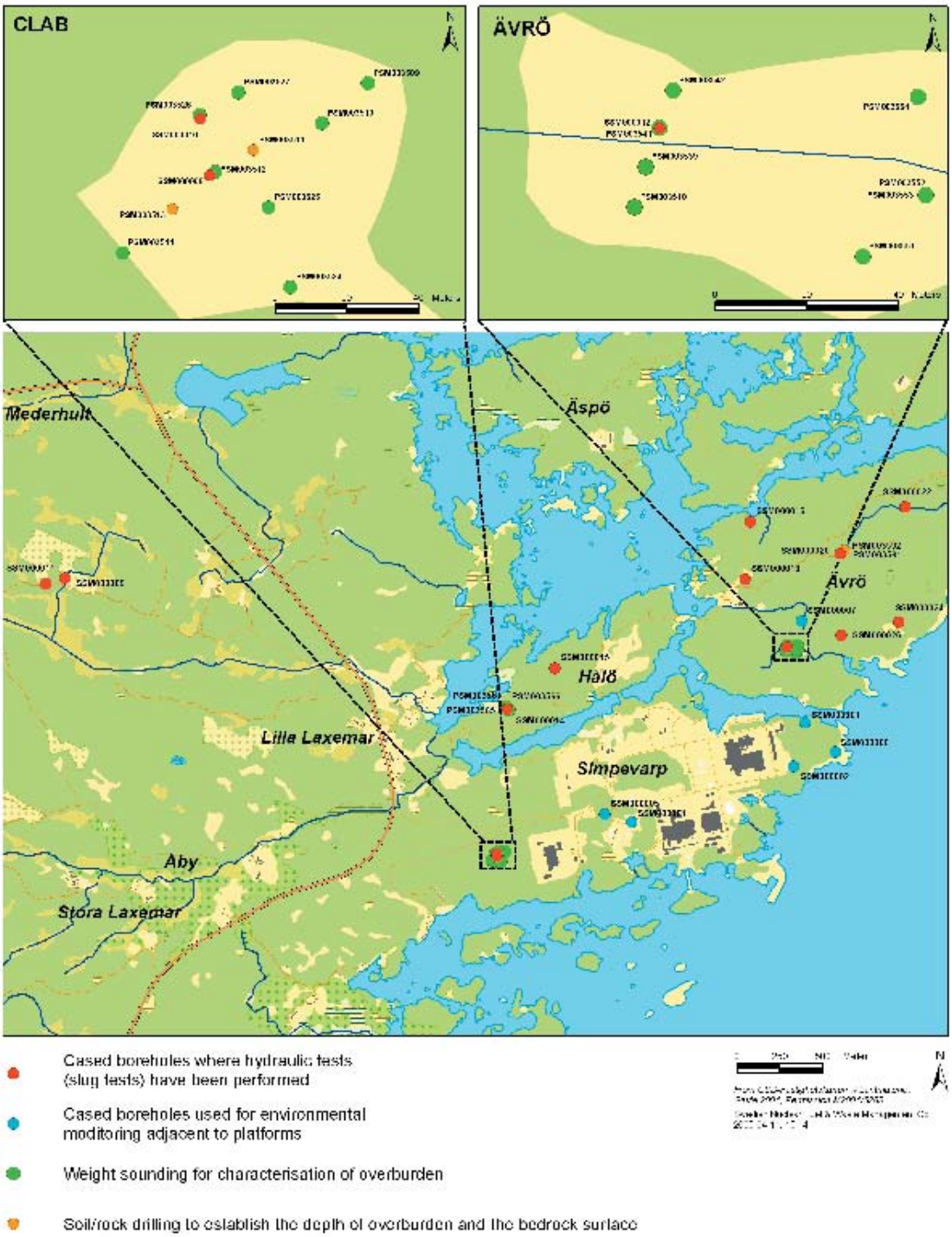

Figure 2-2. *Overview map of boreholes completed in the overburden, coded by types of investigations made in them.*

2.5.1 Borehole investigations during and immediately after drilling

Cored boreholes

Borehole investigations during and immediately subsequent to core drilling should normally include /SKB, 2001a/:

- Monitoring of drilling parameters (rate of penetration, together with flushing and return water parameters: flow rates, pressure, electric conductivity and concentration of dye tracer additive, etc.).

- Overview mapping of the drill core.
- Hydraulic tests employing a special test tool (the wireline probe).
- Measurements of absolute pressure using the wireline probe.
- Water sampling using the wireline probe.
- Borehole deviation measurements.
- Weighing of drill cuttings (and fine material).
- Rock stress measurements using the overcoring technique (HSH02, KAV04 and KLX04 only).

Specific comments regarding cored borehole KSH01A

Borehole KSH01A is a chemistry-prioritised borehole, which means that a complete hydrochemical characterisation programme is performed after drilling. However, during drilling water samples were also taken and the cleaning of drilling equipment was to a higher level than standard. Drilling of KSH01A followed the general approach employed for most deep boreholes completed during the site investigations /Ask et al. 2003/. The borehole has a varying diameter, with the upper 100.24 m of the borehole percussion drilled with a large diameter (φ = 200 mm). The remainder of the borehole, 100.24–1,003 metres, was core drilled using the triple-tube technique and a diameter of 76 mm (50.2 mm core). The use of both percussion- and core-drilling techniques implies that the methodologies applicable to both types of ongoing drilling process, as outlined above, were applied.

The wireline tests performed included five tests for absolute pressure and nine pumping tests for hydrogeological characterisation which were conducted at different length intervals (of which six resulted in useful transmissivity data). Three water samples were collected in three intervals of variable length between 197 and 620 m and analysed according to SKB Class 3 requirements. After drilling was completed, an airlift pumping and recovery test of the entire borehole was conducted.

The drilling of KSH01A and measurements during drilling were performed according to specified routines. As it was the first cored borehole in the site investigation of the Simpevarp subarea, the technical system and routines were not fully established at the beginning of the process. However, this did not negatively affect the result of the drilling. One specified measurement was, however, not performed, namely the weighing of drilling cuttings as accumulated in sedimentation containers for pumped out drilling water.

Specific comments regarding cored borehole KSH01B

KSH01B is a 100 m cored borehole drilled at the same drill site as KSH01A /Ask et al. 2003/. The purpose of KSH01B was to produce drillcore from ground surface to 100 m depth, as KSH01A was percussion-drilled for the first 100 m. KSH01B was conventionally core drilled, ie not using a variable diameter as at KSH01A. The core drilling was made with the same drill rig and downhole equipment as used for borehole KSH01A, hence resulting in the same type of core as for KSH01A.

Specific comments regarding cored borehole KSH02

The drilling of KSH02 /Ask et al. 2004/, conducted between January and June 2003, was slightly different from that of KSH01. First, no B hole was drilled. The upper 100 m was first core drilled and then reamed up to the wider diameter required. As the borehole wall was somewhat unstable, it was decided to install a casing. However, the casing installation was stopped at 66 m depth and the borehole was plugged with cement. The plugged interval was re-drilled before the drilling was continued to 1,000 m depth. The resulting borehole design therefore is casing of 200 mm inner diameter down to 66 m, whereas the rest of the hole has a diameter of 76 mm.

The drilling was made with the same drilling machine and down-hole equipment as used in the KSH01 A and B holes and employing the same procedures as for the KSH01. In KSH02, the following tests and water sampling during drilling were performed:

- Continuous monitoring of drilling parameters and flushing water parameters with the drilling monitoring system throughout the core drilling phase.
- Eleven pumping tests, of which nine gave interpretable transmissivity values.
- Nine water pressure measurements.
- Acquisition of four water samples – only one sample from the core drilling phase had a sufficiently low drilling water content to ensure representative analysis results.

As the borehole was specifically allocated for rock stress measurements, the overcoring technique was used during the core drilling at the three intervals, 250–300 m and around 450 m level. Due to a relatively high frequency of sealed factures only one measurement resulted in useful data /Sjöberg, 2004/.

Specific comments regarding cored borehole KSH03A/B

Drilling of KSH03 was performed between August and November 2003. The hole was cored to a depth of 1,000.7 metres with 76 mm equipment (this hole is denoted KSH03A). The uppermost section, to a depth of 100.5 metres, was constructed as a telescopic section with an inner diameter of 200 mm. In order to retrieve cored material from ground surface to full depth, a separate cored hole was drilled close to the telescopic section from the surface to 100.86 metres (this hole is denoted KSH03B). The following tests were performed in KSH03A:

- Pumping tests were performed with a wireline equipment, typically with one hundred metres intervals.
- An airlift pumping test in the telescopic section was performed when the cored hole was at its full length.
- Continuous monitoring of drilling parameters and flushing water parameters with the drilling monitoring system was conducted throughout the core drilling phase.
- Water samples for chemical analysis were collected during drilling. Only two samples, out of four samples taken, had a sufficiently low drilling water content to ensure representative analysis results.

Specific comments regarding cored borehole KAV04

Drilling of KAV04 /Ask et al. 2005/ was performed between October 6, 2003 and May 3, 2004. The hole was cored to a depth of 1,004.0 metres with 76 mm equipment The uppermost section, to a depth of 100.2 metres, was constructed as a telescopic section with an inner diameter of 200 mm. Borehole KAV04 was labelled a borehole dedicated to rock stress measurements. In order to retrieve core from surface to full depth a separate cored hole was drilled close to the telescopic section from the surface to 101.03 metres, this hole was called KAV04B.The following tests were performed in KSH04A:

- Two results from the final run with the Maxibor borehole deviation method covering the entire length of borehole KAV04A were obtained. A deviation measurement of the shallow part was also made.
- Overcoring measurements were made on three length intervals, 249–273 metres, 429–456 metres and 447–463 metres.
- Fourteen pumping tests using the wireline probe resulted in ten successful results.
- Five measurements of absolute pressure using the wireline probe were conducted.
- Water samples were successfully collected in conjunction with nine of the fourteen pumping tests performed.
- One air lift pumping and recovery test was conducted.
- Data were collected continuously during drilling using the Drill monitoring system (DMS).

Percussion-drilled boreholes in bedrock

Borehole investigations during (and immediately after) percussion drilling followed general guidelines for the site investigations /SKB, 2001a/. For the percussion-drilled boreholes HSH01, HSH02 and HSH03, the following procedures were applied /Ask and Samuelsson, 2004/:

- Sampling of the soil during drilling through the overburden (very thin soil cover resulted in one sample from each of boreholes HSH01 and HSH02).
- Sampling of drill cuttings (and fine material) with a frequency of one sample every third metre (preliminary inspection on location).
- Manual measurement of penetration rate.
- Registration of notable changes in the flow rate of the return drilling water with intermediate measurements in case of an observed increase in flow.
- Recording of the colour of the return water.
- Measurement of borehole deviation after completion of the borehole.

Boreholes in overburden

Details on drilling procedures in conjunction with completion of boreholes are provided by /Ask, 2003; Johanssson and Adestam, 2004/. Aspects on hydrogeochemical sampling and hydraulic investigation (water level monitoring and hydraulic tests) are provided by /Ericsson and Engdahl, 2004; SKB, 2004c/ and /Werner et al. 2005/. The boreholes completed in the overburden which have contributed primary data to the Simpevarp 1.2 modelling are shown in Figure 2-2.

2.5.2 Borehole investigations after drilling

Following completion of drilling, a base programme of characterisation was carried out in all core-drilled and percussion-drilled boreholes. Depending on the assigned priority (rock mechanics or hydrochemistry), the supplementary investigations to the base programme may differ amongst the cored boreholes /SKB, 2000b, 2001a/.

Data from the base programme of characterisation were available from core-drilled borehole KSH01A/B, KSH02 and KSH03A/B, whereas only early data in conjunction with drilling of KAV04 were available at the time of data freeze Simpevarp 1.2.

Percussion-drilled sections of cored boreholes

The following investigations were made and reported as part of the data freeze for Simpevarp 1.2:

- BIPS borehole imaging.
- Borehole radar (dipole antenna).
- Conventional suite of geophysical well logs.

Core-drilled borehole sections

The following investigations were made and reported as part of data freeze for Simpevarp 1.2:

- BIPS borehole imaging, in both the A and B holes.
- Borehole radar (dipole antenna), in both the A and B holes.
- Boremap logging (using BIPS and drill core), in both the A and B holes.
- Hydrochemical logging, in the A hole.
- Difference flow logging, in the A hole.
- Complete hydrogeochemical characterisation, in the A hole.
- Resistivity logs in the A-hole.

- Sampling of the drill core for geological, thermal, rock mechanical, geochemical and transport properties, from the A hole only.
- Rock stress measurements using the hydrofracturing technique (KSH01A only).

Percussion-drilled boreholes

The investigation methods listed below were employed in the three percussion-drilled boreholes. The resulting data formed part of data freeze for Simpevarp 1.2.

- BIPS borehole imaging.
- Borehole radar (dipole antenna).
- Conventional suite of geophysical well logs.
- Hydraulic tests (pump tests and flow logging), in HSH01 and HSH03.

Soil boreholes

Measurements include manual groundwater level measurements and sampling for chemical analyses.

2.5.3 Complementary measurements in old cored boreholes

Complementary tests have been undertaken in two existing cored boreholes at Laxemar (KLX02) and on the island of Ävrö (KAV01). Complementary investigations were also planned for borehole KLX01 (also at Laxemar). These plans were not realised because it proved impossible while a futile attempts were made to remove a steel casing stuck in the borehole between 268.3 and 700 m. The casing is cut at 270, 280, 300, 400, 500 and 600 m, respectively.

The investigations performed in the two boreholes included BIPS, Boremap logging, geophysical logging, borehole radar (RAMAC) and Posiva flow logging (PFL), the latter only in borehole KAV01.

2.6 Other data sources

Other relevant data sources are “old” data that are either already stored in relevant official SKB databases, or are listed in the version 0 report /SKB, 2002b/ and remain to be input into the databases. One obvious extensive source of information is that provided by the characterisation data and associated descriptive models available from the Äspö HRL. The position taken by the site descriptive modelling project is to make use of selective information important for filling voids in the data needs of the modelling process. The ambition is by no means to integrate the vast Äspö HRL database in full, see below. Examples of data of interest are various generations of geological and structural models and compilations of transport properties relevant to Äspö HRL conditions (and the associated data on geology/mineralogy). Additional old data include surface and borehole information from investigations performed on the islands of Ävrö and Hålö. Old data are also available from the construction of the three nuclear power reactors on the Simpevarp peninsula (and associated tunnels and storage caverns). A third source of old data is related to the site characterisation and construction of the central storage facility for spent nuclear fuel (Clab I and Clab II). The old data used as input to the descriptive modelling for Simpevarp 1.2 are summarised in Section 2.7.

Relationship to data from Äspö HRL

As indicated in the previous section, the designated Local Model area for the Simpevarp subarea partially includes the Äspö island and the Äspö HRL. There consequently exists a need to define a relationship to the wealth of data available from Äspö and the Äspö HRL to be employed in the site descriptive modelling. A full inclusion and integration of the Äspö data set would be prohibitive for the realisation of the site modelling project and would introduce a significant bias and imbalance in the density of data. Instead, the project has adapted a flexible relationship to Äspö data and associated descriptive and conceptual models.

The site modelling project does not have to address the Äspö data base in its entirety, rather the ground rule is that Äspö data primarily are used for qualitative comparisons with data collected elsewhere in the model area(-s). However, initial lack of data, primarily in the local model area, can be compensated by import of selected data from Äspö. Thus, in cases where relevant data or statistics are absent in the site-specific database, such information may be imported from Äspö. This could e.g. be rock mechanics, thermal or transport-related information. However, in all cases, such import has to be motivated and constrained on the basis of appropriate geological analogies and relationships.

Studies performed during the characterisation, construction and operational (experimental) phases of the Äspö HRL have resulted in various kinds of conceptual models that could be of use for the site modelling project. Examples of such models are; mechanistic models of geological structure evolution, mechanical stability, hydraulic anisotropy, hydrogeochemical evolution and microbial processes. Experiments focused on the natural barriers have produced conceptual microstructural models of fractures and their immediate environs (including infillings) and conceptual models for transport and retention in fractured rock, including identification of dominant processes and immobile zones involved. Similarly to the import of data, import/use of conceptual models developed at Äspö HRL has to be motivated and justified by geological, petrophysical and geochemical similarities.

2.7 Databases

This section summarises the data that were available at the time of the data freeze for Simpevarp 1.2 and distinguishes data used and data not used in the site descriptive modelling. The basis for the presentation is a series of tables developed for each discipline. In each table, the first two columns set out the data available, columns 3 and 4 identify the data that were used, whereas column 5 identifies data not used, and presents arguments in support of their not being used. It is noted that the use of data from individual boreholes by the various disciplines vary depending on the state of down-hole discipline-wise characterisation in the individual boreholes.

Table 2-1. Available bedrock geological and geophysical data and their handling in Simpevarp 1.2.

Available primary data Data specification	Ref.	Usage in S1.2 Analysis/Modelling	cf. Section	Not utilised in S1.2 Arguments/Comments
Surface-based data				
Bedrock mapping – outcrop data (rock type, ductile and some brittle structures at 353 observation points. Frequency and orientation of fractures at 16 outcrops)	P-04-102	Rock type, ductile deformation in the bedrock, fracture statistics and identification of possible fracture zones at the surface	5.2.2 5.2.3 5.2.4 5.3.3	
Detailed fracture mapping at four sites	P-04-35	Fracture orientation, tracelength and other geologcical parameters (mineral infilling, alteration etc.)	5.2.2	
Modal analyses and geochemical analyses	P-04-102	Mineralogical and geochemical properties of the bedrock. Assessment of thermal properties	5.2.1 11.2	
Petrophysical rock parameters and in situ gamma-ray spectrometric data	P-03-97	Physical properties of the bedrock	5.2.4 11.2	
Airborne geophysical data (magnetic, EM, VLF and gamma-ray spectrometric data)	P-03-25 P-03-63 P-03-100	Identification of lineaments/ deformation zones and lithological boundaries	5.2.4	
Detailed topographic data from airborne photography	P-02-02 P-03-99	Identification of lineaments/ deformation zones	5.2.2	

High resolution reflection seismics	P-03-71 P-03-72 TR-97-06 TR-02-19 R-01-06	Identification of inhomogeneities in the bedrock that may correspond to boundaries between different types of bedrock or to deformation zones. Supportive information used from previous models (Laxemar, Ävrö and Äspö 96)	5.4	
Surface geophysical data (magnetic and EM data)	P-03-66	Identification of lineaments/ deformation zones	5.2.4 5.4	
Regional gravity data				Not utilised in Simpevarp 1.2. Too few and scattered measurements
Interpretation of airborne geophysical and topographical data (linked lineament map)	P-03-100 P-03-99 P-04-49	Deterministic structural model	5.2.2 5.4	
Simevarp site descriptive model v.0	R-02-35	Lithological model and deterministic structural model	5.3.1 5.4.1 5.5.1	
Laxemar area – testing the methodology for site descriptive modelling	TR-02-19	Deterministic structural model	5.4.1	
RVS modelling, Ävrö	R-01-06	Deterministic structural model	5.4.1	
Cored borehole data				
Geophysical, radar and BIPS logging, Boremap data, single-hole interpretation in KSH01A/B	P-03-15 P-03-16 P-03-73 P-04-32 P-04-01 P-04-218	Fracture statistics (including mineralogical analyses), rock type distribution down to borehole depth 1,000 m in DFN (Discrete Fracture Network), lithological and deformation zone models	5.2.5 5.3.3 5.4.3 5.5	
Geophysical, radar and BIPS logging, Boremap data, single-hole interpretation in KSH02	P-04-131 P-04-133 P-04-218	Fracture statistics (including mineralogical analyses), rock type distribution down to borehole depth 1,000 m in DFN, lithological and deformation zone models	5.2.5 5.3.3 5.4.3 5.5	
Geophysical, radar and BIPS logging, Boremap data, single-hole interpretation in KSH03A/B	P-04-132	Fracture statistics (including mineralogical analyses), single hole interpretation, rock type distribution down to borehole depth 1,000 m in DFN lithological and deformation zone models	5.2.5 5.3.3 5.4 5.5	
Geophysical, radar and BIPS logging, Boremap data, single-hole interpretation in KAV01	P-04-130 P-04-133 P-04-218	Fracture statistics (including mineralogical analyses, rock type distribution down to borehole depth 1,000 m in DFN, lithological and deformation zone models	5.2.5 5.3.3 5.4 5.5	
Geophysical, radar and BIPS logging, Boremap data, single-hole interpretation in KLX02	P-04-129	Fracture statistics (including mineralogical analyses), single hole interpretation, rock type distribution down to borehole depth 1,000 m in DFN, lithological and deformation zone models	5.2.5 5.3.3 5.4 5.5	
Geophysical, radar and BIPS logging, Boremap and single-hole interpretation in HSH01, HSH02 and HSH03	P-04-02 P-04-32 P-04-218		5.2.6 5.2.7	

Table 2-2. Available rock mechanics data and its handling in Simpevarp 1.2.

Available primary data Data specification	Ref.	Usage in S1.2 Analysis/Modelling	cf. Section	Not utilised in S1.2 Arguments/Comments
Cored borehole data				
Stress measurement with overcoring, KSH02 KAV04 KLX04	 P-04-23 P-04-84 Prel. report	Estimation of in situ stress field and uncertainty in data	6.2.5	
Stress measurement with hydraulic fracturing in borehole KSH01A	Prel. report	Estimation of in situ stress field and uncertainty in data	6.2.5	
Geological single hole interpretation of boreholes KSH01A and KSH01B KLX02 KSH02 and KAV01 KSH03A	 P-04-32 Prel. report P-04-133 Prel. report	Division of drill core data into rock domains and deformation zones	6.2.3	
Boremap logging of KSH01A and KSH01B KLX02 KAV01 KSH02 KSH03A	 P-04-01 P-04-129 P-04-130 P-04-131 P-04-132	Calculation of empirical rock mass quality indices and estimation of rock mass properties	6.2.3	
Laboratory uniaxial and triaxial tests of intact rock samples KSH01A and KSH02	P-04-107 P-04-108 P-04-109 P-04-110	Estimation of intact rock mechanical properties	6.2.1	
Laboratory indirect tensile strength tests of intact rock samples KSH01A KSH02	 P-04-62 P-04-63	Estimation of intact rock mechanical properties	6.2.1	
Direct shear tests and normal stiffness test of fracture rock samples KSH01A KSH02 KAV01	 P-04-185 P-05-06 P-05-07 P-05-05	Estimation of single fracture mechanical properties	6.2.2	
Tilt tests and Schmidthammer tests, KSH01A KSH02 KAV01 KLX02	 P-03-107 P-04-10 P-04-42 P-04-44	Estimation of intact rock and fracture mechanical properties	6.2.2	
P-wave velocity, transverse borehole core, KSH01A KSH02 KAV01 KLX02	 P-03-106 P-04-11 P-04-43 P-04-45	Identification of potentially high in situ stress conditions	6.2.5	
Other borehole, construction, tunnel data and models				
Stress measurements from boreholes in the region	PR-25-89-17 PR U-97-27 IPR-02-01 IPR-02-02 IPR-02-03 IPR-02-18 R-02-26	Estimation of in situ stress field and uncertainty in data	6.2.5	
Laboratory test data. Core samples from Äspö and Clab	SICADA database	Estimation of intact rock strength properties	6.2.1	

Table 2-3. Available bedrock thermal data and its handling in Simpevarp 1.2.

Available primary data Data specification	Ref.	Usage in S1.2 Analysis/Modelling	cf. Section	Not utilised in S1.2 Arguments/Comments
Cored borehole data				
Laboratory thermal test on cores from Simpevarp and old boreholes at Äspö HRL	R-03-10 IPR-99-17 R-02-27 P-04-53 P-04-54 P-04-55 Preliminary report used /Sundberg et al. 2005/	Estimation of thermal conductivity and specific heat capacity	7.2.1 and 7.2.4 and 7.2.5	
Density logging KSH01A, KAV01 and KLX02	P-04-232 P-03-111 P-03-16 P-04-77 P-04-214 P-04-28	Estimation of thermal conductivity	7.2.3 and 7.2.4	
Laboratory test of thermal expansion	P-04-59 P-04-60 P-04-61	Estimation of the thermal expansion coefficient	7.2.6	
Boremap logging KSH01A, KAV01, KSH02 and KLX02	SICADA	Dominating and subordinate rock type distribution	7.2.3 and 7.3	
Temperature and gradient logging KSH01A, KSH02, KSH03A, KAV01, KLX01 and KLX02	P-03-16 P-04-50 P-04-232 P-03-111 P-04-28 P-04-77		7.2.7	
Modal analyses KLX01, KLX02, KSH01A, KAV01, KSH02 and KSH01B	P-04-53 P-04-54 P-04-55	Estimation of thermal conductivity	7.2.2 and 7.2.4	
Surface based data				
Modal analyses	P-04-102	Estimation of thermal conductivity	7.2.2 and 7.2.4	

Table 2-4. Available meteorological, hydrological and hydrogeological data and its handling in Simpevarp 1.2.

Available primary data Data specification	Ref.	Usage in S1.2 Analysis/Modelling	cf. Section	Not utilised in S1.2 Arguments/Comments
Meteorological data				
Summary of precipitation, temperature, wind, humidity and global radiation up to 2000	TR-02-03 R-99-70	Base for general description and modelling of surface runoff and groundwater recharge	4.3	
Surface based data				
Explore water courses for suitable point of measuring the run-off	P-03-04		4.3	Not used. Document only for planning
Ground elevation and bathymetry of the Baltic sea	SKB GIS-data base	Topography and bathymetry	4.1	
Bathymetry of lakes				No data are available

Hydrological data				
Inventory of private wells 2002. Hydrogeological inventory of the Oskarsahamns area	P-03-05 P-04-277		4.3	Not used. Document only for planning of environmental impact follow-up
Topographical information for delineation of run-off areas	SKB GIS-data base	Definition of run-off areas. Numerical groundwater flow simulations	4.3, 8	
Regional run-off data	TR-02-03 R-99-70	Characteristics of run-off areas	4.3	
Regional oceaographic data	TR-02-03 R-99-70	Characteristics of oceanographic conditions	4.3	
Cored borehole data				
Wireline tests in KSH01A	P-03-113	Borehole data and (prel) transmissivity distribution in large scale	8.2	
Wireline tests in KSH02	P-04-151	Borehole data and (prel) transmissivity distribution in large scale	8.2	
Wireline tests in KSH03	P-xxxx	Borehole data and (prel) transmissivity distribution in large scale	8.2	
Difference flow logging in KSH01A	P-03-70	Conductive parts of the borehole, Statistics of conductive fractures	8.2	
Difference flow logging in KSH02	P-03-110	Conductive parts of the borehole, Statistics of conductive fractures	8.2	
Difference flow logging in KAV01	P-04-213	Conductive parts of the borehole, Statistics of conductive fractures	8.2	
Difference flow logging in KLX02	IPR-01-06 R-01-52		8.2	
Hydraulic injection tests, KSH01A	P-04-247	Transmissivity distribution along the borehole in different scales	8.2	
Hydraulic injection tests, KSH02	P-04-289	Transmissivity distribution along the borehole in different scales	8.2	
Hydraulic injection tests, KSH03	P-04-290	Transmissivity distribution along the borehole in different scales	8.2	
Hydraulic injection tests, KLX02	P-04-288	Transmissivity distribution along the borehole in different scales	8.2	
Percussion hole data				
Drilling, HSH01, HSH02, HSH03	P-03-114	Soil depth, soil samples, Preliminary interpretation of borehole	8	
Hydraulic tests and water sampling in HSH03	P-03-56	Transmissivity of bh. Conductive parts of the borehole	8	
Hydraulic tests and water sampling in KSH03A and HSH02	P-04-212	Transmissivity of bh. Conductive parts of the borehole	8	
Monitoring of water levels in rock holes	SICADA database		8	Brief overview for version S1.2
Other borehole, construction, tunnel data and models				
Hydraulic tests in areas Äspö, Ävrö, Hålö, Simpevarp, Mjälen and Laxemar areas	TR-97-06, TR-02-19, R-98-55, SICADA database	Prevous made evaluations compared to new data.	8	Not used in detail

Table 2-5. Available hydrogeochemical data and their handling in Simpevarp 1.2. For further detailes see Appendix 9 in SKB R-04-74.

Available primary data Data specification	Ref.	Usage in S1.2 Analysis/Modelling	cf. Section	Not utilised in S1.2 Arguments/Comments
Surface based data				
Preciptation, soil pipes Sea water samples	R-04-74	All Hydrchemical modelling and visualisation	9.2	
Cored borehole data				
KSH01, KSH02, KSH03 KAV01, KAV04	P-04-12 R-04-74 P-03-89 P-03-89 P-03-87	All hydrochemical modelling and visualisation	9.2	
Percussion hole data				
HSH02/03; HAV04/05/06/07; HAV09/10	P-03-113 R-04-12 R-04-12	All hydrochemical modelling and visualisation	9.2	
Other available data				
Äspö, Laxemar and other Nordic Sites	R-04-74	All hydrochemical modelling	9.2	

Table 2-6. Available data on transport properties and their handling in Simpevarp 1.2.

Available primary data Data specification	Ref.	Usage in S1.2 Analysis/Modelling	cf. Section	Not utilised in S1.2 Arguments/Comments
Cored borehole data				
Formation factors measured in situ and in the laboratory, KSH01A and KSH02	P-05-27 SICADA	Assignment of porosity and diffusion parameters	10.5	
Results from through-diffusion tests and porosity measurements on samples from KSH01A and KSH02	P-05-18	Assignment of porosity and diffusion parameters	10.5	
Input from other disciplines				
Geological data and description: – lithology and mineralogy of rock mass – fracture mineralogy – porosity data from surface samples and boreholes (KSH01A, KSH02)	Prel. report, P-04-102 P-04-250 P-03-97 P-04-28 P-04-77	Identification of site-specific rock types, fractures and fracture zones, and properties of site-specific geological materials, as a basis for Retardation model and descriptive Transport model	10.4	
Hydrogeological data and description	Prel. report, P-03-70 P-03-110	Identification of conductive fractures and description of their properties	10.4	
Hydrogeochemical data and description	R-04-74 SICADA	Identification of site-specific water types (and water-rock interactions)	10.4	
Other borehole data and models				
Data and models from TRUE project and Äspö Task Force (Task 6C)	TR-98-18 ICR-01-04 IPR-03-13	Conceptual modelling Assignment of sorption and diffusion parameters	10.3 10.5	Some old data not used due to differencies in methods and/or insufficient characterisation
Data from other research at Äspö and Laxemar	SKI 98:41 Research papers	Assessment of spatial variability	S1.1	
SR 97 sorption and diffusion databases	R-97-13 TR-97-20	Used for comparative purposes	S1.1	

Table 2-7. Available abiotic data from the surface system and their handling in S1.2.

Available site data Data specification	Ref.	Usage in S1.2 Analysis/Modelling	cf. Section	Not utilised in S1.2 Arguments/Comments
Geometrical and topographcal data				
Digital Elevation Model (DEM)	P-04-03 SICADA	Basic input to flow and mass transport models	4.3	
Geological data				
Map of Quaternary deposits	P-04-22 R-98-55	Description of surface distribution of Quaternary deposits in the Simpevarp subarea	4.4	
Helicopter borne survey data	P-03-100	Description of surface distribution of Quaternary deposits in the Simpevarp subarea	4.4	
Electric soundings	P-03-17	Description of depth of overburden in the Simpevarp regional model area	4.4	
Stratigraphy of Quaternary deposits	P-04-22	Description of stratigraphical distribution and total depth of deposits in the Simpevarp subarea	4.4	
Drilling and sampling in Quaternary deposits	P-04-121 P-04-46 P-03-80	Description of stratigraphical distribution and total depth of deposits in the Simpevarp subarea	4.4	
Map of Quaternary deposits at the sea bottom	SKB-GIS	Description of surface distribution of Quaternary deposits at the sea bottom	4.4	
Stratigraphy of Quaternary deposits from the sea bottom	SKB-GIS	Description of stratigraphical distribution and total depth of Quaternary deposits in the sea	4.4	
Stratigraphy of water laid Quaternary deposits from the sea bottom	R-02-47			
Old maps of Quaternary deposits	SGU Ac 5 (1904)		4.4	Old map with low geographic accuracy
Map of soils	P-04-243 SICADA	Distribution of soil types in the Simpevarp regional model area	4.4	
Meteorological data				
Regional data (Version 0)	TR-02-03 R-99-70	General description Flow modelling	4.5	
Data from meteorological station on Äspö (Oct. 2003 – Sept. 2004)	SICADA	Comparison with regional meteorological data	4.5	
Hydrological data				
Regional discharge data (Version 0)	TR-02-03 R-99-70	General description Water balance	4.5	
Investigation of potential locations for discharge stations	P-03-04		4.5	Not used explicitly; used as general information and for planning purposes only
Geometric data on catchment areas, lakes and water courses	P-04-242	Delineation and characterics of catchment areas and lakes	4.5	
Simple discharge measurements in water courses, lakes and the sea	P-04-13 P-04-75	Description of temporal variability in runoff	4.5	

Hydrogeological data				
Inventory of private wells	P-03-05	Description of available hydrogeological information	4.5	No attempt made to infer hydraulic parameters from capacity data
Manually measured groundwater levels	SICADA	Basis for estimating depth of unsaturated zone	4.5	
Data on installed groundwater monitoring wells	P-04-121 P-04-46 P-03-80	Description of measurements and evaluation of hydraulic properties	4.5	
Hydraulic conductivity of Quaternary deposits	P-04-122 SICADA	Basis for assigning hydraulic conductivity of Quaternary deposits in conceptual and mathematical models	4.5	
Modelled hydraulic conductivity and pressure distributions in the upper part of the rock	R-04-65	Parametrisation and identification of boundary conditions in flow model	4.5	
Oceanographic data				
Regional oceanographic data	TR-02-03 R-99-70	Quantitative modelling	4.6x	
Chemistry data				
Surface water sampling	P-04-13 P-04-75	Description	4.7	

Table 2-8. Available biotic data from the surface system and their handling in S1.2.

Available site data Data specification	Ref.	Usage in S1.2 Analysis/Modelling	cf. Section	Not utilised in S1.2 Arguments/Comments
Terrestrial biota				
Compilation of existing information 2002	R-02-10	Description	4.8 4.10	
Bird population survey	P-04-21	Description	4.8 4.10	
Mammal population survey	P-04-04, /Svensk Viltförvaltning, 2003/	Description, modelling	4.8 4.10	
Amphibians and reptiles	P-04-36, /Andrén, 2004/	Description, modelling	4.8 4.10	
Soil fauna	/Lohm and Persson, 1979/	Generic description	4.8 4.10	
Vegetation inventory	P-04-20	Description	4.8 4.10	
Vegetation mapping	P-03-83	Description, modelling	4.8 4.10	
Biomass and NPP of the vegetation	NFI	Modelling, tree layer	4.8 4.10	
Biomass and NPP of the vegetation	/Gower et al. 2001/	Modelling, shrub layer	4.8 4.10	
Biomass and NPP of the vegetation	P-03-90, /Bisbee et al. 2001/	Modelling, field layer and ground layer	4.8 4.10	
Biomass and NPP of the vegetation	/Vogt et al. 1982/	Modelling, fungi	4.8 4.10	
Biomass of the vegetation	P-04-20, /Berggren et al. 2004/, P-03-90	Modelling, dead organic material	4.8 4.10	
Data from soil mapping	P-04-243	Description, modelling	4.8 4.10	

Limnic biota			
Limnic producers	P-04-242 P-04-253	Description, modelling	4.8 4.10
Limnic consumers	P-04-253 P-04-251	Description, modelling	4.8 4.10
Marine biota			
Compilation of existing information 2002	R-02-10	Description	4.8 4.10
Habitat borders	P-04-242	Description	4.8 4.10
Barythymetical measurements	P-04-254	Description, modelling	4.8 4.10
Light penetration depth	P-04-13 and field measurements (SICADA)	Description	4.8 4.10
Zooplankton, phytoplankton	P-04-253	Description, modelling	4.8 4.10
Identification of dominating species	P-03-68	Description	4.8 4.10
Macrophyte communities	P-03-69	Description, modelling	4.8 4.10
Soft bottom infauna	P-04-17	Description, modelling	4.8 4.10
Bentic fauna	P-04-251	Description, modelling	4.8 4.10
Reed	P-04-316	Description, modelling	4.8 4.10
Fish surveys	P-04-19	Description, modelling	4.8 4.10
Bird population survey	P-04-21	Description	4.8 4.10
Humans and land use			
Humans and land use	R-04-11	Description, modelling	4.9

Table 2-9. Reports in the SKB P, IPR, ICR, R, and TR-series referenced in Tables 2-1 through 2-8).

P-02-02	**Wiklund S.** Digitala ortofoton och höjdmodeller. Redovisning av metodik för platsundersökningsomr ådena Oskarshamn och Forsmark samt förstudieområdet Tierp Norra (in Swedish).
P-03-04	**Lärke A, Hillgren R.** Rekognoscering av mätplatser för ythydrologiska mätningar i Simpevarpsområdet (in Swedish).
P-03-05	**Morosini M, Hultgren H.** Inventering av privata brunnar i Simpevarpsområdet, 2001-2002 (in Swedish).
P-03-07	**Curtis P, Elfström M, Stanfors R.** Oskarshamn site investigation Compilation of structural geological data covering the Simpevarp peninsula, Ävrö and Hålö.
P-03-15	**Nilsson P, Gustafsson C.** Simpevarp site investigation. Geophysical, radar and BIPS logging in borehole KSH01A, HSH01, HSH02 and HSH03.
P-03-16	**Nielsen U T, Ringgaard J.** Simpevarp site investigation. Geophysical borehole logging in borehole KSH01A, KSH01B and part of KSH02.
P-03-17	**Thunehed H, Pitkänen T.** Simpevarp site investigation. Electrical soundings supporting inversion of helicopterborne EM-data. Primary data and interpretation report.
P-03-25	**Rønning H J, Kihle O, Mogaard J O, Walker P.** Simpevarp site investigation. Helicopter borne geophysics at Simpevarp, Oskarshamn, Sweden.
P-03-31	**Green M.** Platsundersökning Simpevarp. Fågelundersökningar inom SKB:s platsundersökningar 2002 (in Swedish).

P-03-56 **Ludvigson J-E, Levén J, Jönsson S.** Oskarshamn site investigation. Hydraulic tests and flow logging in borehole HSH03.

P-03-63 **Byström S, Hagthorpe P, Thunehed H.** Oskarshamn site investigation. QC-report concerning helicopter borne geophysics at Simpevarp, Oskarshamn, Sweden.

P-03-66 **Triumf C-A.** Oskarshamn site investigation. Geophysical measurements for the siting of a deep borehole at Ävrö and for investigations west of Clab.

P-03-67 **Borgiel M.** Makroskopiska organismers förekomst i sedimentprov. En översiktlig artbestämning av makroskopiska organismer (in Swedish).

P-03-68 **Tobiasson S.** Tolkning av undervattensfilm från Forsmark och Simpevarp (in Swedish).

P-03-69 **Fredriksson R, Tobiasson S.** Simpevarp site investigation. Inventory of macrophyte communities at Simpevarp nuclear power plant. Area of distribution and biomass determination.

P-03-70 **Rouhiainen P, Pöllänen J.** Oskarshamn site investigation. Difference flow measurements in borehole KSH01A at Simpevarp.

P-03-71 **Vangkilde-Pedersen T.** Oskarshamn site investigation. Reflection seismic surveys on Simpevarpshalvön 2003 using the vibroseismic method.

P-03-72 **Juhlin C.** Oskarshamn site investigation. Evaluation of RAMBØLL reflection seismic surveys on Simpevarpshalvön 2003 using the vibroseismic.

P-03-73 **Aaltonen J, Gustafsson C, Nilsson P.** Oskarshamn site investigation. RAMAC and BIPS logging and deviation measurements in boreholes KSH01A, KSH01B and the upper part o KSH02.

P-03-74 **Barton N.** Oskarshamn site investigation. Q-logging of KSH 01A and 01B core.

P-03-83 **Boresjö Bronge L, Wester K.** Vegetation mapping with satellite data of the Forsmark, Tierp and Oskarshamn regions.

P-03-87 **Wacker P.** Oskarshamn site investigation. Hydrochemical logging in KSH01A.

P-03-88 **Berg C.** Hydrochemical logging in KSH02. Oskarshamn site investigation.

P-03-93 **Lindqvist L, Thunehed H.** Oskarshamn site investigation. Calculation of Fracture Zone Index (FZI) for KSH01A.

P-03-97 **Mattsson H, Thunehed H, Triumf C-A.** Oskarshamn site investigation. Compilation of petrophysical data from rock samples and in situ gamma-ray spectrometry measurements.

P-03-99 **Triumf C-A.** Oskarshamn site investigation. Identification of lineaments in the Simpevarp area by the interpretation of topographical data.

P-03-100 **Triumf C-A, Thunehed H, Kero L, Persson L.** Interpretation of airborne geophysical survey data. Helicopter borne survey data of gamma ray spectrometry, magnetics and EM from 2002 and fixed wing airborne survey data of the VLF-field from 1986. Oskarshamn site investigation.

P-03-106 **Chryssanthakis P, Tunbridge L.** Borehole: KSH01A. Determination of P-wave velocity, transverse borehole core. Oskarshamn site investigation.

P-03-107 **Chryssanthakis P.** Borehole: KSH01A. Results of tilt testing. Oskarshamn site investigation.

P-03-110 **Rouhiainen P, Pöllänen J.** Oskarshamn site investigation – Difference flow measurements in borehole KSH02 at Simpevarp.

P-03-111 **Nielsen T, Ringgaard J, Horn F.** Geophysical borehole logging in boreholes KSH02 and KLX02. Svensk kärnbränslehantering AB.

P-03-113 **Ask H, Morosini M, Samuelsson L-E, Stridsman H, 2003.** Oskarshamn site investigation – Drilling of cored borehole KSH01. SKB P-03-113. Svensk Kärnbränslehantering AB.

P-03-114 **Ask H, Samuelsson L-E, 2003.** Oskarshamn site investigation – Drilling of three flushing water wells, HSH01, HSH02 and HSH03. SKB P-03-113. Svensk Kärnbränslehantering AB.

P-04-01 **Ehrenborg J, Stejskal V, 2004.** Oskarshamn site investigation. Boremap mapping of core drilled boreholes KSH01A and KSH01B.

P-04-02 **Nordman C, 2004.** Oskarshamn site investigation. Boremap mapping of percussion boreholes HSH01-03

P-04-04 **Cederlund G, Hammarström A, Wallin K.** Surveys of mammal populations in the areas adjacent to Forsmark and Oskarshamn. Results from 2003.

P-04-10 **Chryssanthakis P.** Oskarshamn Site Investigation – Borehole KSH02, Results of tilt testing,

P-04-11 **Chryssanthakis P, Tunbridge L**. Borehole: KSH02A Determination of P-wave velocity, transverse borehole core. Oskarshamn site investigation.

P-04-12 **Wacker P.** Complete hydrochemical characterization in KSH01A.

P-04-13 **Ericsson U, Engdahl A.** Surface water sampling at Simpevarp 2002–2003. Oskarshamn site investigation,

P-04-14 **Ericsson U.** Sampling of precipitation at Äspö 2002–2003.

SKB P-04-17 **Fredriksson R.** Inventory of the soft-bottom macrozoobenthos community in the area around Simpevarp nuclear power plant. Oskarshamn site investigation.

P-04-21 **Green M, 2004.** Bird surveys in Simpevarp 2003. Oskarshamn site investigation,

P-04-22 **Rudmark L.** Investigation of Quaternary deposits at Simpevarp peninsula and the islands of Ävrö and Hålö. Oskarshamn site investigation.

P-04-20 **Andersson, J.** Vegetation inventory in part of the municipality of Oskarshamn.

P-04-23 **Sjöberg J.** Overcoring rock stress measurements in borehole KSH02. Oskarshamn Site Investigation.

P-04-28, **Mattsson H, Thunehed H.** Interpretation of geophysical borehole data from KSH01A, KSH01B, KSH02 (0–100 m), HSH01, HSH02 and HSH03 and compilation of petrophysical data from KSH01A and KSH01B.

P-04-32 **Mattsson H, Stanfors R, Wahlgren C-H, Stenberg L, Hultgren P.** Geological single-hole interpretation of KSH01A, KSH01B, HSH01, HSH02 and HSH03. Oskarshamn site investigation.

P-04-35 **Hermanson J, Hansen L, Wikholm M, Cronquist T, Leiner P, Vestgård J, Sandah K-A.** Detailed fracture mapping of four outgrops at the Simpevarp peninsula and Ävrö. Oskarshamn site investigation.

P-04-36 **Andrén Claes.** Oskarshamn site investigation, Amphibians and reptiles in SKB special area of investigation at Simpevarp.

P-04-37 **Triumf C-A.** Joint interpretation of lineaments in the eastern part of the site descriptive model area. Oskarshamn site investigation.

P-04-42 **Chryssanthakis P.** Oskarshamn Site Investigation – Borehole KAV01, Results of tilt testing,

P-04-43 **Chryssanthakis P, Tunbridge L.** Borehole: KAV01 Determination of P-wave velocity, transverse borehole core. Oskarshamn site investigation.

P-04-44 **Chryssanthakis P.** Oskarshamn Site Investigation – Borehole KLX02, Results of tilt testing**,**

P-04-45 **Chryssanthakis P, Tunbridge L.** Borehole: KLX02 Determination of P-wave velocity, transverse borehole core. Oskarshamn site investigation.

P-04-53 **Adl-Zarrabi B.** Drill hole KSH01A Thermal properties: heat conductivity and heat capacity determined using the TPS method and mineralogical composition by modal analysis

P-04-62. **Jacobsson L.** Oskarshamn Site Investigation – Drill hole KSH01A, Indirect tensile strength tests,

P-04-63 **Jacobsson L.** Oskarshamn Site Investigation – Drill hole KSH02, Indirect tensile strength tests.

P-04-54 **Adl-Zarrabi B**. Drill hole KSH02 Thermal properties: heat conductivity and heat capacity determined using the TPS method and mineralogical composition by modal analysis. Svensk kärnbränslehantering AB.

P-04-55 **Adl-Zarrabi B.** Drill hole KAV01 Thermal properties: heat conductivity and heat capacity determined using the TPS method and mineralogical composition by modal analysis

P-04-49 **Triumf C-A.** Oskarshamn site investigation**.** Joint interpretation of lineaments

P-04-50 **Nielsen T, Ringgaard J, 2004.** Geophysical borehole logging in borehole KSH03A, KSH03B, HAV09 and HAV10.

P-04-77 **Mattsson H, Thunehed H.** Oskarshamn site investigation. Interpretation of geophysical borehole data and compilation of petrophysical data from KSH02 (80–1,000 m) and KAV01.

P-04-84 **Sjöberg J.** Overcoring rock stress measurements in borehole KAV04. Oskarshamn Site Investigation.

P-04-102 **Wahlgren C-H, Ahl M, Sandahl K-A, Berglund J, Petersson J, Ekström M, Persson P-O.** Oskarshamn site investigation. Bedrock mapping 2003 – Simpevarp subarea. Outcrop data, fracture data, modal and geochemical classification of rock types, bedrock map, radiometric dating.

P-04-110 **Rouhiainen P, Pöllänen J.** Oskarshamn site investigation. Difference flow measurements in borehole KSH02 at Simpevarp.

P-04-129 **Ehrenborg J, Stejskal V.** Oskarshamn site investigation. Boremap mapping of core drilled borehole KLX02

P-04-130 **Ehrenborg J, Stejskal V.** Oskarshamn site investigation. Boremap mapping of core drilled borehole KAV01

P-04-131 **Ehrenborg J, Stejskal V.** Oskarshamn site investigation. Boremap mapping of core drilled borehole KSH02

P-04-132 **Ehrenborg J, Stejskal V.** Oskarshamn site investigation. Boremap mapping of core drilled boreholes KSH03A and KSH03B.

P-04-133 **Mattsson H, Stanfors R, Wahlgren C-H, Carlsten S, Hultgren P.** Oskarshamn site investigation**.** Geological single-hole interpretation of KSH02 and KAV01.

P-04-151 **Ask H, Morosini M, Samuelsson L-E, H Stridsman.** Oskarshamn site investigation – Drilling of cored borehole KSH02

P-04-185 **Chryssanthakis P.** Simpevarp Site Investigation – Drill hole: KSH01A, The normal stress and shear tests on joints.

P-04-207 **Jacobsson L.** Oskarshamn Site Investigation – Drill hole KSH01A, Uniaxial compression test of intact rock.

P-04-208 **Jacobsson L.** Oskarshamn Site Investigation – Drill hole KSH01A, Triaxial compression test of intact rock.

P-04-209 **Jacobsson L.** Oskarshamn Site Investigation – Drill hole KSH02, Uniaxial compression test of intact rock.

P-04-210 **Jacobsson L.** Oskarshamn Site Investigation – Drill hole KSH02, Triaxial compression test of intact rock.

P-04-212 **Svensson T.** Oskarshamn site investigation, Pumping tests and flow logging in boreholes KSH03 and HSH02.

P-04-213 **Rouhiainen P, Pöllänen J.** Oskarshamn site investigation – Difference flow measurements in borehole KAV01 at Ävrö.

P-04-214 **Mattsson H.** Interpretation of geophysical borehole data and compilation of petrophysical data from KSH03A (100–1,000 m), KSH03B, HAV09, HAV10 and KLX02 (200–1,000 m).

P-04-218 **Carlsten S.** Oskarshamn site investigation**.** Geological interpretation of borehole radar reflectors in KSH01, HSH01–03, KAV01 and KSH02

P-04-232 **Nielsen T, Ringgaard J, Horn F.** Geophysical borehole logging in borehole KAV01.

P-04-242 **Brunberg A-K, Carlsson T, Brydsten L, Strömgren M.** Identification of catchments, lake-related drainage parameters and lake habitats. Oskarshamn site investigation.

P-04-247 **Rahm N, Enachescu C.** Hydraulic injection tests in borehole KSH01A, 2003/2004, Simpevarp.

P-04-250 **Drake H, E-L Tullborg.** Oskarshamn site investigation. Fracture mineralogy and wall rock alteration. Results from drill core KSH01A+B.

P-04-251 **Engdahl A, Ericsson U.** Sampling of freshwater fish. Description of the fish fauna in four lakes.

P-04-253 **Sundberg I, Svensson J-E, Ericsson U, Engdahl A.** Phytoplankton and zooplankton. Results from sampling in the Simpevarp area 2003–2004. Oskarshamn site investigation.

P-04-254 **Ingvarson N, Palmeby A, Svensson O, Nilsson O, Ekfeldt T.** Oskarshamn site investigation, Marine survey in shallow coastal waters Bathymetric and geophysical investigation 2004.

P-04-277 **Nyborg M, Vestin E, Wilén P,** Oskarshamns site investigation. Hydrogeological inventory in the Oskarshamn area.

P-04-288 **Rahm N, Enachescu C.** Hydraulic injection tests in borehole KLX02, 2003, Laxemar.

P-04-289 **Ludvigson J-E, Levén J, Källgården J.** Oskarshamn site investigation. Single-hole injection tests in KSH02.

P-04-290 **Rahm N, Enachescu C.** Hydraulic injection tests in borehole KSH03, 2004, Simpevarp.

P-04-316 **Alling V, Andersson P, Fridriksson G, Rubio Lind C.** Biomass production of Common reed (Phragmites australis), infauna, epiphytes, sessile epifauna and mobile epifaunal, Common reed biotopes in Oskarshamn's model area.

P-05-05 **Jacobsson L.** Oskarshamn Site Investigation – Drill hole KAV01, Normal loading and shear tests on joints.

P-05-06 **Jacobsson L.** Oskarshamn Site Investigation – Drill hole KSH01A, Normal loading and shear tests on joints.

P-05-07 **Jacobsson L.** Oskarshamn Site Investigation – Drill hole KSH02, Normal loading and shear tests on joints.

P-05-18 **Gustavsson E, Gunnarsson M.** Oskarshamn site investigation. Laboratory data from the site investigation programme for the transport properties of the rock. Boreholes KSH01A, KSH02 and KLX02.

P-05-27 **Löfgren M, Neretnieks I.** Oskarshamn site investigation. Formation factor logging in situ and in the laboratory by electrical methods in KSH01A and KSH02. Measurements and evaluation of methodology.

PR-25-89-17 **Bjarnason B, Klasson H, Leijon, B, Strindell L, Öhman T, 1989.** Rock stress measurements in boreholes KAS02, KAS03 and KAS05 on Äspö.

PR U-97-27 **Ljunggren C, H Klasson, 1997.** Drilling KLX02 – Phase 2 Lilla Laxemar Oskarshamn – Deep hydraulic fracturing Rock stress measurements in Borehole KLX02, Laxemar.

IPR-99-17 **Sundberg J, Gabrielsson A.** Laboratory and field measurements of thermal properties of the rock in the prototype repository at Äspö HRL.

IPR-02-01 **Rummel F, Klee G, Weber U.** Äspö Hard Rock Laboratory. Rock Stress measurements in Oskarshamn. Hydraulic fracturing and core testing in borehole KOV01.

IPR-02-02	**Klee G, Rummel F.** Äspö Hard Rock Laboratory. Rock Stress measurements at the Äspö HRL. Hydraulic fracturing in boreholes KA2599G01 and KF0093A01.
IPR-02-03	**Collin M, Börgesson L.** Äspö Hard Rock Laboratory. Prototype Repository. Instrumentation of buffer and backfill for measuring THM processes.
IPR-02-18	**Klasson H, Lindblad K, Lindfors U, Andersson S.** Äspö Hard Rock Laboratory. Overcoring rock stress measurements in borehole KOV01, Oskarshamn.
IPR-03-13	**Dershowitz W, Winberg A, Hermanson J, Byegård J, Tullborg, E-L, Andersson P, Mazurek M.** Äspö Hard Rock Laboratory. Äspö Task Force on modelling of groundwater flow and transport of solutes. Task 6c. A semi-synthetic model of block scale conductive strctures at the Äspö HRL.
ICR-01-04	**Byegård J, Widestrand H, Skålberg M, Tullborg E-L, Siitari-Kauppi M.** First TRUE Stage. Complementary investigations of diffusivity, porosity and sorbtivity of Feature A-site specific geologic material.
R-97-13	**Carbol P, Engkvist I.** Compilation of radionuclide sorption coefficients for performance assessment.
R-98-55	**Follin S, Årebäck M, Axelsson C-L, Stigsson M, Jacks G.** Förstudie Oskarshamn. Grundvattnets rörelse, kemi och långsiktiga förändringar (in Swedish).
R-99-70	**Lindell S, Ambjörn C, Juhlin B, Larsson-McCann S, Lindquist K.** Available climatological and oceanographical data for site investigation program.
R-01-06	**Markström I, Stanfors R, Juhlin C.** Äspölaboratoriet RVS-modellering, Ävrö Slutrapport (in Swedish).
R-02-06	**Boresjö Bronge L, Wester K.** Vegetation mapping with satellite data of the Forsmark and Tierp regions.
R-02-10	**Berggren J, Kyläkorpi L.** Ekosystemen i Simpevarpsområdet Sammanställning av befintlig information (in Swedish).
R-02-10	**Berggren J, Kyläkorpi L.** Ekosystemen i Simpevarpsområdet – Sammanställning av befintlig information (In Swedish: Ecosystems in the Simpevarp area – A list of available information).
R-02-26	**Janson T, Stigsson M.** Test with different stress measurement methods in two orthogonal bore holes in Äspö HRL.
SKB R-02-27	**Sundberg J.** Determination of thermal properties at Äspö HRL. Comparison and evaluation of methods and methodologies for borehole KA 2599 G01.
R-02-35	**SKB.** Simpevarp – site descriptive model version O.
R-02-47	**Risberg J.** Holocene sediment accumulation in the Äspö area. A study of a sediment core.
R-04-74	Laaksoharju S1.2.
R-03-10	**Sundberg J.** Thermal Site Descriptive Model. A strategy for the model development during site investigations. Version 1.0.
R-04-11	Miliander S, Punakivi M, Kyläkorpi L, Rydgren B. Human population and activities at Simpevarp.
R-04-12	**Kyläkorpi L, 2005.** Tillgänglighetskartan (Map of accessibility).
R-04-16	**Laaksoharju M, Smellie J, Gimeno M, Auqué L, Gómez J, Tullborg E-L, Gurban I.** Hydrogeochemical evaluation of the Simpevarp area, model version 1.1.
TR-97-06	**Rhén I (ed.), Gustafson G, Stanfors R, Wikberg P.** Äspö HRL – Geoscientific evaluation 1997/5. Models based on site characterization 1986–1995.
TR-97-20	**Ohlsson Y, Neretnieks I.** Diffusion data in granite. Recommended values.
TR-98-18	**Byegård J, Johansson H, Skålberg M, Tullborg E-L.** The interaction of sorbing and non-sorbing tracers with different Äspö rock types. Sorption and diffusion experiments in the laboratory scale.
TR-02-03	**Larsson-McCann S, Karlsson A, Nord M, Sjögren J, Johansson L, Ivarsson M, Kindell S.** Meteorological, hydrological and oceanographical information and data for the site investigation program in the community of Oskarshamn.
TR-02-19	**Andersson J, Berglund J, Follin S, Hakami E, Halvarson J, Hermanson J, Laaksoharju M, Rhén I, Wahlgren C-H.** Testing the methodology for site descriptive modelling. Application for the Laxemar area.
SKI 98:41	**Xu S, Wörman A.** Statistical Patterns of Geochemistry in Crystalline Rock and Effect of Sorption Kinetics on Radionuclide Migration.

2.8 Model volumes

The site descriptive modelling is performed using two different model volumes (or domains) of different scales, the *regional* and the *local* scale model volumes. Generally, the local model is required to cover the volume within which the repository is expected to be positioned, including accesses and the immediate environs. In addition to the description on the local scale, a description is also devised for a much larger volume, the regional model. The latter model provides boundary conditions and puts the local model in a larger context. It is noted that the defined modelling areas and their vertical extents, which in combination defined three-dimensional modelling domains, are the areas for which a parameterised description in some form is expected. They are by no means to be regarded as strict domains for e.g. numerical hydrogeological modelling. In the latter case, other considerations come into play when defining the modelling domain, e.g. topographical considerations (groundwater divides) and/or the positioning of interpreted deformation zones.

This section presents and justifies the model volumes selected for the Simpevarp area for the Simpevarp 1.2 model version, including the Simpevarp and Laxemar subareas.

2.8.1 General

By necessity, the site characterisation efforts need to focus on the volumes of primary interest for the repository location. Demands for high information density are higher in these volumes than outside. The local volume description should be detailed enough for the needs of the repository engineering and safety assessment groups. It is primarily these users of the descriptions who can judge whether the local volume is sufficiently large. However, the site modelling needs to ensure a sufficient understanding of the evolution of the natural system. This means that the size and level of resolution needed, especially in the regional volume, should be dictated by what is required in order to capture the most relevant physical phenomena for describing this evolution.

In selecting the model volumes for version 1.1 models for Simpevarp and Forsmark the following rules of thumb, taken from the SKB strategy document for integrated evaluation /Andersson, 2003/ were applied:

- The local site descriptive model should cover an area of about 5–10 km^2, i.e. large enough to include the potential repository and its immediate surroundings. This also means that the location of this model area needs to be agreed upon by both the design and site modelling groups.
- The regional descriptive model should be large enough to allow for a sensitivity analysis of boundary conditions and to provide site understanding to the local model.
- If possible, model domains selected in previous versions should be retained. Deviations should be well motivated and their basis fully documented.
- The models should include the main sources of new information (e.g. deep boreholes and areas of extensive surface geophysics).
- The local domain should be large enough to allow meaningful hydrogeological flow simulations within the domain, though information for boundary conditions or an encompassing regional scale hydrogeological model will often need to be taken from the regional domain – or beyond.
- Potentially important features, such as lineaments, rock type boundaries etc., should be considered when selecting the size of the model volumes.

These rules also apply for model versions 1.2. It needs also be understood that the distinct model sizes primarily concern the development of the geological model in the SKB Rock Visualisation System, RVS. The following clarifications are possibly motivated:

- Model boundaries for numerical simulations, e.g. in the hydrogeological model, are to be set to suite the purpose of these simulations and do not need to be restricted to the size of the RVS-representation.
- In modelling the hydrogeological and hydrogeochemical evolution, the numerical model assesses the importance of the location of boundaries and the importance of different boundary conditions at these boundaries, see Chapter 8. These studies are in principle not restricted by the size of the regional volume for the RVS representation.

The regional and local model volumes differ with respect to amount of detailed data and degree of determinism, but not with regard to the scale of resolution of the spatial variability. For example, outside the local model volume the geological model only have large deterministic deformation zones, whereas small zones are represented by expanding the DFN-model in this volume, see Chapter 5. This means that in the regional hydrogeological modelling, see Chapter 8, the resolution is the same in the entire model domain, whereas, of course the uncertainty in the domain outside the local volume is indeed much higher than inside this volume

2.8.2 Regional model volume

Generally, the geographic scope of the regional models depends on the local premises and requirements and is controlled by the basic need to achieve understanding of the conditions and processes that determine the conditions at the site /SKB, 2001a/. The regional model volume should encompass a sufficiently large area that the geoscientific conditions that can directly or indirectly influence the local conditions, or help in understanding the geoscientific processes in the repository area, are included. In practical terms, this may entail a surface area of "a few hundred square kilometres".

Figure 2-3 shows the regional model area selected for Simpevarp 1.2. It is the same model area used in the version-0 report /SKB, 2002b/ and for the version Simpevarp 1.1 modelling /SKB, 2004b/. The depth of the model volume is set to 2.2 km (from 100 m above sea level and extending down to 2,100 m below).

The regional model volume has been selected on the basis of the following considerations and arguments:

- It includes the prioritised area for site investigations in the Simpevarp area /SKB, 2001b/ and it is not prohibitively large, with an approximate surface area of 273 km^2.
- It captures the extensive regional deformation zones, that strike in northnortheasterly and near east-west directions, and surround the prioritised area for site investigations. Any expansion of the regional model area to the east or west would not provide any significant changes in the regional geological picture.
- It adequately covers the variations in rock type in the candidate area and its immediate surroundings.
- It captures the main features in the region interpreted to be of hydrogeological importance as the east-west boundaries are judged to be sufficiently well separated in space not to influence the groundwater flow in the region. Furthermore, the western boundary lies on the western side of a local topographic divide and the boundary to the east lies in the Kalmar Sund strait (between the mainland and the island of Öland). The area includes potential discharge areas for groundwater resulting from future shoreline displacement. Due to the very steep topographic relief close to the shoreline, a reduction of the extent of the regional model towards the east in the Kalmar Sund strait was considered for the Simpevarp 1.1 description. However, for convenience and easy back reference it was decided to retain the regional model boundaries used for the v0 modelling. This applies also to the Simpevarp 1.2 modelling. The proper locations of the boundaries in the regional hydrogeological model – as well as the proper boundary conditions are assessed through a series of sensitivity analyses in the hydrogeological modelling, see Chapter 8.
- A depth of 2.2 km (of which 100 m is above sea level) is considered to provide a reasonable context for the local description. Furthermore, this depth is considered the maximum down to which any meaningful extrapolations of deformation zones can be made.

The coordinates outlining the surface area of the Regional model for Simpevarp 1.2, cf. Figure 2-3, are (in metres):

(X, Y):
(1539000, 6373000), (1560000, 6373000), (1539000, 6360000), (1560000, 6360000).

Z: +100 m, –2,100 m.

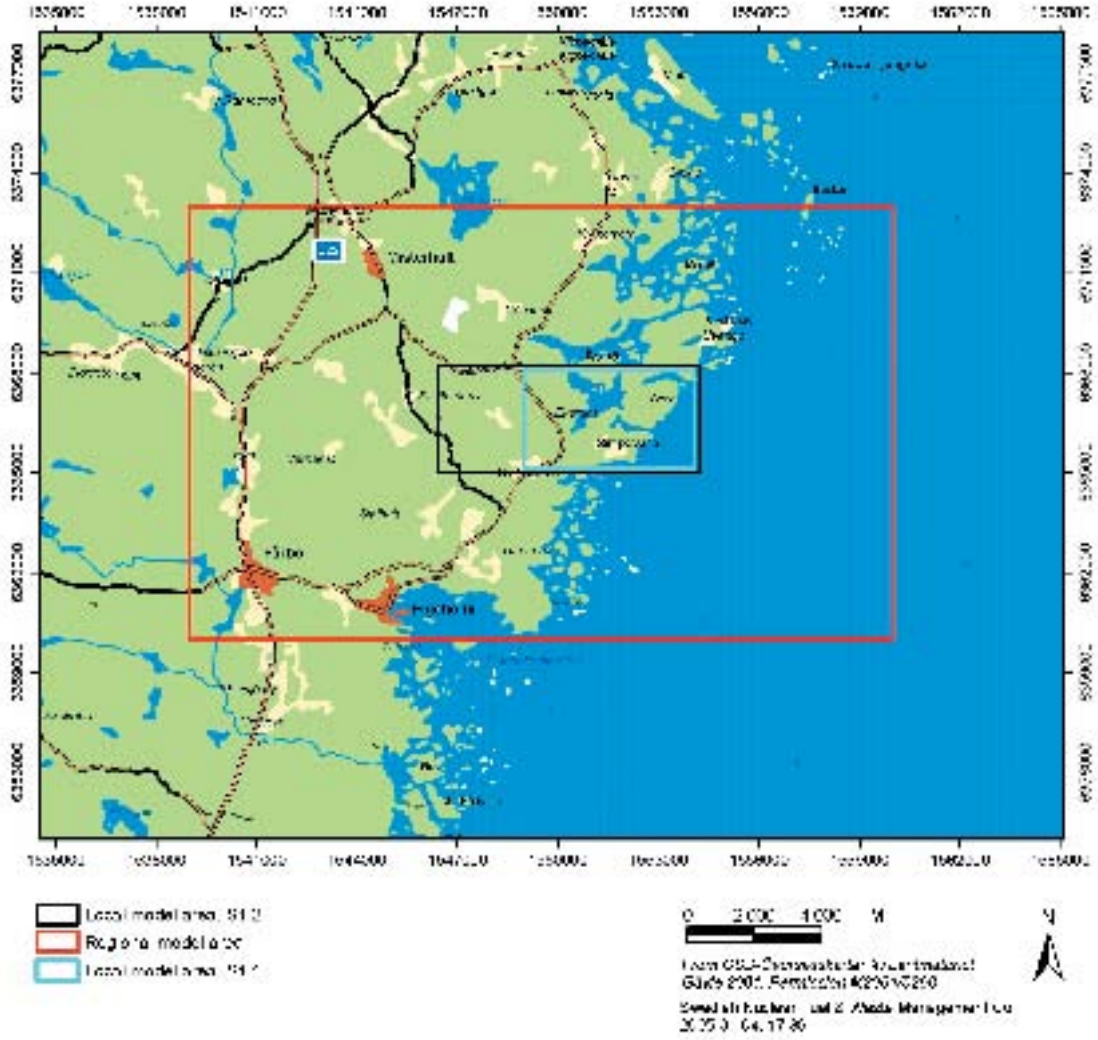

Figure 2-3. *Regional and local model areas used for Simpevarp version 1.1. The areal coverage of the regional model is the same as that used in version 0 /SKB, 2002b/ and for the SDM Simpevarp 1.1 /SKB, 2004b/.*

2.8.3 Local model volume

The area covered by the deep repository (at repository depth) should ideally not be more than about 2 km^2. This assumes a fully constructed repository with approximately 4,000 canisters, a 90% utilisation of possible canister positions and centrally located space for the required infrastructure. The surface facility and the access to the deep repository are not included in this area, as their areal needs depend on whether a straight ramp, a spiral ramp or a shaft access will be employed. A geometrically ideal case will not be achieved in reality, since the layout of the deep repository will be adapted to conditions in the bedrock (deformation zones, etc.). The more deposition subareas the deep repository is made up of, and the more irregular these are, the greater the total repository area that will be required, since intervening unutilised "corridors" must also be included in the total "encompassing" area. The local (investigation and) model area should be considerably larger than the repository area, above all because it is not otherwise possible to try out alternative repository layouts and gradually arrive at the optimal placement and adaptation to the rock conditions. The local model volume should therefore encompass a surface area of 5–10 km^2 /SKB, 2001a/.

In the version 0 report /SKB, 2002b/, a near circular-shaped "candidate area" with a size of some 50 km^2 was presented. The ambition of subsequent characterisation and analysis has been to reduce the candidate area to a "prioritised area for site investigation". In the case of the Simevarp area, the prioritised area for site investigations is made up of two separate subareas. The first area,

where drilling commenced during the summer of 2002, is denoted the “Simpevarp subarea” and is made up of major portions of the Simpevarp peninsula, together with the islands of Ävrö, Hålö and Bockholmen. The second, the “Laxemar subarea” was selected early in 2003 /SKB, 2003b/ following complementary regional investigations and subsequent evaluation /Wahlgren et al. 2003/, cf. Figure 1-1. The two areas are in essence neighbouring one another. This suggested that including the two “subareas” in one single local model would provide synergy and facilitate co-interpretation of data which will emerge from the two sites over time. Characterisation of the Laxemar subarea commenced in late 2003 and in this context comes second in time to the Simepvarp subarea. Also, the area of Hålö/Bockholmen, positioned inbetween the two subareas, is a natural candidate area for the surface installations associated with a future deep repository. By including the two subareas in one local model volume, satisfactory coverage is also provided for any type of access tunnel and/or tunnel connection from a shaft access to either of the two.

For Simpevarp version 1.1, a local scale model area was employed which only included the area east of the Äspö shear zone. This was argued for on the basis of there not being any new data available for the Laxemar subarea. For Simpevarp 1.2 new complementary data are available from borehole KLX02, but the surface information essentially remains the same. Still, with the Laxemar 1.2 modelling soon due, it was decided to enlarge the local scale model area to incorporate both the Simpevarp and Laxemar subareas for the version Simpevarp 1.2 modelling. This way, the local scale modelling is up and running for Laxemar 1.2. For the complete site investigation stage, it is however possible to reduce the locals scale model area to a more optimal size.

The coordinates (X,Y,) outlining the surface area of the local scale model for Simpevarp 1.2, cf. Figure 2-3, are (in metres):

(1546400, 6368200), (1554200, 6368200), (1554200, 6365000), (1546400, 6365000).

Figure 2-3 shows the local model area for the Simpevarp subarea as embedded in the Regional Scale Model. The vertical extent of the local model is set to 1,200 m, 1,100 m below sea level and 100 m above sea level. It is noted that the southern parts of the Äspö island is included in the model, cf. Section 2.6. For comparison, also the local model area employed for Simpevarp 1.1 is shown in Figure 2-3.

The local model volume has been selected on the basis of the following considerations:

- It provides a volume that includes the Simpevarp subarea and the area for potential surface facilities, access ramps and tunnels connecting from the islands of Hålö and Bockholmen.
- In addition it contains the Laxemar subarea. This allows co-interpretation of data emerging from the two subareas in an efficient and flexible manner. However, as the site investigation progresses, it will be equally possible to diminish the size of the local model accordingly.
- The east-west boundaries are positioned along one interpreted v.0 fracture zone (ZSM0002A0, The Mederhult zone), cf. Table 5-15 and associated Figure 5-54, and a topograhically/ geophysically identified lineament, respectively. The north-south boundaries of the model are not associated with any particular geographical feature.
- A depth of 1,100 m below sea level will permit inclusion of all information from the deep boreholes that will be completed at the site.
- The area has a surface area of approximately 24 (8×3) km^2 (see Figure 2-3).

3 Evolutionary aspects

3.1 Crystalline bedrock

3.1.1 Introduction

The following brief outline of the geological evolution in the Oskarshamn region is a slightly modified version of that presented in /Andersson et al. 2002b/. It is mainly based on results published in reports in various SKB series as well as in research papers in scientific journals. The Oskarshamn region is put into a regional geological context, but the description is focussed on the geological evolution of rock types and structural elements that characterize the bedrock in the Oskarshamn municipality and its immediate surroundings.

The geological evolution of cratonic (stabilised) bedrock regions is generally the result of consecutive large-scale processes, e.g. orogenies, which have operated over a considerable period of time. In order to understand the geological development of the bedrock in southeastern Sweden, it is necessary to take into account also post-cratonization (after c. 1,750–1,700 Ma Before Present (BP)), i.e. large-scale processes more or less remote from the Oskarshamn region that might have had a far-field effect on the already cratonised crust.

The geological development in the Oskarshamn region, including the formation of existing rocks, as well as structural and tectonic overprinting, is complex and spans a period of c. 1,900 Ma. The following text gives a brief summary and for further information of the geological evolution and processes that might have affected the bedrock in the Oskarshamn region and the rest of the southern part of the Fennoscandian Shield, the reader is referred to e.g. /Larson and Tullborg, 1993/ and /Milnes et al. 1998/.

As a reference for the following text, the geological time units and nomenclature used are displayed in Figure 3-1.

In order to put the Oskarshamn region in a large-scale geological evolutionary perspective, the successive growth of the Fennoscandian Shield and subsequent formation of Phanerozoic cover sequences from c. 1,910 Ma until the Quaternary period is displayed in Figure 3-2 through Figure 3-6. In each figure, previously formed rocks are marked in grey. The following abbreviations are used:

GP = granite-pegmatite

GDG = granitoid-dioritoid-gabbroid

GSDG = granite-syenitoid-dioritoid-gabbroid

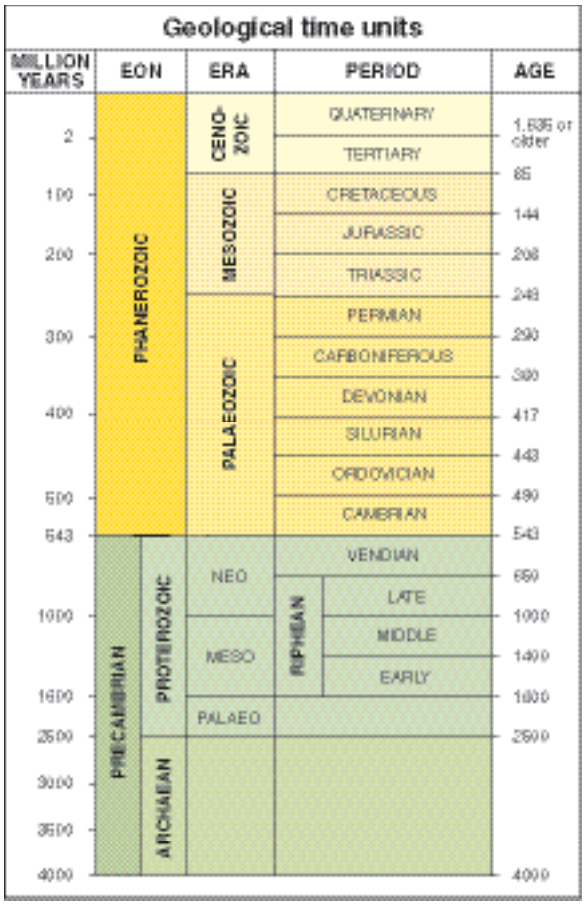

Figure 3-1. *Geological time scale. Modified after /Koistinen et al. 2001/.*

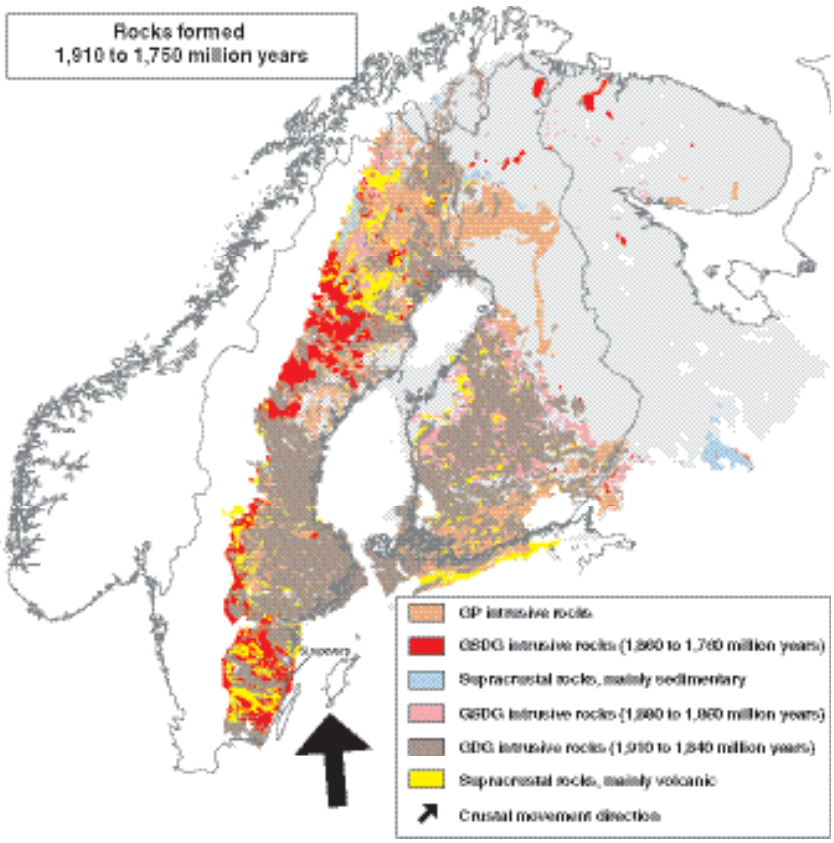

Figure 3-2. *Rocks formed in the time interval 1,910–1,750 Ma BP. The figure is based on the database presented by /Koistinen et al. 2001/.*

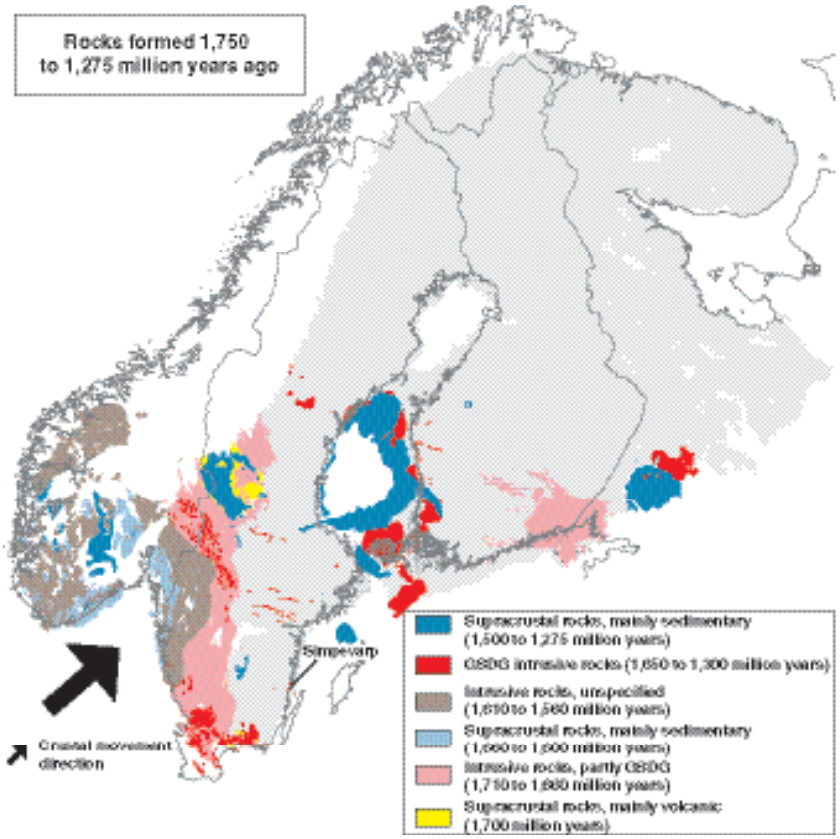

Figure 3-3. *Rocks formed in the time interval 1,750–1,275 Ma BP. The figure is based on the database presented by /Koistinen et al. 2001/.*

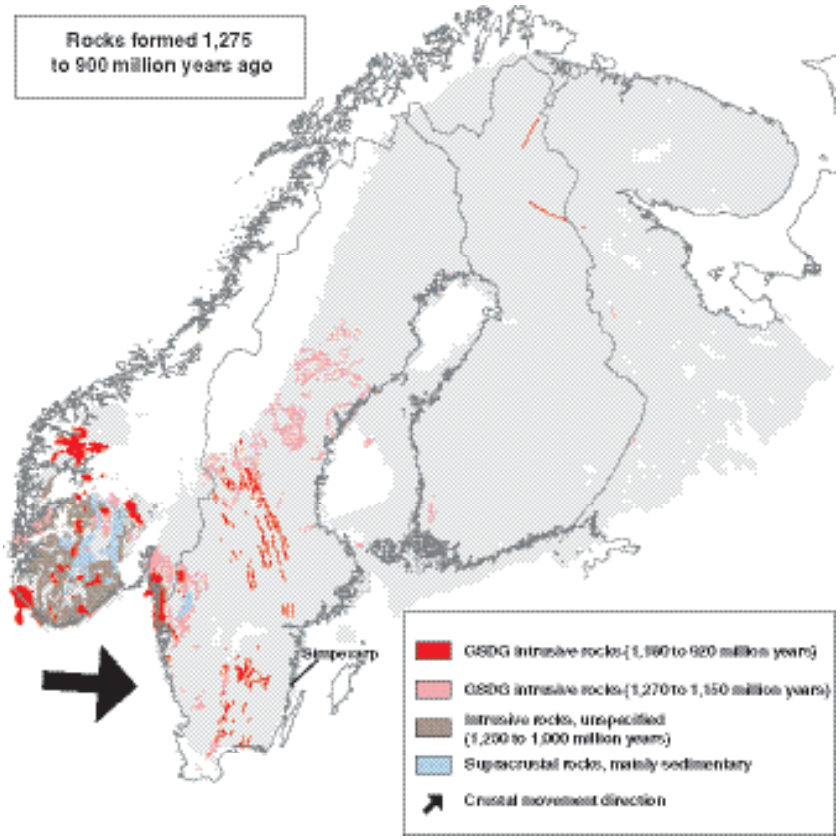

Figure 3-4. *Rocks formed in the time interval 1,275–900 Ma BP. The figure is based on the database presented by /Koistinen et al. 2001/.*

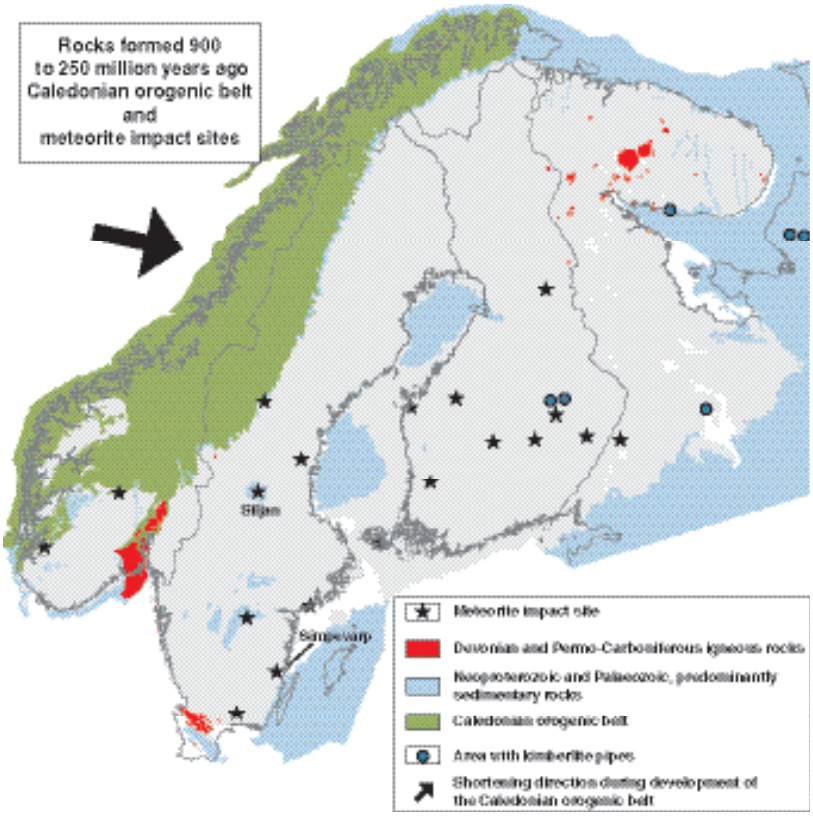

Figure 3-5. *Rocks formed in the time interval 900–250 Ma BP. The figure is based on the database presented by /Koistinen et al. 2001/.*

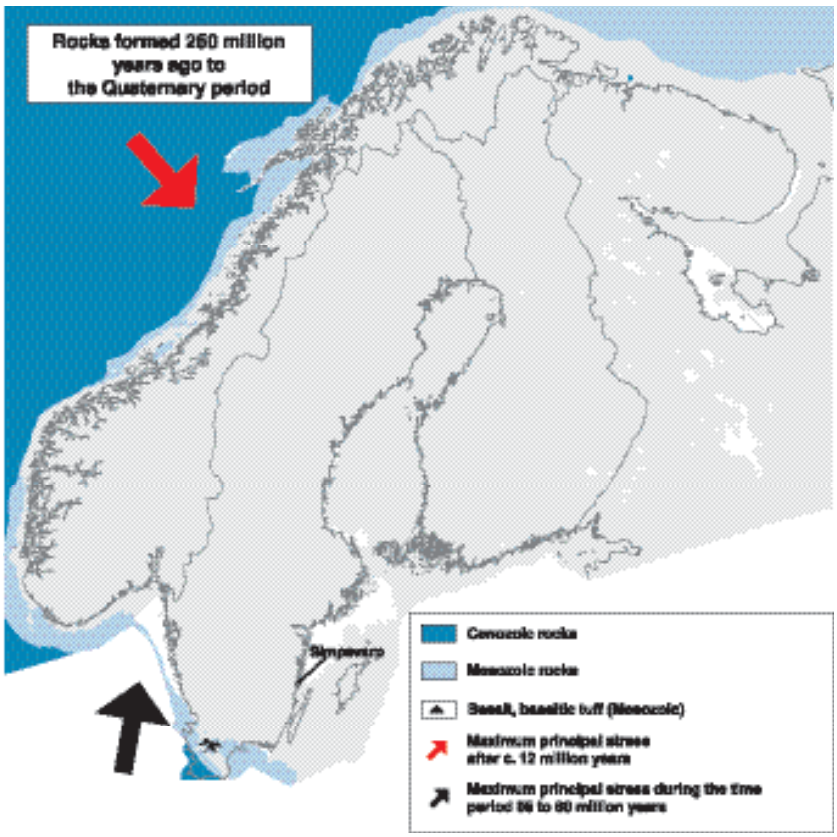

Figure 3-6. *Rocks formed in the time interval 250 Ma BP to the Quaternary period. The figure is based on the database presented by /Koistinen et al. 2001/.*

3.1.2 Lithological development

The position of the Oskarshamn region in a regional geological-evolutionary perspective can be seen in Figure 3-2 through Figure 3-7. The oldest rocks in the Oskarshamn region, though subordinate, comprise more or less strongly deformed and metamorphosed supracrustal rocks of predominantly sedimentary but also of volcanic origin. The formation of the metasedimentary rocks is constrained to the time interval c. 1,870–1,860 Ma BP /Sultan et al. 2004/, and the rocks have their main expression in the Blankaholm-Västervik area, cf. Figure 3-8 /Bergman et al. 1998, 1999, 2000/.

In the area immediately north of Oskarshamn and westwards, metagranitoids belonging to the E-W to WNW-ESE trending so-called Oskarshamn-Jönköping belt /Mansfeld, 1996/ constitute an important lithological component. These rocks were formed c. 1,834–1,823 Ma ago /Mansfeld, 1996; Åhäll et al. 2002/ and display a varying degree of tectonometamorphic overprinting and in many places they are relatively well-preserved.

The majority of the rocks at the present day erosional level in southeastern Sweden were formed during a period of intense igneous activity c. 1,810–1,760 Ma ago /e.g. Wikman and Kornfält, 1995; Kornfält et al. 1997/, during the waning stages of the Svecokarelian orogeny. The dominant rocks comprise granites, syenitoids, dioritoids and gabbroids, as well as spatially and compositionally related volcanic rocks. The granites and syenitoids, as well as some of the dioritoids are by tradition collectively referred to as Småland “granites”. Both equigranular, unequigranular and porphyritic varieties occur, and the compositional variation is displayed in Figure 3-9. Hence, the Småland “granites” comprise a variety of rock types regarding texture, mineralogical and chemical composition.

This generation of igneous rocks belongs to the so-called Transscandinavian Igneous Belt (TIB), which has a NNW extension from southeastern Sweden through Värmland and Dalarna into Norway, where it finally disappears beneath the Scandinavian Caledonides (Figure 3-7). It is characterised by repeated alkalicalcic-dominant magmatism during the period c. 1,860–1,650 Ma ago. Magma-mingling and -mixing processes, exemplified by the occurrence of enclaves, hybridization and diffuse transitions etc. between different TIB rocks indicate a close time-wise and genetic relationship between the different rock types. At mesoscopic scale, these processes often resulted in a more or less inhomogeneous bedrock regarding texture, mineralogical and chemical composition. However, if larger rock volumes are considered, these may be regarded as being more or less homogeneous, despite some internal variations.

Locally, fine- to medium-grained granite dykes and minor massifs, and also pegmatite occur frequently. Though volumetrically subordinate, these rocks constitute essential lithological inhomogeneities in parts of the bedrock in the Oskarshamn region, e.g. in the Simpevarp area. They are roughly coeval with the TIB host rock /Wikman and Kornfält, 1995; Kornfält et al. 1997/, but have been intruded at a late stage in the magmatic evolution. Furthermore, TIB-related mafic and composite dykes occur locally.

After the formation of the TIB rocks, the next rock-forming period in the Oskarshamn region, including southeastern Sweden, did not take place until c. 1,450 Ma ago. It was characterised by the local emplacement of granitic magmas in a cratonized crust. However, this granitic magmatism was presumably a far-field effect of ongoing orogenic processes elsewhere, presumably farther to the southwest of present Scandinavia. In the Oskarshamn region, the c. 1,450 Ma BP magmatism is exemplified by the occurrence of the Götemar, Uthammar and Jungfrun granites, cf. Figure 3-8 /Kresten and Chyssler, 1976; Åhäll, 2001/. Fine- to medium-grained granitic dykes and pegmatites that are related to the c. 1,450 Ma granites occur as well, e.g. in the Götemar granite. However, these dykes are inferred to occur only within the granite and in its immediate surroundings.

The youngest magmatic rocks in the region are scattered dolerite dykes that presumably are related to the regional system of N-S trending, c. 1,000–900 Ma old dolerites that can be followed from Blekinge in the south to Dalarna in the north /Johansson and Johansson, 1990; Söderlund et al. 2004/. The dykes are emplaced in and to the east of the frontal part of the Sveconorwegian orogen. Due to the generally high content of magnetite, they usually constitute linear, positive magnetic anomalies, and their occurrence and extension may, thus, be identified on the magnetic anomaly maps. Time-wise they are related to the c. 1,100–900 Ma Sveconorwegian orogeny which is responsible for the more or less strong reworking and present structural geometry in the bedrock of southwestern Sweden.

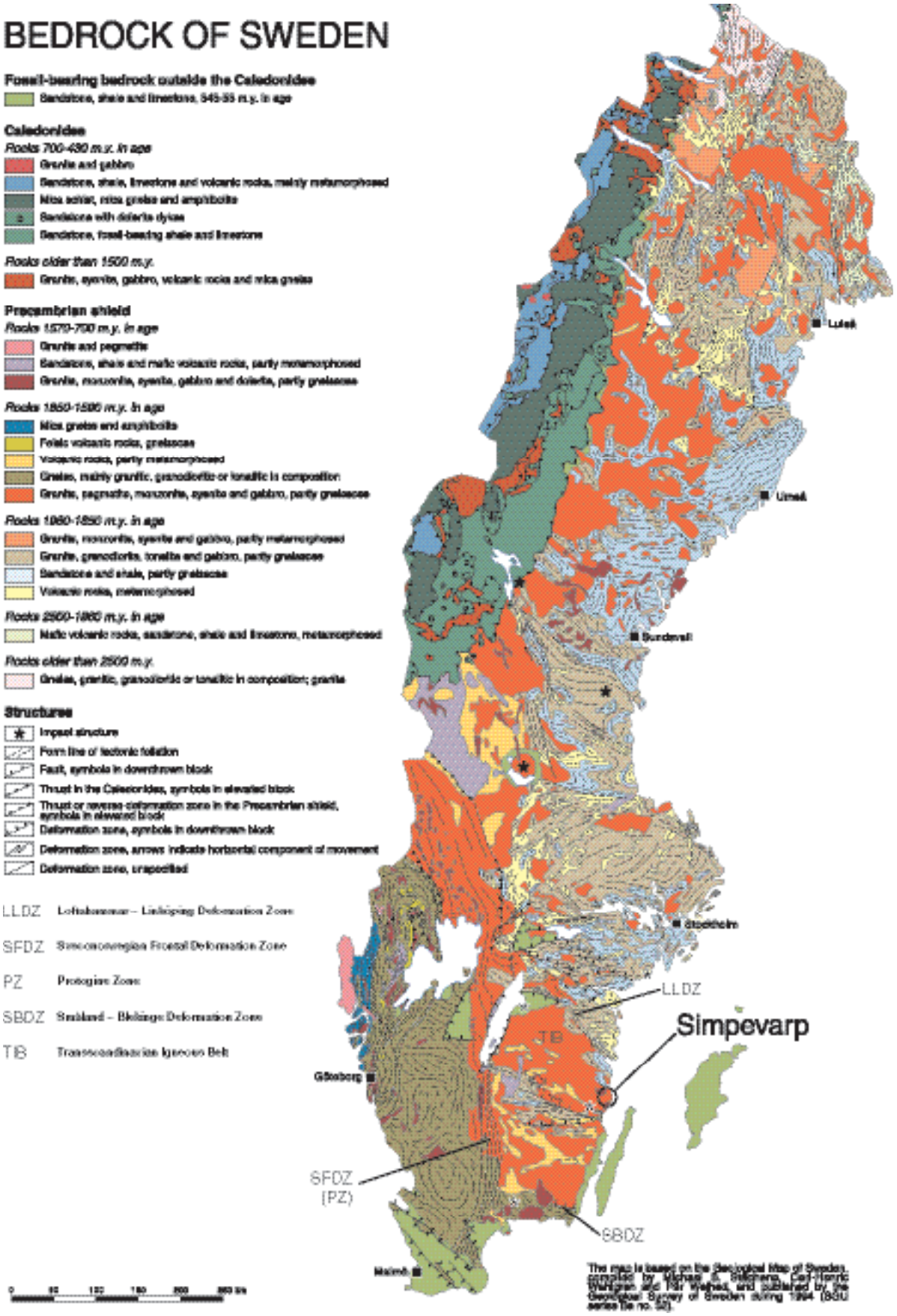

Figure 3-7. *Simplified bedrock map of Sweden. The geological province in which the Simpevarp area lies is bounded by major deformation zones along its northern (LLDZ), southern (SBDZ) and western (SFDZ) boundaries. Modified after /Stephens et al. 1994/.*

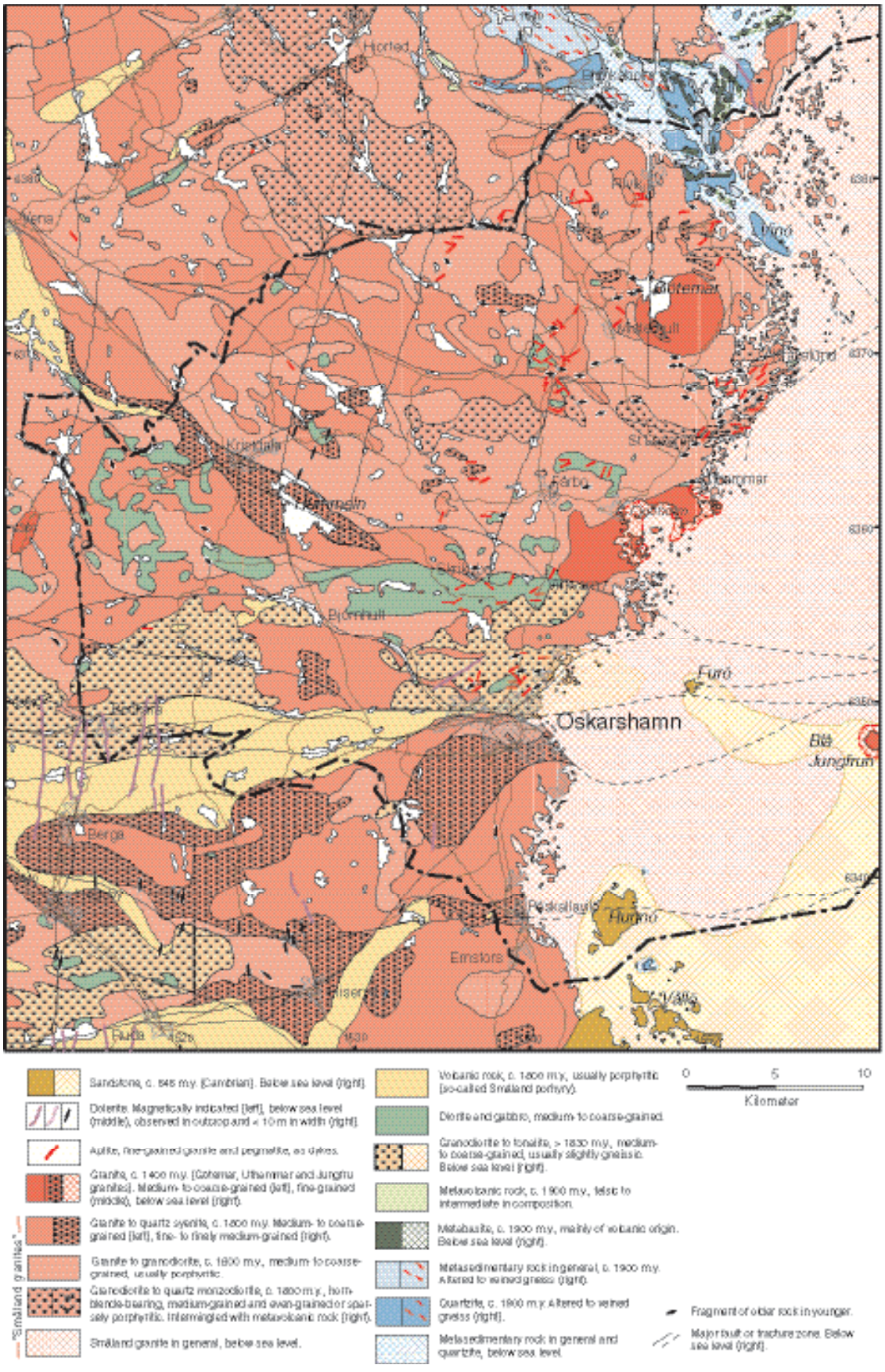

Figure 3-8. *Bedrock map of the Oskarshamn municipality and the surrounding area. Slightly modified after /Bergman et al. 1998/.*

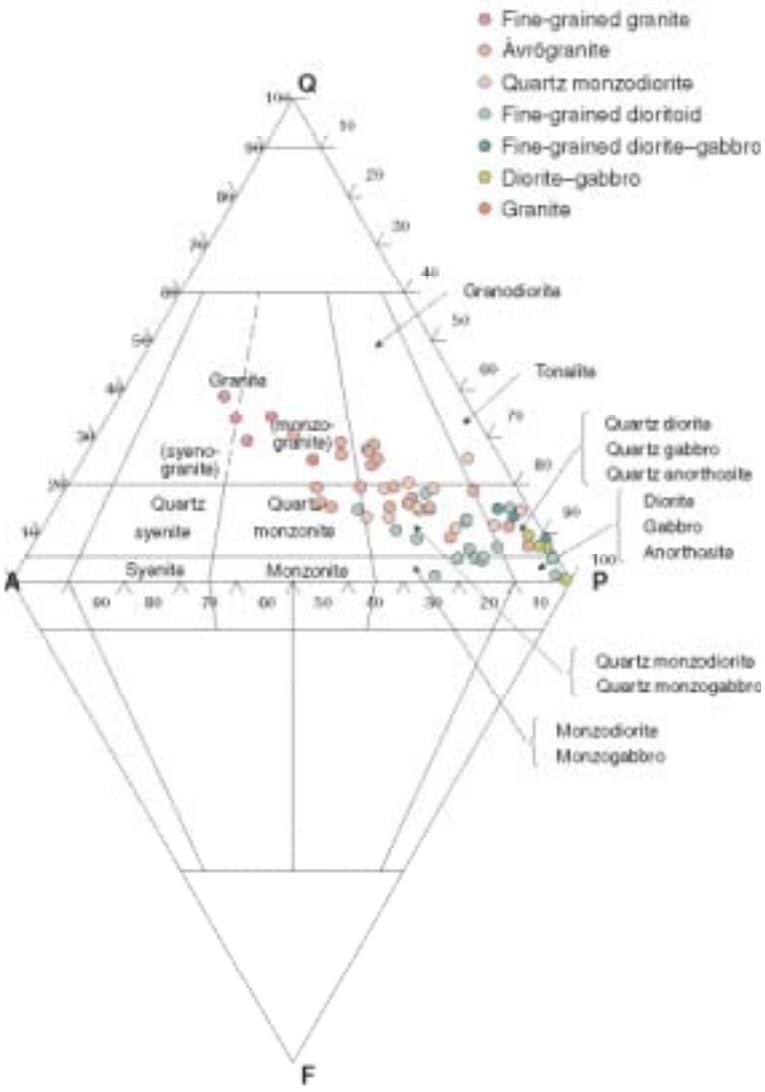

Figure 3-9. *QAPF-diagram displaying the compositional variation of magmatic rocks, exemplified with modal analyses of rocks from the Simpevarp subarea.*

In late Precambrian and/or early Cambrian time, i.e. c. 600–550 Ma ago, arenitic sediments were deposited on a levelled bedrock surface, the so-called sub-Cambrian peneplain. The sediments were subsequently transformed to sandstones, which constitute the youngest rocks in the region, cf. Figure 3-7 and Figure 3-8. The remainder of these former extensively occurring sedimentary rocks covers the Precambrian crystalline rocks along the coast of the Baltic Sea from the area south of Oskarshamn in the north to northeastern Blekinge in the south. Furthermore, fractures filled with sandstone are documented in the Oskarshamn region in e.g. the Götemar granite, east of the N-S trending fault (cf. Figure 3-8) that transects the granite /Kresten and Chyssler, 1976/ and at Enudden, c. 4 km northeast of Simpevarp /Talbot and Ramberg, 1990; see also Röshoff and Cosgrove, 2002/. During the ongoing site investigation in Oskarshamn, sandstone of presumed Cambrian age has been documented in a cored borehole. The sandstone occurs in a deformation zone and occupies c. 0.1 m of the drill core (cf. Sections 5.2.7 and 5.4.3).

In general, the sandstone infilling has been intruded by force downward into the basement /Röshoff and Cosgrove, 2002/. A close spatial relationship between the sandstone dykes, the sub-Cambrian peneplain and Cambrian cover rocks indicates that the sandstone dykes are Cambrian in age. A characteristic feature is the local occurrence of fluorite (+/–calcite and galena) mineralisations within the pores of the sandstone dykes and along the dyke/country rock interface. The timing of formation

of the mineralisations is uncertain, but they post-date the formation of the sandstone dykes. /Alm and Sundblad, 2002/ claimed that the mineralisations are post-Cambrian and pre-Silurian in age, whereas /Röshoff and Cosgrove, 2002/ suggested that they are pre-Permian in age.

3.1.3 Structural development

Ductile deformation

The bedrock of southeastern Sweden has gone through a long and complex structural development, including both ductile and brittle deformation, since the formation of the oldest c. 1,890–1,850 Ma supracrustal rocks. The oldest deformation, which was developed under medium- to high-grade metmorphic conditions, is of regional, penetrative character, and is recorded in the supracrustal rocks in the Blankaholm-Västervik area. It pre-dates the intrusion of the c. 1,860–1,850 Ma generation of TIB rocks which, however, are deformed themselves. At variance from the more or less penetrative pre-1,860 Ma deformation in the supracrustal rocks, the deformation that has affected the 1,860–1,850 Ma generation of TIB rocks, as well as the older supracrustal rocks, was heterogeneous in character. It was caused by dextral transpression under medium-grade metamorphic conditions in response to c. N-S to NNW-SSE regional compression (see Figure 3-2), is constrained to the time-interval c. 1,850–1,800 Ma BP, and is exemplified by the dextral, strike-slip dominated Loftahammar-Linköping deformation zone, cf. Figure 3-7 /Stephens and Wahlgren, 1996; Beunk and Page, 2001/. However, the folding of the foliation in the pre-1,850 Ma rocks was also supposedly developed in response to the same stress field /Stephens and Wahlgren, 1996; Beunk and Page, 2001/.

The 1,810–1,760 Ma BP generation of TIB rocks, that dominates the bedrock in the Oskarshamn region, is post-tectonic in relation to the regional, penetrative deformation related to the peak of the Svecokarelian orogeny. However, they are characterised by a system of ductile deformation zones of the same character as the Loftahammar-Linköping deformation zone, though developed during more low-grade metamorphic conditions, i.e. at shallower levels in the crust, than the initial phase of shearing in the Loftahammar-Linköping deformation zone. However, the latter zone displays ductile reactivation during low-grade metamorphic conditions, which presumably is contemporaneous with the shearing in the 1,810–1,760 Ma TIB rocks. In the Oskarshamn region, these low-grade, ductile deformation zones are exemplified by the E-W trending Oskarshamn-Bockara and NE-SW trending Oskarshamn-Fliseryd deformation zones /Bergman et al. 1998/. Presumably, also the NE-SW trending Äspö shear zone /Gustafson et al. 1989; Bergman et al. 2000/, which is characterised by a sinistral strike-slip component, belongs to this system of ductile deformation zones.

Independent of the syn-deformational metamorphic grade, the dextral and sinistral strike-slip component in the WNW-ESE to NW-SE and NE-SW trending ductile deformation zones, respectively, indicate that a regional, c. N-S to NNW-SSE compression prevailed during their formation and subsequent ductile reactivation. Consequently, this regional stress field is inferred to have prevailed for a considerable period, at least from the time of the intrusion of the 1,850 Ma TIB generation, or possibly earlier, until c. 1,750 Ma ago. Most of the lithological contacts in the region, and also in the whole of southeastern Sweden, are more or less concordant with the orientation of the ductile deformation zones, which indicates that the emplacement of the TIB magmas was facilitated by ongoing shear zone activity. Together with the subsequent deformation of the TIB rocks, this testifies to the influence of the deformation zones in the present structural and lithological framework in the bedrock of southeastern Sweden.

The structural and metamorphic overprinting in rocks in the Oskarshamn region in relation to their age of formation is summarised in Table 3-1.

Apart from the mylonitic foliation in the ductile deformation zones, the 1,810–1,760 Ma TIB rocks locally display a more or less well-developed foliation /Kornfält and Wikman, 1987/, e.g. preferred orientation of feldspar phenocrysts, mafic enclaves, biotite etc. However, it is often difficult to decide whether the foliation is syn-intrusive or caused by a subsequent tectonic overprinting. Independent of origin, the orientation of the foliation suggests that there is a genetic relationship between foliation development outside the ductile deformation zones and the shear zone activity.

Table 3-1. The relation between age of rock types and the structural and metamorphic overprinting.

Age (Ma BP)	Structural and metamorphic overprinting
1,880–1,870	Penetrative, ductile deformation under medium- to high-grade metamorphic conditions.
1,860–1,850	Inhomogeneous ductile deformation under medium-grade metamorphic conditions.
1,834–1,823	Inhomogeneous ductile deformation under low- to medium-grade metamorphic conditions.
1,810–1,760	Spaced ductile shear zones developed under low-grade metamorphic conditions. Although the majority of the rocks are structurally more or less well-preserved, a low- to very low-grade metamorphic alteration occurs.
1,450	Brittle deformation. The rocks are well-preserved.
1,100–900	Brittle deformation. The rocks are well-preserved.
540	Brittle deformation. The rocks are well-preserved.

Brittle deformation

Since no ductile deformation has been observed in the c. 1,450 Ma granites /e.g. Talbot and Ramberg, 1990; Munier, 1995/ or younger rocks, it is evident that only deformations under brittle conditions have affected the bedrock in the Oskarshamn region during at least the last c. 1,450 Ma. However, the transition from ductile to brittle deformation presumably took place during the time interval c. 1,750–1,700 Ma, i.e. during uplift and stabilization of the crust after the Svecokarelian orogeny.

To unravel the brittle tectonic history in the bedrock in southeastern Sweden during the last c. 1,450 Ma is difficult. It is plausible that tectonic activities that are related to more or less remote large-scale processes, such as e.g. the Gothian, Hallandian, Sveconorwegian and Caledonian orogenies, the opening of the Iapetus Ocean, the Late Palaeozoic Variscan and the Late Mesozoic to Early Cenozoic Alpine orogenies, as well as the opening of the present Atlantic Ocean, have had a far-field effect within the shield area, cf. Table 3-1. In a global tectonic perspective, the Sveconorwegian orogeny, which corresponds to the Grenville orogeny in North-America and elsewhere, ultimately resulted in the assembly of the supercontinent Rodinia c. 900 Ma ago. Likewise the Caledonian orogeny (collision between the Laurentian and Fennoscandian Shields) was the first step in the formation of the supercontinent Pangaea, the latter part of which was finally assembled in connection with the Hercynian-Variscan orogeny in central Europe c. 250 Ma ago.

To what degree these large-scale processes have affected the bedrock in the Oskarshamn region and the rest of southeastern Sweden, and especially which brittle structure belongs to which process is difficult to decipher. The main reason for this uncertainty is the great lack of time markers for relative dating, except for the sub-Cambrian peneplain and the Cambro-Ordovician cover rocks, and the difficulties in dating brittle structures radiometrically.

The first brittle faults in the region probably developed in connection with the emplacement of younger, c. 1,450 Ma granites. During the subsequent geological evolution, faults and older ductile deformation zones have been reactivated repeatedly, due to the increasingly brittle behaviour of the bedrock. Brittle reactivation of ductile deformation zones is a general phenomenon. The Oskarshamn-Bockara, Oskarshamn-Fliseryd and Äspö shear zones display clear evidence of being reactivated in the brittle régime /see also e.g. Munier, 1995/. An inversion of the strike-slip component in the Äspö shear zone from sinistral during the older ductile deformation, to dextral during the younger brittle reactivation has been proposed by /Talbot and Munier, 1989/ and /Munier, 1989/.

K-Ar dating of biotites from the “Småland granites” /Åberg, 1978/ has yielded ages of c. 1,500–1,400 Ma. According to /Åberg, 1978/, the obtained ages are caused by the c. 1,500–1,400 Ma BP magmatic activity in southern Sweden. However, /Tullborg et al. 1996/ considered the closure of the K-Ar system in this time interval to be the result of an uplift scenario. Independent of the explanation, there is no information about any explicit tectonic features that can be related to this time period.

The occurrence of c. 1,000–900 Ma BP dolerites in southeastern Sweden testifies to a Sveconorwegian tectonic influence, as the intrusion of the parent magmas was tectonically controlled. However, whether individual faults or fracture zones, which were not injected by mafic magma, were formed or reactivated during the Sveconorwegian orogeny, and if so which of them, is uncertain.

On the basis of titanite and zircon fission track studies in the Oskarshamn region, it has been suggested that sediments that were derived from the uplifted Sveconorwegian orogenic belt and deposited in a Sveconorwegian foreland basin reached a thickness of c. 8 km in southeastern Sweden at around 850 Ma BP /Tullborg et al. 1996; Larson et al. 1999/. Subsequent exhumation of southeastern Sweden and erosion of the sedimentary pile were completed by the establishment of the sub-Cambrian peneplain at the end of the Neoproterozoic. Remnants of this sedimentary pile are found in the Almesåkra Group in the vicinity of Nässjö /Rodhe, 1987a/. Furthermore, apatite fission track ages in the Oskarshamn region indicate that Upper Silurian to Devonian sediments, which were derived from the uplift of the Caledonian orogenic belt and deposited in a Caledonian foreland basin, covered most of Sweden and reached a thickness exceeding 2.5 km /Tullborg et al. 1995, 1996; Larson et al. 1999/. Exhumation and subsequent erosion during the Early Mesozoic removed the sedimentary cover almost completely /Tullborg et al. 1995, 1996; Larson et al. 1999/. During the Cretaceous, a transgression occurred which resulted in a thin cover of marine sediments. In the Oskarshamn, region the sedimentary cover was not completely removed until the Tertiary /Lidmar-Bergström, 1991/.

The above-mentioned repeated large-scale events of subsidence, deposition of sediments, and subsequent exhumation and erosion, reasonably must have been accompanied by tectonic activity, i.e. movements along faults. However, there is no information that helps to decipher which fracture zones (faults) formed or were reactivated during these periods.

A recent (U-Th)/He geochronological study on apatites from rocks sampled in the access tunnel to the Äspö Hard Rock Laboratory and the cored boreholes KLX01 and 02 in the Laxemar area, yields decreasing ages with increasing depth (c. 270 Ma at the surface and c. 120 Ma at 1,700 m). This indicates that exhumation took place primarily during Late Palaeozoic to Mid Mesozoic /Söderlund, et al. in prep./. Crustal movements younger than 120 Ma are plausible in the area, although not possible to constrain until deeper borehole samples are available. The data also suggests that movement occurred during Late Palaeozoic to Mid Mesozoic time along fault zones between Äspö and the Laxemar area, e.g. reactivation in the Äspö shear zone. In future studies, this method will be used to try to estimate offset of some of the faults in the area.

According to /Milnes and Gee, 1992/ and /Munier, 1995/, the Ordovician cover rocks along the northwestern coast of Öland are tectonically undisturbed, except for displacements at the centimetre scale. This suggests that the E-W trending fracture zones/faults in the Oskarshamn-Bockara deformation zone, which can be seen in the magnetic anomaly maps to continue eastwards under Öland, have not affected the Cambro-Ordovician cover sequences on Öland. Thus, this indicates that these brittle deformation zones of regional character were not active in post-Cambrian time, but are related to the Precambrian tectonic evolution. However, post-Cambrian fracture zones/faults do occur in the Oskarshamn region. On the northwestern part of Furö, cf. see Figure 3-8, a small island c. 10 km east of Oskarshamn, a fault contact between a brecciated Cambrian sandstone and a brecciated red granite is recorded /Bergman et al. 1998/. Furthermore, the observed sandstone in the deformation zone in a cored borehole as mentioned above indicates fault movements in post-Cambrian time. Another indication of post-Cambrian deformation is the occurrence of joints filled with sandstone only east of the N-S trending fault in the western part of the Götemar granite, i.e. the eastern block has been down-faulted in relation to the western block /Kresten and Chyssler, 1976; Bergman et al. 1998/.

As mentioned above, the sub-Cambrian peneplain is a potential marker to demonstrate post-Cambrian brittle tectonics. In general, all pronounced depressions and distinct differences of topographic level in the sub-Cambrian peneplain constitute potential fracture zones or faults. /Tirén et al. 1987/ studied the relative movements of regional blocks in southeastern Sweden which were bounded by fracture zones and ranged in size between 25 km^2 and 100 km^2. Differential movements were interpreted to have occurred along existing faults both during periods of uplift and subsidence.

A general problem is to decipher the relation between the formation and subsequent reactivation of faults and fracture zones. Especially the mutual age relationship between fracture zones with different orientation is difficult to determine, mainly due to the complex relationship between age of formation and age of (latest?) reactivation. Another, and perhaps the most important and complicating, factor is that brittle deformation zones are very poorly exposed, since they mostly constitute topographical depressions filled with glacial cover, rivers, swamps etc.

The brittle deformation history of a region can be regarded as the combined effect of generation of new fractures or faults and reactivation of old fractures or faults. The ratio between generation of new structures and reactivation of older structures is presumed to decrease with time, since the orientation spectrum of pre-existing structures increased with every new event of brittle deformation /Munier, 1995/. Relative age determinations of fractures, based on orientation and a succession of mineral filling with decreasing age, have been recorded on Äspö /e.g. Munier, 1995/, and it is reasonable to assume that these findings can be extrapolated to the surrounding parts of the Oskarshamn region. The oldest fractures are epidote- and quartz-bearing, and with decreasing age chlorite, zeolite and calcite appear as fracture fillings. Since the mineralogy in individual fractures within fracture zones is essentially similar to that of fractures in the intervening blocks /Munier, 1995/, the fracture filling is a tool for relative age determination of movement (reactivation) of the former. Consequently, the calcite-bearing fracture zones/faults represent the youngest reactivation, but its absolute age is uncertain. However, an ongoing study of fracture fillings shows that different generations of calcite occurs, while zeolite represents the youngest fracture filling (see Section 5.2.6).

Based on data from Äspö, the orientation of the maximum compressive stress during the formation of the epidote- and quartz-bearing fracture zones was N-S/subhorizontal /Munier, 1989/, but had changed orientation to NE-SW when the chlorite-filled fracture zones/faults formed /Talbot and Munier, 1989/. The maximum horizontal compression was still NE-SW when the fractures formed which are filled with Cambrian sandstone /Talbot and Munier, 1989/. The orientation of the maximum horizontal compressive stress during the subsequent tectonic evolution is presumed to have been NW-SE, i.e. the same as the present stress régime. Consequently, a roughly NW-SE maximum compressive stress is inferred to have prevailed for a considerable period of time, i.e. possibly for hundreds of million of years.

Attempts have been made to use palaeomagnetic, electron spin resonance (ESR) and isotopic dating (K-Ar, Rb-Sr) techniques on some brittle structures at the Äspö site /Maddock et al. 1993/, in order to constrain the minimum age of the most recent movements. Characterization of the sampled fault gouge material demonstrated that many fracture zones contain sequentially developed fault rocks and verifies that reactivation has occurred.

The ages given by the various dating methods reflect both inherent differences in the techniques and differences in the phase or phenomenon being dated. The interpretation of the ESR dating, which was limited by the resolution of the method, yielded minimum ages of movements in the order of several hundred thousand to one million years. The results of the palaeomagnetic and K-Ar analyses strongly suggest that growth of the fracture infilling minerals took place at least 250 million years ago. The most recent fault movements are interpreted to have preceded this mineral growth. /Maddock et al. 1993/ concluded that any Quaternary and Holocene activity had little effect on the fracture zones.

According to /Mörner, 1989/, a great number of supposed post-glacial faults occur on Äspö. However, none of the faults reported showed any positive evidence of kinematics /SKB, 1990/. Some of the reported faults did not display any disturbance of Precambrian markers, others had their bases exposed by excavation and ice plucking could be positively demonstrated. /Talbot and Munier, 1989/ discussed post-glacial faults in connection with studied fault scarps, i.e. abrupt steps in the glacially polished bedrock surface on Äspö. According to /Munier, 1995/, post-glacial reactivation of individual fractures has most likely occurred, but despite searches no evidence of such features has been found on outcrops.

Ongoing tectonic activity is manifested in seismic events and aseismic slip /Larson and Tullborg, 1993/. According to /Slunga et al. 1984/, the so-called Protogine Zone of southern Sweden, cf. Figure 3-7, has been shown to be the border between a more seismic western Sweden and the more aseismic southeastern Sweden. Even though southeastern Sweden is a seismically very quiet area (Figure 3-10), an earthquake of magnitude 3.3 and a focal depth of 5.0 kilometres was recorded c. 100 kilometres south of Gotland in December 2002 /Bödvarsson, 2003/. In addition, an earthquake of magnitude 1.0 and focal depth of c. 16 kilometres was recorded c. 30 kilometres south of Oskarshamn in September 1988 /Slunga and Nordgren, 1990/. The orientation of the maximum horizontal principal stress relaxed by this earthquake, as well as other seismic events in Sweden, was c. NW-SE /Slunga et al. 1984; Slunga and Nordgren, 1990/. This is in agreement with the results from rock stress measurements at depths of more than 300 metres /Stephansson et al. 1987/, and also with the stress field generated by the plate movements in the North Atlantic Ocean /cf. Slunga, 1989; Gregersen et al. 1991; Gregersen, 1992/. According to /Slunga and Nordgren, 1990/, recent seismic activity in southeastern Sweden is related to plate-tectonic forces and not directly to land upheaval subsequent to and consequent on the last glaciation. /Gregersen et al. 1991/ and /Gregersen, 1992/ came to the same conclusion based on focal mechanisms for present-day earthquakes in Fennoscandia. However, /Muir-Wood, 1993/ and /Wu et al. 1999/ suggested that post-glacial rebound appears to be the cause of the post-glacial seismic activity in Fennoscandia.

The geological evolution in southeastern Sweden, with focus on the Oskarshamn region, is tentatively summarized in Table 3-2.

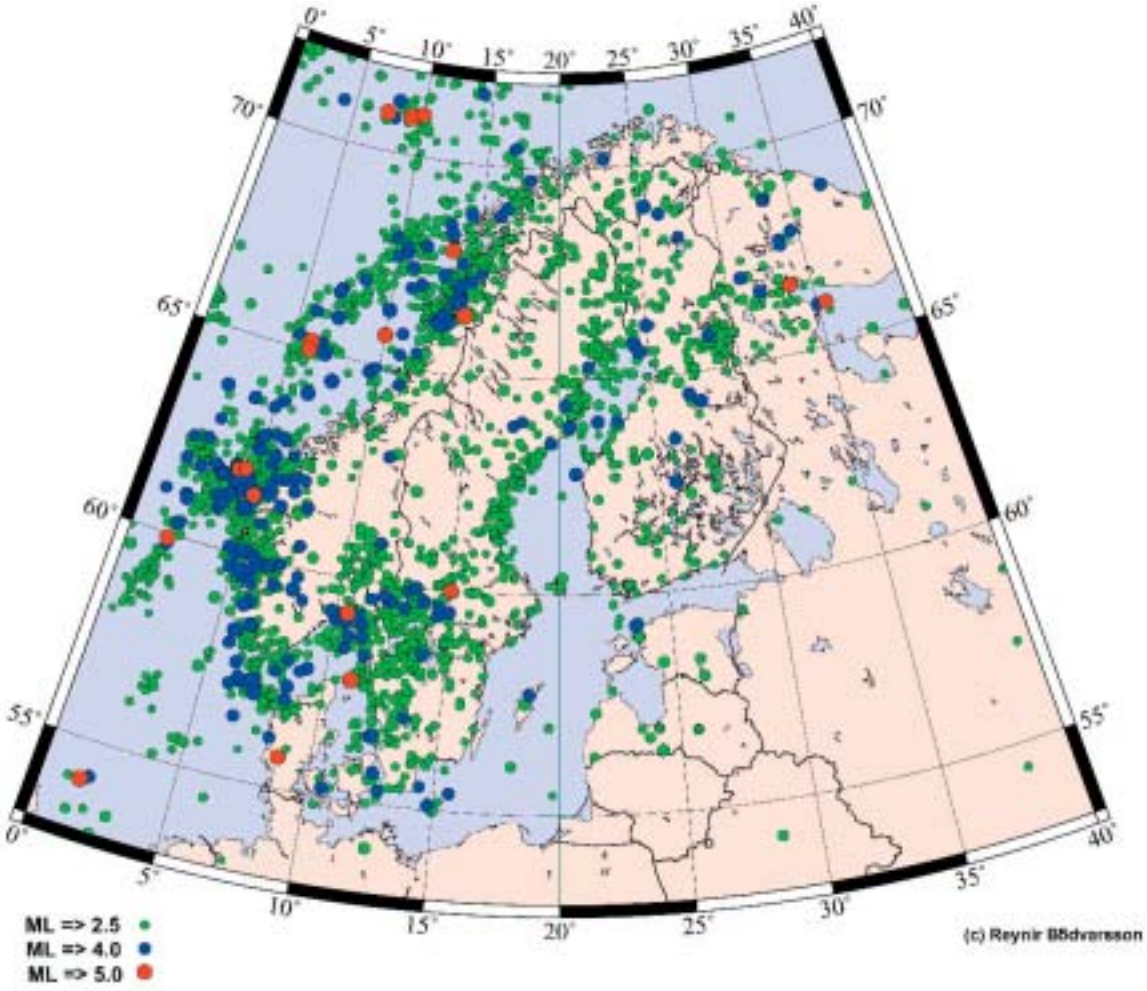

Figure 3-10. *Earthquake epicentra in Scandinavia and Finland 1375–2003. Data from the University of Uppsala*

Table 3-2. Tentative synopsis of the geological evolution in southeastern Sweden with a focus on the Oskarshamn region.

Age (Ma)	Geological event
0.115-0	Glaciation; syn- to post-glacial fault movements?; NW-SE to WNW-ESE maximum horizontal principal stress
95-0	**Alpine orogeny** (central Europe); Final break-up of the supercontinent Pangaea; opening and spreading of the North Atlantic Ocean; *brittle deformation in the cratonic Oskarshamn region as a far-field effect?*
>250	*Latest fault movements at Äspö?* (K-Ar dating of gouge material)
295-60	Tectonic activity in the Tornquist Zone (Fennoscandian border zone); *brittle deformation in the cratonic Oskarshamn region as a far-field effect?*
360-295	**Hercynian-Variscan orogeny** (central Europe). Final assembly of the supercontinent Pangaea; *Brittle deformation in the cratonic Oskarshamn region as a far-field effect?*
420-220	Subsidence related to the development of a Caledonian foreland basin, sedimentation followed by exhumation and erosion; *brittle deformation in the cratonic Oskarshamn region?*
510-400	**Caledonian orogeny**; closure of the Iapetus Ocean; formation of the Scandinavian Caledonides; WNW-ESE shortening (regional compression?) followed by extensional collapse; *brittle deformation in the cratonic Oskarshamn region as a far-field effect of orogenic deformation in western Baltica?*
600-550	Peneplanation; Sub-Cambrian peneplain; Marine transgression and extensive sedimentation
700-600	Final break-up of the supercontinent Rodinia and opening of the Iapetus Ocean; *far-field effect in the cratonic Oskarshamn region?*
900-700	Subsidence related to the development of a Sveconorwegian foreland basin, sedimentation followed by exhumation and erosion; Almesåkra group; Rifting, graben formation, sedimentation in the Vättern area; Visingsö group; *brittle deformation in the cratonic Oskarshamn region?*
1,100-900	**Sveconorwegian orogeny**; formation of the Sveconorwegian Frontal Deformation Zone ("Protogine Zone"); WNW-ESE to E-W regional compression; intrusion of dolerites - E-W extension; Assembly of the supercontinent Rodinia; *Brittle deformation in the cratonic Oskarshamn region as a far-field effect of orogenic reworking of the crust in southwestern Sweden?*
1,460-1,420	**Hallandian orogeny**; *Brittle deformation in the cratonic Oskarshamn region as a far-field effect?*
1,450	Intrusion of granite (e.g. Götemar and Uthammar granites)
1,610-1,560	**Gothian orogeny**; *Brittle deformation in the cratonic Oskarshamn region as a far-field effect?*
1,750-1,700	Transition from ductile to brittle tectonic régime
1,800-1,750	Formation of transpressive, ductile deformation zones in response to c. N-S to NNW-SSE regional compression under low-grade conditions. Deformation zones with NW-SE to WNW-ESE and NE-SW direction display dextral and sinistral horizontal component, respectively.
1,810-1,760	Intense igneous activity; Intrusion of granite-syenitoid-dioritoid-gabbroid ("Småland granite"), composite dykes; Sedimentation and volcanic activity
1,830-1,810	Regional, inhomogeneous deformation under (low)- to medium-grade conditions
1,830-1,820	Intrusion of granitoids; volcanic activity?
1,850(-1,800)	Formation of transpressive, ductile deformation zones with a dextral horizontal component of movement, in response to c. N-S to NNW-SSE regional compression under medium-grade metamorphic conditions; folding of foliation in pre-1,850 Ma rocks
1,850	Intrusion of granite-syenitoid-dioritoid-gabbroid
1,890-1,850	Volcanic activity and sedimentation; regional deformation under medium- to high-grade conditions
1,960-1,750	**Svecokarelian orogeny**

3.2 Overburden including Quaternary deposits

3.2.1 Introduction

This section discusses the Quaternary history of Simpevarp area in a local and regional perspective. A more thorough description is presented in /SKB, 2005/. The Quaternary Period is the present geological period and is characterised by alternating cold glacial and warm interglacial stages. The glacial periods are further subdivided into cold phases, stadials and relatively warm phases, interstadials. A combination of climatic oscillations of high amplitude, together with the intensity of the colder periods, is characteristic of the Quaternary Period. At the Geological Congress in London, 1948 the age of the Tertiary/Quaternary transition, as used here, was determined to be 1.65 million years. More recent research, however, suggests that the Quaternary period started 2.4 million years /e.g. Šibrava, 1992; Shackelton, 1997/. The Quaternary Period is subdivided into two epochs: the Pleistocene and the Holocene. The latter represents the present interglacial, which began c. 11,500 years BP.

Results from studies of deep-sea sediment cores suggest as many as fifty glacial/inter-glacial cycles during the Quaternary /Shackelton et al. 1990/. The climate during the past c. 900,000 years has been characterised by 100,000 years long glacial periods interrupted by interglacials lasting for approximately 10,000–15,000 years. The coldest climate occurred toward the end of each of the glacial periods. Most research indicates that the long-term climate changes (> 10,000 years) are trigged by variations in the earth's orbital parameters. However, there is not universal agreement on this point. Quaternary climatic conditions have been reviewed by e.g. /Morén and Påsse, 2001/.

The most complete stratigraphies used in Quaternary studies are from the well-dated cores from the deep sea that have been used for studies of e.g. oxygen isotopes /e.g. Shackelton et al. 1990/. The marine record has been subdivided into different Marine Isotope Stages (MIS), which are based on changes in the global climatic record. Quaternary stratigraphies from before the Last Glacial Maximum (LGM) from areas that have been repeatedly glaciated, such as Sweden, are sparse. Furthermore, these stratigraphies are often disturbed by erosion and are difficult to date absolutely. Our knowledge of pre-LGM Quaternary history of Sweden is, therefore, to a large extent based on indirect evidence from non-glaciated areas.

In most parts of Sweden, the relief of the bedrock is mainly of Pre-Quaternary age and has only been slightly modified by glacial erosion /Lidmar-Bergström et al. 1997/. The magnitude of the glacial erosion seems to vary considerably geographically. Pre-Quaternary deep weathered bedrock occurs in areas such as the inland of eastern Småland, southern Östergötland and the inner parts of northernmost Sweden /Lundqvist, 1985; Lidmar-Bergström et al. 1997/. Such saprolites indicate that these areas have only been affected to a small extent by glacial erosion.

In some areas, such as in large parts of inner northern Sweden, deposits from older glaciations have been preserved, which indicates that the subsequent glaciations have had a low erosional capacity /e.g. Hättestrand and Stroeven, 2002; Lagerbäck and Robertsson, 1988/.

Saprolites of Pre-Quaternary age occur 50 km west of the Simpevarp regional model area /Lidmar-Bergström et al. 1997/. Also the occurrence of such "old" deposits in the regional model area cannot be excluded.

3.2.2 The Pleistocene

The preserved geological information from the early Quaternary in Sweden is, as mentioned above, fragmentary. However, inorganic deposits such as glacial till have not been dated with absolute methods and deposits from early stages of the Quaternary Period may therefore exist. Although, as mentioned above, the oxygen isotope record indicates numerous glaciations it is impossible to state the number of glaciations reaching as far south as the Simpevarp area.

There are traces of three large glaciations, the Elster (MIS 8), Saale (MIS 6) and Weichsel (MIS 2–5d), that reached northern Poland and Germany. /e.g. Fredén, 2002/. The Saale had the largest maximum extension of any known Quaternary ice sheet. There were two interstadials, the Holstein and Eem, between theses three glacials.

The oldest Quaternary deposit in Sweden, dated by fossil composition, was probably deposited during the Holstein interglacial (MIS 7, c. 230,000 years ago) /e.g. Ambrosiani Garcia, 1990/. The till underlying the Holsteinian deposits is the oldest known Quaternary deposit in Sweden.

Deposits from the interglacial Eem (MIS 5e, 130,000–115,000 years ago) are known from several widely spread places in Sweden /e.g. Robertsson et al. 1997/. The climate was periodically milder than it has been during the present interglacial, Holocene. It is likely that the Simpevarp regional model area was covered by brackish water during large parts of the Eem interglacial.

3.2.3 The latest glaciation

The latest glacial, the Weichsel, started c. 115,000 years ago. It was characterised by colder phases, stadials, interrupted by milder interstadials. The model presented by e.g. /Fredén, 2002/ and /Lundqvist, 1992/ is often used to illustrate the history of Weichsel (Figure 3-11). Two interstadials took place during the early part of Weichsel, approximately 100,000–90,000 (MIS 5c)

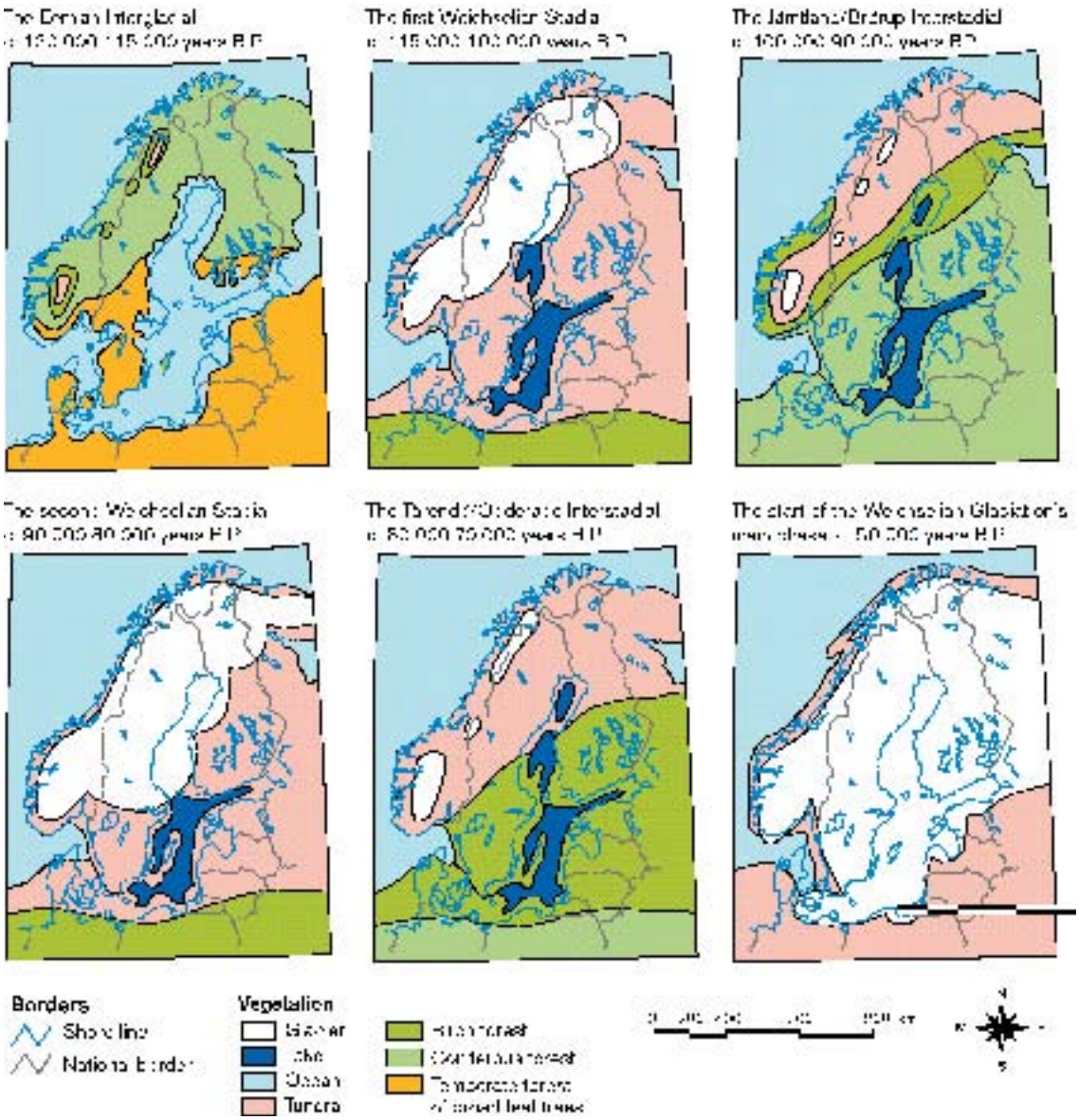

Figure 3-11. *The development of vegetation and ice cover in northern Europe during the latest interglacial (Eem) and first half of the latest ice age (Weichsel). The maps should be regarded as hypothetical due to the lack of well dated deposits from the different stages (from: Sveriges Nationalatlas, www.sna.se).*

and 80,000–70,000 years ago (MIS 5a). Most of Sweden was free of ice during these interstadials, but the climate was considerably colder than today and tundra conditions probably characterised northern Sweden. The ice did not reach further south than the Mälaren Valley during the Early Weichselian stadials. The ice advanced south and covered the Simpevarp area first during the Mid Weichselian (c. 70,000 years ago).

Most of Sweden, including Simpevarp, was then covered by ice until the deglaciation at around 14,000 years BP. The accuracy of the model presented by /Fredén, 2002/ and /Lundqvist, 1992/ has been questioned. Most researchers agree that at least two interstadials, with ice-free conditions, did occur during the Weichselian glaciation. However, since the dating of such old deposits is problematic, the timing of these interstadials is uncertain. Investigations from both Finland and Norway suggest that most of the Nordic countries were free of ice during parts of Mid Weichselian (MIS 3–4) /e.g. Olsen et al. 1996; Ukkonen et al. 1999/. That may imply that one of the interstadials attributed to Early Weichselian by /Fredén, 2002/ may have occurred during Mid Weichsel. In Simpevarp, the total time of ice cover during Weichsel may therefore have been considerably shorter than previously has been thought.

Continental ice reached its maximum extent c. 20,000 years ago (MIS 2), cf. Figure 3-12. The Weichselian ice reached as far south as the present Berlin, but had a smaller maximal extent than the two preceding glacials (Saale and Elster). According to mathematical and glaciological models, the maximum thickness of the ice cover in the Oskarshamn region was more than 1.5 km at 18,000 years BP /Näslund et al. 2003/. Glacial *striae* on bedrock outcrops as well as the orientation of eskers indicate a main ice movement direction from NW-NNW in the Simpevarp region. Subordinate older *striae* indicate more westerly and northerly directions.

3.2.4 Deglaciation

A marked improvement in climate took place about 18,000 years ago and the ice started to melt a process that was completed after some 10,000 years. The deglaciation of southeastern Sweden has been studied by using clay-varve chronologies /Kristiansson, 1986; Ringberg et al. 2002/.

The timing of the deglaciation of Sweden has been dated using several methods. These dates have recently been calibrated to calendar years /e.g. Fredén, 2002; Lundqvist and Wohlfarth, 2001/. According to the calibrated clay-varve chronology, the Oskarshamn area was deglaciated almost 14,000 years ago /Lundqvist and Wohlfarth, 2001/. The velocity of the retreat of the ice margin was c. 125–300 m/year /Kristiansson, 1986/.

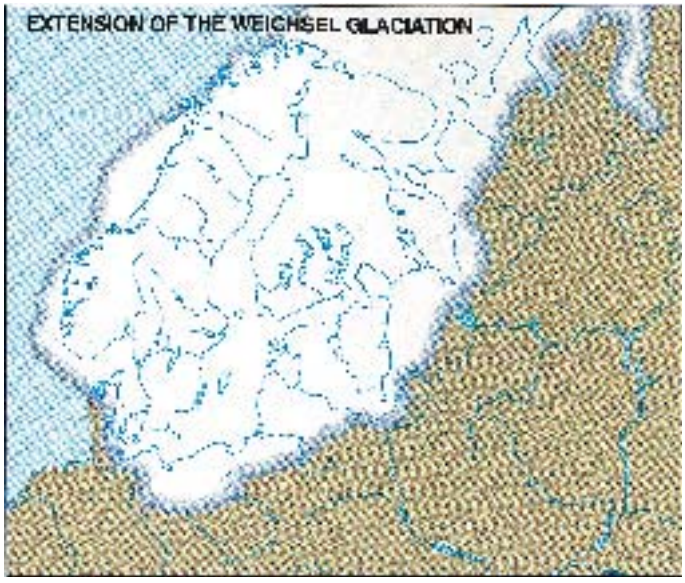

Figure 3-12. *The maximum extent of the Weichselian ice sheet approximately 20,000 years ago (from: Sveriges Nationalatlas, www.sna.se).*

3.2.5 Climate and vegetation after the latest deglaciation

Pollen investigations from southern Sweden have shown that a sparse *Betula* (birch) forest covered the area soon after the deglaciation /e.g. Björck, 1999/. There was a decrease in temperature during a cold period called Younger Dryas (c. 13,000–11,500 years ago) and the deglaciated parts of Sweden were consequently covered by a herb tundra. At the beginning of Holocene c. 11,500 years ago, the temperature increased and southern Sweden was first covered by forests dominated *Betula* and later by forests dominated by *Pinus* (pine) and *Corylus (*hazel*)*. The timing and climatic development of the transition between Pleistocene and Holocene has been discussed by e.g. /Björck et al. 1996/ and /Andrén et al. 1999/.

Between 9,000 and 6,000 years ago the the summer temperature was approximately 2° warmer than at present and forests with *Tilia (*lime*)*, *Quercus (*oak*)* and *Ulmus* (elm) covered large parts of southern Sweden. The temperature has subsequently decreased, after this warm period, and the forests became successively more dominated by coniferous trees. The ecological history of Sweden during the last 15,000 years has been reviewed by e.g. /Berglund et al. 1996/.

3.2.6 Development of the Baltic Sea after the latest deglaciation

A major crustal phenomenon that has affected and continues to affect northern Europe, following the latest melting of continental ice, is the interplay between isostatic recovery on the one hand and eustatic sea level variations on the other. During the latest glaciation, the global sea level was in the order of 120 m lower than at present /Fairbanks, 1989/.

In northern Sweden, the heavy continental ice depressed the Earth's crust by as much as 800 m below its present altitude. As soon as the pressure started to decrease, due to the deglaciation, the crust started to rise (isostatic land uplift). The highest identified traces of the shoreline are at different altitudes throughout Sweden depending on how much the crust had been depressed. The highest shoreline in the Oskarshamn region is c. 100 m above sea level /Agrell, 1976/, and, thus the whole Simpevarp regional model area is situated below the highest shoreline.

The development of the Baltic Sea since the last deglaciation is characterised by changes in salinity and its history has therefore been divided in four main stages /Björck, 1995; Fredén, 2002/, which are summarised in Table 3-3. The most saline period occurred 6,000–5,000 years ago when the surface water salinity was 10–15‰ compared with approximately 7‰ today /Westman et al. 1999/.

Along the southern part of the Swedish east coast, the isostatic component was less and declined earlier during the Holocene, resulting in a complex shore line displacement with alternating transgressive and regressive phases. In the Simpevarp region, shoreline regression has prevailed and the rate of land uplift during the last 100 years has been c. 1 mm/year /Ekman, 1996/.

The estimated shore line displacement since the last deglaciation has been reviewed and modified by /Påsse, 1997, 2001/ (Figure 3-13). Påsse's curve is similar to a curve presented by /Svensson, 1989/, who undertook stratigraphical investigations in the Oskarshamn area. However, according to /Svensson, 1989/, the shoreline dropped instantaneously c. 20 m due to drainage of the Baltic Ice Lake 11,500 years ago. Påsse, on the other hand, suggests a fast isostatic shoreline displacement at that time. The ^{14}C method does not have accuracy enough to tell if the drainage did occur or if the fast shoreline displacement during that time was caused by a fast isostatic rebound. Påsse's curve (Figure 3-13) shows that the shoreline displacement has been regressive for most of the time since the deglaciation. There were, however, two transgressive periods, 10,000 years ago in the Ancylus Lake phase and 7,000 years ago in the Littorina Sea phase, cf. Table 3-3.

Table 3-3. The four main stages of the Baltic Sea.

Baltic stage	Calender year BP	Salinity
Baltic Ice Lake	15,000–11,550	Glacio-lacustrine
Yoldia Sea	11,500–10,800	Lacustrine/Brackish/Lacustrine
Ancylus Lake	10,800–9,500	Lacustrine
Littorina Sea *sensu lato*	9,500–present	Brackish

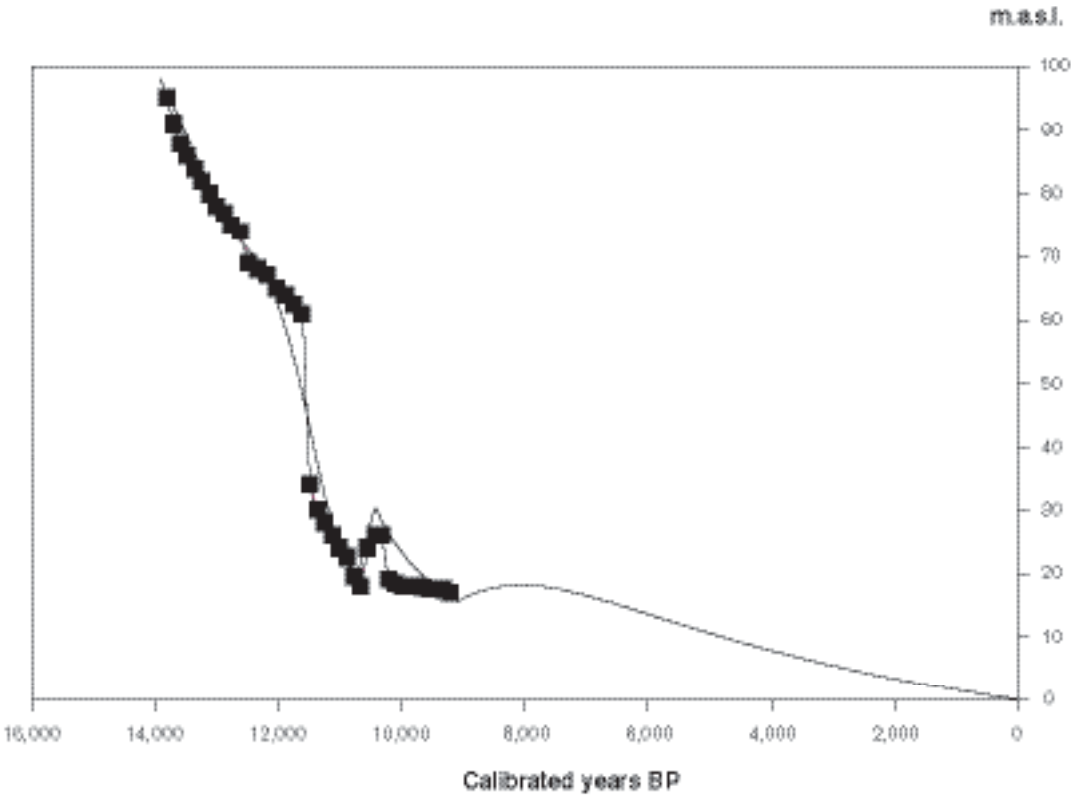

Figure 3-13. *The shore line displacement in the Oskarshamn area after the latest deglaciation. The blue symbols show a curve established by /Svensson, 1989/ after a study of lake sediments in the region. The curve without symbols has been calculated by the use of a mathematical model /Påsse, 2001/.*

/Risberg, 2002/ has studied a five meter long sediment core from Borholmsfjärden south of Äspö. The core comprises two main sediment sequences, the first accumulated in the Yoldia Sea (11,500–10,800 years ago) and the second during the last 3,000 years. As the site was exposed to the sea, there was no accumulation of sediment between the time of the Yoldia Sea and 3,000 years ago, The islands surrounding Borholmsfjärden emerged from the sea some 3,000 years ago, which caused more sheltered conditions and the onset of sedimentation.

3.3 Premises for surface water and groundwater evolution

3.3.1 Premises for surface and groundwater evolution

The first step in the groundwater evaluation is to construct a conceptual postglacial scenario model for the site (Figure 3-14) based largely on known palaeohydrogeological events from Quaternary geological investigations. This model can be helpful when evaluating data since it provides constraints on the possible groundwater types that may occur. Interpretation of the glacial/postglacial events that might have affected the Simpevarp area is based on information from various sources including /Fredén, 2002; Påsse, 2001; Westman et al. 1999/ and /SKB, 2002b/. This recent literature provides background information which is combined with more than 10 years of studies of groundwater chemical and isotopic information from sites in Sweden and Finland in combination with various hydrogeological modelling exercises of the postglacial hydrogeological events /Laaksoharju and Wallin, 1997; Luukkonen, 2001; Pitkänen et al. 1998; Svensson, 1996/. The presented model is therefore based on Quaternary geological facts, fracture mineralogical investigations and groundwater observations. These facts have been used to describe possible palaeo events that may have affected the groundwater composition in the bedrock.

3.3.2 Development of permafrost and saline water

When the continental ice sheet was formed at about 100,000 BP permafrost formation ahead of the advancing ice sheet probably extended to depths of several hundred metres. According to /Bein and Arad, 1992/ the formation of permafrost in a brackish lake or sea environment (e.g. similar to the Baltic Sea) produced a layer of highly concentrated salinity ahead of the advancing freezing front. Since this saline water would be of high density, it would subsequently sink to lower depths and potentially penetrate into the bedrock where it would eventually mix with formational groundwaters of similar density. Where the bedrock was not covered by brackish lake or sea water similar freeze-out processes would occur on a smaller scale within the hydraulically active fractures and fracture zones, again resulting in formation of a high-density saline component which would gradually sink and eventually mix with existing saline groundwaters. Whether the volume of high salinity water produced from brackish waters by this freeze-out process would be adequate to produce such widespread effects is presently under debate.

With continued evolution and movement of the ice sheet, areas previously subjected to permafrost would be eventually become covered by ice accompanied by a rise in temperature and slow decay of the underlying permafrost layer. Hydrogeochemically, this decay may have resulted in distinctive signatures being imparted to the groundwater and fracture minerals.

3.3.3 Deglaciation and flushing by meltwater

During subsequent melting and retreat of the ice sheet the following sequence of events is thought to have influenced the Simpevarp area (see Figure 3-14).

During the recession and melting of the continental ice sheet, glacial meltwater was hydraulically injected into the bedrock (> 14,000 BP) under considerable head pressure close to the ice margin. The exact penetration depth is still unknown, but depths exceeding several hundred metres are possible according to hydrodynamic modelling /e.g. Svensson, 1996/. Some of the permafrost decay groundwater signatures may have been disturbed or destroyed during this stage.

Different non-saline and brackish lake/sea stages then transgressed the Simpevarp area during the period c. 14,000–4,000 BP. Of these, two periods with brackish water can be recognised; Yoldia Sea (11,500 to 10,800 BP) and Littorina Sea starting at 9,500 and continuing to the present. The Yoldia period has probably resulted in only minor contributions to the subsurface groundwater since the water was very dilute to brackish because of the large volumes of glacial meltwater it contained. Furthermore, this period lasted only for 700 years. The Littorina Sea period in contrast had a maximum salinity of about twice that of the present Baltic Sea and this maximum prevailed at least from 6,500 to 5,000 BP; during the last 2,000 years the salinity has remained almost equal to the present Baltic Sea values /Westman et al. 1999 and references therein/. Because of increased density, the Littorina Sea water was able to penetrate the bedrock resulting in a density turnover which affected the groundwater in the more conductive parts of the bedrock. The density of the intruding seawater in relation to the density of the groundwater determined the final penetration depth. As the Littorina Sea stage contained the most saline groundwater, it is assumed to have had the deepest penetration depth, eventually mixing with the glacial/brine groundwater mixtures already present in the bedrock.

When the Simpevarp region was subsequently raised above sea level 5,000 to 4,000 years ago, fresh meteoric recharge water formed a lens on top of the saline water because of its low density. However, local hydraulic gradients resulting from higher topography to the west of the Simpevarp area may have flushed out varying amounts of these older waters, at least to depths of 100–150 m, with the freshwater lens mostly occupying these depths today depending on local hydraulic conditions.

Many of the natural events described above may in the future be repeated several times during the lifespan of a repository (thousands to hundreds of thousands of years). As a result of these events, brine, glacial, marine and meteoric waters are expected to be mixed in a complex manner at various levels in the bedrock, depending on the hydraulic character of the fracture zones, groundwater density variations and borehole activities prior to groundwater sampling. For the modelling exercise which is based on the conceptual model of the site, groundwater end members reflecting, for example, Glacial meltwater and Littorina Sea water composition, were added to the data set /cf. Appendix 5 in Laaksoharju et al. 2004b/.

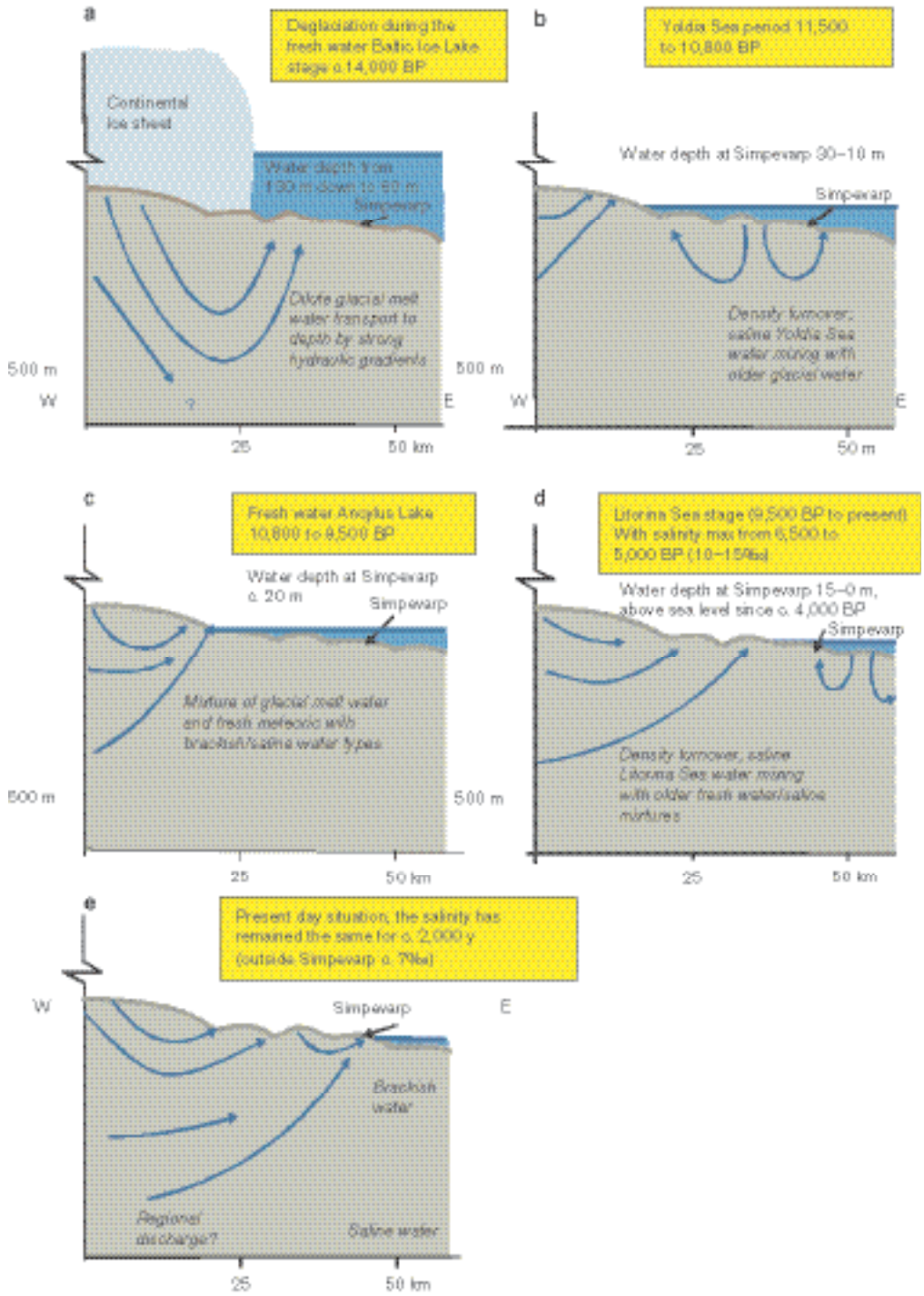

Figure 3-14. *Conceptual postglacial scenario model for the Simpevarp area. The figures show possible flow lines, density driven turnover events and non-saline, brackish and saline water interfaces. Possible relation to different known postglacial stages such as land uplift which may have affected the hydrochemical evolution of the site is shown: a) deglaciation of the continental ice, b) Yoldia Sea stage, c) Ancylus Lake stage, d) Littorina Sea stage, and e) present day Baltic Sea stage. From this conceptual model it is expected that glacial melt water and deep and marine water of various salinities have affected the present groundwater. Based on the shoreline displacement curve compiled by /Påsse, 2001/ and information from /Fredén, 2002; Westman et al. 1999/ and /SKB, 2002b/.*

The uncertainty of the updated conceptual model increases with modelled time. The largest uncertainties are therefore associated with the stage showing the flushing of glacial melt water. The driving mechanism behind the flow lines in Figure 3-14 is the shore level displacement due to the land uplift.

3.4 Development of surface ecosystems

In this section, some illustrative results from the region are presented. For further details see /Jansson et al. 2004/ or /SKB, 2005/.

Data sources used include historical maps, cadastral material, interviews and field work. The investigated areas in the Simpevarp area consist of parishes. This is due to the fact that most of the sources for historical periods are organised in parishes. It is also a level that enables us to study local human activities, e.g. follow the use of forests in the context of a village.

3.4.1 Population

In the year 1571, the estimated population in the three investigated parishes in Småland was c. 1,266 persons. The population growth was quite moderate in the parishes of Misterhult, Döderhult and Kristdala until the middle of the 18th century. However, after c. 1800, there was rapid population growth, especially in Döderhult. Kristdala and Misterhult showed a quite similar population trend, although Misterhult's population size generally was larger. Döderhult follow the same trend as Kristdala and Misterhult, until c. 1865, when a very high rate of population growth began in Döderhult and lasted until c. 1900. This peak might be explained by the fact that the town of Oskarshamn was established in 1856. During the 20th century there has been a negative population trend in the three investigated parishes. After 1960, the trend has turned into a population growth in Döderhult, and the same thing happened in Misterhult after 1980. In 1990, the population size was calculated to 10,640 persons in Misterhult, Döderhult and Kristdala, taken together.

3.4.2 Farms and land use

The number of farms has changed over the years in Småland. In Döderhult nearly 50% of the settlement units were wholly or partially deserted in 1631 according to the cadastral book of the same year. In Kristdala, the deserted farms reached c. 17% and in Misterhult c. 22% of the farmsteads were deserted at this time. A possible explanation for this can perhaps be found in the expensive Swedish wars that had a great impact on the population.

In Oskarshamn, the changes in the landscape were dramatic between 1940 and 1980. About 74 million square metres of arable land were abandoned over that interval. According to the calculations, only 3.8 million new square metres were ploughed in 1980. Of the original 114 million square metres of arable in 1940, only 41 million remained in 1980. If we study the changes spatially, we can detect that some areas were more affected than others. A lot of the smaller fields have been completely abandoned.

During the 18th and 19th century, the arable land and meadows increased. This was particularly true of the number of meadows. Drained wetlands in the woods were now used as meadows. At the same time the old meadows, near the settlements, were transformed into arable land. The increase of the population and the increase of the number of farms during the period may partly explain this. Another explanation may be that fishery and incomes from the sea decreased in relation to other incomes and agriculture increased as the source for incomes at the same time.

In the mid-18th century enclosure (Swe. *laga skifte*) took place in Ekerum and Lilla Laxemar. At that time, the number of farms in the area had increased and the arable land had increased even more. A consequence of the enclosure in Ekerum and Lilla Laxemar was that some farms were forced to move from the former toft of the villages. Another direct consequence of enclosure was the establishment of the boundaries of the properties. From that time, all the farms in the area were single farms, managing their lands on their own.

4 The surface system

This chapter constitutes a description of the work that has been performed within the site modelling for Simpevarp 1.2 concerning the surface system, i.e. meteorology, overburden characterisation, hydrology, hydrochemistry, oceanography, biota and development of ecosystem models. A comprehensive surface description is reported separately in /Lindborg, 2005/ and the modelling and description strategy in /Löfgren and Lindborg, 2003/.

The surface system starts where the deep bedrock ends, except were the bedrock reaches the surface and thereby becomes a part of the surface system as outcrops, and extends to the atmosphere which affects the site, e.g. through the climate. This means that a number of different disciplines are represented in covering discipline specific patterns and processes at various spatial and temporal scales. Each discipline-specific description (e.g hydrology should be considered independent aiming at a deepened understanding of the patterns and processes at the site.

In the end of this chapter, three descriptive ecosystem models are presented, describing terrestrial, limnic and marine environments. The overall aim of the ecosystem modelling is to describe the carbon cycle for the different environments. This is done in two steps; 1) a conceptual model is presented for the three environments, 2) site specific quantitative data are used to create carbon budgets for the terrestrial part of a discharge area, a lake and three marine basins. These descriptive ecosystem models use data from a number of disciplines e.g. overburden characterisation (Quarterary deposits), hydrology, biota etc., that have been presented in the previous sections within the surface ecosystem description. These carbon budgets will be one important tool to estimate and predict flows and accumulations of matter at a landscape scale (regional or sub regional) in the subsequent safety assessment.

The overall aim of the modelling is to produce a detailed description of the present conditions at the site. However, it is equally important to know the history of the studied site, not only to understand the present patterns, but also to be able make predictions about future conditions.

4.1 State of knowledge at previous model version

In the Simpevarp 1.1 site-descriptive model, the modelling of the abiotic components of the surface system was included in the discipline-specific geological, hydrogeological and hydrogeochemical modelling. In addition, an integrated description of the surface system was provided in Chapter 7 of the Simpevarp 1.1 report /SKB, 2004b/. The site data available for the descriptions of the abiotic components were quite limited. The geology of the Quaternary deposits was described based on the detailed map of the Quaternary deposits within the Simpevarp subarea, and available data from soil drillings within the Simpevarp subarea. The descriptions of surface hydrology and oceanography were based on regional (version 0) data only, and as no hydraulic tests in the Quaternary deposits had been performed the hydrology model was based on literature data.

The Simpevarp 1.1 description of the biotic components of the surface system included a vegetation map over the regional model area, results of biomass and production calculations for different vegetation types, some data on aquatic producers, and a description, to large extent based on generic data, of terrestrial and aquatic consumers. In addition, an assessment of the available information on humans and land use was provided. No quantitative ecosystem models were presented in the Simpevarp.1.1 site-descriptive model .

4.2 Evaluation of primary data

A complete list of abiotic and biotic data from the surface system available for use in Simpevarp 1.2 is found in Tables 2-7 and 2-8.

4.2.1 Overburden including Quaternary deposits

The overburden model is based on results from field mapping in both the Simpevarp subarea and also larger parts of the sea floor in the Simpevarp regional scale model area (Table 2-7). Most of the interpretations of the overburden in the remaining parts of the Simpevarp regional model area are based on geophysics (mainly helicopter-borne) and other types of old information, often with uncertain geographical references (Table 2-7). The uppermost part of the overburden, the soil, has, however, been carefully described at 20 selected sites distributed over the regional model area. The readers are referred to /Lindborg, 2005/ for a thorough description of the data used in the description of the overburden in the Simpevarp regional model area. The terrain relief was modelled by interpolation of elevation data creating a DEM (digital elevation model) /Brydsten, 2004/.

4.2.2 Climate, hydrology and hydrogeology

As the Simpevarp version 0 model /SKB, 2002b/ was developed before commencing the site investigations in the Simpevarp area, it was based on information from the feasibility study /SKB, 2000a/, selected sources of "old" data, and additional data collected and compiled during the preparatory work for the site investigations. The investigations that provided the basis for Simpevarp 1.1 in terms of climate, surface hydrology, and near-surface hydrogeology included airborne photography, airborne and surface geophysical investigations, and mapping of Quaternary deposits. In addition, monitoring boreholes were established in the overburden in conjunction to drill sites. The limited amount of site-specific data implied that Simpevarp 1.1 was based mostly on regional and/or generic meteorological, hydrological and hydrogeological data.

Meteorological, hydrological and hydrogeological investigations

Between the Simpevarp 1.1 and 1.2 data freezes, the additional meteorological, surface hydrological and near-surface hydrogeological investigations comprised the following major components:

- Establishment of one local meteorological station on the island of Äspö.
- Delineation and description of catchment areas, water courses and lakes.
- Establishment of local surface-hydrological stations for discharge measurements.
- "Simple" discharge measurements in water courses.
- Drilling and hydraulic tests (slug tests) performed in groundwater monitoring wells.
- Manual groundwater level measurements.

These investigations and available data are summarised in Table 2-7.

Other investigations contributing to the modelling

In addition to the reports on investigations listed in Table 2-7, the Simpevarp 1.2 modelling is based on data from the official SKB databases as well as data used and/or listed in the Simpevarp version 0 and Simpevarp 1.1 reports /SKB, 2002b, 2004b/. In particular, the following SKB databases are used in the Simpevarp 1.2 modelling:

- Topographical and other geometrical data.
- Data from surface-based geological investigations.
- Data from investigations in boreholes in Quaternary deposits.
- Data on the hydrogeological properties of the bedrock.

Summary of available data

Table 2-7 provides references to site investigations and other reports that contain meteorological, hydrological and hydrogeological data used in the Simpevarp 1.2 modelling. The table also provides the corresponding information with respect to other disciplines or types of investigations.

4.2.3 Chemistry

A comprehensive description of the chemical properties in surface ecosystems will eventually include a wide array of parameters (concentrations of elements and compounds) and processes, varying both in time and space in several different media. Water is by far the most important medium for transport, and the site investigations concerning hydrogeochemical properties in the surface system have so far concentrated on obtaining analyses of samples from surface water and near-surface groundwater. The site investigation programme for 2005 is planned to include analyses of chemical properties also in the overburden and in biota. No new information concerning chemical properties of precipitation or atmospheric deposition in the Simpevarp area is available for the current version of the site descriptive model.

The results presented in this chapter represent only a part of the total data produced within the programme, and the aim is mainly to give a first characterisation and understanding of the site-specific data. The surface water sampling programme is described in detail in /Ericsson and Engdahl 2004a,b/, together with a compilation of primary data from the first year of sampling. For the current modelling, all available data at the Simpevarp 1.2 data freeze have been included in the analyses, unless an explicit statement to the contrary is made. However, since no thorough evaluation of the surface water chemistry in the regional model area has been performed yet, some of the results presented here rely on the report by /Ericsson and Engdahl, 2004a/.

4.2.4 Biota

Terrestrial producers

The descriptive model contains a large number of components that describe biomass, NPP (Net Primary Production) and turnover of plant tissues. For information about the site specificity of the data, where it is published and some information about the method used to estimate/calculate results, see /Lindborg, 2005/. The sources from where the data are taken are also shown in Table 2-8.

Terrestrial consumers

Site-specific data and generic data obtained from different reports are listed in Table 2-8. Other data used, such as weight figures for many species and consumption data, have been gathered from Internet sites, such as Svenska Jägareförbundet (Swedish Association for Hunting and Wildlife Management), Jägarnas Riksförbund (The National Association of Huntsmen), BBC-Nature wildfacts, and the Mammal Society. The production figures have been calculated very roughly and are therefore associated with uncertainties.

Limnic producers

The Simpevarp area contains relatively few lakes. In total six lakes, situated partly or entirely within the regional model area, have been investigated for habitat characterisation during the site investigations, and for some lakes there are also other biotic data. Many of the data has been collected during 2004, and the results from some of the investigations have not been reported yet. The most comprehensive dataset available at the time of the data freeze concerning limnic biota in the area is from Lake Frisksjön, and the current description will give an account of data only from Lake Frisksjön. Future versions of the surface description will compile all available data also from the other lakes, as well as from streams in the area.

In the habitat characterisation, the borders between different habitats within the lakes have been defined /Brunberg et al. 2004/. Phytoplankton data from three sampling occasions (July 2003, December and April 2004) in lake Frisksjön 2003–2004 were available at the time of the data freeze /Sundberg et al. 2004/.

Limnic consumers

Zooplankton data from three sampling occasions (July 2003, December 2003 and April 2004) in lake Frisksjön were available /Sundberg et al. 2004/. Benthic macroinvertebrates have been investigated in two watercourses and four lakes in the Simpevarp area /Ericsson and Engdahl, 2004c/, while fish data have been collected for four lakes in the area (Lake Jämsen, Lake Söråmagasinet, Lake Frisksjön and Lake Plittorpsgöl) in August 2004 /Engdahl and Ericsson, 2004/, cf. Figure 4-3. Here, only an account of data from Lake Frisksjön is provided.

Marine producers

Data from six site-specific studies were used for the description of primary producers (Table 2-8). All studies were a part of the ongoing site investigation programme.

The major source for the description of the shallow parts of the marine environment was the vegetation map presented by /Fredriksson and Tobiasson, 2003/. This map is based on three different data sets: (i) a general survey of 1,280 discrete sites with recordings of dominant macrophytes and coverage, (ii) twenty diving transects and (iii) 40 video recordings and data from the nautical charts. The map was drawn by hand and its accuracy is considered to be dependent on the density of observations. Generally, there is a higher density of observations in the inner bays and coastal areas and lower in the offshore area. The site observations and diving transects present data as "degree of coverage", i.e. the percentage of the sea bottom that is covered by macrophytes of a certain type. Data on phytoplankton presented by /Sundberg et al. 2004/ were used as temporal averages from three sampling occasions (December 2003, April and June 2004) in four areas. Data were presented per taxon (or species) and in dry weight per litre. The sampling sites were the same as those used for water chemistry samples taken during the year 2002.

Marine consumers

Data from five site-specific studies were used for the description of the consumers (Table 2-8). All studies were part of the site investigation programme.

There are two main sources of biomass data used in the descriptions: (i) the vegetation mapping study by /Fredriksson and Tobiasson, 2003/ where epifauna associated with the vegetation were sampled, and (ii) a study of the soft bottom fauna by /Fredriksson, 2004/. The quantitative data presented in these reports, i.e. biomass per unit biomass of vegetation (g dry weight per 100 g dry weight) and biomass per unit area (g dry weight per m^2), respectively, were used to calculate the total biomass per functional group and basin. The species were grouped into functional groups according to the classification given in /Kautsky, 1995/. The soft bottom fauna was sampled in 40 locations, and the result was presented per habitat, either vegetation community or bare sediment in archipelago (inshore) or offshore.

4.2.5 Humans and land use

In order to arrive at an overall assessment of the human population and human activities in the model area, a wide range of different human-related statistics were acquired from Statistics Sweden. These statistics include data and times series on demography, labour, health situation, land use, agriculture etc. Beside this, some additional information was searched for and acquired from other sources, such as the National Board of Fisheries, the Swedish Association for Hunting and Wildlife Management, the County Administrative Board. A detailed presentation of the data and results is given in /Miliander et al. 2004/.

4.3 Model of the overburden including Quaternary deposits

4.3.1 Background

The aim of the data evaluation presented in this section is to construct models of the surface and stratigraphical distribution of the overburden in the Simpevarp regional scale model area. However, the present data set only provide detailed information from the Simpevarp subarea and the remainder of the Simpevarp regional model area (including the Laxemar subarea) will therefore have to be more thoroughly analysed and discussed in conjunction with future model versions (after the data freeze for version Laxemar 1.2).

The overburden includes marine and lacustrine sediments and peat. Knowledge of the composition of the overburden is of crucial importance for the understanding of the hydrological, chemical and biological processes taking place in the uppermost part of the geosphere. The overburden is sometimes, for convenience, referred to as Quaternary deposits in the following text.

The topmost part of the overburden is referred to as soil. Soils are formed as a consequence of interactions between the overburden, ambient climate, hydrology and biota over timescales of hundreds to thousands of years. Different types of soils are characterised by horizons with typical chemical and physical properties. It often takes many thousands of years for soil horizons to form. The properties of the soils are of crucial importance for the composition and richness of the vegetation. In Sweden, the soils formed after the latest deglaciation, which is a relatively short period of time for soil formation. At the lowest altitudes in the Simpevarp area the time available for soil-forming processes has been even shorter, since these areas have quite recently been raised above the sea level.

4.3.2 The surface distribution and stratigraphy of Quaternary deposits

All known Quaternary deposits in the Simpevarp regional model area were formed during, or after, the latest glaciation. The oldest deposits are of glacial origin and have been deposited either directly by the ice, or by water from the melting ice. The whole regional model area is located below the highest coastline and fine-grained water-laid glacial and post-glacial sediments have been deposited in sheltered localities. In more exposed positions, the overburden has been partly eroded and redeposited by waves and streams when the water depth became shallower, as a consequence of the isostatic land uplift. The Simpevarp regional model area, in its present state, is a relatively flat area with a coastline highly exposed to the Baltic Sea. Isostatic land uplift is still an active process (1 mm yr^{-1}) and coastal processes are continuously changing the properties and distribution of the overburden. Accumulation of gyttja clay is an ongoing process in the present narrow bays along the coast. For a more detailed account of the present knowledge of Quaternary deposits in the Simpevarp regional model area the reader is referred to /Lindborg, 2005/.

A relatively large part of the Simpevarp subarea (Figure 4-1) is characterised by exposed bedrock. The areas situated at the highest altitudes are almost entirely characterised by exposed bedrock. There are probably several reasons for the relatively low coverage of Quaternary deposits in this area. One reason may be that a relatively small amount of glacial till was deposited in the area during the latest ice age. Another reason is that large parts of the investigated area are exposed towards the open Baltic Sea. This condition has caused erosion and redeposition of overburden by waves and streams.

Glacial till is the oldest known component of the overburden in the area and was deposited directly by glaciers during Quaternary. It may be assumed, but not concluded, that most of the till in the regional model area was deposited during the latest glaciation and rests directly on the bedrock surface. Till is the dominant Quaternary deposit and covers about 35% of the Simpevarp subarea (cf. Table 4-1). The morphology of the till in the subarea normally reflects the morphology of the bedrock surface. The thickness of the till varies between 0.5 and 4 m in the Simpevarp subarea. Most of the till has a sandy matrix, but gravelly till also occurs.

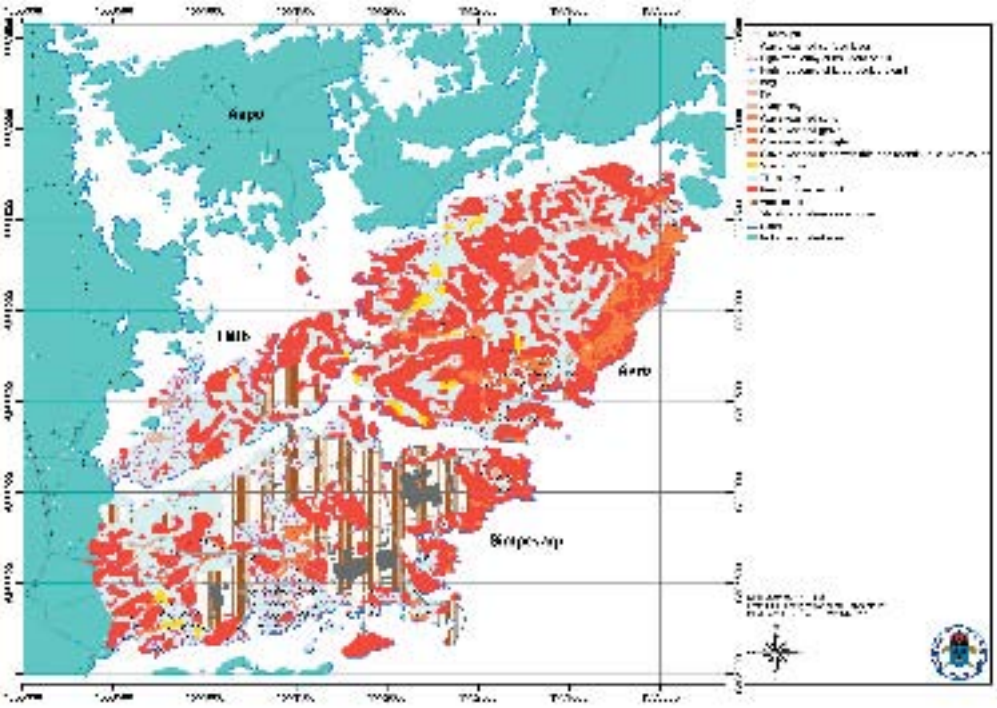

Figure 4-1. *The superficial distribution of Quaternary deposits and bedrock exposures in the Simpevarp subarea. Areas with a wave-washed surface layer and the superficial boulder frequency of the till are also shown. The map has been produced at the scale 1:10,000 and shows deposits with an area larger than 10×10 metres.*

Table 4-1. The proportional surface distribution of Quaternary deposits and exposed bedrock in the terrestrial part of the Simpevarp subarea /from Rudmark, 2004/.

Quaternary deposit	Coverage (%)
Peat	1.89
Gyttja sediment	0.05
Glacial clay	1.06
Postglacial sand and gravel	5.80
Glacial till	35.04
Man-made fill	17.93
Precambrian bedrock	38.22

The distribution of bedrock and fine-grained deposits in the Laxemar subarea and its surroundings are shown in /Lindborg, 2005/. Areas in-between the two surveyed subareas are probably dominated by till (white areas on the map). An old map of Quaternary deposits in the whole regional model area /Lindborg, 2005/, indicates that there is a more coherent till coverage in the south-western and western part of the regional model area. The marine geological map indicates that only a small fraction of the seafloor is covered by till (Figure 4-2). It is, however, possible that the till areas were underestimated in those investigations.

Glaciofluvial deposits are restricted to the western and northern parts of the regional model area. These deposits may have hydrological importance and will be a focus for studies during the forthcoming investigations. Special focus will be put on studying the properties and extension of a glaciofluvial deposit found in the northern part of the Laxemar subarea.

Peat covers c. 2% of the Simpevarp subarea and is restricted to some of the narrower valleys. The peat is often found in mires, which are distinguished into two types: bogs and fens. The bogs are poorer in nutrients than the fens. Fen peat is the most common peat type in the Simpevarp subarea. There are, however, a number of small, but not raised, bogs, which often occur in depressions in areas dominated by exposed bedrock. The bog peat is often underlain by fen peat. Results from the soil investigation have shown that several wetlands in the Simpevarp regional model area consist of peat.

The total depth of overburden, observed at 15 soil drillings and two weight soundings in the Simpevarp subarea varies between 1.5 and 8.6 metres. The average thickness of these observations is 3.6 m. The drillings were, however, carried out in the lowest topographical areas where the total depth of overburden probably exceeds the average for the whole area.

The results from the marine geological investigation show that the thickest overburden cover is restricted to long narrow valleys, but even here the total thickness of overburden is often less than 10 m. Also, according to the geophysical investigations carried out in the regional model area, the thickest overburden is situated in the valleys.

The overburden cover in the higher topographical areas, characterised by numerous bedrock exposures, is probably only one or a few metres thick at most. Further drillings, excavations and geophysical investigations will give more information regarding the thickness of overburden, especially in the Laxemar subarea.

Most of the stratigraphical information is at present concentrated to the Simpevarp subarea. A general tentative stratigraphy for the whole regional model area has, however, been constructed (Table 4-2, see also Table 4-3 on hydraulic soil domains). This stratigraphy is based on results from the marine geological survey and older stratigraphical investigations in the Simpevarp regional model area, e.g. /Borg and Paabo, 1984; Risberg, 2002/ and its surroundings e.g. /Svantesson, 1999; Rudmark, 2000/. It may, however, need modifications in the future, e.g. if Quaternary deposits older than the latest deglaciation are found. The glaciofluvial sediments have not yet been included in this stratigraphy due to the lack of information.

Table 4-2. The stratigraphical distribution of Quaternary deposits in the Simpevarp regional model area.

Quaternary deposit	Relative age
Bog peat	Youngest
Fen peat	↑
Gyttja clay/clay gyttja	
Sand/gravel	↑
Glacial clay	
Till	↑
Bedrock	Oldest

4.3.3 Soils

The Simpevarp regional model area has, except for a short time period, continuously and monotonically been raised above sea level due to post-glacial land uplift (see Section 3.2.6). The lowest investigated parts of the area are situated more than one metre above the present sea level and have consequently been exposed to soil forming processes for at least thousand years.

The forthcoming soil map will give information regarding the relative distribution of the different soil types. It is, however, possible to make some preliminary observations regarding the distribution of soil types. Till is the most common Quaternary deposit in the Simpevarp regional model area /Svedmark, 1904; Rudmark, 2004/. Podzol and regosol are the most common soil types in areas covered by glacial till. It is, therefore, likely that these soil types also are the most common soil types in the whole Simpevarp regional model area. Regosol and podzol are also common in areas with coarse-grained glaciofluvial material.

In the Simpevarp area, most wetlands have been above sea level long enough for a distinct peat layer to form. Histosol is therefore the dominating soil type in the wetlands. This soil type is probably common also in drained wetlands. Land used as arable land and meadows seems to be dominated by gleysol and umbrisol. Gleysol is typically formed in areas with gyttja sediments, which seems to be common in the inner parts of the Simpevarp subarea. These initial conclusions will be reviewed when a comprehensive soil map has been developed.

4.3.4 Descriptive model

Two main type areas, with Quaternary deposits, can be distinguished in the Simpevarp subarea based on the present knowledge. These two areas occur both on the present land and at the sea floor.

1) The highest topographic areas, which are dominated by exposed bedrock and till. Results from the Simpevarp subarea show that small peat lands are common in these areas. The overburden in these areas is generally one or a few metres thick. It is possible that small pockets with thicker overburden occur.
2) Narrow valleys dominated by clay, which is underlain by till. The total thickness of Quaternary deposits is several meters in these areas.

A relatively large part of the Simpevarp subarea comprises of exposed bedrock, especially at the higher altitudes (cf. Figure 4-1). There are probably several reasons for the relatively low coverage of Quaternary deposits. One reason may be that a relatively small amount of glacial till was deposited in the area during the latest ice age. Another reason is the fact that large parts of the investigated area are exposed towards the open Baltic Sea. This has caused erosion and redeposition of overburden elsewhere by waves and streams. The distribution of Quaternary deposits is mainly an effect of the local bedrock morphology. It is mainly the highest areas that have been subjected to strong erosion, but periods of erosion have occurred also in the lower areas. It is evident, however, that long periods with deposition of fine-grained material have taken place in the lowest areas. The processes of erosion and deposition are still active along the present coast and at the sea floor.

The erosive impact of streams and waves on the sea floor increases as the water depth progressively decreases. In wave-exposed positions, the fine-grained fractions have, therefore, often been washed out from the uppermost sequence of the till deposits, which then has a resulting stony and/or gravelly surface layer. The material eroded from the older deposits, e.g. sand and gravel, is subsequently deposited at more sheltered localities. Such deposits of sand and gravel often cover the glacial clay within the investigated area. Results from the marine geological investigation show that the glacial clay is covered by sand also at deep bottoms, which indicates a high carrying capacity of streams also at large water depths (20–30 m).

After the deglaciation of the Simpevarp area, the sea level was c. 100 m higher than at present and the whole area was consequently covered with water. Fine-grained sediments, such as glacial clay, were deposited at the deep or sheltered bottoms. There are several distinct valleys in the Laxemar subarea, which, according to interpretations from geophysics (electric conductivity) are comprised of peat, clay or other fine-grained deposits. Also on the present sea floor, the deepest areas are covered with clay (Figure 4-2). Post-glacial gyttja clay was, and still is, successively deposited in sheltered bays along the coast. These gyttja sediments seem to be common deposits in the present bays along the coast (Figure 4-2) and in the narrow valleys found in the inner parts of the Simpevarp regional model area.

One important aim of future versions of the site descriptive model will be to describe and delineate the glaciofluvial deposits, since these may have a significant hydrological importance. When more data are available it may be necessary to define additional type areas, beside the two types used in the current model version.

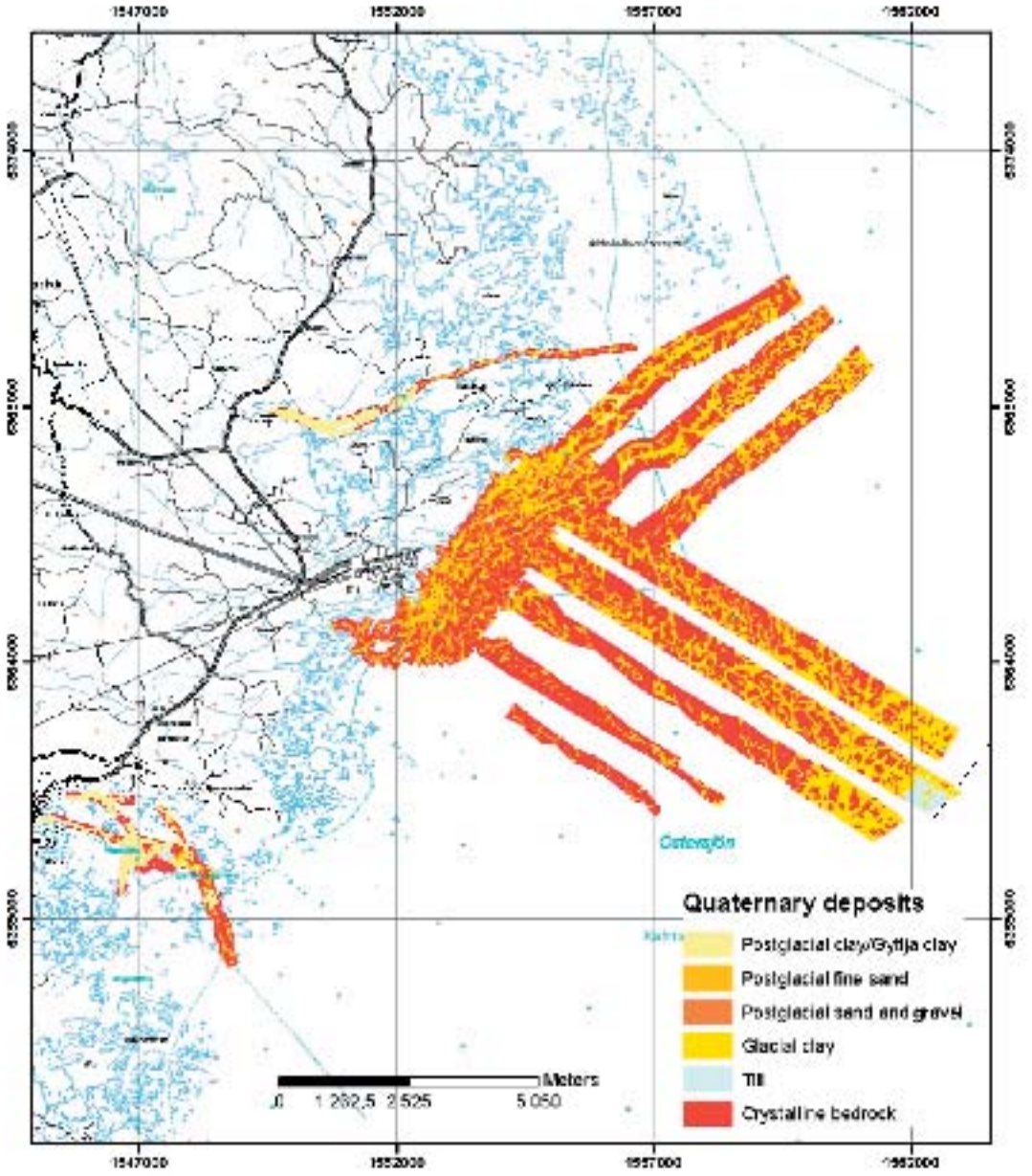

Figure 4-2. *The superficial distribution of Quaternary deposits and bedrock exposures on the sea floor.*

4.4 Description of climate, hydrology and hydrogeology

4.4.1 Overview of data evaluation

This section gives a brief overview of the processing of primary data in the Simpevarp1.2 modelling. For a detailed presentation and evaluation of the meteorological, hydrological and hydrogeological data used, the reader is referred to /Werner et al. 2005/.

In the Simpevarp 1.2 dataset, local meteorological data are available from a station on the island of Äspö (established as a part of the site investigations) for the one-year period from September 2003 to September 2004. During this period, the measured mean air temperature was 7.4°C and the measured (uncorrected) precipitation 671 mm at the Äspö station. Both values are slightly larger than the long-term average values reported by /Larsson-McCann et al. 2002/. The measured precipitation corresponds to a corrected (“true”) annual precipitation of approximately 800 mm.

The available hydrological data include simple discharge measurements in water courses, whereas near-surface hydrogeological data include manual groundwater level measurements in groundwater monitoring wells. Two other important contributions to the Simpevarp1.2 modelling are the delineation and description of catchment areas /Brunberg et al. 2004/, and the hydraulic tests performed in groundwater monitoring wells installed in Quaternary deposits /Johansson and Adestam, 2004/.

The boundaries of the 26 identified catchment areas in the Simpevarp area, which were controlled in the field, are shown in Figure 4-3. These areas are further divided into 96 sub-catchments. Basic data (including land use) of the catchment areas, and a description of the main water courses and lakes in the area, are also available /Brunberg et al. 2004/. As the groundwater table in the area generally is shallow /Werner et al. 2005/, the boundaries of the identified catchment areas (surface water divides) are assumed to coincide with those of the corresponding groundwater divides used in the Simpevarp 1.2 quantitative flow modelling.

Hydraulic conductivity data for till (the dominating type of Quaternary deposit in the area, cf. Section 4.3) are available from hydraulic (slug) tests /Johansson and Adestam, 2004/ performed in 13 groundwater monitoring wells (11 in the Simpevarp subarea and 2 in the Laxemar subarea; see Figure 2-2). The slug tests gave values of hydraulic conductivity, K, between 1.95×10^{-6} and 1.83×10^{-4} m s^{-1}. Based on the tests, the till is assigned a K-value of 1.5×10^{-5} m s^{-1} in the Simpevarp 1.2 modelling, which can be considered a low value compared to K-values of similar materials in literature. For other types of Quaternary deposits in the area, generic (literature) data are currently used to describe the hydraulic properties.

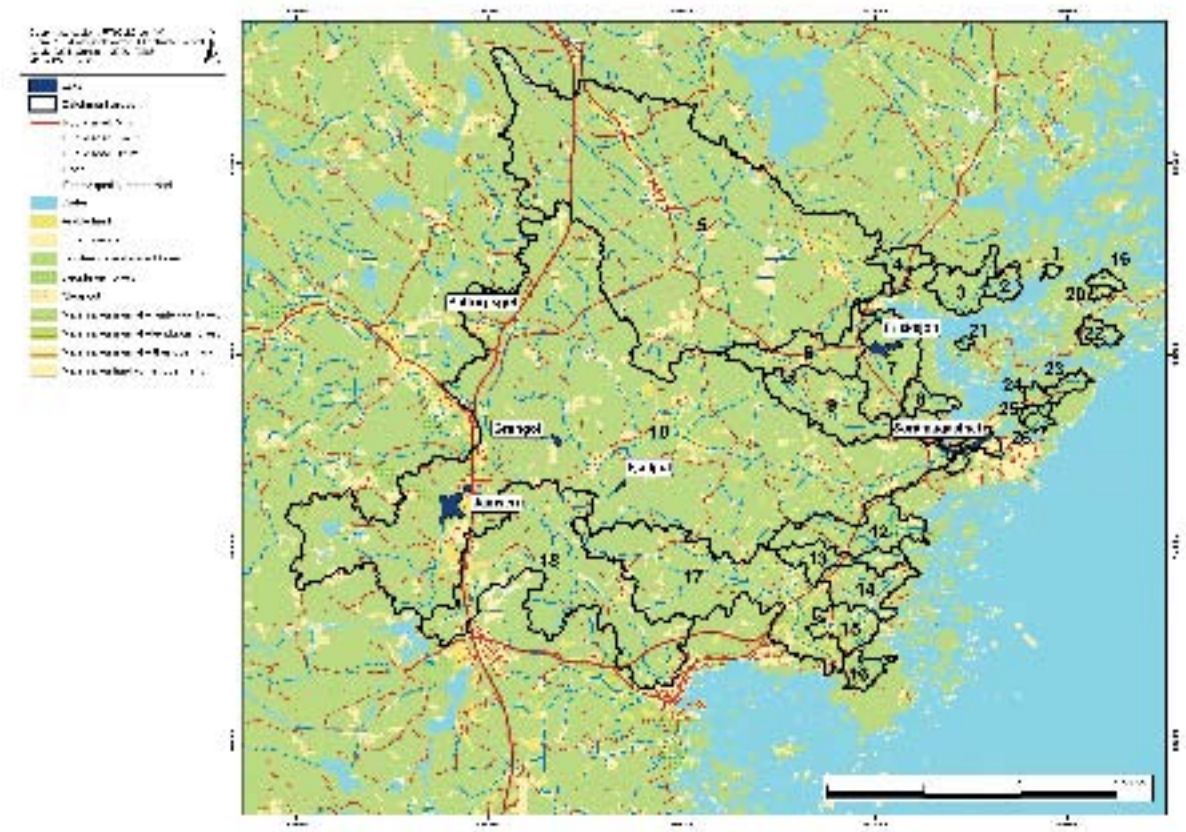

Figure 4-3. *Delineation and numbering of the 26 catchment areas in the Simpevarp regional model area /SKB GIS, 2004/. The map also shows the locations of the 6 identified lakes in the area.*

4.4.2 Conceptual and descriptive modelling

The conceptual and descriptive modelling of the meteorological, surface hydrological and near-surface hydrogeological conditions in the Simpevarp area is presented in /Werner et al. 2005/. Five different types of hydraulic soil domains have been identified in the Simpevarp1.2 modelling performed as part of the surface system modelling (Table 4-3). The Quaternary deposits are mainly located in the valleys, whereas the higher-altitude areas are dominated by exposed bedrock, or thin layers of till and peat (Figure 4-4).

The Quaternary deposits in the Simpevarp area are mainly located in the valleys, whereas the higher-altitude areas are dominated by exposed bedrock, or thin layers of till and peat. Near-surface groundwater flow mainly takes place in the valleys, and is of a local character within each catchment area. The presently available "simple" discharge measurements indicate that the discharge in water courses (located in the valleys) mainly takes place in association with precipitation events and/or snow melt periods. In between these events/periods, the water courses are dry during long periods of the year.

After data freeze for Simpevarp 1.2, continuous discharge measurements have been initiated in the main water courses in the area. These measurements will provide much more detailed discharge data for use in the forthcoming modelling work.

Table 4-3. Assignment of hydraulic properties to hydraulic soil domains (HSDs) in Simpevarp 1.2; detailed references to the literature data are given by /Werner et al. 2005/. Values within parentheses are used in the flow modelling (cf. below).

Domains (HSDs)	Type of Quaternary deposit	Thickness (m)	Hydraulic conductivity (K_H; m s^{-1})	K_H/K_V	Specific yield, S_Y (–)[2]	Storage coefficient S_S (m^{-1})[2]
1	Till (sandy)[1]	0.5–3 (1)	1.5×10^{-5}	1	0.16	0.001
2	Fine-grained glacial and post-glacial sediments: clay and gyttja clay[2]	~ 1 (larger in some valleys) > 1.5 on Ävrö (4)	1×10^{-10}–1×10^{-8} (1×10^{-8})	1	0.03	0.001
3	Sand/gravel[2]	0.2 ~ 3 on Ävrö	10^{-4}–10^{0}	1	0.30–0.40	0.001
4	Peat[2]	0.5–1	10^{-7}–10^{-4}	0.1–3	0.44	0.001
5	Glaciofluvial deposits: coarse sand, gravel[2]	< 30 (large esker in W part of reg. model area)	10^{-4}–10^{0}	1	0.30–0.40	0.001

[1] Site-specific data from slug tests /Johansson and Adestam, 2004/.
[2] Generic data from the literature.

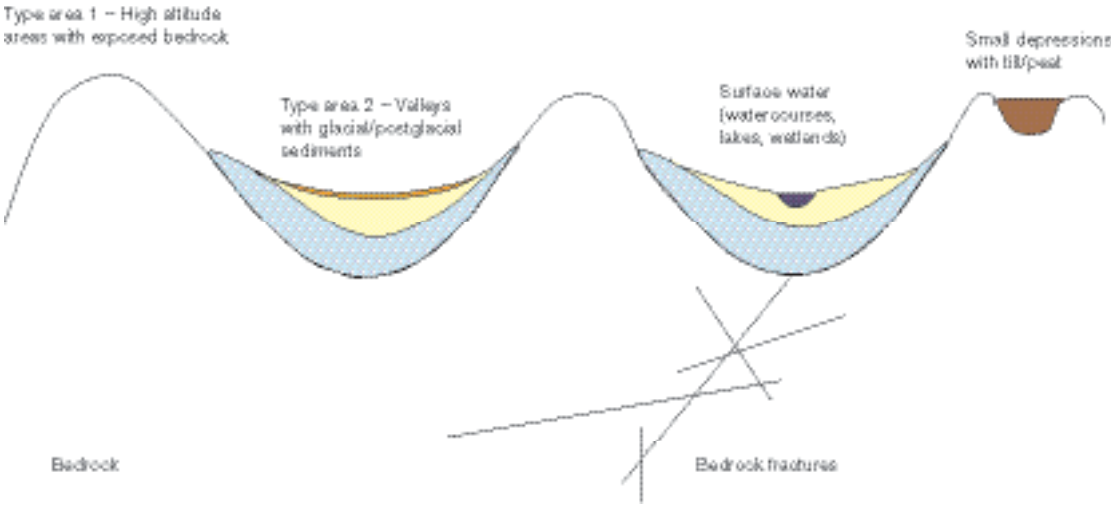

Figure 4-4. Schematic cross section illustrating the basics of the descriptive model of type areas and domains. Not all identified type areas or domains are shown in the figure.

4.4.3 Quantitative flow modelling

Quantitative flow modelling was performed in order to support the descriptive modelling and to provide specific outputs (i.e. calculated flow rates) to other modellers within the surface system modelling. The modelling included GIS-based hydrological modelling, in which the flow pattern is determined by the topography only, and detailed modelling of surface hydrological and hydrogeological processes (evapotranspiration, surface water flow and subsurface unsaturated and saturated flows) using the MIKE SHE code; these tools are described in /Werner et al. 2005/ where also further references to code documentation are given.

The GIS model was used to investigate the locations of catchment area boundaries and water courses, and to estimate discharges in the outlets to the sea. Another important model application is the identification of recharge and discharge areas. Figure 4-5 shows the distribution of these areas in the regional model area, calculated by the GIS model. The results show that the detailed locations of recharge and discharge areas are strongly influenced by the local topography, which creates a small-scale recharge-discharge pattern within most of the regional model area.

In Figure 4-5, areas of other colours than blue and red are “intermediate areas”, i.e. neither recharge nor discharge areas. It should be noted that the spatial extents of recharge, “intermediate” and discharge areas depend on definitions made by the modeller. In this case, recharge areas were defined such that their extent represented a minimum at the used grid resolution (10 m by 10 m), whereas areas receiving water from an upstream area larger than 0.05 km^2 were defined as discharge areas.

Process-based modelling with the MIKE SHE code was performed for a model area corresponding to the “Simpevarp 7” catchment area, i.e. the area where Lake Frisksjön is located. Regional, high-resolution data for a selected year (1981), identified by /Larsson-McCann et al. 2002/ as representative for the Simpevarp area, were used as meteorological input. Furthermore, data from the Simpevarp 1.1 hydrogeological modelling were used to describe the rock underlying the Quaternary deposits down to the bottom model boundary at 150 metres below sea level.

As an example of the results from the process-based modelling, Figure 4-6 shows “snapshots” of the distribution of recharge and discharge areas during a wet (left) and a dry period of the modelled year. It can be seen that the distribution of permanent recharge (higher-altitude) areas and permanent discharge areas (e.g. Lake Frisksjön and the water course in the valley) depends on the topography. However, in “intermediate” areas the results show that the extent of recharge and discharge areas varies during the year, due to the temporally variable meteorological conditions.

The total (corrected) precipitation during the selected representative year was 576 mm, whereas the calculated total evapotranspiration (averaged over the model area) for the one-year period was nearly 430 mm. The total runoff, i.e. discharge from the model area to the sea, was calculated to 150–160 mm/year (depending on how flow crossing model boundaries at depth was handled), which is within the range of the estimates (150–180 mm/year) provided by /Larsson-McCann et al. 2002/.

Given the present status of the modelling these results should not be taken as a confirmation of the previous estimates, or as evidence supporting better constrained site-specific estimates of the main components of the water balance. The modelling was performed for only a part of the regional model area using regional meteorological data, and no site-specific data, neither groundwater levels nor surface water discharges, were available to test the model. Longer time series of meteorological data and discharge data from the recently initiated measurements will, together with groundwater level measurements and additional data on hydrogeological properties, provide a basis for updating the water balance calculations in future model versions.

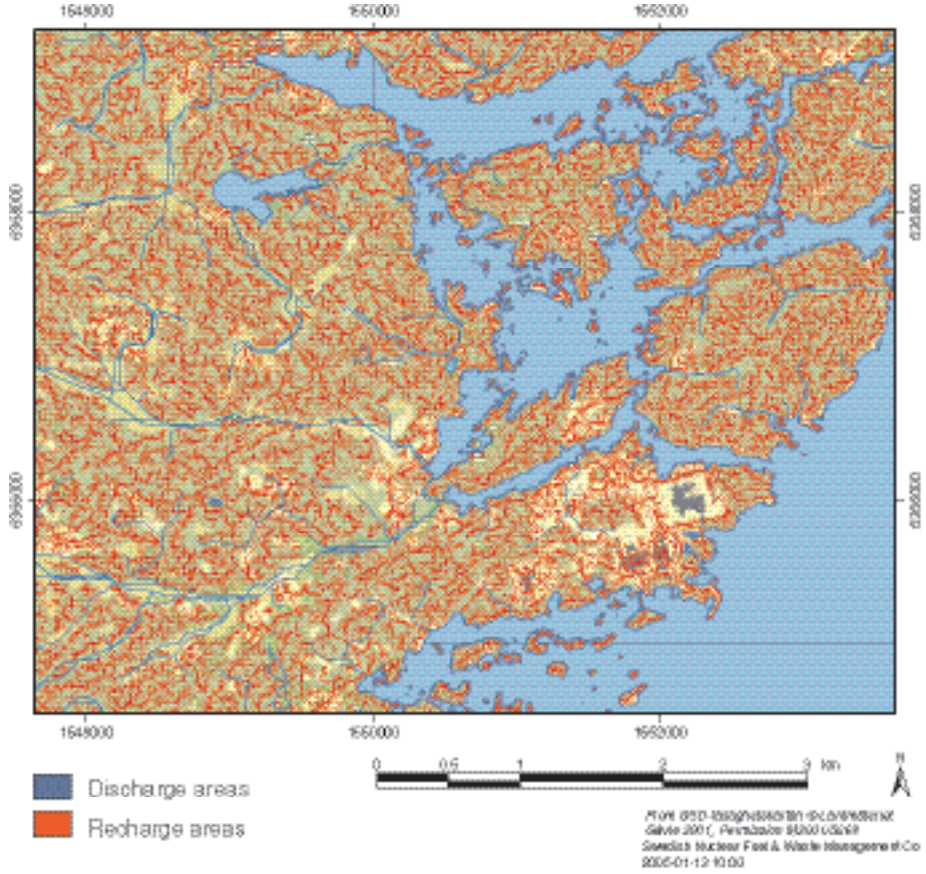

Figure 4-5. *Identification of recharge- and discharge areas using a GIS model. Areas with colours other than blue and red are "intermediate areas", i.e. neither recharge nor discharge areas based on the definitions of those in the modelling.*

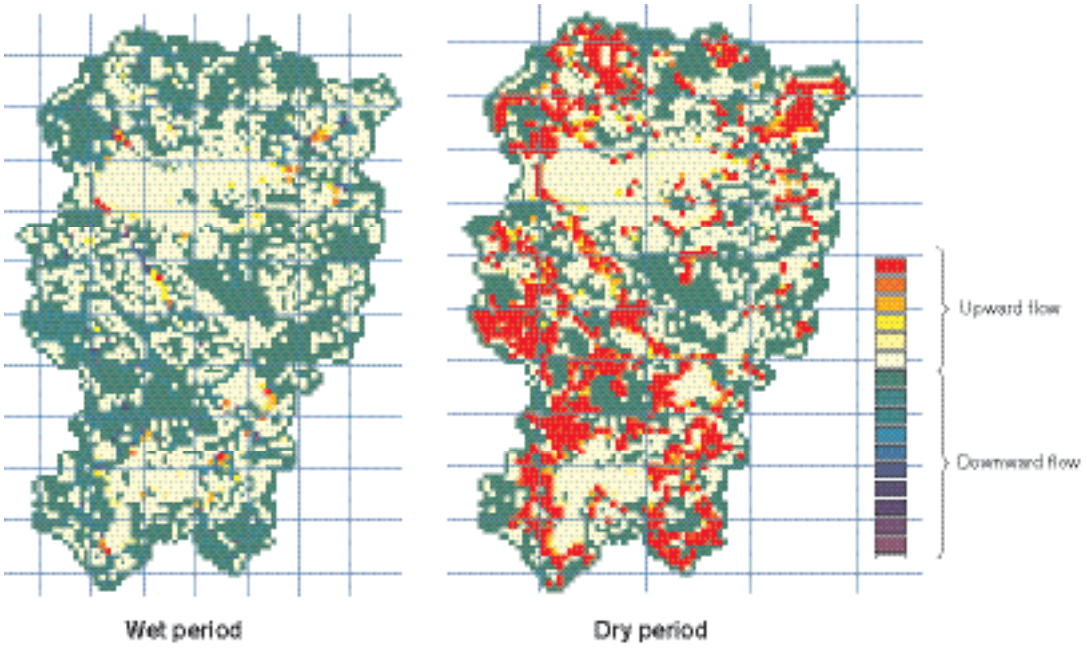

Figure 4-6. *Example of results from detailed process modelling of the Simpevarp 7 catchment area using MIKE SHE, illustrating the calculated distribution of recharge- and discharge areas during a wet (left) and a dry period. In the interpretation of the results, yellow and red areas are defined as discharge areas.*

4.5 Chemistry

4.5.1 Methodology

Data on surface water chemistry has been collected biweekly to monthly from October 2002, and the sampling programme includes 18 stream, 4 lake and 4 sea sampling sites. Analysed parameters include, for most samples, major cations and anions, nutrients, organic compounds and O_2. Water temperature, pH, conductivity, salinity and turbidity were determined in the field. Moreover, trace elements were analysed for one sampling occasion (June 2003) whereas stable and radiogenic isotopes were analysed at 1–4 sampling occasions per year. For a more detailed description over the parameters analysed in the site investigation programme, see /Lindborg, 2005/.

Data on near-surface groundwater have been collected from 13 wells (shallow boreholes), all situated in the Simpevarp subarea. Each well has been sampled once, springs of 2003 or 2004. The forthcoming groundwater chemical program will include a series of analysed samples from each well, and an evaluation of the seasonal variation in groundwater chemistry will be performed later when longer time series are available.

Data on the water chemistry of precipitation have been collected regularly from one sampling location; however, no evaluation of the chemical composition of the precipitation has been performed yet. No data on the chemistry of the overburden or in biota has so far been collected in the site investigations.

4.5.2 Description and conceptual model

Surface water

The lakes and streams in the Simpevarp regional model area are, similar to most surface waters in the northern parts of the County of Kalmar, relatively poor in nutrients while they are rich in organic matter, mainly humic compounds, which give the water a brownish colour. The catchment areas in the regional model area are generally small, which means that some of the streams periodically show very low discharge, or are even ephemeral. Most of the surface water from the regional model area drains into a few, relatively confined, coastal basins, and the water chemistry of these basins will therefore differ considerably from the water chemistry of the outer parts of the archipelago.

Generally, the stream sites in the regional model area show only minor differences from average values for the 26 stream sites in the County of Kalmar which were included in the National Survey of lakes and streams, performed in 2000. Only a few lakes are situated within the regional model area. Four of these, Lake Frisksjön, Lake Jämsen, Lake Söråmagasinet and Lake Götemar, cf. Figure 4-3, are included in the programme for surface water chemistry. In a regional comparison (see /Lindborg, 2005/ for details), nutrient concentrations in the first three lakes are intermediate and they can be characterised as mesotrophic with brown water. Lake Götemar shows considerably lower concentrations of nutrients and can be classified as an oligotrophic clearwater lake.

The five investigated sea sites can be divided into two different types. The first type represents the open sea and outer archipelago and consists of three sites; Kråkelund, Ekö and Fågelöfjärden. These sites are situated quite close to the open sea and show similar electrical conductivity and similar concentrations of most analysed parameters. The other type of site is situated in relatively confined bays close to the mainland and consists of two sites; Borholmsfjärden and Granholmsfjärden. These sites show lower concentrations of ions than the open sea sites, whereas the concentrations of organic compounds and nutrients, especially the nitrogen fractions, are considerably higher. For a comprehensive compilation of selected chemical parameters in stream, lake and sea sites in the regional model area of Simpevarp, the reader is referred to /Lindborg, 2005/.

Near surface groundwater

The chemical composition of the near surface groundwater is an integrated result of both present and past processes (cf. Section 3.2). Results from the investigation of surface groundwater chemistry in the Simpevarp subarea are summarised in Table 4-4. The results for Mg, Ca, HCO_3, Cl, SO_4, Mn and pH were compared with the median values for groundwater from open aquifers in till, or wave-washed sediments situated on the west and south coasts of Sweden /Naturvårdsverket, 1999/.

Table 4-4. The chemical composition of surface groundwater in the Simpevarp subarea. The samples were collected in 13 wells completed in the overburden during the springs of 2003 and 2004.

	Average	Median	Max	Min	N
Na (mg/l)	34.4	10.1	232	4.6	13
Ca (mg/l)	33.2	30.2	91.2	9.1	13
Mg (mg/l)	10.1	9.2	28.8	2.3	13
HCO_3 (mg/l)	113	82	371	2	15
Cl (mg/l)	25.3	7.1	157	3.2	13
SO_4 (mg/l)	35.1	15.4	130	4.1	13
Si (mg/l)	11.4	10.8	22.2	4.9	13
Mn (mg/l)	0.80	0.3	6.0	0.09	13
Li (mg/l)	0.018	0.015	0.041	0.009	11
Sr (mg/l)	0.13	0.10	0.28	0.03	13
Cond. (mS/m)	38.8	25.7	121	11.9	13
pH	6.8	6.51	7.91	6.28	13

The results from the Simpevarp subarea were also compared with values for the whole of Sweden /Aastrup et al. 1995/. These comparisons show that the chemical composition of the groundwater is normal in most of the wells, except for Mn which shows one order of magnitude higher median concentrations than the normal /cf. Naturvårdsverket, 1999/. For a more detailed discussion of the results, see /Lindborg, 2005/.

4.6 Biota

4.6.1 Terrestrial

Producers

The vegetation is the dominant biotic component of the terrestrial environments making it the most important primary producer. The vegetation is strongly influenced by the characteristics of the bedrock, Quaternary deposits and human land management. The bedrock mainly consists of granites. The Quaternary deposits are mainly glacial till, silt and clay, the latter two deposited in the valleys. This pattern is clearly manifested in the vegetation, where pine forests dominate on till, and all the arable land and pastures (abandoned arable land) are located in the valleys. The dominating wetland type is the poor mire (low in nutrients) that is accumulating peat /Rühling, 1997; SNV, 1984/. As a consequence of the forestry activities in the area, there are a lot of clear-cuts found in different success ional stages. The spatial distribution of different vegetation types is presented in the vegetation map. A more detailed description of the different vegetation types is found in /Lindborg, 2005/.

Species composition and red listed species

The flora in this region has been investigated within the project “The flora of Oskarshamn” /Rühling, 1997/. The flora has also been investigated using the same methodology for taxa as “National survey of forest soil and vegetation” /Andersson, 2004/. All red listed plants from the site are presented in /Kyläkorpi, 2004/. Further information concerning the red listed species is presented by /Berggren and Kyläkorpi, 2002/.

Protected areas

A number of sensitive areas of conservational interest are located within the regional model area. Some areas have an extensive protection whereas others are so far unprotected but are under planning. These areas are listed in /Kyläkorpi, 2004/. There are today three areas that are legally protected as nature reserves. These are Stenhagen, Talldungen and Misterhults archipelago (more information about the nature reserves and other protected areas can be found in /Lindborg, 2005/.

Woodland key habitats

Woodland key habitats are areas where red listed animals and plants exist, or could be expected to exist /Nitare and Norén, 1992/. A nationwide survey of these habitats has been conducted in Sweden administrated by the Swedish Board of Forestry /SBF, 1999/. As a complement to this survey, SKB initiated a more comprehensive survey in the Simpevarp area. In the latter case, a total of 46 habitats were identified with a total area of 61 ha /Sturesson, 2003/. The dominating key habitat type in the area, both in number of objects and total area, is old semi-natural grasslands or meadows with old pruned ("hamlade" in Swedish) deciduous trees in close proximity to old settlements.

Descriptive biomass and NPP models – introduction

The vegetation constitutes a major part of the living biomass and comprises the primary producers in terrestrial ecosystems. The biomass and necromass will therefore be an important measure of how much carbon may be accumulated in a specific ecosystem. Similarly, the net primary production (NPP) will be an estimate as to the rate at which carbon (and other elements) is incorporated in primary producers. Thus, combining net primary production and decomposition rates will give a rough estimate of the carbon turnover in the ecosystem. The primary producers covering the terrestrial landscape are described using biomass and NPP in order to feed a conceptual ecosystem model with data (cf. Section 4.10). This section describes the components, the resolution and the methodology that is used to build the quantitative descriptive models of biomass and NPP that are further treated in 4.10.

The plant biomass in an area consists of a number of different components that all have to be measured, or estimated, in order to correctly estimate the total biomass (Figure 4-7).

The photosynthesis provides the carbon and the energy that are essential for most important processes in ecosystems. The measure of photosynthesis at an ecosystem level is termed gross primary production (GPP). Approximately half of the GPP is respired by plants to provide the energy that supports the growth and maintenance of biomass /Chapin et al. 2002/. The net carbon gain is termed net primary production (NPP) and is the difference between GPP and plant respiration. However, GPP cannot be measured directly and total respiration is difficult to measure, especially in multi-species forests /Gower et al. 1999/. The different components constituting the NPP for a certain ecosystem may be measured separately /Clark et al. 2001/ (Figure 4-8).

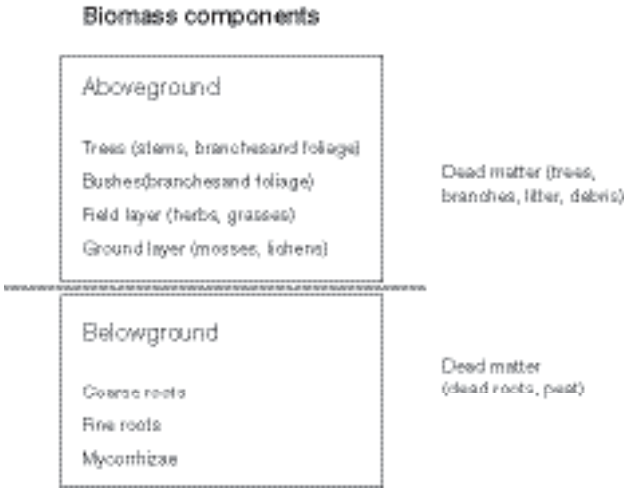

Figure 4-7. *The different components of biomass in a forest.*

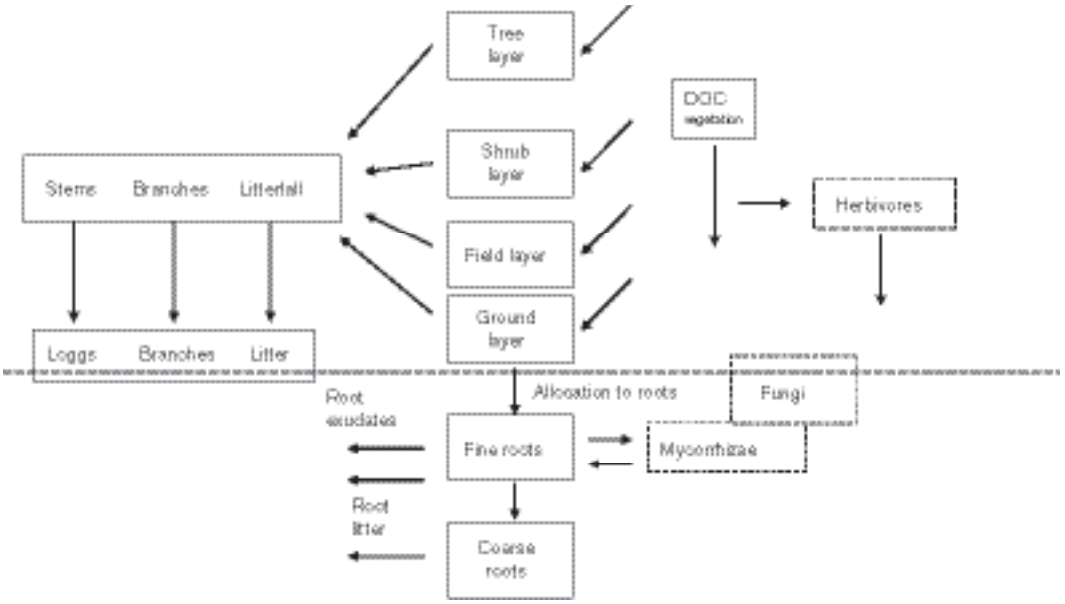

Figure 4-8. *An illustration of the different pools and fluxes of matter in a terrestrial ecosystem with the focus on the producers. Boxes with broken lines are consumers.*

NPP is sometimes (e.g. for trees) equated to the net accumulation of biomass during one year. In those cases, the NPP and the biomass turnover are different. Sometimes the NPP and turnover are set equal, as a simplification, implying that there is no net accumulation of biomass between years.

Quantitative descriptive models

Below the methodology and procedure applied in the modelling are tentatively described. The results are given in /Lindborg, 2005/ and the quantitative figures are used in the corresponding terrestrial ecosystem model, as described in Section 4.10.

Tree layer

Biomass and NPP for four fractions of the tree layer have been calculated (woody parts (above ground), green parts, coarse roots and fine roots). Furthermore, the annual amount of litterfall and other falling components have been calculated for four forest classes. The forest classes used to describe the tree layer (young-, dry- and old- coniferous forest and deciduous forest) and the GIS sources from which the information has been obtained to construct the classes are described in /Lindborg, 2005/, as well as the methodology and the data used in the calculations.

Shrub layer

Biomass and NPP of the shrub layer have been calculated. Field inventories /Andersson, 2004/ indicated that the shrub layer most often is insignificant when a tree layer is present in the area. A habitat that had a very significant shrub layer was clear cuts of varying age where *Betula pendula* (silver birch) is very dominant. *Salix sp.* can be abundant on mires and was identified by /Boresjö Bronge and Wester, 2002/ in their shrub layer. Therefore, the focus is on *Betula* (Birch) and *Salix* (Willow) in the shrub layer. However, due to lack of biomass and NPP data for *Salix sp.* (willow sp.) the values for Birch are used throughout.

The classes used to describe the shrub layer and the GIS sources from where the information was obtained to construct the classes is described in /Lindborg, 2005/ jointly with the methodology and the data used in the calculations.

Dead wood

The biomass of dead wood has been calculated according to the description in /Lindborg, 2005/, and is presented in dw gC m^{-2} for different vegetation types.

Field and ground layer

Biomass and NPP of the field and ground layer have been calculated. The classes used to describe field and ground layer and the GIS sources from where the information is obtained to construct the classes is described in /Lindborg, 2005/ as well as the methodology and the data used in the calculations. The results, assigning biomass and NPP values in dw gC/m^2 and dwgC$m^{-2}y^{-1}$ for the different field and ground layer classes are presented in /Lindborg, 2005/.

Fungi/mycorrhizae

Biomass and NPP for fungi in the forest habitats (young-, dry- and old- coniferous forest and deciduous forest) have been calculated according to the approach described in /Lindborg, 2005/.

Consumers

Mammals

The most common mammal species in the Simpevarp regional model area is roe deer (5 deer/km^2) /Cederlund et al. 2004/. Moose is also fairly common (0.8 moose km^{-2}), but unevenly distributed, which is normal for this part of Sweden due to hunting pressure, snow depth and distribution of food. European and mountain hare are fairly low in abundance, compared to other regions (see Table 4-5). A more detailed description of the mammals is found /Lindborg, 2005/.

Birds

In total, 126 species were found in the regional model area in 2003 (112 in 2002), and 28 of these are noted in the Red List as endangered bird species in Sweden /Green, 2004/. The most common species on land were Chaffinch and Great Tit. A major part of the nesting species were small birds, associated with the open or semi-open landscape.

Cattle

A significant part of the terrestrial biomass for consumers in the Simpevarp area is domestic animals. There were 4.3 cows and calves per km^2 in the Simpevarp area /Miliander et al. 2004/, which can be compared with the densities given in Table 4-5.

Table 4-5. Estimated abundances of mammal species in the Simpevarp regional model area /Cederlund et al. 2004/.

Species	Animals per km^2
European hare (field)	3.51
Mountain hare (forest)	0.52
Fox	Observed
Marten (Swe: Mård)	0.13
Mink	Observed
Moose	0.8
Red deer	0.03
Roe deer	5.0
Small mammals field (mice and voles)	2,200
Small mammals forest (mice and voles)	3,110
Wild boar	0.26

No observations of Badger, Beaver, Fallow deer, Lynx, Otter or Wolf were made during the investigations in 2003.

Amphibians and reptiles

Site-specific data concerning the species that are likely to occur in the Simpevarp area have been obtained through field studies by /Andrén, 2004a/. There are no site-specific density data for amphibians and reptiles. Generic data concerning these species have been obtained from /Andrén, 2004b/. These data are compiled in /Lindborg, 2005/.

Soil fauna

Three examples of soil fauna densities and biomass figures have been obtained from Tryggve Persson, professor in Soil biology at SLU. The three examples come from a pine moor in Gästrikland, a deciduous forest in Uppland (Andersby-Ängsbacka in Dannemora) and a grassland in Uppland /Lohm and Persson,1979/. The densities and biomass for the different soil species are given in /Lindborg, 2005/.

Quantitative model

A carbon budget for the terrestrial consumers in the drainage area of Lake Frisksjön has been calculated based on the site-specific density data for mammals and humans. There is no active agriculture in the Lake Frisksjön drainage area, but as there is some grazing- and arable land in the area, five milk cows have been included in the model. The applied methodology with carbon pools and flows are presented in /Lindborg, 2005/. The results are illustrated in Figure 4-9 and the numbers are used in the terrestrial ecosystem model, described in Section 4.10. No biomass figures have been calculated for birds, as no site-specific density data are available for Simpevarp 1.2.

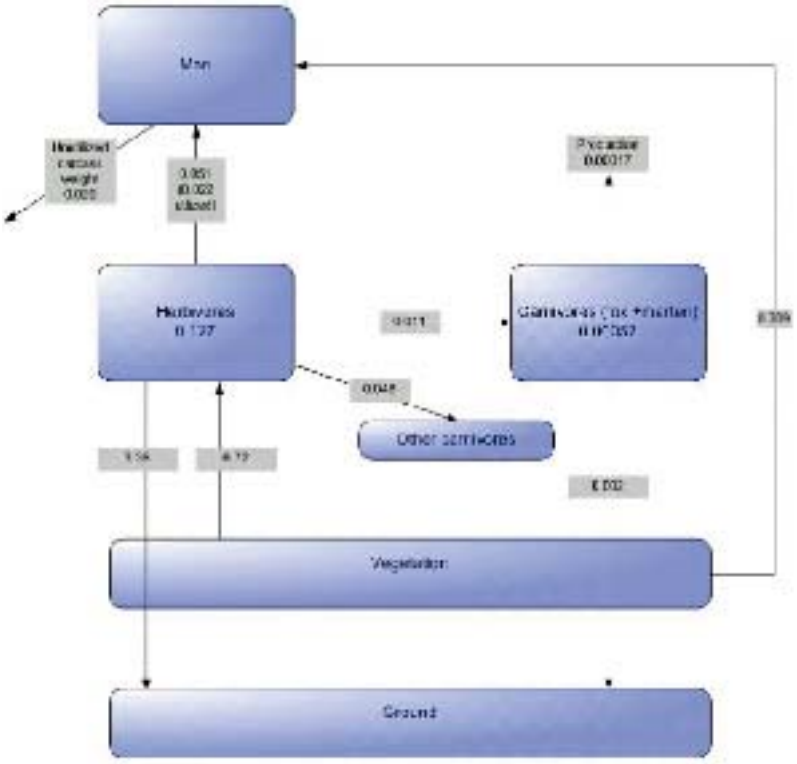

Figure 4-9. *A carbon budget for the terrestrial fauna in the Lake Frisksjön drainage area (Simpevarp 7), expressed as gC m^{-2} y^{-1}.*

4.6.2 Limnic producers

Methodology

The *lake characterisation* includes, besides the identification of watersheds, a recording of lake morphometric parameters using a Differential Geographical Position System and an echo-sounder equipment /Brunberg et al. 2004/. From these data, bathymetric maps, depth grids were constructed for each lake. Using the same equipment, the distribution of different lake habitats was determined in the field.

Phytoplankton was sampled at 12 occasions during the period July 2003–June 2004 /Sundberg et al. 2004/. Three of the samples were analysed (July and December 2003, April 2004). Phytoplankton samples were taken with a so-called "Ramberg-rör" (a 2 m tube sampler with a diameter of 3.5 cm). Five sub-samples were taken within a radius of 50 meters. Species composition and biomass of phytoplankton were determined using an inverted phase-contrast microscope.

Description/models

The lakes in the Simpevarp area have been divided into five different habitat types; the Littoral types I, II and III, Pelagial and Profundal /Brunberg et al. 2004/.

Littoral type I: The littoral habitat with emergent and floating-leaved vegetation. This habitat is developed in wind-sheltered, shallow areas where the substrate is soft and allows emergent and floating-leaved vegetation to colonise.

Littoral type II: The littoral habitat with hard substrate. This habitat develops in wind-exposed areas of larger lakes, but also in smaller lakes, where the lake morphometry includes rocky shores. The photosynthesising organisms colonising these areas include species that are able to attach to the hard substrate, e.g. periphytic algae.

Littoral type III: The littoral habitat with submerged vegetation. This habitat is found in deeper areas of the lakes, where light enough to sustain photosynthetic primary production penetrates down to the sediment.

The profundal habitat: This habitat develops in the sediments of lakes where light penetration is less than that required to sustain a permanent vegetation of primary producers. Non-photosynthesising organisms dominate this habitat. The profundal organisms are dependent on carbon supplies imported from other habitats of the lake, or from allocth sources.

The pelagic habitat: This habitat includes the open lake water, where a pelagic food-web based on planktic organisms is developed. Depending on the availability of light, these plankton are dominated by either photosynthetic production (i.e. by autotrophic phytoplankton) or, if the water is strongly coloured or turbid, by heterotrophic carbon processing (e.g. by heterotrophic or mixotrophic bacterioplankton and phytoplankton). The pelagic habitat covers the same area as the sum of areas corresponding to littoral type II, littoral type III and profundal habitats within a lake.

Below, the habitat characterisation of Lake Frisksjön is presented. The same types of data are available for the other 4 investigated lakes, i.e. Lake Fjällgöl, Lake Plittorpsgöl, Lake Jämsen and Lake Söråmagasinet, Figure 4-3.

Lake Frisksjön

All five major habitats are present in Lake Frisksjön (Figure 4-10). Despite the relative shallowness of this lake (maximum depth 2.8 m), the brown colour of the water prevents light from penetrating some parts. Thus, the profundal habitat covers a substantial part of the bottom area (41%). The dominant littoral habitat is of type III.

The highest phytoplankton biomass in Lake Frisksjön was recorded in July 2003 (5.2 mg ww L^{-1}). In December 2003, the biomass was 0.1 mg ww L^{-1} and in April 2004 biomass was 0.4 mg ww L^{-1}. Compared with other humic lakes, phytoplankton biomass in July was very high, whereas the values for December and April were very low. Dinophytes dominated phytoplankton biomass in July, whereas diatoms dominated in December 2003 and in April 2004. The results are reported in more

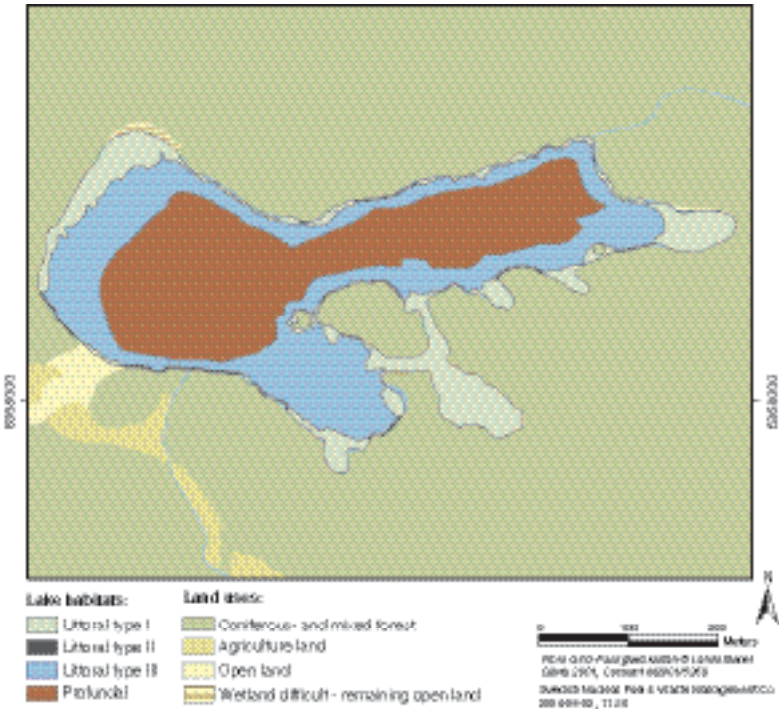

Figure 4-10. *Distribution of major habitats in Lake Frisksjön /Brunberg et al. 2004/.*

detail with tables and figures in /Lindborg, 2005/. Several species found in Lake Frisksjön are typical for humic lakes. Moreover, several species of bluegreen algae (cyanophyceae) were recorded from the lake, although in very low biomasses, and none of the observed species has been documented as potentially toxic.

4.6.3 Limnic consumers

Detailed information on the composition and biomass of zooplankton, benthic fauna and fish in Lake Frisksjön are found in /Lindborg, 2005/. The fish community can be regarded as typical for small brownwater lakes in the area. It contains six species (with Swedish translation in italics); perch *(abborre)*, bream *(braxen)*, ruffe *(gärs)*, roach *(mört)* and pike *(gädda)*, of which perch is dominating both in number and in biomass.

4.6.4 Marine

The marine system in the Simpevarp area encompasses three major habitats; enclosed bay areas (to a varying degree affected by the fresh water discharge), coastal archipelago with sheltered areas, and a Baltic Sea coastal habitat exposed to sea currents and wave action.

The basins have a variable geometry, large shallow areas (depth < 1 m) are found as well as depths down to 18 m. The three habitats have mean depths of 0.8, 3.4 and 4.5 m, respectively. The average surface salinity varies between 3.5–4.5‰ in the basins whereas the bottom water (> 16 m) has a salinity close to the surrounding offshore area of about 6‰. The area is characterised by humic water with low transparency conditions, averaging a light penetration of 2–3 m in enclosed bays, 4–7 m in the archipelago and 12 m in the open sea. The bay areas have a content of nutrients of 600–700 µg tot-N/l, decreasing to roughly 300 µg tot-N/l in the coastal areas and 20–30 µg tot-P/l, in the Baltic sea /Ericsson and Engdahl, 2004a/.

The inner soft bottom parts of the archipelago north of the Simpevarp peninsula (around the island of Äspö) are dominated by *Chara sp.* West of Ävrö a large area is covered by the Xanthophyceae *Vaucheria sp.* On corresponding bottoms in the southern area the vegetation is dominated by vascular plant communities, dominated by *Potamogeton pectinatus* and *Zostera marina*. The

sheltered inner coastal waters, particularly south of the Simpevarp peninsula, are dominated by *P. pectinatus*. Further out, towards more exposed areas *P. pectinatus* and *Z. marina* occur together in a patchy appearance. On hard substrates, in shallow areas, the vegetation is dominated by *Fucus vesiculosus* and in deeper areas red algae cover the hard substrata, with a common degree of coverage of 25% /Fredriksson and Tobiasson, 2003/. *Fucus sp.* in low abundance are recorded to approximately 10 m depth and red algae down to approximately 30 m /Tobiasson, 2003/. The benthic fauna is in all basins dominated by detritivores. Detritivores, often *Macoma baltica* or *Hydrobia sp.*, often constitutes 50–80% in the three selected basins. In total, 45 species associated with the vegetation occurred in the area around Simpevarp and 41 in the sediments. The *Fucus sp.* communities are the most diverse concerning associated fauna and harbour 31 species or higher taxa, whereas the soft bottoms without vegetation have 14 species.

Primary producers in the pelagic habitat, which accounts for a relatively small part of the carbon flow of the ecosystem, seems to be dominated by the diatoms. Copepods are the dominating zooplankton, and zooplanktons are more abundant in the inner bays than in the coastal areas.

From the general survey, different vegetation communities were defined on the basis of dominating species or higher taxa. For the area around Simpevarp, nine vegetation communities were defined. The red algae community covered the largest area with almost 6 million square metres. Second highest coverage was associated with the *Potamogeton pectinatus*-community with an area of almost 2 million square metres. Regarding coverage, the *P. pectinatus* community was followed by the *Chara sp.* and *Fucus vesiculosus*-communities with coverage of about 1.3 and 1 million square metres, respectively.

The vegetation communities consist of sub-areas of different composition of species and degree of coverage. Species occurring in the vegetation communities are presented in Table 4-6. The highest number of species, 23 species or higher taxa, is found in the vegetation community dominated by filamentous algae (Table 4-6). The community with the second highest number of species is the *F. vesiculosus* community which included 19 other taxa. The lowest number of species was recorded in the *P. perfoliatus* and *Vaucheria sp.* communities, with only one and three species respectively (Table 4-6).

The most common species in the samples were *Cladophora sp.* and *Ceramium* gobii which occurred in 6 of the 9 vegetation communities (Table 4-6). Other common species were the red algae *Polysiphonia fucoides* and *Polysiphonia fibrillosa* which along with the phanerogams *Myriophyllum spicatum* and *Ruppia sp.* was found in the samples from five different vegetation communities.

Reed, *Phragmites australis*, was sampled at six sites in the three basins during 2004. The mean biomass for reed in the Simpevarp area was 1.3×10^3 g dry weight m^{-2} and the average value for reed rhizome biomass in the same area was 3.7×10^3 g dry weight m^{-2}. The result from the standing crop biomass measurement corresponds with earlier studies of reed biomass, but the mean biomass value for the rhizome is doubled, which could be due to the fact that this study included both dead and living roots.

Table 4-6. Macrophyte species present in various vegetation communities. o = occurrence.

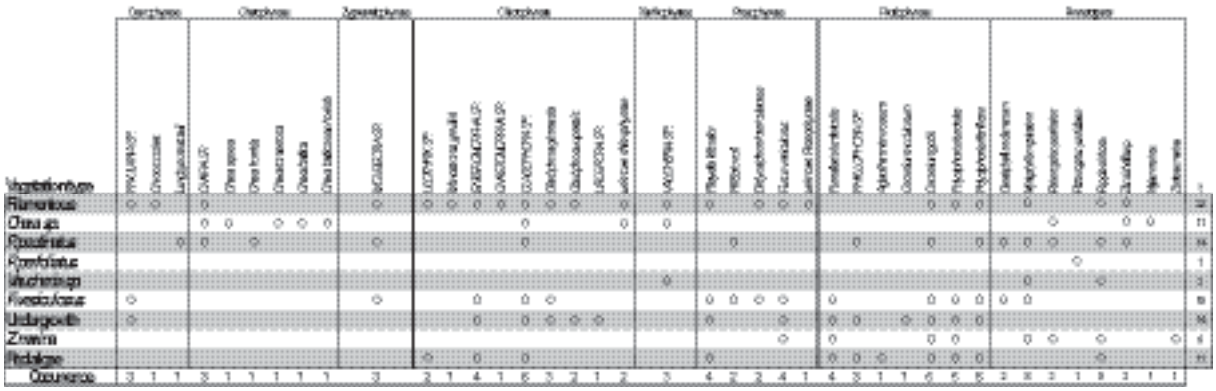

Basin Borholmsfjärden

In this section, the basin Borholmsfjärden is used as an example of the description of the marine environment that have been developed. For a more detailed description, and for descriptions of Gransholmsfjärden and Getbergsfjärden, see /Lindborg, 2005/.

Benthic vegetation

The benthic macrophyte vegetation is to a large extent composed of *Chara*-communities in the shallower parts and *Vaucheria*-communities in the deeper parts (depths of 4–6 m, see Figure 4-11). The *Chara*-communities covers an area that is about twice as large as the *Vaucheria*-communites and they dominate also in dry weight biomass (g dry weight). However, when biomass is recalculated into carbon (gC) *Vaucheria* dominates in biomass in the basin due to a denser constitution. The *Chara*-community consists of sub-areas with different composition in *Chara*-cover and also different amounts of associated species, such as *P. pectinatus*, *Myriophyllum sp.* and *Najas marina*. About one fifth of the *Chara*-community is not dominated by *Chara* but by *Najas marina*. The *P. perfoliatus*- and *Vaucheria*-communities are much more homogenous. All associated macrophyte species are presented in Table 4-6. Reed covers only a small area in Borholmsfjärden but contributes with a large biomass. Area cover and biomass are presented in Table 4-7 and in Figure 4-11.

Benthic fauna

The domination of the *Chara*-community is reflected by the nature of benthic fauna in the basin (see Figure 4-12). Detritivores are the largest contributor to the benthic fauna biomass and most of it is found associated with the *Chara*-vegetation, most of it being the snail *Potamopyrgus antipodarum*. In the infauna, *Macoma baltica* is dominant in all communities, except the *Chara*-community. Herbivores and carnivores, respectively, are found in approximately the same quantity (50% of the detritivores). Whereas the carnivores were evenly spread among the different communities, most of the herbivores are found in the *Chara*- and *Vaucheria*-communities. *Lymnea sp.* is the most common herbivore. Carnivores are represented by *Donacia sp.* (a beetle larvae) and the fish *Syngnathus typhle* in *Potamogeton* communities, by *Sphaeroma hookeri* and the shrimp *Palaemon adspersus* in the *Chara*-community.

The differences between *Potamogeton*-communities in amounts of infauna and epifauna, respectively, depends the difference in density of macrophytes. For instance, *P. perfoliatus* covers a large area, but was much sparser than *P. pectinatus*.

Zooplankton

In basin Borholmsfjärden, the zooplankton community (total biomass was 0.074 mg dry weight l^{-1}) was dominated by rotifers in July 2003 (Figure 4-13). The most important species was *Keratella cochlearis*. In December 2003 (0.061 mg dry weight l^{-1}), calanoid copepods are most important (adults and juveniles of *Acartia sp.* and *Eurytemora sp.*), and in April 2004 (0.352 mg dry weight l^{-1}) large cyclopoid copepods, i.e. *Cyclops sp.* dominated strongly. Tintinnids and macro-invertebrate larvae were absent or very scarce at all sampling dates /Sundberg et al. 2004/.

Table 4-7. Area coverage (m^2) and biomass (g dry weight and gC) of benthic vegetation in basin Borholmsfjärden.

Vegetation type	Area (m^2)	Macrophytes (g dry weight)	Macrophytes (gC)
Vegetation cover less than 5%	2.76×10^5	–	–
Chara sp.	6.46×10^5	1.64×10^8	2.26×10^7
Potamogeton pectinatus	6.54×10^3	4.62×10^5	1.49×10^5
Potamogeton perfoliatus	1.39×10^5	1.18×10^6	3.81×10^5
Vaucheria sp.	3.02×10^5	7.90×10^7	3.09×10^7
Reed, *Phragmites australis*	9.23×10^3	1.16×10^7	4.57×10^6
Not examined	1.78×10^3	–	–

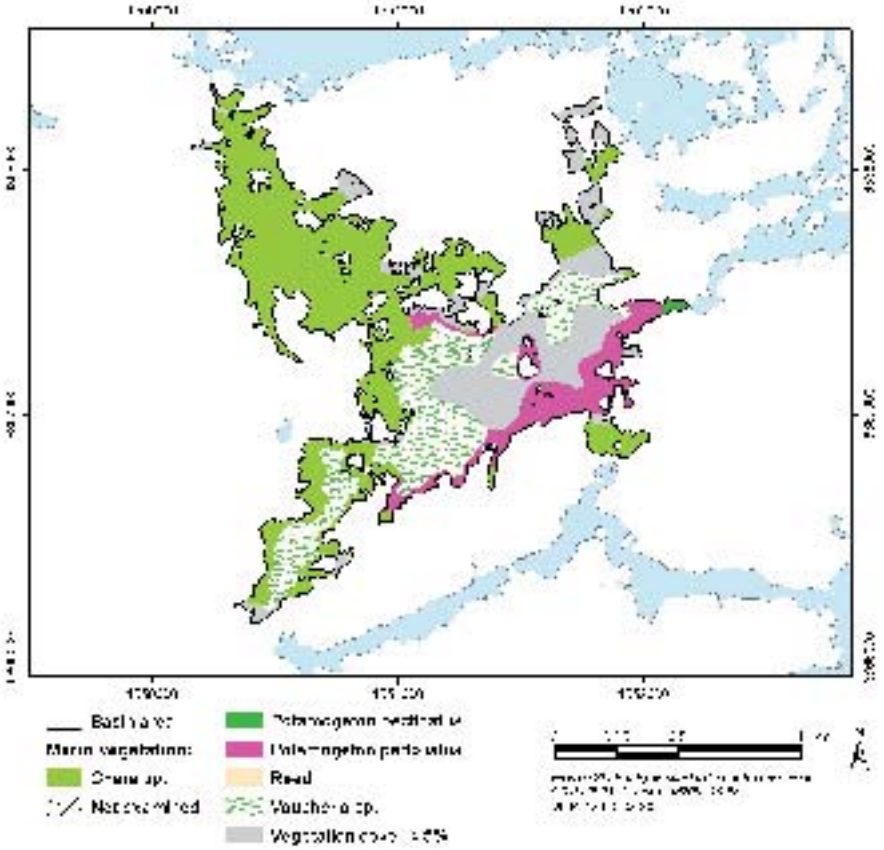

Figure 4-11. *Distribution of different vegetation communities in Basin Borholmsfjärden.*

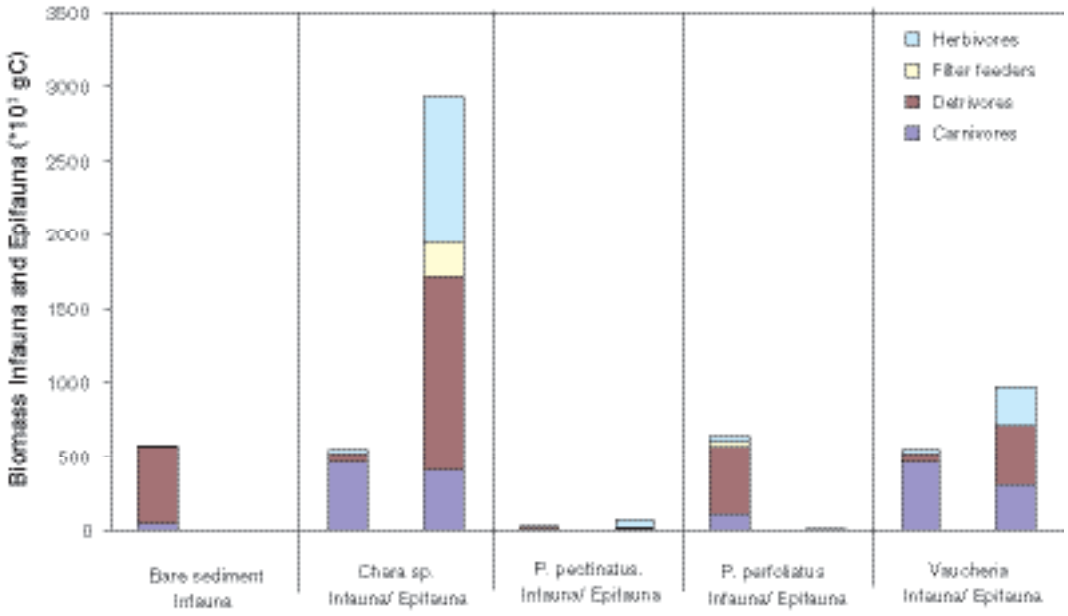

Figure 4-12. *Biomass (gC) of benthic functional groups of infauna and epifauna in different communities: bare sediment (vegetation cover < 5%),* Chara-, P. pectinatus-, P. perfoliatus- *and* Vaucheria-*community.*

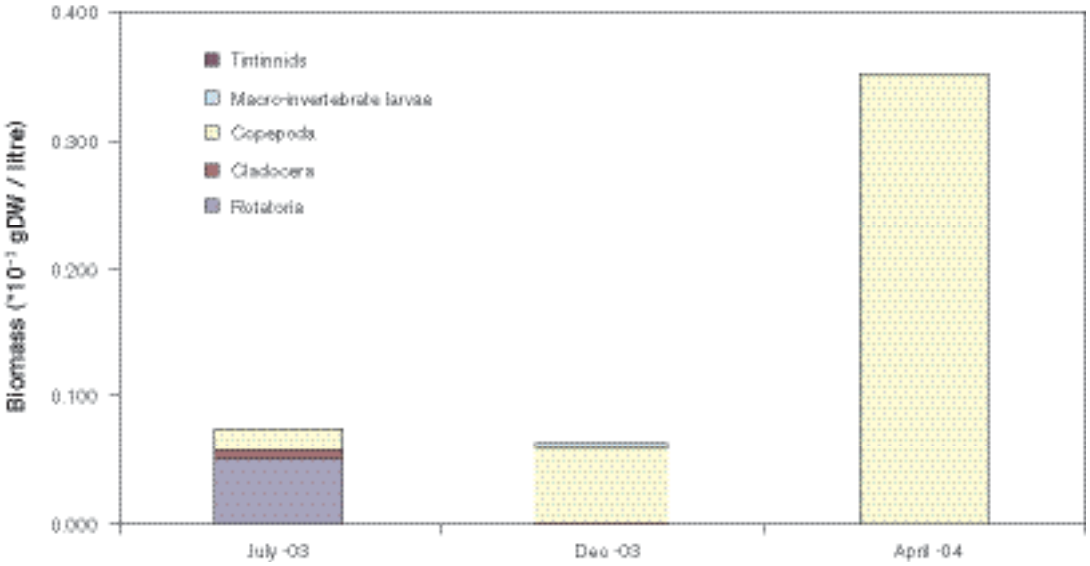

Figure 4-13. *Biomass of different zooplankton taxa in the whole water column in basin Borholmsfjärden (0–3 m) /Sundberg et al. 2004/.*

4.7 Humans and land use

Input data sources and calculated numbers for the variables used to describe humans and land use in the Simpevarp area and its surroundings are shown in great detail in /Miliander et al. 2004/ and more briefly in /Lindborg, 2005/. The short description below illustrates the situation in the parish of Misterhult, since many of the data were available on the parish level.

The assessment of the data acquired can be summarised as follows:

- The parish has a low density of population (6.6 individuals km^{-2} in 2002) and the number of inhabitants has diminished slowly during the 1990s.
- The main employment sector is within electricity production. There is a clear net influx of commuting individuals to the region due the dominant employer (the OKG Power Company that operates the Oskarshamn nuclear power plant).
- Mining (decoration stone) and manufacturing are the main employment sectors among the inhabitants of the parish.
- There are proportionately more holiday-houses in the parish than in the Municipality of Oskarshamn and the County of Kalmar as a whole, which indicates that the region has a proportionally larger holiday population. The number of holiday-houses has increased since 1996 (6%).
- The land use is dominated by forestry and the extraction of wood is the only significant human related outflow of biomass from the area.
- The dominant outdoor activity is hunting. Besides this, the coastal area is well used for leisure activities such as hiking, canoeing, fishing and boating. The entire coast is of national interest for outdoor life and nature conservation.
- The agriculture in the area is of limited extent. The arable land comprises 3.5% of the total land area, compared with 11.5% in the county as a whole. A wide spectrum of crops is cultivated, but the major crop is barley. Its significance has grown during the 1990s. The second most important crop, oats, is decreasing in importance.

The flow of carbon to humans from the drainage area of Lake Frisksjön (drainage area number 7, cf. Figure 4-3 and Figure 4-14) has been calculated according to the methodology described in /Lindborg, 2005/. The result is presented in /Lindborg, 2005/ and in Figure 4-9. The figures are used in the terrestrial ecosystem model that is described in Section 4.8.1.

4.8 Development of the ecosystem models

The drainage area of Lake Frisksjön (Figure 4-14) was chosen as the model area when developing a terrestrial and limnic ecosystem model. The drainage area is 2.06 km^2 and the lake has a total surface area of 0.13 km^2. Basin Borholmsfjärden, west and south of the Äspö HRL, was used for the marine modelling. The ecosystem models were developed as stand-alone models. No efforts have been made in this version to link the models.

4.8.1 Terrestrial ecosystem description

The dominating vegetation types in the drainage area are forests, primarily pine on acid rocks (granites) and pine forest of mesic-moist type. Some agricultural land is also present.

A considerable amount of information describing elemental and nutrient pools and fluxes of matter, and the various degrees of spatial resolution of this information, called for implementation of the conceptual model on a number of the vegetation types, before a carbon budget could be presented for the complete catchment area. These data are presented with commentaries in /Lindborg, 2005/.

The descriptive ecosystem model is applied at the landscape level (regional or subregional) covering the discharge area. Pools and fluxes for all vegetation types are summed using the GIS tool. The descriptive model has been reduced to a limited number of boxes and fluxes, and is presented in Figure 4-15. The carnivore box is the sum of all carnivores presented in Figure 4-9. Where measures of biomass, faecal transfers and mortality were missing, the simple assumption was made that these were, on average, the same as for those animals for which these quantities were known. The

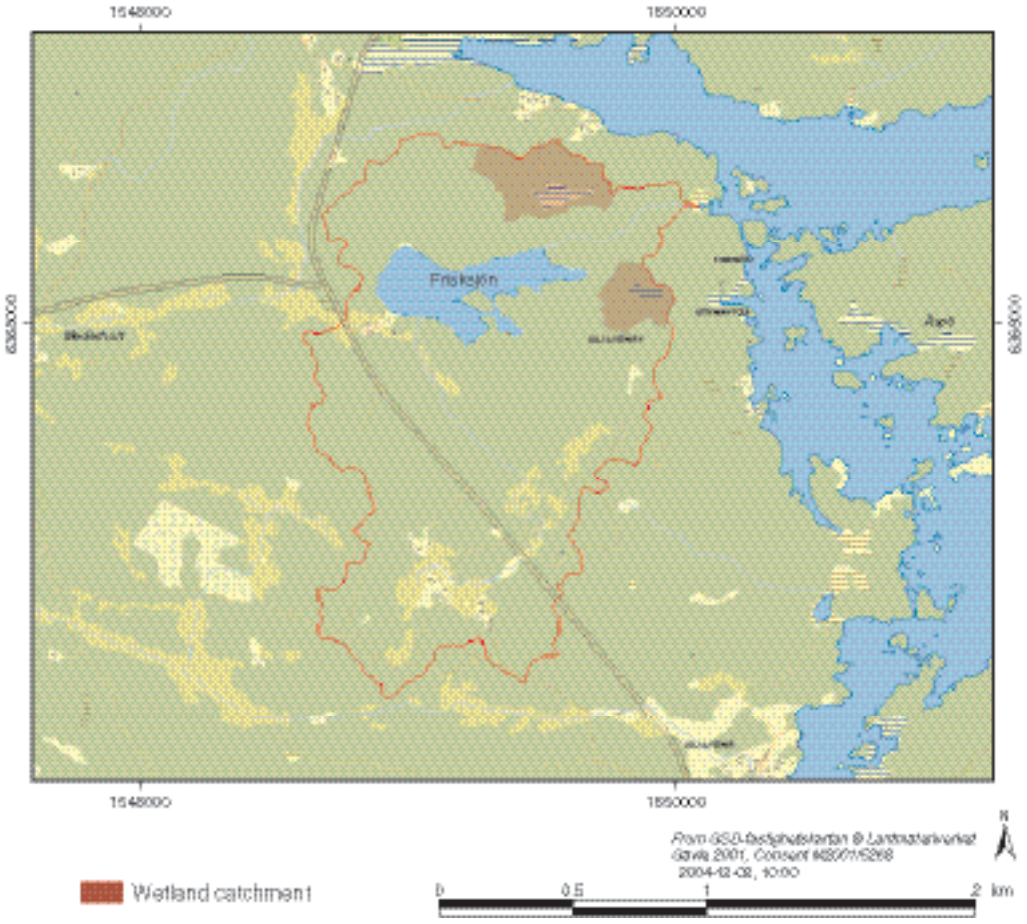

Figure 4-14. *The drainage area of Frisksjön (drainage area 7) near the coast at the Simpevarp area.*

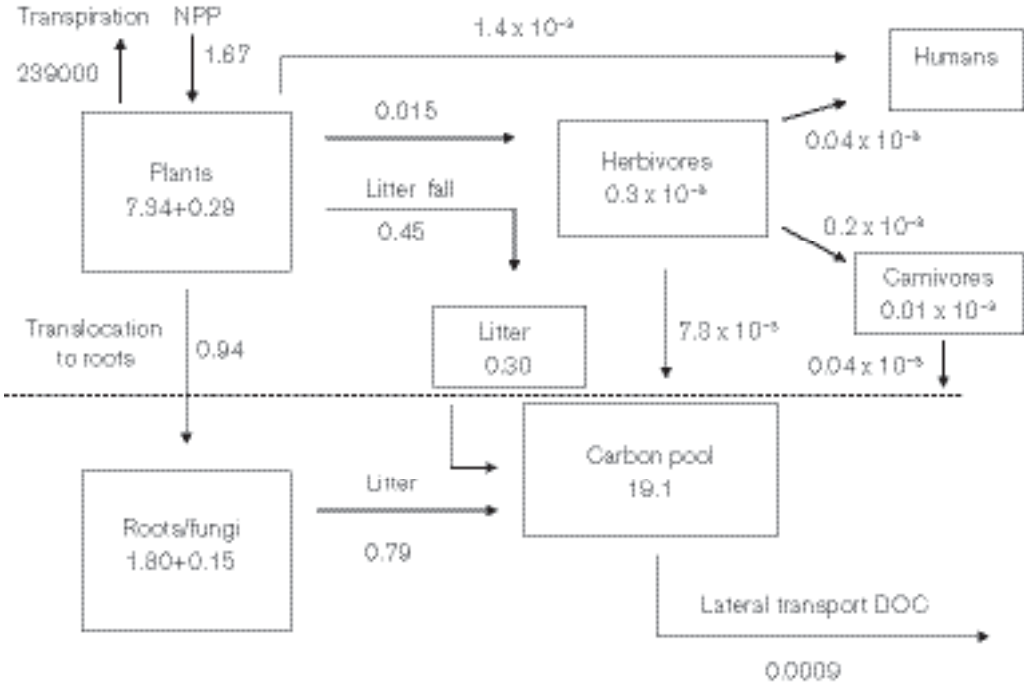

Figure 4-15. *Major pools and net fluxes of carbon for the drainage area Frisksjön. Transpiration is in m^3y^{-1}, number in boxes are in 1×10^9 gC and numbers describing fluxes in 1×10^9 gCy^{-1}. Annual net changes (in 1×10^9 gCy^{-1}) for plants and roots/fungi are shown within the boxes.*

transfer from vegetation to humans represents crops from the agricultural land in the discharge area, and berries and fungi that are utilised, see /Lindborg, 2005/ for more information underlying these numbers. The flux from herbivores to humans is the utilised meat after slaughter. If a steady state between carbon input to Soil Organic Carbon (SOC) and C-mineralisation is assumed, the C-mineralisation should approximate 1.24×10^9 gCy^{-1}.

The total lateral transport of DOC was calculated using a number from /Canhem et al. 2004/ that estimated leaching of DOC from conifer forests into lakes to 3.5 $gCm^{-2}y^{-1}$. This number was multiplied with the total discharge area (lake area of 0.13 km^2 subtracted). This resulted in the total amount of 0.94×10^6 gCy^{-1} transported as DOC from the terrestrial land types in the discharge area.

4.8.2 Limnic ecosystem description

Lake Frisksjön is the only lake in the selected drainage area. The lake has a total surface area of 0.13 km^2, a maximum depth of 2.8 m and a mean depth of 1.7 m. Similar to most lakes in the region, the water colour is brown, and despite the relatively shallow water depth, large areas of the bottom are below the light penetration depth. The theoretical turnover time for the lake is 264 days. For a detailed description of the hydrological, chemical and biological characteristics of the lake, see /Lindborg, 2005/.

Food web matrix for Lake Frisksjön

For the development of an ecosystem model, the major functional groups, producers and consumers, were further divided into a number of subgroups based on taxonomy, choice of habitat and food preferences. The consumption of different food sources for each functional group was obtained by first identifying the food-web relationships between all groups in the system. Consumers were assumed to eat in proportion to what is available of their food item/prey (in terms of biomass). The food-web relationships, together with food availability, were used to calculate the food-web matrix for Lake Frisksjön (Table 4-8).

Table 4-8. Food web matrix for Lake Frisksjön, including estimated food proportions of different food sources (columns) for the different organism groups (rows). DOC = Dissolved Organic Carbon, POC = Particulate Organic Carbon, DIC = Dissolved Inorganic Carbon.

	Phytoplankton	Macrophytes	Epiphytic algae	Epiphytic bacteria	Epiphytic fauna	Bacterioplankton	Zooplankton	Z-fish	B-fish	C-fish	Benthic bacteria	Benthic fauna	DOC	POC	DIC
Phytoplankton						0.22					0.28				0.50
Macrophytes															1.00
Epiphytic algae															1.00
Epiphytic bacteria													0.96	0.04	
Epiphytic fauna			0.50	0.50											
Bacterioplankton													0.96	0.04	
Zooplankton	0.44					0.15	0.41								
Z-fish (zooplanktivore)							1.00								
B-fish (benthivore)			0.06	0.06	0.00							0.88			
C-fish (carnivore)								0.03	0.50	0.47					
Benthic bacteria														1.00	
Benthic fauna	0.02					0.01	0.03				0.81	0.05		0.08	

Primary producers obtain their carbon from the DIC (Dissolved Inorganic Carbon) pool. However, since phytoplankton partly consists of mixotrophic species, they can also use other carbon sources, mainly bacteria. The estimated biomass of benthic bacteria in the lake is very high and, since organisms are assumed to eat in proportion to what is available of their potential food sources, bacteria is estimated to contribute more than a quarter of the phytoplankton carbon need. This high proportion of heterotrophic carbon may be an overestimate and has to be evaluated in future work. Humans and birds are not included in the food web matrix, as quantitative data for these groups are lacking.

Carbon budget for Lake Frisksjön

Both biomass and production of primary producers in Lake Frisksjön are dominated by macrophytes (Table 4-9). Lake respiration is strongly dominated by bacteria, both benthic and pelagic, which together made up 92% of the total respiration in the lake. Accordingly, bacteria also make up the main part of the consumption in the lake (84%).

Taken on an annual basis, almost all groups of organisms show a carbon excess when subtracting respiration and grazing from production/consumption. Since there is no increase in biomass over time, this excess carbon is assumed to contribute to the POC pool (Particulate Organic Carbon).

The carbon budget indicates that respiration in Lake Frisksjön is about 10 times higher than primary production. Thus, the lake must be sustained with carbon from allochtonous sources, e.g. inflow of humic substances from the surroundings. This agrees well with the brown water colour of the lake and the high concentrations of dissolved organic substances. The net inflow and outflow of organic carbon (DOC and POC) to and from the lake has not been included in the calculations. A rough estimate of carbon transport, based on measured TOC (total organic carbon) in lake surface water and modelled discharge, indicates that the annual transport of organic carbon from the lake is approximately 4.7×10^6 g. Thus, annual carbon outflow is in the same order of magnitude as both the annual primary production and the average carbon pool in lake water, while it is about 10 times lower than the total annual respiration.

Table 4-9. Total average biomass (gC) and annual metabolic rates (gC year^{-1}) of functional organism groups in Lake Frisksjön. Note that phytoplankton includes both autotrophic and mixotrophic species and hence show primary production, as well as respiration and consumption.

Functional group	Biomass		Prim. prod.		Respiration		Consumption	
	gC	%	gC y^{-1}	%	gC y^{-1}	%	gC y^{-1}	%
Pelagic habitat	**1.8E+5**	**6.8**	**1.8E+6**	**27.2**	**2.6E+7**	**48.9**	**3.9E+7**	**51.5**
Phytoplankton	3.8E+4	1.4	1.8E+6	27.2	9.1E+5	1.7	1.8E+6	2.4
Bacterioplankton	1.3E+4	0.5			2.2E+7	41.6	2.9E+7	38.4
Zooplankton	7.0E+4	2.6			2.5E+6	4.8	7.6E+6	9.9
Z-fish (zooplanktivore)	2.0E+3	0.06			9.0E+3	0.02	1.5E+4	0.02
B-fish (benthivore)	3.1E+4	1.2			1.8E+5	0.3	3.1E+5	0.4
C-fish (carnivore)	2.9E+4	1.1			1.7E+5	0.3	2.9E+5	0.4
Benthic habitat	**1.8E+6**	**66.3**	**0**	**0**	**2.7E+7**	**50.9**	**3.7E+7**	**48.2**
Benthic bacteria	1.7E+6	62.1			2.6E+7	49.7	3.6E+7	45.8
Benthic fauna	1.1E+5	4.2			6.3E+5	1.2	1.9E+6	2.5
Littoral habitat	**7.2E+5**	**26.9**	**4.9E+6**	**72.8**	**1.7E+5**	**0.3**	**2.3E+5**	**0.3**
Macrophytes	7.1E+5	26.3	4.5E+6	67.8				
Epiphytic algae	7.0E+3	0.3	3.4E+5	5.1				
Epiphytic bacteria	7.0E+3	0.3			1.7E+5	0.3	2.3E+5	0.3
Epiphytic fauna	1.4E+2	0.0			6.0E+2	0.0	1.8E+3	0.0
Lake total	**2.7E+6**		**6.7E+6**		**5.3E+7**		**7.6E+7**	
Carbon pools in lake water (kgC)								
DIC	4.8E+5							
DOC	3.6E+6							
POC	1.6E+5							

4.8.3 Marine ecosystem description

Basin Borholmsfjärden is located west and south of the island of Äspö and has a total surface area of 1.37 km^2 and water volume of 0.024 km^3. The maximum depth in this basin is about 4.2 m, the average depth is 1.7 m and light penetration depth is about 2.2 m (based on field measurements). As the photic zone is assumed to be twice the light penetration depth, the whole basin is assumed to be photic. The average water retention time over a year in this basin is about 9 days.

Food web matrix for Borholmsfjärden

Assuming that the functional groups in the basin Borholmsfjärden consume in proportion to the available biomass of their respective food source, the resulting food web matrix for the basin is shown in Table 4-10 and Table 4-11.

Carbon budget for Borholmsfjärden

The biomass and primary production is clearly dominated by macrophytes and microphytes (Table 4-11). Phytoplankton plays a minor role in terms of carbon flow in the system. The same pattern, in which benthic organisms dominate over the pelagic, is also found among consumers. In terms of biomass, benthic organisms (especially detritivores) are the largest group.

All modelled compartments, except zooplankton and benthic bacteria, are in excess on an annual scale, i.e. the supply of biomass from the compartment was higher than the demand of its predators. The possible explanation for benthic bacteria being extinct in the model evaluation is an overestimation of the predation by the large group of benthic detritivores. It might also be due to an underestimation of the importance of POC (particulate organic carbon) as a food source for benthic detrivores.

Table 4-10. Food web matrix showing food proportions (estimated from the food web matrix and the identified available biomass of their respective food source) for Basin Borholmsfjärden in the Simpevarp area. DIC = Dissolved Inorganic Carbon, POC = Particulate Organic Carbon.

	Phytoplankton	Microphytes	Macrophytes	Bacterio-plankton	Zooplankton	Zooplanktivore fish	Benthivore fish	Carnivore fish	Benthic herbivores	Benthic filter feeders	Benthic detrivores	Benthic carnivores	Benthic bacteria	DIC	POC
Phytoplankton														1.00	
Microphytes														1.00	
Macrophytes														1.00	
Bacterioplankton															1.00
Zooplankton	0.53			0.47											
Zooplanktivore fish					1.00										
Benthivore fish									0.20	0.04	0.53	0.22			
Carnivore fish						0.75	0.20	0.05							
Benthic herbivores		0.11	0.89												
Benthic filter feeders	0.04			0.04	0.12										0.81
Benthic detrivores													0.53		0.47
Benthic carnivores									0.26	0.06	0.68				
Benthic bacteria															1.00
Fish feeding birds						0.75	0.20	0.05							
Benthic feeding birds			0.90						0.02	0.00	0.05	0.02			
Seals						0.75	0.20	0.05							
Humans						0.75	0.15	0.10							
DIC															
POC															

Table 4-11 also presents a deficit of POC (negative excess) which probably is due to the fact that neither the influx of POC from terrestrial runoff, nor the water exchange with other basins of the sea, has been included in the calculations. Taking the POC inflow from these sources into account would probably lead to a positive excess of POC in the budget. This would also lead to a higher proportion of the consumption of POC by benthic detrivores and, consequently, the predation pressure on benthic bacteria would decrease and they would be able to sustain a non-zero population. However, the data on bacteria are not site-specific which may contribute to an underestimated standing stock in the area. The reason for the estimated "negative excess" for the zooplankton compartment is possibly due to an overestimation of the fish feeding biomass and/or their consumption rate. The fish biomass data are not site-specific and the estimations of the metabolic rates of fish are not attributed high confidence.

A summary of the biomass, annual primary production or consumption, respiration, supply (available for consumption), consumption and excess in the ecosystem by each functional group are summarised in Table 4-11. The carbon budget is illustrated graphically as a food web in /Lindborg, 2005/.

In the calculations presented in this section the net inflow of DIC (dissolved inorganic carbon) and POC from run-off and exchange with other sea basins have not been included. For basin Borholmsfjärden the annual terrestrial runoff contributes approximately 1.6×10^7 gPOC. The basin has a modelled retention (residence) time of 9 days which possibly generates an exchange of 4.8×10^7 gPOC. Together, run-off and water exchange could provide about 6.3×10^7 gPOC to the basin which correlates quite well with the calculated depletion of POC of -5.69×10^7 gPOC (Table 4-11). However, the total excess of biota, i.e. supply – available for grazing or predation, also contributes to the POC pool and thus, the total annual contribution of POC is almost 9×10^8 gC, which also indicate that there is a net sedimentation of carbon in the analysed area.

Table 4-11. Biomass (gC basin^{-1}), annual primary production or consumption of carbon by each functional group (gC basin^{-1} yr^{-1}), respiration (gC basin^{-1} yr^{-1}), supply (available for grazing or predation) (gC basin^{-1} yr^{-1}), grazing or predation on the functional groups (gC basin^{-1} yr^{-1}) and excess (gC basin^{-1} yr^{-1}) in the ecosystem in the basin Borholmsfjärden. Seals have been excluded due to lack of data.

Borholmsfjärden	Biomass gC	Prod. or Cons. gC yr^{-1}	Respiration gC yr^{-1}	Supply[1] gC yr^{-1}	Graz. or pred.[2] gC yr^{-1}	Excess[3] gC yr^{-1}
Phytoplankton	6.45×10^4	4.27×10^6	–	4.27×10^6	4.26×10^6	1.13×10^4
Microphytes	7.31×10^6	1.03×10^8	–	1.03×10^8	1.69×10^6	1.01×10^8
Macrophytes	5.86×10^7	7.19×10^8	–	7.19×10^8	1.48×10^7	7.04×10^8
Bacterioplankton	5.69×10^4	9.20×10^6	4.60×10^6	4.60×10^6	3.76×10^6	8.40×10^5
Zooplankton	1.89×10^5	7.79×10^6	2.60×10^6	5.19×10^6	9.42×10^6	-4.22×10^6
Zooplankton feeding fish	7.62×10^5	9.05×10^6	3.02×10^6	6.04×10^6	6.74×10^5	5.36×10^6
Benthic feeding fish	2.03×10^5	2.41×10^6	8.05×10^5	1.61×10^6	1.70×10^5	1.44×10^6
Carnivorous fish	5.08×10^4	6.04×10^5	2.01×10^5	4.02×10^5	5.46×10^4	3.48×10^5
Benthic herbivores	1.37×10^6	1.53×10^7	5.08×10^6	1.02×10^7	5.38×10^6	4.79×10^6
Benthic filter feeders	2.89×10^5	3.09×10^6	1.03×10^6	2.06×10^6	1.13×10^6	9.25×10^5
Benthic detrivores	3.58×10^6	4.44×10^7	1.48×10^7	2.96×10^7	1.41×10^7	1.55×10^7
Benthic carnivores	1.47×10^6	1.86×10^7	6.20×10^6	1.24×10^7	5.59×10^5	1.18×10^7
Benthic bacteria	1.45×10^6	2.55×10^7	1.28×10^7	1.28×10^7	2.34×10^7	-1.07×10^7
Fish feeding birds	5.80×10^2	1.01×10^5	3.38×10^4	6.76×10^4	–	6.76×10^4
Benthic feeding birds	1.52×10^4	1.33×10^6	4.43×10^5	8.87×10^5	–	8.87×10^5
Humans	–	1.94×10^5	–	1.94×10^5	–	1.94×10^5
DIC	2.76×10^7	–	–	2.76×10^7	8.26×10^8	-8.04×10^8
POC	1.30×10^6	–	–	1.30×10^6	5.82×10^7	-5.69×10^7
Total (only biota)	7.54×10^7	(prod.) 8.26×1^8	5.16 × 107	9.12×10^8	7.94×10^7	8.33×10^8
	–	(cons.) 1.38×10^8	–	–	–	–

[1] Supply = consumption – respiration.

[2] Grazing or consumption upon the respective functional group.

[3] Excess = supply – grazing or predation.

4.9 Evaluation of uncertainties

In this section we are discussing the uncertainties involved in the description of the surface systems. The uncertainties are also summarised in Chapter 12.

4.9.1 Abiotic descriptions

Uncertainties in the present descriptions of the climate, and the geology, hydrology and hydrogeology of the surface system are discussed in /Lindborg, 2005/. The main uncertainties are related to the limited availability of site data, especially for areas outside the Simpevarp subarea and for temporally variable parameters for which time series so far are short or non-existent. In particular, both the geological and hydrogeological descriptions are uncertain due to the limited information on the surface distribution and stratigraphy of Quaternary deposits currently available for most of the regional model area.

Important uncertainties identified in the modelling of surface hydrology and near-surface hydrogeology are associated with the geometrical description of the system (the DEM, the Quaternary deposits and the description of the water courses), the limited data on the hydrogeological properties of site-specific materials, and the limited data available for assessing the temporal variations of the hydrological and hydrogeological processes. The next “data freeze”, for Laxemar 1.2, will contain data from geological and hydrogeological investigations of Quaternary deposits within the Laxemar subarea, and extended time series of meteorological and hydrological data. It is expected that these data will reduce the uncertainties associated with the abiotic descriptions.

4.9.2 Biotic description

Terrestrial ecosystem

For the overall carbon budget, the importance of the different pools and fluxes is set by their relative size. This means that large variations or uncertainties in relatively large pools/fluxes overshadow the influence of relative smaller pools/fluxes. This has often been an argument to justify why some smaller pools or fluxes have been left out. There is a large spatial variation within the regional area as an effect of different abiotic conditions and due to disturbances, such as logging and thinning in the forestry industry. The biomass of trees is probably the type of data that has the best estimate in this carbon budget, since it is sampled from a fairly large regional area covering a large number of age classes and abiotic conditions.

It should be noticed that the production figures of mammals, given as a percentage of the biomass, are roughly calculated and are not to be regarded as well-established values.

The largest stocks and flows are associated with trees (except for Soil Organic Carbon). This means that a low confidence in these values will have a large effect on the overall confidence in the descriptive models. The estimates of tree properties are, however, the best estimates there are (compared with all the data used), in the sense of number of replicates, coverage of the region and the allometric functions used within the National Forest Inventory to calculate biomass for the fractions above ground. However, there is a large variation of standing crop depending on a number of factors such as nutrient status and wetness.

An assumption of a steady state has repeatedly been applied when quantifying turnover of plant tissue. This assumption in some cases entails an overestimation of the actual turnover because there some net accumulation in perennial taxa, but there is a lack of data describing these processes on the community level. In other cases, the assumption is more justified, e.g. root turnover /Majdi, 2001/.

Interestingly, few or no single studies have been able, or designed, to estimate all the properties that are treated above. Partly, because of the laborious work involved, but also because many of the pools and fluxes are small in comparison, and are therefore expected to have a small influence on the overall carbon budget.

Limnic ecosystem

The conclusion that Lake Frisksjön is dominated by respiration can be considered highly realistic. Humic lakes with high water colour favour heterotrophic bacteria, whereas phytoplankton and primary production tends to be light limited. However, biomass, production and respiration of bacteria have not been measured in Lake Frisksjön and, therefore, the magnitude of these parameters may be under- or overestimated. Literature values have been taken from lakes as similar to Lake Frisksjön as possible, although studies of epiphytic and benthic bacteria are not as common as for bacterioplankton and thus these values are associated with some uncertainties.

The production of phytoplankton has been taken from a mean of several coloured lakes and can be assumed to be in the right order of magnitude. The biomass was calculated from chlorophyll a measurements in the lake. The ratio of chlorofyll a:C may vary with status of the algal community and, therefore, the biomass could be under- or overestimated. The biomass of phytoplankton was relatively high and was probably somewhat overestimated. This agrees well with the observation that there is not enough of phytoplankton production, but an excess of bacterioplankton consumption, in our budget. As grazing is related to the biomass of the prey, smaller biomass would also lead to smaller grazing pressure and the phytoplankton production would be enough to sustain the standing stock.

Zooplankton biomass usually has a high seasonal variation. However, biomass has only been measured on three occasions. Moreover, on one occasion the biomass was extremely high, whereas it was low on the other two occasions. This makes it difficult to elucidate the biomass and respiration and consumption of this consumer. In this budget the biomass of zooplankton is high. This seems reasonable, as there is a large pool of bacteria and phytoplankton for the zooplankton to utilise as food and a low predation pressure from zooplanktivore fish, which in turn is most probably suppressed by carnivorous fish.

In conclusion, despite there being many parameters that are not measured in the lake, this carbon budget is thougt to be close to reality. When data were lacking, data have been obtained from lakes as similar to Lake Frisksjön as possible, and the main pattern seen in other humic lakes with a dominance of respiration from bacteria was seen also here when using these literature values.

Marine ecosystem

Carbon transport to and from the basins is based on modelled oceanographic water movement (turnover- or residence time), which is described in detail along with modelled run-off from land in /Lindborg, 2005/. Concentrations of DIC and POC were based on a 2.5 year monitoring sampling programme with samples taken every third week. The estimation of total carbon flow is considered to be of low quality, since the variation of concentration of carbon and run-off is great and these two parameters are normally covariates and only averages for each parameter are used here. In later versions of the site-descriptive modelling of the Simpevarp area, site-specific high resolution data on run-off will become available.

The quality and representativity of the used data have been summarised in Table 4-12 and are discussed in more in detail below.

The bathymetric data used to estimate the *areas* and *volumes* of the basins originate from a combination of recent site-specific measurements and existing digital nautical charts and have a very high quality /Lindborg, 2005/.

The estimates of the extensions of the *photic* and *aphotic zones* are based on the rough assumption that the photic zone is twice the light penetration depth (which has been measured in the field).

Table 4-12. Estimations of the quality of input data and their representativeness for the basins in the Simpevarp area. High values indicate high quality or better representativity.

Functional group	Quality of data (1–4)	Representativity of data (1–4)
Areas and volumes	4	4
Photic zone	3	4
Carbon transport	2	2
DIC	2	4
POC	2	4
Phytoplankton	2	4
Macrophytes	3	4
Bacterioplankton	3	2
Zooplankton	2	4
Z- fish (zooplankton feeding fish)	2	1
B- fish (bentic fauna feeding fish)	2	1
C- fish (carnivorous fish)	2	1
Benthic herbivores	3	3
Benthic filter feeders	3	4
Benthic detrivores	3	4
Benthic carnivores	3	3
Benthic bacteria	3	2
Fish feeding birds	1	4
Benthic feeding birds	1	4
Humans	2	2

The primary production was generally estimated from the biomass, conversion factors, and the insolation during the year. It would have been optimal to measure the primary production at the sites during the year. However, the calculated primary production probably has a sufficiently good quality, since the conversion factors used are species-specific and mostly obtained from the Baltic Sea, and the insolation measurements used in the calculations are site-specific. The assumption that the epiphyte biomass and primary production were included in the macrophyte estimates probably contributes to an underestimation in biomass, but all more to an underestimate of primary production.

The reasoning applicable for the estimates of the primary production also applies to the estimates of the respiration, i.e. that real measurements would have given a better estimate than the calculations used in this study. However, as in the case of primary production, species-specific conversion factors indicated that the calculations are fairly correct. The assumption that the respiration to consumption ratio is approximately 1:3 is a fairly accepted relationship, as is also that it is less for bacteria (1:2), since their metabolism has a higher rate.

Human population description

Most of the data in /Miliander et al. 2004/ were obtained from Statistics Sweden (SCB). When only a single object is found within a geographic area, SCB adjusts this single object to a “false” zero for reasons of secrecy. If two objects are found, the count is adjusted to three (SCB, 2003). This can result in incoherence between the sum of values for different categories and the total number (as an example the total number of inhabitants and the sum of inhabitants per age class). Also, for sparsely populated areas the data becomes more statistically unreliable, irrespective of the above deliberate reporting bias.

Furthermore, there are some uncertainties concerning the data from the Department of Fisheries (Fiskeriverket). The catch statistics within the offshore grid (EU-grid) only comprise the catch from the logbook-keeping vessels, as they report the tackle position. Second, the catch is registered in the square where the tackle is placed, but that does not necessarily mean that the fish have been caught in that particular square. Fishing boats can trawl a long distance and, therefore, catch the main part of the fish in a neighbouring square. Therefore the catch data at each EU-square varies, considerably between the years.

5 Bedrock geology

The bedrock geological model consists of three components; the rock domain model, the deterministic deformation zone model, and the statistical analysis of fractures and lineaments, the so-called discrete fracture network (DFN) model. The work has been carried out according to the strategy described in /Munier et al. 2003/. In contrast to the version Simpevarp 1.1 model, the rock domain and deterministic deformation zone models are presented for the whole regional model volume. The DFN model has utilised fractures essentially from within the local model volume. Only fractures that are situated outside deformation zones have been included in the DFN model. Alternative models are presented only for the geological DFN model.

One or more components of the bedrock geological model provide a foundation for the modelling work in rock mechanics, thermal properties, hydrogeology (bedrock) and, to less extent, even hydrogeochemistry (bedrock) and transport properties (bedrock). All components of the geological model have a direct impact on the location and design of the repository volume. They also provide a significant input for the safety analysis work.

5.1 State of knowledge at the previous model version

The Simpevarp version 1.1 only comprised the eastern part of the local scale model area, i.e. principally the Simpevarp subarea /SKB, 2004b/.

In contrast to the reconnaissance character of the surface geological information in the version 0 part of the model area in the Simpevarp 1.1 model version, the age, character and surface extension of the dominant rock types are well established within the Simpevarp subarea. However, this variation in quality of the surface geological data and the restricted subsurface information are the two most important factors that govern the uncertainties associated with the modelling of the seventeen rock domains in the Simpevarp version 1.1. This uncertainty will to a great extent also remain in the modelling for the Simpevarp 1.2 descriptive model. Consequently, the confidence of occurrence and geometry of the rock domains at the surface was judged to be medium to high in the part of the local model area that is covered by the Simpevarp subarea, whereas it is judged to be low to medium outside the Simpevarp subarea. Due to the restricted subsurface information, the confidence of occurrence and geometry at depth is medium to low for most rock domains, except for the interpreted dominating rock domain RSMA01 (dominated by Ävrö granite) which forms the matrix in the local scale model volume. However, the geometrical relationships between rock domain RSMA01 and the other rock domains, in particular the major rock domains, are highly uncertain.

The main uncertainties that are related to the Simpevarp 1.1 lithological model are listed below:

- Lithology below sea and outside the Simpevarp peninsula, Äspö and Ävrö (lower quality data in these areas).
- Three dimensional extension of dioritoid and mixed type domains.
- Proportion of rock types in domains (not evenly distributed at the 50–100 m scale and below, as veins, patches, dykes and occur minor bodies). There could also be statistical anisotropy in their occurrence.
- Distribution, volumetric shape of mafic bodies.
- Three-dimensional extent of “secondary red staining” (hydrothermal alteration).

The Simpevarp 1.1 model included a base case three-dimensional model of deformation zones in the local-scale model. The recognised zones were interpreted with variable confidence. Only zones with a length of 1 km or more were addressed in the deterministic structural model. Older existing structural models, a variety of new surface and sub-surface data, and the interpreted “linked lineaments” were used in the modelling procedure. A total of 63 interpreted deformation zones were included in the local-scale model volume.

The main uncertainties related to the Simpevarp 1.1 deformation zone model were:

- Existence of deformation zones (only some zones are identified with high confidence) – are all lineaments really deformation zones?
- Potentially non-included zones (mainly sub-horizontal).
- Extension (length and depth) of deformation zones (e.g. “linked lineaments”).
- Dip of deformation zones.
- Termination of zones – against each other.
- Character and properties – even in the well-established (e.g. from Äspö) zones there is strong spatial variation of properties (width, fracturing, also hydraulic properties).

A Geological discrete fracture network (DFN) model was developed as part of the Simpevarp 1.1 model which explores the geological and structural controls on evaluated fracture parameters. Two groups of fracture sets were identified: Group 1, consisting of three subvertical sets observed on outcrops and in boreholes, which were related to present-day lineament orientations; and Group 2, consisting of three subvertical fracture orientations and one subhorizontal set observed on outcrop and in boreholes unrelated to current lineament orientations. Intensity was found to be a function of rock type and possibly also alteration. However, alteration may be an effect of fracturing and is not included in the proposed model values.

The main uncertainties related to the Simpevarp 1.1 fracture statistical (DFN) model are listed below:

- Fracture set identification.
- Fracture size distribution – interpolation between lineament and mapped outcrop data and for some sets of fractures only local information could be used making extrapolation to larger sizes highly uncertain.
- Fracture intensity – based largely on surface data – leading to questions of the representativity of these data at depth.
- Spatial model.
- Spatial distribution in different rock domains.

5.2 Evaluation of primary data

No new detailed bedrock information from the surface has been generated in conjunction with the ongoing site investigation programme between the datafreezes for the Simpevarp Site Descriptive Model (SDM) versions 1.1 and 1.2. Apart from the Simpevarp subarea, where the quality of the surface bedrock data is judged to be high, the bedrock geological information in the regional model area, as well as in the western part of the local-scale model area is based on the Site Descriptive Model version 0. It is difficult to judge the quality of the bedrock information in this area, since it is partly based on bedrock maps on the scale 1:250,000 /Bergman et al. 1998, 1999; SKB, 2002b/. Accordingly, the available bedrock data relating to the distribution and description of rock types within the regional model area are of variable quality, whereas the ages of the rock types are judged to be fairly well-constrained. In order to visualise the differences between the bedrock map of the Simpevarp subarea and the bedrock map from model version 0 in a simplified manner, these maps are merged in. The obvious mismatch between the two maps is noted in the western part of the Simpevarp peninsula.

In the Simpevarp subarea of the regional and local scale model areas, the distribution, description and age of the various rock types have been documented with the help of the following information that, to a major extent, has been generated during recently performed site investigation activities:

- An outcrop database with numerical and descriptive data from 353 observation points /Wahlgren et al. 2004/.
- 46 modal analyses (mineral composition) of surface samples, 7 modal analyses from KSH01A, one modal analysis from KSH01B and nine modal analyses from KSH02, recalculated and plotted in a QAPF diagram in order to classify the various rock types /Wahlgren et al. 2004/.

- Chemical analyses of 31 surface samples, 8 analyses from borehole KSH01A, one analysis from KSH01B and eight analyses from borehole KSH02, which have been used to characterise the various rock types /Wahlgren et al. 2004/.
- Petrophysical data from laboratory measurements of samples from ten locations /Mattsson et al. 2003/.
- In situ gamma-ray spectrometry data from 32 locations, including locations on the Äspö island /Mattsson et al. 2003/.
- U-Pb zircon and titanite dating of two of the dominant rock types /Wahlgren et al. 2004/.
- Bedrock geological mapping compiled with the help of the outcrop database and magnetic data from airborne geophysical measurements /Wahlgren et al. 2004/, cf. Figure 5-3. In this report, attention is focussed on the composition, grain size and texture of the rock types in the regional model area. However, the characterisation of the rock types is mainly based on data from the Simpevarp subarea, since no additional bedrock information from the surface has been generated after the completion of the Simpevarp 1.1 report. The petrophysical properties are only briefly discussed since the available information is very limited. Furthermore, the content of uranium is reported since, in particular, anomalously high values ($\geq$ 16 ppm) of the dominant isotope ^{238}U can give rise to high values of ^{222}Rn.

5.2.1 Outcrop mapping

As mentioned above, no new bedrock mapping at the surface has been carried out in between the datafreezes for the Simpevarp model versions 1.1 and 1.2. Accordingly, no detailed bedrock information stored in e.g. an outcrop database exists for the regional and local scale modelling, except for the Simpevarp subarea (Figure 5-1 and Figure 5-2), the latter of which was the base information for site descriptive modelling and the description of the bedrock geology in the Simpevarp 1.1 report.

Rock type distribution on the surface

The bedrock in the Simpevarp regional model area is dominated by intrusive igneous rocks that belong to the approximately 1,810–1,760 Ma old generation of granite-syenitoid-dioritoid-gabbroid rocks in the 1,860–1,650 Ma old so-called Transscandinavian Igneous Belt (TIB), cf. Figure 5-3. The rocks are mostly well preserved and more or less isotropic, but a weak foliation is locally developed. However, low-grade ductile shear zones of mesoscopic to regional character do occur. Another conspicuous rock type in the regional model area is a younger, c. 1,450 Ma old granite.

The distribution of the rock types in the regional and Laxemar part of the local scale model area is based on the Version 0 model, whereas the distribution of the rock types in the Simpevarp subarea is based on documentation produced in connection with the bedrock mapping during 2003 /Wahlgren et al. 2004/, cf. Simpevarp 1.1 /SKB, 2004b/. Due to the lack of detailed bedrock information, the characterisation of the rock types in the regional model area is based on the documentation in the Simpevarp subarea /Wahlgren et al. 2004/ and follows the presentation in the Simpevarp 1.1 report. New information from the ongoing bedrock mapping in the Laxemar subarea and the regional model area, including analytical work, will be presented in the Laxemar 1.2 site-descriptive model report.

It should be mentioned that the bedrock nomenclature employed in the regional model area does not follow that used in the Simpevarp Version 0 /SKB, 2002b/. Rather, an updated nomenclature has been established by SKB (see Appendix 1) and is applied during the ongoing site investigation programme at Oskarshamn. It's relation to nomenclature in the SGU outcrop database is further explained in Appendix 3.

The *regional model area* is composed of six dominant rock types, cf. Figure 5-3, namely:

- Ävrö granite (granite to quartz monzodiorite), medium-grained, generally porphyritic.
- Quartz monzodiorite, medium-grained, equigranular to weakly porphyritic.
- Granite, medium- to coarse-grained.
- Diorite to gabbro.
- Dioritoid, fine-grained, unequigranular.
- Götemar type granite, coarse-grained and fine- to medium-grained.

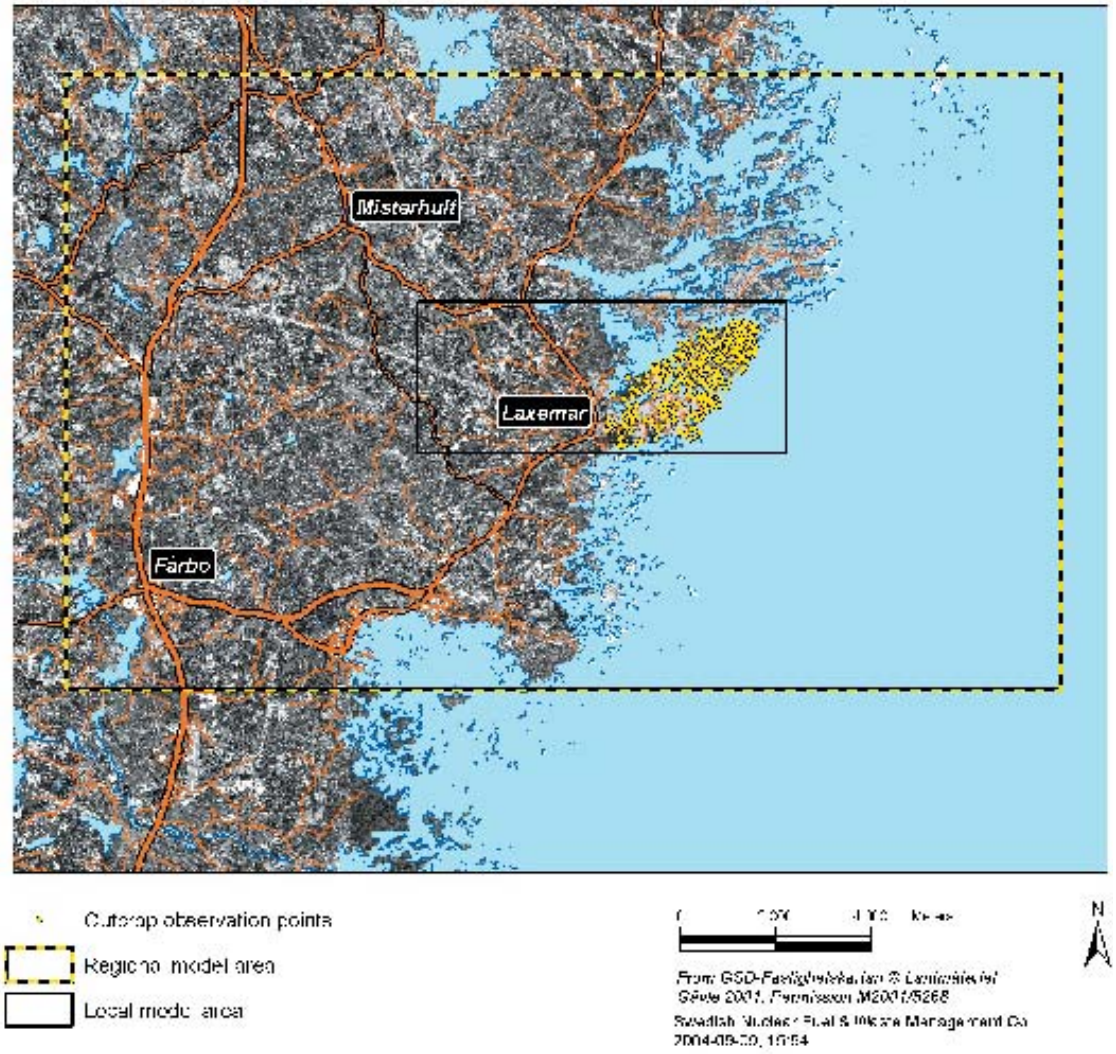

Figure 5-1. *Observation points (yellow) where bedrock outcrop data have been documented during the ongoing site investigation programme /Wahlgren et al. 2004/. The background map is constructed from orthophotography.*

Subordinate rock types in the *regional model area* comprise:

- Granite, fine- to medium-grained.
- Pegmatite.
- Mafic rock, fine-grained (fine-grained diorite to gabbro).

In contrast, only three rock types predominate in the *local scale model area*, cf. Figure 5-3 and Figure 5-2, namely:

- Dioritoid, fine-grained, unequigranular.
- Ävrö granite (granite to quartz monzodiorite), medium-grained, generally porphyritic.
- Quartz monzodiorite, medium-grained, equigranular to weakly porphyritic.

Subordinate rock types in the *local scale model area* comprise:

- Granite, fine- to medium-grained.
- Pegmatite.
- Mafic rock, fine-grained (fine-grained diorite to gabbro).
- Granite, medium- to coarse-grained.
- Diorite to gabbro, medium-grained.

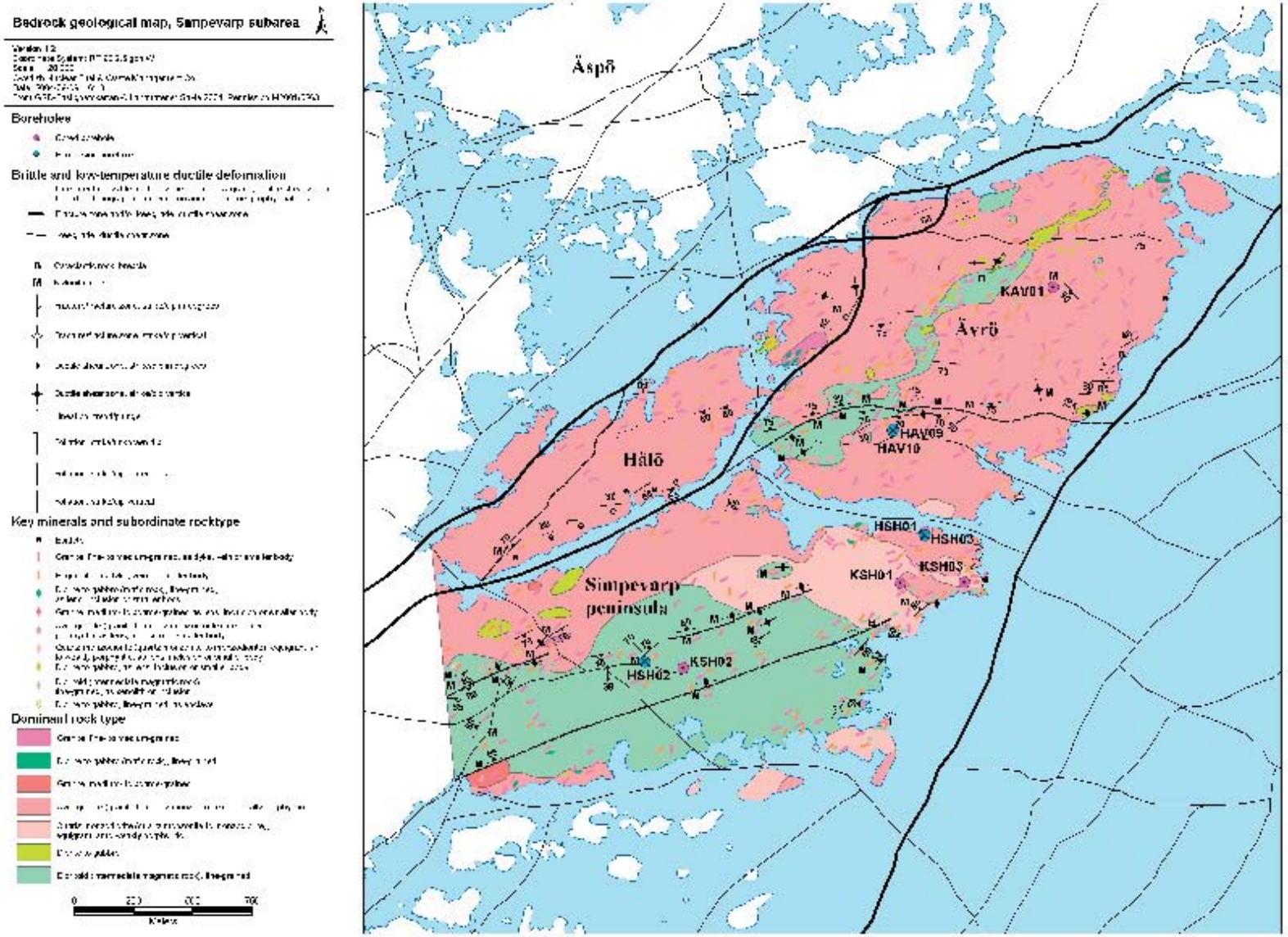

Figure 5-2. *Bedrock map of the Simpevarp subarea.*

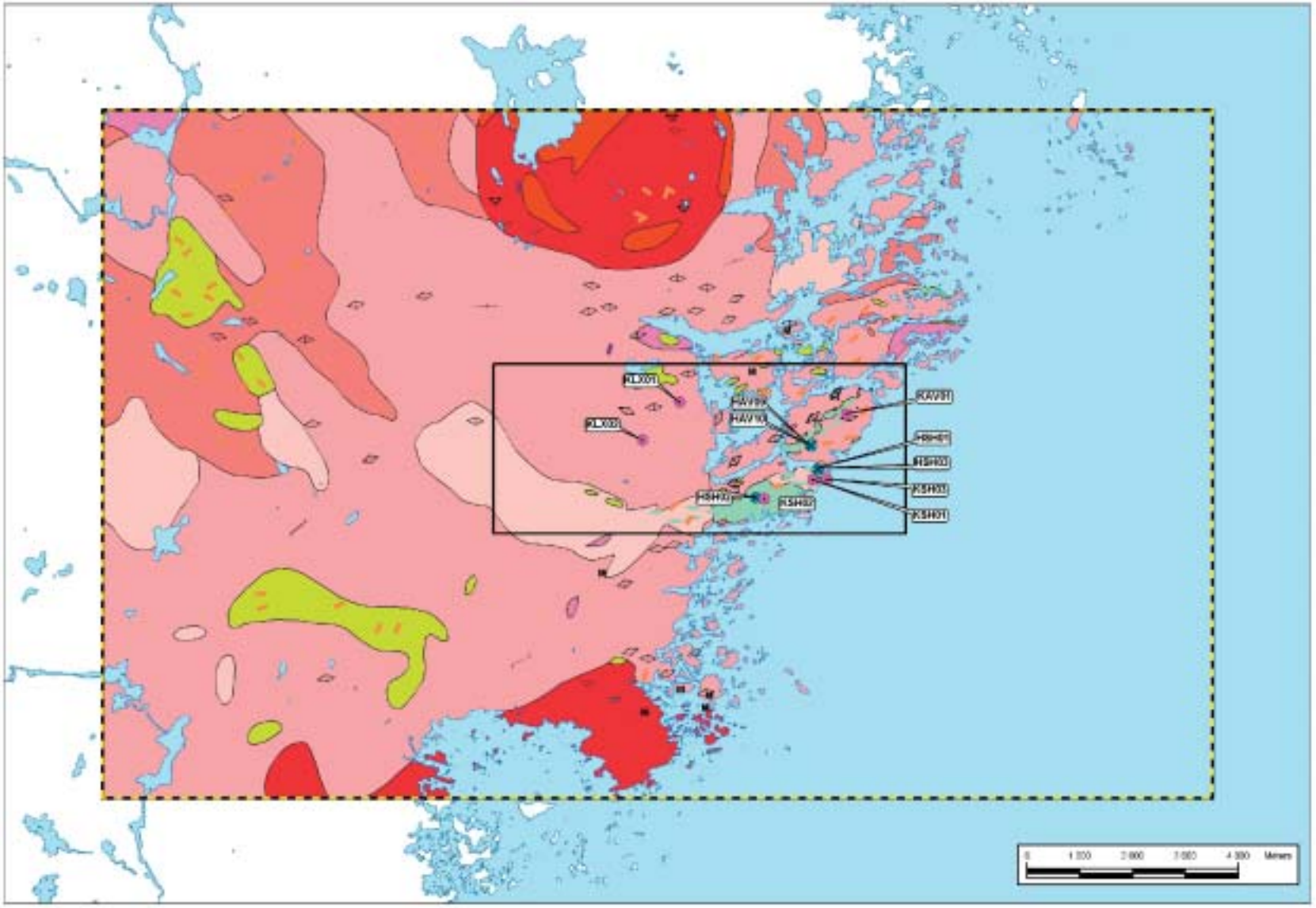

Figure 5-3. *Combination of the bedrock map from the model version 0 in the regional model area and the bedrock map of the Simpevarp subarea (cf. legend in Figure 5-2). Brownish red and red colours mark the Götemar type granites. The solid black frame indicates the local scale model area.*

As can be seen in the QAPF and geochemical classification diagrams (see Figure 5-4, Figure 5-5 and Figure 5-6), the dominant rock types in the Simpevarp subarea display similar and overlapping compositional variations. Petrophysical data obtained from surface samples of the rock types in the Simpevarp subarea are very limited. However, the documentation of the magnetic susceptibility during the bedrock mapping of the Simpevarp subarea displays supporting similar and overlapping values (Figure 5-7). The most important criteria employed in distinguishing between different rock types are texture and grain size.

According to the International Union of Geological Sciences /LeMaitre, 2002/, the classification of rocks should be based on the modal composition. Thus, the geochemical classification diagrams, cf. Figure 5-5 and Figure 5-6, should not be used strictly for classification purposes, but merely as an indication of the compositional trends of the different rock types.

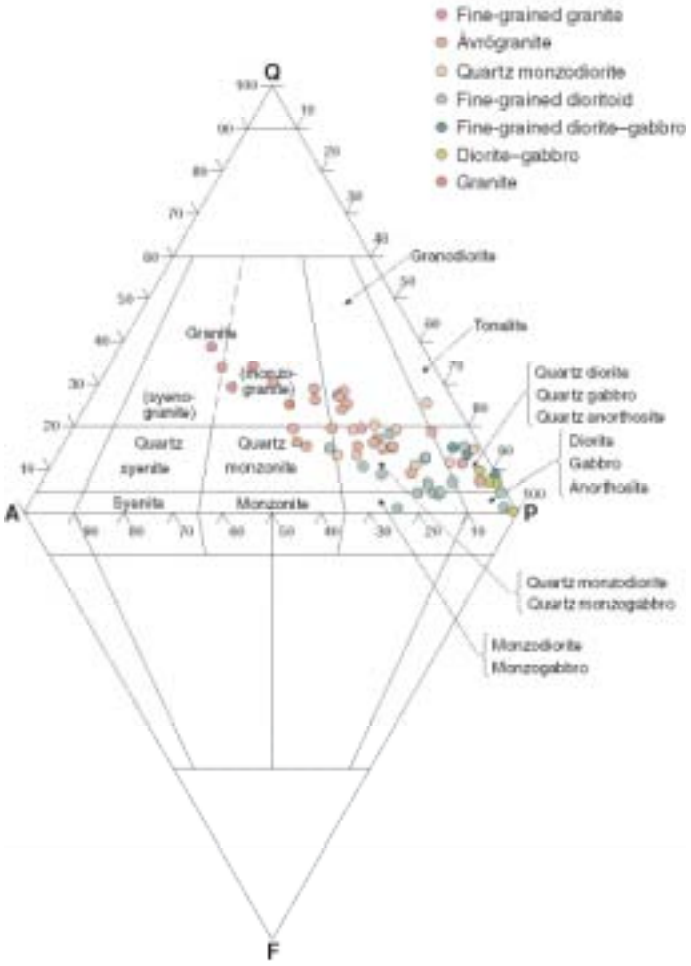

Figure 5-4. *QAPF modal classification /Streckeisen, 1976, 1978/ of rock types in the Simpevarp subarea. Modal analyses of samples from boreholes KSH01A, KSH01B and KSH02 are also included.*

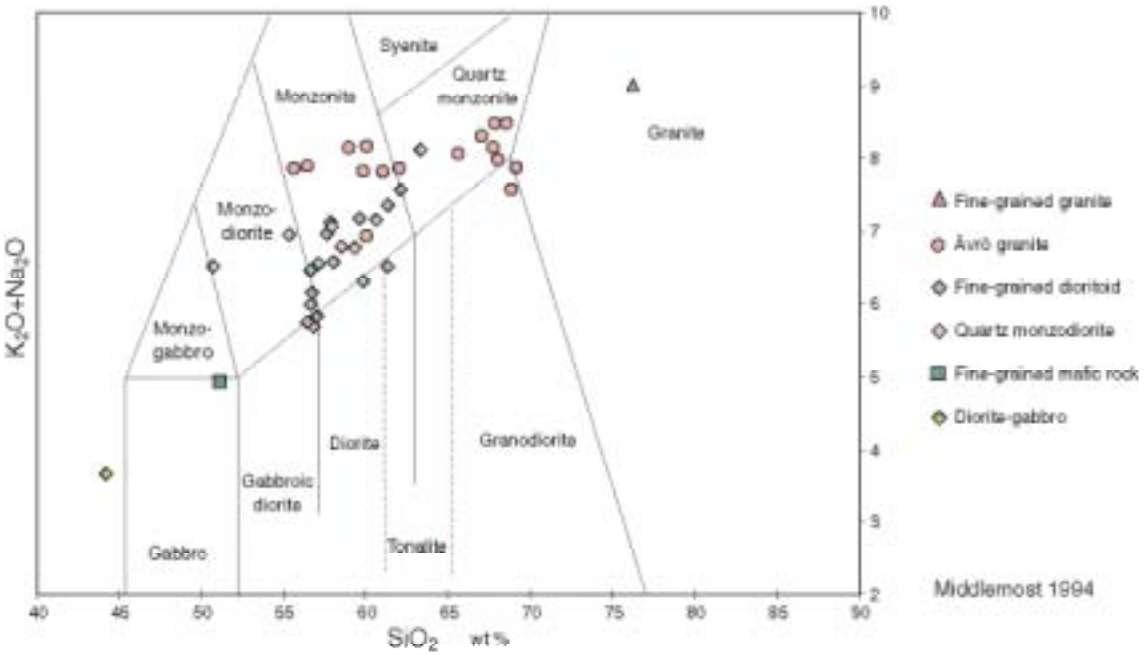

Figure 5-5. *Geochemical classification of rocks from the Simpevarp subarea according to /Middlemost, 1994/. Analyses data from boreholes KSH01A, KSH01B and KSH02 are also included.*

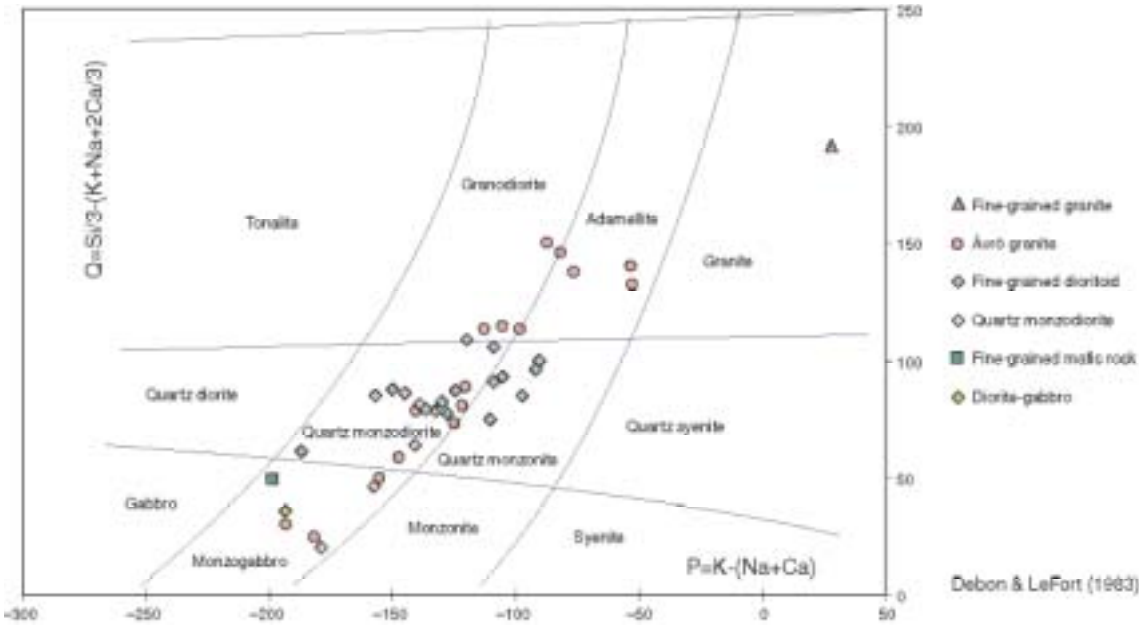

Figure 5-6. *Geochemical classification of rocks in the Simpevarp subarea according to /Debon and Le Fort, 1983/. Analyses data from boreholes KSH01A, KSH01B and KSH02 are also included.*

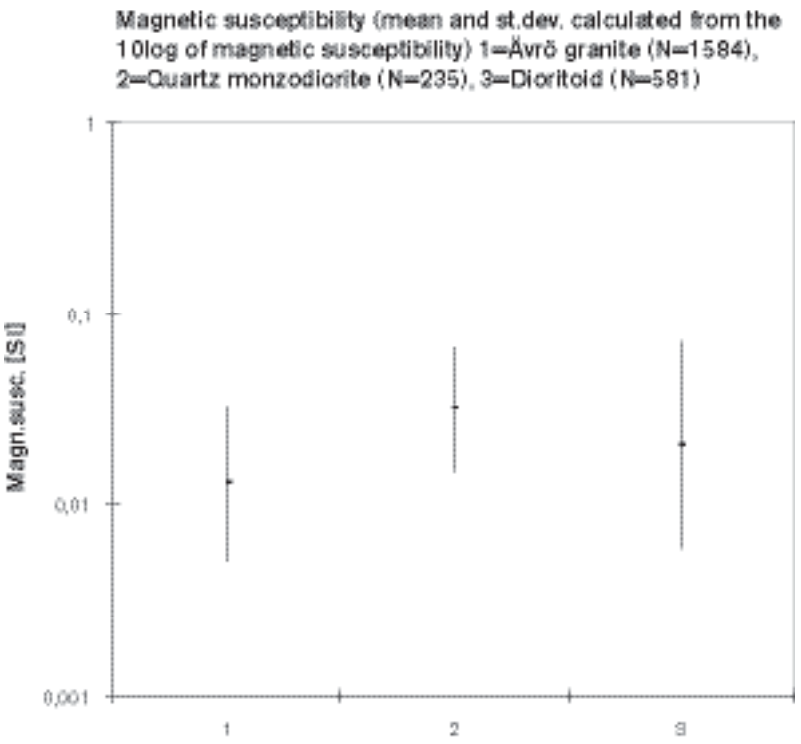

Figure 5-7. *Magnetic susceptibility of the dominant rock types (Ävrö granite, Quartz Monzodiorite and Fine-grained dioritoid) in the Simpevarp subarea. Based on field measurements during bedrock mapping.*

The fine-grained dioritoid dominates the southern part of the Simpevarp peninsula, and the central part of Ävrö island as a NE-trending, narrow, undulating belt (Figure 5-2 and Figure 5-3). It is also verified to constitute the dominating rock type in the cored borehole KSH02 on the Simpevarp peninsula (see Section 5.2.7). The westward extension of the fine-grained dioritoid (cf. Figure 5-3) is uncertain, but this question-mark will be resolved when the detailed bedrock mapping of the Laxemar subarea is completed. Furthermore, the fine-grained dioritoid occurs as minor bodies and inclusions in the Ävrö granite and the quartz monzodiorite.

The fine-grained dioritoid is grey and commonly unequigranular, with up to 3 mm large (exceptionally 5 mm) megacrysts of hornblende and plagioclase (Figure 5-8). Locally, megacrysts of pyroxene and biotite also occur. However, the pyroxene is generally more or less altered to hornblende. Thus, most of the hornblende megacrysts are inferred to be secondary after pyroxene.

A characteristic feature in the fine-grained dioritoid is an inhomogeneous coarsening of the grain size (Figure 5-9). It appears as diffusely delimited vein-like aggregates and patches. The coarsening makes the fine-grained dioritoid resemble the quartz monzodiorite, and consequently, these two rock types are occasionally difficult to distinguish from one another.

The contacts between the dioritoid and the country rocks are usually gradual, but locally the contact is sharp (Figure 5-10).

The compositional variation of the fine-grained dioritoid is displayed in the QAPF modal classification diagram in Figure 5-11. The average density is 2,803 ± 52 kg/m^3.

Figure 5-8. *Fine-grained dioritoid with megacrysts of hornblende (dark grains) and plagioclase (white to light grey grains).*

The fine-grained dioritoid has traditionally been classified as a volcanic rock of dacitic to andesitic composition /SKB, 2002b and references therein/. However, except for being fine-grained, no characteristic criteria indicating that the rock is of volcanic origin were found during the bedrock mapping of the Simpevarp subarea. An alternative interpretation is that the rock constitutes a high-level intrusion that subsequently was intruded by its parent magma, which is represented by the neighbouring quartz monzodiorite in the country rock. The characteristic, inhomogeneous coarsening in the fine-grained dioritoid is inferred to be a late-magmatic phenomenon, presumably due to a thermal input during the emplacement of the quartz monzodiorite and possibly also the Ävrö granite. The uncertainty in the interpretation of the origin of this fine-grained rock of intermediate composition is the primary cause of the more neutral classification as a dioritoid. However, this does not exclude that the rock may be of volcanic origin.

Figure 5-9. *Inhomogeneously coarsened, fine-grained dioritoid.*

Figure 5-10. *Contact between fine-grained dioritoid (lower part) and quartz monzodiorite (upper part).*

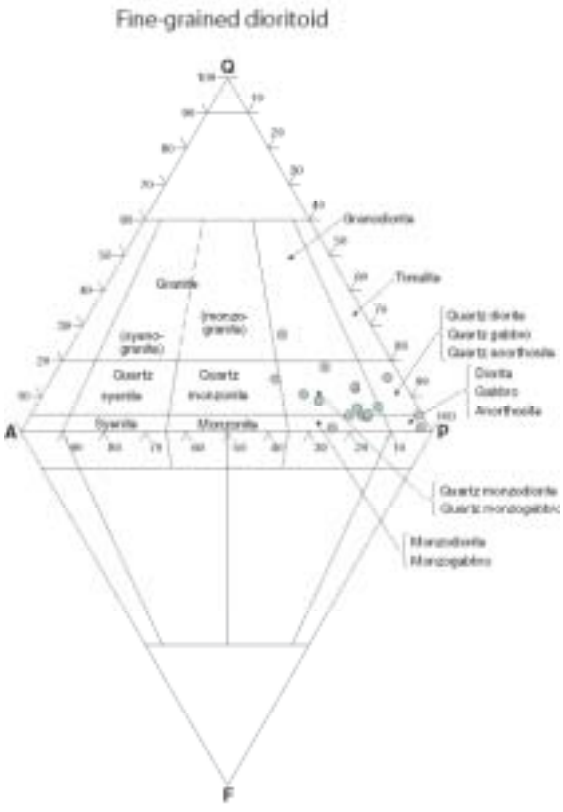

Figure 5-11. *QAPF modal composition of the fine-grained dioritoid.*

The *quartz monzodiorite* occurs in the eastern part of the Simpevarp peninsula and neighbouring parts in southernmost Ävrö (Figure 5-2 and Figure 5-3). However, the largest body occurs in the southwestern part of the local scale model area and neighbouring parts of the regional model area /Bergman et al. 2000; SKB, 2002b/. The quartz monzodiorite has also been documented to dominate the last c. 300 metres, i.e. from c. 1,450 to 1,700 metres borehole length in the cored borehole KLX02 in the Laxemar subarea (unpublished simplified mapping of the drillcore between 1,000 and 1,700 metres). Based on the Simpevarp Version 0 model, it is also inferred to constitute isolated bodies elsewhere in the regional model area (Figure 5-3). It is grey to reddish grey, medium-grained, commonly equigranular (Figure 5-10) and exhibits a relatively restricted compositional range (Figure 5-12), which is similar to that of the fine-grained dioritoid. As can be seen in Figure 5-12, tonalitic and quartz dioritic varieties occur as well. Transitional varieties between typical quartz monzodiorite and fine-grained dioritoid occur, which further strengthens the inferred close relationship between these two rock types (see also Figure 5-15).

Ävrö granite is a collective name for a suite of more or less porphyritic rocks that vary in composition from quartz monzodiorite to granite, including quartz dioritic, granodioritic and quartz monzonitic varieties (Figure 5-13). It is the dominating rock type in the entire regional model area (Figure 5-3) and in the cored boreholes KAV01 on Ävrö, KSH03A on the Simpevarp peninsula and KLX02 in the Laxemar subarea (see Section 5.2.7). The Ävrö granite is reddish grey to greyish red, medium-grained and the phenocrysts are usually 1–2 cm in size but scattered larger phenocrysts exist (Figure 5-14). A characteristic feature in the Ävrö granite is the occurrence of scattered cm to 0.5 metre large enclaves of intermediate to mafic composition. The average density is 2,681 ± 16 kg/m^3. In the present context, the so-called Äspö diorite, due to textural and compositional similarities, is included in the Ävrö granite category.

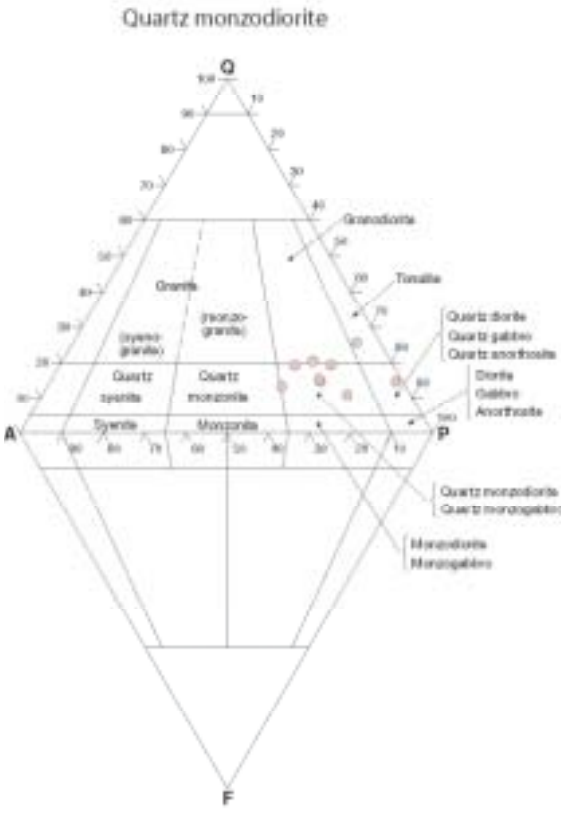

Figure 5-12. *QAPF modal composition of the quartz monzodiorite.*

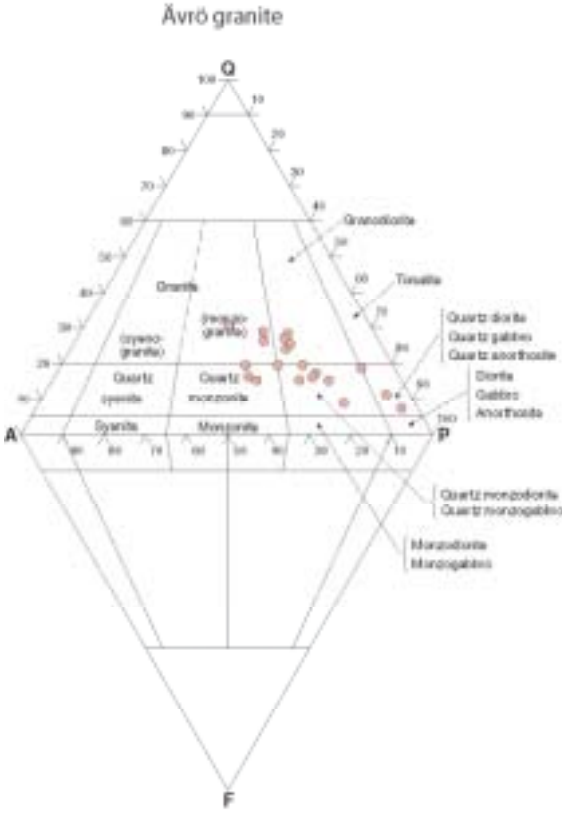

Figure 5-13. *QAPF modal composition of the Ävrö granite.*

Figure 5-14. *Sparsely porphyritic Ävrö granite.*

In the easternmost part of the Simpevarp peninsula, the quartz monzodiorite is mixed and mingled with the Ävrö granite. This is also evident in the cored boreholes KSH01A, KSH03A and KSH03B (see Section 5.2.7). Gradual contact relationships are characteristic and strongly indicate that the quartz monzodiorite and the Ävrö granite formed more or less synchronously.

Diorite to gabbro occurs as separate larger bodies in the western part of the regional model area, and as scattered, minor bodies principally along the coast in the Simpevarp-Ävrö-Äspö and neighbouring area (Figure 5-3). Furthermore, inclusions of diorite to gabbro occur in the Ävrö granite and fine-grained dioritoid. These minor bodies and inclusions usually display mixing and mingling relationships with the country rock.

The mean value of the mineralogical composition of the dominant rock types in the Simpevarp subarea is shown in Figure 5-15.

Red to greyish red, *medium- to coarse-grained granite* occurs as more or less large bodies in the northern and northwestern part of the regional model area (cf. Figure 5-3), /SKB, 2002b/. Furthermore, it occurs as both minor bodies in the western part of the Simpevarp subarea and as mixed and mingled, diffusely delimited small occurrences in the Ävrö granite (Figure 5-2).

A conspicuous rock type in the regional model area is the occurrence of two large bodies of approximately 1,450 Ma old granite, the so-called *Götemar granite* in the northern part and the so-called *Uthammar granite* in the southern part (Figure 5-3, Table 5-1). The granites are red to greyish red and commonly coarse-grained, but fine- to medium-grained varieties occur in the Götemar granite (Figure 5-3).

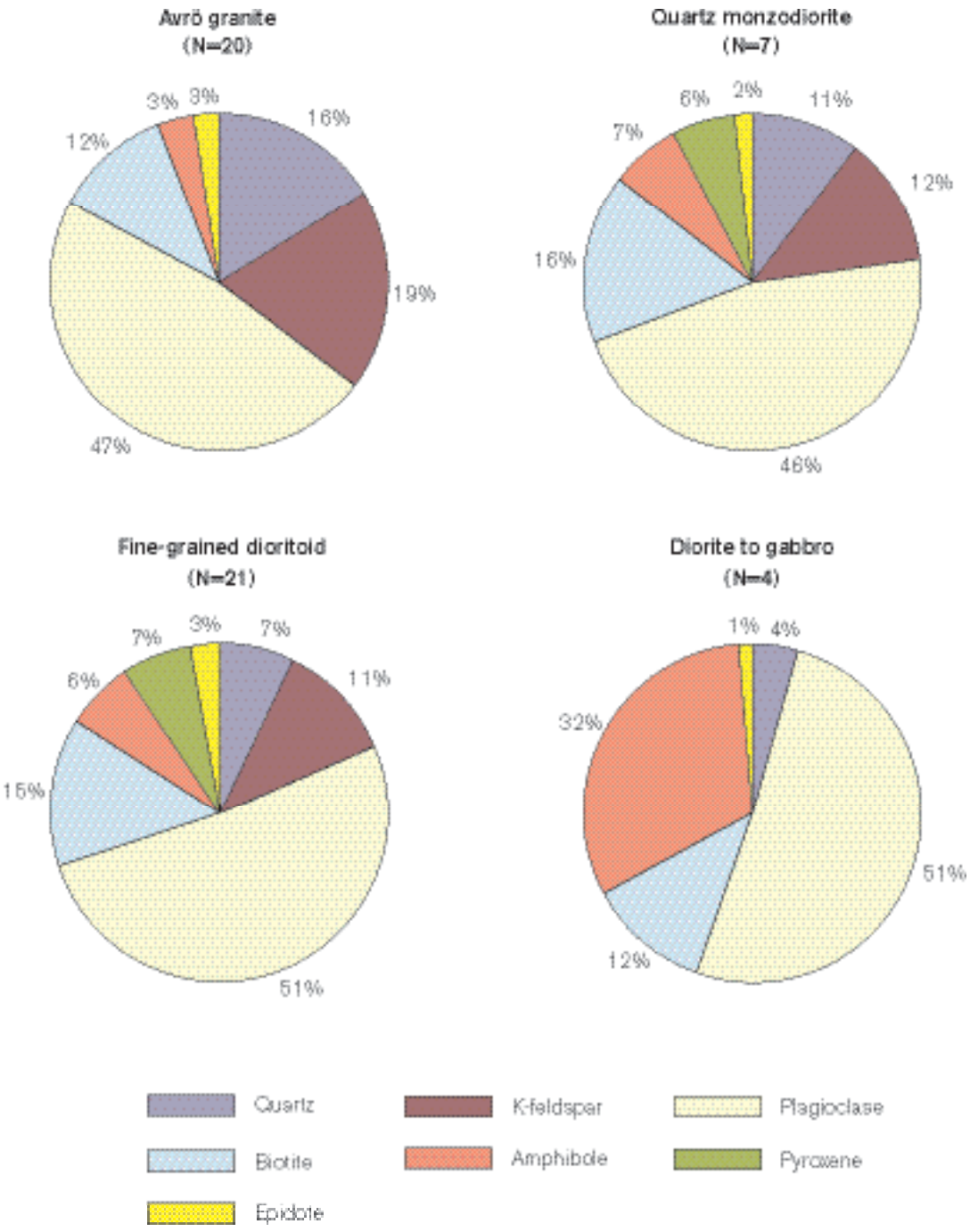

Figure 5-15. *Diagrams showing the mineralogical composition (mean value) of the dominant rock types, including diorite to gabbro, in the Simpevarp subarea.*

A characteristic feature in the Simpevarp subarea is the frequent occurrence of *fine- to medium-grained granite*, usually as dykes but also as veins and minor bodies (cf. Figure 5-2 and Figure 5-16, Figure 5-17 and Figure 5-18). In situ gamma-ray spectrometric measurements have shown that it has a higher content of thorium than the other rock types in the Simpevarp subarea /Mattsson et al. 2002, 2003/. Fine- to medium-grained granite has also been documented to be a characteristic rock type in the regional model area /see Wahlgren et al. 2003/. Furthermore, fine- to medium-grained granite occurs as separate larger bodies in the regional model area (Figure 5-3).

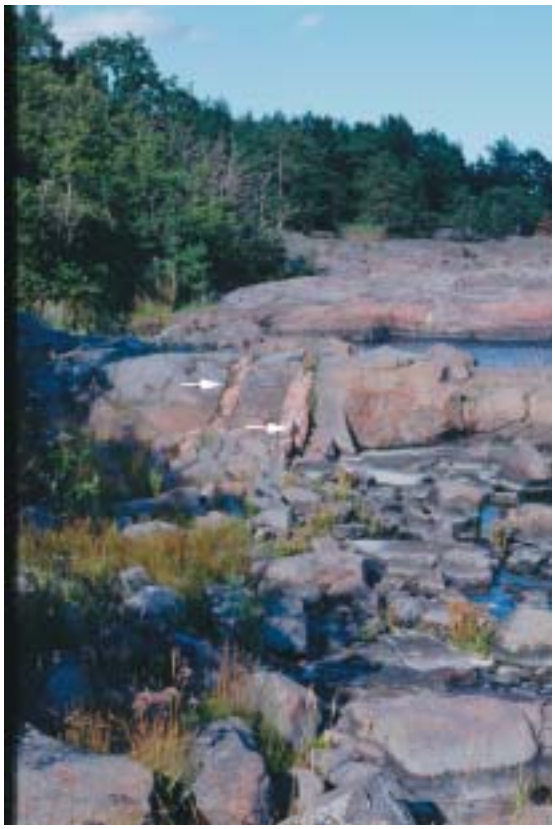

Figure 5-16. *Dykes of fine- to medium-grained granite and pegmatite (cf. arrows in the central part of the picture).*

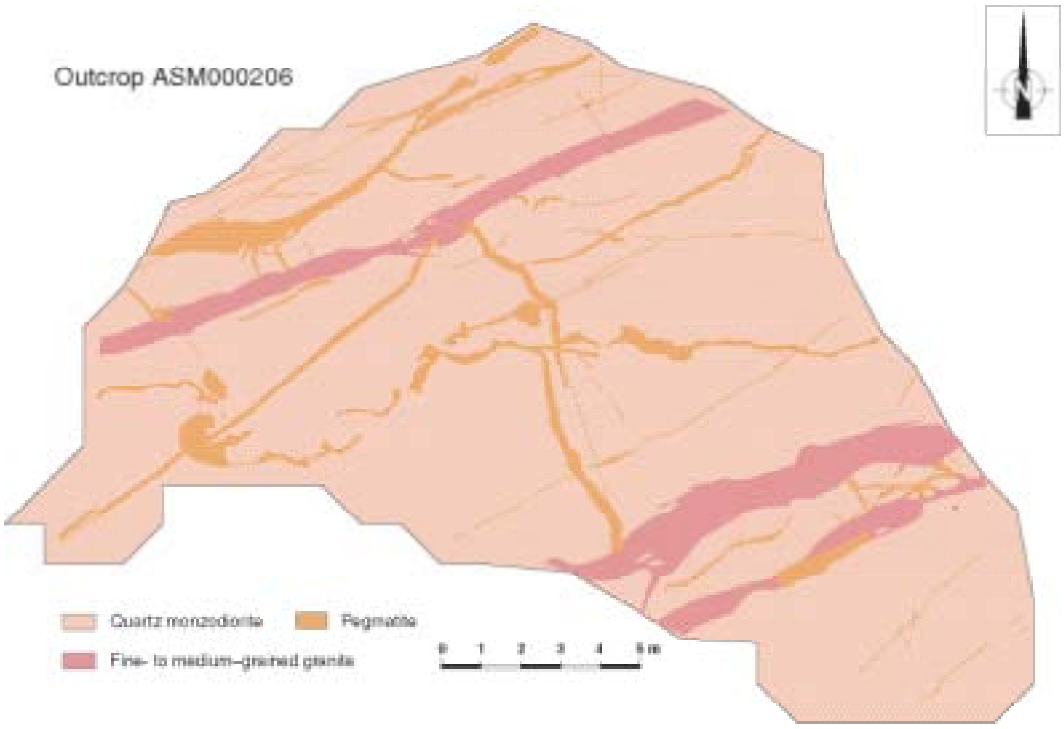

Figure 5-17. *Overview of a cleared outcrop on the Simpevarp peninsula showing the appearance of subordinate rock types. Note the high frequency of pegmatite and fine- to medium-grained granite in the quartz monzodiorite in this outcrop. This is an example of one of the outcrops where detailed fracture mapping has been carried out.*

Figure 5-18. *Dyke, cf. arrow, of fine- to medium-grained granite cross-cutting quartz monzodiorite. Same outcrop as depicted in Figure 5-17. The size of the black note book (lower centre left) is 16.5×13 cm).*

Pegmatite frequently occurs (Figure 5-2, Figure 5-16, Figure 5-17 and Figure 5-19) and pegmatite cross-cutting granitic dykes and vice versa are observed in the Simpevarp subarea. Consequently, at least two generations of fine- to medium-grained granite as well as pegmatite occur. However, they are all interpreted to belong to the waning stages of the igneous activity that formed the majority of the rocks in the region.

Figure 5-19. *Pegmatite cross-cutting quartz monzodiorite. Same outcrop as depicted in Figure 5-17. The size of the black note book is 16.5×13 cm.*

Locally, a fine-grained *mafic (diorite to gabbro) rock* occurs as sheets, dykes or minor bodies in the Simpevarp subarea (Figure 5-2). Generally, it is mixed (net-veined) with fine- to medium-grained granite, and, thus, they constitute composite intrusions (Figure 5-20).

Based on information from the Simpevarp subarea, and as mentioned above, the contacts between the dominant rock types are mostly diffuse in character, i.e. they grade into each other. In contrast to the dominant rock types, the contacts between, in particular, fine- to medium-grained granite dykes and pegmatites and the surrounding bedrock are generally not sealed but open in character.

The mixing and mingling relationships and diffuse contacts between the dominant rock types observed in the Simpevarp subarea strongly support the view that they were formed more or less synchronously, i.e. they belong to the same magmatic generation (cf. Table 5-1). However, based on field relationships, the following chronostratigraphy is indicated for the dominant and subordinate rock types:

Fine- to medium-grained granite and pegmatite	**Youngest**
Fine-grained mafic rock	↑
Medium- to coarse-grained granite	
Ävrö granite	↑
Quartz monzodiorite	
Diorite to gabbro	↑
Fine-grained dioritoid	**Oldest**

In conjunction with the bedrock mapping of the Simpevarp subarea, the Ävrö granite and the quartz monzodiorite were sampled for *U-Pb zircon and titanite dating*. The Ävrö granite was sampled at the stripped outcrop at the site for the cored borehole KAV01. The quartz monzodiorite was sampled in a road cut north of the OIII nuclear reactor, in the eastern part of the Simpevarp peninsula.

Zircon and titanite was analyzed in both samples. The Ävrö granite yielded an upper intercept zircon and titanite age of 1,800 ± 4 Ma, and the quartz monzodiorite yielded an upper intercept zircon age of 1,802 ± 4 Ma and a slightly younger titanite upper intercept age of 1,793 ± 4 Ma. The obtained ages are in good agreement with earlier reported ages for intrusive rocks in the region (Table 5-1).

Figure 5-20. *Composite intrusion of fine-grained mafic (diorite to gabbro) rock and fine- to medium-grained granite in fine-grained dioritoid at the outcrop ASM000205, cf. Figure 5-30, where detailed fracture mapping has been carried out. The size of the black note book is 16.5×13 cm.*

Table 5-1. Radiometric ages for intrusive rocks in the Simpevarp regional model area and surroundings.

Rock type	Northing (m)	Easting (m)	Depth (m.a.s.l.)	U-Pb zircon age	Reference
Fine-grained granite	6367111.8	1551572.7	–124.8	1,794 + 16/–12 Ma	/Kornfält et al. 1997; Wikman and Kornfält, 1995/
Fine-grained granite	6367985.2	1551588.6	–395.7	1,808 + 33/–30 Ma	/Kornfält et al. 1997; Wikman and Kornfält, 1995/
Äspö diorite	6367669.2	1551455.3	–318.4	1,804 ± 3 Ma	/Kornfält et al. 1997; Wikman and Kornfält, 1995/
Uthammar granite	636207	154827		1,441 + 5/–3 Ma	/Åhäll, 2001/
Jungfru granite	63473	12590		1,441 ± 2 Ma	/Åhäll, 2001/
Götemar granite	637280	154980		1,452 + 11/–9 Ma	/Åhäll, 2001/
Gersebo granite	637310	155148		1,803 ± 7 Ma	/Åhäll, 2001/
Virbo granite	6353848	1543959		c. 1,790 Ma	/Bergman et al. 2000/
Quartz monzodiorite	6366200	1552295		1,802 ± 4 Ma	/Wahlgren et al. 2004/
Quartz monzodiorite	6366200	1552295		1,793 ± 4 Ma (titanite)	/Wahlgren et al. 2004/
Ävrö granite	6367281	1553063		1,800 ± 4 Ma (zircon+titanite)	/Wahlgren et al. 2004/

All rock types in the Simpevarp subarea display low contents of uranium, except for pegmatite in which the uranium content locally exceeds 16 ppm. The latter is a critical value that corresponds to radium index=1, which must not be exceeded in rocks that will be used for the construction of buildings in which people are continuously present /BFS, 1990/. Consequently, it is not a site discriminatibng factor.

Bedrock heterogeneity can be assessed at different scales. The subordinate rock types in the Simpevarp subarea have been registered in the outcrop database /see Wahlgren et al. 2004/ at every observation point during the bedrock mapping. The bedrock map in Figure 5-2 and the detailed bedrock map of the cleared outcrop in Figure 5-17 reveals schematically the high content of subordinate rock types, especially fine-to medium-grained granite and pegmatite. The high content of fine- to medium-grained granite in particular, but also pegmatite, is characteristic for at least the Simpevarp subarea, and constitutes the most important factor in heterogeneity.

5.2.2 Lineament identification

Primary data and types of inferred lineaments

Lineaments in the regional model area have been identified on the basis of a joint integrated interpretation of different sets of lineaments, each of which has been identified separately from the following data sets /Rönning et al. 2003; Triumf et al. 2003; Wiklund, 2002; Elhammer and Sandkvist, 2005/:

- Helicopter-borne geophysical survey data, i.e. data on the total magnetic field, electromagnetic (EM) multifrequency data and very low frequency electromagnetic (VLF) data.
- Fixed-wing airborne, very low frequency electromagnetic (VLF) data.
- Detailed topographic data (terrain model).
- Terrain model of the sea bottom and bedrock surface in the sea area outside Simpevarp.

The helicopter-borne magnetic, EM multifrequency and VLF data were obtained during 2002 /Rönning et al. 2003/. Measurements were performed along north-south flight lines with a spacing of 50 m. The nominal instrument flight altitude during the measurements was 30–60 m. In a smaller area immediately east of the Simpevarp nuclear power plants, measurements were made along 36 lines perpendicular to the coast with a line spacing of 100 m. No measurements were carried out over the area occupied by the power plants (Figure 5-21), which implies that a large portion of the Simpevarp peninsula is devoid of airborne geophysical data. Furthermore, there are local disturbances in the measured data induced along existing power lines.

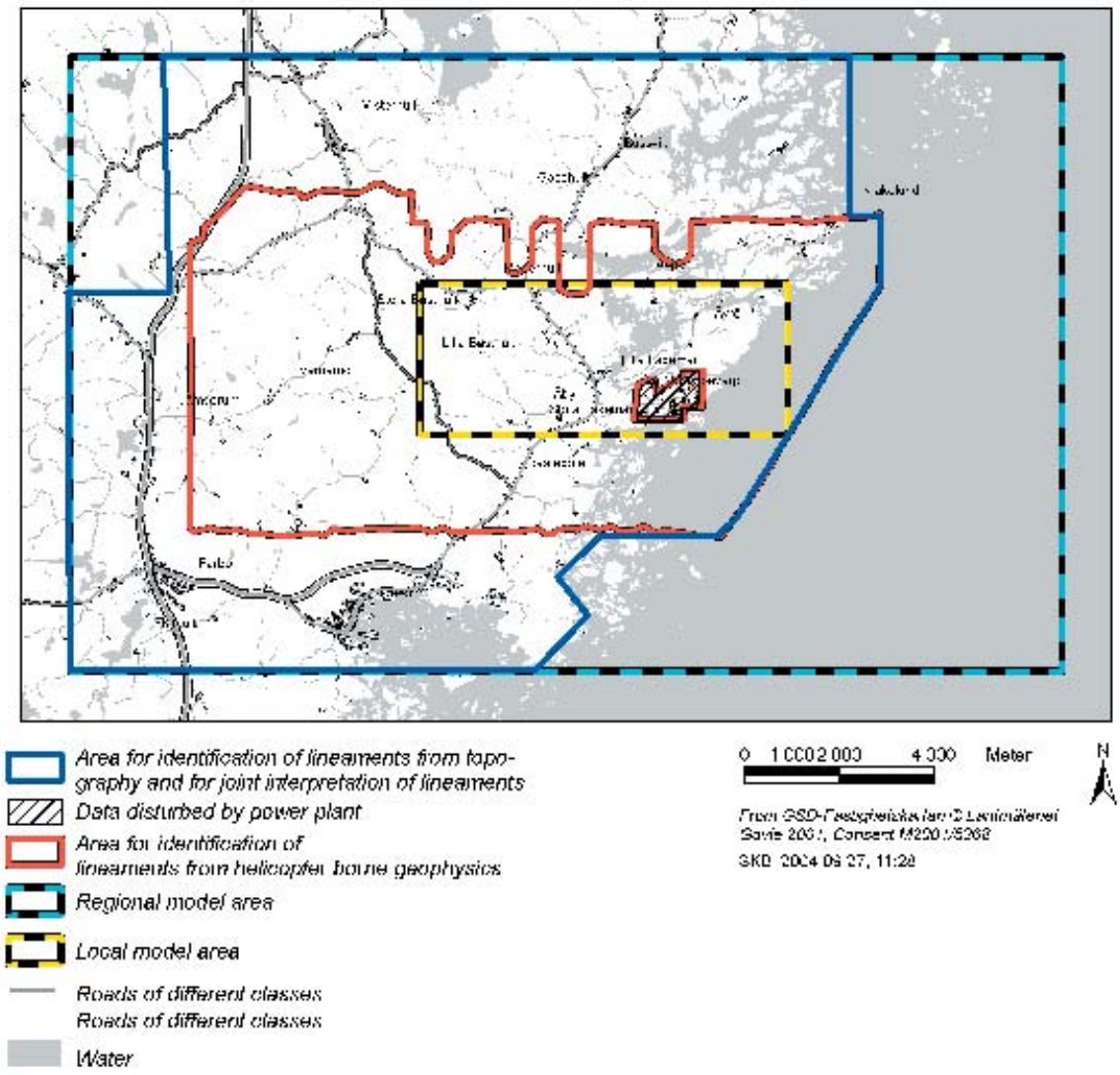

Figure 5-21. *Map showing helicopter-borne geophysical and topographic data coverage. Note that no data were acquired in the area that is occupied by the nuclear power plants and their infrastructure. Permission was not granted to carry out helicopter-borne measurements in certain areas. This accounts for the irregular outline of the northern boundary of these measurements.*

The data processing and methodology used in the interpretation of the helicopter- and fixed-wing borne geophysical survey data and the resulting different sets of identified lineaments are described in /Triumf et al. 2003/. Maps of the total magnetic field, apparent resistivity calculated from fixed-wing VLF data and apparent resistivity calculated from EM multi-frequency data are shown in Figure 5-22, Figure 5-23 and Figure 5-24, respectively.

The topographic data are based on detailed airborne photography carried out in 2001 with an instrument flight altitude of 2,300 m and a spatial resolution of 0.2 m /Wiklund, 2002/. The processing of the data resulted in a new detailed digital terrain model. The latter forms the basis for the identification of topographic lineaments. The processing of the topographic data, the methodology used in the interpretation work and the identified topographic lineaments are reported by /Triumf, 2003a/.

The terrain model of the sea floor and bedrock surface offshore Simpevarp are based on a detailed marine geological survey carried out in 2002 /Elhammer and Sandkvist, 2005/. (Note: This report is not distributed yet because of security restrictions imposed by Swedish authorities.) In the primary investigation area, i.e. close to the coast off the Simpevarp peninsula), the survey line spacing was 100 m, whereas the line spacing was 1,000 m in the remainder of the investigation area. The lineaments interpreted offshore are reported by /Triumf, 2004/.

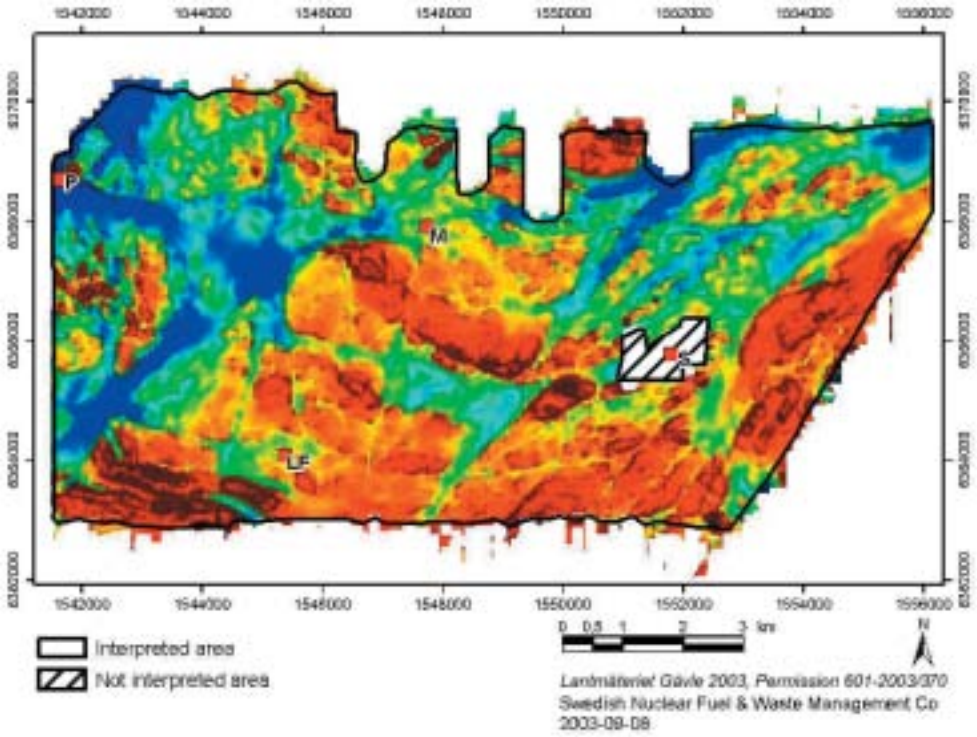

Figure 5-22. *Map showing the total magnetic field from the helicopter survey. Reddish brown colour = strongly magnetic bedrock, blue colour = weakly magnetic bedrock.*

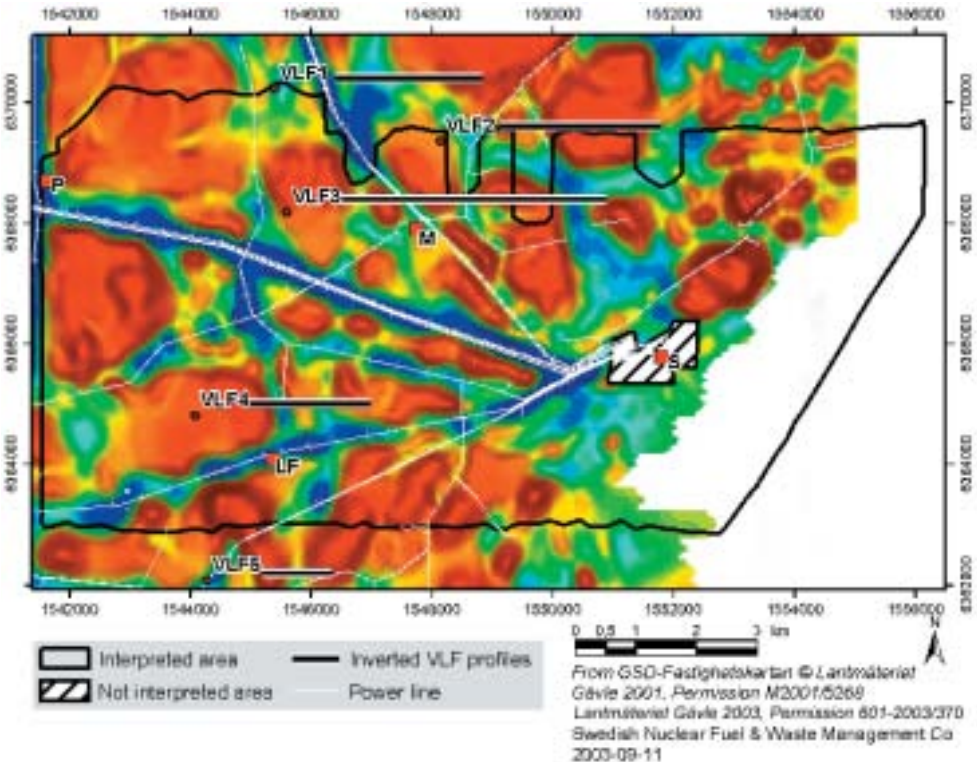

Figure 5-23. *Map showing apparent resistivity calculated from fixed-wing VLF data. Reddish brown colour = high resistivity, blue colour = low resistivity.*

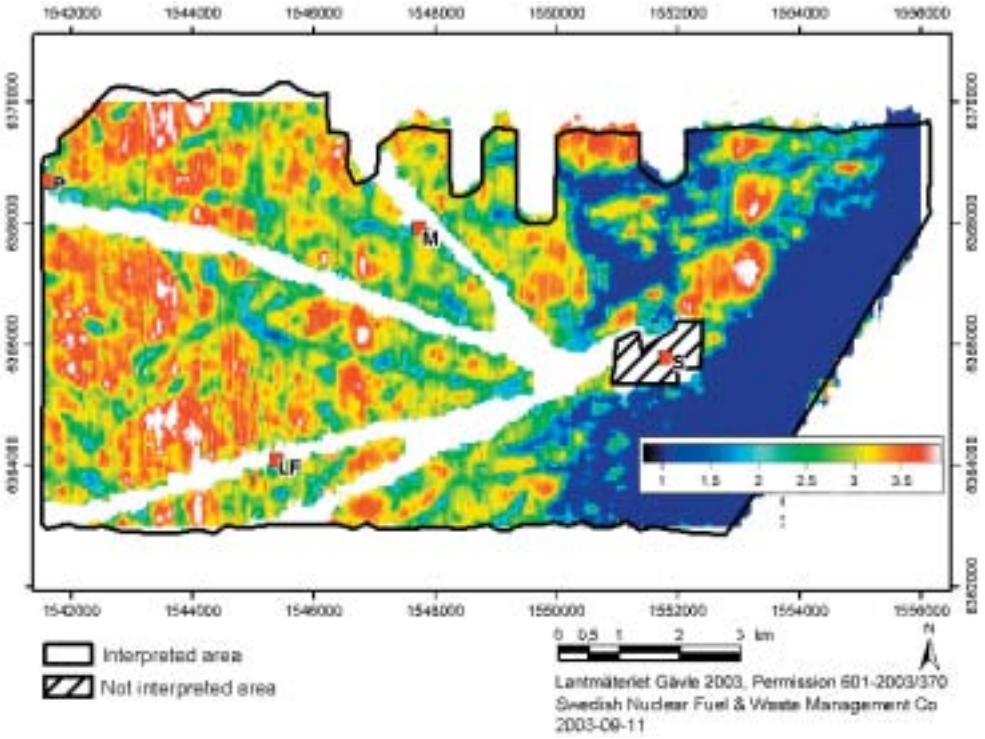

Figure 5-24. *Map showing apparent resistivity calculated from helicopter-borne EM multi frequency data. Reddish colour = high resistivity, blue colour = low resistivity.*

Evaluation

The process of joint interpretation of lineaments consists of the following major steps (cf. Figure 5-25 and definitions in the adjoining text):

- Construction of “co-ordinated lineaments” from “method-specific lineaments”.
- Parameterisation of the “coordinated lineaments”.
- Construction of “linked lineaments”.
- Parameterisation of “linked lineaments”.

A “method-specific lineament” is a lineament identified in a single specific type of data set, e.g. topography, helicopter-borne magnetic data, multifrequency electromagnetic (EM) data or data from the marine geological measurements (e.g. bathymetric data). A “coordinated lineament” is a single interpreted lineament that accounts for all “method-specific lineaments” along a segment of a given single lineament. A “linked lineament” here implies a lineament composed of one or several “coordinated” lineaments with a total extension in most cases longer than the underlying interpreted coordinated lineaments, cf. Figure 5-25.

The final result of the joint interpretation is the map of linked lineaments where the latter have been assigned attributes relating to their origin and character /Triumf, 2004/. The linked lineaments identified in the Simepvarp regional model area are presented in Figure 5-26, where their assigned class (regional > 10 km or local major 1–10 km) are identified. The latter is an expert judgement that relates to the degree of clarity in surface expression of the lineaments where 1=low, 2=medium and 3=high uncertainty. A weighted average is calculated according to the length of each segment in the linked lineament. For a more detailed explanation, see /Triumf, 2004/.

The map of linked lineament covers a smaller area than the regional scale model area, cf. Figure 5-26. For modelling purposes, lineaments from earlier work (Simpevarp version 0) have been evaluated and combined with the linked lineaments in areas with no detailed coverage.

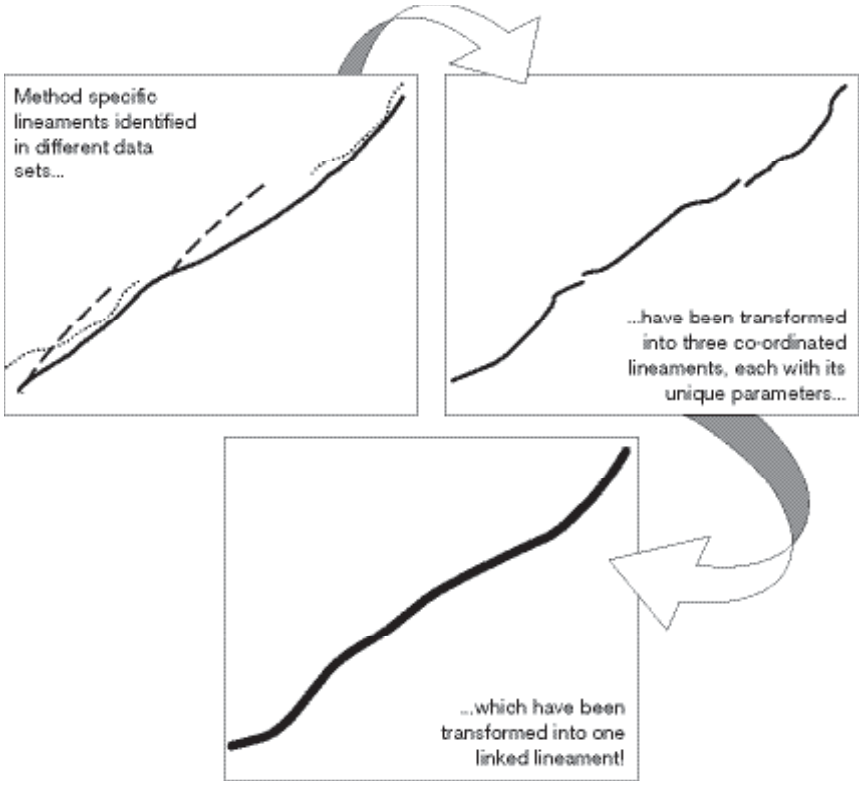

Figure 5-25. *Schematic explanation of the joint lineament interpretation process.*

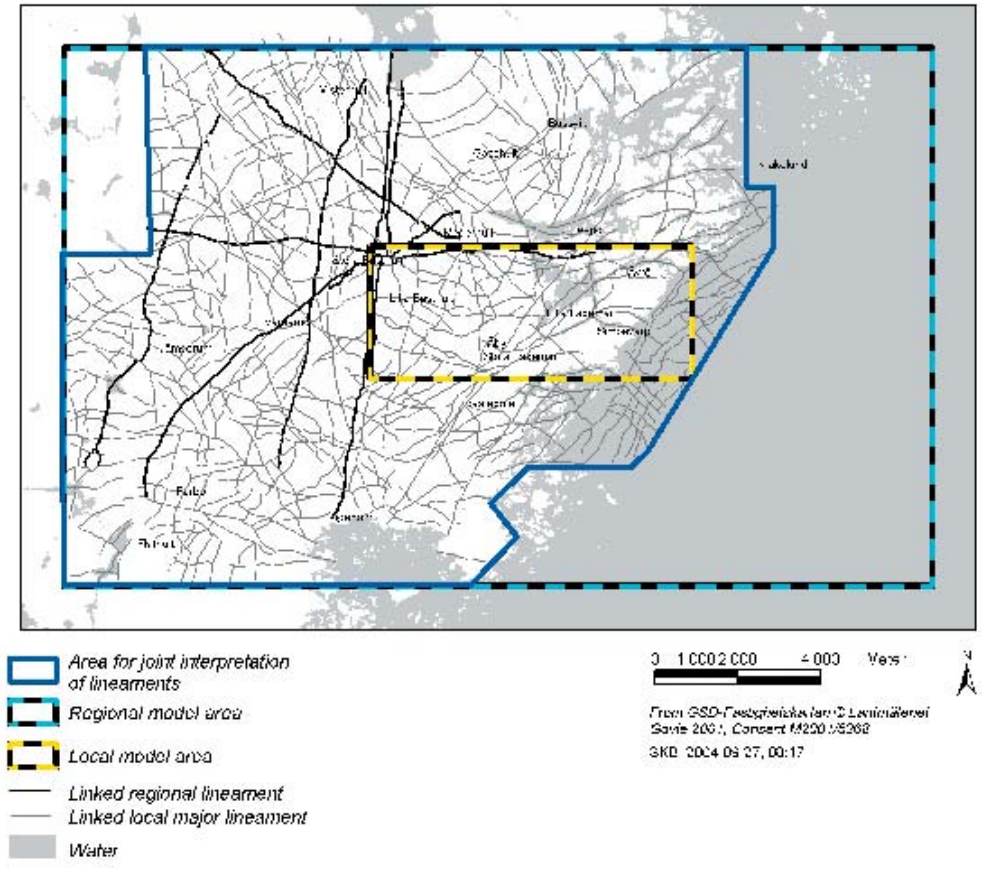

Figure 5-26. *Interpreted linked lineaments in the Simpevarp regional model area.*

The linked lineament interpretation was evaluated also on more structural geological grounds. Several connections were suggested to lineaments that were;

- segmented going from land to sea,
- segmented but still approximately linear and continuous.

Each suggested connection (see Figure 5-27) was reviewed by the geophysicist responsible for the original interpretation of the linked lineaments. The resulting “merged linked lineament map” covers the whole regional model domain, cf. Figure 5-28, and was aimed to be used as the common surface data deck for developing the 3D deformation zone model and the evaluation of DFN parameters.

However, due to time constraints, the merged lineament evaluation was not completely finished when the deformation zone modelling and DFN analysis was initialised. The DFN analysis was consequently based only on available data at the time, i.e. merged and linked lineaments in the high resolution area (cf. Figure 5-26), whereas the deformation zone model utilised early versions of, and later also the final, merged linked lineament map inside the whole regional model domain as shown in Figure 5-28.

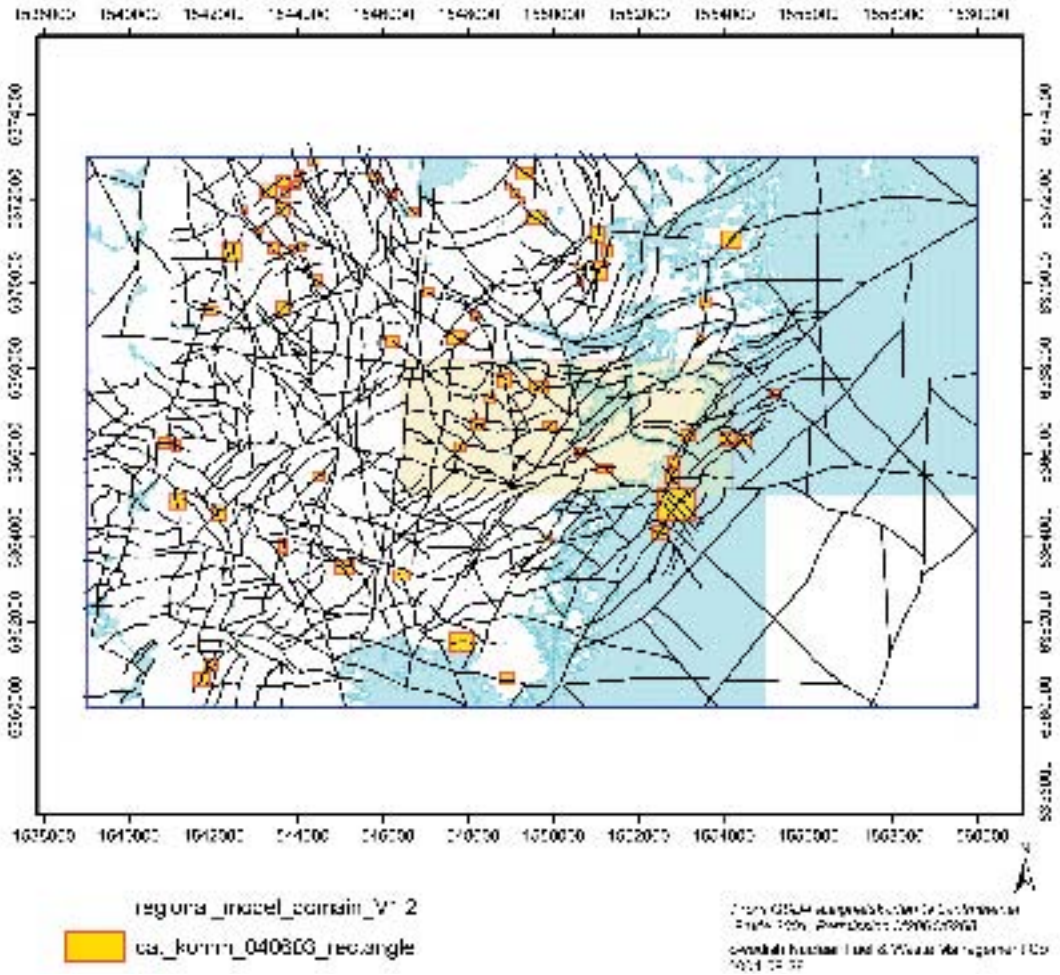

Figure 5-27. *Geometrical improvements to the linked lineament map (small yellow rectangles) combined with the Version 0 lineament map in areas outside of the area of detailed linement coverage.*

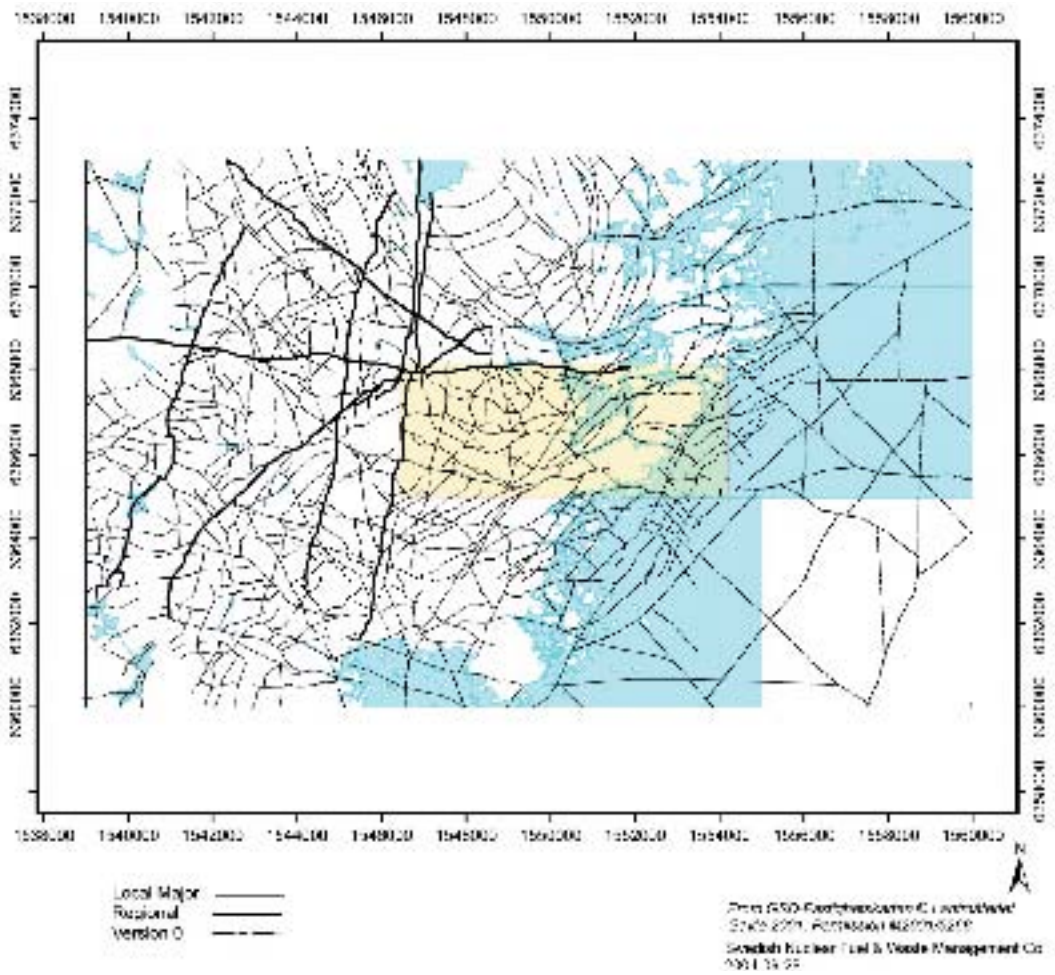

Figure 5-28. *The lineament map (merged linked lineament map) used for the regional scale model area.*

It is important to note that the true natures of the interpreted lineaments are more or less unknown at this stage, except for a few where there is strong evidence from other independent sources of direct or indirect information as to their being basement structures, e.g. borehole data and/or seismic reflections or refractions. It is considered likely that many, but not all, of the interpreted lineaments are associated with basement structures given that the overburden in Simpevarp is very thin or non-existing over large areas. However, at the moment it is not possible to discard lineaments as possible deformation zones, even if there are no data to support this interpretation. All merged and linked lineaments have therefore been considered in the modelling of deformation zones and evaluation of DFN parameters.

5.2.3 Observation of ductile and brittle structures from the surface

Data that document the character and orientation of ductile and brittle structures at the surface are based mainly on observations made in conjunction with the bedrock mapping of the Simpevarp subarea during 2003. Available data comprise:

- Measurements of mainly ductile structures, as well as some brittle structures and bedrock contacts at 91 of the 353 observation points that were documented during the bedrock mapping /Wahlgren et al. 2004/.
- Laboratory measurements of the magnetic susceptibility (including anisotropy) of samples from 10 outcrops in the Simpevarp 1.1 local scale model area /Mattsson et al. 2003/.
- Documentation of fracture fillings by visual inspection at 100 of the 353 observation points referred to above /Wahlgren et al. 2004/.

- Detailed mapping of fractures (including fracture fillings) that are longer than 50 cm at four cleaned or (stripped) outcrops which are approximately 600 m^2 in areal extent /Hermanson et al. 2004/.
- Scan-line mapping of frequency and orientation of fractures that are longer than 100 cm at 16 of the 353 observation points referred to above /Wahlgren et al. 2004/ – fracture fillings were also noted.

Ductile structures

It is noted that the rocks in the Simpevarp subarea generally are well-preserved and more or less isotropic (this is presumably valid also for the rocks in the remainder of the local model area and the regional scale model area). However, locally a weak foliation is developed that is defined by the preferred orientation of biotite and, in the case of porphyritic Ävrö granite, also by oriented feldspar phenocrysts as well. The foliation is principally oriented in an east-west to northeast direction. Its dip is generally steep to vertical, but locally it is difficult to decipher.

However, the most spectacular and characteristic structures in the overall relatively well-preserved rocks are mesoscopic, low-grade ductile to brittle-ductile shear zones of the same character as the regional Äspö shear zone, cf. Table 5-15 and Figure 5-56 (see Section 5.4.1). These are documented at 47 of a total of 353 observation points in the Simpevarp subarea. The recorded widths vary from a decimetre to several metres and the shear zones are characterized by strong protomylonitic to mylonitic foliation (Figure 5-29). The dip is subvertical to vertical and the majority of the observed shear zones have E-W to NE strike. Kinematic indications suggest a sinistral strike-slip and a south-side-up dip-slip component. The alignment of some of the observed shear zones implies that they form part of one and the same zone of local major character (see Figure 5-2).

The anisotropy of the magnetic susceptibility (AMS) measurements constitute a means to calculate the principal directions and principal susceptibilities ($K_1 \geq K_2 \geq K_3$) of the magnetic susceptibility anisotropy ellipsoid for each sample /Mattsson et al. 2003/. By analysing the mean values of the principal magnetic susceptibilities, the degree of anisotropy and the shape of the anisotropy ellipsoid can be estimated. The latter may be prolate (dominated by magnetic lineation), spherical or oblate (dominated by magnetic foliation). By analysing the principal directions, it is possible to estimate the magnetic fabric orientation in 3D, which is related to structural parameters of the rocks such as lineation and foliation. Thus, the AMS data may be an important and useful tool in revealing an anisotropic fabric in rocks that appear well-preserved and lack a clear visible tectonic fabric.

Figure 5-29. *Decimetre-wide, low-grade ductile shear zone in Ävrö granite.*

Despite a limited number of AMS measurements from the Simpevarp regional model area, the results are very consistent. The orientation of the mean magnetic foliation planes and the foliation documented during the bedrock mapping in the Simpevarp subarea are very similar, i.e. they display an east-west to northwesterly strike. Furthermore, the magnetic foliation, as well as the foliation measured during the bedrock mapping, shows an orientation similar to the interpreted major lithological boundaries. However, the majority of the magnetic foliation planes display gentle to intermediate northerly dips, whereas the foliation documented during the bedrock mapping is characterised by steep to vertical dips. With few exceptions, the magnetic lineation is consistently west to northwest plunging between 0º and 53º. Due to the similarities in the orientation of the magnetic foliation and the lithological boundaries, it is inferred that the rocks carry a magnetic fabric related to the stress field that prevailed during the emplacement of the igneous rocks in the Simpevarp subarea. The documented magnetic foliations and lineations in the remaining part of regional model area /Mattsson et al. 2003/ display a similar orientation to those found in the Simpevarp subarea. Thus, the measured magnetic foliations and lineations, though relatively few, display a very uniform orientation across the entire model area.

The AMS data will be more fully evaluated in future model versions when more data are expected to be available, particularly for the local scale model area.

Brittle structures

Detailed fracture mapping has been carried out at 4 sites in the Simpevarp subarea. The sites were chosen on both a geographical and lithological basis, i.e. the sites were distributed between different parts of, and between the various dominant rock types in, the Simpevarp subarea (Figure 5-30). These fracture maps was utilised already in Simpevarp 1.1 but have been re-analysed for this model version.

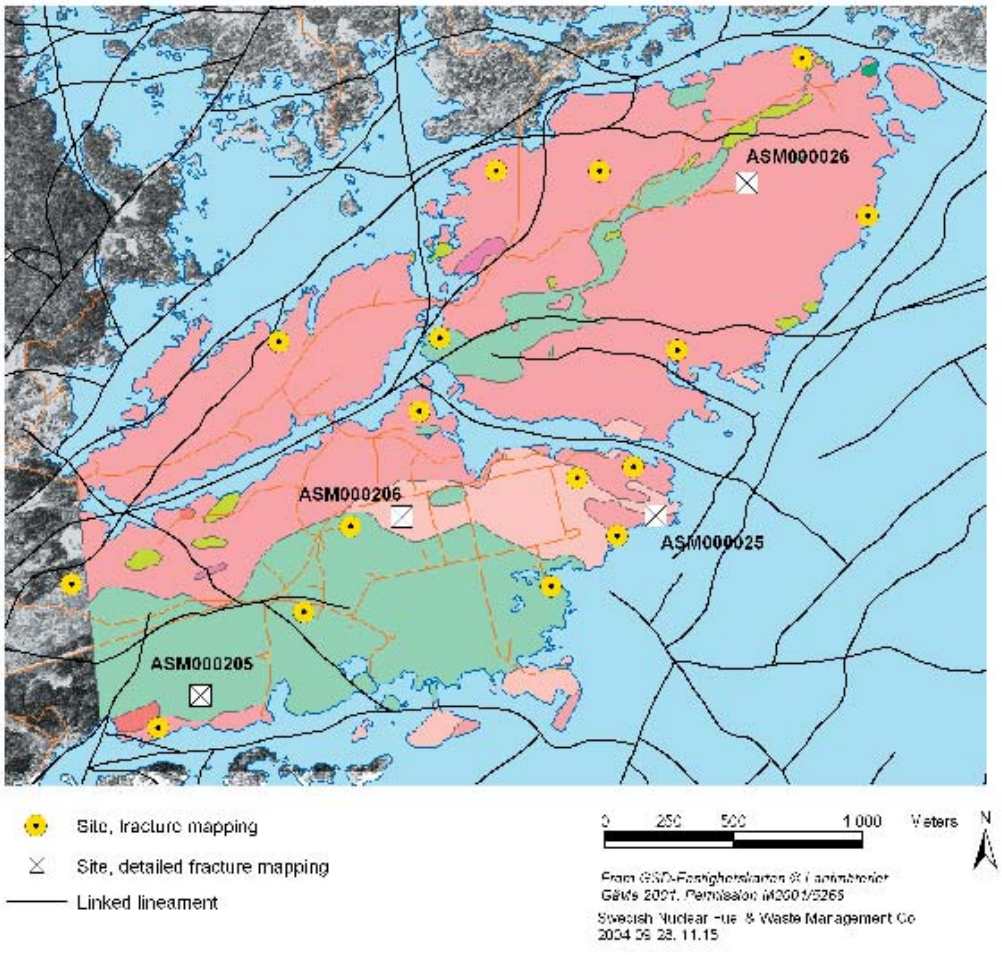

Figure 5-30. *Sites where detailed and scan line mapping of fractures have been carried out. For explanation of the bedrock legend (coloured areas), see Figure 5-2.*

Fracture trace maps that show fracture trace geometry, were produced for each outcrop during the detailed fracture mapping (cf. Figure 5-31). The assembled data include the 3D geometry of fracture traces and their associated geological parameters, including mineralogy, undulation, trace length and characteristics of termination. The truncation (minimum) mapped length were 50 cm long traces, and the maximum length were limited to the size of the cleared outcrop. The number of fractures mapped at each site varied between 876 and 1,175 (Table 5-2). Scan line measurements were also completed at each site along NS and EW directions, employing a mapped truncation length of 20 cm. The analysis of the data from the detailed mapping of fractures is presented in Section 5.5.

Table 5-2. The amount of fractures measured by the detailed fracture mapping, see also Section 5.5 for necessary definitions, cf. Figure 5-31.

Outcrop ID	All fractures	Open Fractures	Sealed Fractures
ASM000025	917	147	770
ASM000026	876	138	738
ASM000205	1,175	126	1,049
ASM000206	940	200	740

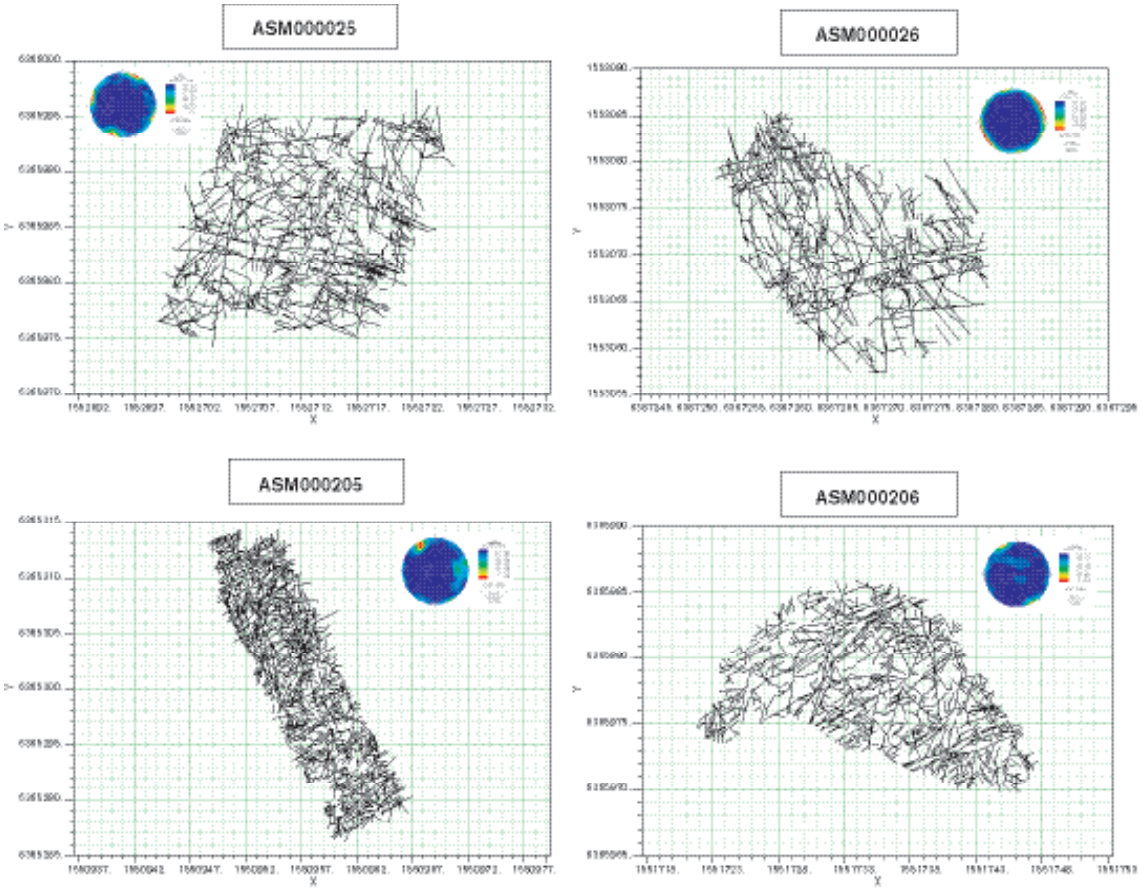

Figure 5-31. *Fracture trace maps and fracture lower hemisphere contour plots of fracture poles of the four outcrops where detailed fracture mapping has been carried out, cf. Figure 5-30, for geographical reference.*

The simplified scan-line mapping of fractures at the 16 locations (Figure 5-30) completed in conjunction with the bedrock mapping of the Simpevarp subarea, was carried out along two orthogonal lines with N-S and E-W orientation. The location and orientation of fractures, with a truncation length of 100 cm, were recorded during the mapping. In total, 616 fractures were measured. The fracture frequency varies between a minimum of 0.6 to a maximum of 3.5 fractures/metre, with an average of 1.9 fractures/metre. In Figure 5-32, rosette diagrams indicate the fracture frequency and strike for fractures with a dip steeper than 45° at each location. The dominance of fractures striking c. NW and NE is clearly evident. However, the fracture set that dominates varies between the different locations mapped in the Simpevarp subarea. Further fracture statistics are provided in Section 5.5.

Epidote is the dominant fracture filling mineral observed during the bedrock mapping of the Simpevarp subarea Another common fracture filling is greyish white and is inferred to be dominated by prehnite. Furthermore, quartz, chlorite and calcite have been observed. Larger veins of hydrothermal quartz are also present.

So far, there are not sufficient data to evaluate the relationship between the fracture filling minerals and the orientation of the fractures. The fracture filling mineralogy is more extensively described in Section 5.2.7.

A characteristic phenomenon in the Simpevarp subarea is an extensive, inhomogeneous, red staining (oxidation) of the bedrock (Figure 5-33; cf. Section 5.2.7). The red staining may at least partly have obliterated the primary magnetisation of the dominant rock types. At least in part, the inhomogeneouos oxidation is inferred to have caused the apparently overlapping magnetic susceptibility values recorded for the dominant rock types (see Figure 5-7). Petrophysical data from the cored borehole KSH02 show that strong alteration affects the physical properties of the fine-grained dioritoid /Mattsson and Thunehed, 2004/. The density, induced and remanent magnetisation and electric resistivity decrease significantly, while the porosity increases. Similar observations have also been reported from reddish alteration zones at Äspö /Eliasson, 1993/.

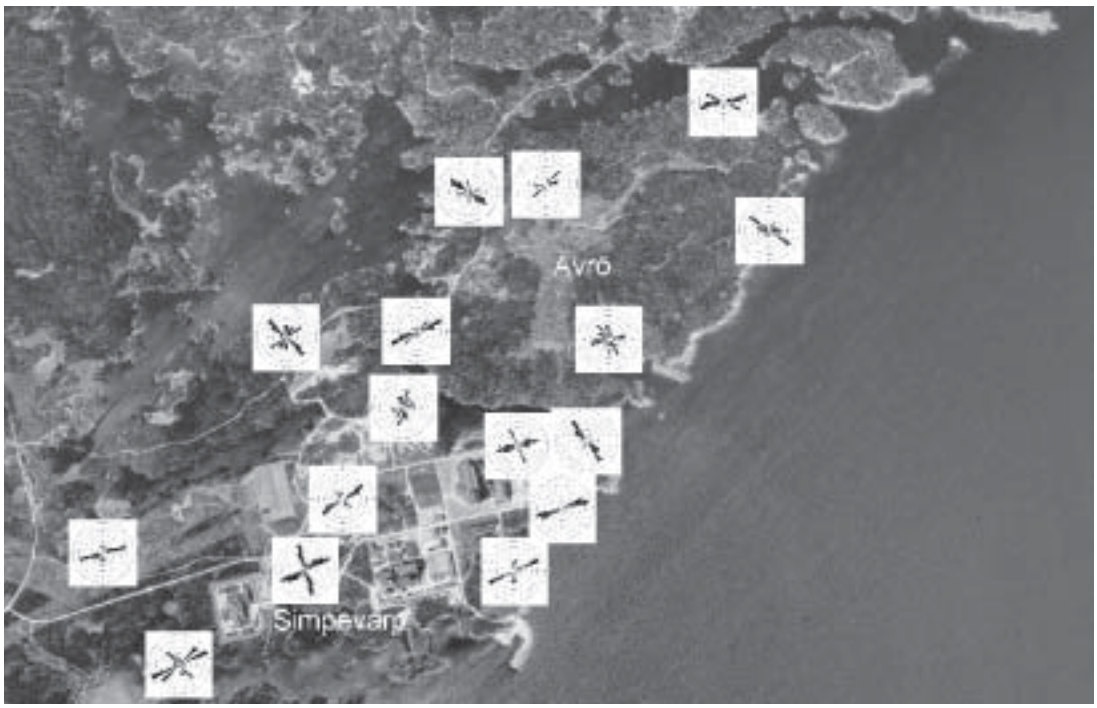

Figure 5-32. *Orthophoto with diagrams showing fracture strike and frequency for fractures dipping 45 degrees or more at each outcrop.*

Figure 5-33. *Red staining along sealed fractures in quartz monzodiorite, Simpevarp peninsula. The mineral filling is presumed to be dominated by prehnite. Outcrop ASM000206 where detailed fracture mapping has been carried out (cf. Figure 5-17 and Figure 5-30). The size of the black note book is 16.5×13 cm.*

The red staining is caused by hydrothermal processes, and is principally concentrated along fractures. However, in many places the red staining has also affected the rock volumes in between mesoscopic fractures. Numerous, small-scale, sealed fractures occur in these rock volumes, and presumably these fractures acted as conduits for the penetrating hydrothermal fluids.

5.2.4 Surface geophysics

Ground magnetic and slingram measurements were carried out during 2003 for the siting of the cored borehole KAV04 in the southern part of the island of Ävrö, and west of Clab on the Simpevarp peninsula in order to improve knowledge of the position and geometry of fracture zones interpreted in Simpevarp 1.2 /Triumf, 2003b/. The results from measurements west of the Clab facility have been evaluated in the present modelling.

Within the Simpevarp peninsula, many surface geophysical measurements were carried out during the investigation phases of OKG I–III and Clab 1–2. The resulting interpretations of major structures have been considered in the current project. However, due to the lack of the original raw data, no reassessment or reinterpretation of these data has been possible. In addition, since these surveys were followed up by drilling and actual excavation, a greater emphasis has been given to the results of tunnel and excavation mapping.

In order to test whether identified lineaments in the sea area around Ävrö and the Simpevarp peninsula constitute actual deformation zones, refraction seismic measurements have been carried out along 14 profiles. The identification of specific low-velocity zones along the profiles indicates that the identified lineament reflects the existence of a deformation zone. The results of the refraction seismic profiling have however not been evaluated in the deformation zone modelling while the full evaluation was not available at the time of the data freeze for Simpevarp 1.2.

5.2.5 Fracture statistics from borehole data

Table 5-3 shows boreholes evaluated as part of this model version. Cored boreholes KSH01A, KSH01B and percussion boreholes HSH01, HSH02 and HSH03 have already been utilized in Simpevarp 1.1 /SKB, 2004b/. However, new and updated BOREMAP data have been delivered for these boreholes applying a new terminology for open and sealed fractures, which has necessitated a renewed analysis of data from these boreholes.

All analysed borehole data now conform to the new terminology, which is significantly different from that employed in the preceeding analysis in Simpevarp 1.1 /SKB, 2004b/. In essence, this terminology distinguishes fractures into groups of open, partly open and sealed fractures according to the following criteria:

- Open fractures separates the core, have an aperture, and are mineral coated.
- Partly open fractures do not necessarily separate the core but have open “channels” with a measurable aperture and mineral coating over a part of the core.
- Sealed fractures are visible in the core, but do not separate the core and contain a mineral infilling.

All three types are attributed a confidence level in the classification (certain, possible and probable).

Table 5-4 shows analysed fracture parameters. For practical reasons, a number of key fracture parameters have been selected and cross-referenced to lithology and to single-hole interpretations in the extracted data from SICADA. The premises and principal results of the statistical analysis are presented in Section 5.5. Below follows only presentations of the general fracture density, fracture orientation and fracture mineralogy.

Table 5-5 shows the number of all, open, partly open and sealed fractures for the analysed boreholes. The number of fractures in the cored boreholes KSH01A and KSH01B has changed slightly since Simpevarp 1.1 as a consequence of the re-mapping process. The reason for this is mainly related to a different classification of engineered (man-induced) fractures.

Table 5-3. Boreholes analysed in Simpevarp 1.2.

Borehole	Borehole depth	Fracture data from (depth m)	Fracture data to (depth m)
KSH01A	100–1,000 m*	101.8	1,000.5
KSH01B	0–100 m	6.2	99.8
KSH02	0–1,001 m	19.8	999.5
KSH03A	100–1,001 m*	101.6	998.6
KSH03B	0–101 m	0.7	100.3
KAV01	0–757 m	2.5	742.9
KLX02	0–1,700 m**	202.8	1,005.6
HSH01	0–200 m	11.6	196.1
HSH02	0–200 m	12.1	146.3
HSH03	0–201 m	12.0	195.0

* The first 100 m telescope drilled. ** Fracture data mapped according to the new terminology between approx. 200–1,006 m.

Table 5-4. Analysed fracture parameters.

Parameter	Comments
BHID	Borehole ID
Orient1	Strike orientation (deg)
Orient2	Dip, right hand rule (deg)
SEC_UP	Fracture location in terms of depth along borehole (m)
TYPE	Open, Partly open or Sealed fracture
CONFIDENCE	Certain, Possible and Probable
ROCKTYPE	Rocktype at fracture location
DZID	Deformation zone at fracture location (from single hole interpretation). Presented in Section 5.5.
RD	Rock domain (from the lithological model). Presented in Section 5.5.
MIN1	Dominant mineral coating

Table 5-5. All fractures analysed in boreholes for Simpevarp 1.2.

Borehole	Total number of fractures	Open fractures	Partly open fractures	Sealed fractures	Ratio of open fractures in the borehole	P_{10} all (m^{-1})	P_{10} open (m^{-1})
KSH01A	9,576	2,153	23	7,400	22%	10.7	2.4
KSH01B	691	141	1	549	20%	7.4	1.5
KSH02	11,872	3,787	2	8,083	32%	12.1	3.9
KSH03A	5,846	2,159	13	3,674	37%	6.5	2.4
KSH03B	795	131	2	662	16%	8.0	1.3
KAV01*	4,292	2,477	1	1,813	58%	5.8	3.3
KLX02	3,070	2,103	105	862	69%	3.8	2.6
HSH01	1,284	569	84	631	44%	7.0	3.1
HSH02	1,198	815	35	348	68%	8.9	6.1
HSH03	843	354	53	436	42%	4.6	1.9

* One fracture missing type (blank).

The ratio of open fractures changes significantly with the new terminology. For example, the cored borehole KSH01A had 706 open and partly open fractures based on aperture measurements in Simpevarp 1.1, whereas it now contains 2,176 open and partly open fractures based on the new terminology. This implies that the ratio of open fractures in borehole KSH01A increased from 7% in Simpevarp 1.1 to 22% of all mapped fractures in this model version. The ratio of open fractures is even higher in the other mapped boreholes, with a mean value of 41% open fractures (36% excluding percussion boreholes).

The average fracture spacing (m) in Figure 5-34 illustrates the density of fractures in each borehole. Spacing has been calculated using the interval between the top and lowermost mapped fracture in each borehole to avoid the uncertainty of exactly where mapping of the borehole has been initiated. The average fracture spacing in Figure 5-34 gives a biased picture of the “background” rock mass fracturing as sections of increased fracturing, i.e. potential deformation zones, have not been identified and removed from the data. This is especially true in shorter boreholes where the impact of sections of increased fracturing will be greater than the deep cored boreholes.

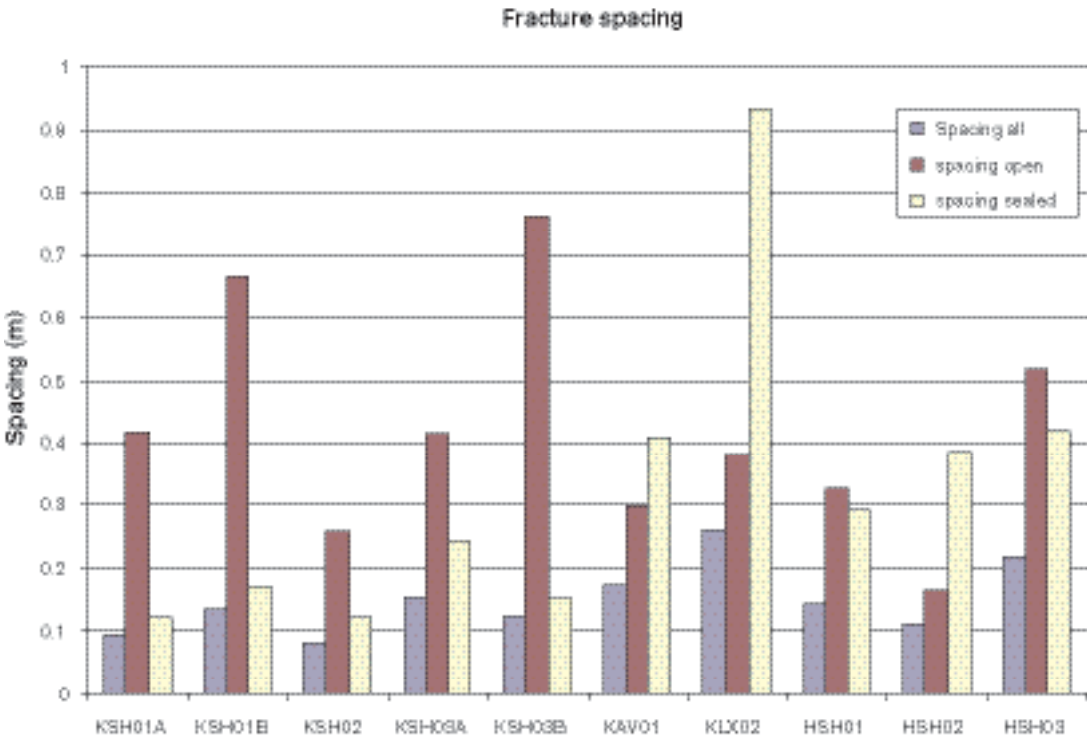

Figure 5-34. *Overall fracture spacing in each borehole. Fractures within sections corresponding to inferred deformation zones identified through single hole interpretation have not been removed.*

The percussion borehole HSH02 and the cored boreholes KSH02 and KSH01A show the highest density of fractures, whereas KLX02 and HSH03 show relatively lower density. The cored borehole KSH02 and the percussion hole HSH02 resides for the most part in the fine-grained dioritoid which is known for its higher fracture intensity as inferred from surface observations. The percussion boreholes HSH01 and HSH03 are drilled next to one another in the same host rock, but show very different behaviour due to intersections of one or several smaller deformation zones in HSH01.

Table 5-6 shows fracturing in cored and percussion-drilled boreholes after removal of fractures within sections interpreted as being deformation zones (see also Table 5-10). Deformation zones in this context include both the interpreted deterministic zones which are part of the deformation zone model and minor (stochastic) deformation zones which are not. Boreholes KSH01B and KSH03B do not contain any interpreted deformation zones. The single-hole interpretation of borehole KLX02 is at present still lacking and consequently no fractures have been removed. Frequency plots in Appendix 2 illustrate the gaps in the fracture frequency in boreholes KSH01A, KSH02, KSH03A, KAV01 and KLX02, after exclusion of fractures in deformation zones as outlined above.

The exclusion of fractures in deformation zones also decreases the ratio of open fractures in all boreholes, but most significantly in the percussion boreholes, cf. Table 5-6. This is possibly an effect of the sampling methodology in percussion boreholes which by default is based only on indirect observation of a BIPS images (no core available).

Table 5-6. Fractures analysed in boreholes for Simpevarp 1.2 excluding interpreted deformation zones inferred by the single hole geological interpretation (see also Table 5-10 below).

Borehole	Total number of fractures	Open fractures	Partly open fractures	Sealed fractures	Ratio of open fractures in the borehole	P_{10} all (m^{-1})	P_{10} open (m^{-1})
KSH01A	6,348	1,085	13	5,250	17%	7.1	1.2
KSH01B**	691	141	1	549	20%	7.4	1.5
KSH02	10,128	3,182	2	6,944	31%	10.3	3.2
KSH03A	3,998	1,325	10	2,663	33%	4.5	1.5
KSH03B**	795	131	2	662	16%	8.0	1.3
KAV01	2,845	1,611	1	1,233	57%	3.8	2.2
KLX02*	3,070	2,103	105	862	69%	3.8	2.6
HSH01	1,032	384	67	581	37%	5.6	2.1
HSH02	544	278	16	250	51%	4.1	2.1
HSH03	512	145	29	338	28%	2.8	0.8

* No single hole interpretation, and therefore no sections of deformation zones. ** No identified deformation zones.

Fracture orientations of the cored borehole KSH01A is presented in Figure 5-35. The data are dominated by subhorizontal fractures together with a steeper northwesterly set. Sealed and open fractures tend to have similar orientations (see also Appendix 2). The orientations of fractures in the three topmost deformation zones in borehole KSH01A are shown in Figure 5-36, showing relatively more subvertical fractures striking NW to NNW, indicating that deformation zones are steeply dipping. Appendix 2 presents similar plots of open, partly open and sealed fractures as well as for all analysed boreholes. Further orientation analysis of sets, association to rock type etc., is presented in Section 5.5.

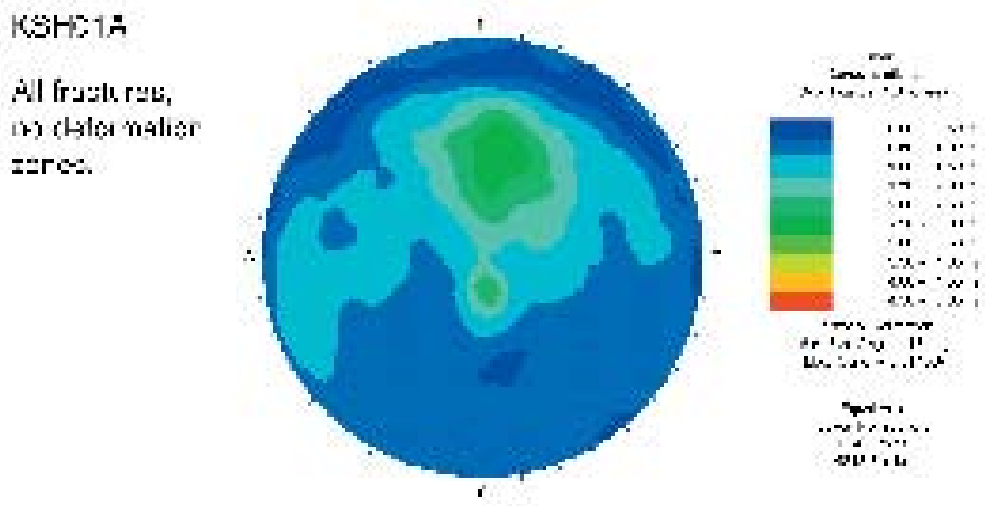

Figure 5-35. *Equal area, lower hemisphere projection of contoured poles to fracture planes in borehole KSH01A (fractures associated with interpreted deformation zones excluded).*

KSH01A

All fractures (no crush) in deformation zone (DZ1) between 136 to 160 m borehole depth.

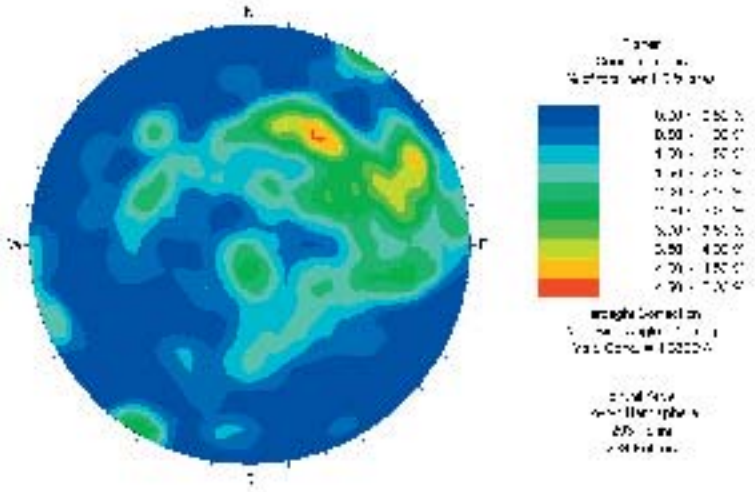

KSH01A

All fractures (no crush) in deformation zone (DZ2) between 239.5 to 281.5 m borehole depth.

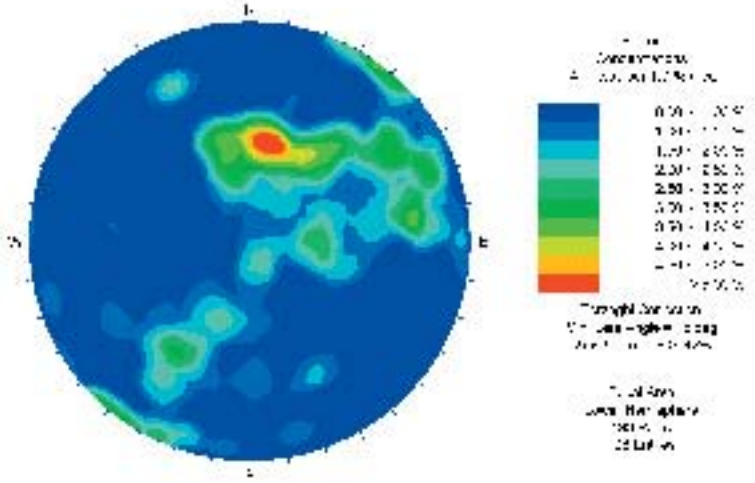

KSH01A

All fractures (no crush) in deformation zone (DZ4) between 259 to 287 m borehole depth.

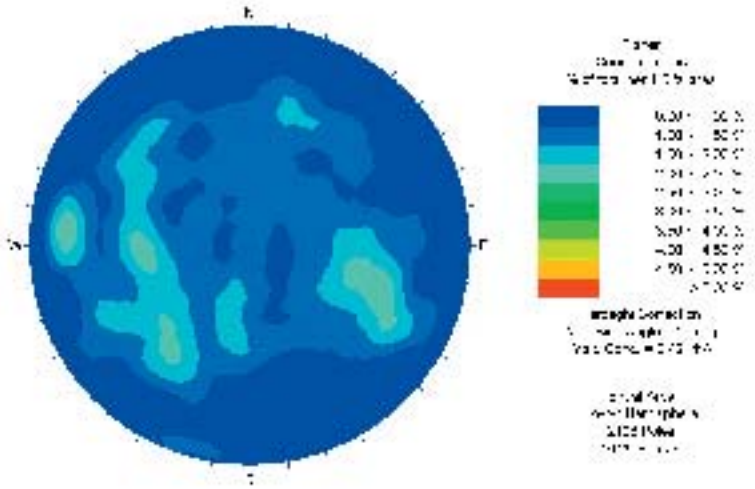

Figure 5-36. *Equal area, lower hemisphere projection of contoured poles of all fractures in a selection of interpreted deformation zones in borehole KSH01A.*

5.2.6 Geologic interpretation of borehole data

Rock types in cored boreholes

The distribution of rock types from the Boremap mapping of the cored boreholes KSH01A, KSH02, KSH03A on the Simpevarp peninsula, KAV01 on the Ävrö island and KLX02 /Ehrenborg and Stejskal, 2004a,b,c,d,e/ in the Laxemar subarea is displayed in the diagrams in Figure 5-37.

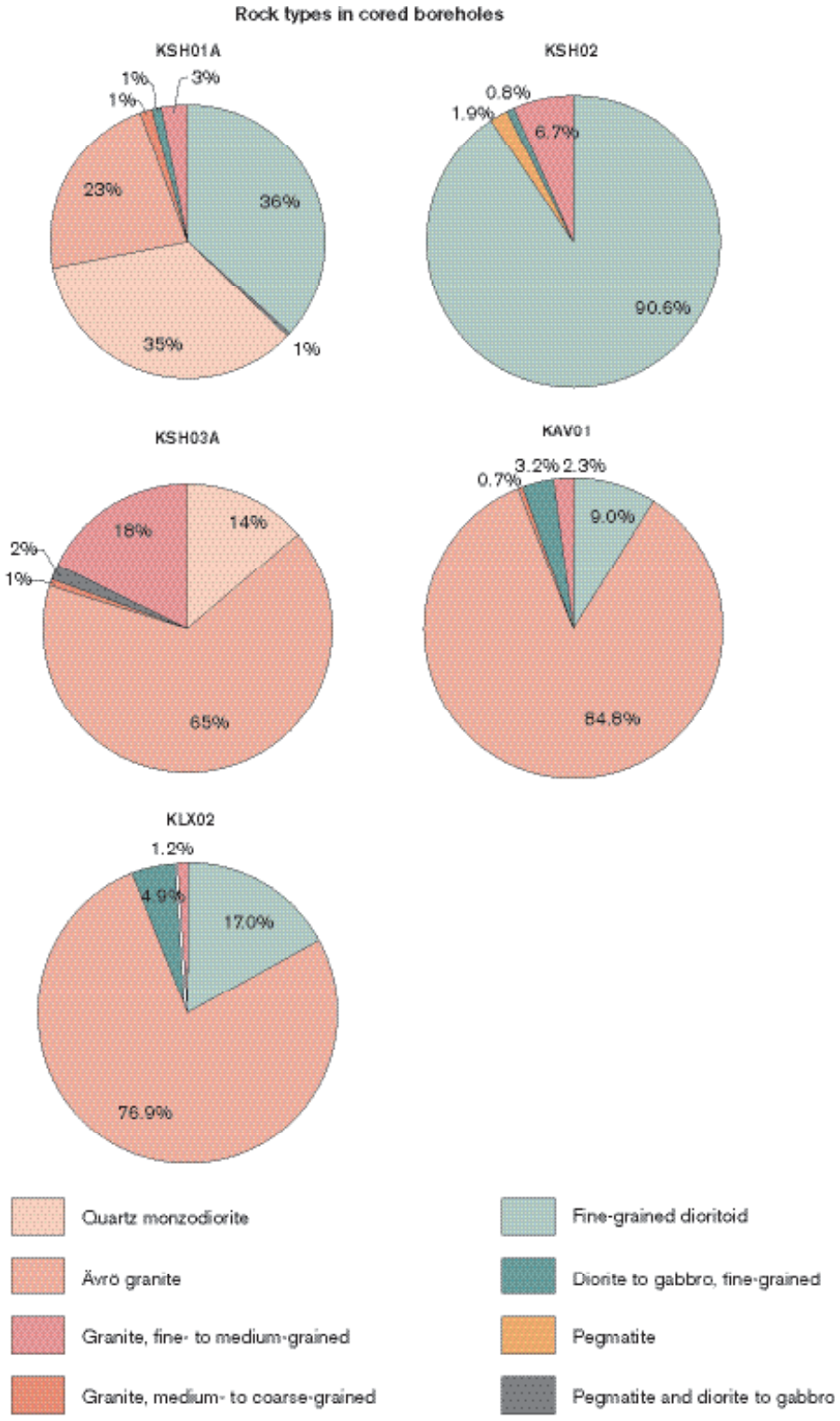

Figure 5-37. *Distribution of rock types in cored boreholes.*

Note that the Boremap mapping of KLX02 only comprises the section 200–1,000 m, although the borehole is c. 1,700 m deep. The percentage of each rock type represents the sum of all portions of the rock type along each borehole. This implies that a particular rock type may be distributed in several more or less long sections in the boreholes mixed with other rock types as is shown in Figure 5-38 and Figure 5-39. As is evident in Figure 5-37, Ävrö granite (granite to quartz monzodiorite, generally porphyritic), quartz monzodiorite and fine-grained dioritoid are the dominant rock types, although they occur in different proportions and are not recorded in every borehole.

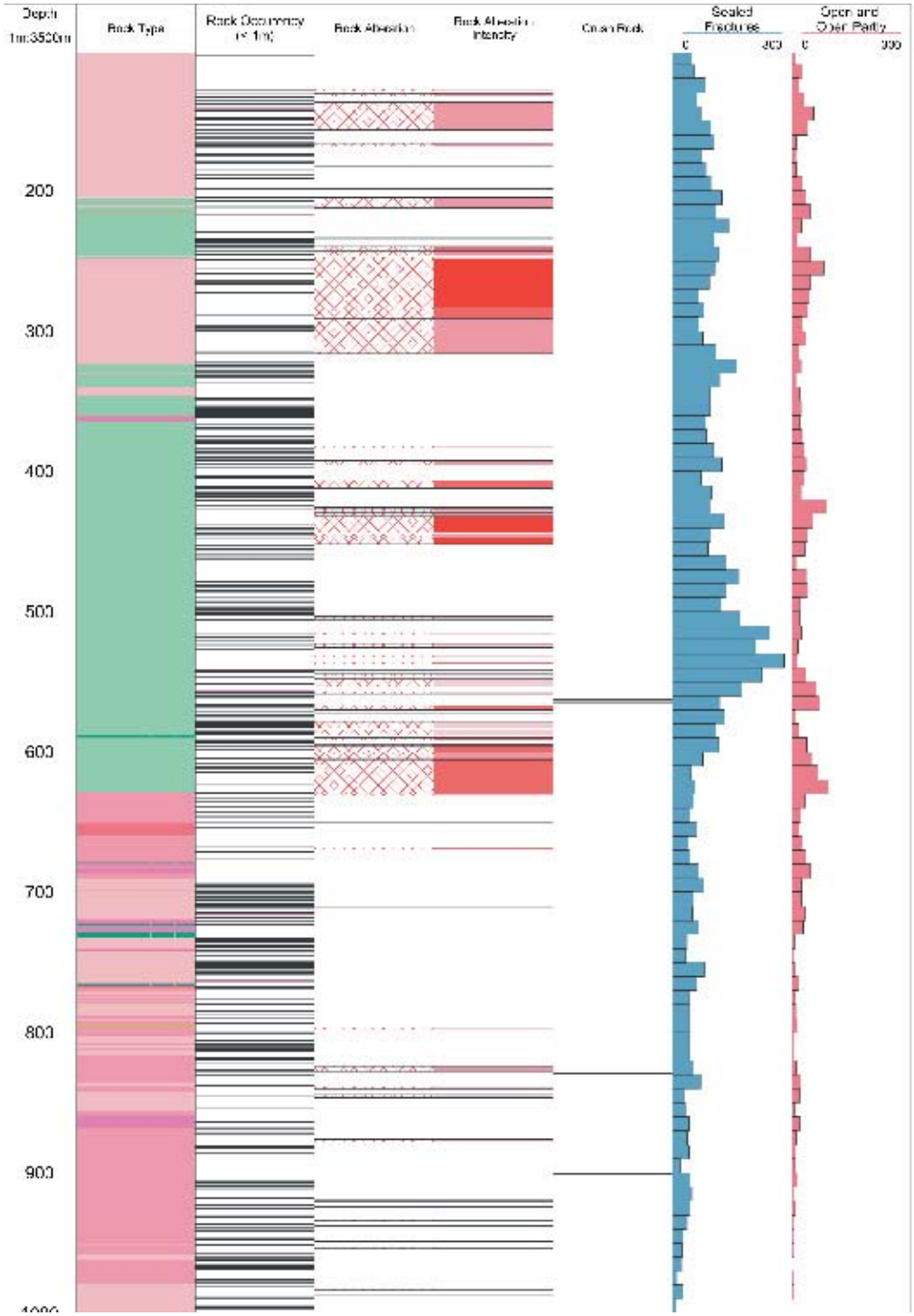

Figure 5-38. *Overview of the distribution of rock types in the cored borehole KSH01A. Legend of rock types according to Figure 5-37.*

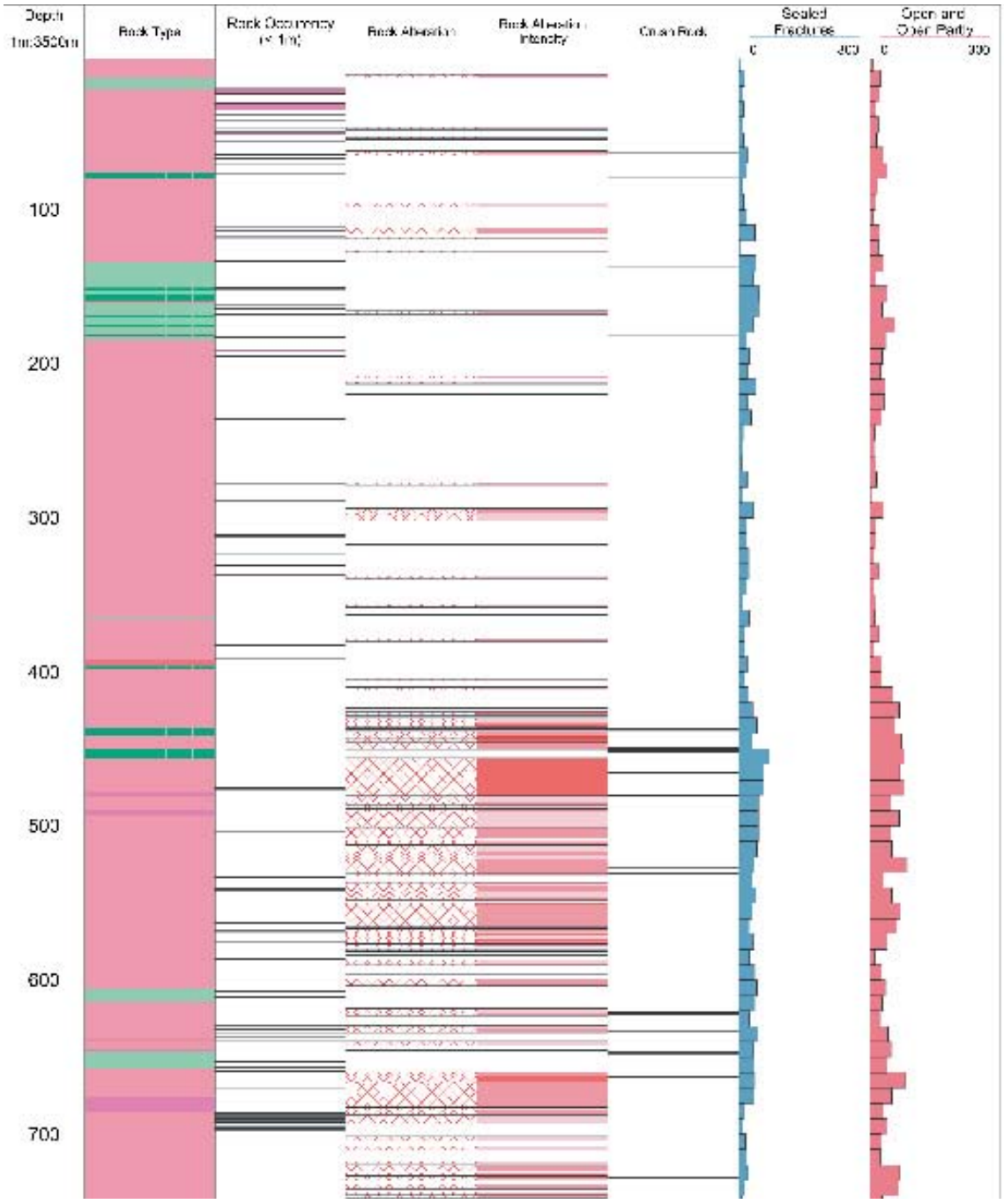

Figure 5-39. *Overview of the distribution of rock types in the cored borehole KAV01. Legend of rock types according to Figure 5-37.*

The Ävrö granite is a dominant rock type in all boreholes except for KSH02, which is totally dominated by the fine-grained dioritoid. The quartz monzodiorite only constitutes a dominant rock type in boreholes KSH01A and KSH03A, whereas the fine-grained dioritoid is documented as an important lithological component in all boreholes except KSH03A.

Note that the fine- to medium-grained granite constitutes almost 20% of the total borehole length in KSH03A.

In the cored borehole KSH01A, fine-grained dioritoid is the predominating rock type between c. 322 and 631 metres (cf. Section 12.1). The remaining part of KSH01A is characterised by alternating sections of variable length made up by Ävrö granite and quartz monzodiorite. The latter also applies for the upper c. 270 m of KSH03A/B.

A conspicuous rock type observed in KSH03A is sandstone, presumably Cambrian in age, that occupies c. 0.1 m of the drill core at a borehole length of approximately 270 m, i.e. within and close to the lower contact of the documented deformation zone ZSMNE024A in this borehole, (cf. Section 3.1 and 5.4.3).

For the description and characterisation of the different rock types, see Section 5.2.2.

Geological and geophysical logs

There are thirty-six identified radar reflections in boreholes KSH01A, HSH01, HSH02 and HSH03, evenly distributed over the sampled depth interval 0–200 m, cf. Table 5-7. There are seventy-one reflections in KSH02. In KSH03A over 100 radar reflectors were identified (Table 5-8) and most of them also orientated (strike/dip). About 20 radar reflectors were identified in KSH03B. The radar information has not been analysed in detail in support of model version Simpevarp 1.2, but has been incorporated indirectly through the usage of the single-hole interpretations from the corresponding boreholes.

Fracture mineralogy

Fracture minerals are determined macroscopically and are mapped within the Boremap system. However, many of the minerals are difficult to identify and small crystals are easily overlooked. Therefore, fracture mineral analyses have been carried out on samples from boreholes KSH01A and KSH01B for identification. These analyses have mainly comprised:

X-ray diffractometry; especially used for identification of clay minerals and gouge material composition; 23 samples have been analysed by XRD;

Table 5-7. Distribution of identified structures from the radar investigations in boreholes KSH01A and KSH02 /from Gustafsson and Gustafsson, 2004a; Nilsson and Gustafsson, 2003/.

Intersection depth	KSH01	Intersection depth	KSH02
0–50	–	0–50	1
50–100	–	50–100	2
100–150	3	100–150	5
150–200	4	150–200	7
200–250	6	200–250	2
250–300	3	250–300	2
300–350	4	300–350	3
350–400	5	350–400	2
400–450	2	400–450	4
450–500	1	450–500	5
500–550	3	500–550	2
550–600	4	550–600	3
600–650	2	600–650	4
650–700	3	650–700	3
700–750	3	700–750	5
750–800	3	750–800	2
800–850	3	800–850	7
850–900	1	850–900	3
900–950	2	900–950	5
950–1,000	1	950–1,000	4

Table 5-8. Distribution of identified structures from the radar investigation in borehole KSH03A /from Gustafsson and Gustafsson, 2004b/.

Depth (m)	No. of structures
100–150	10
150–200	6
200–250	4
250–300	5
300–350	9
350–400	6
400–450	7
450–500	6
500–550	7
550–600	5
600–650	5
650–700	5
700–750	3
750–800	2
800–850	4
850–900	5
900–950	5
950–1,000	5
1,000–	4

Microscopy of fracture fillings; around 30 fractures from borehole KSH01A have been sampled and 30 thin sections and 5 fracture surfaces have been studied by SEM /Drake and Tullborg, 2004/.

The most common fracture minerals are chlorite and calcite, which occur in several different varieties and are present in most of the open fractures. Other common minerals are epidote, prehnite, laumontite, quartz, adularia (low-temperature K-feldspar), fluorite, hematite and pyrite. A barium-zeolite named harmotome has been identified in some fractures and apophyllite has been identified in a few diffractograms.

Clay minerals identified are, in addition to chlorite, made up of corrensite (mixed-layer chlorite/smectite or chlorite/vermiculite clay, the smectite or vermiculite layers are swelling), illite, mixed-layer illite/smectite (swelling) and a few observations of smectites.

Results from XRD analyses

Samples for XRD identification have mainly been taken from open and usually water conducting fractures with loose and clayish coatings, often of fault gouge type. All the fractures sampled are located in the uppermost 600 metres of the borehole (KSH01A+B) as the deeper part shows very low hydraulic conductivity and a low frequency of open fractures. The fine fraction from each sample has been separated and oriented samples on glass were prepared for clay mineral identification.

Most of the samples contain quartz, K-feldspar, and albite in addition to calcite, chlorite and clay minerals (cf. Table 5-9). From earlier studies of open fractures at Äspö (e.g. material from the TRUE experimental sites), it is known that altered rock fragments dominate the gouge material, /Andersson et al. 2002c/. It is, therefore, probable that most of the quartz and feldspars together with the few observations of amphibole and biotite belong to these rock fragments, although contamination due to incorporation of material from the wall rock cannot be ruled out. The total clay mineral content in the open fractures is very difficult to determine in an appropriate way and the XRD analyses should not be regarded as necessarily being representative for the entire filling, but more of the specific sample. However, in fractures filled with fault gouge, a reasonable estimate of the amount of clay mineral (chlorite not included) does not exceed 10–20 weight %. Thin coatings attached to the fracture wall can consist of 90–100% chlorite and clay minerals. The amounts are relatively small, as these coatings are usually thin (< 100 µm) but their surface(-s) can be very large (cf. SEM photo of mixed-layer clay coating cf. Figure 5-42.

Minerals constituting less than 5–10% of a sample by weight may not be detected in the diffractograms and particular minerals, e.g. hematite and pyrite, which have been detected in some of the XRD samples, are likely to be present in several of the other samples as well.

Smectite which is a significant swelling clay mineral, has been identified in three of the samples from KSH01A (at 3.7 m, 24 m and 289.8 m).

Table 5-9. XRD analyses of fracture material from open fractures in borehole KSH01A+B (Analyses carried out by the Geological Survey of Sweden, Uppsala).

Sample Core length	Qtz	Kfsp	Alb	Ca	Chl	Py	Hem	Amp	Bi	Pre	Epi	Apo	Clay	Corr	M-l Clay	Ill	Smec
3.7–3.87	x			xxx	(x)								xx	yy'			y
24.0	xx	xx	x		x	x		x					x				yy
67.8–67.9	xx	xx	xx	x	xx								x		yy	(y)	
81.35	xx	xx	xx	x	x								x		y	yy	
82.2	xx	xx	xx	x	xx								x		yy	y	
95.0		xx	xx	xxx	x			x			x		x	y	y	(y)	
130.83	xx		x	xxx	x			x					(x)*				
159.20 m (I)	xx	x	x	xxx	xx			x					x	yy			
159.20 m (II)	xx	xx	x	xx	xxx			x					xx*			y	
178.25–178.35			xx	xx	x							xxx	x	yy			
249.0	x	x	x	xx	x								(x)*				
250.4	xx	xx		x	xx		x						(x)			(y)	
255.78–255.93	xx	xx		x	xx		x						x	yy'			
259.3	xx	xx		xx	xx		x						x		yy	y	
267.97–268.02	xx	xx		xx	xx		x						xx	yy			
289.8–289.95	xx	xx			xxx								x				yy
290.9	xx	x	xxx	xx	xx								x	yy			
306.77	x	x	x	xxx	x								x	yy			
325.93	xx		x		x				xx			xx	x	yy			
447.34	xx	x			xx					xx	x	xx	x	yy			
514.46	xx			xx	xx								x	y	yy		
558.60–558.65	xx	xx		x	xx		x						x	yy			
590.35–590.52	xx	xx	xx		xx								x		y	yy	

Qtz = quartz, Kfsp = K-feldspar usually adularia, Alb = Na-plagioclase (albite), Ca = calcite, Chl = chlorite, Py = pyrite, Hem = hematite.

Amp = amphibole, Bi = biotite, Pre = prehnite, Ep = epidote, Apo = apophyllite, Clay = presence of clay minerals indicated in the random oriented sample, the clay minerals are identified in the fine fraction oriented sample, results are marked with y.

Corrensite = swelling mixed layer clay with chlorite/smectite or chlorite/vermiculite regularly interlayered, M-l clay = mixed layer clay with illite/smectite layers, ill = illite, Smec = smectite * = indicates swelling chlorite, ‘ = indicates corrensite without 1:1 layering.

xxx = dominates the sample, xx = significant component, x = minor component, OBS this is only semi-quantitative.

yy = dominating clay mineral in the fine fraction, y = identified clay mineral in the fine fraction.

( ) = potentially present.

Results from microscopy and SEM studies

The fractures sampled for microscopy comprise open as well as sealed fractures from the entire length of borehole KSH01A with a focus on the uppermost 600 metres (example shown in Figure 5-40). All sample descriptions and results from the SEM/EDS analyses of different fracture minerals are provided in /Drake and Tullborg, 2004/. The aim of the microscopy, in addition to identification of minerals, is to determine different mineral parageneses and their sequences of formation and also to establish the different chemical varieties of minerals present (primarily chlorite and calcite).

The fracture mineralogy as revealed in drill core KSH01A+B (cf. Figure 5-41) shows several generations of mineralisations ranging from epidote facies (epidote, albite, quartz, calcite, pyrite and muscovite) in combination with ductile deformation, over to brittle deformation in combination with oxidation and formation of hematite, causing extensive red-staining of the wall rock along the fractures. Subsequent breccia sealing by prehnite-fluorite, calcite and Fe-Mg chlorite has occurred followed by adularia, hematite, Mg-chlorite and calcite formation. The latest hydrothermal mineralisation shows a series of decreasing formation temperature as follows; Mg-chlorite, adularia, laumontite (Ca-zeolite), pyrite, hematite, harmotome (Ba-zeolite), Fe-chlorite (sperulitic), calcite + REE-carbonates and clay minerals. There is an ongoing pilot study to attempt dating of the hydrothermal mineralisations using Rb-Sr and Ar-Ar techniques. Early results may be available for the Laxemar 1.2 modelling. Furthermore, indirect dating of calcites using stable isotopes is ongoing and results will also become available for the Laxemar model version 1.2.

Figure 5-40. *Drillcore sample KSH01A:603.11 m showing fracture sealed by prehnite (greenish) and cut by discordant calcite filling (white). Note the red staining and chloritisation of the wall rock. Blue line shows location of thin section.*

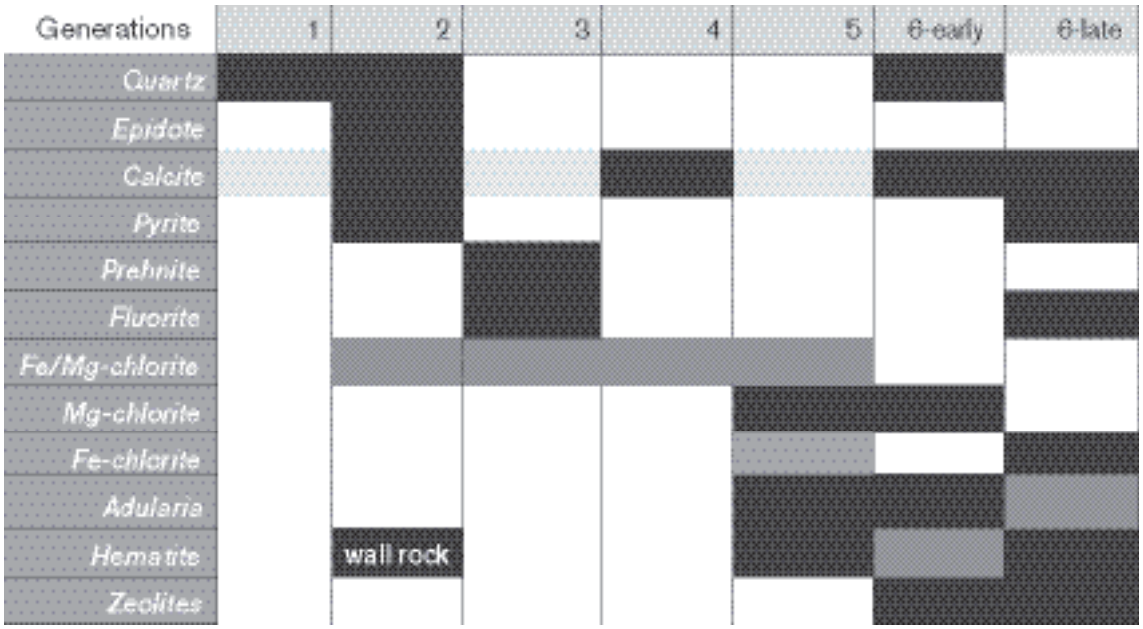

Figure 5-41. *Compiled results showing the paragenesis and different generations determined from microscopy and SEM/EDS /Drake and Tullborg, 2004/. Black colour represents major mineral present in a generation. Dark and light grey represents minerals that are present, but not dominant and possibly present, respectively.*

The outermost coatings along the hydraulically conductive fractures consist mainly of clay minerals of illite and mixed layer clays (corrensite = chorite/smectite and illite/smectite), cf. Figure 5-42, together with calcite and minor grains of pyrite. It is assumed that especially the calcite and pyrite formation is an ongoing process although the amounts of possible recent precipitates are low.

From the fracture mineral data available to date the following can be concluded.

The over all fracture mineralogy is very similar to earlier observations in the Äspö HRL /cf. e.g. Landström and Tullborg, 1995; Andersson et al. 2002c/.

The drill core KSH01A+B is well preserved (flushing and grinding have been minimised), which has facilitated sampling of relatively undisturbed clay mineral samples.

Furthermore, it has been possible to study calcite and pyrite that have grown fracture edges as well as soft or brittle zeolites minerals. This has, for example, resulted in the identification of the previously overlooked Ba-zeolite harmotome.

The red-staining of the wall rock around many fractures and mapped fractures zones, corresponds to hydrothermal alteration/oxidation, which has resulted in saussuritisation of plagioclase, breakdown of biotite to chlorite and oxidation of Fe(II) to form hematite, mainly present as micrograins giving rise to the red colour. However, there is not always a perfect correspondence between the extent of hydrothermal alteration and red-staining /cf. also Landström et al. 2001/.

In the fractures, several generations of hematite and pyrite are present. The finding of small pyrite grains in the outermost layers of the fracture coatings is in agreement with the groundwater chemistry, indicating reducing conditions /cf. Laaksoharju et al. 2004b/. More detailed studies of the redox-sensitive minerals and the timing of the hydrothermal oxidation event/-s is ongoing and needs to be assessed in the next model version.

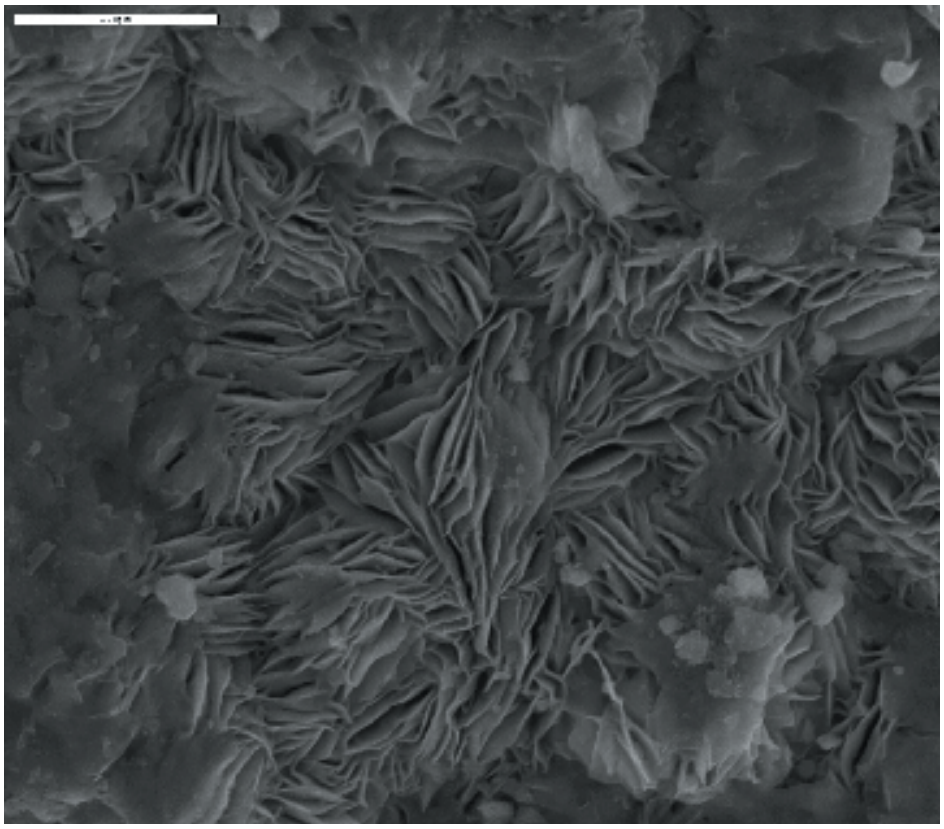

Figure 5-42. *SEM photo showing mixed layer clay on a fracture surface from borehole KSH01A (scale bar = 20 mm).*

It has, so far, not been possible to link different fracture minerals to different fracture orientations. The same difficulty was experienced in a corresponding analysis of a larger data set from Äspö /cf. Munier, 1993; Mazurek et al. 1997/;

- The sequence of minerals, going from epidote facies in combination with ductile deformation, over to brittle deformation and breccia sealing during prehnite facies and subsequent zeolite facies and further decreasing formation temperature series, indicates that the fractures were initiated relatively early in the geological history of the host rock and have been reactivated during several different periods of various physiochemical conditions.
- The locations of the hydraulically conductive fractures are mostly associated with the presence of gouge-filled faults produced by brittle reactivation of earlier ductile precursors or hydrothermally sealed fractures. The outermost coatings along the hydraulically conductive fractures consist mainly of clay minerals, usually illite and mixed layer clays (corrensite = chorite/smectite and illite/smectite) together with calcite and minor grains of pyrite.

Resulting single-hole interpretation

Geological single-hole interpretations were developed for all analysed boreholes given in Table 5-3 except KLX02 and are presented in /Mattson et al. 2004a,b/. The single-hole interpretation supplies, among several things, the sections of potential deformation zones, cf. Table 5-10, which have been used for evaluation of fracturing within deformation zones, cf. Appendix 2 and of fracturing in the rock mass, cf. Section 5.5. The logs also present simplifications of the rock mass into rock units, which are incorporated directly into the lithological modelling.

The rock units are numbered independently in the various holes, where each unit may have its own unique interpretation (Table 5-11). These rock units have then been simplified further to support the same division of the rock mass as used on the geological bedrock map at the surface. This simplified characterisation is described in Section 5.3.

Table 5-10. Sections of mapped deformation zones as obtained from available single hole interpretations. Note that the interpretation of borehole KLX02 was not available for this model version.

Borehole	Secup (m)	Seclow (m)	Typical host rock (dominating)	Comment
HSH01	35.00	50.00	Quartz monzonite to monzodiorite, equigranular to weakly porphyritic	Increased fracturing and alteration indicated by high penetration rate, BIPS, drill cutting and geophysical logging data.
HSH01	160.00	171.00	Quartz monzonite to monzodiorite, equigranular to weakly porphyritic	Increased fracturing indicated by high penetration rate, low susceptiblity and low resistivity. Aleration indicated by drill cuttings.
HSH02	15.00	30.00	Fine-grained dioritoid	Increased fracturing and alteration. Indicated by high penetration rate, BIPS and geophysical logging data.
HSH02	82.00	90.00	Fine-grained dioritoid	Increased fracturing
HSH02	100.00	109.00	Fine-grained dioritoid	Increased fracturing.
HSH02	126.00	147.00	Fine-grained dioritoid	Increased fracturing.
HSH03	58.50	98.50	Quartz monzonite to monzodiorite, equigranular to weakly porphyritic	Increased fracturing and alteration indicated by BIPS, drill cuttings, high penatration rate and geophysical logging data.
KAV01	426.50	437.50	Granite to quartz monzodiorite, generally porphyritic	Increased fracturing.
KAV01	437.50	464.00	Granite to quartz monzodiorite, generally porphyritic	Alteration, low susceptibility and resistivity.
KAV01	464.00	565.00	Granite to quartz monzodiorite, generally porphyritic	Increased fracturing, low density and susceptibility.
KSH01A	136.50	160.00	Quartz monzonite to monzodiorite, equigranular to weakly porphyritic	Increased, fracturing. Indication: Low susceptibility, sonic, density and resistivity.
KSH01A	239.50	251.50	Fine-grained dioritoid	Increased fracturing. Partly alteration. Indication: Low susceptibility, density, sonic and resistivity.
KSH01A	259.00	287.00	Quartz monzonite to monzodiorite, equigranular to weakly porphyritic	Increased fracturing. Partly alteration. Indication: Low susceptibility, density, sonic and resistivity.
KSH01A	420.00	455.00	Fine-grained dioritoid	Partly increased fracturing. Heavy alteration. Indication: Low susceptibility and resistivity.
KSH01A	540.00	608.50	Fine-grained dioritoid	Partly increased fracturing. Partly heavy alteration. Indication: Low susceptibility and resistivity.
KSH01A	614.00	631.00	Fine-grained dioritoid	Partly increased fracturing. Partly heavy alteration. Indication: Low susceptibility and resistivity.
KSH01A	672.00	686.50	Granite to quartz monzodiorite, generally porphyritic	Increased fracturing. Indication: Low susceptibility and density.
KSH01A	692.50	693.00	Quartz monzonite to monzodiorite, equigranular to weakly porphyritic	Increased fracturing. Indication: Low susceptibility and density.
KSH01A	251.50	259.00	Quartz monzonite to monzodiorite, equigranular to weakly porphyritic	Low-grade, ductile shear-zone.
KSH01A	608.50	614.00	Fine-grained dioritoid	Low-grade, ductile shear-zone.
KSH01A	686.50	692.50	Granite to quartz monzodiorite, generally porphyritic	Low-grade, ductile shear-zone.
KSH01A	766.00	767.00	Mafic rock, fine-grained	Low-grade, ductile shear-zone.
KSH01A	833.50	834.50	Granite to quartz monzodiorite, generally porphyritic	Low-grade, ductile shear-zone.
KSH02	233.50	280.50	Fine-grained dioritoid	Increased fracturing.
KSH02	280.50	303.50	Fine-grained dioritoid	Alteration, low density and susceptibility.
KSH02	511.00	532.00	Fine-grained dioritoid	Alteration, low density and susceptibility.

Table 5-11. Example of rock units interpreted in boreholes KSH01A and KSH02 as obtained from single hole geological interpretations /Mattson et al. 2004a,b/.

Idcode	Secup (m)	Seclow (m)	RU	Comment
KSH01A	100.00	136.50	RU1	Rock unit dominated by quartz monzodiorite (quartz monzonite to monzodiorite) with subordinate sections of fine-grained granite pegmatite and sparsely porhyritic Ävrö granite (granite to quartz monzodiorite).
KSH01A	160.00	205.00	RU1	Rock unit dominated by quartz monzodiorite (quartz monzonite to monzodiorite), with subordinate sections of fine-grained granite, pegmatite and sparsely porhyritic Ävrö granite (granite to quartz monzodiorite).
KSH01A	205.00	239.50	RU2	Rock unit dominated by fine-grained dioritoid (fine-grained, intermediate, magmatic rock) with subordinate sections of quartz monzodiorite (quartz monzonite to monzodiorite), fine- to medium-grained granite, pegmatite and fine-grained diorite to gabbro (fine-grained mafic rock).
KSH01A	287.00	322.50	RU1	Rock unit dominated by quartz monzodiorite (quartz monzonite to monzodiorite), with subordinate sections of fine-grained granite, pegmatite and sparsely porhyritic Ävrö granite (granite to quartz monzodiorite).
KSH01A	322.50	420.00	RU2	Rock unit dominated by fine-grained dioritoid (fine-grained, intermediate, magmatic rock)with subordinate sections of quartz monzodiorite (quartz monzonite to monzodiorite), fine- to medium-grained granite, pegmatite and fine-grained diorite to gabbro (fine-grained mafic rock).
KSH01A	455.00	540.00	RU2	Rock unit dominated by fine-grained dioritoid (fine-grained, intermediate, magmatic rock) with subordinate sections of quartz monzodiorite (quartz monzonite to monzodiorite), fine- to medium-grained granite, pegmatite and fine-grained diorite to gabbro (fine-grained mafic rock).
KSH01A	631.00	672.00	RU3	Rock unit characterized by a mixture of sparsely porphyritic Ävrö granite (granite to quartz monzodiorite) and quartz monzodiorite (quartz monzonite to monzodiorite), with subordinate sections of fine- to finely medium-grained granite, medium- to coarse-grained granite, fine- grained diorite to gabbro (fine-grained mafic rock) and pegmatite.
KSH01A	693.00	766.00	RU3	Rock unit characterized by a mixture of sparsely porphyritic Ävrö granite (granite to quartz monzodiorite) and quartz monzodiorite (quartz monzonite to monzodiorite), with subordinate sections of fine- to finely medium-grained granite, medium- to coarse-grained granite, fine- grained diorite to gabbro (fine-grained mafic rock) and pegmatite.
KSH01A	767.00	833.50	RU3	Rock unit characterized by a mixture of sparsely porphyritic Ävrö granite (granite to quartz monzodiorite) and quartz monzodiorite (quartz monzonite to monzodiorite), with subordinate sections of fine- to finely medium-grained granite, medium- to coarse-grained granite, fine- grained diorite to gabbro (fine-grained mafic rock) and pegmatite.
KSH01A	834.50	839.00	RU3	Rock unit characterized by a mixture of sparsely porphyritic Ävrö granite (granite to quartz monzodiorite) and quartz monzodiorite (quartz monzonite to monzodiorite), with subordinate sections of fine- to finely medium-grained granite, medium- to coarse-grained granite, fine- grained diorite to gabbro (fine-grained mafic rock)and pegmatite.
KSH01A	839.00	958.00	RU4	Rock unit dominated by sparsely porphyritic Ävrö granite (granite to quartz monzodiorite), with subordinate sections of fine- to finely medium-grained granite, fine-grained diorite- to gabbro (fine-grained mafic rock), pegmatite and diorite to gabbro.
KSH01A	958.00	1,001.00	RU3	Rock unit characterized by a mixture of sparsely porphyritic Ävrö granite (granite to quartz monzodiorite) and quartz monzodiorite (quartz monzonite to monzodiorite), with subordinate sections of fine- to finely medium-grained granite, medium- to coarse-grained granite, fine- grained diorite to gabbro (fine-grained mafic rock) and pegmatite.
KSH02	80.00	233.50	RU1	Rock unit completely dominated by fine-grained dioritoid (fine-grained, intermediate,magmatic rock) with a few < 5 m long sections of pegmatite. Furthermore, a few scattered thin sections of fine- to medium-grained granite occur. Sealed fracture frequency very high!

Idcode	Secup (m)	Seclow (m)	RU	Comment
KSH02	303.50	470.00	RU1	Rock unit completely dominatedby fine-grained dioritoid (fine-grained, intermediate,magmatic rock) with a few < 5 m long sections of pegmatite. Furthermore, a few scattered thin sections of fine- to medium-grained granite occur. Sealed fracture frequency very high!
KSH02	470.00	511.00	RU2	Rock unit characterized by a mixture of fine-grained dioritoid (fine-grained, intermediate,magmatic rock) and up to 20 m long sections of fine- to medium-grained granite. Furthermore, a few < 4 m long sections of pegmatite occur. Sealed fracture frequency very high.
KSH02	532.00	654.00	RU2	Rock unit characterized by a mixtureof fine-grained dioritoid (fine-grained, intermediate,magmatic rock) and up to 20 m long sections of fine- to medium-grained granite. Furthermore, a few < 4 m long sections of pegmatite occur. Sealed fracture frequency very high.
KSH02	681.00	743.00	RU2	Rock unit characterized by a mixtureof fine-grained dioritoid (fine-grained, intermediate,magmatic rock) and up to 20 m long sections of fine- to medium-grained granite. Furthermore, a few < 4 m long sections of pegmatite occur. Sealed fracture frequency very high.
KSH02	743.00	1,007.00	RU3	Rock unit very similar to rock unit 1, i.e. completely dominated by fine-grained dioritoid (fine-grained, intermediate, magmatic rock). An exception is a c. 10 m long section of fine-grained diorite to gabbro (fine-grained, mafic rock) between c. 970 and 980 m.

5.3 Lithological model

5.3.1 Modelling assumptions and input from other disciplines

In the Simpevarp 1.1 model, no three-dimensional modelling of rock domains was presented for the regional model area or the entire local-scale model area, but only for the Simpevarp local scale model area (which is smaller in area than that employed for Simpevarp 1.2) /SKB, 2004b/. The Simpevarp 1.1 site descriptive lithological model forms the basis for the present modelling, which covers the entire regional model area. In the version 0 report /SKB, 2002b/, no three-dimensional model was presented. A lithological model as a vertical section across Äspö is presented in /Rhén et al. 1997a/. Also, a tentative three-dimensional lithological model has been presented for Ävrö /Markström et al. 2001/. Furthermore, as a result of the testing of the methodology for the site descriptive modelling procedure, a three-dimensional lithological model was presented for Laxemar /Andersson et al. 2002b/, i.e. the westernmost part of the local scale model area used for the Simpevarp 1.1 modelling. However, this model has not been evaluated and incorporated in the present lithological model, mainly because the Laxemar project was designed only as a methodology test. Furthermore, there were significant limitations in the input data and the scope of analysis.

Six deep cored boreholes (KLX01, KLX02, KSH01, KSH02, KSH03 and KAV01) and a number of shallow percussion boreholes are available in the present Simpevarp local scale model area. Furthermore, geophysical modelling has been used to establish the geometric relationships between rock domains in the Laxemar area /Triumf et al. 2003/, and for the geometry of the Götemar and Uthammar granites in the regional model area /Nisca, 1987/. However, the construction of the rock domain model is principally based on existing bedrock data from the surface, i.e. the bedrock map of the Simpevarp subarea and the version 0 bedrock map in the remaining part of the model area (see Section 5.2.2).

5.3.2 Conceptual model with potential alternatives

This section describes how the three-dimensional lithological model of the Simpevarp regional model area has been constructed. The terms rock units and rock domains are used here according to the terminological guidelines for geological site descriptive modelling given in /Munier et al. 2003/. Rock units are defined on the basis of the mineralogical composition, grain size, texture, and age of the dominant rock type. In particular, composition and grain size are judged to have some relevance for the construction of a repository. Rock domains are defined on the basis of an integration of the rock units taking into account these geological criteria, i.e. rock units of the same character have been put together into one and the same rock domain. In addition, a complex and intimate mixing of rock types, i.e. the degree of homogeneity in the bedrock, has also been used as a criterion in the definition of a given rock domain.

The first stage in the modelling procedure is the identification of rock domains at the surface. This involves the use of six principal rock units distinguished on the basis of the composition, grain size, texture and also age of the dominant rock type (Table 5-12)). Note that these rock units should not be confused with the simplified units introduced in the geological single-hole interpretation of borehole KSH01A, cf. Section 5.2.7.

Since the bedrock in the regional model area employed for the Simpevarp 1.2 modelling is dominated by more or less pristine igneous rocks, there are no ductile structural frameworks that can be adopted as a guide for the three-dimensional geometric modelling of the rock domains. If no subsurface data exist, e.g. from cored boreholes and/or geophysical modelling, that relate to depth extension (geometry) of the interpreted rock domains, the following assumption has been adopted in the modelling procedure:

- Rock domains have been extended to a depth that equals the width of the rock domain at the surface. In addition, the width of the rock domains decreases gradually with increasing depth.

The above assumption is the basis for the geometric three-dimensional modelling of the rock domains in the regional model volume. The three-dimensional model is presented in conjunction with the description of the site (cf. Section 11.2)

An alternative assumption is that the larger rock domains, if subsurface data are lacking, extend vertically to the bottom of the model volume, whereas the minor rock domains are only modelled to a depth that equals their width at the surface.

Table 5-12. Bedrock components used in the lithological modelling procedure and their principal characteristics and encoding.

Rock units − composition, grain size and texture of dominant rock type			
Code (SKB)	**Composition**	**Complementary characteristics**	
501044	Granite to quartz monzodiorite	Medium-grained	Porphyritic
501036	Quartz monzodiorite	Medium-grained	Equigranular
501030	Dioritoid	Fine-grained	Unequigranular
501058	Granite	Medium- to coarse-grained	Equigranular to slightly porphyritic
511058	Granite	Fine- to medium-grained	Equigranular
501033	Diorite to gabbro	Medium-grained	Equigranular
521058	Granite (“Götemar type”)	Coarse-grained and fine- to medium-grained	Equigranular to slightly porphyritic

5.3.3 Division into rock domains and property assignment

Geometric modelling

The geometrical modelling follows the same principles that were applied in the Simpevarp 1.1 modelling. The latter lithological model has not been modified and is extended to comprise the entire regional model volume. Based on the Simpevarp 1.1 modelling, the following working stages have been followed during the geometric modelling:

- The Simpevarp 1.1 lithological model forms the basis for the present modelling /SKB, 2004b/.
- Integration of the bedrock map of the Simpevarp subarea with the bedrock map that was used in the version 0 report /SKB, 2002b/.
- Definition of the areal extension of rock domains at the surface using the bedrock components defined above (Table 5-12).
- Projection of the rock domains downward in the regional model volume.

In order to carry out the modelling properly, it was necessary to simplify the version 0 bedrock map before definition of and integration with the rock domains that were defined in the Simpevarp 1.1 model. The most important simplification is the integration of the medium- to coarse-grained granite in the northern and northwestern parts of the regional model area (Figure 5-3) with the Ävrö granite (cf. Figure 5-3 and Figure 5-43). This was judged to be reasonable, partly because the version 0 bedrock map is provisional in character and partly because the Ävrö granite includes granitic varieties (cf. Figure 5-4). Furthermore, some minor bodies of fine-to medium-grained granite and diorite to gabbro were included as subordinate rock types in the surrounding principal rock unit.

The next stage in the modelling involved an integration of the bedrock map of the Simpevarp subarea with the bedrock map compiled in conjunction with the Simpevarp version 0 /SKB, 2002b/. As the fine-grained dioritoid was not separated as a mappable unit in the version 0 bedrock map, the extension of the fine-grained dioritoid west of the Simpevarp subarea is based on the bedrock map by /Kornfält and Wikman, 1987/. Note that the fine-grained dioritoid has been extended further to the west compared with the Simpevarp 1.1 model.

The simplification and integration procedures applied to the surface data have yielded a geological map that shows rock domains in the local scale and regional scale model areas (Figure 5-43). The rock domains have been given different denominations (Figure 5-43), where rock domains denominated with the same capital letter are dominated by the same rock type.

On this basis, 36 rock domains have been identified in the regional model volume, and 17 of these rock domains make up the local scale model volume. All these domains have subsequently been modelled at depth. Note that the resolution is much higher in the eastern part of the local scale model volume than in the remaining part of the model area. This is due to the much higher resolution in the bedrock map of the Simpevarp subarea.

The final stage in the modelling work concerns the projection of the rock domains that have been recognised at the surface to a depth of –1,100 metres above sea level (m.a.s.l.) in the local scale model volume and to –2,100 m.a.s.l. in the regional scale model volume, i.e. to the respective bases of the two defined model volumes. The key assumptions adopted in this procedure have been summarised earlier in this section.

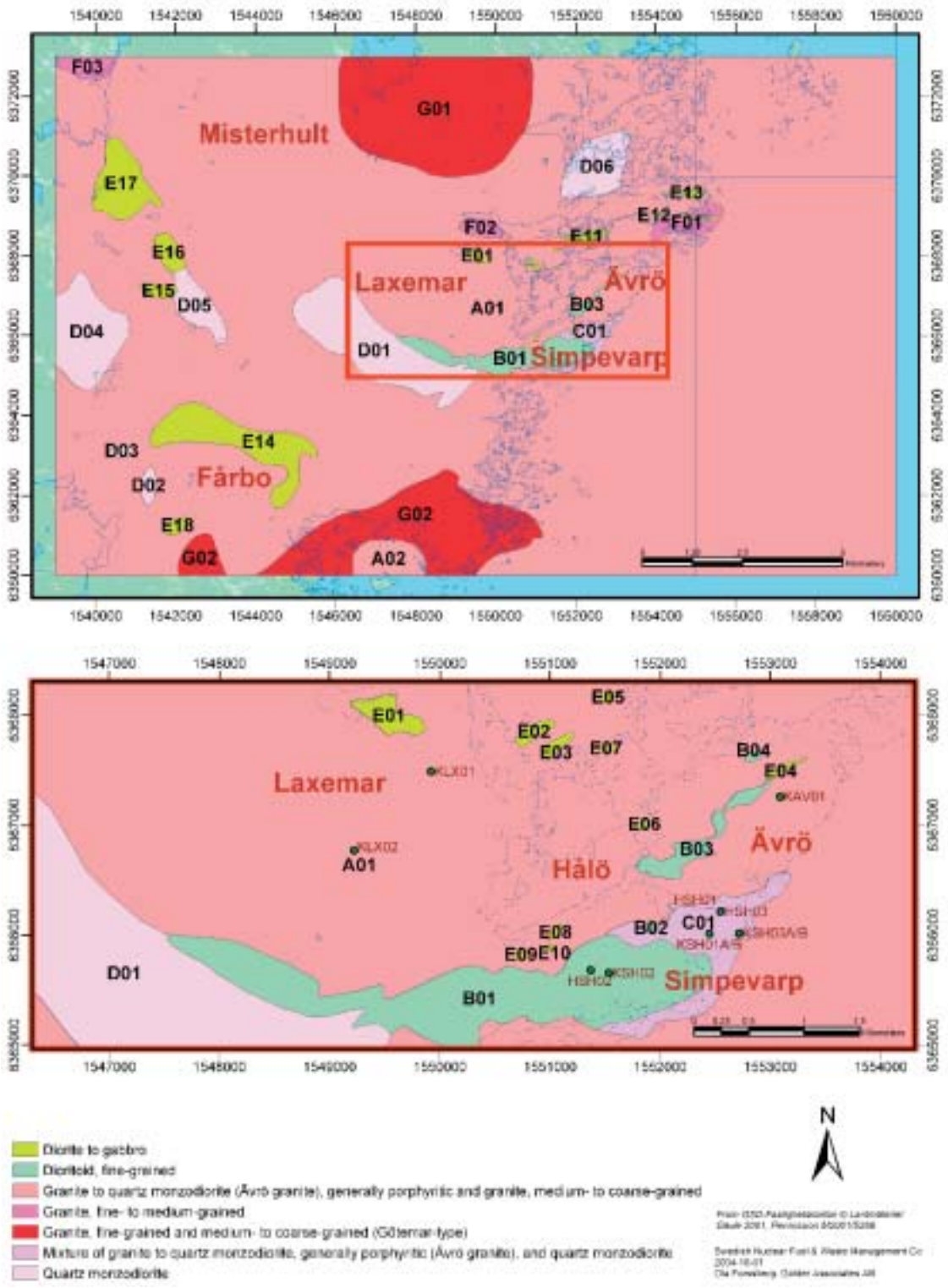

Figure 5-43. *Surface view of the rock domains used in the modelling procedure. Local scale model area (N=17) and regional scale model area (N=36), including the rock domains in the local scale model area).*

Assignment of properties

Each rock domain has been assigned a set of properties (Table 5-13), including the dominant and subordinate rock types in the domain. Furthermore, the properties of the different rock types have also been defined. All these properties are presented in tabular format in the summary description of the site (Section 11.2).

For the rock domains situated within the Simpevarp subarea, the properties of the rock domains (Table 5-13) have been extracted from the outcrop database (see Section 5.2.2). The key properties that define the rock types have been obtained from the petrographic, geochemical and petrophysical analyses of surface samples or, in the case of the gamma-ray spectrometric data, from the measurements carried out directly on the outcrop (see Section 5.2.2). Mean and standard deviation values as well as the number of samples analysed are provided for each property (Section 11.2).Additional information is available in the data from the cored boreholes KSH01A/B, KSH02, KSH03A/B, KAV01, KLX02 and the percussion boreholes HSH01 and HSH03. Only limited information is available from the bedrock compilation for rock domains or those parts of rock domains that are situated outside the Simpevarp subarea (see Section 5.2.2).

Important properties are the composition, grain size and texture of the different rock types in the various domains. By using the information in the outcrop database from the Simpevarp subarea (see Section 5.2.2), it has been possible to estimate qualitatively the relative amounts of the different rock types in each domain.

For example, in rock domain RSMA01, the lithology that forms the dominant rock type is the Ävrö granite, i.e. medium-grained, porphyritic granite to quartz monzodiorite (Figure 5-44). However, fine-grained granite, pegmatite, fine-grained dioritoid, diorite to gabbro, fine-grained diorite to gabbro, granite and quartz monzodiorite form subordinate rock types (Figure 5-44). Similar semi-quantitative information concerning the proportions of dominant and subordinate rock types in most of the remaining rock domains within the Simpevarp subarea are presented in Appendix 3.

Table 5-13. Properties assigned to each lithological rock domain.

Rock domain ID (RSM***, according to the nomenclature recommended by SKB)
Property
Dominant rock type
Mineralogical composition
Grain size
Age (million years)
Structure
Texture
Density
Porosity
Magnetic susceptibility (SI units)
Electric resistivity in fresh water (ohm m)
Uranium content based on gamma ray spectrometric data (ppm)
Natural exposure (µR/h)
Subordinate rock types
Degree of inhomogeneity
Metamorphism/alteration (%)
Mineral fabric (type/orientation)

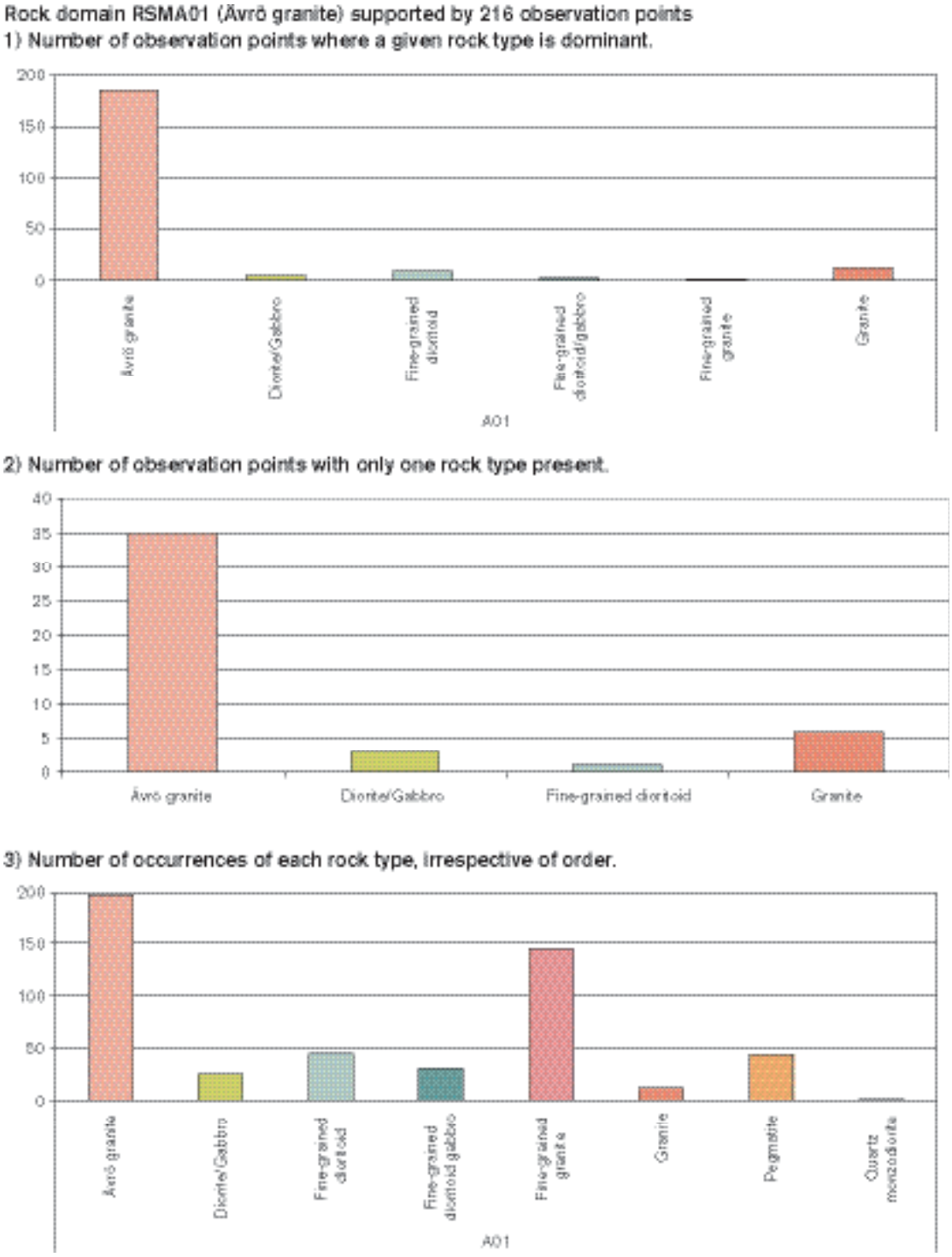

Figure 5-44. *Qualitative assessment of dominant and subordinate rock types in rock domain RSMA01 (Ävrö granite) based on surface outcrop data from the Simpevarp subarea. The translation of the rock codes to rock type is provided in Appendix 3.*

Based on the mapped rock types in the cored boreholes KSH01A (RSMC01), KSH02 (RSMB01), KSH03 (RSMC01 and RSMA01), KAV01 (RSMA01) and KLX02 (RSMA01), it has been possible to quantify the total occurrence in terms of borehole length in metres and the percentage of the total length of the core for the different rock types (Figure 5-45, Figure 5-46 and Figure 5-47; see Section 5.2.7). This quantification is another estimate of the relative amounts of different rock types in the rock domains that complements the estimate based on the outcrop database.

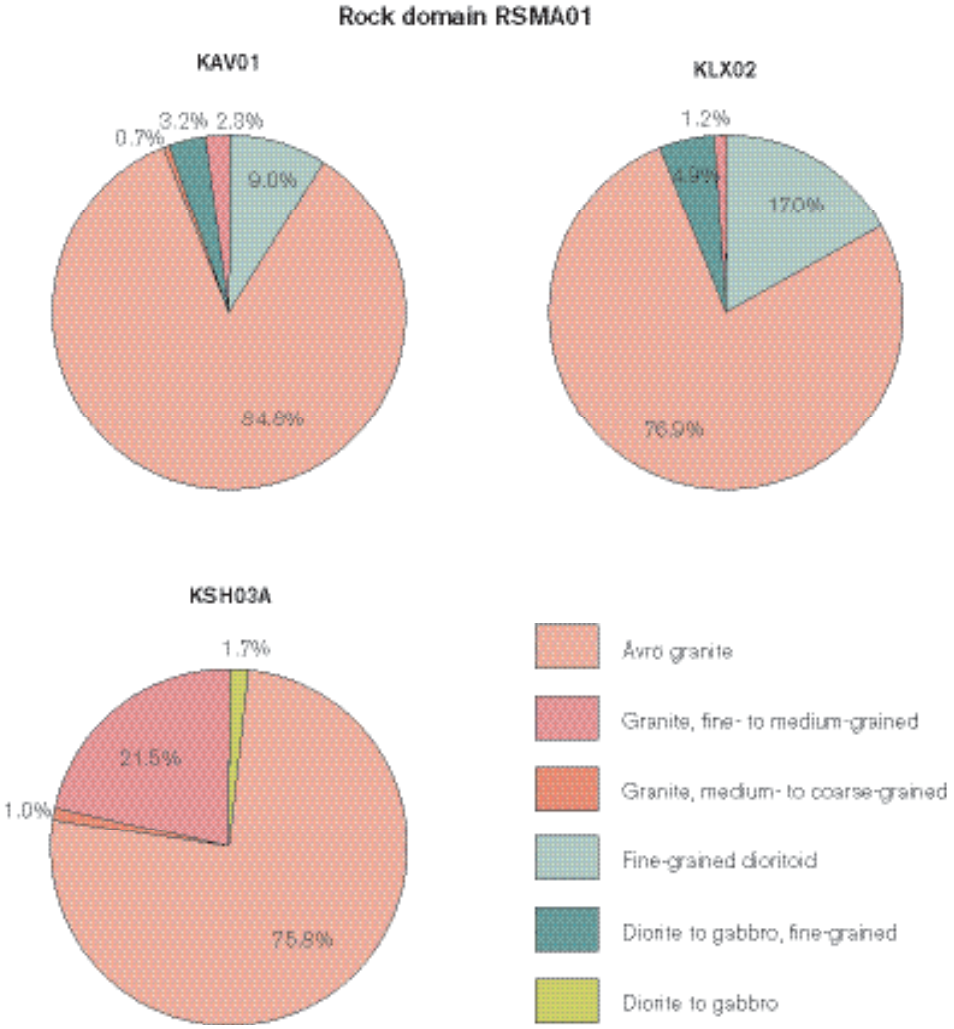

Figure 5-45. *The distribution of different rock types in the rock domain RSMA01 based on the cored boreholes KAV01, KLX02 and KSH03A.*

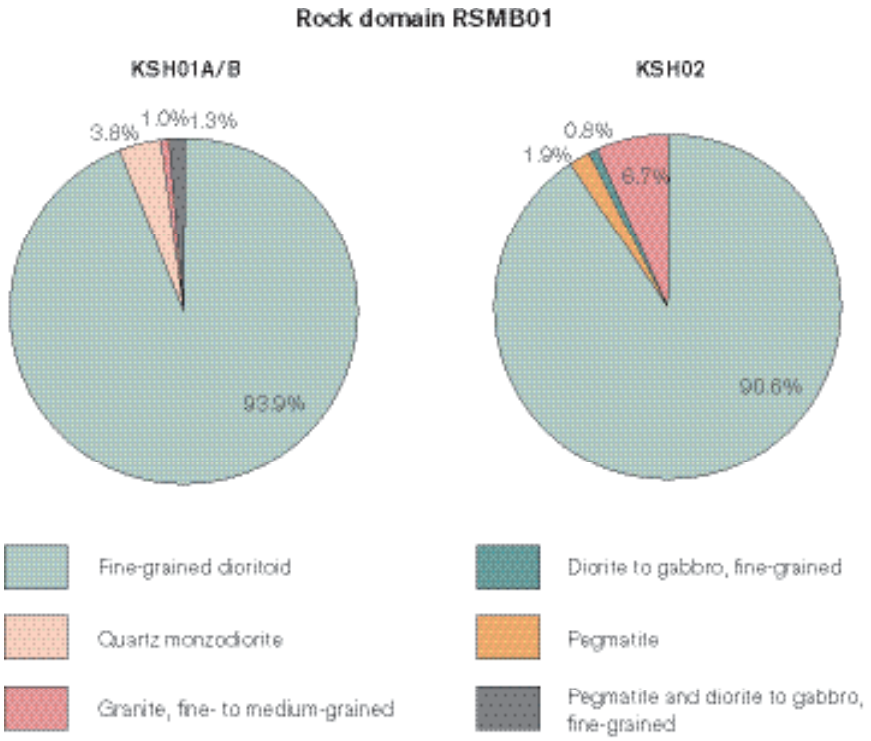

Figure 5-46. *The distribution of different rock types in the rock domain RSMB01 based on the cored boreholes KSH01A/B and KSH02.*

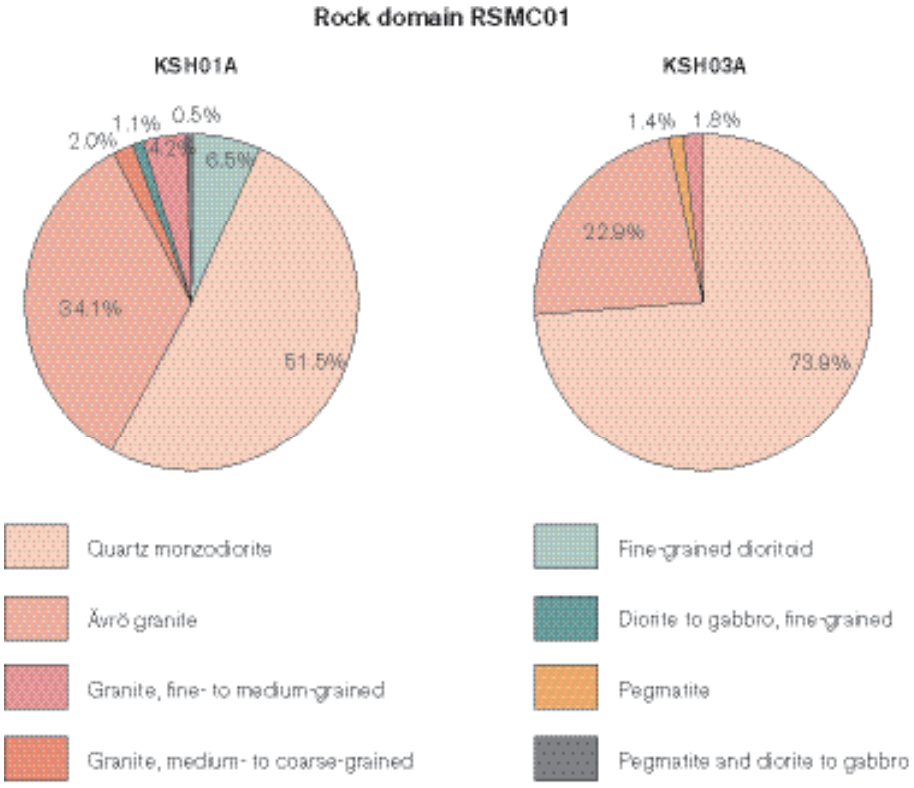

Figure 5-47. *The distribution of different rock types in the rock domain RSMC01 based on the cored boreholes KSH01A and KSH03A.*

An estimation of percentage distribution of rock types in the rock domains have also been carried out based on the areal distribution in the cleared outcrops used for the detailed fracture mapping (Figure 5-48; cf. Figure 5-17 and Figure 5-30).

Another type of inhomogeneity that has to be considered is the inhomogeneously distributed secondary red staining (hydrothermal alteration) and accompanied small-scale fracturing (see Section 5.2.2). Estimate for the rock domains RSMA01, RSMB01 and RSMC01, based on the length of the sections that display red staining (faint to strong) in the cored boreholes KSH01A/B, KSH02, KSH03A/B, KAV01 and KLX02, are displayed in Figure 5-49, Figure 5-50 and Figure 5-51.

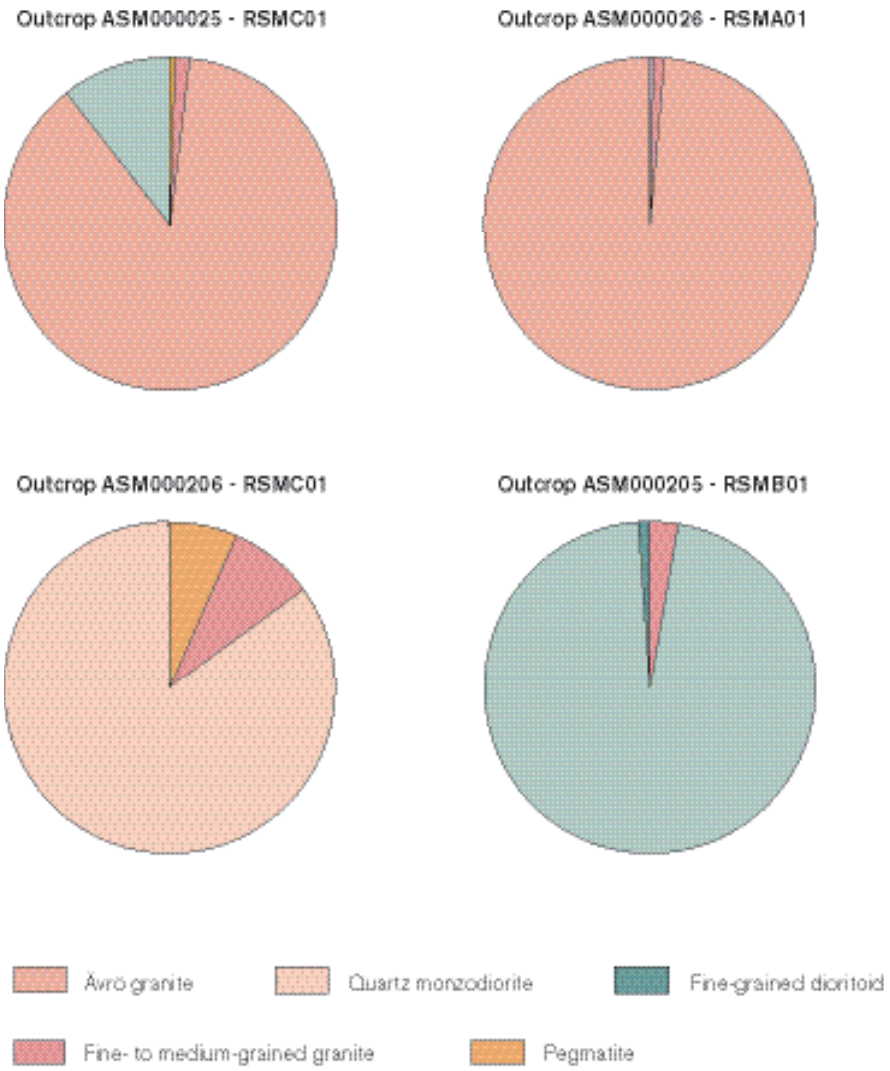

Figure 5-48. *Distribution of rock types in outcrops where detailed fracture mapping has been carried out.*

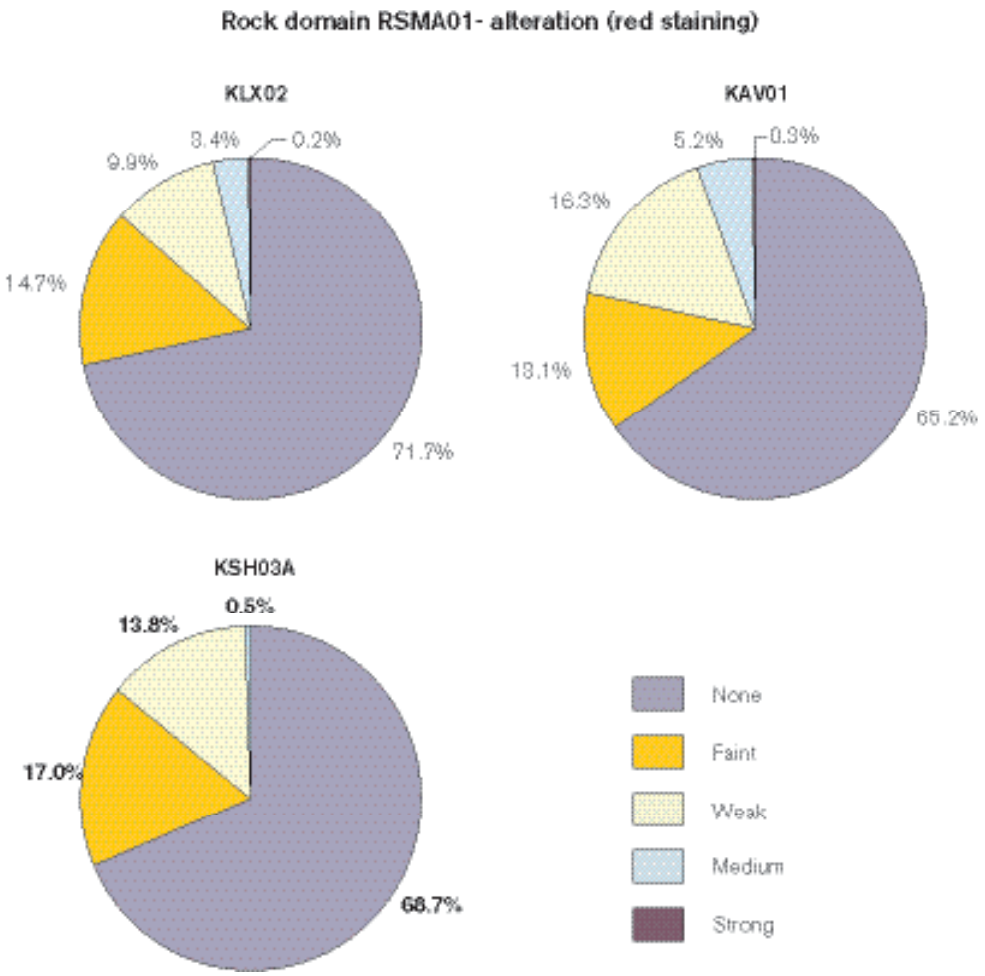

Figure 5-49. *Alteration (red staining) in rock domain RSMA01. Estimates are based on length of altered sections in the cored boreholes KLX02, KAV01 and KSH03A.*

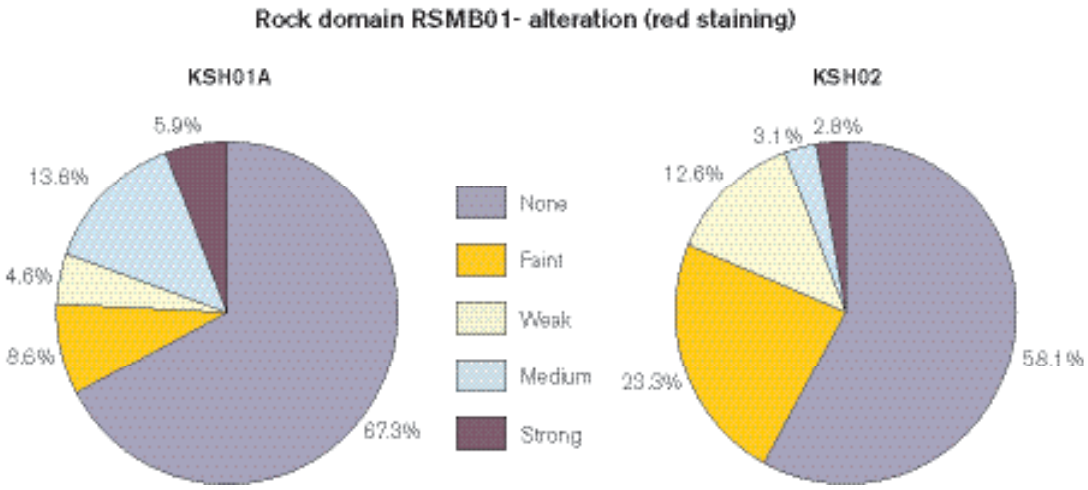

Figure 5-50. *Alteration (red staining) in rock domain RSMB01. Estimates are based on length of altered sections in the cored boreholes KSH01A and KSH02.*

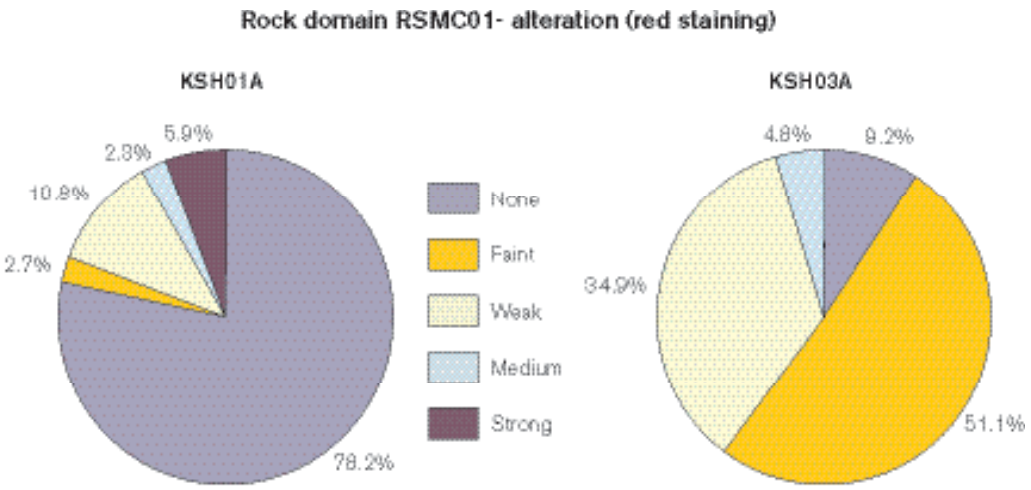

Figure 5-51. *Alteration (red staining) in rock domain RSMC01. Estimates are based on length of altered sections in the cored boreholes KSH01A and KSH03A.*

5.3.4 Evaluation of ore potential

The Simpevarp regional model area is dominated by intrusive rocks, i.e. dioritoids-syenitoids and granites that belong to the c. 1,810–1,760 Ma generation of the Transscandinavian Igneous Belt (TIB), which by experience is more or less devoid of metallic mineralisations. The only candidate for metallic mineralisations in the Simpevarp regional model area is the c. 1,450 Ma old Götemar type granite, that is judged to have a potential for tin (Sn) and tungsten (W), although no mineralisations of this type have so far been found. Consequently, the Simpevarp regional model area may be considered as sterile with respect to ores and metallic mineralisations /Lindroos, 2004/.

5.3.5 Evaluation of uncertainties

The variation in the quality of the surface geological data across the regional model area (cf. Section 5.2.2) is important to consider in the modelling procedure. Since no additional surface information has been made available for the Simpevarp local scale and regional model areas since the compilation of the Simpevarp 1.1, the uncertainties described in the latter remain valid also for the version Simpevarp 1.2 site descriptive model. Apart from some possible local updating of the lithologies outside the local scale model area, the attributed uncertainties in the regional model area will presumably persist throughout the site investigation programme.

The uncertainties mainly concern the location of the boundaries between the different rock units, especially outside the Simpevarp subarea where only reconnaissance bedrock information is available. Furthermore, there remains an uncertainty as to whether some minor inhomogeneous rock domains possibly could be treated as subordinate rocks and be integrated in the surrounding major rock domain. There is also insufficient information concerning the character of the inhomogeneity of the rock domains. In particular, this concerns the frequency and spatial distribution of subordinate rock types. The estimates of the proportion of subordinate rocks presented above (Section 5.3.3) indicate that the local variation may be high, i.e. specific parts of a rock domain may contain a high frequency, while other parts may be more or less devoid of subordinate rocks. Accordingly, the estimate of the degree of inhomogeneity is scale dependent. If for instance the entire rock domain RSMA01 is considered it may be judged to contain a fairly moderate amount of subordinate rock types. However, specific parts of the rock domain may contain a large amount of subordinate rock types.

As there is a limited amount of subsurface lithological data, there remain considerable uncertainties concerning the extension and geometry of rock domains at depth. Apart from:

- The dominating rock domain RSMA01 (Ävrö granite), which constitutes the “matrix” in the lithological model.
- The rock domain RSMB01 that has been verified to a depth of 1,000 metres in the cored borehole KSH02.
- The rock domain RSMC01 (mixture of Ävrö granite and quartz monzodiorite), which has been verified to a depth of 1,000 metres in the cored borehole KSH01A and to a borehole length of c. 168 metres in the cored borehole KSH03.
- The boundary between the rock domains RSMA01 and RSMD01 (quartz monzodiorite) defined at a borehole length of c. 1,375 metre in the cored borehole KLX02.

The depth extensions of the remaining rock domains are uncertain. Even though the rock domains have been verified to a certain depth, the geometrical relationships between the different rock domains are considered highly uncertain. This problem will presumably persist throughout the site investigation programme for most of the rock domains, especially in the regional model area. However, reduction of this uncertainty may be achieved by future modelling of airborne or ground geophysical data and information collected from cored and percussion-drilled boreholes. The uncertainty associated with the surface extension of rock domain RSMB01 (see above) west of the Simpevarp subarea will be resolved during the detailed mapping of the Laxemar subarea.

With the above considerations in mind, an attempt has been made to assess, at least qualitatively, the confidence in the occurrence and geometry of the interpreted 36 rock domains (Table 5-14). Confidence is expressed at three levels; “high”, “medium” and “low”.

The information concerning the properties of the different rock domains (Table 5-13) originates primarily from the surface outcrop data from the Simpevarp subarea (cf. Section 5.2.2). Subsurface data are only available for rock domains RSMA01, RSMB01 and RSMC01 (cf. Section 5.2.7). Despite the fact that it has been possible to estimate the relative importance of the different rock types in a specific domain from the surface data, there remains an uncertainty concerning the quantitative proportions of the different rock types, i.e. how much of a specific rock domain is occupied by subordinate rock types. This characteristic is a basis for the uncertainty assessment related to the bedrock heterogeneity in the rock domains. Based on a qualitative estimation at the present stage of the site investigation, subordinate rock types, particularly the frequently occurring fine- to medium-grained granite, are judged to occur in more or less the same amounts both in individual rock domains and between the various rock domains. However, local variations in the frequency of subordinate rock types are to be expected.

Due to the lack of data from the regional model area, the assigned properties of most rock types are incomplete and are based only on available data from the Simpevarp subarea. Whether the properties of the rock types of the Simpevarp subarea are also valid for the rock types in the remaining part of the local-scale and regional-scale model areas is a factor contributing to uncertainty. This will be evaluated in forthcoming site descriptive models.

Table 5-14. Table of confidence related to existence of interpreted rock domains in the regional and local-scale model volume employed for the Simpevarp 1.2 site-descriptive model.

Domain ID	Basis for interpretation	Confidence at the surface	Confidence at depth
RSMA01	Bedrock geological map, version 1.1 of the Simpevarp subarea and version 0 in the remaining area, KAV01, KLX02, KSH03A	High	High
RSMA02	Bedrock geological map, version 0	Low	Low
RSMB01	Bedrock geological map, version 1.1 of the Simpevarp subarea, /Kornfält and Wikman, 1987/, KSH01A, KSH02, HSH02	Medium	Medium
RSMB02	Bedrock geological map, version 1.1 of the Simpevarp subarea	Medium	Low
RSMB03	Bedrock geological map, version 1.1 of the Simpevarp subarea	High	Low
RSMB04	Bedrock geological map, Simpevarp 1.1 /based on Kornfält and Wikman, 1987/	Medium	Low
RSMC01	Bedrock geological map, Simpevarp 1.1, KSH01A, KSH01B, KSH03A, KSH03B, HSH01, HSH03	High	Medium
RSMD01	Bedrock geological map, version 0, KLX02	Medium	Low
RSMD02	Bedrock geological map, version 0	Medium	Low
RSMD03	Bedrock geological map, version 0	Medium	Low
RSMD04	Bedrock geological map, version 0	Medium	Low
RSMD05	Bedrock geological map, version 0	Medium	Low
RSMD06	Bedrock geological map, version 0	Medium	Low
RSME01	Bedrock geological map, version 0	Medium	Low
RSME02	Bedrock geological map, version 0	Medium	Low
RSME03	Bedrock geological map, version 0	Medium	Low
RSME04	Bedrock geological map, Simpevarp 1.1	High	Low
RSME05	Bedrock geological map, version 0	Medium	Low
RSME06	Bedrock geological map, Simpevarp 1.1	High	Low
RSME07	Bedrock geological map, version 0	Medium	Low
RSME08	Bedrock geological map, Simpevarp 1.1	Medium	Low
RSME09	Bedrock geological map, Simpevarp 1.1	Medium	Low
RSME10	Bedrock geological map, Simpevarp 1.1	Medium	Low
RSME11	Bedrock geological map, version 0	Medium	Low
RSME12	Bedrock geological map, version 0	Medium	Low
RSME13	Bedrock geological map, version 0	Medium	Low
RSME14	Bedrock geological map, version 0	Medium	Low
RSME15	Bedrock geological map, version 0	Medium	Low
RSME16	Bedrock geological map, version 0	Medium	Low
RSME17	Bedrock geological map, version 0	Medium	Low
RSME18	Bedrock geological map, version 0	Medium	Low
RSMF01	Bedrock geological map, version 0	Medium	Low
RSMF02	Bedrock geological map, version 0	Medium	Low
RSMF03	Bedrock geological map, version 0	Medium	Low
RSMG01	Bedrock geological map, version 0	High	Medium
RSMG02	Bedrock geological map, version 0	High	Medium

5.4 Deterministic deformation zone modelling

5.4.1 Modelling assumptions and input from other disciplines

There are some fundamental assumptions underlying the deformation zone model.

It is assumed that:

- deformation zones can be interpreted through both indirect sources of data such as geophysical maps (magnetics, VLF, slingram, gravimetric), topography, seimic reflections and refractions, and
- through direct data in boreholes, tunnels and from surface field observations. The geological character and possible extent (length and width) of deformation zones inferred from indirect data sources is lower than for zones identified from direct observations,
- different sources of data can complement each other and increase the confidence in the interpreted deformation zone. Several types of observations, both indirect and direct also increase the degree of detail in which the zone can be described,
- the interpreted deformation zones can be interpolated between points of observations if there is reasonable data to suggest this,
- deformation zones are variable in their geological width, but can be modelled as surfaces without thickness,
- deformation zones interpreted on ground surface can be extended toward depth and that the extent at depth is related to the interpreted length of the surface trace.

The local scale model of deformation zones has made use of:

- The deformation zone model presented in Simpevarp 1.1 site descriptive model /SKB, 2004b/.
- The interpretation of linked lineaments completed during the ongoing site investigation programme (see Section 5.2.2).
- The regional structural model presented in version 0 of the site descriptive model /SKB, 2002b/.
- The structural model of Äspö HRL (Äspö 96 model), /Rhén et al. 1997a/.
- GEOMOD structural model /Berglund et al. 2003/.
- Ävrö RVS model /Markström et al. 2001/.
- Laxemar model test /Andersson et al. 2002b/.
- Measurements of mainly ductile structures, as well as some brittle structures and bedrock contacts at 91 of the 353 observation points documented during the bedrock mapping carried out during 2003 /Wahlgren et al. 2004/.
- A variety of structural geological data covering the Simpevarp peninsula and the islands of Hålö and Ävrö, as compiled in /Curtis et al. 2003a/ and /Curtis et al. 2003b/.
- Borehole and seismic reflection data compiled in conjunction with the ongoing site investigation programme (see Sections 5.2.5 and 5.2.6, respectively).

The Simpevarp 1.2 deformation zone model has addressed deformation zones in the regional model area which is equivalent to that used for the version 0 model /SKB, 2002b/. The local scale model contains deformation zones that are inferred to be of length 1 km or longer, i.e. local major and regional deformation zones according to the terminology of /Andersson et al. 2000/.

Presently, surface data coverage in parts of the area outside the local model area has a lower resolution, which limits the possibilities to modelling zones of 1 km length or more. The offshore and north-western parts of the regional model area are covered only by the lineament map from the version 0 model of relatively low resolution /Andersson et al. 2000/. In order to provide a regional model based on an even resolution of data, inferred deformation zones outside the local model area have, therefore, been limited to be of length 1.6 km or longer. This approach produces a model which has an increased level of resolution around the area of highest interest, i.e. the local model area.

Structures that are considered to be shorter than the modelled deformation zones in the local and regional areas are handled in a statistical way and are presented as part of the stochastic description in Section 5.5. That means that all lineaments shorter than 1 km are treated as part of the stochastic fracture network and their evaluatation is presented in Section 5.5.

For the modelling of deformation zones, it is assumed that the merged extended linked-lineaments (see Section 5.2.2) can provide the necessary detailed information about the location and extent at the surface of possible deformation zones and are regarded as the preferred surface information in comparison with existing older lineament data.

The version Simpevarp 1.1, version 0, Laxemar model test, GEOMOD and Ävrö models have been checked systematically relative to the merged extended linked-lineament map of the regional model domain. Interpretations that are related to the new merged extended linked-lineament map are always preferred, unless there is other additional supporting information from geophysics, boreholes or tunnels.

A key question in the modelling procedure concerns the extension of the deformation zones towards depth. It is assumed that the deformation zones which are vertical or steeply dipping, and can be recognised at the surface as linked lineaments, extend downwards the same distance that can be traced as a lineament at the surface. This assumption implies that the frequency of deterministically modelled deformation zones decreases with depth.

Each interpreted deformation zone has also been ranked according to the confidence of its existence being high or possible. Zones that have high confidence ratings have, in addition to lineament indications, also supportive information from other sources of indirect data such as geophysics and from sources of direct data, such as boreholes or tunnels.

Interpreted zones with assigned confidence “possible” are only supported by indirect sources of information such as lineament indications of variable strength, either from topography, magnetics, EM or other indirect indications such as seismics or ground geophysics.

5.4.2 Identification of deformation zones with alternatives

This section describes how the three-dimensional deformation zone model of the Simpevarp regional model area has been constructed.

An initial step in the modelling procedure made use of the previous version Simpevarp 1.1 model established in the Simpevarp area /SKB, 2004b/. Each of the zones in this model was checked against the linked-lineaments and against new information from borehole data and updated interpretations were assessed in each case.

The subsequent modelling work was executed by introducing the following groups of deformation zones in the regional model volume, in the order indicated below:

- The regional deformation zones, and their associated splays, which are supported by direct data observations through new boreholes, linked-lineament support and have been included in older existing structural models.
- The regional deformation zones, and their associated splays, which have linked-lineament support and have been included in older existing structural models.
- The local major fracture zones, which are supported by direct data observations in new boreholes, linked-lineament support and have been included in older structural models or are supported by new borehole data.
- The local major fracture zones, which are supported by linked-lineament data and have been included in older structural models.

The possible deformation zones that have been inferred solely on the basis of the interpretation of linked lineaments.

The modelling procedure has made use of the key assumptions concerning the relationships between dip and the along-strike and down-dip extents of a single deformation zone, as outlined in the previous section.

Twenty-two (N=22) deformation zones, interpreted as deformation zones of high confidence, have been included in the model. Each one of these interpreted zones is observed both indirectly, through lineament or geophysical data, and directly through borehole or tunnel observations. The exception to this is the Mederhult zone (ZSMEW002A) which has not been observed in boreholes or tunnels. These high confidence deformation zones, as interpreted in model version Simpevarp 1.2, are summarised in Table 5-15 and are illustrated in Figure 5-52 and Figure 5-53.

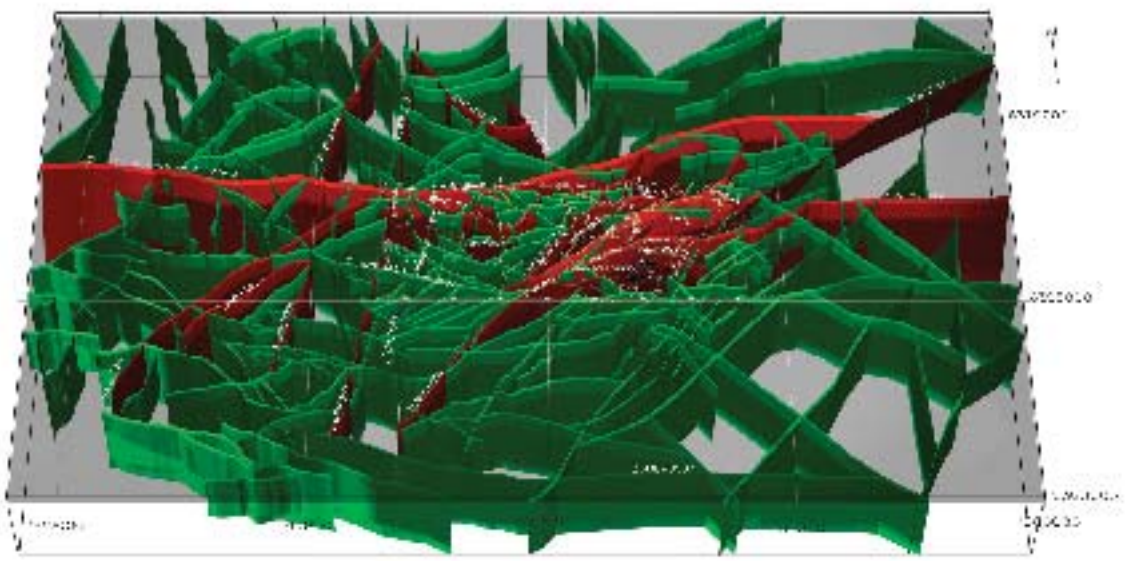

Figure 5-52. *The interpreted twenty-two (N=22) high confidence deformation zones in the Simpevarp 1.2 regional model domain (red) together with interpreted possible deformation zones in the regional and local model domains (green).*

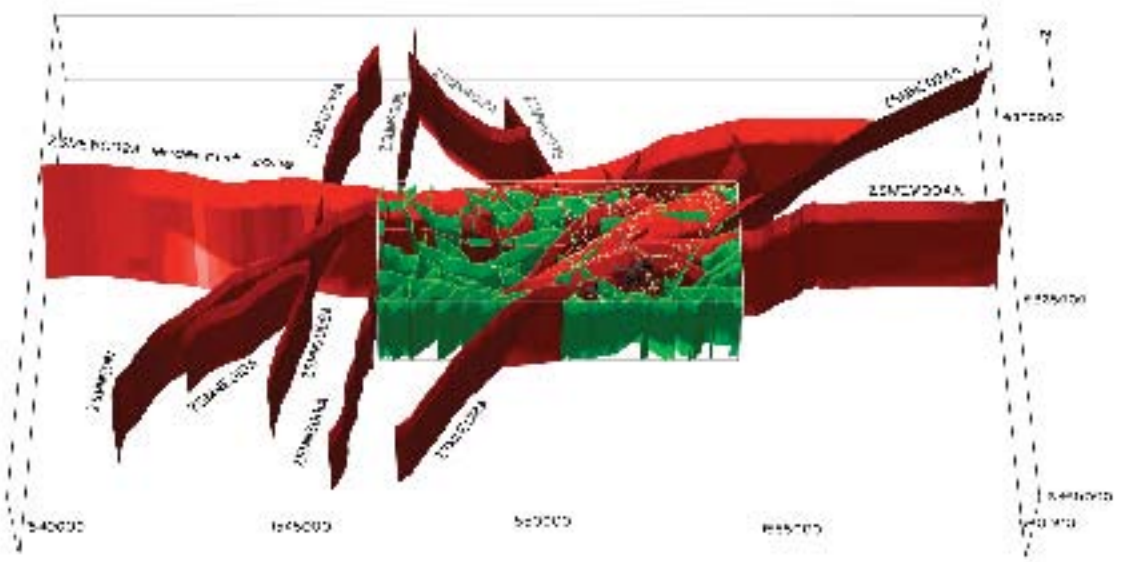

Figure 5-53. *The interpreted twenty-two (N=22) high confidence deformation zones in the Simpevarp 1.2 regional model domain (red). The small box outlines the local scale model volume also including possible zones in the local scale (green).*

Table 5-15. Summary of high confidence deformation zones (N=22) included in the Simpevarp 1.2 deterministic deformation zone model.

Zone ID	Alternative name	Zone ID, in other models	Class	Basis for interpretation
ZSMEW002A	Mederhult zone	Position on surface: combination of a short section of XSM013A0 with v0 ZSM0002A0.	Regional	Linked lineaments, VLF, seismic refraction. Ground geology.
ZSMEW004A		XSM0010A0, B0 and XSM0016A0 in v0 model.	Regional	Airborne geophysics (magnetic 100% along the length, low uncertainty), tunnel, v0.
ZSMEW007A		ZLEW02 in Laxemar model test.	Local Major	Airborne geophysics (magnetic 100% along the length, electrical data, low uncertainty), topography. borehole.
ZSMEW009A		EW3 in Geomod model.	Local Major	Topography, ground geology, tunnel, borehole.
ZSMEW013A		ZLXNW04 in Laxemar model test.	Local Major	Airborne geophysics (magnetic 100% along the length, electrical data, low uncertainty), topography, borehole.
ZSMEW028A			Local Major	Airborne geophysics and borehole evidence.
ZSMNE005A	Äspö shear zone	NEHQ3, EW1b in Geomod model, ZSM0005A0 and ZSM0004A0 in v0 model, ZLXNE01 in Laxemar model test.	Local Major	Airborne geophysics (magnetic 100% along the length, low to medium uncertainty), ground geology, ground geophysics, borehole, Äspö HRL data.
ZSMNE006A	NE1	NE1 in Geomod model, ZSM0006A0 in v0, ZLXNE06 in Laxemar model test.	Local Major	Airborne geophysics (magnetic 100% along the length, low to medium uncertainty), tunnel, boreholes, Äspö HRL data.
ZSMNE010A		ZSM0010A0 in v0.	Local Major	Airborne geophysics, topography, field control.
ZSMNE011A		ZSM0011A0 in v0.	Local Major	Airborne geophysics, topography, ground geophysics.
ZSMNE012A	NE4	Linked lineaments XSM0012A0, (part of B0), A1, A3 and B1. NE4 in Äspö 97 Z15 in Ävrö model.	Local Major	Airborne geophysics, tunnel, borehole.
ZSMNE016A		Only north section of lineament XSM0016A0, ZSM0004A0/B0 in v0.	Local Major	Airborne geophysics, topography, tunnel.
ZSMNE018A			Local Major	Airborne geophysics, borehole.
ZSMNE024A		Z13 in Ävrö model.	Local Major	Airborne geophysics, tunnel, borehole.
ZSMNE040A		ZSM0003A0 in v0, ZLXNE04 (part ZLXNE03) in Laxemar model test.	Local Major	Airborne geophysics boreholes.
ZSMNS001A		ZSM0001A0/B0 in v0.	Regional (A–D)	Airborne geophysics, ground geophysics, topography.
ZSMNS001B		ZSM0001A0/B0 in v0.	Regional (A–D)	Airborne geophysics, topography.
ZSMNS001C		ZSM0001A0/B0 in v0.	Regional (A–D)	Airborne geophysics, topography.
ZSMNS001D		ZSM0001A0/B0 in v0.	Regional (A–D)	Airborne geophysics, topography.
ZSMNS009A		ZSM0009A in v0.	Regional	Airborne geophysics, topography.
ZSMNS017A		NNW4 in Geomod model.	Local Major	Topography, borehole and tunnel evidence.
ZSMNW004A		Z14 in Ävrö model.	Local Major	Airborne geophysics, ground geophysics, boreholes, topography.
ZSMNW007B		ZSM0007A0 in v0, ZLXNS01 in Laxemar model test.	Local Major	Airborne geophysics, topography.
ZSMNW012A		ZSM0012A0 in v0.	Local Major	Airborne geophysics, topography.
ZSMNW025A			Local Major	Airborne geophysics, borehole evidence.

Possible deformation zones based solely on the interpretation of linked lineaments that was completed during the ongoing sisite investigation programme

The dip of each of these twenty-two zones has been estimated using identified observations based on geophysical data, borehole or tunnel observations. These observations are in several cases identical to observations made use of for the Simpevarp 1.1 model, but the redefined lineaments on the surface result in changes to the position and therefore to the dip of the zones.

One hundred and sixty-six (N=166) deformation possible zones have also been included in the deformation zone model. These zones are interpreted only on basis of the linked lineament interpretation presented in Section 5.2.2.

Thirteen of the high confidence deformation zones where already identified in the Simpevarp 1.1 model /SKB, 2004b/. Nine more deformation zones have been identified in boreholes or tunnels, together with surface data, cf. Table 5-15. This is partly an effect of the fact that the local scale model domain is larger in the present model version, cf. Figure 5-54, and extends further west, including the Laxemar subarea.

Below follows a description, in order of consecutive numbering, of all interpreted high confidence deformation zones in the Simpevarp 1.2 model;

The regional Mederhult deformation zone, ZSMEW002A, follows the interpretation made in model version 0 (zone ZSM0002A0) and a short section of the linked-lineament XSM013A0. The zone can be traced westward to the boundary of the regional model domain following the version 0 interpretation. The surface extent is interpreted to be at least 30 km. It is argued here that the linked lineament XSM013A0 provides a more precise description of the extension eastward than the previous interpretation used in version 0. The detailed lineament map shows that there are no indications from magnetics or topography to suggest a zone extension eastward as suggested in version 0. The linked-lineament XSM013A0, on the other hand, is well indicated by topography, magnetics and EM. The zone has been verified by ground magnetic and VLF measurements /Stenberg and Sehlstedt, 1989/, a refraction seismic survey /Rydström and Gereben, 1989/ and surface geology /Stanfors and Erlström, 1995/. Results from the VLF measurements indicate that the zone has a steep southerly dip, whereas observations on the surface suggest a more gentle dip to the southeast. The zone is not interpreted to intersect borehole KLX02, but to pass underneath the bottom of this borehole. The interpreted mean geometry in terms of strike and dip of the zone in the local scale model of deformation zones is 85/55. The conclusion in the version 0 model regarding dextral movements during the Phanerozoic has not been verified and remains an open issue. Update of properties from version Simpevarp 1.1 includes a change of width, now ranging from 20 m up to to 70 m.

The local major zone ZSMEW004A, is based on the magnetic lineaments XSM0010A0, XSM0010B0 and XSM0016A0. The 70 degree dip towards the south of the zone is observed in the Äspö HRL access tunnel at chainage 0/318 m, which intersection also corresponds with the version 0 zone ZSM0004A0, cf. Figure 5-55. The interpretation of ZSMEW004A deviates from version 0 zone ZSM0004B0 on the Ävrö island, mainly based on the more pronounced nature of the XSM0010A0 lineament together with surface observation on Ävrö. The lateral extension is estimated to be at least 8 km. Update of properties from version Simpevarp 1.1 includes a change of width, now ranging from 30 m up to 50 m based on the tunnel intercept at Äspö HRL (chainage 0/318 m).

The regional Äspö shear zone, ZSMNE005A, is reinterpreted from the version 0 model zone ZSM0005A0 based on the new linked lineament data, cf. Figure 5-56. The southernmost section of the Äspö shear zone is interpreted to link into the southern part of version 0 zone ZSM0004A0 due to a better defined linked lineament that runs through the whole local scale model domain (XSM0005A0). The lineament is a strong magnetic anomaly that does not follow the earlier south-west extension of the shear zone, but turns more west along version 0 zone ZSM0004A0. This zone also corresponds (further north) with zones NEHQ3 and EW-1b in the GEOMOD model and zone ZLXNE01 in the Laxemar model. Update of properties from version Simpevarp 1.1 includes a change of width, which is set to 40 m, where the ductile part is estimated to be varying between 10 to 40 m and the brittle part from 70 to 200 m wide.

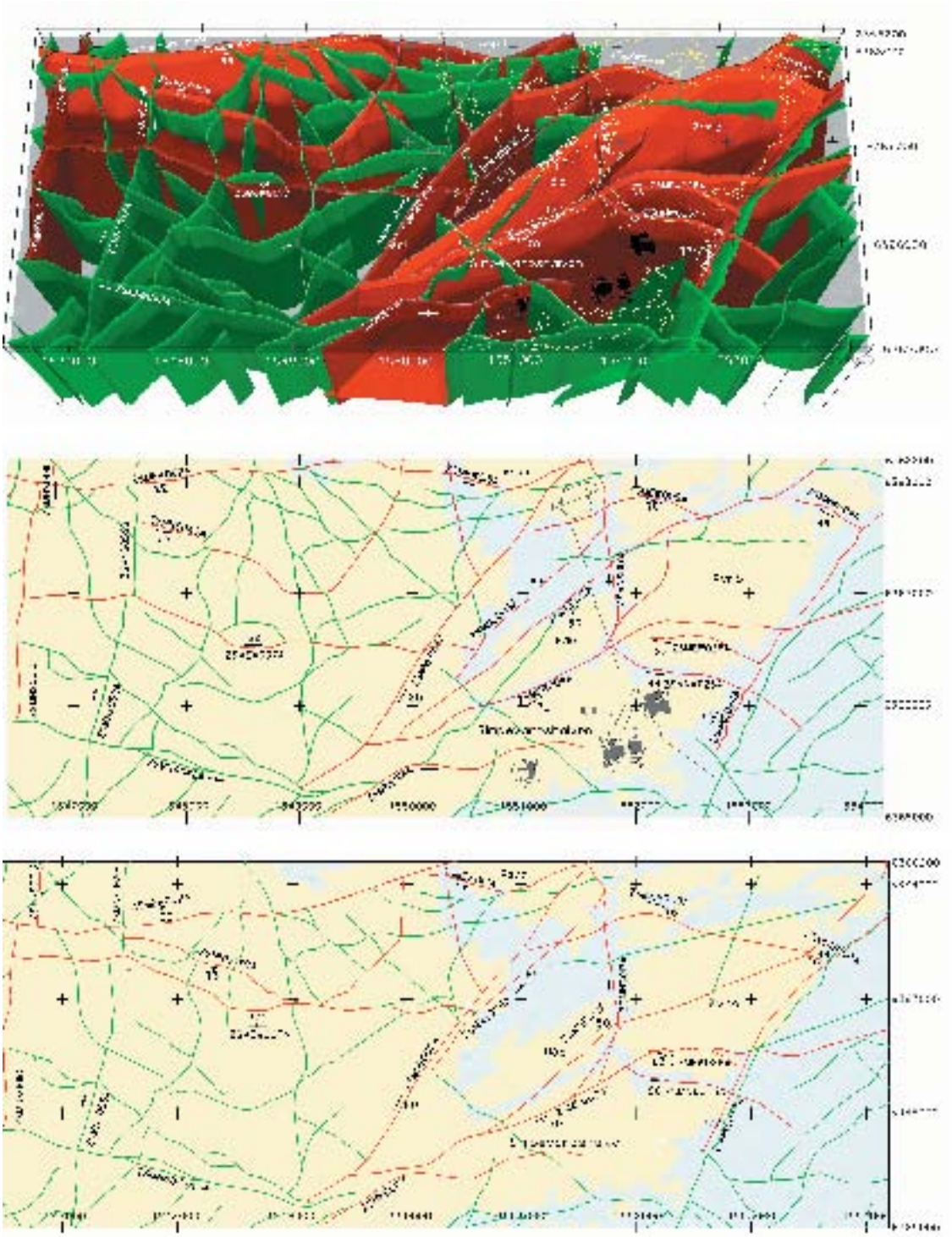

Figure 5-54. *Interpreted high confidence (red) and possible (green) deformation zones in the local model domain. The top illustration (a) shows the model in perspective, (b) shows a top view corresponding to sea level (c) shows the situation at Z=–500 m.a.s.l.*

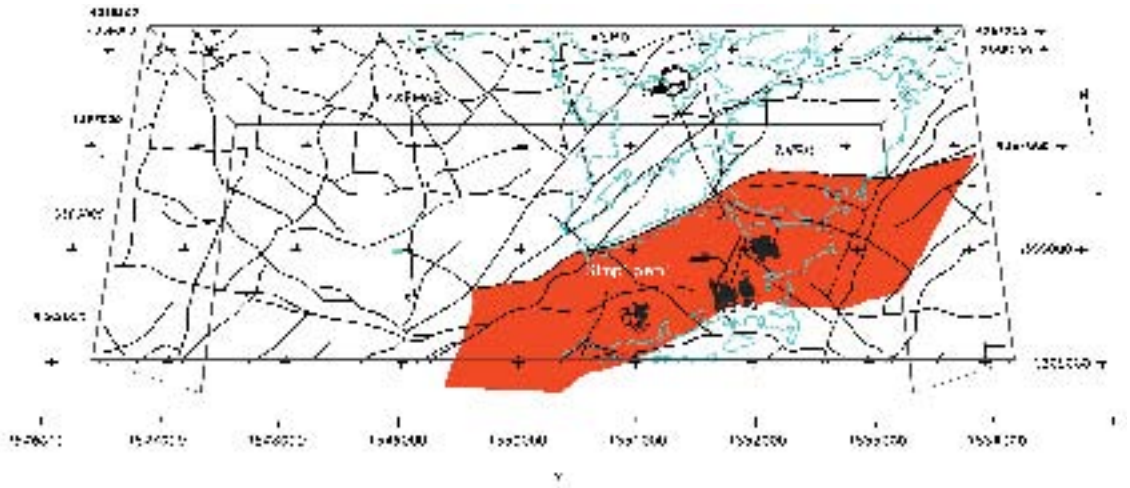

Figure 5-55. *Interpretations of zone ZSMEW004A in model version Simpevarp 1.2 (red) and ZSM0004A0 and ZSM0004B0 in version 0 (grey). The linked lineaments are shown in black.*

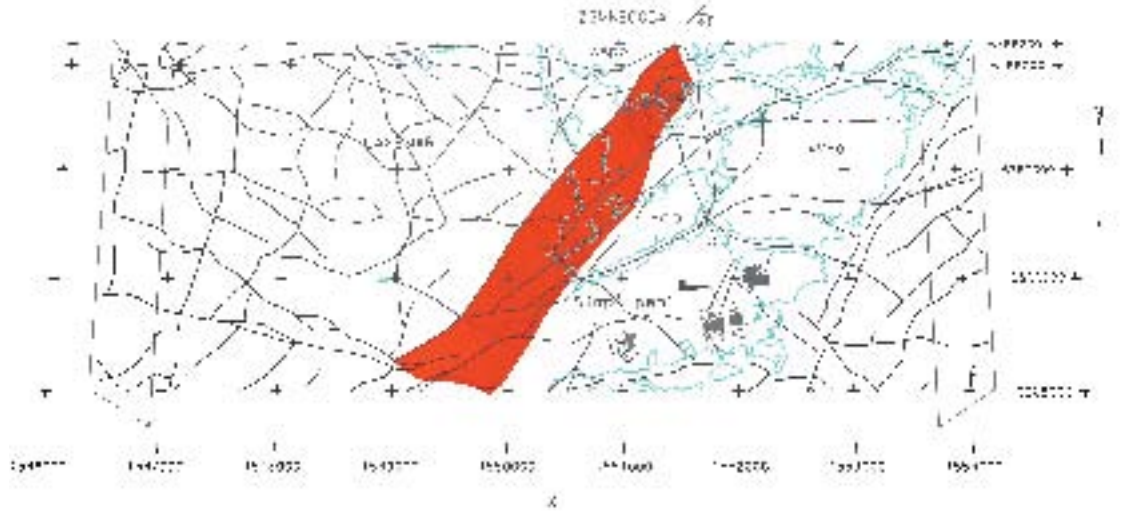

Figure 5-56. *Interpretations of zone ZSMNE005A (Äspö shear zone) in model version Simpevarp 1.2. The linked lineaments are shown in black.*

The surface outcrop of the local major zone ZSMNE006A (NE-1) is based on the linked lineament XSM0015B0, which corresponds well with the version 0 surface outcrop of zone ZSM0006A0. The dip of the zone is adjusted based on the GEOMOD model and the Äspö access tunnel at chainage 1/290 m. The reinterpreted dip is 65 degrees towards the NW compared to 70 degrees in the version 0 model. This zone also corresponds with zone ZLXNE06 in the Laxemar model test and zone NE-1 in the GEOMOD model. Update of properties from version Simpevarp 1.1 includes a change of width, which is set to 28 m based on the intersection with the Äspö tunnel (TASA ch. 1/290). However, the intersection in the tunnel shows a complex zone with at least three branches over a 60 m tunnel interval. The core of this zone is partially clay-altered (5–8 m wide). This deformation zone is particularly well confirmed through at least nine cored boreholes at Äspö.

The deformation zone ZSMEW007A (Figure 5-57) is based on a topographic and magnetic EW-lineament with an intersection in KLX02 at 340 m together with a seismic reflector dipping north. The fracturing at the intersection of the zone in KLX02 supports a northerly dip and a general strike NW to EW. The width of the zone, 2 m (ranging from 1 to 10 m), is estimated from crush, increased fracturing and alteration in the core of KLX02. This interpretation also coincides with the interpretation of zone ZLEW02 in the Laxemar model /Andersson, 2000/.

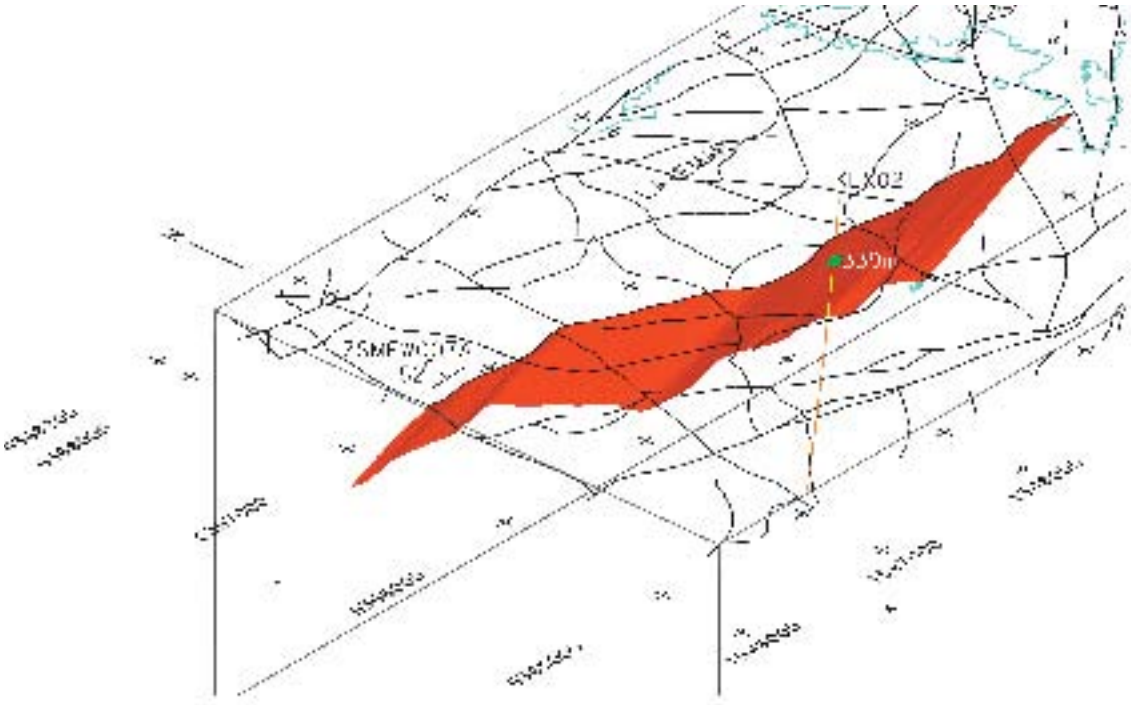

Figure 5-57. *Interpretations of zone ZSMEW007A in model version Simpevarp 1.2 The linked lineaments are shown in black.*

The deformation zone ZSMEW009A (EW3) is based on a EW topographic and magnetic lineament, tunnel and borehole intersections at Äspö HRL, as well as surface observations in one of the trenches cutting over the Äspö Island. The orientation, 85/76, is estimated from tunnel observations at Äspö (TASA ch. 1/407 m) and corresponds to zone EW3 in the Geomod model, cf. Figure 5-58. This deformation zone is recognised as a re-activated ductile zone with a crushed and altered mylonitic core as observed in borehole KAS06 at 66 m depth. It is also a major hydraulic conductor with reported inflows to the tunnel in the order of 90 litres per minute. The width, estimated from the tunnel intersection, is 12 m, with an anticipated variability ranging from 5 m to 20 m.

The local major deformation zone ZSMNE010A is based on the topographic and magnetic lineament XSM0077A0 and is verified by geological field control where epidote-healed fractures where found. The width is set to a default value of 20 m and is regarded as highly uncertain.

The local major deformation zone ZSMNE011A is based on the topographic and magnetic lineament XSM0011A0 interpreted already in version 0 with the same name. This zone is verified by ground magnetics, VLF measurements and observation of increased fracturing, mesoscopic ductile and brittle deformation zones and epidote healed fractures.

The local major zone ZSMNE012A is based on the merged extended lineament XSM0012A0, previously separated in lineament segments A0, B0, A1, B1 and A3. The part of the zone based on lineament XSM0012A0 is correlated with zone ZLXNE02 of the Laxemar model test and zone Z15 in the Ävrö model. The zone section based on lineament XSM0012B1 is correlated with the Äspö access tunnel, chainage 0/827 m and zone Z15 in the Ävrö model. The portions of the zone based on lineaments XSM0012A3 and XSM0012A1 are correlated with zone Z15 in the Ävrö model. The strike derives from the lineament orientation whereas the dip comes from the Äspö tunnel (ch. 0/827). This zone is found in boreholes KAV01 (413 m) and HAV07 (98 m) and in three reflectors from Ävrö and has a dip which extends the interpreted zone under the Simpevarp Peninsula.

Figure 5-58. *Interpretations of zone ZSMEW009A (EW3) in model version Simpevarp 1.2 The linked lineaments are shown in black.*

The local major zone ZSMEW013A is based on the linked lineament XSM0013A0 which shows a magnetic anomaly along its full extent with a medium confidence of existence. The interpreted zone is modified to terminate against ZSMEW002A (western boundary) and at the eastern end of the linked lineament XSM0014A0. This zone corresponds to zone ZLXNW04 in the Laxemar model test, which has been possibly indicated in the percussion borehole HLX02 /Andersson et al. 2002b/. Update of properties from Simpevarp 1.1 includes a change of width, which is set to a default value of 20 m with low confidence.

The interpreted surface outcrop of the local major zone ZSMNE016A is based on the north section of lineament XSM0016A0 and shows a medium-strong magnetic anomaly and a strong topographic depression. The interpreted surface outcrop corresponds well with the southern part of version 0 zone ZSM0004B0. However, with the current orientation and northern termination of zone ZSMNE016A, it does not intersect borehole KAV01, as does the corresponding version 0 zone ZSM0004B0. At this stage it is not clear if any of the interpreted zones from the single-hole interpretation in borehole KAV01 can be associated with zone ZSMNE016A. The zone is bounded in the south by zone ZSMEW004A and in the north by zone ZSMNE012A.

The surface intersection of the local major zone ZSMNE018A is based on the north section of lineament XSM0018A0 and shows a medium-strong magnetic anomaly and a topographic depression. The zone intersects percussion borehole HSH02 (85 m). The borehole data indicate that this is a complex zone with several branches.

The local major zone ZSMNE024A is based on the linked lineament XSM0024B0, which is indicated by a strong offshore magnetic and topographic anomaly immediately east of the island of Ävrö and the Simpevarp peninsula, cf. Figure 5-59. There are also four seismic reflectors on Ävrö and an inferred intersection in borehole KSH03 between 180 and 280 m borehole depth. This zone is reinterpreted in the current model version to stop short of the OKG power plant water intake tunnel. It is also correlated with zone Z13 of the Ävrö model in its northern part. The zone is interpreted to dip 73 degrees NW under the Ävrö Island. The zone shows a complex geological width c. 80 m with a clearly anomalous RQD (Rock Quality Designation index). The intersection in borehole KSH03 contains both ductile precursors, clay and increased fracturing over large intervals.

The local major deformation zone ZSMEW028A is based on the topographic and magnetic lineament XSM0028A0 and is interpreted to intersect percussion borehole HAV09 between 70 and 105 m. The borehole shows a very low resistivity anomaly over much of this interval. The orientation is EW strike with a steep dip towards the south (095/83). The inferred length is close to 1 km.

The deformation zone ZSMNE040A is interpreted to follow the relatively complex topographic and magnetic lineament XSM0040A0, cf. Figure 5-60. The underlying interpretation is suggested to combine the linked lineaments XSM0040A0 and XSM0053A0 to reflect the curved nature of lineaments surrounding the Götemar granite. Curved deformation zones are indicative of for example a protruding magma from underneath, such as the Götemar granite. This is clearly seen in lineaments XSM0257C1, XSM0258C0 and XSM0259C0, north of ZSMNE040A. However, alternative interpretations may be equally justifiable, such as splitting the zone in two branches, one NE and one NW, at the intersection with ZSMNS046A.

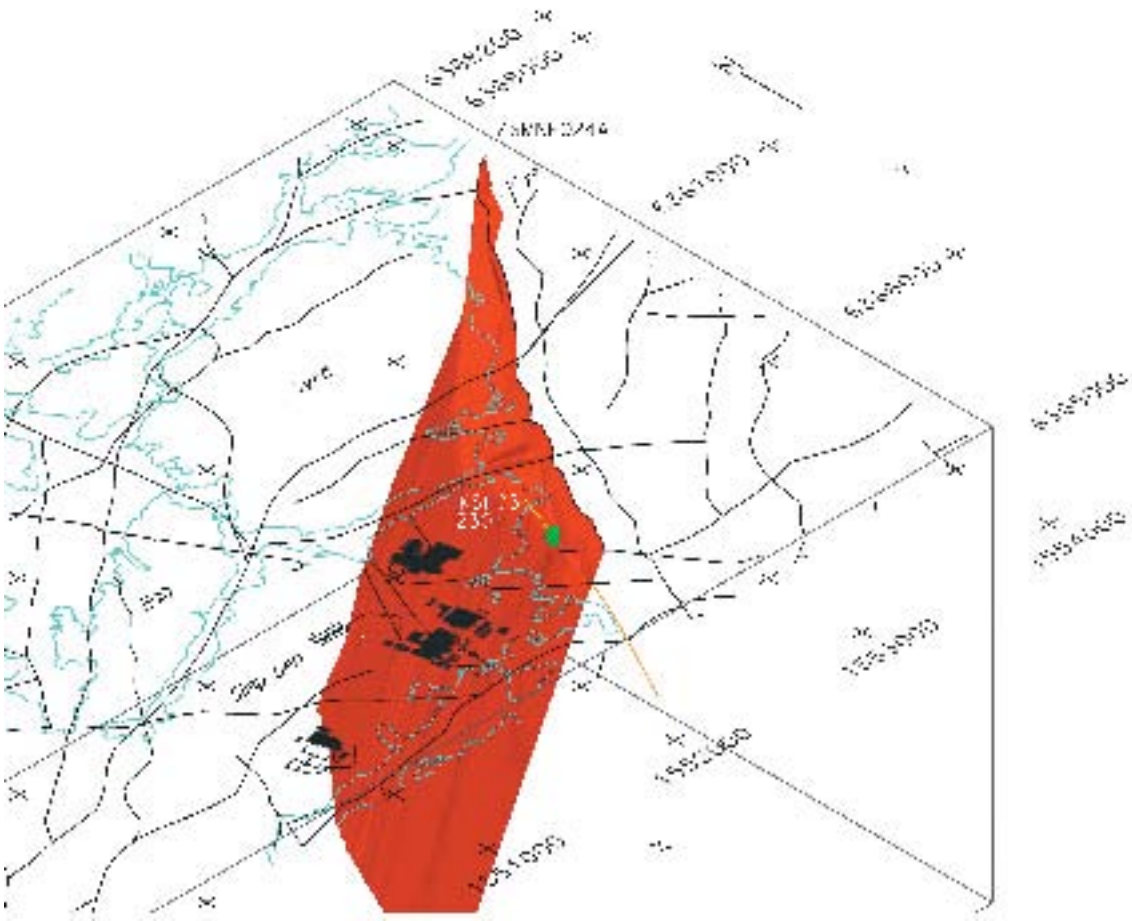

Figure 5-59. *Interpretations of zone ZSMNE024A in model version Simpevarp 1.2. The interpreted linked lineaments are shown in black.*

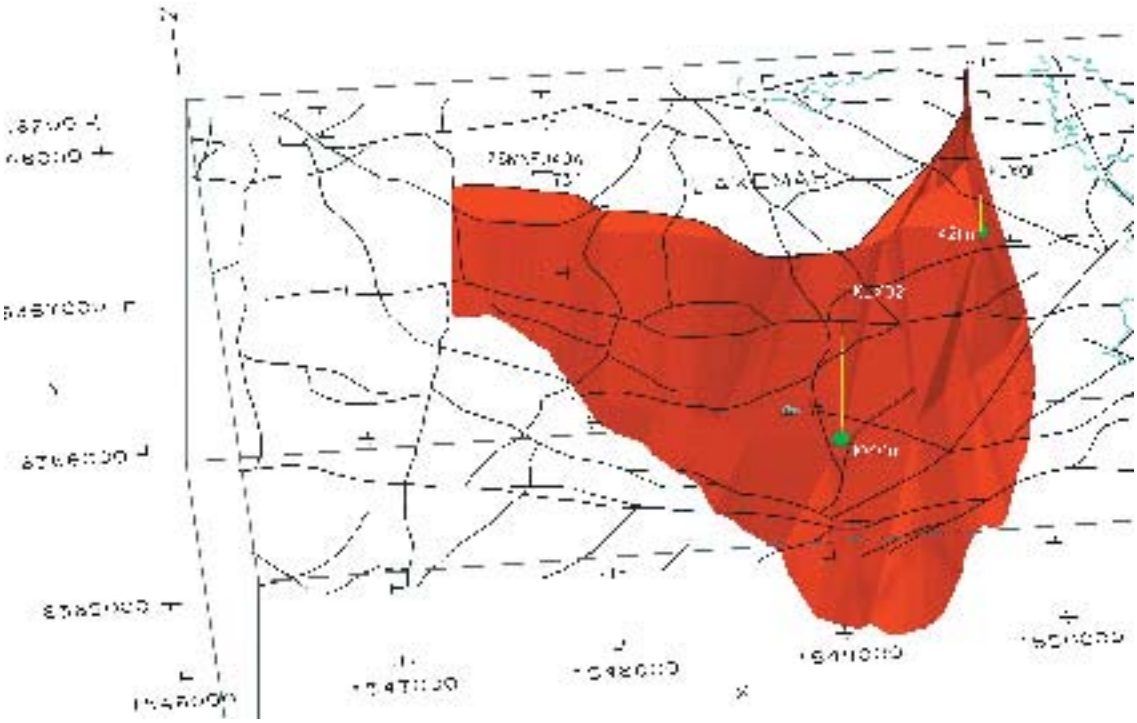

Figure 5-60. *Interpretations of zone ZSMNE040A in model version Simpevarp 1.2. The linked lineaments are shown in black.*

The deformation zone ZSMNE040A is also identified in boreholes KLX01 (421 m) and KLX02 (1,040 m), where cataclastic brittle deformation and alteration dominates the borehole intervals. The dominant fracture orientation in these borehole sections is NNE. The width is estimated to 15 m in KLX01 and KLX02, with a variability from 1 to 30 m. The zone also coincides with zones ZLXNE03 and ZLXNE04 in the Laxemar model.

The regional deformation zone ZSMNS001A–D is identified through a series of north-south trending lineaments which are offset by an apparent dextral movement. These lineaments have been verified by VLF and direct observations of mesoscopic brittle-ductile zones along, or close to, the marked fracture zone. The dip is interpreted to be vertical from VLF measurements, and the strike is approximately NS. The width is extracted from the version 0 deformation zone ZSMN0001A/B.

The regional deformation zone ZSMNS009A is based on a topographic and magnetic lineament XSM0056A0, which has been verified by ground magnetic and VLF observations together with increased small scale fracturing, mesoscopic brittle and brittle-ductile deformation zones and epidote-healed fractures. This zone already present in the version 0 model.

The local major zone ZSMNS017 was divided into two segments, A and B in model version Simpevarp 1.1. This deformation zone is now interpreted to be one continuous zone which is correlated with zone NNW4 in the GEOMOD model and is identified in the Äspö access tunnel at chainages 1/876 m, 1/979 m and 3/083 m, as well as in several boreholes at Äspö.

The local major zone ZSMNW004A is based on the topographic linked lineament XSM0004B0 and is sub-parallel to zone Z14 of the Ävrö model. The width, based on expert judgement, is estimated to be 50 m (± 20 m).

The local major zone ZSMNW007B is based on the linked lineament XSM0003A1, which exhibits strong magnetic and topographic anomalies. This zone corresponds to the version 0 zone ZSM0007A0, but has a slightly different mean orientation because of the detailed lineament interpretation. The new orientation (165/90) also corresponds well with the Laxemar zone ZLXNS01, alternative model. The width is estimated to be 50 m (± 20 m).

The local major deformation zone ZSMNW012A is interpreted to follow lineament XSM0270C1 and has been verified by ground magnetics and VLF and coincides with the version 0 deformation zone ZSM0012A0. The width is estimated to be 40 m.

The local major deformation zone ZSMNW012A is interpreted to follow lineament XSM0025A0 and intersect percussion borehole HSH01 at 160 to 171 m depth. The zone is identified in the single hole interpretation as DZ2 in this percussion borehole. The width is estimated to be 5 m.

There remains a clear possibility that one or more additional deformation zones will be recognised/ interpreted in a later modelling phase, following completion of more surface and borehole investigations in the Simpevarp and Laxemar subareas.

The remaining 166 possible deformation zones (made up of 183 segments) included in the regional deformation zone model correspond to the map of linked lineaments. It is assumed that the strike of the possible deformation zones correspond to the trends of the corresponding lineaments. All these deformation zones are assumed to be vertical (90^{o} dip).

The presented Simpevarp 1.2 model of deformation zones consists of only one “base case” model. Alternative models for deformation zones have not yet been considered, mainly due to time constraints. Alternative models are likely to be presented for the subsequent site-descriptive model version Laxemar 1.2.

5.4.3 Assigment of properties to interpreted deformation zones

Key properties, and numerical estimates of the uncertainty in some of these parameters, have been attributed to each of the twenty-two high confidence deformation zones that are based on a variety of geological and geophysical information, or deduced from older models (Table 5-16). The properties of the deformation zones are presented in tabular format in the description of the regional model domain (Section 11.2).

The properties of the twenty-two high confidence deformation zones have been extracted primarily from the version 0 /SKB, 2002b/, version Simpevarp 1.1 /SKB, 2004b/, the Laxemar model test report /Andersson et al. 2001/ and the report on the Ävrö model /Markström et al. 2001/. The GEOMOD model was provided without any description and therefore references are made to properties related to the Äspö model /Rhén et al. 1997a/.

There are few data available at present relating the properties (including numerical estimates of uncertainty) of the interpreted possible deformation zones, which are based solely on the interpretation of linked lineaments (Table 5-17). The data available are presented for each orientation set − NW, NE, NS and EW − in the description of the site (Section 11.2). Both the NW and NS orientation sets are divided into two subsets that include the regional and local major deformation zones, respectively.

An estimate of the mean value of the strike and dip of the possible deformation zones for each of these sets (or subsets) is provided on the basis of the statistical analysis of fractures and lineaments in the DFN model (see Section 5.5). The estimate of width is based solely on a comparison with the twenty-two deformation zones where more data are available.

Assigned properties to deformation zones are provided in Appendix 4.

Table 5-16. Properties assigned to the twenty-two high confidence deformation zones of the Simpevarp 1.2 model, along which there are, to variable extents, supporting geological and geophysical data.

Property	Comment
Deformation zone ID	ZSM******, in two places with additional letter A, B, C, D and E (according to the nomenclature recommended by SKB).
Position	With numerical estimate of uncertainty.
Strike and dip	With numerical estimate of uncertainty.
Width	With numerical estimate of uncertainty.
Length	With numerical estimate of uncertainty.
Ductile deformation	Indicated if present along the zone.
Brittle deformation	Indicated if present along the zone.
Alteration	Indicated if present along the zone.
Fracture orientation	In places, with numerical estimate of uncertainty.
Fracture frequency	With numerical estimate of uncertainty.
Fracture filling	Mineral composition.

Table 5-17. Properties assigned to the 166 possible deformation zones that are based solely on the interpretation of linked lineaments.

Property	Comment
Orientation set	Each zone within the set is identified with a ZSM****** code, in two places with additional letters A and B or A, B and C (according to the nomenclature recommended by SKB).
Position	With numerical estimate of uncertainty.
Strike and dip	With numerical estimate of uncertainty. Statistical analysis.
Width	With numerical estimate of uncertainty. Assumption – no data available.
Length subset	Regional (> 10 km) or local major (1–10 km).
Ductile deformation	Indicated if present along the zone.
Brittle deformation	Indicated if present along the zone.

5.4.4 Evaluation of uncertainties

An expert judgement concerning the level of confidence for the occurrence of the various deformation zones is provided in Table 5-18. Twenty-two (N=22) deformation zones are attributed a high confidence of occurrence. One hundered and sixty-six (N=166) deformation zones are interpreted as possible

All the twenty-two zones that are based, at least in part, on supporting geological and geophysical data are included in the deformation zone model with a high confidence of occurrence. Since there is considerable uncertainty concerning the interpretation of the geological significance of the linked lineaments, the 166 deformation zones that are based solely on the interpretation of lineaments are judged to have a lower degree of confidence. Strictly, they form a group of possible deformation zones. The majority of the latter zones are found in the western part of the local scale model volume and in the regional model volume. For the reasons outlined in the evaluation of the primary data, both the character and the clarity of the linked lineaments are used to assess the confidence level of the respective possible deformation zones that have been identified solely from these lineaments.

Table 5-18. Table of confidence for the deformation zones attributed a high confidence of occurence.

Zone ID	Basis for interpretation	Class	Confidence	Comments
ZSMEW002A (Mederhult zone)	Linked lineaments, VLF, seismic refraction, ground geology.	Regional	High	Position on surface: combination of a short section of XSM013A0 and zone ZSM0002A0 in v0.
ZSMEW004A	Airborne geophysics (magnetic 100% along the length, low uncertainty), tunnel. v0.	Regional	High	Position on surface and Äspö tunnel. Based on lineaments XSM0010A0, B0 and XSM0016A0in v0.
ZSMEW007A	Airborne geophysics (magnetic 100% along the length, electrical data, low uncertainty), topography. borehole.	Local Major	High	Zone ZLEW02 in Laxemar model test.
ZSMEW009A (EW3)	Topography, ground geology, tunnel, borehole.	Local Major	High	Zone EW3 in Geomod model.
ZSMEW013A	Airborne geophysics (magnetic 100% along the length, electrical data, low uncertainty), topography, borehole.	Local Major	High	Zone ZLXNW04 in Laxemar model test.
ZSMEW028A	Airborne geophysics and BH evidence.	Local Major	High	
ZSMNE005A (Äspö shear zone)	Airborne geophysics (magnetic 100% along the length, low to medium uncertainty), Ground geology, ground geophysics, Borehole, Äspö data.	Local Major	High	Also known as the 'Äspö shear zone'. Zones NEHQ3 and EW1b in Geomod model. Zones ZSM0005A0 and ZSM0004A0 in v0. Ref: ZLXNE01 alternative Laxemar model.
ZSMNE006A (NE1)	Airborne geophysics (magnetic 100% along the length, low to medium uncertainty), tunnel, boreholes, Äspö data.	Local Major	High	Zone NE1 in Geomod model. Zone ZSM0006A0 in v0. Zone ZLXNE06 in Laxemar model test.
ZSMNE010A	Airborne geophysics, topography, field control.	Local Major	High	Zone ZSM0010A0 in v0.
ZSMNE011A	Airborne geophysics, topography, ground geophysics.	Local Major	High	Zone ZSM0011A0 in v0.
ZSMNE012A (NE4)	Airborne geophysics Tunnel, borehole.	Local Major	High	Linked lineaments XSM0012A0, (part of B0), A1, A3 and B1. Zone NE4 in Äspö 96 model /Rhén et al. 1997a/. Zone Z15 in Ävrö model, /Markström et al. 2001/.
ZSMNE016A	Airborne geophysics, topography, tunnel.	Local Major	High	Only north section of lineament XSM0016A0. Zone ZSM0004A0/B0 in v0.
ZSMNE018A	Airborne geophysics borehole.	Local Major	High	Complex zone, single hole interpretation.
ZSMNE024A	Airborne geophysics, tunnel, borehole.	Local Major	High	Modified geometry, cross checked with boreholes KSH03, does not intercept KSH01. Zone Z13 in Ävrö model.
ZSMNE040A	Airborne geophysics boreholes.	Local Major	High	Zone ZSM0003A0 in v0. Zone ZLXNE04 (part ZLXNE03) in Laxemar model test.
ZSMNS001A	Airborne geophysics, ground geophysics, topography.	Regional (A–D)	High	Zone ZSM0001A0/B0 in v0. General agreement in alignment

ZSMNS001B	Airborne geophysics, topography.	Regional (A–D)	High	Zone ZSM0001A0/B0 in v0. General agreement in alignment.
ZSMNS001C	Airborne geophysics, topography.	Regional (A–D)	High	Zone ZSM0001A0/B0 in v0. General agreement in alignment.
ZSMNS001D	Airborne geophysics, topography.	Regional (A–D)	High	Zone ZSM0001A0/B0 in v0. General agreement in alignment.
ZSMNS009A	Airborne geophysics, topography.	Regional	High	Zone ZSM0009A in v0.
ZSMNS017A	Topography, borehole and tunnel evidence.	Local Major	High	Zone NNW4 in Geomod.
ZSMNW004A	Airborne geophysics, ground geophysics, boreholes, topography.	Local Major	High	Zone Z14 in Ävrö model.
ZSMNW007B	Airborne geophysics, topography.	Local Major	High	Zone ZSM0007A0 in v0. Zone ZLXNS01 alternative Laxemar model.
ZSMNW012A	Airborne geophysics, topography.	Local Major	High	Zone ZSM0012A0 in v0.
ZSMNW025A	Airborne geophysics, borehole evidence.	Local Major	High	

5.5 Statistical model of fractures and deformation zones

The statistical model of fractures and deformation zones is presented in detail in /Lapointe and Hermanson, in prep./. Below follows a general presentation of the assumptions, statistical analysis, basic results and conceptual model. An alternative geological DFN model of the Simpevarp subarea has been produced by /Darcel et al. 2004/. The results of the latter alternative DFN modelling is not reported or discussed in the current site-descriptive model, but will be further assessed in the subsequent Laxemar 1.2 modelling.

5.5.1 Modelling assumptions and input from other disciplines

There are several assumptions that have been made in order to construct the stochastic DFN model for the Simpevarp site. Each assumption is described below, along with its projected impact on the model, a rationale for why the assumption is regarded reasonable, and recommendations for future re-evaluation of the assumption.

Assumption 1: Lineaments represent fractures, or traces of deformation zones.

Much care was taken to ensure that the lineaments in the GIS file with primary data were structural features likely to be fractures /see Triumph, 2004/, but this does not guarantee that each and every lineament trace is a manifestation of a true mechanical fracture. Because of the care and protocols followed, however, it is likely that a very high proportion of the interpreted lineaments do represent mechanical fractures, and the error in subsequent orientation and size statistics that may arise from considering the presumed few data that in reality are not representing fractures, is likely to be small.

Assumption 2: The length of a linked lineament or a linked fracture in outcrop is an accurate and appropriate measure of a fracture's trace length for the purpose of building a stochastic DFN model.

This assumption contains two parts: that the linked lineament is a sufficiently accurate measure of a fracture's length; and that it is the appropriate one for computing size statistics. One purpose of linking lineaments is to develop a DFN model that incorporates fracture sizes and intensities that i.a. adequately reproduce flow and transport over large and small scales. It is not adequate to base the DFN model only on (non-linked) lineament segment lengths, because many of these segments, cannot be proven to be truly unique rupture events, which could provide linked flow paths and failure surfaces, and thus are important for transport calculations and mechanical stability estimates.

Moreover, the segments as seen in maps may also reflect effects of the geophysical acquisition and processing procedures, and gaps or misalignments may reflect inadequacies in those procedures.

Although the size model depends on the lengths of the linked lineaments and the way outcrop segments are linked, the uncertainty can be bracketed and quantified. The potential uncertainties in trace lengths at the outcrop scale are manifested (along with other uncertainties) as the variance among area-normalized frequency values for the outcrops. It is likely that the variance due to outcrop differences is greater than the uncertainty produced by the linkage algorithm, and in any case, the uncertainty is quantified by calculating an envelope of parameters for the size of a specific fracture set.

Assumption 3: Fractures in outcrop may represent the smaller portion of a much larger population of fractures if the orientation of the sets in outcrop is similar to the orientation of linked lineaments (i.e. inferred two-dimensional deformation zone traces).

The size calculation for lineament-related sets is based on fitting a power law curve to lineament trace length values and outcrop trace length values. It is possible that most lineaments are actually faults, while most outcrop fractures are mostly joints, which could be in different orientations and have different size characteristics.

However, the fracturing at Simpevarp is likely to be very old /Munier, 1993/, and whatever the origin of the outcrop fracturing may be, it is likely to have been re-activated many times. In this respect, large-scale deformation zones which are assumed to have been subject to more intense reactivatation by multiple events at alternate stress states (variable stress magnitudes and stress orientations), partly enhanced by reduced rock strength strength properties, still share a common tectonic evolution with the fractures mapped in outcrop rock between the major deformation zones.

Assumption 4: Variations in fracture intensity as a function of rock type, alteration or other geological controls can be estimated for unsampled rock units based on the inference of the controlling parameters for those units.

Thus far, information on geological controls for fracture intensity variation suggests that lithology and degree of alteration may be important controls. However, data from the four outcrops and the limited number of boreholes has not provided data for all possible lithology/alteration degree combinations. In order to specify fracture intensity throughout the model region, it is necessary to infer similarity of yet unsampled rock types to sampled ones, or to adjust sampled rock types to reflect assumed unsampled rock type characteristics. It would be useful to verify this extrapolation to unsampled rock types by acquiring data in one of these unsampled domains and comparing with predictions made.

5.5.2 Derivation of statistical model with properties

Introduction

The strategy for calculating the parameter values required for the geological DFN focuses on first defining fracture sets, and then on calculating properties for each set. Because each set may have its own distinct parameter values, the specification of the sets impacts on the uncertainty in the parameter values. The separation of fractures into multiple sets makes it possible to reduce the parameter variance associated with each group, thereby lowering the overall uncertainty in the DFN model.

After the sets have been specified, it is necessary to determine the stochastic geometrical description of each set. For each set, this geometry is composed of:

- fracture orientations, expressed as the trend and plunge of the mean pole, with variability quantified by one of the following models and its associated parameters: either Fisher, Bivariate Fisher, Bingham, Bivariate Normal or Bootstrap models,
- fracture sizes, expressed as a size-frequency distribution following one or more of the following distributions and their associated parameters: either normal, lognormal, exponential, power law or uniform models; and any imposed minimum or maximum truncation values,

- fracture shape,
- fracture intensity, specified as P_{32}, the amount of fracture surface area per unit volume of rock,
- fracture spatial controls. These might be such models as Poissonian, fractal, geostatistical, or more complex combinations of these processes within specific geological domains,
- fracture terminations.

The work flow for analyzing the individual borehole, outcrop and lineament data sets (Figure 5-61) is presented within the context of achieving the overall characterisation objectives, which are to determine regional controls on fracture pattern geometry. In particular, to develop a predictive algorithm for specifying fracture intensity, orientation and size throughout the Simpevarp local model domain.

The workflow diagram begins with the analysis of data sets for each individual borehole, outcrop trace map or lineament data set. These individual data sets are described as “local”, in the sense that it is not initially known whether the fracture controls and geometry determined for each individual set is found elsewhere; they may not show any regional consistency among boreholes or outcrops. The results from the analyses for each borehole or outcrop are initially assumed to only represent the fracturing in the rock in the immediate proximity of the outcrop or borehole. This position is maintained unless comparative analysis later demonstrates that fracture orientations, geological controls on intensity, etc. exhibit a consistency over the whole local model domain. The term, local fracture set should not be confused with the DFN model of the local model domain. The local DFN model is independent of whether it is composed of local fracture sets, where individual borehole or outcrop data sets show little spatial consistency, regional sets, which show great spatial consistency, or some combination of regional and local sets.

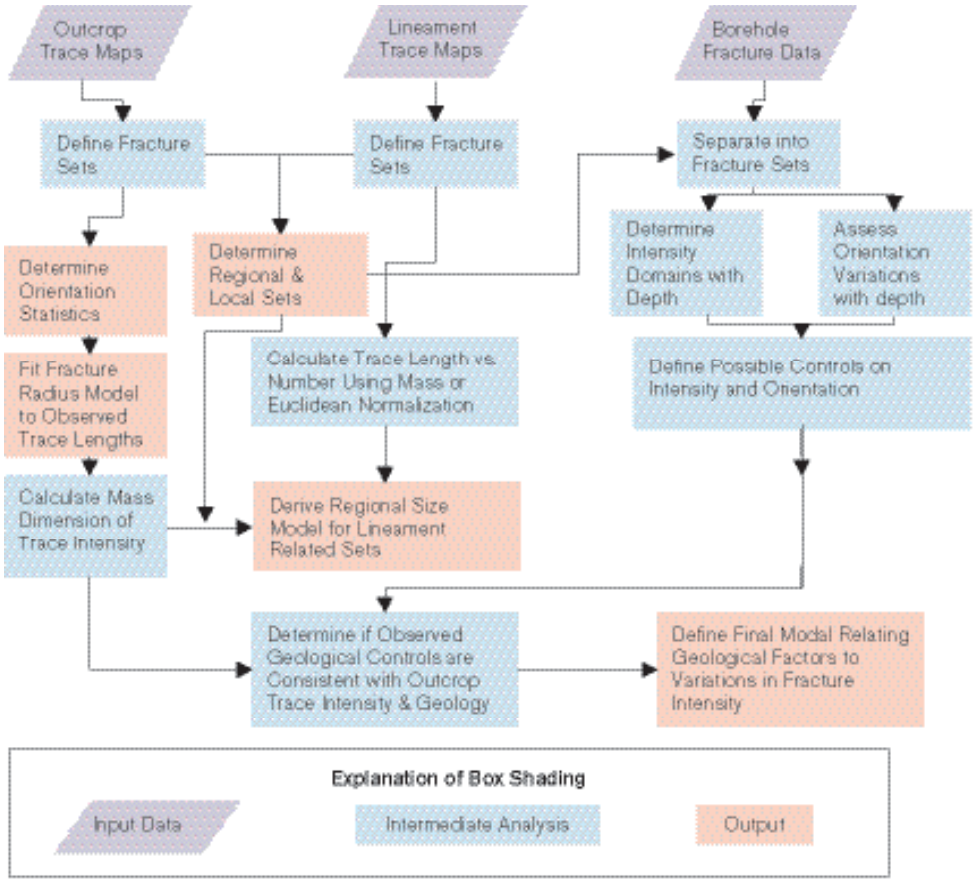

Figure 5-61. *Geological DFN analysis – flow chart of data analysis.*

The flow chart shows the components of the analysis of the local data sets. Any box that can be traced to an original input data source without connection to another data source is part of the local fracture data set analyses. For example, the chart shows that calculating the mass dimension of the trace intensity is part of the local data analysis for the outcrop trace data, but the derivation of the regional size model for lineament-related sets is not, as it relies upon the joint analysis of both the lineament and outcrop trace data sets, and whether the outcome of these analyses suggest that lineaments and smaller-scale fracturing ought to be combined. In contrast, the stages in determining the possible regional controls on fracturing are based on the borehole data, as these data sets contain the most detailed geological information. Any controls identified in the borehole data set are then extended to the outcrop data to see if the controls appear to persist for these data sets as well. All of the analyses eventually lead towards the conceptual basis and parameter values for the local stochastic DFN model. This model consists of all of the pink-shaded output data sets and relations.

Orientation determination and statistics – subvertical sets

The subvertical sets were determined from the outcrop trace data and the lineament data. Figure 5-62 shows the outcrop trace patterns in which each identified set is shown by colours. The analysis of the sets suggested two alternative conceptual models for the fracturing: Alternative 1, in which three vertical sets were related to the lineaments, and another three vertical sets were not; and Alternative 2, in which all of the six vertical sets were related to corresponding lineaments. In both alternatives, there was one additional subhorizontal set. There were six sets found for each outcrop with the exception of ASM000206, where seven sets were identified.

A relative chronology, based upon a visual assessment of termination relations, is given in Table 5-19. Colors were selected to visually accentuate the differences of sets with similar azimuths, (and this varied from outcrop to outcrop). This table and figure shows that there appear to be consistent, dominant older sets in each of the outcrops. The oldest set typically strikes northeast or north-northeast. There are also prominent, older sets striking west-northwest and northwest.

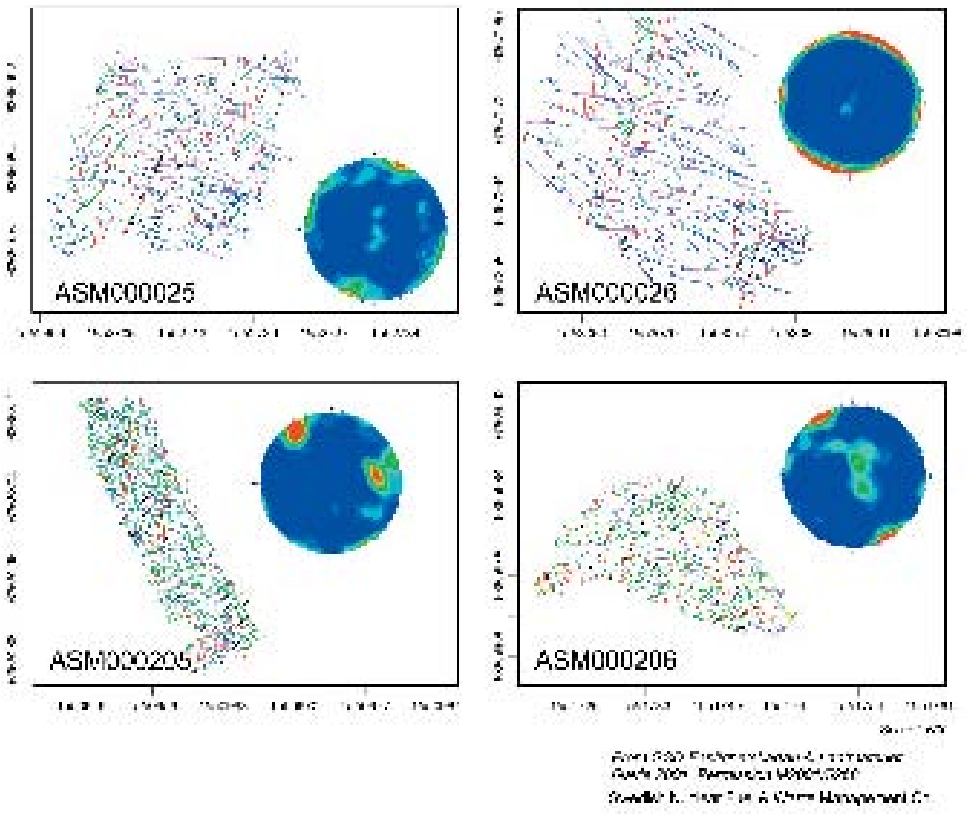

Figure 5-62. *Trace maps for outcrops ASM000025, ASM000026, ASM000205 and ASM000206. Colors represent different fracture sets.*

Table 5-19. Relative chronology of sets in outcrop inferred from abutting relations, length and spatial homogeneity, cf. Figure 5-62.

ASM000025	Black & Blue (NNE & WNW Sets; NNE older than WNW) Cyan & Red (NW & NS Sets; NW older than NS) Purple & Green (ENE & NE Sets)
ASM000026	Red (NS Set) Blue (NW Set) Purple (EW Set) Cyan (NNW Set) Black & Green (NNE & NE Sets)
ASM000205	Red (NS Set) Green & Black (ENE & NE Sets) Cyan & Blue (NNW & NW Sets) Purple (EW Set)
ASM000206	Red (NNE Set) Green & Black (ENE & NE Sets) Purple & Blue (EW & WNW Sets) Cyan (NW Set) Yellow (NNW Set)

However, there is enough variation in the set azimuths to conclude that the oldest sets do not have constant mean orientations for all four outcrops.

The next step in determining sets was to see what fracture sets might be present in the lineament data (Figure 5-26), /SDE, 2004/. The lineaments have been classified by /Triumph, 2004/ as either regional or local major lineaments. The local major lineaments are systematically mapped within the local region, whereas the regional lineaments intersect the local domain, but extend outside. The regional lineaments also often truncate against the outer perimeter of the regional model domain. As a result, the bias in the regional lineament set makes it inappropriate for the systematic calculations of fracture trace length, but is useful in a qualitative manner for assessing the definition of the lineament trace sets. Figure 5-63 shows the rosette for traces from the local major set of lineaments.

Two sets are interpreted to be present in the regional lineament group, whereas there are three sets present in the local major lineament group.

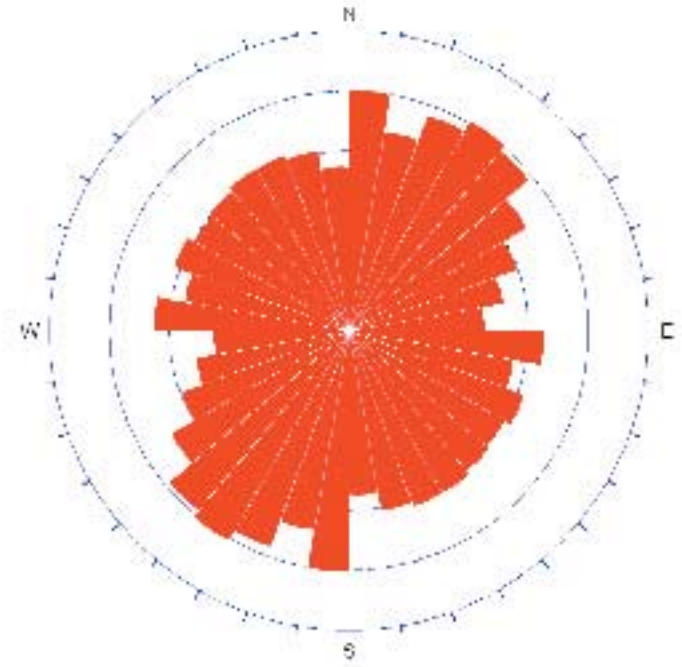

Figure 5-63. *Rosettes for local major lineaments for the Simpevarp and Laxemar region.*

The relation between the orientations of mapped fractures in outcrop and the orientations of the lineaments suggests two possible alternative conceptual models. In the first alternative, three of the outcrop sets are related to the lineament sets, whereas the remainder is not. This alternative conceptual model is consistent with the interpretation of the three dominant local major lineament classes in the local major lineament group rosette (Figure 5-63). The lineament-related fracture sets are denoted Group 1 sets.

In terms of developing a regional model, this implies that:

- Some fracture sets identified in outcrop appear to be related to nearby lineaments in terms of orientations.
- Orientations of lineament-related fracture sets, whether at the scale of meters or kilometres, change locally according to the dominant orientations of adjacent lineaments.
- Assignment of a mean orientation for any lineament-related fracture set would be inaccurate. Orientations should be assigned based on adjacent lineament trends, using the dispersion values calculated from the outcrop analyses of the respective sets (Table 5-20).

The remaining fracturing that is not part of the lineament-related sets forms the Group 2 sets. /Lapointe and Hermanson, 2004/ show that group 2 sets consist of three main orientations as shown in Table 5-21 (BGNE, BGNS and BGNW).

The broad range of azimuths of the lineament sets and visual inspection of the lineament trace maps suggests that there might be up to six lineament trace sets as well. These six lineament trace sets correspond reasonably well to the six outcrop trace sets. In the second alternative, all subvertical fracture sets have lineament counterparts. The relation between the outcrop data sets and the lineament data sets for Alternative Model 2 is given in Table 5-22.

Table 5-20. Mean dispersion (κ) for lineament-related fracture sets based on averaging outcrop values for each set.

Lineament-Related Fracture Set Identifier	Dispersion Averaged from Outcrop Sets
NNE-NE	17.3
EW-WNW	11.2
NW-NNW	13.7

Table 5-21. Orientation parameters for Alternative Model 1 – subvertical fracture sets.

ORIENTATION			
Set Name	**MeanPole Trend/ Plunge/Dispersion**	**Model/K-S**	**Relative % of total population of sub-vertical fractures (Terzhaghi corrected)**
NNE-NE	118.0/1.9/17.3	Fisher Not significant	18.99%
EW-WNW	17.1/7.3/11.2	Fisher Not significant	17.75%
NW-NNW	73.1/4.7/13.7	Fisher Not significant	22.50%
BGNE	326.3/5.5 K1:17.65 K2:18.14	Bivariate Fisher 0.041/45.4%	18.60%
BGNS	96.8/3.8/20.32	Fisher Not significant	15.44%
BGNW	22.1/2.4 K1:5.36 K2: 6.66	Bivariate Fisher 0.051/61.3%	6.71%

Table 5-22. Orientation for Alternative Model 2 – subvertical fracture sets.

ORIENTATION			
Set Name	**MeanPole Trend/ Plunge/Dispersion**	**Model/K-S**	**Relative % of total population of sub-vertical fractures (Terzhaghi corrected)**
NS	99.7/6.9/9.63	Fisher Not significant	13.74%
NE	128.4/2.6/8.92	Fisher Not significant	12.32%
ENE	331.7/5.4/10.2	Fisher Not significant	23.72%
EW	6.0/3.1/6.97	Fisher Not significant	15.75%
NW	39.0/0.7/7.78	Fisher Not significant	21.16%
NNW	74.5/9.2/9.17	Fisher Not significant	13.30%

Orientation determination and statistics – subhorizontal set

Sub-horizontal fractures in outcrops with dips equal or less than 25 degrees constitute about 3% (unweighted) or 9% (Terzaghi corrected) of the sampled population. The mapping of these fractures is difficult in outcrop due to the intersection angle with the horizontal outcrop, weathering and erosion. The sub-sample is also quite small (129 fractures in all four outcrops out of more than 3,000 fractures). Therefore it is considered that borehole data may provide a more comprehensive data source for sub-horizontal fractures.

Borehole data from KSH01A, KSH01B, KSH02, KSH03A, KSH03B, KAV01 and KLX02 as well as HSH01, HSH02 and HSH03 provide around 30,000 fractures with dips less than 25 degrees. A visual analysis of the clustering of all fractures in all orientations in these boreholes indicates that there is no clear set of sub-horizontal fractures. Rather, it is a concentration of sub-horizontal fractures that gradually changes orientation towards steeper fracture orientations. This pattern prevails even after orientation bias has been corrected for. For simplistic reasons, it was decided to capture the slight offset of the sub-horizontal set centre and at the same time provide a set definition that was easy to use for modelling. The sub-horizontal set was defined by all fractures with dips equal to or less than 20 degrees and fractures dipping equal to or less than 25 degrees in the interval NW25 to N80E, cf. Figure 5-64. Sub-horizontal fractures in this interval constitute about 20% (unweighted) or 12% (Terzaghi corrected) of the fractures in the boreholes. Table 5-23 presents statistics for the sub-horizontal set.

Table 5-23. Orientation parameters for subhorizontal fracture set in Alternative Models 1 and 2.

ORIENTATION			
Set Name	**MeanPole Trend/Plunge/ Dispersion**	**Model/K-S**	**Relative % of total population in boreholes** **Unweighted** **(Terzhagi corrected)**
SubHZ	33/86/31.3	Fisher	20.1% (12.4%)

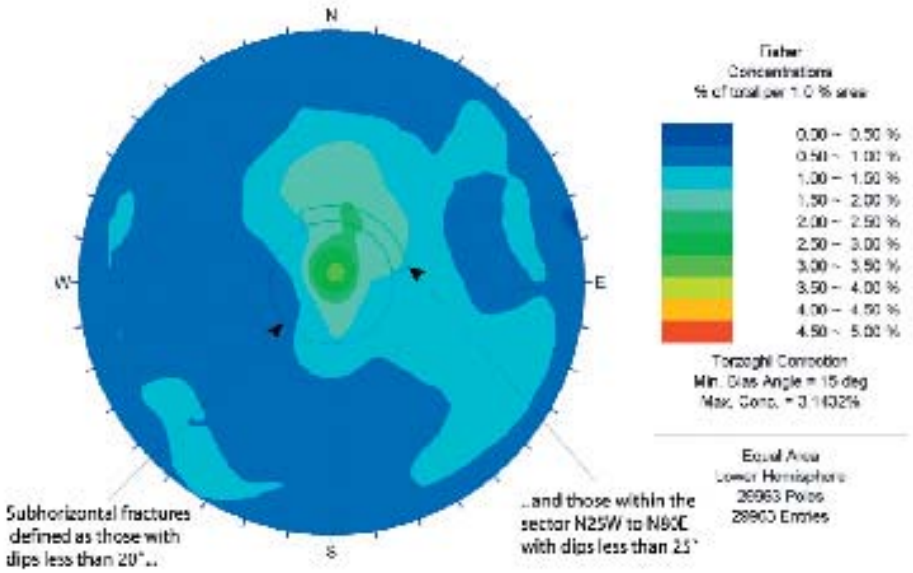

Figure 5-64. *Definition of horizontal fractures from borehole data. The plot shows open and sealed fractures from boreholes KSH01A/B, KSH02, KSH03A/B, KAV01 and KLX02 as well as HSH01, HSH02 and HSH03.*

Estimation of fracture sizes

The size distribution parameters were estimated in two different ways, depending upon whether they were lineament-related (Group 1) or not.

The calculations on fractures Group 1 were carried out by first computing the mass dimension, and then using the mass dimension for detemining the appropriate area renormalisation scaling. If the mass dimension was close to 2.0, then the scaling is approximately Euclidean and the area renormalisation is accomplished by simply dividing the number of fractures by the area of the outcrop or lineament map. For the Group 2 fractures, the size was determined by employing the ISIS approach, /Dershowitz, 1996/, on the outcrop data alone.

The mass dimension analyses for each outcrop fracture data set showed that intensity does not scale, except in rare cases, linearly with area. In other words, the scaling behaviour is rarely Euclidean. In general, the regression through the locus of the mean for each mass dimension plot indicates that a fractal scaling behavior is a valid model for the fracture sets.

The trace length scaling plots (example in Figure 5-65) show the renormalised data and three lines fit visually to the data. The lines labelled as “Upper” and “Lower” represent the upper and lower bounds on the data, and constitute a measure of the uncertainty in the trace length scaling calculations. The median line is the visual best fit to the data. The statistics reported in each plot consist of the slope of the line, labelled as k_t for the power law distribution. These two trace length parameters are used to calculate the parameters for the parent radius distribution according to Equation 5-1;

$$\mathrm{Prob}(x \geq x_{t0}) = \left(\frac{x_{t0}}{x}\right)^{k_t}$$

$$k_r(radius) = k_t(traces) + 1.0$$

$$x_{r0}(radius) = x_{t0}(traces) * \frac{2}{\pi}$$

Equation 5-1

where
x_{t0} is the minimum trace length;
x is any trace length greater than or equal to x_{t0};
k_t is the shape parameter of the Trace Length distribution, and
$Prob(x \geq x_{t0})$ is the probability that x is greater than or equal to x_{t0}.

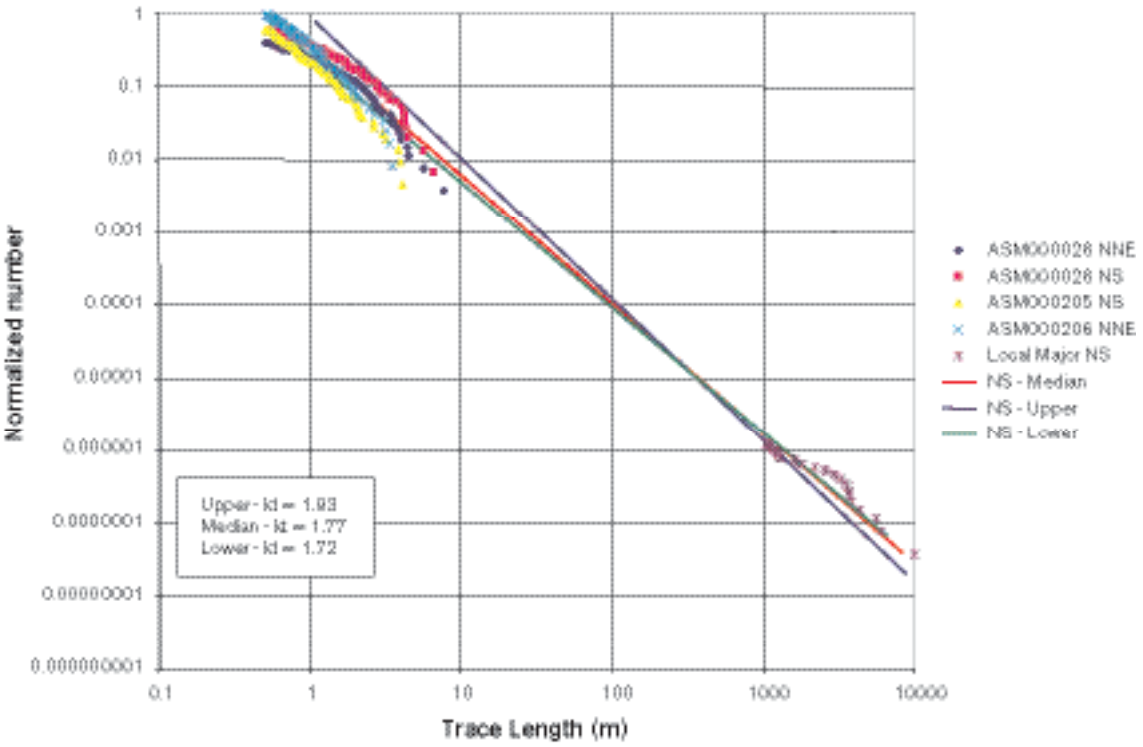

Figure 5-65. *Trace length scaling plot for the NS set (Alternative Model 2 only).*

The results for Model 1 are given in Table 5-24. This table gives the parameters for the parent fracture radius distribution for the upper, median and lower bound lines. Values are also given for both mass dimension and Euclidean scaling. The values for the Group 1 sets were estimated from the area renormalisation plots. In all cases for the Group 2 sets, the best fitting distribution was a lognormal distribution. Parameters were also estimated for power law distributions for the Group 2 fracture sets in order to facilitate comparisons with other studies of fracturing that have been carried out in the past in the Simpevarp area. However, the preferred size model for Group 2 fractures is lognormal based upon statistical significance /LaPointe and Hermanson, 2004/.

The size calculations for Alternative Model 2 are given in Table 5-25.

Table 5-24. Fracture size parameters for fracture sets of Alternative Model 1.

SET	Size model preferred, (alternative)	Lognormal (radius distribution)			Powerlaw (radius distribution)		
		Arithmetic space	Log^{10} space	LN space	Upper	Median	Lower
		Mean [(1/n) Σ x_i] (meter)/ Standard deviation	Mean [(1/n) Σ log^{10} x_i]/ Standard deviation	Mean [(1/n) Σ ln x_i]/ Standard deviation	k_r/X_{r0} (mass) (euc)	k_r/X_{r0} (mass) (euc)	k_r/X_{r0} (mass) (euc)
NNE-NE	Powerlaw				2.68/0.38 2.85/0.27	2.58/0.23 2.82/0.20	2.50/0.13 2.69/0.10
EW-WNW	Powerlaw				2.93/0.40 2.99/0.45	2.80/0.23 2.82/0.20	2.67/0.11 2.78/0.13
NW-NNW	Powerlaw				2.97/0.48 3.02/0.35	2.87/0.31 2.91/0.22	2.62/0.08 2.83/0.10
BGNE	Lognormal (Powerlaw)	0.48/0.55	–0.50/ 0.60	–1.15/ 0.92	2.86/0.55 3.07/0.51	2.77/0.35 3.00/0.36	2.61/0.17 2.78/0.11
BGNS	Lognormal (Powerlaw)	0.67/0.82	–0.37/0.63	–0.86/0.96	2.93/0.60 2.99/0.36	2.77/0.35 2.95/0.29	2.72/0.28 2.95/0.23
BGNW	Lognormal (Powerlaw)	0.45/1.00	–0.73/0.88	–1.69/1.33	3.05/0.69 3.14/0.55	2.82/0.28 2.94/0.24	2.80/0.23 2.89/0.18
SubH	Lognormal	0.57/1.86	–0.78/1.03	–1.79/1.57			

Table 5-25. Fracture size parameters for the fracture sets of Alternative Model 2.

SET	Size model preferred, (alternative)	Powerlaw (radius distribution)		
		Upper	Median	Lower
		k_r/X_{r0} (mass) (euc)	k_r/X_{r0} (mass) (euc)	k_r/X_{r0} (mass) (euc)
NE	Powerlaw	2.68/0.38 2.85/0.27	2.58/0.23 2.82/0.20	2.50/0.13 2.69/0.10
EW	Powerlaw	2.93/0.40 2.99/0.45	2.80/0.23 2.82/0.20	2.67/0.11 2.78/0.13
NNW	Powerlaw	2.97/0.48 3.02/0.35	2.87/0.31 2.91/0.22	2.62/0.08 2.83/0.10
NS	Powerlaw	2.93/0.60 2.99/0.36	2.77/0.35 2.95/0.29	2.72/0.28 2.95/0.23
NW	Powerlaw	3.05/0.69 3.14/0.55	2.82/0.28 2.94/0.24	2.8/0.23 2.89/0.18
ENE	Powerlaw	2.86/0.56 3.07/0.52	2.77/0.36 3.00/0.36	2.61/0.17 2.78/0.12
SubH	Lognormal	0.57/1.86	–0.78/1.03	–1.79/1.57

Intensity

Analysis of fracture intensity as a function of lithology and rock domain shows that both potentially consitute controls that could be used to subdivide the data and reduce model uncertainty.

Examination of fracture intensity with depth for the cored boreholes showed no significant differences between sealed fractures and open fractures in terms of variations with depth. Areas that had a high intensity of sealed fractures with depth also showed a high intensity of open fractures, and similarly with zones of lower intensity.

Rigorous statistical tests suggest that rock domain can be used to reduce model uncertainty, as the variability of intensity between domains is greater than the variability within domains /LaPointe and Hermanson, 2004/. The results are shown in Table 5-26 and Table 5-27 and provide estimates of mean fracture intensity by rock domain for each group (vertical and horizontal) of fracture sets. In order to determine the appropriate P_{32} for an individual subvertical fracture set for a specified rock domain, all that needs to be done is to multiply the rock domain P_{32} value shown in the table by the set's proportion as given in Table 5-21 for the Alternative model 1 and in Table 5-22 for the Alternative Model 2.

Spatial model

The spatial model is closely related to the intensity model. The results of the calculation of mass dimension suggest that the spatial pattern at the outcrop level is Euclidean to "mildly fractal". This suggests that a Poisson Point process (which has a mass dimension of 2.0) is a reasonable fit to much of the mass dimension data. Until further results suggest otherwise, it appears that the Poisson model, at least at the outcrop scale, is a reasonable model given the existing trace length data.

Another issue concerns how fracture intensity may vary with depth. One of the key issues is whether fractures seen in outcrop or near the surface are representative of fractures at repository depths hundreds of meters below the surface. If surficial stress relief has produced increased fracturing near the surface, the latter fracturing should have certain characteristics, such as increased horizontal fracture intensity and also characteristics like low temperature mineral fillings or relatively unaltered walls relative to fracturing at depth. To test these hypothesises, fractures from boreholes KAV01, KSH01A, HSH01, HSH02 and HSH03 were evaluated in several different ways:

- Variation of intensity with depth as a function of "open" or "sealed".
- Variation of intensity with depth as a function of dip for open fractures.
- Variation of intensity with depth as a function of mineral fillings for open fractures.

Table 5-26. Intensity (P_{32}) for subvertical sets.

Rock Domain	P32 Sub-vertical (All)	P32 Sub-vertical (Open fractures)	Comments
A	2.10	0.47	Outcrop ASM000026
B	4.86	0.69	Outcrop ASM000205
C	2.92–3.27	0.65–0.93	Two outcrops, ASM000025 and ASM000206, both close to boundary of C domain
D	No data	No data	No data

Table 5-27. Intensity (P_{32}) for the horizontal set. The * mark represent intensities where the lower 95% confidence limit, based on the assumption of normality, is below 0.0. It has been set to 0.0 as negative intensities are not physically possible.

Fractures by domain	P_{32}				
	Mean	SD	SE	95% CI of Mean	
All by Domain – A	0.924	0.1611	0.0930	0.524	to 1.324
All by Domain – B	2.798	0.1318	0.0932	1.614	to 3.982
All by Domain – C	2.008	0.9178	0.4105	0.868	to 3.147
All by Domain – D	No Data				
Open by Domain – A	0.491	0.1498	0.0865	0.118	to 0.863
Open by Domain – B	0.726	0.4690	0.3316	0.000*	to 4.940
Open by Domain – C	0.429	0.2510	0.1122	0.117	to 0.741
Open by Domain – D	No Data				
Partly Open by Domain – A	0.008	0.0144	0.0083	0.000*	to 0.044
Partly Open by Domain – B	0.000	–	–	–	to –
Partly Open by Domain – C	0.006	0.0093	0.0041	0.000*	to 0.017
Partly Open by Domain – D	No Data				
Sealed by Domain – A	0.425	0.2968	0.1714	0.000*	to 1.163
Sealed by Domain – B	2.072	0.6008	0.4248	0.000*	to 7.470
Sealed by Domain – C	1.573	0.6836	0.3057	0.724	to 2.422
Sealed by Domain – D	No Data				

Results show little evidence of enhanced fracture intensity near the surface. KAV01 shows lower intensity in the upper 100 m compared to the interval from about 125 m to 250 m measured depth. The intensity as seen in the three percussion boreholes (HSH01, HSH02 and HSH03) shows little intensity variation with depth. In addition, the intensity of open and sealed fractures generally are very similar, as are those of the open horizontal and all open fractures. Data for the deep-penetrating boreholes (KSH01A, KAV01 and KLX02) have their zones of highest intensity at the deeper intervals.

5.5.3 Verification tests of developed geological DFN models

Two verification approaches have been performed;

Verification of conceptual Alternative Model 1 was made using outcrop data and borehole data from domain A. This approach was made with a thorough re-examination of fracture intensity on outcrop ASM000026 and in borehole KLX02 and has been focused on open, sub-vertical fracturing.

Verification of conceptual Alternative Model 2 using estimated parameters for subvertical and sub-horizontal fractures. This approach has made use of the presented tables for orientation, size and intensity for the alternative 2 conceptual model.

In both conceptual alternatives, sub-vertical sets are estimated only from surface observations, as has been described previously. Verification tests show that estimates of simulated intensity for sub-vertical sets are about 50% (simulating all fractures) to an order of magnitude (only open fractures) smaller than observed in boreholes.

The major reason for this may be due to the different resolution in mapping of fractures in outcrop and boreholes. If the intended use of the DFN model is to estimate sub-vertical intensity in boreholes, it is suggested that the minimum radii of the powerlaw size distributions are lowered to 5–10 cm when simulating open fractures. Complete conditioning of all sets has not been performed due to time constraints.

In both conceptual alternatives, sub-horizontal fractures are estimated partly on surface data (size) and partly on borehole data (orientation and intensity). Verification tests show that sub-horizontal fractures are currently over-estimated about two times compared to observations in boreholes.

The main reason for this may be the poor definition of subhorizontal fracture orientation and the size estimation. Relatively small samples of subhorizontal traces from outcrop have been used for estimating size, and these traces are considered to be highly uncertain due to the low angle of intersection with the outcrops. The orientation of the subhorizontal set is basically estimated by hard sector definition, as exemplified in Figure 5-64, which is converted to a Fisher distribution in the model. When simulating fractures, this approach may produce a higher intensity than intended.

If the intended use of the DFN model is to estimate open and sealed subhorizontal fracture intensity in boreholes, it is currently suggested to lower the estimated P_{32} for subhorizontal fractures by about 50%. Complete conditioning of the subhorizontal set has not been performed.

5.5.4 Evaluation of uncertainties

Uncertainty in the developed model (and its alternative) derives from several sources, including the uncertainty inherent in the data variability among the various outcrops and boreholes, as well as in the conceptual model in which the data is analysed.

The uncertainty in fracture orientation has been quantified in two different ways: the conceptual model uncertainty has been addressed by evaluating two alternative models for fracture sets; the uncertainty in orientations within each set has been quantified by calculating the orientation dispersion for each set at each of the four outcrops. Since there are many alternative ways to aggregate the data at each outcrop, for example, by weighting by area or by fracture intensity, it is left to the users of the results to decide the best way to propagate the uncertainty for their own purposes.

The uncertainty in size is quantified in two different ways. For local fracture sets, the size model for the parent fracture radius distributions is based on aggregating all of the outcrop data for that set, and estimating a model for the distribution of fracture radii. For the lineament-related sets, three values are given: two bounding cases and a “best-guess”. Because of the artifacts having to do with truncation of trace length data, the trace length model fit to the normalized data is done visually rather than through non-linear regression. The “best-guess” is the best visual fit through all of the outcrop and lineament data. The two bounding cases are lines that approximate the shallowest and steepest lines that could be fit through the data. These represent the span of possible size variation given the existing data. As in the case of orientations, it is up to the user of these data to decide which parameter values to select. It may be worthwhile to further evaluate the fractures mapped in outcrop to determine what evidence for reactivation there exists, and perhaps to construct an alternative size model based only on outcrop fractures than have clear evidence for re-activation or shear movement.

The intensity of fracturing is specified, where data allows, as a function of the geological factors in terms of the mean and standard deviation of P_{32}. However, for the vertical sets there exist only one outcrop in each rock domain, except in one case, the C domain, where there are two outcrops.

6 Rock mechanics model

The rock mechanics model describes the properties of the intact rock and the single fractures as well as the properties of the bedrock on a larger scale, i.e. as a composite material, what we denote the 'rock mass'. The rock mechanics model also includes a description of the in situ stress conditions in the Simpevarp subarea. These properties and states together are of importance since they may affect the design and depth location of a possible repository and may introduce requirements on the necessary space. The starting point for the modelling work is an evaluation of the primary data, i.e. laboratory tests on core samples, measurements in boreholes and geological mapping of the drill cores. The estimation of rock mechanics properties for the rock mass is based both on empirical and theoretical approaches. While based on measurement observations, the stress model is supported by a numerical model of the site. The result of the modelling work is a list of predicted parameter values, for each rock domain defined within the local model area, including an estimation of variability and uncertainties. The presented rock mechanics model is developed in accordance with the Strategy report /Andersson et al. 2002a/.

6.1 State of knowledge at previous model version

In the Simpevarp 1.1 model report /SKB, 2004b/ a description of the rock mechanics properties and the in situ state of stress was included. The description consisted of estimates for deformation and strength parameters, both for intact rock and for the rock mass of various defined lithological rock domains. The description was mainly based on data from one single cored borehole (KSH01A) and on empirical classifications. Old laboratory test data from the Äspö HRL were another important input to this model. The rock mass in the area was described as having, on the average, normal strong mechanical properties for Swedish crystalline rocks, but being relatively inhomogeneous, with a large spread in fracturing characteristics, giving large spans for parameter values. This was in accordance with the geological description showing that the defined rock domains were intersected by many smaller deformatiosn zones. The stress model presented showed quite large uncertainty, due to a large spread in the available measurement data.

6.2 Evaluation of primary data

The primary data used for the rock mechanics modelling is briefly described in the following paragraphs. A list of the different data sources is given in Table 2-2.

6.2.1 Laboratory tests of intact core samples

To test the intact rock strength, uniaxial and triaxial loading tests were performed on samples from boreholes KSH01A and KSH02 (samples from other boreholes were not available for the Simpevarp 1.2 data freeze). These tests are standard tests developed for drillcore samples. The resulting load deformation curves have been interpreted to provide several standard parameters that have been put into the SICADA database. Some of the available test results from SICADA are shown in Table 6-1 and a more detailed compilation is given in /Lanaro and Fredriksson, 2005/.

It may be noted from Table 6-1 that the mean uniaxial strength (UCS) is 161 MPa and 205 MPa for quartzmonzodiorite and fine-grained dioritoid, respectively. These values are within the expected range for Swedish crystalline rocks. Similarly, the stiffness of the fine-grained diorite is slightly higher than that of the quartzmonzodiorite. Also, note that the samples that include sealed fractures show fairly high strength and stiffness values, indicating that the fractures are very well healed by the infilling minerals.

The rock types of samples from Äspö Hard Rock Laboratory (Äspö HRL) vary but are expected to be for the most part either quartzmonzodiorite or the Ävrö granite according to the current nomenclature (Section 5.2). The rock type at the Clab facility is dominated by the fine-grained dioritoid, and therefore old data in columns 4 and 5 of Table 6-1 may be compared to the new data in columns 1 and 2, respectively. Old data were also used since the number of new data was limited and the old data were found to roughly support the results seen from new tests.

The whole distributions of results for the UCS values are shown in Figure 6-1. Although the number of new tests is limited at this stage of investigation, the distributions seem to be roughly normal and the spread is larger for the Äspö HRL data compared with other data. This may be explained to some extent by a larger mix of rock types in these data, but also by an expected larger variation in texture, and thus strength, of the Ävrö granite samples (Section 5.2). New laboratory test from Ävrö granite were not available at the time of data freeze for Simpevarp 1.2.

Table 6-1. Laboratory test results on mechanical properties of intact rock samples. Mean values are provided. For further statistical details cf. /Lanaro and Fredriksson, 2005/.

Laboratory test results	Quartz-monzonite to monzodiorite	Fine-grained dioritoid	Finegrained dioritoid including sealed fractures	Data from Äspö HRL (Old data, See S1.1)	Data from Clab (Old data, See S1.1)
Number of uniaxial tests	10	10	5	70*	40*
Number of triaxial tests	16	16	11	–	–
Mean UCS (uniaxial compressive strength), MPa	161	205	126	183	187
Mean σ_{ci} (crack initiation stress), from uniaxial tests, MPa	77	88	–	–	–
Mean E (Young's modulus) from triaxial tests, GPa	77	78	81	–	–
Mean (Poissons ratio) from uniaxial tests	0.27	0.26	0.24	0.23	0.27
Mean friction angle*	59.5	52.7	49.3	–	–
Mean apparent cohesion*, MPa	20.3	33.0	19.2	–	–

* For best fit Mohr-Coulomb failure criterion.

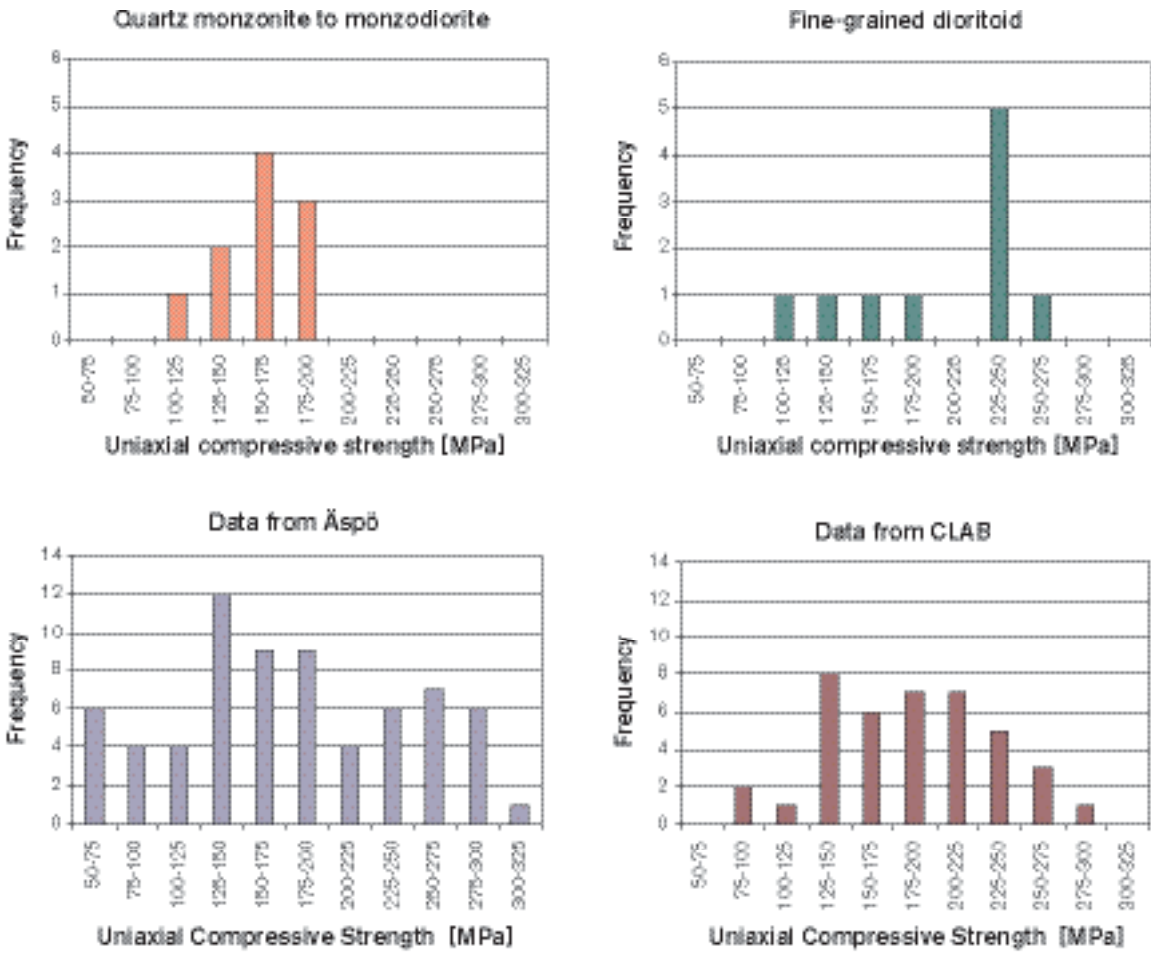

Figure 6-1. *Histograms of the uniaxial compressive strength (UCS) obtained from uniaxial loading tests on rock core samples collected from boreholes KSH01A and KSH02 (as sorted by rock type), and from Äspö HRL and Clab, respectively.*

6.2.2 Laboratory tests on fracture samples

As a part of the standard testing program of drillcore samples from the boreholes, normal stiffness tests and shear tests have been performed. The results from the testing, cf. Table 6-2 and Table 6-3, indicate fairly constant properties. No differences correlated to the identified fracture sets have been found so far. For further details on the test results refer to the compilation in /Lanaro and Fredriksson, 2005/.

Table 6-2. Summary of results on peak friction angle and cohesion for fracture samples. Further details are given in /Lanaro and Fredriksson, 2005/.

Laboratory test results	Number of tests	Peak friction angle		Peak cohesion	
		Mean	St. Dev.	Mean	St. Dev.
Direct shear test on samples from KSH01A, KSH02 and KAV01 performed at SP /Jacobsson, 2004a–c/	28	32	4.3	0.5	0.35
Direct shear test on samples from KSH01A performed at NGI /Chryssanthakis, 2004d/	18	34.3	3.5	1.16	0.19
Tilt test, samples from KSH01A, KSH02, KAV01 and KLX02. /Chryssanthakis, 2003, 2004a–c/ (Estimated from basic friction angle, JRC and JCS)	142	33.7	3.5	0.37	0.12

Table 6-3. Summary of results on normal and shear stiffness for fracture samples. Further details are given in /Lanaro and Fredriksson, 2005/.

Laboratory test results	Number of tests	Normal stiffness		Shear stiffness	
		Mean MPa/mm	St. Dev.	Mean MPa/mm	St. Dev.
Direct shear test on samples from KSH01A, KSH02 and KAV01 performed at SP /Jacobsson, 2004a–c/	28	100.2	31.9	29.3	10.6

6.2.3 Rock mechanics interpretation of borehole data

Rock mechanics modelling employing empirical classification systems have been applied to the available borehole data. The data used are the Boremap logging data in the SICADA database. The applied methodology is described by /Andersson et al. 2002a/ and the results from each borehole are reported by /Lanaro, 2005b/. A compilation of the results from all boreholes which are part of the data freeze for the current model version, and a summary for the defined lithological rock domains, is provided by /Lanaro, 2005a/.

The empirical index Q is determined according to /Barton, 2002/ and the empirical index RMR is determined according to /Bienawski, 1989/. As an example, the results for Q along all studied boreholes are given in Figure 6-2. The mean value and the most frequent value of Q and RMR, for the different lithological domains are given in Table 6-4. The indices were determined for each 5 m long section of the boreholes.

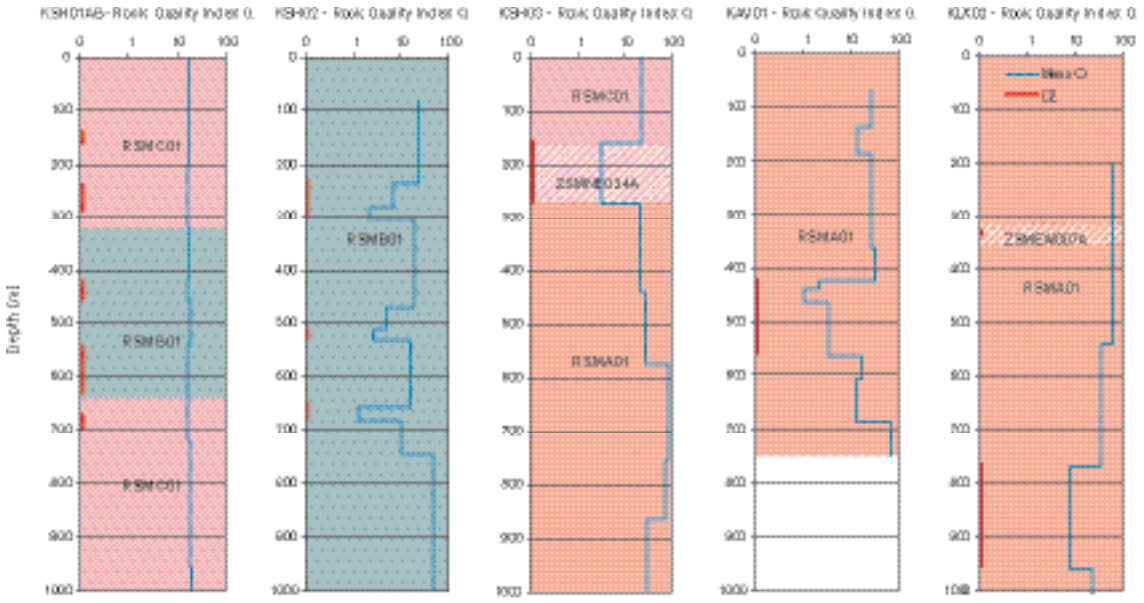

Figure 6-2. *The mean of the empirical index Q for each interpreted unit along the boreholes, shown by the blue vertical line. The division of boreholes into units is based on the geological single hole interpretation. Note that the axis for the Q given in a logarithmic scale /Lanaro, 2005/.*

Table 6-4. Mean empirical rock classification indices for the rock mass in the defined lithological rock domains and inside the interpreted deformation zones, respectively /Lanaro, 2005a/.

Index Based on 5 m long sections	Rock Domain A (Ävrö granite)	Rock Domain B (Fine-grained dioritoid)	Rock Domain C (Ävrö granite + Quartzmonzo-diorite)	Minor deformation zones'	Deterministic deformation zones
	'Competent'	'Competent'	'Competent'		
	Mean value [Most freq.]	Mean value [Most freq.]	Mean value [Most freq.]	Mean value [Most freq.] Dom. A; B; C	Mean value [Most freq.] ZSMNE024
Q [–]	42 [24]	23 [13]	25 [12]	5; 6; 6 [3]; [4]; [5]	3 [1]
RMR [–]	74	70	72	64; 65; 64	57

6.2.4 Other data

Other data used are the analyses performed as part of the construction of the Clab II facility. This underground works is situated within the local scale model area, (cf. Figure 2-3 and 2-1) at shallow depth. The deformation modulus was, in this case, back-calculated from observed convergences and an estimated stress field /Fredriksson et al. 2001/. The most probable deformation modulus for the rock mass at Clab was estimated at 40 GPa.

Further results from back-analysis of the deformation modulus of the rock mass at the Äspö HRL have been used to compare with the results from the empirical and theoretical approaches. At the site of a the Äspö HRL Pillar Strength Experiment (APSE) the deformation modulus has been estimated at 55 GPa, using results from tunnel convergence and stress measurements /Staub et al. 2004/. This site is situated at a depth of 470 metres below sea level.

The general stability situation at the Äspö HRL has been reported by /Andersson and Söderhäll, 2001/. From the results of this study we may compare, at least qualitatively, the modelled mechanical properties for Simpevarp 1.2 with the observed behaviour at depth in the Äspö HRL experimental excavations. Also, a part of the experimental excavation for the Äspö HRL was empirically characterised by /Makurat et al. 2002/.

6.2.5 Stress measurements

Rock stresses have been measured in 4 new cored boreholes as part of the site investigation program at the Simpevarp and Laxemar subarea (KSH01, KSH02, KAV04 and KLX04 (NB. Data from KLX04 were not part of the overall datafreeze for Simpevarp 1.2. However, stress data available in due time for the rock mechanics modelling were retained and used), see Figure 2-1). All other existing measurement data from within the Simpevarp area have also been compiled jointly with the newer data. Figure 6-3 and Figure 6-4 show the measurement results for the maximum, intermediate and minimum principal stresses, respectively. Every point in the diagram represents one single measurement point and measurements in the same borehole are given the same symbol. Since the results showed a large spread, a grouping of the data based on the geographical location of the borehole in relation to interpreted stress domain (cf. Section 6.4.2) was attempted and the red and blue symbols indicate these two groups. The orange symbols are associated with data from an experimental borehole lying outside the Simpevarp local model area in the town of Oskarshamn (borehole KOV01).

Figure 6-5 shows the orientation of the major principal stress from overcoring measurements together with the orientation for the major horizontal stress from hydrofracturing measurements (the major principal stress is normally fairly horizontal). The overall spread in the stress orientation data is large, but there is a clear concentration around the NW-SE orientation. For further details about the input data to the stress model see /Hakami and Min, 2005/.

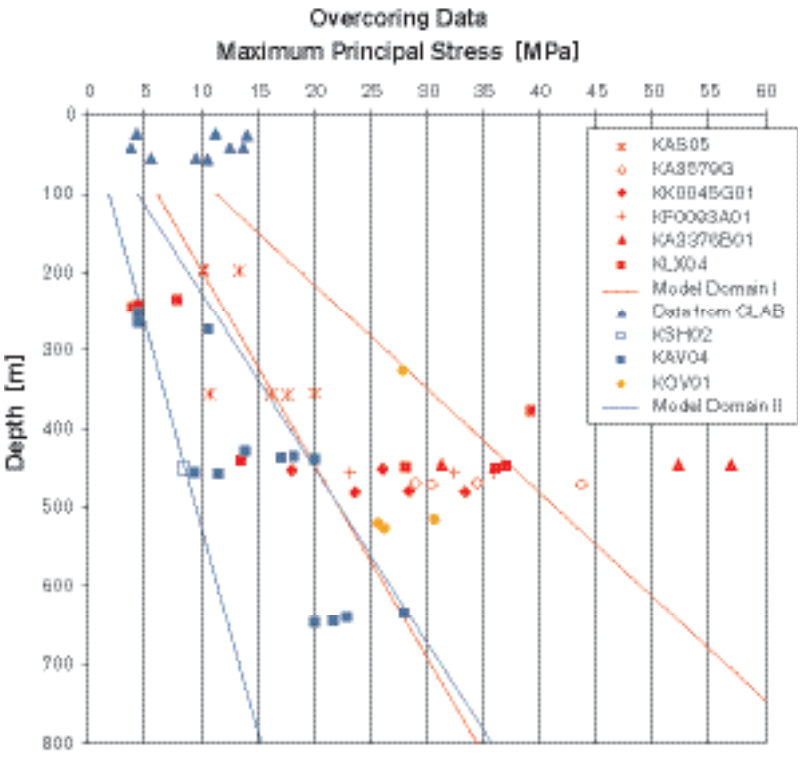

Figure 6-3. *Results from overcoring stress measurements, maximum principal stress magnitudes. The solid lines show the final model span (see Section 6.4.4)*

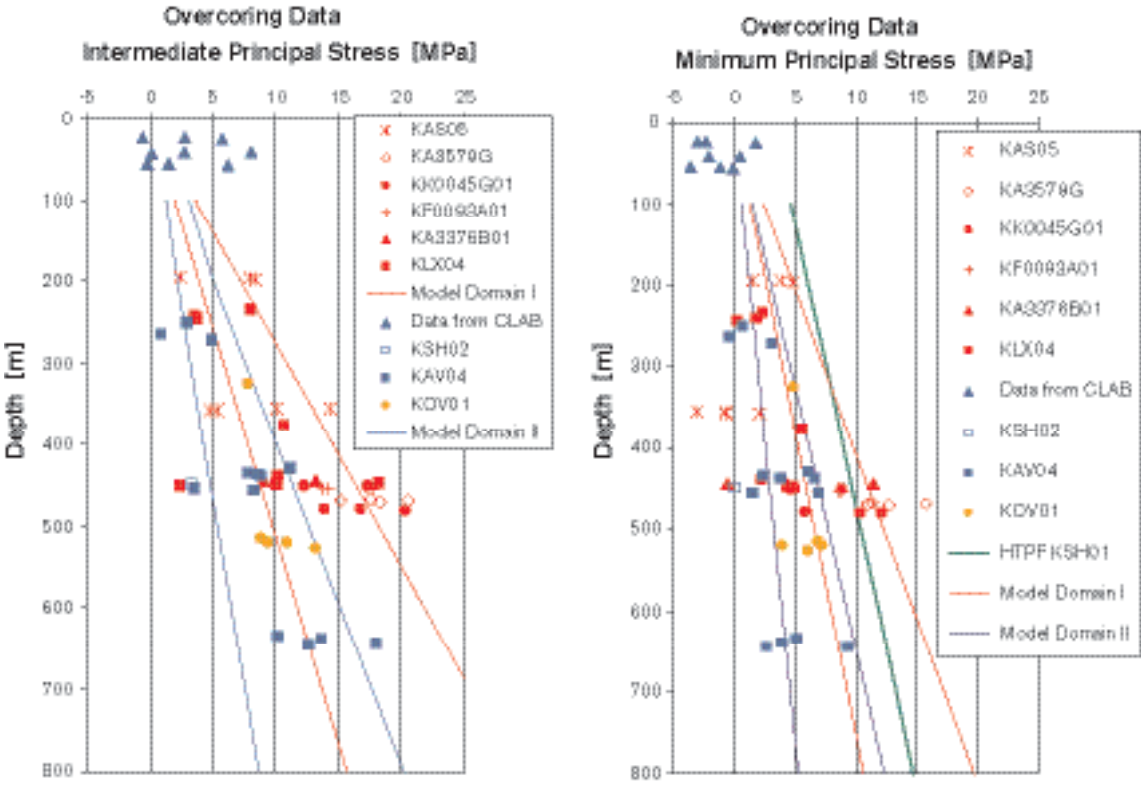

Figure 6-4. *Results from overcoring stress measurements, a) intermediate and b) minimum principal stress magnitudes. The solid lines show the final model span (see Section 6.4.4)*

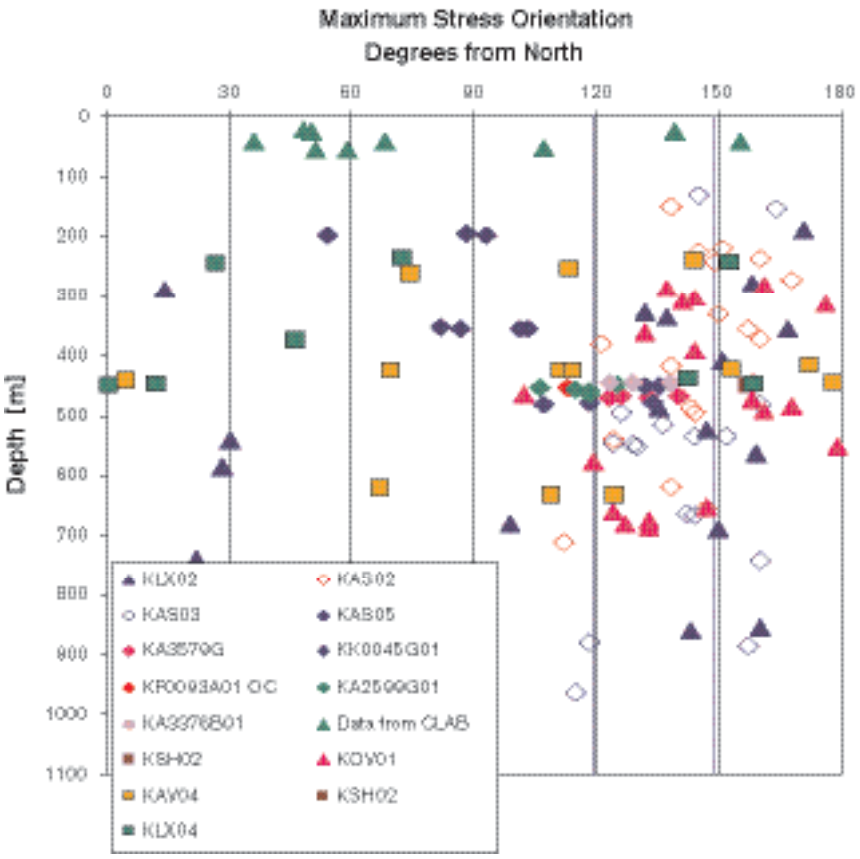

Figure 6-5. *Orientation of maximum principal stress measured in the Simpevarp area.*

The scatter in stress magnitudes seen in Figure 6-3 and Figure 6-4 may be explained either as a result of the uncertainty in the measurement method itself, or as a result of a true spread in the stresses. It is not possible, however, to prove how much the two factors influences data in this case. In the modelling, it is assumed that the scatter in data is representing a real stress variation and also that there is no systematic errors in the measurement data. How the measurement data were used to establish the final descriptive model is described in Section 6.4

6.3 Rock mechanics properties

6.3.1 Assignment of properties for the intact rock

For Simpevarp 1.2, new laboratory data are only available for two rock types (fine-grained dioritoid and quartz monzonite to monzodiorite), despite the fact that there are more rock types in the local model area (see geological model description in Chapter 5). New laboratory data for Ävrö granite, which is by and large dominating in the local and regional scale model areas, will become available for the next model version. However, as a predicted estimate of the intact rock properties of Ävrö Granite, the properties determined for the Quartz monzodiorite are used, because this rock type is expected to be closest in characteristics to the Ävrö granite. Also looking at the data from Äspö HRL (Figure 6-1) one can note that the results fit fairly well to the suggested distribution (Table 6-5). The mean UCS (uniaxial compressive strength) value for the old data at Äspö HRL was 183 MPa, and the mean for the new tests on quartz monzonite to monzodiorite was 161 MPa. A mean value of 165 MPa, with a standard deviation of 30 MPa, was selected for the model. The model values were all selected as rounded off numbers, not to give a false impression of certainty in the estimations.

Table 6-5. Estimated rock mechanics properties for intact rock (matrix) of the dominating rock types (i.e. small pieces of rock without any fractures). Properties of the Ävrö granite are interpreted to correspond with those of the quartz monzonite to monzodiorite.

Parameter for intact rock (drill core scale)	Quartz monzonite to monzodiorite and Ävrö granite		Finegrained dioritoid	
	Truncated normal distribution Mean / standard dev.	Min (trunc.) – Max (trunc.)	Truncated normal distribution Mean / standard dev.	Min (trunc.) – Max (trunc.)
Uniaxial compressive strength, UCS*	165 MPa / 30 MPa	110–200 MPa	210 MPa / 50 MPa	120–265 MPa
Crack initiation stress, σ_{ci}	0.47 × UCS	0.47 × UCS	0.47 × UCS	0.47 × UCS
Young's modulus	80 GPa / 10 GPa	70–90 GPa	85 GPa / 10 GPa	70–110 GPa
Poisson's ratio	0.27 / 0.05	0.18–0.33	0.26 / 0.03	0.19–0.31
Tensile strength	17 MPa / 4 MPa	12–24 MPa	20 MPa / 2 MPa	14–24 MPa
Moh-Coulomb, F	60° / 3°	57°–62°	55° / 6°	35°–60°
Mohr-Coulomb, c*	22 MPa / 3.2 MPa	14 –29 MPa	32.5 MPa / 5.4 MPa	20–42 MPa

* The UCS should not be used as input to the Mohr-Coulomb model.

The parameters are all described with truncated normal distribution functions. (This is different from version Simpevarp 1.1 where only a span was given.) The truncated distributions are used because there is a limit on how low and high we expect each parameter to possibly be, even in the extreme cases. The truncation values are not necessarily symmetrical with respect to the mean as they are selected not only based on the observed data but also on expert judgement. This is because the amount of data and the judged quality and representativeness of available data may differ (i.e. there is no particular relation between standard deviation and truncation levels).

The crack initiation stress is modelled as a function of the USC value, based on the data compilation showing clear correspondence. The crack initiation stress appears to to be close to 47% of the maximum stress at uniaxial failure.

The estimated assignment of mechanical properties for intact rock of different rock types in the area is provided in Table 6-5. The rock type mixtures in the rock domains are described in Section 5.3. Domain A is dominated by Ävrö granite and Domain B is dominated by fine-grained dioritoid.

6.3.2 Assignment of properties for the single fractures

The properties of the single fractures are described by the parameters: normal and shear stiffness, and by friction angle and cohesion of the common Coulomb slip model. Two different laboratory results show fairly similar results on friction angle and cohesion (Table 6-2). Because the accuracy and set-up for the SP stiffness measurements were considered better, it was judged that the model should simply be taken as the results from these tests, for all parameters and with rounded-off numbers. The number of tests is not high (N=28 in total, including different normal load levels) and it is therefore interesting to note that the spread in the results from the many more (N=147) tilt tests, is almost the same as in the results from the direct shear tests, thus supporting the model chosen. It is noted from the test results /Lanaro and Fredriksson, 2005/ that the friction angle and the cohesion are correlated and therefore the model for cohesion is chosen as a function of the friction angle. The values given for the friction angle and cohesion are applicable above a normal stress of 0.5 MPa, while this was the stress level above which the tests were performed. Below this stress level a connecting slip envelope starting from origo is suggested (see footnote to Table 6-6). The dilation was not part of the description for the current model version.

Table 6-6. Estimated rock mechanics properties for single fractures. The prediction is the same for all fractures, independent of rock domain or fracture set.

Parameter for single rock fractures	All Domains, All fracture sets	
	Truncated normal distribution Mean ; standard dev.	Min (trunc.) – Max (trunc.)
Normal stiffness, MPa/mm	100 ; 32	49–179
Shear stiffness, MPa/mm	29 ; 11	10–49
Peak friction angle, ϕ[1)]	32° ; 4°	24°–40°
Peak cohesion, c[1)], MPa	$c_{mean} = 2.35–0.058 \cdot \phi$; 0.25	$c_{min} = c_{mean} – 0.37$ MPa $c_{max} = c_{mean} + 0.69$ MPa

[1)] For normal stresses smaller than 0.5 MPa, a linear envelope should be assumed. This envelope should have zero cohesion and should equal the shear strength obtained from the properties in this table when the normal stress of 0.5 MPa is considered. A maximum friction angle of 70° should be adopted when higher values are obtained from the linear envelope for low normal stresses.

6.3.3 Conceptual models for rock mass characterisation

The actual behaviour of a rock mass under different loading conditions is very complicated. The rock mass is a composite of elements of many different kinds and scales (grains, micro fissures, joints, faults, infillings etc.) and the actual geometry of the different elements is not possible to describe in detail. A gross simplification of the rock mass and its behaviour is needed. For the current site-descriptive model the aim is to describe the rock mass in sufficient detail that a preliminary repository design and safety analysis of the investigated site is possible. Following the strategy report /Andersson et al. 2002a/, a few common parameters have been selected, although additional parameters and details may be needed for analysis performed as part of future design and safety assessment work.

The selected parameters for the rock mass are: deformation modulus, Poisson's ratio, tensile strength and three parameters associated with to the Mohr-Coulomb strength model, friction angle, cohesion and "uniaxial compressive strength" (UCS_m). Note in particular that the UCS_m parameter for rock mass is chosen such that it fits to a simplified linear model (Mohr-Coulomb) of the rock mass, and not to a real situation of zero confining stress. (This choice was made to make it easier for the user to select parameters for continuum modelling, that would give a realistic strength for higher stress levels.) Also note that these numbers do not provide any "standard description"; the values will be dependent on what stress levels that are chosen to fit the linear Mohr-Coulomb model. In our case, the stress range 10–30 MPa is chosen because it is considered relevant for most analyses for a conceived deep geological repository. Importantly, exactly the same definitions of parameters are being used for the version 1.2 site description of the Forsmark site, such that possibilities for comparison are facilitated.

Furthermore, predictions have been made of the empirical indices Q and RMR for the different lithological domains and interpreted deformation zones. These may be used for a preliminary judgement on the rock engineering conditions and for the estimation for reinforcement of underground excavations.

6.3.4 Empirical approach to rock mass mechanical properties

The use of two empirical systems enabled comparison of the outcome in terms of the estimated rock mechanics parameters. Figure 6-6 shows an example for lithological domain A concerning the deformation modulus (E_m) for the rock mass. The differences between E_m(RMR) and E_m(Q) are not large. This supported a decision that only results from one of the systems should be retained and used in the further compilation and presentation of results, i.e. there was no need to carry two alternative models forward, and consequently the values determined from RMR are the ones shown in the following results tables.

One empirical index value was calculated for each 5 meter section of a borehole, giving about 200 values in each borehole. The data were sorted depending on which lithological domain it belongs to, and the data associated with interpreted deformation zones were also sorted out into a separate group. The E_m(RMR) results are shown in the form of histograms in Figure 6-7. It can be seen that there is a fairly large spread in the data. Also, E_m in the minor deformation zones (SDZ) and in the deterministic deformation zones (DDZ) are clearly lower than the E_m of the rock mass between interpreted zones (COMP). The differences between the defined rock domains are minor. Based on this result it was decided to describe the local scale model area with separate sets of rock mechanics parameters for the “competent” rock (rock mass with natural background fracturing) the minor deformation zones and the deterministic zones, respectively.

Figure 6-7 (lower right) also shows the variation of the estimated deformation modulus (E_m) (using the empirical approach), between boreholes. Interesting to note here is that there is a difference between boreholes KAV01 and KLX02, which are both sunk in the lithological rock domain A (Ävrö granite). The reason for this is interpreted to be the fracture intensity being larger in borehole KAV01.

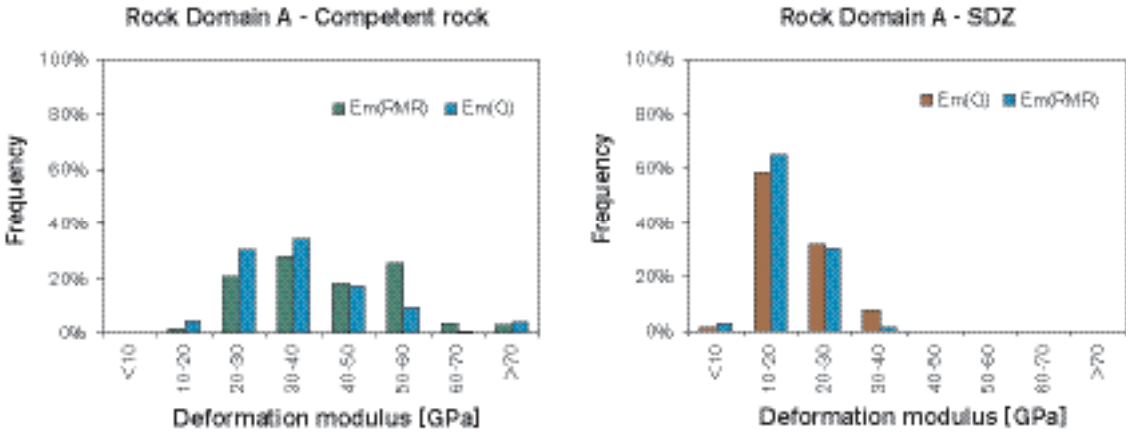

Figure 6-6. *Comparison of the deformation modulus (E_m) determined for lithological rock domain A (Ävrö granite), using two different empirical systems, Q /Barton, 2002/ and RMR /Serafim and Pereira, 1983/. The diagram to the right corresponds to the rock mass of the minor deformation zones (SDZ) inside lithological domain A.*

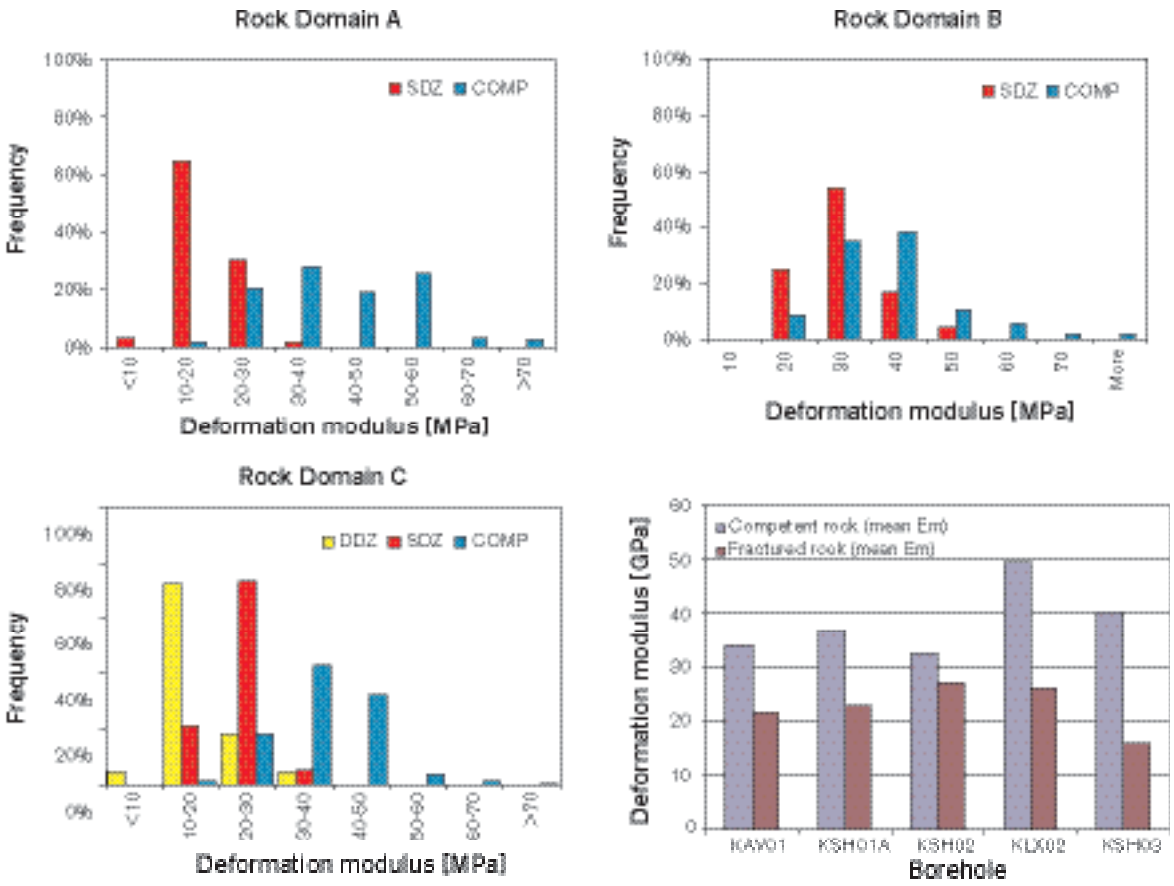

Figure 6-7. *The deformation modulus determined with the empirical approach for different lithological rock domains A, B and C, respectively in a) through c). Figure d) shows the mean values for the data sorted by boreholes and separate for the competent rock and deformation zones (based on the single hole interpretation).*

6.3.5 Theoretical approach to rock mass mechanical properties

The second approach used to estimate the mechanical property parameters for the rock mass was to calculate the composite behaviour based on knowledge about the intact rock and the fractures. This approach is denoted the “theoretical approach” and the methodology is outlined in /Olofsson and Fredriksson, 2005/.

The basic assumption here is that the developed geological DFN model may be used to simulate a fracture network that in turn may be used to create numerical models of the rock mass. A simulated fractured rock block is subsequently numerically loaded until it fails upon which the stresses and strains in the block are determined (cf. example in Figure 6-8 and Figure 6-9). Since the description of the fracture network is stochastic, a number of realisations of the geometry are generated and each model is subjected to a “loading test”. The compiled results for each simulated rock mass then provide a spread in results due to the inherent geometrical differences. So far, the numerical modelling, based on a preliminary DFN model, has not addressed the effect of varying fracture intensity or the situation with very low confining stress, but this will be considered in future work.

The intact rock properties and fracture properties have also been described as stochastic functions (cf. Section 6.3.2 and 6.3.3), and the effect on the deformations and strength due to these variations are also included in the theoretical approach. Furthermore, a sensitivity study has been performed to identify which parameters (apart from the intensity) have the largest influence on the results /cf. Fredriksson and Olofsson, 2005/. As an example, some of the results are given in Figure 6-10. The results show a slightly larger spread for the strength for the rock mass in domain B compared with domain A.

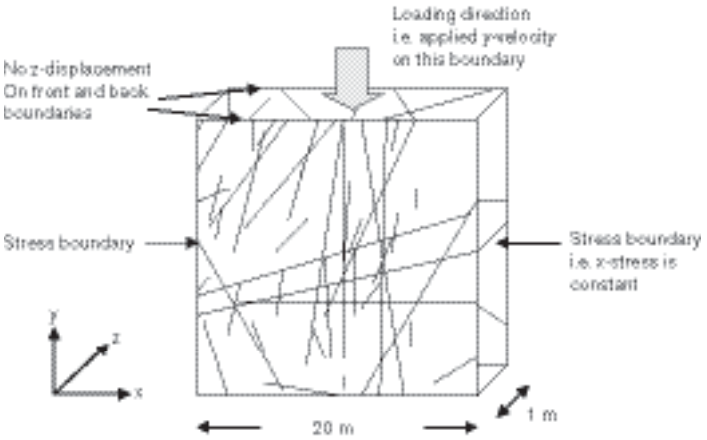

Figure 6-8. *Theoretical approach to estimation mechanical properties of the rock mass. The numerical model (3DEC) is a thin rock block with intersected by a number of fractures. The left and right boundaries of the loaded block were confined with a constant stress, and the block was compressed in the y-direction. The fracture network is built based on the DFN model and 20 different networks were analysed for /cf. Olofsson and Fredriksson, 2005/.*

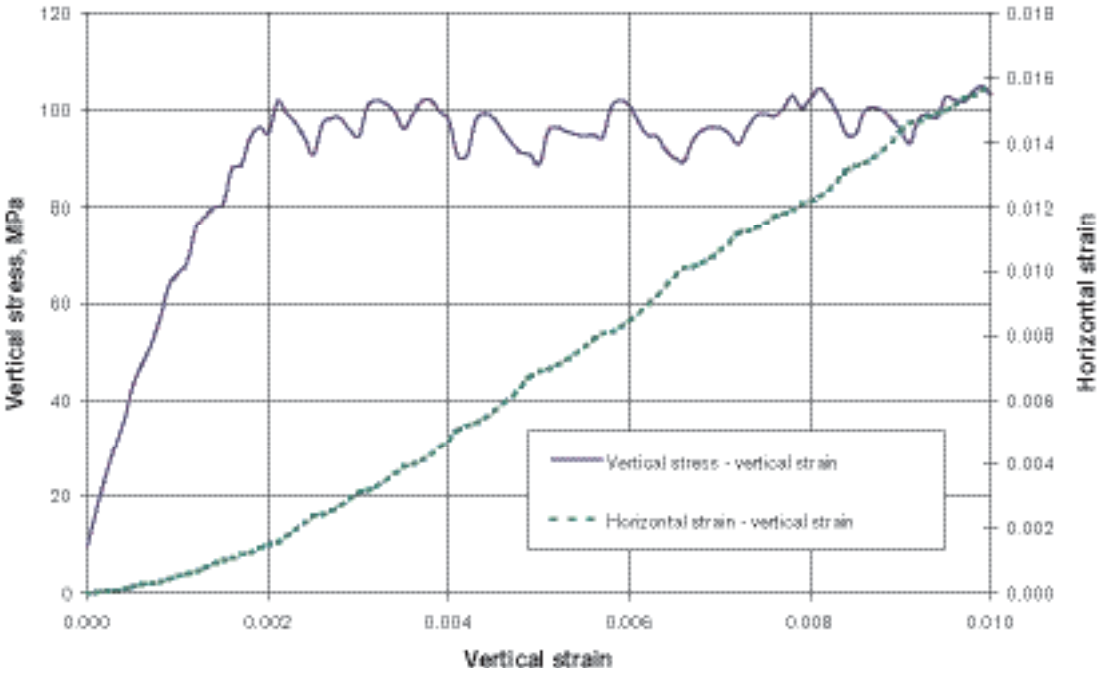

Figure 6-9. *When the rock mass block is compressed the fractures will first deform elastically and finally slip. Deformation modulus, Poisson's ratio and the compressive strength of the rock mass have been calculated from the stress strain curves resulting from the numerical loading tests described in Figure 6-8. The vertical stress is the mean axial stress along a section parallel to the 20 m side, going through the centre of the model.*

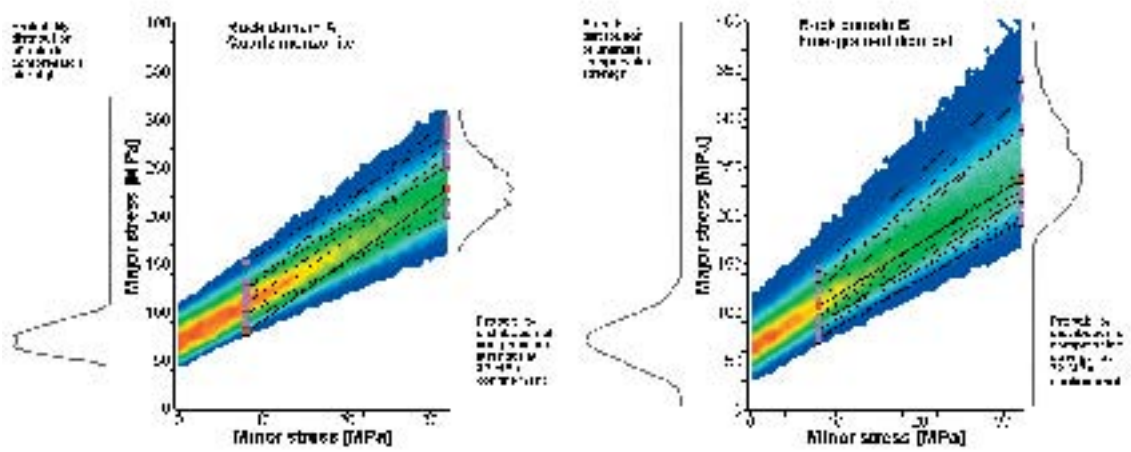

Figure 6-10. *Probability distributions of simulated triaxial test for rock mass of rock domains A (Ävrö granite) and B (fine-grained dioritoid), respectively. The x-axis is the confining stress and the y-axis shows the vertical stress in the model at failure. Pink boxes are results from 3DEC modelling using different DFN realisations at confining stress levels 8 MPa and 32 MPa, respectively /Fredriksson and Olofsson, 2005/.*

6.3.6 Assignment of rock mass mechanics properties in the model volume

Each of the two approaches provided separate individual predictions (estimates) for the selected characterisation parameters. These estimates are fully independent from one another, and are clearly different, since the empirical approach utilises the borehole mapping data and the theoretical approach uses the developed geological DFN model and subsequent numerical modelling. However, the intact rock data used as input were the same for both approaches.

To make the final assignment of properties to the local scale rock mass model, the results from both approaches have been considered. This has been done by making the following overall assumptions and steps:

- The empirical modelling provides only one value for deformation modulus and the Poisson's ratio, i.e. the empirical relation assumes no explicit stress dependence. It was assumed here that the E_m values were best estimates for the condition where the confining stresses are low, because it was believed that the empirical systems were built up based mostly on excavation cases from shallow depth. Therefore, the empirical results were assumed to correspond to a situation with minor principal stress (confining stress) of 1.5 MPa, roughly corresponding to 50 metres depth.
- The results from both approaches were plotted together and compared. Model values (assuming a truncated normal distribution function) were selected based on these results, giving a good visual fit to all the results. The model functions were selected such that the values were rounded off, not to give any false impression of certainty in the descriptive model. Symmetry in standard deviation and min-max truncation values was preferred, for reasons of simplicity.
- The spread due to the spatial variation was assumed contained in the standard deviation value and the min and max values, whereas the uncertainty was assumed to be covered by the uncertainty value estimated for the mean value. This uncertainty was selected based on the differences seen in the approaches, such that mean results for both approaches would "come out true", i.e. would fall within the uncertainty span. No weighting between the two approaches was consequently applied.
- In the cases where data were lacking (domains C and D), the actual numbers were selected based on the assumption that the behaviour should be similar to other geologically similar domains. In these cases, the uncertainty was taken to be higher, but selected by judgement.

The diagrams in Figure 6-11 through Figure 6-16 show the obtained results following the modelling steps above. In the diagrams the mean values are given with box symbols. The selected model is shown as solid red lines (cf. legends). As was expected, the values from the empirical approach are lower than those of the theoretical approach, but as discussed previously this is considered as being an effect of the difference in confining stress.

The choice of a bilinear model for the stress-dependent parameters, makes the results from the two approaches independent from each other (the empirical results govern the lower stress part and the theoretical results govern the high stress part), and it is therefore not possible to say directly if the approaches give coherent results or not. However, the results seem reasonable in that the empirical approach consistently yields lower values.

Also, the estimated model values for E_m compare well with the absolute magnitude and relative difference for E_m at the shallow Clab excavations, and at the deeper Äspö HRL, 40 and 55 GPa (Section 6.2.4), respectively. These values were obtained by the back-analysis approach. Another noteworthy result is that the spread in values is fairly similar. It may be that this is a coincidence, and that they in reality are not representing the same type of spread. However, it made the choice of standard deviation for the parameter model easier.

For the deformation modulus, it is noted that the predicted estimates are given as different values depending on the stress situation. The first value given in Table 6-7 is a constant value given for a fairly high level of confinement (minor principal stress), > 10 MPa. For the situation when the confining stress is estimated to be < 10 MPa, the predicted deformation should be calculated with the given function. This means that the prediction of the deformation modulus is a bilinear function of confining stress.

The parameters of the final models are summarised in Table 6-7.

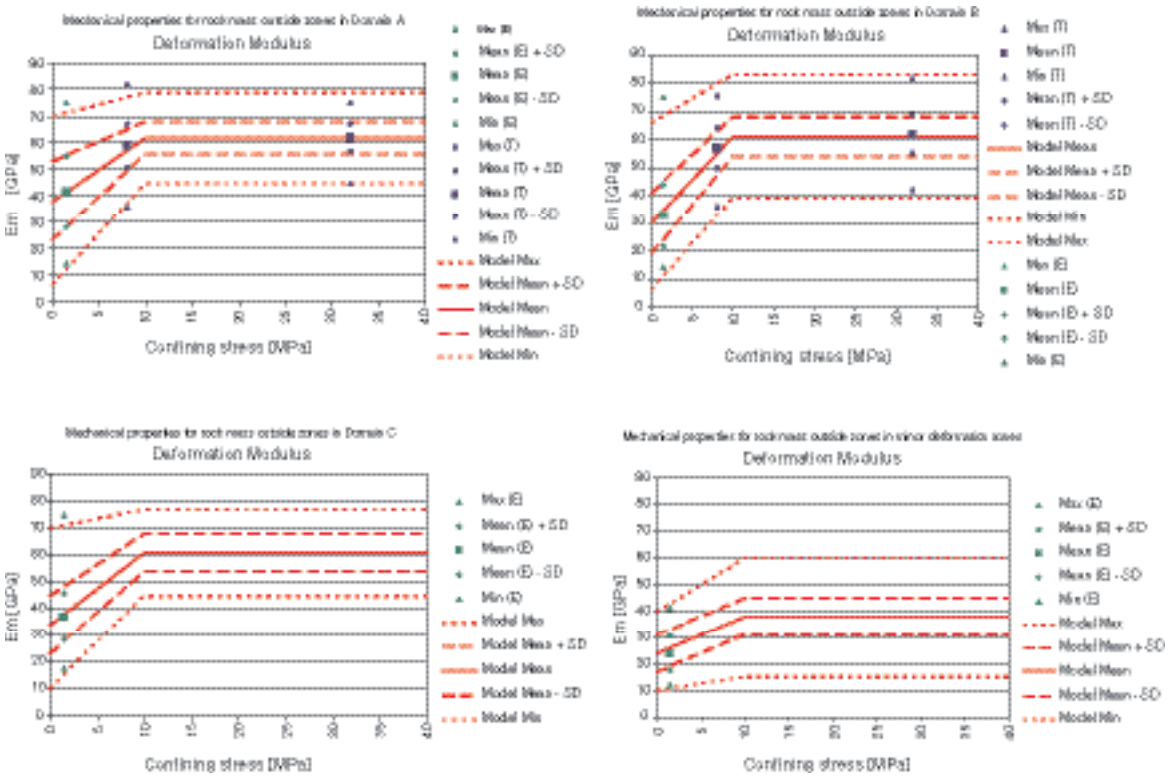

Figure 6-11. *Diagrams showing the results from empirical approach and theoretical approach for the deformation modulus in the lithological rock domains A, B, C, and for the rock corresponding to interpreted minor deformation zones.*

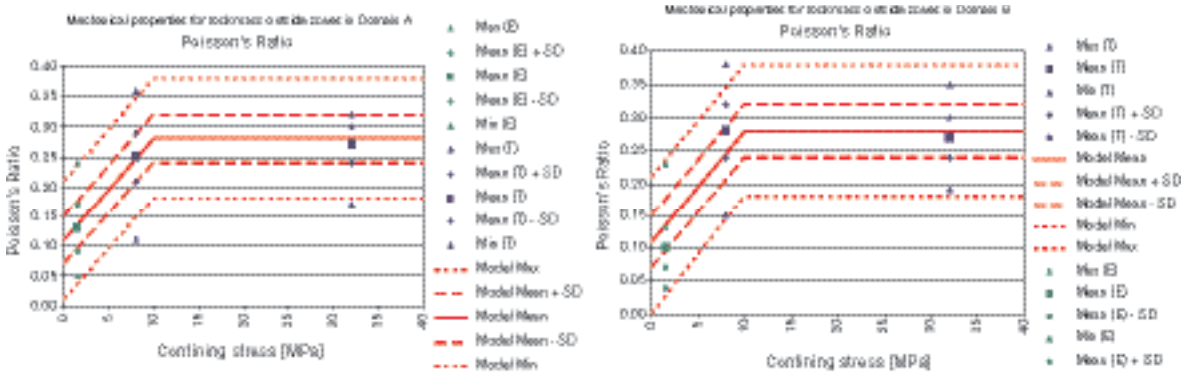

Figure 6-12. *Diagrams showing the results from empirical approach and theoretical approach for the Poisson's ratio in lithological domains A and B.*

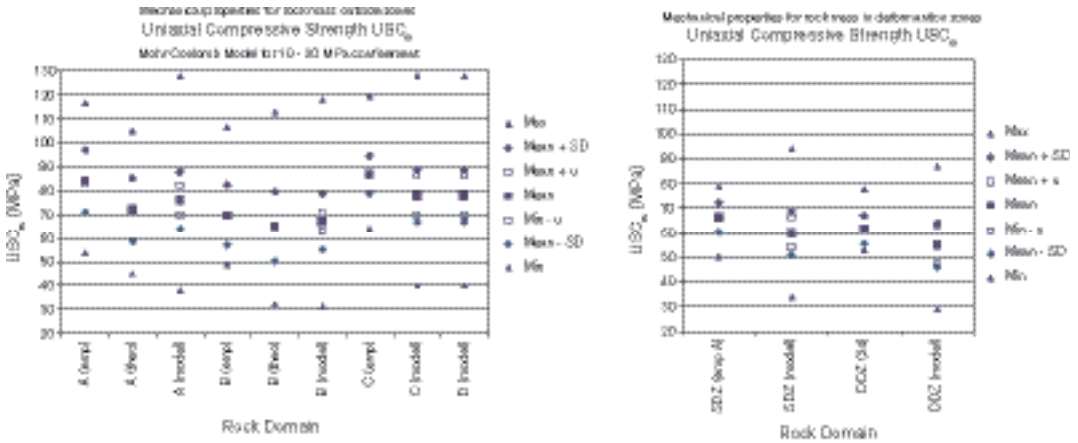

Figure 6-13. *Results from empirical and theoretical approach for the Uniaxial Compressive strength for the rock mass in (a) all domains and (b) in the deformation zones.*

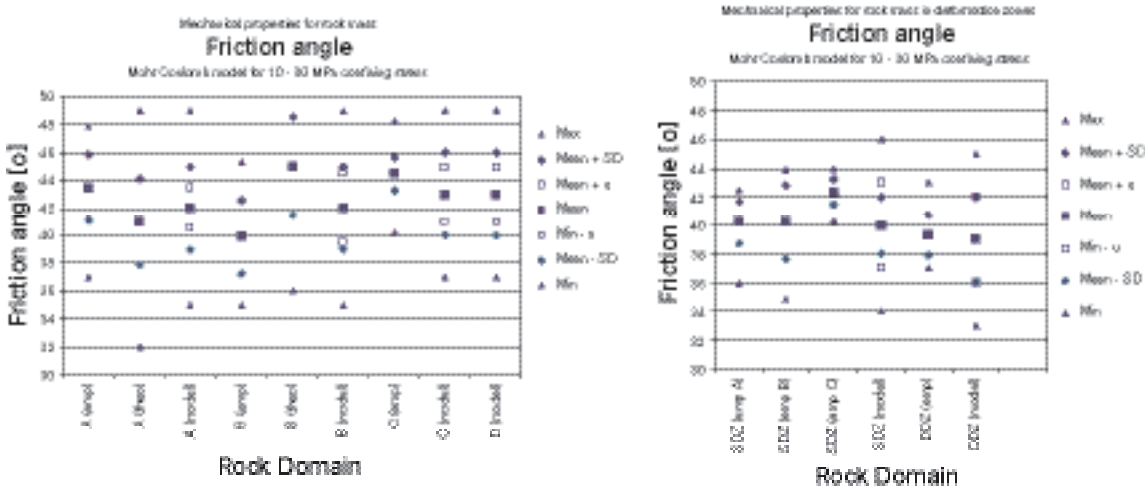

Figure 6-14. *Diagrams showing the results from empirical approach and theoretical approach for the rock mass friction angle in (a) all domains and (b) in the deformation zones.*

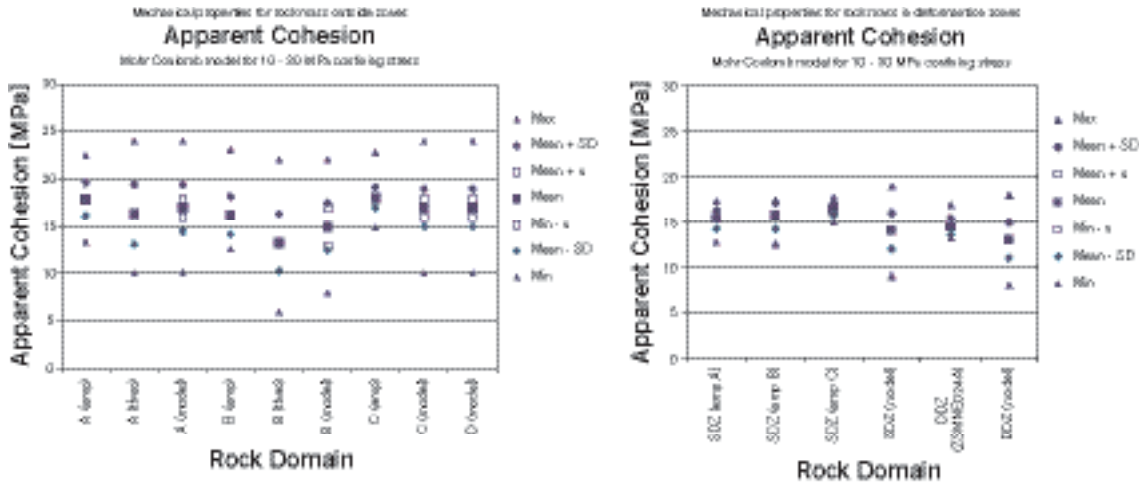

Figure 6-15. *Diagrams showing the results from empirical approach and theoretical approach for apparent cohesion of the rock mass in (a) all domains and (b) in the deformation zones.*

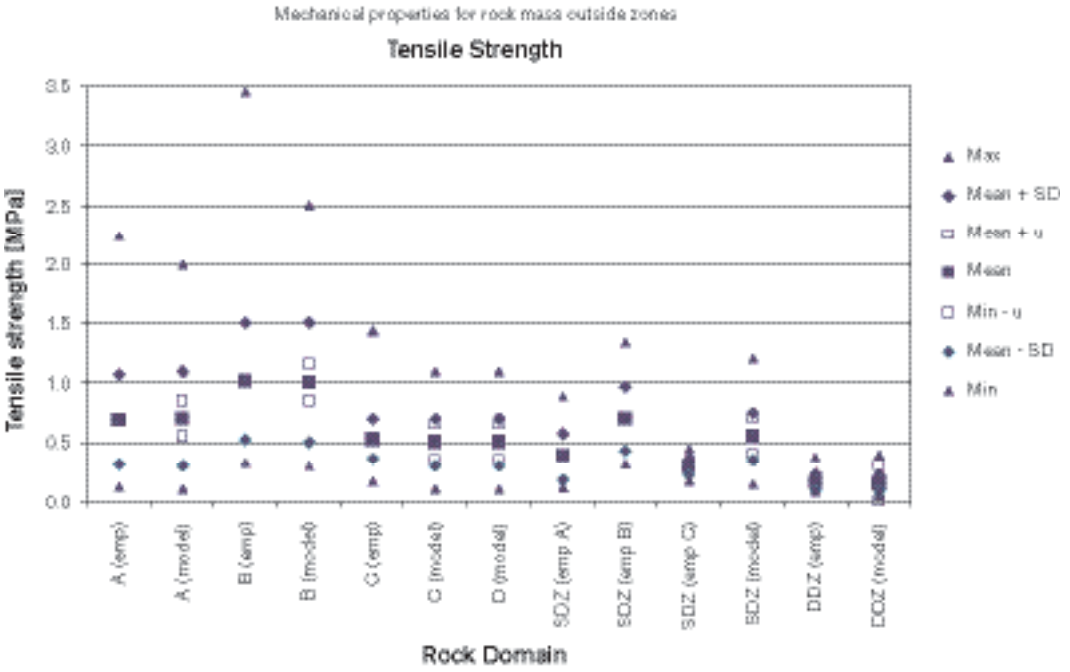

Figure 6-16. *Results from empirical approach to estimation of tensile strength in all rock domains and in the deformation zones. The selected model parameters are also shown.*

6.3.7 Evaluation of uncertainties

Table 6-7 includes a value to describe the uncertainty in the prediction (in italics). This value gives the expected possible difference between the given model mean and the real mean value of the actual distribution. The figure thus describes the certainty attributed to any given mean value of a parameter.

The shape of the normal distribution is assumed unchanged if the mean value is increased or decreased, i.e. the standard deviation should be the same, whereas the min and the max truncation values should be adjusted with an amount equal to the adjustment of the mean value.

The uncertainty value is selected such that it reflects the difference found between the empirical and the theoretical parameter estimation. Also, the uncertainty value has been compared with the uncertainty value given for the empirical prediction itself. The uncertainty is in most cases of the same order as the given empirical uncertainty /Lanaro, 2005a/.

Table 6-7. Simpevarp 1.2 – Estimated rock mechanics properties for the rock mass in lithological rock domains and in rock mass in interpreted deformation zones, respectively. For location and geometry of lithological domains, see Figure 5-43.

Parameter for the rock mass (30×30×30 m scale)	Rock Domain A (Ävrö granite) 'Competent' Mean; St.Dev. Min–Max truncation *Uncertainty in Mean*	Rock Domain B (Fine-grained dioritoid) 'Competent' Mean; St.Dev. Min–Max truncation *Uncertainty in Mean*	Rock Domain C and D 'Competent' Mean; St.Dev. Min–Max truncation *Uncertaintyinf Mean*	All Domains'Stochastic (minor) deformation zones' Mean; St.Dev. Min–Max truncation Uncertainty in Mean	All Deterministic deformation zones of the deformation zone model Mean; St.Dev. Min–Max truncation *Uncertainty in Mean*
Def Modulus s^3 > 10M Pa[2]	62 ; 6 45–79	61 ; 7 39–81	61 ; 7 39–81	38 ; 7 15–60	*26 ; 5* 10–60
s^3 < 10M Pa[2] [GPa]	E_{mean}= 38+2.4s^3; SD= 15–0.9s^3 E_{min}= 6+3.9s^3 – E_{max}= 70+0.9s^3	E_{mean}= 30+3.1s^3 SD= 11–0.4s^3 E_{min}= 6+3s^3 – E_{max}= 70 +1.1s^3	E_{mean}= 35+2.6s^3 SD= 11–0.4s^3 E_{min}= 6+3s^3 – E_{max}= 70 +1.1s^3	E_{mean}= 24+1.4s^3 SD= 7 E_{min}= 10*0.5s^3 – E_{max}= 40+2s^3	E_{mean}= 16+s^3 SD= 5 E_{min}= 5+0.5s^3 – E_{max}= 35+ 2.5s^3
	± *4*	± *4*	± *4*	± *6*	± *8*
Poisson's ratio s^3 > 10 MPa[2]	0.28 ; 0.04 0.18–0.38	0.28 ; 0.04 0.18–0.38	0.28 ; 0.04 0.18–0.38	0.28 ; 0.04 0.18–0.38	0.28 ; 0.04 0.18–0.38
s^3 < 10 MPa[2]	ν_{mean}= 0.11+0.017s^3 SD= 0.04 ν_{min}= ν_{mean} – 0.1 ν_{max}= ν_{mean} + 0.1	ν_{mean}= 0.11+0.017s^3 SD= 0.04 ν_{min}= ν_{mean} – 0.1 ν_{max}= ν_{mean} + 0.1	ν_{mean}= 0.11+0.017s^3; SD= 0.04 ν_{min}= ν_{mean} – 0.1 ν_{max}= ν_{mean} + 0.1	ν_{mean}= 0.06+0.017s^3; SD= 0.04 ν_{min}= 0 ν_{max}= ν_{mean} + 0.1	ν_{mean}= 0.04+0.017s^3; SD= 0.04 ν_{min}= 0 ν_{max}= ν_{mean} + 0.1
	± *0.02*	± *0.03*	± *0.03*	± *0.03*	± *0.03*
Uniaxial compressive strength[1) 3)] [MPa]	76 ; 12 38–128 ± *6*	67 ; 12 31–118 ± *4*	78 ; 11 40–128 ± *8*	60 ; 9 34–94 ± *6*	55 ; 9 29–87 ± *8*
Mohr-Coulomb, Friction angle, φ	42 ; 3 35–49	42 ; 3 35–49	43 ; 3 37–49	40 ; 2 34–46	39 ; 3 33–45
	± *1.5*	± *2.5*	± *2.0*	± *3.0*	± *3.0*
Mohr-Coulomb, Apparent cohesion, c'[4)] [MPa]	17 ; 2.5 10–24 ± *1*	15 ; 2.5 8–22 ± *2*	17 ; 2 10–24 ± *1*	14 ; 2 9–19 ± *3*	13 ; 2 8–18 ± *3*
Tensile strength [MPa]	0.7 ; 0.4 0.1–2.0 ± *0.15*	1.0 ; 0.5 0.1–2.0 ± *0.15*	0.5 ; 0.2 0.15–1.2 ± *0.15*	0.55 ; 0.2 0.15–1.2 ± *0.15*	0.15 ; 0.07 0.05–0.4 ± *0.15*

[1)] This parameter to the strength of a rock mass block assuming that a Mohr-Coulomb strength criterion is applied. The M-C model is fitted to confining stress levels 10–30 MPa.

[2)] Note that the model is a bilinear function. The first given constant values are expected for confining stress (s^3) of 10 MPa or higher. The second group of values should be used for lower stress levels.

[3)] Uniaxial strength, friction angle and apparent cohesion are correlated parameters and should be selected to fit each other in each case. If other material model is used the cohesion should be adjusted to the choice of model.

Apart from the predicted values from each approach (see Figure 6-11 through Figure 6-16), it was also considered what the results from the theoretical method would have been, given that the observation for Domains A and B would be general for the behaviour in all domains. For rock domain C (Ävrö granite + Quartz monzodiorite) the underlying data are less, and for domain D (Quartz monzodiorite) no data were available, and, therefore, the uncertainty values are taken to be larger. The uncertainties are given as absolute values in the same unit as the mean value.

The main uncertainty factor for the theoretical approach is the uncertainty in the input data, such as the fracture intensity and the fracture properties. These uncertainties are discussed, mainly in qualitative terms, by /Olofsson and Fredriksson, 2005/ and /Fredriksson and Olofsson, 2005/.

6.4 State of stress

6.4.1 Modelling assumptions and input from other disciplines

The stress modelling is mainly based on the stress measurement data presented in Section 6.2.5. As the measurement data show a large spread, the issue of finding a geological explanation for this condition is desirable. Following the developed methodology, the most probable explanation for the noted variation was expected to be associated with the existing structures (i.e. the modelled deformation zones). The deformation zone model, presented in Section 5.4, includes both the interpreted geometry and a description of the properties of the interpreted major zones.

6.4.2 Conceptual model with potential alternatives

It was recognised that the essentially northeast trending deformation zones on either side of the Simpevarp peninsula-Hålö-Ävrö (zones ZSMNE012A and ZSMNE024A) could form a wedge-shaped body of rock that could represent a different stress regime from that experienced further to the west. When the measured stress data are sorted into two different groups representing these assumed geographical domains (cf. Figure 6-3) it is noted that the spread within each group is significantly less than the overall spread of the two groups merged together. This fact provides some support for the hypothesis and the assumption was consequently made that the measurement data as such, although being associated with some uncertainty, are sufficiently reliable to make the conjecture that the stress state is dissimilar between the two suggested stress domains.

An alternative stress model would be that the stresses are locally very much more variable and that the variation is unrelated to the existing deformation zones. This alternative model is by far the simplest and was also employed for the version Simpevarp 1.1 model, when data were very scarce. Yet another alternative could be that there indeed are structurally controlled stress domains, but that the positions and geometry of these important structures are different from the ones indicated above. If the model of deterministic deformation zones changes in later versions of the site-descriptive model, this latter alternative should be considered.

6.4.3 Modelling of stress distribution

To evaluate the hypothesis of a structure-controlled explanation for the noted stress variation in the local scale model area, a numerical model study was performed. The underlying approach is further described in the strategy report /Hakami et al. 2002/ and the details of this modelling is presented by /Hakami and Min, 2005/. The modelled three-dimensional mechanical block model includes the major interpreted deformation zones in the area, cf. Section 5.4. The zones are for the purpose of the present analysis simplified geometrically, whereby deformation zones are simulated as planes, as shown in Figure 6-17 and Figure 6-18 (compare with Figure 5-54).

When a stress field is applied to the model, the orientation of the modelled zones in combination with the strength properties given, induce displacements and some of the zones reach slip failure. Due to this process, the stresses in the model are, at equilibrium, distributed in a way that is regarded as a model of the present stress distribution in the Simpevarp area, resulting from tectonic compression in the direction (NW-SE), assumed prevailing during the latest evolutionary period as described in Chapter 3 (cf. Table 3-2).

From the modelling results, it can be seen that, as expected, the wedge-shaped rock mass surrounded with weak structures is not able to sustain high horizontal stresses, the stress will become lower inside the wedge and higher in areas outside (as illustrated in Figure 6-19). The results support the notion of describing the stress state in the area as being made up of two different stress domains.

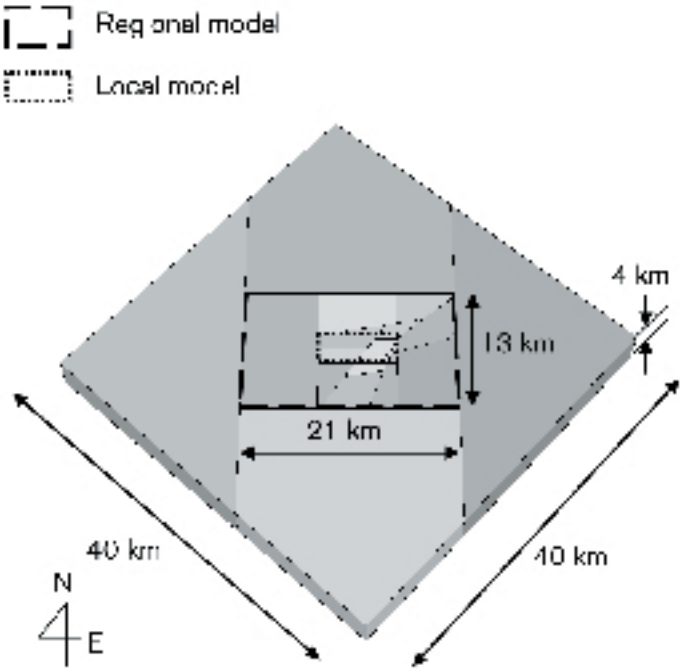

Figure 6-17. *Perspective view of the 3D numerical model (3DEC) with the embedded representation of the regional scale model area (21×13) and the rectangular local model area in the centre, cf. Figure 6-18. The numerical modelling explores the stress distribution inside the local model area only. The largest deformation zones extend to the boundaries of the regional model area (cf. Figure 6-18).*

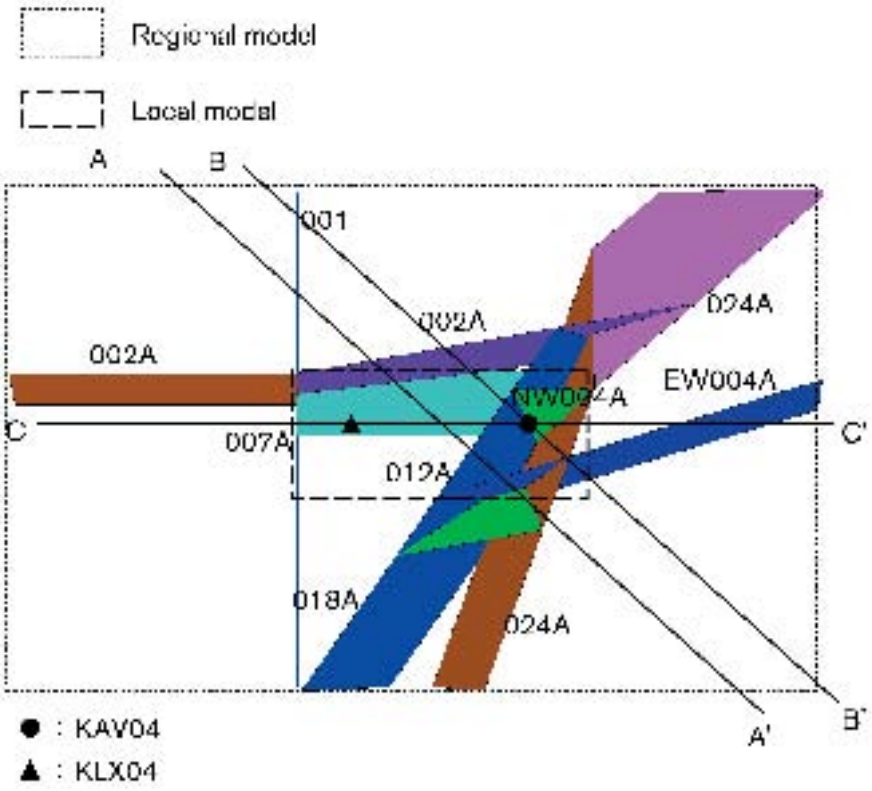

Figure 6-18. *Top view of the deformation zones interpreted for the regional model area, as included in the 3D numerical model. Each zone, including label, is a simplified representation of the zones included in the geological model, cf. Figure 5-54, and consists of one or two planar fractures in the model. The locations of sections (A-A', B-B', C-C') used for presenting the modelling results are indicated. The locations of two boreholes where stress measurements have been performed are also marked /Hakami and Min, 2005/.*

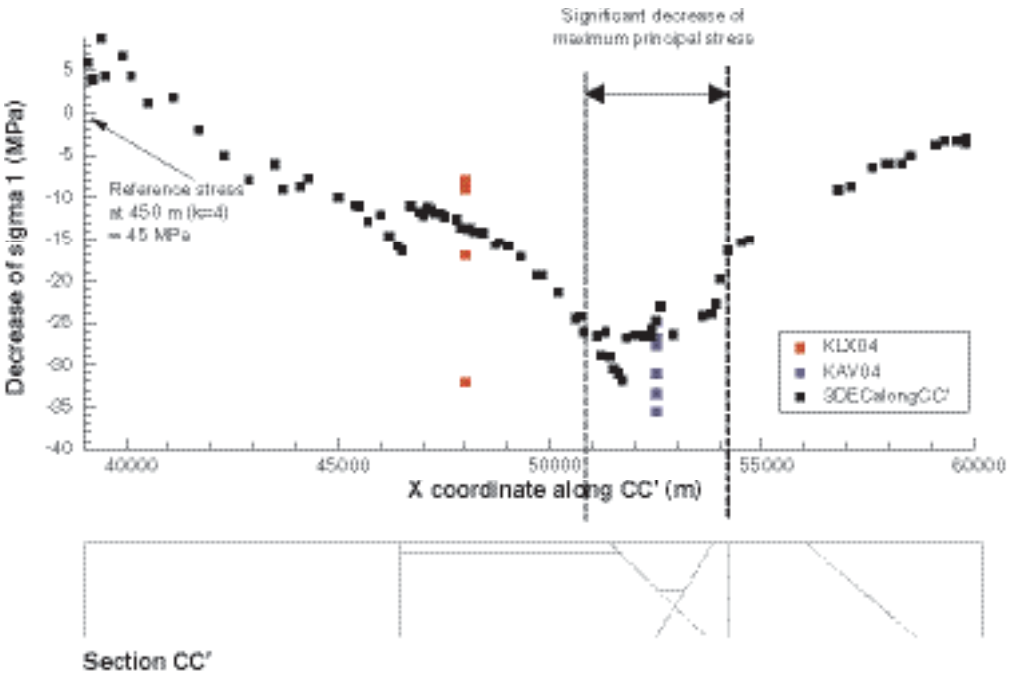

Figure 6-19. *Modelled major principal stress magnitudes along section C-C' (cf. Figure 6-18). The section is parallel to the direction of major principal stress.*

6.4.4 Resulting stress model

In Table 6-8 through Table 6-11, the stress estimations are presented for the two defined stress domains included in the local scale model area. The locations of the two stress domains are explained in Figure 6-20. In this figure, the deformation zones of version Simpevarp 1.2 are shown, and the defined stress domains are related to two of the major zones in this model oriented northeast as explained in Section 6.4.3.

Note that division into two stress domains is based on available information up till now, which includes overcoring in one borehole in the Laxemar subarea (in the domain with assumed higher stress). This model may be changed at later stages of the site investigation (later model versions) as new measurement data will become available.

The mean principal stress magnitudes are estimated to be within a span and the magnitudes are furthermore assumed to increase with depth. The model is intended to describe the stress state between 100 and 1,100 m depth. The mean stress values as given are the expected mean stress values in a rock volume of 30×30×30 m size. The uncertainty is described as a ± percentage span of the mean value.

Table 6-8. Model of in situ stress magnitudes in the Simpevarp 1.2 stress domain I.

Parameter	σ1	σ2	σ3
Mean stress magnitude, z = depth below ground surface	0.058·z+3 MPa	0.028·z MPa	0.019·z MPa
Uncertainty, 100–1,100 m	± 30%	± 30%	± 30%
Spatial variation in rock domains	± 15%	± 15%	± 15%
Spatial variation in or close to deformation zones	± 50%	± 50%	± 50%

Table 6-9. Predicted in situ stress orientations in the Simpevarp 1.2 stress domain I.

Parameter	σ1, trend	σ1, dip	σ2, trend	σ2, dip	σ3, trend	σ3, dip
Mean stress orientation	132°	0°	90°**	90°	42°	0°
Uncertainty	± 15°	± 10°	± 90°	± 15–45°*	± 15°	± 15–45°*
Spatial variation, rock domains	± 15°	± 15°	± 15°	± 15°	± 15°	± 15°
Spatial variation inside or close to deformation zones	± 25°	± 30°	± 25°	± 30°	± 25°	± 30°

* At some level σ2 and σ3 may have similar magnitude and the dip can then be any. The tree principal stresses are in each point oriented perpendicular to each other.

** Since the direction is expected to be subvertical, i.e. the dip 90, the trend of the tensor may therfore be any.

Table 6-10. Model of in situ stress magnitudes in the Simpevarp 1.2 stress domain II.

Parameter	σ1	σ2	σ3
Mean stress magnitude, z = depth below ground surface	0.032·z MPa	0.018·z MPa	0.011·z MPa
Uncertainty, 100–1,100 m	40%	40%	40%
Spatial variation in rock domains	15%	15%	15%
Spatial variation in or close to deformation zones	50%	50%	50%

Table 6-11. Predicted in situ stress orientations in the Simpevarp 1.2 stress domain II.

Parameter	σ1, trend	σ1, dip	σ2, trend	σ2, dip	σ3, trend	σ3, dip
Mean stress orientation	132°	0°	90°	90°	42°	0°
Uncertainty	± 20°	± 20°	± 90°**	± 15–45°*	± 20°	± 15–45°*
Spatial variation, rock domains	± 15°	± 15°	± 15°	± 15°	± 15°	± 15°
Spatial variation inside or close to deformation zones	± 25°	± 30°	± 25°	± 30°	± 25°	± 30°

* At some level σ2 and σ3 may have similar magnitude and the dip can then be any. The three principal stresses are in each point oriented perpendicular to each other.

** Since the direction is expected to be subvertical, i.e. the dip 90, the trend of the tensor may therfore be any.

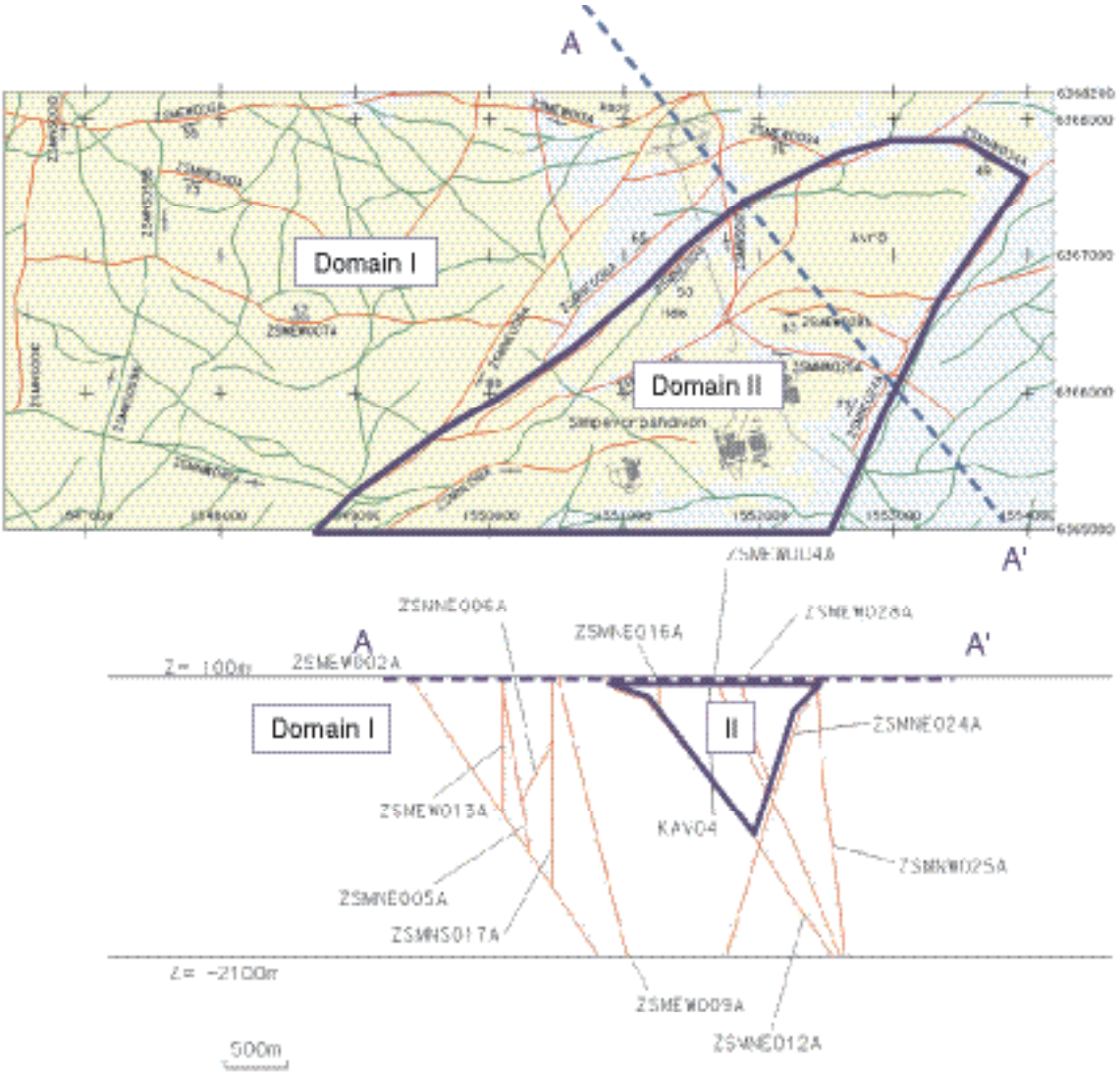

Figure 6-20. *Stress domain I is located NW of zone ZSMNE012A (dipping SE) and SW of zone ZSMNW024A (dipping NW). Domain II is located in the wedge-shaped domain between the zones, located below the Simpevarp peninsula, Hålö and Ävrö islands.*

6.4.5 Evaluation of uncertainties

The reasons for uncertainty in the stress model are several. Firstly, the accuracy of the measurements themselves is limited. The overcoring method is dependent on accuracy in biaxial tests for the interpretation of magnitudes and the hydrofracturing method is dependent on the sometimes ambiguous interpretation of pressure build-up curves. Secondly, the amount of data is not large, from a statistical viewpoint, and the fitted linear stress model functions have an uncertainty due to this. Thirdly, the assumptions made regarding the stress domains and the need to extrapolate the available measurement results over large areas also contribute to the uncertainty. The value selected for the total uncertainty thus includes different components and is selected based on a judgement for each. The selected spans are shown graphically in Figure 6-3 and Figure 6-4 and it can be seen that most of the observed data are enclosed in the model uncertainty span.

The spatial variation, is described with another percentage span around the mean value prevailing, here implied as the local variation at a smaller scale (from data point to data point, < $1m^3$ scale) at the same depth. Inside the rock mass (including naturally occurring fractures), but outside the major deformation zones the spatial variation of the stress is expected be less than in the immediate vicinity of deformation zones.

7 Bedrock thermal model

The bedrock thermal model describes thermal properties at a domain level, which is of importance since the thermal properties of the rock mass affects the possible distance, both between canisters and deposition tunnels, and therefore puts requirements on the necessary repository volume. Of main interest is the thermal conductivity, since it directly influences the design of a repository. Measurements of thermal properties are performed at the cm scale, but values are required at the canister scale, where due consideration of the spatial variability is required. Therefore, the thermal modelling includes elements of upscaling of thermal properties from measurements on specific rock types to the lithological domain level, described in more detail in a supporting document for the thermal model version Simpevarp 1.2 /Sundberg et al. 2005b/. The work has been performed according to a strategy presented in /Sundberg, 2003a/.

7.1 State of knowledge at previous model version

The only thermal conductivities available in Simpevarp version 1.1 were values estimated from mineral composition, no laboratory measurements were available. The upscaling from calculated values at cm scale to domain scale (1×11 m) was performed based on the simplified assumption that the variance reduction of small scale variations, when going from cm scale to domain scale, is equitable to the variance contribution resulting from the fact that a domain consists of several different rock types. Therefore the cm scale was used for modelling of the domain scale. Thermal conductivity properties were reported separately for each lithological domain and seemed to be fairly low, 2.7 W/(m·K) or lower. No distinction was made between different domains for specific heat capacity and thermal expansion coefficient. The specific heat was given the range 2.0–2.3 MJ/(m³·K) and the thermal expansion coefficient the range 6.0–8.0×10^{-6} m/(m·°C). The in situ temperature of the Simpevarp subarea was determined to be 15.5–16°C at a depth of 600 m.

In model version Simpevarp 1.1 the thermal properties at the regional scale were assumed to be identical with those of the local scale model.

The main uncertainties of the thermal model in version Simpevarp 1.1 concerned modelling, from mineral composition, thermal properties on domain level and upscaling from core samples to rock domains.

7.2 Evaluation of primary data

Table 2-3 presents data on thermal properties used in the Simpevarp 1.2 modelling of thermal properties.

7.2.1 Thermal conductivity from measurements

Laboratory measurements of the thermal conductivity on rock samples have been performed with the Transient Plane Source method (TPS), see description in /Sundberg, 2003a/. The measurements are made on a defined rock volume (approximately 10 cm³) determined by the size of the sensor. The variability in the data is relatively large, due to the small measurement scale. Results from the laboratory measurements are presented in Table 7-1. Observe that samples from rock type Ävrö granite (501044) are gathered from both the Simpevarp subarea /Adl-Zarrabi, 2004a,b,c/ and the Äspö HRL /Sundberg and Gabrielsson, 1999; Sundberg, 2002; Sundberg et al. 2005a/. Samples from rock type Fine-grained dioritoid (501030) and Quartz monzodiorite (501036) all comes from the Simpevarp subarea /Adl-Zarrabi, 2004a,b,c/. Some of the samples are spatially located closed to each other with approximately 2–5 samples in each group. For illustration, see /Sundberg et al. 2005b/. The temperature dependence is small with a decrease in thermal conductivity of 1.1–3.4% per 100°C increase in temperature for the investigated rock types.

Table 7-1. Measured thermal conductivity (W/(m·K)) of samples using the TPS method. Samples are from boreholes KAV01, KSH01A, and KSH02 (Simpevarp) together with borehole KA2599G01 (Äspö HRL) and boreholes from the prototype repository tunnel (Äspö HRL).

Rock name	Rock type	Sample location	Mean	St. dev.	Number of samples
Fine-grained dioritoid	501030	(borehole KSH01A and KSH02)	2.79	0.16	26
Quartz monzodiorite	501036	(borehole KSH01A)	2.83	0.07	10
Ävrö granite	501044	(borehole KAV01, KA2599G01, Äspö HRL prototype tunnel)	2.73	0.35	37

7.2.2 Thermal conductivity from mineral composition

The thermal conductivity of rock samples can be calculated with the SCA method (Self Consistent Approximation) using mineral compositions from modal analyses and reference values of the thermal conductivity of different minerals /Sundberg, 1988, 2003a/. The calculations are performed in mm scale and values have earlier been shown to be in good agreement with measured values /Sundberg, 1988, 2002/.

The following data were used for calculations with the SCA method:

- Modal analyses from the Sicada database performed in conjunction with Simpevarp version 1.1, reclassified rock types (62 samples).
- Modal analyses made in conjunction with measurements of thermal properties on samples from boreholes KAV01, KSH01A, and KSH02 (6 samples).
- Modal analyses on samples from boreholes KLX01 and KLX02 (39 samples).

The results of the SCA calculations are presented in Table 7-2, subdivided according to rock type. Samples from the Simpevarp subarea show a certain degree of alteration which results in an increase in the thermal conductivity. The variability at the SCA scale is probably overestimated compared with the canister scale.

Table 7-2. Thermal conductivity (W/(m·K)) of samples from different rock types, calculated from the mineralogical compositions (SCA method).

Rock name	Rock type	Mean	St. dev.	Number of samples
Fine-grained dioritoid	501030	2.43	0.33	31
Quartz monzodiorite	501036	2.46	0.27	11
Ävrö granite	501044	2.72	0.33	39
Fine-grained diorite-gabbro	505102	2.57	0.23	10
Diorite/gabbro	501033	2.46	0.21	6
Fine-grained granite	511058	3.26	0.35	8
Granite	501058	2.59	0.65	2

7.2.3 Thermal conductivity from density

The relationship between rock density and thermal conductivity for Ävrö granite (501044) as reported by /Sundberg, 2003b/ (Equation 7-1 in Figure 7-1) has been further developed using new measurements on thermal properties (Equation 7-2 in Figure 7-1). It is assumed that the developed relationship is valid within the density interval 2,600–2,850 kg/m³, which corresponds to the thermal conductivity interval 1.90–3.69 W/(m·K), that is slightly outside the data interval. Figure 7-2 illustrates the relationship applied to the density logging of borehole KAV01.

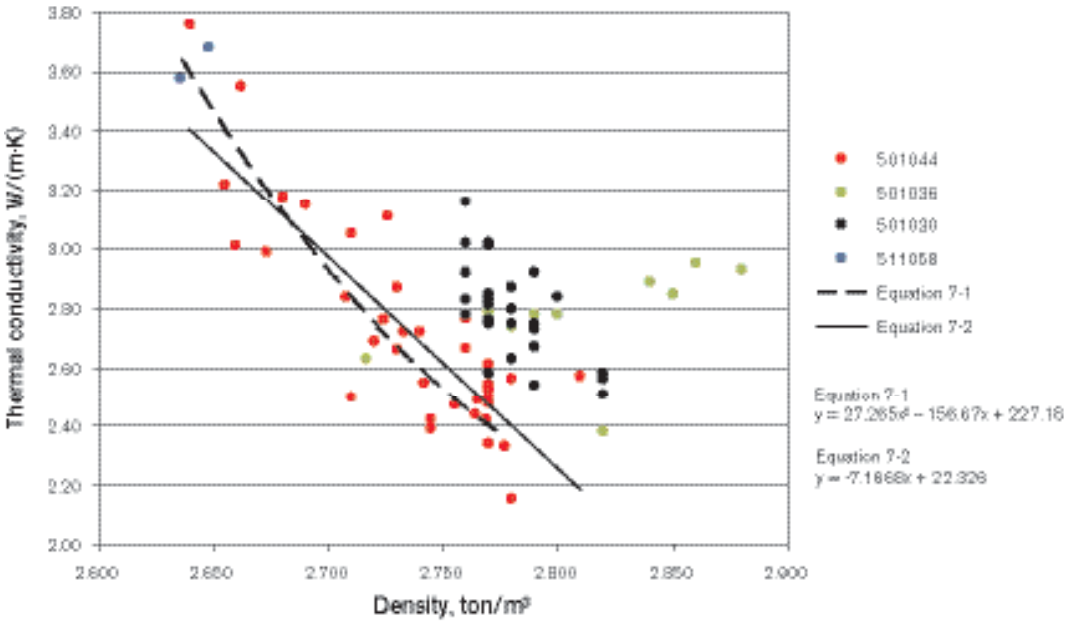

Figure 7-1. *Relationships between density and thermal conductivity. Equation 7-1 is the relationship from /Sundberg, 2003b/ derived by polynomial regression and equation 7-2 is the improved relationship based on a linear regression which is used for Simpevarp 1.2. The validity of both relationships is limited to rock type Ävrö granite (501044) and data from the other rock types are not used in the regression. A key to the rock type codes is presented in Table 7-2.*

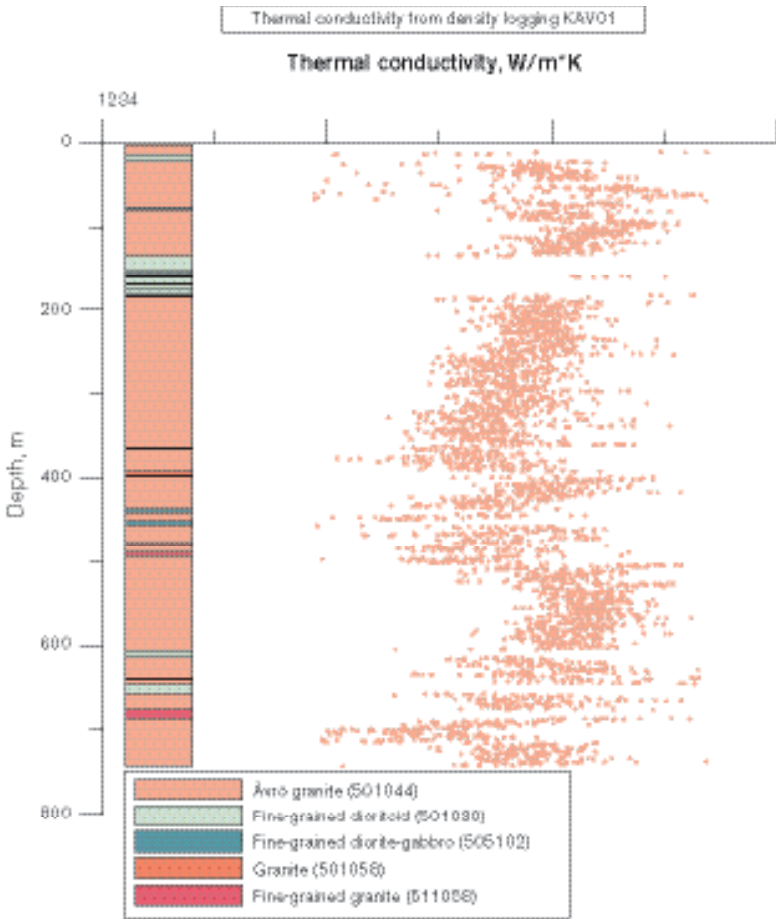

Figure 7-2. *Thermal conductivity of Ävrö granite in KAV01 estimated from density logging alongside a generalised geological borehole log.*

In order to evaluate how well the model in Equation 7-2 (cf. Figure 7-1) reflects the actual thermal conductivity in the borehole, a comparison between measured samples (TPS) and estimated values from density logging was performed /Sundberg et al. 2005b/. The comparisons indicate a fairly large uncertainty in the method, but it is noted that the comparison is based on a small number of samples, only reflecting a small interval of the borehole.

7.2.4 Modelling of thermal conductivity (rock type)

There are different data sets of thermal conductivity for the dominating rock types. The most reliable data comes from TPS measurements, but these samples are probably not representative of the rock type due to limited number of samples and the sample selection, see also discussion in Section 7.3.4. Therefore, also SCA calculations from the mineral distribution have to be included in the rock type model, since they have a larger spatial distribution in the rock mass.

In Table 7-3, thermal conductivity values calculated using the SCA method are compared with measured values of the same sample (not always the identical sample although closely located). For the Fine-grained dioritoid and Quartz monzodiorite, a total of only six samples were available for comparison. To be able to compare values for the Ävrö granite, measurements from the Äspö HRL were used. Table 7-3 indicates a potential bias in the SCA calculations for some rock types (deviations between measurements and calculations).

Rock type models have been developed for the different rock types, see Table 7-4. To eliminate or reduce the effect of a potential bias in the SCA calculations, a correction of the SCA values was done, based on the data in Table 7-3. SCA determinations of rock type Fine-grained dioritoid (501030) are corrected with a multiplicative factor of 1.10 and Ävrö granite (501044) with a factor of 1.04. Distributions of different data sets and the rock type model for Ävrö granite (501044) are specified in Figure 7-3. For other rock types, see illustrations in /Sundberg et al. 2005b/.

The rock type models are used to model thermal properties for domains, see Section 7.3. Density loggings have not been used for the rock type models, but are applied in the domain modelling in order to include spatial variability. All rock types are assumed to be characterised by normal (gaussian) PDF:s, as indicated by the data /Sundberg et al. 2005b/.

Table 7-3. Comparison of thermal conductivity for samples with different rock types calculated from mineralogical compositions with the SCA method and measured with the TPS method.

Method	Fine-grained dioritoid 5 samples Mean λ (W/(m·K))	Quartz monzodiorite 1 sample Mean λ (W/(m·K))	Ävrö granite 18 samples Mean λ (W/(m·K))
Calculated (SCA)	2.56	2.78	2.57
Measured (TPS)	2.85	2.79	2.68
Diff. (SCA-TPS)/TPS	–10.1%	0.4%	–4.1%

Table 7-4. Model properties of thermal conductivity (W/(m·K)) from different methods and combinations divided by rock type. All rock type models are based on normal (Gaussian) distributions (PDF:s).

Rock name (rock type)	Samples	Mean	St. dev.	Number of samples	Comment
Ävrö granite (501044)	Therm. cond. from density logging	2.96	0.36	13037	The st. dev. of therm. cond. from density logging is partly a consequence of the restricted interval for the density vs. thermal conductivity relationship. Potential bias in density data, see Section 7.3.4.
	TPS	2.74	0.35	37	
	SCA	2.72	0.33	39	
	Rock type model: 1.04*SCA+TPS	**2.79**	**0.35**	**76**	
Quartz monzodiorite (501036)	TPS	2.83	0.07	10	
	SCA	2.44	0.26	12	
	Rock type model: SCA+TPS	**2.62**	**0.28**	**22**	
Fine-grained dioritoid (501030)	TPS	2.79	0.16	26	
	SCA	2.40	0.35	26	
	Rock type model: 1.1*SCA+TPS	**2.72**	**0.30**	**52**	
Fine-grained granite (511058)	TPS	3.63	0.07	2	
	SCA	3.26	0.35	8	
	Rock type model: SCA+TPS	**3.33**	**0.34**	**10**	
Fine-grained diorite-gabbro (505102)	Rock type model: SCA	**2.57**	**0.23**	**10**	
Diorite/gabbro (501033)	Rock type model: SCA	**2.46**	**0.21**	**6**	
Granite (501058)	Rock type model: SCA	**2.59**	**0.65**	**2**	

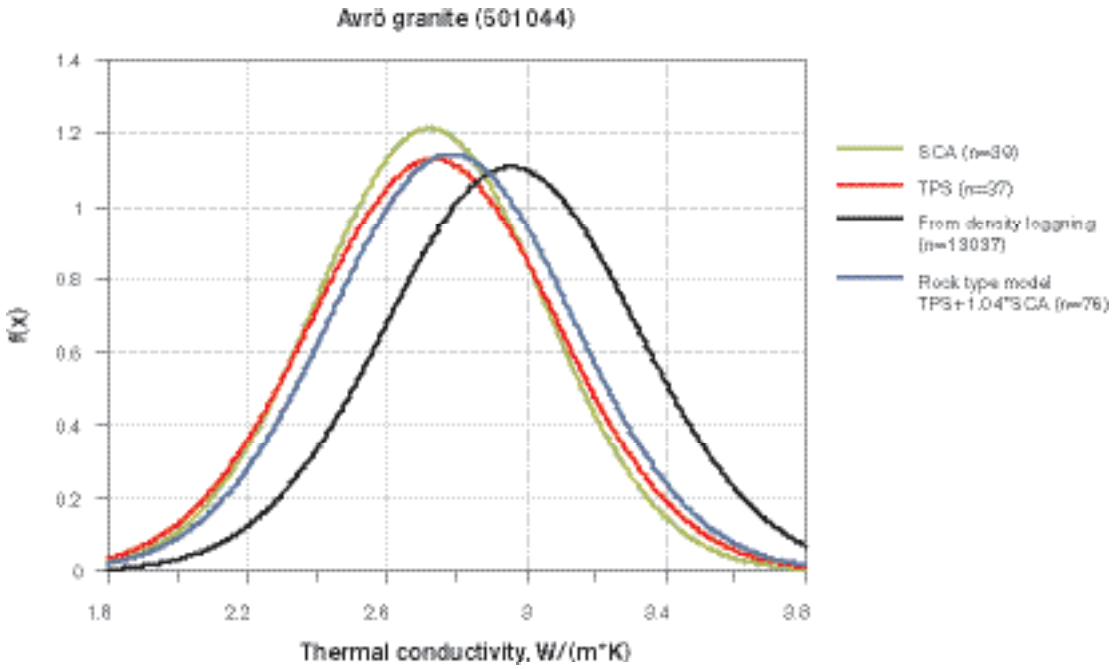

Figure 7-3. *PDF:s for calculated values (SCA), measured values (TPS), density logging for rock type Ävrö granite (501044) and a summarising rock type model where SCA values are corrected with a factor of 1.04. Data from the density loggings result in a higher mean value than TPS and SCA data, see also Section 7.3.4.*

7.2.5 Heat capacity

No direct laboratory measurements of the heat capacity have been carried out, but the heat capacity has been calculated from conductivity and diffusivity measurements performed with the TPS method. Results are presented in Table 7-5. Determination of heat capacity has been performed on the same samples as used for measurement of thermal conductivity, cf. Section 7.2.1. Therefore, the same problem concerning representativeness of the rock mass exists. There are no other sources for heat capacity values and therefore rock type models are based on the data in Table 7-5 /Sundberg et al. 2005b/. Heat capacity exhibits a large temperature dependence which is shown in Table 7-6.

Table 7-5. Determined heat capacity (MJ/(m³·K)) of samples from different rock types, using the TPS method. Samples are from boreholes KAV01, KSH01A, and KSH02 (Simpevarp subarea) together with borehole KA2599G01 (Äspö HRL) and boreholes from the prototype repository tunnel (Äspö HRL).

Rock name (sample location)	Mean	St. dev.	Number of samples
Fine-grained dioritoid (borehole KSH01A, KSH02)	2.23	0.10	26
Quartz monzodiorite (borehole KSH01A)	2.25	0.06	10
Ävrö granite (borehole KAV01, KA2599G01, Äspö HRL prototype tunnel)	2.18	0.21	37

Table 7-6. Determined temperature dependence of heat capacity (per 100°C temperature increase) on samples from different rock types in boreholes KAV01, KSH01A, and KSH02 in the Simpevarp subarea. The mean of the temperature dependence is estimated by linear regression.

Rock name (sample location)	Mean	St. dev.	Number of samples
Fine-grained dioritoid (boreholes KSH01A and KSH02)	25.6%	0.035	11
Quarz monzodiorite (borehole KSH01A)	25.3%	0.033	5
Ävrö granite (borehole KA2599G01)	32.0%	0.056	4

7.2.6 Coefficient of thermal expansion

The coefficient of thermal expansion was measured on samples from three different boreholes; KAV01, KSH01A and KSH02 in the Simpevarp subarea /Åkesson, 2004a,b,c/. Results as obtained for three rock types, are presented in Table 7-7. Other measurements from Äspö HRL are reported in /Staub et al. 2004; Sundberg and Ländell, 2002/.

Table 7-7. Measured thermal expansion (m/(m·K)) between 20°C and 80°C on samples of different rock types from boreholes KAV01, KSH01A, and KSH02 in the Simpevarp subarea.

Rock name (sample location)	Mean	St. dev.	Number of samples
Fine-grained dioritoid (boreholes KSH01A and KSH02)	6.9 E–6	1.5 E–6	17
Quartz monzodiorite (borehole KSH01A)	8.0 E–6	1.4 E–6	10
Ävrö granite (borehole KAV01)	6.0 E–6	0.5 E–6	5

7.2.7 In situ temperature

The temperature of the borehole fluid was logged in boreholes KSH01A, KSH02, KSH03A, KAV01, KLX01, and KLX02. Measured temperature results are presented in Figure 7-4. For method description and presentation of borehole results see /Sundberg et al. 2005b/. Temperature vs. depth is presented in Table 7-8. There is an uncertainty in the temperature logging results due to disturbance from the drilling and water movements along the boreholes. Thus, there is a potential error in the loggings and this is indicated by the noted difference in temperature for the same borehole logged on different occasions. Although this difference in temperature is relatively small for a specified depth, the influence on the design of a repository may be significant. The temperature of borehole KSH03A is deviant and the reason in unknown. The borehole is not included in the calculation of mean temperature in Table 7-8.

Table 7-8. Measured temperature (°C) at different vertical depths; 400, 500, and 600 m from ground surface. Approximate inclination of the boreholes is also indicated.

Borehole, year	400 m	500 m	600 m	Approximate inclination (°)
KSH01A, 2003	12.97	14.34	15.80	74
KSH02, 2003	13.31	14.69	16.12	87
KSH03A, 2003	11.34	12.69	14.09	56
KAV01, 2003	12.55	14.62	16.31	88
KAV01, 1986	12.10	14.40	15.90	87
KLX01	13.67	15.35	16.92	86
KLX02, 2003	13.36	14.82	16.32	84
KLX02, 2002	12.98	14.46	16.06	84
KLX02, 1993	12.57	14.07	15.58	83
Mean	**12.8**	**14.4**	**15.9**	(KSH03A excluded in calculation of mean temperatures)

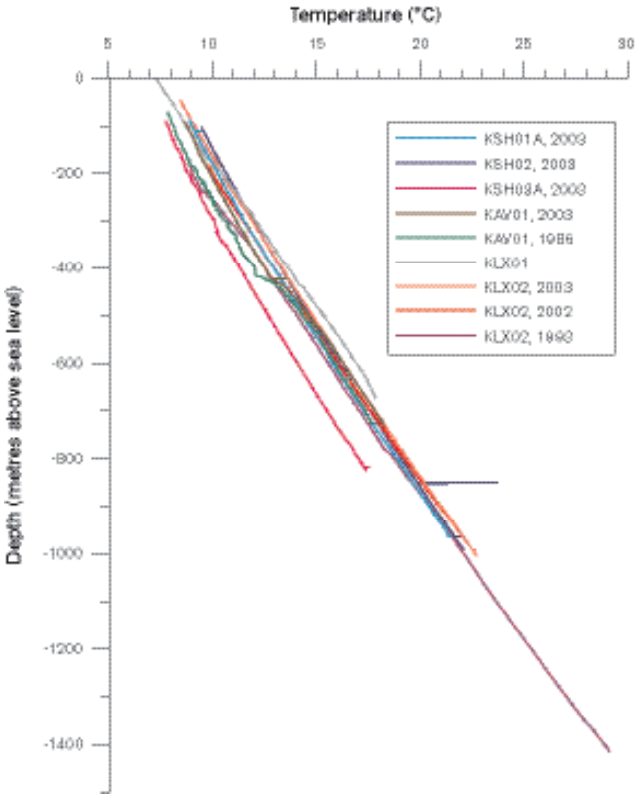

Figure 7-4. *Temperature measurements in boreholes.*

7.3 Thermal modelling (lithological domains)

7.3.1 Modelling assumptions and input from other disciplines

The lithological model for Simpevarp 1.2 is the geometrical base for the thermal model and is described in Section 5.3. The geological Boremap log of the boreholes, showing the distribution of dominant and subordinate rock types, has been used as input to the thermal modelling jointly with a lithological domain classification of borehole intervals. However, the resulting rock type distributions per domain used in the thermal domain modelling differ from those presented in Section 5.3, due to slightly different data (for example rock occurrences less than 1 m from Boremap are included in the thermal modelling). Furthermore, density loggings of boreholes within domain RSMA01 (dominated by Ävrö granite) have been used.

7.3.2 Conceptual model

There are three main causes for the spatial variability of thermal conductivity at the domain level; (1) small scale variability between minerals, (2) spatial variability within each rock type, and (3) variability between the different rock types making up the domain. The first type entails variability in small samples (based on TPS measurements and modal analysis). At this scale, the small scale variability can be substantial. However, the variability is rapidly reduced when the scale increases.

The second type of variability is associated with variability in sample data from a rock type and cannot be explained by small scale variations. This is believed to be especially important for the rock type Ävrö granite, where this (spatial) variability is large. The reason for the variability within a rock type is associated with the process of rock formation, but also the system of classifying the rock types. This variability cannot be reduced, but the uncertainty in the variability may be reduced. This is achieved by collecting large number of samples at varying distances from each other, so that reliable variograms can be created.

Spatial variability of thermal conductivity within rock types has only been studied for rock type Ävrö granite (501044), where density loggings could be used. For other rock types, it was not possible to study the spatial variability because of few measurements and the lack of a reliable relationship between density and thermal conductivity. Variograms of thermal conductivity for different boreholes and separation distances are presented in /Sundberg et al. 2005b/. As an example, variograms for Ävrö granite in borehole KAV01 are illustrated in Figure 7-5. About 50% of the variability occurs at scales of less than about 2 m. However, there are relatively large differences of spatial variability within the rock type Ävrö granite between the different boreholes in the Ävrö granite domain (RSMA01).

The third type of variability is due to the presence of different rock types in the lithological domain. This variability is more pronounced where the difference in thermal conductivity is large between the most common rock types of the domain. Large variability of this type can also be expected in a domain of many different rock types. It is believed that the variability between rock types is important for all defined domains. It is only reduced significantly when the scale becomes large compared to that of the spatial occurrence of the rock type.

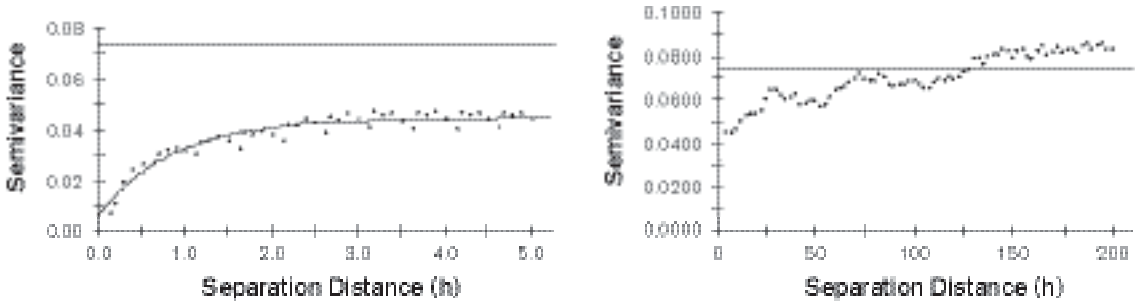

Figure 7-5. *Variogram of thermal conductivity of Ävrö granite (501044) in KAV01, estimated from density logging; 0–5 m and 0–200 m separation distance. The straight line indicates the total variance in data. Increasing semivariance indicates correlation between samples at the actual separation distance. The variograms indicate correlation at different scales.*

Of importance at the domain level is the scale representative for the canister, i.e. at which the thermal conductivity is important for the heat transfer from the canister. At present knowledge, this scale is not known in detail, but it is believed to be in the order of 1 to 10 meters. Therefore, the approach in the domain modelling is to use different scales to study the scale effect, and to draw conclusions of representative thermal conductivity values from that. However, there are large uncertainties and relatively small scales are used in modelling and analysis.

7.3.3 Modelling approaches

The methodology for domain modelling and the modelling of scale dependency were developed for the Prototype Repository at the Äspö HRL /Sundberg et al. 2005a/. In parallel, the domain modelling of Simpevarp was performed /Sundberg et al. 2005b/. Different approaches are used in the modelling. Modelling of the mean for the thermal conductivity at domain level is performed according to the main approach (Approach 1) described in Figure 7-6. This approach is applied to geological domains RSM01A (Ävrö granite), RSM01B (Fine-grained dioritoid), and RSM01C (mixture of Ävrö granite and quartz monzodiorite). Rock domain RSM01D (Quartz monzodiorite) is not represented by any boreholes and is therefore handled differently, see approach below. In order to evaluate the spatial variability at domain level, three alternative/complementary approaches were applied (Approaches 2–4). Mean value results on a domain level and concluding standard deviations are presented in Table 7-11.

It would be useful to develop a spatial model of thermal conductivity and its variability for the domains. However, in this version of the site descriptive modelling the spatial variability has only been modelled for Ävrö granite in specific boreholes.

Approach 1: Main approach

The main approach for domain RSMA01 (Ävrö granite), RSMB01 (Fine-grained dioritoid) and RSMC01 (mixture of Ävrö granite and quartz monzodiorite) is as follows:

Measured and calculated values from modal analysis are used to produce a PDF (Probability Density Function) model for rock types present in the domains, according to Table 7-4. Density loggings are transformed into thermal conductivity estimates according to the model described in Section 7.2.3.

The summed up length of boreholes, or parts of boreholes, belonging to a domain is assumed to be a representative realisation of the domain. Each borehole belonging to a domain is divided into 0.1 m long sections and each section is assigned a thermal conductivity value according to the lithological classification of that section. Both dominating and subordinate rock types are considered in this context. The principles for the assignment of thermal properties are as follows for rock type 501044 (Ävrö granite):

- Primary, the thermal conductivity values calculated from density loggings are used. This implies that the spatial variability within rock type Ävrö granite is considered.
- If the density value is outside the valid range as stipulated by the correlation between density and thermal conductivity, a value of the thermal conductivity is randomly selected from the rock type model (PDF).

Other dominating and subordinate rock types are assigned thermal properties according to:

- A value of thermal conductivity is randomly selected according to the rock type model (PDF), see Table 7-4.

An example showing the principle for assigning thermal conductivity for the rock types is shown in Figure 7-7.

For rock types where no rock type model (PDF) is available (due to lack of data), no value is assigned to that 0.1 m section (section ignored in the calculations). Such rock types, primarily pegmatite, have a low degree of occurrence in the domains and are therefore assumed not to influence the results significantly.

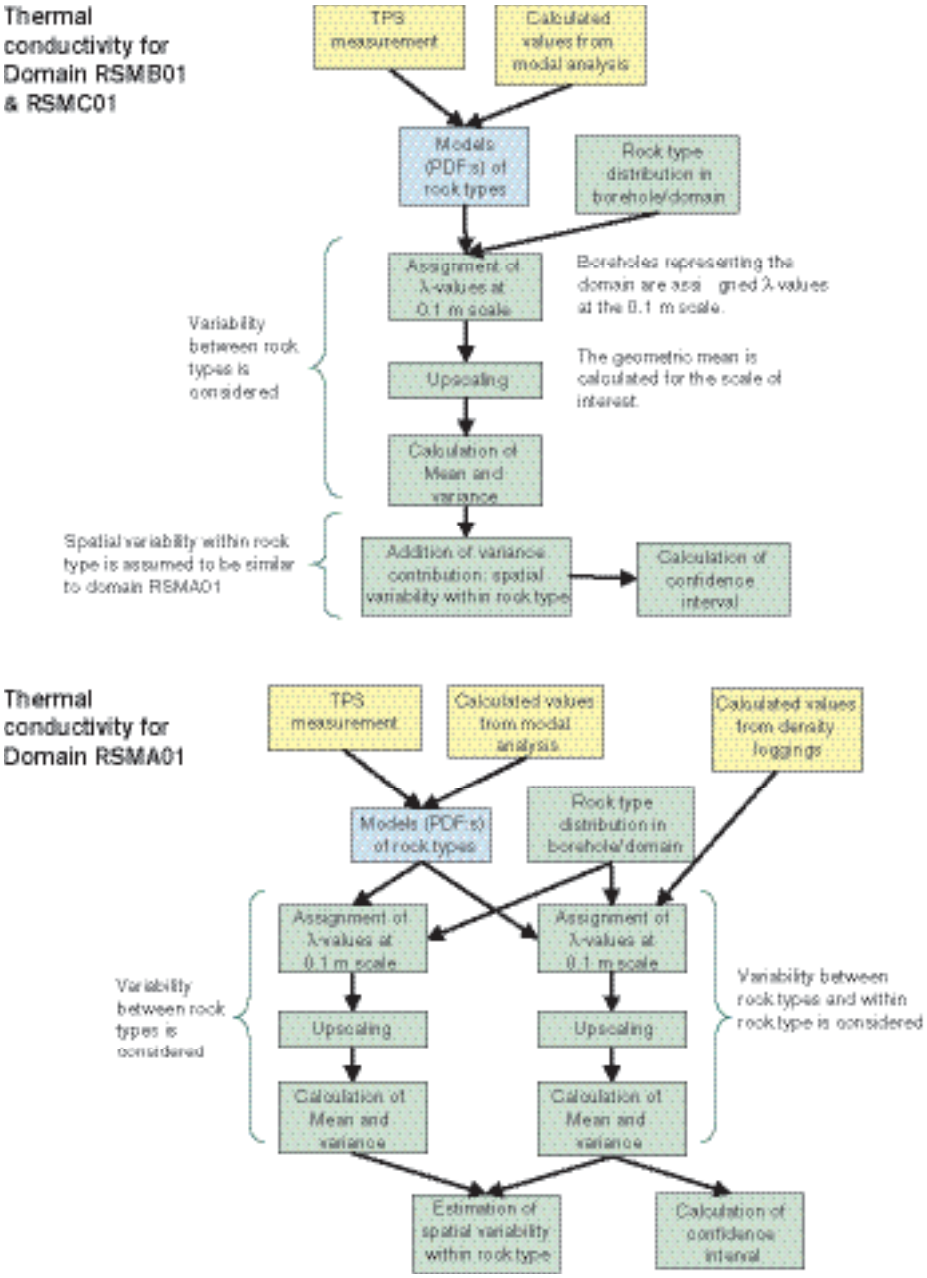

Figure 7-6. *Approach for estimation of thermal conductivity for domain RSMA01 (Ävrö granite), RSMB01 (Fine-grained dioritoid), and RSMC01 (mixture of Ävrö granite and quartz monzodiorite). Yellow colour indicates the data level, blue the rock type level, and green the domain level. The parameter λ refers to thermal conductivity.*

The next step is the upscaling from 0.1 m scale to the appropriate scale of the canister. The significant scale for the canister has not yet been determined in detail and therefore upscaling is performed on scales ranging from 0.1 m to 60 m. The upscaling is performed in the following way:

1. The boreholes representing the domain are divided into a number of sections with a length according to the desired scale (0.1–60 m).
2. Thermal conductivity is calculated for each section by geometric mean calculations of the values at the 0.1 m scale.

3. The mean and the variance for all sections of the domain are calculated. For each scale, the calculations are repeated at least 10 times with different assignments of thermal conductivity values at the 0.1 m scale, according to principle in Figure 7-7. This produces representative values of the mean and the standard deviation for the desired scale.
4. The calculations are repeated for the next scale.

The principle for upscaling of data for different rock types is illustrated both in Figure 7-7 and Figure 7-8. In Figure 7-7, 25 sections are indicated, each with a length of 0.1 m. For the scale 0.5 m, the thermal conductivity $\lambda_{0.5-1}$ is estimated as the geometric mean of the five 0.1 m sections, $\lambda_{0.5-2}$ as the geometric mean for the next five 0.1 m sections, and so on. The mean and variance is then easily computed for the 0.5 m scale. This sequence is repeated for the other scales of interest. In Figure 7-8 the effects of upscaling are shown. The geometric mean is often applied for estimation of average transport properties /Dagan, 1981; Sundberg, 1988/.

As illustrated in Figure 7-6, the approach is slightly different between domain RSMA01 (dominated by Ävrö granite) and the other domains. The reason is that density loggings can be used for domain RSMA01 to take into account spatial correlation within the dominating rock type. This is not possible for domain RSMB01 (Fine-grained dioritoid) and only to a limited degree for domain RSMC01 (mixture of Ävrö granite and quartz monzodiorite), because the two latter rock domains are dominated by other rock types, for which no reliable relationship between density and thermal conductivity is presently available. Therefore, the variance for domain RSMB01 and RSMC01 is grossly underestimated in the approach described above. This is solved in the following way, as illustrated in Figure 7-6:

1. Variance caused by spatial variability within rock type 501044 is estimated for domain RSMA01 (Ävrö granite). This is performed by a second simulation where all thermal conductivity values are randomly selected from the rock type PDF models and no data from density loggings are used. The variance contributed by spatial correlation within rock types is assumed to be the difference between simulation 1 and 2, see Figure 7-9.
2. For domain RSMB01 (Fine-grained dioritoid) and RSMC01 (mixture of Ävrö granite and quartz monzodiorite), no density loggings are used, see Figure 7-6. Instead it is assumed that the variance caused by spatial variability within rock types is identical to that of domain RSMA01. Therefore, the spatial contribution of variance in Figure 7-9 is added to the variance for domain RSMB01 and RSMC01.

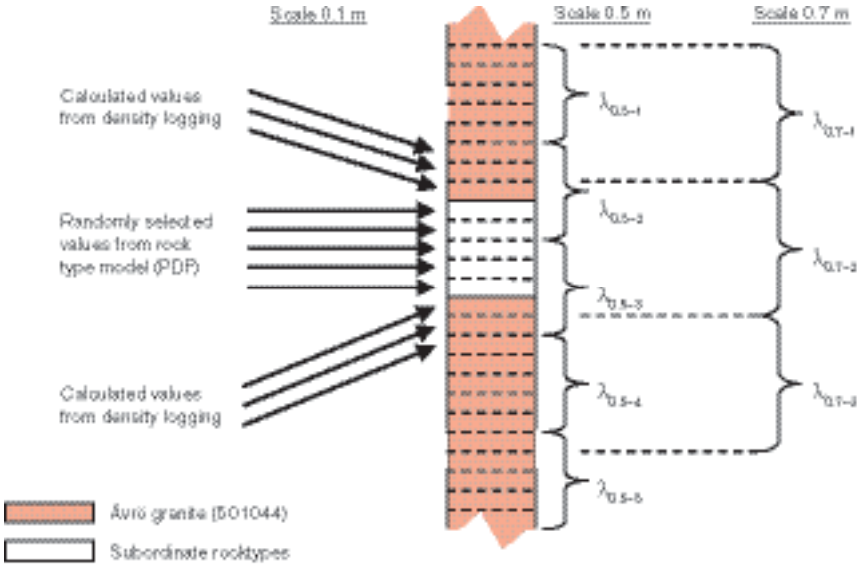

Figure 7-7. *Thermal conductivity is assigned to 0.1 m sections by calculation from density loggings or randomly selected from the rock type models. Upscaling is done by calculating geometric means for different scales, for example 0.5 and 0.7 m.*

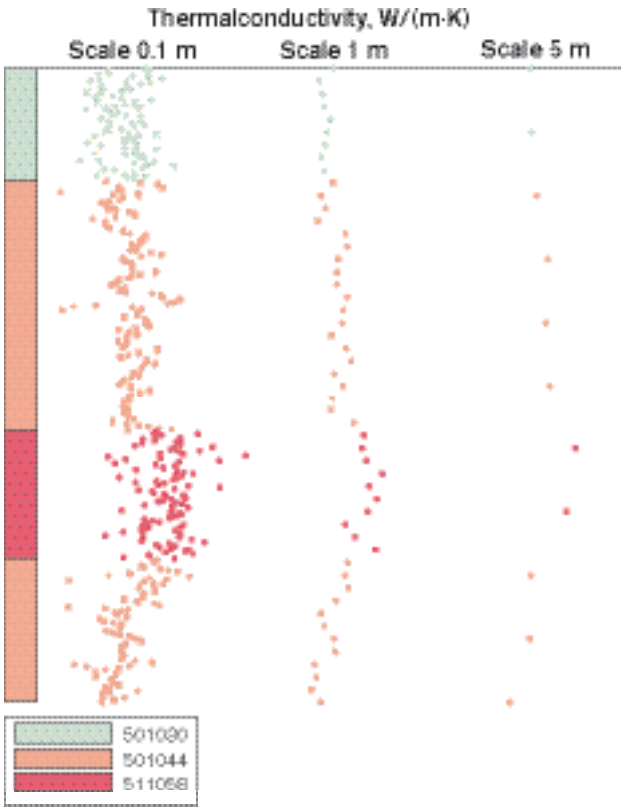

Figure 7-8. *Conceptual illustration of effects of applying the principle for upscaling of thermal conductivity, as given in Figure 7-7, where mean values, standard deviations, and lower and upper confidence intervals for the domains are calculated for different scales.*

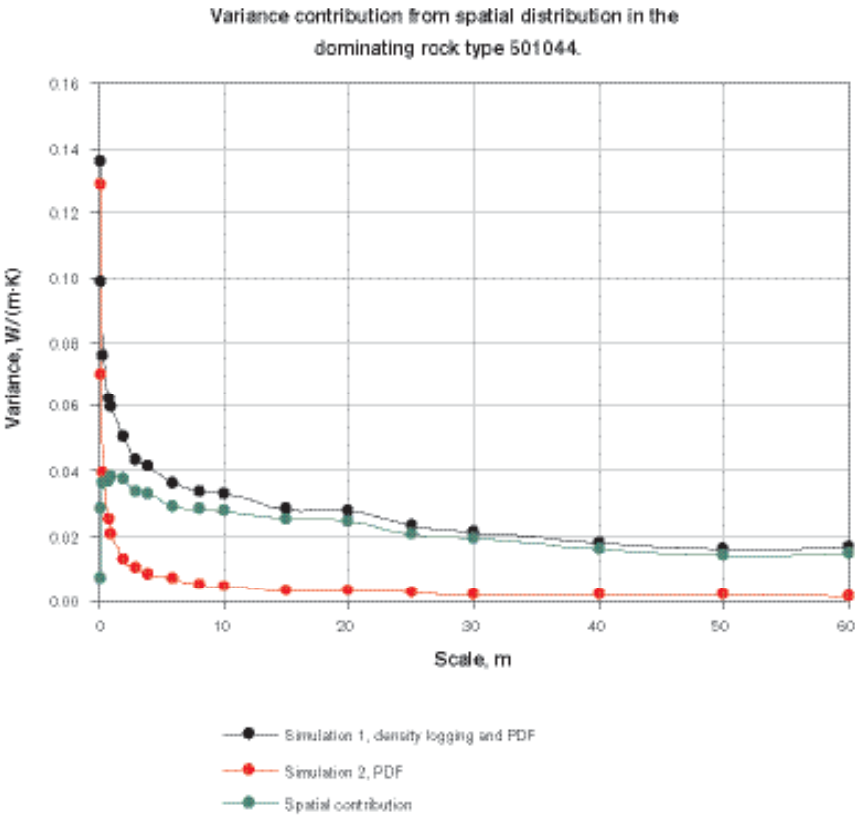

Figure 7-9. *Variance contribution from spatial distribution in the dominating rock type 501044 of domain RSMA01.*

The addition of variances is assumed valid because:

- The processes behind spatial variability within rock types and between rock types can be regarded as the effects of stochastic processes resulting in stochastic variables. It is reasonable to assume that these variables are fairly independent, at least for the purpose of the modelling.
- Addition of variances of stochastic variables is possible if they are independent.

Domain RSMD01 (Quartz monzodiorite) is handled differently because no borehole data from this domain were available. An assumption is made that the domain solely consists of quartz monzodiorite (501036). The PDF model for this rock type is used to estimate the variability at the 0.1 m scale. No direct upscaling is possible due to lack of borehole data (lithology etc.).

Approach 2: Extrapolation – spatial variation in all rock types

When modelling domain RSMA01 (dominated by Ävrö granite) according to the main approach described above, spatial distribution was only considered for 71.3% of the borehole length since not all 0.1 m sections of the domain contained density logging data within the range of validity. For the remainder of the borehole, 28.7%, thermal conductivity values were randomly assigned from the rock type models. Therefore, an approach was made to correct for this (it is assumed that all rock types have the same spatial variation as Ävrö granite, 501044). By randomly replacing thermal conductivity values estimated from density logging with random PDF values it is possible to study the effect of ignoring the spatial variability for 28.7% of the borehole. Figure 7-10 shows an extrapolation of the standard deviation for the scale 0.75 m as a function of the percentage of spatial data used in the modelling of domain RSMA01. If the whole spatial variation is considered, the standard deviation of domain RSMA01 at 0.75 m scale is estimated to be 0.32 W/(m·K), which corresponds to a variance of about 0.10. The variance contribution due to spatial variability within rock types is then 0.073, which differs from 0.037 used in the modelling main approach, see Figure 7-10.

However, it is reasonable to assume that this approach of correction overestimates the total variance since the spatial variation of other rock types than Ävrö granite probably is significantly smaller, which is not considered in the correction.

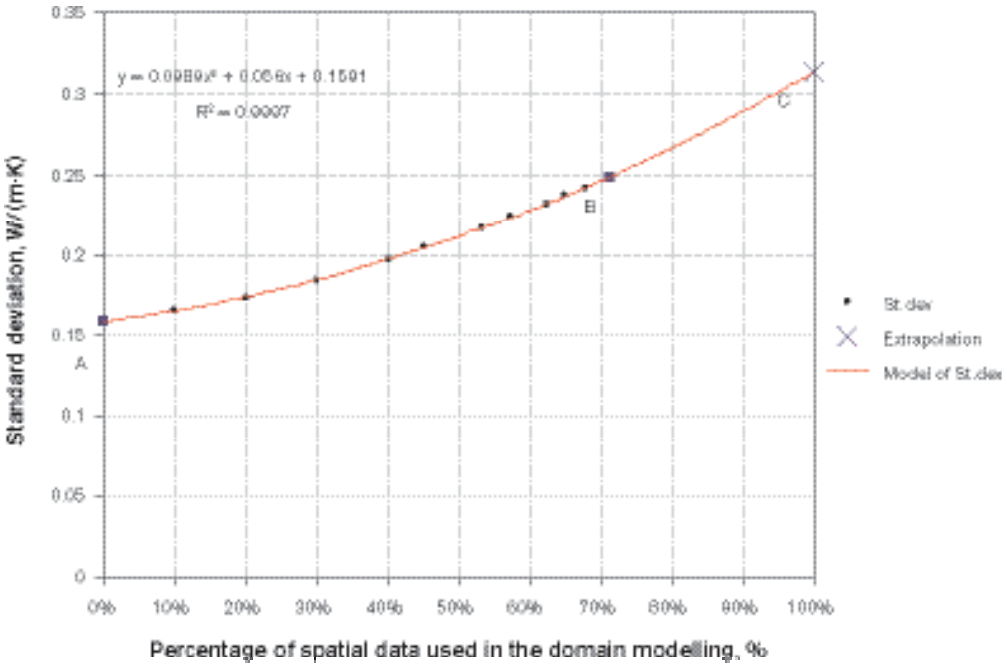

Figure 7-10. *Extrapolation of standard deviation for thermal conductivity at scale 0.75 m for domain RSMA01. At point A, all data are randomly assigned without consideration of spatial variability within Ävrö granite. Point B corresponds to 71.3% of the values estimated from density loggings and thus considering spatial variability. Point C is extrapolated and corresponds to 100% spatial data values, assuming the same spatial variability as in Ävrö granite.*

Approach 3: Reduction of small scale variability

In the third approach, variograms presented in Figure 7-5 and in /Sundberg et al. 2005b/ are used to estimate the small scale variance of 501044 in RSMA01 (dominated by Ävrö granite). The variograms are based on data from boreholes KAV01 and KLX02, both of which belong to domain RSMA01.

In this approach, the small-scale variability for the scale of interest within 501044 is subtracted from the total variability of the same rock type (from PDF:s). This residual variability is assumed to be the variance after averaging to the desired scale. The basis for the approach is that variability in scales smaller than the desired is evened out. Table 7-10 illustrates rough estimations of the variance at different scales based on variograms and PDF:s, and also the variance after averaging to the desired scale. The variograms of borehole KAV01 (Figure 7-5) and KLX02 /Sundberg et al. 2005b/, however, do illustrate that there is a difference between the boreholes regarding spatial correlation. This means that there is uncertainty about the representativeness of the two boreholes for the domain.

For other lithological domains this approach was not applied since no variograms could be established. An attempt was made to calculate a variogram of 501030 (Fine-grained dioritoid) from TPS measurements, but the variogram became very unstable due to sparse data.

There is a reason to believe that this approach may underestimate the variance because only the dominating rock type is considered and the others are ignored.

Approach 4: Addition of "between rock type" and "within rock type" variance

The approach of randomly selecting thermal conductivity values from rock type models (PDF:s) without consideration of spatial variability was described in the main approach. This modelling resulted in estimates of thermal conductivity at different scales, see Table 7-10. This variance includes variability due to rock type changes in the boreholes ("between rock type" variability) but the variability within each rock type is effectively and rapidly reduced when the scale is increased because of the random assignment of thermal conductivity values. The resulting variance is therefore mainly a result of the presence of different rock types in the boreholes. Below, this variance is denoted as V_1.

One way of compensating for the variance reduction caused by ignoring spatial variability is to add the spatial variability within the dominating rock type in the domain. This is a similar, although not identical, approach to the main approach for domain RSMB01 (Fine-grained dioritoid) and RSMC01 (mixture of Ävrö granite and quartz monzodiorite). The spatial variability within the dominating rock type can be estimated in different ways. For Ävrö granite (501044) the calculated values from density loggings can be used and for Fine-grained dioritoid (501030) TPS measurements can provide a rough estimate of the spatial variability within the rock type. The variances as a function of scale were calculated in these ways (geometric mean for the actual scale) and the results are presented in Figure 7-11 for Ävrö granite and Fine-grained dioritoid. This type of variance is denoted V_2 below.

The total variance for the domain can be estimated as the sum of variances due to different rock types /Sundberg et al. 2005b/ and the variance due to spatial variability within the dominating rock type: $V_{tot} = V_1 + V_2$

For domain RSMC01 there are two dominating rock types. Therefore, the variance V_2 is estimated slightly differently, as a weighted sum of the spatial variance for the two dominating rock types, where the weighting factors are the fractions of each rock type in the domain. Although this approach only provides a rough estimate of the total variability it encompasses all the major types of variability within the domain.

The estimated mean thermal conductivity and the total variance estimated for each domain using the four defined approaches are presented in Table 7-9 and Table 7-10, respectively.

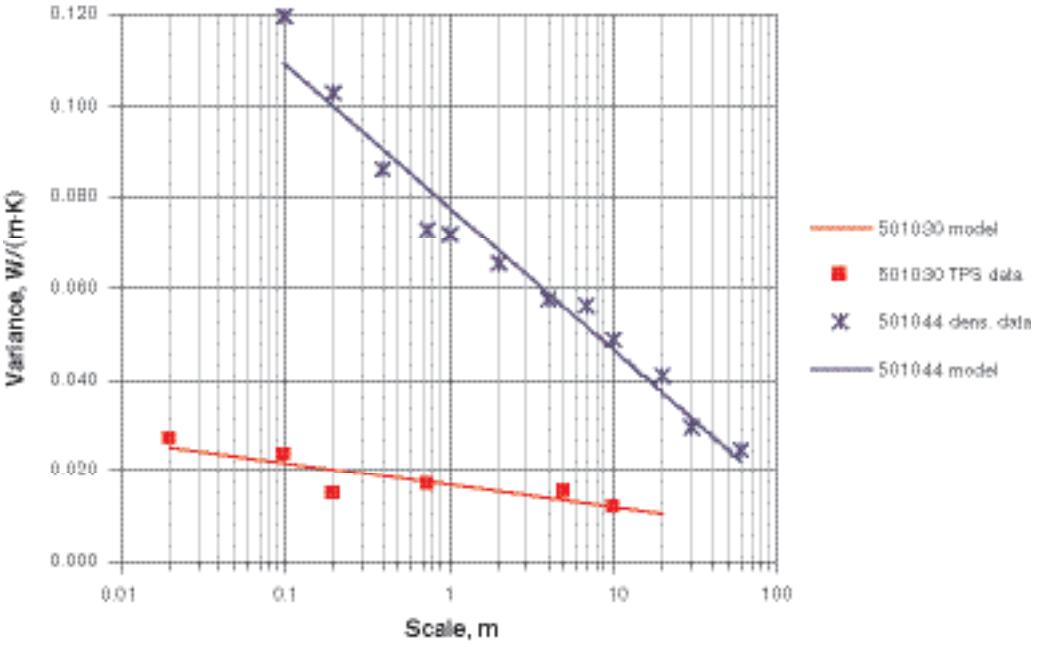

Figure 7-11. *Comparison between variability within rock type 501030 and 501044 (V_2). Note that data for 501030 are sparse and based on 26 TPS measurement, while data for 501044 are based on calculated values determined from density loggings.*

For domain RSMB01 and RSMC01 the difference between approach 1 and 4 is in the way the "variability within rock type" is estimated. For approach 1 it is performed by looking at domain RSMA01 (Ävrö granite), but in approach 4 it is achieved by studying the dominating rock type in the domain.

It is not easy to assess whether this approach under- or overestimates the total variance for the domain. There are several factors that may influence this, such as the spatial variability in subordinate rock types compared with the dominating rock type. In addition, the variance V_2 in Figure 7-11 is rather uncertain due to relatively few measurements and questions of representativeness. Still, it is believed that this approach gives a quite reasonable estimate of the variability compared to the other approaches.

Conclusions – modelling results

Mean values representative of the thermal conductivity on domain level is presented in Table 7-9 based on modelling according to the main approach. The thermal conductivity of domain RSMA01 (Ävrö granite) has been corrected by a subtraction of 0.1 W/(m·K), which is motivated by a potential bias in the relationship between density and thermal conductivity, used for the dominating rock type in this domain.

Table 7-9. Thermal conductivity (W/(m·K)) by lithological domain.

Domain	Mean	Comment
RSMA01, Ävrö Granite	2.80	Mean value substracted by 0.1 W/(m·K)
RSMB01, Fine-grained dioritoid	2.74	
RSMC01, Mix of Ävrö granite and quartz monzodiorite	2.74	
RSMD01, Quartz monzodiorite	2.62	Modelled with Monte Carlo simulation

The standard deviations for the different domains were estimated with three alternative or complementary approaches, where the results are summarised in Table 7-10. For approach 1, mean values and standard deviations are calculated for each scale under the assumption of normally distributed data at the scale of interest /Sundberg et al. 2005b/. As described in the table, and also in previous sections, approach 2 probably overestimates the standard deviation and approach 3 underestimates it. Approach 1 is believed to underestimate the standard deviation for domain RSMA01, although it probably overestimates it for domain RSMB01 (Fine-grained dioritoid) and RSMC01 (mixture of Ävrö granite and quartz monzodiorite). Therefore, the standard deviation of domain RSMA01 is given the concluding value of 0.28 W/(m·K), which is the result from approach 4 at the 2 m scale and is a value in between approaches 1 and 2.

For domains RSMB01 and RSMC01 the standard deviation according to approach 1 in Table 7-10 probably overestimates the variability. Therefore, the standard deviation is suggested to be identical to approach 4 at the 2 m scale, in the same way as for RSMA01. For domain RSMD01 (Quartz monzodiorite) no changes have been made in the standard deviation compared with the simulation results.

Table 7-10. Summary of standard deviations (W/(m·K)) from modelling results at the domain level with the main approach (Approach 1) compared with the three alternative/complementary approaches (Approaches 2–4). Numbers within brackets are calculated variances with the resulting standard deviation in bold.

Appr.	Scale (m)	RSMA01 (Ävrö granite)	RSMB01 (Fine-grained dioritoid)	RSMC01 (Mixture of Ävrö granite and quartz monzodiorite)	RSMD01 (Quartz monzodiorite)	Comment
1	0.75	**0.25** (0.025+0.037=0.062) (random+71.3% spatial variation)	**0.27** (0.035+0.037=0.072) (random+spatial variation from RSMA01)	**0.28** (0.042+0.037=0.079) (random+spatial variation from RSMA01)	**0.28** Monte Carlo sim.	Underestimation of RSMA01 and overestimation of RSMB01 and RSMC01. RSMD01 result of Monte Carlo simulation.
	2	–	–	–	–	
2	0.75	**0.31** (0.025+0.073=0.098) (random+100% spatial variation)	–	–	–	Overestimation
	2	–	–	–	–	
3	0.75	**0.22** (0.12–0.07=0.07) (total variance within rock type-small scale variance)	–	–	–	Underestimation
	2	**0.20** (0.12–0.08=0.04)	–	–	–	
4	0.75	**0.31** (0.025+0.073=0.098) (random+internal spatial)	**0.23** (0.035+0.018=0.053) (random+internal spatial)	**0.28** (0.042+0.035[1]=0.077) (random+internal spatial)	–	
	2	**0.28** (0.013+0.066=0.079)	**0.20** (0.024+0.014=0.038)	**0.24** (0.026+0.030[2]=0.056)	–	

[1] Internal spatial variance within the rock types in the domain calculated with a composition of 30% Ävrö granite and 70% Fine-grained dioritoid (0.3×0.073+0.7×0.018=0.035), see /Sundberg et al. 2005b/.

[2] Internal spatial variance in 2 m scale calculated as above (0.3×0.066+0.7×0.014=0.030).

Table 7-11 summarises the mean and suggested standard deviation of thermal conductivity per domain at the assumed canister scale.

A comparison of the results on domain level presented in model version Simpevarp 1.1 /SKB, 2004b/ and the model version Simpevarp1.2 is given in Table 7-12.

Table 7-11. Mean value and revised standard deviation of thermal conductivity (W/(m·K)) per domain in canister scale (compare with Table 7-9). Two-sided 95% confidence intervals are indicated.

Domain	Mean	St. dev.	Lower confidence limit	Upper confidence limit
RSMA01	2.80	0.28	2.25	3.35
RSMB01	2.74	0.20	2.35	3.13
RSMC01	2.74	0.24	2.27	3.21
RSMD01	2.62	0.28	2.04	3.20

Table 7-12. Comparison of modelling results (the mean and the standard deviation) from Simpevarp versions S1.1 and S1.2

Domain	Mean (W/(m·K))		Diff. (S1.2-S1.1)/S1.1	St. dev. (W/(m·K))	
	Version S1.1	Version S1.2		Version S1.1	Version S1.2
RSMA01	2.67	2.80	4.9%	0.25	0.28
RSMB01	2.23	2.74	22.9%	0.08	0.20
RSMC01	2.50	2.74	9.6%	0.09	0.24
RSMD01	2.38	2.62	10.1%	0.10	0.28

Heat capacity

Modelling of heat capacity on domain level is performed as a Monte Carlo simulation where the occurrence of different rock types in the domain is weighted together with the rock type models. Results are presented in Table 7-13 and rock type models with an extended methodology are presented in /Sundberg et al. 2005b/.

Table 7-13. Heat capacity (MJ/(m³·K)) per domain with two-sided 95% confidence intervals under assumption of normal distribution.

Domain	Mean	St. dev.	Lower confidence limit	Upper confidence limit
RSMA01	2.23	0.120	2.00	2.46
RSMB01	2.23	0.097	2.04	2.42
RSMC01	2.24	0.090	2.04	2.42
RSMD01	2.25	0.060	2.11	2.38

Coefficient of thermal expansion

No domain modelling performed. For all domains a mean value for the coefficient of thermal expansion is suggested as 6–8 $\times 10^{-6}$ m/(m·K), see Section 7.2.6.

In situ temperature

No domain modelling performed. For all domains, a mean of the in situ temperature at 400, 500 and 600 m depth is estimated at 12.8, 14.4 and 15.9°C, respectively, see Section 7.2.7.

7.3.4 Evaluation of uncertainties

A general description of uncertainties is provided in the strategy report for the thermal site descriptive modelling /Sundberg, 2003a/. In /Sundberg et al. 2005a/ conceptual uncertainty model is presented. In the supporting document for thermal model version 1.2 /Sundberg et al. 2005b/, uncertainties are further described. For additional discussion of uncertainties also refer to Chapter 12 and Table 12-4. To obtain an overview at what stages uncertainties are introduced, the reader is referred to Figure 7-6. Uncertainties are introduced at the following levels/stages:

- Data level
- Rock type level
- Domain level

Thermal conductivity

Data level

– TPS data.

The accuracy of TPS measurements is better than 5% and the repeatability is better than 2%, according to the manufacturer of the measurement equipment /Sundberg, 2002/. Note that this uncertainty refers to the measurement volume (approx. 10 cm^3) and not the volume of the sample, since only a subvolume of the sample is subject to measurement. If the TPS-measurement is supposed to represent the sample scale (approx. 0.1 dm^3) the uncertainty is larger and depends on the small-scale heterogeneity of the rock.

There is a potential bias (underestimation) in thermal conductivity data. The reason is that stress dependence has not been assessed. Measurements are made on stress released samples. However, the effect is assumed to be low since the samples are water saturated before measurement.

– SCA data.

The uncertainty associated with SCA data is significantly larger than for TPS data. For SCA data there are three important sources of uncertainty; (1) alteration of minerals, (2) determination of the volume fraction of each mineral in the sample, and (3) representative values of thermal conductivity of the different minerals. An example of the first type of uncertainty is that parts of the plagioclase and biotite in fine-grained dioritoid and quartz monzodiorite are partly sericitised and chloritised.

– Density data.

Thermal conductivities are calculated for Ävrö granite based on density loggings using the relationship in Figure 7-1. These values are more uncertain than both TPS and SCA data. The main sources of uncertainty are; (1) uncertainty in the density logging technique, (2) uncertainty in filtering and recalibration of density data, and (3) uncertainty in the statistical relationship between density and thermal conductivity. There is a potential bias in the calculated values from density measurement. One reason could be extrapolation slightly beyond the density range of the data for the statistical relationship. On the other hand, the difference in mean values between density loggings and calculated/measured data could be a natural result of the large scale heterogeneity of the Ävrö granite in relation to sample locations.

Rock type level

– Representativeness of data.

The representativeness of samples selected for TPS measurements can be questioned. The samples are not taken with the purpose of statistically representing the rock mass. For both measured and calculated data, non-probabilistic selection of samples has resulted in bias of unknown magnitude. However, samples were taken in order to characterise the rock type – not to find odd varieties. The potential for bias, due to TPS and SCA data sets with low representativeness, is largest for rock types with high spatial variability, such as Ävrö granite.

– Rock type models.

For fine-grained granite and quartz monzodiorite the rock type models are based on TPS data and corrected SCA data. The correction is based on comparison of SCA data with TPS data. Because the comparison is based on only a few samples, there is uncertainty in the accuracy of this correction.

The rock type models were chosen as normal distributions (PDF:s). There is a slight deviation between data and model and one reason for this can be the question of representativeness of the samples. Generally, the rock type models slightly overestimate the occurrence of small thermal conductivity values and underestimate the number of large values. The rock type models are required in the domain modelling.

The data set is very small for several rock types, which implies that these rock type models are highly uncertain. This applies to quartz monzodiorite, fine-grained diorite-gabbro, diorite/gabbro, granite, and fine-grained granite.

Domain level

– Representativeness of boreholes.

It is not known how representative the boreholes are for the different domains. Since the number of boreholes in a domain is low, it is reasonable to believe that there is a bias present. This is supported by borehole data showing large differences in e.g. spatial variability, especially for domain RSMA01 (Ävrö granite). This bias can only be reduced with additional boreholes, or a more complete understanding of the lithology.

– Anisotrophy.

Anisotropy has not been considered in the domain modelling. Anisotropic effects may result due to presence of subordinate rock types occurring as dykes of significant extension, consisting of a rock type with different thermal characteristics. The effect of structure and foliation in dominating rock types is assumed to be small.

– Significant scale.

At the present state of knowledge it is not known at which scale thermal conductivity is significant for the heat emitted from the canister. This implies a major source of uncertainty in the thermal modelling.

– Upscaling methodology.

For all rock types except Ävrö granite, thermal conductivity values are randomly assigned at the 0.1 m scale based on the rock type models. These rock type models probably overestimate the variance at the 0.1 m scale. The reason is that TPS and SCA data represent a smaller scale. At the 0.1 m scale, some reduction of variance should already have taken place. Therefore, this approach overestimates the likelihood of small values.

In the main modelling approach, spatial variability within other rock types than Ävrö granite is ignored. This results in too large a variance reduction when the scale increases. To compensate for this, the approach was modified such that the variance due to spatial variability within other rock types was assumed to be equal the spatial variability within Ävrö granite. This is probably on overestimation of the variance.

There is also a potential bias in the modelling approach for the same rock type (Ävrö grante). The assigned values based on density loggings are higher than predicted by the rock type model of Ävrö granite. In the modelling the results have been corrected for this potential bias.

There are several other uncertainties in modelling approaches 2–3. These include the procedure used in approach 2 for adjustment of spatial variability, the addition and subtraction of variances in approaches 1–4, and the estimation of spatial variability from variograms (approach 3) and TPS data (approach 4). These uncertainties all arise from lack of knowledge of spatial variability within the rock types and within the domains. The most straight-forward way of reducing this uncertainty is to collect more data.

The confidence intervals calculated for each domain are based on the assumption that domain data at the significant scale are normally distributed. This is an uncertain assumption. As long as knowledge of spatial variability is insufficient, it is not possible to check the validity of this assumption.

Influences from fractures and deformation zones on thermal properties have not been considered. No thermal data are presently available from the deformation zones.

The rock type models have been considered as normal distributions although the data are somewhat skewed. This results in a too small change of the mean value for the domain when the scale increases. The effect is however insignificant compared to the other uncertainties.

Heat capacity

There exists a problem with the representativeness for measured values (TPS data). The samples are few and focused on certain parts of the rock volume.

Subordinate rock types have not been considered when modelling the heat capacity.

No direct laboratory measurements of heat capacity have been performed. Instead, heat capacity has been determined through conductivity and diffusivity measurements performed with the TPS method.

In situ temperature

Temperature loggings from different boreholes show a variation in temperature at specified depth. The difference implies an uncertainty in temperature loggings and even small uncertainties may influence the design. Possible sources of uncertainty are timing of the logging after drilling (drilling adds to temperature disturbance), water movements along the boreholes, uncertainty in the temperature logging or in the measured inclination of the boreholes. The uncertainty imposed by water movements may be evaluated jointly with the hydrogeologists. However, the latter has not yet been done.

Thermal expansion

Problem with the representativeness for measured samples. The samples are few and focused to certain parts of the rock volume.

There are differences in the results of thermal expansion measurements since different methods and laboratories have been used.

There is a potential bias (underestimation) in thermal expansion data. The reason is that stress dependence has not been assessed. Measurements are made on stress released samples.

8 Bedrock hydrogeology

A primary objective of the hydrogeological description is to provide a general conceptual "understanding of the Site" and to determine and justify the assignment of hydraulic properties, boundary and initial conditions based on primary data and numerical simulations, useful for Repository Design, Safety Assessment, and Environmental Impact Assessment studies.

The conductive elements of the bedrock hydrogeological model of Simpevarp are divided into two types of domains, hydraulic rock domains (HRD) and hydraulic conductor domains (HCD). The geometries of the HRDs and HCDs coincide by and large with the geological rock domains and the deterministically modelled deformation zones, respectively. The HRDs consist of two components, the geology-based stochastic description of rock fractures and lineaments, the so-called discrete fracture network (GeoDFN), and the "rock mass" between the rock fractures included in the DFN.

Numerical simulation models are used to underpin the development of the bedrock hydrogeological model. The hydraulic parameterisation of the conceptual model is based on data from the site investigations. The level of detail by which the HCDs and HRDs are represented in a continuous numerical simulation model depends largely on the information at hand (data freeze version), the size of the model domain and the chosen grid resolution. As in Simpevarp 1.1, the treatment of the bedrock hydrogeological model follows that of the geological model (cf. Chapter 5), which effectively means that the hydrogeological modelling in Simpevarp 1.2 is done on a regional scale although the body of the data used for the hydraulic parameterisation come from the site investigations within the candidate area.

The development of the bedrock hydrogeological model is carried out according to the methodology described in /Rhén et al. 2003/. The data used by the two modelling teams conducting the regional numerical simulations /Hartley et al. 2005; Follin et al. 2005/ is specified in an internal steering document entitled "Task Description". The focus of the numerical simulations in Simpevarp 1.2 is to establish integration with hydrogeochemistry.

One or more components of the bedrock hydrogeological model provide a foundation for the integration with, and modelling work in rock mechanics, bedrock hydrogeochemistry and bedrock transport properties. Being strongly coupled to the geological model, all components of the bedrock hydrogeological model have a direct impact on the location and design of the shafts and tunnels for the deep repository. They also provide a significant input for the safety analysis work in terms of hydraulic properties relevant for transport simulations.

8.1 State of knowledge at previous model version

The hydrogeolological model of the bedrock in Site Descriptive Model Simpevarp version 1.1 covered the entire regional area /SKB, 2004b/. Groundwater flow modelling was presented in /Hartley et al. 2004/ and /Follin et al. 2004/.

The Hydraulic Conductor Domains (HCDs), corresponding to the interpreted deterministic deformation zones were in the hydrogeological model based on version 0 of the regional scale structural model, which consisted of 171 deformation zone segments. Some of the deformation zones in the regional scale model area, in the vicinity of the island of Äspö, were considered as high-confidence deformation zones (concerning their existence) and several of them had been hydraulically tested. However, most HCDs had attributed hydraulic properties based on other sources. A simplified approach was employed in the assignment of properties to the HCDs as the model was based on version 0 model and not the actual version 1.1 model, which arrived late in the Simpevarp 1.1 work.

No statistics for a HydroDFN model were available at the time of the Simpevarp 1.1 groundwater flow modelling. Approximate statistical values of parameters for the HydroDFN model were estimated on the basis of parameters evaluated from boreholes KLX01 and KLX02 (in the Laxemar subarea) and parameters estimated for the Forsmark 1.1 descriptive model. The working hypothesis

embedded in the HydroDFN model employed for Simpevarp 1.1 was that it coupled an inferred power-law size distribution of fractures (up to the size of local minor fracture zones) to hydraulic properties by assuming that transmissivity is dependent on size through a power-law relationship. The same hydraulic DFN model was assigned to all HRDs and one common size distribution was used for all interpreted fracture sets. The applied HydroDFN in the regional model used a minimum size of 100 m, so the stochastically modelled features represented rather a distribution of deformation zones, all of which are assumed to be brittle, i.e. fracture zones. The fracture centres were assumed be Poisson distributed in space.

The main uncertainties in the Simpevarp version 1.1 hydrogeological model concerned the following:

- The DEM model was not correct in the vicinity of the shoreline. The error was in the bathymetric data between 0 and –3 masl. (This could however be seen as a minor uncertainty).
- All assumptions made in the geological structural model were directly transferred to the hydrogeological model. In particular, there was an uncertainty in the interpretation of lineaments as representing deformation zones (confidence level) and in the assignment of hydraulic properties at depth. (i.e. the upscaling of hydrogeologic data is entirely based on the geologic features). The deformation zones were also extended to the bottom of the modelled domain (depth 2,100 m), which also is an assumption associated with uncertainty.
- The assigned transmissivity distribution to deformation zones and the spatial variability within the zones were considered uncertain.
- The hydraulic DFN model and resulting connectivity were considered highly uncertain. It was not based on the resulting version 1.1 geological DFN-model. It is assumed that the transmissivity distributions were the same for all fracture sets. Furthermore, the model had an assumed correlation between transmissivity and size and an assumed spatial distribution. This “interpretation” was considered unsatisfactory and the data analysis was judged to require strengthening in coming versions of the site-descriptive model.
- The current distribution of groundwater salinity was known at depth only from a few boreholes. This in turn made it difficult to test the importance of the initial hydrogeological condition (paleohydrogeology) on present salinity. There was also an uncertainty associated with the conditions after the last glaciation. The significance of this situation was recommended through sensitivity analyses.
- The boundary conditions at the regional scale were regarded as uncertain, but could be handled by sensitivity analyses in simulations.

The most important uncertainties are related to the HydroDFN models and the deformation zone model (existence and properties) as flow paths, transport times and construction issues are coupled to these models and are essential for both Safety Assessment and Repository Engineering.

8.2 Evaluation of primary data

Data from field investigations, here called primary data, avalible for the present model version are compiled and commented in this section. These primary data, used for the analysis and subsequent hydrogeological modelling, are provided in Table 2-4 in Chapter 2 and presented in some detail in this section.

8.2.1 Hydraulic evaluation of of single hole tests

Methods for measurement of hydraulic parameters

A number of hydraulic tests are used as (more or less) standardised methods in boreholes drilled during the site investigations. These are summarised in Table 8-1.

Table 8-1. Principal methods used during initial site investigations for measurement and evaluation of hydraulic parameters.

Measurement equipment	Acronym for method	Acronym for method variant	Type of test performed	Comments
Pipe String System	PSS		Pumping or injection tests performed as constant rate tests. Impulse test is an option.	Transient data collected. Evalution based on transient or stationary conditions. Test in cored boreholes. Injection tests before the Site investigations were made with other equipment than PSS but are indicated in tables as “PSS”.
Hydraulic test system percussion boreholes	HTHB		Pumping or injection tests performed as constant rate tests. Flow logging with impeller is an option.	Transient data collected. Evalution based on transient or stationary conditions.
Wire Line Probe	WLP	WLP-pt	Pumping tests with WLP in cored boreholes.	Transient data collected. Evalution based on transient or stationary conditions.
		WLP-ap	Absolute pressure measurement with WLP in cored bore holes.	Transient data collected.
Posiva Flow Log	PFL	PFL-s	Difference flow logging (section). Electrical conductivity (EC) and temperature of the borehole fluid as well as Single Point resistance (SP) is measured during different logging sequences.	Purpose is to estimate test section transmissivity and undisturbed pressure. Two logging sequences. Evalution is based on stationary conditions.
		PFL-f	Difference flow logging (flow-anomaly).	Purpose is to estimate flow distribution and use PFL-s to estimate transmissivity for fractures/features. One single logging sequence.
Slug test			Slug or bail test.	Normally just performed in boreholes completed in the overburden.

Data available

Cored boreholes KSH01A, KSH02, KSH03A, KAV01 and percussion boreholes HSH01–03 have been tested during the early stages of the initial site investigations and were available for the Simpevarp 1.2 modelling cf. Figure 2-1. In the cored boreholes hydraulic tests with the wire-line probe (WLP), the Posiva flow logging tool (PFL) and the Pipe String System (PSS) were performed in most boreholes. In percussion holes HSH01–03, hydraulic tests with HTHB equipment were performed.

Single-hole hydraulic tests and interference tests conducted prior to the onset of the ongoing initial site investigations (historical data) were carried out at Äspö, Ävrö, Hålö, Mjälen, Laxemar and the Simpevarp peninsula /e.g. Rhén et al. 1997a,b/. Some of these existing data are commented on in this section, but have not been re-evaluated and are only partly included in the analysis for Simpevarp 1.2. However, it is judged that the most significant results from /Rhén et al. 1997b/ of relevance for consideration of hydraulic conductor domains (HCD), cf. Section 8.3, are incorporated in the Simpevarp 1.2 modelling.

The single-hole hydraulic tests conducted in the cored boreholes and percussion boreholes are listed in Table 8-2 through Table 8-6. The hydraulic tests conducted in the percussion boreholes were performed as open-hole pumping tests combined with flow logging. Some tests were also conducted with a single packer, making it possible to pump the section above or below the packer. The hydraulic tests performed in the cored boreholes were made during drilling, as pumping tests and included measurements of absolute pressure made using the SKB-developed Wire-Line Probe (WLP).

Table 8-2. Hydraulic tests performed in cored borehole KSH01A (WLP: WireLine probe (tests during drilling), PFL: Posiva Flow Logging).

Borehole ID	Borehole length	Upper limit	Lower limit	No. of tests	Type of test performed	Test scale	Step length (for moving test section)
	(m)	Secup (m)	Seclow (m)			(m)	(m)
KSH01A	1,003	102.79	997.98	179	PFL-s, difference flow logging-section	5	5
		102.8	730	–	PFL-f, difference flow logging-flow-anomaly	5	0.1
		12.1	1,003	1	Pumping test	≈1,000	–
		197	1,003	7	Pumping tests with WLP	≈100	–
		300	700	81	PSS – transient injection	5	–
		103	999	45	PSS – transient injection	20	–
		103	999	9	PSS – transient injection	100	–

Table 8-3. Hydraulic tests performed in cored borehole KSH02 (WLP: WireLine probe (tests during drilling), PFL: Posiva Flow Logging).

Borehole ID	Borehole length	Upper limit	Lower limit	No. of tests	Type of test performed	Test scale	Step length (for moving test section)
	(m)	Secup (m)	Seclow (m)			(m)	(m)
KSH02	1,001.11	81.52	997	183	PFL-s, difference flow logging-section	5	5
		82.8	995.2	–	PFL-f, difference flow logging-flow-anomaly	5	0.1
		80	1,001.11	1	Pumping test	≈1,000	–
		80.1	1,001.11	7 (9)	Pumping tests with WLP (2 airlift test)	≈100	–
		301.50	701.50	80	PSS – transient injection	5	–
		81.50	961.50	45	PSS – transient injection	20	–
		101.50	997	9	PSS – transient injection	100	–

Table 8-4. Hydraulic tests performed in cored borehole KSH03A (WLP: WireLine probe (tests during drilling), PFL: Posiva Flow Logging).

Borehole ID	Borehole length	Upper limit	Lower limit	No. of tests	Type of test performed	Test scale	Step length (for moving test section)
	(m)	Secup (m)	Seclow (m)			(m)	(m)
KSH03A	1,000.70	101.4	1,000.70	1	Pumping test	≈1,000	–
		11.8	1,003	8(9+3)	Pumping tests with WLP (1 with submersible pump or airlift test: 1 in scale 100 m +3 tests with test scale < 100 m)	≈100	–
		102.5	995	9	PSS – transient injection	100	–

Table 8-5. Hydraulic tests performed in cored borehole KAV01 (WLP: WireLine probe (tests during drilling), PFL: Posiva Flow Logging).

Borehole ID	Borehole length	Upper limit	Lower limit	No. of tests	Type of test performed	Test scale	Step length (for moving test section)
	(m)	Secup (m)	Seclow (m)			(m)	(m)
KAV01	757.31	71.40	732.26	132	PFL-s, difference flow logging-section	5	5
		70.1	651.3	–	PFL-f, difference flow logging-flow-anomaly	5	0.1
		70.4	757.31	1	Pumping test	≈1,000	–
		22.6	438.5	175	PSS – transient injection	2	–
		20	710	69	PSS – transient injection	10	–

Table 8-6. Hydraulic tests performed in percussion boreholes HSH01–HSH03.

Borehole ID	Borehole length	Upper limit	Lower limit	No. of tests	Type of test performed	Test scale	Step length (for moving test section)
	(m)	Secup (m)	Seclow (m)			(m)	(m)
HSH01	200	12.03	200	1	Airlift test	≈200	–
HSH02	200	12.03	200	1	Pump test	≈200	–
		12.03	200	2	Pump test	≈100	
HSH03	201	12.03	201	1	Pumping test	≈200	
HSH03		29	198.7	1	Flow logging		≈2 , anomalies 0.5
HSH03		12.03	103	1	Pumping test	≈100	
HSH03		80.5	201	1	Injection test	≈100	
HSH03		12.03	201	1	Step-drawdown test (after hydr.fract)	≈200	

After completion of the drilling, the Posiva Flow Log (PFL) was generally applied in the cored borehole. The section logging (PFL-s) was made with a test section length of 5 m and a step length of 0.5 m (5/0.5), with the purpose to measure transmissivity in 5 m sections and to indicate flowing sections with a resolution of 0.5 m, useful for planning the hydrogeochemistry sampling and the flow-anomaly logging. The flow-anomaly logging (PFL-f) was made with a test section length of 1 m and a step length of 0.1 m (1/0.1) when moving the test section along the borehole, with the purpose to identify individual flowing fractures. The flow logging (1/0.1) logging was performed where (5/0.5) logging identified flow anomalies. Estimates of transmissivity based on PFL-s are based on two established heads (or drawdowns) (h_1, h_2). The head h1 is established without pumping (h_1 = undisturbed water level in borehole) and h_2 with pumping (h_2 generally = h_1–10 m) in the borehole associated with two corresponding flow rates (Q_{s1}, Q_{s2}) from the test section. If the upper measurement limit of the flow rate is reached in a test, the test in that test section is later repeated with a smaller drawdown.

The flow-anomaly logging, PFL-f, is only performed with one head (h_2) and and the fracture flow (Q_{f2}) is measured, therefore the h_1 and flow Q_{f1} must be aproximated as follows. The same h_1 as for the corresponding section with (5/0,5) measurement, that straddles the flow anomaly, is used as well as setting $Q_{f1}=Q_{s1}$, if Q_{s1} was possible to estimate for the section. If no value was possible to estimate it is assumed that $Q_{f1}=0$.

Thiems equation /e.g. in Kruseman and de Ridder, 1991/ is used to calculate the transmissivity (T_s for PFL-s representing a 5 m section and T_f for PFL-f representing a fracture, or hydraulic feature, that is rather distinct, within a dm or so, in the borehole) and the undisturbed hydraulic head in the formation outside the test section (h_s for PFL-s and h_f for PFL-f). If Q_{f1}=0 only the fracture (or hydraulic feature) transmissivity (Tf) is estimated. It is assumed that the influence radius divided by the borehole radius is can be approximated to 500 (corresponding to influence radius of 19 m with a borehole with diameter 0.076 m. It is thus assumed that undisturbed formation pressure exists at a radial distince of c. 19 m). As a steady state solution is used the evaluated transmissivity may be affected by a skin factor.

(A test employing the same test section length and step length as well as two draw downs, has been called “sequential flow logging with PFL” and tests with a step length smaller than test section length as PFL-o have been denoted “overlapping flow logging with PFL” in some earlier reports).

In the first two boreholes, KSH01A and KSH02A, two flow rates were only measured for even 5 m sections (step length of 5 m used) for PFL-s.

Subsequently, injection tests with the Pipe String System (PSS) were made starting with 100 m test section, then 20 m sections within all 100 m sections with flow rates above the measurement limit and then 5 m sections in the borehole section 300–700 m in all 20 m sections with flow rates above measurement limit. The 20 and 5 m sections not measured for the above reason were assigned the value of the measurement limit of the specific capacity (Q/s) for the 100 m and 20 m sections, respectively. These Q/s values were then applied in the steady state solution by /Moye, 1967/ to estimate a measurement limit as a transmissivity value. The tests were evaluated as transient tests giving Transmissivity (T_T) and skin factor (assuming a storage coefficient S=1E–6). Steady state evaluation of transmissivity (T_M) based on /Moye, 1967/ was also made. If it was not possible to evaluate T_T, the T_M values were used as “best choice” for the test section in question.

The drilling process and the tests during drilling in cored boreholes are described by /Ask et al. 2003, 2004a,b/. The drilling and some simple hydraulic tests in percussion boreholes were reported by /Ask, 2003/. Hydraulic tests after drilling in HSH03 were reported by /Ludvigson et al. 2003; Svensson, 2003/ and the PFL measurements by /Rouhiainen, 2000; Rouhiainen and Pöllänen, 2003a,b, 2004/. PSS tests were reported by /Rahm and Enachescu, 2004a,b,c/ and /Ludvigson et al. 2004/. Evaluation methods and data are presented in those reports.

Overview of results from hydraulic tests

In Figure 8-2 through Figure 8-4 the results from the PFL-f is show together with Boremap data (open fractures, partly open fractures and crush zones) and the interpreted rock domains and deformations zones. In the coremapping each fracture is classified as “Sealed”, “Open” or “Partly open” and with a judgement of how certain the geologist is of this classification – expressed as “Certain”, “Probable” and “Possible”. “Partly open” refers to observations of the borehole wall with BIPS that indicates being on the edge of a fracture – these observations are few. The existence of a PFL flow anomaly is classified as “certain” or “uncertain”. Both the core mapped data and the PFL anomalies are rigorously length corrected and it is expected that the positions of objects along the boreholes normally can be correlated to within 0.1 m. As a first assumption when correlating core-mapped data and flow anomalies, all open and partly open fractures as well as crush zones are assumed to be possible flowing features. In most cases one or several open fractures were identified within 0.2 m from a given flow anomaly. Only in a few cases no “open fractures”, “partly open fractures” or “crush zones” could be linked to within 0.5 m of a flow anaomaly, probably indicating that a fracture mapped as “sealed” should have been classified as “open”. In such cases one could generally find “sealed fractures” classified as “Probable” or “Possible” near the flow anomaly.

As the flow-anomalies in most cases could be correlated to individual open fractures, assigned fracture properties, e.g. orientation can be coupled to the flow anomaly. Figure 8-1 illustrates a fracture system coupled to a flow anomaly. The uncertainty classification of fractures and flow anomalies also opens up for sensitivity analysis. This is to be focus of future work. Details of this evaluation are presented in /Forsman et al. 2005/. The data shown in Figure 8-2 through Figure 8-4 have been the main input data for the HydroDFN model presented in Section 8.3.

In Figure 8-5 through Figure 8-8, the results from some of the PSS injection- and pumping tests are shown together with interpreted rock domains and deformation zones from the geological model (see Chapter 5). In Appendix 5 all PSS measurements are shown as transmissivity as well as hydraulic conductivity. In this context "T-BC" stands for "Transmissivity – best choice"; If a transient evaluation is available for a test section this value is used as representative (best choice) value for the section, otherwise the steady state value (T-Moye) is used. The PSS measurements in KSH01A (Figure 8-2 and Figure 8-5) can here be compared with the PFL measurements, and as can be seen the correspondence is good.

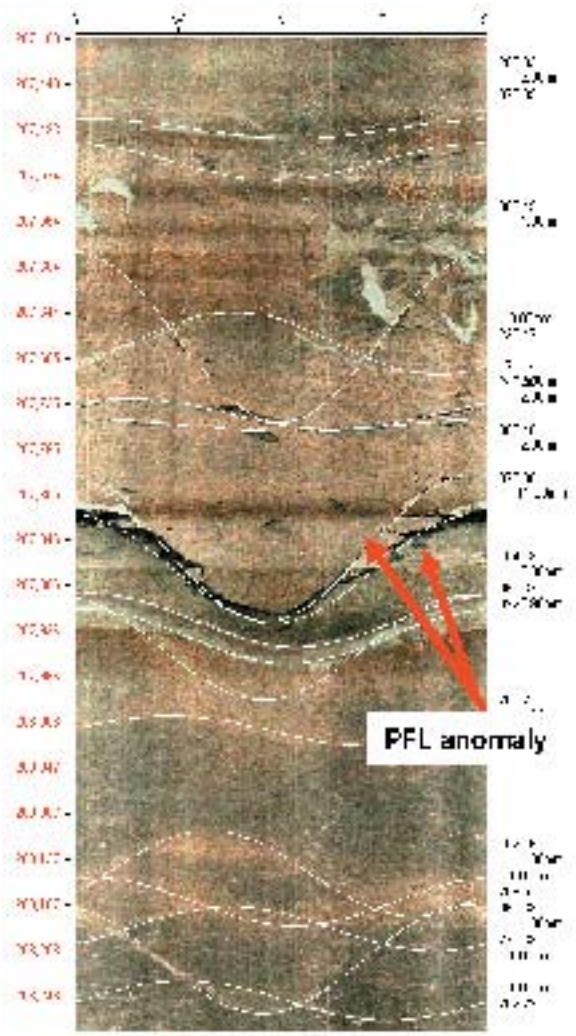

Figure 8-1. *Close-up of BIPS image of a borehole section in borehole KSH01A. Shown object: T (m_2/s) = 1.72E–7 Generally open fractures cannot be seen in BIPS as in the example above. White lines represents different mapped objects as open and sealed fractures, rock contacts etc. /Forsman et al. 2005/.*

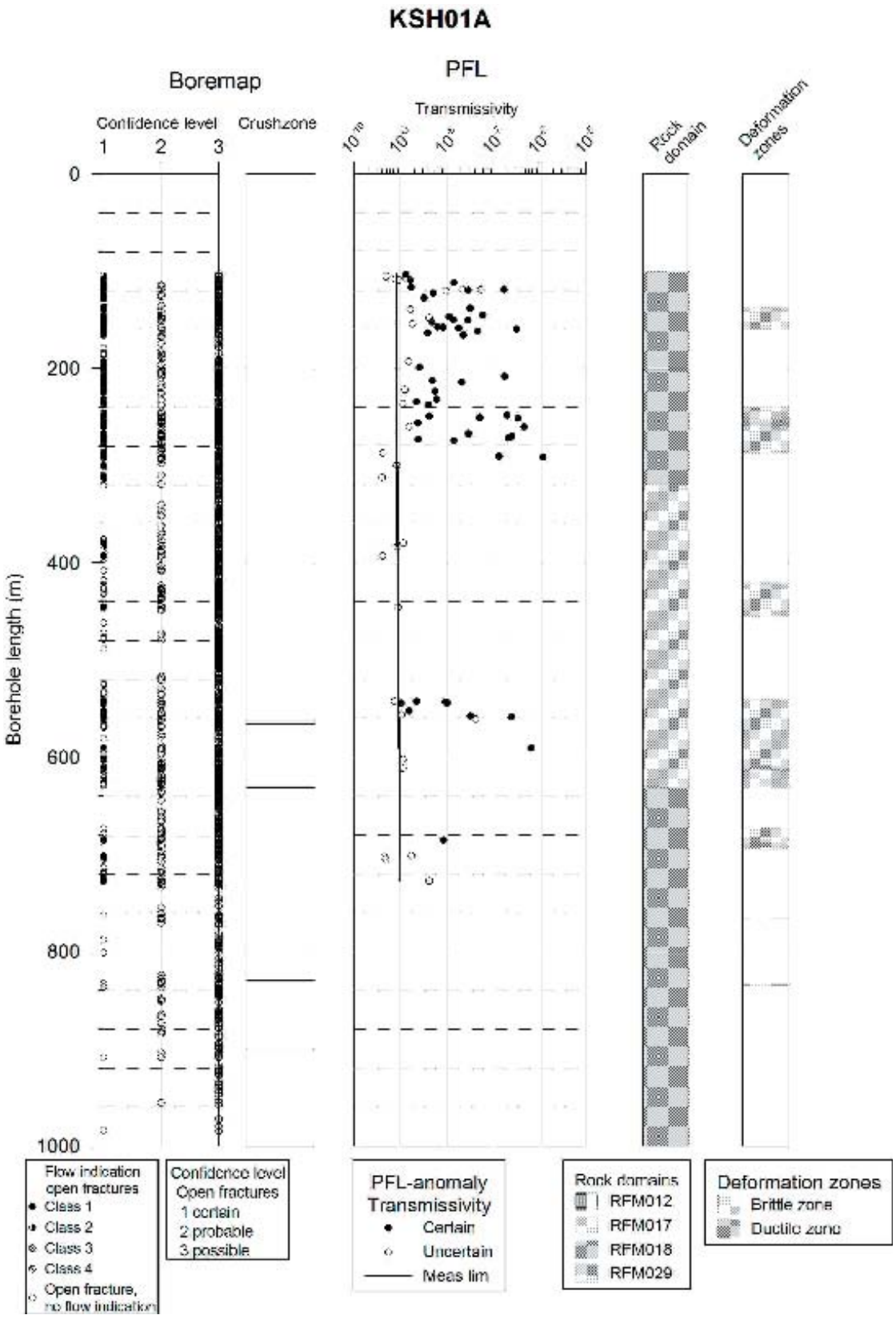

Figure 8-2. *Transmissivity of hydraulic features of borehole KSH01A based on PFL-f data, Boremap data (open fractures, partly open fractures and crush zones) and the interpreted rock domains and deformations zones /Forsman et al. 2005/.*

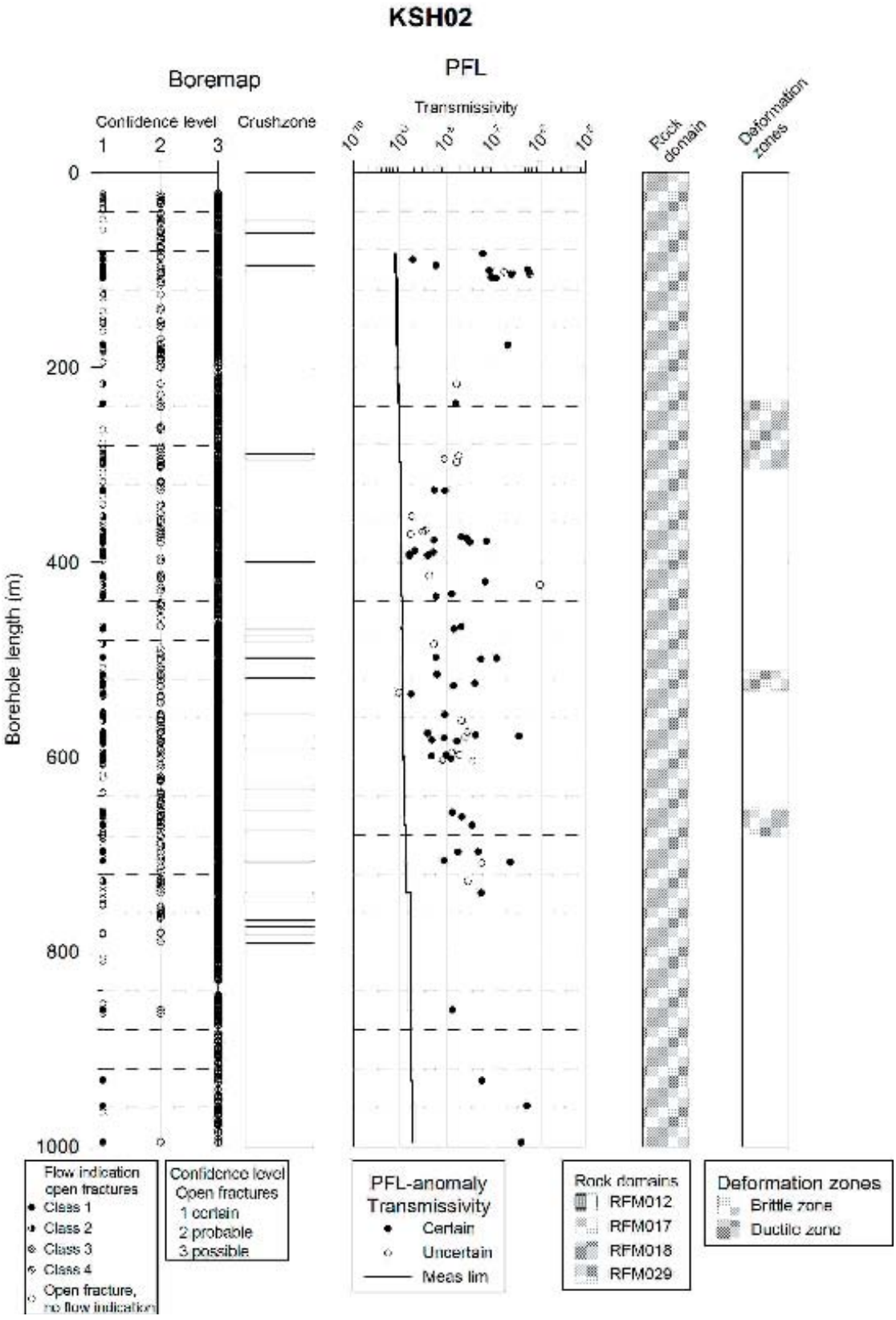

Figure 8-3. *Transmissivity of hydraulic features in borehole KSH02 based on PFL-f data, Boremap data (open fractures, partly open fractures and crush zones) and the interpreted rock domains and deformations zones /Forsman et al. 2005/.*

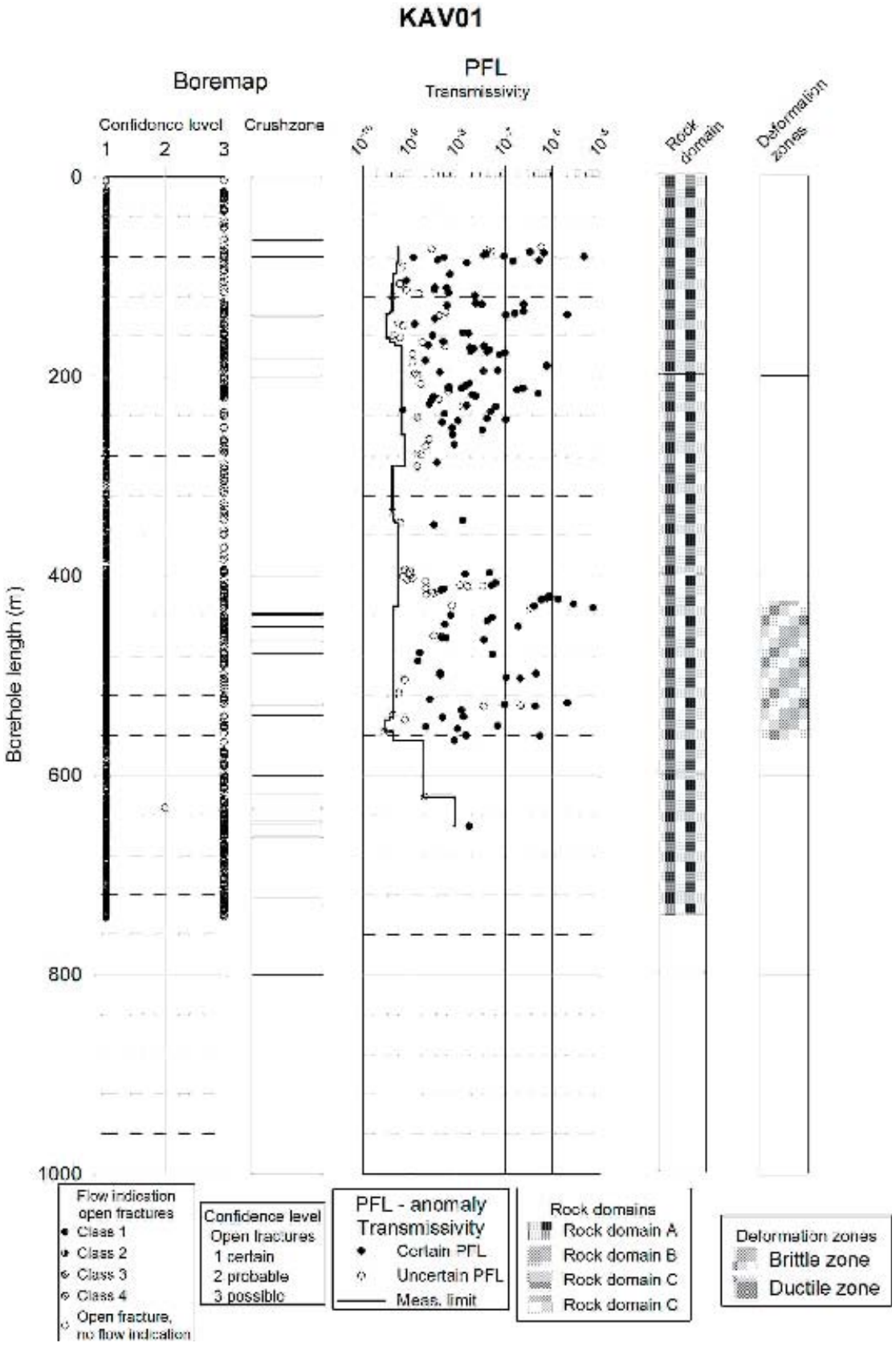

Figure 8-4. *Transmissivity of hydraulic features of borehole KAV01 based on PFL-f data, Boremap data (open fractures, partly open fractures and crush zones) and the interpreted rock domains and deformations zones /Forsman et al. 2005/.*

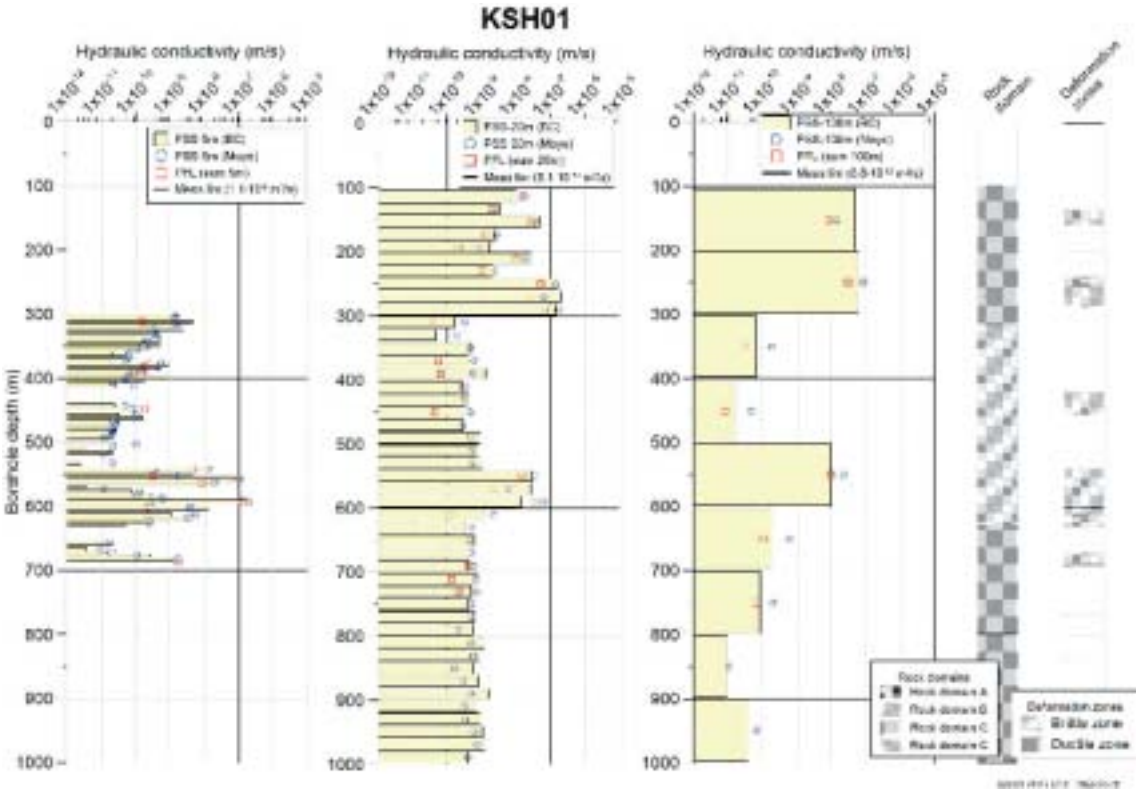

Figure 8-5. *Hydraulic conductivity of borehole KSH01A based on PSS data and evaluated rock domains and deformation zones. (Borehole depth: length along the borehole.)*

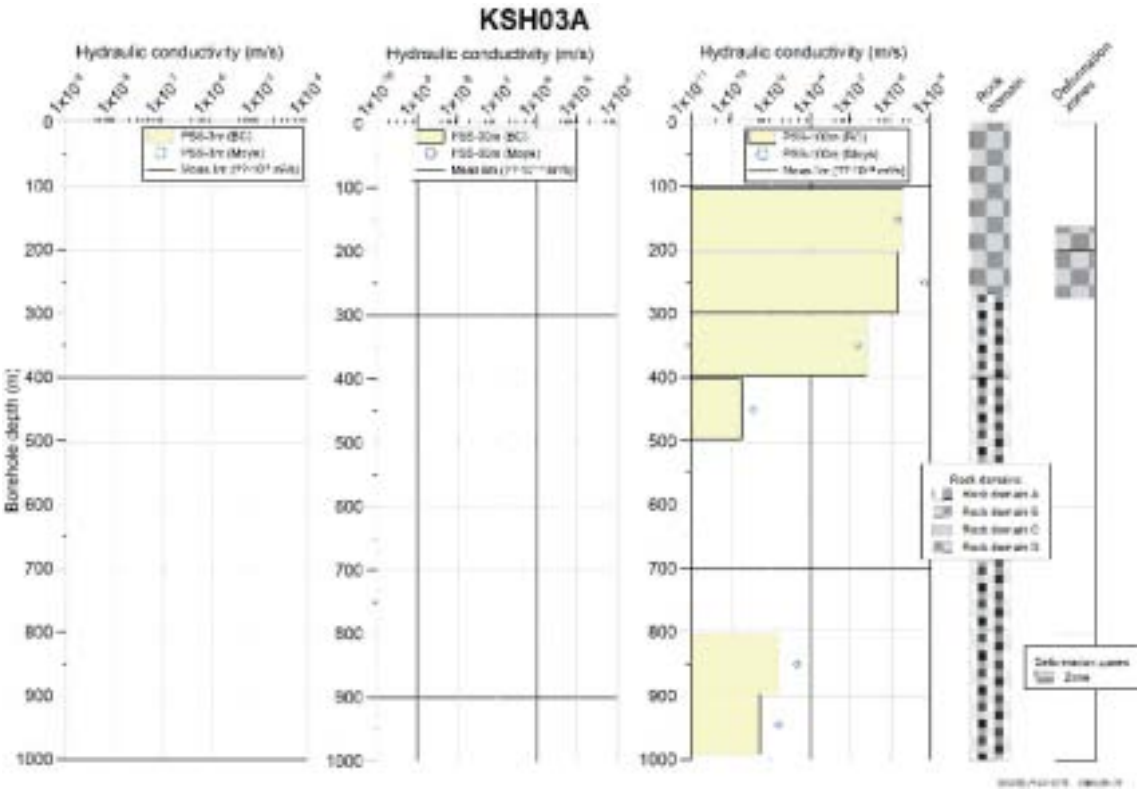

Figure 8-6. *Hydraulic conductivityof borehole KSH03A based on PSS data and evaluated rock domains and deformation zones. (Borehole depth: length along the borehole.)*

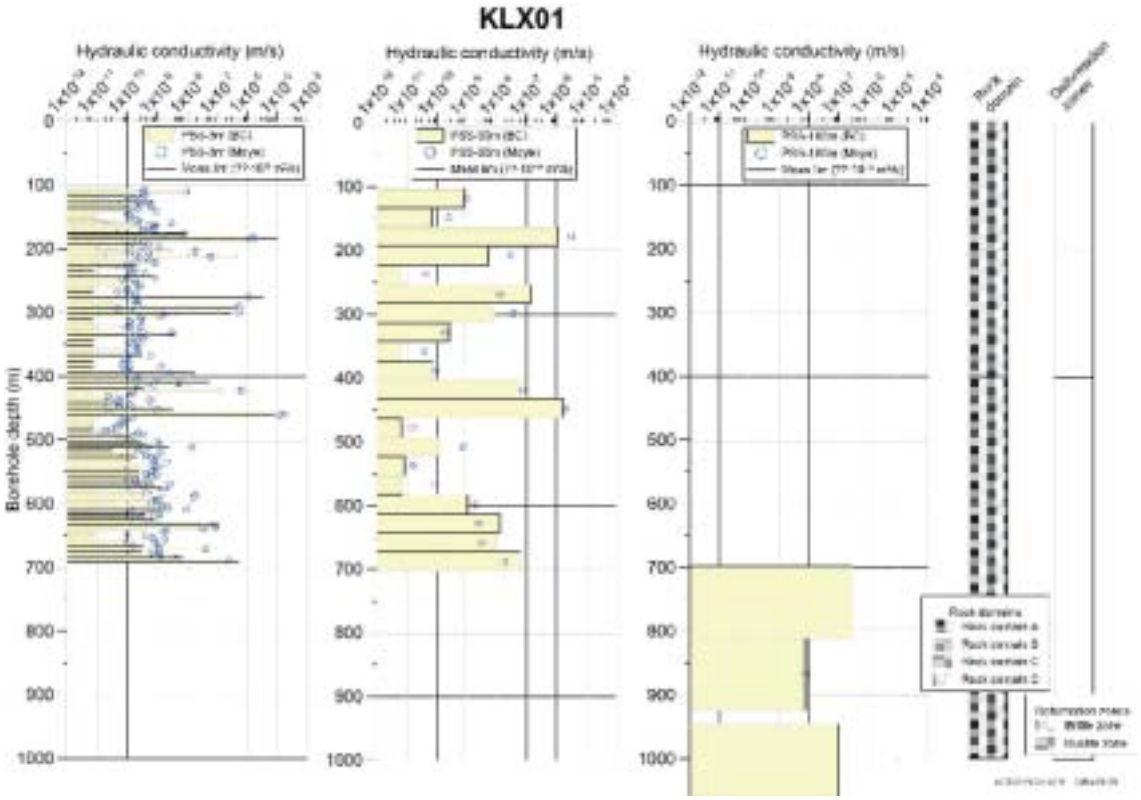

Figure 8-7. *Hydraulic conductivityof borehole KLX01 based on PSS data and evaluated rock domains and deformation zones. (Borehole depth: length along the borehole.)*

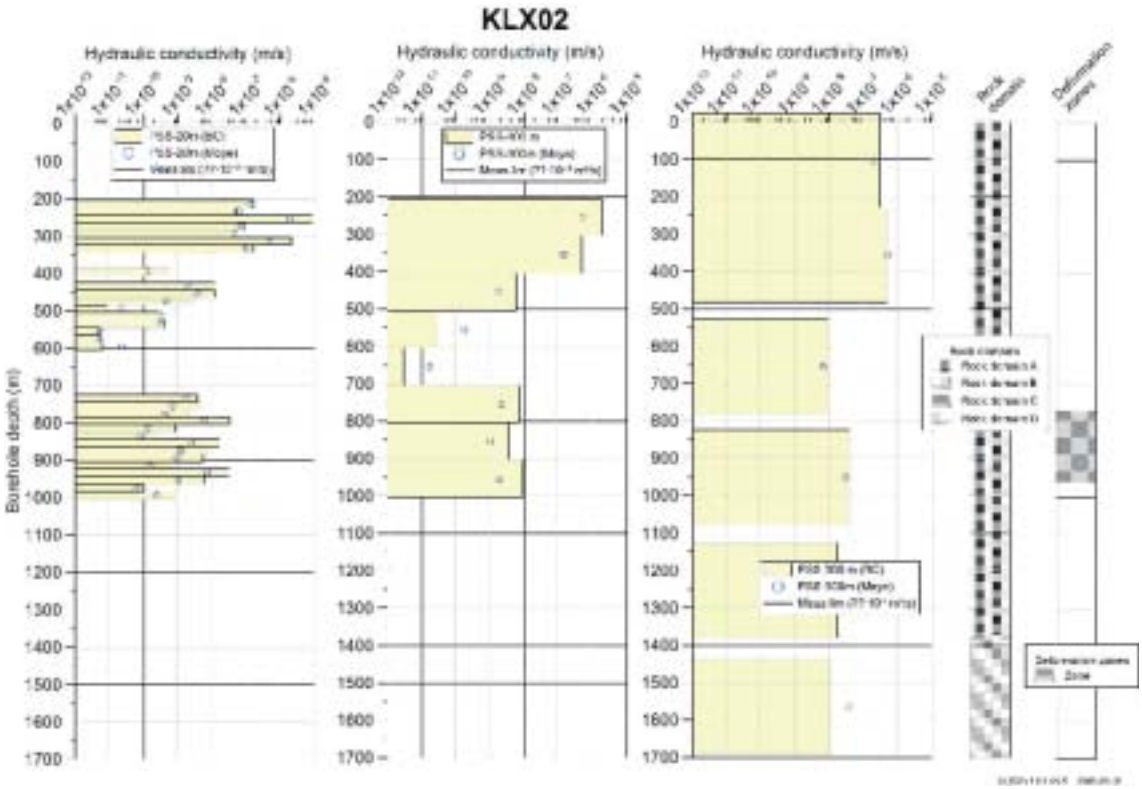

Figure 8-8. *Hydraulic conductivity of borehole KLX02 (20 m/100 m) based on PSS data and evaluated rock domains and deformation zones. (Borehole depth: length along the borehole.)*

Comparing test methods and evaluation methodologies

The flow logging with PFL is performed in two modes as decribed above. The evaluated transmissivities for the individual hydraulic features (PFL-f) were summed up to the corresponding 5 m sections measured by PFL-s and are shown in Figure 8-9. As can be seen, the PFL-s compare well with the PFL-f summed transmissivities for the individual hydraulic features. The simplified approach for PFL-f appears to be accurate.

The transmissivities evaluated from PFL have also been compared to transmissivities from PSS data. In boreholes KSH01A and KSH02 all tests or loggings are length-corrected giving high accuracy of the position of individual tests in the boreholes. Transmissivity evaluated using /Moye, 1967/ (T_M) from PSS is compared with the evaluated transient transmissivities (T_T) from PSS and the summed transmissivities from the hydraulic features based on PFL-f, see Figure 8-10. Despite use of different test methods and different evaluation methods, most of the transmissivities plot close to the 1:1 line within 0.2 to 5 of the value on the x-axis. The transmissivity estimates therefore seem robust.

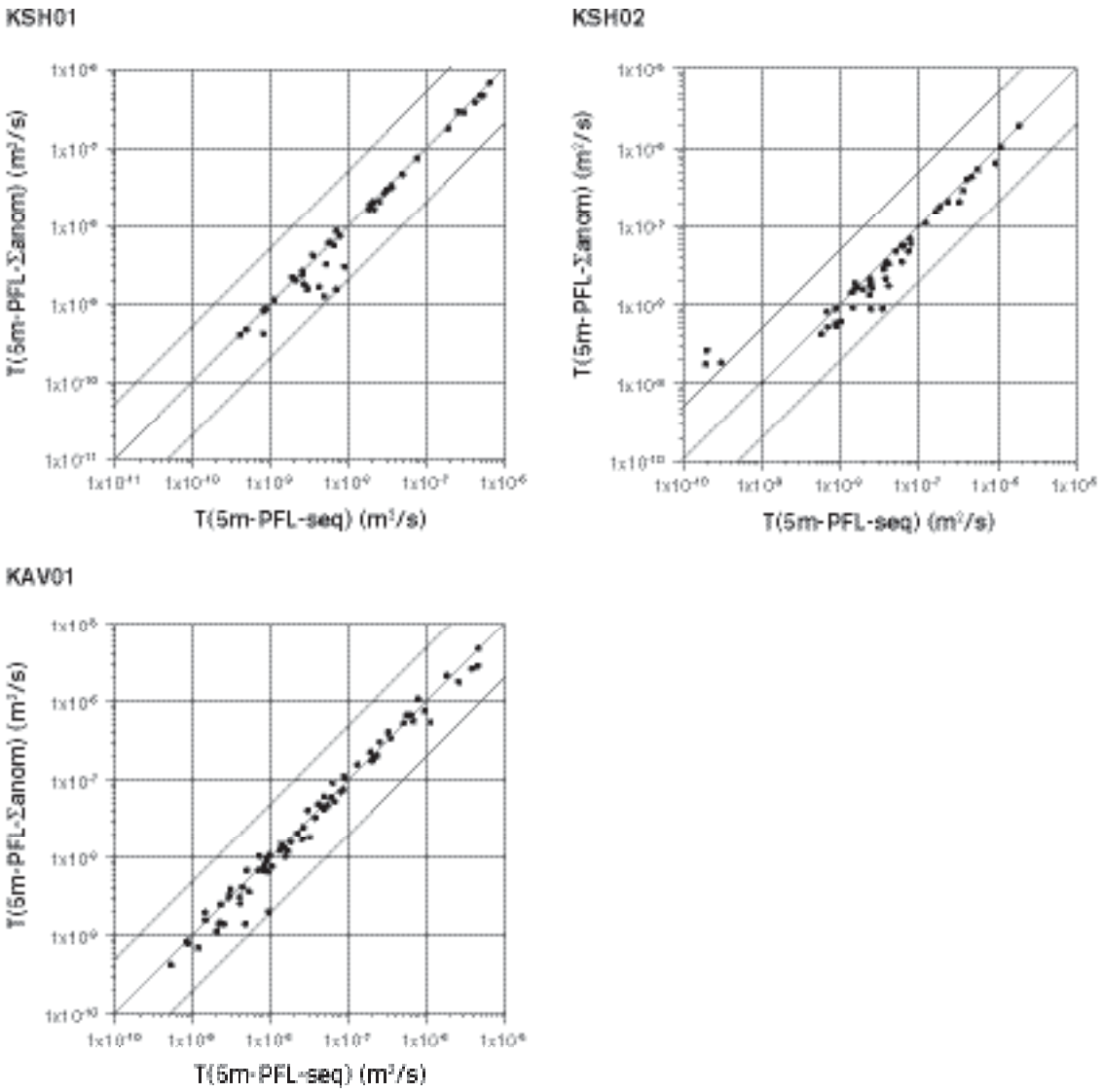

Figure 8-9. *Cross plott of transmissivity from PFL: Transmissivities evaluated for 5 m sections, section logging (PFL-s) (T(5 m-PFL-seq)in the plot) versus transmissivities for the individual hydraulic features (PFL-f) summed up to 5 m sections (T(5 m-PFL-Σ anom) in the plot). (The bounding lines to the 1:1 line: 0.2 and 5 times 1:1 value.)*

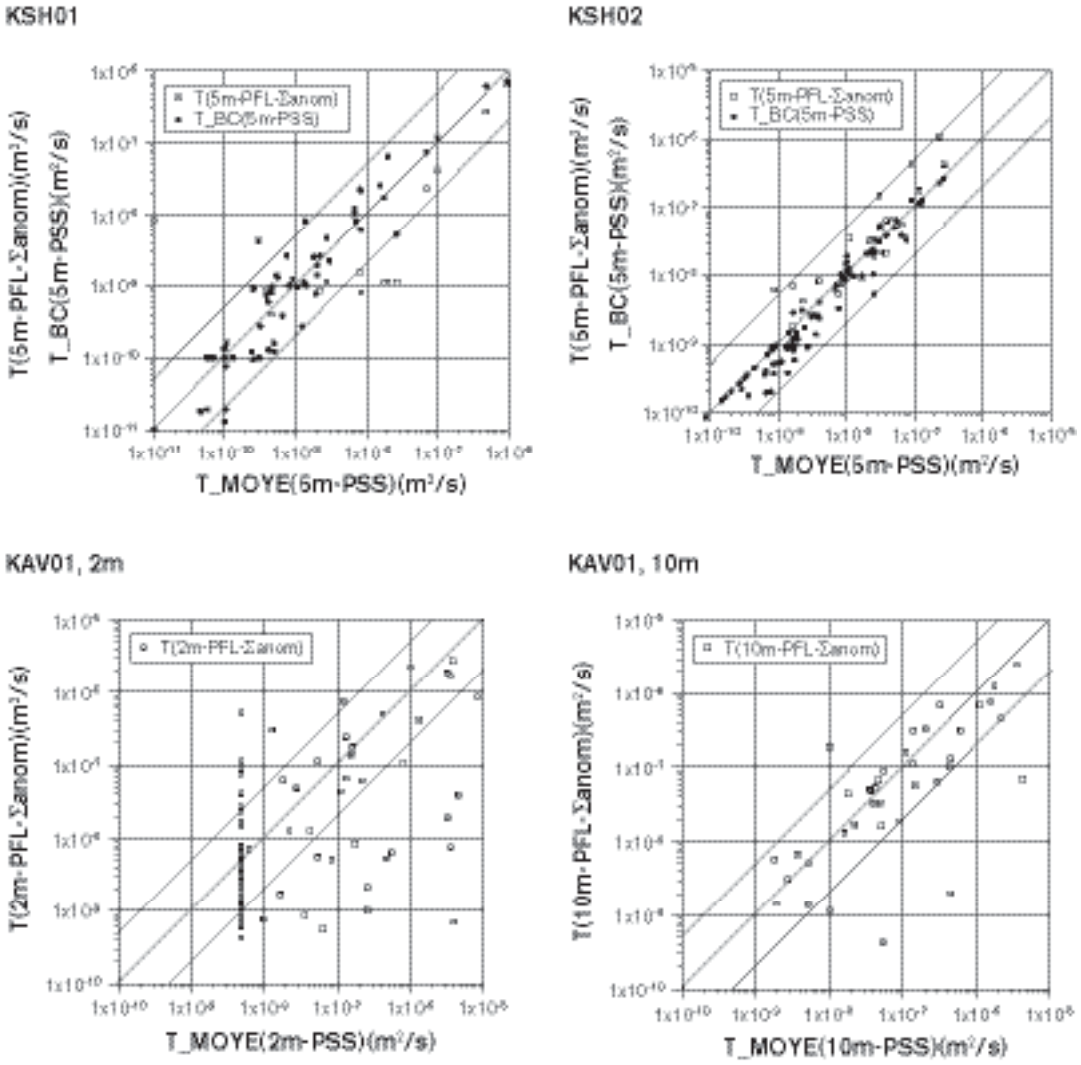

Figure 8-10. *Cross plott of transmissivity PFL vs. PSS: Transmissivitis based on PSS data and steady state evaluation ((T_Moye) in the plot) versus transmissivities for the individual hydraulic features (PFL-f) summed up to 2, 5 or 10 m sections (PFL-f) (T(Xm-PFL-Σanom) in the plot) and transmissivities based on PSS and transient evaluation ((T-BC(5 m-PSS)) in the plot). (The bounding lines to the 1:1 line: 0.2 and 5 times 1:1 value.)*

The injection tests in borehole KAV01 were made before the site investigations began and no length correction can be applied to these data. This is interpreted as being the main reason for the large scatter noted for this borehole. Comparing the tests in 10 m sections, however, shows that the transmissivities correspond rather well.

Statistics of single hole test results – general

Data from the hydraulic tests performed in the cored boreholes have been compiled and univariate statistics have been calculated and compared with data from other cored boreholes in the Simpevarp area, where similar tests have been conducted.

Hydraulic conductivity (or transmissivity) evaluated from hydraulic tests with the same test section length often fit rather well to a lognormal distribution. When the test section length decreases, the number of tests below the lower measurement limit increases. The data set is henced “censored”, which has to be taken into account when choosing a statistical distribution that should describe the measured values above the measurement limit as well as possible. Below the measurement

limit the fitted distribution can predict the properties, but of course it is not known whether it is a good prediction. When performing modelling based on the fitted distribution it has to be decided if extrapolation is reasonable and if there also is a lower limit (below the lower measurement limit) for the property in question due to e.g. conceptual considerations. In crystalline rock, the matrix permability sets the limit, cf. e.g. /Brace, 1980/.

The standard procedure in describing the hydraulic material properties from single-hole test data is to fit the logarithm of the data to a normal distribution, also taking the censored data into account. The associated statistics normally include the mean and standard deviation (std) of Y, $Y=\log_{10}(X)$, X = hydraulic conductivity (K) or transmissivity (T), where the mean of $\log_{10}(X)$ corresponds to the geometric mean of X. Occasionally, the number of measurements below the lower measurement limit is greater than the number above the measurement limit, and it is here argued that the methodology above (fitting the statistical distribution to values above the lower measurement limit, but also just values below the upper measurement limit (if there exist such data) – the "known values"). is an appropriate way by which to describe a dataset with censord values. Instead of a lognormal distribution a power law may work equally well. This has not been tested here.

Statistics of single hole tests

In Table 8-7 through Table 8-10 the univariate statistics are shown for the PFL-s and PSS tests for each borehole. In Appendix 5 details of the statistical distributions are shown and in Figure 8-11 an example of distributions for the PFL-s measurements are shown.

The difference flow logging (PFL-f) conducted in borehole KSH01A indicates that the rock is of very low transmissivity below the casing shoe at c. –100 masl. Out of a total of 179 test intervals, only 46 intervals were found to yield a flow above the lower measurement limit of the test equipment, corresponding to a hydraulic conductivity of approximately K=8 E–11 m/s (T=4 E–10 m^2/s) in this particular borehole /Rouhiainen and Pöllänen, 2003a/. The "theoretical" lower measurement limit for PFL (under optimal conditions) is estimated at c. T=1.7 E–10 m^2/s, based a minimum flow rate of 6 mL/h, 10 m drawdown and 19 m influence radius applied in Thiems equarion. (Theoretical measurement limit outlined in /Pöllänen et al. 2004/). Due to effects of fine particles or gas in the water-filled borehole, the measurement limit that is considered in the evaluation is in general higher and may vary along the borehole. In boreholes KSH02, KAV01 and KLX02 135, 58 and 276 sections, respectively, were below the measurement limit and the measurement limit varies between and along the boreholes, see Figure 8-2 through Figure 8-4.

The measurement limit for PSS is more stable and generally lower than that for PFL-s. The tests using PSS are therefore essential, especially for confirming the conductivity of the rock in the lower transmissivity range.

Table 8-7. Univariate statistics for hydraulic tests performed in cored boreholes (Method employed: PFL-s, Section Posiva Flow Logging) (K: m/s).

Bore hole	Test type	Secup (m)	Seclow (m)	Test scale (m)	Sample size	Lower meas. limit[1], [2] Log10 K (m/s)	Mean Log10 K (m/s)	Std Log10 K (m/s)
KSH01A	PFL-s	102.79	997.98	5	179	(–10.5)	–11.2	2.06
KSH02	PFL-s	81.52	997	5	183	(–10.5) – (–10)	–9.9	1.47
KAV01	PFL-s	71.40	732.26	5	132	(–10.1) – (–8.8)	–9.3	1.58
KLX02	PFL-s	205.92	1,399.92	3	398	(–10) – (–8.3)	–9.9	1.34

[1] Measurement limit estimated from field results. The measurement limit may vary along the borehole.

[2] PFL-s: Theoretical lower measurement limit (under optimal conditions) is K=3.3E–11 m/s (Log_{10}(K(m/s))=–10.5) for test section length 5 m (or rather T=1.7E–10 m^2/s).

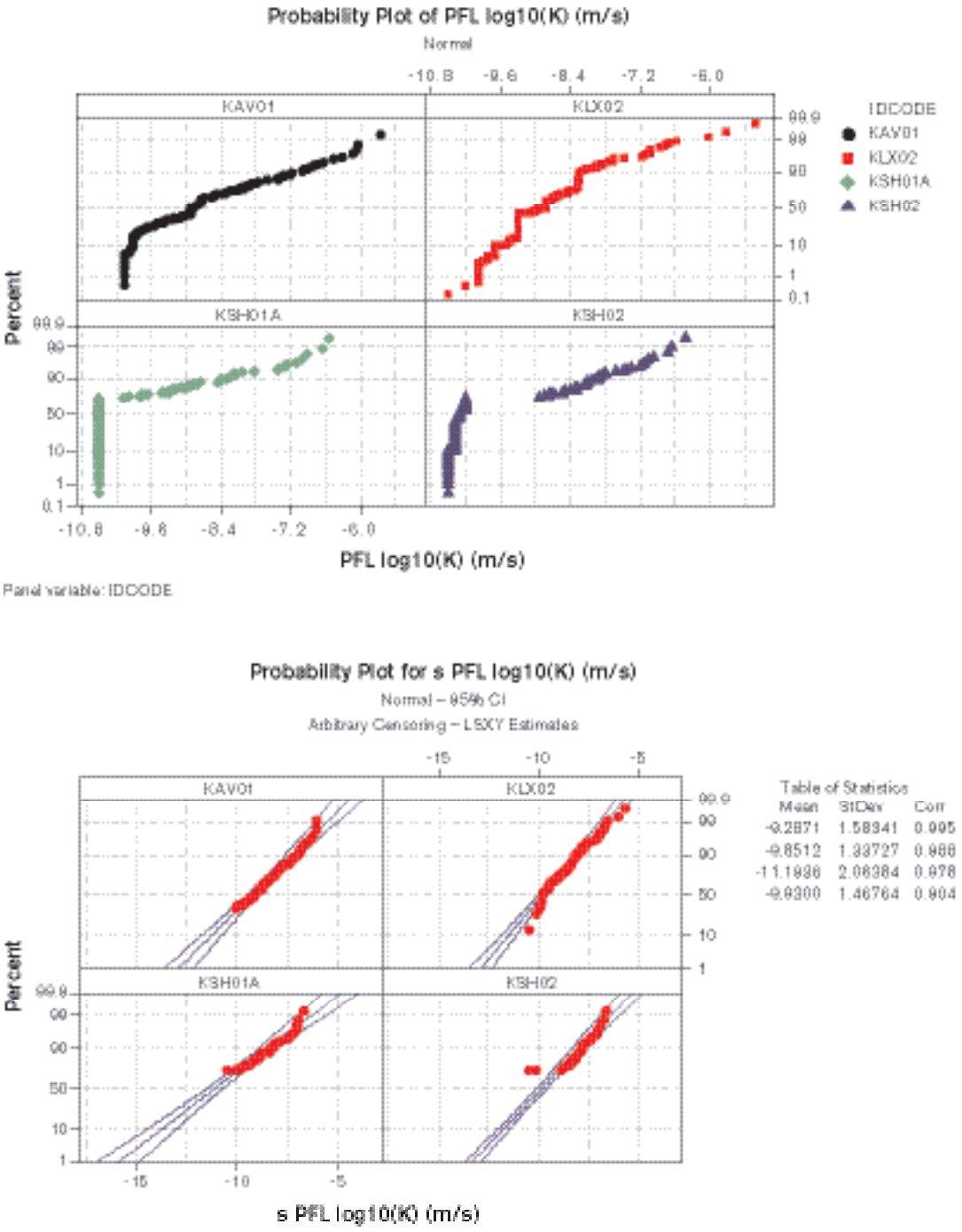

Figure 8-11. *Hydraulic conductivity based on PFL-s data from boreholes KAV01, KLX02, KSH01A and KSH02 (individual sample size are given in Table 8-5), Top: all measurement includingvalues at the measurement limit. Bottom: Fitted distributions. Values at measurement limit are not plotted.*

Table 8-8. Univariate statistics for hydraulic tests performed in cored boreholes. Method employed: PSS.

Borehole	Test type	Secup	Seclow	Test scale	Sample size	Lower meas. limit[1] Log10 K	K Log10(K)	Mean Log10 K	Std Log10 K
		(m)	(m)	(m)		(m/s)	(m/s)	(m/s)	(m/s)
KSH01A	PSS	300	700	5	81	(–11.7)		–10.4	1.51
	PSS	103	999	20	45	(–10.4)		–8.8	0.76
	PSS	103	999	100	9	(–11.2)		–9.7	1.53
	Pump t.	12.1	1,003	1,000	1	–	–8.6		
KSH02	PSS	301.50	701.50	5	80	(–10.8) – (–9.7)		–9.4	0.99
	PSS	81.50	961.50	20	45	(–10.4)		–9.2	1.06
	PSS	101.50	997	100	9	(–11.2)		–8.8	0.68
	Pump t.	80	1,001.11	1,000	1	–	–8.5		
KSH03A	PSS	102.5	995	9	9	(≈ –12)		–9.7	3.63
KAV01	PSS[2]	22.6	438.5	2	175	(–8.6)		–9.1	1.81
	PSS[2]	20	710	10	69	(–10.7)		–8.5	1.69
	Pump t.	70.4	757.31	≈1,000	1		–7.25		
KAV02	PSS[2]	13.5	94.5	2	41	(–8.4)		–7.2	1.69
KAV03	PSS[2]	10	225	10	22	(–10.7 ?)		–6.3	1.47
KLX01	PSS[2]	106	691	3	197	(–11.1)		–10.6	2.06
	PSS[2]	103	702.11	30	20	(≈ –12)		–9.3	2.14
	PSS[2]	701	1,077.99	100	3	(≈ –12)		(–7.6)	(1.3)
	Pump t.	101.3	702.11	≈1,000	1		–6.9		
KLX02	PSS	300	545	5	49	(–11.7) – (–9.5)		–11.2	2.50
	PSS	204	1,004	20	48	(–11.3) – (–10.8)		–9.7	2.08
	PSS	204	1,004	100	8	(≈ –11.7)		–8.34	1.78
	PSS[3]	0	1,700.5	100–300	11	(≈ –11)			
	Pump t.	202.95	1,700.5	≈1,000	1		–7.1		

[1] Measurement limit estimated from field data.

[2] Old data from tests made with equipment similar to PSS.

[3] Old test data + new PSS test data.

Table 8-9. Compilation of data from boreholes at Äspö from /Rhén et al. 1997b/.

Bore hole	Test type	Secup	Seclow	Test scale	Sample size	Lower meas. limit[1] Log10 K	Mean Log10 K	Std Log10 K
		(m)	(m)	(m)		(m/s)	(m/s)	(m/s)
KAS02–KAS08	Inj.test	c. 100	500–800	3	1,105		–7.8 to –9.7	1.12 to 2.08

[1] Measurement limit estimated from field results.

Table 8-10. Univariate statistics for hydraulic tests performed in percussion-drilled boreholes. Methods used: HTHB-p: Pumping test or injections test, HTHB-f: flowlogging, cf. Table 8-1.

Borehole ID	Test type	Upper limit in bh	Lower limit in bh	Test scale	Lower meas. limit[1]	Sample size	K Log10(K)	K Mean Log10K	K Std Log10K
		Secup (m)	Seclow (m)	(m)	(m/s)		(m/s)	(m/s)	(m/s)
HSH01, 02, 03[1]	HTHB-p	12	200	≈200	≈2 E–8	3		(–8.3)	(1.2)
HSH01	HTHB-p	12	200	≈200	–	1	–8.9		
HSH02	HTHB-p	12	200	≈200	–	1	–7.8		
HSH03	HTHB-p	12	201	≈200	≈2 E–8	1	–7.1		

[1] Mixed tests: airlift tests and pumping tests. Parameters evaluated from airlift tests are regarded as being uncertain.

[2] Preliminary values.

Only one percussion-drilled borehole, HSH03, was tested with HTHB, cf. Table 8-6. The other two percussion boreholes, HSH01 and HSH02, were judged as being low-conductive from the flushing after drilling, and only rough values of the specific capacity Q/s are available. In borehole HSH03, one major hydraulic anomaly at a depth of 58.5–59.5 m and one minor anomaly at a depth of 53–56 m were observed.

/Rhén et al. 1997b/ estimated a geometric mean K=1.6E–8 m/s with a standard deviation ($Log_{10}K$) of 0.96 for well data obtained from the well archive of the Swedish Geological Survey (area approximately corresponding to the NE part of the municipality of Oskarshamn) and percussion holes located at Äspö, Ävrö, Mjälen. Hålö and Laxemar. The test scale was approximately 100 m. Subsequently, /Follin et al. 1998/ estimated a geometric mean K=6.3E–8 m/s for wells sunk in the bedrock within the municipality of Oskarshamn as found in the SGU well archive. The test scale in this case varied between 10 and 100 m. Both analyses included wells intercepting fracture zones, if present.

8.2.2 Hydraulic evaluation of interference tests

No new interference tests were available for the Simpevarp 1.2 modelling.

8.2.3 Joint hydrogeology and geology single hole interpretation

As part of the geological single-hole evaluation, borehole sections with deformation zones (DZ) were identified. Lithological Rock Domains (RD) along the borehole were also identified. A few of the deterministically modelled deformations zones intersect some of the tested boreholes and are also included in the analyses of the deformation zones below. As test scales of 10, 20 and 30 m cover the most part of the borehole lengths, these test scales have been used to estimate properties of the RDs, with or without DZ, see Table 8-11and Appendix 5.

The geometric mean of the hydraulic conductivity (K) of the deformation zones (mostly considered brittle, that is “fracture zones”, but some are considered as “ductile”, see Figure 8-2 trough Figure 8-8) is about ten times higher than that of the surrounding rock. According to /Bergman et al. 1999/ the “fracture zones” in the Götemar granite in the depth interval 300–600 m are interpreted to have 100–1,000 times greater hydraulic conductivity than the surrounding rock.

Defined rock domains have almost the same geometric mean value, but the standard deviation differs considerably. The difference in hydraulic properties between the rock domains is relativly small such that it is not considered relevant to defines several HRDs at this stage of the investigations.

Table 8-11. Univariate statistics for hydraulic tests performed in cored boreholes. Hydraulic conductivity is shown for Rock Domains (RD) excluding borehole sections with interpreted deformation zones (No DZ) and for parts of the boreholes corresponding to Deformation zones (DZ) interpreted in the single-hole geological evaluation. (DZs in this analysis include both the minor ones from the single-hole geological evaluation and those deterministically interpreted, included in the deformation zone model, cf. Chapter 5.

Bore hole	Test type	RD	DZ/ No DZ	Test scale	Sample size	Lower meas. limit[1], Log10 K	Mean Log10 K	Std Log10 K
				(m)		(m/s)	(m/s)	(m/s)
KSH01A, KSH02, KLX01, KLX02, KA01, KAV03	PSS[2]	A	No DZ	10.20.30	120	(–12) – (–10.4)	–8.9	2.18
KSH01A, KSH02, KLX01, KLX02, KA01, KAV03	PSS[2]	A	DZ	10.20.30	39	(–10.4) – (–10)	–7.8	1.62
KSH01A, KSH02, KLX01, KLX02, KA01, KAV03	PSS[2]	B	No DZ	10.20.30	45	(–12) – (–10.4)	–9.2	1.0
KSH01A, KSH02, KLX01, KLX02, KA01, KAV03	PSS[2]	B	DZ	10.20.30	16	(–10.4) – (–10)	–9.2	0.97
KSH01A, KSH02, KLX01, KLX02, KA01, KAV03	PSS[2]	C	No DZ	10.20.30	20	(–12) – (–10.4)	–9.0	0.41
KSH01A, KSH02, KLX01, KLX02, KA01, KAV03	PSS[2]	C	DZ	10.20.30	9	(–10.4) – (–10)	–8.3	1.32
KSH01A, KSH02, KLX01, KLX02, KA01, KAV03	PSS[2]	A+B+C	No DZ	10.20.30	185	(–10.4) – (–10)	–9.0	1.84
KSH01A, KSH02, KLX01, KLX02, KA01, KAV03	PSS[2]	A+B+C	DZ	10.20.30	64	(–10.4) – (–10)	–8.2	1.54

[1] Approximate measurement limit estimated from field results.

[2] Old test data + new PSS test data.

8.3 Hydrogeological model – general conditions and concepts

This section describes the modelling strategy and conceptuel models used. It forms the basis for the hydrogeological modelling presented in the following sections.

8.3.1 Modelling objectives and premises

The hydrogeological descriptive model should provide data that are useful for variable-density groundwater flow modelling. More specifically, groundwater flow models should be able to simulate groundwater flow within a given volume under natural (undisturbed) conditions. Hydrogeological modelling, that includes the fully open or back-filled deep repository is subsequently carried out by Repository Engineering and Safety Assessment. In the undisturbed system, the flow paths to the potential repository area are of interest, as they provide a description of the rate at which potential corrodants are introduced. Likewise, the flow paths from the recharge areas to the

potential repository area within the modelled volume are important for a reasonable assessment the paleo¬hydrogeological evolution and hydrogeochemical interpretation, while the flow paths from the repository area to discharge areas are important for Safety Assessment. Of particular importance in this context is the shoreline displacement which must be taken into account when modelling the long-time evolution of the groundwater flow (and chemical evolution).

The numerical groundwater flow modelling serves three main purposes:

- Model testing: Simulations of different major geometric alternatives or boundary conditions in order to disprove a given geometric interpretation or boundary condition, and thus reduce the number of alternative conceptual models of the system.
- Calibration and sensitivity analysis: to explore the impact of different assumptions of hydraulic properties, boundary and initial conditions.
- Description of flow paths and flow conditions: useful for the general understanding of the groundwater flow system (and hydrogeochemistry) at the site.

The numerical groundwater flow simulations are thus helpful for the description of the hydraulic properties, boundary and initial conditions and associated uncertainties, as well as for enhancing the general understanding of the site. The interaction between the geology and hydrogeology disciplines, but also involving the disciplines of hydrogeochemistry, transport and surface ecosystems, in interpreting the available data, is essential in order to obtain consistent models, and the numerical groundwater flow models play an important role in this context.

A given version of the site description, with its groundwater flow models, subsequently forms the basis for further analysis by Repository Design and Safety Assessment and for the planning of new investigations. Exploratory groundwater flow simulations are considered when planning field investigations or addressing specific Repository Engineering and Safety Assessment questions.

Overview of work done for Simpevarp 1.2

The hydrogeological model version 1.2 presented in the subsequent sections is based on the current geological descriptive model as presented in Chapter 5.

The modelling done for Simpevarp 1.2 comprises estimates of hydraulic properties based on data from the Simpevarp and Laxemar subareas, including data from the Äspö HRL, as well as numerical groundwater flow simulations. The numerical groundwater flow modelling based on structural model version Simpevarp 1.2 and the estimations of hydraulic properties were performed by two different modelling teams using the numerical codes DarcyTools /Svensson et al. 2004; Svensson and Ferry, 2004; Svensson, 2004/ and ConnectFlow /Hartley et al. 2003a,b; Hartley and Holton, 2003; Hoch and Hartley, 2003; Hoch et al. 2003/, respectively.

8.3.2 General modelling assumptions and input from other disciplines

The descriptive hydrogeological model is based on four different sources of information. These sources are: (i) mapping of Quaternary deposits and bedrock geology (rock type, lineaments and deformation zones) (ii) meteorological and hydrological investigations, (iii) hydraulic borehole investigations and monitoring, and (iv) hydrogeological interpretation and analysis. The model may be described by means of parameters, boundary conditions and initial conditions, which detail:

- The geometrical description and hydraulic properties of the crystalline bedrock and the Quaternary deposits.
- The hydrological processes that govern the hydraulic boundary conditions and the hydraulic interplay between surface water and groundwater, including groundwater flow at repository depth.

Figure 8-12 illustrates schematically SKB's general systems approach to hydrogeological modelling of groundwater flow. The division into three hydraulic domains (overburden (soil), rock and conductors (deformation zones)) constitutes the basis for the numerical simulations carried out in support of the site descriptive model.

From a hydrogeological perspective, the geological data and related interpretations constitute the basis for the geometrical modelling of the different hydraulic domains. Thus, the investigations and documentation of the bedrock geology and the overburden (Quaternary deposits) provide input to:

- The geometry of deterministic deformation zones (HCD) and the bedrock in between (HRD).
- The distribution of Quaternary deposits (overburden) (HSD), including genesis, composition, stratification and thickness.

HCDs are important large features that may be modelled with constant properties or with a with defined distributions of properties. HRDs are generally the lithological Rock Domains (RD) defined by the discipline geology, cf. Chapter 5, but several RDs may also be merged into one HRD or one RD may be divided into several HRD. HRDs are generally modelled as Discrete Fracture Networks (DFN), but if considered relevant, other model application can of course be applied /Rhén et al. 2003/.

Likewise, the investigations and documentation of the present-day meteorology, hydrology and near-surface hydrogeology (in terms of mapping of springs, wetlands and streams, surveying of land use (ditching and dam projects), resources for water supply, etc.), together with the shoreline displacement throughout the Holocene, constitute the basis for the hydrological process modelling. This information provides input to:

- Present-day interpretation of drainage areas, as well as the distribution of recharge and discharge areas.
- Estimates of the average present-day precipitation and run-off, distribution of hydraulic head and flow in watercourses.
- Estimates of boundary conditions since the last glaciation.

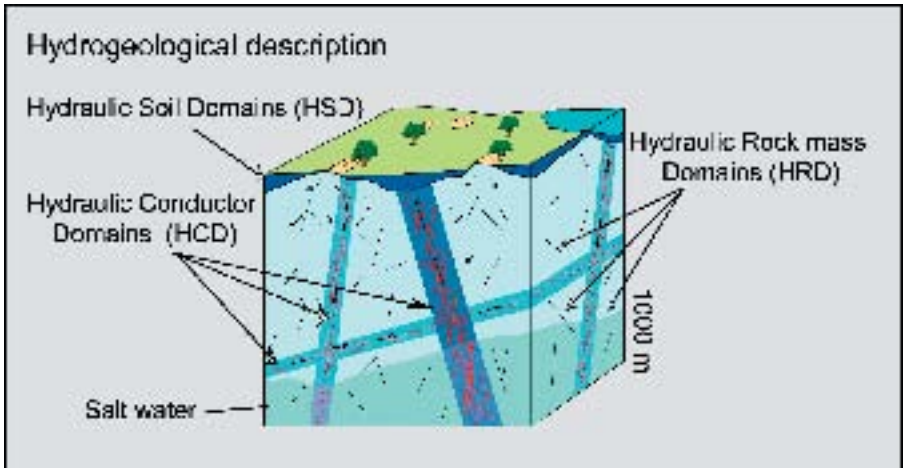

Figure 8-12. *Division of the crystalline bedrock and the overburden (Quaternary deposits) into hydraulic domains representing the overburden,(HSD) and the rock mass volumes (HRD) between major fracture zones (conductors, HCD). Within each domain, the hydraulic properties are represented by mean values, or by spatially distributed statistical distributions /Rhén et al. 2003/.*

Results from hydraulic borehole investigations and monitoring are of interest for the assignment of hydraulic properties to the different hydraulic domains. There are basically two main sources of information for the bedrock hydrogeological properties:

- Hydraulic tests and hydrogeological monitoring in deep boreholes within the Simpevarp area, cf. Section 8.2.
- Hydraulic tests and other hydrogeological observations in boreholes drilled in overburden (Quaternary deposits) in the Simpevarp area.

Hydrogeological interpretation and analysis form the hydrogeological part of site descriptive model. The work has three main parts.

- Primary interpretation of hydrogeological data.
- Integrated evaluation between disciplines to obtain consistent models.
- Groundwater flow simulations for testing and evaluating the implications of the site descriptive model.

8.3.3 General modelling strategy

The applied modelling strategy is illustrated in Figure 8-13. The HydroDFN model(-s) representing the HRD(s), the HCD model, the HSD model applied in a regional scale forms the Regional model. The HydroDFN parameters are applied in a hydraulic DFN model at a given block scale to estimate block-scale parameters and analyse anisotropy in flow. The block scale parameters are requested by Repository Engineering, but these simulations also serve to guide implementation of the HydroDFN in the regional scale model using a Equivalent Porous Media (EPM) approach. In the latter case the HydroDFN model is transferred to the regional model grid (at the selected discretisation) and EPM parameters are calculated for the respective grid blocks of the HRDs. The EPM regional model is calibrated with hydraulic test data and hydrogeochemical data, as e.g. chemical elements (salinity), water types or isotopes. The calibrated EPM regional model is then used for sensitivity analysis of ground water flow (GWF) paths and transport of solutes (particle tracking).

Conceptual models, assumptions and details of the modelling approaches are presented in /Hartley et al. 2005/ and /Follin et al. 2005/.

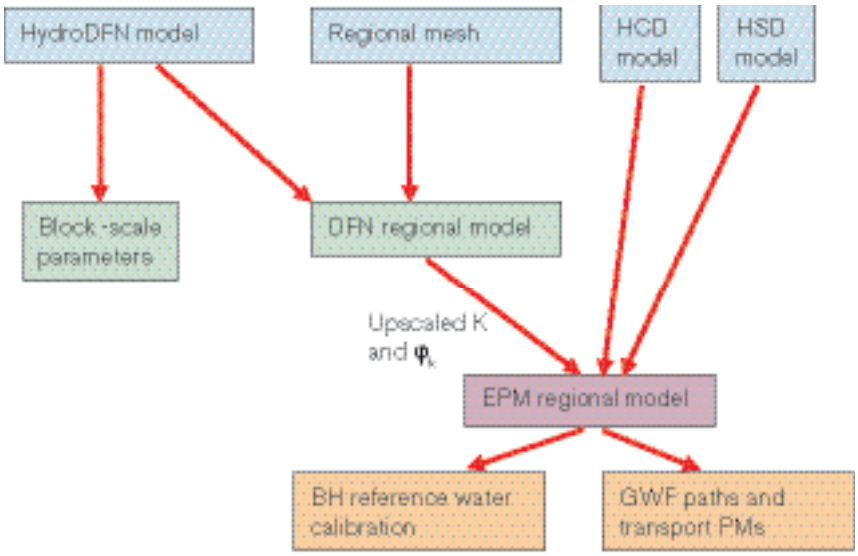

Figure 8-13. *A schematic workflow for the modelling /Hartley et al. 2005/.*

8.3.4 Conceptual model with potential alternatives

Concepts and assignment of hydraulic properties to the HRDs

The rock domains between the deterministically defined deformations zones are modelled as fracture networks. The fracture models are defined in Chapter 5 (GeoDFN) and those models are the basis for constructing conductive fracture networks (HydroDFN). The basic concepts for the construction of HydroDFN models are outlined below.

1. Potential conductive fractures: Open and partly open fractures

All naturally open and partially open fractures seen in a cored borehole are considered potential candidates for flow. Sealed fractures, on the other hand, are considered impervious. The site characterisation of open and partially open fractures allows for three levels of geological confidence – "Certain", "Probable" and "Possible". All naturally open and partially open fractures or a subset based on "Certain" and "Probable" have been used as alternative basis for analysis so far.

2. Conductive features: Deformation zones and conductive fractures

Potentially flowing stochastic deformation zones are simulated as single planar features, see Figure 8-14. This means that the fracturing within a given deformation zone is not studied in terms of its components, but treated as one single object. Both (minor) stochastic and interpreted deterministic deformation zones are treated in the same way.

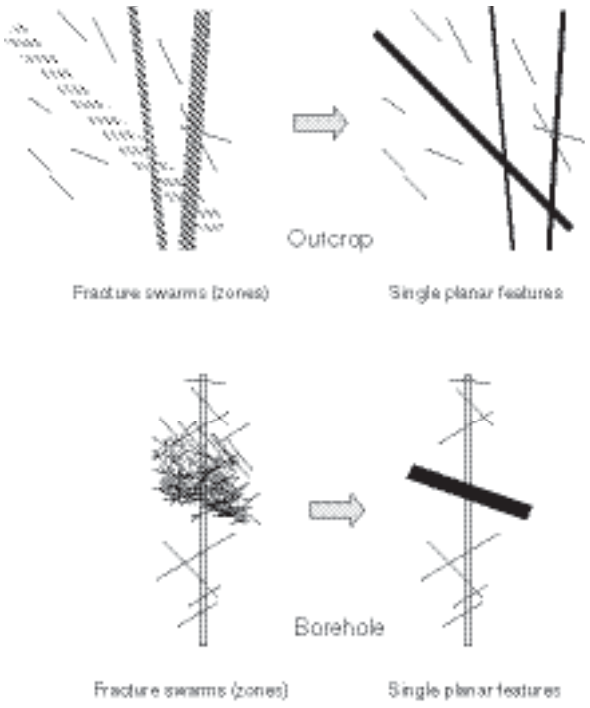

Figure 8-14. *Potentially flowing stochastic deformation zones consisting of fracture swarms (clusters) are simulated as single planar features and are considered homogeneous with regards to their hydraulic properties /Follin et al. 2005/.*

If N_{TOT} is the total number of potentially flowing fractures in a borehole and N_{DZ} is the number of potentially flowing fractures in an intercepted deformation zone, the remaining number of potentially flowing fractures in the borehole ("the geological fracture intensity") to be matched in the modelling process may be written as,

$$N_{CAL} = N_{TOT} - \sum_{DZ} (N_{DZ} - 1)_i \qquad (8\text{-}1)$$

In equation (8-1) 1 is subtracted from the numberof fractures in a deformation zone as the zone it self is making up one feature to be included in the modelling process. The transmissivity of a potentially flowing stochastic deformation zone is considered equal to its geological thickness-hydraulic conductivity product and the storativity is equal to its geological thickness-specific storativity product. This implies that the transmissivity of a deformation zone, as determined by its intersection with a borehole, is equal to the sum of the transmissivities of the flowing fractures,

$$T_{DZ} = \sum_{f} (T_f)_i \qquad (8\text{-}2)$$

In case of heterogeneous deformation zone properties, equivalent homogeneous values are considered.

3. Conductive fractures are assumed planar and homogenous

Potentially flowing single fractures between deterministically modelled deformation zones are simulated as stochastic (uncertain) planar features and are considered homogeneous with regards to their hydraulic properties, i.e. transmissivity T_f, storativity S_f. In case of heterogeneous fracture properties equivalent homogeneous (effective) values are considered.

In reality, the flow is through channels distributed across the fracture plane. Possibly, also intersections between fractures can be considered as potential channels. The physical channels are formed by the undulating fracture surfaces (spatial distribution of the fracture asperity) that don't exactly match, thus creating channels. The distribution of flow channels are, however, governed by the acting boundary conditions. The flow channels in the fracture plane occupy only a minor part of the fracture volume, and parts of the fracture surface is closed due to the undulating fracture surface. Exchange of solutes to stagnant pools of water, outside the flow channels, is by diffusion, which is faster than the diffusional exchange with the rock matrix. It can also be expected that parts of the fracture is filled with fault gauge material, i.e. fine-grained, clayey material. All threes characteristics cannot, and need not always, be modelled in detail, but must be approximated in some way. For the diffusion processes, DarcyTools can handle multiple diffusion processes (at different rates) and ConnectFlow incorporate one diffusion process (the presently most common approach). Details how these processes are treated in ConnecFlow and DarcyTools is found in /Hartley et al. 2005/ and /Follin et al. 2005/.

4. Conductive fracture: a subset of all fractures mapped as open or partly open

It is assumed that the conductive and connected fracture network may be characterised as a subset of all open and partly open fractures. Fractures mapped as sealed are not considered.

5. Distribution of size of conductive features

The sizes (L) of the potentially flowing fractures are assumed to be power law (base case, see Figure 8-15), or lognormally distributed.

Fracture shapes are modelled as squares with side length L. This is the what is meant by "size" in this context. (Assuming circular shape the corresponding radius r is $r = \sqrt{L^2/\pi}$.

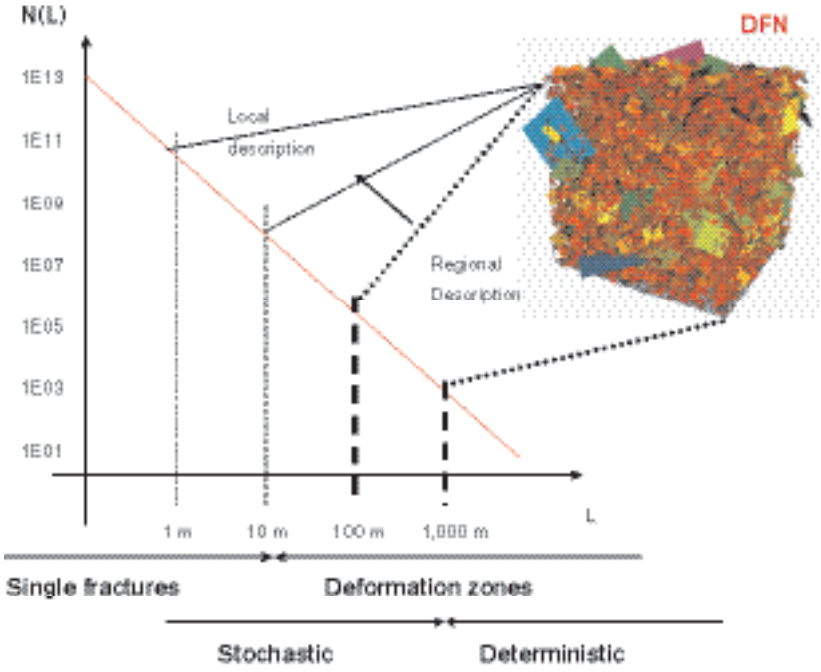

Figure 8-15. *The frequencies of occurrence of single fractures and deformation zones are assumed to be power law distributed. The shift from single fractures to deformation zones is here semantic since the deformation zones are treated as single features (cf. Assumption 1) /Follin et al. 2005/.*

When describing the intensity of a fracture set in terms of P_{10} (fractures/length along a scan line/or borehole), (1/m), P_{21} (trace length/area, (m/m^2) or P_{32} (fracture surface area/volume, (m^2/m^3)) it is always important to describe the size interval considered, as especially the small sizes tends to affect the intensity measures significantly.

6. Minimum fracture size

The minimum size of open fractures is a difficult issue. Observations of fracture traces on outcrops down to 0.5 m can be made and shorter can be observed but it is clear that it is difficult. Most probably, one cannot really observe all small fractures on outcrops but, if present, they will show up in the borehole. Therefore, one should test different assumptions and see what implication they have. This has an effect on the length distributions that are estimated in the DFN analysis. Two assumptions have been tested:

1. The number of potentially flowing fractures seen in a cored borehole (the geological fracture intensity) is assumed to be dependent on the borehole diameter, which is 0.076 m.
2. Due to practical reasons, generally the lower trace length threshold on outcrops is around 0.5 m. Smaller fractures can be observed, but they are difficult to map. One assumption is that the minimum size corresponds to about 0.5 m. Trace length on outcrops depends on several geometrical parameters that describes the spatial distribution of fracures. However, assuming Poisson distributed fractures in space, circular shape with radius r generates mean trace length = $r \cdot \pi/2$ for fractures with radius r. That is, a trace length of 0.5 m should approximately correspond to a fracture with a radius r=0.32 m)

7. Spatial distribution of fractures and deformation zones: Poisson distribution

The spatial pattern of potentially flowing stochastic fractures and deformation zones in the rock mass between the deterministically modelled deformation zones is assumed to be Poissonian when generating the DFN. However, the resulting connected conductive feature network may be non-Poissonian, due to the fact that groups of non-connected fractures (but “potentially flowing” in terms of that they are part of all “open or partly open” fractures) are excluded.

8. Transmissivity distribution models for HydroDFN

Several models for the fracture transmissivity have been considered, see Figure 8-16 and below:

1. The fracture transmissivity Tf is assumed to be uncorrelated to the fracture size L, with a log-normal distribution of Tf.

$$T = 10^{[\mu + \sigma N(0,1)]} \quad (8\text{-}3)$$

2. The fracture transmissivity Tf is assumed to be positively and fully correlated to the fracture size L.

$$T = a\,L^{b} \quad (8\text{-}4)$$

3. The fracture transmissivity Tf is assumed to be positively correlated to the fracture size L, with a superimposed random log-normal spread.

$$T = 10^{[\log_{10}(a\,L^{b}) + \sigma N(0,1)]} \quad (8\text{-}5)$$

where:
μ: Mean of log10(T) distribution.
σ: Standard deviation of log10 (T) distribution.
a, b: Factor and exponent describing the power-law relation between transmissivity T and size L.
N(0,1): Normalised normal distribution.

The last two assumptions imply that the fracture transmissivities are power-law distributed, provided that the length distribution is a power-law distribution. In addition, it is assumed that the geologically inferred size distribution can be used to estimate the transmissivity distribution and that the measured transmissivities interpreted are free from boundary effects.

9. Transmissivity range of hydraulic features versus observations

Only the most transmissive of the potentially flowing open and partially open fractures are assumed to be detected by the Posiva Flow Log (PFL-f) due to the measurement limit, i.e.

$$N_{PFL} \leq N_{CAL} \quad (8\text{-}6)$$

N_{PFL} is here referred to as for the number of PFL-f flow anomalies and N_{CAL} is the number of conductive features in a generated model that is intersected by a borehole. It is noted that the magnitude of the lower measurement threshold of the PFL is sensitive to various disturbances such as drilling debris or dissolved gases in the borehole fluid, as pointed out in previous sections. The PSS has a somewhat lower measurement threshold and is also less sensitive to disturbances.

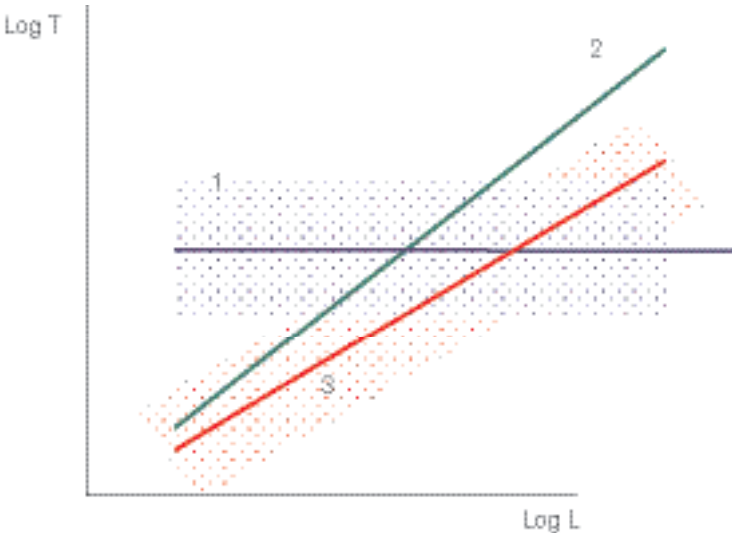

Figure 8-16. *Schematic of transmissivity models: 1) Uncorrelated, 2) Correlated, and 3) Semi-correlated /Hartley et al. 2005/.*

Another concern related to the PFL is that large flow anomalies are occasionally not detected. This problem can occur if the flow anomalies coincide with "cavities" in the borehole. This type of problem is less frequent with the PSS. In conclusion, the two methods should be run in parallel as they provide mutual support.

Sum of T_f (ΣT_f), for the generated model, over the same test section length as the PSS data must be used when comparing model to PSS data. Also here one must expect that the model can produce test sections with transmissivities below the measurement limit.

More details of the assumptions made for the HydroDFN modelling is found in /Hartley et al. 2005/ and /Follin et al. 2005/.

General assumptions regarding HCD, HRD, HSD, initial and boundary conditions

The primary concepts and assessments used in the regional scale groundwater flow modelling are:

- The current hydrogeological and hydrogeochemical situation in the Simpevarp area has resulted from natural transient processes that have evolved over the post-glacial period;
- The hydrogeochemical conditions can be modelled in terms of four reference waters ("Rain 1960, Brine, Marine and Glacial") using the reference water (mixing) fractions as "conservative tracers";
- The natural transient processes (land-rise, marine transgressions, dilution/mixing of sea water) can be modelled by appropriate choice of flow and reference water boundary conditions;
- The spatial variability of hydraulic properties can be represented in an equivalent porous media (EPM) model by appropriate upscaling of bedrock fracturing and downscaling of deformation zones on a suitable grid resolution;
- The properties of the hydraulic rock domains (HRD) are represented as EPM properties underpinned by a regional scale stochastic HydroDFN model. The HRD properties (hydraulic conductivity tensor (ConnectFlow) of grid-cell wall-conductivities (DarcyTools) and porosity) are calculated explicitly for each element in the EPM model by an upscaling method. One HydroDFN model was applied to the whole model domain;
- For the hydraulic conductor domains (HCD) the properties (transmissivity, thickness, and porosity) are constant over each modelled deformation zone.
- For the hydraulic surface domains (HSD) the properties (hydraulic conductivity, thickness, and porosity) are constant over the whole top surface of the model.

8.4 Assignment of preliminary hydraulic properties

The geometrical model of the overburden, the defined geological domains, and the hydraulic tests coupled to these domains constitute the basis for defining hydraulic domains and assigning hydraulic properties to them. This process is described in this section.

With "preliminary hydraulic properties" in the section title, we here imply that the assignment is based on hydraulic test results applied directly to the geological model in 3D. To some extent these properties may be updated (fairly locally) by numerical modelling of hydraulic test results, see Section 8.5, or updated in relevant parts of the regional model area by numerical simulations including matching to hydrogeochemical data, see Section 8.8 where the Resulting groundwater flow model is discussed. The necessary updates and the associated uncertainties in the hydraulic properties are described in Sections 8.8 and 8.9.

8.4.1 Overburden – assignment of hydraulic properties to the HSDs

The overburden is described in detail in Chapter 4. For Simpevarp 1.2, no site specific values of the hydraulic properties were available on the outset of the groundwater flow modelling. The limited information on the overburden in Simpevarp 1.2 has led to use of a simplified two-layer model for the regional hydrogeological flow models. Below, the compiled results used as a basis for input to the regional groundwater flow modelling are shown.

Table 8-12. Hydraulic properties assigned to Hydraulic Soil Domain (HSD). Based on /Knutsson and Morfeldt, 2002/ and /Carlsson and Gustafson, 1997/.

HSD	Type of Quaternary deposits	Thickness (m)	Hydraulic conductivity (m/s)	Expected range of hydraulic conductivity (K) (m/s)	Comment
HSD1	Sandy till , near surface	1	1.0 E–5	1.0E–7 to 1.0E–3	
HSD2	Sandy till, below HSD1	2	1.0 E–7	1.0E–8 to 1.0E–6	

HSD	Type of Quaternary deposits	Thickness (m)	Specific storage (S_s) (1/m)	Expected range of Specific storage (S_s) (1/m)	Comment
HSD1	Sandy till , near surface	1	1.0E–4	1.0E–5 to 1.0E–3	
HSD2	Sandy till, below HSD1	2	1.0E–4	1.0E–5 to 1.0E–3	

HSD	Type of Quaternary deposits	Thickness (m)	Specific yield (SY) (–)	Expected range of Specific yield (S_Y) (–)	Comment
HSD1	Sandy till , near surface	1	1.0E–1	1.0E–2 to 3.0E–1	
HSD2	Sandy till, below HSD1	2	1.0E–1	1.0E–2 to 3.0E–1	

HSD	Type of Quaternary deposits	Thickness (m)	Kinematic porosity, n_e (%)	Expected range of Kinematic porosity, n_e (%)	Comment
HSD1	Sandy till , near surface	1	5.0E–2	1.0E–2 to 1.0E–1	
HSD2	Sandy till, below HSD1	2	5.0E–2	1.0E–2 to 1.0E–1	

8.4.2 Deterministic deformation zones – assignment of hydraulic properties to the HCDs

All deterministic deformation zones in the regional scale model presented in geological model, see Chapter 5, constitute the base case (Case 1) for HCDs. These deformation zones are mostly based on geological and/or geophysical indications. Some of the deformation zones are intercepted by boreholes, and hydraulic test data from these boreholes are the base for the assigning material properties. However, just a few boreholes drilled during the site investigations have penetrated deformation zones deterministically modelled in Simpevarp 1.2.

Hydraulic tests in borehole KSH03A, drilled through zone ZSMNE024A, gave clear indication of the deformation zone's importance. Other zones penetrated by new boreholes were: ZSMEW002A (by HLX20), ZSMEW007A (by HLX11 and HLX13), ZSMNE012A (by HAV13 and HAV14), ZSMNE018A (by HSH02), ZSMNE024A (also by HAV11) and ZSMNE025A (by HSH01). No new interference tests were available to support the deformation zone model.

According to the deformation zone model, several old boreholes intersect a number of deformation zones, see Table 8-22. The deformation zones corresponding to zones in the Äspö site investigation model, based on the pre-construction investigation and the construction of the Äspö HRL, /Rhen et al. 1997b/ were assigned properties according to /Rhén et al. 1997b/. A few intersections between old existing boreholes and deformation zones were used to assign properties.

Base case (case 1) and two alternative models cases (case 2 and case 3), were suggested for modelling, see Figure 8-17:

Case 1: Model incuding all deformation zones. Case 2: Model including all HCD of high confidence of existence and HCD of low confidence of existence with lengths > 1,600 m. Case 3: Model including all HCD of high confidence of existence and HCD of low confidence of existence with lengths > 3,000 m.

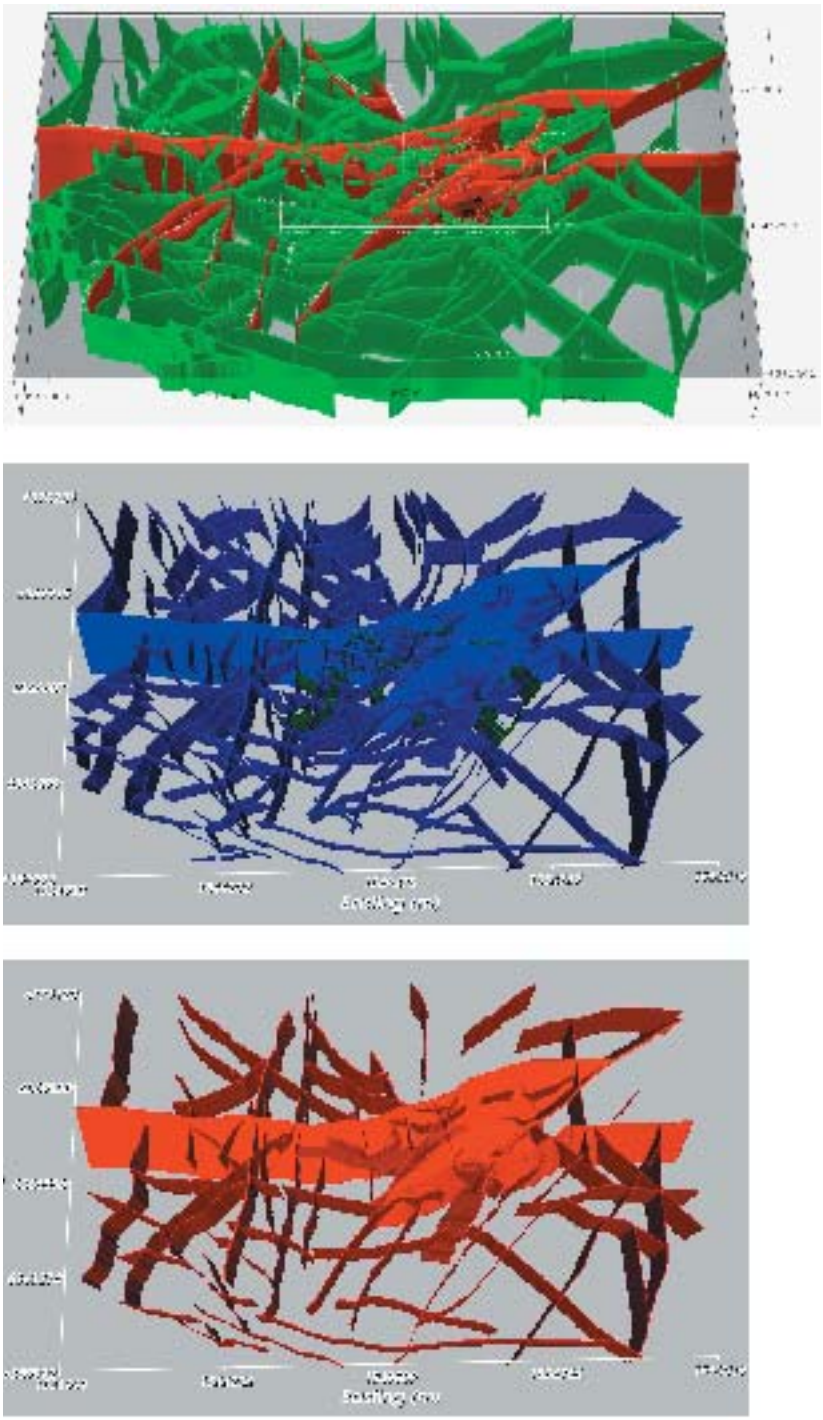

Figure 8-17. *Top: Case 1: Model incuding all HCDs. Middle: Case 2: Model including all HCD of high confidence of existence and HCD of low confidence of existence with lengths > 1,600 m. Bottom: Case 3: Model including all HCD of high confidence of existence and HCD of low confidence of existence with lengths > 3,000 m /Hartley et al. 2005/.*

Table 8-13 summarises the hydraulic properties of the HCDs included in the Simpevarp 1.2 descriptive hydrogeological model. The properties are based on results from the pre-construction investigation and the construction of the Äspö HRL and the ongoing Site Investigations in the Simpevarp area. The geometric mean of the transmissivities of HCDs from Äspö HRL /Rhen et al. 1997b/ was used if no site-specific value was available for a specific HCD. The properties are assumed to be constant within each HCD.

Table 8-13. Summary of the properties (base case) assigned to the HCDs in the Simpevarp 1.2 model.

Name of HCD RVS ID	Geological confidence High/Medium/Low	Hydraulic thickness (b) (m)	Transmissivity (T) (m^2/s)	Storage coefficient (S) (–)	Mean transport aperture (e_T) (–)
ZSMEW002A, (Mederhult zone)	High	45	1.0E–05	S[2]	e_T[3]
ZSMEW004A	High	30	1.26E–05[1]	S[2]	e_T[3]
ZSMEW007A	High	2	2.29E–04	S[2]	e_T[3]
ZSMEW009A, (EW3)	High	12	1.70E–05	S[2]	e_T[3]
ZSMEW013A	High	20	4.00E–07	S[2]	e_T[3]
ZSMEW028A	High	10	8.45E–08	S[2]	e_T[3]
ZSMNE005A, (Äspö shear zone)	High	40	6.63E–07	S[2]	e_T[3]
ZSMNE006A, (NE1)	High	28	2.20E–04	S[2]	e_T[3]
ZSMNE010A	High	20	1.26E–05[1]	S[2]	e_T[3]
ZSMNE011A	High	10	1.26E–05[1]	S[2]	e_T[3]
ZSMNE012A, (NE4)	High	41	1.06E–04	S[2]	e_T[3]
ZSMNE016A	High	13	1.26E–05[1]	S[2]	e_T[3]
ZSMNE018A	High	30	2.94E–06	S[2]	e_T[3]
ZSMNE024A	High	80	3.64E–04	S[2]	e_T[3]
ZSMNE040A	High	15	3.74E–06	S[2]	e_T[3]
ZSMNS001A	High	10	1.26E–05[1]	S[2]	e_T[3]
ZSMNS001B	High	10	1.26E–05[1]	S[2]	e_T[3]
ZSMNS001C	High	10	1.26E–05[1]	S[2]	e_T[3]
ZSMNS001D	High	10	1.26E–05[1]	S[2]	e_T[3]
ZSMNS009A	High	50	1.26E–05[1]	S[2]	e_T[3]
ZSMNS017A	High	20	6.50E–05	S[2]	e_T[3]
ZSMNW004A	High	50	1.26E–05[1]	S[2]	e_T[3]
ZSMNW007B	High	50	1.26E–05[1]	S[2]	e_T[3]
ZSMNW012A	High	40	1.26E–05[1]	S[2]	e_T[3]
ZSMNW025A	High	5	2.60E–07	S[2]	e_T[3]
ZSMxxxxxx (All other det. zones)	Low	20	1.26E–05[1]	S[2]	eT[3]

[1] Properties based on geometric mean for deformation zones at Äspö HRL (Rhen et al. 1997b).

[2] Based on correlation to T, see Table 8-14.

[3] Based on correlation to T, see Table 8-15.

The hydraulic thicknesses of the individual deformation zones were based on the geological interpretation of zone thickness made for the Simpevarp 1.2 deformation zone model, cf. Chapter 5.

Information on the storage coefficient is essential for estimating influence radius of tests and planning and interpreting of interference tests. In the regional groundwater flow modelling the storage coefficient is of minor importance, unless the task is to test the model against interference tests.

There is rather limited information concerning storage coefficients of fracture zones in the Simpevarp area. In /Rhén et al. 1997b/ the storage coefficient of fracture zones was estimated based on large-scale interference tests, and in /Rhén and Forsmark, 2001/ the storage coefficient (S) was estimated for larger and smaller fracture zones. In conjunction with the TRUE Block Scale experiment at Äspö HRL, a large number of hydraulic interference tests have been made and the storage coefficient (S) was estimated for larger and smaller fracture zones, e.g. /Andersson et al. 2000;

Andersson et al. 1998/. Data were compiled from these projects and a relation was estimated for the correlation between T and S, see Table 8-14. The variation along the regression line can be expected to be within ± one order of magnitude of the S calculated with the formula in Table 8-11.

Likewise, the database for the kinematic porosity (n_e) (= Mean transport aperture/Hydraulic thickness of HCD, $n_e = \frac{e_T}{b}$) is also very limited. The equation given in Table 8-15 is based on the hydraulic aperture presented in /Dershowitz et al. 2003/. It gives similar values to those reported in /Rhén et al. 1997b/ with a=1.428 and b=0.523, based on a compilation of tracer tests in crystalline rock ranging from fracture, densely fractured rock and fracture zones. Kinematic porosity is considered as a calibration parameter, but the base case value should be as in to Table 8-15 combined with Table 8-13.

Table 8-14. Estimation of storage coefficient (S) from transmissivity (T). $S=aT^b$. T (m^2/s), S (–).

Approx. test scale (m)	a	b	Reference
5–100	0.0007	0.5	/Rhén et al. 1997b/ /Rhén and Forsmark, 2001/ /Andersson et al. 1998, 2000/

Table 8-15. Estimation of mean transport aperture from transmissivity (T). $e_t=aT^b$. T (m^2/s), e_t(m).

Approx. test scale (m)	a	b	Reference
5–100	0.5	0.5	/Dershowitz et al. 2003/

8.4.3 Rock mass between the deterministic deformation zones – assignment of hydraulic properties to the HRDs

These properties are are assigned by modelling, see section below.

8.5 Simulation/calibration against hydraulic tests

Hydraulic properties are generally, as a first step, estimated from the evaluation of hydraulic test results related to the geological rock domains, as shown in Section 8.4. The next phase is to set up a numerical groundwater flow model by applying geometrical domains with preliminary properties and calibrate the model versus relevant measured responses. This section summarises these efforts.

8.5.1 Overburden – HSDs

No simulations or calibrations have been made to adjust the assigned hydraulic properties of the HSDs.

8.5.2 Deterministic deformation zones – HCDs

No simulations or calibrations have been made to adjust the assigned hydraulic properties of the HCDs.

8.5.3 Fracture model – HRDs – HydroDFN

The HydroDFN modelling undertaken by /Hartley et al. 2005/ and /Follin et al. 2005/ included four main steps:

1. Assessment of geological data.
2. Assessment of hydraulic data.
3. Geological simulation and assessment of preliminary hydraulic fracture properties.
4. Hydraulic simulation.

Step 1 covered the division of borehole data into the entities deformation zones and rock outside the deformation zones and subsequently into rock domains, followed by examination of the fracture properties and intensities (P_{10}) as well as orientations for each zone or domain.

Step 2 included analysis of hydraulic data to obtain a representative value for each deformation zone treated as a part of the HydroDFN model. Deterministically defined deformation zones intersecting the borehole were excluded from the analysis. A second component was to define the transmissivity distribution of hydraulic features, as defined in Section 8.3, along the borehole. A third component (that was not really included in the Simpevarp 1.2 modelling) is to test if the hydraulic features have defined sets with different orientations and different transmissivity distributions.

Step 3 aims first at generation of a fracture model that compares with the mapped open and partly open fractures (the GeoDFN model provided was used, but the fracture intensities required adjustment to better represent the specific boreholes studied). Then the non-connected fractures are excluded (by /Follin et al. 2005/ but not by /Hartley et al. 2005/), see Figure 8-18. Subsequently, a preliminary relationship for the transmissivity model was derived (last step is employed by /Follin et al. 2005/ based on the power law relationship)

Step 4. The hydraulic simulation begins with a relationship between T_f and L. Secondly, a sufficiently large model domain is constructed with appropriate boundary conditions for the hydraulic tests to be used. So far the inflow rate distribution along the boreholes as obtained from the PFL

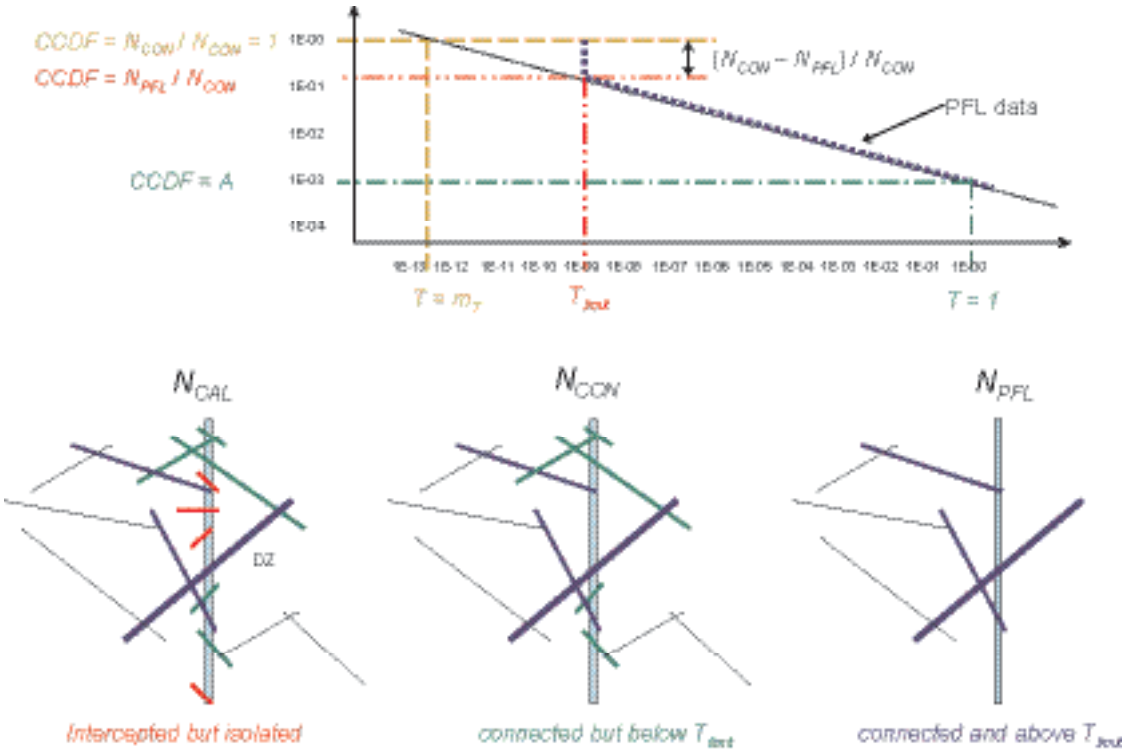

Figure 8-18. *Top: Illustration showing how the CCDF plot of the measured fracture transmissivities is used. Bottom: Illustration of the intensity principle underpinning the work reported here,* $N_{PFL} \leq N_{CON} \leq N_{CAL} \leq N_{TOT}$ */Follin et al. 2005/.*

measurement has been used. These PFL measurements are conducted under pumping test conditions which lasts about a week. Simulated inflows to the modelled borehole are then cross-plotted against the measured inflows. The procedure is repeated a couple of times for each transmissivity model tested, see Figure 8-19. A typical result from the simulations is exemplified in Figure 8-20.

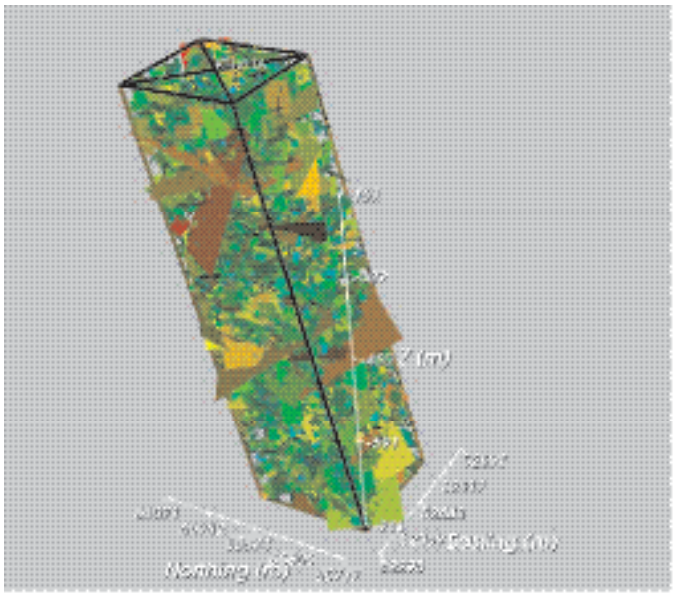

DFN realisation for a 100 m radius region around the inclined borehole KSH01A. All fractures (145,000) are shown and coloured by log(T) (in this case T is lognormally distributed and not correlated to L).

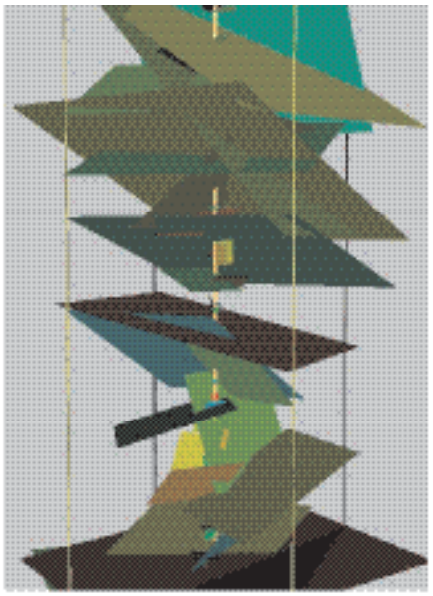

Close-up of fractures intersected by borehole KSH01A to show different scales of fractures seen in borehole. Fractures are coloured by log(T) (in this case T is lognormally distributed and not correlated to L).

DFN realisation for a 100 m radius region around KSH01A used in the PFL simulation. For the case shown here, it is assumed that only 30% of open and partly-open fractures are actually open. Also, only fractures with length greater than 1 m are used. Fractures are coloured by the average head on the fracture or grey where they are either isolated or dead-ends.

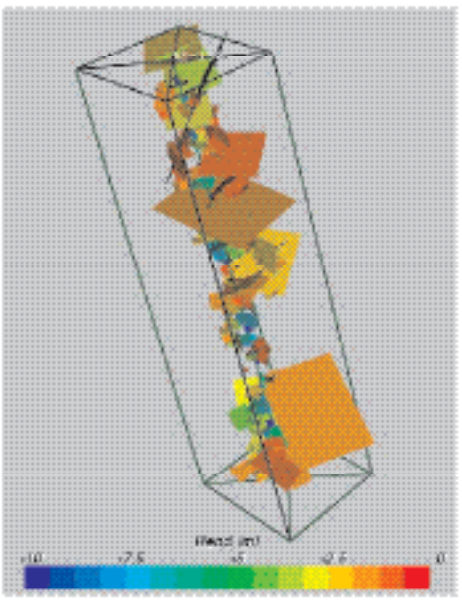

DFN realisation as for the figure to the left, but only showing the fractures around the borehole with a significant drawdown.

Figure 8-19. *Iterative process to match T-distribution:1: Simulate a HydroDFN in a 200×200×1,000 m³ block. Fracture geometry is modelled with applied T-distribution. (ConnectFlow:s block size. Darcy-Tools used a larger block) 2: Model a borehole applying a head difference and compare flow rates with measured. (Figures from /Hartley et al. 2005/).*

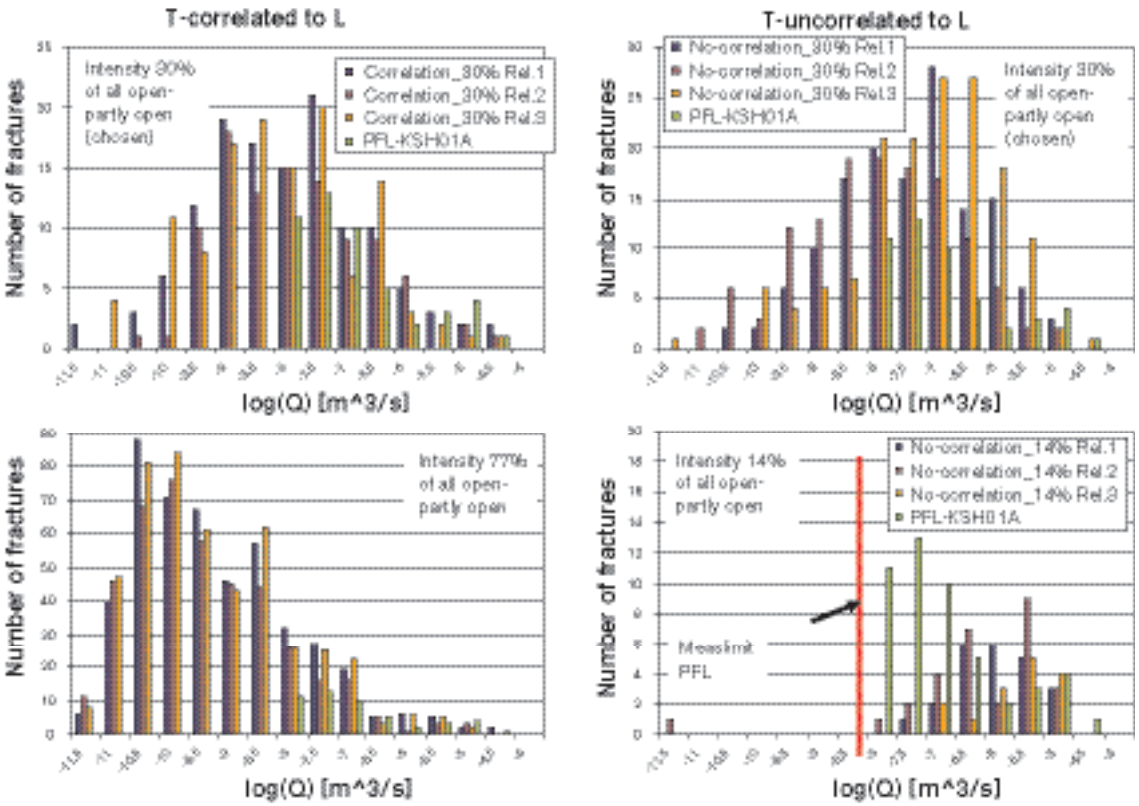

Figure 8-20. *Example of simulated flow rates (several realisations-bars in blue, brown and orange)) compared with measured (bar in green). KSH01A. (Figures from /Hartley et al. 2005/).*

The HydroDFN model parameters resulting from the analysis are:

- Fracture set with: orientation (mean trend and plunge of fractures poles, concentration (fracture pole dispersion parameter)).
- Length distribution model (power law, lognormal).
- Fracture intensity of conductive fractures for each set.
- Transmissivity model (Uncorrelated to fracture size (mean, std), Correlated to fracture size (Intercept, slope), Semi-correlated to size (Intercept, slope, standard deviation).

Based on a limited number of realisations and cases for the sensitivity analysis, the resulting models from the DarcyTools and ConnectFlow teams are presented in Table 8-16 and Table 8-17. A few key numbers are summarised in Table 8-18.

A difference between the teams is that the ConnectFlow team made some modifications of the GeoDFN fracture set considering the orientations. The DarcyTools team used only a power-law length distribution, and, furthermore, the size interval for the modelled fractures differed between the teams, see Table 8-16 through Table 8-18. The transmissivity-length models are also illustrated in Figure 8-21.

Table 8-16. Description of DFN parameters used in ConnectFlow simulation of fractures in the Simpevarp sub-area for calculating block properties The model is also the base for the regional flow simulations. Orientation sets are numbered: 1=NE, 2=EW, 3=NW, 4=BGNE (Background NE, see Chapter 5 for explanation of "background" fractures), 5=BGNS (Background NS), 6=BGNW(EW)(Background NW (to EW), 7=HZ(Horizontal). Transmissivity model parameters are given for each of the cases, denoted in italics. $P32_t$ is the total fracture intensity m^2/m^3, $P32_c$ is the connected fracture intensity m^2/m^3 /Hartley et al. 2005/.

Rock domain	Fracture set name	Orientation, Set pole: (trend, plunge), concentration	Length model, Constants: lognormal (μ, σ), power-law (L_0, k_r) (m)	Intensity, (P_{32t}, P_{32c}), valid length interval: (L_0, L_{max}) (m^2/m^3)	Relative intensity of P32	Transmissivity model Eq. No, constants T(m^2/s)
All	1. NE	(128, 4) 19.1	(L_0, kr) (0.5,2.58)	(0.71, 0.29) (0.5, 1,000)	0.036	Uncorrelated: (μ, σ) (–6.7,1.3)
	2. EW	(182, 2) 11.0	(L_0, k_r) (0.5,2.80)		0.079	Correlated: (a,b) (1.5 10^{-10}, 1.5)
	3. NW	(237, 1) 18.5	(L_0, k_r) (0.5,2.87)		0.096	Semi-correlated: (a,b,σ) (2.0 10^{-10}, 1.5, 1.0)
	4. BGNE	(128, 4) 19.1	(μ, σ) (0.58,0.6)		0.035	
	5. BGNS	(271, 0) 18.1	(μ, σ) (0.58,0.88)		0.055	
	6. BGNW(EW)	(182, 2) 11.0	(μ, σ) (0.58,0.63)		0.030	
	7. HZ	(30, 81) 4.5	(L_0, k_r) (0.5,2.6)		0.669	

Table 8-17. Description of DFN parameters used in DarcyTools simulation of fractures in the Simpevarp sub-area for calculating block properties. The model is also the base for the regional flow simulations. Orientation sets are numbered: 1=NE, 2=EW, 3=NW, 4=BGNE, 5=BGNS, 6=BGNW(EW), 7=HZ. Transmissivity model parameters are given for each of the cases, denoted in italics. $P32_t$ is the total fracture intensity m^2/m^3, $P32_c$ is the connected fracture intensity m^2/m^3 /Follin et al. 2005/.

Rock domain	Fracture set name	Orientation, Set pole: (trend, plunge), concentration	Length model, Constants: lognormal (μ, σ), power-law (L_0, k_r) (m)	Intensity, (P_{32t}, P_{32c}), valid length interval: (L_0, L_{max}) (m^2/m^3)	Relative intensity of P32	Transmissivity model Eq. No, constants T(m^2/s)
All	1. NE	(118, 1.9) 17.3	(L_0, k_r) (0.5,2.6)	(0.77,0.29) (0.5, 300)	0.07	Correlated: (a,b) (5×10^{-13}, 2.63)
	2. EW	(17.1, 7.3) 11.2			0.20	alt.
	3. NW	(73.1, 4.7) 13.7			0.11	(5×10^{-12}, 2) (recommended)
	4. BGNE	(316.3, 5.5) 17.9			0.12	
	5. BGNS	(96.8, 3.8) 20.3			0.01	
	6. BGNW(EW)	(22.1, 2.4) 6.0			0.07	
	7. HZ	(125, 75) 5.0			0.43	

Table 8-18. Comparison of some key results from the ConnectFlow (CF) and DarcyTools (DT) modelling. P_{32T}: Volumetric fracture (feature) intensity for all ("total") fractures. P_{32C}: Volumetric fracture (feature) intensity for all conductive and hydraulically connected fractures.

Modelling team	Size interval (m)	P_{32T} (m^2/m^3)	P_{32C} (m^2/m^3)	Comments
CF	0.5–1,000	0.71	0.29	
DT(2)	0.5–300	0.77	0.29	Recalculated DT(1) to Lmin 0.5 m for comparison with CF
DT(1)	0.067–300	2.58	0.97	

The conclusions from the results of the modelling teams are as follows:

ConnectFlow- results:

- If the intensity (P_{32}) is adjusted all three T-models parameter settings can be fitted such that the model simulations generate flow rate distributions similar to the measured ones.
- As PSS has a lower measurement limit than PFL, it is possible to identify a narrower range for P_{32} (Comparison of T-distributions)
- Suggest intensities of 30–40% of total intensity of conductive fractures (KSH01A) for correlated and uncorrelated T-model.
- Correlated model seems to provide somewhat better match than the uncorrelated T-model.

DarcyTools-results:

- DarcyTools simulated fracture sizes down to L_{min}=0.067 m, which is the area-equivalent size of a square for a borehole diameter 0.076 m. This the reason for difference in parameter estimates for the T-correlated model when compared to CF.
- Intensities for conductive fractures for L>0.5 m are similar to those of ConnectFlow.

A general comment is that it has only been possible to make a limited number of simulations. This indicates that the suggested models possibly are associated with more uncertainty, than if a larger number of realisations and cases had been analysed.

The database of the core mapping of the boreholes that were PFL-logged was updated late summer 2004. These changes affected the statistics for fractures associated with PFL-flow anomalies, but the changes are considered to be of minor importance for the result presented here given other uncertainties.

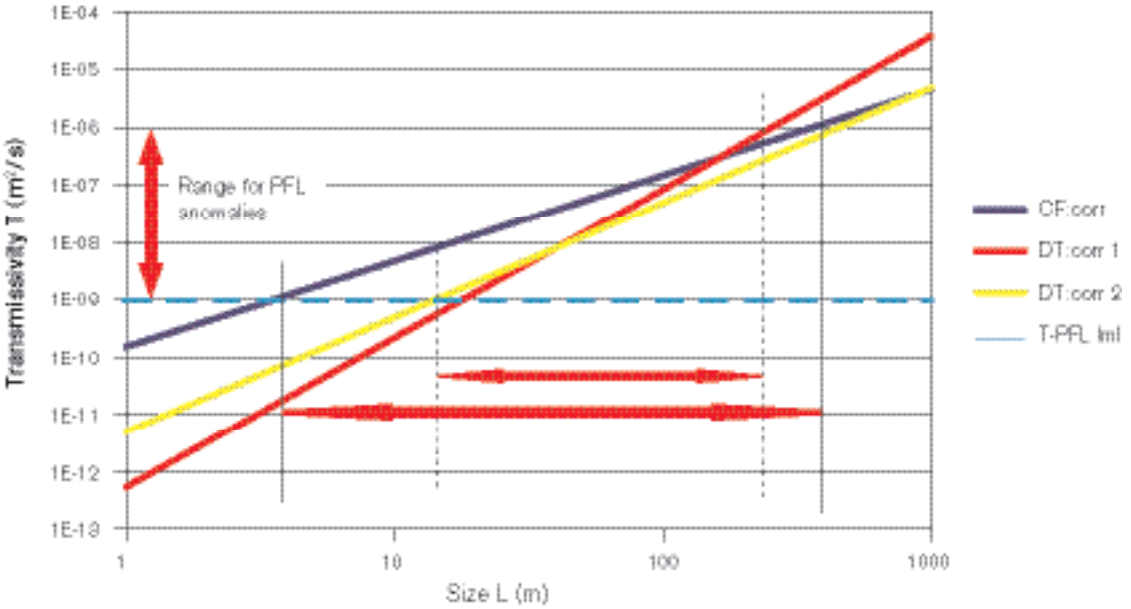

Figure 8-21. *Recommended models for the correlated case and illustration of the ranges of measurements. DarcyTools recommends "DT: corr 2". (Based on /Follin et al. 2005/ and /Hartley et al. 2005/).*

8.5.4 HRDs – HydroDFN – Block modelling

The purpose with the Block modelling is to:

- Test implications of the truncation of the size distribution on the properties of the selected numerical grid.
- Estimate hydraulic conductivity distributions at different scales (20 and 100 m) and under varius anisotropy conditions (for Repository Engineering).

Figure 8-22 illustrates a block of size 1 km^3 that is discretised into 20 m blocks and a HydroDFN model that is used to generate the block properties for each 20 or 100 m block. An example of results is presented in Figure 8-23 and a summary of results in Table 8-19.

Table 8-19. Block modelling. Comparison of some key results from the ConnectFlow team (CF) and DarcyTools team (DT). Block-effective hydraulic conductivity (K_b). K_h: Hydraulic conductivity within a horizontal plane.

Modelling team	T-model	Block size	Mean Log10(K_b)	Std Log10(K_b)	(K_{hmax}/K_{hmin})	Trend of K_{hmax}	(K_{hmax}/K_z)
		(m)	(m/s)	(m/s)	(–)	(° from N)	
CF	Uncorr.	20	–8.5	1.4	≈1	–	2.5
	Correl.	20	–8.5	1.1	≈2.2	100–140	3.8
	Semi-corr	20	–8.5	1.1	≈3.2	120–160	2.6
	Uncorr.	100	–8.9	1.3	≈1	–	2.6
	Correl.	100	–8.2	0.6	≈2.0	90–130	2.4
	Semi-corr	100	–8.5	0.7	≈3.0	120–150	2.6
DT	Correl.	20	–8.8 (–8.0)[1]	1 (0.6)[1]	(≈1)[2]	(≈90 ?)[2]	≈1
	Correl.	100	–8.2 (–7.7)[1]	0.6 (0.2)[1]	(≈1)[2]	(≈90 ?)[2]	≈1

[1] Based on data from borehole KSH02 – considered not representative.

[2] No clear trend for the lumped model.

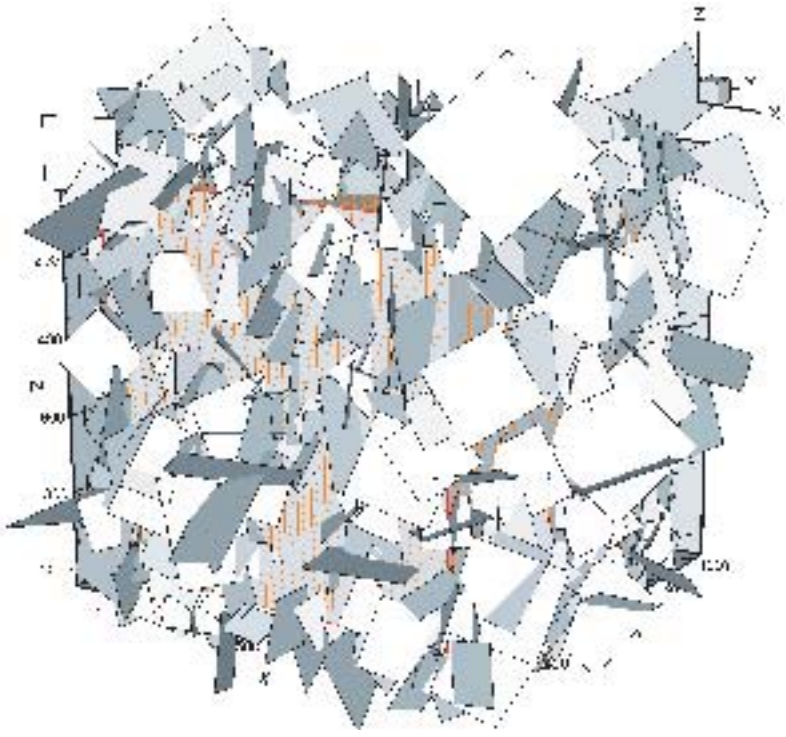

Figure 8-22. *Caclulating block properties. Superimpose two different grids on the HydroDFN and analyse the properties of the blocks. The two different grids used were used; 20 m and 100 m, and the 20 m grid is indicated in this illustration /Follin et al. 2005/*

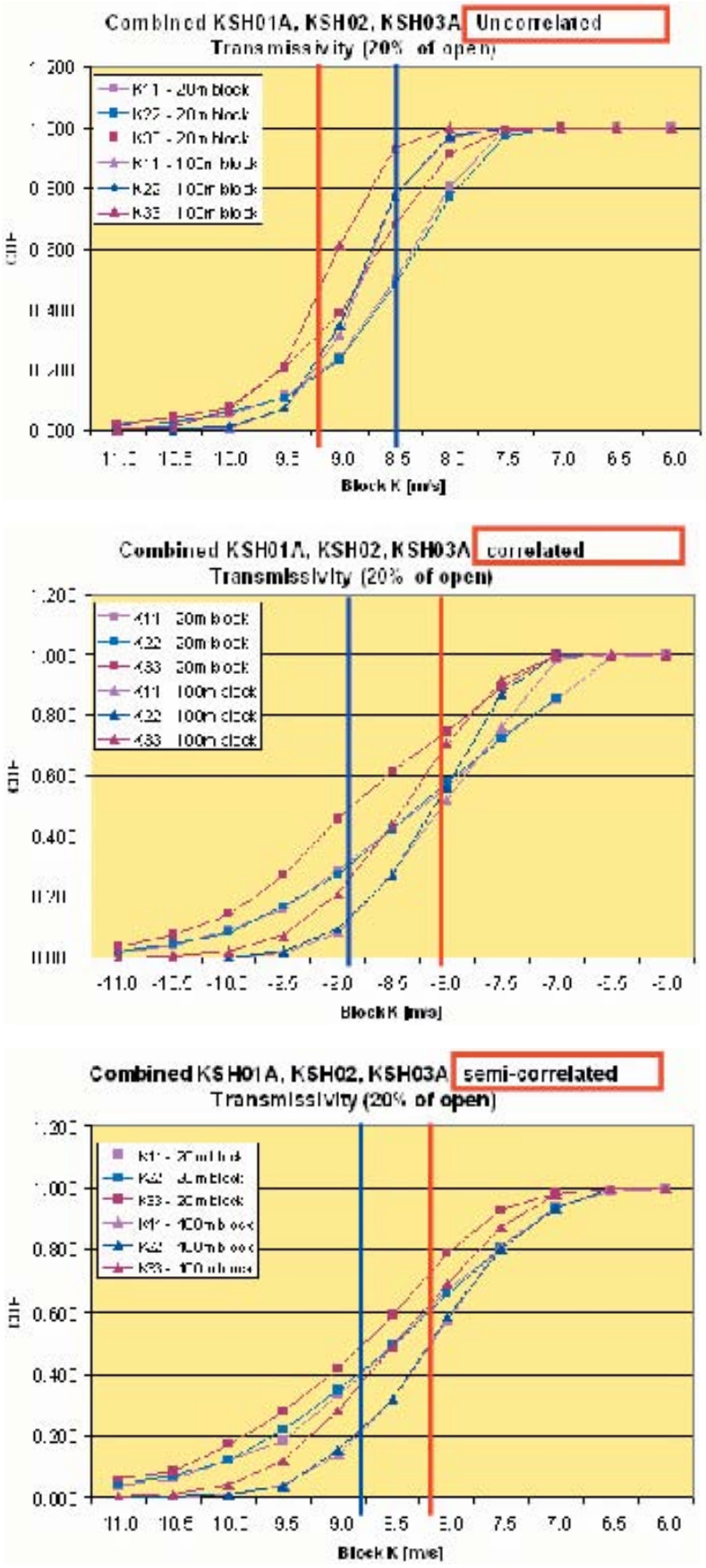

Figure 8-23. *Example of estimates hydraulic conductivity distributions at different scales (20 and 100 m) and under varius anisotropy conditions. Blue vertical line indicate geometric mean for the scale 20 m and red line scale 100 m. 20% of the total fracture intensity of the open fractures was used in the simulation. (Figures from /Hartley et al. 2005/).*

Conclusions from the block modelling:

- There is a trend of horizontal anisotropy but this is considered weak.
- ConnectFlow: The correlated model gives larger variance and higher mean compared with the uncorrelated model.
- ConnectFlow: The correlated model gives greater heterogeneity of the hydraulic conductivity, but also a greater spatial correlation between blocks associated with large stochastic deformation zones.
- Median K_b(20 m) < Median K_b(100 m), i.e. opposite to the results based on the uncorrelated model (cf. Figure 8-23), but similar to that seen for Äspö HRL data /Rhén et al. 1997b/.
- ConnectFlow: Kinematic porosity has a median of Log(n_e)=–4.8 for a 100 m block. For the correlated case it does not have a strong dependence on Lmin, but does for the uncorrelated case.
- ConnectFlow: A L_{min} < 50 m has to be used for a 100 m block size for the correlated T model, but must be less than 50 m for the uncorrelated T model. As a general rule of thumb, fractures down to a length at least as small as half the block-size need to be included.
- ConnectFlow: Some bias is introduced whether the models are based on the PSS data from borehole KLX01 or the combined PFL/PSS data from the Simpevarp boreholes KSH01A, KSH02 and KSH03A. The median hydraulic conductivities are very similar, but there is less variability for the KLX01 case, i.e. it is more homogeneous.

The evaluated anisotropy is different from the experiences at Äspö HRL. In the latter case it was found that the highest permeability in the horizontal direction is WNW-NW /Rhén et al. 1997b/. These data were further analysed in /Munier et al. 2001/. Evaluation of hydraulic data from the Prototype Repository at Äspö HRL also showed similar results, but also indicated that the most conductive fracture set was sub-vertical, with strike about WNW /Rhén and Forsmark, 2001/. The ratio between the maximum and the minimum hydraulic conductivity was c. 100, thus considerably larger than the corresponding ratio estimated for the boreholes in the Simpevarp subarea.

An examination of the orientation of the fractures interpreted to correspond to PFL anomalies in the boreholes presented in Section 8. 2, indicate that steeply dipping fractures with strike NW and sub-horizontal fractures dominate. This will be looked into in more detail in the continued site modelling.

8.6 Initial and boundary conditions

Boundary conditions have to be assessed when performing steady state groundwater flow simulations and the initial conditions need also be assessed if transient groundwater flow simulations are required. The initial and boundary conditions are equally important as the hydraulic properties presented in Sections 8.4 and 8.5.

8.6.1 Boundary conditions

Top boundary

The applied boundary conditions are used to mimic the transient processes of shoreline displacement due to post-glacial rebound and the variations in the salinity of the Baltic Sea. The evolutions of these two quantities over the post-glacial period are shown in Figure 8-24 and Figure 8-25. The general modelling approach was to hold the model domain fixed (i.e. same x, y and z coordinates), but vary the head and salinity on the top surface with time. One clear characteristic of the land-rise scenario is the very sharp change in shoreline of about 40 m corresponding to rapid melting of the ice sheet occurring around 9,700 BC. This may have implications for the numerics during the early part of the simulations. Figure 8-25 illustrates the uncertainty in the salinity of the sea. There is also an uncertainty inherent in when the different stages of Baltic started, which will be analysed further in future modelling efforts.

Figure 8-24. *The shore line displacement at Simpevarp /after Påsse, 2001 in Hartley et al. 2005/.*

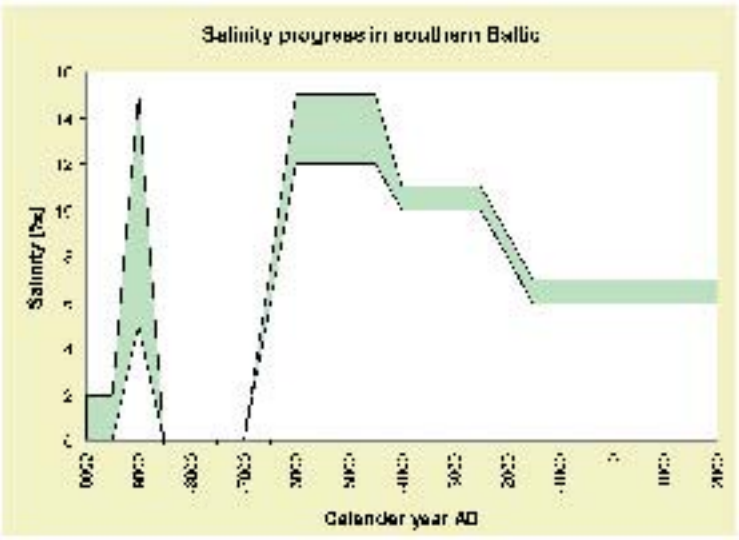

Figure 8-25. *The salinity evolution in the southern Baltic Sea. Two possible scenarios are shown (The uncertainty shown in green). Only the lower scenario was used by ConnectFlow. (Baltic ice lake: 12,000–9,500 BC, Yoldia sea: 9,500–8,800 BC, Ancylus Lake: 8,800–7,500 BC, Littorina Sea: 7,500 BC–) /modified after Stigsson et al. 1999 in Hartley et al. 2005/.*

The evolution of salinity in the Baltic informs how the “Marine” and “Rain 1960” references waters have mixed in different fractions over time. It is also important to have a more general hypothesis of the evolution of surface and sub-surface reference waters. The current understanding is illustrated in Chapter 3.

For flow, the head on the top surface was set to the topographic height that evolves with time due to changes in the location of the shoreline (see Figure 8-24). It may be argued that the water level should be below the top surface, but, as can be seen in /SKB, 2005/ the probable location of the water table should mimic the topography rather well. (A surface connecting all discharge areas has an elevation that looks rather similar to the topographic surface.) Offshore, the head was set equal to the depth of the sea multiplied by the relative density of the Baltic Sea to freshwater. A variant using a flux-type boundary condition for above sea-level surfaces with a potential infiltration of

c. 165 mm/year corresponding to run-off for the Simpevarp area /Werner et al. 2005/ was tested by Connect Flow team /Hartley et al. 2005/, and more simulations with this boundary condition will be made in future modelling.

Vertical and bottom boundaries

The vertical boundaries and bottom boundary were assigned as no-flow boundaries.

8.6.2 Initial conditions

It is assumed that only Glacial and Brine water types were present as groundwater after the last glaciation, see Figure 8-26. The depth of 100% "Glacial water" and the depth interval of the linear transition between "Glacial" and "Brine" toward pure "Brine" are calibration parameters for the modelling of the past evolution and comparisons with the present situation of water types in sampled in borehole sections.

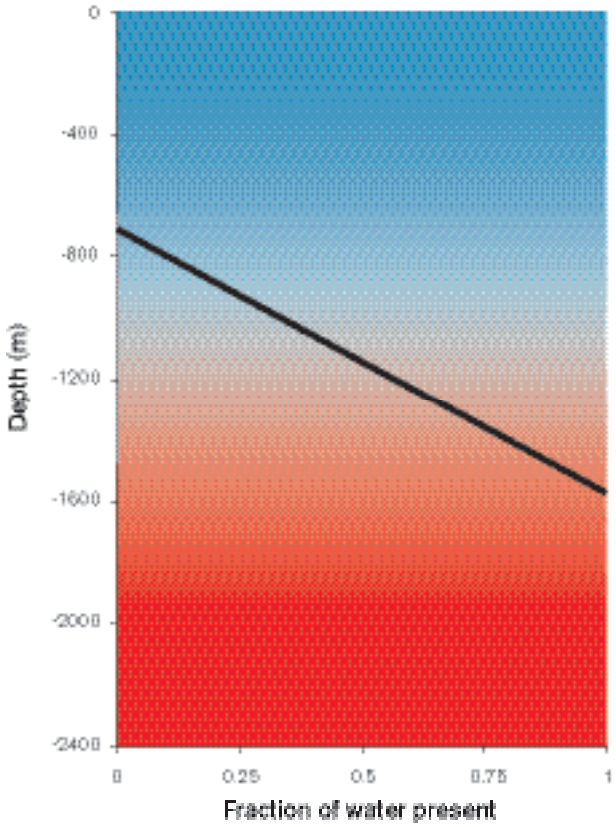

Figure 8-26. *Initial condition for reference water transport, at 12,000 BP. Above 700 m the water is pure Glacial (coloured cyan). There is a linear transition between Glacial and Brine (coloured red) toward pure Brine below 1,500 m (One test case is shown). No other water types were considered as initial conditions /Hartley et al. 2005/.*

8.7 Effects of model size and model resolution

To some extent the results from a numerical groundwater flow model depend on the model size and model resolution, and therefore it is needed to explore the effects and judge if they are small enough so they do not affect the overall results that are looked for, to meet the modelling objectives.

8.7.1 Model domain size

To minimise the computational effort one task was to test the model size, required. ConnectFlow tested smaller models than the pre-set regional scale model domain (cf. Figure 8-27) and DarcyTools tested a larger model domain (cf. Figure 8-28). Hence, part of the study concentrated on quantifying the sensitivity of the calibration targets to domain size with the aim of finding a minimum size for the regional model for which stable calibration results could be obtained. The primary calibration targets used were the profiles of salinity along boreholes KLX01, KLX02, KSH01A, KSH02 and KSH03A. The salinity was also considered in borehole KAV01 and a hypothetical borehole in the centre of the Äspö HRL.

The smaller model sizes tested by ConnecFlow tested showed that it significantly differed from the salinity distution in the large scale model Simpevarp 1.1 and the Simpevarp 1.2 regional model domain. The “smaller regional domain” showed minor differences, see orange curve in Figure 8-29.

The advective travel time from 500 m depth up to surface for particles released from the areas shown in Figure 8-30 were calculated for the regional model domain and the extended model domain, using a low and a high fracture frequency in the HydroDFN model, see Figure 8-31.

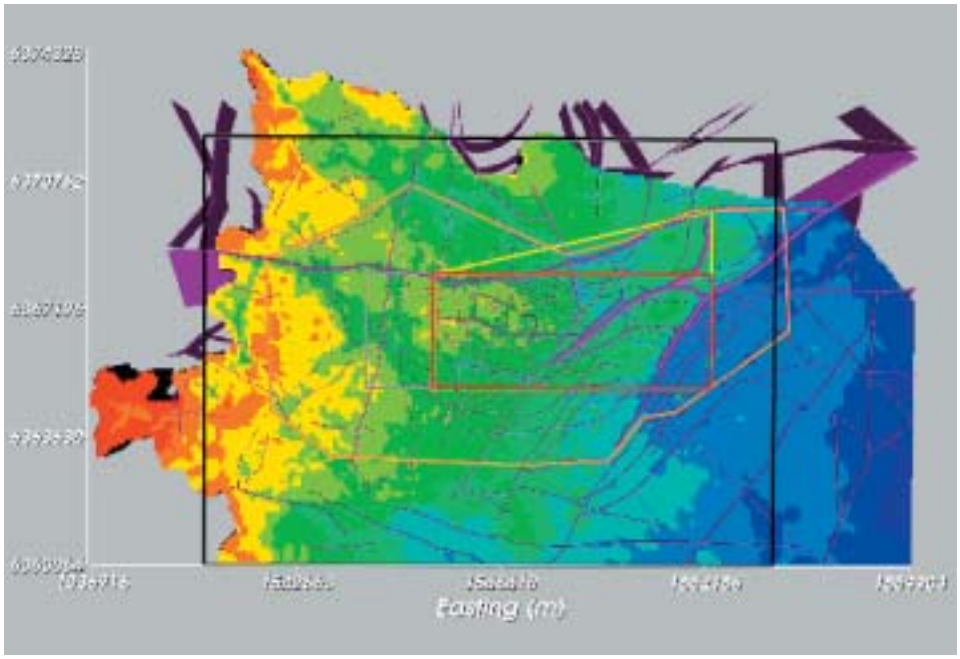

Figure 8-27. *ConnectFlow: The alternative regional model domains considered for version Simpevarp 1.2 superimposed on the Simpevarp 1.1 ConnectFlow model domain coloured by elevation. Simpevarp regional model in black (21×13 km^2), Simpevarp local model in red (8×3 km^2) – cf. Chapter 2. “Small regional model” in orange, was used in most ConnectFlow simulation cases /Hartley et al. 2005/.*

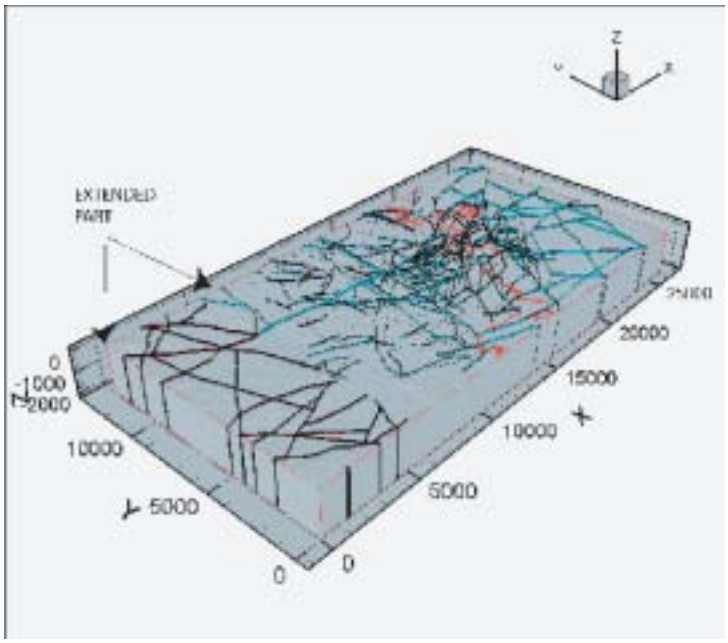

Figure 8-28. *DarcyTools: The alternative regional model domain considered for Simpevarp 1.2 was extended 5 km to the west of the regional model domain defined for Simpevarp 1.2. The "extended part" runs from X=0 to X=5,000 m, where the X-axis is oriented W-E.The applied deformation zones for the extended part are vertical and based on the interpreted lineaments /Follin et al. 2005/.*

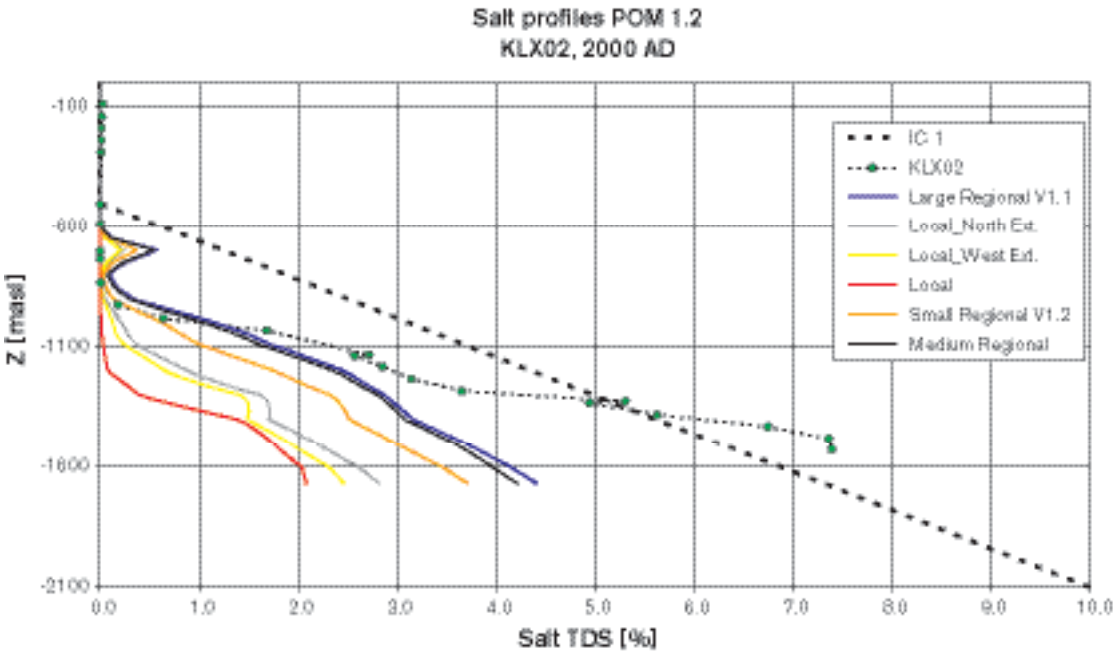

Figure 8-29. *ConnectFlow: "Small regional model" considered to give approximately the same TDS distribution as the "Large regional model V1.1" ("Small regional model" was also used as a base case for Simpevarp 1.2) /Hartley et al. 2005/.*

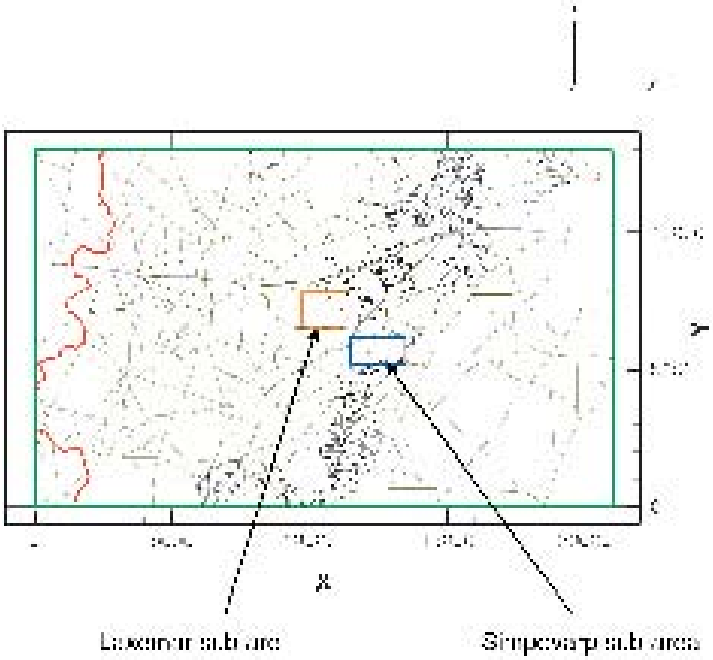

Figure 8-30. *Definition of the Simepvarp (blue rectangle) and Laxemar (orange rectangle) release areas employed for particle tracking calculations.*

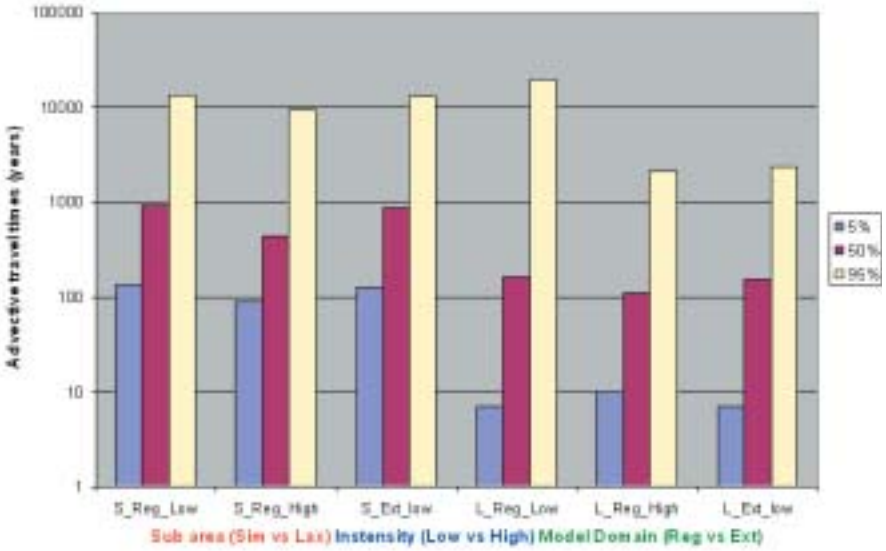

Figure 8-31. *DarcyTools: The flow paths from Simpevarp release area are not affected by an increased model size but to some extent the flow paths from the Laxemar release area are /Follin et al. 2005/.*

The conclusions were as follows (cf. Figure 8-29 through Figure 8-31):

- ConnectFlow: ”Small-regional domain” ~ 14 km (E-W) by 7 km (N-S) constitutes the minimum model size for obtaining an adequate reference water calculation.
- ConnectFlow: The latter constraint may not be sufficient for transport pathways for all site scale or local scale applications. This will need to be investigated further.
- DarcyTools: The regional scale model as defined for Siimpevarp 1.2 is sufficient for adequate reference water calculations.
- DarcyTools: Flow paths from the Laxemar release area, cf. Figure 8-31, (95 percentile of the advective travel time) are to some extent affected by the model size, but the median advective time is about the same for the tested models.

The “optimal” model size is still an open question that has to be further tested even though the employed regional model domain possibly is sufficient. Using a larger model size than the regional model domain can probably be made with larger grid sizes toward the boundaries. Both ConnectFlow and the new version of DarcyTools can handle this transition of the grid.

8.7.2 Model resolution

The grid size used was for DarcyTools 100 m, see illustration in Figure 8-32, and for ConnectFlow 100 m and 50 m (embedded grid) see Figure 8-33. The figures illustrates that the 100 m grid smears out the deterministic zones rather severely (the size of the grid blocks are so large compared to the thickness of the deformation zones), which has an impact in regions with many deterministic zones; the effect of the stochastic fracture network on the flow field becomes small. This is illustrated in Figure 8-32 with the large number of deterministic zones around boreholes KLX01 and KLX02.

A finer grid resolution than 100 m within the local model area, and probably down to a depth of 1,000 m , where most of the hydrogeochemistry data is available, is required to capture the heterogeneity that is present and probably is relevant for the long-time and large-scale simulations of the groundwater flow after last glaciation.

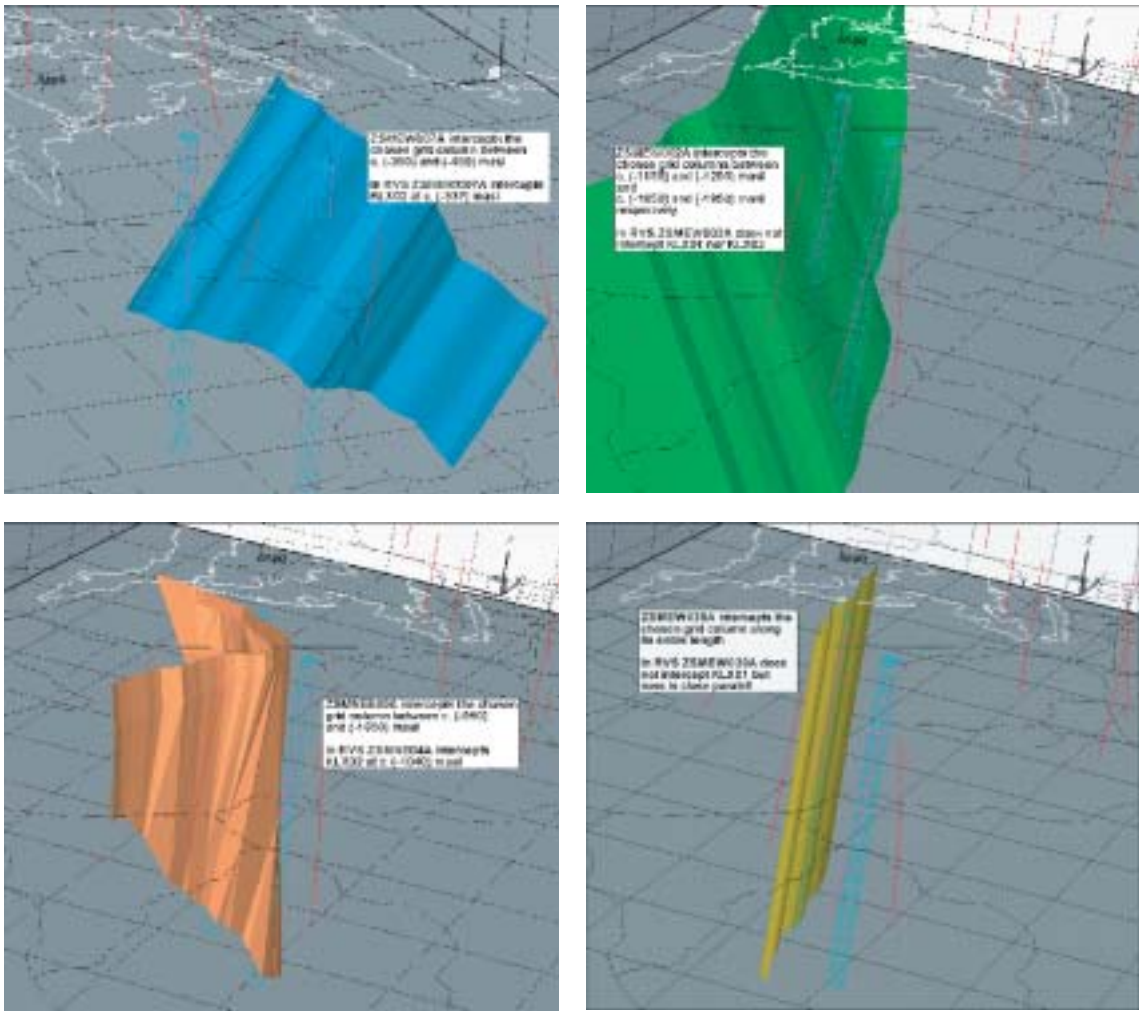

Figure 8-32. *DarcyTools: The grid size used is 100 m. The grid size affects the resolution near boreholes and may also significantly affect the hydraulic connection between the borehole and near-by deformation zones (less distinct connection than possibly in reality) /Follin et al. 2005/.*

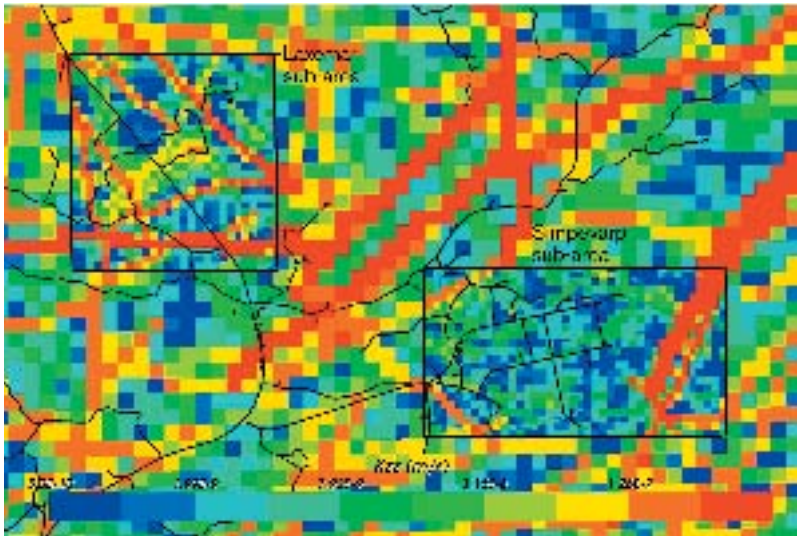

Figure 8-33. *Vertical hydraulic conductivity Kzz (m/s) mapped on a horizontal slice at z=–50 m showing the representation of the HRD and HCD (mainly mapped in red) on the regional- and site-scales using an embedded grid: Grid size 50 and 100 m. Simpevarp and Laxemar release areas, with the finer grid, are outlined /Hartley et al. 2005/.*

8.8 Resulting groundwater flow model

In this section the resulting groundwater flow model is presented together with some results from sensitivity studies. First the base case properties are presented together with a brief summary of how sensitive the model is to different properties/conditions applied. Subsequently, the evolution of the groundwater flow system since last glaciation is described, followed by an overview of the present groundwater flow conditions at the site.

8.8.1 Base case properties – and sensitivity to calibration targets

The ConnectFlow and DarcyTools-teams used the model parameters as given in Table 8-20 and Table 8-21, respectively. The following general conclusions can be made on the initial and boundary conditions and the hydraulic properties:

Initial and boundary conditions:

- Glacial water was probably injected at high pressures to about 1 km depth during the early parts of the post-glacial period.
- Possibly there should be a large Glacial water component in early freshwater arising during the Baltic Ice Lake and Ancylus Lake periods.

HRD, HCD, HSD:

- HydroDFN properties give block-scale hydraulic conductivities in the correct order of magnitude for prediction of hydrogeochemistry.
- Smaller, low confidence deformation zones have limited effect on regional-scale flow, but do affect hydrogeochemistry in the vicinity of individual boreholes. Possibly hydrogeochemistry can be used to confirm the extent and properties of individual deformation zones.
- A reduced assigned hydraulic condictivity at depth may give a better hydrogeochemistry, but the average K from the HydroDFN needs to be preserved. The depth decrease of K should only be a within a factor < 10.

Observe in the figures below that ”Rain 1960” in DarcyTools is the meteoric water infiltrated after 1960 and “Meteoric” represents the meteoric water before 1960, whereas ConnectFlow used the water type “Rain 1960” defined by the hydrogeochemists for their M3 analysis, in which it is considered to represent all the meteoric water after the last glaciation.

The estimates of the porosity of the fracture system (the flow porosity in fractures with advective flow and the porosity related to the stagnant pools in the same fractures) and the matrix porosity (micro fractures extending from the fracture with the advective flow) are uncertain, but most probably the matrix porosity is significantly higher than the flow porosity, and this should have a an influence of the evolution of water composition. This has been tested, but more efforts will be made in future modelling.

Table 8-20. ConnectFlow: Summary of hydraulic parameters and conditions used in calibration of Base Case model with an indication of the possible range of alternative parameters that may also give a match to the borehole hydro-geochemistry.Details are presented in /Hartley et al. 2005/.

Parameter	Calibration value	Comments alt. parameter range
Model domain	Small regional model – about 14 (E-W) × 7 km (N-S)	This constitutes the minimum. 16 km (E-W) × 12 km (N-S) to get good stable results
Grid resolution	50 m necessary on the site-scale	100 m necessary on regional-scale
Initial condition	Full Glacial 0–700 m; then linear gradient to non-Glacial, full Brine below 1,500 m	Glacial has to go to about 1 km depth then full Brine below 1,500 m
Top surface flow BC	Topography	Try specified infiltration to calibrate infiltration and HSD K
Top surface waters	Baltic Ice Lake (Glacial), Yoldia Sea (Marine/Glacial), Ancylus Ice Lake (Glacial), Litorina Sea (Marine), Baltic Sea/Precipitation with land rise (Marine diluting with Rain 1960)	Onshore – Ice Lakes could be mixture of Brine and Rain 1960. Offshore, Litorina could occur at slightly different time or strength (not very sensitive)
HydroDFN HRD K	CF, DT, KLX01 all calibrated This had block-scale properties of $K_{50\%} \sim 5\times10^{-9}$ m/s, $K_{10\%} = 5\times10^{-10}$ m/s	All conditioned HydroDFN models calibrated, but the model is probably sensitive to changing K by a factor of 5
Depth dependence	None	Weak slope (factor 5 over 2 km) may improve results, but keep mean at 1 km same
Kinematic HRD porosity n_{etb}	Based on DFN value, $e_t = 0.5T^{0.5}$ (T: transmissivity, m^2/s, e_t = transport aperature, m)	Fairly insensitive. Can increase by factor 10
Matrix porosity n_m	5×10^{-3}	$2–5\times10^{-3}$
Kinematic HCD porosity n_{et}	$e_t = 5T^{0.5}$	a=1–5 in $e_t=aT^b$, or could make b higher to be continuous with HRD
FWS for RMD (FWS=$2\times P_{32c}$) (m^2/m^3)	2.0	0.5–2.0
Maxtrix diffusion length L_D (m)	0.5	0.5–2
Intrinisic diffusion coefficient into matrix D_e (m^2/s)	5×10^{-13}	$1–5\times10^{-13}$

Table 8-21. DarcyTools: Summary of hydraulic parameters and conditions used in calibration of Base Case model with an indication of the possible range of alternative parameters that may also give a match to the borehole hydro-geochemistry. Details are presented in /Follin et al. 2005/.

Parameter	Calibration value	Comments alt parameter range
Model domain	210×130×2.1 km^3	(210–260)×130×2.1 km^3
Grid resolution	100 m	No alternative tested
Initial condition	Full Glacial 0–950 m; then linear gradient to no Glacial, full Brine at 1,450 m; full Brine below 1,450 m	Glacial has to go to about 1 km depth then full Brine by 1,500 m
Top surface flow BC	Topography	No alternative tested
Top surface waters	Baltic Ice Lake (Glacial), Yoldia Sea (Marine/Glacial), Ancylus Ice Lake (Glacial), Littorina Sea (Marine), Baltic Sea/Precipitation with land rise (Marine diluting with Rain 1960)	Tested also the sensitivity of the flow model to the initial situation and the situation of maximum salinity of the Littorina Sea
HydroDFN HRD K	CF, DT, KLX01 all calibrated Block-scale properties of $K_{50\%} \sim 5\times10^{-9}$ m/s, $K_{10\%} = 5\times10^{-10}$ m/s	Tested also an alternative DFNmodel with a much lower fracture intensity (about a factor of four less)
Depth dependence	None	Tested also an alternative model where the conductivity decreased by a factor of 10 per kilometre
Kinematic HRD porosity n_{etb}	1E–4 for the background rock 0.5% for the stochastic deformation zones (100–1,000 m)	No alternative tested
Matrix porosity n_m	Used a multi-rate diffusion model A global value of the ratio between the immobile to mobile pore volume of 2 was assumed	Tested also 0.1, 1, 10 and 100
Kinematic HCD porosity n_{et}	1% for the deterministic deformation zones	No alternative tested
FWS for RMD (m^2/m^3)	2 $m^2/(b\cdot m^2)$ where b is the geological thickness of the fracture zone	No alternative tested
Maxtrix diffusion Used a multi-rate diffusion model	10 storage volumes of different time scales for modelling	No alternative tested
Multi-rate diffusion model coefficients	αmax = 1E–3 s^{-1} and αminm = 1E–10 s^{-1}	No alternative tested

Generally, it seems the model gives a good reproduction of the overall profiles for the reference waters (see e.g. Figure 8-34), although some local differences to the HCD model around boreholes KLX01 and KSH02 would probably greatly improve the match in this area. It should be noted that the modelled water type “Marine” corresponds to sum of the identified water types “Marine sediments” and “Littorina”.

Apart from comparing the interpreted hydrogeochemistry from the M3 approach, a comparison was made with the environmental isotopes, considering them as conservative tracers. The Oxygen-18 isotope ratios and Deuterium isotope ratios are shown for boreholes KLX01, KLX02, KSH01A and KSH02 in Figure 8-35. High negative values of $\delta^{18}O$ and δD are associated with Glacial water. Hence, the model at KLX02 predicts the correct shape of the change, but there is somewhat too much Glacial water, whereas the model is not predicting enough Glacial in KLX01, due to too much mixing in the model. Still, the shapes of the profiles down the boreholes seem to generally mirror those of the data.

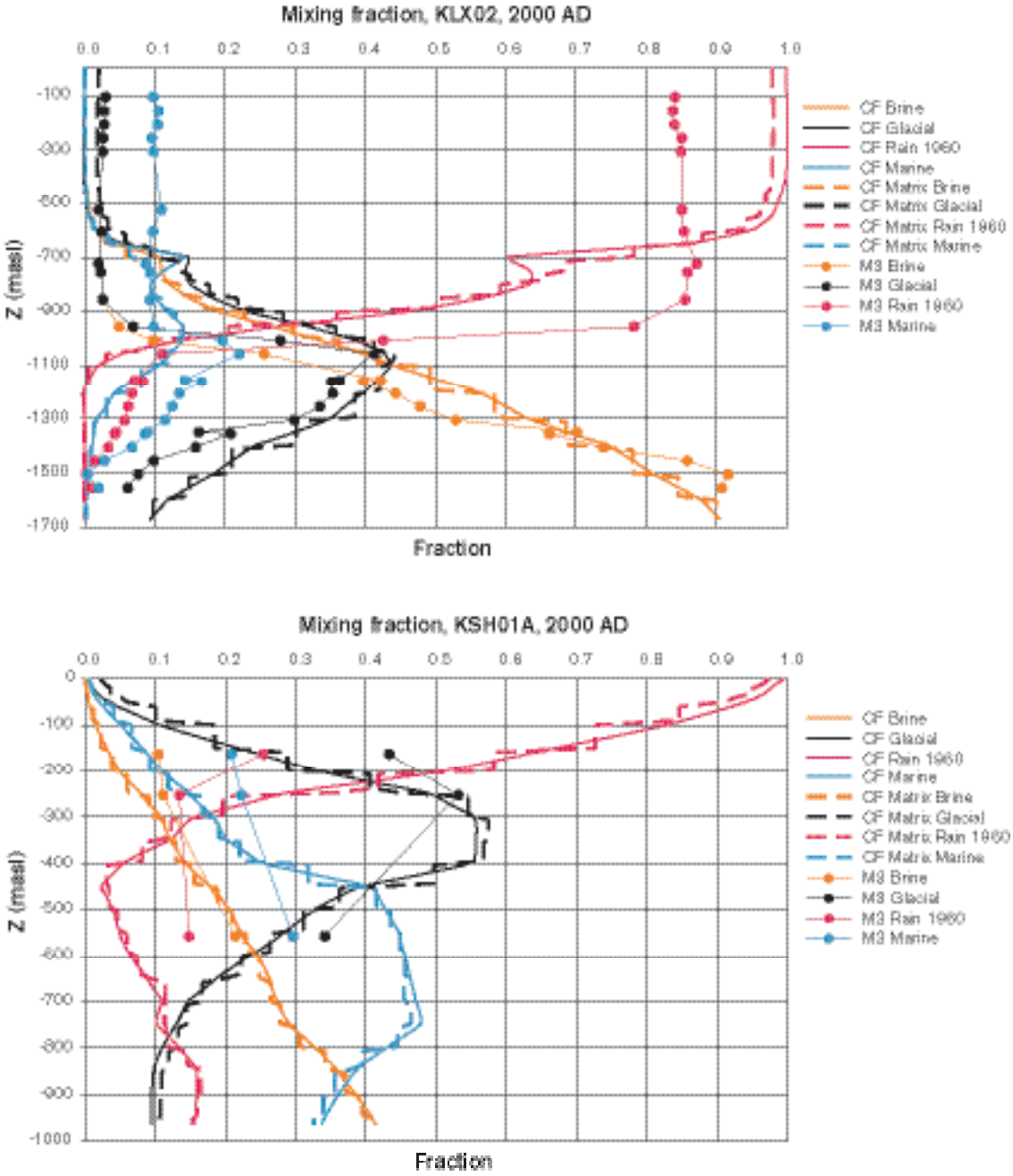

Figure 8-34. *ConnectFlow: Comparison of 4 calcualted reference water fractions in boreholes KLX02 and KSH01A for Base Case (SReg_4Component_IC2). The mixing fractions in the fracture system are shown by solid lines and those in the matrix by dashed lines, and the measured data by points /Hartley et al. 2005/.*

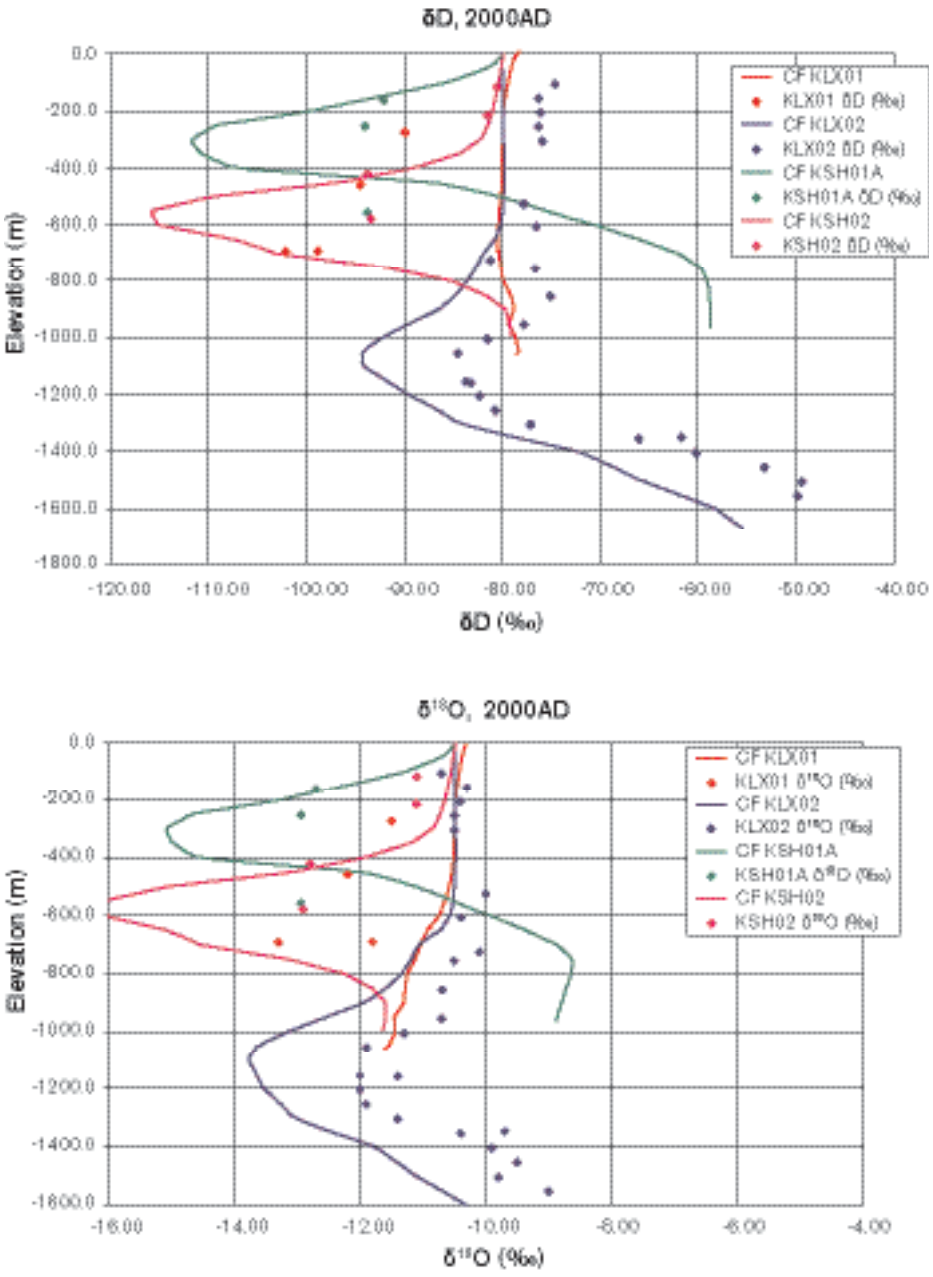

Figure 8-35. *ConnectFlow: Comparison of calculated hydrogen isotope ratio δD (top) and Oxygen isotope ratio $\delta^{18}O$ (bottom) in boreholes KLX01, KLX02, KSH1A and KSH02 for Base Case (SReg_ 4Component_IC2). $\delta^{18}O$ in the fracture system is shown by solid lines and measured data by points /Hartley et al. 2005/.*

Figure 8-36 illustrates the impact of a lower fracture intensity compared to what was suggested in the HydroDFN model by DarcyTools. As can be seen, the overall pattern is the same, but there are differences looking at the modelled “1960 rain”, “Meteoric” , “Glacial” and “Littorina” water types.

Figure 8-37 shows a model with no depth dependency and a model with decreasing hydraulic conductivity by depth. As can be seen the match between the simulated and the calculated fractions of water types is better for the model with a decreasing hydraulic conductivity.

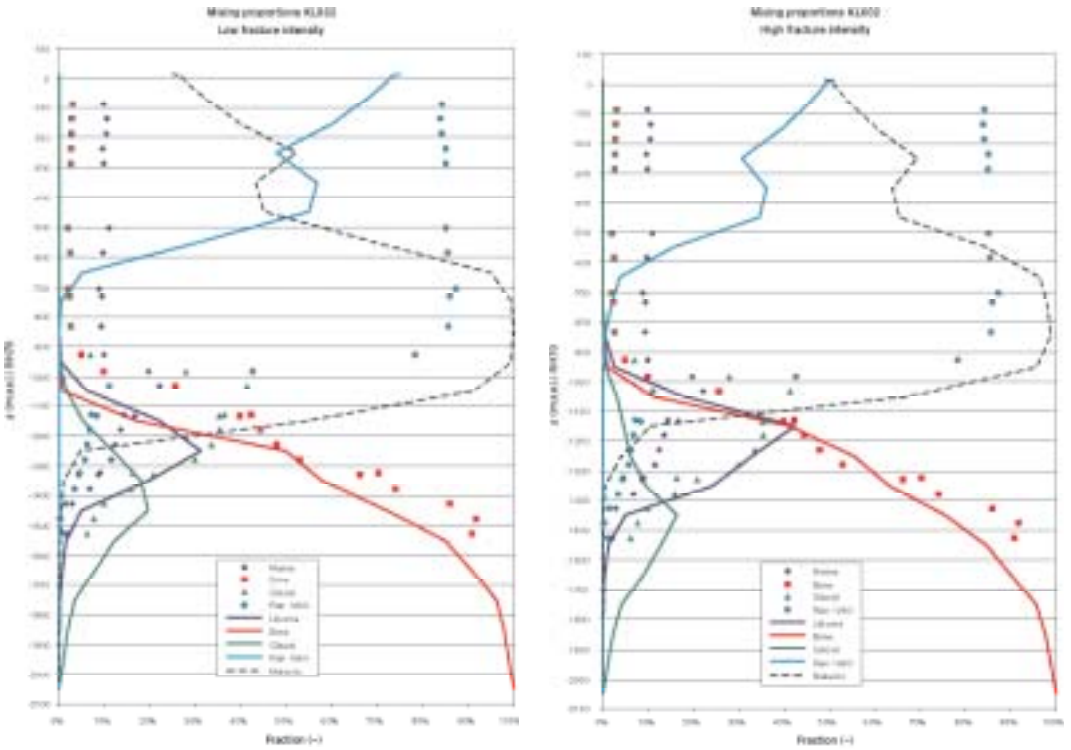

Figure 8-36. *DarcyTools: Comparison of effects of high fracture network intensity (base case in HydroDFN model, DT) and low fracture intensity. Modelled and measured (based on water samples) water types in borehole KLX02. Water after 1960 was in the model given its own "signature" – therefore modelled "Rain 1960" + "Meteoric" should be compared to M3-modelled "Rain 1960". See Chapter 9 for detailes concerning water types /Follin et al. 2005/.*

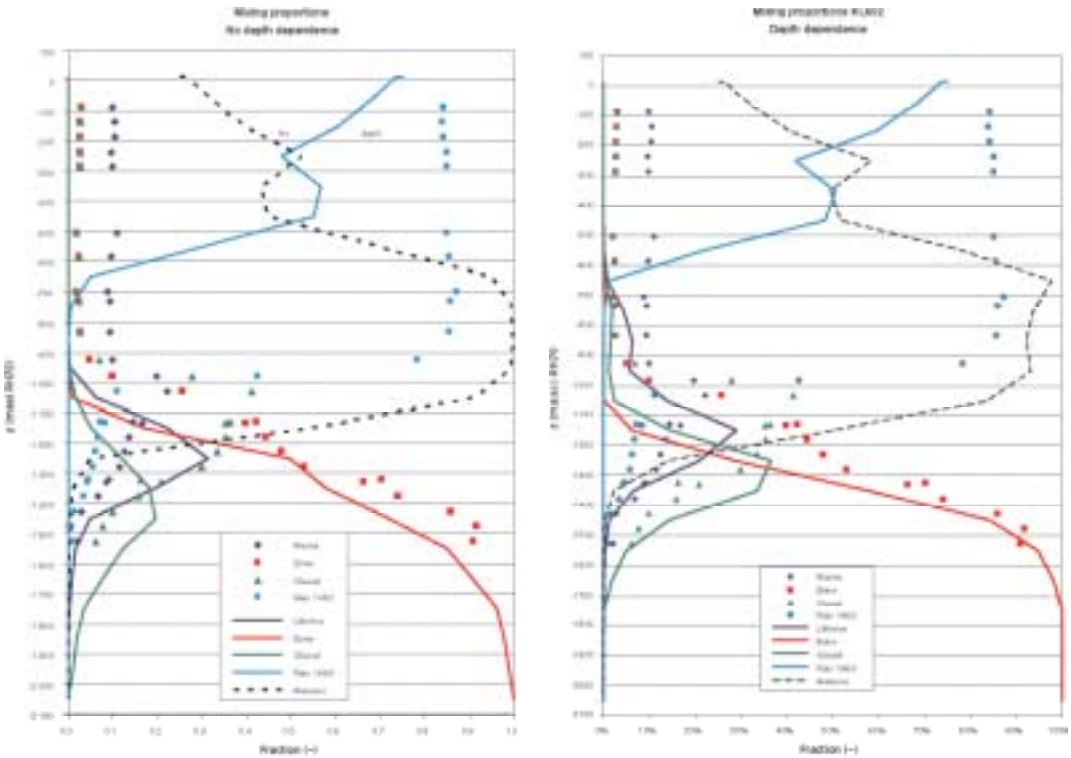

Figure 8-37. *DarcyTools: Comparison of effects of depth dependence of hydraulic conductivity. Modelled and measured (based on water samples) water types in borehole KLX02. Water after 1960 was in the model given its own "signature" – therefore modelled "Rain 1960" +" Meteoric" should be compared with calculated "Rain 1960" See Chapter 9 for detailes concerning water types /Follin et al. 2005/.*

8.8.2 Calibration against past evolution of hydrogeochemistry

The groundwater flow simulations start after the last glaciation with the initial conditions according to Section 8.3. Calibration targets have been the water type and isotope distribution in boreholes, and material properties as well as initial conditions have been varied to match the model with measured values.

Figure 8-38 illustrates the evolution of the water types “Rain 1960” and Glacial water. As can be seen the Glacial water is “washed” out by the infiltrating Littorina water (not shown in Figure 8-30, see the modelling reports /Follin et al. 2005/ and /Hartley et al. 2005/) and infiltrating meteoric water (Observe, as pointed out earlier, that the definition of “Rain 1960” is different between the modelling teams). The models indicate that large amounts of Glacial water should be present beyond the present shore line and in minor amounts in “pockets” below the surface, immediately west of the shoreline (shown in more detail in Section 8.7.3).

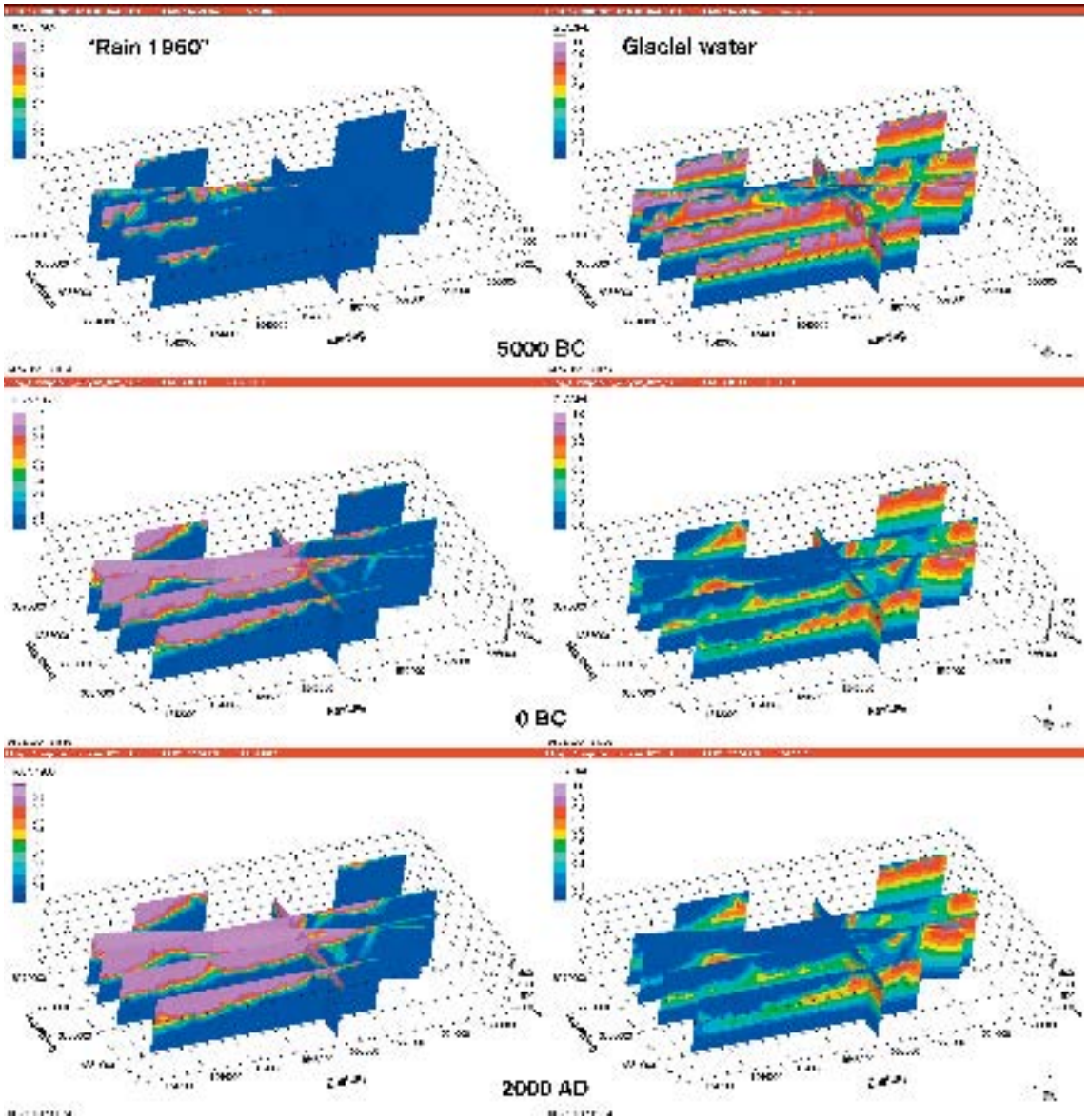

Figure 8-38. *ConnectFlow. Example of the the evolution of the water types “Rain 1960” and Glacial water after the last glaciation. Base Case (SReg_4Component_IC2) /Hartley et al. 2005/.*

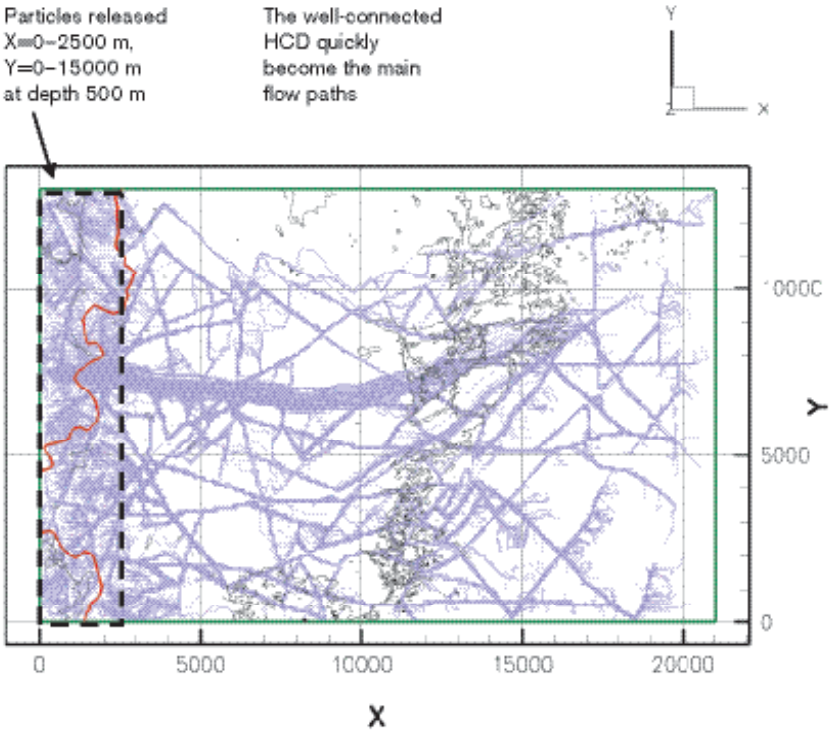

Figure 8-39. *DarcyTools: The deterministic deformation zones in the model controls the flow paths. Particles travel 10–1,000 m in a stochastic network and then discharge into the large, well-connected HCDs to their respective final discharge points /Follin et al. 2005/. The red curve indicates the western water divide and the blue lines show the particle traces.*

The base case for the HCDs is to include all interpreted deterministic deformation zones. These are all well connected and were, if no hydraulic tests were available, given the geometric mean transmissivity of the HCDs in the vicinity of the island of Äspö,. This system of large and fairly conductive hydraulic features controls much of the groundwater flow and thus the evolution of the water types. Figure 8-39 illustrates how particles released at a depth of 500 m after some 100–1,000 m reach a HCD and then follows the HCDs to their respective discharge points.

8.8.3 Present-day flow conditions

This section presents the present-day (2,000 AD) flow conditions in terms of distribution of the water types and groundwater fluxes as predicted by the numerical models. Details are found in /Hartley et al. 2005/ and /Follin et al. 2005/.

Figure 8-40 shows that the Brine reaches as high up as about –200 masl in the model. At a depth of –1,000 masl the fraction of Brine is about 50% in the eastern part, corresponding to a TDS of about 40g/l, whereas the western part of the modelled area still contains freshwater originating from the “Rain 1960” and “Glacial water”.

Marine water is only present in the eastern part of the modelled area underneath the sea. A few very transmissive deterministic deformation zones in this area transports Marine water deep into the rock. In the remaining rock, there is little or no Marine water present at 2,000 AD.

Water originating from the “Rain 1960” (Equal to Meteoric water since last glaciation in ConnectFlow reporting) penetrates the rock down to about –1,500 masl in the western area where land first rose above the sea level. In the top layers the Rain 1960 covers almost the entire model domain since the dominant part of the model has risen above the sea at close to the present-day.

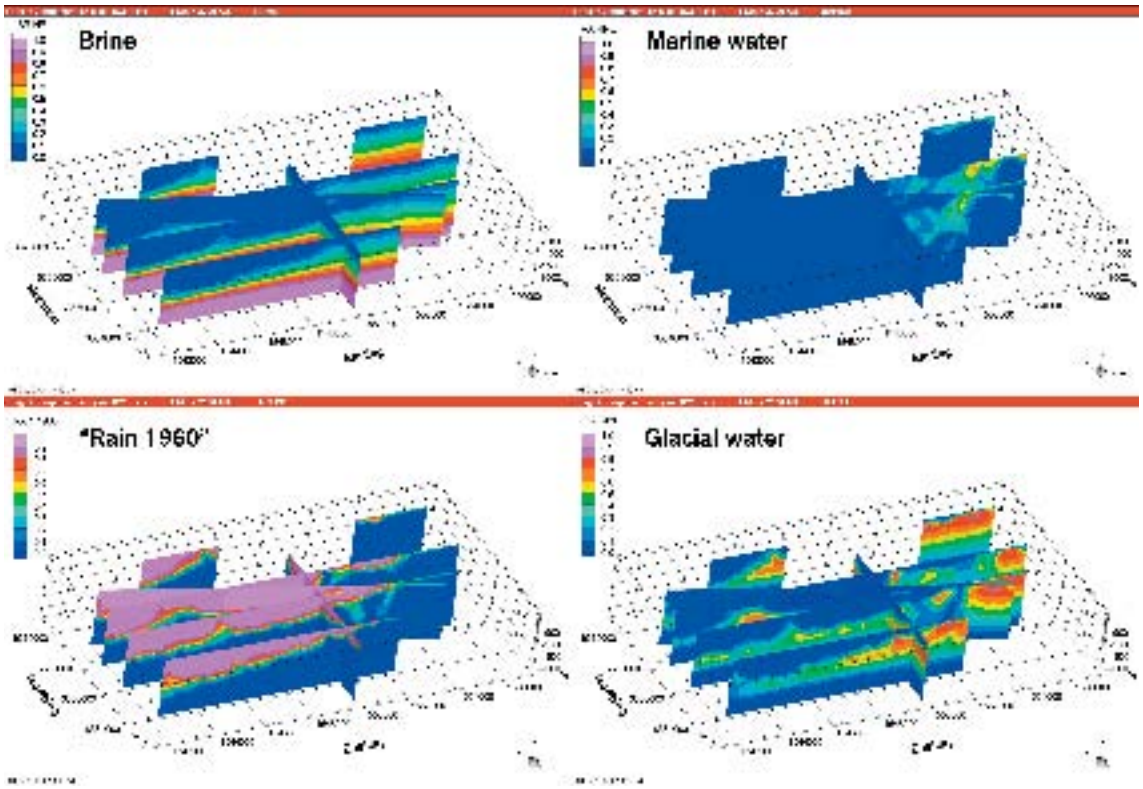

Figure 8-40. *ConnectFlow: Present day distribution of Brine, Marine water , Rain 1960 and Glacial water. Base Case (SReg_4Component_IC2) /Hartley et al. 2005/.*

The Glacial water that covered the upper part of the model at 10,000 BC has been flushed out by Rain 1960 and Marine waters down to more than –500 masl. Between –500 masl and –1,000 masl there is, however, Glacial water present in the eastern part.

Figure 8-41 and Figure 8-42 show the modelled water types at depths –100 and –500 masl. They illustrate possible targets for boreholes if one would better confirm the spatial distribution of water types. This is also true for Figure 8-44, which is the DarcyTools illustration of the possible distribution of Littorina and Glacial water types.

Figure 8-43 illustrates the downward (recharge) or upward (discharge) flow direction as well as the flow rate. Close to the surface at –10 and –100 masl the flows are mainly downward (recharge) around –0.1 to –0.001 m/year in the rock mass. The discharge is located towards the Baltic Sea in the eastern part of the modelled area and around deformation zones onshore. In the deformation zones, the vertical Darcy velocity is around 0.1 m/year. The flow field near the surface is very heterogeneous indicating development of very local flow cells. At –500 masl, the flow rates are generally around 0.01–0.0001 m/year in the recharge as well as in the discharge areas. This is an order of magnitude lower than for the flow above –100 masl. The flow field also tends to be more homogeneous at this depth. At –1,000 masl, the flow rates are generally less than 0.0001 m/year. Most of the flow is directed downwards at this depth.

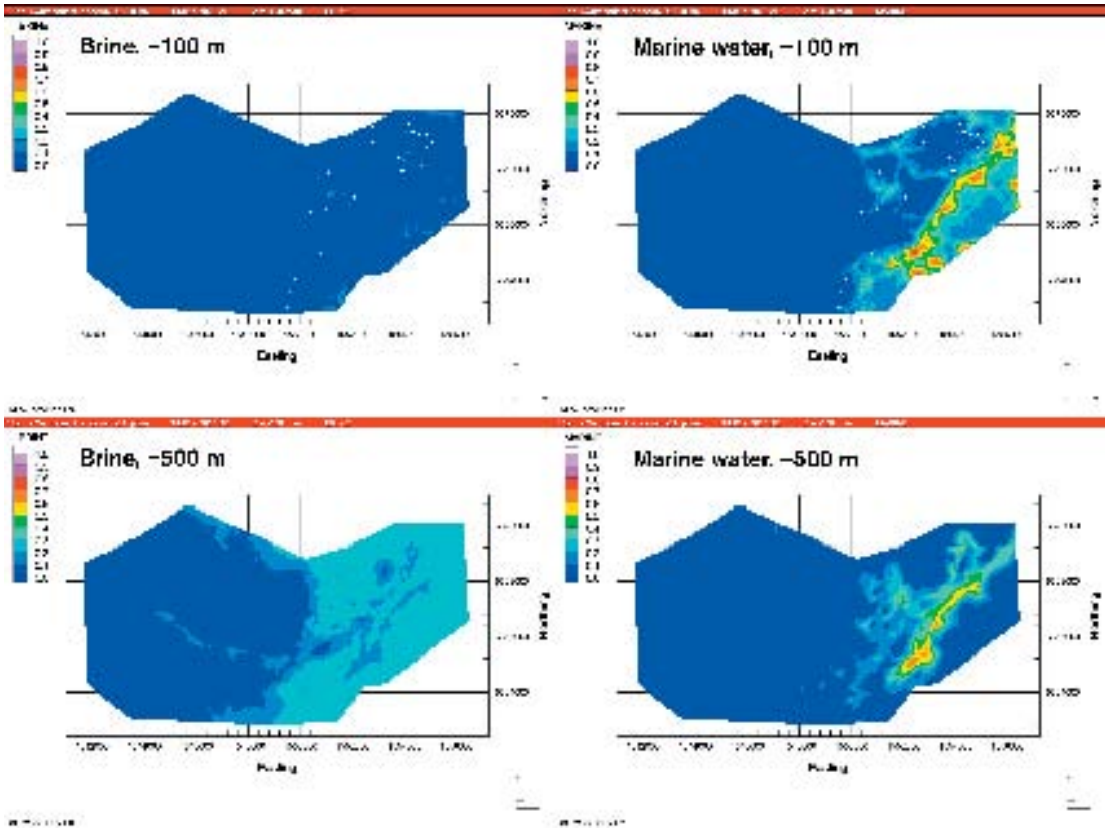

Figure 8-41. *ConnectFlow: Present day distribution of Brine and Marine water at depth –100 masl and –500 masl. Base Case (SReg_4Component_IC2) /Hartley et al. 2005/.*

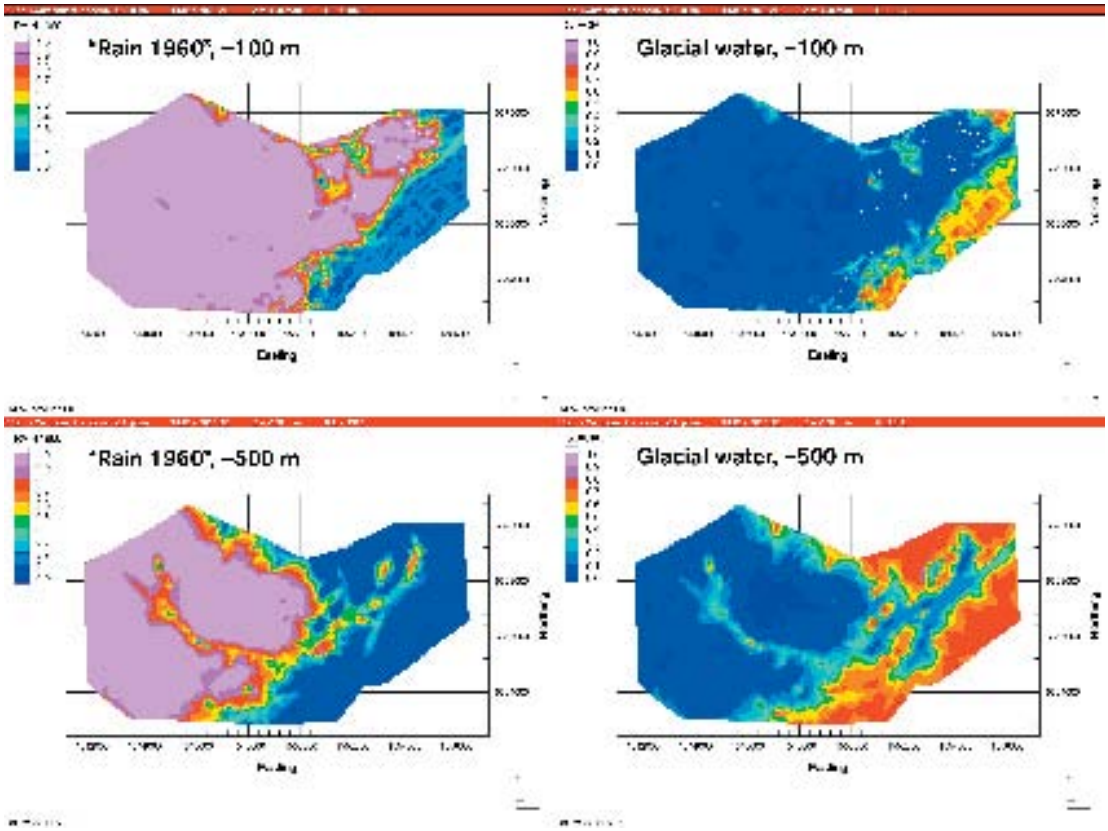

Figure 8-42. *ConnectFlow: Present day distribution of Rain 1960 and Glacial water at depth –100 masl and –500 masl. Base Case (SReg_4Component_IC2) /Hartley et al. 2005/.*

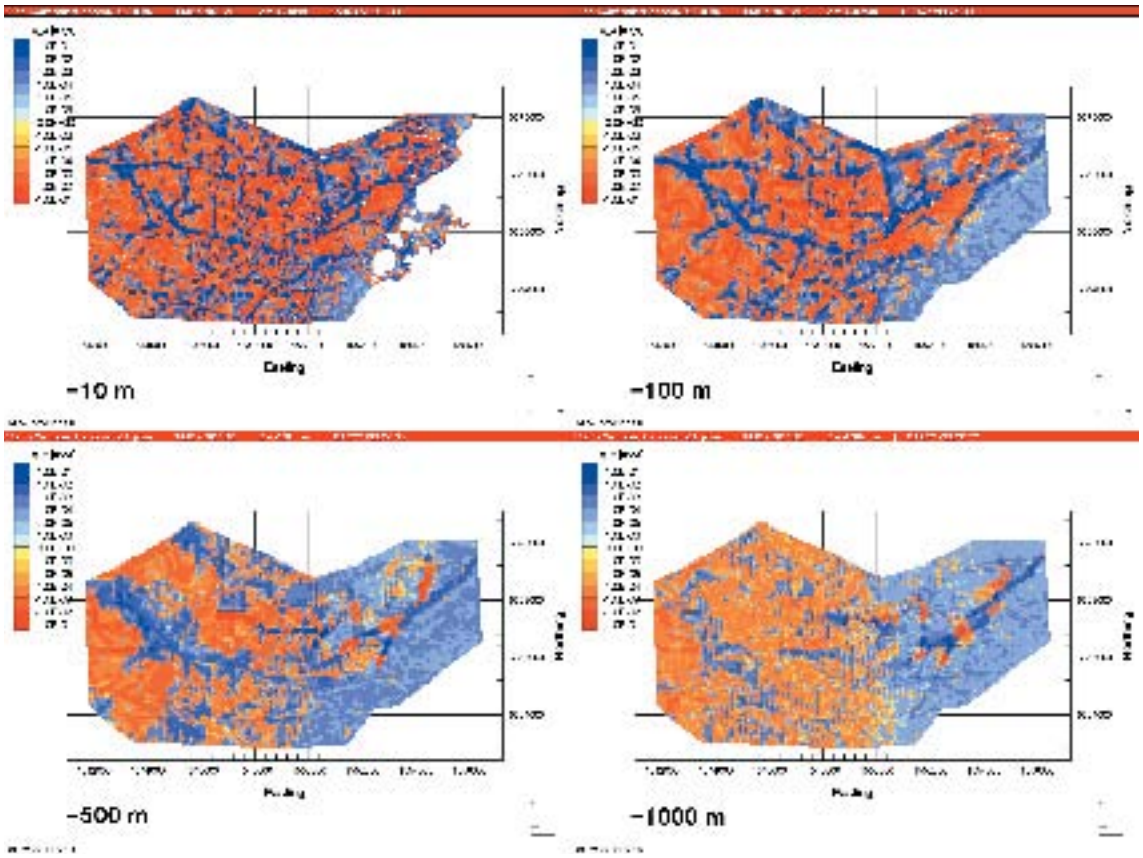

Figure 8-43. *ConnectFlow: Present day vertical Darcy flux at different vertical depths. Orange-red: flow downwards. Blue: flow upwards – 0 m/y yellow, 0.1 m/y dark blue, –1e–4 m/y orange, –0.1 m/y dark red. Base Case (SReg_4Component_IC2) /Hartley et al. 2005/.*

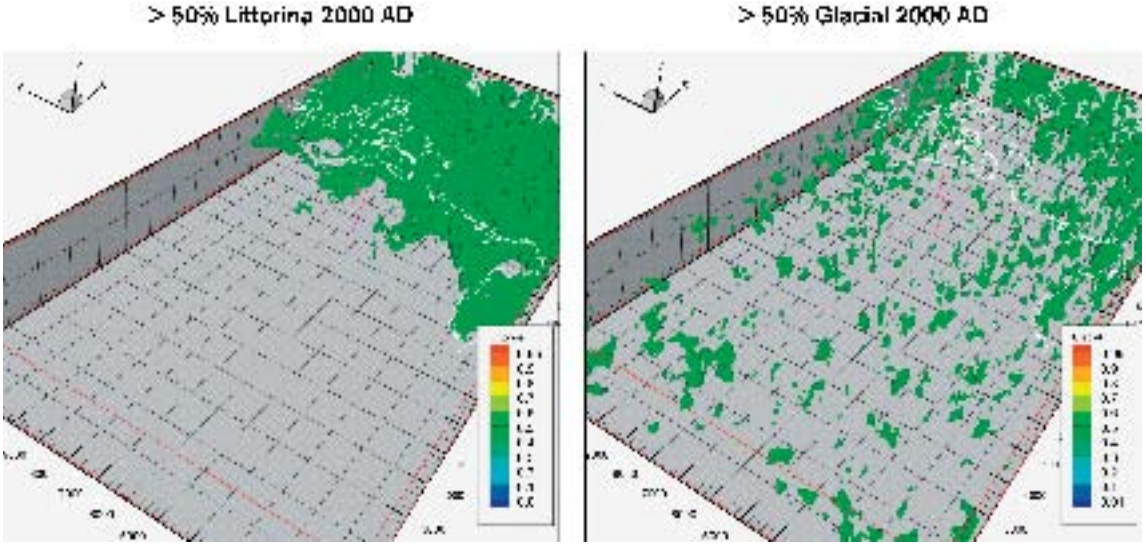

Figure 8-44. *DarcyTools: Present day distribution of Littorina and Glacial water types. Littorina water type is according to the model is supposed to be found near or east of the present coast line /Follin et al. 2005/.*

ConnectFlow: The model is not very sensitive to the changes considered. The distributions of the four reference waters and the vertical Darcy velocity are not affected much in the different cases compared with the Base Case. There are however a few parameters that clearly have significant effects on the results:

- Using a more shallow **initial condition** (IC1) where there is a linear transition between full Glacial at –500 masl and full Brine at –1,000 masl. Because the Brine is present higher up in the rock from the start, it is also found there to a higher degree at the present-day compared with the Base Case.
- **Decreasing K with depth.** Even a small decrease in K (a factor 5) significantly changes the flow distribution. Due to the decrease in Darcy velocities, the Brine now stays deeper in model and the flow is shallower.
- Most parameters did not need to be changed from the initial values specified in the Task Description. An exception was the **kinemeatic porosity of the HCD** that needed to be modified significantly from the initial guess, e.i. increased by factor 10 from the HCD definition.
- The **transport pathway** studies suggest discharge areas are **strongly linked to the HCD structures** including the eastern end of defomation zone ZSMEW007A in the centre of the local-scale area, ZSMEW004A in the south around the shore, and ZSMEW013A immediately north of Simpevarp. Based on the present day boundary conditions, the flow paths from release areas located within the Laxemar and Simpevarp subareas at 500 m depth were simulated. It was found that the released particles travel a short distance before reaching a HCD, and subsequently followed the system of HCDs to discharge points below the Baltic Sea. The discharge points for release in the Laxemar subarea are located mainly around the Äspö island, whereas discharge points for particles released in the Simpevarp subarea are found to the south and east of the subarea, as expected.

DarcyTools: The stipulated stochastic fracture intensity (or rather fracture zone intensity as features larger than 100 m was simulated), which was one of the key results from the HydroDFN analysis, renders a fairly continous medium, not very “DFN-like” with lots of cells more or less impermeable, on a 100 m scale, with at least one 100 m large DFN feature in all principal flow directions. Using this value there is almost no need for a DFN as the spatial model is Poissonian. Sensitivity studies show, however, that a lower intensity in the DFN model is also quite feasible from a calibration point of view, yet renders a quite different flow system with isolated volumes of Glacial and Littorina waters, see Figure 8-44 possible explanation for this result is that the calibration area where the deepest and most significant boreholes are situated is densely intersected by deterministically modelled deformation zones, which by and large make the properties of the stochastic DFN redundant. However, if one looks at fictive borehole locations, which are at a distance from the nearest deterministically modelled deformation zone, the simulated chemical profile versus depth show significant variability between realisations. This result is not reproduced for a high DFN intensity. Due to the great dependence on the deterministically modelled deformation zones, the model is quite sensitive to a decrease (depth dependence) in the grid cell conductivities.

As it stands from the simulations, it is of great interest to know more about the in situ occurrence of isolated volumes of different water types, in particular, Glacial, Brine and Littorna. The occurrence of isolated volumes of different water types could suggest a lower DFN intensity than the one originally stipulated value for Simpevarp 1.2 (as provided by the geological DFN model). Another property of key interest is pore matrix water chemistry.

The occurrence of “Rain 1960” water, which did not start to infiltrate until 1960 in contrast to the Meteoric water type, which began to infiltrate as soon as land rose above the sea level, is a very interesting geochemical tracer. The occurrence of Tritium rich water in the rock at great depth could suggest that the HCDs are quite permeable at depth. As shown above, the transport pathway studies suggest that the flow paths of the advective transport are strongly linked to the HCD structures.

The flow porosity of the HCD was increased to a value much greater than the value suggested, the latter based on tracer experiments in single features, cf. Table 8-13 and Table 8-15. The main reason for the increase was the aforementioned high frequency of HCDs in the near proximity of the boreholes of interest for calibration in combination with high transmissivity values of the HCD at depth.

This caused an unrealistic flushing of the water types at depth. It is noted that the current version of DarcyTools does not account for matrix diffusion of the water types but for the salinity solely.

8.9 Evaluation of uncertainties

Uncertainties in hydraulic properties, boundary conditions and initial conditions to variable extent govern the overall uncertainty of results of the numerical groundwater flow simulations. Their identification further promotes the discussion of how and where the the uncertainty should be decreased, and why.

8.9.1 Overburden – HSDs

The model suggested has low confidence as the geological decription of the overburden is very simplified in Simpevarp 1.2, and also the site-specific information on hydraulic properties is very limited.

8.9.2 Deterministic deformation zones – HCDs

The general confidence in the existence and properties of all suggested possible deformations zones is low, as most possible deformation zones are only based on lineaments and no hydraulic tests for the deformation zones are available. High confidence for existence has been judged for some of the deformation zones, cf. Chapter 5. For these zones, the confidence in some of the hydraulic properties is judged in Table 8-22.

The confidence in the hydraulic thickness is very low, based on one or a few intercepts of deformation zones by boreholes. Also, the hydraulic thickness may vary over the extent of the individual deformation zone “plane”. However, the width is judged to be of minor importance as it is the transmissivity that controls the capacity for flow in the deformation zone.

The confidence in the transmissivity is medium to low due to zero, one or a few intercepts of individual deformation zones. Having 1–2 hydraulic test results in a deformation zone, the confidence is set to low to medium. Having 3 up to c. 5 hydraulic test results, the confidence is set to medium. The transmissivity can be expected to vary along the “plane” of the deformation zones and as most zones are larger than 1 km one can expect that there will always be great difficulties to obtain a high confidence in the properties by drilling and borehole testing. Several observations have been judged as low to medium, despite three or more borehole intercepts. The reason is that the borehole intercepts have to be examined in more detail. More deformation zones than shown in Table 8-22 are associated with intercepts with boreholes, which also have been used to assign hydraulic parameters. However, as the geological confidence is regarded as low, the associated data have been excluded from this table.

The confidence in the storage coefficient is low, and will be low to a greater degree than transmissivity, due to difficulties in making proper tests. However, it is judged that this is of minor importance, as it controls the transient responses on time scales of days-months when pumping and during drawdown caused by tunnelling, which is of minor importance. The variation of the storage coefficient is less than transmisivity making it easier to analyse using sensitivity studies. However, the storage coefficient is important when size of hydraulic features is assessed, which is an essential component when studying the transmissivitry models suggested for the HydroDFN models. The storage coefficient is also important when judging results from interference tests.

The confidence in the mean transport aperture (giving the flow porosity jointly with the hydraulic thickness) is low, and probably will be rather low for individual deformation zones. There are data from Äspö HRL and some other places that gives indications of possible realistic values. However, some new data will be collected and probably the confidence in how transport aperture should be assigned will be increased during the continued site investigations, but still the confidence will probably be low-medium, demanding sensitivity studies to investigate the significance uncertainties in this property.

Table 8-22. Table of confidence of the hydraulic properties (base case) assigned to the HCDs in Simpevarp 1.2. Hydraulic thickness (b) Transmissivity (T), Storage coefficient (S), Mean transport aperture (e_T).

Name of HCD RVS ID	Geological confidence High/Medium/Low	(b) (m)	T (m^2/s)	S (–)	e_T (–)	Comment (intersection boreholes and other comments)
ZSMEW002A, (Mederhult zone)	High	low	low-medium	low	low	HLX20 and KAS03
ZSMEW004A	High	low	low	low	low	
ZSMEW007A	High	low	medium	low	low	HLX10, HLX11, HLX13. KLX02, KLX04
ZSMEW009A, (EW3)	High	low	medium	low	low	HAS13, HAS21, KAS06, KAS07
ZSMEW013A	High	low	low-medium	low	low	HAS01, HLX02, KAS04
ZSMEW028A	High	low	low	low	low	HAV09
ZSMNE005A, (Äspö shear zone)	High	low	low	low	low	KAS04, KAS12
ZSMNE006A, (NE1)	High	low	medium	low	low	KA1061, KA1131, KAS02, KAS07, KAS08, KAS09, KAS10, KAS11, KAS14, KAS16, KBH02. Many borhos but fairly local.
ZSMNE010A	High	low	low	low	low	
ZSMNE011A	High	low	low	low	low	
ZSMNE012A, (NE4)	High	low	Medium	low	low	HAV02, HAV07, HAV13, HAV14, HMJ01, KAV01, KAV04A, KBH02
ZSMNE016A	High	low	low	low	low	(HAV14 ?)
ZSMNE018A	High	low	low	low	low	HSH02
ZSMNE024A	High	low	low	low	low	HAV11, KSH03A
ZSMNE040A	High	low	low-medium	low	low	HLX01, HLX02, HLX04, KLX01, KLX02. The zone has an unusual shape. Other interpretation possible?
ZSMNS001A	High	low	low	low	low	
ZSMNS001B	High	low	low	low	low	
ZSMNS001C	High	low	low	low	low	
ZSMNS001D	High	low	low	low	low	
ZSMNS009A	High	low	low	low	low	
ZSMNS017A	High	low	low	low	low	KA2048B
ZSMNW004A	High	low	low	low	low	
ZSMNW007B	High	low	low	low	low	
ZSMNW012A	High	low	low	low	low	
ZSMNW025A	High	low	low	low	low	HSH01
ZSMxxxxxx (All other det. zones)	Low	low	low	low	low	Based on statistics from identified deformantions zone near Äspö HRL.

Issues concerning properties of deformation zones

The defined deformation zones (with high and low confidence) create a well-connected system, partly because of the geometrical definition (assumed to intersect or stop mutually and to be continuous over the plane) and partly because of the assigned hydraulic properties (assumed to be constant over the plane and to have a rather high transmissivity). The latter was based on a geometric mean value from Äspö data, if no hydraulic tests are available. There are several issues that should be looked at e.g.

- Can new investigations (mainly geological and geophysical) give a more general view of the existence of deformations zones?
- The spatial distribution of properties within HCDs is difficult to assess (generally very few samples), but depth dependency and heterogeneity within deformation zones should be assessed and tested with groundwater flow simulations. Possibly, geological and rock mechanical conceptual models can strengthen the assessment?

8.9.3 HydroDFN model – HRDs

The general confidence in the HydroDFN models is rather low due that data processed for the HydroDFN model represents mainly a smaller domain within the regional model domain and it is recognized that more tests and analysis can be made. Below some characteristics of the HydroDFN models is outlined and discussed.

- All three proposed conceptual transmissivity models can be used as alternative cases. However:
  - The correlation transmissivity – length seem to fit the data better when using PSS data.
  - Estimated geometric mean hydraulic conductivity at different test scales from the Äspö HRL investigations seems to support a correlation transmissivity – size.
- For the correlated transmissivity model it was possible to get different matches for P32, when adjusting the parameters of the T to L correlation. This suggests that:
  - This uncertainty may be addressed by the PSS data.
  - Size distribution and transmissivity should be examined for the large features.
- The rock is most conductive in direction EW to NW, but the difference is small.
- Horizontal K (Kh) is higher than the vertical K (Kv).
  - The reason is the higher intensity of the horizontal fracture set and possibly this may change if different T-models are applied for different fracture sets.
- The body of the PFL anomalies can be associated with 4 of the 7 fracture sets (Sub-vertical sets: E-W to WNW, NW, NW-NNW and a subhorizontal set).
  - This probably leads to a higher K in direction NW and may change the relation Kh/Kv. (Data from Äspö Laboratory also show a strong anisotropy due to conductive subvertical fractures with strike WNW-NW dominating.)
  - Modelling using different T-models for different fracture sets remains to be tested (Based on PFL-f data).

Issues concerning properties of the rock mass

- The suggested HydroDFN models have considerable differences in intensitiy. A high intensity creates more or less a continuum with block size of 100 m and with hardly any “pockets” of Glacial water. The low intensity model, however, generates a more heterogeneous system where “pockets” of Glacial water develop. To find evidence whether the connected and conductive fracture system is a “low intensity” one is essential and several possibilities are available:
  - If it can be argued that the hydrochemical data that indicate a highly heterogeneous distribution of Glacial water is a good evidence of a low intensity system.
  - The PSS data have only been used to a minor extent. Possibly the PSS tests with different test scales and test times, as well as a lower measurement limit than PFL, can be useful to discriminate between models.

  - The HydroDFN model is firmly linked to the GeoDFN model. Conceptual issues such as minimum fracture size that is observed in boreholes, the methodology to link surface data to borehole data and a "stronger" (useful for the disciplines of rock mechanics and hydrogeology) definition of deformation zones intersecting boreholes should be revisited. Seven fracture set were suggested in the GeoDFN, one group linked to lineaments and the other not linked to lineaments. Several sets were similar, and when trying to avoid coupling of the generation of the fracture network to each individual determintically defined deformation zone, it seems reasonable to use fewer fracture sets in the type of modelling presented here.

- Is there a depth dependence of properties?
  - Simulations indicate that a decreasing hydraulic conductivity with depth may provide a better match to the interpreted water types. An increased hydraulic conductivity in the upper 100 m of the rock may also have a significant effect on the distribution of water types. However, from the hydraulic data used so far this is not obvious, but data will be re-examined and new data will become available.
- What are the "background properties" in grid cells not intersected by a fracture (Considering that a minimum fracture size is adopted, L_{min}, and that smaller fractures are taken into account in the "background properties")?
  - This is a partly a code specific issue that needs to be tested more in coming model versions.
- The magnitudes of matrix porosity, porosity coupled to stagnant water in fractures and flow porosity of the fracture system are important for the evolution of the water types. Questions remain with regards to reasonable estimates of each of these porosities and how to best treat them in the models. For example, the current version of DarcyTools does not consider matrix diffusion of water types.
- PFL data seem to support the observation that the most conductive fractures are parallel to the main stress direction. However, no detailed evaluation has yet been made.

8.9.4 Boundary and initial conditions

- Initial and boundary conditions have a significant impact on the results.
  - Limits for the initial depth distribution for Glacial and Brine distribution is reasonable well constrained.
  - The size of suitable regional model should be further tested.
- The well connected system of HCDs (deterministically defined deformation zones). Different realisations of a HydroDFN model as well as different HydroDFN models presented by ConnectFlow and DarcyTools teams have only a minor effect on the overall distribution of water types. Locally, different realisations or HydroDFN models generate minor changes of the water types, but with a low fracture-intensity model significant differences are seen some distance away from the HCDs.
- Depth dependence of conductive properties has an effect on the flow field and the water type distribution.
  - A decrease in the hydraulic conductivity with depth seems to give a better match between simulated and calculated water types regardless of other parameter value settings.

8.10 Feedback to other disciplines

Some of the observed uncertainties may be related to data (or lack of data) and models coming from other disciplines, and others to lack of hydrogeological field data. The first part is solved by communicating and sicussiong the model issues with other disciplines to identify actions to be taken. The second part is resoved by communicating with responsible for the planning and execution of future site investigations. In this section the main issues are highlighted for further discussion.

8.10.1 Can new boreholes resolve some of the issues raised?

- New hydrochemical data may contribute significantly on the understanding of the flow system and basic properties of the HydroDFN.
- New boreholes within the regional model area could be useful:
  - Borehole near the Baltic sea: Do we find significant amounts of Littorina water component below the Baltic sea?
  - Deep borehole to the west in an area free from large deterministic deformation zones. Do we find Brine and Glacial water components similar to KLX02 data? Inland and east below Baltic sea – Do we find "pockets" of Glacial water and higher amount to the East? (Examination of old data may also be useful.)
  - Boreholes in larger discharge areas (depth 100–300 m). Do we find a Brine water component?
- A deeper examination of the earlier and new groundwater flow simulations may provide guidance where drilling should be made to get the most useful additional information.
- New, 100–200 m long, cored boreholes, with different orientations, from surface are essential to better link the fracture trace maps to the mapped fractures in boreholes. Fracture information of the upper 100 m of rock is sparse, due to the technique generally chosen by SKB for deep core-holes. With the purpose to minimise the contamination of the groundwater with drilling fluids, the upper 100 m of the rock is drilled with percussion drilling, followed by core drilling for rock deeper than 100 m. In these new short cored boreholes injection tests should also be made in test scales 5 and 20 m from surface to borehole bottom.

8.10.2 What other data or tests can discriminate between models?

- The Tritium data provides a fairly well-defined boundary condition, but have only been tested briefly by the ConnectFlow team /Hartley et al. 2005/ for the regional groundwater flow simulations. These data should be taken into account in future modelling.
- Other environmental isotopes should be tested in the regional groundwater flow simulations. Assessment of time series since the last glaciation of $\delta^{18}O$ and use of these data in modelling will probably be one task.
- The modelling using "Littorina" and "Marine sediments" as water types for boundary conditions have raised questions and, if possible, some "unique" components of Littorina should be defined, if possible, by the hydrogeochemists.
- The hydraulic connectivity is a major issue and may be tested as indicated above. These tests may be non-conclusive and raise the question if other methods are available. Interference tests may be helpful. The planned interference tests are on a large scale, mainly to indicate existence and connectivity of HCDs to support the structural model of the deterministically defined deformation zones, but also to provide hydraulic properties of some HCDs and useful data for testing groundwater flow models. Ideally one would like to have a large number of observation sections and (especially as data set for numerical models) to have pseudo-steady state data, so one can neglect the storage component. This may be difficult to achieve, at least in the near future, but it is essential to start with the possibilities available. Boreholes within c. 1 km from an ongoing drilling or ongoing pumping test should be monitored, and responses measured may give support for interpreting of deformations zones orientation/position or indications of anisotropy. Longer pumping tests (days) should be made rather frequenly as the number of observation points (boreholes) have increased.
- Another type of interference test is the "Single-hole interference test", using one test-section for injection/pumping water and observing pressure responses in a few test sections surrounding the test section. No equipment for this purpose is available at present, but can possibly be developed for the PSS.The main idea is to use 3 or 5 packed off sections with pressure measurements and with injection in the middle section. The tests are performed for the test scale 5 and 20 m (injection section length). The possibility to make this type of interference test will be investigated. This type of interference test may be useful for discriminating between different HydroDFN models.

9 Bedrock hydrogeochemistry

The evaluation of the hydrogeochemical data has been carried out by considering not only the samples from Simpevarp subarea, but also in relation to available samples from the Laxemar subarea, Äspö HRL and, in some cases, also in relation to the whole Fennoscandian hydrochemical dataset. For example, selecting the water end members describing other Fennoscandian sites in order to see how well they compare with the general Simpevarp trend, and whether or not Simpevarp can be interpreted as part of the regional hydrogeochemical system. Consequently, information from hydrogeochemical model versions based on previously investigated sites in Sweden and elsewhere, and information from ongoing geological and hydrogeological modelling at Simpevarp, where included in the evaluation when motivated and possible.

The data evaluation and modelling becomes a complex and time-consuming process when the wealth of information has to be decoded. Manual evaluation (Section 9.2), expert judgment and mathematical modelling (Section 9.3) must normally be combined when evaluating groundwater information. A schematic presentation of how a site evaluation/modelling is performed and its components is put forward and discussed in Section 9.3. The methodology applied in this report is described in detail by /Smellie et al. 2002/. The outcome of the hydrogeochemical modelling is used e.g. in the hydrogeological modelling (Chapter 8), transport modelling (Chapter 10) and subsequent safety assessment. The results of the detailed hydrogeochemical modelling are intergrated to produce a hydrogeochemical site descriptive model as presented in Section 11.6.

9.1 State of knowledge at previous model version

The first model of the Simpevarp area was the Site Descriptive Hydrogeochemical Model version 0 /SKB, 2002b/. Although there were few data from the Simpevarp regional model area to support a detailed hydrogeochemical site descriptive model, postglacial events believed to have affected the groundwater evolution and chemistry at Simpevarp were described in a conceptual model.

The model version Simpevarp 1.1 /Laaksoharju et al. 2004b/ represented the first evaluation of the available Simpevarp groundwater analytical data. The complex groundwater evolution and patterns at Simpevarp were modelled to be a result of many factors such as: a) the flat topography and proximity to the Baltic Sea, b) past changes in hydrogeology related to glaciation/deglaciation and land uplift associated with repeated marine/lake water regressions/transgressions, and c) organic or inorganic alteration of the groundwater composition caused by microbial processes or water/rock interactions. The sampled groundwaters reflected various degrees of modern or ancient water/rock interactions and mixing processes. Higher topography to the west of Simpevarp had resulted in hydraulic gradients which had partially flushed out old water types.

Except for seawater, most surface waters and some groundwaters from percussion boreholes represented fresh, non-saline waters according to the classification used for Äspö groundwaters. The rest of the groundwaters were brackish (Cl < 5,000 mg/L), except for three samples from KSH01A (at 253 m and 439 m depth) which were saline. Most surface waters were of Ca-HCO_3 or Na-Ca-HCO_3 type and naturally the seawater was of Na-Cl type. The deeper groundwaters were mainly of Na-Ca-Cl type.

The modelling indicated three water types, one dominated by meteoric water, another affected by marine water and the third affected by glacial water. The surface meteoric type shows seasonal variations. Closer to the coast the influence of marine water is detected. With depth, the saline groundwater has been affected by glacial melt water and meteoric water.

Knowledge of the reactive system in the Simpevarp 1.1 model version was that the main water-rock interaction processes affecting the chemistry in the fresh meteoric waters were: a) decomposition of organic matter, b) calcite, plagioclase, biotite and sulphide dissolution, c) Na-Ca ion exchange, and d) phyllosilicate precipitation probably extremely slow in the present low temperature environment. In contrast, for the brackish-saline groundwaters, the water/rock interaction processes seemed to be less evident although this could not be confirmed because of a lack of data. Multiple end-member mixing between marine water, glacial meltwater and deeper saline water seemed to play a significant role.

9.2 Evaluation of primary data

This section describes the evaluation of the primary hydrogeochemical data forming the basis of the Simpevarp 1.2 hydrogeochemical model. Most of these data are from waters sampled at various surface locations and in boreholes. The evaluation essentially aims at identifying representative datasets which are used for further analysis and providing a first conceptualisation of the origin and evolution of the Simpevarp groundwaters.

9.2.1 Hydrogeochemical data evaluation

The groundwater data in the evaluation consist of data derived from the so-called *Simpevarp subarea*, i.e. the Simpevarp peninsula, Ävrö island and Hålö island (for geographical reference see Figure 9-1). Where the groundwater description refers to a certain geographical location the *name* of the site (e.g. Simpevarp, Ävrö, Hålö) is used in the text and in the figures. Groundwater data from surrounding locations such as the Laxemar subarea and Äspö (prior to tunnel construction), and also in some cases Oskarshamn (KOV01), were included and referred to as data from the *Simpevarp area*. The data from the Nordic sites (e.g. Forsmark and Olkiluoto) are included in the overall comparison and referred directly by their names. The data used in the groundwater evaluation are listed in /Appendices 7 and 8 in SKB, 2004c/. The use of the data in the different modelling activities is described in /Appendix 9 in SKB, 2004c/.

The data freeze for Simpevarp 1.2 also includes older existing data. In total the dataset consists of 1,518 water samples from four sites: 964 from Simpevarp, 302 from Laxemar, 152 from Äspö, and 100 from Ävrö. Samples reflecting surface conditions (precipitation, streams, lakes and seawater) comprise a total of 822 samples (766 from Simpevarp and 56 from Laxemar). Of the remaining 696 samples, 63 samples are from percussion-drilled boreholes and 633 from core-drilled boreholes; some of these borehole samples represent repeated sampling from the same isolated location or samples in a non-sealed, open borehole (tube sampling = 168 samples) and shallow soil pipe waters (23 samples).

From the total dataset only 174 surface samples and 144 groundwater samples were analysed for all the major elements, stable isotopes and tritium at the time of the Simpevarp 1.2 data freeze. There are some samples with additional information, mainly on colloids, dissolved gasses and microbes, which are also listed in /SKB, 2004c/. This means that 21% of the samples could be used for a detailed evaluation concerning the origin of the waters.

The detailed representativity check of the samples show that only 81 out of 144 samples with complete chemical data have been considered representative. The representative data are labelled in /SKB, 2004c/. How this dataset has been used in the different models is listed in the same report /SKB, 2004c/.

Analysed data include the same set of parameters as in the previous stages. The pH and electrical conductivity values used in the evaluation were those determined in the laboratory. There are no data for Eh and temperature for the surface waters but there are data from some continuous logging of Eh, pH and temperature from several boreholes at different depths. The selected Eh, pH and temperature values are included in the table of the chemical analysis.

Groundwater chemistry data sampled in boreholes

The borehole sampling locations at the Simpevarp area are shown in Figure 9-1 (the complete analytical data is found in /SKB, 2004c/) and the groundwater sampling and analytical data have been reported by /Wacker, 2003; Berg, 2003a,b/; draft versions of a report /Wacker et al. 2004/ were available at the time for the data freeze. The analytical programme included: major cations and anions (Na, K, Ca, Mg, Si, Cl, HCO_3^- SO_4^{2-}, S^{2-}), trace elements (Br, F, Fe, Mn, Li, Sr, DOC, N, PO_4^{3-}, U, Th, Sc, Rb, In, Cs, Ba, Tl, Y and REEs) and stable (^{18}O, ^{2}H, ^{13}C, ^{37}Cl, ^{10}B, ^{34}S) and radioactive-radiogenic (^{3}H, ^{226}Ra, ^{228}Ra, ^{222}Rn, ^{238}U, ^{235}U, ^{234}U, ^{232}Th, ^{230}Th and ^{228}Th) isotopes, microbes, gases and colloids.

The different analytical results obtained with contrasting analytical techniques for Fe and S have been confirmed with speciation-solubility calculations and checking their effects on the charge balance. The values selected for modelling were those obtained by ion chromatography (SO_4^{2-}) and spectrophotometry (Fe) assuming no colloidal contribution. The selected pH and Eh values correspond to available downhole data.

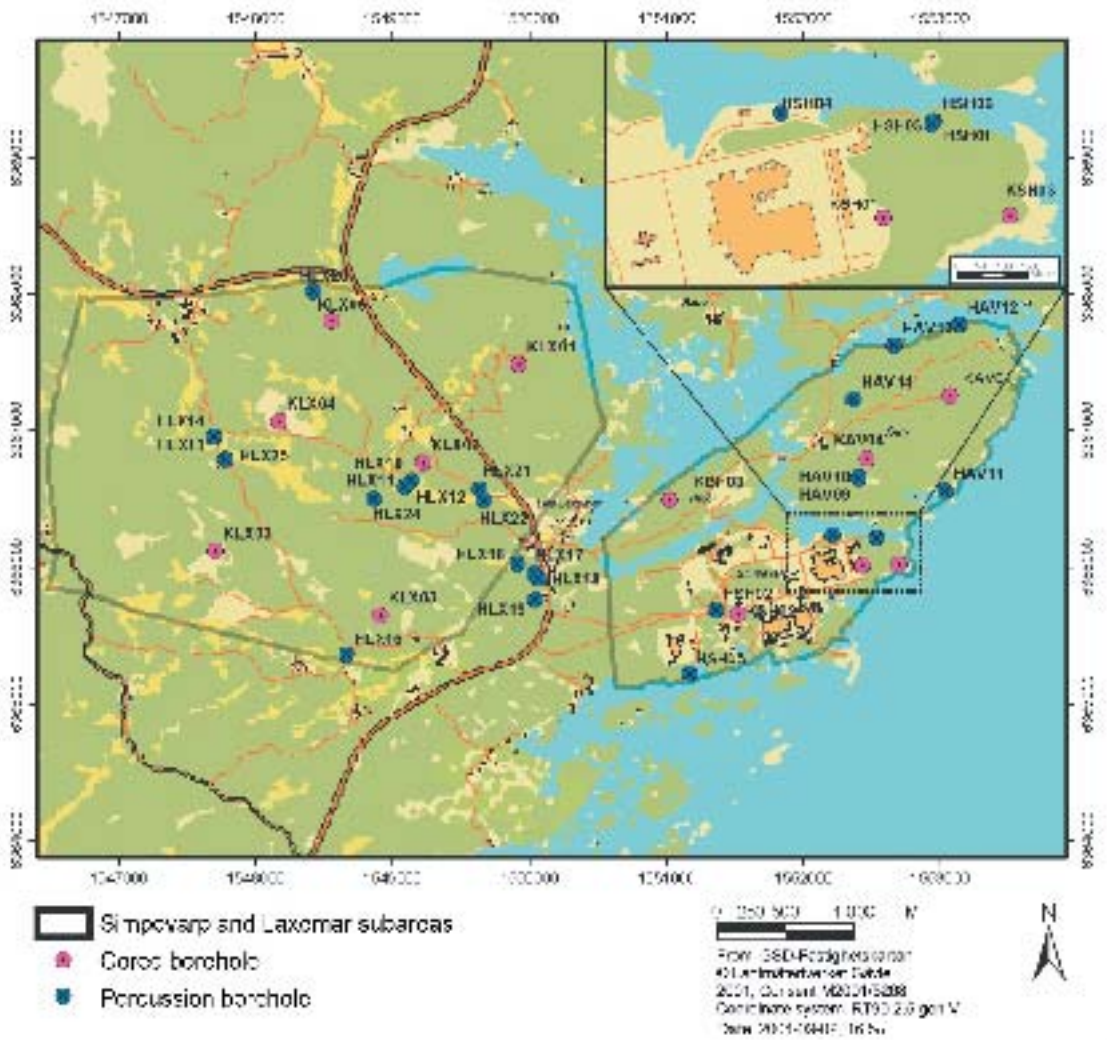

Figure 9-1. *The groundwater sampling locations at the Simpevarp subarea (right). Laxemar subarea (left) and Äspö site data were included in the evaluation in the so called groundwater data from the Simpevarp area. The dotted line indicates the orientation of the vertical section used for the visualisations.*

Representativeness of the data

By definition, a high quality sample is considered to be that which best reflects the undisturbed hydrological and geochemical in situ conditions for the sampled section. A low quality sample may contain in situ, on-line, at-line, on-site or off-site errors such as contamination from tubes of varying compositions, air contamination, losses or uptake of CO_2, long storage times prior to analysis, analytical errors etc. The quality may also be influenced by the rationale in locating the borehole and selecting the sampling points. Some errors are easily avoided, others are difficult or even impossible to avoid. Furthermore, chemical responses to these influences are sometimes, but not always, apparent.

Simpevarp area

Included in the Simpevarp version 1.2 evaluation are data representing surface and near-surface waters collected from the Baltic Sea, Lakes, Streams, and also from shallow Soil Pipes placed in the overburden. These data, because of the complex nature of the sampling locations (i.e. subject to annual and seasonal trends, potential recharge/discharge areas etc.) have been evaluated based only on charge balance (Lake and Stream waters), charge balance and observed contamination during sampling (Soil Pipe waters) and charge balance and salinity (Baltic Sea waters). Some precipitation values are also included but have not undergone any representativity check because of unpredictable annual and seasonal trends and possible evaporation.

The Simpevarp groundwater analytical data are compiled in the SICADA database and form the basis of the hydrochemical evaluation. The data have undergone an initial screening process by field and laboratory personnel based on sampling, sample preparation and analytical criteria /Wacker, 2003a/. The next stage in the hydrogeochemical site descriptive modelling process is to assess these screened data in more detail to derive a standard set of representative groundwater data for hydrogeochemical modelling purposes.

For this assessment the initial most important stage is to check for groundwater contamination. To accomplish this stage a detailed knowledge of the borehole site is required which entails borehole geology and hydrogeology and a detailed log of borehole activities. These latter activities are a major source of groundwater contamination and include:

- drilling and borehole cleaning,
- open hole effects,
- downhole geophysical/geochemical logging,
- downhole hydraulic logging/testing/pumping, and
- downhole sampling of groundwaters.

In /SKB, 2004c/ these potential sources of contamination have been addressed and documented systematically for each borehole drilled and for each borehole section sampled. The degree of contamination has been judged, for example, by plotting tritium against percentage drilling water and using measured values with specifically defined limits, i.e. charge balance (± 5%) and drilling water component (< 1%), and supported qualitatively by expert judgement based on detailed studies of the distribution and behaviour of the major ions and isotopes. The final selection of data which best represents the sampled borehole section is based on:

- Identifying as near as possible a complete set of major ion and isotope (particularly tritium, ^{18}O and deuterium) analytical data. This is not always the case, however, and a degree of flexibility is necessary in order to achieve an adequate dataset to work with. For example:
- A charge balance of ± 5% was considered acceptable. In some cases groundwaters exceeding this range were chosen to provide a more representative selection of groundwaters. These groundwaters should therefore be treated with some caution when used in the modelling.

- In many cases the drilling water content was either not recorded or not measured. Less than 1% drilling water was considered acceptable. In some cases groundwaters were chosen when exceeding this range to provide a more representative selection of groundwaters. These groundwaters should be treated with some caution when used in the modelling exercises.
- Some of the older tritium data were analysed with a higher detection limit of 8 TU; the detection limit lies around 0.02 TU for recent analyses. For some groundwaters an approximate tritium value is suggested where no recorded value is available. This value is selected normally from the same borehole section but representing an earlier or later sample.

/SKB, 2004c/ shows a summary of the Simpevarp area data indicating the use of selected criteria (charge balance; drilling water content; tritium content) to identify the samples considered representative. Resulting from this assessment, two groundwater sample types were highlighted one type considered representative, the other type less representative but suitable when used with caution. In the data set these are toned orange and green respectively.

The drilling event is considered to be the major source for contamination of the formation groundwater. During drilling large hydraulic pressure differences can occur due to uplifting/lowering of the equipment, pumping and injection of drilling fluids. These events can facilitate unwanted mixing and contamination of the groundwater in the fractures, or the cutting at the drill bit itself can change the hydraulic properties of the borehole fractures. It is therefore of major importance to analyse the drilling events in detail. From this information not only the uranine spiked drilling water can be traced, but also the major risk of contamination and disturbances from foreign water volumes can be directly identified. Insufficient or excessive extraction of water from a fracture zone prior to sampling can be calculated by applying the DIS (Drilling Impact Study) modelling /Gurban and Laaksoharju, 2002/.

In the absence of suitable data from any of the new borehole sections, a hydraulically active fracture zone in one isolated section in borehole KSH01A:548–565 m was the subject of the DIS modelling (sections 156.5–167 m and 245–261.5 m were investigated as part of Simpevarp version 1.1). The modelling carried out for this fracture zone was based on the DIFF (differential flow meter logging) measurements and the main aim was to model the amount of the contamination (Figure 9-2) for this particular fracture zone /cf. SKB, 2004c/. The DIS calculations show that the section was contaminated with 22.4 m^3 of foreign water during the drilling of this section of which a maximum of 23.61% consisted of drilling water. The maximum uranine lost to the fracture during drilling was 0.04 mg/L, which represents 23.6% drilling water. Later drilling activities could have increased the amount of contamination. The result from the sampling shows 18.7% remaining drilling water in the first chemical sample after pumping 336 hours, and 10.7% remaining drilling water in the last sample after pumping 1,675 hours. The average flow rate was 200 mL/min /Wacker et al. 2004/. The volume removed was calculated to be 20 m^3. This can be compared with the maximum 22.4 m^3 volume of water that contaminated the fracture. The average amount of drilling water remaining in the fracture is 2.4 m^3. The DIS calculations show that pumping should have continued further for about 8 days in order to remove the additional 2.4 m^3.

One fundamental question in modelling is whether the uncertainties lead to a risk of misunderstanding the information in the data. Generally the uncertainties from the analytical measurements are lower than the uncertainties caused by the modelling but the variability during sampling is generally higher than the model uncertainties.

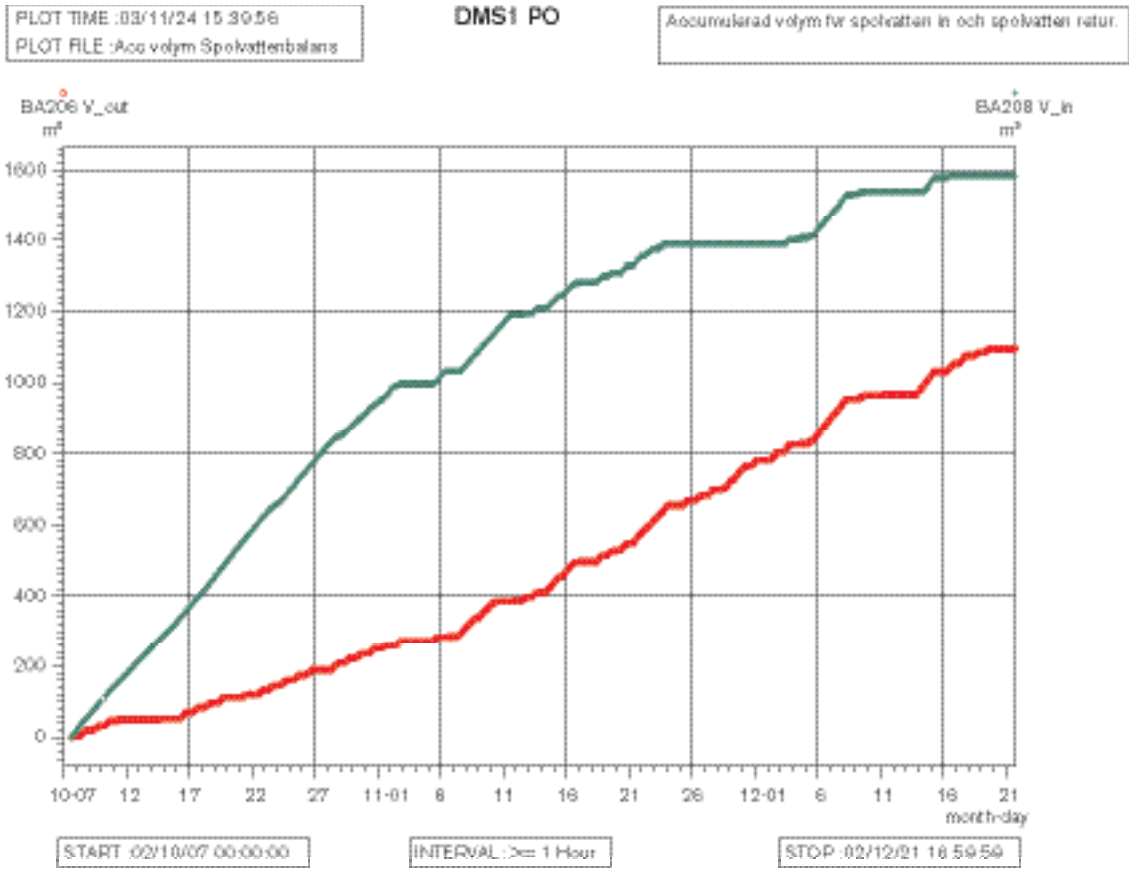

Figure 9-2. *Accumulated drilling water volume pumped in (in green) and drilling water volume pumped out (in red) in borehole KSH01A+B with time. The monitoring of the amount of drilling water pumped into the borehole is of varying quality indicated by 2 or 3 plateaus with no inflow. During the "plateau period" drilling was conducted and water is still pumped in. The error is due to a sensor problem.*

Nordic sites

The Nordic sites, in addition to Simpevarp area, comprise Forsmark and all remaining Swedish sites studied over the last 20–25 years; Olkiluoto in Finland is also included. Most of these sites have undergone earlier detailed assessments as to groundwater quality and representativeness, e.g. Gideå, Kamlunge, Klipperås, Fjällveden, Svartboberget, Finnsjön /Smellie et al. 1985, 1987; Smellie and Wikberg, 1991/, Lansjärv /Bäckblom and Stanfors, 1989/ and Olkiluoto /Pitkänen et al. 1999, 2004/. Based on this information the Nordic Table has been highlighted with respect to representative and less suitable groundwater samples /SKB, 2004c/. In accordance with the Simpevarp area evaluation, the representative groundwaters are toned orange and the less suitable samples green. These latter groundwaters do not meet all of the criteria for representativeness but are deemed sufficiently important to be included. The importance of early or 'First Strike' samples is emphasised in the evaluation discussed in /SKB, 2004c/. These less suitable groundwaters involve one or more of the following deviations from being considered 'representative':

- lack of important ions – especially Br,
- lack of ^{18}O and deuterium data,
- few or an absence of time-series measurements, and
- variation in salinity during the time-series measurements.

Explorative analysis

A commonly used approach in groundwater modelling is to start the evaluation by explorative analysis of different groundwater variables and properties. The degree of mixing, the type of reactions and the origin and evolution of the groundwater can be indicated by applying such analyses. Also of major importance is to relate, as much as possible, the groundwaters sampled to the near-vicinity geology and hydrogeology.

Borehole properties

Figure 9-3, Figure 9-4 and Figure 9-5 represents a schematic representation of boreholes KSH01, KSH02 and KSH03 and the intercepted structures and their hydraulic conductivities; groundwater sampling locations are indicated and the sampled chloride contents are shown. The results from drillcore mapping, BIPS measurements, differential flow measurements and electric conductivities together with groundwater quality and representativeness of the samples are discussed in great detail for all investigated boreholes in /SKB, 2004c/.

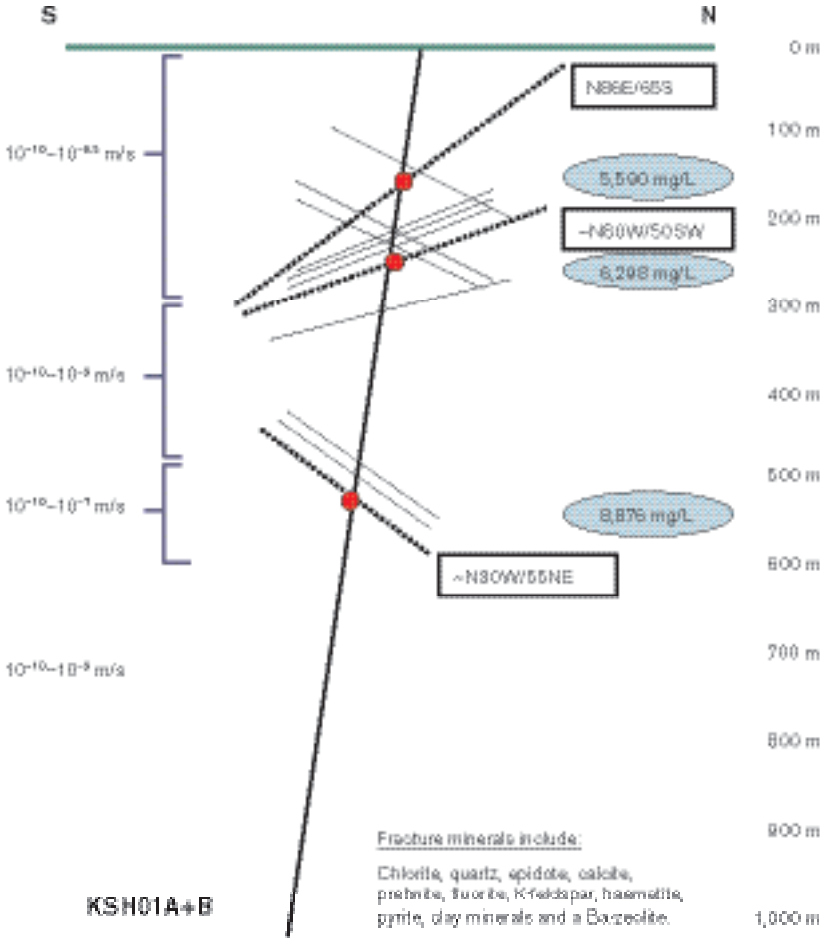

Figure 9-3. *Borehole KSH01 (in the figure the initial percussion drilled portion is referred to as 'B' and from 100 m to the hole bottom by core drilling is referred to as 'A') showing intercepted structures and their hydraulic conductivities (m/s); groundwater sampling locations are indicated in red with the chloride content (mg/L) in blue. Dotted lines represent sampled structures.*

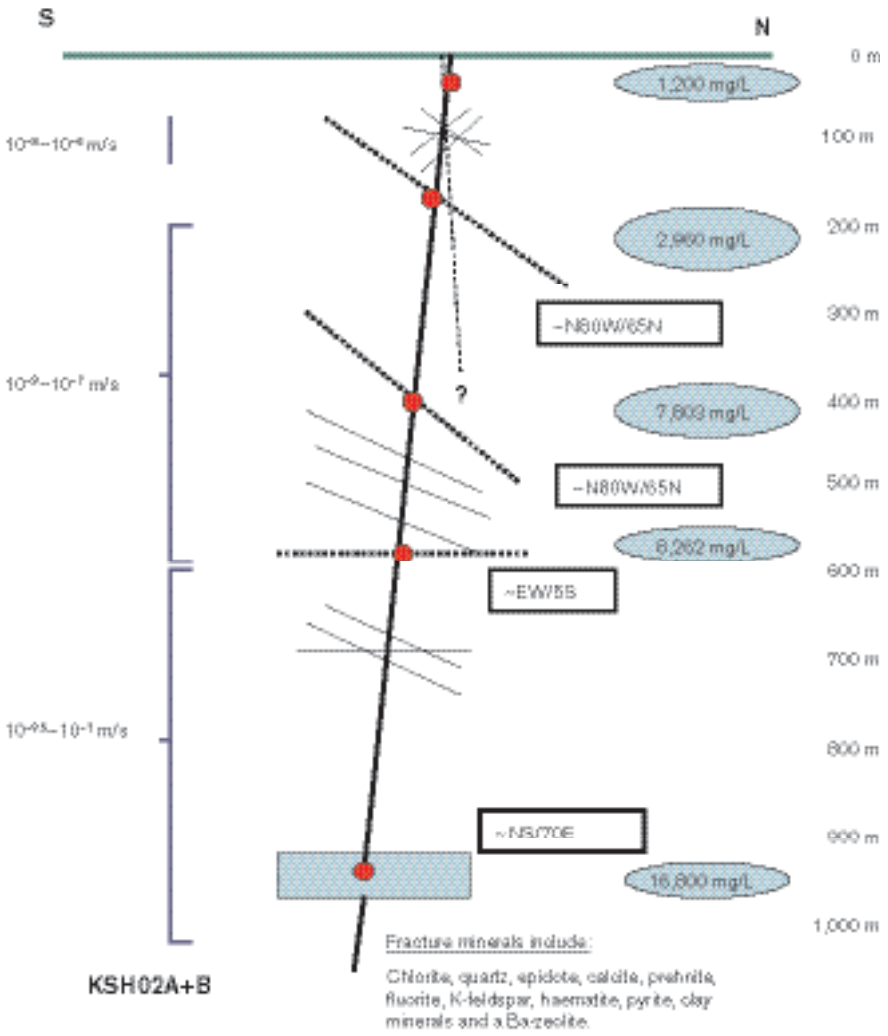

Figure 9-4. *Borehole KSH02 showing intercepted structures and their hydraulic conductivities (m/s); groundwater sampling locations are indicated in red with the chloride content (mg/L) in blue. Dotted lines represent sampled structures.*

Evaluation of scatter plots

The hydrochemical data have been expressed in several X-Y plots to derive trends that may facilitate interpretation. Since chloride is generally conservative in normal groundwater systems its use is appropriate to study hydrochemical evolution trends when coupled to ions, ranging from conservative and non-conservative, to provide information on mixing, dilution, sources/sinks etc. Many of the X-Y plots therefore involve chloride as one of the variables.

The hydrogeochemical evaluation presented below follows a systematic approach /see Smellie et al. 2002/ commencing with traditional plots (e.g. Piper Plots) to group the main groundwater types characterising the Simpevarp area and to identify general evolutionary or reaction trends. Comparisons are made with hydrochemical information from other sites, i.e. Äspö, Laxemar, Ävrö, Oskarshamn and Bockholmen. Importantly, the hydrogeochemistry is related also to the regional and local geology and hydrogeology in order to understand the overall (i.e. large- and small-scale) dynamics and evolution of the groundwater systems which characterise the Simpevarp subarea. A more detailed evaluation of the major components and isotopes can be found in /SKB, 2004c/. Discussion of the reactive elements is presented in the modelling part of this report and also in /SKB, 2004c/.

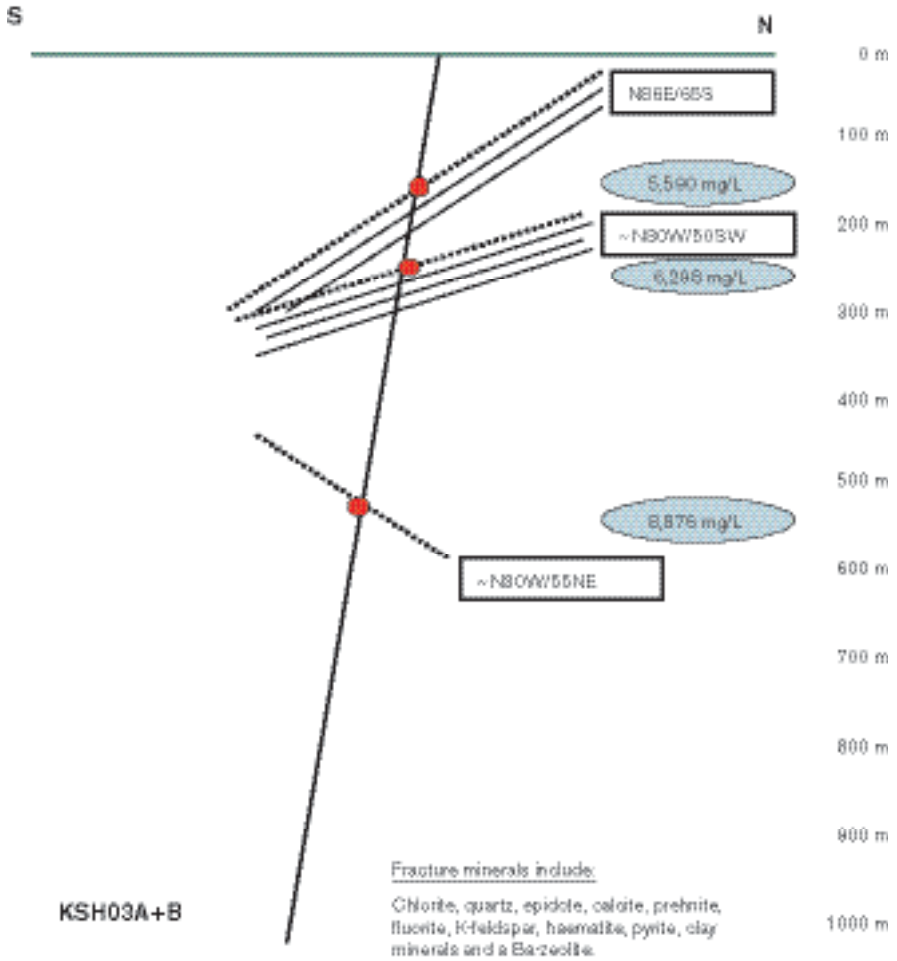

Figure 9-5. *Borehole KSH03A+B showing intercepted structures and their hydraulic conductivities (m/s); groundwater sampling locations are indicated in red with the chloride content (mg/L) in blue. Dotted lines represent sampled structures.*

Piper Plot

The main groundwater groups characterising Simpevarp area are: a) shallow (< 200 m) Na-HCO_3 to Na-Cl-HCO_3 to Na-Ca-Cl-HCO_3 to Na-Ca-Cl types, b) intermediate (approx. 200–600 m) Na-Ca-Cl (with some enhanced SO_4 and Br) types, and c) deep (> 600 m) with increasingly enhanced Na-Ca-Cl(Br, SO_4). The variation in compositions, especially in the upper 200 m of the bedrock, is due to local hydrodynamic flow conditions leading to mixing of varying proportions. Microbially mediated reactions are also important influencing both HCO_3 and SO_4, especially in the 200–600 m interval.

Set in a more regional context (Figure 9-6), the Simpevarp subarea groundwaters (red infilled circles) generally conform in chemistry to similar depth-related groupings representing the Simpevarp area data. The deep highly saline Laxemar groundwaters show a clear differentiation from all the other sites.

Comparison of Simpevarp waters, representing the Baltic Sea (SW), Lakes (LW) and Streams with the Laxemar surface waters, shows some degree of grouping. This is suggested also in many of the following diagrams. Here the Baltic Sea is clearly differentiated with a concentrated cluster at high Cl+SO_4 which reflects a representative Baltic Sea composition for the Simpevarp latitude. The plot also separates the Simpevarp Lake waters from the Stream waters, the latter clearly indicating a lower Na+K content, and the main Lake water cluster suggesting a slightly higher Cl+SO_4 content. There is a wide distribution of Stream waters and, as would be expected, some degree of overlap between the Lake waters, which occurs particularly at higher Cl+SO_4 contents. The Laxemar surface waters are scattered throughout the diagram although with a more dense clustering close to the Simpevarp Lake waters, but with a significant overlap with the Stream waters.

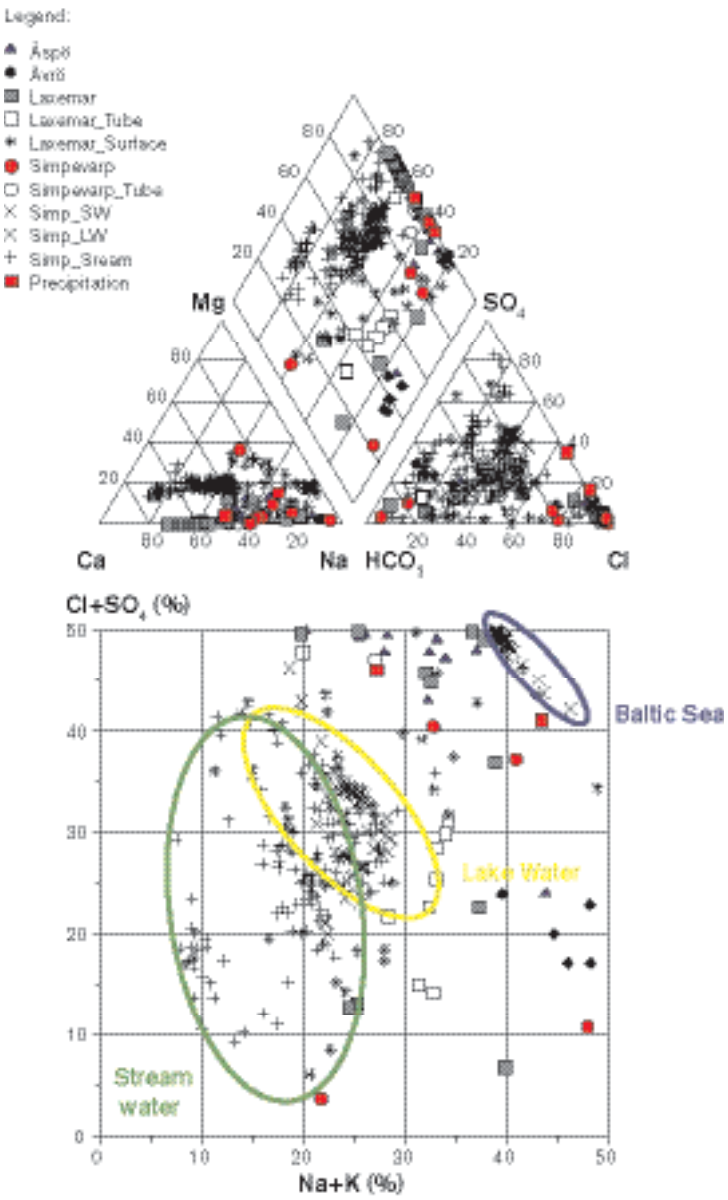

Figure 9-6. *Piper and Ludwig-Langelier plots of surface, near-surface and groundwaters from the Simpevarp subarea compared with other groundwater data. Indicated on the diagram are surface water groupings involving Baltic Sea (blue), Stream (green) and Lake (yellow) waters.*

General comparison of Cl vs. depth with other sites

Comparison of the Simpevarp subarea chloride data with some of the Simpevarp area data together with Forsmark and Olkiluoto, is shown in Figure 9-7. It may be argued that such a comparison should be treated with caution since Forsmark and Olkiluoto are geographically distant, have a differing palaeo-evolution and represent different hydrogeological regimes. Furthermore, Laxemar, although close by, represents more a mainland environment and involves greater depths. However, since the Fennoscandian basement hydrogeochemistry probably shares general similarities irrespective of geographic location, Figure 9-7 may serve a useful purpose particularly with respect to establishing whether a Littorina component is present in the Simpevarp subarea groundwaters.

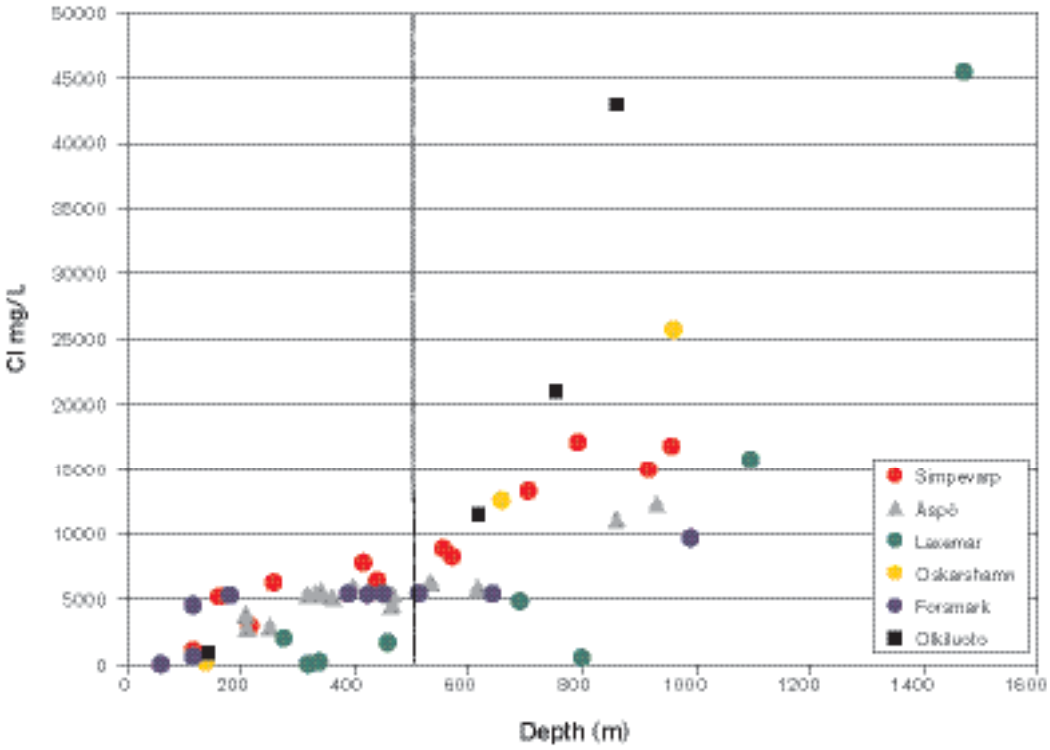

Figure 9-7. *Depth comparison of chloride between different Swedish and Fennoscandian sites.*

The Laxemar data show mostly dilute groundwaters (< 2,000 mg/L Cl) extending to approx. 600 m for KLX01 and to around 1,000 m for KLX02 before a rapid increase in salinity to maximum values of around 47 g/L Cl at 1,500 m. Olkiluoto shows an initial sharp increase in chloride at around 150 m to a levelling off at 5,000 mg/L Cl which continues to 450 m; here there is a relatively steady increase to maximum values of around 20 g/L Cl at 900 m depth (one maximum value of 45.5 g/L Cl was recorded). The available Forsmark data so far show a close similarity to the initial Olkiluoto trends, although the levelling off at approx. 5,000 mg/L Cl continues to around 650 m where a small increase to 10,000 mg/L Cl is achieved at 1,000 m; there are no deeper groundwater data to compare ultimate salinity contents. In addition the Äspö trends generally are close to those of Forsmark.

The Simpevarp data fall along the general plateau characterised to approx. 500 m depth by chloride ranging from around 5,100–6,300 mg/L Cl (Figure 9-7). In addition the Simpevarp profile so far shares a close similarity with Oskarshamn (borehole KOV01) and shares with Äspö and Forsmark similar trends over the first approx. 600 m.

Tracing the Littorina Sea signature with Mg, Br, and $\delta^{18}O$

The Littorina stage in the postglacial evolution of the Baltic Sea commenced when the passage to the Atlantic Ocean opened through Öresund in the southern part of the Baltic Sea. The relatively high sea level together with the early stages of isostatic land uplift led to a successively increasing inflow of marine water into the Baltic Sea. Salinities twice as high as modern Baltic Sea have been estimated for a time period of about 2,000 years starting some 7,000 years ago (cf. description of the post glacial scenario). From shore displacement curves it is clear that Simpevarp and Laxemar in part were covered by the Littorina Sea. Due to the topography of the area and the on-going isotstatic land uplift, the Laxemar area was probably influenced only to a small degree, whereas the Simpevarp peninsula was covered for several thousands of years until eventual emergence during uplift initiated a recharge meteoric water system some 4,000 to 5,000 years ago. This recharge system effectively flushed out much of the Littorina Sea water that had penetrated the bedrock.

The Forsmark area, in contrast, has been covered by the Littorina Sea for a much longer period of time and the low topography implies that it reached several tens of kilometres further inland. Furthermore, the present meteoric recharge stage following uplift and emergence has only prevailed for less than 1,000 years such that any flushing out of the Littorina Sea component is less pronounced. Stronger evidence of a Littorina Sea water signature can therefore be expected in groundwaters at Forsmark.

Comparison of Forsmark data with the Simpevarp-Äspö-Laxemar-Oskarshamn (KOV01 is one of the characterised boreholes from the Oskarshamn site, situated within the town of Oskarshamn near the harbour) data indicates large differences in the character and origin of the groundwaters, especially for brackish groundwaters with chloride contents of around 4,000–6,000 mg/L Cl. This is exemplified in three plots showing chloride versus magnesium, bromide and $\delta^{18}O$ (Figure 9-8, Figure 9-9 and Figure 9-10). The magnesium versus chloride plot (Figure 9-8) clearly shows the difference between the Forsmark and Simpevarp groundwaters characterised by chloride contents up to 5,500 ppm Cl; characteristically the Forsmark samples closely follow the modern marine (Baltic Sea) trend. Those few groundwaters that plot within the Simpevarp group are from greater depths in the bedrock and, as such, have been influenced by mixing with deeper non-marine saline groundwaters. A few samples from Äspö (KAS06 and HAS02; Figure 9-8) also show relatively high Mg contents, although not as high as in the Forsmark groundwaters with similar chloride contents. Compared with the Forsmark groundwaters, most of the Simpevarp area groundwaters show low Mg values although increases (peaking at 150 mg/L) are observed for samples in the chloride interval 4,000–6,300 mg/L.

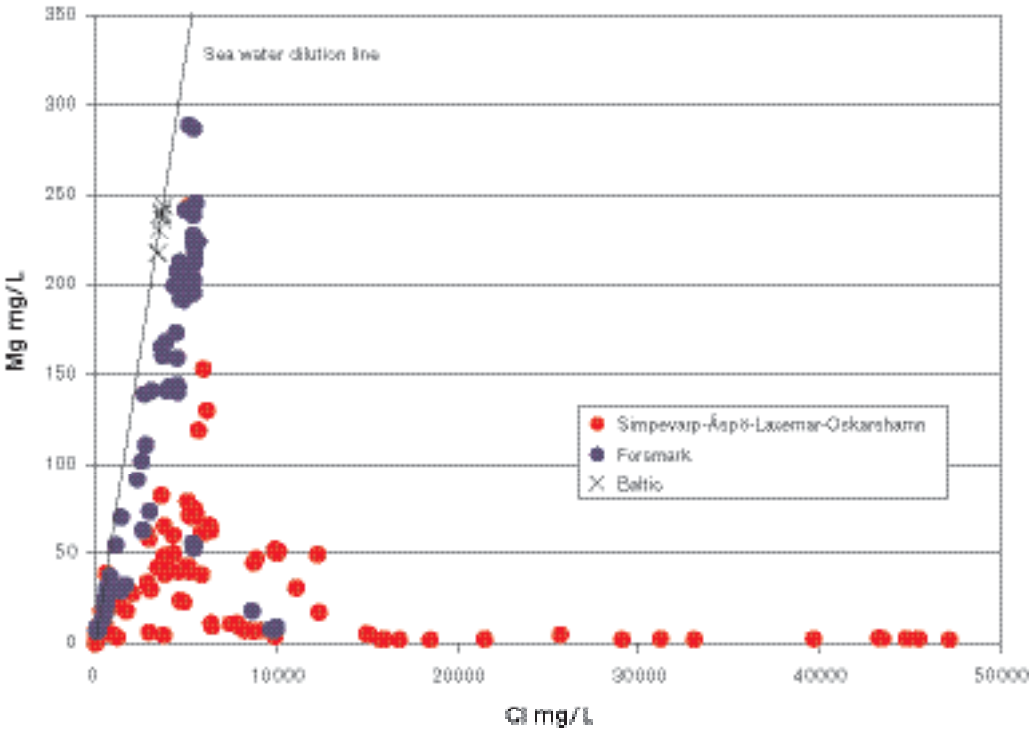

Figure 9-8. *Mg versus Cl for groundwaters from Forsmark and other sites within the Simpevarp area. Baltic Sea waters from the Simpevarp and Forsmark areas are included for reference.*

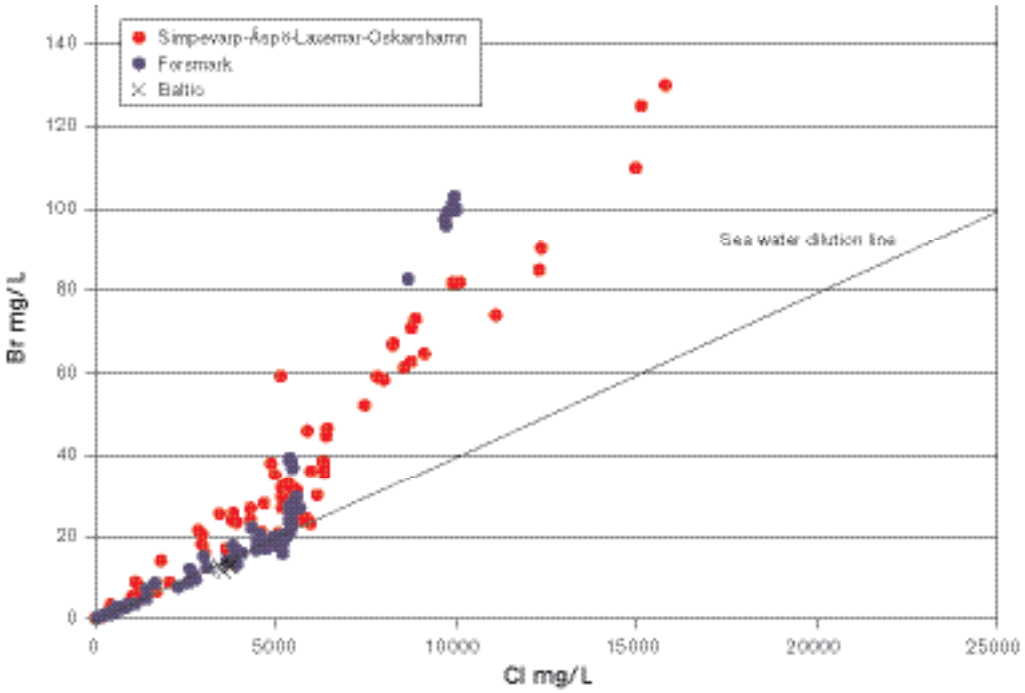

Figure 9-9. *Br versus Cl for groundwater samples from Forsmark and other sites within the Simpevarp area. Baltic Sea waters from Forsmark and Simpevarp areas are included for reference.*

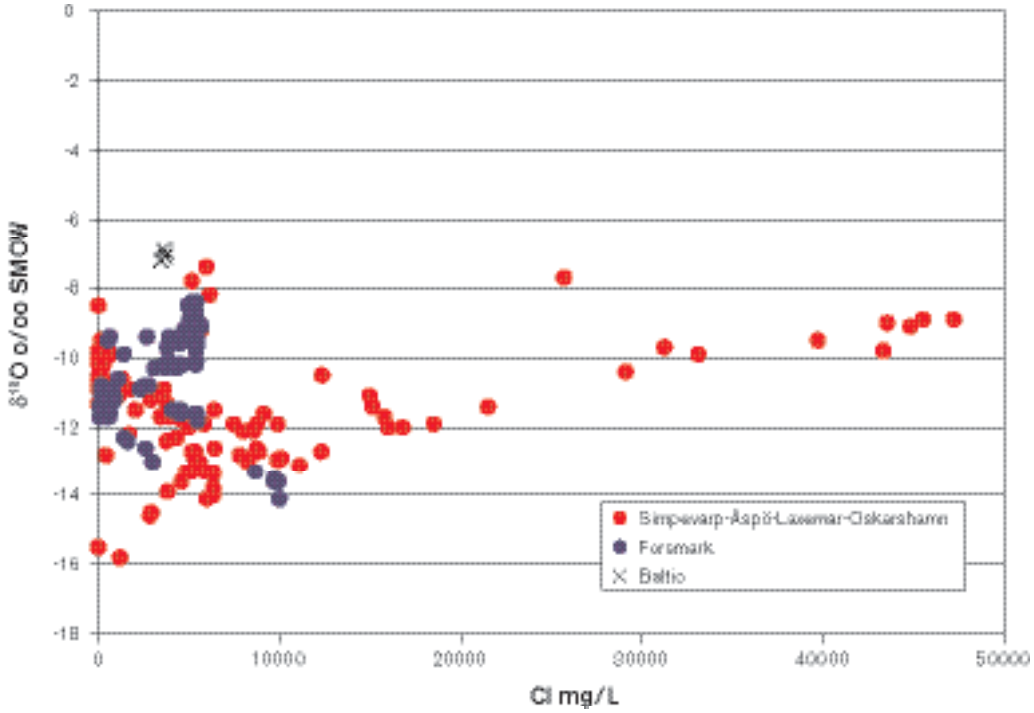

Figure 9-10. *$\delta^{18}O$ versus Cl for groundwaters from Forsmark and other sites within the Simpevarp area. Baltic Sea waters from the Simpevarp area are included for reference.*

The bromide versus chloride plot (Figure 9-9) underlines the marine signature for most of the Forsmark groundwaters up to contents of 5,500 mg/L Cl, whereas marine signatures only are obtained in a few of the Simpevarp area groundwaters. This observation is strengthened in the $\delta^{18}O$ versus chloride plot (Figure 9-10) which shows deviating groundwater trends for Forsmark and Simpevarp.

Generally, with a few exceptions, the brackish to saline groundwaters up to 5,500 mg/L Cl at Forsmark show indications of a marine origin in terms of: a) Br/Cl ratios, b) Mg values ≥ 100 mg/L, and c) $\delta^{18}O$ values higher than meteoric waters (due to in-mixing of marine waters). In contrast, for the Äspö-Simpevarp/Laxemar groundwaters these criteria are only fulfilled in samples from KAS06 (Äspö) and one sample in KSH03A. In both cases the groundwater samples have been collected from fracture zones outcropping close to the shoreline or under the Baltic Sea.

The chloride content and $\delta^{18}O$ value for the Littorina Sea at maximum salinity is difficult to determine precisely. Interpretations of salinities based on fossil fauna together with $\delta^{18}O$ analyses of the fossils has resulted in suggested salinities around 6,500 mg/L Cl and $\delta^{18}O$ values ~ –4.5‰ SMOW /Donner et al. 1999; Pitkänen et al. 2004/. In Figure 9-11 (Cl versus $\delta^{18}O$) groundwaters from the Simpevarp area show Br/Cl ratio < 0.0045 and magnesium values > 100 mg/L. For comparison are included a small set of samples from Forsmark and the values for selected groundwaters at Olkiluoto considered to contain the largest proportion of Littorina Sea water /Pitkänen et al. 2004/. As can be seen in the figure these values cluster along a mixing line from the suggested Littorina Sea composition to a typical glacial meltwater. Notably, none of the Simpevarp bedrock groundwaters sampled so far show values in total agreement with a Littorina Sea component (i.e. lower Mg content). At least two explanations can be suggested: 1) the cluster represents the Littorina Sea at the time when the water intruded, and 2) the Littorina Sea water was mixed with glacial meltwater in the bedrock.

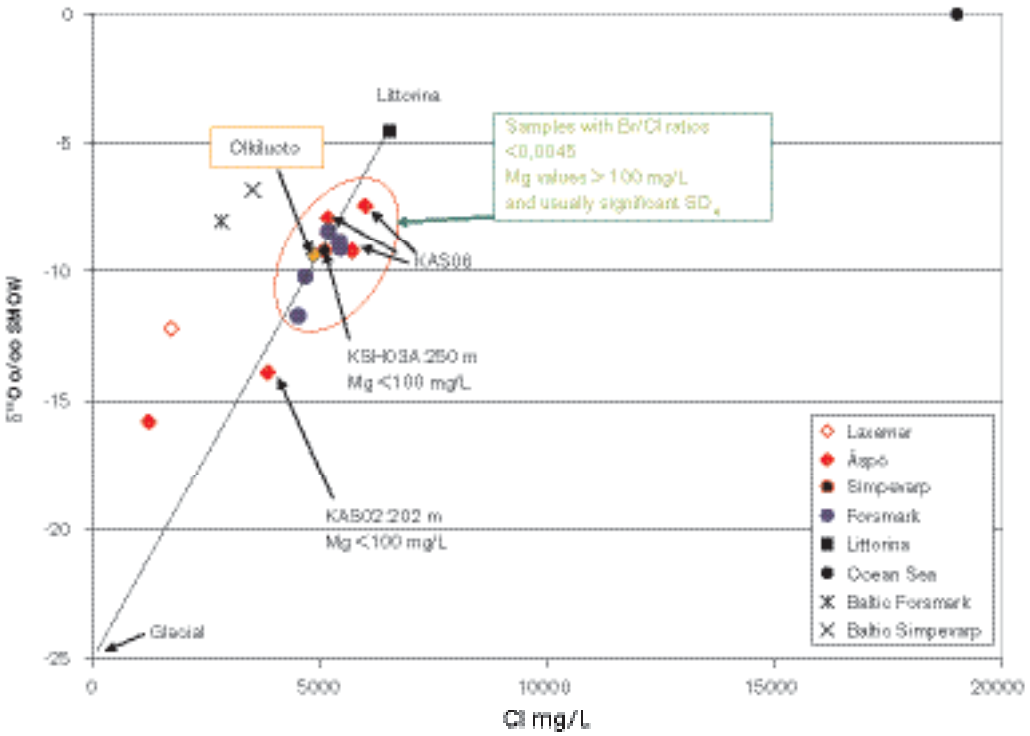

Figure 9-11. *$\delta^{18}O$ versus chloride content for potential marine groundwaters from the Simpevarp (KSH03A:250 m), Forsmark and Olkiluoto areas, the latter from /Pitkänen et al. 2004/.*

In conclusion, groundwaters from the Äspö, Laxemar and Simpevarp sites at best only show a weak presence of a Littorina Sea water component. However, based on the post glacial scenario for the region, it is reasonable to assume that Littorina Sea water penetrated into the bedrock but has been flushed out subsequently by later recharge meteoric waters during early uplift. This has been facilitated by the fact that the maximum penetration of these Littorina waters appear to have been restricted to shallow depths (approx. 150–300 m). Greater penetration depths may have occurred along some of the sub-vertical structures in the area, but to date there is an absence of data to support this.

Some contributions of ion exchange processes to enhanced magnesium contents in a number of the Simpevarp area groundwaters must also be considered. The nature of such magnesium sources are presently uncertain, but water/rock interaction through weathering processes and/or removal by ion exchange processes of earlier marine sources from near-surface sediments to subsequent recharging meteoric waters could be invoked.

Plot of oxygen-18 versus deuterium

Figure 9-12 details the stable isotope data which plot on or close to the Global Meteoric Water Line (GMWL) indicating a meteoric origin. In accordance with many of the other plots, two main groundwater groups are indicated: a) shallow dilute groundwaters ranging from $\delta^{18}O$ = –11.3 to –9.8‰ SMOW, δD = –80.4 to 74.3‰ SMOW, and b) brackish to saline groundwaters ranging from $\delta^{18}O$ = –14.0 to –12.7‰ SMOW, δD = –100.0 to –93.8‰ SMOW. The two tube samples plot within group (a). The heavier group (a) isotopic values suggest a modern meteoric recharge component. The lighter isotopic values of group (b) indicate the presence of a cold recharge meteoric component (glacial melt water?). The limited data suggest there is no major Baltic Sea influence on the sampled Simpevarp groundwaters.

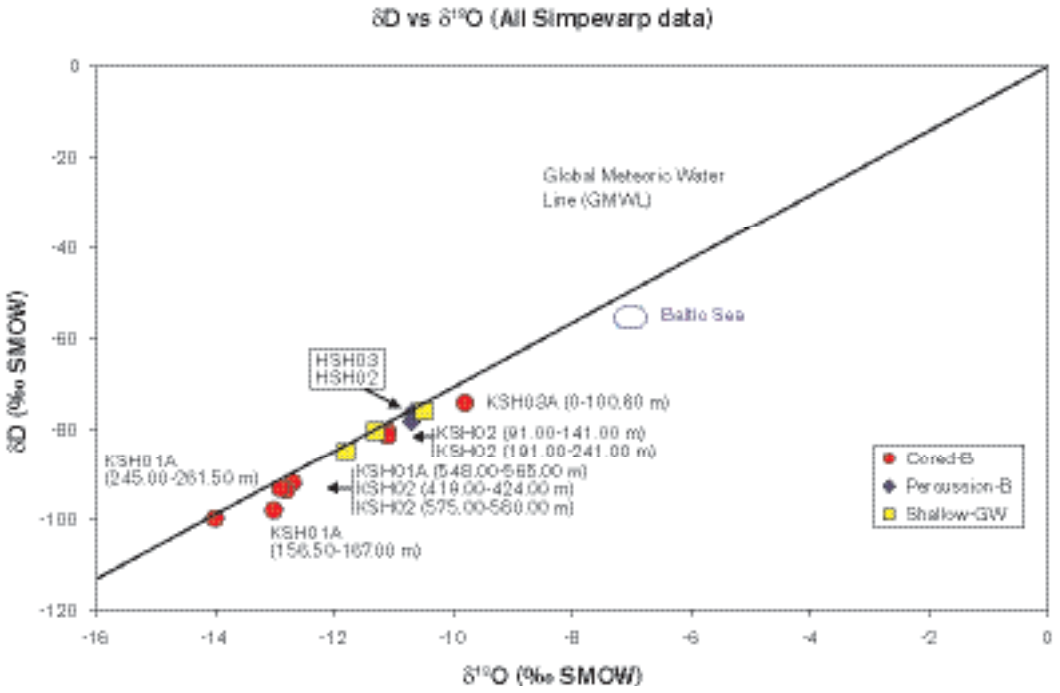

Figure 9-12. *Plot of $\delta^{18}O$ versus δD for all data collected within the Simpevarp area.*

Plot of calcium/magnesium versus bromide/chloride

By plotting Ca/Mg versus Br/Cl, Figure 9-13 provides an opportunity to differentiate those groundwaters of modern marine origin (e.g. Baltic Sea) from non-marine or non-marine/old marine mixing origin. The figure clearly shows the Baltic Sea group of modern marine waters and also the deepest non-marine saline groundwaters from Laxemar and Oskarshamn (KOV01). Between these two extreme end-members lie most of the groundwater data. The red arrow shows the direction towards the deep saline non-marine types, and much of the data plotting along this pathway represent groundwaters which contain an increasing component of the deep saline non-marine end-member. Likewise, at the other extreme, some of the plotted data closest to the modern marine end-member may well comprise groundwaters with a modern marine water signature, although in this case there is not a clear transition zone as might be expected if mixing processes were occurring. The other possibility is the presence of an older marine component (e.g. Littorina Sea) in the shallower brackish groundwaters which persist from 100–500 m depth, depending on local conditions. These groundwaters are circled in blue and indicate enhancements of, for example, Mg and Br.

Plot of oxygen-18 versus chloride

The Simpevarp groundwaters show a systematic decrease in $\delta^{18}O$ (from a maximum of approx. –10‰ SMOW) with increasing salinity (i.e. depth) to a levelling out at approx. –13‰ SMOW at 5,500 mg/L Cl; at greater salinity/depth $\delta^{18}O$ remains steady. Figure 9-14 compares the Simpevarp data with the other sites. The light $\delta^{18}O$ Simpevarp groundwaters from the deeper cored boreholes fall within the same range as many of the Äspö groundwaters, the latter known for their cold climate recharge signatures.

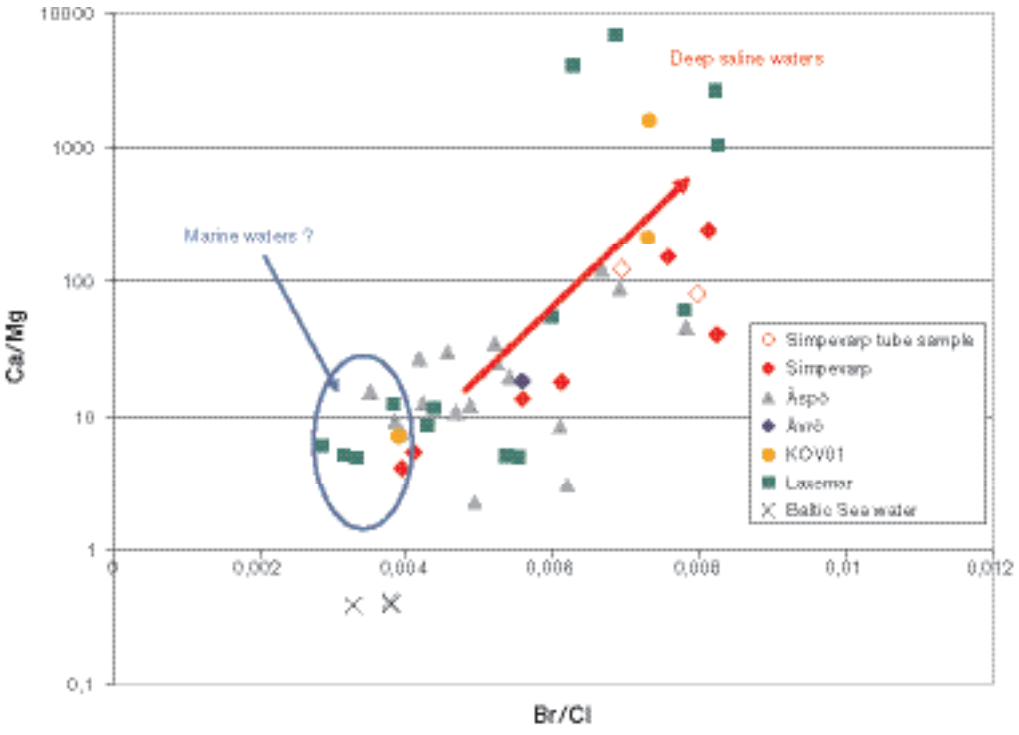

Figure 9-13. *Plot comparing all Simpevarp Ca/Mg vs. Br/Cl data with data from within the Simpevarp area.*

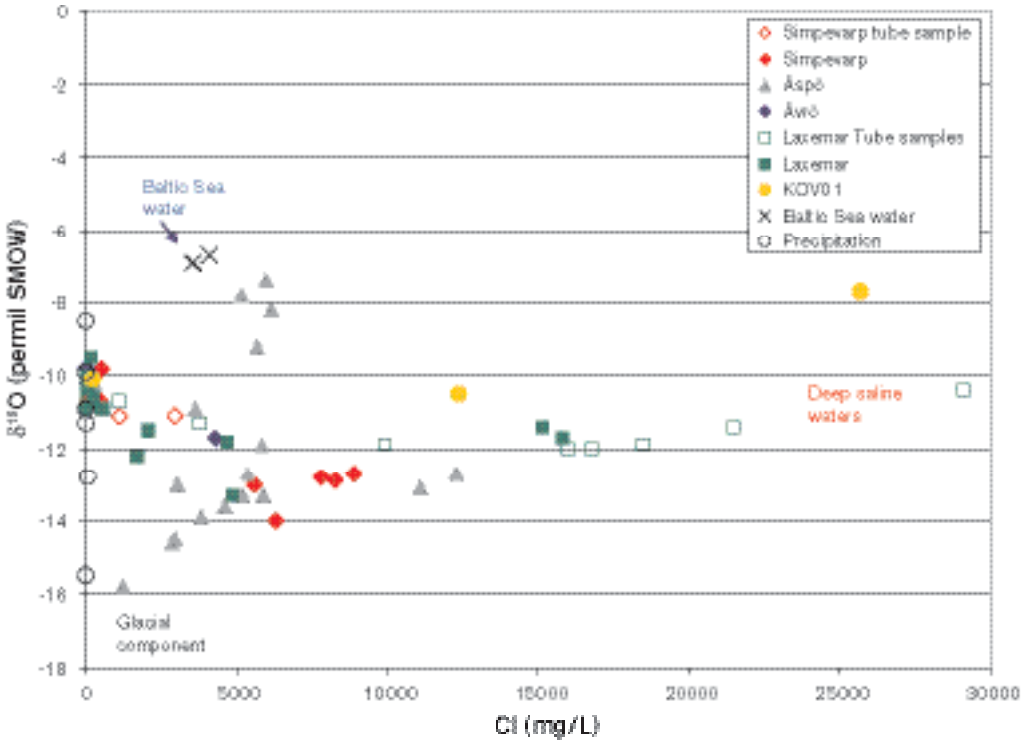

Figure 9-14. *Plot comparing all Simpevarp $\delta^{18}O$ versus Cl data with the other sites.*

Tritium

Tritium produced by bomb tests during the early 1960's is a good tracer for waters recharged within the past four decades. As part of an international monitoring campaign, peak values between 1,000 and 4,300 TU were recorded at Huddinge near Stockholm in the years 1963–1964 and values reaching almost 6,000 TU were recorded 15th of June 1963 at Arjeplog and Kiruna in northern Sweden (IAEA database). Due to decay (half life of ^{3}H is 12 years) and dispersion, in addition to a cessation of the nuclear bomb tests, precipitation tritium values decreased so that the measurements carried out at Huddinge (Stockholm) during 1969 showed that values had dropped to between 74 and 240 TU.

Present day surface waters from the Simpevarp and Forsmark show values of 7–20 TU with exceptions of a few Lake and Stream water samples from Forsmark (Figure 9-15). Generally, the Baltic Sea samples (10.3–19.3 TU) show somewhat higher values compared to the meteoric surface waters (7.8–15 TU) for precipitation. The Forsmark Baltic Sea samples show some values that are higher than the Simpevarp Baltic Sea samples but the spread is large for both sites. The successive lowering of tritium contents versus time elapsed since the bomb tests may explain the higher values in the Baltic Sea (due to reservoir effects) compared with precipitation. The difference between the Simpevarp and Forsmark Baltic Sea samples can be a latitude effect, with higher tritium values in the north compared to the south. However this is not demonstrated by the precipitation values (Figure 9-15). Moreover, the ^{14}C content in the Baltic Sea water is relatively similar between the two sites (Figure 9-16). It should be emphasised that the precipitation values are very few, show a large variation in tritium and therefore are not considered very conclusive. Continued systematic sampling of precipitation for tritium analyses is encouraged. One problem in using tritium for the interpretation of near-surface recharge/discharge is, as mentioned above, the variation in content in the recharge water over time, which implies that near-surface groundwaters with values around 15 TU can be 100% recent, or a mixture of old meteoric (tritium free) and a small portion (10%) of water from the sixties at the height of the atmospheric nuclear bomb tests.

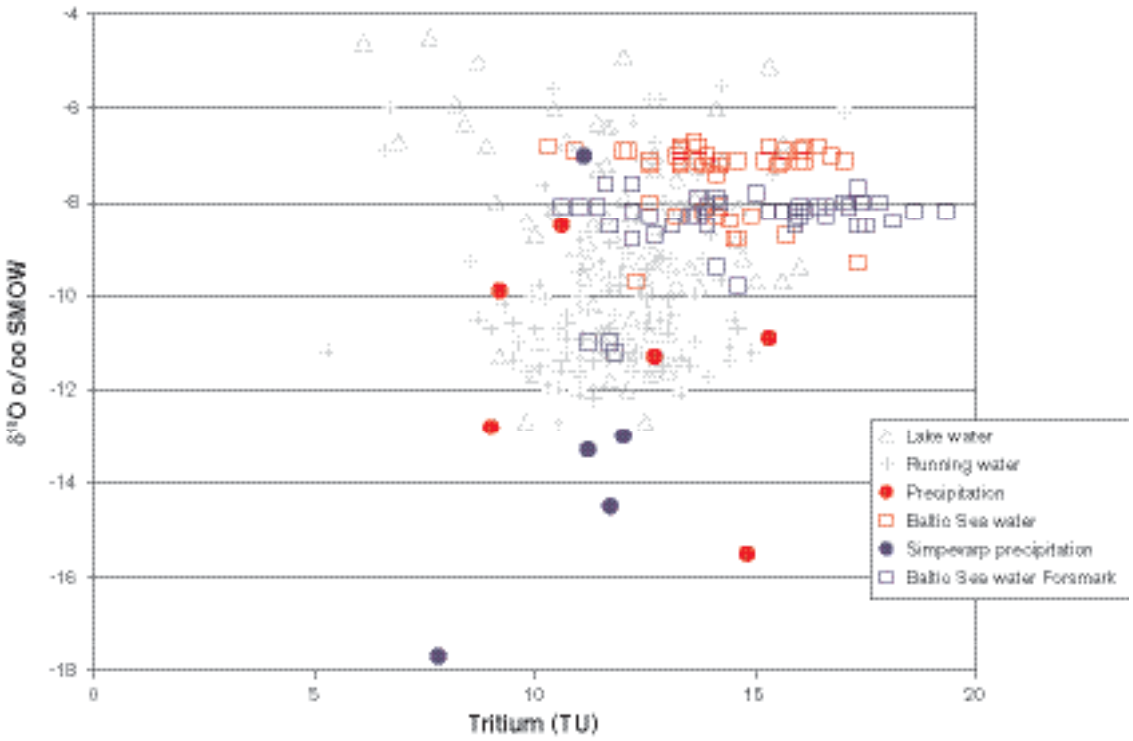

Figure 9-15. *Plot of $\delta^{18}O$ versus tritium in surface water samples from the Simpevarp and Forsmark areas.*

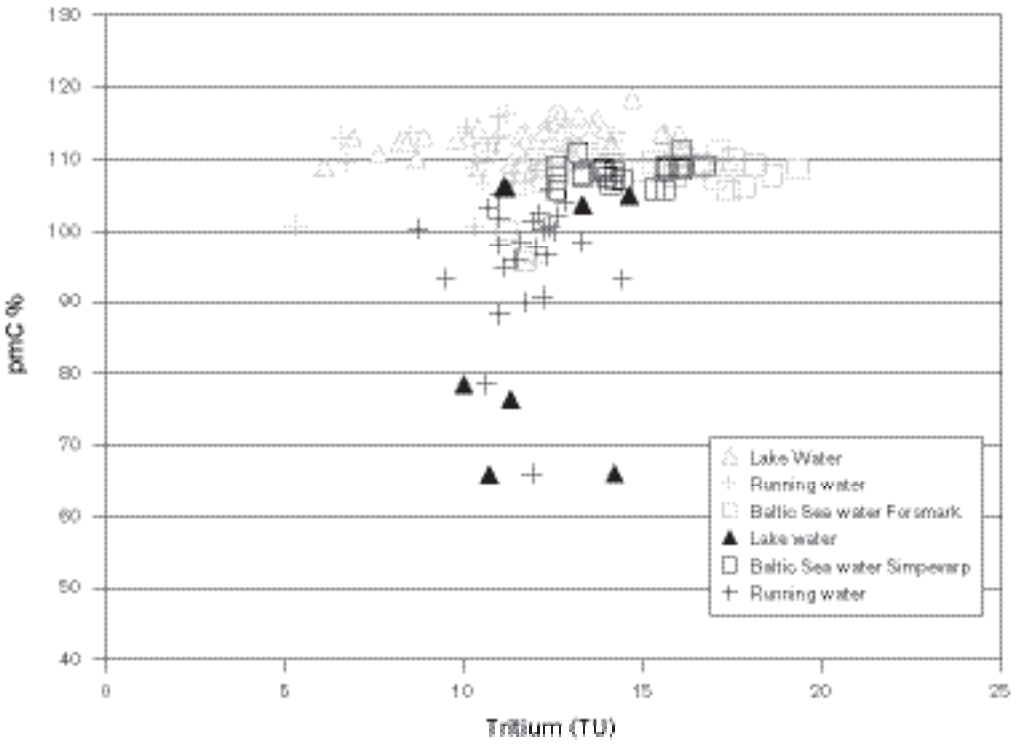

Figure 9-16. *Plot of ^{14}C (pmC) versus tritium in surface waters from the Simpevarp (shown in black and green) and Forsmark (in grey) areas.*

The plot of tritium versus ^{14}C for surface waters from Forsmark and Simpevarp show large differences concerning the Lake and Stream waters of the two sites. At Simpevarp the Lake and Stream waters show a distinct decrease in ^{14}C content whereas the tritium values remain the same or show a small decrease. They can be explained by HCO_3 added to the waters originating either from calcites devoid of ^{14}C or due to microbial oxidation of organic material with lower (or no) ^{14}C. This is the pattern expected for near-surface waters. At Forsmark, in contrast, most Lake and Stream waters have higher ^{14}C values compared with Baltic Sea waters whereas the tritium values range from 5–15 TU. The reason for this is not clear and several explanations are possible.

An additional problem in using tritium for groundwater modelling for the Simpevarp site is shown in Figure 9-17 where percentage drilling water content is plotted against tritium content. The drilling water used from percussion borehole HSH03 has tritium values in the range of 4.7 to 9.4 TU. Since the subsurface production of tritium is expected to be very low in the granitoids of the Simpevarp area, a linear relation between drilling fluid portion and tritium would be expected for the deeper samples. As can be seen, the tube samples from borehole KSH01A (750–1,000 m) deviate from this trend. Two different explanations are possible: 1) surface waters of other sources than the drilling fluid have entered and mixed within the borehole, or 2) the uranine tracer used to spike the drilling fluid has not been added uniformly throughout the drilling phase resulting in erroneous determinations of drilling water content in the sampled groundwaters. High tritium values compared to drilling fluid portion are also obtained in some groundwaters from the upper 200 m of the bedrock and are probably explained by inmixing (artificially or natural) of young meteoric recharge waters.

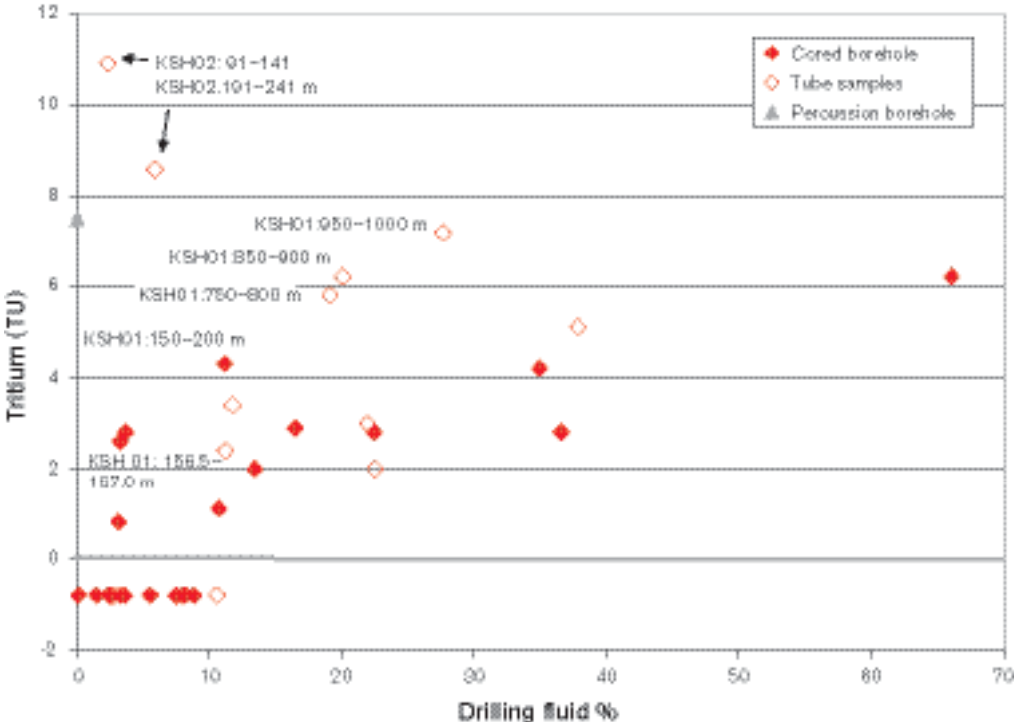

Figure 9-17. *Plot of tritium versus drilling fluid for boreholes HSH03, KSH01A, KSH02 and KSH03A.*

Carbon and carbon isotopes

Review of existing data from Äspö and Ävrö

Interpretation of the carbon inventory /see SKB, 2004c/ and how this inventory has evolved contributes to understanding of the nature of the principle groundwater contributors, key geochemical processes and possibly in some cases to the origin and age of the contributors. The work thus aims at contributing to provision of confidence in the hydrological interpretation and determination of key geochemical processes.

The objectives were: (i) to provide a methodology for interpretation of the groundwater carbon inventory, (ii) to provide tools for extending the database by relevant carbon inventory descriptors, and (iii) to outline future activities.

The approach used is a very simple and straightforward one. It makes use of simple assumptions such as the DIC (Dissolved Inorganic Carbon) biogenic inventory having a ^{13}C value of –27‰, the same as in the source material for recharge under normal plant material, soil and vegetation. If there are recharge contributions from lakes or wetlands with standing water with DIC exchange/isotopic fractionation with the atmosphere, such simple approaches are not valid. The same is true if there is microbial activity in the subsurface producing methane or carbon dioxide or considerable precipitation of DIC. Another problem is the heterogeneous carbon isotope composition of the fracture calcites that are partly dissolved in the upper part of the flow paths. The main idea, however, is that by using this simple approach, systems/samples can be identified that basically follow this simple route in the development of the DIC inventory and deviations can be identified for further clarification. However, because the available carbon isotope data from the Simpevarp 1.2.data freeze are still very limited, especially concerning groundwaters, no tests have therefore been performed within this model version.

Carbon and carbon isotope data from Simpevarp

The stable carbon isotope ratios, expressed as $\delta^{13}C$ ‰ PDB, and radiocarbon contents (^{14}C) expressed as pmC (percentage modern carbon), and HCO_3^-, have been analysed from surface waters and groundwaters. The tritium versus ^{14}C for surface waters has been discussed already in the previous section. Figure 9-18 shows $\delta^{13}C$ versus tritium for the Simpevarp waters.

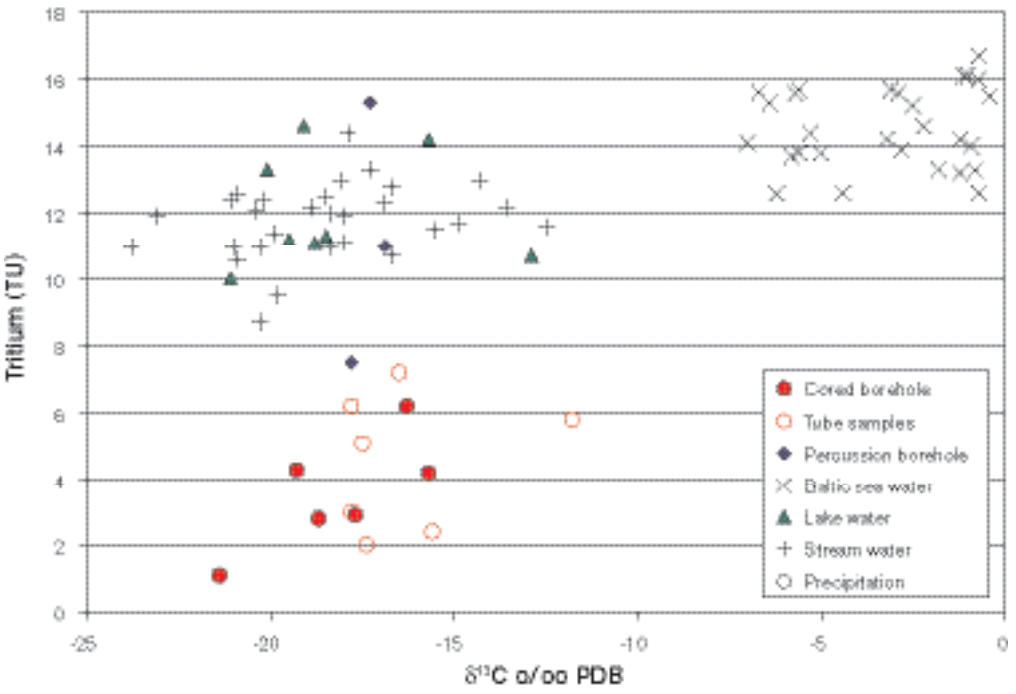

Figure 9-18. *Plot of tritium versus $\delta^{13}C$ in surface waters and groundwaters from the Simpevarp subarea.*

The Baltic Sea water has high carbon isotope values produced by equilibria with atmospheric CO_2; this contrasts with all the other waters, both surface and groundwaters, which show significantly lower values. CO_2 produced in the soil cover due to breakdown and oxidation of organic material usually results in $\delta^{13}C$ values of around –20‰ PDB which can partly explain the dissolved $\delta^{13}C$ (HCO_3^-). However, the lowering in $\delta^{14}C$ accompanying the decrease in $\delta^{13}C$ in some Lake and Stream waters indicate that calcite dissolution may have taken place as well, and/or breakdown of old organic material.

The fracture calcites show no homogeneous $\delta^{13}C$-values and it is therefore not possible to model calcite dissolution as a two end member mixing. Since to date only six ^{14}C analyses of groundwaters from packed-off sections are available from the Simpevarp area, existing data from Laxemar, Äspö and Ävrö have been included in two plots showing $\delta^{13}C$ (HCO_3^-) versus ^{14}C (Figure 9-19) and $\delta^{13}C$ (HCO_3^-) versus HCO_3^- (Figure 9-20). The plots show that there is no real correlation between ^{14}C and $\delta^{13}C$, i.e. there is no indication of a change in $\delta^{13}C$ with age. Instead, most groundwater samples show values in the range of –15 to –22‰ $\delta^{13}C$ indicating that breakdown of organic material plays a major role and has occurred either in the near-surface (being transported downwards) or that in situ production has taken place. An organic origin is also supported by the $\delta^{13}C$ versus HCO_3^- plot where the groundwater samples with the highest HCO_3^- content show relatively homogeneous $\delta^{13}C$ values clustering at –16 to –20‰ $\delta^{13}C$.

Figure 9-21 shows the "^{14}C-derived ages" of fresh groundwater samples assuming different initial values of pmC at the recharge water (100 and 85 pmC, respectively). The hypothesis is that after the initial carbon uptake in the soil zone by infiltrating water, some ^{14}C dilution could occur through the addition of ^{14}C-free carbon. Then the "initial" value for ^{14}C activity of the aqueous carbonate dissolved in the recharge water actually reaching the phreatic surface would be lower than 100 pmC. Thus, the water age is determined from the decay equation "corrected" with a dilution factor (q), as:

$$t = -8267 \ln \frac{a^{14}C_{DIC}}{q a_o{}^{14}C} \qquad (9\text{-}1)$$

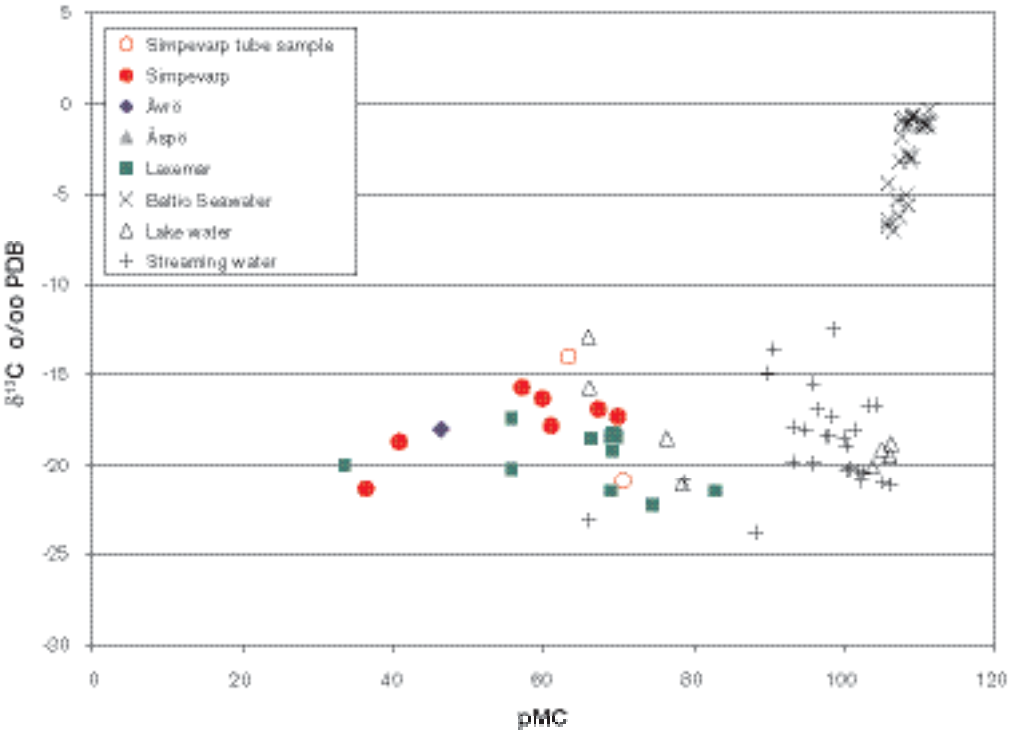

Figure 9-19. *$\delta^{13}C$ (HCO_3^-) versus ^{14}C in surface waters and groundwaters from the Simpevarp area.*

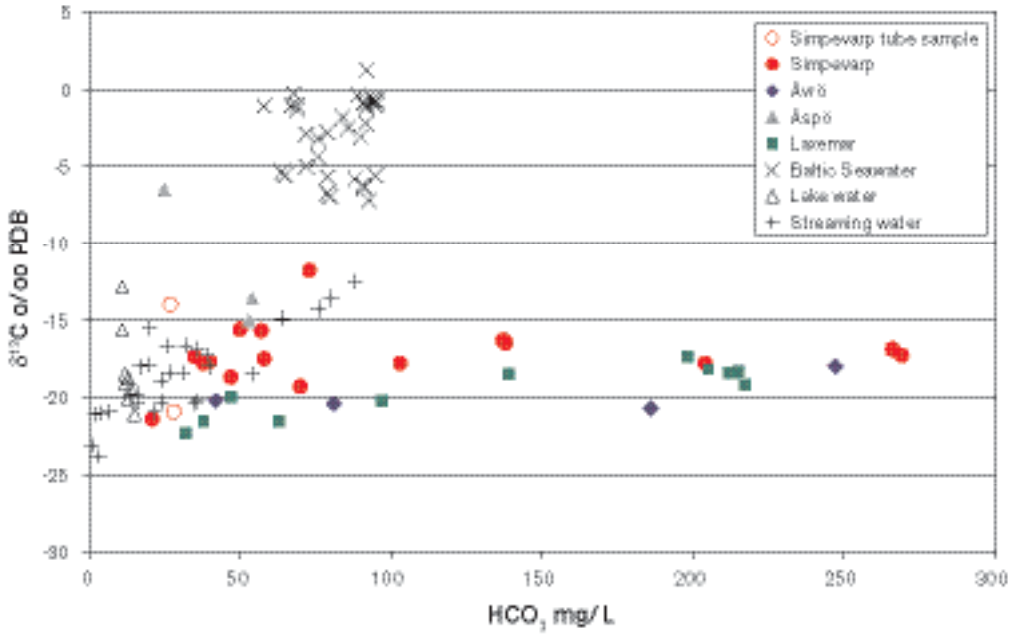

Figure 9-20. *$\delta^{13}C$ (HCO_3) versus HCO_3 in surface waters and groundwaters from the Simpevarp area.*

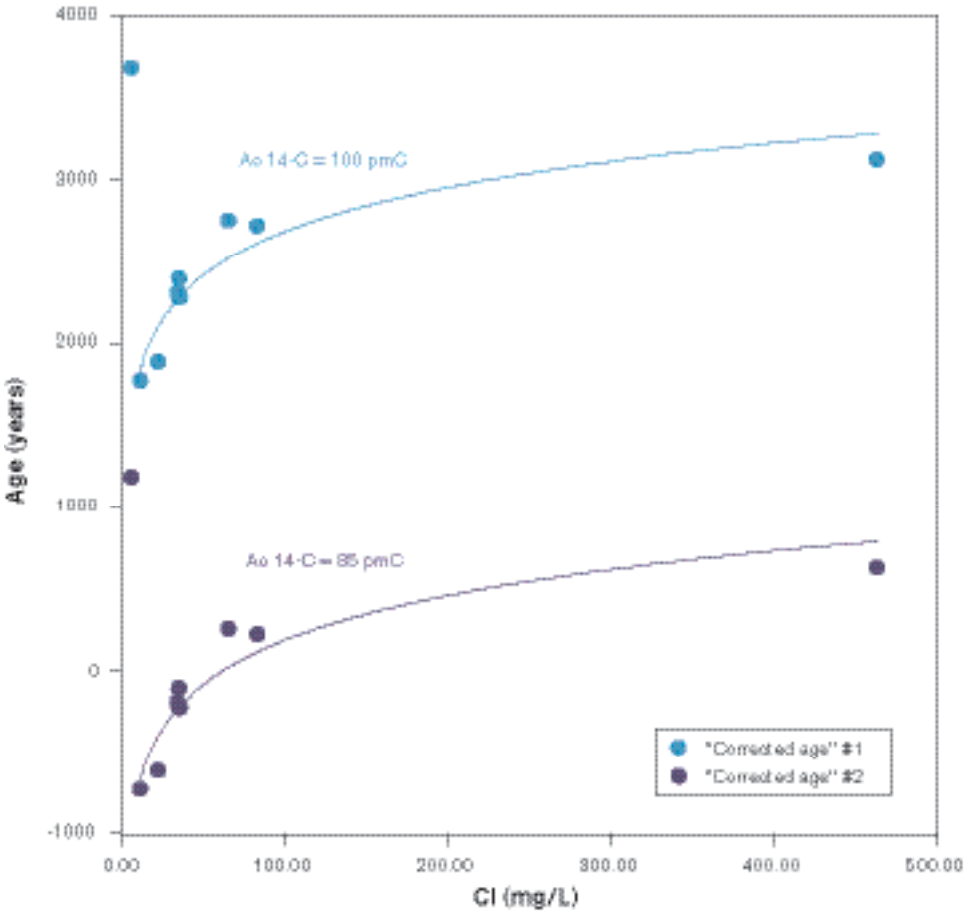

Figure 9-21. *^{14}C-derived ages of fresh groundwater samples from the Simpevarp area assuming initial values of 100 pmC and 85 pmC.*

/Vogel, 1970/ reported q values for different hydrogeologic systems ranging from 0.65 to 1.00. Figure 9-22 shows the computed radiometric water age using q values of 1.00 and 0.85 (corrected ages #1 and #2, respectively). Both calculations assume that the initial ^{14}C activity in the soil (a_0 ^{14}C) is 100 pmC. The data shown in Figure 9-22 correspond to all available data fulfilling the following conditions: (1) collected at the first 100 m of the granitic bedrock, (2) having chloride contents lower than 500 mg/L, and (3) being judged as representative samples.

Modelling the distribution of groundwater ages was based on (1) geochemical evidence of calcite dissolution, (2) ^{13}C values of fresh groundwater, and (3) previous experience and published data of other granitic aquifers, it is believed that an initial value of 100 pmC for recharge water in Simpevarp is highly unlikely.

The modelling shown in Figure 9-21 indicates that the age of fresh groundwater at Simpevarp (at a depth of 100–200 m) could be in the order of magnitude of some decades to hundreds of years, instead of thousands of years as estimated from uncorrected ^{14}C measurements.

Sulphur isotopes

Sulphur isotope ratios, expressed as $\delta^{34}S$ ‰ CDT, have been measured in dissolved sulphate in Baltic Sea waters, surface waters and groundwaters from the Simpevarp area. Over 200 analyses have been performed of which 30 are groundwaters from boreholes KSH01 and KSH02 at Simpevarp with two exceptions; one from Laxemar (HLX10) and one from Ävrö (KAV04). The isotope results are plotted versus SO_4^{2-} contents (Figure 9-22) and versus Cl contents (Figure 9-23). Unfortunately, neither SO_4^{2-} nor Cl contents were measured in 10 of the groundwater samples analysed for $\delta^{34}S$. Better coordination of these measurements is considered essential for continued sampling and analyses in the area.

The recorded values vary within a wide range (–1 to +24‰ CDT) indicating different sulphur sources for the dissolved SO_4^{2-}. For the surface waters (Lake and Stream waters) the SO_4^{2-} content is usually below 50 mg/L and the $\delta^{34}S$ relatively low but variable (–1 to +15‰ CDT) with most of the samples in the range 2–9‰ CDT. These relatively low values indicate that atmospheric deposition and oxidation of sulphides in the overburden is the origin for the SO_4^{2-}. The Baltic Sea waters cluster around the 20‰ CDT marine line but show a relatively large spread (16–23‰ CDT). The reason for this is not fully understood but suggestions include: a) contribution from land discharge sources (e.g. streams) to various degrees (low values), and b) potential bacterial modification creating high values in the remaining SO_4^{2-}.

The borehole groundwaters (Figure 9-22) show $\delta^{34}S$ values in the same range as the Baltic Sea waters but with a clear indication of $\delta^{34}S$ values greater than +21‰ CDT in samples with low SO_4^{2-}. These latter values are interpreted as a product of sulphate reduction taking place in groundwaters identified in Figure 9-23 with a chloride content between 5,000 and 6,300 mg/L. The five groundwaters with higher salinities share lower $\delta^{34}S$ but higher SO_4 contents. The $\delta^{34}S$ values of these groundwaters are, however, still within the range for the analysed Baltic Sea waters. The SO_4^{2-} contents are still not high enough to invoke dissolution or leaching as a mechanism, more likely processes are in-mixing of marine waters although in-mixing of SO_4^{2-} from deep brine waters cannot be excluded. Deep saline SO_4^{2-} sources may have resulted from the leaching of sediments and/or dissolution of gypsum previously present in fractures. Lowering of the $\delta^{34}S$ signature by oxidation of sulphides seems to be less probable for the groundwater samples and is not supported by fracture mineral investigations /Drake and Tullborg, 2004, P-report in press/.

The SO_4 content in deep groundwaters from the Oskarshamn area (borehole KOV01) show different trends versus Cl content /cf. Appendix 1 in SKB, 2004c/. The Laxemar samples show relatively high SO_4 content in the saline waters, whereas the KOV01 samples show extremely low values. The most saline water at Simpevarp (16,800 mg/L Cl) has a SO_4 content of around 600 mg/L. Geochemical modelling indicates dissolution of gypsum as a possible source for SO_4 in the groundwaters. A few observations of fracture gypsum in the lower part of borehole KSH03A have been documented. Unfortunately, no $\delta^{34}S$ measurements are so far available from this gypsum or from the waters at Simpevarp with chloride contents greater than 9,000 mg/L.

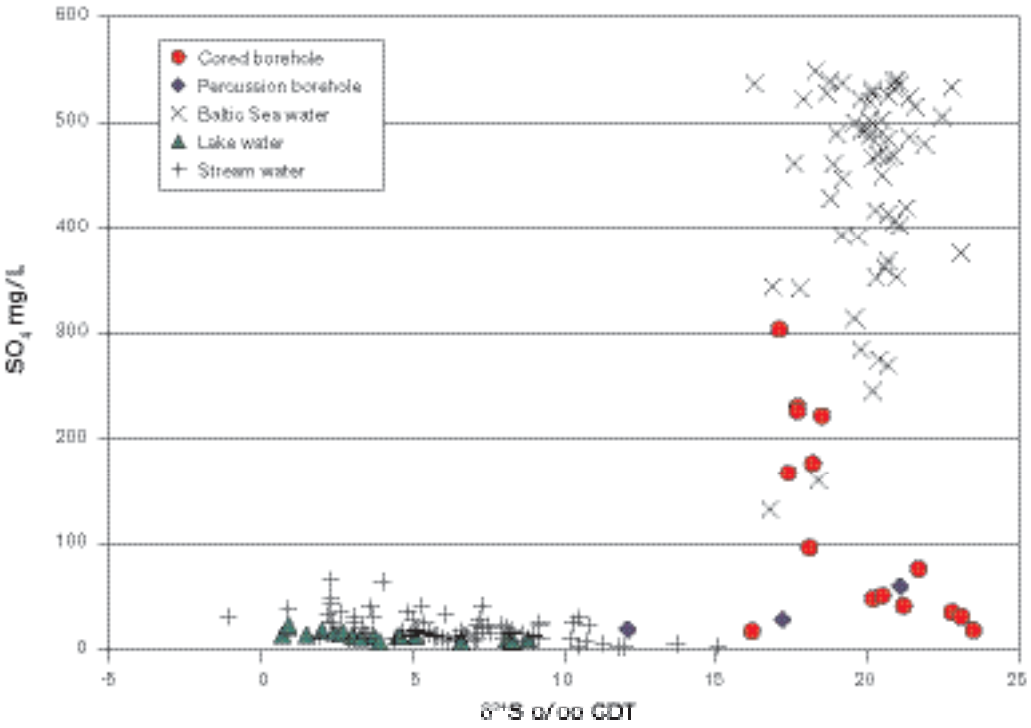

Figure 9-22. *Plot of $\delta^{34}S$ versus SO_4^{2-} in surface waters and groundwaters. The grey line indicates the marine value at around 20‰ CDT.*

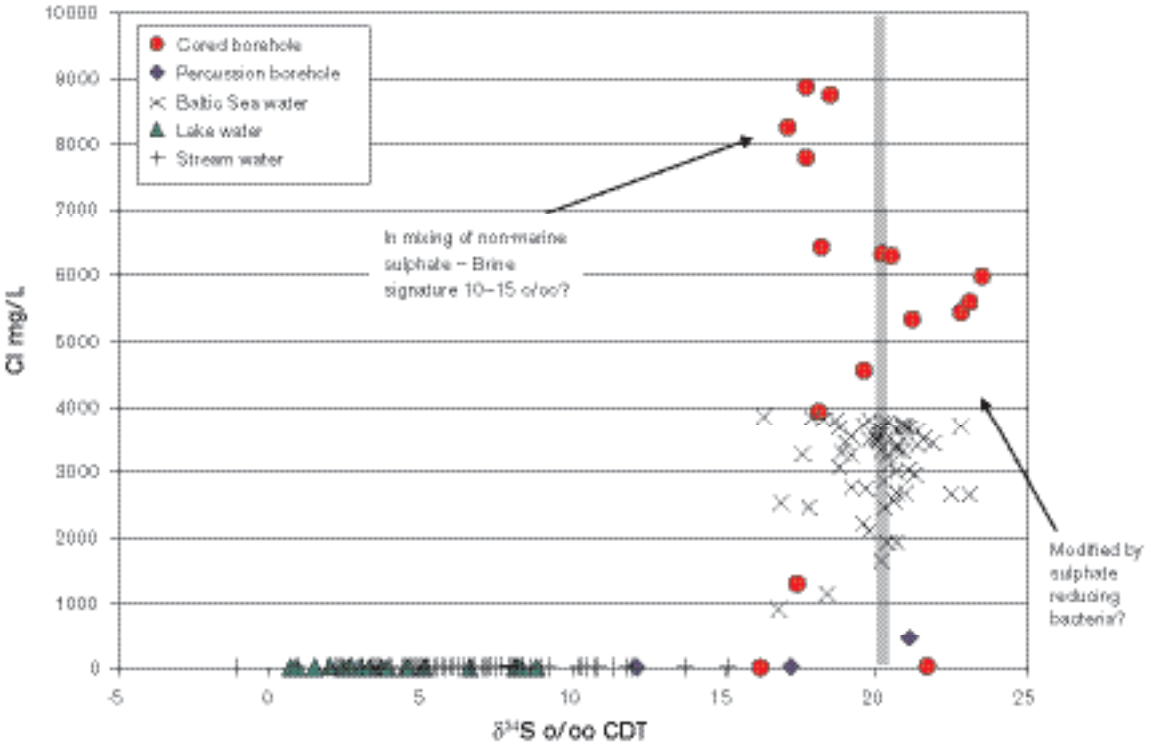

Figure 9-23. *Plot of $\delta^{34}S$ versus Cl in surface waters and groundwaters. The grey line indicates the marine value at around 20‰ CDT.*

Strontium isotopes

Strontium isotope ratios ($^{87}Sr/^{86}Sr$) have been measured in groundwater samples and Baltic Sea waters from the Simpevarp area and these are plotted versus strontium content in Figure 9-24. Also included in this diagram are groundwater analyses from Forsmark.

^{87}Sr is a radiogenic isotope produced by the decay of ^{87}Rb (half-life 5×10^{10}a). Marine waters show a distinct Sr isotope signature (0.7092) which is very close to the measured values in the Baltic Sea waters, whereas groundwaters from the different sites (Figure 9-24) show values significantly more enriched in radiogenic Sr. Water/rock interaction processes involving Rb-containing minerals are the reason for this. The relatively small variation in Sr isotope ratios within each area, particularly at the Simpevarp, Ävrö and Laxemar is probably an indication that ion exchange reactions with clay minerals along the groundwater flow paths is an important process. For the Simpevarp and Laxemar subareas there is a tendency towards higher contents of radiogenic Sr in the groundwaters with greatest salinity (and thus the highest Sr contents measured). Because of the limited data it is not possible to explain this observation, but in the absence of any mineralogical reasons, it is likely that longer residence times for these deep saline groundwaters result in more extensive mineral/water interactions. The higher $^{87}Sr/^{86}Sr$ ratios in the Forsmark samples are most probably due to differences in the composition of the bedrock and fracture minerals compared to the Simpevarp area.

The possibility of tracing marine components by the use of Sr isotopes is often debated. Clay minerals in the fractures may, however, make such interpretations difficult. For example, the strong present-day major ion Littorina Sea signature in the Forsmark groundwaters is not reflected by any marine Sr isotope imprint. Instead, modification of the Sr isotope values is probably attributable to ion exchange processes.

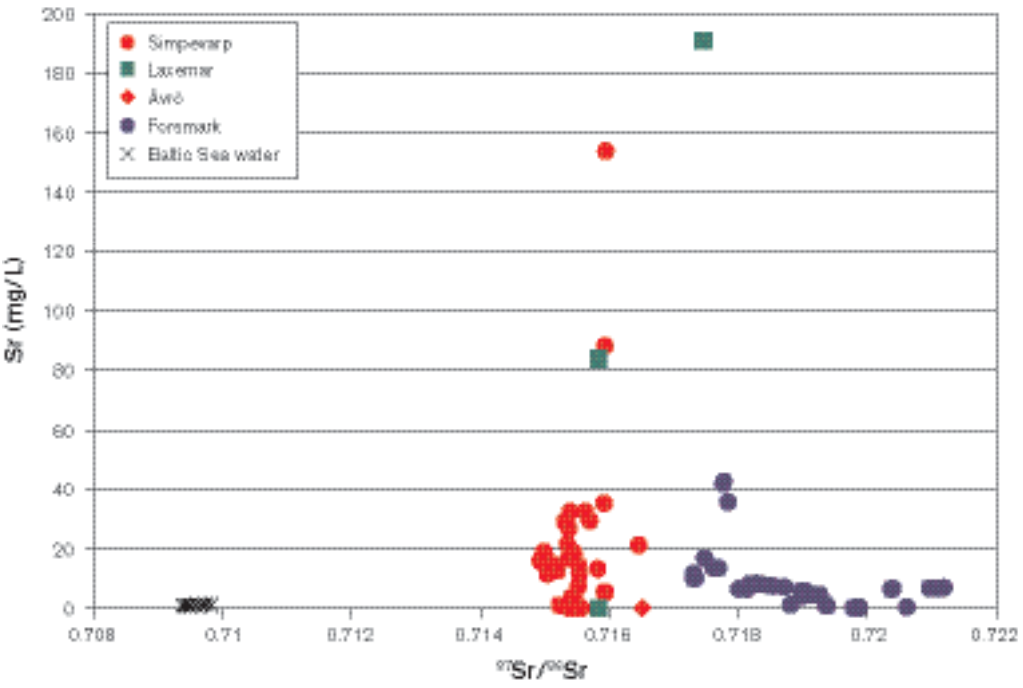

Figure 9-24. *Plot of $^{87}Sr/^{86}Sr$ ratios versus Sr in groundwaters from the Simpevarp area. Also included are Baltic Sea waters from the Simpevarp and Forsmark areas.*

Chlorine isotopes

Stable chlorine isotopes have been analysed on waters from the Simpevarp area. Figure 9-25 plots $\delta^{37}Cl$ vs. Cl for the Simpevarp, Laxemar, Ävrö and Forsmark sites, including Baltic Sea and surface Lake and Stream waters from the Simpevarp subarea. According to /Frape et al. 1996/ modern Baltic and possibly palaeo-Baltic waters may be recognised by negative $\delta^{37}Cl$ signatures related to salt leachates from Palaeozoic salt deposits south of the Baltic Sea; influence by water-rock interaction tends to result in positive $\delta^{37}Cl$ signatures. /Clark and Fritz, 1997/ also show a clear distinction between the Fennoscandian and Canadian Shield crystalline rock groundwaters and groundwaters from sedimentary aquifers.

Taking into consideration the analytical uncertainty of around ± 0.2‰, Figure 9-25 shows that the Simpevarp cored borehole groundwaters are characterised by positive values (+0.14 to +0.75‰ SMOC). The Baltic Sea waters fall within the range of –0.28 to +0.27‰ SMOC and the surface Stream waters and the percussion borehole groundwaters with very low Cl contents show the largest spread in $\delta^{37}Cl$ values (–0.03 to +0.44‰ SMOC). These data suggest that the deeper cored borehole groundwaters are characterised by water/rock interaction processes, whilst the near-surface percussion borehole groundwaters are mainly marine derived. The distribution of Baltic Sea and surface Lake and Stream waters suggest some mixing components of marine-derived and deeper groundwater sources.

When the $\delta^{37}Cl$ values for groundwaters from the Laxemar subarea and Forsmark are compared with the Simpevarp data, groundwaters with Cl contents around 5,000 mg/L show a large variation in $\delta^{37}Cl$ values; most of the Forsmark samples show slightly negative values whereas the Simpevarp samples show values on the positive side. For groundwaters with higher Cl contents (> 6,000 mg/L) the Simpevarp and Laxemar subarea samples show values greater than 0.3‰ SMOC. The Forsmark sample (only one available so far) shows 0.09‰ SMOC. This suggests that for groundwaters containing around 5,000 mg/L Cl, the Forsmark data indicate a greater marine signature involved (Littorina Sea?). This is emphasised by plotting the Br/Cl ratios against $\delta^{37}Cl$ (Figure 9-26). This plot shows that groundwaters significantly enriched in Br (i.e. Simpevarp and Laxemar subareas),

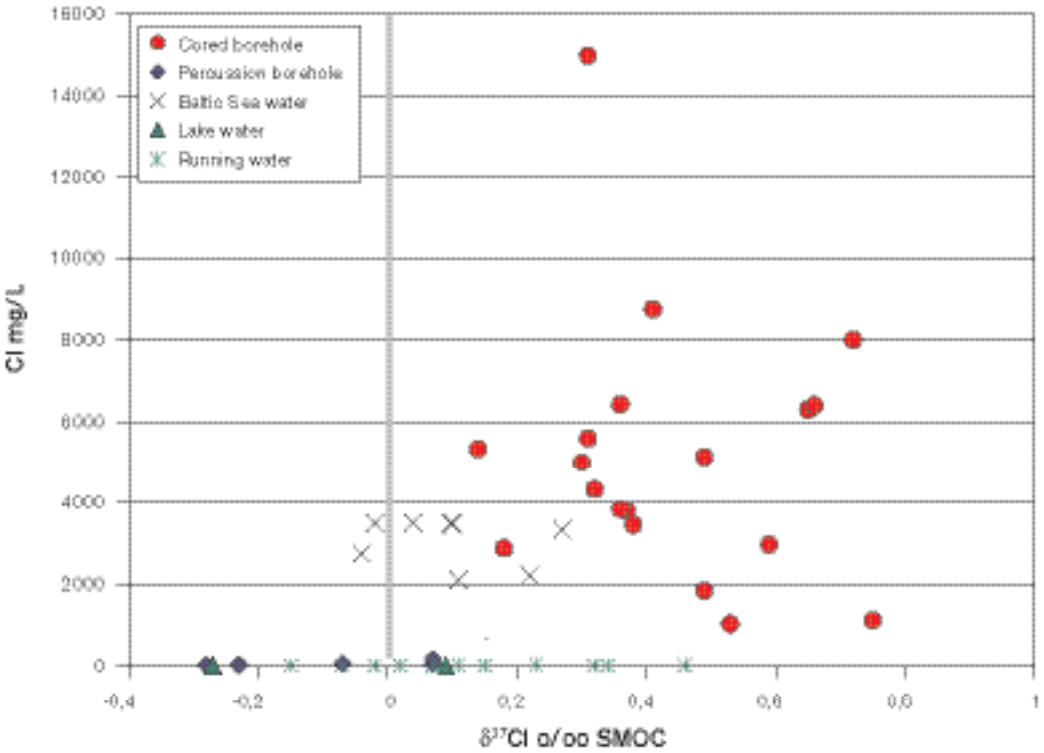

Figure 9-25. *Plot of $\delta^{37}Cl$ versus Cl in surface and near-surface waters, groundwaters, and Baltic Sea waters from the Simpevarp subarea.*

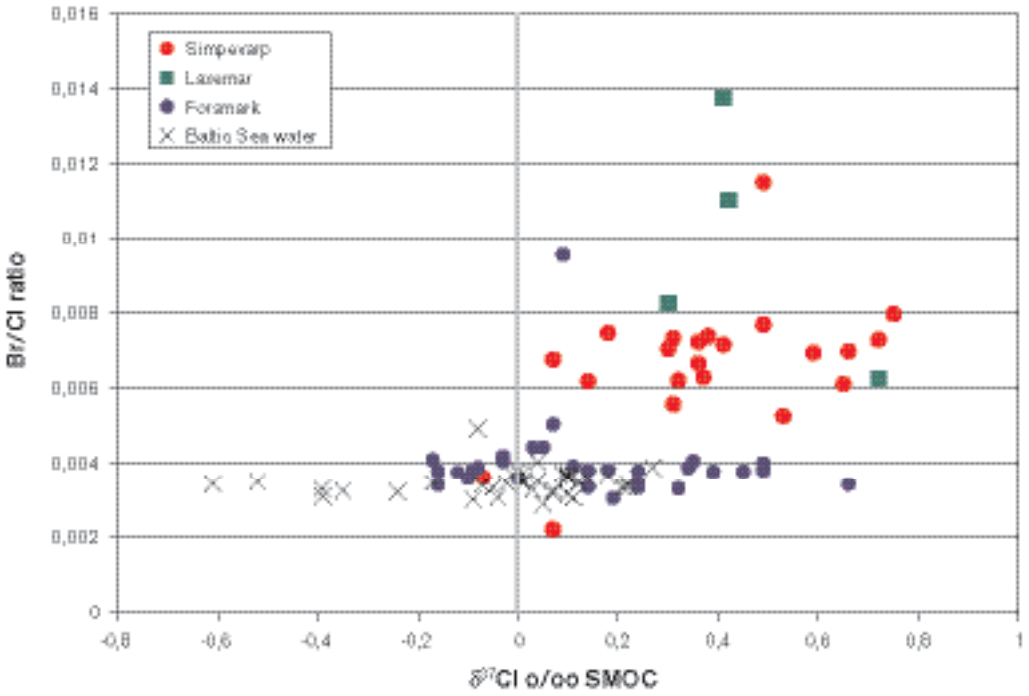

Figure 9-26. *Plot of $\delta^{37}Cl$ versus Br/Cl ratio in groundwaters from the Simpevarp and Forsmark areas. Baltic Sea waters from the Simpevarp and Forsmark areas included for reference.*

compared to marine waters (i.e. Baltic Sea) and those groundwaters with a marine signature (i.e. Forsmark), display positive $\delta^{37}Cl$ values. The Forsmark groundwaters characterised by more marine-derived Br/Cl ratios cluster closer to 0‰ SMOC with a similarly large spread of values as for the Baltic Sea samples. At Forsmark the more positive values reflect deeper groundwaters from the cored boreholes where mixing with marine waters is less marked.

Trace elements

Only a few data exist for the majority of groundwaters and even some of these are incomplete. The following was concluded from the evaluation:

- Sr, Cs and Rb show a positive correlation with depth (and therefore Cl).
- Ba varies considerably but a negative correlation with SO_4^{2-} is indicated, possibly explained by the solubility control of barite.
- Mn contents show large variations in near-surface waters, usually uniform or slightly decreased values in groundwaters down to 600 metres depth, and decreasing values at greater depths.
- The uranium contents are below 2 µg/L in all the analysed waters. The surface waters show values between 0.16 and 1.9 µg/L whereas the Baltic Sea waters all display values around 0.8 µg/L; most of the groundwater samples are low in uranium (≤ 0.2 µg/L). Higher uranium in surface and near-surface waters is usually observed and is caused by oxidising conditions at the surface. The mobility of the oxidised and dissolved uranium is highly dependent on access to complexing agents, mostly in form of HCO_3^- which is produced in the soil cover and the near-surface environment.

Calcites

Isotopic evidence from calcites sampled from borehole KSH01A supports the results from the hydrogeological and hydrochemical studies which show that the upper part of the bedrock in the Simpevarp subarea is much more hydraulically conductive and dynamic than the deeper part (> 300 m) and have probably been so for a very long time. The number of open fractures and the amounts of calcite in the deeper fractured bedrock is limited. Furthermore, the stable isotope ratios

support the decreased interaction with biogenic carbonate at depths greater than 300 metres in KSH01A. The morphology of the calcites formed in open fractures show crystal shapes typical for recent brackish or saline groundwater carbonates with one exception. This is in agreement with the present groundwater chemistry where saline groundwaters (> 5,000 mg/L Cl) are sampled already at a depth of 150 m.

Microbes

Figure 9-27 shows the distribution of the different microbial groups found at the three sampled levels in KSH01A and the measured redox potentials. The right part of the Figure 9-27 shows a so-called redox ladder with different microbial respiration redox couples placed at their respective E_0'. The red line in this figure marks the redox interval measured in KSH01A. These redox values coincide where sulphate reducers and methanogens can be found and correlates very well with the Most Probable Number (MPN) /American Public Health Association, 1992/ results for this borehole. If iron- and manganese reducers were to be found, the measured redox values had to be at least 50 mV higher. Redox calculations show that the redox pairs $SO4^{2-}/S^{2-}$ and CH_4/CO_2 give values that agree with the measured redox potentials and by that also with the microorganisms found.

In Figure 9-28 the MPN data are plotted versus depth. Here it can be seen that a higher number of microorganisms were found in the depth interval 101–300 m, that is the two shallowest sampling points, than at the deepest, 548–565.5 m section. Since there are two sampled depths at the 101–300 interval, the sum of MPN values was divided by 2. This finding indicates that the activity of microorganisms is higher in the groundwater from the shallower sites.

Figure 9-29 shows a one-dimensional redox model of borehole KSH01A including the 3 sampling depths and intercepting structures. Flow measurements showed that the fracture zone at 245–261.6 m covers a large area but each fracture had a low flow. The low flow velocity was probably due to clay formation in the fractures /Laaksoharju et al. 2004b/. Figure 9-29 shows that in the shallowest part of the borehole, 156.5–167 m, the sulphate reducing bacteria were dominant.

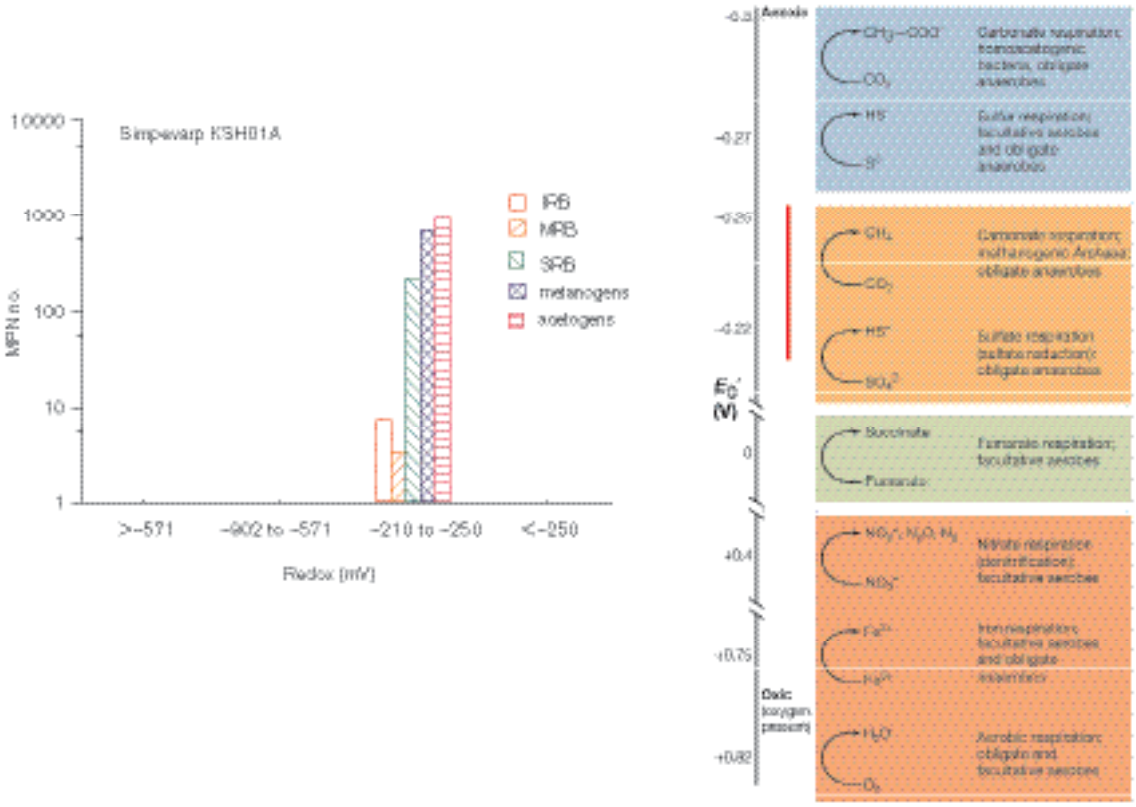

Figure 9-27. *The sum of the most probable number of microorganisms plotted versus redox intervals. The data are from sampling of ground water in borehole KSH01A in the Simpevarp subarea.*

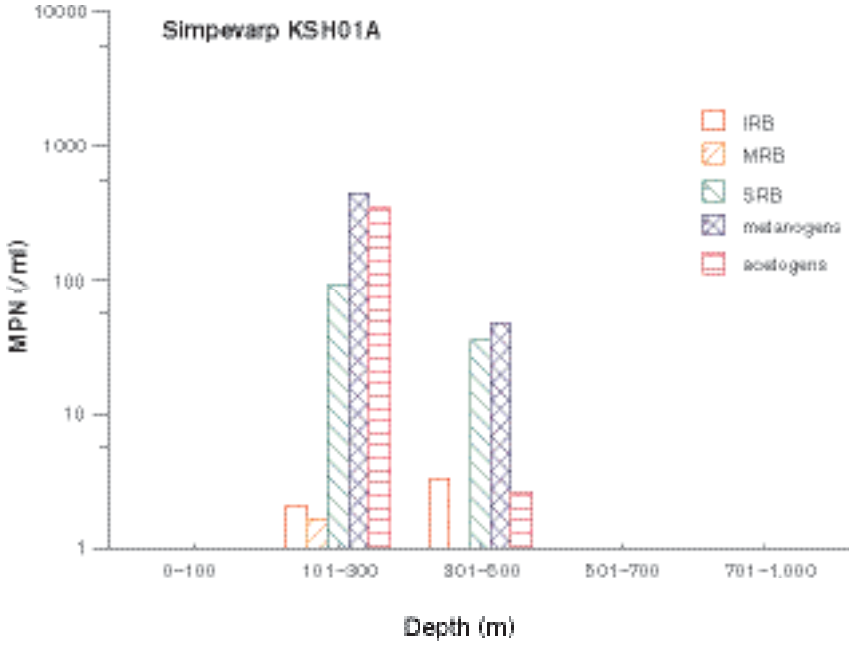

Figure 9-28. *The sums of most probable number of microorganisms plotted versus depth intervals. The data are from sampling of groundwater in borehole KSH01A in the Simpevarp subarea.*

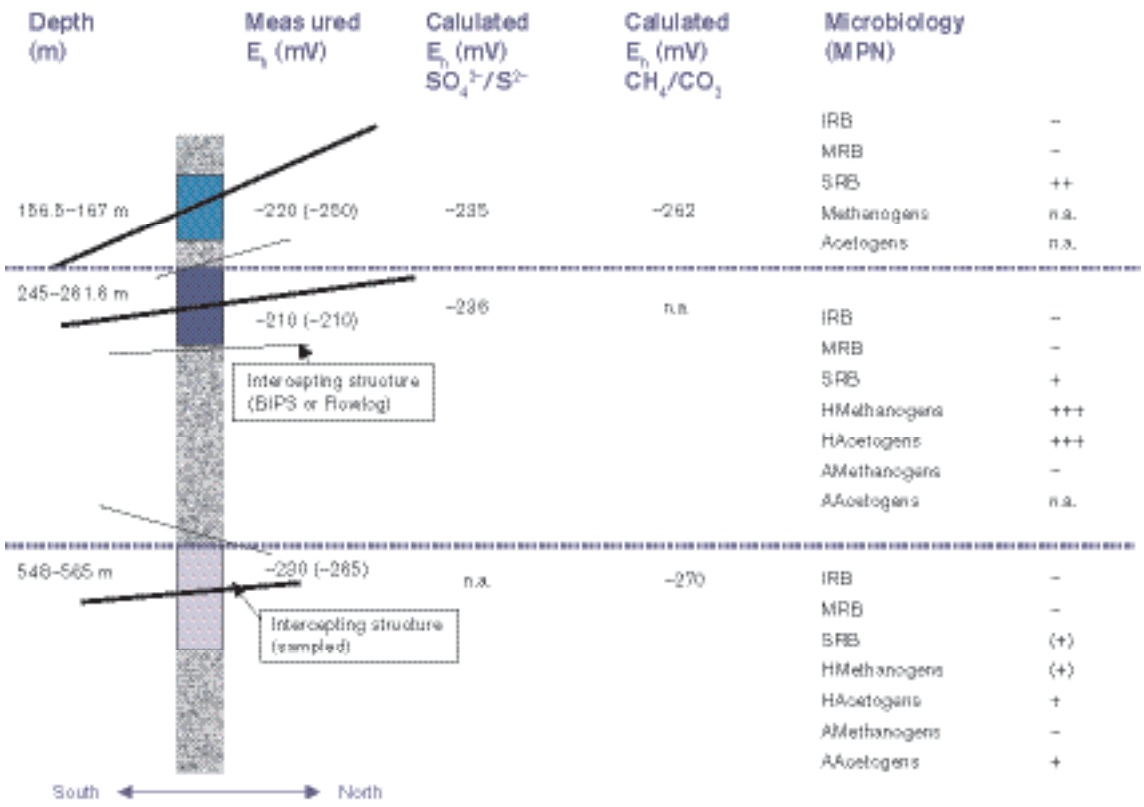

Figure 9-29. *Biogeochemical model of borehole KSH01A in Simpevarp (n.a.= not analysed). Bracketed numbers inidcate redox measurements conducted at different times than the microbial sampling.*

The measured and the calculated redox values with the redox pair SO_4^{2-}/S^{2-} support this finding. In version Simpevarp 1.1 pyrite was reported as one of the minerals found in fracture fillings and this too supports the microbiological data and gives an explanation as to why the measured sulphide data at this depth were very low.

At the next sampling depth, 245–261.6 m, heterotrophic methanogens and acetogens dominated. The measured and calculated redox values, this time with CO_2/CH_4 as redox pair, corresponds with the redox interval where these types of microorganisms can be found.

Finally, the deepest section has in general very low activity. Groundwater flow at this location was lower than that at the depth above and the redox value was low. The lowest measured redox value at this depth was –265 mV. The E_0' where autotrophic acetogenesis takes place is around –300 mV and the measured low redox strengthens the suggestion that acetogens would be the most active at this depth even though MPN numbers were very low. The reason for this might be that the MPN method is difficult to apply to autotrophic organisms and that the MPN method therefore gave lower values than in realty.

Colloids

Colloid data have been evaluated from the Simpevarp area where the data represent mostly old data sampled during the last 10 years, since few new data were available at the time of the Simpevarp 1.2 data freeze.

It was detected that the amount of colloids decreases with depth in KLX01 but not in KAV01. Furthermore, the amount does not vary much at the different depths. The sampled depths were 422.5 m, 525.5 m and 560.5 m and they differ only 140 m in depth, which is not large in relation to the total depth explored (Figure 9-30). The average concentration of colloids in this study is 63 ± 49 µgL^{-1} and is in agreement with colloid studies from Switzerland (30 ± 10 and 10 ± 5 µgL^{-1} /Degueldre, 1994/) and Canada (300 ± 300 µgL^{-1} /Vilks et al. 1991/) where they used the same approach as at Simpevarp /Laaksoharju et al. 1995a/.

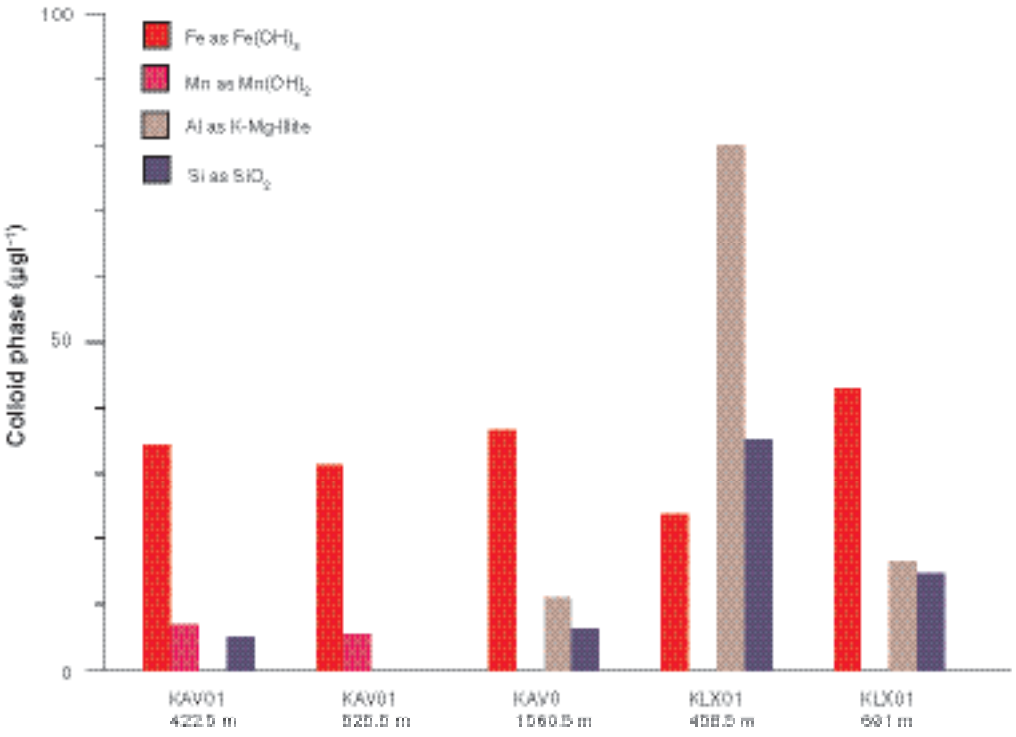

Figure 9-30. *The composition of colloids sampled from 2 boreholes, KAV01 and KLX01, in the Simpevarp area. Calcite and sulphur values are omitted in this figure.*

However, because of the few data available it is difficult to draw far-reaching conclusions from this analysis. In particular, the lack of data for numbers of particles makes it difficult to make calculations of possible binding sites for radionuclides in the different colloid fractions.

Gas

In the current study /SKB, 2004c/ up to 12 gases were analysed: helium, argon, nitrogen, carbon dioxide, methane, carbon monoxide, oxygen, hydrogen, ethyne, ethene, ethane and propane. Borehole KSH01A is the only one that was complete regarding analysed gas components. Data for the total volume of gas were available only for five depths in two of the boreholes. They contain between 44 and 80 mL L^{-1} and this is in accordance with volumes found at other locations in the Fennoscandian shield. The highest amounts of gas have been found in deep groundwater in Olkiluoto in Finland with volumes up to above 1,000 mL L^{-1} /Pitkänen et al. 2004/. The high gas content is due to the high pressure at the 900–1,000 m depth. The gas volume data from KLX01 does not include propane (C_3H_8), oxygen, argon or hydrogen and therefore the volume from this borehole should not be compared to the volumes from KSH01A.

Figure 9-31 shows that the amount of nitrogen decreases with depth in KLX01 but in KSH01A it is the opposite trend. It is noticed that the data from KSH01A are from shallower water and from KLX01 below 600 m. The nitrogen concentration in groundwater from Olkiluoto, Finland showed an increasing trend with depth down to 1,100 m /Pitkänen et al. 2004/.

Helium concentration in both boreholes in the Simpevarp area showed a slight decrease with depth but there is little variation among the data. Helium concentrations in Olkiluoto increased with depth following the concentration of nitrogen.

The origin of nitrogen and helium in groundwater is considered to be crustal degassing of the bedrock. Another source for helium can be radioactive decay, also from the bedrock.

Carbon dioxide in groundwater is a dissociation product of dissolved carbonates in fractures in the bedrock. The carbon dioxide concentrations in samples from the Simpevarp area are fairly constant in the different boreholes with values below 0.1 mM (Figure 9-32). There is a slight tendency that the concentration decreases with depth down to 500–600 m and below that the values are more or less constant. This pattern has also been observed for carbon dioxide concentrations in groundwater from the Olkilouto Site in Finland /Pitkänen et al. 2004/.

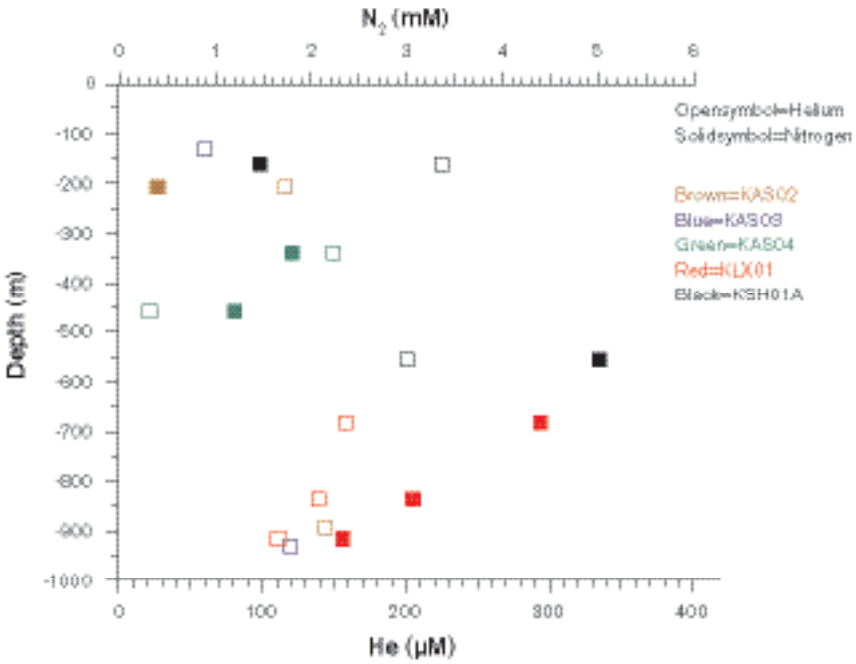

Figure 9-31. *The concentrations of nitrogen and helium plotted versus depth in samples from boreholes in the Äspö (KAS02, 03, 04), Laxemar (KLX01) and Simpevarp (KSH01A) sites.*

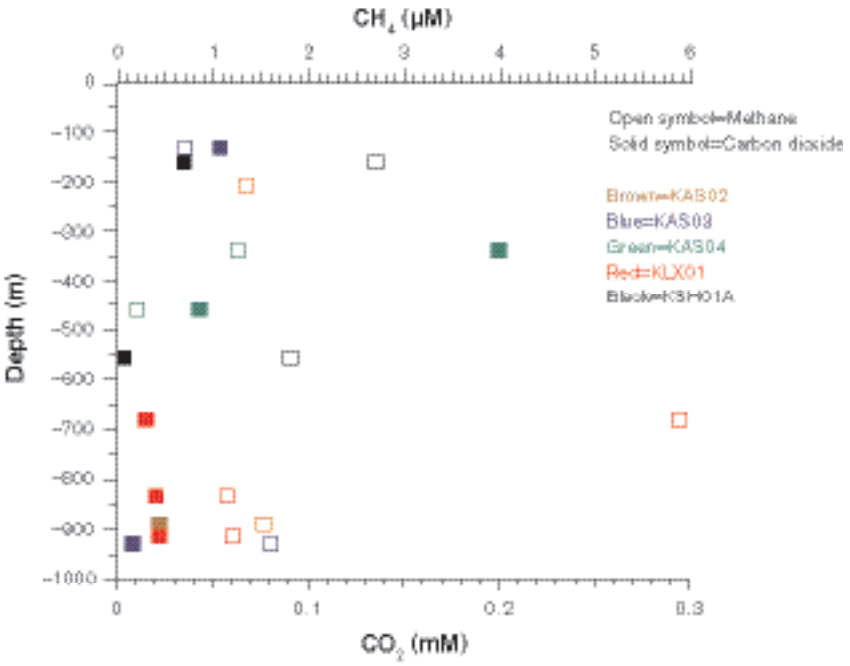

Figure 9-32. *Carbon dioxide and methane plotted versus depth in samples from boreholes in the Äspö (KAS02, KAS03 and KAS04) Laxemar (KLX01) and Simpevarp (KSH01A) sites.*

Methane is found in low concentrations, 0.5–3 µM, in all boreholes at all depths but no trend in concentration can be seen due to the very restricted amount of available data (Figure 9-32). In KSH01A, the value for the greatest depth 556.5 m sampled is lower than for 161.75 m, i.e. 1.8 µM compared to 2.7 µM, respectively.

The origin of methane in groundwater can be either biotic or abiotic. The biotic methane is produced by methanothrophic Achaea, a group of prokaryotic organisms. They can utilise either chlorine compounds or acetate. They can also fixate carbon dioxide with hydrogen gas as an energy and electron source. The origin of their substrate can be biodegraded organic matter as in sea and lake sediments or composts. Carbon dioxide and hydrogen can also originate in the mantle /Apps and Van de Kamp, 1993/.

Abiogenic methane is produced in, for example, hydrothermal systems during water-rock interactions.

9.3 Modelling assumptions and input from other disciplines

The modelling assumption is that the obtained groundwater compositions are a result of mixing and reactions including different water types. The water types are a result of palaeohydrogeology and modern hydrogeology (see Section 3.3). A schematic presentation of how a hydrogeochemical site evaluation/modelling is performed, its components, and the interaction with other geoscientific disciplines, is shown in Figure 9-33. The methodology applied in this report is described in detail by /Smellie et al. 2002/.

For the groundwater chemical calculations and simulations the following standard tools were used:

For evaluation and explorative analyses of the groundwater:

- AquaChem: Aqueous geochemical data analysis, plotting and modelling tool (Waterloo Hydrogeologic).

Mathematical simulation tools:

- PHREEQC with the database WATEQ4F: Chemical speciation and saturation index calculations, reaction path, advective-transport and inverse modelling /Parkhurst and Appelo, 1999/.
- M3: Mixing and Massbalance Modelling /Laaksoharju et al. 1999/.
- Flow and reactive transport simulations: CORE^{2D} /Samper et al. 2000/.

Visualisation/animation:

- TECPLOT: 2D/3D interpolation, visualisation and animation tool (Amtec Engineering Inc.).

Hydrogeochemical modelling involves the integration of different geoscientific disciplines such as geology, hydrogeology and transport properties. This information is used as background information, supportive information or as independent information when models are constructed or compared.

Geological information is used in hydrogeochemical modelling as direct input in mass-balance modelling but also to judge the feasibility of the results from, for example, saturation index modelling. For this particular modelling exercise geological data were summarised, the information was reviewed and the relevant rock types, fracture minerals and mineral alterations were identified.

The underlying model of interpreted deformation zones provides important information of water-conducting fractures used for the understanding and modelling of the hydrodynamics. The vertical cross section used for visualisation of groundwater properties is generally selected with respect to the geological model and the hydrogeological simulations. The available hydrogeological information and the results from hydrogeological modelling is directly used in the coupled flow and transport modelling. The measured values of Cl, ^{18}O, ^{2}H, ^{14}C and the results from the M3 mixing calculations were provided to the hydrogeologists to be used in their modelling.

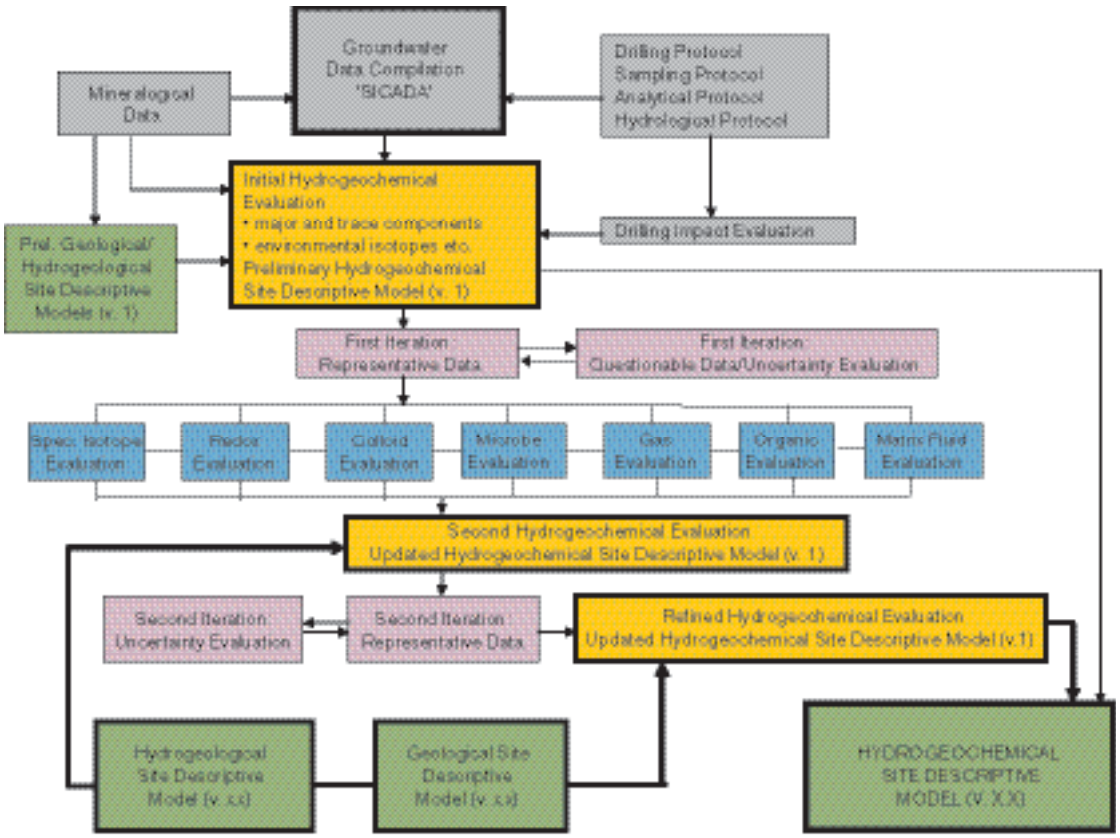

Figure 9-33. *The evaluation and modelling steps used /after Smellie et al. 2002/.*

9.4 Conceptual model with potential alternatives

The alternative conceptual models tested included different reference waters and local and regional models, and various modelling tools and approaches were applied on the data set /SKB, 2004c/. In addition the concept where the water composition is a result of reactions rather than mixing is discussed in the sections below.

9.5 Hydrogeochemical modelling, mass-balance and coupled modelling

9.5.1 Hydrogeochemical modelling

Hydrogeochemical modelling has been carried out with PHREEQC /Parkhurst and Appelo, 1999/ using the WATEQ4F thermodynamic database. The modeling focused on speciation-solubility calculations, reaction path modelling and redox system analysis. The calculations are used to investigate the processes that control water composition in the Simpevarp area. This section is divided into two main sections, the first one concerning the state of non-redox elements and phases, and the second focussed on the redox state of the system.

Carbonate system

Superficial fresh waters show a wide range of pH values as a consequence of their multiple origins (Figure 9-34). The lowest values are associated with waters with a marked influence of atmospheric and biogenic CO_2; the highest values (up to 8.5 pH units) are associated with the most diluted groundwater. Overall this gives a decreasing pH trend with chloride when the rest of the groundwater samples are taken into consideration. Nevertheless, this trend is affected by uncertainties in pH measurements in the laboratory and there are not enough data from in situ logging of pH to make a more careful evaluation.

Alkalinity (HCO_3^-) is, together with chloride and sulphate, the third major anion in the system, and is the most abundant in the non-saline waters. Its concentration increases in the shallower groundwaters (Figure 9-35a) as a result of atmospheric and biogenic CO_2 influence and/or calcite dissolution. The alkalinity content reaches equilibrium (or super saturation) with calcite in the fresh groundwaters (Figure 9-35a and Figure 9-35b) and then decreases dramatically with depth as it is consumed by calcite precipitation, whereas calcium keeps increasing as a result of mixing (Figure 9-35b).

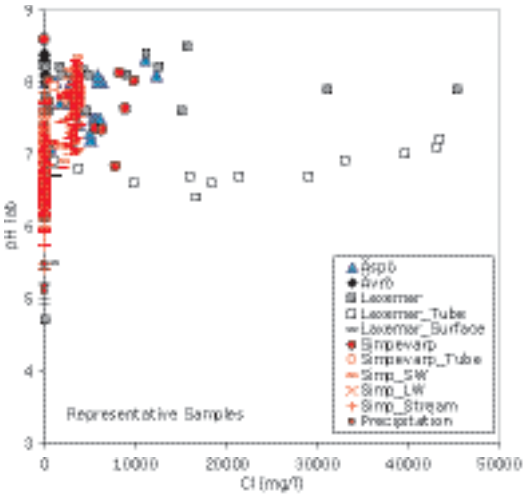

Figure 9-34. *pH vs. chloride content in mg/L (increasing with depth) in waters from the Simpevarp area.*

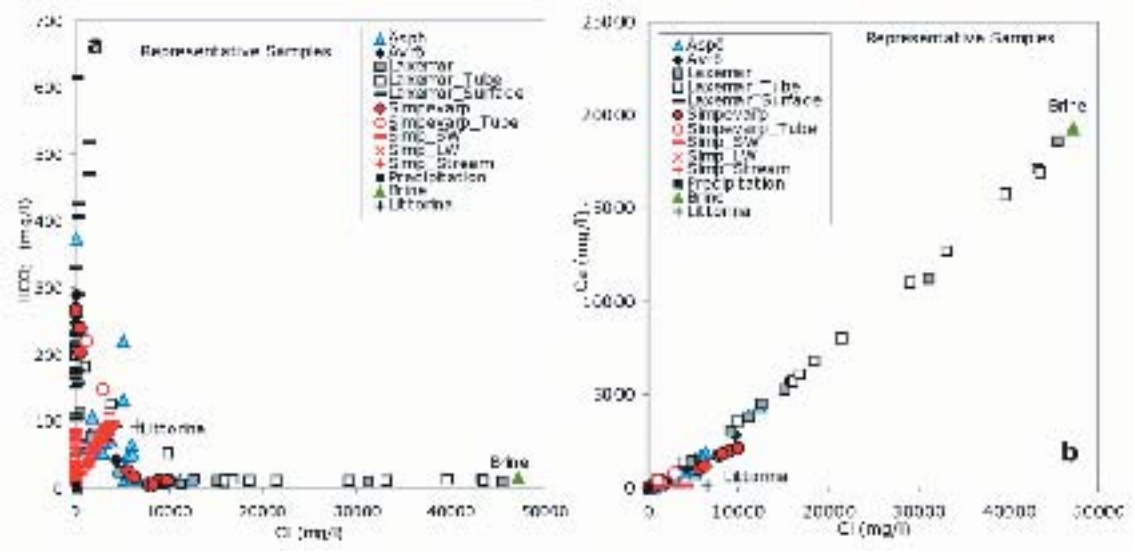

Figure 9-35. *Alkalinity (a) and calcium (b) vs. Cl in waters from the Simpevarp area.*

As can be seen in Figure 9-35b, calcium shows a good positive correlation with increasing chloride concentration in saline groundwaters, suggesting that mixing is the main process controlling this element. In spite of the extent of reequilibrium with calcite affecting Ca, the high Ca content of the mixed waters (originating from the brine end member) obliterates the effects of mass transfer with respect to this mineral. This fact justifies the quasi-conservative behaviour of calcium, at least in waters with chloride contents higher than 10,000 mg/L. Simple theoretical simulations of mixing between a brine end member and a dilute water, with and without calcite equilibrium, have shown the negligible influence of reequilibrium on the final dissolved calcium contents.

Figure 9-36 shows the calcite saturation index in the groundwaters. The alkalinity trend described above can be readily explained in this plot. The uncertainty associated with the saturation index calculation (± 0.5) is higher than that usually considered (± 0.3). This is due to problems during the laboratory measurements of pH (CO_2 outgassing and ingassing), as was described in the report for the version Simpevarp 1.1 /Laaksoharju et al. 2004a,b/.

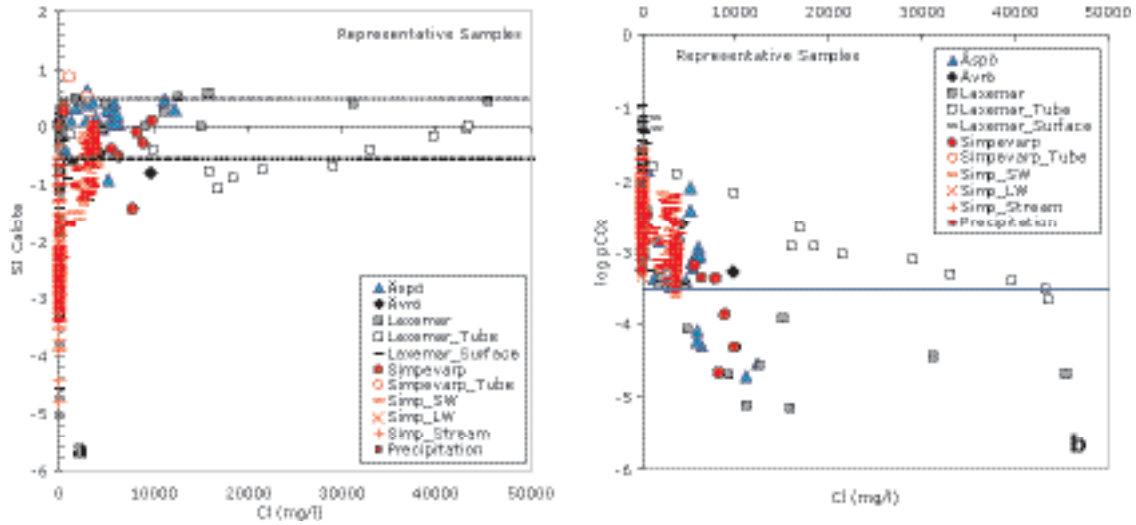

Figure 9-36. *a) Calculated calcite saturation indexes and b) partial pressure of CO_2 against chloride for waters from the Simpevarp area. The dashed lines in the figure represent the uncertainty associated with SI calculations. The blue line in figure b represents the value in the atmosphere.*

Silica system

The content of dissolved SiO_2 in surface waters indicates a typical trend of weathering, while in groundwaters it has a narrow range of variation indicative of partial reequilibrium (Figure 9-37a). The general process evolves from an increase in dissolved SiO_2 by dissolution of silicates in surface waters and shallow groundwaters to a progressive decrease related to the participation of silica polymorphs and aluminosilicates which control dissolved silica, as the residence time of the waters increases. This can be seen in Figure 9-37b.

The weathering of rock-forming minerals is the main source of dissolved silica. Superficial waters have a variable degree of saturation with respect to silica phases (quartz and chalcedony), compatible with the weathering hypothesis, and a rather unclear control by secondary phases. This is a rough generalisation, useful for this general description but it should be noted that surface waters come from diverse systems (streams, lakes and soil zones) involving contrasting processes (evaporation, biological uptake, etc. /Laaksoharju et al. 2004b/) that affect silica concentrations.

Saline groundwaters are oversaturated with quartz and close to equilibrium with chalcedony (Figure 9-37b). Saturation indices are relatively constant and independent of the chloride content; this suggests that the groundwater has already reached, at least, an apparent equilibrium state associated with the formation of aluminosilicates or secondary siliceous phases like chalcedony, which seems to be controlling dissolved silica.

The lack of quality assured aluminium data for the Simpevarp area groundwaters precludes a speciation-solubility analysis of aluminosilicates. Therefore, activity diagrams were used to study the relationship between silicate minerals and their stability. This analysis will be discussed later in this chapter.

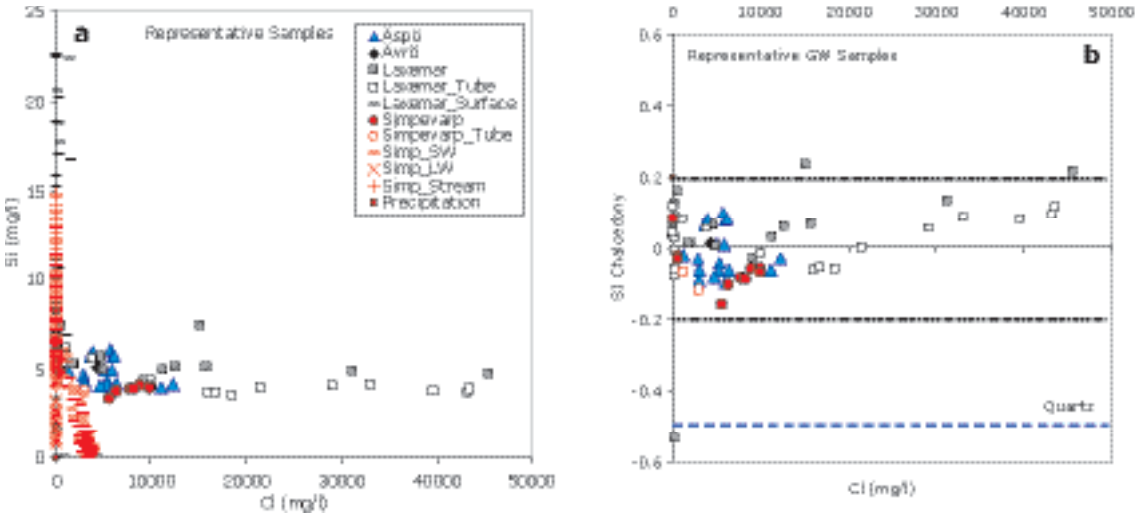

Figure 9-37. *(a) Plot of SiO_2 vs. Cl for all Simpevarp area waters. (b) Saturation indexes of chalcedony and quartz as a function of Cl in the waters. The dashed lines represent the uncertainty associated with SI calculations /Deutsch et al. 1982/.*

Sulphate system

Figure 9-38a, showing SO_4 vs. Cl, indicates an obvious modern Baltic Sea water dilution trend affecting some of the groundwater samples. In general, these groundwater data lend support to the absence of a significant postglacial marine component, suggesting instead the mixing with deeper, more saline waters of a non-marine origin. Perhaps the most interesting aspect is the different evolution shown by sulphate in all Simpevarp area waters (which increases with salinity) compared with the sulphate behaviour at other sites. Figure 9-38b shows the sulphate contents in Olkiluoto and Forsmark[1] sites. In both cases, after an initial increase in sulphate (reaching the maximum values when salinity is around 5,000–6,000 mg/L of Cl) there is a clear decrease towards zero. For the same chloride content, sulphate concentrations of the Simpevarp area waters are clearly higher.

This contrasting behaviour must be related to the process controlling the sulphate content in these waters. Analysing the saturation state of waters with respect to gypsum (Figure 9-39b) some conclusions can be drawn. For the whole set of Simpevarp area groundwaters, the gypsum SI trend indicates a clear evolution towards equilibrium (Figure 9-39a) which is reached at chloride values of 10,000 mg/L and maintained even in the most saline waters. This equilibrium, defined mainly in the most saline and deepest groundwaters from the Laxemar subarea, introduces a new controlling phase in the groundwater system. Moreover, it can help to solve the uncertainties reported in previous works /Laaksoharju and Wallin, 1997/ on the unusual sulphate behaviour in the Laxemar site waters. In fact, /Laaksoharju et al. 1995/ reported the presence of gypsum as a fracture filling mineral in the Laxemar subarea, though in small amounts. In addition, the influence of gypsum as the sulphate limiting phase has been already reported in the Canadian Shield /Gascoyne, 2004/.

The behaviour of other sulphate minerals, like celestite ($SrSO_4$), was also checked. The SI trend is similar to the one shown by gypsum and, therefore, celestite should be considered as another possible new controlling phase in this groundwater system. Celestite has not yet been identified in the Simpevarp area bedrock. Some consequences of these new equilibrium situations with respect to other phases (Strontianite) and to the Ca/Sr ratio are discussed in /SKB, 2004c/.

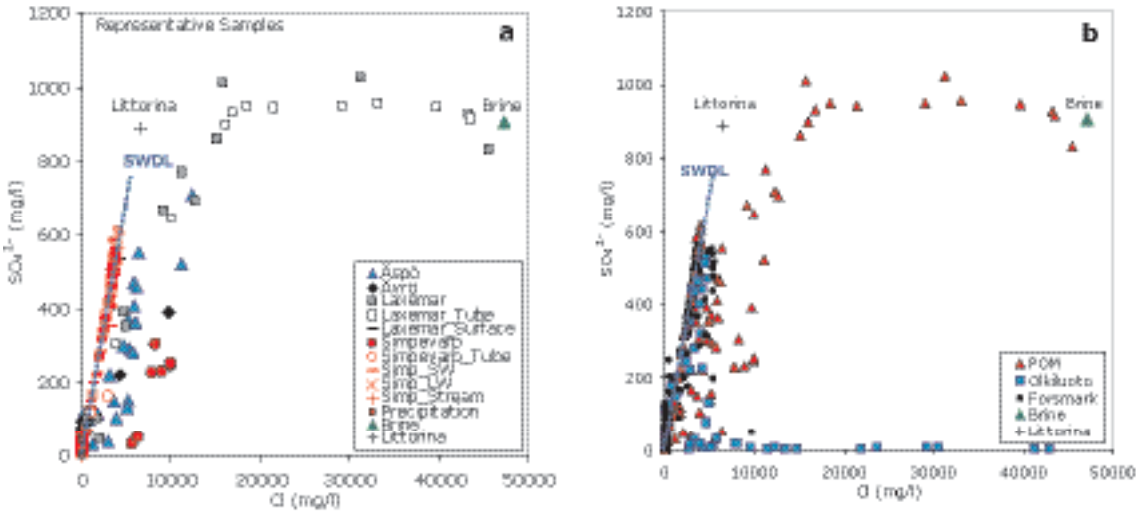

Figure 9-38. *(a) Plot of SO_4 vs. Cl for all data. (b) Plot comparing Simpevarp area data with Forsmark and Olkiluoto samples.*

[1] Forsmark data shows a lower salinity than Olkiluoto data, but the trend shown by the more saline waters in Forsmark follows the same evolution as in Olkiluoto.

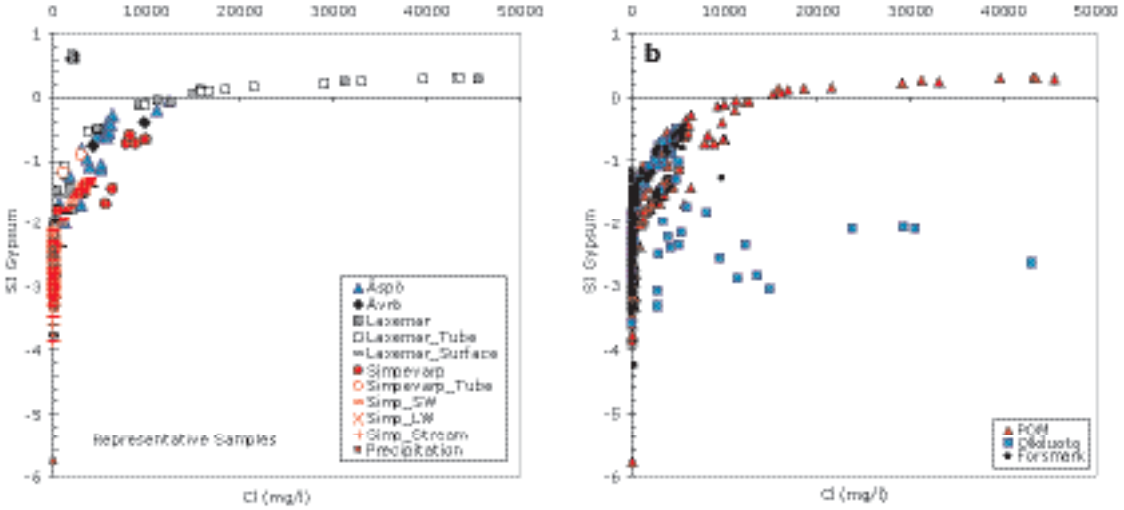

Figure 9-39. *(a) Plot of Gypsum saturation index vs. Cl for the Simpevarp area data. (b) Scatter plot comparing Simpevarp area data with Forsmark and Olkiluoto data.*

Aluminosilicate system

The mineralogical results from KSH01A and KSH01B have demonstrated the presence of a complex sequence of fracture fillings. Apart from chlorite and calcite, epidote, prenhite, laumontite, Ba-zeolite, adularia, albite, haematites and pyrite have also been reported. Small amounts of outermost coatings with smectite, interstratified clay minerals and illite, with high surface area, have also been identified. This set of minerals is common to the other sites (e.g. Äspö).

Besides the granite rock-forming minerals, some of these fracture-filling phases are aluminosilicate minerals with which groundwaters have been in contact during their geochemical evolution. Therefore they are important water-rock interaction phases. However, as already pointed out, the lack of aluminium data for the Simpevarp area groundwaters precludes a speciation-solubility analysis, limiting their analysis to stability diagrams.

The accuracy of these diagrams depends on pH and is therefore affected by uncertainties in its value. Uncertainties in the equilibrium constants of the aluminosilicates (especially the phyllosilicates) also affect the conclusions drawn from these diagrams and the results of any theoretical model performed with them /e.g. Laaksoharju and Wallin, 1997; Trotignon et al. 1997, 1999/. In this context the study of aluminosilicate phases has been limited to those with lower uncertainties and using thermodynamic data that have already given reasonable results in systems similar to the one studied here. That means that the aluminosilicate system studied here is limited to adularia, albite, kaolinite, and the selected thermodynamic data are the ones calculated at 15°C by /Grimaud et al. 1990/ for the Stripa groundwaters.

Stability diagrams

The following description includes a general evaluation of the groundwaters sampled in the Simpevarp area based on their position in the stability diagrams and a discussion on the effects of mixing and reaction in the more saline, older groundwaters[2]. This discussion is illustrated with a theoretical equilibrium modelling. The question of the origin of the saline groundwaters (brine end member) is not discussed here, and the model simply assumes that they are already in the system, participating in mixing processes. Nevertheless, the last part of this section deals with the potential use of this modelling approach to predict the chemical characteristics of these very old saline groundwaters.

[2] In this section different diagrams and computer simulations for Simpevarp area groundwaters are presented, in some of the cases together with other sites (Olkiluoto and Stripa).

Figure 9-40 shows the stability diagram kaolinite-albite-adularia for the Simpevarp area waters. Green and blue arrows show the main trends that can be distinguished. The first trend (green arrows) crosses the kaolinite stability field and goes towards the limit with adularia. This trend is defined by surface and shallow groundwaters. They are modern waters with low chloride contents and whose geochemical evolution is the result of water-rock interaction.

The evolution path of these waters in the kaolinite field shows a slope around 2, typical of weathering-alteration processes in granitic materials. This trend represents the effects of a progressive dissolution of the rock-forming minerals (calcite, chlorite, plagioclase, K-feldspars, etc.). Along this process, partial reequilibria with phyllosilicates (e.g. kaolinite) can be reached. Ionic exchange and, finally, calcite precipitation can also take place.

Waters close to or on the kaolinite-adularia boundary would correspond to the more evolved samples in this water-rock interaction process. A special case are certain groundwaters sampled in the Laxemar subarea, which are highly diluted (30–150 mg/L Cl) but at great depths (up to 700 m in KLX02 borehole). The position of these samples in the diagram would support a meteoric origin without a mixing component with more saline waters, but with a residence (reaction) time longer than the shallower groundwaters.

Laxemar subarea groundwaters taken by tube sampling are placed in the kaolinite field but this is uncertain due to the possible “artificial mixing” during sampling, and, probably, also to the pH measurements.

The second trend (blue arrow) evolves parallel to the adularia-albite limit indicating an equilibrium situation. Brackish and saline groundwaters from the Simpevarp area follow this second trend. This result is very similar to Stripa waters but there is an important difference: maximum chloride contents in Stripa only reach 700 mg/L, whereas Simpevarp area groundwaters, plotted in the same position, reach chloride values up to 45,000 mg/L. Stripa groundwaters’ residence time has been estimated as being approximately 100,000 years /Fontes et al. 1989/. That means that even in that time, water-rock interaction provides only 700 mg/L of chloride. It is clear, therefore, that an additional source of salinity is needed in the Simpevarp area groundwaters to justify much higher chloride values in much younger waters. This source is the mixing with a saline component (marine and/or non marine).

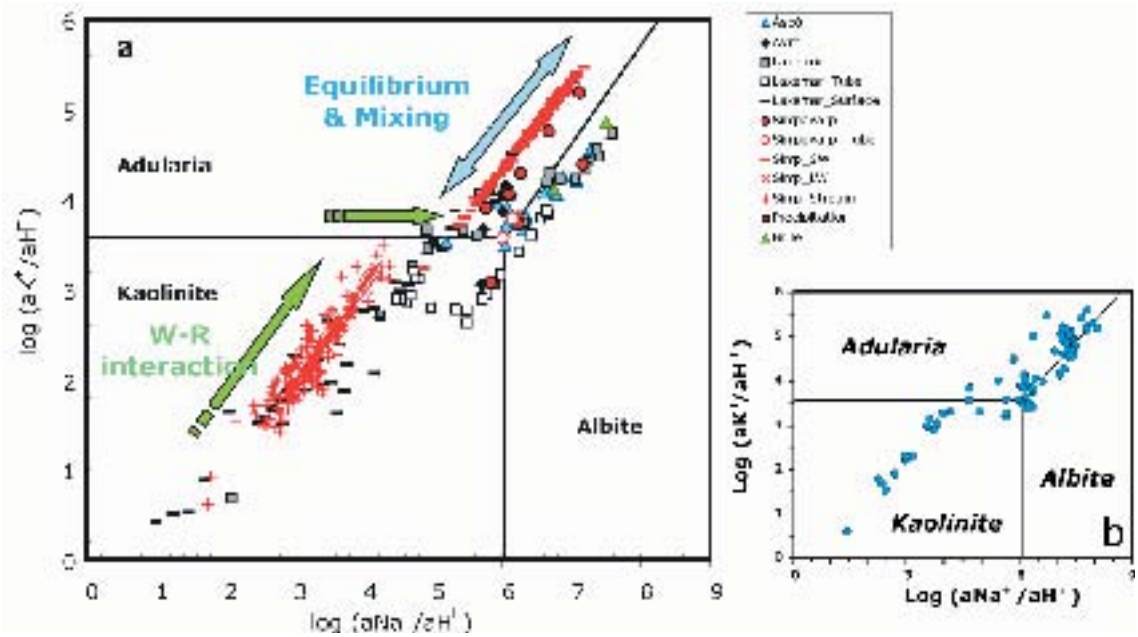

Figure 9-40. *Stability diagrams for kaolinite, adularia and albite in the Simpevarp area groundwaters (a) and in the Stripa groundwaters (b).*

Another interesting finding is that in the trend parallel to the adularia-albite limit the range of salinity in the Simpevarp area groundwaters is very broad, including not only the most saline waters (close to brine end member composition), but also waters with around 5,000 mg/L Cl. This again points to the important effects of mixing in these waters.

In Figure 9-41 the Simpevarp area samples have been plotted together with those of Olkiluoto /Pitkänen et al. 2004/. Olkiluoto waters occupy the same location as the Simpevarp area waters. Olkiluoto samples in the kaolinite stability field and in the kaolinite-adularia boundary correspond to subsurface or shallow groundwaters whose chemistry is controlled by water-rock interaction. Samples located on the adularia-albite boundary correspond to brackish and saline groundwaters characterised by having undergone complex mixing processes (between Meteoric, Littorina, Glacial and Saline end members, /Pitkänen et al. 2004/).

The position of the theoretical end members is also shown in Figure 9-41 (Brine, Littorina and Glacial; Meteoric is close to Glacial). It is fairly clear that the evolutionary path of these waters is the result of (a) reaction between diluted waters (surface and shallow groundwaters) and rock, (b) mixing in depth with more saline groundwaters in different proportions as a function of location and residence time, and (c) the simultaneous interaction of these deep waters with the rock.

Simulating the Brine water composition

The thermodynamic approach described in /SKB, 2004c/ to assess mixing and reaction processes provides an ideal tool for predicting the composition of groundwaters with long residence times. This is the case of the "old brine end members" found in the Scandinavian Shield. These groundwaters can be considered as having reached a "global" equilibrium with calcite, chalcedony and different aluminosilicaltes. This kind of approach was used by Michard and co-workers /e.g. Michard, 1980; Michard et al. 1986/ to predict the composition of some granitic thermal groundwaters assuming thermodynamic equilibrium between the water and a selected mineral assemblage, as a function of chemical contents not controlled by mineral equilibria (e.g. Cl). This model was also applied by /Grimaud et al. 1990/ to the low temperature granitic groundwaters at Stripa.

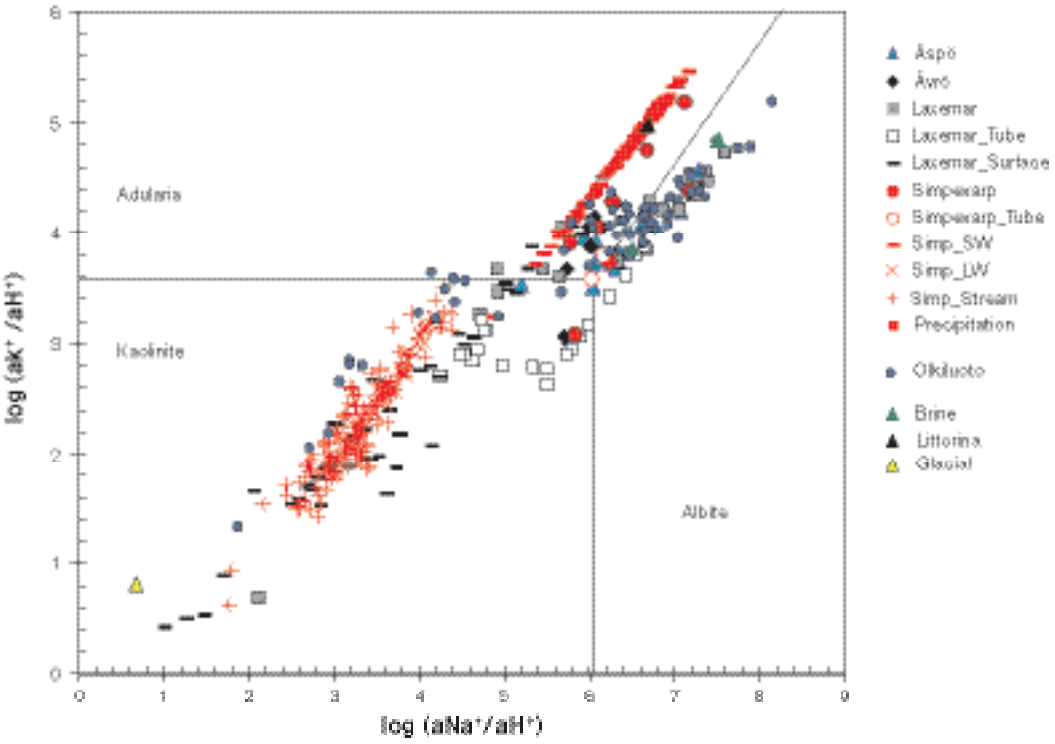

Figure 9-41. *Stability diagram for kaolinite, adularia and albite. Waters from the Simpevarp area, the Olkiluoto groundwaters /Pitkänen et al. 2004/ plotted together with the theoretical end members (Brine, Littorina and Glacial).*

More recently, /Trotignon et al. 1997, 1999/ applied the same concept to Äspö groundwaters (from KAS02 and KAS03 boreholes) and reported a high sensitivity of the predictions to the mineral equilibrium constants, mainly from laumontite. They found a reasonable fit between the predicted values and the measured concentrations for the assemblage calcedony + kaolinite + albite + adularia + laumontite with the selected equilibrium constants.

Here, the approach of /Trotingon et al. 1997, 1999/ was extrapolated to calculate "brine compositions" using the same assemblage (calcedony, kaolinite, albite, adularia and laumontite) plus calcite and gypsum (saline waters in Simpevarp area are in equilibrium with these minerals as explained above), and the thermodynamic data from /Grimaud et al. 1990/ except for kaolinite and laumontite. The equilibrium constants for these minerals were taken from the best fit of /Trotignon et al. 1997, 1999/.

The procedure consists of the following steps: pure water (Glacial end member) was equilibrated with the selected mineral assemblage imposing, simultaneously, different chloride concentrations up to "brine" values. PHREEQC was then used to simulate this process. The results obtained for the Brine end member and for the more saline water in Olkiluoto /Pitkänen et al. 2004/ are shown in Table 9-1.

Comparing the predicted values with the measured ones, it is clear that in most cases the fit is quite good (pH, Na, Ca, SiO_2). But, more interestingly, the predictions are able to reproduce and quantify the main groundwater features: pH values close to 8 and very low alkalinity. Considering the thermodynamic uncertainties associated to these calculations, one can say that in general the results are fairly good.

A plot of the concentration data in Table 9-1 as a function of chloride concentration (Figure 9-42) shows some other interesting facts. It makes clear that the concentration of elements controlled by equilibrium with the mineral assemblage depends on chloride content. This conclusion is not new /Michard, 1987/ but it has important implications in the context of the mixing and reaction processes that affect this kind of system. For the oldest mixing event, it clearly shows that chloride is a useful conservative element to compute mixing proportions. Therefore, it could be concluded that in the Simpevarp area mixing is the main irreversible process. It controls the chloride concentration which, in turn, determines the re-equilibrium path (water-rock interaction) triggered by mixing.

Table 9-1. Predicted and observed concentrations for the brines in the Simpevarp area (Brine end member) and in Olkiluoto.

Increasing chloride concentration

	Initial water	Equilibrium with the selected mineral assemblage	Prediction		Equilibrium with the selected mineral assemblage	Prediction
	Glacial		Olkiluoto Brine	Olkiluoto Br (Theor)	Brine end member	Brine (Theor)
mCl	1.41E-05		0.8754	0.8833	1.442	1.443
pH	5.8		8.3	7.95	7-8	7.8
mNa	7.39E-06		0.366	0.375	0.400	0.490
mK	1.02E-05		0.0005	0.00145	0.00126	0.00213
mCa	4.49E-06		0.258	0.261	0.521	0.490
mH_4SiO_4	1.42E-04		9.79E-05	9.30E-05	6.67E-05	7.40E-05
mAlkalinity	1.97E-06		1.32E-04	5.39E-05	2.50E-04	4.56E-05
mSO_4	5.20E-06		5.38E-05	7.27E-03*	5.14E-03	5.36E-03

* The equilibrium with gypsum assumption is not valid in these waters as they are clearly undersaturated.

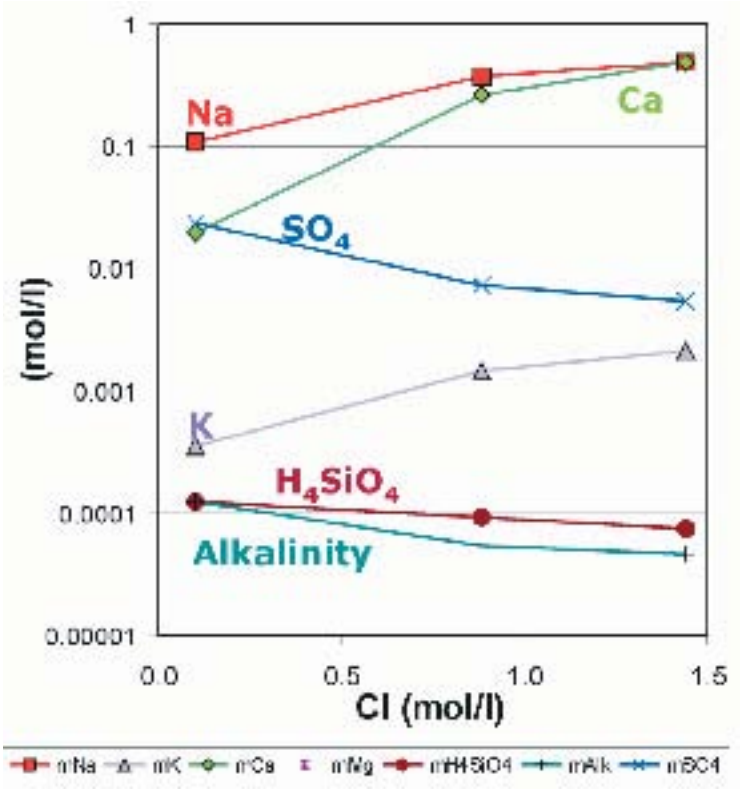

Figure 9-42. *Evolution of chemical contents as a function of chloride, maintaining the equilibrium with the selected mineral assemblage.*

Redox modelling

For Simpevarp 1.2, the amount of suitable data for a redox study is greater than for Simpevarp 1.1 and, therefore, this study is more complete. The two possibilities suggested in previous studies about the redox state of the groundwaters have been reassessed, namely: (a) the iron system controls the redox state /Grenthe et al. 1992/; and (b) the sulphur system controls the redox state /e.g. Nordstrom and Puigdomenech, 1986/. Some of the samples supplied with data freeze Simpevarp1.2 have been used previously to support both interpretations /Grenthe et al. 1992; Glynn and Voss, 1999/.

For this modelling exercise samples with adequate redox data were selected. This includes Eh and pH data from continuous logging (from this data freeze and from previous reports, /Smellie and Laaksoharju, 1992; Laaksoharju et al. 1995/, analytical data[3] for Fe^{2+}, S^{2-} and CH_4, and microbiological information. The selected samples cover four of the site locations in the Simpevarp area (Äspö, Ävrö, Laxemar and Simpevarp) and a wide range of depths (130 to 930 m).

Redox pair calculations

More than one redox couple is active in the groundwaters of the Simpevarp subarea and the results from redox pair calculations are summarised in Figure 9-43 and Figure 9-44. The Eh calculated with the $Fe(OH)_3/Fe^{2+}$ redox pair and Grenthe's calibration agrees reasonably well with most of the Eh values measured in the Ävrö and Äspö sites. This good fit was expected as these samples were used by Grenthe and co-workers to perform the calibration. The Eh calculated with the same redox pair but for microcrystalline $Fe(OH)_3$ is much more oxidising. On the contrary, the microcrystalline phase gives the best results in the case of the Simpevarp and some Laxemar subarea samples, whereas Grenthe's calibration gives much more reducing Eh values (Figure 9-43). This observation was already made in the previous Simpevarp 1.1 modelling /Laaksoharju et al. 2004b/; and for Forsmark 1.1 /Laarksoharju et al. 2004a/. This fact suggests that the groundwater redox state can be controlled by iron oxides and oxyhydroxides with different degrees of crystallinity.

[3] The range of analytical concentrations (mol/L) are: $Fe^{2+} = 8.9\times10^{-8} – 3.6\times10^{-4}$; $S^{2-} = 3.12\times10^{-7} – 2.3\times10^{-4}$; $SO4^{2-} = 9\times10^{-6} – 1.3\times10^{-2}$; $CH_4 = 2.5\times10^{-7} – 3.8\times10^{-6}$.

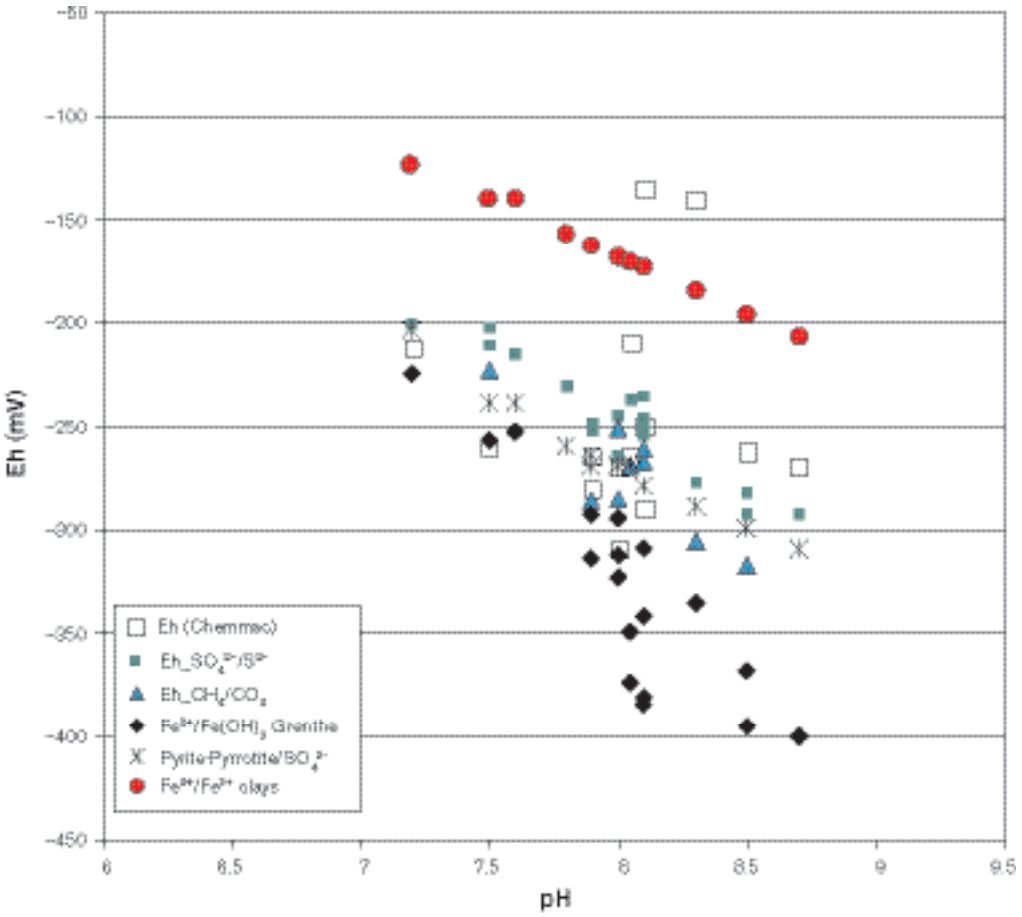

Figure 9-43. *Comparison of redox results for different redox pairs.*

Except for a few samples, the different "sulphur system" redox pairs provide Eh values coincident with the potentiometrically measured Eh. The SO_4^{2-}/S^{2-} homogeneous redox pair gives Eh values similar to the ones obtained from the heterogeneous pairs (Pyrite/SO_4^{2-} and FeS/SO_4^{2-}; Figure 9-44) as calculated with the WATEQ4F thermodynamic data. A sensitivity analysis carried out comparing these data to those of /Bruno et al.1999/ shows only minor differences.

As expected, Eh values obtained with the CH_4/CO_2 pair are close to the ones obtained with SO_4^{2-}/S^{2-} (and also to the remaining sulphur redox pairs). Therefore, they also agree well with the potentiometrically measured Eh.

For the Äspö and Ävrö samples there is good agreement between the potentiometrically measured Eh and the value calculated from the following redox pairs: heterogeneous and homogeneous sulphur pairs, CH_4/CO_2 and Grenthe's calibration for $Fe(OH)_3/Fe^{2+}$. In the Simpevarp area, the redox pair results also agree very well with the measured Eh values; however, the iron system seems to be controlled by a microcrystalline hydroxide instead of by an intermediate phase (Grenthe's calibration). Finally, in Laxemar the sulphur redox pairs show good agreement with potentiometric Eh. In common with the iron hydroxide pair, the best agreement with the measured value is not always obtained with the same pair, for example, in some cases Grenthe's calibration is the one which better agrees with the measured Eh and in other cases is the microcrystalline phase which agrees better. Some samples have a potentiometric Eh considerably lower than any other calculated using the redox pairs.

The results given by the sulphur system are more homogeneous and in better agreement with each other than those obtained from the $Fe(OH)_3/Fe^{2+}$ redox pair. This suggests that the sulphur system is the main controller of the groundwater redox state, as reported previously /Nordstrom and Puigdomenech, 1986; Glynn and Voss, 1999; Laaksoharju et al. 2004 a,b/. The CH_4/CO_2 redox pair gives results in good agreement with the sulphur pairs. This conclusion is supported by the

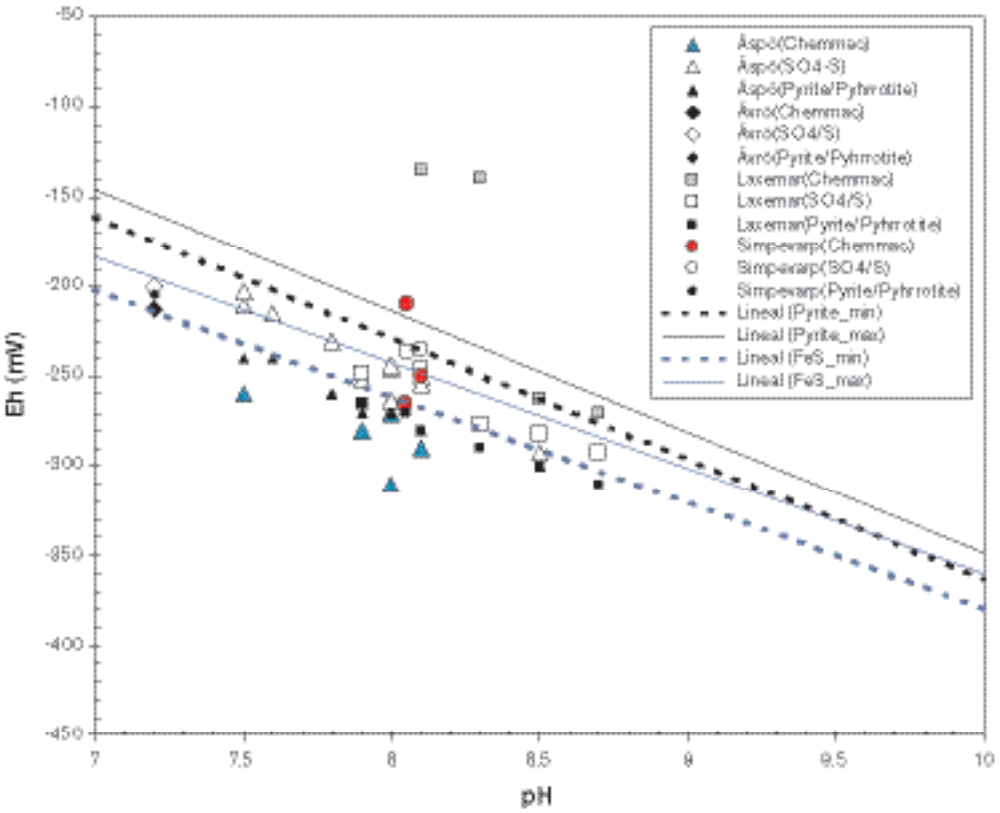

Figure 9-44. *Eh-pH diagram showing the calculated Eh values for the Simpevarp area samples. The Eh values obtained from potentiometric measurements are included in the figure. The Eh values from the SO_4^{2-}/S^{2-} redox pair are represented with open symbols and the values obtained with the pyrite-pyhrrotite/SO_4^{2-} pair, with a filled black symbol. "Pyrite_min" and "Pyrite_max" lines represent the equilibrium situation for the range of SO_4^{2-} and Fe^{2+} concentration found in the Simpevarp area groundwaters. The same is valid for the FeS/SO_4^{2-} equilibrium.*

microbial measurements in KSH01A. In summary, all these redox pairs should be used when characterising the redox state of the groundwaters. However, the variable results obtained with the $Fe(OH)_3/Fe^{2+}$ pair do not mean that the iron system does not participate in the redox control of these waters.

Conceptual model for the redox system

The redox state of groundwaters in the Simpevarp area appears to be well described by sulphur redox pairs in agreement with some previous studies in this area /Glynn and Voss, 1999; Laaksoharju et al. 2004a,b/ and in other sites from the Fennoscandian Shield /Nordstrom and Puigdomenech, 1986; Laaksoharju et al. 2004b; Pitkänen et al. 2004/. Besides, from the analysis performed here it can be concluded that CH_4/CO_2 is another important redox pair in determining the redox state.

The presence of sulphate reducing bacteria and methanogens is widely distributed at the Äspö site and in the Simpevarp subarea can be related to the above discussion and supports the probability that the sulphur and methane redox pairs could be the prevailing ones in controlling a microbiologically mediated redox state. High quality measurements of S^{2-} and CH_4 are needed to pursue this approach.

However, in agreement with /Grenthe et al. 1992/, the work presented here also supports the fact that the iron system contributes to the control of the redox state through different oxide-oxyhydroxides. The issue is to clearly identify the real contribution of the iron system due to the variable crystallinity of the phases involved and their evolution by, probably fast, recrystallisation. This fact indicates that more than one iron phase could be controlling the Eh in different groundwaters, although theoretically, with enough time, they could all eventually tend to an equilibrium with goethite and therefore to lower Eh values than the measured ones.

The interaction between the iron and sulphur systems is evident through sulphate reducing bacteria and sulphide mineral precipitation. Several lines of reasoning indicate that this process is effective at different levels in the investigated Simpevarp area. For instance, recent pyrite coatings have been identified in the fracture fillings of Simpevarp, which is an additional support to the good results of sulphur redox pairs. However, the influence of iron oxyhydroxide crystallinity on sulphide precipitation has also been rated in the Simpevarp subarea as an important factor.

Therefore, although the sulphur system can be considered the best suited to characterise the redox state of the groundwaters, a better understanding of the iron system is needed to assess its particular contribution to the redox state or to the reductive capacity of these groundwater systems.

9.5.2 Mixing modelling using M3

Introduction

An additional modelling approach which is useful in helping judge the origin, mixing and major reactions influencing groundwater samples is the M3 modelling concept (Multivariate Mixing and Mass-balance calculations) detailed in /Laaksoharju et al. 1995b/ and /Laaksoharju et al. 1999b/ and applied on the Simpevarp 1.1 data /Laaksoharju et al. 2004b/.

Model results

The M3 method consists of 4 steps where the first step is a standard principal component analysis (PCA), selection of reference waters, followed by calculations of mixing proportions, and finally mass balance calculations.

The reference waters used in the M3 modelling have been identified from: a) previous site investigations (e.g. at Äspö and Laxemar), b) evaluation of the Simpevarp primary data set, and c) selecting possible compositions of endmembers which according to the post glacial conceptual model (see Section 3.3) may have affected the site. The selected reference waters are more extreme than actually present at Simpevarp (e.g. Rain-60 or Littorina Sea). Their function is a) to be able to compare differences/similarities of the Simpevarp groundwaters with possible endmembers, b) to be able to describe all available data used in the local and regional models, and c) to facilitate comparison with the results from the hydrogeological modelling. The analytical composition of the selected reference waters are listed in /SKB, 2004c/. The reference waters should not be regarded as point sources of flow but rather as possible contributors to the obtained water type. The reference waters have the following features:

- **Brine water:** Represents the sampled deep brine type (Cl = 47,000 mg/L) of water found in KLX02: 1,631–1,681 m /Laaksoharju et al. 1995a/. An old age for the Brine is suggested by the measured ^{36}Cl values indicating a minimum residence time of 1.5 Ma for the chloride component /Laaksoharju and Wallin, 1997/. The sample contains some tritium (TU 4.2) which is believed to be contamination from borehole activities. In the modelling 0 TU was used for this sample.
- **Glacial water:** Represents a possible melt-water composition from the last glaciation > 13,000 BP. Modern sampled glacial melt water from Norway was used for the major elements and the $\delta^{18}O$ isotope value (−21‰ SMOW) was based on measured values of $\delta^{18}O$ in calcite surface deposits /Tullborg and Larsson, 1984/. The $\delta^{2}H$ value (−158‰ SMOW) is a calculated value based on the equation ($\delta H = 8 \times \delta^{18}O + 10$) for the global meteoric water line.
- **Littorina Sea:** Represents old marine water and its calculated composition has been based on /Pitkänen et al. 1999/. This water is used for modelling purposes to represent past Baltic Sea water composition.
- **Modified Sea water (Sea sediment):** Represents sea water affected by microbial sulphate reduction.
- **Precipitation:** Corresponds to infiltration of meteoric water (the origin can be rain or snow) from 1960. Sampled modern meteoric water with a modelled high tritium (2,000 TU) content was used to represent precipitation from that period.

The results of the PCA modelling are shown at regional scale (Data from the Simpevarp area are compared with Forsmark data and other Nordic sites data) in Figure 9-45.

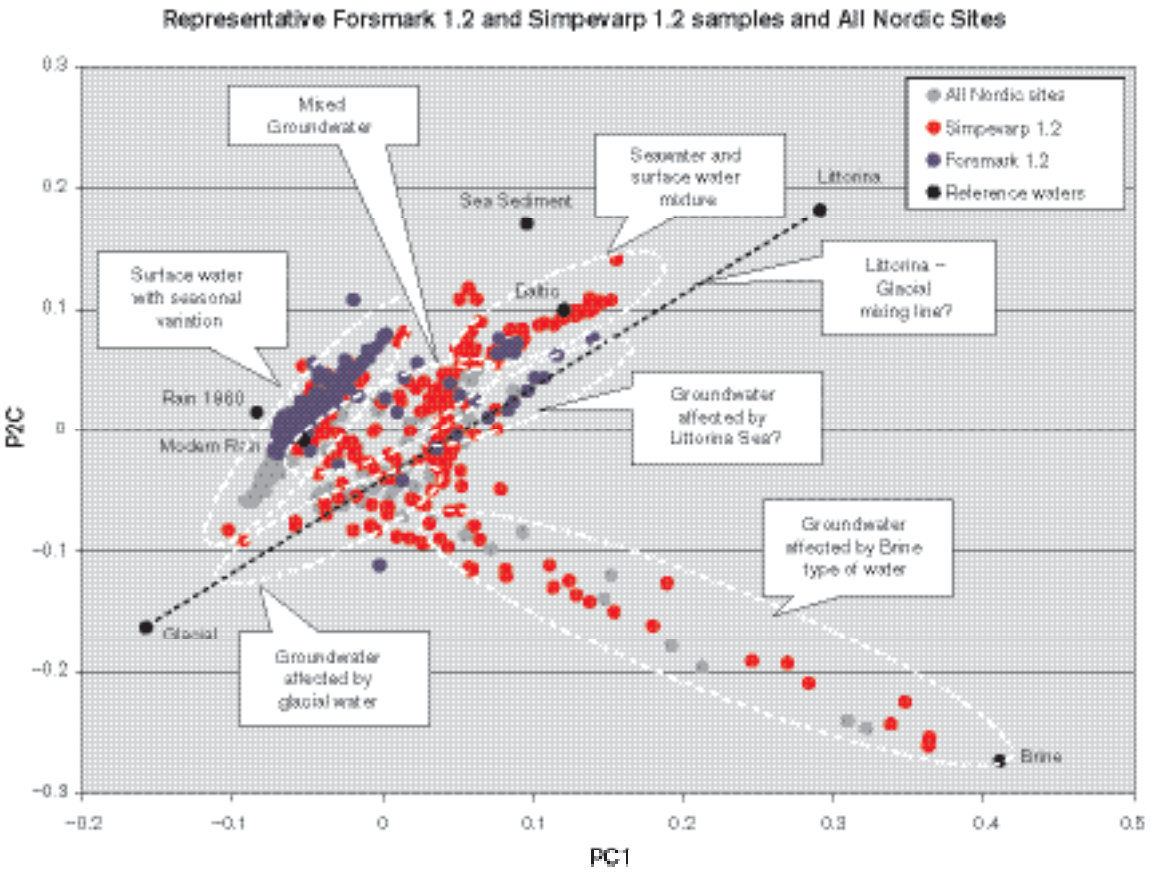

Figure 9-45. *PCA modelling of the representative Simpevarp area-, Forsmark- and Nordic-data. The reference waters used in the modelling are indicated and the possible influences from different end members on the samples are indicated.*

The M3 modelling shown in Figure 9-45 indicates that the Simpevarp area samples are affected by all the reference waters: Meteoric, Marine, Glacial and Brine. Forsmark 1.2 data are lacking a clear indication of Brine component. Only a few samples from Forsmark indicate a Glacial-Brine component. The Littorina signature is much clearer at Forsmark compared with the data from the Simpevarp area. Figure 9-45 shows that four water types occurs at the Simpevarp area, one dominated by meteoric water, the second affected by marine water, the third saline groundwater affected by glacial water, and finally a deep water affected by brine type groundwater. The surface meteoric groundwater type shows seasonal variations. Closer to the coast the influence of marine water is detected for the shallow samples. With depth the glacial, meteoric and brine type of waters have affected the saline groundwater. Only a few samples from Äspö and one from Simpevarp are showing a possible Littorina Sea water influence. The deviation calculations in the M3 mixing calculations show potential for organic decomposition/calcite dissolution in the shallow water. Indications of ion exchange and sulphate reduction have been modelled. These M3 results support the initial evaluation of primary data and the general modelling results described in previous sections.

9.5.3 Visualisation of the groundwater properties

Measured Cl content and the calculated M3 mixing proportions based on representative samples are shown for two cored boreholes within the modelling domain (Figure 9-46). The results for all the boreholes are shown in /SKB, 2004c/. The specific purpose of the plots is to show the water type, changes with depth, and to facilitate comparison of hydrochemical results with hydrogeological results. Due to the fact that the hydrogeologists use only 4 reference waters, the marine components (Littorina and Sea Sediment reference waters) were here combined and referred to as “Marine water”.

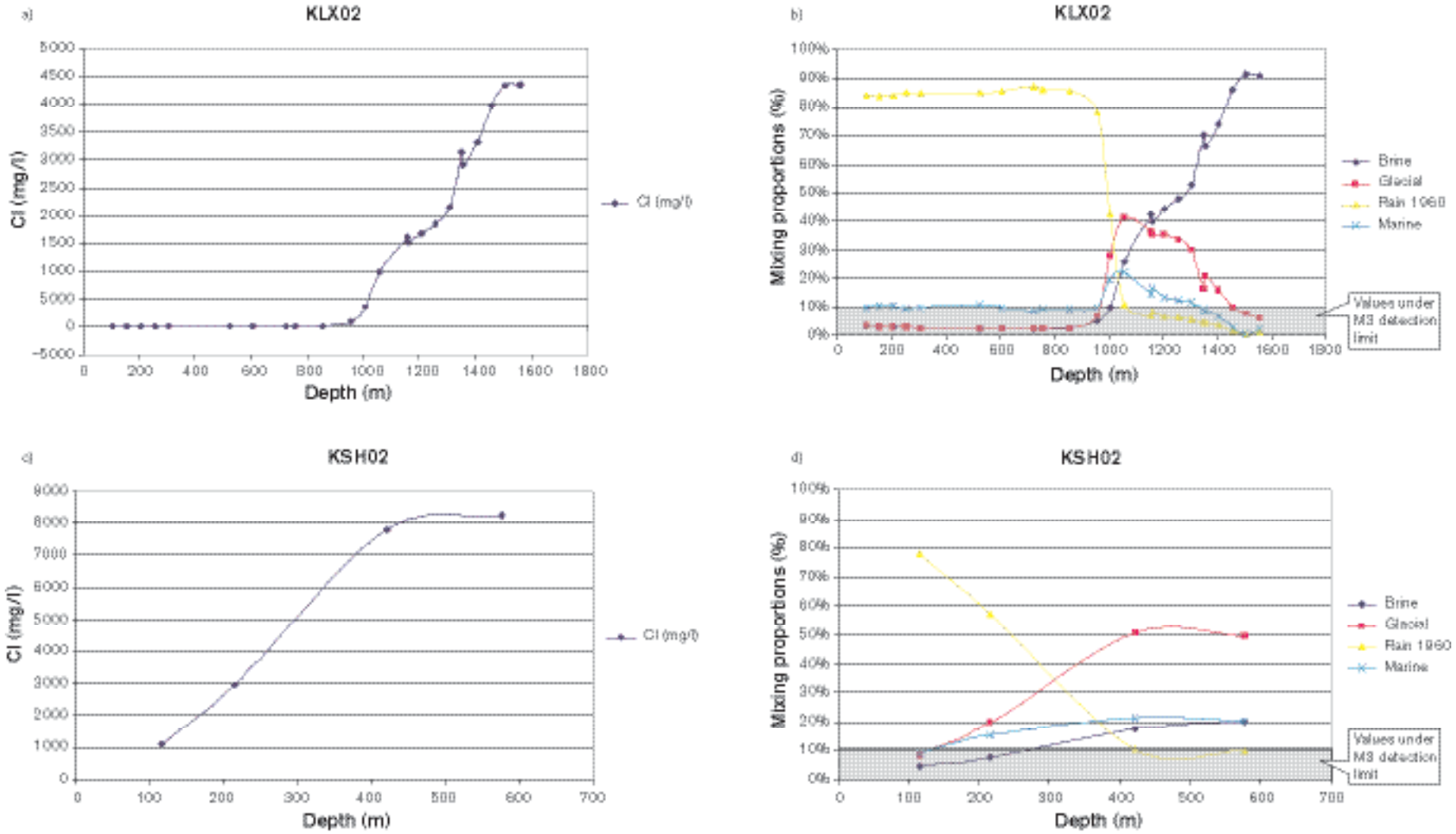

Figure 9-46. *(a) and (b) scatter plot of the Cl content and mixing proportions with depth for borehole KLX02. (c) and (d) scatter plot of the Cl content and mixing proportions with depth of borehole KSH02. A mixing proportion of less than 10% is regarded as being under the detection limit of the M3 method and is therefore shaded. The mixing proportions have an uncertainty range of ± 0.1 mixing units /Laaksoharju et al. 1999/.*

The 3D/2D visualisation of the Simpevarp Cl values was performed using the Tecplot code and employing the inverse distance algorithm. Figure 9-47 shows the 3D and the 2D visualisation of Cl in the sampling points for both representative and non-representative samples and for the M3 mixing proportions based on representative samples. The Cl figures (Figure 9-47a, b) reflect the possible uncertainties in the interpolations if the non-representative samples are included but also the effect from sampling artefacts on the site description. The relatively few observations in the 3D space results in uncertainties; only in the near-vicinity of the observations are the uncertainties low.

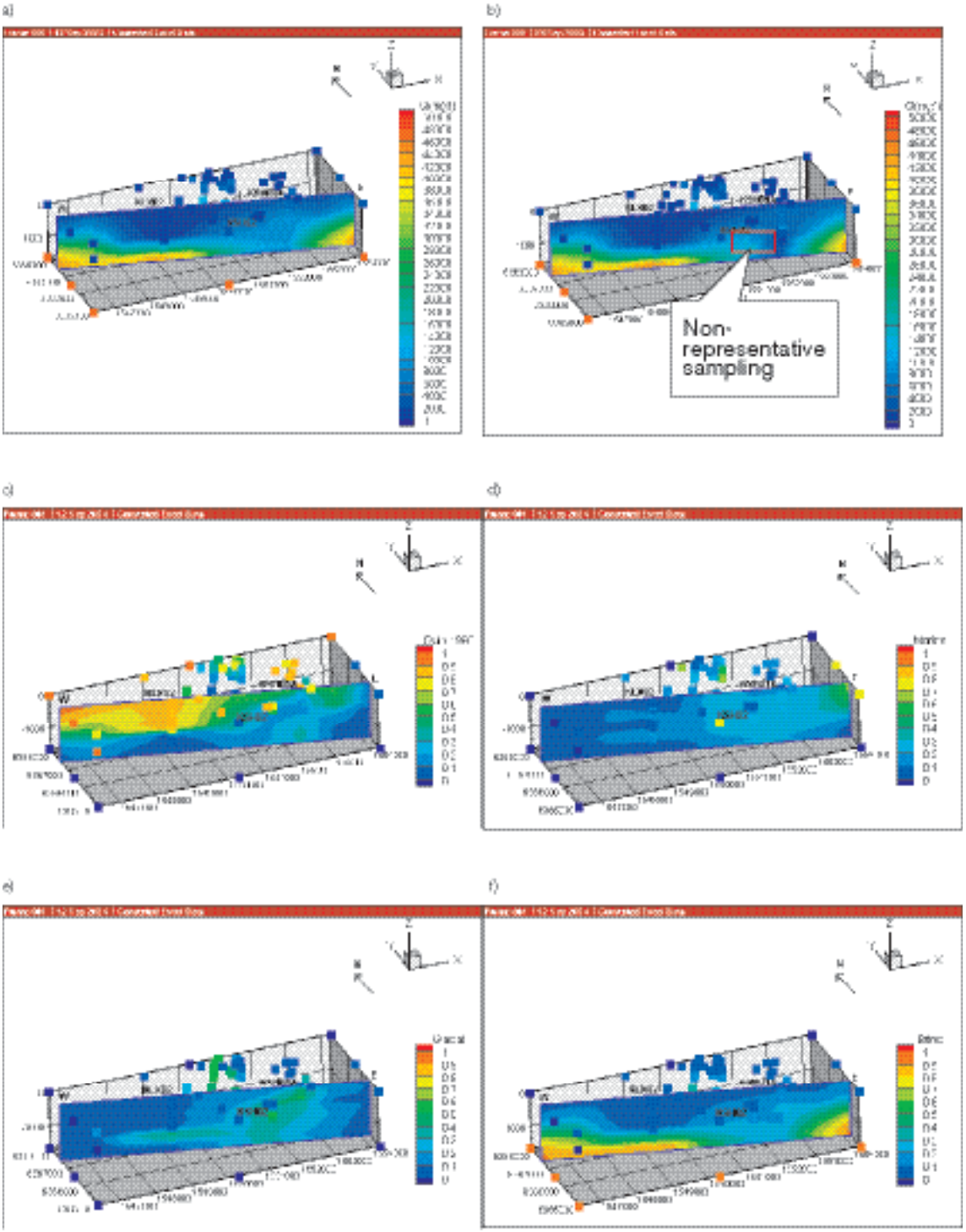

Figure 9-47. *3D interpolation and 2D visualisation of the groundwater properties along the W-E cutting plane, for orientation see Figure 9-1. (a) Cl interpolation based on representative samples (b) Cl interpolation including representative and non-representative samples. Figures c, d, e and f show the mixing proportions for the water types Rain 1960, Marine, Glacial and Brine. The x, y, z coordinates represent the Easting (m), Northing (m) and elevation (metres above sea levell).*

However, the interpolations can still be used to indicate the major occurrence of the different water types at the site. For example, a) Meteoric water is dominating in the west part and in the middle part of the cutting plane, b) Marine water is found towards the coast and under the sea in the east part of the cutting plane, c) Glacial water is found in the middle part of the cutting plane, and d) Brine type water is dominating at depth. The interpolation is discussed in more detail in /SKB, 2004c/.

9.5.4 Coupled modelling

A first attempt to combined hydrogeological and hydrochemical model analysis of the Simpevarp subarea is described in /SKB, 2004c/. The main objective of this exercise is to develop a framework to integrate available hydrogeological and hydrochemical information, with special emphasis on the assessment of consistency between them.

Present time hydrogeological conditions of the Laxemar/Simpevarp area consist of a dynamic fresh-groundwater aquifer overlying a deeper and virtually stagnant saline groundwater system. The present work focuses on the coupling between groundwater flow, solute transport and geochemical processes interpreted to take place within the dynamic aquifer.

Qualitative analysis of environmental isotopes of the fresh groundwater samples from the Simpevarp area suggests an average water age from several decades to 100 years. The Simpevarp subarea appears, therefore, to be the discharge area of a dynamic fresh water aquifer. Tritium activities measured are consistent with mixing between recent, modern and sub-modern fresh groundwaters. The mixing is produced by the convergence of flow lines discharging on the Baltic Sea coast.

Combined analyses of isotopic and hydrochemical information of fresh groundwater samples allows identification of some trends which are consistent with the hydrogeological conceptual model of the area. The distributed recharge (recent water) of the granitic fresh aquifer is supported through the analysis of shallow groundwater samples. These recharge groundwaters are Ca-CO_3 in type, have high ^{14}C contents, tritium values are close to actual precipitation, and the waters are undersaturated with respect to calcite. On the other hand, deep fresh-groundwater samples from the Simpevarp subarea (at depths of 100–200 m) could correspond to the granitic aquifer discharge (older water). These waters are Na-HCO_3 type and show a calculated average age of decades up to one hundred years. Tritium values are mainly between 10–15 TU and the water is saturated in respect with calcite. Midway between recharge to discharge the deep groundwaters from the Laxemar subarea show a clear influence of recharge from the 1960's and 1970's and characterised by 'intermediate' brackish hydrochemical signatures. However this conclusion is based on the presently available set of tritium data, the credibility of which, as pointed out in /SKB, 2004c/ has been partly questioned. A larger set of new and dependable tritium data from the Laxemar subarea will be used in the forthcoming modelling where also information from the hydrogeological model version Simpevarp 1.2 can be used to further test the above assumptions.

It has been detected that some lake waters show isotopic signatures very similar to groundwater in the Simpevarp subarea. This could be reflecting the presence of lakes constituting local discharge areas of the granitic aquifer.

Numerical modelling of groundwater flow and solute transport has been performed in order to simulate groundwater age and tritium concentration (Figure 9-48). As expected, kinematic porosity has been identified as the most sensitive parameter affecting the transport model results. Measured activities of environmental isotopes can only be reproduced numerically by using the same porosity values (order of magnitude of 10^{-3}) proposed by hydrogeological models of Simpevarp version 1.1, which were calibrated using salinity data. Thus, the present model results provide additional support to hydrogeological models by using independent hydrochemical information.

A first attempt at coupled groundwater flow and reactive solute transport modelling has been performed. The hydrogeochemical part of the model consists of a set of 23 homogeneous reactions (aqueous complexes), calcite dissolution/precipitation and cation exchange. A calcite dissolution front /Appendix 6 in SKB, 2004c/ was computed by flushing saline water with fresh recharge (infiltrated) water, in agreement with one of the main processes described by other hydrochemical models as reported in earlier sections of this chapter. However, computed calcite dissolution cannot explain the measured concentrations of bicarbonate and calcium. By including Ca-Na exchange

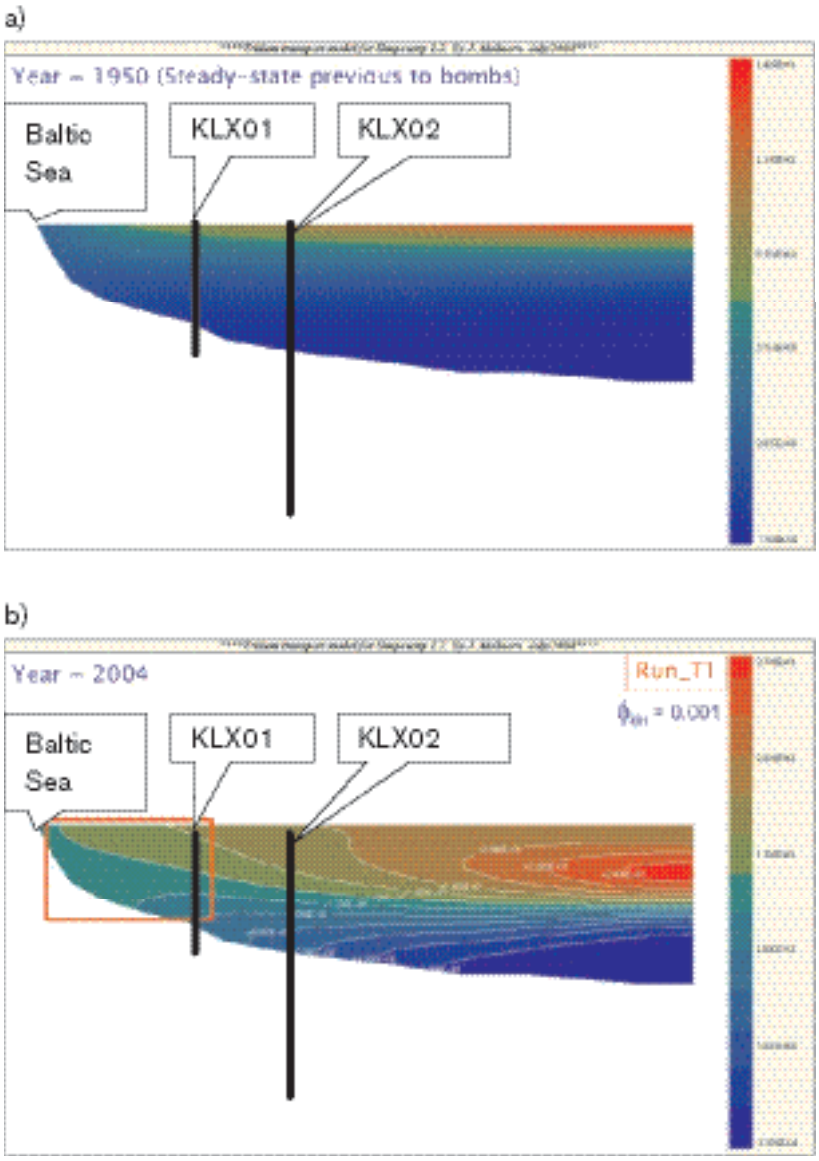

Figure 9-48. *(a) Simulated tritium contents in the Laxemar/Simpevarp fresh-water aquifer at year 1950. It can be seen that maximum tritium contents of near 15 TU are computed at the subsurface levels. The depth down to 100–200 m consists of fresh groundwater which is tritium free at year 1950. (b) Simulated tritium contents at year 2004, by using a kinematic porosity value of 0.001. The red square represents the equivalent area of fresh groundwaters at Simpevarp. The location of boreholes KLX01 and KLX02 are shown and the depth of the simulation is 1,000 m. The bottom of the model domain corresponds to the saline-fresh water interface computed by /Svensson, 1996/.*

the computed results are in good agreement with calcium and sodium concentrations measured at Simpevarp. The measured bicarbonate concentrations are higher than computed ones. A possible explanation could lie in the microbially-mediated decomposition of organic matter. This process has been described in the Äspö site groundwaters /Banwart, 1999; Banwart et al. 1999/, and successfully modelled by coupled hydro-bio-geochemical approaches /Molinero et al. 2004/. The current version of the reactive transport model underestimates dissolved silica and sulphate, and overestimates dissolved iron. Most probably this is due to the occurrence of water-rock interaction processes involving silicates, pyrite, iron oxides and phyllosilicates, as already proposed by the hydrochemical model version Simpevarp 1.1 /Laaksoharju et al. 2004b/.

9.6 Evaluation of uncertainties

At every phase of the hydrogeochemical investigation programme – drilling, sampling, analysis, evaluation, modelling – uncertainties are introduced which have to be accounted for, addressed fully and clearly documented to provide confidence in the end result, whether it will be the site descriptive model or repository safety analysis and design /Smellie et al. 2002/. The proposed handling of the uncertainties involved in constructing a site descriptive model has been documented in detail by /Andersson, 2003/. The uncertainties can be conceptual uncertainties, data uncertainty, spatial variability of data, chosen scale, degree of confidence in the selected model, and error, precision, accuracy and bias in the predictions. Some of the identified uncertainties recognised during the modelling exercise are discussed below.

The following data uncertainties have been estimated, calculated or modelled for the Simpevarp subarea data; these are based on models used for the Simpevarp 1.1 model version and for the nearby Äspö site where similar uncertainties are believed to affect the present modelling (the percentages indicate possible deviations from reported values):

- disturbances from drilling; may be ± 10–70% (cf. DIS modelling),
- effects from drilling during sampling; is < 5%,
- sampling; may be ± 10%,
- influence associated with the uplifting of water; may be ± 10%,
- sample handling and preparation; may be ± 5%,
- analytical error associated with laboratory measurements; is ± 5% (the effects on the modelling was tested in /SKB, 2004c/),
- mean groundwater variability during groundwater sampling (first/last sample); is about 25%.

The M3 model uncertainty; is ± 0.1 units within 90% confidence interval (the effects on the modelling were tested in /SKB, 2004c/.

Conceptual errors can occur in, for example, the palaeohydrogeological conceptual model. The influence and occurrences of old water end members in the bedrock can only be indicated by using certain elements or isotopic signatures. The uncertainty is therefore generally increasing with the age of the end member. The relevance of an end member participating in the groundwater formation can be tested by introducing alternative end member compositions or by using hydrodynamic modelling to test if old water types can reside in the bedrock at prevailing hydrogeological conditions. In this model version the validation is checked by comparison with hydrogeological simulations.

Uncertainties in the PHREEQC code depend on which code version is being used. Generally the analytical uncertainties and uncertainties concerning the thermodynamic databases are of importance (in speciation-solubility calculations). Care is also required to select mineral phases which are realistic (even better if they have been positively identified) for the systems being modelled. These errors can be addressed by using sensitivity analyses, alternative models and descriptions. A sensitivity analysis was performed concerning the calculations of activity coefficients in waters with high ionic strength and also the uncertainties of the stability diagrams were discussed in /SKB, 2004c/.

The uncertainty due to 3D interpolation and visualisation depends on various issues, i.e. data quality, distribution, model uncertainties, assumptions and limitations introduced. The uncertainties are therefore often site specific and some of them can be tested such as the effect of 2D/3D interpolations. The site specific uncertainties can be tested by using quantified uncertainties, alternative models, and comparison with independent models such as hydrogeological simulations.

Uncertainties in the coupled reactive transport modelling are numerous at the present site investigation stage. No systematic tests of the uncertainties have been conducted at this preliminary stage of the modelling. The uncertainties can be of two main types: (a) conceptual model uncertainties and (b) parameter uncertainties. Reactive transport modelling is based on version Simpevarp 1.1 hydrogeological and current hydrochemical conceptual models. Hence, possible conceptual uncertainties are directly translated into the reactive transport model results. Conceptual uncertainties are mainly related to the extent and nature of boundary conditions (i.e. dimensions and geometry of the model, water recharge values, etc.), and the selection of physical-chemical processes included in the calculations. Parameter uncertainties are also present in the model (permeability, porosity, cation exchange capacity, amount of calcite in the granite, etc.). However, reactive transport model has been used

as a tool for testing the consistency (or plausibility) of different assumptions. It is considered that parameter uncertainty is less relevant than conceptual uncertainties at the present stage.

The discrepancies between different geochemical modelling approaches can be due to differences in the boundary conditions used in the models or in the assumptions made. The discrepancies between models should be used as an important validation and confidence building opportunity to guide further modelling efforts. In this work the use of different modelling approaches starting from manual evaluation to advanced coupled modelling can be used as a tool for confidence building. Arrival at the same type of process descriptions independent of the modelling tool or approach increases confidence in the modelling.

How the above uncertainties affect the site descriptive model are described in detail in Chapter 12.

9.7 Feedback to other disciplines

9.7.1 Comparison between the hydrogeological and hydrogeochemical models

Since hydrogeology and hydrogeochemistry deal with the same geological and hydrodynamic properties, these two disciplines should be able to complement each other when describing/modelling the groundwater system. Testing such an integrated modelling approach was the focus of a SKB project (Äspö Task Force Task 5) based on the Äspö HRL /Wikberg 1998; Rhén and Smellie, 2003/. The advantages with such an approach were identified as follows:

- Hydrogeological models will be constrained by a new data set. If, as an example, the hydrogeological model, which treats advection and diffusion processes in highly heterogeneous media, cannot produce any Meteoric water at a certain depth and the hydrogeochemical data indicate that there is a certain fraction of this water type at this depth, then the model parameters and/or processes has to be revised.
- Hydrogeological models are fully three dimensional and transient processes such as shoreline displacement and variable-density flow can be treated, which means that the spatial variability of flow related hydrogeochemical processes can be modeled, visualised and communicated. In particular, the role of the nearby borehole hydraulic conditions for the chemical sampling can be described.
- Hydrogeochemical models generally focus on the effects from reactions on the obtained groundwater rather than on the effects from transport. An integrated modelling approach can describe flow directions and hence help to understand the origin of the groundwater. The turn over time of the groundwater system can indicate the age of the groundwater and, knowing the flow rate, can be used to indicate the reaction rate. The obtained groundwater chemistry is a result of reactions and transport, and therefore only an integrated description can be used to correctly describe the measurements.
- By comparing two independent modelling approaches a consistency check can be made. As a result greater confidence in active processes, geometrical description and material properties can be gained.

Major recent developments in hydrogeological modelling of the Simpevarp area, cf. Chapter 8, represents further progress since the Äspö Task Force Task #5 exercise /Rhén and Smellie, 2003/. The current Simpevarp 1.2 modelling has further developed the comparison and integration between hydrochemistry and hydrogeology. The hydrogeological model provide predictions of the groundwater components and isotopes such as Cl, ^{18}O and ^{2}H in the immobile zones of the rock and the mobile water, including dynamic predictions over time for the different water types (meteoric, marine, glacial and brine). Furthermore, the hydrodynamic model can, independently from chemistry, predict these salinity features at any point of the modelled rock volume, and the predictions can be checked by direct hydrogeochemical measurements or calculations. The mixing proportions from the hydrogeological model can, for example, be directly compared with the mixing calculations from the hydrogeochemical modelling (Figures 8-34, 8-36 and 8-37) or, conversely, the hydrogeochemical model can be used to predict the chemistry which results from mixing alone and which, in turn, can be compared with that obtained from reactions. The modelling will increase the understanding of transport, mixing and reactions and will also provide a tool for predicting future chemical changes due to climate changes. The coupled transport modelling presented in /SKB, 2004c/ can be used as an independent validity tool to check different processes and transport hypotheses.

10 Bedrock transport properties

The main objectives of the investigations and modelling of the transport properties of the bedrock are to provide parameters to the radionuclide transport calculations performed by Safety Assessment, and to present a description of the site-specific transport conditions that can be used to support the selection of processes and parameters in radionuclide transport models developed by Safety Assessment and others. In relation to Safety Assessment, the role of the site modelling is to describe the site-specific parameters and conditions; Safety Assessment may use other parameters, depending on the scenarios investigated. In addition, the results of the transport properties modelling are used as qualitative and/or quantitative input to transport modelling within site descriptive hydrogeological and hydrogeochemical modelling.

The strategy for site descriptive modelling of transport properties has been changed between model versions Simpevarp 1.1 and 1.2. In version Simpevarp1.2, flow-related transport parameters are not presented as a part of the site description. This implies that all calculations of flow-related transport parameters, including quantifications of retention variability along flow paths, will be handled by Safety Assessment, whereas the site descriptive model is focused on retardation parameters (diffusivity, D_e, and sorption coefficient, K_d) and their representation within the framework of the geological site descriptive model.

The main reasons for this change in strategy is the experience gained during and after the version Simpevarp 1.1 modelling, in combination with the fact that Simpevarp 1.2 does not include more detailed groundwater flow modelling than the previous model version. Specifically, it was found difficult to communicate, internally as well as externally, the difference between F-values and travel times (t_w) obtained from the large-scale flow models in the site descriptive modelling, and the "actual performance measures", also expressed in terms of F and t_w, that were calculated with the higher-resolution flow models (including repository layouts) developed by Safety Assessment.

10.1 State of knowledge at previous model version

The Simpevarp 1.1 modelling of transport properties is described in /SKB, 2004b/. The main uncertainty identified in Simpaverp 1.1 was related to the fact that no site investigation transport data were available. As further discussed below, this uncertainty is only partly resolved in the Simpevarp 1.2 model.

The Simpevarp 1.1 modelling was focused on an evaluation of transport data from research projects at Äspö HRL and their potential use within the site descriptive modelling. However, the complete Simpevarp version 1.1 geological model was not available at the time for the transport modelling. Based on the limited geological comparisons that could be made, it was concluded that the diffusion and sorption data from Äspö HRL provided information on only one of the main rock types (quartz monzodiorite, interpreted as equivalent to Äspö diorite) and one of the less frequent rock types (fine-grained granite) within the Simpevarp subarea. The potential for further "import" of data from Äspö HRL has been investigated in the present model version.

The version 1.1 modelling considered intact rock only; no attempt was made to relate transport data from fractures and deformation zones at Äspö HRL to those within the Simpevarp area. For the intact rock, the results of the 1.1 modelling, which also included a comparison with the SR 97 databases /Ohlsson and Neretnieks, 1997; Carbol and Engkvist, 1997/, emphasised the need for site-specific data on the diffusion properties of, in particular, the fine-grained dioritoid, and on sorption properties of site-specific materials in general.

10.2 Modelling methodology and input from other disciplines

The process of site descriptive modelling of transport properties is described by /Berglund and Selroos, 2003/. Essentially, the description consists of three parts:

- Description of rock mass and fractures/deformation zones, including relevant processes and conditions affecting radionuclide transport; the description should express the understanding of the site and the evidence supporting the proposed model.
- Retardation model: Identification and description of "typical" rock materials and fractures/deformation zones, including parameterisation.
- Transport properties model: Parameterisation of the 3D geological model and assessment of understanding, confidence and uncertainty.

The methods used within the transport programme produce primary data on the retardation parameters, i.e. the porosity, θ_m, the effective diffusivity, D_e, and the linear equilibrium sorption coefficient, K_d. These retardation parameters are evaluated, interpreted and presented in the form of a retardation model; the strategy for laboratory measurements, data evaluation and development of retardation models is described by /Widestrand et al. 2003/. In the three-dimensional modelling, the retardation model is used to parameterise the various geological "elements" (rock mass, fractures and deformation zones) in the site-descriptive geological model.

The development of retardation models relies to large extent on interactions with other disciplines, primarily Geology and Hydrogeochemistry. Specifically, Geology provides lithological and structural models where the rock types, fractures and deformation zones are described, as well as the mineralogical compositions of intact and altered materials. Hydrogeochemical information is used as a basis for the selection of water compositions in laboratory measurements of retardation parameters. Furthermore, hydrogeochemical data, together with results from geological-hydrogeochemical analyses of fracture materials, are important inputs to the development of the retardation model and the description of the understanding of the retention processes at the site.

10.3 Conceptual model with potential alternatives

10.3.1 Basic conceptual model

The conceptual model underlying the present descriptive model is based on a description of solute transport in discretely fractured rock. Specifically, the fractured medium is viewed as consisting of mobile zones, i.e. fractures and deformation zones where groundwater flow and advective transport take place, and immobile zones in rock mass, fractures and deformation zones where solutes can be retained, i.e. be removed, temporally or permanently, from the mobile water /Berglund and Selroos, 2003/. In the safety assessment framework that provides the basis for identification of retention parameters in the site descriptive models, retention is assumed to be caused by diffusion and linear equilibrium sorption. These processes are reversible and are here referred to as retardation processes.

The conceptualisation outlined above implies that radionuclide transport takes place along flow paths consisting of connected "sub paths" in fractures and deformation zones of different sizes. In this model, advection is the dominant process for moving the radionuclides in the transport direction, whereas the main role of diffusion is to remove the solutes from the mobile zone and transport them within the immobile zones. It should be noted that this conceptual model, and the present methodology for site descriptive modelling in general, are to large extent based on the experience from the Äspö Hard Rock Laboratory (Äspö HRL), primarily the TRUE project /Winberg et al. 2000; Poteri et al. 2002/, which is not necessarily fully applicable to the transport conditions at the Simpevarp site. This means that also the conceptual and methodological implications of the observations made during the site investigation must be considered.

10.3.2 Alternative models

Alternative conceptual models could involve additional processes and/or more refined descriptions of the presently considered processes. Furthermore, different conceptualisations of the radionuclide transport paths, i.e. as advective flow paths in accordance with the basic conceptual model described above or with, for instance, diffusive transport in the mobile zone, could be considered. For radionuclide retention, consideration of more refined representations of sorption (process-based sorption models) and additional retention processes (e.g. precipitation and co-precipitation) are of particular interest.

Modelling activities involving process-based sorption models have been initiated during the Simpevarp 1.2 transport modelling. This modelling constitutes a first attempt at reactive-transport simulations in a single fracture, using data from Äspö HRL /Dershowitz et al. 2003/. The aims are to gain experience of this type of modelling in a transport context, and to investigate whether the process-based sorption models show qualitative differences or specific features that cannot be reproduced with K_d-based models. Whereas such differences and features can be observed in the presently available results, it remains to be evaluated whether these effects may occur under realistic conditions. Hence, no conclusive results that could support, or provide alternatives to, the K_d-based model presented here are currently available.

10.4 Description of input data

The Simpevarp 1.2 data evaluation and retardation model are presented in a background report /Byegård et al. 2005/. The background report is summarised in this and the following sections; for further details the reader is referred to that report.

10.4.1 Data and models from other disciplines

/Byegård et al. 2005/ summarise and evaluate data from Geology and Hydrogeochemistry with the aim of identifying and describing relevant materials and conditions for transport analyses. The results provide a basis for the continued sample selection and laboratory investigations (primarily related to fractures and deformation zones), and for interpretations of experimental results and modelling.

Geology – rock types

Of the five core-drilled boreholes available at the time for the Simpavarp1.2 data freeze (KSH01–03, KAV01 and KAV04), only the boreholes on the Simpevarp peninsula (KSH01–03) have been sampled for transport parameters and fracture mineralogy, and only KSH01 for full hydrogeochemical characterisation /SKB, 2004c/. Therefore, the following discussion is focused on the three boreholes on the Simpevarp peninsula.

As described in Chapter 5, the following three rock types make up most of the local model area: Ävrö granite (usually porphyritic in texture and with composition ranging from granite to quartz monzodiorite), quartz monzodiorite (medium-grained) and fine-grained dioritoid. Minor rock types occur as dikes, lenses and xenlithes; these include fine-grained granite, medium- to coarse-grained granite, pegmatite, fine-grained diorite to gabbro, and equigranular diorite to gabbro. In the Simpevarp 1.2 geological model, the Simpevarp peninsula consists of three rock domains (see Chapter 5): RSMA01, dominated by Ävrö granite, RSMB01, where fine-grained dioritoid is the dominant rock type, and RSMC01, with 50% Ävrö granite and 50% quartz monzodiorite as dominant rock types.

The results presented in Chapter 5 show that the frequency of sealed fractures is not always correlated to the frequency of open fractures. However, the open fracture frequency seems to be correlated to the altered and oxidised part of the bedrock. This implies that transport and retention along the open fractures will, to large extent, take place in altered wall rock. Figures 5-45 to 5-47 show the volume of altered rock compared to fresh rock. Relatively large parts of the different rock domains at the Simpevarp peninsula and Ävrö are affected by alteration, but large variations in intensity among and along boreholes are observed.

The hydrothermal alteration/oxidation is the cause of the wide-spread red-staining of the rock. The altered parts of the rock can be assumed to have different transport properties from the unaltered rock, due to, e.g. low biotite content but rather higher content of sericite and illite (influencing the sorption capacity), and usually higher porosity and possibly also changed structure of the porosity (influencing the diffusivity). It is therefore an important consideration that all rock domains in all the boreholes show alteration (rated as weak/medium/strong) in more than 13% of the rock mass.

Fractures and deformation zones

The most common fracture minerals found in drillcores from the Simpevarp subarea are chlorite and calcites, which occur in several different varieties and are present in most of the open fractures. A compilation of the available fracture mineral results is presented in the hydrogeochemical modelling report for Simpevarp 1.2 /Appendix 1 in SKB, 2004c/. Identified clay minerals include, in addition to chlorite, corrensite, illite, mixed-layer illite/smectite, and a few observations of smectites. Conclusions of importance for the transport modelling (mainly based on /Drake and Tullborg, 2004/) can be summarised as follows:

- It has so far not been possible to relate different fracture minerals to different fracture generations.
- The sequence of mineral paragenesis shows the transition from epidote facies in combination with ductile deformation, over to brittle deformation and breccia sealing during prehnite facies and subsequent zeolite facies. A further decreasing formation temperature series, indicates that the fractures were initiated relatively early in the geological history of the host rock and have been reactivated during several different periods of various physiochemical conditions.
- The locations of the hydraulically conductive fractures are mostly associated with the presence of fault gouge-filled faults produced by brittle reactivation of earlier ductile precursors or hydrothermally sealed fractures. The outermost coatings along the hydraulically conductive fractures consists mainly of clay minerals, usually illite and mixed layer clays (corrensite = chorite/smectite and illite/smectite) together with calcite and minor grains of pyrite.
- Isotopic evidence from the calcites (KSH01A+B) indicates that the upper part of the bedrock is far more hydraulically conductive than the deeper part (> 300 m depth), and that these conditions have prevailed for a very long time. The number of open fractures at depths > 300 m and the amounts of calcites within these fractures are small. So far, however, no conclusive evidence of a strong depth dependence of the hydraulic properties of the rock has been obtained from the hydrogeological investigations (cf. Chapter 8). The stable isotope ratios indicate a decreased interaction with biogenic carbonate at depths lower than 300 meters in KSH01. The morphology of the calcites grown in open fractures show crystal shapes typical for brackish or saline water carbonates (with one exception). This is in agreement with the present groundwater chemistry, where saline waters (< 5,000 mg/l) are sampled already at depths of about 150 m.

/Byegård et al. 2005/ present an evaluation of the occurrence of different fracture and clay minerals, expressed as percentages of the open fractures in the core logs. Most of the open fractures contain chlorite and calcite. Other hydrothermal Al-silicates like prehnite, epidote and adularia are common but subordinate, and are not expected to give significant contributions to the sorption capacity. Clay minerals and hematite, in contrast, are expected to have comparably higher sorption capacity, and for this reason the percentages of these fracture coatings in the open fractures are given as well. The Ca-zeolite laumontite is found in many fractures in the area, and zeolites may have high sorption capacity. Therefore, the frequency of laumontite has been evaluated as well.

In /Byegård et al. 2005/, the strategy for sampling of fracture coatings for batch sorption measurements is described, and five different coatings are selected. Fracture coatings representing chlorite+ calcite constitute the base, and fractures containing these two minerals in addition to other minerals of interest have been selected in order to determine the importance of some common fracture minerals. The strategy is to test the selected five coatings in terms of their sorption properties and after that, if possible, to reduce the laboratory programme by concentrating on fewer fracture coatings.

For the modelling of local minor deformation zones, each zone is assumed to be built up of one or several types of altered wall rock. The conductive parts of the zones usually consist of several fractures that can be referred to some of the identified fracture types, or to a broader fault gouge-filled section. Therefore, four types of altered rocks, referred to as fault gouge, chlorite, porous episyentic wall rock, and cataclasite, have been selected for porosity, diffusion and batch sorption measurements; they are described in detail by /Byegård et al. 2005/.

Hydrogeochemistry

The results of hydrogeochemical sampling in KSH01–03 and nearby percussion boreholes are described and modelled in Chapter 9, see also /SKB, 2004c/. Water of salinity close to the one measured at repository depth has been used for the diffusivity measurements. A water composition (described as composition III below) was chosen; however, only the major components (i.e. Ca^{2+}, Na^{+}, Cl^{-} and SO_4^{2-}) were included for the diffusion experiments. For the batch sorption experiments, the groundwater composition is considered to be more important. Four different groundwater compositions have been selected, as follows:

I. Fresh diluted Ca-HCO_3 water (present water in the upper 100 m of the rock).

II. Groundwater of marine character, Na-(Ca)-Mg-Cl type (5,000 mg/L Cl).

III. Groundwater of Na-Ca-Cl type (8,800 mg/L Cl; present water at repository depth in the Simpevarp peninsula).

IV. Brine type water of very high salinity, Ca-Na-Cl type (45,000 mg/L Cl).

The detailed compositions of these waters are given by /Byegård et al. 2005/.

10.4.2 Transport data

Available data

The data available for the Simpevarp 1.2 modelling are summarised in Table 2-6, see also /Gustavsson and Gunnarsson, 2005/ and /Löfgren and Neretnieks, 2005/. About 130 rock samples from boreholes KSH01, KSH02 and KSH03 on the Simpevarp peninsula have been selected for the laboratory investigations within the Transport programme. The sample selection has been made in accordance with the laboratory strategy report /Widestrand et al. 2003/, and primarily includes major rock types, fractures and deformation zones, but also some samples of minor rock types and altered bedrock. The selection of samples from fractures/deformation zones has mainly been determined by indications of water flow, as recorded in flow logs.

Since diffusion experiments and batch sorption experiments are still in progress, the data available for use in the transport modelling are rather limited. PMMA (polymethylmethaacrylate; an impregnation method for studying the pore system, see /Hellmuth et al. 1993, 1994; Byegård et al. 1998/) porosity measurements and He-gas through-diffusion measurements are to be done during winter/spring 2005. The site investigation data available for this report include data from the water saturation porosity measurements on major rock types, a few preliminary diffusivity data, and some BET surface area data (BET – a method for determining the specific surface area of a solid material by use of gas adsorption, cf. /Brunauer et al. 1938/) on the major rock types.

Application of Äspö HRL data to Simpevarp

The potential for "importing" Äspö HRL data for use within the site descriptive modelling has been further evaluated in the Simpevarp 1.2 modelling /Byegård et al. 2005/. Due to the lack of data for the "rock types of the Simpevarp subarea" it has been necessary to import transport data to get an initial retardation model. The imported data are from through diffusion and batch sorption laboratory measurements on the "Äspö rock types", particularly Äspö diorite and fine-grained granite /Byegård et al. 1998; Dershowitz et al. 2003/.

Ävrö granite is generally unequigranular and porphyritic in texture and ranges in composition from granite to quartz monzodiorite with a majority of the samples plotting in the granodiorite/quartz monzodiorite fields (Chapter 5). The porosities of the Ävrö granite samples are in better agreement with the data for the Äspö diorite and it is therefore considered that diffusivity data for the Äspö diorite can be used for the Ävrö granite.

Concerning the sorption properties, which are more closely related to the mineralogical composition than to the texture, the use of Äspö diorite data for Ävrö granite is not perfect, but still a best choice since no data are available on Ävrö granite or equivalent rock type from the earlier investigations at Äspö. Of largest importance for the K_d-values is the biotite content, which is lower in the Ävrö granite samples from Simpevarp (11.4 ± 5.4%) than in the Äspö diorite samples in the imported data (15%). Quartz monzodiorite, on the other hand, has a higher biotite content (16%), which better corresponds to that of the Äspö diorite. This suggests that the Äspö diorite data primarily should be used for the Simpevarp quartz monzodiorite, see further discussion in Section 10.5.4.

10.5 Evaluation of transport data

The Simpevarp 1.1 evaluation of transport data, which was focused on data from Äspö, is described in /SKB, 2004b/. Below, only a brief account of the Simpevarp 1.2 data evaluation is given, primarily consisting of summary tables of the available data. The details of the data evaluation procedure are described by /Byegård et al. 2005/, who also provide additional comments and references.

10.5.1 Methods and parameters

The main laboratory methods used within the Transport programme are through-diffusion tests on slices of rock samples for determining the effective matrix diffusivity, D_e, and batch sorption tests on crushed rock and fracture-filling materials for determining the equilibrium sorption distribution coefficient, K_d. Most of the through-diffusion tests are performed with HTO (tritiated water) as a tracer. The formation factor, F_m, which is related to the diffusivity as $F_m = D_e/D_w$ (D_w is the free diffusivity in water), is evaluated from the measured diffusivities, and is then used to calculate the diffusivities of all tracers/nuclides of interest, see /Widestrand et al. 2003/.

Electrical resistivity measurements are also used to determine the formation factor. This is a relatively fast method, which enables testing of large numbers of samples. Thus, the majority of the laboratory formation factor data are from resistivity measurements. In addition, the laboratory programme includes measurements of the porosity, θ_m, by the water saturation technique, and for some samples also by PMMA measurements. The through-diffusion tests also provide estimates of the porosity by means of the "capacity factor" calculated from the experimental results.

The in situ methods within the Transport programme include in situ electrical resistivity measurements (in situ formation factor logging), tracer tests in single boreholes (SWIW = Single-Well Injection Withdrawal, cf. review in /Nordqvist and Gustavsson, 2002/) and multi-well configurations, and in situ borehole sorption/diffusion experiments. Some of these methods are still under development. Method tests with in situ resistivity measurements and SWIW have been performed in Simpevarp during 2004. Formation factor logs have been obtained from resistivity measurements in boreholes KSH01A and KSH02; the results are discussed below. The SWIW results will be reported as part of the Laxemar 1.2 site-descriptive model.

10.5.2 Porosity

A summary of porosity data obtained from samples selected for though-diffusion and batch sorption measurements within the site investigation programme is presented in Table 10-1. No porosity measurements on altered rock materials close to the fractures are available. However, results from previous measurements reported by /Byegård et al. 2001/ on a material that can be concluded to represent altered Äspö diorite are included. Clearly, the large standard deviations of the datasets in Table 10-1, with sample mean minus one standard deviation showing negative values in some cases, indicate that log-normal distributions are more appropriate than normal distributions for describing the data.

The geological binocular microscope characterisation shows a great number of small cracks that are 3–15 mm in length and with a width of ≤ 0.5 mm, in both fresh and altered rock samples. Table 10-1 includes results where the samples with cracks have been excluded. Comparisons with the corresponding "complete" data sets indicate that these cracks may increase the porosity. The effect of the sample length is presented in Table 10-2, where it can be seen that the porosity increases with decreasing sample length. It can be noted, however, that the statistical significance of the data in Table 10-2 is questionable (few samples), which is also the case for some of the results presented in Table 10-1.

Table 10-1. Porosities (%) of different rock types in the Simpevarp area. The values are given as mean ±1σ of the experimental dataset (non-log and log_{10} values).

Rock type	All rock samples (n)	Rock samples without cracks (n)
Fine-grained dioritoid	0.21 ± 0.21 (87) $10^{(-0.82\pm0.38)}$	0.17 ± 0.15 (63) $10^{(-0.90\pm0.35)}$
Quartz monzodiorite	0.26 ± 0.31 (23) $10^{(-0.75\pm0.35)}$	0.20 ± 0.13 (22) $10^{(-0.80\pm0.28)}$
Ävrö granite	0.40 ± 0.13 (19) $10^{(-0.43\pm0.19)}$	No samples excluded
Fine-grained granite	0.29 ± 0.23 (17) $10^{(-0.70\pm0.34)}$	0.22 ± 0.09 (15) $10^{(-0.73\pm0.31)}$
Altered Äspö diorite (Äspö data from /Byegård et al. 2001/)	0.33 (1)	No samples excluded

Table 10-2. Porosities (%) for rock samples of different lengths. The values are given as mean ±1σ of the experimental dataset.

Rock type	Samples ≤ 1 cm (n)	Samples 3 cm (n)	Samples 5 cm (n)
Fine-grained dioritoid	0.32 ± 0.18 (12)		0.17 ± 0.16 (6)
Quartz monzodiorite			
Ävrö granite	0.52 ± 0.6 (6)	0.34 ± 0.12 (11)	
Fine-grained granite			

10.5.3 Diffusion

For the Simpvarp 1.2 modelling, diffusivity values are available from through-diffusion tests in the laboratory, and from resistivity measurements in situ and in the laboratory /Löfgren and Neretnieks, 2005/. The through-diffusion results from the site investigation should be considered preliminary, because steady state conditions, necessary for final evaluation, have not been reached in most samples.

Since no site-specific data are available for Simpevarp rock types other than Ävrö granite, fine-grained dioritoid and quartz monzodiorite (resistivity data only), the possibilities for importing Äspö data have been investigated. Based on the reasoning in Section 10.4.2, import of data from Äspö diorite for the Ävrö granite and of data for the fine-grained granite can be justified. However, Ävrö granite is here parameterised using site investigation data. For the remaining rock types, i.e. granite and fine-grained diorite-gabbro, no data are available, implying that the diffusivities of these rock types must be considered pending in the present model version.

Table 10-3 summarises the Simpevarp 1.2 diffusion data, expressed as formation factors. Thus, the diffusivities obtained from the through-diffusion tests have been converted to formation factors using the diffusivity of tritiated water in pure water (2.13E–9 m^2/s). The data from the electrical resistivity measurements are expressed in terms of statistics of both non-log and log_{10} values. As described by /Byegård et al. 2005/, log-normal distributions provide better fits to the experimental data than normal distributions, although the deviations from log-normal behaviour are also relatively large in some cases. Similar to the porosity data presented above, “sample” standard deviations are in many cases of the same order as, or even larger than, the mean values.

The relatively large amount of data that is available from the resistivity measurements in KSH01A and KSH02 has been used to investigate various aspects of the diffusion properties of the rock, such as the relations between porosity and formation factor, between depth and formation factor, and between formation factors measured in situ and in the laboratory /Byegård et al. 2005/. The following observations can be made:

- The formation factor tends to increase with increasing porosity.
- The results show a large spread in the laboratory data. Due to the large scatter, it is difficult to identify trends indicating, for instance, depth dependence or consistent differences between rock types.
- The in situ formation factors show less spread than those measured in the laboratory. This could, to some extent, be an effect of the insufficient measurement range of the equipment used for the in situ measurements, or the limited in situ data available for some rock types /Löfgren and Neretnieks, 2005/.
- The evaluation of the relation (ratio) between laboratory and in situ formation factors shows no conclusive evidence of a depth trend that would demonstrate increasing effects of stress release in the laboratory samples. As indicated by Figure 10-1, a regression line showing increasing values with depth could probably be fitted to the data. However, the deviations from such a trend line would be large, and the trend uncertain. Therefore, the main observation made at this stage is that data from depths larger than 800 m could be taken as indications of such stress release effects (see Figure 10-1).

Table 10-3. Summary of the formation factor determinations for the Simpevarp rock types. The values are given as mean ±1σ of the considered datasets (non-log and log_{10} values).

Method	Fine-grained dioritoid	Quartz monzodiorite	Ävrö granite	Fine-grained granite	Altered Äspö diorite
HTO through-diffusion	(9±10)E–5	Pending	(5.3±0.6)E–4	(6±4)E–5	(8±4)E–5
Electrical resistivity, lab	(1.0±1.7)E–4	(1.1±1.6)E–4	(2.9±2.9)E–4	Pending	Pending
	$10^{(-4.69\pm0.89)}$	$10^{(-4.45\pm0.73)}$	$10^{(-3.85\pm0.66)}$	Pending	Pending
Electrical resis-tivity, in situ	(1.1±0.9)E–5	(2.1±1.1)E–5	(7.4±4.5)E–5	Pending	Pending
	$10^{(-5.05\pm0.31)}$	$10^{(-4.72\pm0.20)}$	$10^{(-4.20\pm0.30)}$	Pending	Pending

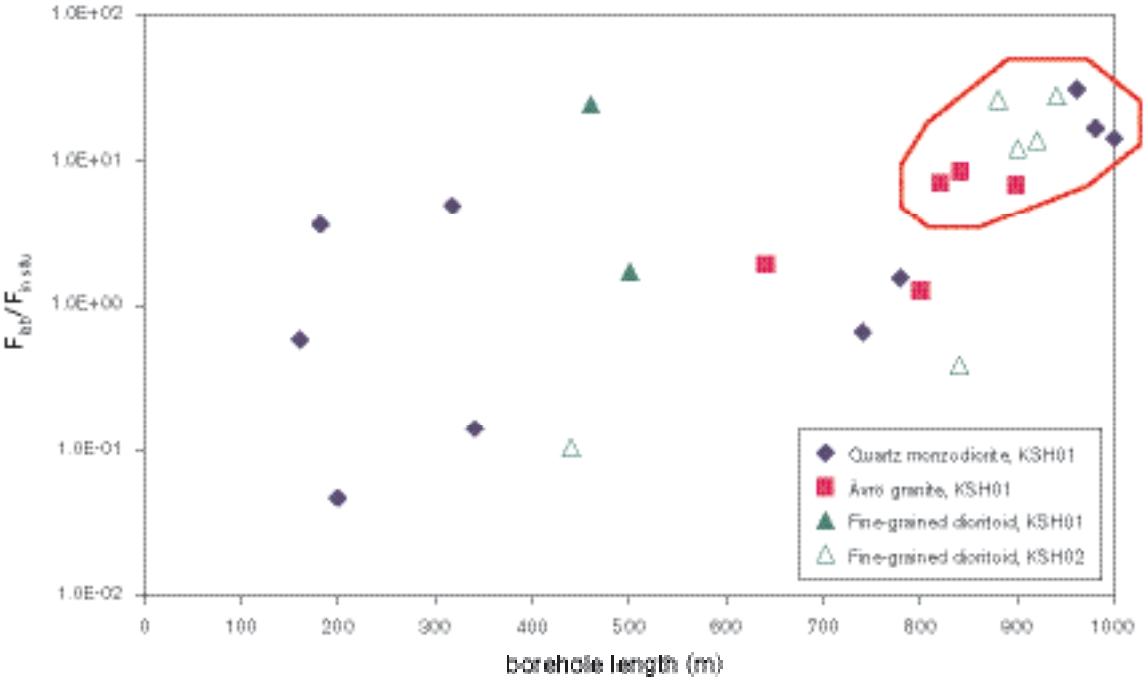

Figure 10-1. *Ratio of the formation factors measured with electrical resistivity in the laboratory and in situ versus the borehole length.*

10.5.4 Sorption

BET measurements

Since the adsorption of radionuclides is taking place on the surfaces of the rock material, the quantification of available surface areas is an important estimation of the sorption capacity of the rock material. Although at this stage no method is available for establishing a relationship between specific surface areas and sorption coefficients, the results of the BET surface measurements are included here as qualitative data important for the understanding of the sorption processes. Results of BET measurements on site-specific materials are shown in Table 10-4.

Table 10-4. Measured BET surface areas for the fractions 0.045–0.090 mm and 1–2 mm presented together with the result of an extrapolation of the results in order to obtain an inner surface area (concept equivalent to the concept in the K_d extrapolation).

Rock type	BET surface area 0.045–0.090 mm (m^2/g)	BET surface area 1–2 mm (m^2/g)	Extrapolated inner BET surface area (m^2/g)
Fine-grained dioritoid	0.57	0.048	0.036
Ävrö granite	0.32	0.041	0.034
Quartz monzodiorite	0.33	0.042	0.035
Fine-grained granite	0.34	0.075	0.069

Sorption data

The lack of site investigation sorption parameters implies that Äspö data are the only data that could provide input on the properties of site-specific rock types. In the Simpevarp 1.1 model, it was recommended to import sorption data from the Äspö rock type "fine-grained granite" to Simpevarp "fine-grained granite", and from the Äspö rock type "Äspö diorite" to Simpevarp "quartz monzodiorite".

However, based on the Simpevarp 1.2 mineralogical investigation of the different major rock types, it can be observed that the biotite and plagioclase contents are similar for Ävrö granite, quartz monzodiorite and fine-grained dioritoid. Calculations have indicated that more than 90% of the cation exchange capacity of the Äspö diorite can be attributed to the biotite and plagioclase contents /Dershowitz et al. 2003/. Therefore, it has been decided that sorption coefficients for cation exchange sorbing radionuclides determined for Äspö diorite should be valid for Ävrö granite, quartz monzodiorite and fine-grained dioritoid. The results of the BET surface area measurements, cf. Table 10-4, also indicate a similarity between these three rock types from a sorption perspective.

As discussed in Section 10.4.1, and in more detail in /Byegård et al. 2005/, a significant part of flow and transport can be assumed to take place in fractures within altered major rock types (i.e. altered fine-grained dioritoid, quartz monzodiorite and Ävrö granite). The altered Äspö diorite from KXTT2 in the Äspö HRL /Byegård et al. 1998/ has been selected to represent these altered rock types in the sorption model.

The sorption data for the non-altered and altered rock types have been evaluated in accordance with the proposed strategy for laboratory measurements /Widestrand et al. 2003/, see /Byegård et al. 2005/ for details. This evaluation includes a separation of the total sorption, as quantified by the measured mass distribution in the batch experiments, into sorption on outer surfaces (quantified by the parameter K_a) and inner surfaces (quantified by K_d) of the matrix. The resulting parameter values are summarised in Table 10-5. It can be noted that the K_d-values for altered rock are lower than those for non-altered rock. A reasonable explanation for this difference, supported by observations in /Byegård et al. 1998/, is that it is related to differences in the biotite content of the materials.

The water used in the used in the Äspö HRL sorption experiments had a composition that makes the results applicable for groundwater composition III in Section 10.4.1 (see also /Byegård et al. 2005/). For the other groundwater compositions identified as relevant for the transport modelling, there are no experimental results that can be imported. It follows that the present Simpevarp 1.2 retardation model is restricted to sorption under hydrochemical conditions equivalent to groundwater composition III, and to the two radionuclides in Table 10-5 (Sr and Cs).

Table 10-5. Sorption coefficients (K_a- and K_d-values) imported and selected for the Simpevarp 1.2 site descriptive model according to the procedure described by /Byegård et al. 2005/.

	Sr		Cs	
Rock type	**K_d (m³/kg)**	**K_a (m)**	**K_d (m³/kg)**	**K_a (m)**
Non-altered Ävrö granite Quartz monzodiorite Fine-grained dioritoid	(4.2±0.8)E–5	(2.0±0.5)E–6	0.06±0.03	0.012±0.002
Altered Ävrö granite Quartz monzodiorite Fine-grained dioritoid	(1.2±0.2)E–5	(6±1)E–7	0.013±0.006	0.002±0.0004
Non-altered Fine-grained granite	(1.5±0.1)E–5	(2.12±0.08)E–6	0.007±0.001	0.00155±0.00008

10.6 Transport properties of rock domains

10.6.1 Methodology

The parameterisation of the retardation model is based on the following considerations and parameters:

- **Rock matrix porosity, θ_m (–):** The results from the water saturation porosity measurements on site-specific rock materials have been selected in this work. A log-normal distribution has been considered to describe the system somewhat better (although not perfectly) than a normal distribution, and has therefore been selected for the representation.
- **Rock matrix formation factor, F_m (–):** This parameter is used to multiply literature values of the radionuclide-specific free diffusivities in water (D_w (m²/s); tabulated, e.g. by /Ohlsson and Neretnieks, 1997/) to obtain the effective diffusivities, D_e (m²/s), for the different radionuclides. Since the results of the laboratory electrical resistivity measurements are based on a larger number of samples and have been found not to deviate significantly from the through-diffusion results, they have been selected for the retardation model. For consistency with the closely related porosity parameter, a log-normal distribution has been selected also for the formation factor representation.
- **Rock matrix sorption coefficient, K_d (m³/kg):** All available data (all from Äspö HRL investigations) are imported for use in the retardation model. Site-specific data on the BET surface areas of the different rock types are given as supporting data.

10.6.2 Description of rock domains

The geological model is based on rock domains, whereas the sampling for the transport programme is based on rock types and mainly focused on the three major rock types. The samples represent both fresh and altered samples of these rocks. Also minor rock types have been sampled, but no data on these are available so far. The greater importance of the fine-grained granite for transport, indicated by observations of its percentage of open fractures and deviating transport properties in previous investigations at Äspö HRL /Byegård et al. 1998/, has not been addressed in the present work.

As discussed in previous sections, large parts of the rock are hydrothermally altered, which is expected to affect the transport parameters. This alteration occurs in all three major rock types, but based on observations in boreholes KSH01A, KSH02, KSH03A and KAV01 to a lesser extent in the Ävrö granite than in the two other major rock types (cf. Chapter 5).

Table 10-6 presents parameters for the fresh and altered major rock types. The percentages quantify the portions of the rock types that are altered; they are estimated from data in the geological description (Chapter 5). The parameterisation of the major rock types can then be used to parametrise to the different rock domains. Three different domains constitute the rock volume of the Simpevarp subarea; these domains consist of mixtures of the different rock types according to Table 10-7, which is based on borehole data on the proportions of different rock types within the rock domains.

Tables 10-6 and 10-7 provide a basis for parametrisation of the rock domains RSMA01, RSMB01 and RSMC01. The parameterisation of each rock domain could range from a simple selection of a single parameter value for the dominant rock type in that domain to, for instance, volume averaging using data for fresh or altered rock, or both. For the diffusion parameters of the major rock types, statistical distributions are given that can be used as a basis for stochastic parameterisation of transport models.

However, no specific recommendations on the selection of data from the retardation model are given here. This implies that the present model does not provide detailed guidelines on how to "dress" the geological model with transport parameters using the parameters in the retardation model. At this stage of model development, the retardation model should be viewed as a presentation of the interpreted site-specific information on retardation parameters, intended to provide a basis for the formulation of alternative parameterisations within the Safety Assessment modelling.

Table 10-6. Suggested transport parameters for the major rock types in the Simpevarp subarea.

Rock type	Porosity (vol-%)	Formation factor (–)	K_d Sr (m^3/kg) (GW type III)	K_d Cs (m^3/kg) (GW type III)
Ävrö granite, Fresh (90%)	$10^{(-0.43\pm0.19)}$	$10^{(-3.85\pm0.66)}$	(4.2±0.8)E–5	0.06±0.03
Ävrö granite, Altered (10%)	0.33	8E–5	(1.2±0.2)E–5	0.013±0.006
Quartz monzodiorite, Fresh (80%)	$10^{(-0.80\pm0.28)}$	$10^{(-4.45\pm0.73)}$	(4.2±0.8)E–5	0.06±0.03
Quartz monzodiorite, Altered (20%)	0.33	8E–5	(1.2±0.2)E–5	0.013±0.006
Fine-grained dioritoid, Fresh (80%)	$10^{(-0.90\pm0.35)}$	$10^{(-4.69\pm0.89)}$	(4.2±0.8)E–5	0.06±0.03
Fine-grained dioritoid, Altered (20%)	0.33	8E–5	(1.2±0.2)E–5	0.013±0.006

Table 10-7. Estimated percentages of different rock types in the rock domains of the Simpevarp subarea.

Rock domain	Ävrö granite	Quartz monzo-diorite	Fine-grained dioritoid	Fine to medium grained granite	Pegmatite	Diorite and gabbro	Fine-grained mafic rock
RSMA01	76–85		9–17	1–22		0–1.7	3.0–4.9
RSMB01		0–4	91–94	1–7	0.8–1.0		0.6–0.8
RSMC01	23–34	52–74	6	2–4	0.3–1.4	0.2	1.2

10.7 Transport properties of fractures and deformation zones

10.7.1 Methodology

According to the retardation model concept proposed by /Widestrand et al. 2003/, the aim is to prepare retardation models for the identified fractures and deformation zone types by describing and quantifying retardation parameters for the different layers of geological materials present in (and adjacent to) the fractures and deformation zones. The geological materials in the fractures/deformation zones could consist of, e.g. fault fault gouge, fracture coatings, mylonite and altered wall rocks. Additional parameters in the retardation model include the thickness of each layer and the hydraulic properties and preferential directions of each fracture type.

In the Simpevarp 1.2 modelling, an identification and quantitative description of different fracture types is presented, whereas deformation zone types cannot be identified due to the limited data available. The limited amount of data also implies that some parameter values are missing in the tables for the identified fracture types. The the on-going site investigation programme will improve the basis for parameterisation of fractures and deformation zones. It should be noted, however, that the present Safety Assessment transport modelling uses retardation parameters for fresh (non-altered) rock. Therefore, this modelling is not directly dependent on the availability of parameters for fault gouge, fracture coatings and altered rock.

10.7.2 Description of fractures

The following quantitative estimates are used as a basis for the identification and parameterisation of different fracture types:

Chlorite + calcite is the overall dominating coating in the open fractures. Also hematite is present in about 20% of the open fractures in boreholes KSH01A and KSH02, and in more than 40% of the fractures in borehole KSH03A. Clay minerals are present in less than 5% of all open fractures according to the core logging, but this is probably an underestimation. Laumontites are documented in less than 2% of the fractures.

According to the presently available data, the presence of different fracture coatings cannot be related to specific rock types. This is important for the application of the identified fracture types in transport models.

Concerning the host rock, it has been found that between 46 and 68% (according to data from boreholes KSH01–KSH03) of the open fractures are situated within altered parts of the rock. If considering the nearest cm to the fracture only, this is probably an underestimation, as most of the fracture coatings documented by thin sections show hydrothermal alteration.

Based on the core mapping only, the following quantification and description of different fracture types is suggested:

A. 40% have chlorite and calcite as fracture coating (max 0.5 mm thick on each side) and fresh wall rock.

B. 20% have chlorite and calcite as fracture coating (max 0.5 mm thick on each side) and altered wall rock $\geq$ 5 cm (on each side of the coating).

C. 30% have chlorite+calcite+hematite as fracture coating (max 0.5 mm thick on each side); all of these fractures have altered wall rock $\geq$ 5 cm (on each side of the coating).

D. 10% have chlorite+ calcite + clay minerals as fracture coating (max 1 mm thick on each side); all of these fractures have altered wall rock $\geq$ 5 cm (on each side of the coating).

The quantitative descriptions of the identified fracture types, including the available retardation parameters, are given in Tables 10-8 to 10-11. The fracture types in the present retardation model could be used as a basis for modelling radionuclide transport along flow paths in the fractured medium. However, the model could also be viewed as primarily proposing a basic structure, for discussion and further development, which from the viewpoint of numerical transport modelling

will become more useful when more data are at hand. Concerning the parameterisation of transport models, it should also be noted that at present there are no data supporting, for instance, quantitative correlations between fracture types and hydraulic properties.

Table 10-8. Retardation model for Fracture type A.

	Fracture coating	Fresh host rock
Distance	Max 0.5 mm	0.5 mm –
Porosity	Pending	According to Table 10-6
Formation factor	Pending	According to Table 10-6
Sr, Kd (m^3/kg) Groundwater type III	Pending	According to Table 10-6
Cs, Kd (m^3/kg) Groundwater type III	Pending	According to Table 10-6
Mineral content	Chlorite, Calcite	See geological description
Grain size	Pending	Pending
Proportion of conducting structures	40%	
Transmissivity interval	Pending	
Direction	Pending	

Table 10-9. Retardation model for Fracture type B.

	Fracture coating	Altered wall rock	Fresh host rock
Distance	Max 0.5 mm	0.5 mm – ≥ 5 cm	≥ 5 cm –
Porosity	Pending	According to Table 10-6	According to Table 10-6
Formation factor	Pending	According to Table 10-6	According to Table 10-6
Sr, Kd (m^3/kg) Groundwater type III	Pending	According to Table 10-6	According to Table 10-6
Cs, Kd (m^3/kg) Groundwater type III	Pending	According to Table 10-6	According to Table 10-6
Mineral content	Chlorite, Calcite	See geological description	See geological description
Grain size	Pending	Pending	Pending
Proportion of conducting structures	20%		
Transmissivity interval	Pending		
Direction	Pending		

Table 10-10. Retardation model for Fracture type C.

	Fracture coating	Altered wall rock	Fresh host rock
Distance	Max 0.5 mm	0.5 mm – ≥ 5 cm	≥ 5 cm –
Porosity	Pending	According to Table 10-6	According to Table 10-6
Formation factor	Pending	According to Table 10-6	According to Table 10-6
Sr, Kd (m^3/kg) Groundwater type III	Pending	According to Table 10-6	According to Table 10-6
Cs, Kd (m^3/kg) Groundwater type III	Pending	According to Table 10-6	According to Table 10-6
Mineral content	Chlorite, Calcite, Hematite	See geological description	See geological description
Grain size	Pending	Pending	Pending
Proportion of conducting structures	30%		
Transmissivity interval	Pending		
Direction	Pending		

Table 10-11. Retardation model for Fracture type D.

	Fracture coating	Altered wall rock	Fresh host rock
Distance	Max 0.5 mm	0.5 mm – ≥ 5 cm	≥ 5 cm –
Porosity	Pending	According to Table 10-6	According to Table 10-6
Formation factor	Pending	According to Table 10-6	According to Table 10-6
Sr, Kd (m^3/kg) Groundwater type III	Pending	According to Table 10-6	According to Table 10-6
Cs, Kd (m^3/kg) Groundwater type III	Pending	According to Table 10-6	According to Table 10-6
Mineral content	Chlorite, Calcite, Clay minerals	See geological description	See geological description
Grain size	Pending	Pending	Pending
Proportion of conducting structures	10%		
Transmissivity interval	Pending		
Direction	Pending		

10.7.3 Description of deformation zones

Local minor deformation zones

Based on the information available at this stage of the site investigation, it is not possible to provide a retardation model for the local minor deformation zones. This is due to the lack of transport data, but also to uncertainties in the evaluation of deformation zone data from the core logs. The only deterministic data available so far are for the local major deformation zones.

A few things can, however, be pointed out:

- The local minor deformation zones are hosted in altered rocks.
- Fault gouge is common, and in four zones in boreholes KSH01A and KSH02 several cm-wide fault gouge-filled sections hosted in metre-wide parts of cataclastic rocks are observed (e.g. at 248–250 m core length in borehole KSH01A). Also smaller zones with only mm-thick fault gouge-filled fractures in altered or cataclastic rocks are observed.
- Chlorite- and clay-rich zones (on the order of < 1 cm), hosted in altered wall rock (dm-wide), are also found.
- The available data are too limited to allow conclusions on the abundances of different types of deformation zones.

Local major deformation zones

Only one local major deformation zone is penetrated by the Simpevarp boreholes, the ZSMNE0024A zone transected by borehole KSH03A at 200 to 300 m core length. The rock is severely altered; biotite is altered to chlorite. No porosity measurements are available, but a significantly higher porosity is expected in this section of the drill core. In the centre of the zone, some smaller parts are highly porous, with an episyenitic structure. Other parts are cataclastic with sections of clay-rich fault gouge (dm-wide). Hematite is a common mineral in many of the fractures in this section, together with clay minerals and chlorite.

10.8 Evaluation of uncertainties

General discussions on the uncertainties related to the site-descriptive transport model are given in the transport modelling guidelines /Berglund and Selroos, 2003/ and in the Simpevarp 1.1 modelling report /SKB, 2004b/. Similar to the other geoscientific disciplines, spatial variability is considered an important potential source of uncertainty in the modelling of transport properties. Quantitative results from previous studies on Äspö /Byegård et al. 1998, 2001; Löfgren and Neretnieks, 2003; Xu and Wörman, 1998/, demonstrating spatial variability along flow paths and within the matrix, are briefly summarised in /SKB, 2004b/.

The main uncertainties identified in the Simpevarp 1.1 modelling were related to the absence of site-specific transport data. As described above, this uncertainty has been partly resolved in the Simpevarp 1.2 model, although significant data gaps still remain. In particular, no site-specific sorption parameters are available for the Simpevarp 1.2 modelling. Furthermore, the available data are insufficient for establishing quantitative relations between transport parameters and other properties of fractures and deformation zones, e.g. lengths, orientations and hydraulic properties. However, it should be noted that the basis for importing transport data from Äspö HRL have been improved by the geological/mineralogical-transport evaluation undertaken as a part of the Simpevarp 1.2 modelling.

The uncertainties relevant for present description of transport properties can be categorised as follows:

- Uncertainties in the data and models obtained from other disciplines, primarily Geology and Hydrogeochemistry.
- Uncertainties in the interpretations and use of data and models from other disciplines, i.e. in interpretations of the relations between transport properties and various underlying properties, and the simplifications made when identifying and parameterising “typical” materials and fractures.
- Data uncertainties related to measurements and spatial variability of transport parameters, including the “extrapolation” of small-scale measurements to relevant model scales.
- Conceptual uncertainties related to transport-specific processes and process models (see Section 10.3.2).

This model provides quantitative information on transport data uncertainties only. Uncertainty ranges, in most cases taken directly from the experimental data, are given in the data tables above. Essentially, these ranges incorporate both random measurement errors and the spatial variability associated with the particular dataset. The uncertainties introduced by the inputs from other disciplines and by the “expert judgement” utilised to interpret and use these data have not been addressed in the transport description. Whereas the uncertainties in the description devised by Geology and Hydrogeochemistry are discussed in Chapter 5 and Chapter 9, respectively, no attempt has been made to formulate alternative interpretations or otherwise address the “expert judgment” aspects of the work.

Regarding the uncertainties related to spatial variability and scale, it may be noted that all measurements providing data to the retardation model have been obtained in the laboratory, on a millimetre- to centimetre-scale. The proper means of “upscaling” these parameters is by integrating them along flow paths in groundwater flow models, implying that the scale of the flow model is the relevant model scale. The approach is here to present the data on the measurement scale, thereby providing a basis for further analysis in connection with the numerical flow and transport modelling.

11 Resulting description of the Simpevarp area

This chapter provides condensed accounts of the version 1.2 site-descriptive model of the Simpevarp subarea. The resulting description follows the consecutive order of the discipline-wise presentation in preceding chapters. In the case of the disciplines Geology (Section 11.2) and Hydrogeochemistry (Section 11.6) , the presentation is somewhat more elaborate than for the other disciplines. This is fully intentional, and motivated by the multi-component modelling aspects of these models, and their relative complexity.

11.1 Surface properties and ecosystems

11.1.1 Quaternary deposits and other regoliths

The terrestrial parts of the Simpevarp area are relatively flat, and are dominated by exposed bedrock and glacial till. The Quaternary deposits are mainly located in the valleys, whereas the high-altitude areas are dominated by exposed bedrock, or thin layers of till and peat. All known Quaternary deposits in the area were formed during or after the latest glaciation, which declined subsequent to its peak some 14,000 years ago. The whole area is located below the highest coastline, and the overburden has partly been eroded and redeposited by waves and streams when the water became shallower as a consequence of the isostatic land uplift.

After the deglaciation of the Simpevarp area, the sea level was c. 100 m higher than at present and the whole area was consequently covered with water. Fine-grained sediments, such as glacial clay, were deposited at the deep and sheltered bottoms. There are several distinct valleys in the Laxemar subarea where the overburden is comprised of peat, clay or other fine-grained deposits. Also on the present sea floor, the deepest areas are covered with clay (Figure 4-2).

Based on the present knowledge of the Simpevarp area, two main type areas with Quaternary deposits, which occur both on the present land and at the sea floor, can be distinguished:

1. The highest topographic areas, which are dominated by exposed bedrock and till. The overburden in these areas are generally thin (up to a few metres), although small pockets of thicker overburden may occur. Results from the Simpevarp subarea show that small peatlands are common in these areas.
2. Narrow valleys dominated by clay, which is underlain by till. The total thickness of Quaternary deposits in these areas is generally several metres.

11.1.2 Climate, hydrology and hydrogeology

The hydrological conditions in the Simpevarp area have changed considerably since the last glaciation. An important component in these changes is the shoreline displacement, discussed in Section 3.2. Another component is the changing salinity of the Baltic, from the time of the Baltic Ice Lake to the present Baltic Sea (see Section 3.3), that probably has affected the present spatial distribution of the salinity in the groundwater and thus constitutes an important conditioning constraint for the groundwater flow modelling.

Climate

The present regional meteorological conditions in the Simpevarp area are described by /Larsson-McCann et al. 2002/. In short, the annual mean temperature is 6–7°C, with monthly mean temperatures between –2°C (January–February) and 16–17°C (July). The annual precipitation, corrected for losses in the measurements, is usually 600–700 mm, with a slight tendency to increase inland. During the one-year period from September 2003 to September 2004, the average air temperature measured at the meteorological station on the Äspö island (established as a part of the site investigations) was 7.4°C. The measured (uncorrected) precipitation at this station during the same period was 671 mm, which corresponds to a corrected (“true”) precipitation of approximately 800 mm.

Catchment areas and run-off

The Simpevarp regional model area is characterised by a relatively small-scale topographical undulation and by relatively shallow Quaternary deposits (see below). Almost the entire regional model area is below 50 metres above sea level, and the whole area is located below the highest coastline. Hydrologically, the area can be described as consisting of a large number of relatively small catchments, and it also contains a relatively large number of water courses (most of them are small).

Estimates of the specific discharge (i.e. the area-normalised total runoff) for the regional model area were presented by /Larsson-McCann et al. 2002/. For the present model version, hydrological process modelling was performed for one catchment, ("Simpevarp 7" where Lake Frisksjön is located), using meteorological data from a station some distance away from the present model area for a selected representative year /Werner et al. 2005/. The calculated runoff was 150–160 mm/year, which is within the range of the previous estimates. Since this modelling concerns only a part of the regional model area and is based on regional (non site-specific) meteorological data, it does not provide a sufficient basis for updating the previous runoff estimates. However, the on-going meteorological measurements and the recently initiated discharge measurements within the model area will be used as basic inputs to water balance calculations in forthcoming model versions

Near-surface groundwater flow mainly takes place in Quaternary deposits in the valleys, and is of a local character within each catchment area. Groundwater levels are probably shallow, usually less than a few metres below ground in recharge areas and < 1 m in discharge areas. Simple discharge measurements available today indicate that the discharge in water courses (located in the valleys) mainly takes place in association with precipitation events and/or snow melt periods; in between, the water courses are dry during large parts of the year.

Recharge and discharge areas

An important model application in this version of the Site Descriptive Model is the identification of recharge- and discharge areas (Figure 4-5). The results show that the detailed locations of recharge- and discharge areas are strongly influenced by the local topography. Moreover, detailed modelling shows that the extent of recharge and discharge areas may vary considerably during the year, due to the temporally variable meteorological conditions (Figure 4-6). The lakes are considered to be permanent discharge areas, whereas the streams are considered to be discharge areas during water-bearing periods. The wetlands can either be in direct contact with the groundwater and constitute typical discharge areas, or be separate systems where low-permeable bottom materials imply little or no hydraulic contact with the underlying aquifer.

11.1.3 Chemistry

Near surface groundwater chemistry

Results from the investigation of near-surface groundwater chemistry show that the chemical composition in the Simpevarp subarea does not deviate considerably from the typical composition of groundwater in Sweden, except for manganese (Mn) which showed ten times higher median concentrations than normal /cf. Naturvårdsverket, 1999/. For a more detailed discussion of these results, see /Lindborg, 2005/.

11.1.4 Ecosystem description

The surface ecosystem is described using a large number of properties which, when combined, will constitute the ecosystem site descriptive model /cf. Löfgren and Lindborg, 2003/. The surface ecosystem is divided into different subsystems based on the presence of system-specific processes and properties, and also on the collection, measurement and calculation of data that may differ between different subsystems. Accordingly, three different subsystems are characterised: (1) the *terrestrial system* which includes all land and wetland areas, (2) the *limnic system*, i.e. lakes and rivers, and (3) the *marine system*. The amount of data describing both the abiotic and the biotic parts of the ecosystem has increased considerably since Simpevarp 1.1, and these data are presented in

detail in /Lindborg, 2005/. A brief summary of our present knowledge of the different subsystems is given below. Detailed carbon budgets have been developed for each of the three subsystems and these are presented in Section 4.8.

Terrestrial system

Generally, the vegetation is strongly influenced by the type of bedrock, Quaternary deposits and human land management present. The bedrock in the area mainly consists of granites, and the Quaternary deposits are mainly till, while silt and clay have been deposited in the valleys. This pattern is clearly manifested in the vegetation, where pine forests dominate on till, and all the arable land and pastures are found in the valleys. The wetlands are characterised by mires poor in nutrients. The land management is today mainly restricted to forestry activities that are, among other things, seen as numerous clear-cuts in different success ional stages. Many traces of a more intensive management is seen in the landscape. This is particularly illustrated with the dominating woodland key habitat type that is old semi-natural grasslands or meadows with old pruned deciduous trees in close proximity to old settlements.

The most common mammal species in the Simpevarp regional model area is roe deer (5 deer/km^2). Moose is also fairly common (0.8 moose/km^2), but unevenly distributed, which is normal for this part of Sweden due to hunting pressure, snow depth and distribution of food. European and mountain hare are fairly low in abundance, compared to other regions (see Table 4-5). However a significant part of the mammals in the area is domestic animals and there are 4.3 cows and calves per km^2 in the Simpevarp area. In total, 126 species were found in the regional model area in 2003, and 28 of these are noted in the Red List of endangered bird species in Sweden. The most common species on land are Chaffinch and Great Tit.

Limnic system

The lakes and streams in the Simpevarp regional model area are, as most surface waters in the northern parts of the County of Kalmar, relatively poor in nutrients but rich in organic matter, mainly humic compounds, that give the water a brownish colour. The catchment areas within the regional model area are generally small, which means that some of the streams periodically show very low discharge or are even ephemeral. Most of the streams in the area are more or less affected by human activities, such as straightening or ditching, and many of the present lakes have been lowered in order to reclaim more land for agriculture.

Streams

Generally, the chemical composition of stream water in the regional model area shows only minor differences from typical stream sites in the County of Kalmar. Mean values for major ions and electrical conductivity are somewhat lower for sites in the regional model area, whereas mean values for C/N/P-fractions, and especially for total nitrogen, are somewhat higher for sites in the regional model area. This is partly due to high nutrient concentrations in some sampling points situated in farming areas. Mean values of alkalinity and pH for stream sites in the Simpevarp area are low, especially for upstream sites with small sub-catchment areas.

Lakes

Only a few, relatively small and shallow lakes are situated within the regional model area. The concentrations of nutrients in these lakes are moderate and they can be characterised as mesotrophic with brown water. One larger lake in the northern part of the area, Lake Götemar, shows considerably lower concentrations of nutrients and can be classified as an oligotrophic clearwater lake. Compared to typical values for lakes in the County of Kalmar, the Simpevarp lakes show higher concentrations of ions associated with marine water and of total nitrogen. The buffering capacity of the investigated lakes, measured as HCO_3-concentration, is generally good and the pH values are close to neutral and stable over the season. Accordingly, there are no signs of anthropogenic acidification affecting the lakes.

All lakes develop a thermal stratification during summer, and the oxygen levels in the bottom water become low during stagnant conditions, both in summer and in winter. Despite the relative shallowness, the brown water prevents light from penetrating down to the bottom in the deeper parts, and substantial parts of the bottom in all lakes is free from vegetation. This means that primary production by phytoplankton and submerged macrophytes in the lakes is low, and the limnic food web is to a large extent sustained by energy (i.e. organic carbon) from the terrestrial system.

The fish community of the investigated lakes can be regarded as typical for small brownwater lakes in the area; it is dominated by perch both in number and biomass. Pike and roach occur in all investigated lakes, and the total number of species in a lake varies between 3 and 7.

Marine system

Most of the surface water from the regional model area drains into a few, relatively confined, coastal basins, and the water chemistry of these basins differ considerably from the water chemistry of the outer parts of the archipelago. The marine system in the area can therefore be divided into two different types, the first type representing the open sea and outer archipelago (two sub types), and the second type the relatively confined bays close to the mainland. The bays show lower concentrations of ions than the open sea, whereas the concentrations of organic compounds and nutrients, especially the nitrogen fractions, are considerably higher. As a consequence of the relatively high concentration of organic compounds (humus) in the bays, water transparency is rather low throughout the year. The oxygen concentration in the bottom water of the open sea is high throughout the year, whereas almost anoxic conditions seem to be common in the bottom water of bays in late summer.

From the general survey, different vegetation communities were defined on the basis of dominating species or higher taxa. For the area around Simpevarp, nine vegetation communities were defined. The red algae community covered the largest area with almost 6 million square metres. Second highest coverage was associated with the *Potamogeton pectinatus*-community with an area of almost 2 million square metres. Regarding coverage, the *P. pectinatus* community was followed by the *Chara sp.* and *Fucus vesiculosus*-communities with coverage of about 1.3 and 1 million square metres, respectively.

The benthic fauna in all basins is dominated by detritivores. Detritivores, often *Macoma baltica* or *Hydrobia sp*., often constitutes 50–80% in the three selected basins. In total, 45 species associated with the vegetation occurred in the coastal area of f the Simpevarp subarea and 41 in the sediments. The *Fucus sp*. communities are the most diverse concerning associated fauna and harbour 31 species or higher taxa, whereas the soft bottoms without vegetation have 14 species /Lindborg, 2005/.

11.1.5 Humans and land use

The Simpevarp area is a sparsely populated area located in a relatively lightly populated county. In 2002, the population density was 7.4 inhabitants/km^2, three times lower than in the County of Kalmar as a whole. The demographic statistics show no upward trend, instead there is a slow downward trend in Simpevarp area as well as in the Municipality of Oskarshamn and the County of Kalmar. Most (83.6%) of the people that work within Simpevarp area (employed day-time population) are occupied within the sectors of electricity-, gas- and water supply, sewage and refuse disposal. This dominance is due to the Oskarshamn nuclear power plant (OKG) /Miliander et al. 2004/.

The forests are influenced by active and ongoing forestry; approximately one third of the forests within the regional model area are younger than 30 years. The average age of the productive forest is approximately 53 years. About 1/4 of the logging products are used for pulp production, and the rest as timber. The Simpevarp area is a frequently visited area for outdoor activities, such as hunting, fishing, hiking as well as picking of wild berries and mushrooms /Miliander et al. 2004/.

11.2 Bedrock geological description

In the following subsections, the descriptive models of lithology, deformation zones and geological discrete feature networks (DFN) are presented.

11.2.1 Lithological model

A three-dimensional lithological model for the Simpevarp version 1.2 description consists of 36 rock domains in the regional model area, of which 17 occupies the local scale model area. The modelled rock domains have been distinguished on the basis of their composition, grain size, texture and/or age.

More or less pristine igneous rocks belonging to the c. 1,800 Ma generation of the Transscandinavian Igneous Belt (see Section 3.1) predominate in the Simpevarp regional and local scale model areas. Magma mixing and mingling and diffuse contact relationships are characteristic features. The dominating rock types display a compositional variation between diorite to gabbro and granite. Mean values of recalculated quartz content that are used in the QAPF-diagrams, cf. Section 5.2.2, vary between approximately 11 and 20%. Thus, the true quartz content is lower since only the relative proportions of quartz, alkali feldspar and plagioclase are represented in the QAPF-diagram; other minerals are not accounted for in this diagram. The fine-grained dioritoid that dominates in the southern part of the Simpevarp peninsula has a quartz content that is locally < 5%. The uranium content is low, except for some pegmatites that display a slightly higher content. A conspicuous rock type in the regional model area is a c. 1,450 Ma old granite that occurs in two major bodies, one in the northern (Götemar granite) and one in the southern part (Uthammar granite) of the model area.

Information concerning the properties, e.g. composition, grain size, texture, age and physical properties as well as the uranium content of the dominant rock type, of all 36 rock domains, in accordance with the procedures outlined in Section 5.3.3 is summarised in tables, one for each rock domain (Appendix 6). However, the properties of the three the rock domains are also illustrated in Table 11-1 through Table 11-3. These domains are:

- RSMA01 (Ävrö granite) penetrated by the cored boreholes KSH03A, KAV01, KLX01 and KLX02, which dominates and forms the “matrix“ of the three-dimensional lithological model,
- RSMB01 (fine-grained dioritoid), penetrated by the cored boreholes KSH01A and KSH02, and
- RSMC01 (mixture of Ävrö granite and quartz monzodiorite), penetrated by the cored boreholes KSH01A/B and KSH03A/B.

All rock codes according to SKB’s nomenclature are listed in Appendix 1.

Table 11-1. Properties of rock domain RSMA01 (Ävrö granite).

RSMA01				
Property	**Character**	**Quantitative estimate**	**Confidence**	**Comment**
Dominant rock type (%)	Ävrö granite (501044)	75.8–84.7	High	Quantitative estimate based on occurrence in KSH03A, KAV01, KLX02 and the Äspö tunnel (section 2,265–2,874 m)
Mineralogical composition (%) (dominant minerals)	Quartz	16.4±6.1	High	N=20. Quantitative estimate based on modal analyses of surface samples from the Simpevarp subarea and KSH01A. Mean value ± std
	K-feldspar	18.5±8.0		
	Plagioclase	47.1±7.8		
	Biotite	11.4±5.4		
Grain size	Medium-grained		High	
Age (million years)		1,800	High	
Structure	Isotropic to weakly foliated. Scatttered mesoscopic, ductile shear zones		High	
Texture	Unequigranular to porphyritic		High	
Density (kg/m^3)		2,681±16		N=5. The quantitative estimate is based on surface samples from the Simpevarp subarea. Mean value ± std
Porosity (%)		0.57±0.12		N=5. The quantitative estimate is based on surface samples from the Simpevarp subarea. Mean value ± std
Magnetic susceptibility (SI units)		3.12±0.16		N=5. The quantitative estimate is based on surface samples from the Simpevarp subarea. Average value in logarithmic scale ± std
Electric resistivity in fresh water (ohm m)		4.16±0.18		N=5. The quantitative estimate is based on surface samples from the Simpevarp subarea. Average value in logarithmic scale ± std
Uranium content based on gamma ray spectrometric data (ppm)		4.9±2.2		N=25. The quantitative estimate is based on measurements from the Simpevarp subarea. Mean value ± std
Natural exposure (microR/h)		9.5±1.4		N=25. The quantitative estimate is based on measurements from the Simpevarp subarea. Mean value ± std
Subordinate rock types (%)	Fine- to medium-grained granite (511058)	0.8–21.5	High	Quantitative estimate based on occurrence in KSH03A, KAV01, KLX02 and the Äspö tunnel (section 2,265–2,874 m)
	Pegmatite (501061)	No data		
	Fine-grained dioritoid (501030)	9.0–17.0		
	Diorite to gabbro (501033)	0–1.7		
	Fine-grained mafic rock (505102)	3.0–4.9		
	Quartz monzodiorite (501036)	No data		
Degree of inhomogeneity	Medium		High	Based on outcrop database for the Simpevarp subarea and KAV01, KLX02, KSH03
Metamorphism/alteration (%)	Inhomogeneous hydrothermal alteration (secondary red staining)	14–22	High	Quantitative estimate based on KSH03A, KAV01, KLX02. No data from ther major part of the regional model area
Mineral fabric (type/ orientation)				

Table 11-2. Properties of the rock domain RSMB01 (fine-grained dioritoid).

RSMB01				
Property	**Character**	**Quantitative estimate**	**Confidence**	**Comment**
Dominant rock type (%)	Fine-grained dioritoid (501030)	90.6–94.2	High	Quantitative estimate based on occurrence in KSH01A and KSH02. High confidence that this rock type is dominanting at the Simpevarp peninsula but lower in the western part of the local model area
Mineralogical composition (%) (dominant minerals)	Quartz	7.4±5.0	High	N=21. Quantitative estimate based on modal analyses of surface samples from the Simpevarp subarea, KSH01A and KSH02. Mean value ± std
	K-feldspar	11.3±6.4		
	Plagioclase	51.4±8.7		
	Biotite	14.7±7.6		
	Amphibole	0–14		
	Pyroxene	0–22		
Grain size	Fine-grained		High	
Age (million years)		1,800	High	
Structure	Isotropic to weakly foliated. Scatttered mesoscopic, ductile shear zones		High	
Texture	Unequigranular		High	
Density (kg/m^3)		2,803±52		N=5. The quantitative estimate is based on surface samples from the Simpevarp subarea. Mean value ± std
Porosity (%)		0.29±0.11		N=5. The quantitative estimate is based on surface samples from the Simpevarp subarea. Mean value ± std
Magnetic susceptibility (SI units)		3.22±0.84		N=5. The quantitative estimate is based on surface samples from the Simpevarp subarea. Average value in logarithmic scale ± std.
Electric resistivity in fresh water (ohm m)		4.58±0.41		N=5. The quantitative estimate is based on surface samples from the Simpevarp subarea. Average value in logarithmic scale ± std
Uranium content based on gamma ray spectrometric data (ppm)		3.7±1.8		N=14. The quantitative estimate is based on measurements from the Simpevarp subarea. Mean value ± std
Natural exposure (microR/h)		11.0±3.3		N=14. The quantitative estimate is based on measurements from the Simpevarp subarea. Mean value ± std
Subordinate rock types (%)	Quartz monzodiorite (501036)	0–3.5	High	Quantitative estimate based on occurrence in KSH01A and KSH02
	Fine-to medium-grained granite (511058)	0.9–6.7		
	Pegmatite (501061)	0.8–1		
	Fine-grained mafic rock (505102)	0.6–0.8		
Degree of inhomogeneity	Medium		High	Based on outcrop database for the Simpevarp subarea, KSH01and KSH02
Metamorphism/alteration (%)	Inhomogeneous hydrothermal alteration (secondary red staining)	13–24	High	Quantitative estimate based on KSH01 and KSH02
Mineral fabric (type/ orientation)				

Table 11-3. Properties of rock domain RSMC01 (mixture of Ävrö granite and quartz monzodiorite).

RSMC01				
Property	**Character**	**Quantitative estimate**	**Confidence**	**Comment**
Dominant rock type (%)	Quartz monzodiorite (501036)	51.5–73.9	High	Mixture of 501036 and 501044. Quantitative estimate based on occurrence in KSH01A and KSH03A
	Ävrö granite (501044)	22.9–34.1		
Mineralogical composition (%) (dominant minerals)				Cf. RSMA01 and RSMD01
Grain size				Cf. RSMA01 and RSMD01
Age (million years)		1,800	High	
Structure				Cf. RSMA01 and RSMD01
Texture				Cf. RSMA01 and RSMD01
Density (kg/m^3)				Cf. RSMA01 and RSMD01
Porosity (%)				Cf. RSMA01 and RSMD01
Magnetic susceptibility (SI units)				Cf. RSMA01 and RSMD01
Electric resistivity in fresh water (ohm m)				Cf. RSMA01 and RSMD01
Uranium content based on gamma ray spectrometric data (ppm)				Cf. RSMA01 and RSMD01
Natural exposure (microR/h)				Cf. RSMA01 and RSMD01
Subordinate rock types (%)	Fine-grained dioritoid (501030)	6.5	High	Quantitative estimate based on occurrence in KSH01A and KSH03A
	Fine- to medium-grained granite (511058)	1.8–4.2		
	Granite (501058)	2.0		
	Fine-grained mafic rock (505102)	1.2		
	Pegmatite (501061)	0.3–1.4		
	Diorite to gabbro (501033)	0.2		
Degree of inhomogeneity	High		High	Based on outcrop database for the Simpevarp subarea, KSH01A, B and KSH03A, B
Metamorphism/alteration (%)	Inhomogeneous hydrothermal alteration (secondary red staining)	19.1–39.7	High	Based on outcrop database for the Simpevarp subarea, KSH01A, B and KSH03A, B. Quantitative estimate based on occurrence in KSH01A and KSH03A
Mineral fabric (type/ orientation)				

The three-dimensional lithological models of the Simpevarp regional and local scale domains are displayed in Figure 11-1 and Figure 11-2, respectively. The rock domains in the modelled three-dimensional geometry of the *regional scale model volume* are dominated by:

- a mixture of porphyritic granite to quartz monzodiorite (Ävrö granite) and medium- to coarse-grained granite (RSMA01),
- fine-grained and medium- to coarse-grained granite (Götemar-type; RSMG01–02),
- quartz monzodiorite (RSMD01–06),
- diorite to gabbro (RSME01–18)

as displayed in Figure 11-1. In the *local scale model volume*, the modelled rock domains are dominated by:

- porphyritic granite to quartz monzodiorite (Ävrö granite; RSMA01),
- quartz monzodiorite (RSMD01),
- fine-grained dioritoid (RSMB01–04),
- a mixture of porphyritic granite to quartz monzodiorite (Ävrö granite) and quartz monzodiorite (RSMC01)

as presented in Figure 11-2, Figure 11-3 and Figure 11-4. With the exception of the local occurrence of low-grade, ductile to brittle-ductile shear zones, commonly of mesoscopic character, and a locally developed weak foliation, all rock types in the rock domains are more or less structurally well preserved.

As can be seen in Figure 11-1, Figure 11-2 and Figure 11-5 the rock domain RSMA01 dominates and constitutes the main “matrix” in both the regional and local scale model volumes.

The eastward extent at depth of the rock domain RSMB01 is based on the documented occurrence of fine-grained dioritoid between approximately 322 and 631 metres in the cored borehole KSH01A (cf. Figure 11-3, Figure 11-4 and Section 5.2.7).

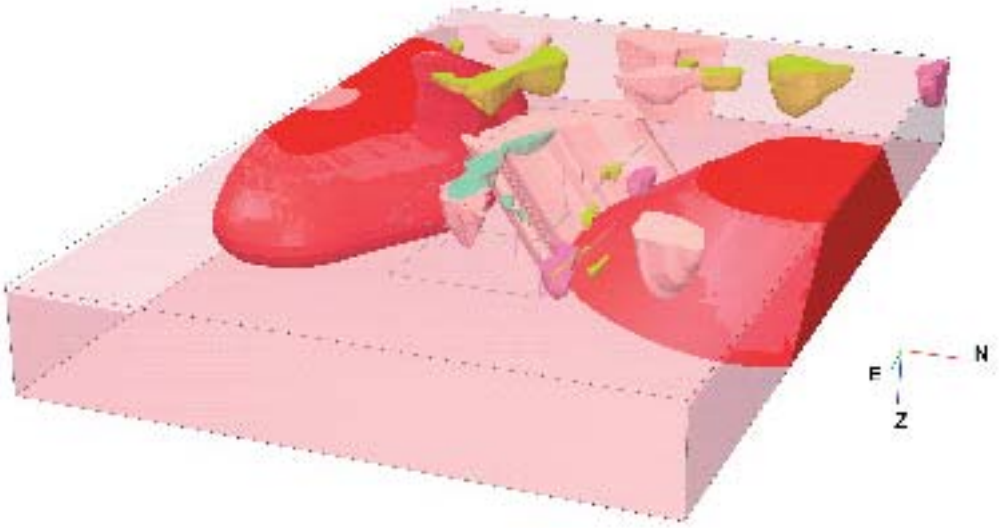

Figure 11-1. *Rock domain model for the Simpevarp 1.2 regional model domain seen from the eastnortheast. The dominant rock type in each domain is illustrated with the help of different colours (see the rock domain map at the surface in Figure 5-43). Outline of local model domain provided in the centre of the regional model domain.*

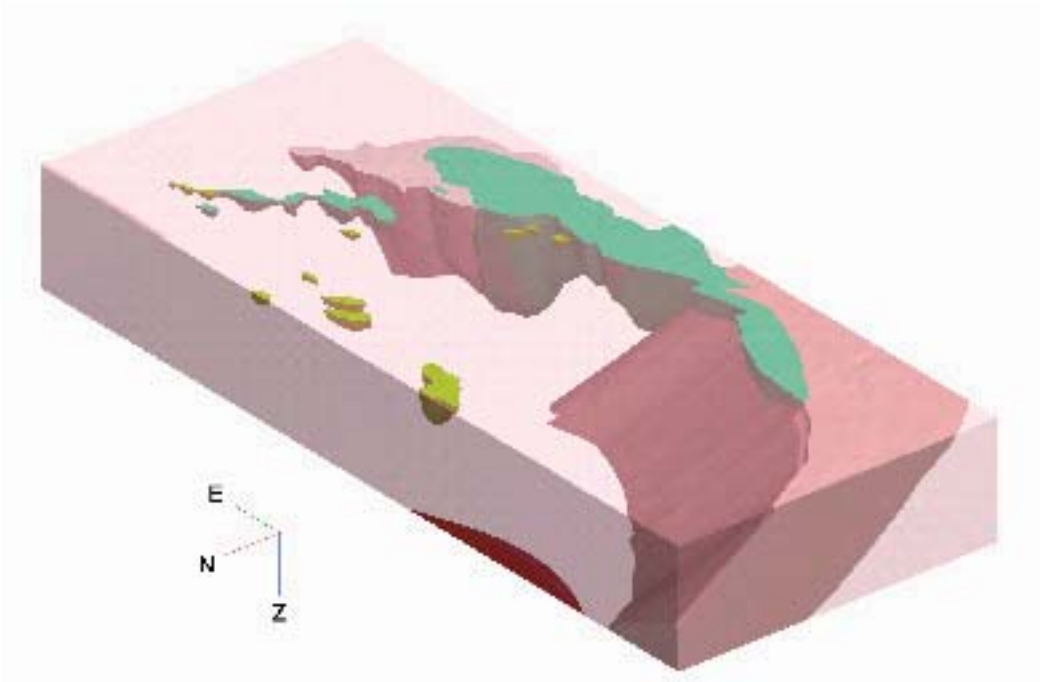

Figure 11-2. *Rock domain model for the Simpevarp 1.2 local scale model domain seen from the northwest. The dominant rock type in each domain is illustrated with the help of different colours (see the rock domain map at the surface in Figure 5-43).*

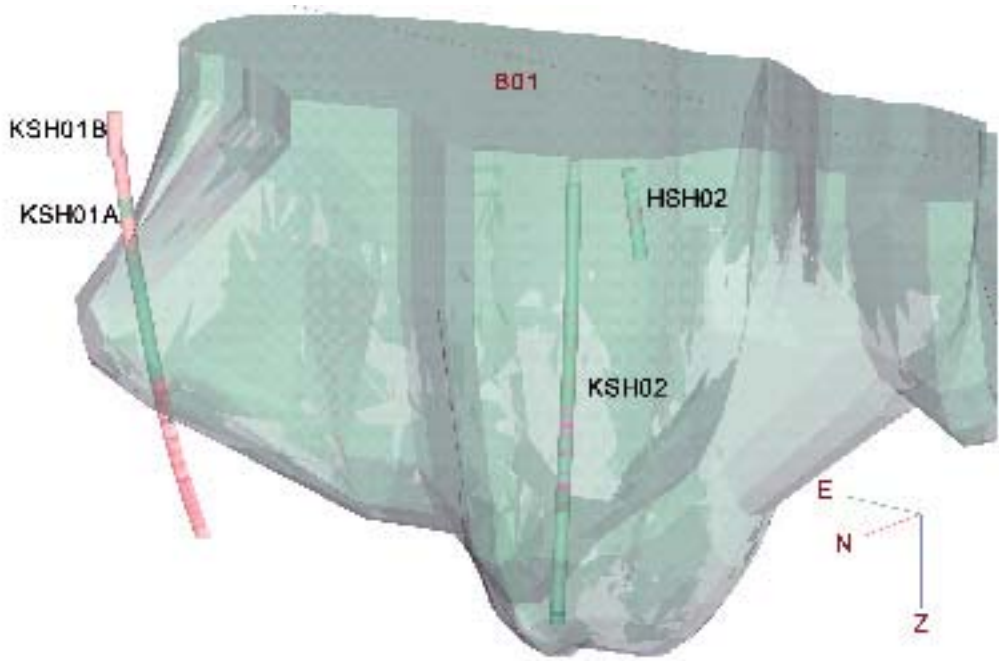

Figure 11-3. *Rock domain RSMB01 that is dominated by fine-grained dioritoid. Simpevarp peninsula. View from the northwest.*

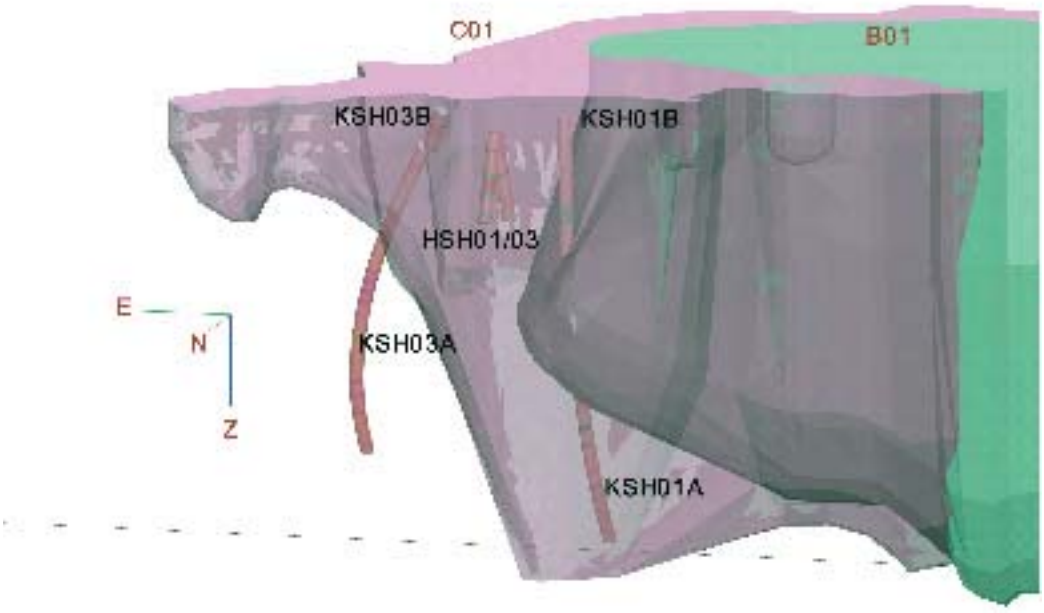

Figure 11-4. *Rock domain RSMC01 which is characterised by a mixture of porphyritic granite to quartz monzodiorite (Ävrö granite) and quartz monzodiorite. Note the geometrical relationship to the fine-grained dioritoid in rock domain RSMB01 and rock domain RSMA01 that occupies the lower part of the cored borehole KSH03A. Eastern part of the Simpevarp peninsula and southern part of Ävrö. View from the north.*

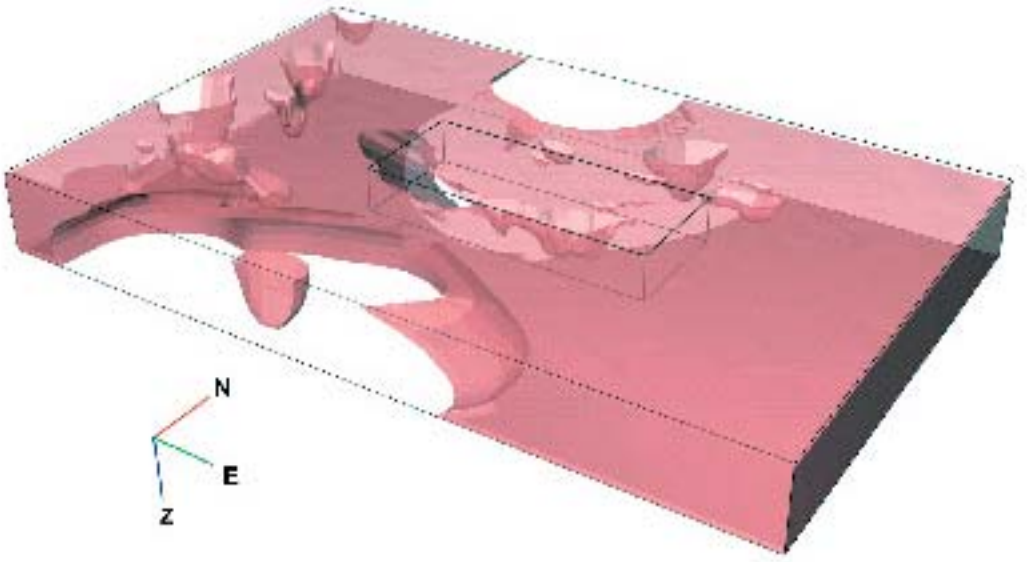

Figure 11-5. *Rock domains RSMA01 and RSMA02 (the isolated small domain in the foreground). View from the southeast. Regional scale model domain with outline of local scale model domain.*

An important result of the present geometrical modelling is that the Götemar granite, apart from occupying a large part of the regional model volume, also occupies the lowermost northern part of the local scale model volume in the Laxemar subarea (Figure 11-2).

The degree of inhomogeneity in the rock domains is related to the frequency of subordinate rock types. Of these, the fine- to medium-grained granite, and to some extent also pegmatite, are the most important ones. They are treated qualitatively and, based on the present state of knowledge, they are judged to be more or less homogeneously distributed within the entire regional and local scale model volumes. Accordingly, they are presumed to occur in all rock domains, though there might be local internal variations in frequency (cf. Section 5.3.3).

The remaining subordinate rock types occur much less frequently. Locally, inclusions or minor bodies of diorite to gabbro and enclaves of intermediate to basic composition are characteristic in the Ävrö granite in the Simpevarp subarea in rock domain RSMA01. However, as pointed out in Section 5.2, it must be noted that the available information on the amount of subordinate rock types is very limited outside the Simpevarp subarea, i.e. in the regional model area including the Laxemar part of the local scale model area.

The red staining (hydrothermal alteration) which is a ubiquitous characteristic in conjunction with fracturing throughout the Simpevarp subarea is presumed to be homogeneously distributed in the eastern part of the local scale model volume (cf. Section 5.3.3). Whether the red staining is characteristic also for the remaining part of the local scale and the regional model area will be treated in the Laxemar SDM 1.2 report.

There are limited site investigation surface data available in the western part of the local scale model area west of the Simpevarp subarea. In this area, the compilation of the bedrock data at the surface, completed in conjunction with the version 0 /SKB, 2002b/, has formed the basis for the Simpevarp 1.2 three-dimensional rock domain model. Furthermore, it must also be emphasised that the offshore area is totally devoid of bedrock geological information. Accordingly, the variation in the quality of the surface geological data and the restricted subsurface information are the two most important factors that govern the uncertainties associated with the modelling of the 36 rock domains. This uncertainty will to a great extent persist in the descriptive modelling of the local scale model area, and particularly for the regional model area, also for the Laxemar 1.2 descriptive model. Based on available information, a judgement concerning the confidence of the occurrence and geometry of individual rock domains was presented earlier (Section 5.1.3). To summarise, the confidence of occurrence and geometry of the rock domains at the surface is judged to be medium to high in the part of the local scale model area that is covered by the bedrock map of the Simpevarp subarea, and low to medium outside the Simpevarp subarea.

The bedrock geological information in the available cored boreholes is highly important and has been utilised in the 3D lithological modelling (cf. Figure 11-3 and Figure 11-4). However, it must be pointed out that a contact between two specific rock domains in a cored borehole is “point information”. Thus, the geometrical relationship between the actual rock domains in the remaining part of the model volume is still associated with high uncertainty. Due to the restricted subsurface information, especially outside the Simpevarp subarea, the confidence of occurrence and geometry at depth is medium to low for most rock domains, except for the dominating rock domain RSMA01 which forms the matrix in the local scale model volume. However, the geometrical relationships between rock domain RSMA01 and the other rock domains, in particular the major rock domains, are highly uncertain. For instance, the geometry at depth of the rock domains RSMG01 (Götemar granite) and RSMG02 (Uthammar granite) is based on gravity modelling /Nisca, 1987/ that in turn is based on sparse gravity data. However, the available information strongly indicates an outward dip of the contacts from the centre of the bodies into the surrounding rock domains.

In Simpevarp 1.1, one alternative to the developed “base case” local scale lithological model was constructed /SKB, 2004b/. In the alternative rock domain model, the contacts between rock domain RSMA01 and the rock domains RSMB01, RSMB03, RSMC01 and RSMD01 were modelled with vertical contacts to the bottom of the local scale model volume. The minor rock domains were retained with a modelled depth extent that equalled their widths at the surface. Similarly, the same assumption could be adopted outside the Simpevarp subarea for rock domains with a width at the surface that exceeds 2 kilometres and where no subsurface information exists. However, no such

model has been constructed in the Simpevarp version 1.2 SDM. Besides the above mentioned alternative assumption, no alternative modelling concept has been considered at the present stage of the site descriptive modelling. However, an infinite number of varieties of the adopted concept are possible. This merely reflects the restricted subsurface information that constrains the geometric relationships between the different rock domains. A presentation of these possibilities is not motivated.

11.2.2 Deterministic model of deformation zones

A three-dimensional deformation zone model, which consists of 22 high confidence and 166 possible deformation zones in the whole regional model domain is presented for the Simpevarp 1.2 description. Deformation zones with a length of 1 km or more in the local model domain and zones with a length of 1.6 km or more in the regional model domain are addressed. The data coverage in the regional scale model domain does not permit the same high level of resolution as in the local scale model domain. Existing old structural models, a variety of new surface and sub-surface data, and new linked lineament data from a larger area have been used in the modelling procedure. For this model version, the linked lineaments have also been further post-processed to reflect geology better and minimise effects of differences in data coverage over land and sea.

Deterministic model of interpreted deformation zones

Several of the interpreted deformation zones have been modelled in segments, due to either geological reasons or due to assessments of confidence inherent in the associated linked lineaments. For this reason, there are 208 underlying zone segments. Twenty-two deformation zones, for which there are supporting geological and geophysical data, are judged to have a high level of confidence for their occurrence. However, the majority of deformation zones in the deformation zone model are based solely on the interpretation of linked lineaments. The confidence as to occurrence of these zones is judged to be possible. The previous model version /SKB, 2004b/ differentiated these zones according to the strength of the lineament expressions. However, it is considered that the way linked lineaments are interpreted makes further differentiation difficult, especially after subsequent post-processing. Therefore, all deformation zones without direct evidence of existence are classified as possible in this model version. The group of 166 possible deformation zones, attributed low or intermediate confidence of occurrence, are interpreted mainly in the western part of the local scale model area, and in larger parts of the regional scale model area. These areas are characterised by a low information density and a high degree of uncertainty.

Detailed information concerning the properties of the deformation zones, in accordance with the procedures outlined in Section 5.4.3, are summarised in a series of tables (Appendix 4). A sample property sheet of the 22 high-confidence zones is illustrated in Table 11-4.

The deformation zone model for the twenty-two high confidence deformation zones is presented in Figure 11-6 (local model domain) and Figure 11-7 (regional model domain). These zones are supported by a variety of geological and geophysical information and are to a lesser extent governed by the interpretation of linked lineaments. Two important types of deformation zones are present within this group:

- Important Regional major deformation zones with northeasterly strike, confirmed already in model version 0 or in other previous models established in the Simpevarp area.
- Local major fracture zones, which have been confirmed either by new borehole information or in previous models in the Simpevarp area.

Smaller zones and fractures , with a surface extent of less than 1 km have not been included deterministically in the model, but are handled in a stochastic way through DFN models.

The Mederhult zone (ZSMEW002A) and the Äspö shear zone (ZSMNE005A), are the two most well known regional deformation zones in the Simpevarp subarea. Low-grade mesoscopic, ductile to brittle-ductile deformation are present along both these zones. Their interpreted lengths suggest that both zones extend to the base of the regional model volume. Kinematically, the Äspö shear zone is characterised by a sinistral strike-slip component of movement. There are also other, smaller ductile

high strain zones in the Simpevarp subarea, usually NE-SW and ENE-WSW striking decimetre wide vertical zones or alternatively with moderate dips /Bergman et al. 2000/. Based on their structural and tectonic similarities, as well as their spatial interrelations, these structures are likely to be related to the Äspö shear zone.

Table 11-4. Properties of fracture zone ZSMNE005A (Äspö shear zone).

ZSMNE005A (Äspö shear zone)					
Property	**Quantitative estimate**	**Span**	**Confidence level**	**Basis for interpretation**	**Comments**
Position		+/–50 m	medium	Linked lineaments, v0	
Orientation (strike/dip)	40/80	dip 70–90 NW ductile sinistral; 60–90 SE brittle dextral	high	Linked lineaments	Ref: NEHQ3, EW1b Geomod; ZSM0005A0, ZSM0004A0 v0; ZLXNE01 Lax'
Width	40 m	Ductile 10–40 m Brittle 70–200 m	high	v0	
Length	5.1 km		low	Linked lineaments	
Ductile deformation	Mylonitic		high	Field data, Äspö data	
Brittle deformation	Cataclastic		High	Field data, ground geophysics, Äspö data	
Alteration	Not yet assessed				
Fracture orientation	Not yet assessed				
Fracture frequency	Not yet assessed				
Fracture filling	Not yet assessed				

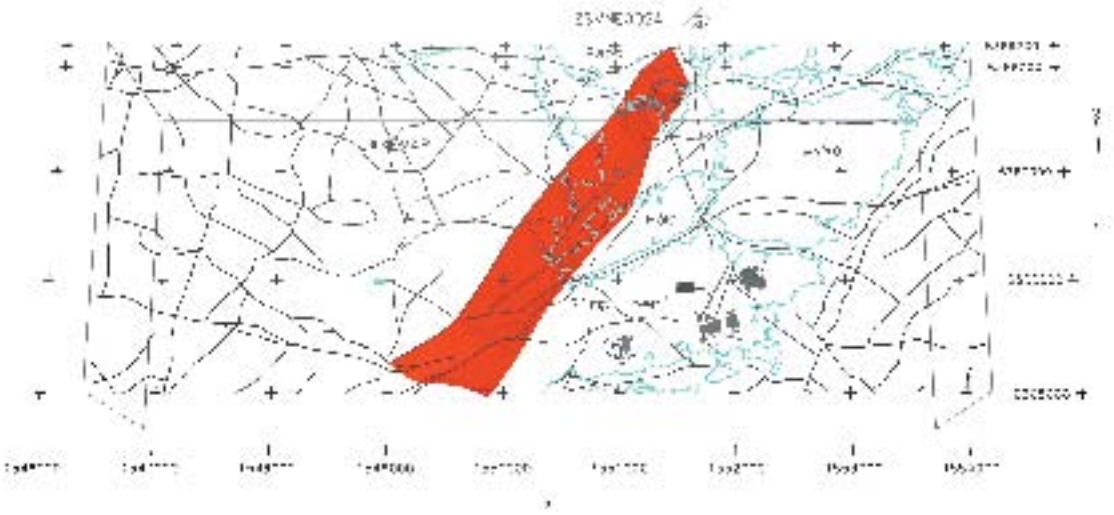

[1] Concerns total length. Extends outside local scale model domain.

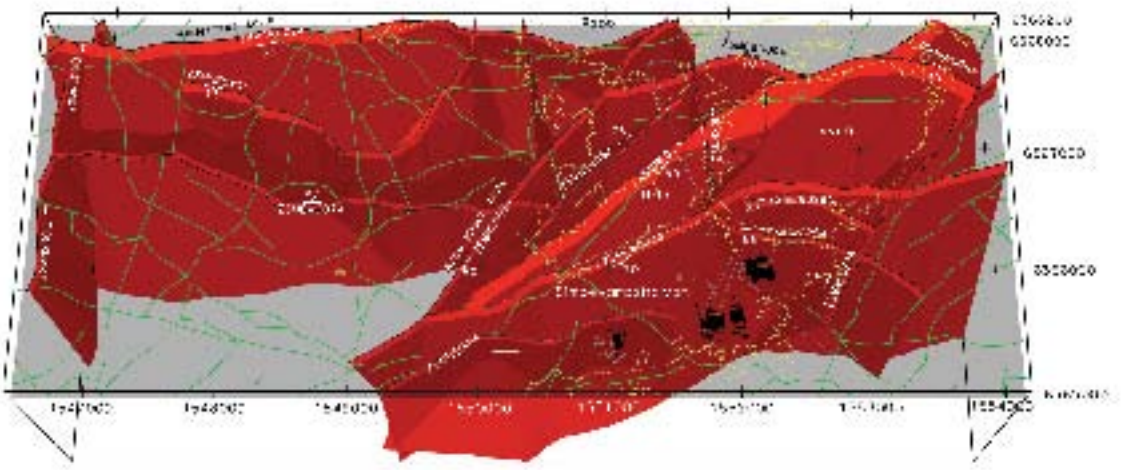

Figure 11-6. *Simpevarp 1.2 deformation zone model of the local model domain showing the interpreted twenty-two deformation zones supported by geological and geophysical data and judged to have a high confidence of occurrence. This figure may be compared with Figure 7-10 in the Simpevarp 1.1 SDM report /SKB, 2004b/.*

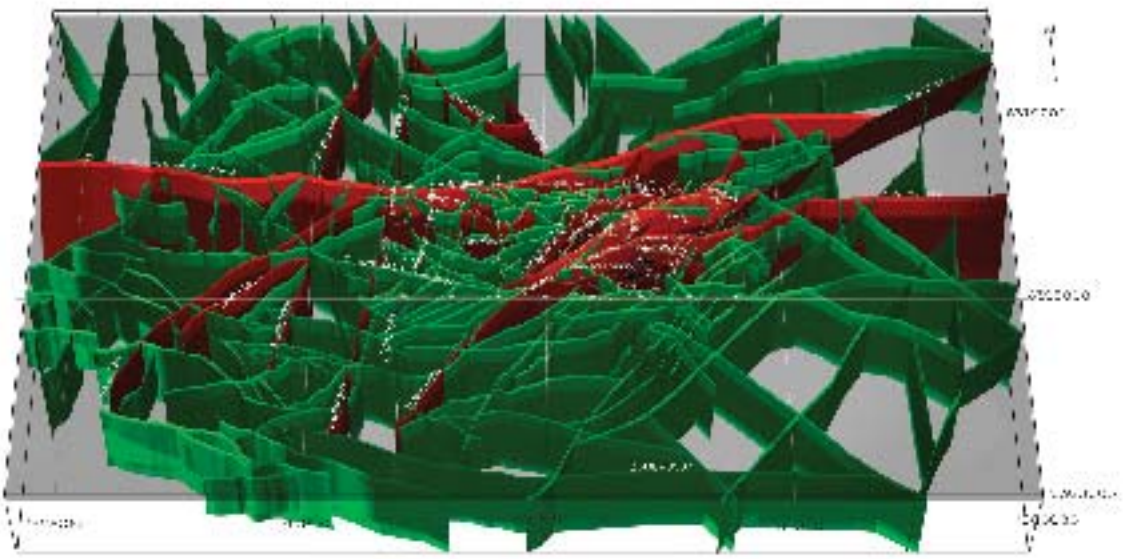

Figure 11-7. *Simepvarp 1.2 regional model domain with interpreted high confidence and possible deformation zones. Interpreted high confidence zones indicated in red, possible zones in green.*

A number of local major zones are also well established in the Simpevarp area, of which most of them have been characterised through investigations performed in and around the Äspö and Ävrö Islands. For example, the local major (or possibly regional) zone ZSMNE024A, which trends along the coast line of Ävrö, is interpreted to dip around 70 degrees towards the NW (underneath the Ävrö island), cf. Figure 11-6 and Figure 11-8. This zone has been better defined in this model version through observations in KSH03A and through a series of strong offshore magnetic and topographic anomalies immediately east of Ävrö and the Simpevarp peninsula. This zone together with other zones located more to the south east seem to form a belt of brittle-ductile deformation zones following the east coast line of Ävrö and the Simpevarp peninsula.

The northern coastline of the Ävrö island is bounded by zones ZSMNW004A and ZSMNE012A (NE4 in Äspö HRL terminology), both of which dip south to southeast. These zones, together with zone ZSMNE024A (dipping to the northwest under the Simpevarp peninsula and the Ävrö island), seem to form a relatively narrow wedge beneath Ävrö extending to around 800 m depth.

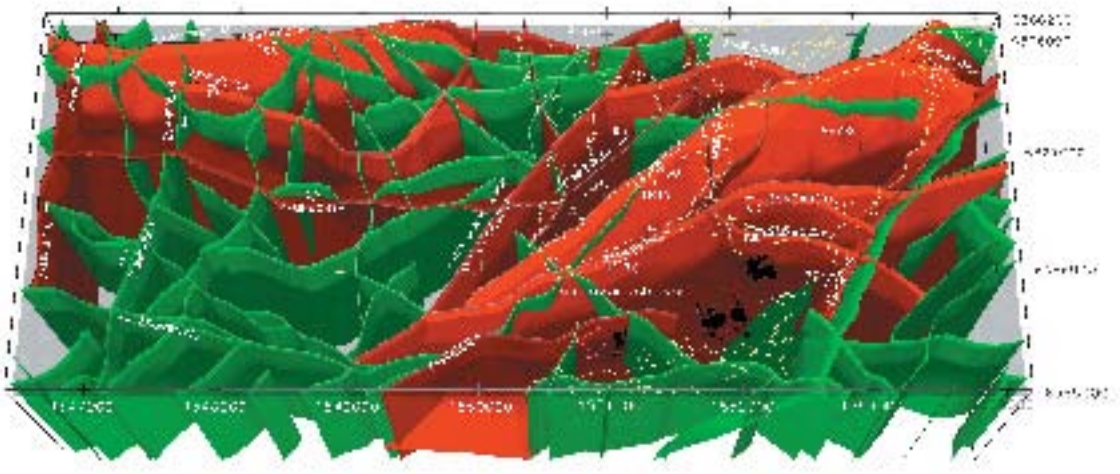

Figure 11-8. *Simepvarp 1.2 local model domain with interpreted high confidence and possible deformation zones. High confidence zones indicated in red, possible zones in green.*

The detailed tectonic evolution of the deformation zones in the model is not well established, and hence little is known about the mutual terminations and sequence of mechanical formation of the individual zones. The interpreted linked lineaments have been used as guide where evidence is lacking. There are several cases where different interpretations can be made to reflect other tectonic sequences. For example, the local major deformation zone ZSMNE040A is interpreted to possibly reflect the curved nature of other lineaments surrounding the near-circular outcrop of the Götemar granite. The modelled curvature of this deformation zone could be connected to tectonic uplift of the host rock at the time of emplacement of the Götemar granite. However, this tectonic interpretation is not supported by any field evidence and is considered to be weak,

The twenty-two deformation zones with high confidence are complemented with 166 possible deformation zones that are based at least in part, on distinct, low-magnetic or topographic lineaments, cf. Figure 11-8 (local model).

The interpreted deformation zones recognised solely on the basis of linked lineaments have been grouped into four different orientation sets − NW, NE, NS and EW. The zones striking NE and EW dominate. The above four principal orientations of deformation zones were identified already in the SDM version 0 /SKB, 2002b/. The occurrence of distinct fracture orientation sets striking NE and EW (cf. Section 5.2.4) provides support for the inference that at least linked lineaments with these orientations represent deformation zones.

Besides the question marks concerning the occurrence of these interpreted possible deformation zones, a key uncertainty concerns their dip. As a consequence, all possible zones have been modelled with a preferential vertical dip.

The along-strike continuity of nearly all the interpreted vertical or steeply dipping deformation zones, irrespective of their confidence of occurrence, is governed by the interpretation of the length of the linked lineament that is related to the deformation zone. It is considered probable that the number of smaller segments that are present along an individual interpreted deformation zone has been underestimated. Such segments may be associated with shorter zones arranged, for example, in an *en echelon* manner along the main zone direction. It is difficult to resolve the individual breaks between such segments, bearing in mind the uncertainty inherent in the location of the lineaments. It is considered likely that the true continuity in the strike direction of many of the deformation zones interpreted in the current Simpevarp 1.2 deformation zone model is far less than is indicated in the produced maps. The recognition of separated segments along the same zone may have important implications in subsequent safety analyses.

Evident from the presented visualisations of the deformation zone model, is that the majority of interpreted “possible” deformation zones are located in the western part of the local model area, corresponding to the Laxemar subarea, areas covered by the Baltic Sea, and larger parts of the regional scale model area. This distribution reflects the uncertainties which largely are associated with the distribution of data/information in the modelled area.

Alternative structural model

No alternative structural model of interpreted deformation zones has been produced for the Simpevarp 1.2 site-descriptive model. Key issues, such as the existence of sub-horizontal zones in Simpevarp or Laxemar may be targets for alternative model development in the future incorporation of new data (especially from reflexion and refraction seismics, and old existing data from Ävrö and Äspö, not yet incorporated in the analysis.

Finally, it should be stated that considerable more work is required to relate more closely the different sets of fracture orientations (see Section 5.5), the different groups of mineral fracture fillings, kinematic data along the various deformation zones and the geological evolutionary model. In this way, a better understanding of the timing of brittle deformation in the Simpevarp area may be achieved.

11.2.3 Statistical model of fractures and deformations zones

The geological data available in cored and percussion boreholes, outcrops and lineament maps have been used to calculate geometrical parameters for geological DFN models within the local model domain.

Major conceptual and data uncertainties have been quantified with the exception of uncertainties as to how fracture intensity and size might vary by rock domain.

The fracturing, both open and sealed, outside of deformation zones, is characterized by six subvertical sets and one horizontal set. There are two possible conceptual models concerning the vertical sets. Alternative Model 1 relates three of these sets to three lineament sets, while the other three are unrelated to lineament sets. In Alternative Model 2, all six vertical sets are related to lineament sets.

The differences between Alternative Models 1 and 2 are in how orientations and size are specified for the DFN model. In Model 1, the three lineament-related sets have mean strikes equal to the local trend of the lineaments, while the three unrelated sets have mean orientations that are fixed throughout the model region. The sizes of the sets unrelated to lineaments are based only on matching outcrop trace lengths, and as such, are very much smaller than the lineament-related sets. On the other hand, the orientations for all six sets in Alternative Model 2 have mean orientations related to the trends of nearby lineaments, and do not have constant mean orientations throughout the model region. In addition, the sizes of the three previously unrelated sets, as they are now lineament related, have a much larger size range.

The mass dimensions of the facture traces suggest that fracture intensity does scale with area, at least for some sets. This implies that a simple Poissonian spatial model may not be appropriate for extrapolating fracture intensities measured in outcrop or borehole to models at the kilometre scale. It also suggests that the trace length distributions derived from the mass dimension renormalisation, rather than the Euclidean renormalisation, more accurately quantify the size distribution of most of the fracture sets.

The orientations of the sub-vertical fractures are relatively constant with depth.

There are distinct zones of higher and lower fracture intensity in the borehole fracture data logs. These zones are of varying length, and can range from a few meters to hundreds of meters. Furthermore, these zones are preferentially associated with certain rock types, rock domains and alteration zones. This implies that the fracture intensity of the DFN model can be further subdivided by rock domain or lithology, both to reduce uncertainty and to reproduce the measured data with minimised error.

There is no evidence for, and much evidence against, the hypothesis that there is recent fracturing within a few tens of meters of the surface due to e.g. glacial unloading, surficial stress unloading or other mechanisms. Rather, all evidence to date from the boreholes suggests that zones of high and low fracture intensity do exist, but may have formed at a much older time, probably prior to 1,700 Ma before present.

Sub-vertical sets are estimated only from surface observations. Verification tests show that simulated intensity for subvertical sets are about 50% (all fractures) to an order of magnitude (open fractures) smaller than that observed in boreholes. The major reason for this may be due to the difference in resolution in mapping of fractures in outcrop and in boreholes. If the intended use of the DFN model is to estimate sub-vertical intensity in boreholes, it is suggested that the minimum radius of the powerlaw size distributions is lowered to 5–10 cm when simulating fractures.

Sub-horizontal fractures are estimated partly on surface data (size) and partly on borehole data (orientation and intensity). Verification tests show that simulated sub-horizontal fractures are currently overestimated about two times compared to observations in boreholes. The main reason for this may be the poor definition of subhorizontal fracture orientation and the size estimation. Relatively small samples of subhorizontal traces from outcrop have been used for estimating size, and these traces are considered to be highly uncertain due to the low angle of intersection with the outcrops. The orientation of the subhorizontal set is estimated by hard sector definition based on compiled borehole data. The hard sector definition is converted to a Fisher distribution in the model. When simulating fractures, this approach may produce a higher intensity than what was intended. If the intended use of the DFN model is to estimate open and sealed sub-horizontal fracture intensity in boreholes, it is currently suggested to lower the estimated intensity for sub-horizontal fractures by 50%. Complete conditioning of the sub-horizontal set has not been performed due to time constraints and needs to be pursued in coming model versions.

The quantified conceptual models, models 1 and 2 compiled in two tables, Table 11-5 and,Table 11-6 showing best estimates of each parameter. More details of each parameter can be found in earlier chapters of the report or in /Lapointe and Hermanson, 2004/.

Table 11-5. Summary table for conceptual DFN model, Alternative Model 1.

Orientation				Size		Intensity, all fractures*			Intensity, open fractures*		
Set Name	MeanPole Trend/Plunge/ Dispersion	Model/K-S	Relative % of total population of fractures (Terzhaghi corrected)	Size model preferred	Radius Powerlaw (kr/Xr0) or Lognormal (mean, stdev in arithmetic space)	A	B	C	A	B	C
NNE-NE	118.0/1.9/17.3	Fisher Not significant	16.64%	Powerlaw	2.58/0.23	0.4	0.92	0.59	0.09	0.13	0.15
EW-WNW	17.1/7.3/11.2	Fisher Not significant	15.55%	Powerlaw	2.80/0.23	0.37	0.86	0.55	0.08	0.12	0.15
NW-NNW	73.1/4.7/13.7	Fisher Not significant	19.71%	Powerlaw	2.87/0.31	0.47	1.09	0.70	0.11	0.16	0.18
BGNE	326.3/5.5 K1:17.65 K2:18.14	Bivariate Fisher 0.041/45.4%	16.29%	Lognormal	0.48/0.55	0.39	0.9	0.58	0.09	0.13	0.15
BGNS	96.8/3.8/20.32	Fisher Not significant	13.53%	Lognormal	0.67/0.82	0.32	0.75	0.48	0.07	0.11	0.12
BGNW	22.1/2.4 K1:5.36 K2:6.66	Bivariate Fisher 0.051/61.3%	5.88%	Lognormal	0.45/1.00	0.14	0.33	0.21	0.03	0.05	0.05
SubH**	33/86/31.3	Fisher	12.40%	Lognormal	0.57/1.86	0.92	2.8	2.01	0.49	0.73	0.43

* Intensity of sub-vertical fractures based on surface data, and intensities will not fit with borehole data. See text.

** Sub-horizontal set is poorly constrained and intensity of sub-horizontal data is over estimated. See text.

Table 11-6. Summary table for conceptual DFN model, Alternative Model 2.

Orientation				Size		Intensity, all fractures*			Intensity, open fractures*		
Set Name	MeanPole Trend/Plunge/ Dispersion	Model/K-S	Relative % of total population of fractures (Terzhaghi corrected)	Size model preferred	Radius Powerlaw (kr/Xr0) or Lognormal (mean, stdev in arithmetic space)	A	B	C	A	B	C
NS	99.7/6.9/9.63	Fisher Not significant	12.04%	Powerlaw	2.77/0.35	0.29	0.67	0.43	0.06	0.09	0.11
NE	128.4/2.6/8.92	Fisher Not significant	10.79%	Powerlaw	2.58/0.23	0.26	0.6	0.38	0.06	0.09	0.10
ENE	331.7/5.4/10.2	Fisher Not significant	20.78%	Powerlaw	2.77/0.36	0.5	1.15	0.73	0.11	0.16	0.19
EW	6.0/3.1/6.97	Fisher Not significant	13.80%	Powerlaw	2.80/0.23	0.33	0.77	0.49	0.07	0.11	0.12
NW	39.0/0.7/7.78	Fisher Not significant	18.54%	Powerlaw	2.82/0.28	0.44	1.03	0.65	0.1	0.15	0.17
NNW	74.5/9.2/9.17	Fisher Not significant	11.65%	Powerlaw	2.87/0.31	0.28	0.65	0.41	0.06	0.09	0.11
SubH**	33/86/31.3	Fisher	12.40%	Lognormal	0.57/1.86	0.92	2.8	2.01	0.49	0.73	0.43

* Intensity of sub-vertical fractures based on surface data, and intensities will not fit with borehole data. See text.

** Sub-horizontal set is poorly constrained and intensity of sub-horizontal data is over estimated. See text.

11.3 Rock mechanics description

11.3.1 Mechanical properties

The mechanical properties are described separately for intact rock, single fractures and for rock mass in the different lithological domains and in deformation zones, Figure 11-9. A detailed description is found in Chapter 6 and a summary is given in the following sections.

Intact rock

The rock types in the model area are crystalline and show the typical stiff, strong and brittle behaviour of crystalline rocks, often found in Sweden. The main rock types occurring in the local model area are expected to have a mean Young's modulus of 80–85 GPa. The mean uniaxial compressive strength (UCS) is expected to be 210 MPa for the fine-grained dioritoid and somewhat lower, 165 MPa, for other rock types. The crack initiation strength is about 47% of the UCS.

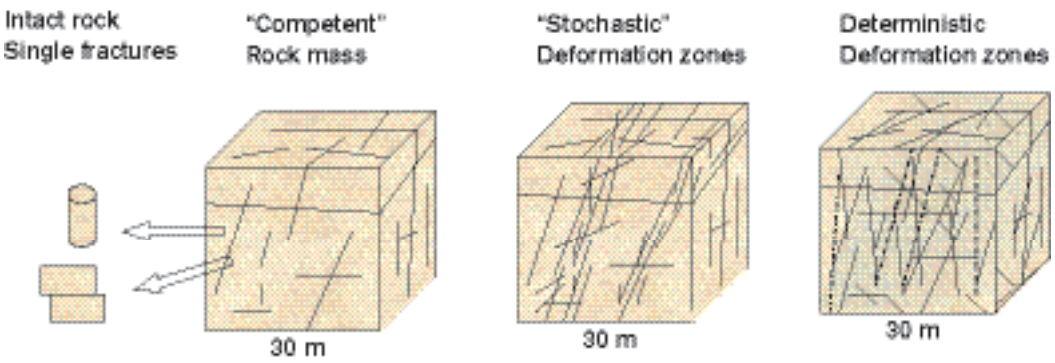

Figure 11-9. *The components of the rock mechanics description.*

The description is provided as truncated normal distribution functions for all parameters, where the standard deviation value describes the variation within the rock type and the truncation values give the expected most extreme values. The standard deviation for Young's modulus is 10 GPa, while the standard deviation for UCS is 50 MPa for fine-grained dioritoid and 30 MPa for other rock types.

For the Poisson's ratio, estimated Mohr-Coulomb strength parameters and the complete description refer to Table 6-5.

Single fractures

The single fracture mechanical properties are described by the Mohr-Coulomb fracture model, using the parameters peak friction angle and cohesion. The available data have not revealed any clear differences between different sets of fractures, and the description therefore applies to all fractures. The mean friction angle is estimated to be 32 degrees with a standard deviation of 4 degrees. The cohesion is described as a function of the friction angle, giving a mean value of 0.5 MPa.

The fracture samples tested show high normal stiffnesses, in the range from 49 to 179 MPa/mm with a mean value of 100 MPa/mm (this description applies to normal stress levels above 0.5 MPa). The shear stiffness is about three times lower than the normal stiffness. For more details cf. Table 6-6.

Rock mass equivalent properties

For Repository engineering and Safety assessment it will be necessary to study the rock mechanics effects for both large and small scales. On the large scale, rock mass is commonly regarded as a continuous material, even though it consists of intact rock and fractures. Such equivalent continuum material properties were also estimated as a part of the description of the rock mass.

The resulting model parameters for the rock mass are given as truncated normal distributions, as for the intact rock. Both the deformation modulus and the Poisson's ratio require estimation with due respect to the stress conditions, as they are stress-dependent parameters. However, above 10 MPa confining stress, the parameters are considered constant in this descriptive model.

The mean for the deformation modulus at depth is 61–62 GPa in the competent parts of the rock domains, and clearly lower, 38 GPa, in the minor deformation zones contained in the domains. The portion of the domain volumes occupied by the minor (stochastic) deformation zones remains to be quantified, but is expected to be in the order of 5–20%. In the major deterministic deformation zones the mean value of the deformation modulus is estimated at 26 GPa.

The spread in rock mass model distributions is fairly large, due to the expected variation in fracturing, and the total range (min and max truncations) for the deformation modulus ranges from 39 to 81 GPa in the competent part of rock domains.

For the rock mass the uncertainty is also quantified, providing a span within which the actual mean value for the parameter distribution is expected. The uncertainty for the deformation modulus is ± 4 GPa in the rock domains outside fracture zones.

The commonly used Mohr-Coulomb material model was chosen for the strength description (cf. Section 6.3.3 for the definition of parameters used). The mean friction angle is fairly similar in all parts of the bedrock, 39–42 degrees, the lower values for the major deformation zones. But cohesion also adds to the difference, 14 MPa in the major deformation zones compared to 17 MPa in the competent parts of the rock mass. The strength is slightly lower in the rock mass of Domain B (fine-grained dioritoid) compared to the other rock domains.

Further details of all the model parameters are given in Table 6-7.

11.3.2 In situ stress conditions

For the description of the rock stresses the local model area has been divided into two "stress domains", as shown in Figure 11-10. The stresses in domain II, the wedge-shaped rock volume outlined by deformation zones below the Ävrö island and the Simepvarp peninsula, are expected to be lower than in the surrounding rock mass, because of an interpreted stress relief in the wedge that is free to move upwards.

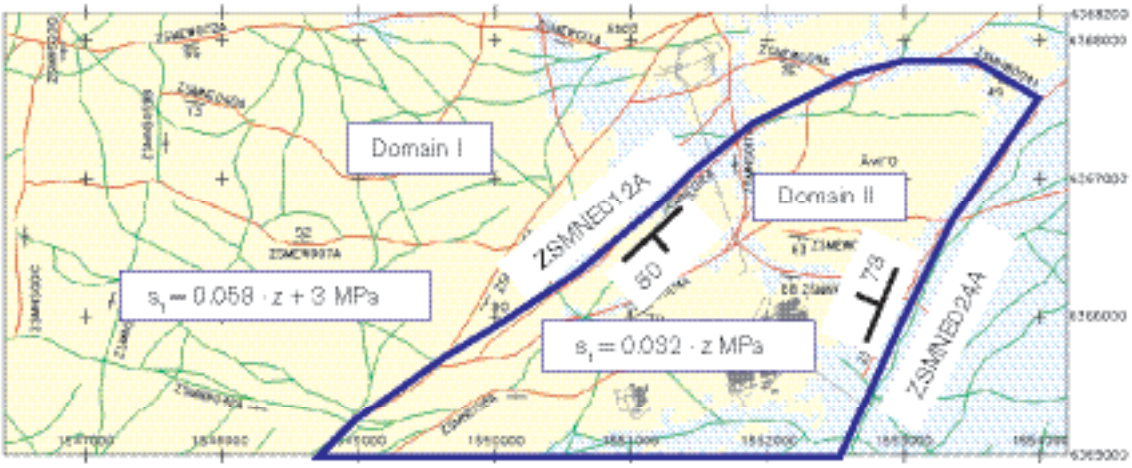

Figure 11-10. *The variation of rock stress in the Simpevarp local model area is described by dividing the area into Domain I and Domain II, depending on the location with respect to the regional deformation zones ZSMNE012A and ZSMNE024A. These zones are expected to dip in below the Simpevarp peninsula, Hålö and Ävrö to form a wedge-shaped volume of rock. The red and green lines on the map are the interpreted deformation zones (cf. Figure 11-8).The magnitude of the major principal stress in Domain I is expected to be higher than in Domain II and increase with depth according functions given (see further Tables 6-8 to 6-11).*

The stress magnitude is described as a linear function with depth. At 500 m depth, the stress model gives a span for the major principal stress of 22–42 MPa in domain I and a span of 10–22 MPa in domain II.

The expected mean orientation of the major horizontal stress is the same, NW-SE, in the whole local model area. Both the trend and dip may vary locally, in particular in the vicinity of deformation zones.

The complete stress model parameters, including quantitative estimations of uncertainty and local variation, are given in Tables 6-8 to 6-11.

11.4 Bedrock thermal properties

11.4.1 In situ temperature

In situ temperature has been measured in six boreholes. The temperature has been logged at different occasions in two of them. Temperature vs. depth is presented in Table 7-8. The mean of all temperature loggings is 14.4°C at 500 m depth, see Table 7-8 (data from one borehole with deviatory results excluded). There is a variation in temperature between the boreholes at a specified depth.

Different temperature loggings in the same borehole give slightly different results, indicating that there is a potential error. Possible sources of uncertainty in the temperature logging results include the timing of the logging after drilling, water movements along the boreholes, and the measured inclination of the boreholes.

11.4.2 Thermal properties

Thermal conductivity at canister scale was modelled for four lithological domains with different modelling approaches. Results indicate that the mean of thermal conductivity is expected to exhibit only a small variation between the different domains, from 2.62 W/(m·K) to 2.80 W/(m·K) (cf. Table 7-9). The standard deviation varies according to the scale considered and for the canister scale it is expected to range from 0.20 to 0.28 W/(m·K) (cf. Table 7-11). Consequently, the lower confidence limit for the canister scale is within the range 2.04–2.35 for all four domains.

The temperature dependence is rather small with a decrease in thermal conductivity of 1.1–3.4% per 100°C increase in temperature for dominating rock types. The dominating rock type is assumed to have isotropic thermal properties due to there are no clear foliation/lineation. However, there is possible anisotropy in a larger scale caused by the orientation of subordinate rock types.

There are a number of important uncertainties associated with these results. One uncertainty is the methodological uncertainties associated with the upscaling of thermal conductivity from cm-scale to canister scale. In addition, the representativeness of rock samples is uncertain and also the representativeness of the boreholes for the domains.

In general, the thermal conductivity is estimated to be higher in the Simpevarp 1.2 model than in Simpevarp 1.1. This applies for all four lithological domains considered (cf. Table 7-12). The difference is 5–23% depending on domain. However, the variability is estimated to be larger in Simpevarp 1.2, substantially larger for all domains except Ävrö granite.

Mean values of heat capacity ranges for the lithological domains are about 2.25 MJ/(m³·K) with a. standard deviation that varies between 0.06 to 0.121 MJ/(m³·K). Heat capacity exhibits a rather high temperature dependence. For the dominating rock types the increase in heat capacity is from 25% to 32% per 100°C temperature increase. The mean of the coefficient of thermal expansion was determined to 6.0–8.0E–6 m/(m·K) for three dominating rock types.

11.5 Bedrock hydrogeological description

11.5.1 Hydraulic properties

Hydraulic properties are described for deformation zones (Hydraulic Conductor Domains, HCD) and the rock mass between the HCDs (Hydraulic Rock Domains, HRD). The properties of the HRDs are treated in an implicit fashion by transferring a stochastic (fracture) network simulation of deformation zones to an equivalent porous medium representation (EPM).

Hydraulic Conductor Domains, HCD

The HCDs in the hydrogeological model are based on the version Simpevarp 1.2 regional scale structural model. Some of the zones in the regional scale model area, particularly in the vicinity of Äspö Island, are to be considered as high-confidence zones (concerning their existence) and several of them have been hydraulically tested. However, most HCDs have been attributed hydraulic properties which are to be regarded as uncertain.

For 13 of all the deformation zones, intersections with boreholes were identified where also hydraulic data were available. The range of the interpreted transmissivity (T) for these HCDs is 8E–8 to 3.6E–4 m^2/s. The geometric mean of the transmissivity of HCDs from the Äspö HRL is T=1.3E–5 m^2/s with a standard deviation $Log_{10}T = 1.55$ /Rhén et al. 1997b/. This geometric mean T was assigned to all the rest of the HCDs in the regional scale model, regardless of their geological genesis.

The hydraulic thickness of the HCDs is based on the geological interpretation of zone thickness made for the regional scale structural model version Simpevarp 1.2.

There is very limited information concerning storage coefficient (S) and kinematic porosities (n_e) (or mean transport aperture (e_t) = kinematic porosity multiplied by the hydraulic thickness) of the deformation zones. In /Rhén et al. 1997b/, /Rhen and Forsmark, 2001/, /Andersson et al. 2000/, /Andersson et al. 1998/ and /Dershowitz et al. 2003/ these parameters were estimated. Based mainly on these results, the storage coefficient and transport aperture were estimated as function of the transmissivity: $S = aT^b$ and $e_t = aT^b$. The properties of S and e_t are assumed to be representative mean values for individual features irresepctive of size, from fracture up to fracture zones. The uncertainty in these values is probably high. See Section 8.3 (Tables 8-13 through 8-15) for details concerning the properties of HCDs.

The calibration of the regional groundwater flow model did not entail modification of the transmissivity of the HCDs or for the HydroDFN models, but it was proposed to increase the kinematic porosity of the HCD and in the HydroDFN.

Hydraulic Rock Domains, HRD

The HydroDFN model is based on the developed version Simpevarp 1.2 GeoDFN model but has been modified (mainly intensities of different fracture sets have been modified but some changes were made also in length distributions and orientations. ConnectFlow and DarcyTools teams did not do exactly the same modifications) in order to match hydraulic data.

The working hypothesis embedded in the hydraulic DFN model employed for Simpevarp 1.2 is that it couples an inferred power-law size distribution of fractures (up to the size of local minor fracture zones) to hydraulic properties by assuming that the transmissivity value is dependent on the size through a power-law relationship. Generally, the hydraulic feature sizes in the regional groundwater flow simulations were within the range 100–1,000 m. Minor fracture zones were simulated rather than small-scale fractures. During the testing of the HydroDFN against hydraulic tests, the minimum fracture size was set to 0.067 m (corresponding to a borehole diameter of 0.076 m).

Alternative geometric models and different transmissivity models for fractures (hydraulic features) resulted in a number of alternative HydroDFN models that all matched the data, see Tables 8-16 and 8-17. However, some tests indicated that the model assuming a positively correlated fracture transmissivity T_f with fracture size L fits the data better than the model that assumes no correlation between transmissivity T_f and fracture size L (with a log-normal distribution of T_f).

The same hydraulic DFN model was assigned to all HRDs. The fracture centres were assumed be Poisson distributed in space.

The tests of the application of the HydroDFN models in the regional groundwater modelling show that all defined HydroDFN models could be used if the flow porosity is increased. However, the storage of different defined hydrogeochemical water types differs between low fracture intensity models compared with high fracture intensity models. The low intensity model results in a more heterogeneous distribution of water types. It remains to see whether new data and more use of hydraulic test data (PSS) can indicate which transitivity model and what intensity and size distributions of the fractures (hydraulic features) are most appropriate.

Mean properties of geologically defined rock domains

The hydraulic conductivity (K) of the rock domains differs somewhat. According to the injection tests at test scales 10–30 m (in boreholes KSH01A, KSH02, KLX01, KLX02, KA01, KAV03) the means of $\log_{10}(K)$, excluding deformation zones, are for rock domains A, B and C: –8.9, –9.2 and –9.0, respectively, see Table 8-11.

The block modelling at 20 m scale based on HydroDFN model with KSH01A data /Follin et al. 2005/ indicated for rock domain B a mean $\log_{10}(K)$ that was higher (c. –8.9) than above and for rock domain C higher (top of the borehole) and lower (bottom part of the borehole) (c. –7.5 and –10, respectively): The block modelling based on KSH02 data representing rock domain B with mean $\log_{10}(K)$ that was higher (c. –8.0) than above, but this borehole is probably affected of a nearby deformation zone and not representative for rock domain B.

Mean properties of rock blocks

The mean $\text{Log}_{10}(K)$ for blocks of size of 20 and 100 m , excluding deterministic deformation zones, were estimated as: $\text{Log}_{10}(K\ (20\ m))$ = –8.8 to –8.5 and $\text{Log}_{10}(K\ (100\ m))$ = (–8.9, case with uncorrelated T vs. L) –8.5 to –8.2, see Table 8-19.

11.5.2 Boundary and initial conditions

Initial conditions for the salt water distribution and water types at the end of the last glaciation were tested. A best fit of simulated results to available measured data was obtained by employing freshwater conditions, mainly of glacial type, down to c. 700 m depth, with a linear increase of Brine below that to 100% at depth of 1,500 m. No other distributions of the water types were assumed as initial conditions.

All other water types were imposed at the upper boundary as a function of time, based on the shore-line displacement due to the land uplift, see Section 8.6.

11.5.3 Groundwater flow pattern

Flow distribution

The topography appears to control much of the flow pattern in the upper part of the rock mass and this is visible also in the salinity distribution, which calls for sensitivity tests of other types of boundary conditions than simply approximating the water table with the topography. At depth, the salinity field decreases the magnitude of the flow rates considerably and hence groundwater fluxes near the ground surface are much higher than those at depth. At –1,000 m.a.s.l., flow rates are very low in magnitude. Near the surface, at –10 m.a.s.l. and –100 m.a.s.l., the vertical flow component is mainly oriented downwards (recharge). Discharge areas are located in the extreme east, associated with the Baltic Sea and onshore discharge areas, the latter mainly located in conjunction with fracture zones.

The results of the groundwater flow simulations undertaken suggest that the Laxemar subarea is predominantly subjected to recharging flow conditions at –500 m.a.s.l. This is in contrast to the Simpevarp subarea, which is predominantly subjected to discharging flow conditions at the same depth. However, it should be remembered that these inferences are based on modelling employing present-day boundary conditions.

Flow paths

Based on the present day boundary conditions, the flow paths from release areas located within the Laxemar and Simpevarp subareas at 500 m depth were simulated. It was found that the released particles rapidly reach a HCD and subsequently followed the system of HCDs to discharge points below the Baltic Sea. The discharge points for release in the Laxemar subarea are located mainly around the Äspö island, whereas discharge points for particles released in the Simpevarp subarea are found to the south and east of the subarea, as expected.

The base case including all deformation zones as HCDs is a well-connected system that more or less controls the groundwater flow. Excluding HCDs of size < 3,000 m (but including HCDs that were considered certain by the geologists) has only a minor effect of the flow field compared with the case including HCDs according to the base case. The reason is that the remaining HCDs are still rather many, well-connected and with fairly high transmissivities in the area of interest.

Hydrogeochemistry of the groundwater

The modelling results suggest the possibility that the Littorina water type may be present near the coast and below the Baltic Sea and, furthermore, that the water chemistry may be quite heterogeneous. Possibly the Glacial water type may be found in “pockets” and in larger quantities near and below the Baltic sea. This heterogeneity in distribution is attributed to an underlying heterogeneity in the distribution of the hydraulic properties.

11.6 Bedrock hydrogeochemical description

The results of the hydrogeochemical modelling described in Chapter 9 are used to produce a hydrogeochemical site descripte model. The model consists of a conceptual hydrochemical model of the modelled area (Section 11.6.1) and of a supporting descriptive part (Section 11.6.2) summarising the most important findings from the modelling.

11.6.1 Hydrogeochemical site descriptive model

One of the objectives of the Initial Site Investigation (ISI) stage is to produce versions of the hydrogeochemical descriptive model on a site scale. Visualisation of the hydrogeochemical evaluation documented in this report is in the form of a vertical transect that run through the Laxemar and Simpevarp subareas (for positioning see Figure 9-1). The vertical extent of the transect is to approximately 1,700 m to accommodate the deepest borehole (KLX02) in the Laxemar site. The approach to locate and construct the transect is described in /SKB, 2004c/. Based on existing geological and hydrogeological information a schematic version of the transect was produced to facilitate illustration of the most important structures/fault zones and their potential hydraulic impact on the groundwater flow (Figure 11-11). This hydraulic information was then integrated with the results of the hydrogeochemical evaluation and modelling results to produce the vertical and lateral changes in the groundwater chemistry (Figure 11-1).

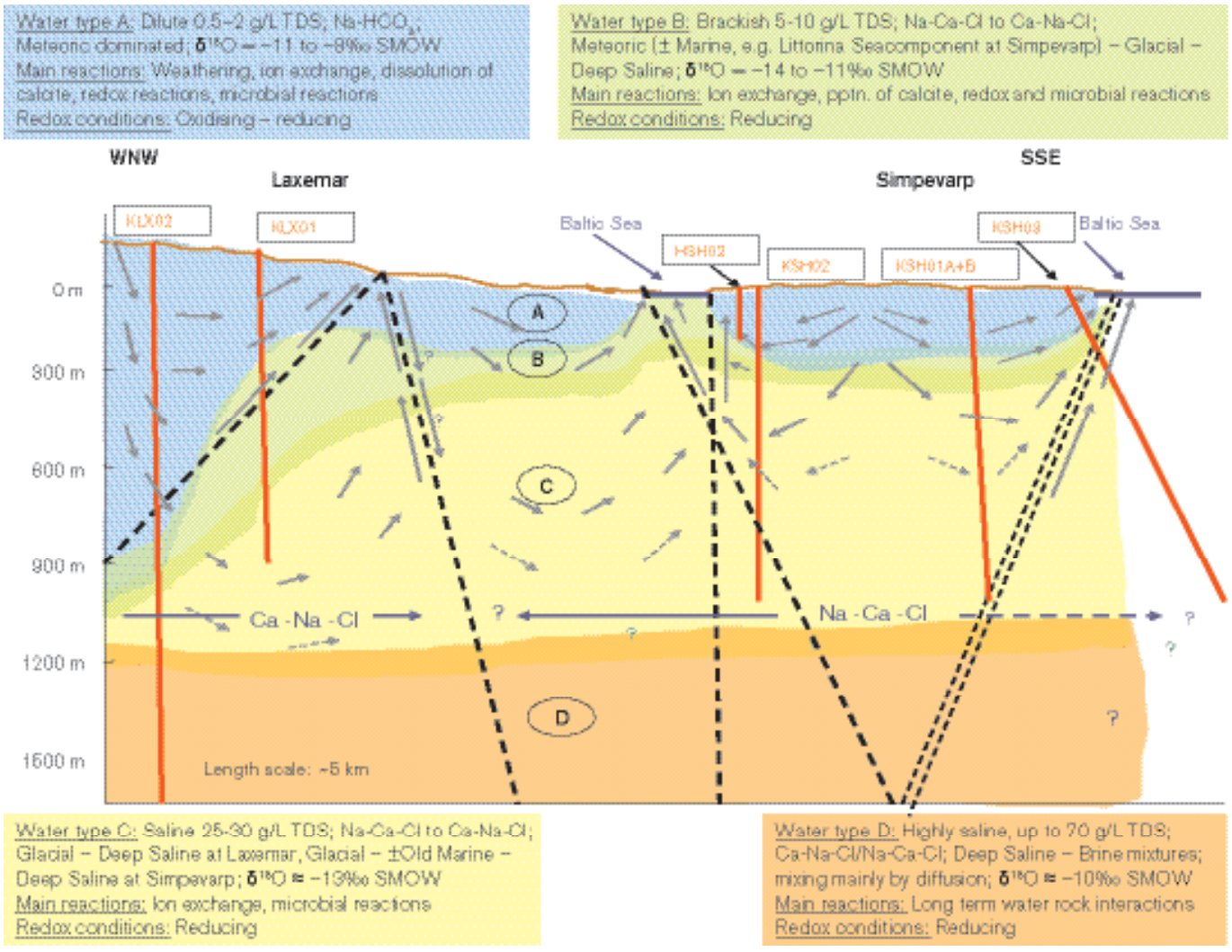

Figure 11-11. *Schematic conceptual hydrogeochemical model based on integrating the major structures, the major groundwater flow directions and the different groundwater chemistries (A–D) and properties.*

In the Simpevarp subarea the main structures intersected by the transect have an approximate NE-SW orientation; in the Laxemar subarea the transect is mostly parallel to the main WNW-SSE structural trends. The former are considered sub-vertical whilst at Laxemar the structures tend to dip at shallower angles to the SW or NE. Combined, these structures effectively divide both the Simpevarp and Laxemar areas into structural compartments as illustrated in Figure 11-11. It is also believed that each major structural compartment will be characterised by its own local hydraulic groundwater flow regime (Figure 11-11). Most of the vertical to sub-vertical fracture zones are considered as discharging groundwater pathways.

Local groundwater flow regimes are assumed to develop at the Laxemar and Simpevarp subareas and are considered to extend down to depths of around 600–1,000 m, depending on local topography. Close to the Baltic Sea coastline, where topographical variation is small, depth penetration of groundwater flow will subsequently be less marked. In contrast, the Laxemar subarea is characterised by higher topography resulting in a much more profound groundwater circulation which appears to extend to 1,000 m depth in the vicinity of borehole KLX02.

The marked differences in the groundwater flow regimes (in terms of depth penetration of local flow cells) between the Laxemar and Simpevarp areas are reflected in the groundwater chemistry. Figure 11-11 shows four major recognised hydrochemical groups of groundwaters denoted by A–D. Questionmarks are inserted where there is a degree of uncertainty, i.e.:

- Groundwater types A and B close to borehole KLX02 at Laxemar: There is some uncertainty whether dilute recharge Na-HCO_3 water extend to the depth indicated. Some short-circuiting of groundwater flow paths by borehole KLX02 may be occurring.
- Groundwater types C and D within the Simpevarp site: The extent of Na-Ca-Cl groundwaters below 1,000 m is unknown. In addition, it is uncertain whether there is a transition to Ca-Na-Cl groundwater types at even greater depths.

In terms of depth location, chemistry, major reactions and main mixing processes, the main features of the four identified groundwater types are summarised below.

TYPE A – Shallow (< 200 m) at Simpevarp but deeper (0–900 m) at Laxemar

Dilute groundwater (< 1,000 mg/L Cl; 0.5–2.0 g/L TDS)

Mainly Na-HCO_3 in type

Redox: Marginally oxidising close to the surface, otherwise reducing

Main reactions: Weathering; ion exchange (Ca, Mg); dissolution of calcite; redox reactions (e.g. precipitation of Fe-oxyhydroxides); microbially-mediated reactions (SRB)

Mixing processes: Mainly meteoric recharge water at Laxemar; potential mixing of recharge meteoric water and a modern sea component at Simpevarp; localised mixing of meteoric water with deeper saline groundwaters at Laxemar and Simpevarp

TYPE B – Shallow to intermediate (150–300 m) at Simpevarp but deeper (approx. 900–1,100 m) at Laxemar

Brackish groundwater (1,000–6,000 mg/L Cl; 5–10 g/L TDS)

Mainly Na-Ca-Cl in type but some Na-Ca(Mg)-Cl(Br) types at Simpevarp; transition to more Ca-Na-Cl types at Laxemar

Redox: Reducing

Main reactions: Ion exchange (Ca, Mg); precipitation of calcite; redox reactions (e.g. precipitation of pyrite), microbial reactions

Mixing processes: Potential residual Littorina Sea (old marine) component at Simpevarp, usually in fracture zones close to or under the Baltic Sea; meteoric and potential glacial component at Simpevarp and Laxemar; potential deep saline (non-marine) component at Simpevarp and at Laxemar

TYPE C – Intermediate to deep (> 300 m) at Simpevarp but deeper (approx. 1,200 m) at Laxemar

Saline (6,000–20,000 mg/L Cl; 25–30 g/L TDS)

Mainly Na-Ca-Cl with increasingly enhanced Br and SO_4 with depth at Simpevarp; mainly Ca-Na-Cl with increasing enhancements of Br and SO_4 with depth at Laxemar

Redox: Reducing

Main reactions: Ion exchange (Ca), microbial reactions

Mixing processes: Potential glacial component at Simpevarp and Laxemar; potential deep saline (i.e. non-marine and/or non-marine/old Littorina marine) component at Simpevarp, deep saline (non-marine) component at Laxemar

TYPE D – Deep (> 1,200 m) only at Laxemar

Highly saline (> 20,000 mg/L Cl; to a maximum of ~ 70 g/L TDS)

Mainly Ca-Na-Cl with higher Br but lower SO_4 compared to Type C groundwaters

Redox: Reducing

Main reactions: Water/rock reactions under long residence times, microbial reactions

Mixing processes: Probably long term mixing of deeper, non-marine saline component driven by diffusion

Deep groundwaters at the Simpevarp subarea (including Äspö) (1,000 m) are Na-Ca-Cl in type; deep groundwaters at Oskarshamn (KOV01; 1,000 m) and at Laxemar (1,700 m) are Ca-Na-Cl in type. Since the Laxemar subarea is inland and Oskarshamn is close to the coast, this could be an indication of very deep discharging groundwaters at Oskarshamn. Therefore, below the Simpevarp subarea (including Äspö), at greater depths than presently sampled, Ca-Na-Cl groundwaters might be expected.

11.6.2 Descriptive and modelled characteristics of the area

Descriptive and modelled observations are included in the hydrogeochemical site descriptive model and they are the fundamental to the overall hydrochemical understanding of the site. The most important characteristics are summarised in the following subsections. The final important overall result of the hydrogeochemical evaluation is the assessment whether the modelled site meets the hydrogeochemical stability criteria defined by SKB. These parameters are discussed in this final subsection.

Descriptive observations

Main elements

- Overall depth trends show increasing TDS with increasing depth. In particular the Ca/Na and Br/Cl ratios increase markedly.
- Sulphate and Mg show an overall decrease with depth with greater dispersion from approx. 200–600 m. Bicarbonate decreases sharply with depth.
- Ca/Mg and Br/Cl ratios versus Cl content indicate a deep, non-marine source of the salinity for most of the borehole samples. This is similar to groundwaters from the Äspö, Laxemar subarea and Oskarshamn (KOV01) boreholes.
- Deep groundwaters at the Simpevarp subarea and Äspö (1,000 m) are Na-Ca-Cl in type; deep groundwaters at Oskarshamn (KOV01; 1,000 m) and at Laxemar (1,700 m) are Ca-Na-Cl in type. Since Laxemar is inland and Oskarshamn is close to the coast, this could be an indication of discharging very deep groundwaters at Oskarshamn. At greater depths below the Simpevarp subarea and Äspö than presently sampled, Ca-Na-Cl groundwaters therefore might be expected.

- A small set of brackish groundwaters (1,000–6,000 mg/L Cl), located around 150–300 m depth, show marine signatures of possible Littorina Sea origin. These are located in fracture zones close to or under the Baltic Sea.
- $\delta^{18}O$ versus Cl indicates a contribution of glacial waters to the brackish and deeper saline water samples.
- The SO_4 contents show a large variation for the brackish and saline groundwaters. In the brackish groundwaters with 5,000–6,300 mg/L Cl, microbially mediated sulphate reduction is taking place. The SO_4^{2-} contents in the more highly saline groundwaters are still not high enough to invoke dissolution or leaching as a mechanism. More likely processes are in-mixing of marine waters although in-mixing of SO_4^{2-} from deep brine waters cannot be excluded. Deep saline SO_4^{2-} sources (> 20,000 mg/L Cl) may have resulted from the leaching of sediments and/or dissolution of gypsum previously present in fractures.

Isotopes

- The isotope data from the boreholes are still relatively few and often do not correspond to the most representative samples. To compensate, most of the available data have been plotted with the objective of determining trends rather than striving for far reaching conclusions.
- With respect to tritium, generally the Baltic Sea samples show somewhat higher values (10.3–19.3 TU) compared to the meteoric surface waters (7.8–15 TU). The successive lowering of the tritium contents versus time elapsed since the bomb tests may explain the higher values in the Baltic Sea (due to reservoir effects). Note that the precipitation values are very few, show a large variation in tritium and therefore are not considered very conclusive. Continued systematic sampling of precipitation for tritium analyses is recommended.
- For carbon, plots of ^{14}C versus $\delta^{13}C$ versus HCO_3^- show that there is no real correlation between ^{14}C and $\delta^{13}C$, i.e. there is no indication of a change in $\delta^{13}C$ with age. Breakdown of organic material plays a major role and has occurred either in the near-surface (being transported downwards) or that in situ production has taken place. An organic origin is also supported by the $\delta^{13}C$ versus HCO_3^- plot where the groundwater samples showing the highest HCO_3 contents show relatively homogeneous $\delta^{13}C$ values.
- The plot of tritium versus ^{14}C for surface waters from the Simpevarp area shows a distinct decrease in ^{14}C content in the Lake and Stream waters, whereas the tritium values remain the same or show a small decrease. The explanation is that HCO_3^- added to the waters originates either from calcites, devoid of ^{14}C, or due to microbial oxidation of organic material with lower (or no) ^{14}C. This is the pattern expected for near-surface waters.
- Marine waters show a distinct Sr isotope signature (0.71) which is very close to the measured values in the Baltic Sea waters, whereas groundwaters from the different sites show values significantly more enriched in radiogenic Sr. Water/rock interaction processes involving Rb-containing minerals are the reason for this. The relatively small variation in Sr isotope ratios within each area, particularly at the Simpevarp and Laxemar subareas, is probably an indication that ion exchange reactions with clay minerals along the groundwater flow paths is an important process. For the Simpevarp area as a whole there is a tendency towards higher contents of radiogenic Sr in the waters with highest salinities (and thus the highest Sr contents measured). Because of the limited data it is not possible to explain this observation, but in the absence of any mineralogical reasons, it is likely that greater residence times for these deep saline groundwaters result in more extensive mineral/water interactions.
- The borehole groundwaters generally show $\delta^{34}S$ values in the same range as the Baltic Sea waters but with a clear indication in the brackish groundwaters of $\delta^{34}S$ values greater than +21‰ CDT in samples with low SO_4^{2-}. This may be explained by modification of the isotope ratios by sulphur-reducing bacteria. The higher saline groundwaters share lower $\delta^{34}S$ but higher SO_4^{2-} contents. The $\delta^{34}S$ values of these deeper groundwaters are, however, still within the range for the analysed Baltic Sea waters.

- The $\delta^{37}Cl$ data suggest that the deeper cored borehole groundwaters are characterised by water/rock interaction processes, whilst the near-surface percussion borehole groundwaters are mainly marine derived. The distribution of Baltic Sea and surface Lake and Stream waters suggest some mixing components of marine-derived and deeper groundwater sources.

Microbes, colloids and gases

- As there were only three sets of microbiological data available from one borehole (KSH01A), the model produced is therefore in essence one-dimensional and preliminary.
- Redox potentials in borehole KSH01A were in general low, below –200 mV at all sampled depths.
- Sulphate reducing bacteria dominated at the shallowest level sampled, 156.5–167 m.
- At the mid level, 245–261.6 m, heterotrophic methanogens and acetogens were dominant.
- At the deepest level autotrophic and heterotrophic acetogens were found but only in low numbers.
- The large numbers of microorganisms at level 245–261.6 m were probably due to the large fracture area with high amounts of fracture surfaces inducing significant perturbations and favourable conditions for life.
- The abundance of microbial species and their activity in borehole KSH01A seem to be closely correlated with the redox potential.
- The numbers of colloids decrease with depth in KLX01 but not in KAV01. Furthermore, the numbers do not vary much at the different depths sampled. The sampled depths were 422.5 m, 525.5 m and 560.5 m respectively, i.e. an extent of only 140 m which is not much in relation the total depth explored. The average number of colloids in this study is 63 ± 49 µg L^{-1} and is in agreement with colloid studies from Switzerland (30 ± 10 and 10 ± 5 µg L^{-1}) and Canada (300 ± 300 µg L^{-1}) where they used the same approach as in the Simpevarp area /Laaksoharju et al. 1995a/.
- Up to 12 gases were analysed: helium, argon, nitrogen, carbon dioxide, methane, carbon monoxide, oxygen, hydrogen, ethyne, ethene, ethane and propane. KSH01A was the only borehole sampled completely regarding analysed gas components. Numbers for the total volume of gas were available only for 5 depths in two of the boreholes. They contain between 44 and 80 mL L^{-1} and this is in accordance with volumes found at other places in the Fennoscandian shield.

Modelled observations

PHREEQC modelling

Groundwater in the Simpevarp area can be divided into three groups based on their salinity:

- **Saline groundwaters.** Mixing with a brine end member is responsible, directly or indirectly, for most of their chemical content, especially from Cl concentrations higher than 10,000 mg/L. Their alkalinity is low, and controlled by equilibrium with calcite. pH is controlled by calcite equilibrium and, possibly, aluminosilicate reactions. In contrast to other Fennoscandian sites, sulphate is controlled by gypsum (supported by gypsum identified in fracture fillings) in high saline groundwaters. These old mixed waters tend, with time, to re-equilibrate with a relatively constant mineral assemblage, irrespective of their initial elemental contents. These reactions are slow and can be approached by equilibrium modelling (with aluminosilicates), although other alternatives can be explored (clay minerals).
- **Brackish groundwaters.** They have been subject to more complex mixing processes involving all possible end-members. A combination of slow and fast chemical reactions (e.g. Na-K-Ca ion exchange, calcite precipitation, etc.) have influenced the mixed waters

- **Non saline groundwaters.** These waters are the result of "pure" water-rock interaction or mixing of the previous types with recent waters. They lack a clear thermodynamic control. Control is by fast chemical reactions (ionic exchange, surface complexation reactions, calcite dissolution-precipitation, etc.) coupled with more important irreversible processes (fracture mineral dissolution, decomposition of organic matter, etc.).

The redox state of groundwaters in the Simpervarp area appears to be well described by sulphur redox pairs in agreement with some previous studies in this area and in other sites from the Fennoscandian Shield. Besides, from the analysis performed here it can be concluded that CH_4/CO_2 is another important redox pair in determining the redox state. Therefore, although the sulphur system can be considered the best suited to characterise the redox state of the groundwaters, a better understanding of the iron system is needed to assess its particular contribution to the redox state or to the reductive capacity of these groundwater systems.

A modelling approach was used to simulate the brine composition concluding that in the Simpevarp area the mixing is the main irreversible process. It controls chloride concentration that, in turn, determines the re-equilibrium path (water-rock interaction) triggered by mixing. This result emphasises the important effort made in the Swedish (and Finnish) framework to characterize the mixing process. Moreover, it justifies the selection of chloride as the main descriptive variable when studying the geochemical evolution of these systems.

M3 and DIS modelling

- M3 modelling helped to summarise and understand the data in terms of origin, mixing proportions and reactions.
- The surface meteoric type waters show seasonal variations and closer to the coast the influence of marine water is indicated. With depth the glacial, meteoric and brine type of waters have affected the groundwater salinity. Only a few samples from Äspö and one from the Simpevarp peninsula show a possible Littorina Sea water influence. The deviation calculations in the M3 mixing calculations show the potential for organic decomposition/calcite dissolution in the shallow water. Indications of ion exchange and sulphate reduction have been modelled. These M3 results support the initial evaluation of primary data and general modelling results.
- The 3D/2D visualisations indicate that meteoric water is dominating in the western part and in the central part of the modelling domain. Marine water is found towards the coast and under the sea in the eastern part of the cutting plane. Glacial water is found in the central part of the cutting plane and Brine type of water is dominating at depth.
- DIS evaluation can help to judge the representativeness of the sampled data. The section 548–565 m in KSH01 was investigated and the results showed that the amount of drilling water remaining in the fracture is 2.4 m^3. The calculations showed that the pumping should have continued further in order to remove the additional 2.4 m^3.

Coupled transport modelling

- Qualitative modelling of environmental isotopes representing the fresh groundwater samples from the Simpevarp area suggests an average water age from several decades to 100 years.
- The Simpevarp subarea appears to be the discharge area of a dynamic fresh water aquifer. Tritium activities measured are consistent with mixing between recent, modern and sub-modern fresh groundwaters. The mixing is produced by the convergence of flow lines discharging on the Baltic Sea coast.
- Combined analyses of isotopic and hydrochemical information of fresh groundwater samples allows the identification of clear trends which are consistent with the hydrogeological knowledge of the area.
- It has been detected that some lake water shows isotopic signatures very similar to groundwaters sampled in the Simpevarp subarea. This could be reflecting the presence of lakes constituting local discharge areas of the granitic aquifer.

- Numerical modelling of groundwater flow and solute transport has been performed in order to simulate groundwater age and tritium concentration. The model results provide additional support to hydrogeological models by using independent hydrochemical information.
- A first attempt to coupled groundwater flow and reactive solute transport modelling has been performed. A calcite dissolution front is computed due to the flushing of saline water by fresh recharge (infiltrated) water, in agreement with one of the main processes detected by previous hydrochemical models. However, computed calcite dissolution cannot explain measured concentration of bicarbonate and calcium. Additional modelling is required in order to have a more accurate description.
- Measured bicarbonate concentrations are higher than those computed. A possible explanation could lie in microbially-mediated decomposition of organic matter. The current version of the reactive transport model underestimates dissolved silica and sulphate, as well as overestimates dissolved iron. Most probably this is due to the occurrence of water/rock interaction processes involving silicates, pyrite, iron oxides and phyllosilicates.

Hydrochemical stability criteria

The most important result of the hydrochemical evaluation and modelling is to assess whether the site meets the SKB hydrogeochemical stability criteria used in the safety assessment. The evaluation and modelling indicate that the groundwater composition at repository depth in the Simpevarp subarea, as seen in the analysed variables of the representative sample from KSH01A:548–565 m and KSH02:575–580 m are such that they meet the SKB chemical stability criteria (Table 11-7) for Eh, pH, TDS, DOC and Ca+Mg /see Anderson et al. 2000/. The analyses are not complete for colloids and Eh. The table will therefore be updated in future modelling versions.

Table 11-7. The hydrochemical stability criteria defined by SKB are valid for the analysed values of the represenative sample KSH01A:548–565 m and KSH02:575–580 m. Note that the analyses are not yet complete for colloids and Eh.

	Eh mV	pH (units)	TDS g/L)	DOC (mg/L)	Colloids (mg/L)	Ca+Mg (mg/L)
Criterion	< 0	6–10	< 100	< 20	< 0.5	> 4
KSH01A:548–565 m	–230	7.6	15.1	< 1	NA	1,947
KSH02:575–580 m	NA	8.1	14.1	< 1	NA	1,797

NA = Not analysed.

11.7 Bedrock transport properties

For the previous Simpevarp 1.1 description of transport properties, no site-specific data on retardation parameters were available. The modelling comprised an evaluation of the potential for using Äspö data, and a description of flow-related parameters obtained from the groundwater flow modelling. The strategy for site descriptive modelling of transport properties has been changed between model versions 1.1 and 1.2, such that flow-related transport parameters are not presented as a part of the Simpevarp 1.2 site description. This implies that the site-descriptive model considers retardation parameters (porosity, diffusivity and sorption coefficient) only.

Site investigation data from porosity measurements and diffusion experiments (in situ and in the laboratory) have been available for the Simpevarp 1.2 modelling. The modelling work has included evaluations of data on rock mass geology, fractures and fracture zones, and hydrogeochemistry, in addition to the evaluation of transport data. In particular, the early access to the Simpevarp 1.2 geological model enabled an improved analysis of the relations between the Simpevarp rock types and the rock types previously investigated at Äspö, improving the basis for data import from the Äspö HRL to Simpevarp. The Simpevarp 1.2 transport modelling is described in a background report /Byegård et al. 2005/, which provides the basis for Chapter 10.

11.7.1 Summary of observations

The main observations from the evaluations of transport data and of data and models from other disciplines can be summarised as follows:

- Relatively large parts of the rock volumes consist of altered rock, and the proportions of altered rock show large variations among and along the boreholes. The altered rock can be assumed to have different transport properties from fresh rock.
- The open fracture frequency appears to be correlated to the altered/oxidised parts of the rock, implying that transport in the open fractures to large extent takes place in the altered parts of the rock.
- The locations of hydraulically conductive structures are mostly associated with the presence of gouge-filled faults, with outermost coatings consisting mainly of clay minerals together with calcite and pyrite grains.
- The presence of different fracture coatings is not related to the rock type in the investigated boreholes on the Simpevarp peninsula.
- Based on similarities in composition, texture and porosity, import of diffusion data from the Äspö HRL can be made by using Äspö diorite data for Ävrö granite. Diffusion data can be imported also for fine-grained granite. Due to similarities in biotite and plagioclase contents, it is proposed that Äspö diorite data are used for modelling the sorption of cation exchange sorbing nuclides on all three major rock types.

11.7.2 Retardation model

A retardation model for rock mass and fractures is presented, in accordance with the proposed modelling strategy. The retardation model for the rock mass contains data for the fresh and altered forms of the major rock types in the Simpevarp subarea (Ävrö granite, quartz monzodiorite and fine-grained dioritoid). Specifically, the retardation model is based on porosity data from water saturation measurements on site-specific rock samples, diffusivities from formation factors measured in laboratory electrical resistivity measurements on site-specific samples, and sorption coefficients imported from Äspö, see Section 10.6.2 and Table 10-6. The sorption dataset is limited to Cs and Sr under hydrochemical conditions corresponding to “Groundwater type III” (as specified by /Byegård et al. 2005/).

Table 11-8 summarises the mean values and standard deviations (expressed as mean value ± one standard deviation) of the transport parameters of the rock mass; for further details, see Table 10-6 (where porosities and formation factors are given as distributions). It can be seen that the porosities and formation factors (normalised diffusivities) for Ävrö granite are larger than those for the other major rock types. Since the same K_d-values, obtained from experiments at Äspö, are used for all three major rock types, no conclusions can be drawn on differences in sorption properties. It can also be noted that the data uncertainty, as quantified by the standard deviations of the experimental populations, in many cases is of the same order as the mean values (or even larger).

As a basis for detailed parametrisations of the rock domains, Section 10.6.2 presents the estimated percentages of the major rock types within the rock domains RSMA01, RSMB01 and RSMC01 (Table 10-7; data from Geology). Estimated proportions of fresh and altered rock for each rock type are also given (Table 10-6). In principle, the parametrisation of each rock domain could range from a simple selection of a single parameter value representing the dominant rock type in that domain to, for instance, volume averaging using data for fresh or altered rock, or both. For the diffusion parameters of the major rock types, statistical distributions are also given.

However, no specific recommendations on the selection of data from the retardation model are given here. At this stage of model development, the retardation model should be viewed as a presentation of the interpreted site-specific information on retardation parameters, intended to provide a basis for the formulation of alternative parametrisations within the Safety Assessment modelling.

Table 11-8. Summary of mean values and standard deviations of porosity, formation factor (diffusivity normalised by the free diffusivity in water) and K_d in the proposed retardation model for the rock mass.

Rock type	Porosity (vol-%)[1]	Formation factor (–)[1]	K_d Sr (m^3/kg)[2] (GW type III)	K_d Cs (m^3/kg)[2] (GW type III)	Comments
Ävrö granite (fresh)	0.40 ± 0.13	$(2.9 \pm 2.9)\times10^{-4}$	$(4.2 \pm 0.8)\times10^{-5}$	0.06 ± 0.03	Dominant rock type in RSMA01. One of the two dominant rock types in RSMC01.
Quartz monzo-diorite (fresh)	0.20 ± 0.13	$(1.1 \pm 1.6)\times10^{-4}$	$(4.2 \pm 0.8)\times10^{-5}$	0.06 ± 0.03	One of the two dominant rock types in RSMC01.
Fine-grained dioritoid (fresh)	0.17 ± 0.15	$(1.0 \pm 1.7)\times10^{-4}$	$(4.2 \pm 0.8)\times10^{-5}$	0.06 ± 0.03	Dominant rock type in RSMB01.
Altered rock	0.33 [3]	$(0.8 \pm 0.4)\times10^{-4}$	$(1.2 \pm 0.2)\times10^{-5}$	0.013 ± 0.006	The same parameter values are assumed for the altered forms of all major rock types.

[1] Site investigation data (except for the altered rock data).

[2] Based on data from Äspö HRL (further evaluated in the site descriptive modelling).

[3] Only one value available.

Four different fracture types have been identified and described in the retardation model, see Section 10.7.2 and Tables 10-8 to 10-11. These fracture types include fractures with fracture coating on fresh rock (Fracture type A) and fractures with altered wall rock between the coating and the fresh rock (Fracture types B, C and D). The estimated percentages of the different fracture types (proportions of all open fractures) are also given. However, it should be noted that retardation parameters are not available for all materials in the model, and that quantitative relations between fracture types and other properties of the fractures (e.g. lengths, orientations and hydraulic parameters) have not been established.

Although somewhat limited in terms of data and correlations to other parameters and properties of the system, the presented model can be used as a basis for parametrisation of numerical transport models and, perhaps more important, as a basic structure that can be subject to further discussions and development. Concerning the parametrisation of transport models, it could be observed that the present data show that the presence of different fracture coatings cannot be related to specific rock types.

No identification or description of deformation zone types is given in the present model. However, the available information and indications related to deformation zones are described in Section 10.7.3.

11.7.3 Implications for future work

A large number of samples have been taken from drill cores from the Simpevarp and Laxemar subareas. Laboratory experiments for determining porosities as well as diffusion and sorption parameters are on-going, and additional in situ measurements have been performed. Thus, the site-specific database will be considerably improved during 2005, filling many of the data gaps identified in the Simpevarp 1.2 model.

However, the additional amount of data contained in the Laxemar 1.2 data freeze is relatively small. For the Laxemar 1.2 modelling, it is proposed that an extraction of data from on-going experiments is made, similar to the one in Simpevarp 1.2, in order to improve the database and the resulting model.

12 Overall confidence assessment

The Site Descriptive Modelling involves uncertainties and it is necessary to assess the confidence in the modelling. Based on the integrated strategy report, /Andersson, 2003/, and experience gained in version 1.1, procedures (protocols) have been further developed for assessing the overall confidence in the modelling. These protocols concern whether all data are considered and understood, uncertainties and potential for alternative interpretations, consistency between disciplines, and consistency with understanding of past evolution, as well as comparisons with previous model versions. These protocols have been used in a technical auditing exercise as a part of the overall modelling work. This chapter reports the conclusions reached after that audit.

12.1 How much uncertainty is acceptable?

A site descriptive model will always contain uncertainties, but a complete understanding of the site is not needed. As set out in the geoscientific programme for investigation and evaluation of sites /SKB, 2000b/ the site investigations should continue until the reliability of the site description has reached such a level that the body of data for safety assessment and repository engineering is sufficient, or until the body of data shows that the site does not satisfy the requirements. Even if the Construction and Detailed Investigation Phase does not imply potential radiological hazards, it would still be required that no essential safety issues remain that could not be solved by local adaptation of layout and design.

12.1.1 Safety assessment needs

The Safety Assessment planning suggests that only certain site properties are really important for assessing the safety. These are

- the intensity and size distribution of deformation zones and fractures in the repository volume,
- whether there is ore potential,
- the intact rock strength and coefficient of thermal expansion,
- the rock thermal conductivity,
- the distribution of hydraulic conductivity (or the transmissivity distribution of the DFN-model) in the repository volume,
- the chemical composition of the groundwater, especially absence of dissolved oxygen and low TDS, at repository depth and
- the porosity and diffusivity of the rock matrix.

Generally, these properties are connected to the preferences and requirements already stated in SKB's criteria for siting and site evaluation /Andersson et al. 2000/. Consequently, there is a need to ensure that the site modelling is able to produce qualified uncertainty estimates of these properties.

Furthermore, it is necessary to develop sufficient *understanding* of the site in order to address questions like; can there be fast flow paths due to channelling, what is the source of the brine at depth, what is the impact of rock stresses on available sorption surfaces in the rock, do we understand the impact of the mixing processes observed during the chemistry sampling etc. However, full understanding of all aspects of a site is neither attainable nor required. In particular, many strongly variable properties like thermal conductivity or rock matrix diffusivity because these data will be averaged. Thus seemingly large variabilities will not have much impact in such cases.

12.1.2 Repository engineering needs

According to current thoughts within Repository Engineering, there are essentially three design issues to be addressed during the Site Investigation phase:

- Is there enough space?
- What is the degree of utilisation (i.e. a subset of the space issue)?
- Are critical tunnel locations (e.g. of problematic deformation zones) properly assessed?

The overriding issue whether there is enough space for the repository may be divided into determining the generally available space and the degree of utilisation within this generally available space. The factors controlling the generally available space are the position and geometry of regional and local major deformation zones. Deposition tunnels must not be placed closer than a certain respect distance from such zones. Working definitions of respect distances exist, but some refinement work is still going on regarding what should be appropriate respect distances, see e.g. /SKB, 2004d/.

The repository layout is not only controlled by the regional and local major deformation zones. For example, deposition holes connected to large fractures or high inflows will not be used and the thermal rock properties affect the minimum allowable distances between deposition tunnels and deposition holes. During site investigations, this is handled in the design by estimating a "degree of utilisation" for the deposition panels already adjusted to the regional and local major deformation zones. Final selection of deposition holes and tunnels will be made locally, underground, during the construction and detailed investigation phase. Distribution of inflow to the deposition tunnels is an important aspect of the degree of utilisation. Apart from water, other factors affect the degree of utilisation. These include heat conductivity and rock mechanics properties affecting bedrock stability and the potential for rock spalling.

For the engineering planning and selection of the surface access point it is necessary to identify and characterise potentially difficult tunnel locations (i.e. where the tunnel would pass deformation zones) in the rock. However, the information needed will be quite detailed, which means that the overall site description will be used to identify potential access locations. At these locations there will later be a need to drill some additional exploration boreholes in order to assess the actual critical passages.

12.1.3 Assessing the importance of the uncertainties

As further discussed by e.g. /Andersson et al. 2004/ there are several planned occasions during the Site Investigation when Safety Assessment will be able to provide organised feedback as regards the sufficiency of the site investigations. The SR-Can project delivered its first interim report in mid 2004 /SKB, 2004d/ but the actual assessment will be published in 2006. Preliminary Safety Evaluations /SKB, 2002c/ of the investigated sites will be made using the respective version 1.2 SDM as input. Quantitative feedback from Safety Assessment could not be obtained before these studies, but the type of feedback to be obtained can still be assessed in relation to its potential impact on decisions related to the site investigation programme.

The Overall Confidence Assessment presented in this chapter concern i) whether all data are considered, understood and what is the accuracy and biases in the data, ii) what are the uncertainties in the models, their cause, potential for alternative interpretations and what further characterisation would reduce uncertainty, iii) consistency between disciplines, iv) consistency with understanding of past evolution, and v) comparison with previous model versions, Figure 12-1.

Less emphasis is put on the importance of the uncertainties. Such an assessment could strictly only be done by the users and is also planned part of the design and safety assessment activities where the Site Descriptive Model is input. Still, some general remarks based on the overall list of important issues as listed above could be made. A more thorough discussion on implications for further work is presented in Chapter 13. This discussion is based on the assessment presented in this chapter.

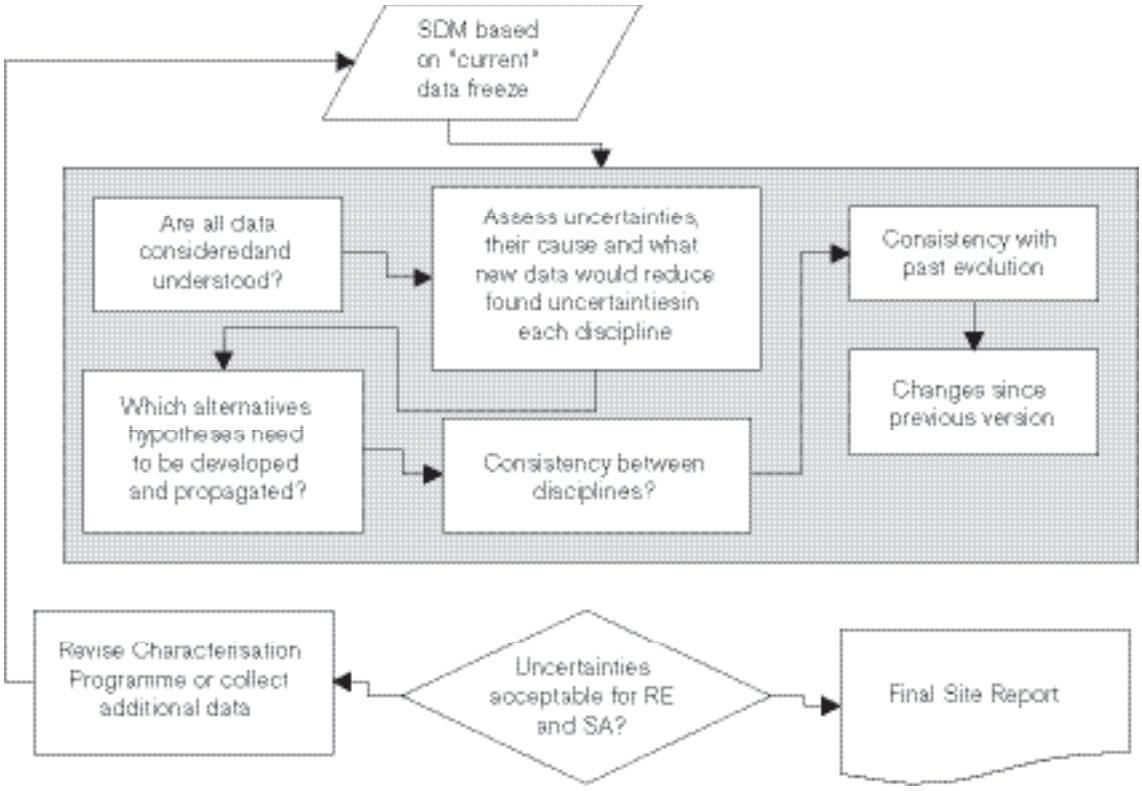

Figure 12-1. *The Overall Confidence Assessment presented in this chapter concern the various aspects inside the blue box in the flow chart above. Whether these uncertainties are acceptable and what would require additional characterisation efforts require input from Repository Engineering and for Safety Assessment and are thus not fully addressed in this report.*

12.2 Are all data considered and understood?

Checking whether all data are considered and understood is the first step in the Overall Uncertainty and Confidence Assessment (see Figure 12-1). A similar and unbiased treatment of all data and interpretations that explains several different observations enhances confidence.

12.2.1 Answers to auditing protocol

A protocol has been developed for checking the use of available data sources. It concerns:

- Data that have been used for the current model version (by referring to tables in Chapter 2).
- Available data that have not been used and the reason for their omission (e.g. not relevant, poor quality, …).
- If applicable – What would have been the impact of considering the non-used data?
- How accuracy is established (e.g. using QA procedures) for the different data. (Essentially by reference to tables in Chapter 2.)
- For data (types) where accuracy is judged low – whether accuracy is quantified (with reference to applicable sections of this report or supporting documents).
- If biased data are being produced, can these be corrected for?

The filled in auditing protocols are provided in Appendix 7. It should be noted that the questions sometimes produce long answers but this does not necessarily mean grave impacts on the uncertainty on key features of the Simpevarp Site. The answers suggest the following overall observations.

Use of data

The database for the modelling is well defined and is accounted for in the tables of Chapter 2.

Generally, all data available at the time of the data freeze for Simpevarp1.2 and as listed in the tables of Chapter 2 have been considered for the modelling. The main exception is that the geological and hydrogeological modelling did not make full use of the substantial amount of old raw data from Äspö, Ävrö and Clab. However, the modelling has used the old models developed for Äspö, Ävrö and Clab, as a starting point and has used the new data from the site investigation to assess the information in these models. Considering all existing raw data would have been practically very resource demanding, and since the resulting existing models have been used, the impact on the modelling of the Simpevarp subarea (including the Simpevarp peninsula and the Ävrö island) is likely to be moderate, possibly with some important exceptions:

- Lineaments on the Simpevarp peninsula and the Ävrö island are short, i.e. the model of deterministic deformation zones is not much affected by the detailed linked lineament interpretation (the indication is that there are no/few large deformation zones in the Simpevarp subarea), but the lineaments and observed minor ("stochastic") deformation zones in Clab and Äspö HRL could possibly resolve existence/non existence of such zones observed in the boreholes. This could prove valuable input to enhancing the DFN-model (see below).
- The old subhorizontal borehole KBH02 (from Hålö to Äspö) has not been fully used. The borehole covers a volume and direction that would reduce bias and uncertainty.
- Also for the hydrogeological modelling the hydraulic DFN-model could have been tested also on the old hydraulic data from Äspö (including data from the TRUE Block Scale experiment), Ävrö and Laxemar, with potential modification of the model and enhanced confidence. Furthermore, the packer test data (PSS) also from the new boreholes were only partially used – although some assessments were made to show the importance of these data to bridge the gap resulting form the relatively high measurement limit of the Posiva Flow Log (PFL).

These data ought to be considered in coming model versions.

Accuracy

Accuracy in field data and interpretation has generally been established using well-defined procedures as is explained in detail in previous chapters of this report. In general the data are taken from the SICADA data base and have been subject to Quality Assurance in accordance with developed method descriptions. In addition, the following remarks could be made:

- For the geological modelling no systematic revisit of the lineament map has been made, unless there was a fully apparent mismatch with observations. For the Borehole data: no systematic check of SICADA data, or of single-hole geologic interpretation was made, the data where used as is.
- Rock Mechanics used the Boremap data as is, but simple checks were made and error corrected. Each shear test and normal loading test was analysed in detailed and improvements of test procedure and interpretation were suggested. The inherent uncertainty in different stress measurement techniques are discussed and considered (by judgement) in the modelling.
- The thermal modelling team made their own check of reasonableness while working with the data.
- Hydrogeological data were checked when used in the modelling.
- In Hydrogeochemistry checking the data is a part of the modelling.

In summary, some of the data are further checked during the modelling, but possibly more such checks could be made to further improve the quality of data.

The potential for inaccuracy stemming from the field data is assessed and is in general judged to be a minor source of uncertainty in the resulting model description. This general statement is true also for the few instances of poor precision found, i.e.:

- Current outcrop data on secondary red-staining (hydrothermal alteration) has poor spatial resolution, which leads to uncertain description of its spatial distribution.
- There is lack of confidence in the lineament interpretation especially their lengths, continuity and density and whether they actually are indications of deformation zones or not. This problem is considered when judging the uncertainty in the deformation zones, see Section 12.3.
- Borehole radar reflectors have low accuracy both in interpreted fracture orientations and in actually detecting fractures and are thus not used very much.
- Interpretation of open/sealed fractures on outcrops is of poor accuracy and is thus not used in the modelling.
- Accuracy of laboratory rock mechanics fracture, normal and shear stiffness, were judged low and an update of the methodology report has been initiated. There was also large scatter in results from tilt test – therefore laboratory shear tests are now used.
- The maximum (horizontal) principal rock stress from hydraulic measurement methods is not quantified, but over-coring data provide estimates of this stress.
- Inaccuracies in modal analyses have led to the position that direct measurements of thermal properties are favoured instead of calculation from the mineral content.
- Results from WL-tests or airlift-pumping generally have less accuracy than other hydraulic tests, but are still useful if no other tests are available.
- Hydrogeochemistry has assessed the accuracy of major components, stable isotopes to about ± 5–10%.
- For the near surface modelling, the accuracy of the data on distribution of till on the seafloor is limited and the geophysical interpretations need field verifications. Also, the regional map of the overburden (primarily the Quaternary deposits) , the transport in overburden and various biota data are judged to have rather low accuracy.

As can be seen from the list above, most of the items are not sources of uncertainty in the model description because they have been recognised as subject to error and therefore not used. Furthermore, this has not necessarily resulted in serious data gaps as the methods previously used have been replaced by alternatives.

Bias

There are biases in the Simpevarp version 1.2 data, but much of the bias noted in Simpevarp version 1.1 is not reduced. Some important examples are discussed here, whereas the filled in tables in Appendix 7 provide a fuller picture.

Few data exist from areas covered by the sea and the bedrock information in the regional and local scale model area outside the Simpevarp subarea is only of a reconnaissance character. Consequently, there are far more lineaments and, thereby, inferred deformation zones on land and in i) areas covered by airborne geophysical measurements and detailed air photography and ii) in the sea area close to the Simpevarp peninsula and Ävrö, than in the remaining part of the sea area. The bias resulting from less detailed data in the sea area will remain in future model versions, but is judged acceptable since it is not very important to model details of deformation zones in the sea.

Bias is introduced by the data gap between lineaments (lower cut-off > 500 m) and outcrop mapping (window < 30 m). It is necessary to consider this when assessing the uncertainty in the size distribution of features in the range 10–1,000 m in the DFN-model.

Directional bias exists in cored borehole data, as all these boreholes, except KSH03, are steep and borehole KLX01 does not have information on oriented fractures. Mapping of fractures at the surface will produce a bias towards steeply-dipping fractures. These directional biases also impact the rock mechanics and hydrogeological modelling. Some correction of the fracture orientation mapping can be applied with the help of a Terzaghi orientation correction, but to really reduce this bias some gently inclined boreholes would be needed. The Terzaghi correction is likely to work best over the small angle range and no correction can fully compensate for the lack of information that arises when the structures of interest are aligned close to parallel to the sampling direction.

Some concerns exist as to the possibly poor representativity of samples for thermal data. However, samples were taken in order to characterise the rock type – not to find odd varieties, but random sampling was not made. There is also an unknown bias resulting from using modal data in the SCA method, SCA data are thus judged to be more uncertain that direct measurements (when available).

Potential sources of bias in chemical data include contamination from drilling fluid. Such biased data have been corrected by using back-calculations, but the representativity of data may be still put in question.

Biases in data for the surface system description could partly be corrected. The effect of ion balance errors and drilling water contamination can be back-calculated but the representativity may be in question. For meteorology, precipitation data are corrected for measurement errors by a standard procedure. Generic information on hydrology variations in small areas, and influence of topography and land use, can be used to infer local discharge estimates from available discharge data in relatively large catchments and potential biases in results of hydrogeology field tests can, to some extent, be identified by comparisons with literature data. This allows identification of possibly anomalous results and to filter them out before use.

12.2.2 Overall judgement

In general the available data have been analysed and treated according to good practices. Inaccuracy and biases are understood and accounted for in the subsequent modelling. However, it is noted that better use could be made of the old data from Äspö and Clab.

12.3 Uncertainties and potential for alternative interpretations?

The next step in the Overall Uncertainty and Confidence Assessment, see Figure 12-1, is to assess the uncertainties in the different disciplines. Small estimated uncertainties and inability to produce many different alternative interpretations from the same database are indications of confidence – although not a strict proof. A related issue is whether new measurements or other tests could resolve uncertainties or distinguish between alternatives and thereby further enhance confidence.

12.3.1 Auditing protocol

The SDM represents an integrated characterisation of a natural rock mass. Uncertainties are an inherent aspect of any such characterisation and thus also of the SDM. There are different types or origins of the uncertainties. Some are conceptual and may depend on unresolved scientific issues or on inadequate understanding (and/or modelling) of the geological, physical or chemical properties or behaviour of the rock mass. Other uncertainties are related with limitations in the available database due to spatial variations, temporal variations, measurement accuracy, the quality of data or with the lack of some data. Uncertainties cannot be avoided. It must be kept in mind that some uncertainties are more important than others. The important uncertainties must be identified and properly assessed and accounted for in the analyses.

The uncertainties need to be identified and the cause for uncertainty should be determined. Are the uncertainties mainly caused by inaccuracy in data, poor information density or is there a limited process understanding. Specifically, confidence in the description could be high, even if there are few measurements, if the geological understanding is high (e.g. if there is a homogenous and evident geology), but could also be low, even with a ‘wealth’ of data, if the geological understanding is poor.

An important support for confidence in a model aspect (parameter/geometry or process) is to what extent it is based on support from different (independent) data rather than being based on "simple" extrapolation of a single measurement. A related issue is whether the selected conceptual model (model process) with associated parameters have been determined through a calibration or verification exercise.

Another issue is whether a certain uncertainty could influence the assignment of uncertainty to another parameter. If two aspects of the SDM (or of the input data) are correlated they cannot be estimated independently of each other. Addressing the issue will also provide input for assessing the need to consider interdisciplinary model interactions (see Section 12.4).

In order to assess the importance of an uncertainty it needs to be quantified. The quantification needs to consider the different causes of uncertainty.

One way of expressing uncertainty is to formulate an alternative representation. In a first step potential alternative hypotheses are to be listed. These are then further evaluated – see Section 12.3.3.

Finally, the uncertainty assessment provides input to the question on if and how the Site Investigation Programme should be continued. Among issues to consider are the questions whether there are already available unused data, which could be used to reduce uncertainty, and what new data would potentially help reduce or resolve uncertainty.

Thus a common philosophy is required for addressing uncertainty and the implementation needs to be audited. There is a need to consider how uncertainties can be identified through uncertainty elicitation. A protocol has thus been developed for checking this. It concerns:

- Listing the main uncertainties in the different disciplines.
- What is the cause of the uncertainty (e.g. data inaccuracy, information density, uncertainty in other discipline model or process understanding), also indications from new data not yet fully analysed is a valid cause.
- Whether the uncertainty has been assessed considering information from more than one data source or through a calibration or validation exercise (a positive answer would be an argument in support for the uncertainty in the quantification).
- Assessing the impact on other uncertainties (in all disciplines).
- Quantification of the uncertainty (with reference to applicable section of the SDM report).
- Whether there is a potential for an alternative representation and whether an alternative actually has been developed (if yes this will be assessed in a subsequent protocol sheet).
- Whether there are unused data, which could be used to reduce uncertainty.
- What new data would potentially help resolve uncertainty.

The filled in auditing protocols are provided in Appendix 7. It should be noted that only some of listed uncertainties really would be of concern for Safety Assessment or Rock Engineering. As already explained assessing the importance of these uncertainties lies outside the scope of current report, but some general assessment is still made below.

12.3.2 Main uncertainties

Bedrock geological model

As already identified and discussed in Chapter 5 and as listed in Table A7-3 of Appendix 7 the main uncertainties in the version 1.2 *Bedrock Geological* model of *Rock Domains* concern:

- Spatial distribution of Rock Domains, outside the Simpevarp subarea.
- Offshore lithology.
- 3D geometry of most of the rock domains.
- Heterogeneity of rock domains, i.e. proportion of rock types in domains, subordinate rock types, veins, patches, dykes, minor bodies, frequency of minor deformation zones.

- Spatial distribution of varieties of rock types.
- 3D distribution of secondary alteration, e.g. “red staining.

For the model area outside the Simpevarp subarea the uncertainty is essentially caused by the lack of a detailed bedrock map and the quality of the surface bedrock information. The uncertainty is difficult to quantify – but is not judged important for other disciplines.

Uncertainty in the three-dimensional geometry of the rock domains inside the Simpevarp subarea is caused by the still rather limited subsurface information and the fact that the overall geology is a pristine igneous bedrock terrain with little structural control. The actual geometry has some impact on disciplines directly using the lithological description (i.e. rock mechanics, thermal properties and transport properties). The uncertainty as such is difficult to quantify, but users could still assess potential impact of the uncertainty by noting that the actual location of a rock domain in space is uncertain (i.e. the spread of mechanical and thermal properties for each rock domain, as provided in Chapters 6 and 7, is a measure of the impact of this uncertainty).

Uncertainty in heterogeneity of the rock domains, in spatial distribution of varieties of rock types and in the three-dimensional distribution of “red staining” (hydrothermal alteration) is mainly caused by the restricted information available. The uncertainties are generally quantified as ranges. Disciplines directly using the lithological description (i.e. rock mechanics, thermal properties and transport properties) are affected by the uncertainty – but also take it into account.

None of the uncertainties in the Rock Domain model are of significant importance for Safety and they are only of limited importance for Repository Engineering. Furthermore, information from new boreholes and detailed investigation of cleaned outcrops concerning the amount, distribution and character of subordinate rock types would reduce the above uncertainties within the Simpevarp subarea. Analysing exiting data with e.g. variography, although already done within thermal analyses, see Chapter 7, could also provide additional insights.

As already identified and discussed in Chapter 5 and as listed in Table A7-3 of Appendix 7, the main uncertainties in Simpevarp version 1.2 *Bedrock Geological* model of *Deformation Zones* concern:

- Existence of deformation zones (only some interpreted with high confidence) – are all lineaments really deformation zones?
- Potentially existence of non-included zones (mainly subhorizontal) (e.g. the Nordenskjöld hypothesis /Nordenskjöld, 1944/.
- Continuity along strike and at depth, dip and termination.
- Character, properties (width, internal structure, fracturing, hydraulic properties, ...) and spatial variability along zones.

Uncertainty in existence – or in non-existence − of deformation zones is essentially due to still rather limited supporting subsurface data and the question whether all interpreted lineaments really represent deformation zones. Hydrogeology and rock mechanics are directly affected by this uncertainty. The deformation zone model provides the geometrical framework for the hydrogeological modelling. The uncertainty is not quantified – but could potentially be handled by formulating alternative descriptions, although this was not yet made, see also Table 12-1.

Uncertainty in continuity along strike and at depth, dip and termination is intrinsic to the modelling process and questions of scale. Hydrogeology is possibly affected by this uncertainty, but the impacts are possibly handled within the uncertainty of properties within deformation zones.

Uncertainty in character and properties also in the well established zones is essentially due to the information density and spread of data. Hydrogeology and rock mechanics are directly affected by this uncertainty – and this in turn causes uncertainty in the distribution of e.g. hydraulic properties in the “plane” of the deformation zones. The uncertainty, regarding the geological heterogeneity, is not quantified.

Uncertainties in the deformation zones have both Safety and Engineering implications, especially as long as these uncertainties remain inside potential repository volumes. However, it should be noted that the uncertainties are comparatively lower inside the Simpevarp peninsula. Several new data would potentially locally (i.e. in the Simpevarp and Laxemar subareas) reduce uncertainty in the deformation zone models, including further analyses of potential borehole intercepts, data from new boreholes, seismic survey results, field control of lineaments performed during field bedrock mapping and feedback from hydraulic tests. It should also be noted that old data from Äspö HRL and Clab have not yet been fully used.

As already identified and discussed in Chapter 5 and as listed in Table A7-3 of Appendix 7 the main uncertainties in the version 1.2 *Bedrock Geological Discrete Fracture Network* model concern:

- Fracture set (orientation) identification.
- Fracture size distribution – interpolation between lineament and mapped outcrop data and for some sets only local information (extrapolation to larger sizes).
- Fracture intensity – coupling surface to subsurface, variability with depth.
- Coupling to the deformation zone model.
- Assumption of fracture intensity and spatial model coupled to rock domains.
- Thickness distribution for larger stochastic features.

Uncertainty in fracture set orientation, size and intensity originates from the assumptions of viewing data from the linked lineaments, outcrop maps and the boreholes to be expressions of the same underlying DFN-model. Furthermore, there are problems with all these data sources. There is a general uncertainty in the relevance of lineaments – do they actually represent expressions of deformation zones. Some fracture sets are only observed in outcrops, requiring extrapolation to larger sizes. Another issue is whether the surface fracturing as observed in outcrops is relevant for the fracturing at depth, as there is currently a lack of analysis of data for the superficial bedrock (0–100 m). Verification analyses have been performed and results shows that the simulated fracture intensity based on surface data can be as much as one order of magnitude lower than observations in boreholes. The major reasons for this *can* be that size estimates are based on truncated surface data in conjunction with borehole mapping done at a much higher resolution than surface mapping. Another major uncertainty factor is the poorly constrained properties (size, intensity) of the sub-horizontal set. Hydrogeology is critically affected by these uncertainties and to some extent also rock mechanics. The uncertainty is quantified to some extent, but as a large portion of the uncertainty is also connected to the underlying conceptual model and the modelling “style”, alternative descriptions are needed. An alternative DFN-model has therefore been developed by an independent modelling team, see below and Section 5.5.

The assumption of a fracture intensity coupled to rock domains, instead of rock type, and assumptions of a weakly Poissonian spatial model, instead of fracturing being correlated to proximity to larger deformation zones, are assumptions and are substantially uncertain. Also these uncertainties impact hydrogeology and rock mechanics modelling. The uncertainty is not quantified and is rather listed as a reason for alternative model hypotheses at this stage.

Uncertainty in the thickness of the (larger) features of the DFN-model is essentially due to lack of analysing this aspect. The thickness has direct implications for rock mechanics and potentially also for hydrogeology. There is currently no quantification of this uncertainty – although it is apparent from the single-hole interpretation that (minor) “stochastic” deformation zones could have significant width. Possibly old data (observations of length, width and property relationship) from Clab etc. could be used to characterise, or at least set bounds on the uncertainty for some of these minor zones.

Uncertainties in the DFN-model have direct Safety and Engineering implications. The current description, with its alternatives, is judged appropriate to get a handle on the situation, but reducing the uncertainties would be useful. There still exist a significant number of old data not yet analysed in full that potentially would reduce the uncertainty in the DFN-model. The most important such data are tunnel mapping from Äspö HRL and the Clab and existing scan-line data. New information that would further reduce uncertainty include data from inclined boreholes in different orientations and rock domains – preferably in conjunction with surface area mapping.

Rock mechanics model

As already identified in Chapter 6 and Table A7-4 of Appendix 7, the main uncertainties in the Simpevarp version 1.2 *rock mechanics stress* model concern:

- Rock stress magnitudes and the spatial variation of stress within the model area. (However, the uncertainty varies in the area, and is lower on the Simpevarp peninsula and even less at Äspö HRL.)
- Uncertainty in the division of the local model area into two stress domains.

Uncertainties in rock stress magnitudes and distribution within the model area are due to data inaccuracy (see Section 12.2.1) and information density (especially outside Äspö HRL, Simpevarp peninsula and parts of the Laxemar subarea). Uncertainty in the deformation zone model also implies uncertainties in the boundaries of the two stress domains. Different measurement types have been used and compared, see discussion in Sections 6.2 and 6.4 and experiences from Äspö HRL confirm that extremely high stress magnitudes do not exist in the local model area , i.e. – an upper bound of stress can be justified. The other model descriptions are little affected by this uncertainty, but varying stress may possibly explain the potential difference in transmissivity anisotropy between Äspö HRL and the Simpevarp peninsula – and reduced uncertainty would thus enhance understanding. (However, at this point it may be a bit premature to conclude whether there are in fact such differences.) Uncertainty in the the stress magnitude is described as a range and there is little need for alternative representations.

All existing data are used to assess the stress distribution. New data that would further reduce uncertainty include additional overcoring measurement data, but no additional data are judged needed, since the current uncertainty span in stress still suggest rather low overall stress levels, which probably are acceptable.

As already identified in Chapter 6 and Table A7-4 of Appendix 7, the main uncertainties in the Simpevarp version 1.2 *rock mechanics properties* model concern:

- Rock mass mechanical properties and especially the extent and occurrence of stochastic (minor) deformation zones, having different mechanical properties compared with the remaining rock mass.
- Rock mechanical properties for intact rock (for Ävrö granite).
- Mechanical properties of deformation zones.

Uncertainty in rock mass mechanical properties originates both from the model uncertainties, see /Andersson et al. 2002a/ and uncertainty in the DFN-model. The latter affects the “theoretical” approach in many different ways. The fracture intensity is one of the most important DFN-model parameters for the prediction of the strength and deformation parameters using the theoretical approach. Therefore, uncertainties or weaknesses in the DFN description of the fracture intensity, and its spatial variation within domains, would cause uncertainties also in the description of expected mechanical properties.

Uncertainty in extent and width of “stochastic” (minor) deformation zones is a larger concern as these zones may make up a significant volume of the rock mass – and have different properties compared with the remaining rock mass. Both the single hole interpretation and results of the DFN-modelling results have been used, but the DFN-model does not (yet) include any width parameter (see above). The resulting uncertainty is thus only qualitatively assessed based on the single hole interpretation (see Section 6.3). An alternative (or more elaborate) DFN-model with a width distribution would be useful for further analysis.

Uncertainties in rock mechanical properties of intact Ävrö granite rock are due to lack of new laboratory tests. Old data from Äspö HRL have been used, but there are uncertainties in the quality of these data. Furthermore, these data have low spatial coverage, i.e. may give bias. However, this uncertainty is judged to only have a minor effect on the assessed rock mass properties.

There are several reasons for the uncertainty of mechanical properties of the deformation zones. There is low data coverage, since only borehole KSH03 intersects a deterministic deformation zone. Furthermore, the current geological description only in a few instances reports whether a deformation zone is brittle or ductile. Further geological characterisation of the zones would thus reduce this uncertainty. The impact on other discipline models is low, but a better description could enhance understanding in the stress modelling. Uncertainties are expressed as ranges – using the empirical approach. There is little reason for alternative models.

The uncertainties are of no importance for Safety and of limited concern for Engineering. Apart from the issue of minor "stochastic" deformation zones, there is probably little need for more data, apart from those already planned for Laxemar 1.2 to further reduce uncertainty in the rock mechanical property modelling.

Thermal model

As already identified in Chapter 7 and Table A7-4 of Appendix 7, the main uncertainties in the Simpevarp version 1.2 *thermal* model concern:

- Thermal conductivity – rock type.
- Scale transformation – from measurement to canister scale.
- Thermal conductivity – rock domains.
- Thermal properties of deformation zones.
- In situ temperature.
- Coefficient of Thermal expansion.

Uncertainty in thermal conductivity occurs at different scales ranging from uncertainty within rock types, uncertainty in upscaling laboratory size data to larger (e.g. canister) scales, spatial variability within rock types, rock type variability within rock domains and the uncertainty in the actual geometry of rock domains, as discussed for the geological model. Furthermore, there are no thermal data from the deformation zones, but this is of little importance if canisters are not to be emplaced in those zones. At the small scale, the representativety of SCA calculations from modal analysis (thermal conductivity of minerals, modal composition, alteration) is questioned. These indirect results have partly been compared with direct thermal (TPS) data. For upscaling it is possible to use the correlation between density logs and thermal conductivity for Ävrö granite, but there is no such correlation for other rock types. For these, there are far fewer data to base upscaling rules on. Nevertheless, the uncertainty of thermal conductivity is quantified as ranges, for different scales, although better understanding of the upscaling could possibly allow further variance reduction at the larger scales.

Uncertainty in temperature data is possibly due to convection in the boreholes (both thermal and due to the "short-circuited" flowpaths created by the borehole). The uncertainty is quantified as a range. It is small in absolute terms, but still important for Engineering and layout.

There is a possible uncertainty in the coefficient of thermal expansion but the results using different measurement methods and laboratories have not yet been reported. The uncertainty is currently quantified as a range, but different conceptual models (linear or not) could be considered.

The uncertainties have little direct implications on Safety, but are important for Repository Engineering as further reduction in the uncertainty of the variability of thermal conductivity and also of the initial temperature would enable a more efficient use of the rock volume. Overall, the uncertainty in thermal properties could be reduced by representative direct measurements of thermal conductivity, more samples with both density and thermal conductivity measurements on the Ävrö granite and sampling of other rock types, including more boreholes, to produce variograms of spatial variability. The methodology for thermal modelling need to be further developed. Also, improved confidence in the Rock Domain model would help. Uncertainty in temperatures would be reduced by more temperature logs and, if possible, developing the measurement procedure to mitigate the effect of the convection in the boreholes. A new laboratory test method, that is now underway, may reduce uncertainties in the coefficient of thermal expansion.

Hydrogeology

As already identified in Chapter 8 and in Table A7-5 of Appendix 7, the main uncertainties in the Simpevarp version 1.2 *hydrogeological* model concern:

- Geometry of deformation zones and their connectivity.
- Transmissivity distribution in zones (spatial variability).
- Hydraulic DFN model and especially the fracture transmissivity distribution.
- Present day salinity conditions and especially its spatial distribution.
- Regional scale boundary and initial conditions.
- The digital elevation model.

The uncertainty in the geological model of the deformation zones, see above, causes uncertainty in the hydrogeological model, especially in the regional area where the uncertainty in the zone geometry is larger. The impact of this uncertainty on regional flow and evolution of groundwater composition is assessed in the numerical regional flow modelling by exploring cases with varying numbers of deformation zones. As discussed in Chapter 8, the uncertainty in the geological model has an effect on the flow field in the regional scale, but the magnitude is dependent on the interplay with the Hydro-DFN model characteristics.

Uncertainty in the transmissivity distribution and spatial variability within zones is essentially due to sparse data. Only a few zones have been measured and even less have more than one measurement (i.e. intersection with a borehole). Some different cases of the transmissivity distribution are explored in the numerical regional flow modelling. In principle each deformation zone can be modelled as Hydro-DFN with effective values as well as spatial correlation models, but it is not judged necessary, see Chapter 8.

Uncertainties in the hydraulic DFN-model originate from the uncertainty in the geological DFN-model (see above) and the uncertainty in the transmissivity distribution between and within fractures and features. The latter uncertainty is due to relatively few measurements, the indirect nature inherent in the measurement methods (PFL and PSS), and the uncertain conceptual models for coupling transmissivity as a function of feature size. Connected to this is the fact that the larger features of the DFN-model usually are made up of many small fractures, and do not represent individual fractures. The relatively high and varying measurement limit of the PFL (within and between boreholes) also adds uncertainty of the low permeability end of the transmissivity distribution. The uncertainty has direct implications for transport, but possibly less for the overall permeability, since the models are anyway calibrated to the known hydraulic data. The uncertainty is assessed and quantified by simulation of the actual tests using alternative transmissivity-size models. Matching both PFL and PSS data potentially offers some possibilities for selecting the more likely model. There are also uncertainties in the intensity and size distribution used in the hydraulic DFN-model.

The spatial distribution of the present day salinity conditions is uncertain as the number and spatial distribution of sampling points are limited, and there are few to no data on the water composition in the intact rock matrix (see hydrogeochemistry below). This means that there are uncertainties in the calibration target for the regional groundwater flow simulations. This is considered when discussing the degree of match between model results and measured data.

Regional scale boundary and initial conditions are also uncertain. There are various hypotheses on the water type distribution at the end of the last glaciation. The impact of these uncertainties is assessed by exploring various locations of, and conditions at, the regional boundary and by exploring various initial conditions, see further discussion in Chapter 8. The estimate of the uncertainties in the present-day calculated relative proportion of each water type and the evolution of the water types after the last glaciation (introduced as boundary conditions) are other uncertainties that should be discussed in more detail in the future models.

There is also some uncertainty in the digital elevation model, including the location of the shoreline, as it is now made up of input from various sources that are not intrinsically consistent with each other. This could affect the modelled distribution of discharge areas. A unified digital elevation model is being developed and will be available for Laxemar 1.2.

The uncertainties in the hydraulic DFN model have direct safety implications. The current description, with its alternatives, is judged appropriate to get a handle on the situation, but reducing the uncertainties would be useful. It would also be useful to get a better understanding of boundary conditions and the properties of the deformation zones in the regional domain, but the implications on safety are less severe since upper bounds on the hydraulic gradients always can be found.

Further analysis of existing data could reduce some of the uncertainties in the hydrogeological model, but the current hypotheses on anisotropy and T versus size correlations stems from previous analyses of data from Äspö HRL. Still it is possible that the PSS data could be used more to test the Hydro-DFN models by simulating existing tests performed at various scales. Further reduction of uncertainty would require more hydraulically tested (both PFL and PSS) boreholes and further integration with the geological modelling. Interference data and cross-hole tests are important in this context.

Hydrogeochemistry

As already identified in Chapter 9 and in Table A7-5 of Appendix 7, the main uncertainties in the Simpevarp version 1.2 *hydrogeochemical* model concern:

- Spatial variability in 3D at depth.
- Groundwater composition in the intact rock matrix.
- Temporal (seasonal) variability in surface water chemistry, which ultimately impacts the groundwater at depth in the bedrock.
- Model uncertainties (e.g. equilibrium calculations, migration and mixing).
- Identification and selection of end-member waters. This is a judgemental aspect of the M3 (principal components) analysis.

There is uncertainty in spatial variability in 3D at depth, as the information density concerning borehole groundwater chemistry is low. Furthermore, samples are mixed and represent an average composition, but a verification test has been conducted where representative/non-representative samples have been interpolated. The uncertainty in spatial distribution must be considered when used as a calibration target for the coupled numerical regional flow and transport modelling of the past groundwater evolution, see Chapter 8. The uncertainty is quantified with a local uncertainty in the order of ± 50% and a site-scale uncertainty in the order of ± 10%, see Section 9.6.

The groundwater composition in the intact rock matrix is uncertain, as there are very few measurements. Knowing the composition would be important for the coupled regional flow and transport modelling of past groundwater evolution, and will thus be important for enhancing the understanding of the role of the rock matrix as a factor on migration (transport) in the rock.

The temporal (seasonal) variability in surface water chemistry ultimately impacts the groundwater at depth in the bedrock, but the sampling may not describe the actual seasonal variation. A detailed surface hydrogeological modelling may be helpful to explore the potential significance of this issue. The uncertainty affects evaluation of the interaction between surface and groundwaters and may affect transport modelling. It is essential to address the bedrock surface interface properly. The effect from seasonal variation has not been quantified but the effects have been identified, see Section 9.3. Model uncertainty is handled by applying different modelling approaches on the same data set to describe the same processes.

There are several model uncertainties e.g. relating to equilibrium calculations, migration and mixing. This is due to inaccurate pH measurements, inaccuracy in the thermodynamic data bases, possible alternative mineral phase selections, possible alternative end-member selection, as well as conceptual model uncertainties. For verification and internal consistency, different modelling approaches are applied on the same data set. The uncertainty may affect the transport modelling and certainly affects the overall hydrogeochemical understanding of the site. The impact is quantitatively assessed by applying different model approaches and through sensitivity analyses, e.g. one unit error in the pH measurements may cause one unit error in the equilibrium calculations, see Sections 9.2, 9.5 and 9.6, but through available in situ measurements of pH at depth, the uncertainties are manageable. As different modelling approaches are applied on the same data set to describe the same processes, confidence is built into the overall hydrogeochemical description.

There is a judgemental aspect of the M3 (principal components) analysis and the identification and selection of end-member waters. There is an ongoing effort to integrate the description with hydrogeology. The uncertainties need to be considered in the coupled numerical regional flow and transport modelling of the past groundwater evolution and impacts on the overall hydrogeochemical understanding of the site. To explore this uncertainty, different end-members have been selected in the regional/local models, but no quantification has been conducted, see Sections 9.5 and 9.6. Nevertheless different modelling approaches are applied to the same data set to describe the same processes, which contributes to enhancing understanding.

There are no direct Safety or Engineering implications stemming from the uncertainties in the hydrogeochemical model. The listed groundwater compositions are well within the bounds of the preferred conditions, see Chapter 9 and 11. Still, reducing the uncertainties would enhance understanding and thus the capability of predicting the future evolution (including assessment of effects of post-emplacement perturbations). More data observations from deep boreholes and analyses of rock matrix samples would reduce uncertainties in the hydrogeochemical model. It should be noted that samples for rock matrix determination have been collected and the results will be available for the Laxemar SDM version 1.2. Sampling reflecting seasonal variation from selected surface and borehole locations in identified recharge/discharge areas would reduce the uncertainty in temporal averaging.

Bedrock transport properties

As already identified in Chapter 10 and Table A7-5 of Appendix 7, the main uncertainties in the Simpevarp version 1.2 model of the *bedrock transport properties* concern:

- Site-specific sorption and diffusion parameters.
- Assignment of parameter values to the “elements” in the geological description (“typical” rock materials and structures).
- Understanding of retention/retardation processes as a basis for selection of parameters in models.
- Correlation between matrix transport properties and flow paths.

A main reason for these uncertainties is the lack of site-specific transport data and that all relevant rock types are not represented in Äspö HRL data, which could be used as an analogue. There are also limitations in the geological description concerning, e.g., porosity, fracture mineralogy and alteration. The uncertainties can still be estimated using data from various geological environments, although current data do not allow for any quantification of the correlation between matrix transport properties and potential flow paths. Concerning the latter correlation, it should be noted that the quantification of flow-related transport parameters, including assessment of spatial variability along flow paths, will be handled by Safety Assessment.

Another reason for uncertainty is the limited conceptual understanding of retention/retardation processes and selection of parameters in models, see Chapter 10. The process understanding could possibly be enhanced. A study of “alternative” processes and process models is currently being performed, but no site-specific conclusions can be drawn based on the results obtained so far. It should also be clearly stated that this is an active research area, and that the potential for progress in terms of site-specific results is somewhat uncertain.

The uncertainties are of importance for Safety but not for Engineering. The current description, with its alternatives, is judged appropriate to get a handle on the situation, especially by further uncertainty assessment with Safety Assessment itself, but further reduction of uncertainties would be useful. Laboratory investigations of site-specific samples are presently being performed. However, the tests take a long time, which implies that most of the results will not be available until after the version 1.2 models have been completed. Additional samples from future boreholes will also be tested, and more results from in situ measurements will become available. Eventually, a considerably improved site-specific database will be at hand, which will reduce the listed uncertainties and provide a basis for further integration with other disciplines.

Surface system

As already identified in Chapter 4 and in Table A7-6 of Appendix 7 the main uncertainties in the Simpevarp version 1.2 model of *the surface system* are related to the lack of certain types of data. Specifically, the most important gaps in the present database concern:

- Overburden (Quaternary deposits) – composition, spatial distribution, depth and thickness of individual strata.
- Meteorology – spatial and temporal variability in precipitation and other meteorological parameters.
- Hydrology – water flows in the surface system, surface water and groundwater levels, water balance components (evapotranspiration, distribution of runoff on surface water and groundwater flows).
- Flora and fauna – biomass and production, chemical composition of biota.

These uncertainties will be reduced as additional data becomes available. Furthermore, uncertainties related to the understanding of site-specific processes will be analysed in future model versions. It is also worth remembering that there is a general conceptual uncertainty in that what is observed in the surface system at present day may not be representative, even under current climate conditions, and that it may be desirable to adopt a modified description (e.g. more cautious) for Safety Assessment.

12.3.3 Alternatives

As discussed by /Andersson, 2003/ alternatives may both concern:

- alternative geometrical framework (e.g. the geometry of deformation zones and rock domains), and
- alternative descriptions (models such as DFN or SC – or parameter values) within the same geometrical framework.

Alternative model generation should be seen as a means for model development in general and as a means of exploring confidence. At least in early stages, when there is little information, it is evident that there will be several different possible interpretations of the data, but this may not necessitate that all possible alternatives are propagated through the entire analysis chain including Safety Assessment (SA). Combining all potential alternatives with all its permutations leads to an exponential growth of calculation cases – variant explosion – and a structured and motivated approach for omitting alternatives at early stages is therefore a necessity.

Compared with model version Simpevarp 1.1 there is an increased attention to alternatives in version Simpevarp 1.2. As can be seen from Tables A7-3 to A7-6 in Appendix 7, some alternative hypotheses have actually been developed into alternative models. Furthermore, the alternative hypotheses are all assessed in order to decide on their treatment. This assessment is based on addressing the following set of questions for each potential alternative identified concerning:

- Is the alternative “resolved in Simpevarp 1.2? (Only concerns hypotheses raised in Simpevarp version 1.1.)
- Will the alternative affect other discipline models of the site descriptive model (or aspects of these models)?

- What are judged to be the gross implications for Engineering in phase D1?
- What are judged to be the gross implications for Safety Assessment analyses in PSE (Preliminary Safety Evaluation) and SR-Can?
- What are judged to be the implications for investigations to “resolve” a particular alternative?

Finally, based on the answers to these questions a recommendation is made whether the alternative should be developed and propagated, be discarded or be put “on hold”, by applying the following criteria:

Reasons to develop/propagate now:

- Potentially large impact on Safety Analysis or Repository Engineering.
- Potentially very expensive to resolve by further data collection.
- Issue judged to be good to put “at rest” early.

Reasons not to propagate/develop:

- “Old hypotheses” which is now resolved.
- Shown to have little impact on Safety Assessment or Repository Engineering (can be directly discarded).
- Could be factored into quantified uncertainty.

Reasons to wait with development/propagation:

- Judged to have little impact on Safety Assessment or Repository Engineering.
- Will be resolved through expected investigations and data made available in later data freezes.

Alternative hypotheses not explored will be “kept on the list” for further scrutiny.

The judgements made for the different alternative hypotheses are summarised in Table 12-1. The judgements regarding importance for Safety Assessment and Engineering are preliminary, but have been reviewed by experts within the Safety Assessment and Rock Engineering teams.

Bedrock geological model

As further explained in Table A7-3 in Appendix 7 identified hypotheses for alternative models of the bedrock geology concern:

- Lineaments.
- Existence of deformation zones.
- Extension (size) of deformation zones.
- Character and properties of deformation zones.
- The geological DFN-model.
- Width of minor deformation zones in the DFN-model.

Some of these alternatives hypotheses have been further assessed, whereas others are discarded or kept, as summarised in Table 12-1.

Other means of carrying out the coordinated lineament interpretation could potentially be a generator for an alternative model. This was noted already in Simpevarp 1.1. However, no alternative lineament interpretation has been made for Simpevarp 1.2, but will be made for Laxemar 1.2. Depending on the results, it will then be assessed how this affects uncertainty and potential alternatives in the deformation zone model.

Table 12-1. Assessment of alternatives.

Potential "Primary" alternatives in SDM (see Tables A7-3 to A7-5) of Appendix 7	Is the need for alternative resolved in Simpevarp 1.2? (Only concerns hypotheses raised in Simpevarp version 1.1)	Impact on other discipline models (or aspects of these models)?	Implications for Repository Engineering in phase D1	Implications for analyses in PSE and Safety Assessment	Implications for investigations to "resolve" alternative	Handling in Simpevarp version 1.2
Surface and near surface description						
None						No alternatives will be developed. The prime objective is to derive a model.
Bedrock geology						
Geometry of Rock Domains in the Simpevarp subarea.	Most of the uncertainty remains, but little need for alternative model, since resulting uncertainty in thermal and mechanical properties can still be estimated (see next col.).	Affects thermal and rock mechanics model. Work implication minor (since 3D extrapolation anyway made in geological model). However, uncertainty is (if needed) already now described as a wider uncertainty range – and not necessarily as alternative models.	May affect space and degree of utilisation.	Changed repository volume. Revised thermal analyses.	Additional boreholes to explore lithological boundaries.	Uncertainty is acknowledged, but no need for an alternative model at all. *Not necessary* to propagate at this point. Implications are straightforward.
Alternative lineament interpretation.	No	May affect deformation zone model (if alternative lineament interpretation is really different compared to "original" lineament interpretation). See also next row.	See next row.	See next row.		Not made for Simpevarp, but will be made for Laxemar 1.2. Depending on results it will then be assessed how this affects uncertainty and potential alternatives in the DZ model.
Changes of existence or geometry of deformation zones (extent and directions) in Simpevarp Peninsula.	No, see Table A7-3 in Appendix 7.	New rock mechanics model (minor update). New hydrogeologic model (major update – all calibrations should be remade with this structure in mind).	Yes, new design – changed repository volume.	Yes, new set of migration calculations (due to new hydrogeological model). May also affect assessment of rock mechanics impacts and respect distances.	see Table A7-3 in Appendix 7 (Review of Clab, OKG, Ävrö and Äspö data – reinterpretation Alternative lineament map Several additional deep boreholes Excavated trenches).	Potentially important to propagate – but implications for RE and SA are relatively straightforward and could be less cost effective for full analysis in 1.2. The issue will anyway be resolved later in the investigations
Changes of geometry of deformations zone (extent and directions) outside Simpevarp Subarea.	Yes	May affect stress calculations (more for understanding). Affects hydrogeology in large scale Sensitivity calculations.	Probably NO IMPACT (although if this results in new stress model – see next row).	Probably NO IMPACT (possibly on future developments).	Potentially unrealistic characterisation efforts would be needed in the regional area.	No need to resolve outside Simpevarp and Laxemar subareas. Updated DZ model of Laxemar in Laxemar version 1.2. No need to RE or SA propagate since implications are trivial.

Potential "Primary" alternatives in SDM (see Tables A7-3 to A7-5) of Appendix 7	Is the need for alternative resolved in Simpevarp 1.2? (Only concerns hypotheses raised in Simpevarp version 1.1)	Impact on other discipline models (or aspects of these models)?	Implications for Repository Engineering in phase D1	Implications for analyses in PSE and Safety Assessment	Implications for investigations to "resolve" alternative	Handling in Simpevarp version 1.2
Character and properties – also in the well established zones.	New	Affects assignment of hydraulic and mechanical properties of these zones.	See hydrogeology and rock mechanics row.	See hydrogeology and rock mechanics row.	See Table A7-3 in Appendix 7.	Not done yet – but there remains potential for alternatives. Impact is partly assessed in hydrogeology.
Alternative (geological) DFN-model.	No, see Table A7-3 in Appendix 7.	Rock Mass Mechanics model (see further discussion under rock mecanics). Hydrogeology: (see further discussion under hydrogeology).	May affect space and degree of utilisation. (Amount of key blocks may be affected by alternative DFN-models.)	Yes, new set of calculations for RN-transport.	See Table A7-3 in Appendix 7.	Alternative DFN-models are being presented (see Table A7-3 in Appendix 7).
Width of minor deformation zones in the DFN-model.	New	Rock Mass Mechanics model (see further discussion under rock mecanics). Hydrogeology: (see further discussion under hydrogeology).	Affects degree of utilisation.	Yes, new set of calculations for RN-transport.	See Table A7-3 in Appendix 7.	Discussed by Engineering. To be developed for the Laxemar model.
Rock Mechanics						
Rock Mechanics Properties – due to alternative DFN-models.	New	No	Impact depends on change of properties.	No – or minor impact expected.	Potentially carry out sensitivity analyses on the SDM-level using different SDM:s.	The quantification of uncertainty using different methods, see Table A7-4 in Appendix 7, is judged sufficient. However, should possibly be reconsidered depending on handling of minor deformation zones in the DFN.
Alternative Stress Model	Of the two alternatives in 1.1, the one with two stress domains is now considered the most likely (due to new data).	No (but stress modelling may provide feedback to deformation zone model).	Affects degree of utilisation (and thus possibly overall layout), but due to the low stress level impact is judged minor at Simpevarp and Laxemar.	Potentially Minor, since stress levels quite low.	See Table A7-4 in Appendix 7.	The current model with two stress domains is considered likely. The alternative hypothesis will not be further pursued. Will instead be handled as quantified uncertainty.
Thermal properties						
Thermal properties	Yes, there is no alternative model. Uncertainty handled by uncertainty range.	No	Would affect canister spacing.	Would affects certainty in temperature calculations.	An upscaling validation test is currently carried out using the prototype repository data.	There is no alternative model. Uncertainty handled by uncertainty range.

Potential "Primary" alternatives in SDM (see Tables A7-3 to A7-5) of Appendix 7	Is the need for alternative resolved in Simpevarp 1.2? (Only concerns hypotheses raised in Simpevarp version 1.1)	Impact on other discipline models (or aspects of these models)?	Implications for Repository Engineering in phase D1	Implications for analyses in PSE and Safety Assessment	Implications for investigations to "resolve" alternative	Handling in Simpevarp version 1.2
Hydrogeology						
Alternative in the geological model of geometry of deformation zones and their connectivity.	No (see Table A7-5).	New regional hydrogeologic model – affects palaeohydrogeological model.	Possibly minor – would affect construction consequence analysis and impact of "open repository".	Possibly minor for radionuclide migration (little transport resistance in zone). Impact of "open repository". Potentially important for evolution of groundwater chemistry, but not very dramatic.		The impact of this uncertainty on regional flow and evolution of groundwater composition is assessed in the numerical regional flow modelling by exploring cases with varying numbers of deformation zones.
Change of hydraulic properties ("transmissivity" and connectivity) of deformation zones in Simpevarp subarea. (Depth dependence, T correlation to orientation.)	New	New regional hydrogeologic model – affects palaeohydrogeological model.	Possibly minor – would affect construction consequence analysis and impact of "open repository".	Possibly minor for radionuclide migration (little transport resistance in zone). Impact of "open repository". Potentially important for evolution of groundwater chemistry and thus on retardation properties and parameters.	See Table A7-5 in Appendix 7.	The need to further resolving this issue essentially depends on how it affects the understanding of regional groundwater flow and the evolution of water composition. Some different cases of the transmissivity distribution are explored in the regional flow modelling, see Chapter 8.
Alternative hydro-DFN, including alternative T vs. Size correlation. Depth dependence, T correlation to orientation. At FM evidence for alternative hypotheses.	Alternative is kept since 1.1.	Affects hydrogeology model (need to remake calibration efforts – but possibly only on smaller scale). Potentially – no need to e.g. update palaeohydrogeology and regional scale descriptions.	May perhaps affect space and degree of utilisation.	Potentially large impact on transport. New set of calculations for RN-transport.	See Table A7-5 in Appendix 7.	Several Hydro-DFN models with different T-models (T correlated/ un-correlated) fractures have been calibrated to the data. The alternatives are propagated to the regional flow modelling and will be propagated to Safety Assessment.
Hydrogeochemistry						
Alternative hypotheses in groundwater composition and processes.	Possibly, but potential for alternatives should still be considered in future versions.	May affect "palaeo-hydrogeological" simulations.	NO IMPACT	Predictions of future groundwater composition (and thus resulting migration data).	Table A7-5 in Appendix 7.	In version 1.2 different modelling approaches are applied on the same data set to describe the same processes Thereby, the most realistic descriptions can be identified and less realistic discarded.

Alternatives with non-included deformation zones (mainly sub-horizontal) as well as alternative extensions (length and depth) of deformation zones were noted already in Simpevarp 1.1. The issue is not resolved, and not fully developed. Some assessment of the importance of zones is carried out in the regional numerical hydrogeological modelling. Apart from the potential impact on the regional groundwater flow, which is being assessed, there is little need to resolve the issue for zones outside the Simpevarp and Laxemar subareas, as implications for Repository Engineering and Safety Assessment are small. Within the subareas, it is eventually important to reduce the spread of alternatives as the deformation zones directly affect the layout, but implications are relatively straightforward and could be of limited cost effectiveness for full analysis in Simpevarp 1.2. The issue will anyway be resolved later in the investigations.

An alternative for describing the character and properties of the zones is a new issue since Simpevarp 1.1, but has not been developed. However, the impact of varying deformation zone properties is partly assessed in hydrogeology.

There are several reasons to develop alternative DFN-models, as was already identified in version Simpevarp 1.1. In version Simpevarp 1.2 some alternatives are presented, including models produced by two independent teams but these have not been considered in the subsequent hydrogeological or rock mechanics modelling. After assessment of the alternative DFN-models, it will be decided whether one of the tried approaches is to be preferred or if all alternatives would need to be propagated. These decisions will possibly be made in time for the development of Laxemar version 1.2.

The width of the minor deformation zones in the DFN-model are currently not assessed, since these zones take up a considerable part of boreholes the issue has been raised. The size is potentially important for Repository Engineering. The issue will be assessed for the Laxemar 1.2 modelling – either as a development of the existing DFN-methodology or as an alternative approach. The impact of the width will be discussed by Repository Engineering already for Simpevarp 1.2.

Finally, in Simpevarp version 1.1 there were alternatives in the extrapolation of the extension of dioritoid and mixed type domains. Most of the uncertainty remains, but it is difficult to formulate any viable alternative. Furthermore, there is little need for an alternative since resulting uncertainty in thermal and mechanical properties can still be estimated (e.g. see Table A7-3 in Appendix 7). In conclusion, the uncertainty is acknowledged, but there is no need for an alternative model.

Rock mechanics model

As explained in Table A7-4 in Appendix 7, possible hypotheses for alternative models of the bedrock geology concern the stress model and the rock mass mechanical properties. However, as summarised in Table 12-1, no alternative hypotheses are formulated in Simpevarp version 1.2.

Version Simpevarp 1.1 presented two alternatives with one or two stress domains. In Simpevarp version 1.2 the alternative with two stress domains is selected, as the one that is much more likely. There is still uncertainty in the extent of these stress domains, due to the uncertainties in the dip of some deformation zones, see above, but there is no reason to maintain alternative stress models. The alternative hypothesis of one stress domain will not be further pursued. The uncertainty in stress will instead be handled as quantified uncertainty.

In principle, alternative DFN-models would also result in alternative models of rock mass mechanical properties. However, the quantification of uncertainty using different methods, see Table A7-4 in Appendix 7, is judged sufficient to handle this issue. However, this standpoint should possibly be reconsidered depending on the handling of the width of minor deformation zones in the DFN.

Thermal model

Version Simpevarp 1.1 stated that if there is an alternative lithological model it will also mean an alternative thermal model. However, as made clear in Table A7-4 in Appendix 7, there is no need for such an alternative. The uncertainty is handled by providing an uncertainty range.

Hydrogeological model

As further explained in Table A7-5 in Appendix 7, identified hypotheses for alternative models of the bedrock hydrogeology concern:

- Impact of alternatives in the geological deformation zone model.
- Hydraulic properties ("transmissivity" and connectivity) of deformation zones.
- Transmissivity distribution in the hydraulic DFN-model of the rock mass.

Some of these alternative hypotheses have been further assessed, whereas others are discarded or kept, as summarised in Table 12-1.

Alternatives in the geological deformation zone (see above) model would potentially also generate alternative hydrogeological models, as was noted already in version Simpevarp 1.1. The impact of this uncertainty on regional flow and evolution of groundwater composition is, at least partially, assessed in the numerical regional flow modelling by exploring cases with varying numbers of deformation zones. As demonstrated in Chapter 8, the number of deterministically defined deformation zones have an impact on the flow field and distribution of TDS and water types but the Hydro-DFN model is equally important for these variables. It could also be noted that a simpler alternative for the hydrogeological model would be to consider a Channel Network Model. In its simplest form it only uses information on the frequency of flowing (conductive) fractures and transmissivity distributions observed in boreholes and does not depend on the details of the uncertain DFN geometry. However, at least so far, this possibility has not been considered within the Site Modelling.

It is possible to envisage different conceptual models for the variability of hydraulic properties within deformation zones. This is a new issue compared with Simpevarp Simpevarp version 1.1. Potentially there is relatively little impact on Safety Analysis and Repository Engineering. The need to further resolve this issue essentially depends on how it affects the understanding of regional groundwater flow and the evolution of water composition. Some different cases of alternative transmissivity distribution are explored in the regional flow modelling, see Chapter 8.

Several conceptual models for the transmissivity distribution in the DFN-model and its correlation to size and orientation can be conceived, as already identified in version 1.1. Such correlations could potentially be very important for radionuclide migration properties and should be considered in the Safety Assessment. In version Simpevarp 1.2, several Hydro-DFN models with different transmissivity models (fully correlated, semi-correlated or uncorrelated to size) have been calibrated to the borehole data. The alternatives are propagated to the regional flow modelling, as none of these alternatives could be discarded. They should thus be propagated to Safety Assessment.

Hydrogeochemical model

Version Simpevarp 1.1 listed alternative hypotheses concerning the hydrochemical processes, e.g. if they essentially are mixing and reactions, only reactions or only mixing. In version Simpevarp 1.2 different modelling approaches are applied on the same data set to describe the same processes, as further explained in Table A7-5 in Appendix 7. Thereby, the most realistic descriptions can be identified and less realistic discarded. Possible alternatives have to be further investigated in future versions.

Bedrock transport properties

Version Simpevarp 1.1 listed some alternative hypotheses concerning the bedrock transport models. These concerned the need to propagate uncertainties and alternatives in the hydrogeological description and uncertainties in the retention models (e.g. sorption vs. co-precipitation). While these issues certainly still are highly important, they are no longer part of the Site Descriptive Modelling, as explained in Chapter 1. The issues will be handled within the Safety Assessment modelling.

Surface system

Formulation and analyses of alternative models is not judged a necessary or useful approach at the present stage of surface and near surface systems modelling, but consistency between the hydrological and hydrochemical description of the surface and the bedrock is desired and should be sought. Due to the rapid development of the surface system Safety Assessment need to apply a more stylised approach. Also, as the surface system is much more accessible than the subsurface, there is less room for overall conceptual uncertainty and most uncertainty can be mapped onto parameter variation.

12.3.4 Overall assessment

Compared with version Simpevarp 1.1, more of the uncertainties are now quantified or explored as alternatives. Some uncertainties remain un-quantified and several alternative hypotheses are still left as hypotheses.

Only some of the uncertainties have direct implications for Safety Assessment or Repository Engineering. However, it will also be important to obtain the feedback from the users of the Site Descriptive Model as to which of these uncertainties really require additional efforts. Such feedback is also expected from e.g. the preliminary design work and the Preliminary Safety Assessments. More data will allow for further quantification and may also reduce many of these uncertainties.

12.4 Consistency between disciplines

Another prerequisite for confidence is consistency (i.e. no conflicts) between the different discipline model interpretations. This checking is the next step of the Overall Uncertainty and Confidence Assessment (see Figure 12-1). A protocol has been developed using an interdisciplinary interaction matrix for documentation. For each interaction, the following questions have been addressed:

- Which aspects of the “source” discipline would it be valuable to consider in developing the “target” discipline SDM? The answer should be based on overall process understanding and the answers to the questions on impacts on uncertainties and alternatives provided in Tables A7-3 to A7-6 in Appendix 7 and in Table 12-1.
- Which aspects of the “source” discipline have actually been used when developing the “target” discipline SDM?
- Are there any discrepancies between answers to the first and second question, and if so why?

It should be noted that this protocol is an expansion of a similar type protocol used in version 1.1. There only the second question, which aspects where actually considered, was asked.

Discrepancies between what would be valuable to consider and what actually is considered affects confidence in the model. Again, it is rather the users that could tell whether these discrepancies are grave or acceptable. Still, an overview assessment of this is done at the conclusion of this section.

12.4.1 Important and actually considered interactions

Table 12-2 provides an overview of the interactions judged to be important (green) and to what extent these where actually considered (black) in version Simpevarp 1.2. Table A7-7 in Appendix 7 lists them in full. In addressing the questions, the efforts are spent primarily on issues judged to be important and not in explaining why unimportant interactions indeed are so.

Table 12-2. Summary of interactions judged to be important (green) and to what extent these where actually considered (black) in version Simpevarp 1.2. (There is a clockwise interaction convention in the matrix, e.g. influence of geology on rock mechanics is located in Box 1,2, whereas the influence of rock mechanics on geology is located in Box 2,1.)

Bedrock Geology	Yes/Yes	Yes/Yes	Yes/Most	Yes/Yes	Yes/Yes	No need	No need	Yes/Yes	No need
Yes/Discussed	**Rock Mechanics (in the bedrock)**	No need	Yes/Discussed	No need.	Yes/Some	No need	No need	No need	No need
Yes/Discussed	No	**Thermal (in the bedrock)**	Yes/Yes	No need	No need	No need	No need	No need	No need
Yes/ Partial	Yes/Discussed	Yes/Yes	**Hydrogeology in the bedrock**	Yes/Yes	Yes/Some	Yes/No	Yes/Yes	No need	No
No need	No need	No need	Yes/Yes	**Hydrogeo-chemistry in the bedrock**	Yes/Yes	Yes/Some	No	No	No
No need	No need	No need	Yes/Some	Yes/Some	**Bedrock Transport Properties**	No need	No need	No need	No need
No need	No need	No need	Yes/Yes	Yes/Some	No need	**Hydrogeo-chemistry (surface and near surface)**	Yes/Some	Yes/Some	Yes/Yes
No need	No need	No need	Yes/Some	Yes/Some	No need	Yes/No	**Surface hydrology and near surface hydrogeology**	Yes/Yes	Yes/Yes
Yes/Some	No need	No need	No need	Yes/Some	No need	Yes/Some	Yes/Yes	**Quaternary Deposits**	Yes/Yes
No need	No need	No need	No need	Yes/Some	No need	Yes/Some	Yes/Yes	Yes/Yes	**Biota**

Impacts on bedrock geology

As can be seen from Table A7-7 in Appendix 7, many disciplines are judged to provide important feedback to the geological modelling. However, it is noted that the geological modelling up till now has not fully used such feedback. On the other hand, an essential part of the modelling philosophy is to base the geometrical framework on geological information and reasoning and not to "fit" the geological model to the other models. Still, the geological model should be useful to other disciplines and could use data from other disciplines as indications, among others, for e.g. identifying deformation zones.

Feedback from *rock mechanics* on stress orientations in relation to fracture sets could give additional confidence in the deformation zone and DFN model. The analysis of rock mechanics properties could affect the division of Rock Domains and Deformation Zones (e.g. less reason to split between domains or reason to split existing domains). In version Simpevarp 1.2 this feedback has been discussed, but not formally considered.

Also the *thermal modelling* could provide feedback on the description of rock domains. Thermal data could be used as input to mineralogical description. In version Simpevarp 1.2 this feedback has been discussed, but not formally considered in the Geological Modelling. Furthermore, it is judged that, in reality, there could only be a minor impact of the thermal data.

Hydrogeology could provide confirmation and indications of deformation zones (i.e. are there hydraulic connections or not) and control of the hydraulic applicability of the DFN-model. In version Simpevarp 1.2, the confidence in the deformation zone (ZSMNE024A) intercepted by borehole KSH03 is enhanced by the associated hydraulic anomaly. Current data do not allow exploration of contacts within or between zones, but such data and analyses have been used to establish the deformation zones at Äspö and Hålö. Assessing the applicability if the geological DFN-model is part of the hydrogeological DFN-analysis.

Impacts on rock mechanics model

As can be seen from Table A7-7 in Appendix 7, it is mainly the *bedrock geology* model that impacts the rock mechanics model through the Rock Domains, deformation zones and DFN-model. This input is used within the rock mechanics modelling.

In principle also *Hydrogeology* would impact the rock mechanics description, since water pressures reduces the rock stress to effective stress. However, this coupling has little effect on the parameters predicted, but is considered by Repository Engineering. Furthermore, the coupling is relatively trivial to take into account since water pressures are close to hydrostatic, i.e. no special hydraulic modelling is needed.

Impacts on thermal model

As can be seen from Table A7-7 in Appendix 7, it is mainly the *bedrock geology* model that impacts the thermal model through the rock type descriptions etc. of the Rock Domains. This input is used within the thermal modelling.

Thermal convection and other groundwater flows (i.e. a formal impact from *hydrogeology*) affects uncertainty in measurement of initial temperature. These effects are considered when assessing uncertainty in in situ temperature.

Impacts on hydrogeology model

As can be seen from Table A7-7 in Appendix 7, many disciplines should inform the hydrogeological modelling and most of this input is considered.

Bedrock geology provides the geometrical framework in terms of Rock Domains, Deformation zones and DFN-geometry for the hydrogeological models. Furthermore, hydrogeology has made some assessments whether there are hydraulic differences between Rock Domains, but this issue is not resolved. Also better used could be made of the description of deformation zones (e.g. whether they are brittle or ductile) in the property assignment.

Stress orientation, i.e. a *rock mechanics* input, is expected to affect hydraulic anisotropy. In version Simpevarp 1.2, there is an attempt to assess anisotropy from the borehole data (using the detailed PFL-data), but the issue is not yet fully resolved. However, since strong anisotropy and correlation with the stress field is found at Äspö HRL – this hypothesis is kept despite unclear evidence in data from the Simpevarp subarea.

Temperature affects water density and viscosity. In version Simpevarp 1.2, the impact is assessed in the regional hydrogeological modelling. The impact is insignificant.

There is a strong coupling between hydrogeology and *hydrogeochemistry,* since it is suggested that mixing is a main process for groundwater evolution. Furthermore, density differences created by varying salinity affect the flow regime. These couplings are certainly considered in the modelling work. The regional hydrogeological simulations in version Simpevarp 1.2 acknowledge density-dependent flow and use present-day salinity and water type distribution as “calibration targets”. However, it should also be noted that mixing is not the only important process controlling the groundwater composition, especially for less conservative species than chlorine. Other parameters, like redox, pH, sulphate and carbonate, are controlled by local and/or global geochemical reactions. These species, however, would not affect the flow.

The understanding of mixing processes is critical to understand groundwater evolution from the hydrogeological point of view, however, the contrary does not apply. Most of the hydrochemistry of the system can be described without taking into consideration the mixing processes.

The regional simulations of past groundwater evolution involves modelling of salt migration. The migration properties should be consistent with assessed migration properties of the *transport model*. Version Simpevarp1.2 includes analyses of the sensitivity to matrix porosity. As discussed in Section 8.5, the models can match TDS in boreholes for the present situation by adjusting flow and matrix parameters but clearly there are uncertainties in the parameterisation of the models.

Impacts on hydrogeochemistry model

As can be seen from Table A7-7 in Appendix 7 many disciplines are judged to provide important feedback to the hydrogeochemical modelling and most of this input is considered.

Fracture mineralogy and the chemical composition of the bedrock, as provided by the *geological model*, should be considered. In version Simpevarp 1.2, these couplings are also used in the modelling of the palaeo effects in the way that fracture mineralogy can be used to independently indicate effects from glacial-, marine- or surface-water intrusions.

As already noted there is a strong coupling between *hydrogeology* and hydrogeochemistry and between hydrogeochemistry and the *transport* model. These couplings are considered in the modelling work, as explained above.

Impacts on transport model

As can be seen from Table A7-7 in Appendix 7, many disciplines are judged to provide important feedback to the transport modelling and most of this input is also considered.

The rock domains of the *bedrock geology* provide the main tool for extrapolating the transport property data into three dimensions. In principle, this coupling is also considered, although the current lack of transport property data in the different rock domains makes the correlation study yet weak. Geology also provides the main inputs needed to identify “type structures” and to justify further import of Äspö HRL data.

It is necessary to consider the impact of stress release (i.e. influence from *rock mechanics*) on the intact rock samples taken for laboratory diffusion and sorption measurements. This consideration is also part of the actual data evaluation. Also comparisons between in situ formation factor logs and formation factors measured in the laboratory contributes to analysis of stress release effects.

Hydrogeology should identify the potential flow paths where the transport description is needed. In version Simpevarp 1.2 this is not done. Furthermore, it should be noted that the strong impact from hydrogeology on flow-related transport parameters is no longer part of the site-descriptive modelling, but will be assessed within the framework of Safety Assessment.

The groundwater composition (i.e. *hydrogeochemistry*) affects diffusivity and sorption values. In the version Simpevarp 1.2, model the groundwater compositions, as assessed within the hydrogeochemical modelling, are used for setting up laboratory tests and for parameterisation of the Retardation model. However, the final selection of parameters for calculating retardation along flow paths is done within Safety Assessment, i.e. not as a part of the site-descriptive modelling, as it needs to consider conceptual model uncertainties and the uncertainties in the future groundwater evolution.

Surface system

As shown in Table A7-7 in Appendix 7 many interactions take place among the different surface disciplines, which is why an integrated modelling approach is adopted for the surface system. However, the table also indicates that these interactions are performed only partially in this model version, (cf. the frequent use of "some" in the table). It is also evident from the table that much feedback is required and considered, in order to produce consistent, integrated models within the disciplines where modelling is performed for both the surface system and the deep rock. Also in these cases, interactions need to be further developed.

12.4.2 Overall assessment

Table A7-7 in Appendix 7 demonstrates the integrated character of the Site Descriptive Modelling. Different disciplines depend on the outcome of other disciplines and provide important feedbacks to other. Furthermore, to a large extent the interactions judged to be important are also considered in the modelling, even if further improvements are identified as being required. In particular, it is observed that the geological modelling could enhance its use of feedback from especially rock mechanics, hydrogeology and hydrogeochemistry, but this also stresses the needs for these latter disciplines to clearly formulate this feedback in a form useful for the geological modelling.

12.5 Consistency with understanding of past evolution

For confidence, it is essential that the naturally ongoing processes considered being important can explain – or at least do not contradict – the model descriptions. The distribution of the groundwater compositions should, for example, be reasonable in relation to rock type distribution, fracture minerals, current and past groundwater flow and other past changes. Such 'palaeohydrogeologic' arguments may provide important contributions to confidence even if they may not be developed into strict 'proofs'.

Table 12-3 lists how the current model is judged to be consistent with the overall understanding of the past evolution of the sites as outlined in Chapter 3. Furthermore, there are no findings from the modelling suggesting a need to update the Evolutionary model.

The following are noted:

- It would be potentially interesting to couple the geologic evolution and the formation of the different fracture sets (the order of formation could be determined) with hydrogeochemical indications (e.g. fracture minerals) of age. Although such studies performed at Äspö HRL were rather inconclusive, they could nevertheless provide some insights into the validity of the conceptual model for groundwater flow and hydrogeochemical development.
- In Simpevarp 1.2 there is no information (in support or against) to be used for assessing potential "neo-tectonic" movements. Such information may potentially be available in later data freezes.
- Stress modelling to see whether current stress model is reasonable in relation to the deformation zone model and past tectonic evolution.

- The existing regional palaeohydrogeology model seems to describe the observed distribution of water types fairly well. The strength of this argument could be discussed since the observed distribution was a calibration target and since the initial and boundary conditions are quite uncertain. The important conclusion to be drawn is that the hydrogeology and the hydrogeochemical models are consistent and provide a plausible description of past evolution.

Table 12-3. Consistency with past evolution.

Site Descriptive Model (SDM) Technical Audit: Consistency with past evolution		
Time period and subject	Is SDM consistent with evolution in this time period?	Are there findings from the modelling suggesting a need to update the Evolutionary model?
1,900 million years to the Quaternary		
Bedock Geology	The Geological model is consistent with the regional geological evolutionary model. It would be potentially interesting, i.e. not done in Simpevarp 1.2, to couple the geologic evolution and the formation of the different fracture sets (the order of formation could be determined) with hydrogeochemical indications (e.g. fracture minerals) of age. However, such studies performed at Äspö HRL were rather inconclusive, but could nevertheless provide some insights into the validity of the conceptual model for groundwater flow and hydrogeochemical development.	There are no new data in 1.2, which would necessitate an update of this evolutionary model.
Rock Mechanics	Stress modelling to see whether current stress model is reasonable in relation to the deformation zone model and past tectonic evolution.	
During the Quaternary period		
Bedrock Geology	In Simpevarp 1.2 there is no information (in support or against) to be used for assessing potential “neo-tectonic” movements. (Such information may potentially be available in later data freezes.) Whether near surface boulder “caves” and “assemblies” are indications of post glacial seismic events is assessed in a – non completed – separate study, not addressed in Simpevarp 1.2.	
Rock Mechanics	No reason to change current view of the conceptual model of stress. Implications from up-lift could possibly be assessed, but are not judged important in the Simpevarp area.	
Thermal model	Not assessed – there is also a lack of historical development data.	
Hydrogeology and Hydrogeochemistry	Groundwater flow and salinity transport simulations cover the period from the melting of the last glaciation, but not alterations before that. Instead, the simulations have explored the impact of various assumptions on initial conditions, properties, events and boundary conditions since the latest deglaciation (approximately 10,000 years ago). In general, analysing the impact of potential changes after the glaciation on the current day groundwater flow and distribution of groundwater composition will affect and support the conceptual groundwater flow model. The interaction between the evolution of the surface water composition and the evolution of the groundwater composition, is described concerning processes and origin of various water types (e.g. meteoric water, glacial melt water, Littorina water, brine.	There are large uncertainties in e.g. initial and boundary conditions: What is the time period for Littorina, see, should the meteoric boundary conditions be divided into several time periods, what is the most appropriate origin of the water type “Marine sediments”:
Surface system	The description of the historical development of the surface system is consistent with the description of the present system.	No

12.6 Comparison with previous model versions

The final evaluation of confidence envisaged in the flow chart of Figure 12-1 concerns to what extent measurement results from later stages of the investigation compare well with previous predictions. This will also be important for discussing the potential benefit of additional measurements. Clearly, if new data compare well with a previous prediction, the need for yet additional data may even further diminish.

12.6.1 Auditing protocol

Again, a Protocol has been developed for checking this. It concerns:

- changes compared to the previous model version (i.e. version Simpevarp 1.1, /SKB, 2004b/),
- whether there were any "surprises" connected to these changes, and
- whether changes are significant or only concern details.

Table 12-4 lists the answers to these questions.

12.6.2 Assessment

As can be seen from Table 12-4 there are significant changes in version Simpevarp 1.2 compared with version 1.1 /SKB, 2004b/, but there are no substantial surprises.

Compared to version Simepvarp 1.1 the main change in the *geological* model are:

- Expansion of the local model area and inclusion of updated regional model (now in 3D) with Rock Domain.
- New boreholes – modified geometries of some RD in Simpevarp subarea.
- Deformation Zone-model is based on more sub-surface information, and locally new surface data with higher resolution.
- Changes to the regional lineaments.
- Within the local model areas – local changes (including new DZ) to zone geometries.
- New data for geological DFN-model.
- Ore potential assessed – and is shown to be low!

Of these changes the Deformation Zone and DFN model are significantly different compared with version Simpevarp 1.1.

Compared with version Simpevarp 1.1 the main changes in the *rock mechanics* model are:

- New and more data, which implies that a full analysis has been possible in accordance with strategy report.
- Division into properties of deformation zones, minor deformation zones and remaining rock mass.
- One alternative selected for the stress model.

None of these changes imply significant differences in the description compared with version Simpevarp 1.1.

Compared with version Simpevarp 1.1 the main changes in the *thermal model* are:

- New approach to describe thermal properties of lithological domains.
- New and more data such that the analysis has been possible in accordance with strategy report (e.g. upscaling relations are considered).
- Scaling relations may allow for some variance reduction.

Of these changes the scaling relations implies a significant difference compared with version Simpevarp 1.1.

Table 12-4. Comparison with previous model version.

Site Descriptive Model (SDM) Technical Audit: Previous model version	
List changes compared to previous model version (i.e. version 1.1 for the Simpevarp subarea and version 0 for the regional model).	**Geology** Expansion of the local model area and inclusion of updated regional model (now in 3D) with Rock Domains (RD). New boreholes – modified geometries of some RD in Simpevarp subarea. Deformation Zone (DZ) model is based on more sub-surface information, and locally new surface data with higher resolution: There were changes to the regional lineaments (significant). Within the local model areas – local changes (including new DZ) to zone geometries (significant). New data for DFN-model. Ore potential assessed – and shown low! **Rock mechanics** New and more data, means that analysis has been possible in accordance with the strategy report (e.g. also theoretical approach). Division into properties of defoemation zones, minor defoermation zones and the remaining rock mass. One alternative selected for the stress model. **Thermal model** New approach to describe thermal properties of RD. New and more data, means that analysis has been possible in accordance with strategy report (e.g. upscaling relations are considered). Scaling relations may allow for some variance reduction. **Hydrogeology** The version Simpevarp 1.2 deformation zone model and geological DFN-model are used and tested against hydraulic data. A Hydrogeological DFN-model (with alternatives) is produced. New boreholes: i.e. better understanding of the spatial distribution. **Hydrogeochemistry** The Simpevarp 1.2 model contains considerable more data from depth and also measurements on microbes, gases and colloids that were not available during Simpevarp 1.1. New modelling approaches such as integrated transport and geochemical modelling have been applied on the Simpevarp 1.2 data. Better description of the hydrogeochemical system and opportunities to compare/integrate the results with the hydrogeological modelling. **Surface systems** In the present model version, a first attempt on an integrated description of the surface system is attempted. The previous model presented the limited dataset available at that time, without integration of different disciplines or system descriptions.
Address whether there were any “surprises” connected to these changes.	No big surprises, but for Hydrogeochemistry it was somewhat surprising that more measurements from the Simpevarp area did not indicate a Littorina water signature.
Address whether changes are significant or only concern details.	**Geology** Significant changes in DZ-model and DFN model. **Rock mechanics** No major change. **Thermal model** Scaling relations may allow for some variance reduction. **Hydrogeology** Significant changes in hydraulic properties of the Deformation Zones and in the Hydro DFN-models. The methodology may suggest that the variability is wider than in Simpevarp 1.1. Unclear importance of sub-horizontal fracture set (see Table A7-5 in Appendix 7). **Hydrogeochemistry** The changes are significant since the model will describe the groundwater evolution down to 1,000 m depth rather than down to 200 m depth as in the version Simpevarp 1.2 **Surface systems** No comparison can be made.

Compared with version Simpevarp 1.1 the main changes in the *hydrogeological model* are:

- The version Simpevarp 1.2 deformation zone and DFN models are used as input to the hydrogeological model.
- A Hydro-DFN-model (with alternatives) is presented.
- The new boreholes provide a better understanding of the spatial distribution of the hydrological properties.

All of these changes imply a significant difference compared with version Simpevarp 1.1.

Compared with version Simpevarp 1.1 the main changes in the *hydrogeochemical* model are:

- Considerably more data from the depth and also measurements on microbes, gases and colloids that were not available during Simpevarp 1.1,
- New modelling approaches such as integrated transport and geochemical modelling has been applied to the Simpevarp 1.2 data,
- Better description of the hydrochemical system and chances to compare/integrate the results with the hydrogeological modelling.

All of these changes imply a significant difference compared with version Simpevarp 1.1. The surprising fact that more measurements from the Simpevarp area did not indicate a Littorina signature, could imply a need to reconsider the model of past evolution, as already suggested in Section 12.5.

The present model version of the *surface system* is a first attempt at an integrated description of the surface system. The previous model presented the limited dataset available at that time, without integration of different disciplines or system descriptions.

13 Conclusions

This chapter summarises the essence of the Simpevarp 1.2 site-descriptive model by starting off with an account of important achievements in the current Simpevarp 1.2 model. This is followed by a resume of the current understanding related to the Simpevarp subarea and a condensed account of the handling of uncertainties and model alternatives in light of the detailed discussion of uncertainty and confidence in Chapter 12. This discussion forms the basis for concluding remarks regarding the overall understanding of the Simpevarp subarea. This is followed by a review of the important steps to be taken in future modelling to improve the site-descriptive model and further reduce uncertainty. Finally, the implications for the ongoing site investigations and early phases of the complete site investigations are discussed. This latter part addresses what additional data or measurements are required to improve the site descriptive model and reduce existing uncertainties.

13.1 Overall changes since the previous model version

The current Simpevarp version 1.2 modelling constitutes a distinct step from the initial local scale description presented in the Simpevarp version 1.1 to the current local scale description that embodies the full analysis chain performed in the correct sequence. The current descriptive modelling is still limited for the Laxemar subarea because of lack of data from this area, and in the regional model area. Information from these areas is expected for the Laxemar version 1.2 model. In the current site description, the developed geological models (lithology, deformation zones and DFN) have constituted the geological and geometrical foundation for the other disciplines as originally planned. This implies that the hydrogeological, rock mechanical and thermal properties modelling have been done in accordance with the developed strategy documents. Furthermore, the availability of data at great depth has also implied that the hydrogeochemical modelling has been performed in accordance with the developed strategy. The surface ecological modelling has been performed under the auspices of a newly formed group (SurfaceNET). In this way, all aspects of the surface system, including topographical description (digital elevation model), overburden, hydrology and chemistry of the surface waters, have been combined under one heading and evaluated in an integrated way.

With regards to the description of the subsurface, the amount of new information compared with version Simpevarp 1.1 is larger, with new data/information from cored boreholes KSH01A/B, KSH02, KSH03A/B, KAV04 (comprehensiveness by discipline varying from hole to hole) and new complementary data from old existing cored boreholes (KLX01, KLX02 and KAV01). In consequence, the availability of data and information at depth for Simpevarp 1.2, is significantly improved from the version 1.1 model of the Simpevarp area.

13.1.1 Important modelling achievements

In the light of the availability of additional data and from more general considerations, a series of important modelling achievements have been made in the version Simpevarp 1.2 description. These are set out below;

- Expansion of the local model area employed in the geological modelling to also include the Laxemar subarea in full and inclusion of the updated regional model (now in 3D) in the lithological rock domain model.
- Interpretation of 36 lithological domains, of which 17 are found in the local scale model domain, and 3 principal domains (A, B and C) and a limited number of small domains are found within the Simpevarp subarea. The geometries of some rock domains in the Simpevarp subarea have been modified as a result of data from new boreholes.
- The ore potential of the Simpevarp area has been assessed.

- Interpretation of 22 deformation zones of high confidence of occurrence and interpretation of 166 “possible” deformation zones, the latter of low to intermediate confidence of occurrence (most of which are located in the Laxemar subarea and in the regional scale model area). The Deformation Zone model is based on more sub-surface information, and locally on new surface data of higher resolution. Within the local model area, (significant) local changes (including new deformation zones) are imposed on earlier interpreted zone geometries.
- An improved geometrical control of the important major deformation zones in the Simpevarp subarea has been achieved through strategic borehole intercepts.
- New and more data have enabled analysis in accordance with the strategy report for Rock mechanics, including division into properties of interpreted deterministic deformation zones, minor (stochastic) deformation zones and the remaining rock mass. The descriptive model of mechanical properties (modulus, strength etc.) is based on a theoretical approach (based on simulated failure tests in a developed DFN model) complemented by an updated empirical model (based on Q and RMR).
- Two rock stress domains have been defined on the basis of existing rock stress measurements, geological inference and numerical modelling.
- A new approach has been applied to describe thermal properties of rock domains. New data have enabled analysis in accordance with the strategy report, including application of relations for upscaling. Scaling relationships may allow for some variance reduction.
- A first hydraulic DFN model based on site-specific data (with alternatives) has been produced. The hydraulic DFN model has been successfully calibrated against available hydraulic tests in boreholes in the Simpevarp subarea (KSH01A and KSH02). The hydraulic DFN model has subsequently been used to estimate block properties at various scales. The block properties have been assigned to regional scale hydrogeological flow models.
- The hydrogeochemical model is based on considerably more hydrogeochemical data from depth and also measurements on microbes, gases and colloids that were not available for version Simpevarp 1.1. New modelling approaches, such as integrated transport and geochemical modelling have been applied to the data. The descriptive Hydrogeochemical model has been updated including descriptions of the distribution of salinity, mixing and a more detailed description of major reactions/processes down to a vertical depth of 1,000 m, compared to 300 m in Simpevarp 1.1.
- A better description of the hydrogeochemical system has been provided and this has resulted in improved opportunities to compare/integrate the results with the hydrogeological modelling.
- The description of transport properties has taken a distinct step towards parameterisation of various rock units and domains. However, the assignment is still largely based on indirect inference. The diffusion characteristics are primarily based on laboratory resistivity measurements (formation factor). Sorption characteristics are at present inferred from Äspö data based on mineralogy and type groundwater compositions.
- The surface ecological model largely describes the situation in the regional area. New elements in the local scale description, with special focus on the Simpevarp subarea, include trial surficial hydrogeological modelling that embodies the current description of the overburden and development of ecosystem models for one selected lake catchment and one shallow bay.

13.2 Current understanding of the site

The understanding of the Simpevarp subarea in model version Simpevarp 1.2 is discussed in Chapter 12, where also the identified uncertainties of the developed discipline models are articulated and an overall confidence assessment is provided in light of the identified model interactions and integration. The following sections summarise the current understanding of the Simpevarp subarea and account for the associated uncertainties, model alternatives and interactions between models.

13.2.1 General understanding of the Simpevarp subarea

In the execution programme for the Simpevarp area /SKB, 2002b/, a number of important site specific questions were formulated. They concerned; *"size and locations of rock volumes with suitable properties, location and importance of fine-grained granite bodies and deformation zones, high rock stresses, thermal conductivity of the bedrock, rock mechanics properties of rock mass, and ore potential"*.

In the following, condensed resumes are given of current understanding on the above issues, but also on other important issues and aspects of the Simpevarp subarea, as inferred from the Simpevarp 1.2 modelling:

On *"topography and overburden characteristics":*

- The parts of the Simpevarp subarea located above sea level are largely outlined by the Simpevarp peninsula and the Hålö and Ävrö islands. The area features a relatively flat topography (c. 0.4% topographical gradient), which largely reflects the surface of the underlying bedrock surface, and is characterised by a high degree of bedrock exposures (38%). Till is the dominant Quaternary deposit which covers about 35% of the subarea.

On the *"development of ecosystem models":*

- First attempts on independent ecosystem modelling in terms of pools and fluxes of carbon have been developed for the terrestrial (e.g. plants and animals) and limnic (e.g. algae and fish) systems using the Lake Frisksjön drainage area. Furthermore, a first marine ecosystem model has been developed for the Basin Borholmsfjärden.
  - In this context we have acquired a general knowledge of the functional aspects of the ecosystems in the regional model area. However, we have no specific knowledge of the Simpevarp subarea.
  - In terms of overall understanding, we have learned that the major pools of carbon in the ecosystem are found in the soils and sediments, where also the longest turnover times for carbon are found. The latter findings are of importance for radionuclide accumulation in subsequent Safety Analysis.

On *"bedrock geology, modelled lithological domains and associated fracturing":*

- Three principal lithological domains have been defined in the subarea, an A domain that is dominated by the *Ävrö granite* and which dominates on the island of Ävrö, Hålö and the northern parts of the peninsula, a domain that is dominated by the *fine-grained dioritoid (B),* one of which dominates the peninsula, a C domain that is characterised by a mixture of of *Ävrö granite* and *quartz monzodiorite* on the cape of the peninsula. A fourth domain is made up a few scattered domains of *diorite* to *gabbro*.
  - Fine-grained granite and pegmatite veins and dykes exist throughout the investigated Simpevarp subarea.
  - Fracture intensities (total and open) are generally higher in the fine-grained dioritoid, compared with the Ävrö granite (and the quartz monzodiorite). The frequency (P_{10}) of interpreted open fractures in KSH02 (completely dominated by fine-grained dioritoid) is 3.2 fractures/m, compared with boreholes KSH01A (1.2 fractures/m) and KSH03A (1.3 fractures/m), both dominated by Ävrö granite.
- On the *"metal ore potential"* in the Simpevarp area:
  - The ore potential has been assessed by an independent exploration company /Lindroos, 2004/. The ore potential is considered negligible, with a real potential only for quarrying of building- and ornamental stone associated with the Götemar and Uthammar granite intrusions to the north and south of the investigated area, respectively.
- On the *"size and locations of rock volumes with suitable properties"* including *"location and importance of fine-grained granite bodies and deformation zones":*
  - The understanding of the deformation zones of the Simpevarp subarea is considered adequate to make a preliminary assessment of available storage volumes. The two most important, and volume-delineating deformation zones are ZSMNE012A, which trends north of the

islands of Hålö and Ävrö, dipping towards the southeast under the Simpevarp peninsula, and ZSMNE024A which strikes along the coasts of the Ävrö island and the Simpevarp peninsula. A number of deformation zones of lower dignity (ZSMEW004A, ZSMNE018A and ZSMNW025A and ZSMNW028A) further divide the modelled subarea. Uncertainties in properties for rock volumes under the sea, southeast of ZSMNE024A, are large and the suitability of these volumes has not been assessed.

  – Data from the cored borehole KSH03A has verified the interpreted deformation zone ZSMNE024A. Similarly, deformation zone ZSMNE012A. is interpreted to be intersected by boreholes KAV01 and HAV07 (*Note : The existence of the zone is also verified by an intercept in borehole KAV04. Geological data from KAV04 were however not part of the Simpevarp 1.2 geological data freeze*).
  – Uncertainty in the presented deformation zone model still exists, but is primarily related to the interpreted "possible" zones (of low or intermediate confidence of occurrence), mainly located in the neighbouring Laxemar subarea and throughout the regional scale model volume.

- On *"rock stresses"* and *"mechanical properties of the rock":*
  – High rock stresses do not appear to be a major concern for the Simevarp subarea. The current stress model indicates two stress domains, one with lower stresses in the Simpevarp subarea, east of deformation zone ZSMNE012A, compared with the area west thereof (including the Laxemar subarea) which shows comparatively higher stress levels. The magnitude of the maximum principal stress (σ_1) at 500 m in the Simpevarp subarea is estimated at 10–22 MPa. This situation, supported by numerical stress modelling, is attributed to unloading of a wedge-formed rock volume underneath the Simpevarp peninsula and Hålö and Ävrö islands, as delineated by the intersecting deformation zones ZSMNE012A and ZSM024A.
  – Quantification of mechanical properties of the naturally fractured rock mass and rock associated with interpreted deformation zones is supported by new laboratory data on intact rock samples, underpinned by empirical and theoretical relationships. The latter approach makes use of the DFN model to perform numerical models of large scale loading tests of fracture rock blocks under confining stress.
  – The results for deformation properties using the empirical approach gives lower values than the theoretical approach and this is explained as a difference caused by different confining stress. The deformation modulus and Poisson's ratio are therefore modelled as stress-dependent parameters. For example, estimated model values for the deformation modulus E_m compare well with the absolute magnitude and relative difference for E_m estimated at the shallow CLAB excavations, and at the deeper Äspö HRL, 40 and 55 GPa (Section 6.2.4), respectively.

- On the *"thermal conductivity"* of the rock mass:
  – The analysis of the *"thermal conductivity"* has developed considerably since Simpevarp 1.1. Our current understanding is that the thermal conductivity in the Simpevarp subarea is generally low. In terms of interpreted global mean values for the identified lithological domains, the thermal conductivity vary within a relatively narrow interval (2.6–2.8 W/(m·K)).
  – A methodology for upscaling of thermal conductivity data from core scale has also been developed. At the canister scale (L=2 m) the standard deviations, at lithological domain level, corresponding to the conductivity data above span between 0.20 and 0.28.

- General on *"bedrock hydraulic properties":*
  – The conductive elements of the bedrock are made up of large scale conductive features, denoted Hydraulic Conductor Domains (HCDs), assumed to coincide with deformation zones in the geological model, and the Hydraulic Rock Domains (HRDs), which represent the rock mass between the HCDs.
  – The hydraulic properties of the HRDs are described in terms of a network of discrete fractures (DFN) with a geometrical description taken from the geological DFN model. A fracture transmissivity distribution is superimposed, and calibrated against existing hydraulic borehole data.

- On the *"hydraulic properties of the rock mass":*
  - The working hypothesis employed is that the hydraulic DFN model couples transmissivity and size through an inferred power-law (main case) or lognormal size distribution of fractures, up to the size of the local minor deformation zones (L < 1,000 m).
  - The basic hypothesis employed by the two modelling teams is to assume full correlation between size and transmissivity. However, tested alternatives included cases with no correlation, and a correlation with a superimposed statistical variation. Calibration of the developed models has resulted in a number of alternative hydraulic DFN models.
  - For the correlated case, and for the size interval 0.5–1,000 m, the two modelling teams report a resulting volumetric fracture intensity of all fractures P_{32T} of 0.7–0.8 m^2/m^3 and a volumetric intensity of all conductive and hydraulically connected fractures P_{32C} amounting to 0.29 m^2/m^3, cf. Table 8-18.
- On the *"transmissivity of interpreted deformation zones":*
  - Some of the interpreted deformation zones in the regional scale model area are assigned high confidence (regarding existence), several have been hydraulically tested, but overall most zones are attributed uncertain hydraulic properties.
  - All together 13 of the interpreted deformation zones have been tested in boreholes. The range of interpreted transmissivity of these tested intercepts range from 10^{-7} to about 4×10^{-4} m^2/s, cf. Table 8-13. The geometric mean transmissivity of the tested HCDs at Äspö HRL, $T=1.3\times10^{-5}$ m^2/s (with a standard deviation $\log_{10}T$ of 1.55) /Rhen et al. 1997b/, has been assigned to the remainder of the HCDs in the regional scale model.
- On *"effective values of hydraulic conductivity":*
  - The different alternative hydraulic DFN models have been used to simulate effective values of hydraulic conductivity at different scales. The simulations are set up by generating discrete fractures in large blocks, applying simple boundary conditions and solving for groundwater flow. Subsequently, the results are averaged over selected grid sizes, typically 20 m and 100 m
  - The results of the generation of block hydraulic conductivities show that 20m blocks on the average are less permeable than 10^{-8} m/s, cf. Table 8-19.
- On aspects of *"regional ground water flow":*
  - Local groundwater flow regimes are assumed to develop at the Laxemar and Simpevarp subareas and are considered to extend down to depths of around 600–1,000 m, depending on local topography, cf. Figure 11-11. In the Simpevarp subarea, close to the Baltic Sea coastline, where topographical variation is limited, depth penetration of local groundwater flow cells will consequently be less marked. In contrast, the Laxemar subarea is characterised by higher topography, resulting in a much more profound groundwater circulation that appears to extend to approximately 1,000 m depth in the vicinity of borehole KLX02.
  - Numerical modelling shows that groundwater flow is controlled by topography and the geometry of the system of modelled deformation zones, also identifying the Simpevarp subarea as an area of groundwater discharge (upward directed flow) at repository depth.
  - Model variants used in the hydrogeological modelling (domain size, boundary conditions, transmissivity vs. size in the hydraulic DFN model, depth dependence in hydraulic conductivity, boundary and initial conditions) all show very similar results, both with regards to flow distribution and particle release locations. In all cases, released particles at depth travel a short distance to reach a modelled deformation zone and subsequently follow the system of connected deformation zones to final discharge in the Baltic Sea.
- On *"hydrogeochemical conditions":*
  - The complex groundwater evolution and patterns noted in the Simpevarp area are a result of many factors such as: a) the present-day topography and proximity to the Baltic Sea, b) past changes in hydrogeology related to glaciation/deglaciation, land uplift and repeated marine/lake water regressions/transgressions, and c) organic or inorganic alteration of the groundwater composition caused by microbial processes or water/rock interactions. The sampled groundwaters reflect, to variable degrees, processes relating to modern or ancient water/rock interactions and mixing.

- Three groundwater types have been identified in the Simpevarp subarea, cf. Figure 11-11; the Type A (dilute and mainly of Na-HCO3) is found at shallow depths (< 100 m), Type B (brackish, mainly Na-Ca-Cl) at shallow to intermediate depths (150–300 m), Type C (saline (6,000–20,000 mg/l Cl, 25–30 g/L TDS), mainly Na-Ca-Cl) at intermediate to deep levels (> 300 m).
- The marked differences in the groundwater flow regimes (in terms of depth penetration of local flow cells, see above) between the Laxemar and Simpevarp subareas are reflected in differences in measured groundwater chemistry.
- Our current understanding is that the hydrochemical stability critera are met for the analysed components, cf. Table 11-7, as inferred from groundwater sampling in two intervals located at approximate repository depth in boreholes KSH01A and KSH02, respectively.

- On "*comparison of paleohydrogeological modelling results and present day hydrogeochemistry and conceptualisation*":
  - Applications of the hydraulic DFN models, and block hydraulic conductivites derived there from, show that all hydroDFN models defined for Simpevarp 1.2 can be made to match measured hydrogeochemical in situ data if the flow porosity is increased. Examples are given in e.g. Figure 8-35 (Deuterium and Oxygen-18), and Figure 8-36 (Water type).
  - Transient simulation of present day salinity distribution on the basis of inferred transient boundary conditions (shore-line displacement due to isostatic land uplift and variable salinity of the water of the Baltic Sea) show results compatible with measured geochemical signatures in selected reference boreholes. The results further suggest that Littorina water, indicated by the characterisation, may be present near the coast and below the Baltic Sea.
- On the "*transport properties*" of the rock matrix:
  - The current retardation model provides a parameterisation for fresh (unaltered) and altered varieties of the rock types and modelled lithological domains identified in the subarea, cf. Table 10-6, and an identification and description of four characteristic fracture types, cf. Section 10.7.2.
  - Suggested porosities for intact fresh rock (in terms mean values in vol-%) on lithological domain level vary from 0.17 (Fine-grained dioritoid) to 0.40 (Ävrö granite, cf. Table 11-8).
  - Suggested formation factors for intact fresh (reflecting diffusion characteristics, mean values) on lithological domain level vary from about 1.0×10^{-4} (Fine-grained dioritoid) to 2.9×10^{-4} (Ävrö granite).
  - Current parameterisation of sorption properties is restricted to Sr and Cs and one type groundwater composition, cf. Table 10-6.

13.2.2 Uncertainties, alternatives and integration of models

As discussed in detail in Section 12.3, important modelling steps have been taken in Simpevarp 1.2 and the main uncertainties are now identified, in some cases quantified, or explored as alternatives. Notwithstanding, some uncertainties still remain unquantified at this stage and alternative hypotheses are retained only as hypotheses. Additional data, collected in the Simpevarp subarea following the Simpevarp 1.2 data freeze, may allow additional quantification, and may help further reduce the observed uncertainties.

For the geological model various possible alternative descriptions are inherent in uncertainties related to geometry (size/extent in lateral and vertical directions, dip and termination), uncertainties in characteristics/properties and confidence of existence of modelled lithological domains and deformations zones. No analysis of possible alternatives has however been pursued explicitly in the current modelling. This applies also to the possible existence of subhorizontal deformation zones. It should however be noted that only limited indications of subhorizontal deformation zones exist in the Simpevarp subarea. Similarly, no major subhorizontal deformation zones have been identified in the boreholes and underground openings of the Äspö HRL.

Alternatives for the geological DFN model have been developed based on alternative size models for the identified fracture sets. In hydrogeology, alternative hydraulic DFN models (with alternative assumptions regarding the correlation between fracture size and transmissivity) have been developed, and subsequently propagated in estimating block hydraulic conductivities and in the assignment of material properties to continuum regional scale hydrogeological flow models.

For the other disciplines, other alternative models (hypotheses) are possible, but have not been elaborated in model version Simpevarp 1.2.

Section 12.4 outlines possible interactions between disciplines, and the interactions considered for version Simpevarp 1.2. It is obvious that changes to the lithological model have a strong impact on most disciplines (e.g. rock mechanics, thermal and transport properties). The deformation zone model in particular influences the hydrogeological and rock mechanics models. Likewise, there is a strong interdependence between hydrogeology and hydrogeochemistry, primarily through the description of mixing, proposed as being mainly responsible for the evolution of the groundwater chemistry, including the distribution of salinity, over time. The hydrogeochemical model in turn is to a limited degree dependent on the chemical composition of the bedrock and the fracture minerals. To this also comes the coupling between geology (mineralogy), hydrogeochemistry and the transport model, for the sorption characteristics of the rock. Other aspects on the transport model stem from rock stress effects, both in virgin rock (affecting in situ measurements to establish the formation factor along boreholes) and in drill core rock samples (effects of unloading of rock stresses on laboratory results), on magnitude and anisotropy of diffusion properties, possibly associated with any existing fabric (foliation) of the bedrock. Many interactions are evident within the surface system, and this is also the reason for integrating the surface analysis. However, what still remains to be better established and quantified are the interactions between the surface system and the bedrock system. This applies primarily to the turnover of water and chemical mass balances.

No qualitative or quantitative transfer of feedbacks from Simpevarp 1.1 rock mechanics, hydrogeology and hydrogeochemistry models to the Simpevarp 1.2 geological modelling (lithology, deformation zones and DFN models) has occurred. However, the basis for such evaluations and transfer in the subsequent Laxemar 1.2 geological modelling is expected to be significantly improved. Of particular interest in this context is evidence of hydraulic connections, as indicated from drilling and/or cross-hole interference test pressure responses. These could potentially help assess the hydraulic properties and connectivity (and extent) of certain interpreted deformation zones. This analysis requires boreholes equipped with packer systems and pressure transducers and appropriate distances between boreholes, and the possibility to resolve hydraulic disturbances.

The Simpevarp 1.2 site descriptive model is in general agreement with current understanding of the past evolution as described in Chapter 3. This applies e.g. to the composition of present groundwater in relation to the bedrock lithology and fracture mineralogy. Furthermore, the hydrogeological modelling of groundwater chemical evolution arrives at reasonable present day groundwater compositions when compared with borehole data. It is identified as potentially interesting to analyse and improve the understanding of the relation between geological evolution, including formation of different fracture sets, with (hydro-)geochemical indicators (including fracture minerals).

No major surprises have been noted in the Simpevarp 1.2 modelling.

In summary, more quantitative data have been produced for Simpevarp 1.2 compared with Simpevarp 1.1. Some alternatives have been explored and even propagated in the analysis, but uncertainty remains, particularly in the Laxemar subarea and the regional scale model volume. The modelling for Simpevarp 1.2 is furthermore characterised by a stronger element of interaction between disciplines.

Important for making priorities in reducing the important uncertainties is the obtaining of direct feedback to investigations and site modelling from the end users of the developed site-descriptive modelling, i.e. from Preliminary Repository Design (D1) /SKB, 2005a, in prep./ and the Preliminary Safety Evaluation /SKB, 2005b, in prep./ based on the version Simpevarp 1.2 models.

13.2.3 Concluding remarks on site understanding

In conclusion, the geometrical basis of the Simpevarp subarea in terms of lithological defined lithological domains and principal volume-delimiting deformation zones is largely well established. Verification and information of properties are still limited with regard to the interpreted deformation zones of less significant stature, which are interpreted to further divide the subarea. In terms of properties at depth, the remaining needs are primarily associated with further detailing of the statistical descriptions of geological, thermal, mechanics, hydrogeological and hydrogeochemical properties. Additional data at depth are also needed north of ZSMNE012A.

It is also noted that informing (verifying) every single interpreted deformation zone in the modelled area by drilling/excavation will never be possible to achieve. It is furthermore identified, that this is not necessary from a safety assessment point of view. This is particularly true for most of the deformation zones in the regional scale model volume, many of which are interpreted as being "possible", i.e. associated with low or intermediate level of confidence.

Prioritisation and optimisation in light of the needs of Safety Assessment and Repository Engineering will, by necessity, be required for making the right priorities regarding any complementary work.

Auxiliary issues which are regarded as means/vehicles to further resolve the remaining issues are; the refinement of the hydraulic DFN model, improved description of an interface between surface and subsurface, and further integration/comparison of hydrogeochemical and hydrogeological data, models and understanding.

13.3 Implications for future modelling

The site-descriptive model Simpevarp 1.2 was originally planned to make up one site-specific component for the safety assessment analysis (SR Can) for the canister encapsulation plant /SKB, 2003, 2004d/. However, due to SKB's intention in principle to pursue complete site investigations only in the Laxemar subarea, a decision was taken to instead use Laxemar 1.2 as a basis for SR Can. This implies that the subsequent Laxemar version 1.2 will have a very important stature. Given that additional data have been collected in the Simpevarp subarea following the Simpevarp 1.2 data freeze, the Laxemar 1.2 site-descriptive model will allow inclusion and reference to this additional data and information in the modelling process.

Modelling for Laxemar version 1.2 is presently under way using data available at the data freeze as of November 1, 2004.

13.3.1 Technical aspects and scope of the Laxemar 1.2 modelling

The needs expressed by Safety Assessment and Repository Engineering define the requirements for resolution and accuracy in parameterisation within the defined regional and local scale model volumes. Expressed needs for higher resolution and reduced uncertainty may call for a reduction in the local scale model domain, with a focus on the area of interest. However, the desire to also incorporate additional data from the Simpevarp subarea, and relating information between the two subareas, calls for retaining the current local scale model domain employed for Simpevarp 1.2 (that includes both defined subareas). This implies that the basic geometrical setting for the ensuing Laxemar 1.2 modelling is essentially set. The idea is to include all available data in the two subareas in the analysis, but with an obvious shift in focus and dedication to the Laxemar subarea. The experience and understanding gained from the two-step analysis of Simpevarp versions 1.1 and 1.2 will serve as an important platform for the analysis of data from the Laxemar subarea. This is particularly true for the geological modelling, which will incorporate the new surface information from the recently concluded bedrock mapping of the Laxemar subarea, and parts of the regional model area. Similarly, the understanding and experience gained from the current regional scale hydrogeological modelling, including that of the paleo-groundwater chemical evolution, serves as an invaluable basis for subsequent analysis of flow and hydrogeochemical conditions in the Laxemar subarea.

When taking the step to the complete site investigation phase, the site investigations will focus on a selected part of the investigated area. A decision will subsequently be taken whether to retain or reduce the size of the local scale model domain, in light of the focusing of the site investigations.

A requirement for the version 1.2 modelling is that more attention should be paid to model alternatives. Such developments have to be made with a close attention to what is important for the principal consumers of the site descriptive models, i.e. Safety Assessment and Repository Engineering. Furthermore, it is foreseen that only one (or two) alternatives can be propagated all the way from geology (geometry) through hydrogeology (property assignment) to assessment of groundwater flow and flow paths. This has been done to some extent for Simpevarp 1.2.

The use of independent modelling approaches within the hydrogeochemical, and to some extent also within the hydrogeological modelling, provides opportunities to compare outcomes and use noted discrepancies to guide future modelling work. This work has to be carried out in an atmosphere of "balanced competition" working towards one common goal. Similarly, alongside the Laxemar 1.2 modelling, alternative geological DFN models and alternative linked lineament maps will be developed by independent groups (outside the SKB site modelling team and supporting NET-groups organised by discipline) applying alternative hypotheses to those used by the SKB site modelling team.

13.3.2 Modelling procedures and organisation of work

A great deal of experience has been gained on procedures and organisation of the modelling work during the Simpevarp 1.2 modelling. Interdisciplinary modelling is a continuous learning process which will continue to develop throughout the site descriptive modelling. This entails that the strategy/methodology described in the developed strategy documents may become out of date, or needs revision/amendment. One such example is the development of the document which details an updated methodology for geological DFN modelling /Munier, 2004/.

Perhaps the most important experience from the presently ongoing modelling work is that the unification of scales (e.g. in devising "universal" fracture length distributions in geology and mathematical expressions that link fracture transmissivity with fracture size in hydrogeology) is non-trivial. This has posed conceptual issues that are being pursued in the continued modelling, cf. Section 8.3.4.

Furthermore, information exchange with the site investigation organisation at Simpevarp ("site") has been regular during the Simpevarp 1.2 modelling. This has been realised by attendance at the Simpevarp site modelling project meetings by representatives of the site. Similarly, representatives of the site modelling team have been present at planning meetings organised by the site.

As observed earlier, one drawback with the data freeze concept is that unlike the modelling team, the site continues to work with a successively evolving model where new data are successively fed in, and used to make decisions about the immediate forward program. In contrast, the site modelling team "lags behind", working with a model that is based on, relatively speaking, an older data set. Despite this fact, in the analysis of Simpevarp 1.2, the two-way dialogue between the site and the site modelling team has worked well. During the work on Simpevarp 1.2, the "gap" between the model worked on by the site and the site modelling team has diminished significantly.

The upcoming work on model version Laxemar 1.2 will require continued improvement and development in the integration of disciplines. Given the sequential nature of the work where geology provides the geometrical skeleton to all disciplines, and e.g. hydrogeology provides results to Repository Engineering, but foremost to Safety Analysis, there is a high demand to adhere to set up plans and milestones to keep the overall schedule.

13.4 Implications for the ongoing investigation programme

One of the objectives of the version Simpevarp 1.2 site modelling of the Simpevarp area is to provide recommendations on continued field investigations during the initial site investigations. With Simpevarp 1.2 completed and the time of data freeze for Laxemar 1.2 passed, and Laxemar 1.2 modelling underway, possibilities only exist to influence investigations during the complete site investigations, which will be analysed as part of the future 2.X site-descriptive modelling. Furthermore, with the decision in principle to continue complete site investigations only in the Laxemar, the recommendations provided here are relevant to the Laxemar subarea (with associated regional scale model volume). However, there still exist possibilities to perform limited complementary investigations in the Simpevarp subarea which are important for the general understanding of the whole Simpevarp area (including both subareas). This may e.g. be related to collection of data that may improve the understanding (in a statistical sense) of deformation zones, and their characteristics and properties.

An account of the recommendations arising from work with the Simpevarp 1.2 modelling is provided in the following sections and is divided into recommendations and/or feedback provided to the site investigation organisation at Simpevarp during the course of the modelling work, and recommendations arising from identified uncertainties in the model version Simpevarp 1.2. The recommendations to site investigations related to the latter uncertainties reflect the availability of data and project understanding as of mid October 2004. The understanding of the Laxemar area at the time was relatively limited, and hence the relatively general nature of the recommendations given. However, many of the general recommendations given have been applied and have resulted in specified actions on the part of the ongoing site investigations. Some of these are also accounted for in the developed tentative program for continued site investigations in the Simpevarp area /SKB, 2004e/.

Aspects of the recommendations by the site modelling team on future investigations in the Simpevarp subarea (were the investigations to continue) given below have already been integrated in the developed tentative program for continued site investigations in the Simpevarp area /SKB, 2004e/.

As a further development of close working modes between the site modelling team and the site, the modelling team will, during the first half of 2005, work intimately with the site to select the part of Laxemar subarea that will be subjected to more focussed investigations during the complete site investigations. This latter work comprises parts of the site modelling work on model version Laxemar 2.1.

13.4.1 Recommendations/feedback given during the modelling work

During the work with Simpevarp 1.2, the site modelling team has had an information exchange with the site investigation team regarding the site investigation programme. These questions have ranged from profound ones (location of drilling sites, location of cored boreholes and their geometries, location of percussion-drilled boreholes for the purpose of verifying deformation zones, location of superficial “type profiles” through the Quaternary, focused on interpreted deformation zones) to details regarding e.g. sampling procedures and methods.

Comments and feedback have been given to draft versions of planning documents and decision papers on specific boreholes produced by the site investigation team. Overall, the feedback to the site investigation team has been given in an “informal” manner via electronic mail, telephone and during meetings, and has not necessarily been fully documented. An electronic log was devised during the work on Simpevarp 1.1 in an attempt to keep track of some of this “informal” exchange of information.

Recommendations concerning drilling of new boreholes

Mid 2003 a draft document was produced by the site investigation team that outlined the plans for drilling deep cored boreholes in the Simpevarp and Laxemar subareas /SKB, 2003c/. This document broadly identified the locations and geometries of boreholes KSH03, KAV04, and drilling sites for boreholes KLX03 and KLX04. During the course of the Simpevarp 1.1 work, the modelling team provided detailed comments on geometries and boreholes KLX03 and KLX04 and recommendations on the further usage of existing drilling sites and possible location of future new drilling sites in the Laxemar subarea. During the first quarter of 2004, the site modelling team also provided feedback on a document concerning detailed plans for drilling short percussion boreholes with the purpose of verifying interpreted deformation zones in the Simpevarp subarea (boreholes HAV11–HAV14, HSH01, HSH04 and HSH05).

Feedback and interaction during the course of work on Simpevarp 1.2 was directed towards finalising plans for the new cored boreholes KLX05 and KLX06. These two boreholes in the Laxemar subarea were drilled on deformation zones ZSMEW0002A (The Mederhult Zone) and ZSMNE042, respectively. The latter constitutes the interpreted eastwest bounding deformation zone in the south, located immediately north of the boundary of the local model area.

Furthermore, the project team provided feedback and input to the program for verification of interpreted deformation zones in the Laxemar area (boreholes HLX21 through HLX29), primarily focused on deformation zones ZSMEW007A and ZSMNE042A, cf. Figure 5-54. The site modelling team also expressed a wish to secure borehole imaging (BIPS) information from percussion boreholes drilled earlier with the corresponding objective in the Simpevarp subarea, see above. The importance of BIPS imagery for the conceptual modelling of deformation zones in the Simpevarp area was emphasised.

To this direct operational feedback and interaction should also be added actions on the part of the site modelling team to optimise the contents of data freezes for Simpevarp 1.2 and Laxemar 1.2. This was primarily related to requests for optimisation of on-site work to ensure delivery of important data at appropriate times. This is particularly important for borehole fracture data and borehole hydraulic data and associated data storage in databases.

13.4.2 Recommendations based on uncertainties in the site descriptive model Simevarp 1.2

The site-specific issues of critical nature raised in the complementary program for research and development (FUD-K) /SKB, 2001a/ and subsequently in the planning document for the site investigations in the Simpevarp area /SKB, 2002c/ are essentially still valid, cf. Section 13.2.2. Model version Simpevarp 1.2 provides additional increase in the understanding of the geological features of the Simpevarp subarea. Uncertainties in the site description are still significant in the remainder of the local scale model domain (i.e. the Laxemar subarea) and also in the regional model area. The main differences to conditions at the time of Simpevarp 1.1 completion are that 1) the geological model for Simpevarp 1.2 has propagated in the modelling of other disciplines (e.g. Thermal properties, Rock mechanics and Hydrogeology), and 2) the issue of ore potential has been resolved, i.e. it is considered negligible and is regarded as a closed issue.

The main noted uncertainties are listed and discussed in Section 12.3 where it is identified that the main reason for the noted uncertainties still is the relative lack of data at depth in the bedrock combined with a low data density. Using these uncertainties as a starting point, the site modelling team has made an effort to assess whether the identified uncertainties can be reduced by additional data, and if so, what are those data, and how they can be collected?

The overall basis for the assessments made below are compiled in Chapter 12 and the associated tables in Appendix 7. In the assessments made, due consideration has been taken to the SKB decision in principle to prioritise the Laxemar subarea in favour of the Simpevarp subarea.

Location of new boreholes

Given that much of the noted uncertainty is associated with lack of data, and in particular data at depth, a continued drilling programme and new borehole information (during and after completion of drilling) is expected to contribute to an improved description of the bedrock. In the case of the Simpevarp subarea, the completion of the deep boreholes KSH03 and KAV04 together with the performed percussion borehole and investigation program for verification of deformation zones, and complementary characterisation in borehole KAV01 completed the borehole characterisation programme in the Simpevarp subarea.

For the Laxemar subarea, and the Laxemar 1.2 modelling, data from two new additional boreholes (KLX03 and KLX04) add to the information at depth already existing from boreholes KLX01 and KLX02. To this list should also be added the program of shallow percussion boreholes targeted on interpreted deformation zones. Data from an additional two deep boreholes (KLX05 and KLX06) will provide additional information on two of the interpreted deformation zones in the Laxemar area (to be fully processed in the subsequent Laxemar version 2.1 modelling).

The cored boreholes listed above complete the planned boreholes within the auspices of initial site investigations in the Laxemar subarea, and the Simpevarp area as a whole. It can be noted that cored boreholes drilled in the future will be required to serve multiple purposes, foremost assessment of geometry and properties of fracture zones at depth, but also assessment of properties of the rock mass. This calls for careful consideration and optimisation of collar locations and geometry of the cored boreholes.

Heterogeneity of lithological domains

The heterogeneity of the interpreted lithological domains (and rock units making up the domains) could potentially affect distribution (variability) of thermal conductivity which in turn may have implications for the actual positioning and layout of the repository. The average thermal conductivity of the identified lithological domains in the Simpevarp subarea vary in a tight span from 2.6–2.8 W/(m·K). Variability will be faced within the individual lithological domain, but the effect of lithological heterogeneity on positioning and layout is deemed manageable. Likewise, the impact of lithology, and lithological variability on the actual construction of a geological repository is deemed minor or negligible. This implies that no specific action to further inform on lithological heterogeneity in the Simpevarp subarea is required. The fact that planned drilling for Laxemar 1.2 is focused on the Laxemar subarea, see above, therefore does not constitute a problem from this perspective.

However, consideration of heterogeneity of the bedrock and associated thermal properties is still required in the future characterisation in the Laxemar subarea.

Occurrence, geometry and properties of deformation zones

Borehole information provided for the Simpevarp 1.2 modelling has enabled improved constraint of deformation zones in the Simpevarp subarea; ZSMNE024A (KSH03A), ZSMNE012A (KAV01). However, both the occurrence and geometry of interpreted deformation zones are associated with uncertainty. This applies in particular to “possible deformation zones”, attributed low or intermediate confidence of occurrence. As for subhorizontal deformation zones, such zones of significant nature have not been identified in available boreholes, nor in the underground openings of the Äspö HRL. Despite the fact that the cored boreholes drilled are all near vertical, and should be optimal for identifying horizontal structures, their existence in some parts of the investigated domain cannot be ruled out. Close scrutiny of the possible existence of such zones will therefore be required in future site investigation work. This is particularly true for subhorizontal structures of minor extent.

Suggested field activities in order to eliminate or reduce uncertainties related to existence and geometry of important deformation zones are:

- Field investigations of selected interpreted deformation zones in order to confirm their occurrence, geometry and properties. This can be partly achieved by indirect means (reflection and refraction seismic surveys). However, geophysical anomalies (reflectors) without direct borehole verifications are always associated with uncertainty, in that they can also be associated with lithological boundaries. Targeted percussion drilling (or short cored boreholes) and excavation on surface of trenches on selected interpreted deformation zones are therefore required. For the Laxemar 1.2 modelling, a series of new reflection seismic surveys, including reprocessing of new and old data in combination will become available,
- Cross-hole hydraulic interference tests between boreholes (where applicable, and possibly supplemented by injections of solute tracers) may provide information on the connectivity (extent) of interpreted deformation zones.

Core drilling for establishing geometry and properties of deformation zones ZSMEW002A (the Mederhult zone, (KLX06)) and ZSMNE042A (KLX05) is presently underway. A percussion drilling campaign was carried out on zones ZSMEW007A and ZSMNE042A. This information will become available for the Laxemar 1.2 modelling. Future drilling activities focused on deformation zones will largely be performed in the Laxemar subarea.

Fracture statistics and DFN modelling

The geological DFN model developed for Simpvarp subarea as part of Simpevarp 1.2 is firmly related to geology and can be seen as an expansion of work done for Simpevarp 1.1. Uncertainty in fracture size is recognised by defining two alternative models which differ in the choice of model for size distribution (power law or log-normal) for the defined fracture sets, cf. Section 5.2.2. Uncertainty in orientation is handled by calculating orientation dispersion for available outcrops. Similarly, fracture intensity is expressed as a function of geological factors. In the case of vertical sets, the information is restricted, with one exception, to only one outcrop per defined lithological domain in the local scale model volume. Consequently, the address of uncertainty requires confirmatory results from short inclined cored boreholes in variable directions and surface statistics from more outcrops. Ideally, the latter two sources of fracture statistics should be closely geographically related. Furthermore, there is a need to better capture the size fraction of structures above the maximum size of fractures possible to map on the surface (constrained by outcrop size) and the minimum size of interpreted lineaments. This can possibly be achieved by high resolution aerial photography using low flight altitude, possibly combined with detailed ground geophysics.

Rock stress distribution – rock mechanics properties

The understanding of the rock stress situation in the Simpevarp subarea is considered satisfactory. The results show firm evidences of low rock stresses in the Simpevarp subarea, supported by stress modelling. No further measurements are foreseen in the Simpevarp subarea. However, the overall uncertainty in rock stress magnitudes at depth will most likely be reduced further by measurements performed for data freeze Laxemar 1.2. The understanding related to deterministic deformation zones in the Simpevarp subarea emerging for Laxemar 1.2 is expected to only marginally reduce uncertainties regarding the division into rock stress domains. Similarly, understanding of the existence and properties of minor (stochastic) deformation zones will be improved through analysis of an improved and further processed geological DFN model. Efforts should be made to improve understanding of mechanical properties of deformation zones, making use of drill core material and material collected from dug trenches. More site-specific test results on intact rock mechanical properties will become available for Laxemar 1.2.

Bedrock thermal conductivity

In order to improve the developed model of thermal conductivity, more representative direct measurements on rock samples are required, as well as corroborating analysis of both density and thermal conductivity, particularly for Ävrö granite. Due consideration to measurement scale and spatial variability should be considered in order to, among other things, improve scale transformations.

Transmissivity distribution – hydraulic tests

The uncertainty in geometry of water-bearing structures and transmissivity distribution in zones and fractures will be reduced by the improved understanding of the geological model of deformation zones, as outlined above, and by interpretation of new information from additional boreholes and hydraulic tests. Additional such data became available for Simpevarp 1.2 from boreholes KSH02, KSH03A and KAV01. However, address of key conceptual issues – like the transmissivity/fracture size relationships – calls e.g. for cross-hole interference tests. Given the potential lack of suitable sink-source pairs of boreholes, there may be a need to consider import of existing data/results from e.g. Äspö HRL. It should however be noted that any inference of fracture/structure size and subsequent coupling to a transmissivity value is associated with uncertainty. The new data for Laxemar 1.2 are expected to include the first site-specific elements of hydraulic interference.

As a complement to the geological efforts described above, any new short inclined cored boreholes with the purpose of obtaining fracture statistics should also be subject to detailed hydraulic tests to facilitate the hydraulic DFN modelling. In addition, the prospects of using single-hole interference tests in boreholes with multi-packer systems to help constrain hydraulic DFN models should be explored.

Groundwater composition – pore water in intact rock matrix

The conceptual understanding of present day hydrogeology and hydrogeochemistry, individually or in combination, is associated with uncertainties concerning past evolution including initial conditions. There is also a general need to obtain more representative chemical data from great depths.

In addition, information on the composition of the rock matrix water and the intact rock matrix porosity will provide valuable input to this understanding of the past, as well as the present hydrogeological and hydrogeochemical conditions at the site. Measurements of these entities are under way and will become available for Laxemar 1.2 and will be useful for inferences about both the Laxemar and Simpevarp subareas.

Furthermore, there is a need to assess, and potentially include the effects of temporal variations in water chemistry in the modelling.

Bedrock transport properties

The assessment and modelling of transport properties suffers from the long times involved in obtaining the necessary laboratory results. Some site-specific data will become available for Laxemar 1.2 (from both the Simpevarp and Laxemar subareas), but most of the data will not become available until the complete site investigation stage. In the meantime strategic use of indirect data (e.g. formation factor from in situ borehole resistivity logs) and data from the Äspö HRL is employed.

Surface system

The current uncertainty in the surface system properties and processes description stems mainly from lack of data. This uncertainty is expected to be partly resolved through the data that will become available by the data freeze for Laxemar 1.2. The subdivision of the overburden (mainly Quaternary deposits) in terms of composition/properties, spatial variability, overall thickness and individual thicknesses of strata will however only be partly resolved for Laxemar 1.2.

Collection of site-specific hydrological data was initiated 2004 and sufficiently long time series will not be available for Laxemar 1.2. Prolongation of the monitoring programmes for e.g. meteorology, hydrology (water levels, run-off etc.), hydrogeochemistry and ecosystems will result in longer time series, which will help reduce uncertainties in future models developed as part of the complete site investigations. Similarly, there exists a need to assess seasonal variation in surface water chemistry.

13.5 General conclusions

In revisit of the specific objectives stated for the version 1.2 modelling of the Simpevarp subarea as given in Chapter 1 it is concluded that the;

- available new primary data have been adequately analysed as part of the Simpevarp 1.2 modelling. Some existing old primary data remain to be included in future modelling,
- three-dimensional descriptive models of lithological domains and deformation zones have been updated, covering defined local and regional scale model volumes. The geological models have formed the basis for the parameterisation of other discipline models and have also formed the geometrical and structural basis for subsequent hydrogeological flow modelling,
- confidence in the developed models has been treated in a systematic way as presented in Chapter 12, including assessment of uncertainties, and interactions and feedback between disciplines. Significant progress is noted in the coupling between hydrogeochemistry and hydrogeological modelling. To be improved in future modelling is the feedback from other disciplines to the geological modelling,
- possible alternative models have been screened and priorities in relation to the needs of repository engineering and safety assessment. In the current modelling the alternative modelling propagated in hydrogeological flow modelling is related to alternative models relating transmissivity to feature size,
- site-specific issues have been addressed and understanding has developed as part of the performed Simpevarp 1.2 modelling as demonstrated in the preceding sections. No new important site-specific issues have been raised,
- modelling results and identified uncertainties have been used to propose complementary investigations to further increase understanding and reduce uncertainties.

14 References

Aastrup M, Thunholm B, Johnson J, Bertills U, Berntell A, 1995. Grundvattnets kemi i Sverige. Naturvårdsverket, rapport 4415, 52 pp (in Swedish).

Adl-Zarrabi B, 2004a. Drill hole KSH01A Thermal properties: heat conductivity and heat capacity determined using the TPS method and mineralogical composition by modal analysis. SKB P-04-53, Svensk Kärnbränslehantering AB.

Adl-Zarrabi B, 2004b. Drill hole KSH02 Thermal properties: heat conductivity and heat capacity determined using the TPS method and mineralogical composition by modal analysis. SKB P-04-54, Svensk Kärnbränslehantering AB.

Adl-Zarrabi B, 2004c. Drill hole KAV01 Thermal properties: heat conductivity and heat capacity determined using the TPS method and mineralogical composition by modal analysis. SKB P-04-55, Svensk Kärnbränslehantering AB.

Agrell H, 1976. The highest coastline in south-eastern Sweden. Boreas 5, 143–154.

Alling V, Andersson P, Fridriksson G, Rubio Lind C, 2004. Biomass production of Common reed (Phragmites australis), infauna, epiphytes, sessile epifauna and mobile epifaunal, Common reed biotopes in Oskarshamn's model area. SKB P-04-316. Svensk Kärnbränslehantering AB.

Alm E, Sundblad K, 2002. Fluorite-calcite-galena-bearing fractures in the counties of Kalmar and Blekinge, Sweden. SKB R-02-42. Svensk Kärnbränslehantering AB.

American Public Health Association, 1992. Estimation of bacterial density, 977–980. In: Standard methods for the examination of water and wastewater, 18th ed. American Public Health Association, Washington, D.C.

Ambrosiani Garcia K, 1990. Macrofossils from the till-covered sediments at Öje, central Sweden. In: Late Quaternary Stratigraphy in the Nordic Countries 150,000–15,000 BP. (Andersen B G and Königsson L-K, eds). Striae 34, 1–10.

Andersson P, Ludvigsson J-E, Wass E, 1998. Äspö Hard Rock Laboratory, True Block Scale Project, Preliminary characterisation. Combined interference tests and tracer tests, SKB IPR-01-44, Svensk Kärnbränslehantering AB.

Andersson P, Ludvigsson J-E, Wass E, Holmqvist M, 2000. Äspö Hard Rock Laboratory, True Block Scale Project, Tracer test stage. Interference tests, dilutiontests and tracer tests, SKB IPR-00-28, Svensk Kärnbränslehantering AB.

Andersson J, Ström A, Svemar C, Almén K-E, Ericsson L O, 2000. What requirements does the KBS-3 repository make on the host rock? Geoscientific suitability indicators and criteria for siting and site evaluation. SKB TR-00-12, Svensk Kärnbränslehantering AB.

Andersson C, Söderhäll J, 2001. Rock mechanics conditions at the Äspö HRL. A study of the correlation between the geology, tunnel maintenance and the tunnel shape. SKB R-01-53, Svensk Kärnbränslehantering AB.

Andersson J, Christiansson R, Hudson J, 2002a. Site Investigations Strategy for Rock Mechanics Site Descriptive Model. SKB TR-02-01, Svensk Kärnbränslehantering AB.

Andersson J, Berglund J, Follin S, Hakami E, Halvarson J, Hermanson J, Laaksoharju M, Rhén I, Wahlgren C-H, 2002b. Testing the methodology for site descriptive modelling. Application for the Laxemar area, SKB TR-02-19, Svensk Kärnbränslehantering AB.

Andersson P, Byegård J, Dershowitz B, Doe T, Hermanson J, Meier P, Tullborg E-L, Winberg A, 2002c. TRUE Block Scale Project. Final report. 1. Characterisation and model development. SKB TR-02-13, Svensk Kärnbränslehantering AB.

Andersson J, 2003. Site descriptive modelling – strategy for integrated evaluation. SKB R-03-05. Svensk Kärnbränslehantering AB.

Andersson J (ed), 2004. T-H-M in Safety Assessments. Findings of DECOVALEX III, SKI Report (in progress).

Andersson J, Munier R, Ström A, Söderbäck B, Almén K-E, Olsson L, 2004. When is there sufficient information from the Site Investigations? SKB R-04-23, Svensk Kärnbränslehantering AB.

Andrén T, Björck J, Johnsen S, 1999. Correlation of the Swedish glacial varves with the Greenland (GRIP) oxygen isotope stratigraphy. Journal of Quaternary Science 14, 361–371.

Andrén C, 2004. Underlag till Energiflöden i ekosystem med grod- och kräldjur. Nature – Artbevarande & Foto (in Swedish).

Andrén C, 2004a. Oskarshamn site investigation, Amphibians and reptiles in SKB special area of investigation at Simpevarp. SKB P-04-36. Svensk Kärnbränslehantering AB.

Andrén C, 2004b. Forsmark site investigation, Amphibians and reptiles. SKB P-04-07. Svensk Kärnbränslehantering AB.

Apps J A, Van de Kamp P C, 1993. Energy gases of abiogenic origin in the Earth's crust. The future of energy gases. US Geological Survey Prof. Pap. 1570, 81–132.

Ask H, 2003. Oskarshamn site investigation. Installation of four monitoring wells, SSM000001, SSM000002, SSM000004 and SSM000005 in the Simpevarp subarea. SKB P-03-80. Svensk Kärnbränslehantering AB.

Ask H, 2003. Oskarshamn site investigation – Drilling of three flushing water wells, HSH01, HSH02 and HSH03. SKB P-03-114. Svensk Kärnbränslehantering AB.

Ask H, Morosini M, Samuelsson L-E, Stridsman H, 2003. Oskarshamn site investigation – Drilling of cored borehole KSH01. SKB P-03-113. Svensk Kärnbränslehantering AB.

Ask H, Morosini M, Samuelsson L-E, Stridsman H, 2004a. Oskarshamn site investigation – Drilling of cored borehole KSH02 (in prep). Svensk Kärnbränslehantering AB.

Ask H, Morosini M, Samuelsson L-E, Stridsman H, 2004b. Oskarshamn site investigation – Drilling of cored borehole KSH03. P-04-233. Svensk Kärnbränslehantering AB.

Ask H, Morosini M, Samuelsson L-E, Ekström L, Håkansson N, 2005. Drilling of cored borehole KAV04. Oskarshamn site investigation. SKB P-05-25. Svensk Kärnbränslehantering AB.

Banwart S A, 1999. Reduction of iron (III) minerals by natural organic matter in groundwater. Geochim. Cosmochim. Acta, 63, 2919–2928.

Banwart S, Gustafsson E, Laaksoharju M, 1999. Hydrological and reactive processes during rapid recharge to fracture zones. The Äspö large scale redox experiment. App. Geoch. 14, 873–892.

Barton N, 2002. Some new Q-value correlations to assist in site characterisation and tunnel design, I.J. Rock Mech. & Min. Eng., Vol. 39, p 185–216.

Bein A, Arad A, 1992. Formation of saline groundwaters in the Baltic region through freezing of seawater during glacial periods. Journal of Hydrology, 140, Elsevier Science B.V. pp 75–87.

Berg C, 2003a. Hydrochemical logging in KAV01. Oskarshamn site investigation. SKB P-03-89. Svensk Kärnbränslehantering AB.

Berg C, 2003b. Hydrochemical logging in KSH02. Oskarshamn site investigation. SKB P-03-88. Svensk Kärnbränslehantering AB.

Berggren J, Kyläkorpi L, 2002. Ekosystemen i Simpevarpsområdet – Sammanställning av befintlig information. SKB R-02-10. Svensk Kärnbränslehantering AB (in Swedish).

Berggren D, Bergkvist B, Johansson M-B, et al. 2004. A description of LUSTRA's common field sites. Department of Forest Soils, Swedish University of Agriculture Sciences, Uppsala, Report 87.

Berglund B E, Digerfeldt G, Engelmark R, Gaillard M-J, Karlsson S, Miller U, Risberg J, 1996. Palaeoecological events during the last 15,000 years, Regional syntheses of palaeoecological studies of lakes and mires in Europe – Sweden. In Berglund B E, Birks H J B, Ralska-Jasiewiczowa M and Wright H E (eds): IGCP Project 158B p. 233–280.

Berglund S, Selroos J-O, 2003. Transport properties site decsriptive model – Guidelines for evaluation and modelling. SKB R-03-09, Svensk Kärnbränslehantering AB.

Berglund J, Curtis P, Eliasson T, Ohlsson T, Starzec P, Tullborg E-L, 2003. Äspö Hard Rock Laboratory – Update of the geological model 2002. SKB IPR-03-34. Svensk Kärnbränslehantering AB.

Bergman T, Isaksson H, Johansson R, Lindén A H, Lindgren J, Lindroos H, Rudmark L, Wahlgren C-H, 1998. Förstudie Oskarshamn. Jordarter, bergarter och deformationszoner. SKB R-98-56, Svensk Kärnbränslehantering AB (in Swedish).

Bergman T, Follin S, Isaksson H, Johansson R, Lindén A H, Lindroos H, Rudmark L, Stanfors R, Wahlgren C-H, 1999. Förstudie Oskarshamn. Erfarenheter från geovetenskapliga undersökningar i nordöstra delen av kommunen. SKB R-99-04, Svensk Kärnbränslehantering AB (in Swedish).

Bergman T, Isaksson H, Rudmark L, Stanfors R, Wahlgren C-H, Johansson R, 2000. Förstudie Oskarshamn. Kompletterande geologiska studier. SKB R-00-45. Svensk Kärnbränslehantering AB (in Swedish).

Beunk F F, Page L M, 2001. Structural evolution of the accretional continental margin of the Paleoproterozoic Svecofennian orogen in southern Sweden. Tectonophysics 339, 67–92.

BFS, 1990. Nybyggnadsregler ändringar. Boverkets författningssamling. BFS 1990:28, Nr. 2, Stockholm, ISBN 91-38-12510-2 (in Swedish).

Bieniawski Z T, 1989. Engineering rock mass classifications. John Wiley & Sons.

Bisbee K E, Gower S T, Norman J M, Nordheim E V, 2001. Environmental controls on ground cover species composition and productivity in a boreal black spruce forest. Oecologia 129: 261–270.

Björck S, 1995. A review of the history of the Baltic Sea, 13.0–8.0 ka BP. Quaternary International 27, 19–40.

Björck S, Kromer B, Johnsen S, Bennike O, Hammarlund D, Lemdahl G, Possnert G, Lander Rasmussen T, Wohlfarth B, Hammer C H, Spurk M, 1996. Synchronized Terrestrial-atmospheric deglacial records around the North Atlantic. Science 274, 1155–1160.

Björck J, 1999. The Alleröd-younger Dryas pollen zone in an 800-years varve chronology from southeastern Sweden. GFF 121, 287–292.

Bolin B, Rodhe H, 1973. A note on the concepts of age distribution and transit term in natural reservoirs. Tellus, 25, 58–62.

Boresjö Bronge L, Wester K, 2003. Vegetation mapping with satellite data of the Forsmark, Tierp and Oskarshamn regions. SKB P-03-83, Svensk Kärnbränslehantering AB.

Borg G Ch, Paabo K, 1984. Area description and sediment investigation of the coastal area between Karlskrona and Oskarshamn S.E. Sweden. Striolae, Uppsala University. 85 pp.

Bossart P, Hermanson J, Mazurek M, 2001. Analysis of fracture networks based on the integration of structural and hydrogeological observations at different scales. SKB TR-01-21. Svensk Kärnbränslehantering AB.

Brace W F, Permeability of Crystalline and Argillaceous Rocks. Int. J. Rock. Mech. & Geomech. Abstr. Vol. 17, pp. 241–251.

Bratt P (ed), 1998. Forntid i ny dager – Arkeologi i Stockholmstrakten, Raster Förlag, Stockholm (in Swedish).

Brunauer S, Emmet P H, Teller E, 1938. Adsorption of gases in multimolecular layers. J. Am. Chem. Soc., 60, 309.

Brunberg A-K, Carlsson T, Brydsten L, Strömgren M, 2004. Oskarshamn Site investigation, Identification of catchments, lake-related drainage parameters and lake habitats. SKB P-04-242. Svensk Kärnbränslehantering AB.

Bruno J, Cera E, Grivé M, Rollin C, Ahonen L, Kaija J, Blomqvist R, El Aamrani F Z, Casas I, de Pablo J, 1999. Redox Processes in the Palmottu uranium deposit. Redox measurements and redox controls in the Palmottu system. Draft. Informe 64023. ENRESA, 76 p.

Brydsten L, 2004. Method for construction of digital elevation models for site investigation program in Forsmark and Simpevarp. SKB P-04-03, Svensk Kärnbränslehantering AB.

Byegård J, Johansson H, Skålberg M, Tullborg E-L, 1998. The interaction of sorbing and non-sorbing tracers with different Äspö rock types – Sorption and diffusion experiments in the laboratory scale. SKB TR 98-18, Svensk Kärnbränslehantering AB.

Byegård J, Widestrand H, Skålberg M, Tullborg E-L, Siitari-Kauppi M, 2001. Complementary investigation of diffusivity, porosity and sorptivity of Feature A-site specific geological material. SKB ICR-01-04. Svensk Kärnbränslehantering AB.

Byegård J, Gustavsson E, Tullborg E-L, Berglund S, 2005. Bedrock transport properties. Preliminary site description Simpevarp subarea – version 1.2. SKB R-05-05, Svensk Kärnbränslehantering AB.

Bäckblom G, Stanfors R, 1989. Interdisciplinary study of post-glacial faulting in the Lansjärv area, northern Sweden. SKB TR-89-31, Svensk Kärnbränslehantering AB.

Bödvarsson R, 2003. Swedish National Seismic Network (SNSN). A short report on recorded earthquakes during the fourth quarter of the year 2002. SKB P-03-02. Svensk Kärnbränslehantering AB.

Canhem C D, Pace M L, Papaik M J, Primack A G B, et al. 2004. A spatially explicit watershed-scale analysis of dissolved organic carbon in Adirondack lakes. Ecological Application 14(3):839–854.

Carbol P, Engkvist I, 1997. Compilation of radionuclide sorption coefficients for performance assessment. SKB R-97-13, Svensk Kärnbränslehantering AB.

Carlsson L, Gustafson G, 1997. Provpumpning som geohydrologisk undersökningsmetodik (ver 2.1), Chalmers Tekniska Högskola, Geologiska institutionen, Publ C62 (in Swedish).

Cederlund G, Hammarström A, Wallin K, 2004. Surveys of mammal populations in the areas adjecent to Simpevarp. Svensk Kärnbränslehantering AB (in prep).

Chapin III F S, Matson P A, Mooney H A, 2002. Principles of Terrestrial Ecosystem Ecology. Springer Verlag New York, Inc. ISBN 0-387-95439-2.

Chryssanthakis P, 2003. Borehole: KSH01A. Results of tilt testing. Oskarshamn site investigation. SKB P-03-107, Svensk Kärnbränslehantering AB.

Chryssanthakis P, 2004a. Oskarshamn Site Investigation – Borehole KSH02, Results of tilt testing, SKB P-04-10, Svensk Kärnbränslehantering AB.

Chryssanthakis P, 2004b. Oskarshamn Site Investigation – Borehole KAV01, Results of tilt testing, SKB P-04-42, Svensk Kärnbränslehantering AB.

Chryssanthakis P, 2004c. Oskarshamn Site Investigation – Borehole KLX02, Results of tilt testing, SKB P-04-44, Svensk Kärnbränslehantering AB.

Clark I, Fritz P, 1997. Environmental Isotopes in Hydrogeology. Lewis Publishers. Boca Raton, Florida. 328 pp.

Clark D A, Brown S, Kicklighter D W, et al. 2001. Measuring net primary production in forests: concepts and field methods. Ecological applications 11(2):356–370.

Curtis P, Elfström M, Stanfors R, 2003a. Oskarshamn site investigation – Compilation of structural geological data covering the Simpevarp peninsula, Ävrö and Hålö. SKB P-03-07. Svensk Kärnbränslehantering AB.

Curtis P, Elfström M, Stanfors R, 2003b. Oskarshamn site investigation. Visualization of structural geological data covering the Simpevarp peninsula, Ävrö and Hålö. SKB P-03-86. Svensk Kärnbränslehantering AB.

Dagan G, 1981. Analysis of flow trough heterogeneous random aquifers by the method of embedding matrix, 1, Steady flow, Water resources res., 17 (1), 107–121.

Darcel C, Davy P, Bour O, de Dreuzy J-R, 2004. Alternative DFN model based on initial site investigations at Simpevarp. SKB R-04-76. Svensk Kärnbränslehantering AB.

Debon F, Le Fort P, 1983. A chemical-mineralogical classification of common plutonic rocks and associations. Transactions of Royal Society of Edinburgh, Earth Sciences 73, 135–149.

Degueldre C, 1994. Colloid properites in groundwaters from crystalline formation. PSI Bericht NP-94-21 Paul Scherrer Institute, Villigen, Switzerland.

Dershowitz W, Lee G, Geier J, Foxford T, LaPointe P, Thomas A, 1996. FracMan Interactive Discrete Feature Data Analysis, Geometric Modeling, and Exploration Simulation User Documentation, Version 2.6, Golder Associates Inc.

Dershowitz W, Winberg A, Hermanson J, Byegård J, Tullborg E-L, Andersson P, Mazurek M, 2003. Äspö Hard Rock Laboratory. Äspö Task Force on modelling of groundwater flow and transport of solutes – Task 6C – A semi-synthetic model of block scale conductive structures at the Äspö HRL. SKB IPR-03-13. Svensk Kärnbränslehantering AB.

Deutsch W J, Jenne E A, Krupka K M, 1982. Solubility equilibria in basalt aquifers: The Columbia Plateau, Eastern Washington, U.S.A. Chemical Geology, 36, 15–34.

Donner J, Kankainen T, Karhu J A, 1999. Radiocarbon ages and stable isotope composition of Holocene shells in Finland. In T. Andrén (ed.), In: Proceedings of the Conference The Baltic – past, present and future. Stockholm 14-16. March, 1994. Stockholm University, Quaternaria A:7, 31–38.

Drake H, Tullborg E-L, 2004. Fracture mineralogy and wall rock alteration. Results from drill core KSH01A+B. Oskarshamn Site investigation. SKB P-04-250. Svensk Kärnbränslehantering AB. 119 pp.

Ehrenborg J, Stejskal V, 2004a. Oskarshamn site investigation. Boremap mapping of core drilled boreholes KSH01A and KSH01B. SKB P-04-01. Svensk Kärnbränslehantering AB.

Ehrenborg J, Stejskal V, 2004b. Oskarshamn site investigation. Boremap mapping of core drilled borehole KLX02. SKB P-04-129. Svensk Kärnbränslehantering AB.

Ehrenborg J, Stejskal V, 2004c. Oskarshamn site investigation. Boremap mapping of core drilled borehole KAV01. SKB P-04-130. Svensk Kärnbränslehantering AB.

Ehrenborg J, Stejskal V, 2004d. Oskarshamn site investigation. Boremap mapping of core drilled borehole KSH02. SKB P-04-131. Svensk Kärnbränslehantering AB.

Ehrenborg J, Stejskal V, 2004e. Oskarshamn site investigation. Boremap mapping of core drilled boreholes KSH03A and KSH03B. SKB P-04-132. Svensk Kärnbränslehantering AB.

Ekman M, 1996. A consistent map of the postglacial uplift of Fennoscandia. Terra-Nova 8/2, 158–165.

Elhammer A, Sandkvist Å, 2005. Oskarshamn site investigation. Detailed marine geological survey of the sea bottom outside Simpevarp. SKB P-05-35. Svensk Kärnbränslehantering AB. In press.

Eliasson T, 1993. Mineralogy, geochemistry and petrophysics of red coloured granite adjacent to fractures. SKB TR-93-06. Svensk Kärnbränslehantering AB.

Engdahl A, Ericsson U, 2004. Sampling of freshwater fish. Description of the fish fauna in four lakes. SKB P-04-251, Svensk Kärnbränslehantering AB.

Ericsson U, Engdahl A, 2004a. Surface water sampling at Simpevarp 2002–2003. SKB P-04-13, Svensk Kärnbränslehantering AB.

Ericsson U, Engdahl A, 2004b. Oskarshamn site investigation. Surface water sampling in Oskarshamn – Subreport October 2003 to February 2004. SKB P-04-75. Svensk Kärnbränslehantering AB.

Ericsson U, Engdahl A, 2004c. Benthic macro invertebrates. Results from sampling in the Simpevarp area 2004. SKB P-04-252, Svensk Kärnbränslehantering AB.

Fairbanks R, 1989. A 17,000-year glacio-eustatic sea level record: influence of glacial melting rates on the Younger Dryas event and deep-ocean circulation. Nature 342, 637–642.

Follin S, Årebäck M, Axelsson C-A, Stigsson M, Jacks G, 1998. Förstudie Oskarshamn, Grundvattnets långsiktiga förändringar. SKB R-98-55, Svensk Kärnbränslehantering AB (in Swedish).

Follin S, Stigsson M, Svensson U, 2004. Variable-density groundwater flow simulations and particle tracking in support of the Preliminary Site Description for the Simpevarp area (version 1.1). SKB R-04-65. Svensk Kärnbränslehantering AB (in press).

Follin S, Stigsson M, Svensson U, 2005. Variable-density groundwater flow simulations and particle tracking – Numerical modelling using DarcyTools. Preliminary site description Simpevarp subarea – version 1.2. SKB R-05-11, Svensk Kärnbränslehantering AB.

Fontes J-Ch, Louvat D, Michelot J-L, 1989. Some constraints on geochemistry and environmental isotopes for the study of low fracture flows in crystalline rocks – The Stripa case. In: International Atomic Energy Agency (eds) Isotopes techniques in the study of the Hydrology of Fractured and Fissured Rocks. IAEA, Vienna, Austria.

Forsman I, Zetterlund M, Rhén I, 2005 (in prep). Oskarshamn site investigation. Correlation of Posiva Flow Log anomalies to core mapped features in KSH01A, KSH02A and KAV01. SKB P-05-XX, Svensk Kärnbränslehantering AB.

Frape S K, Byrant G, Blomqvist R, Ruskeeniemi T, 1966. Evidence from stable chlorine isotopes for multiple sources of chloride in groundwaters from crystalline shield environments. In: Isotopes in Water Resources Management, 1966. IAEA-SM-336/24, Vol. 1, 19–30.

Fredén C, 2002. Berg och Jord, Sveriges Nationalatlas. 208 pp (in Swedish).

Fredriksson A, Hässler L, Söderberg L, 2001. Extension of CLAB – Numerical modelling, deformation measurements and comparison of forecast with outcome. Proceedings of the ISRM Reg Symp EUROCK 2001, Espoo, Finland 4–7, June 2001.

Fredriksson R, Tobiasson S, 2003. Simpevarp site investigation. Inventory of macrophyte communities at Simpevarp nuclear power plant. Area of distribution and biomass determination. SKB P-03-69. Svensk Kärnbränslehantering AB.

Fredriksson R, 2004. Inventory of the soft-bottom macrozoobenthos community in the area around Simpevarp nuclear power plant. Oskarshamn site investigation, SKB P-04-17, Svensk Kärnbränslehantering AB.

Fredriksson R, Tobiasson S, 2004. Inventory of the soft-bottom macrozoobenthos community in the area around Simpevarp nuclear power plant. SKB P-04-17, Svensk Kärnbränslehantering AB.

Fredriksson A, Olofsson I, 2005. Rock mechanics characterisation of the rock mass – Theoretical approach. Preliminary site description Simpevarp subarea – version 1.2. SKB R-05-22, Svensk Kärnbränslehantering AB.

Fridriksson G, Öhr J, 2003. Forsmark site investigation. Assessment of plant biomass of the ground, field and shrub layers of the Forsmark area. SKB P-03-90, Svensk Kärnbränslehantering AB.

Gascoyne M, 2004. Hydrogeochemistry, groundwater ages and sources of salts in a granitic batholith on the Canadian Shield southeastern Manitoba. Appl. Geochem., 19, 519–560.

Glynn P D, Voss C I, 1999. Geochemical characterization of Simpevarp ground waters near the Äspö Hard Rock Laboratory. SITE-94 SKI Report 96:29, 210 p.

Gower S T, Kucharik C J, Norman J M, 1999. Direct and indirect estimations of Leaf Area Index, fAPAR, and Net Primary Production of terrestrial ecosystems. Remote Sensing of Environment 70:29–51.

Gower S T, Krankina O, Olson R J, Apps M, Linder S, Wang C, 2001. Net primary production and carbon allocation patterns of boreal forest ecosystems. Ecological Application 11:1395–1411.

Green M, 2004. Bird surveys in Simpevarp 2003. Oskarshamn site investigation, SKB P-04-21, Svensk Kärnbränslehantering AB.

Gregersen S, Korhonen H, Husebye E S, 1991. Fennoscandian dynamics: Present-day earthquake activity. Tectonophysics 189, 333–344.

Gregersen S, 1992. Crustal stress regime in Fennoscandia from focal mechanisms. Journal of Geophysical Research 97, B8, 11821–1827.

Grenthe I, Stumm W, Laaksoharju M, Nilson A C, Wikberg P, 1992. Redox potentials and redox reactions in deep groundwater systems. Chem. Geol. 98, 131–150.

Grimaud D, Beaucaire C, Michard G, 1990. Modeling of the evolution of ground waters in a granite system at low temperature: the Stripa ground waters, Sweden. Applied Geochemistry, 5, 515–525.

Gurban I, Laaksoharju M, 2002. Drilling Impact Study (DIS); Evaluation of the influences of drilling, in special on the changes on groundwater parameters. SKB PIR-03-02, Svensk Kärnbränslehantering AB.

Gustafson G, Stanfors R, Wikberg P, 1989. Swedish Hard Rock Laboratory. First evaluation of 1988 year pre-investigations and description of the target area, the island of Äspö. SKB TR 89-16, Svensk Kärnbränslehantering AB.

Gustafsson J, Gustafsson C, 2004. RAMAC and BIPS logging in boreholes KSH03A, KSH03B, HAV09, HAV10 and BIPS in KAV01. Oskarshamn site investigation. SKB P-04-48, Svensk Kärnbränslehantering AB.

Gustafsson J, Gustafsson C, 2004a. RAMAC logging with directional radar antenna in boreholes KSH01A, KSH01B and KSH02. Oskarshamn site investigation. SKB P-04-66, Svensk Kärnbränslehantering AB.

Gustavsson E, Gunnarsson M, 2005. Oskarshamn site investigation. Laboratory data from the site investigation programme for the transport properties of the rock. Boreholes KSH01A, KSH02 and KLX02. SKB P-05-18. Svensk Kärnbränslehantering AB.

Hakami E, Hakami H, Cosgrove J, 2002. Strategy for a Rock Mechanics Site Descriptive Model. Development and testing of an approach to modelling the state of stress. SKB R-02-03. Svensk Kärnbränslehantering AB.

Hakami E, Min K-B, 2005. Modelling of the state of stress. Preliminary site description Simpevarp subarea – version 1.2. SKB R-05-19, Svensk Kärnbränslehantering AB.

Hartley L J, Holton D, 2003. ConnectFlow (Release 2.0) Technical Summary Document. SERCO/ERRA-C/TSD02V1.

Hartley L J, Hoch A R, Cliffe K A C, Jackson C P, Holton D, 2003a. NAMMU (Release 7.2) Technical Summary Document. SERCO/ERRA-NM/TSD02V1.

Hartley L J, Holton D, Hoch A R, 2003b. NAPSAC (Release 4.4) Technical Summary Document. SERCO/ERRA-N/TSD02V1.

Hartley L, Gylling B, Marsic N, Holmén J, Worth D, 2004. Preliminary Site Description: Groundwater flow simulations Oskarshamn area (version 1.1) modelled with ConnectFlow. SKB R-04-63. Svensk Kärnbränslehantering AB.

Hartley L, Hoch A, Hunter F, Marsic N, 2005. Regional hydrogeological simulations – Numerical modelling using ConnectFlow. Preliminary site description Simpevarp subarea – version 1.2. SKB R-05-12, Svensk Kärnbränslehantering AB.

Haveman S A, Pedersen K, Ruotsalainen P, 1998. Geomicrobial investigations of groundwaters from Olkilouto, Hästholmen, Kivetty and Romuvaara, Finland. POSIVA Report 98-09, Helsinki, Finland, 40 p.

Helander B, Karlsson O, Lundberg T, 2003. Inventering av gråsäl vid Svenska Östersjökusten 2002. Sälinformation 2003:1 (in Swedish).

Hellmuth K H, Siitari-Kauppi M, Lindberg A, 1993. Study of porosity and migration pathways in crystalline rock by impregnation with ^{14}C-polymethylmethacrylate. J. of Contaminant Hydrology, 13: 403–418.

Hellmuth K H, Lukkarinen S, Siitari-Kauppi M, 1994. Rock matrix studies with carbon-14-polymethylmethacrylate (PMMA). Method, development and applications. Isotopenpraxis Environ. Health Stud. 30: 47–60.

Hermanson J, Hansen L, Wikholm M, Cronquist T, Leiner P, Vestgård J, Sandahl K-A, 2004. Detailed fracture mapping of four outcrops at the Simpevarp peninsula and Ävrö. SKB P-04-35. Svensk Kärnbränslehantering AB.

Hoch A R, Hartley L J, 2003. NAMMU (Release 7.2) Verification Document. SERCO/ERRA-NM/VD02V2

Hoch A R, Hartley L J, Holton D, 2003. NAPSAC (Release 4.3) Verification Document. SERCO/ERRA-NM/VD02V1.

Hättestrand C, Stroeven A, 2002. A preglacial landscape in the centre of Fennoscandian glaciation: geomorphological evidence of minimal Quaternary glacial erosion. Geomorphology 44, 127–143.

Jansson U, Berg J, Björklund A, 2004. A study on landscape and the historical geography of two areas – Oskarshamn and Forsmark, June 2004. SKB R-04-67, Svensk Kärnbränslehantering AB.

Jacobsson O, 1978. Skog för framtid. SOU 1978:7, bilaga 1 pp 200–205 (in Swedish).

Jacobsson L, 2004a. Oskarshamn Site Investigation – Drill hole KAV01, Normal loading and shear tests on joints. SKB P-05-05, Svensk Kärnbränslehantering AB.

Jacobsson L, 2004b. Oskarshamn Site Investigation – Drill hole KSH01A, Normal loading and shear tests on joints. SKB P-05-06, Svensk Kärnbränslehantering AB.

Jacobsson L, 2004c. Oskarshamn Site Investigation – Drill hole KSH02, Normal loading and shear tests on joints. SKB P-05-07, Svensk Kärnbränslehantering AB.

Johansson L, Johansson Å, 1990. Isotope geochemistry and age relationships of mafic intrusions along the Protogine Zone, southern Sweden. Precambrian Research 48, 395–414.

Johansson T, Adestam L, 2004. Oskarshamn site investigation. Slug tests in groundwater monitoring wells in soil in the Simpevarp area. SKB P-04-122. Svensk Kärnbränslehantering AB.

Kautsky U, 1995. Ecosystem processes in coastal areas of the Baltic Sea. Doctoral Thesis, Department of Zoology, Stockholm University, Sweden.

Knutsson G, Morfeldt C-O, 2002. Grundvatten, teori & tillämpning, AB Svensk Byggtjänst, Stockholm (in Swedish).

Koistinen T, Stephens M B, Bogatchev V, Nordgulen O, Wennerström M, Korhonen J, 2001. Geological map of the Fennoscandian Shield, scale 1:2 000 000. Geological Surveys of Finland, Norway and Sweden and the North-West Department of Natural Resources of Russia.

Kornfält K-A, Wikman H, 1987. Description of the map of solid rocks around Simpevarp. SKB PR 25-87-02, Svensk Kärnbränslehantering AB.

Kornfält K-A, Persson P-O, Wikman H, 1997. Granitoids from the Äspö area, southeastern Sweden – geochemical and geochronological data. GFF 119, 109–114.

Kresten P, Chyssler J, 1976. The Götemar massif in south-eastern Sweden: A reconnaissance survey. Geologiska Föreningens i Stockholm Förhandlingar 98, 155–161.

Kristiansson J, 1986. The ice recession in the south-easten part of Sweden. University of Stockholm. Department of Quaternary Research 7, 132 pp.

Kruseman G P, de Ridder N A, 1991. Analysis and evaluation of pumping test data, ILRI publication 47, Wageningen.

Kyläkorpi L, 2004. Nature values and site accessibility maps of Forsmark and Simpevarp. SKB R-04-12, Svensk Kärnbränslehantering AB.

Laaksoharju M, Degueldre C, Skårman C, 1995a. Studies of colloids and their importance for repository performance assessment SKB TR-95-24, Svensk Kärnbränslehantering AB.

Laaksoharju M, Smellie J, Nilsson A-C, Skårman C, 1995b. Groundwater sampling and chemical characterisation of the Laxemar deep borehole KLX02. SKB TR 95-05. Svensk Kärnbränslehantering AB.

Laaksoharju M, Wallin B (eds), 1997. Evolution of the groundwater chemistry at the Äspö Hard Rock Laboratory. Proceedings of the second Äspö International Geochemistry Workshop, June 6–7, 1995. SKB International Co-operation Report ISRN SKB-ICR-91/04-SE. ISSN 1104-3210 Stockholm, Sweden.

Laaksoharju M, Skårman C, Skårman E, 1999. Multivariate Mixing and Mass-balance (M3) calculations, a new tool for decoding hydrogeochemical information. Applied Geochemistry Vol. 14, #7, 1999, Elsevier Science Ltd. pp 861–871.

Laaksoharju M (ed), Gimeno M, Smellie J, Tullborg E-L, Gurban I, Auqué L, Gómez J, 2004a. Hydrogeochemical evaluation of the Forsmark site, model version 1.1. SKB R-04-05, Svensk Kärnbränslehantering AB.

Laaksoharju M (ed), Smellie J, Gimeno M, Auqué L, Gómez J, Tullborg E-L, Gurban I, 2004b. Hydrogeochemical evaluation of the Simpevarp area, model version 1.1. SKB R-04-16. Svensk Kärnbränslehantering AB.

Lagerbäck R, Robertsson A-M, 1988. Kettle holes – stratigraphical archives for Weichselian geology and palaeoenvironment in northernmost Sweden. Boreas 17, 439–468.

Lanaro F, 2005a. Rock mechanics characterisation of the rock mass – Empirical approach. Preliminary site description Simpevarp subarea – version 1.2. SKB R-05-20, Svensk Kärnbränslehantering AB.

Lanaro F, 2005b. Rock Mechanics characterisation of borehole KSH01AB, KSH02, KSH03A, KAV01 and KLX02, Simpevarp Site Investigations (in prep), Svensk Kärnbränslehantering AB.

Lanaro F, Fredriksson A, 2005. Rock mechanics characterisation of the rock mass – Summary of primary data. Preliminary site description Simpevarp subarea – version 1.2. SKB R-05-21, Svensk Kärnbränslehantering AB.

Landström O, Tullborg E-L, 1995. Interactions of trace elements with fracture filling minerals from the Äspö Hars Rock laboratory. SKB TR 95-13, Svensk Kärnbränslehantering AB. ISSN 0284-3757. 65 pp.

Landström O, Tullborg E-L, Eriksson G, Sandell Y, 2001. Effects of glacial/post-glacial weathering compared with hydrothermal alteration – implications for matrix diffusion. SKB R-01-37, Svensk Kärnbränslehantering AB. ISSN 1402-3091.

La Pointe P R, Hermanson J, 2005. Statistical model of fractures and deformations zones. Preliminary site description Simpevarp subarea – version 1.2. SKB R-05-28, Svensk Kärnbränslehantering AB.

Larson S Å, Tullborg E-L, 1993. Tectonic regimes in the Baltic Shield during the last 1,200 Ma – A review. SKB TR 94-05, Svensk Kärnbränslehantering AB.

Larson S Å, Tullborg E-L, Cederbom C, Stiberg J-A, 1999. Sveconorwegian and Caledonian foreland basins in the Baltic Shield revealed by fission-track thermochronology. Terra Nova 11, 210–215.

Larsson-McCann S, Karlsson A, Nord M, Sjögren J, Johansson L, Ivarsson M, Kindell S, 2002. Meteorological, hydrological and oceanographical information and data for the site investigation program in the community of Oskarshamn. SKB TR-02-03, Svensk Kärnbränslehantering AB.

LeMaitre R W (ed), 2002. A classification of igneous rocks and glossary of terms: Recommendations of the International Union of Geological Sciences, Subcommission on the Systematics of Igneous Rocks, 2nd edition, Blackwell, Oxford.

Lidmar-Bergström K, 1991. Phanerozoic tectonics in southern Sweden. Zeitschrift für Geomorphologie N.F. 82, 1–16.

Lidmar-Bergström K, Olsson S, Olvmo M, 1997. Paleosurfaces and associated saprolites in southern Sweden. Geological Society 120, 95–124.

Lindborg T (ed), 2005. Description of surface systems, Preliminary site description Simpevarp subarea – version 1.2. SKB R-05-01. Svensk Kärnbränslehantering AB

Lindén A, 1984. Some ice-marginal deposits in the east-central part of the South Swedish Upland. Sveriges Geologiska Undersöknig C 805, 35 pp.

Lindroos H, 2004. The potential for ore, industrial minerals and commercial stones in the Simpevarp area. SKB R-04-72. Svensk Kärnbränslehantering AB.

Ludvigson J-E, Levén J, Jönsson S, 2003. Oskarshamn site investigation. Hydraulic tests and flow logging in borehole HSH03. SKB P-03-56. Svensk Kärnbränslehantering AB.

Ludvigson J-E, Levén J, Källgården J, 2005. Oskarshamn site investigation. Single-hole injection tests in borehole KSH02. SKB P-04-247. Svensk Kärnbränslehantering AB.

Lundin L, Lode E, Stendahl J, 2004. Soils and site types in the Forsmark area. SKB R-04-08, Svensk Kärnbränslehantering AB.

Lundqvist J, 1985. Deep-weathering in Sweden. Fennia 163, 287–292.

Lundqvist J, 1992. Glacial stratigraphy in Sweden. Geological Survey of Finland Special paper 15. 43–59.

Lundqvist J, Wohlfarth B, 2001. Timing and east-west correlation of south Swedish ice marginal lines during the Late Weichselian. Quaternary Science Reviews 20, 1127–1148.

Luukkonen A, 2001. Groundwaters mixing and geochemical reactions. An inverse-modelling approach. In: A Luukkonen and E Kattilakoski (eds), Äspö hard-rock laboratory. Groundwater flow, mixing and geochemical reactions at Äspö HRL. Task 5. Äspö Task Force on groundwater flow and transport of solutes. SKB IPR-02-041, Svensk Kärnbränslehantering AB.

Löfgren A, Lindborg T, 2003. A descriptive ecosystem model – a strategy for model development during site investigations. SKB R-03-06. Svensk Kärnbränslehantering AB.

Löfgren M, Neretnieks I, 2005. Oskarshamn site investigation. Formation factor logging in-situ and in the laboratory by electrical methods in KSH01A and KSH02. Measurements and evaluation of methodology. SKB P-05-27, Svensk Kärnbränslehantering AB.

Maddock R H, Hailwood E A, Rhodes E J, Muir Wood R, 1993. Direct fault dating trials at the Äspö Hard Rock Laboratory. SKB TR 93-24, Svensk Kärnbränslehantering AB.

Majdi H, 2001. Changes in fine root production and longevity in relation to water and nutrient availability in a Norway spruce forest stand in northern Sweden. Tree Physiology 21:1057–1061.

Makurat A, Løset F, Hagen A W, Tunbridge L, Kveldsvik V, Grimstad E, 2002. Äspö HRL: A Descriptive Rock Mechanics Model for the 380–500 m level. SKB R-02-11. Svensk Kärnbränslehantering AB.

Mansfeld J, 1996. Geological, geochemical and geochronological evidence for a new Paleoproterozoic terrane in southeastern Sweden. Precambrian Research 77, 91–103.

Markström I, Stanfors R, Juhlin C, 2001. Äspölaboratoriet – RVS-modellering, Ävrö – Slutrapport. SKB R-01-06. Svensk Kärnbränslehantering AB (in Swedish).

Mattsson H, Triumf C-A, Wahlgren C-H, 2002. Prediktering av förekomst av finkorniga granitgångar i Simpevarpsområdet. SKB P-02-05. Svensk Kärnbränslehantering AB (in Swedish).

Mattsson H, Thunehed H, Triumf C-A, 2003. Oskarshamn site investigation – Compilation of petrophysical data from rock samples and in situ gamma-ray spectrometry measurements. SKB P-03-97, Svensk Kärnbränslehantering AB.

Mattsson H, Thunehed H, 2004. Interpretation of geophysical borehole data from KSH01A, KSH01B, KSH02 (0–100 m), HSH01, HSH02 and HSH03, and compilation of petrophysical data from KSH01A and KSH01B. SKB P-04-28, Svensk Kärnbränslehantering AB.

Mattsson H, Stanfors R, Wahlgren C-H, Stenberg L, Hultgren P, 2004a. Oskarshamn site investigation. Geological single-hole interpretation of KSH01A, KSH01B, HSH01, HSH02 and HSH03. SKB P-04-32. Svensk Kärnbränslehantering AB.

Mattsson H, Stanfors R, Wahlgren C-H, Carlsten S, Hultgren P, 2004b. Oskarshamn site investigation. Geological single-hole interpretation of KSH02 and KAV01. SKB P-04-133. Svensk Kärnbränslehantering AB.

Mazurek M, Bossart P, Eliasson T, 1997. Classification and characterization of water-conducting features at Äspö: Results of investigations on the outcrop scale. SKB ICR 97-01, Svensk Kärnbränslehantering AB.

Michard G, 1980. Contrôle des concentrations d'éléments dissous dans les eaux thermales et géothermales. J. fr. Hydrol. 11, 7–16.

Michard G, Sanjuan B, Criaud A, Fouillac C, Pentcheva E, Petrov P S, Alexieva R, 1986. Equilibria and geothermometry in hot alkaline waters from granites of SW Bulgaria. Geochem. J. 20, 159–171.

Michard G, 1987. Controls of the chemical composition of geothermal waters. Chemical Transport in Metasomatic Processes, 323–353.

Middlemost E A K, 1994. Naming materials in the magma/igneous rock system. Earth-Science Reviews 37, 215–224.

Miliander S, Punakivi M, Kyläkorpi L, Rydgren B, 2004. Simpevarp site description: Human population and human activities. SKB R-04-11, Svensk Kärnbränslehantering AB.

Milnes A G, Gee D G, 1992. Bedrock stability in southeastern Sweden. Evidence from fracturing in the ordovician limestones of northern Öland. SKB TR 92-23, Svensk Kärnbränslehantering AB.

Milnes A G, Gee D G, Lund C-E, 1998. Crustal structure and regional tectonics of SE Sweden and the Baltic Sea. SKB TR 98-21, Svensk Kärnbränslehantering AB.

Molinero J, Samper J, Zhang G, Yang C B, 2004. Biogeochemical reactive transport model of the Redox Zone Experiment of the Äspö Hard Rock Laboratory in Sweden. Nuclear Technology, 148, 151–165.

Morén L, Påsse T, 2001. Climate and shoreline in Sweden during Weichsel and the next 150,000 years. SKB TR-01-19, Svensk Kärnbränslehantering AB. 67 pp.

Moye D G, 1967. Diamond drilling for foundation exploration. Civil Eng. Trans., Inst. Eng. Australia, p 95–100.

Muir-Wood R, 1993. A review of the seismotectonics of Sweden. SKB TR 93-13, Svensk Kärnbränslehantering AB.

Munier R, 1989. Brittle tectonics on Äspö, SE Sweden. SKB PR 25-89-15, Svensk Kärnbränslehantering AB.

Munier R, 1993. Segmentation, fragmentation and jostling of the Baltic shield with time. Thesis, Acta Universitatus Upsaliensis 37.

Munier R, 1995. Studies of geological structures at Äspö. Comprehensive summary of results. SKB PR 25-95-21, Svensk Kärnbränslehantering AB.

Munier R, Hermanson J, 2001. Metodik för geometrisk modellering. Presentation och administration av platsbeskrivande modeller. SKB R-01-15. Svensk Kärnbränslehantering AB (in Swedish).

Munier R, Follin S, Rhén I, Gustafson G, Push R, 2001. Projekt JADE, Geovetenskapliga studier, SKB R-01-32, Svensk Kärnbränslehantering AB (in Swedish).

Munier R, Stenberg L, Stanfors R, Milnes A G, Hermanson J, Triumf C-A, 2003. Geological Site Descriptive Model. A strategy for the model development during site investigations. SKB R-03-07. Svensk Kärnbränslehantering AB.

Munier R, 2004. Statistical analysis of fracture data, adapted for modelling Discrete Fracture Networks – Version 2. SKB R-04-66. Svensk Kärnbränslehantering AB.

Mörner N-A, 1989. Postglacial faults and fractures on Äspö. SKB PR 25-89-24, Svensk Kärnbränslehantering AB.

Naturvårdsverket, 1999. Bedömning för miljökvalitet. Report 4915. 140 pp, (in Swedish).

Neff J C, Ashner G P, 2001. Dissolved organic carbon in terrestrial ecosystems. Ecosystems 4: 29–48.

Nielsen U T, Ringgaard J, 2003. Simpevarp site investigation. Geophysical borehole logging in borehole KSH01A, KSH01B and part of KSH02. SKB P-03-16. Svensk Kärnbränslehantering AB.

Nilsson P, Gustafsson C, 2003. Simpevarp site investigation – Geophysical, radar and BIPS logging in borehole KSH01A, HSH01, HSH02 and HSH03. SKB P-03-15. Svensk Kärnbränslehantering AB.

Nisca D, 1987. Aerogeophysical interpretation. Bedrock and tectonic analysis. SKB PR 25-87-04. Svensk Kärnbränslehantering AB.

Nitare J, Norén M, 1992. Nyckelbiotoper kartläggs i nytt projekt vid Skogsstyrelsen. Svensk botanisk tidskrift volym 86: 219–226 (in Swedish).

Nordenskjöld C E, 1944. Morfologiska studier inom övergångsområdet mellan Kalmarslätten och Tjust. Medd. Lunds Geog. Inst. Avd. VIII, (in Swedish).

Nordqvist R, Gustavsson E, 2002. Single-well injection-withdrawal tests (SWIW). Literature review and scoping calculations for homogeneous crystalline bedrock conditions. SKB R-02-34, Svensk Kärnbränslehantering AB.

Nordstrom D K, Puigdomenech I, 1986. Redox chemistry of deep ground water in Sweden. SKB TR-86-03. Svensk Kärnbränslehantering AB.

Näslund J O, Rodhe L, Fastook J L, Holmlund P, 2003. New ways of studying ice sheet flow directions and glacial erosion by computer modelling-examples from Fennoscandia. Quaternary Sciences Reviews 22, 245–258.

Ohlsson Y, Neretnieks I, 1997. Diffusion data in granite – Recommended values. SKB TR-97-20, Svensk Kärnbränslehantering AB.

Olofsson I, Fredriksson A, 2005. Strategy for a numerical Rock Mechanics Site Descriptive Model. Further development of the theoretical approach. Svensk Kärnbränslehantering AB (in prep).

Olsen L, Mejdahl V, Selvik S, 1996. Middle and Late Pleistocene stratigraphy, Finnmak, north Norway. NGU Bulletin 429, 111 p.

Parkhurst D L, Appelo C A J, 1999. User's Guide to PHREEQC (Version 2), a computer program for speciation, batch-reaction, one-dimensional transport, and inverse geochemical calculations. U.S. Geological Survey Water-Resources Investigations Report 99-4259, 312 p.

Pitkänen P, Luukkonen A, Ruotsalainen P, Leino-Forsman H, Vuorinen U, 1998. Geochemical modelling of groundwater evolution and residence time at the Kivetty site. POSIVA Report 98-07, Helsinki, Finland, 139 p.

Pitkänen P, Luukkonen A, Ruotsalainen P, Leino-Forsman H, Vuorinen U, 1999. Geochemical modelling of groundwater evolution and residence time at the Olkilouto site. POSIVA Report 98-10, Helsinki, Finland, 184 p.

Pitkänen P, Partamies S, Luukkonen A, 2004. Hydrogeochemical interpretation of baseline groundwater conditions at the Olkiluoto Site. (Technical Report POSIVA 2003-07), POSIVA, Helsinki, Finland, 159 p.

Poteri A, Billaux D, Cvetkovic V, Dershowitz B, Gómez-Hernández J-J, Hautojärvi A, Holton D, Medina A, Winberg A, 2002. TRUE Block Scale Project. Final Report – 3. Modelling of flow and transport. SKB TR-02-15, Svensk Kärnbränslehantering AB.

Puigdomenech I (ed), 2001. Hydrochemical stability of groundwaters sourrunding a spent nuclear fuel repository in a 100,000 year perspective. SKB TR-01-28, Svensk Kärnbränslehantering AB, 83 p.

Påsse T, 1997. A mathematical model of past, present and future shore level displacement in Fennoscandia. SKB TR 97-28, Svensk Kärnbränslehantering AB, 55 pp.

Påsse T, 2001. An empirical model of glacio-isostatic movements and shore-level displacement in Fennoscandia. SKB R-01-41, Svensk Kärnbränslehantering AB, 59 pp.

Pöllänen J, Sokolnicki M, Rouhiainen P, 2004. Forsmark site investigation – Difference flow logging in borehole KFM05A. P-04-191. Svensk Kärnbränslehantering AB.

Rahm N, Enachescu C, 2004a. Hydraulic injection tests in borehole KSH01A, 2003/2004, Simpevarp, SKB P-04-289, Svensk Kärnbränslehantering AB.

Rahm N, Enachescu C, 2004b. Hydraulic injection tests in borehole KLX02, 2003, Laxemar. SKB P-04-288. Svensk Kärnbränslehantering AB.

Rahm N, Enachescu C, 2004c. Hydraulic injection tests in borehole KSH03, 2004, Simpevarp. SKB P-04-290, Svensk Kärnbränslehantering AB.

Rhén I, Bäckblom G, Gustafson G, Stanfors R, Wikberg P, 1997a. Äspö HRL – Geoscientific evaluation 1997/2. Results from pre-investigations and detailed characterization. Summary Report. SKB TR-97-03. Svensk Kärnbränslehantering AB.

Rhén I, Gustafson G, Wikberg P, 1997b. Äspö HRL – Geoscientific evaluation 1997/4. Results from pre-investigations and detailed site characterization. Comparisons of predictions and observations. Hydrogeology, groundwater chemistry and transport of solutes. SKB TR-97-05. Svensk Kärnbränslehantering AB.

Rhén I, Gustafson G, Wikberg P, 1997c. Äspö HRL – Geoscientific evaluation 1997/5. Models based on site characterization 1986–1995. SKB TR-97-06. Svensk Kärnbränslehantering AB.

Rhén I, Forsmark T, 2001. Äspö Hard Rock Laboratory, Prototype repository, Hydrogeology, Summary report of investigations before the operation phase. SKB IPR-01-65, Svensk Kärnbränslehantering AB.

Rhén I, Smellie J (eds), 2003. Task force on modelling of groundwater flow and transport of solutes. Task 5 summary report. SKB TR-03-01. Svensk Kärnbränslehantering AB.

Rhén I, Follin S, Hermanson J, 2003. Hydrological Site Descriptive Model – a strategy for its development during site investigations. SKB R-03-08. Svensk Kärnbränslehantering AB.

Ringberg B, Hang T, Kristiansson J, 2002. Local clay-varve chronology in the Karlskrona-Hultsfred region, southeast Sweden. GFF 124, 79–86.

Risberg J, 2002. Holocene sediment accumulation in the Äspö area. SKB R-02-47, Svensk Kärnbränslehantering AB. 37 pp.

Robertsson A-M, Svedlund J-O, Andrén T, Sundh M, 1997. Pleistocene stratigraphy in the Dellen region, central Sweden. Boreas 26, 237–260.

Rodhe A, 1987a. Depositional environment and lithostratigraphy of the middle Proterozoic Almesåkra Group, southern Sweden. Sveriges geologiska undersökning Ca 69.

Rouhiainen P, 2000. Äspö Hard Rock Laboratory – Difference flow measurements in borehole KLX02 at Laxemar. SKB IPR-01-06. Svensk Kärnbränslehantering AB.

Rouhiainen P, Pöllänen J, 2003a. Oskarshamn site investigation – Difference flow measurements in borehole KSH01A at Simpevarp. SKB P-03-70. Svensk Kärnbränslehantering AB.

Rouhiainen P, Pöllänen J, 2003b. Oskarshamn site investigation – Difference flow measurements in borehole KSH02 at Simpevarp. SKB P-03-110. Svensk Kärnbränslehantering AB.

Rouhiainen P, Pöllänen J, 2004. Oskarshamn site investigation – Difference flow measurements in borehole KAV01 at Ävrö. SKB P-04-213. Svensk Kärnbränslehantering AB.

Rudmark L, 2000. Beskrivning till jordartskartan 5G Oskarshamn NO. SGU Ae 94. 64 pp (in Swedish).

Rudmark L, 2004. Oskarshamn site investigation, Investigation of Quaternary deposits at Simpevarp peninsula and the islands of Ävrö and Hålö. SKB P-04-22, Svensk Kärnbränslehantering AB, 19 pp.

Rühling Å, 1997. Floran i Oskarshamns kommun. Svensk Botanisk Förening, Lund (in Swedish).

Rydström H, Gereben L, 1989. Regional geological study. Seismic refraction survey. SKB PR 25-89-23, Svensk Kärnbränslehantering AB.

Rønning H J S, Kihle O, Mogaard J O, Walker P, 2003. Simpevarp site investigation – Helicopter borne geophysics at Simpevarp, Oskarshamn, Sweden. SKB P-03-25. Svensk Kärnbränslehantering AB.

Röshoff K, Cosgrove J, 2002. Sedimentary dykes in the Oskarshamn-Västervik area. A study of the mechanism of formation. SKB R-02-37. Svensk Kärnbränslehantering AB.

Samper J, Delgado J, Juncosa R, Montenegro L, 2000. CORE2D v 2.0: A Code for non-isothermal water flow and reactive solute transport. User's manual.ENRESA Technical report 06/2000.

SBF, 1999. Nyckelbiotopsinventeringen 1993–1998 – Slutrapport. Swedish Board of Forestry, Jönköping (in Swedish).

SDE, 2004. SKB GIS Layer (SDEADM.GV_SM_GEO_2028 = XSM_Linked_lineament_line.shp).

Serafim J L, Pereira J P, 1983. Consideration of the geomechanics classification of Bieniawski, Proc. Int. Symp. Eng. Geol. & Underground Constr. p 1133–1144.

Shackleton N J, Berger A, Peltier W R, 1990. An alternative astronomical calibration of the lower Pleistocene timescale based on ODP Site 677. Transactions of the Royal Society of Edinburgh: Earth Sciences 81, 251–261.

Shackleton N J, 1997. The deep-sea sediment record and the Pliocene-Pleistocene boundary. Quaternary International 40, 33–35.

Šibrava V, 1992. Should the Pliocene-Pleistocene boundary be lowered? Sveriges Geologiska Undersökning, Ca 81, 327–332.

Sjöberg J, 2004. Oskarshamn site investigation – Overcoring rock stress measurements in borehole KSH02. SKB P-04-23. Svensk Kärnbränslehantering AB.

SKB, 1990. Granskning av Nils-Axels Mörners arbete avseende postglaciala strukturer på Äspö. SKB AR 90-18, Svensk Kärnbränslehantering AB (in Swedish).

SKB, 2000a. Förstudie Oskarshamn – Slutrapport. Svensk Kärnbränslehantering AB (in Swedish).

SKB, 2000b. Geoscientific programme for investigation and evaluation of sites for the deep repository. SKB TR-00-20. Svensk Kärnbränslehantering AB.

SKB, 2001a. Site investigations – Investigation methods and general execution programme. SKB TR-01-29. Svensk Kärnbränslehantering AB.

SKB, 2001b. Geovetenskapligt program för platsundersökning vid Simpevarp. SKB R-01-44. Svensk Kärnbränslehantering AB (in Swedish).

SKB, 2002a. Preliminary safety evaluation, based on initial site investigation data. Planning document. SKB TR-02-28, Svensk Kärnbränslehantering AB.

SKB, 2002b. Simpevarp – site descriptive model version 0. SKB R-02-35, Svensk Kärnbränslehantering AB.

SKB, 2002c. Execution programme for the initial site investigations at Simpevarp. SKB P-02-06. Svensk Kärnbränslehantering AB.

SKB, 2003a. Planning report for the safety assessment SR-Can, SKB TR-03-08, Svensk Kärnbränslehantering AB.

SKB, 2003b. Prioritering av områden för platsundersökningen i Oskarshamn. SKB R-03-12. Svensk Kärnbränslehantering AB (in Swedish).

SKB, 2003c. Planering för fortsatt kärnborrning, våren 2003. Platsundersökning Oskarshamn. SKB P-03-61. Svensk Kärnbränslehantering AB (in Swedish).

SKB, 2004a. Preliminary site description, Forsmark area – version 1.1. SKB R-04-15, Svensk Kärnbränslehantering AB.

SKB, 2004b. Preliminary site description Simpevarp area – version 1.1. SKB R-04-25. Svensk Kärnbränslehantering AB.

SKB, 2004c. Hydrogeochemical evaluation for Simpevarp model version 1.2. Preliminary site description of the Simpevarp area. SKB R-04-74, Svensk Kärnbränslehantering AB.

SKB, 2004d. Interim main report of the safety assessment SR-Can. SKB TR-04-11. Svensk Kärnbränslehantering AB.

SKB, 2004e. Program för fortsatta undersökningar av berggrund, mark och vatten. Platsundersökning i Oskarshamn. SKB P-04-300, Svensk Kärnbränslehantering AB (in Swedish).

SKB, 2005. Description of surface systems – Simpevarp 1.2. SKB R-05-01, Svensk Kärnbränslehantering AB

SKB, 2005a. Deep repository. Underground design Simpevarp, step D1 (in prep). Svensk Kärnbränslehantering AB.

SKB, 2005b. Preliminary safety evaluation for the Simpevarp subarea Based on data and site descriptions after the initial site investigation stage. SKB TR-05-12. Svensk Kärnbränslehantering AB.

Slunga R, Norrman P, Glans A-C, 1984. Baltic shield seismicity, the results of a regional network. Geophysical research letters 11, 1247–1250.

Slunga R, 1989. Analysis of the earthquake mechanisms in the Norrbotten area. In Bäckblom and Stanfors (eds), Interdisciplinary study of post-glacial faulting in the Lansjärv area northern Sweden. 1986–1988. SKB TR 89-31, Svensk Kärnbränslehantering AB.

Slunga R, Nordgren L, 1990. Earthquake measurements in southern Sweden APR 1 1987–NOV 30 1988. SKB AR 90-19, Svensk Kärnbränslehantering AB.

Smellie J A T, Larsson N-Å, Wikberg P, Carlsson L, 1985. Hydrochemical investigations in crystalline bedrock in relation to existing hydraulic conditions: Experience from the SKB test-sites in Sweden. SKB TR-85-11, Svensk Kärnbränslehantering AB.

Smellie J A T, Wikberg P, 1991. Hydrochemical investigations at Finnsjön, Sweden. J. Hydrol. 126, 129–158.

Smellie J, Laaksoharju M, 1992. The Äspö hard rock laboratory: final evaluation of the hydrogeochemical pre-investigations in relation to existing geologic and hydraulic conditions. SKB TR 92-31, Svensk Kärnbränslehantering AB, 239 p.

Smellie J, Laaksoharju M, Tullborg E-L, 2002. Hydrogeochemical site descriptive model – a strategy for the model development during site investigations. SKB R-02-49. Svensk Kärnbränslehantering AB.

SNV, 1984. Våtmarksinventering inom fastlandsdelen av Kalmar Län: Del 1 Allmän beskrivning och katalog över särskilt värdefulla objekt. Statens Naturvårdsverk, Solna, Rapport PM 1787 (in Swedish).

Stanfors R, Erlström M, 1995. SKB Palaeohydrogeological programme. Extended geological models of the Äspö area. SKB AR 95-20, Svensk Kärnbränslehantering AB.

Stanfors R, Erlström M, Markström I, 1997. Äspö HRL – Geoscientific evaluation 1997/1. Overview of site characterization 1986–1995. SKB TR-97-02, Svensk Kärnbränslehantering AB.

Staub I, Andersson C, Magnor B, 2004. Äspö Hard Rock Laboratory – Äspö Pillar Stability Experiment, Geology and mechanical properties of the rock mass in TASQ. SKB R-04-01. Svensk Kärnbränslehantering AB.

Stenberg L, Sehlstedt S, 1989. Geophysical profile measurements on interpreted regional aero-magnetic lineaments in the Simpevarp area. SKB PR 25-89-13, Svensk Kärnbränslehantering AB.

Stephansson O, Dahlström L-O, Bergström K, Sarkka P, Vitinen A, Myrvang A, Fjeld O, Hansen T H, 1987. Fennoscandian Rock Stress Database – FRSDB. Research report TULEA 1987:06, Luleå University of Technology, Luleå.

Stephens M B, Wahlgren C-H, Weihed P, 1994. Geological Map of Sweden, scale 1:3 000 000. SGU series Ba 52, Sveriges Geologiska Undersökning.

Stephens M B, Wahlgren C-H, 1996. Post-1.85 Ga tectonic evolution of the Svecokarelian orogen with special reference to central and SE Sweden. GFF 118, Jubilee Issue, A26–27.

Stigsson M, Follin S, Andersson J, 1999. On the simulation of variable density flow at SFR, Sweden. SKB R-99-08, Svensk Kärnbränslehantering AB.

Streckeisen A, 1976. To each plutonic rock its proper name. Earth Science Reviews 12, 1–33.

Streckeisen A, 1978. IUGS Subcommision on the Systematics of Igneous Rocks. Classification and Nomenclature of Volcanic Rocks, Lamprophyres, Carbonatites and Melilitic Rocks. Recommendations and suggestions. Neues Jahrbuch für Mineralogie Abhandlungen 143, 1–14.

Sturesson E, 2003. Platsundersökning Oskarshamn – Nyckelbiotopsinventering i Simpevarpsområdet. SKB P-03-78, Svensk Kärnbränslehantering AB (in Swedish).

Sultan L, Claesson S, Plink-Björklund P, Björklund L, 2004. Proterozoic and Archaean detrital zircon ages from the Palaeoproterozoic Västervik Basin, southern Fennoscandian Shield. GFF 126, 39.

Sundberg J, 1988. Thermal properties of soils and rocks, Publ. A 57 Dissertation, Doctoral thesis, Geologiska institutionen, Chalmers University of Technology and University of Göteborg.

Sundberg J, Gabrielsson A, 1999. Laboratory and field measurements of thermal properties of the rock in the prototype repository at Äspö HRL. SKB IPR-99-17, Svensk Kärnbränslehantering AB.

Sundberg J, 2002. Determination of thermal properties at Äspö HRL, Comparison and evaluation of methods and methodologies for borehole KA2599G01. SKB R-02-27, Svensk Kärnbränslehantering AB.

Sundberg J, Ländell M, 2002. Determination of linear thermal expansion. Samples from borehole KA 2599 G01. Äspö HRL. SKB IPR-02-63, Svensk Kärnbränslehantering AB.

Sundberg J, 2003a. Thermal Site Descriptive Model, A Strategy for the Model Development during Site Investigations. SKB R-03-10, Svensk Kärnbränslehantering AB.

Sundberg J, 2003b. Thermal Properties at Äspö HRL, Analysis of Distribution and Scale Factors. SKB R-03-17, Svensk Kärnbränslehantering AB.

Sundberg I, Ericsson U, Engdahl A, Svensson J-E, 2004. Phytoplankton and zooplankton. Results from sampling in the Simpevarp area 2003–2004. Oskarshamn site investigation, SKB P-04-253, Svensk Kärnbränslehantering AB.

Sundberg J, Back P-E, Bengtsson A, 2005a. Uncertainty analysis of thermal properties at Äspö HRL prototype repository. Svensk Kärnbränslehantering AB, Stockholm. Report in progress.

Sundberg J, Back P, Bengtsson A, 2005b. Thermal modelling. Preliminary site description Simpevarp subarea – version 1.2. SKB R-05-24. Svensk Kärnbränslehantering AB.

Svantesson S, 1999. Beskrivning till jordartskartan 7G Västervik SO/ 7H Loftahammar SV. SGU Ae 124. 109 pp (in Swedish).

Svedmark E, 1904. Beskrifning till kartbladet Oskarshamn. SGU Ac 5, 85 pp (in Swedish).

Svensk Viltförvaltning AB, 2003. Älgstammens ålderssammansättning och reproduktion i Ankarsrum, mars 2003 (in Swedish).

Svensson N-O, 1989. Late Weichselian and early Holocene shore displacement in the central Baltic, based on stratigraphical and morphological records from eastern Småland and Gotland, Sweden. LUNDQUA 25, 181 pp.

Svensson U, 1996. SKB Palaeohydrogeological programme. Regional groundwater flow due to advancing and retreating glacier-scoping calculations. In: SKB Project Report U 96-35, Svensk Kärnbränslehantering AB.

Svensson T, 2003. Oskarshamn site investigation, Pumping tests and flow logging in boreholes KSH03 and HSH02. P-04-212. Svensk Kärnbränslehantering AB

Svensson U, 2004. DarcyTools, Version 2.1. Verification and validation. SKB R-04-21, Svensk Kärnbränslehantering AB.

Svensson U, Ferry M, 2004. DarcyTools, Version 2.1. User's guide. SKB R-04-20, Svensk Kärnbränslehantering AB.

Svensson U, Kuylenstierna H-O, Ferry M, 2004. DarcyTools, Version 2.1. Concepts, methods, equations and demo simulations. SKB R-04-19, Svensk Kärnbränslehantering AB.

Söderlund U, Patchett P J, Isachsen C, Vervoort J, Bylund G, 2004. Baddeleyite U-Pb dates and Hf-Nd isotope compositions of mafic dyke swarms in Sweden and Finland. GFF 126, 38.

Söderlund P, Juez-Larre J, Dunai T, Page L, in prep. Apatite (U-Th)-He-dating of drill-core samples from Oskarshamn, southeast Sweden.

Talbot C, Munier R, 1989. Faults and fracture zones in Äspö. SKB PR 25-89-11, Svensk Kärnbränslehantering AB.

Talbot C, Ramberg H, 1990. Some clarification of the tectonics of Äspö and its surroundings. SKB PR 25-90-15, Svensk Kärnbränslehantering AB.

Tirén S A, Beckholmen M, Isaksson H, 1987. Structural analysis of digital terrain models, Simpevarp area, southeastern Sweden. Method study EBBA II. SKB PR 25-87-21, Svensk Kärnbränslehantering AB.

Tobiasson S, 2003. Tolkning av undervattensfilm från Forsmark och Simpevarp. SKB P-03-68. Svensk Kärnbränslehantering AB (in Swedish).

Triumf C-A, 2003a. Oskarshamn site investigation – Identification of lineaments in the Simpevarp area by the interpretation of topographical data. SKB P-03-99. Svensk Kärnbränslehantering AB.

Triumf C-A, 2003b. Oskarshamn site investigation. Geophysical measurements for the siting of a deep borehole at Ävrö and for investigations west of CLAB. SKB P-03-66. Svensk Kärnbränslehantering AB.

Triumf C-A, Thunehed H, Kero L, Persson L, 2003. Oskarshamn site investigation. Interpretation of airborne geophysical survey data. Helicopter borne survey data of gamma ray spectrometry, magnetics and EM from 2002 and fixed wing airborne survey data of the VLF-field from 1986. SKB P-03-100. Svensk Kärnbränslehantering AB.

Triumf C-A, 2004. Oskarshamn site investigation. Joint interpretation of lineaments. SKB P-04-49. Svensk Kärnbränslehantering AB.

Trotignon L, Beaucaire C, Louvat D, Aranyossy J F, 1997. Equilibrium geochemical modelling of Äspö groundwaters: a sensitivity study to model parameters. In: Laaksoharju M and Wallin B (eds) Evolution of the groundwater chemistry at the Äspö Hard Rock Laboratory. Report SKB 97-04, Svensk Kärnbränslehantering AB.

Trotignon L, Beaucaire C, Louvat D, Aranyossy J F, 1999. Equilibrium geochemical modelling of Äspö groundwaters: a sensitivity study of thermodynamic equilibrium constants. Appl. Geochem. 14, 907–916.

Tullborg E-L, Larson S Å, 1984. $\delta^{18}O$ and $\delta^{13}C$ for limestones, calcite fissure infillings and calcite precipitates from Sweden. Geologiska föreningens i Stockholm förhandlingar 106(2).

Tullborg E-L, Larson S Å, Björklund L, Samuelsson L, Stigh J, 1995. Thermal evidence of Caledonide foreland, molasse sedimentation in Fennoscandia. SKB TR-95-18, Svensk Kärnbränslehantering AB.

Tullborg E-L, Larson S Å, Stiberg J-A, 1996. Subsidence and uplift of the present land surface in the southeastern part of the Fennoscandian Shield. GFF 118, 126–128.

Tullborg E-L, Byegård J, Gustavsson E, 2005. Retardation model for the Simpevarp 1.2 site description (in prep), Svensk Kärnbränslehantering AB.

Ukkonen P, Lunkka J P, Jungner H, Donner J, 1999. New radiocarbon dates from Finnish mammoths indicating large ice-free areas in Fennoscandia during the Middle Weichselian. Journal of Quaternary Science 14, 711–714.

Vilks P, Miller H, Doern D, 1991. Natural colloids and suspended particles in Whiteshell Research area, Manitoba, Canada, and their potential effect on radiocolloid formation. Applied Geochemistry 8, 565–574.

Vogel J C, 1970. Carbon-14 dating of Groundwater. In: Isotope Hydrology-1970, IAEA Symposium 129, March 1970, Vienna. 225–239.

Vogt K A, Grier C C, Meier C E, Edmonds R L, 1982. Mycorrhizal role in net primary production and nutrient cycling in Abies amabilis ecosystems in western Washington. Ecology 63(2): 370–380.

Wacker P, 2003. Oskarshamn site investigation. Hydrochemical logging in KSH01A. SKB P-03-87, Svensk Kärnbränslehantering AB.

Wacker P, Berg C, Bergelin A, 2004. Complete hydrochemical characterisation of KSH01A (in prep), Svensk Kärnbränslehantering AB.

Wahlgren C-H, Persson L, Danielsson P, Berglund J, Triumf C-A, Mattsson H, Thunehed H, 2003. Geologiskt underlag för val av prioriterad plats inom området väster om Simpevarp. Delrapport 1–4. SKB P-03-06. Svensk Kärnbränslehantering AB (in Swedish).

Wahlgren C-H, 2004. SGU (Geological Survey of Sweden), Personal communication.

Wahlgren C-H, Ahl M, Sandahl K-A, Berglund J, Petersson J, Ekström M, Persson P-O, 2004. Oskarshamn site investigation. Bedrock mapping 2003 – Simpevarp subarea. Outcrop data, fracture data, modal and geochemical classification of rock types, bedrock map, radiometric dating. SKB P-04-102. Svensk Kärnbränslehantering AB.

Werner K, Bosson E, Berglund S, 2005. Simpevarp 1.2. Background report for climate, surface hydrology and near-surface hydrogeology. SKB R-05-04. Svensk Kärnbränslehantering AB.

Westman P, Wastegård S, Schoning K, Gustafsson B, 1999. Salinity change in the Baltic Sea during the last 8,500 years: evidence causes and models. SKB TR 99-38, Svensk Kärnbränslehantering AB. 52 pp.

Widestrand H, Byegård J, Ohlsson Y, Tullborg E-L, 2003. Strategy for the use of laboratory methods in the site investigations programme for the transport properties of the rock. SKB R-03-20, Svensk Kärnbränslehantering AB.

Wikberg P, 1998. Äspö Task Force on modelling of groundwater flow and transport of solutes. SKB progress report HRL-98-07, Svensk Kärnbränslehantering AB.

Wiklund S, 2002. Digitala ortofoton och höjdmodeller. Redovisning av metodik för platsundersökningsområdena Oskarshamn och Forsmark samt förstudieområdet Tierp Norra. SKB P-02-02. Svensk Kärnbränslehantering AB (in Swedish).

Wikman H, Kornfält K-A, 1995. Updating of a lithological model of the bedrock of the Äspö area. SKB PR 25-95-04, Svensk Kärnbränslehantering AB.

Winberg A, Andersson P, Hermansson J, Byegård J, Cvetkovic V, Birgersson L, 2000. Äspö Hard Rock Laboratory. Final report of the first stage of the Tracer Retention Understanding Experiments, SKB TR-00-07. Svensk Kärnbränslehantering AB. ISSN 1404-0344.

Wu P, Johnston P, Lambeck K, 1999. Postglacial rebound and fault instability in Fennoscandia. Geophysical Journal International 139, 657–670.

Xu S, Wörman A, 1998. Statistical patterns of geochemistry in crystalline rock and effect of sorption kinetics on radionuclide migration. SKI Technical Report 98:41. Statens kärnkraftinspektion.

Åberg G, 1978. Precambrian geochronology of south-eastern Sweden. Geologiska Föreningens i Stockholm Förhandlingar 100, 125–154.

Åhäll K-I, 2001. Åldersbestämning av svårdaterade bergarter i sydöstra Sverige. SKB R-01-60. Svensk Kärnbränslehantering AB (in Swedish).

Åhäll K-I, Connelly J, Brewer T, 2002. Transitioning from Svecofennian to Transscandinavian Igneous Belt (TIB) magmatism in SE Sweden: Implications from the 1.82 Ga Eksjö tonalite. GFF 124, 217–224.

Åkesson U, 2004a. Drill hole KSH01A Extensometer measurements of the coefficient of thermal expansion of rock. SKB P-04-59, Svensk Kärnbränslehantering AB.

Åkesson U, 2004b. Drill hole KSH02 Extensometer measurements of the coefficient of thermal expansion of rock. SKB P-04-60, Svensk Kärnbränslehantering AB.

Åkesson U, 2004c. Drill hole KAV01 Extensometer measurements of the coefficient of thermal expansion of rock. SKB P-04-61, Svensk Kärnbränslehantering AB.

Appendix 1

Nomenclature of rock types (in English and Swedish), including associated rock codes applied in the site investigation at Oskarshamn

Nomenclature of rock types applied in the site investigation at Oskarshamn			Colour code		
Rock code	**Rock nomenclature** *(names within parenthesis refer to nomenclature used at the Äspö Hard Rock Laboratory and related studies)*	**Descriptive nomenclature of rock type**	**R**	**G**	**B**
501027	Dolerite Diabas	Dolerite Diabas	152	83	161
531058	Fine-grained Götemar granite Finkornig Götemargranit	Granite, fine- to medium-grained, (”Götemar granite”) Granit, fin- till medelkornig, (”Götemargranit”)	255	0	0
521058	Coarse-grained Götemar granite Grovkornig Götemargranit	Granite, coarse-grained, (”Götemar granite”) Granit, grovkornig, (”Götemargranit”)	200	24	56
511058	Fine-grained granite Finkornig granit	Granite, fine- to medium-grained Granit, fin- till medelkornig	235	122	179
501061	Pegmatite Pegmatit	Pegmatite Pegmatit	241	157	86
501058	Granite Granit	Granite, medium- to coarse-grained Granit, medel- till grovkornig	237	113	116
501044	Ävrö granite *(Småland-Ävrö granite)* Ävrögranit *(Småland-Ävrögranit)*	Granite to quartz monzodiorite, generally porphyritic Granit till kvartsmonzodiorit, vanligtvis porfyrisk	246	162	168
501036	Quartz monzodiorite *(Äspö diorite, tonalite)* Kvartsmonzodiorit *(Äspödiorit, tonalit)*	Quartz monzonite to monzodiorite, equigranular to weakly porphyritic Kvartsmonzonit till monzodiorit, jämnkornig till glest porfyrisk	250	199	193
501033	Diorite/gabbro Diorit/Gabbro	Diorite to gabbro Diorit till gabbro	193	221	53
501030	Fine-grained dioritoid *(Metavolcanite, volcanite)* Finkornig dioritoid *(Metavulkanit, vulkanit)*	Intermediate magmatic rock Intermediär magmatisk bergart	168	216	183
505102	Fine-grained diorite-gabbro *(Greenstone)* Finkornig diorit-gabbro *(Grönsten)*	Mafic rock, fine-grained Mafisk bergart, finkornig	69	185	124
509010	Sulphide mineralization Sulfidmineralisering	Sulphide mineralization Sulfidmineralisering	204	204	204
506007	Sandstone Sandsten	Sandstone Sandsten	217	192	106

Appendix 2

KSH01A	
[redacted]	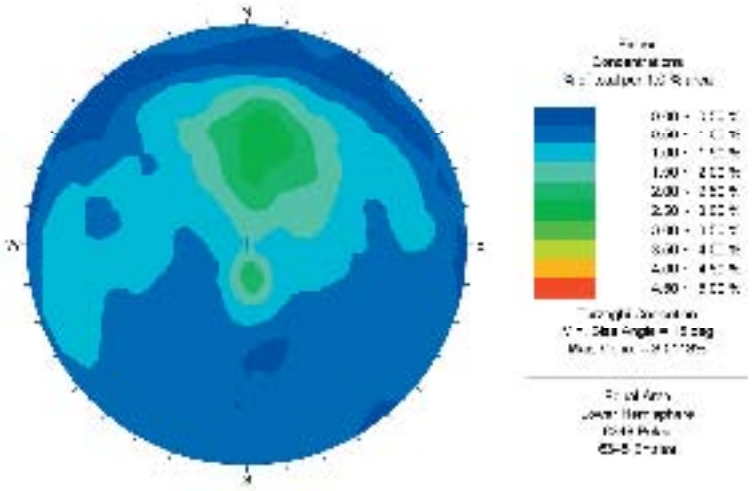
[redacted]	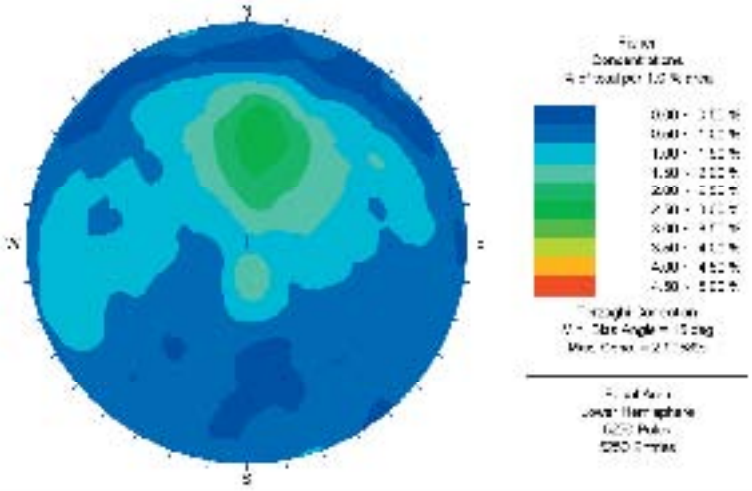
[redacted]	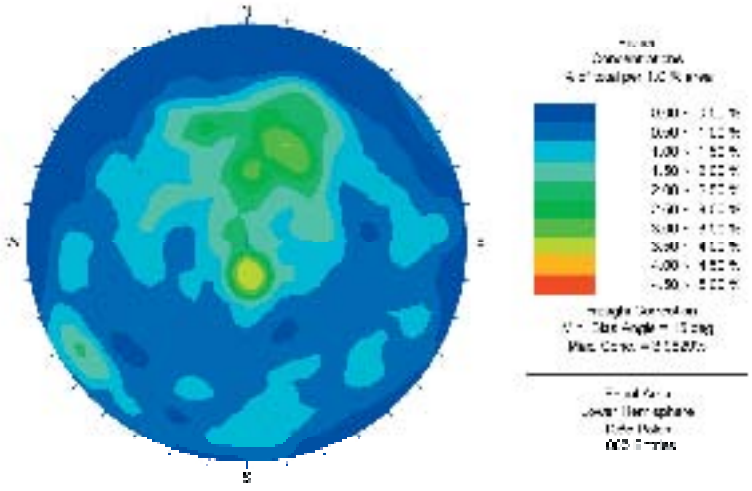

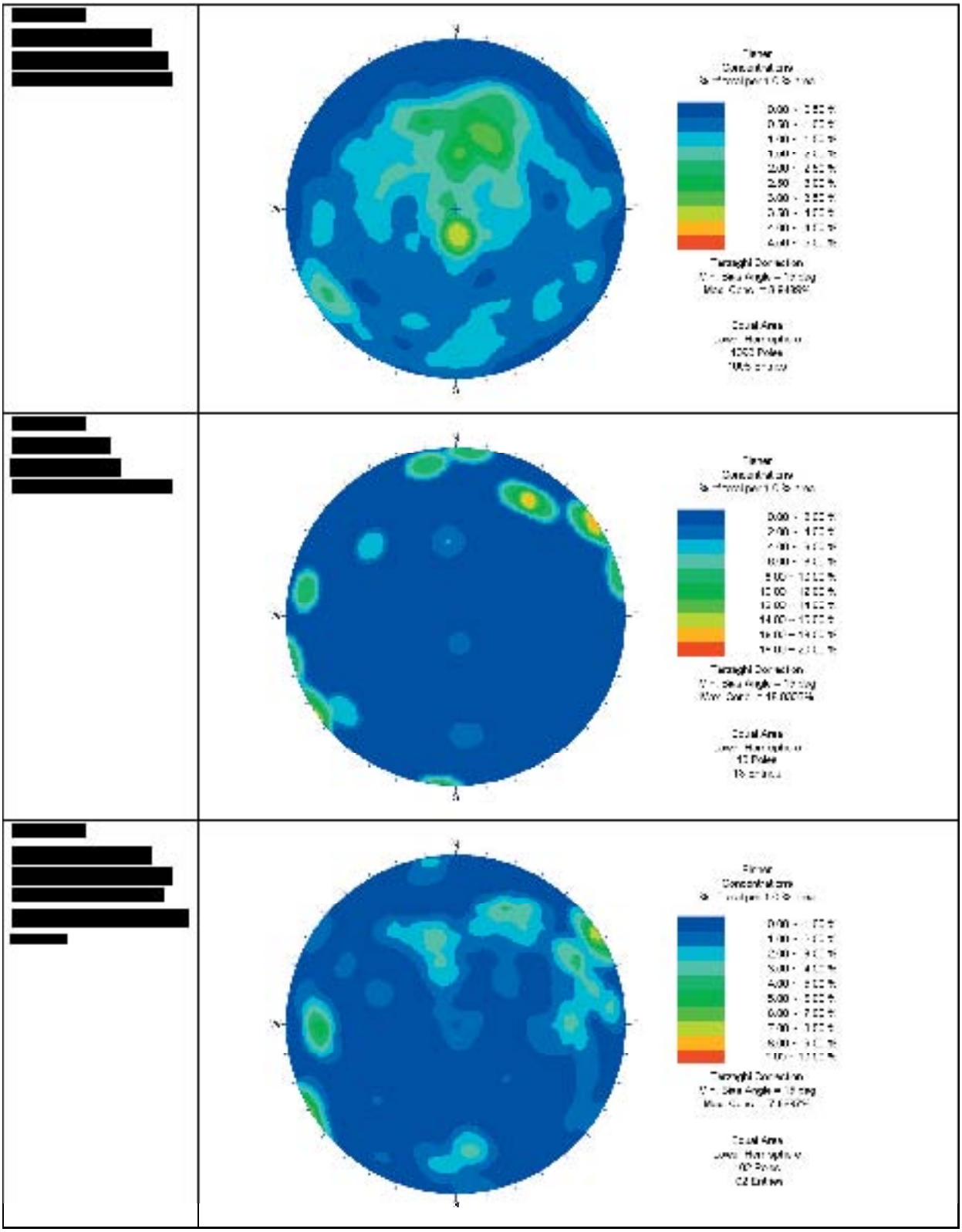

[redacted]	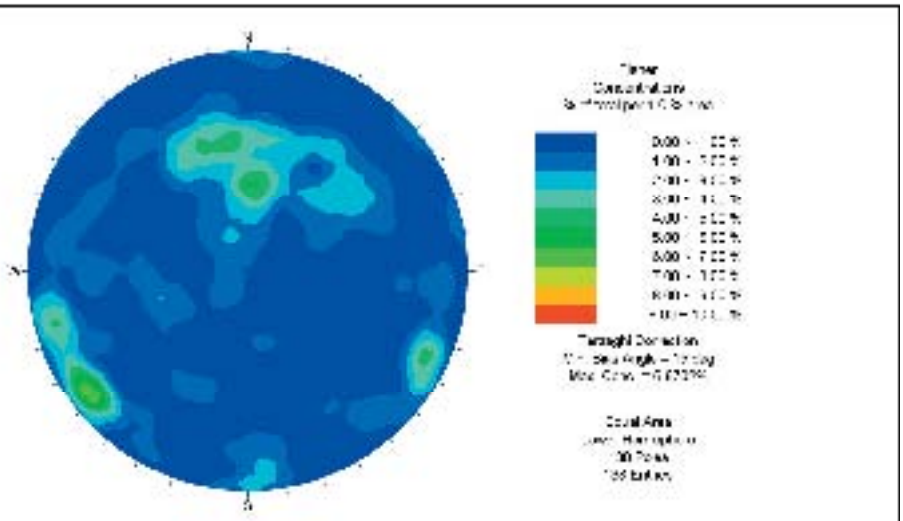
[redacted]	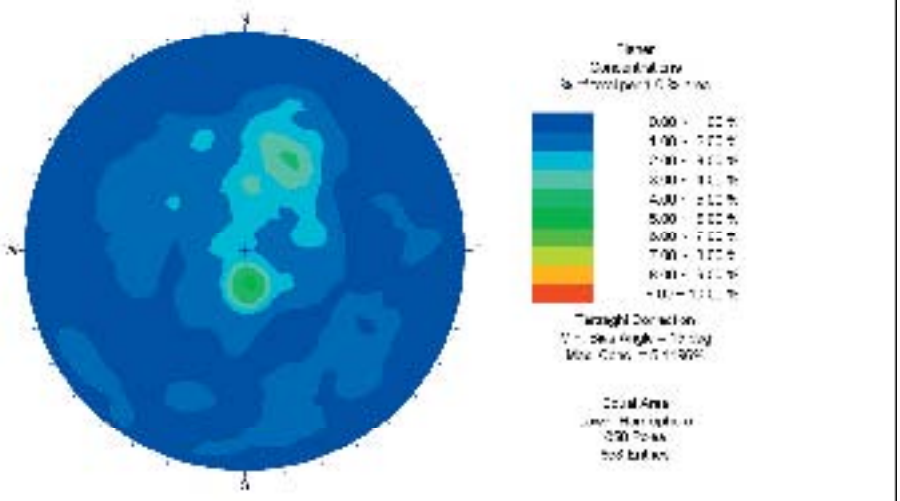
[redacted]	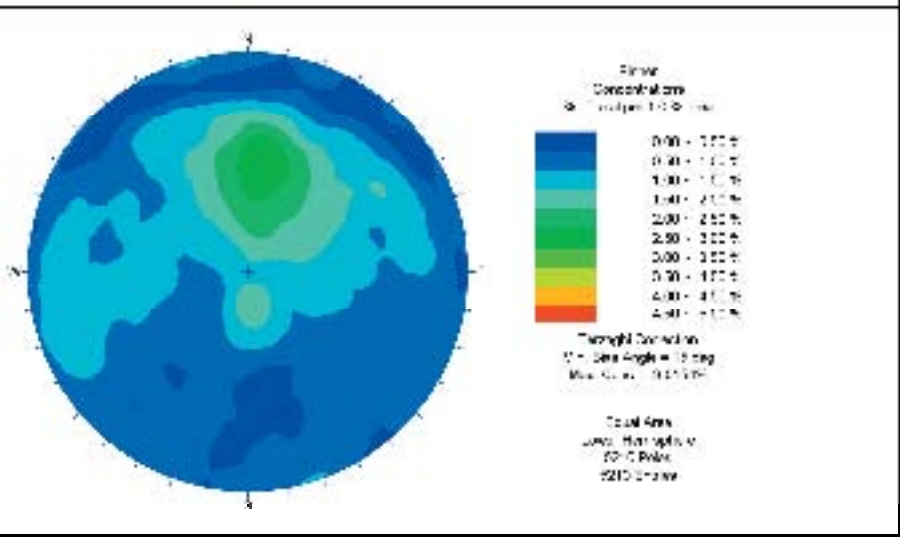

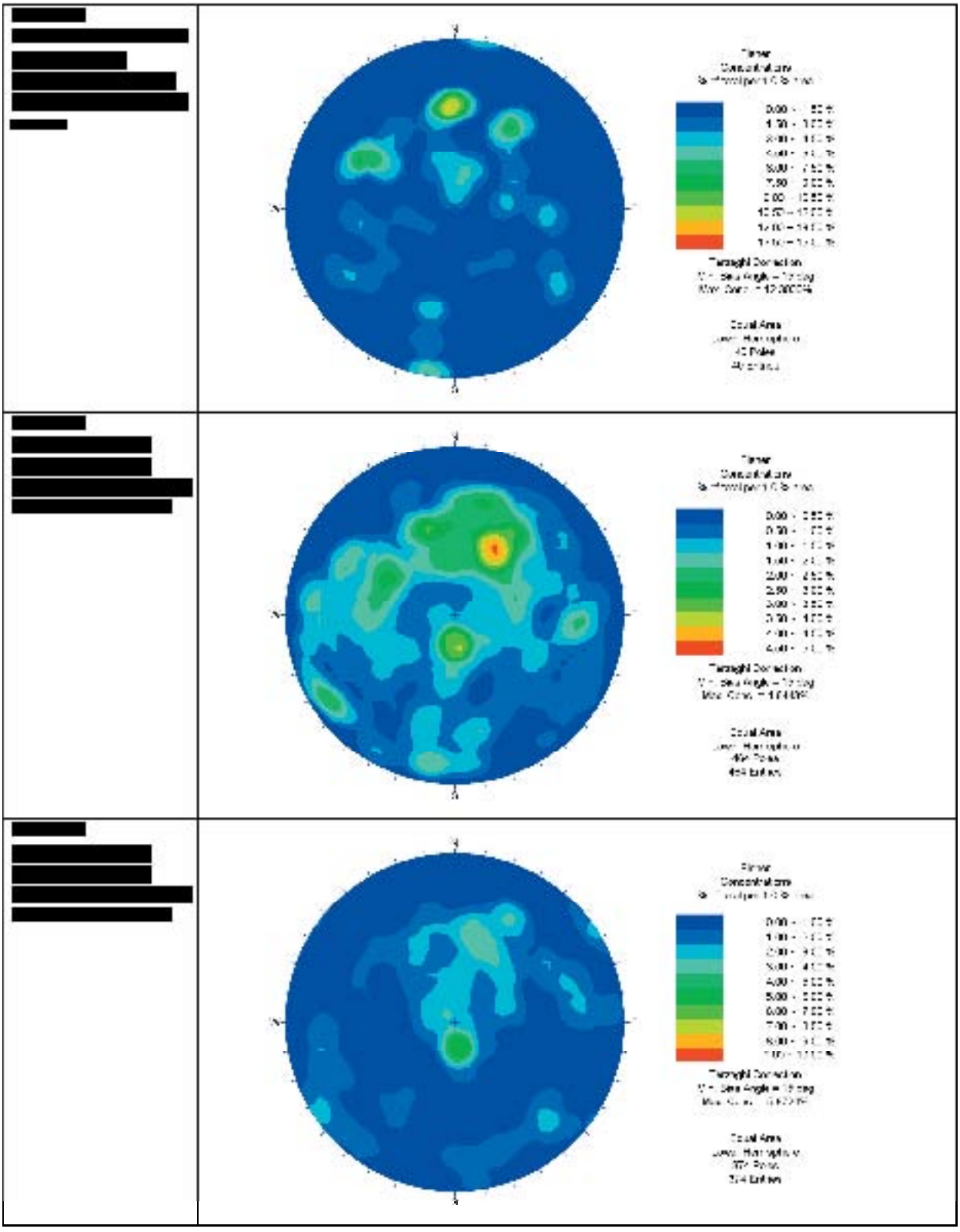

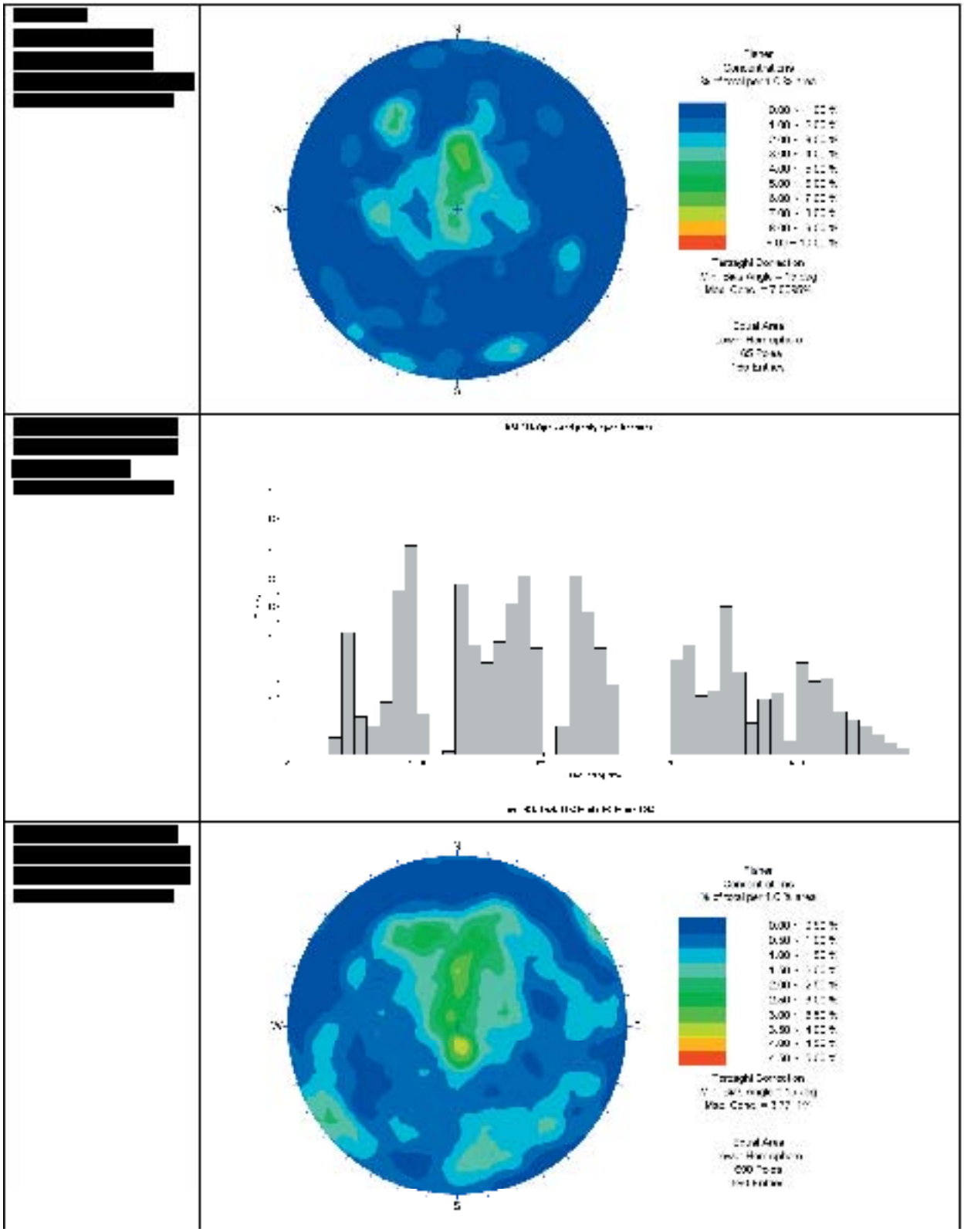

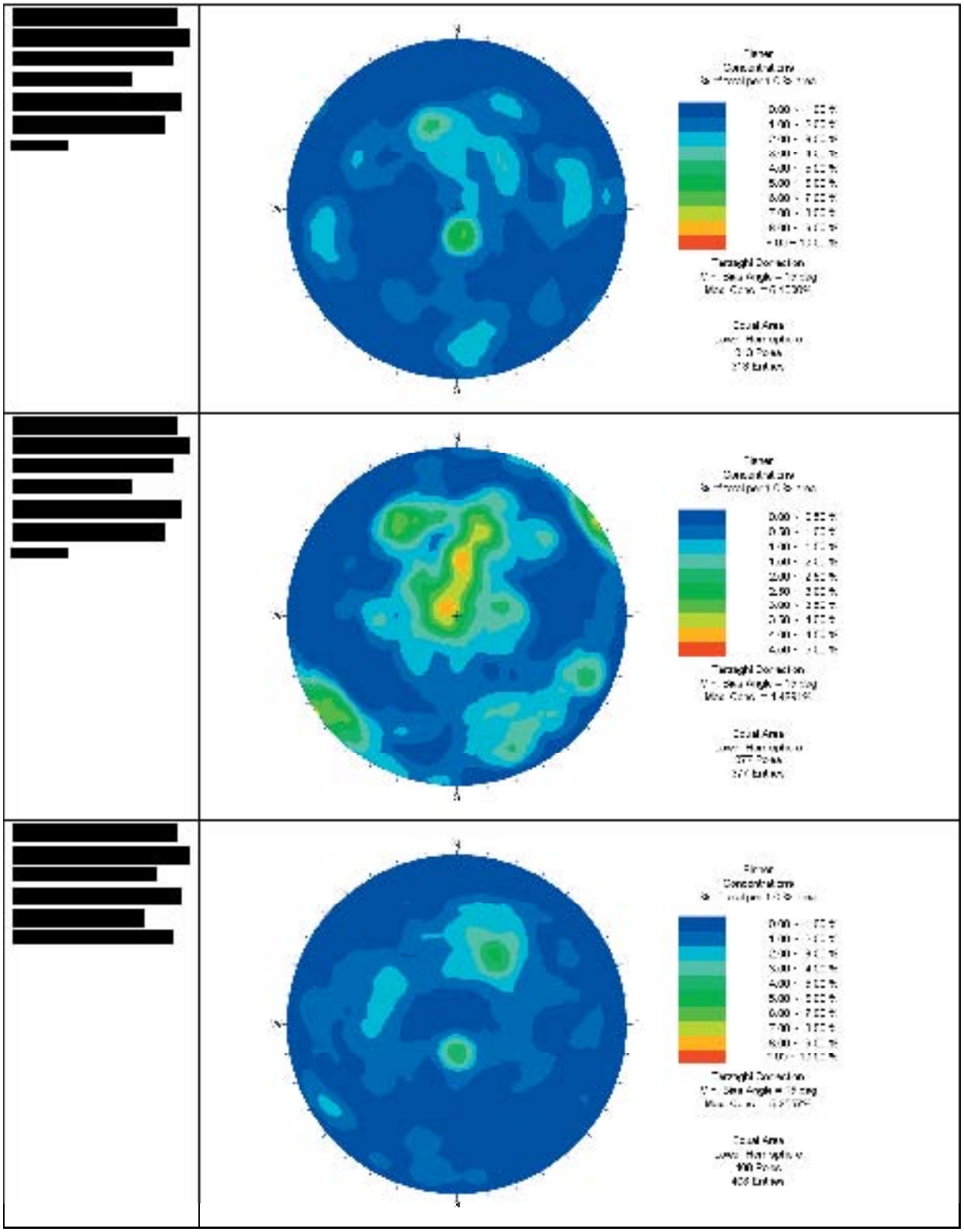

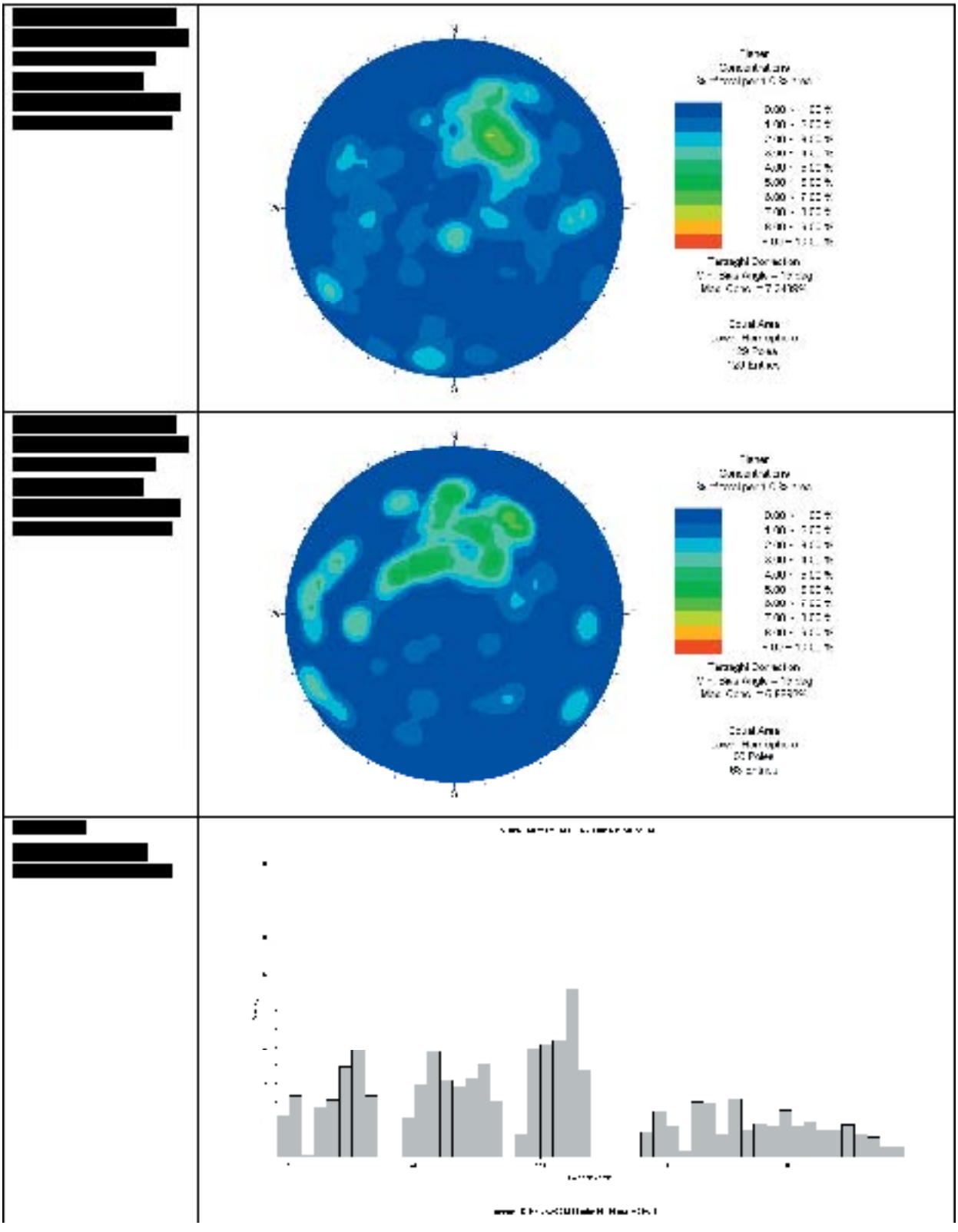

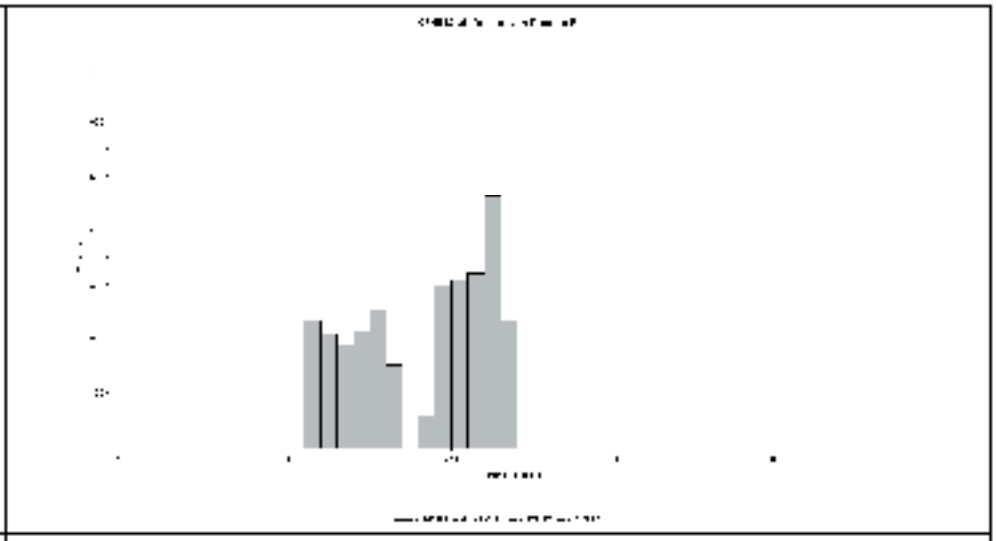

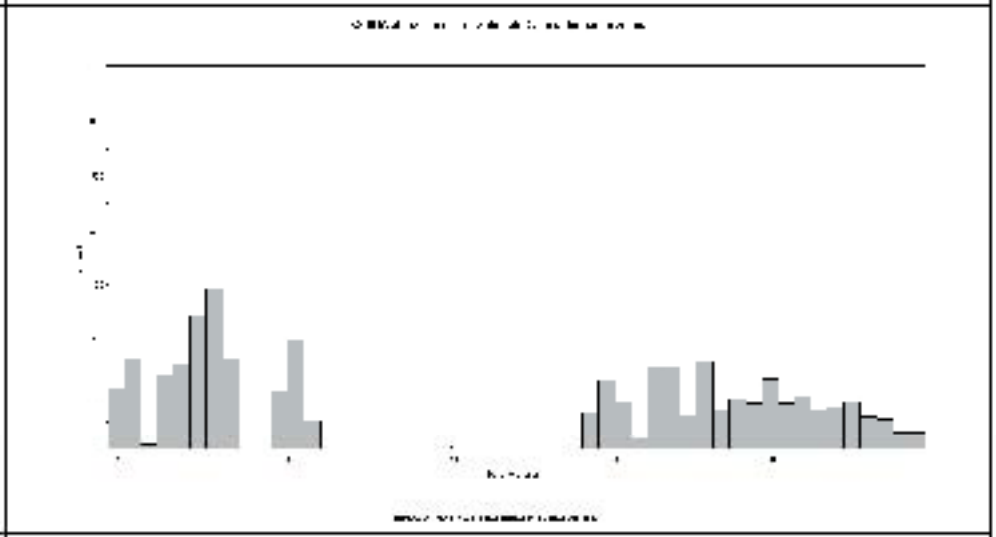

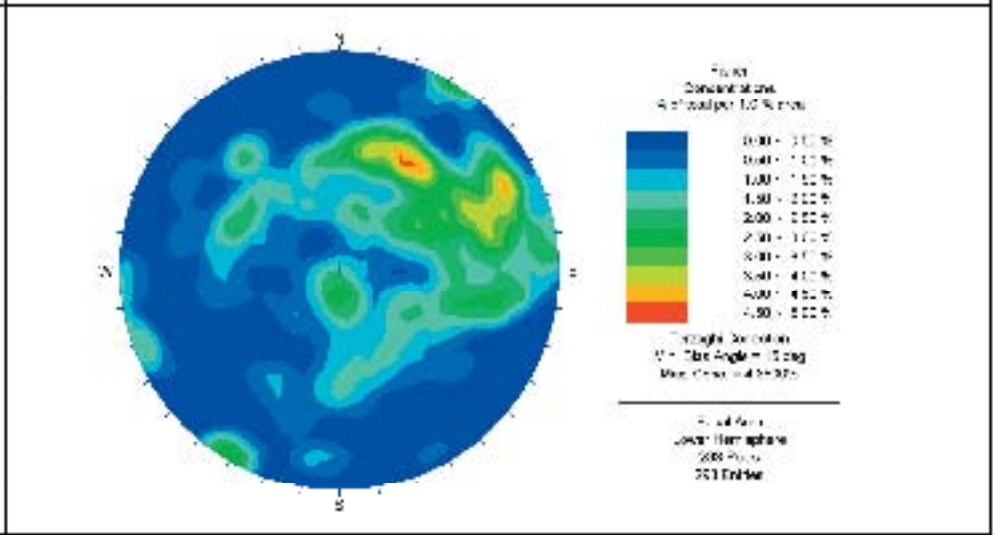

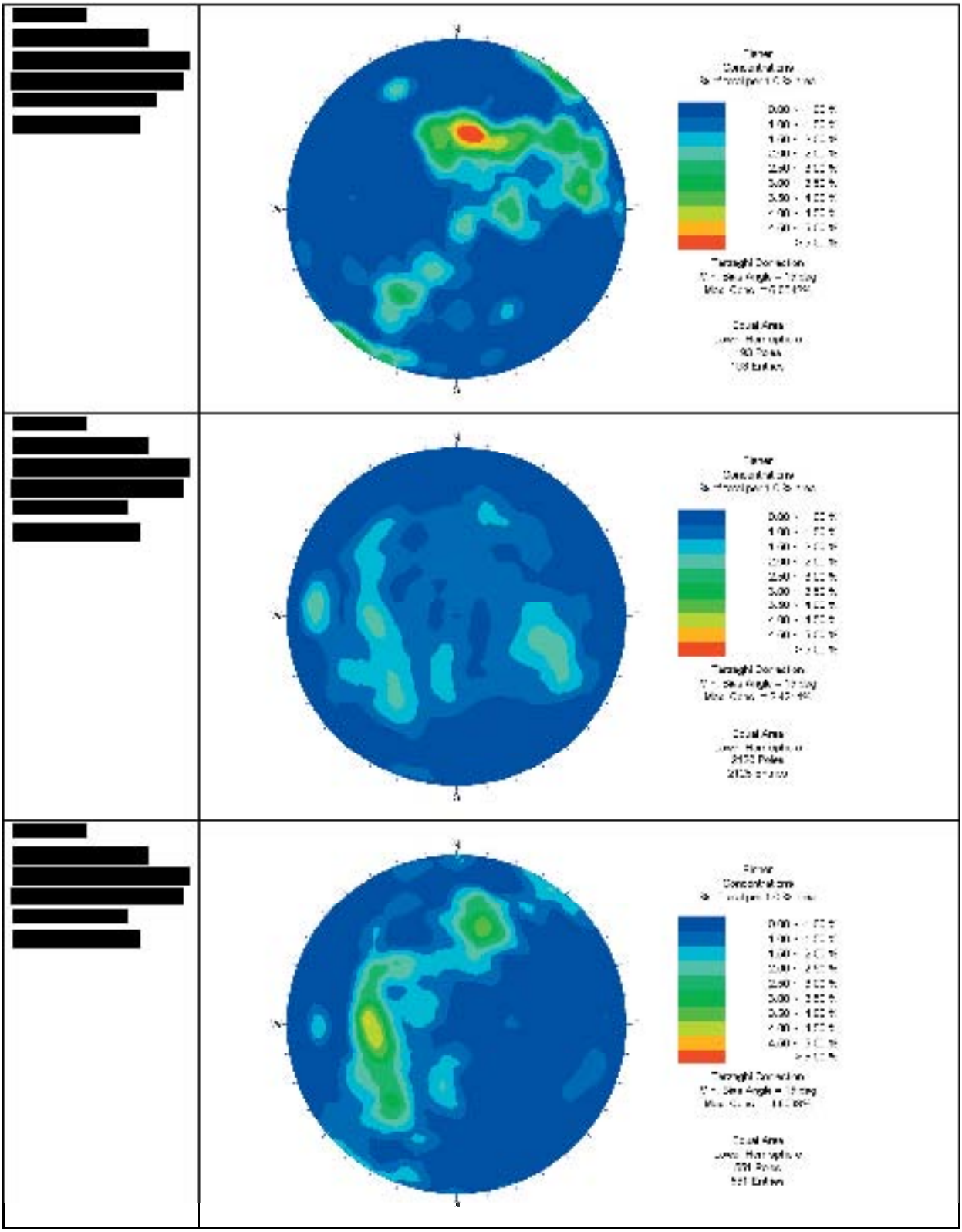

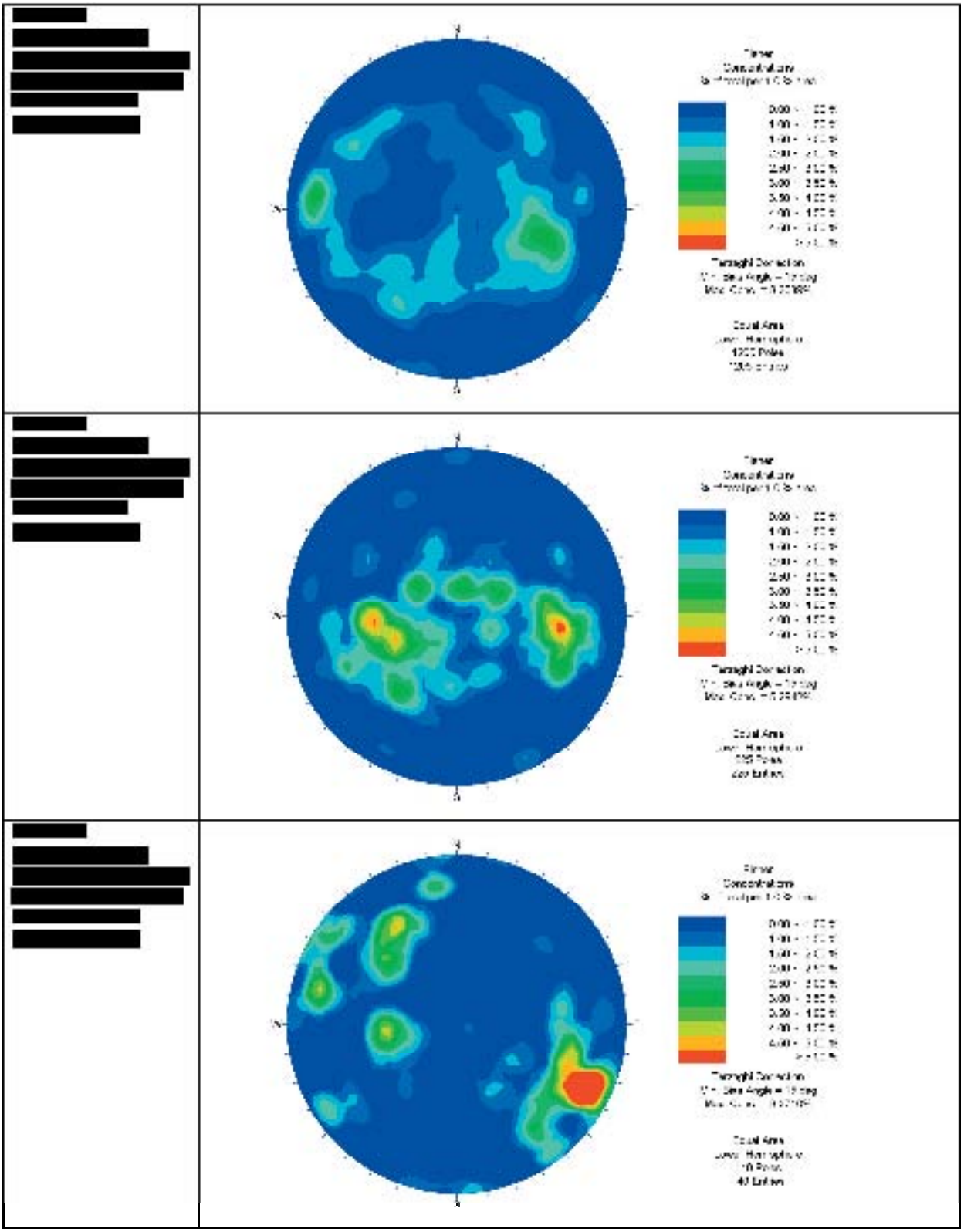

[redacted]

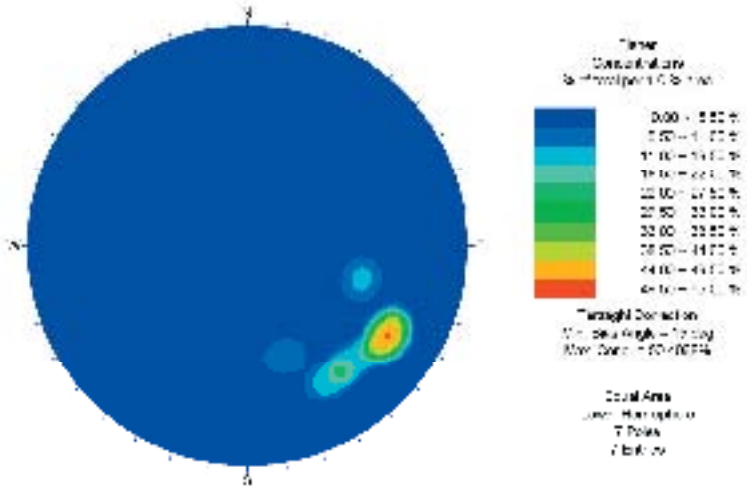

HSH01 and HSH03

[redacted]

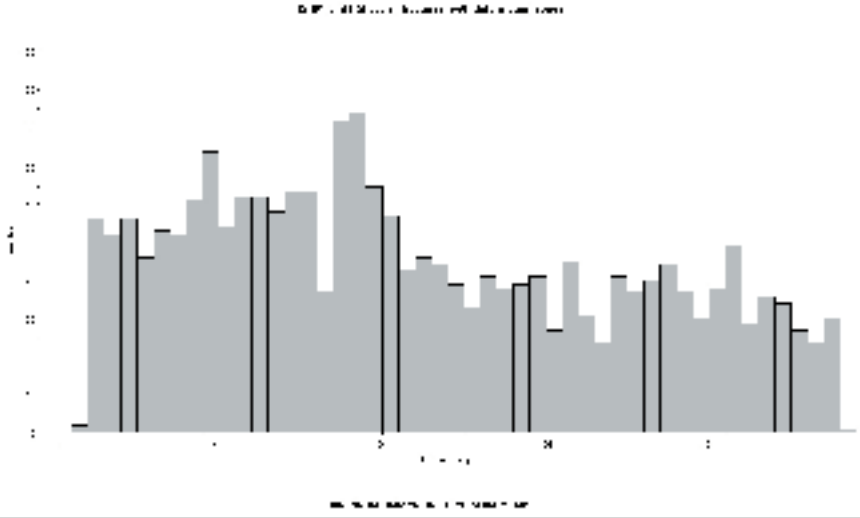

[redacted]

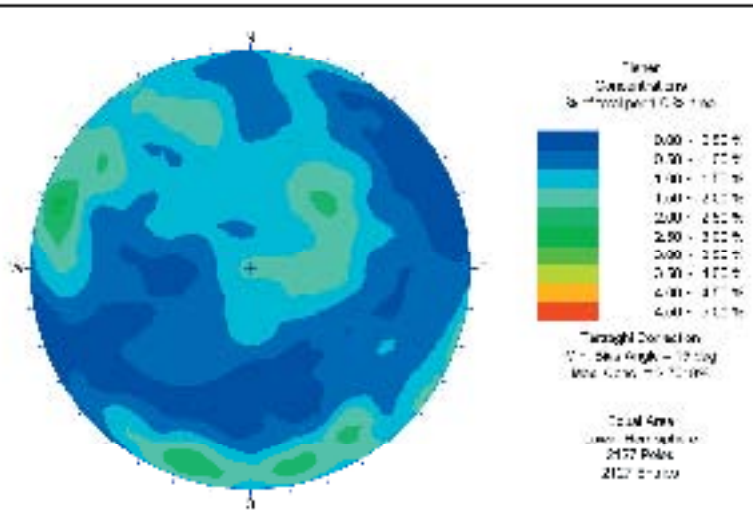

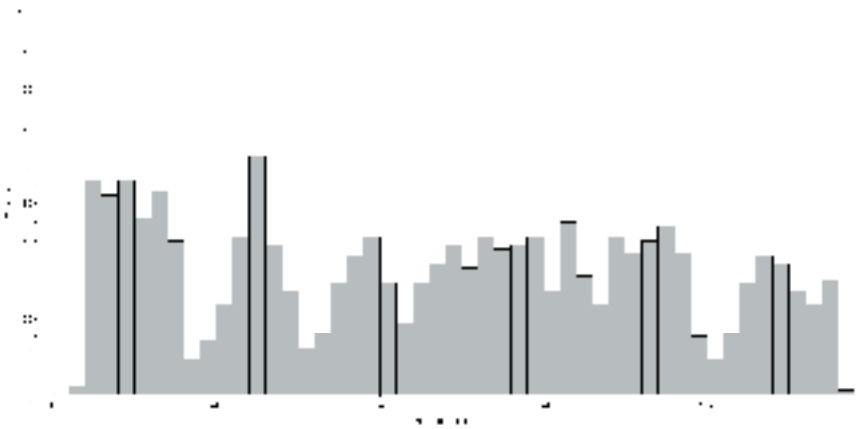

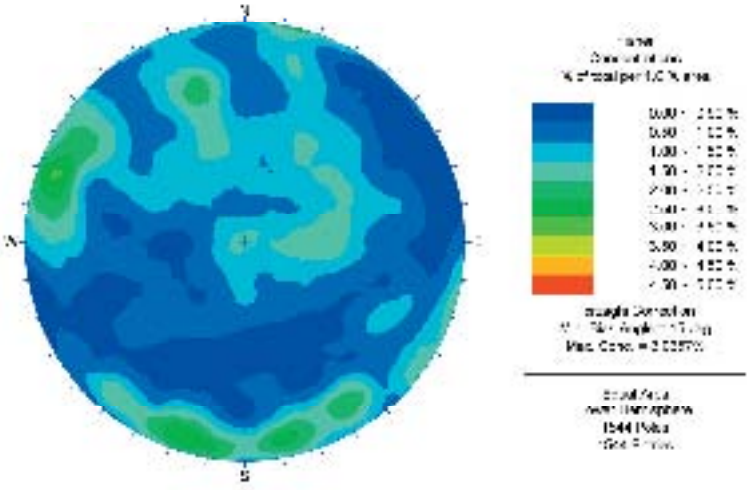

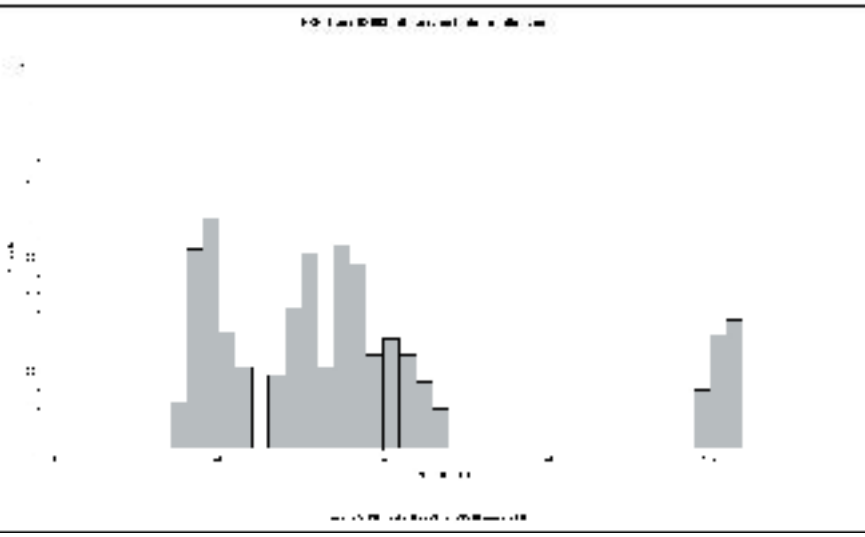

[redacted]	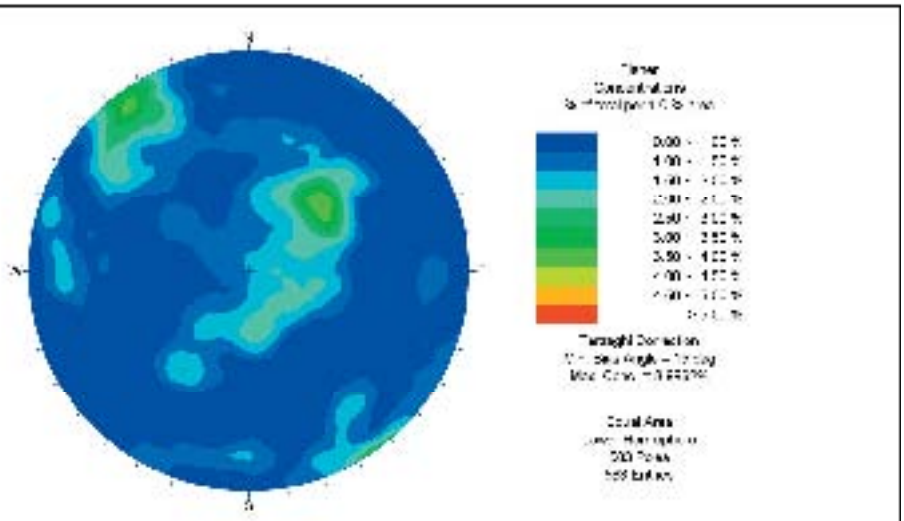
[redacted]	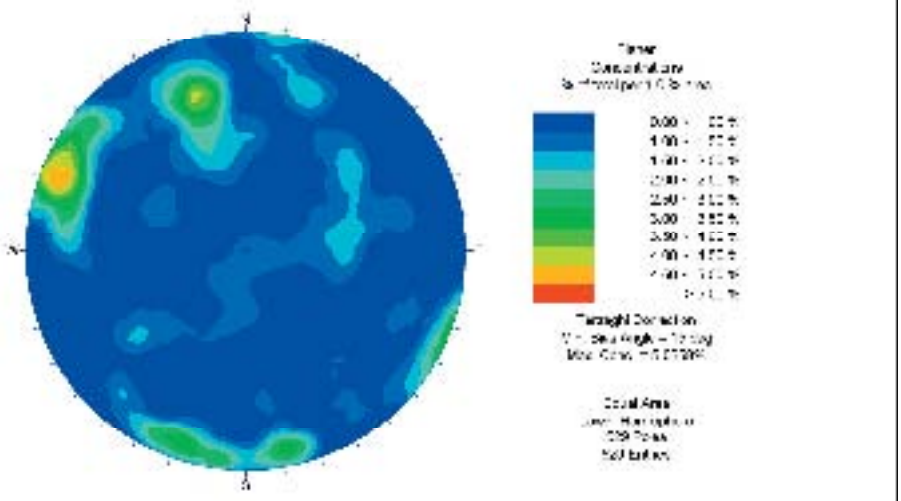
[redacted]	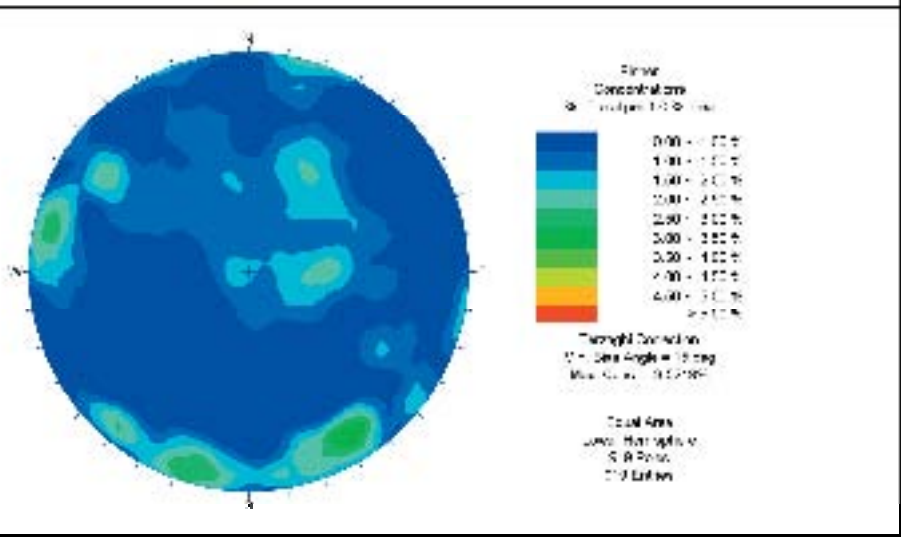

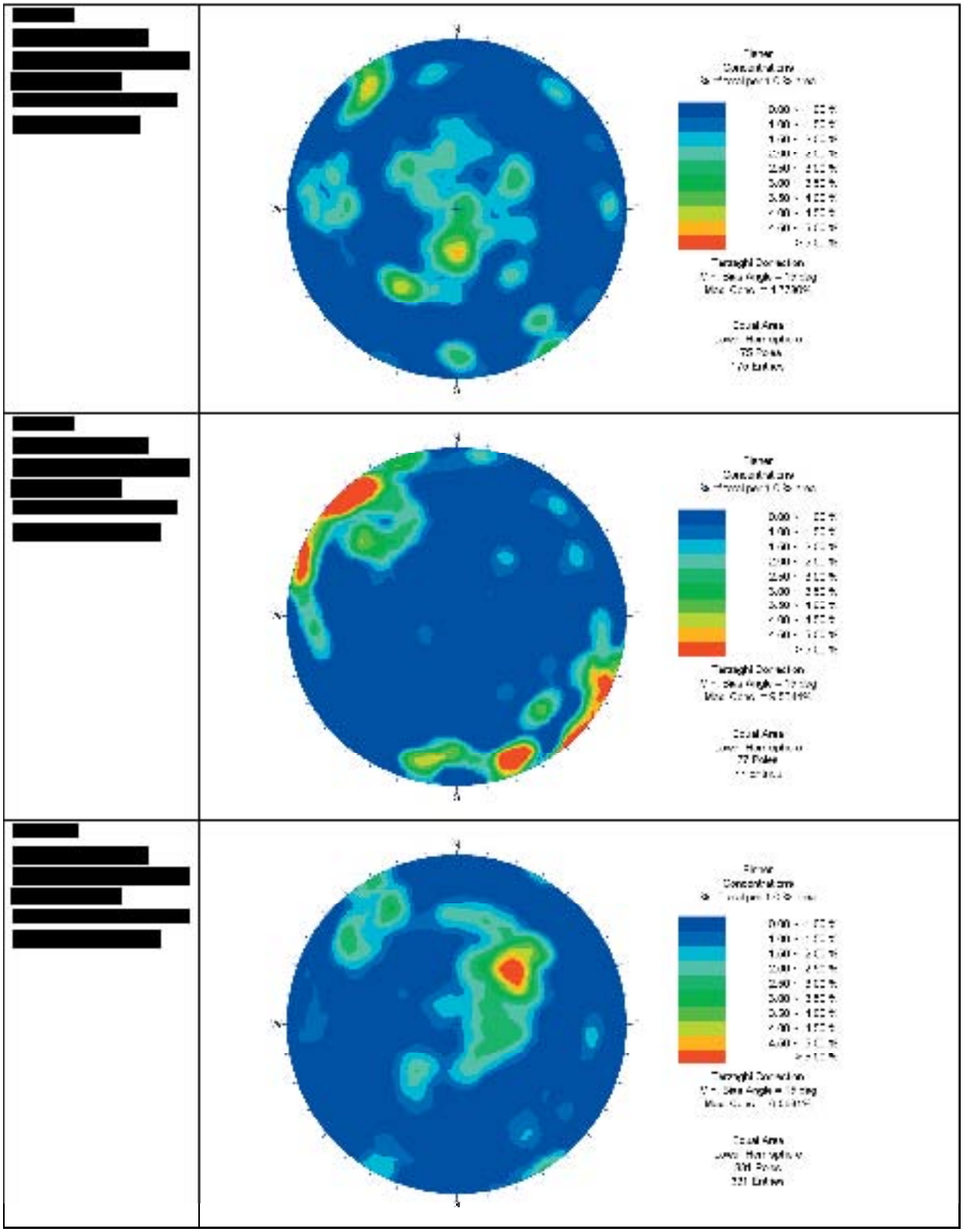

KSH01B	
[redacted]	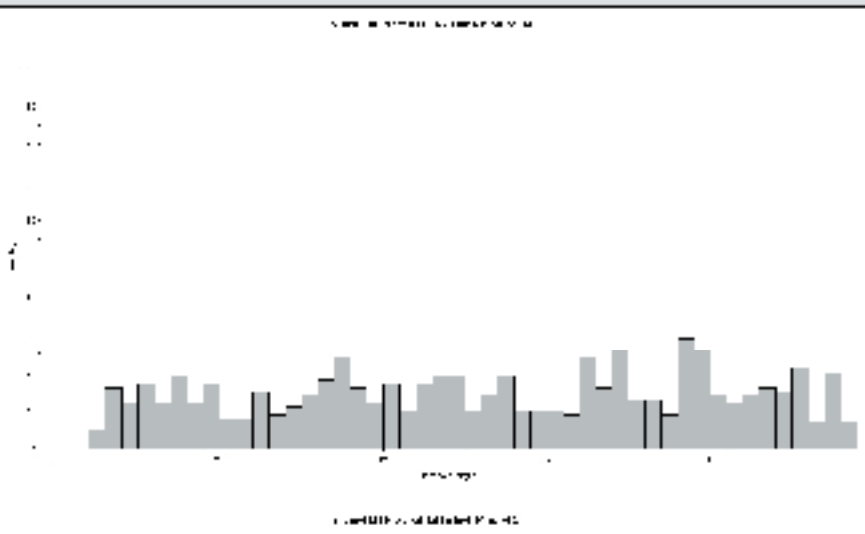
[redacted]	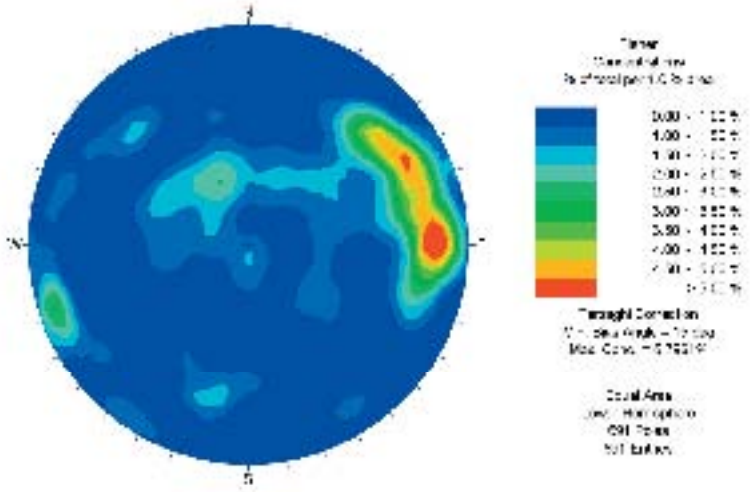
[redacted]	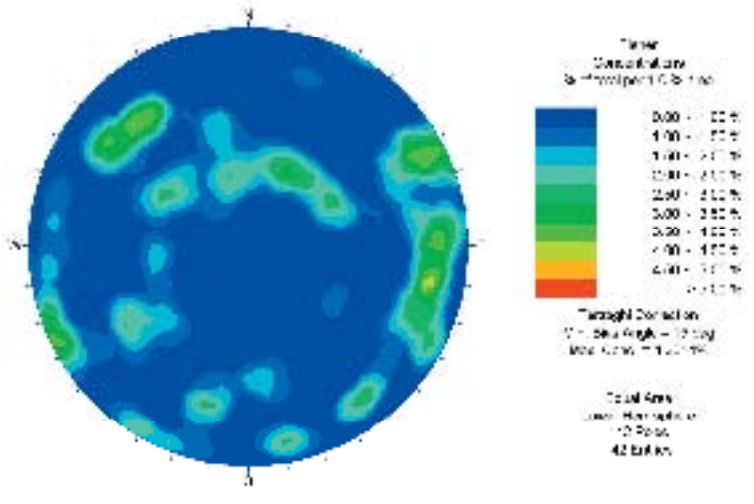

KSH02	
[redacted]	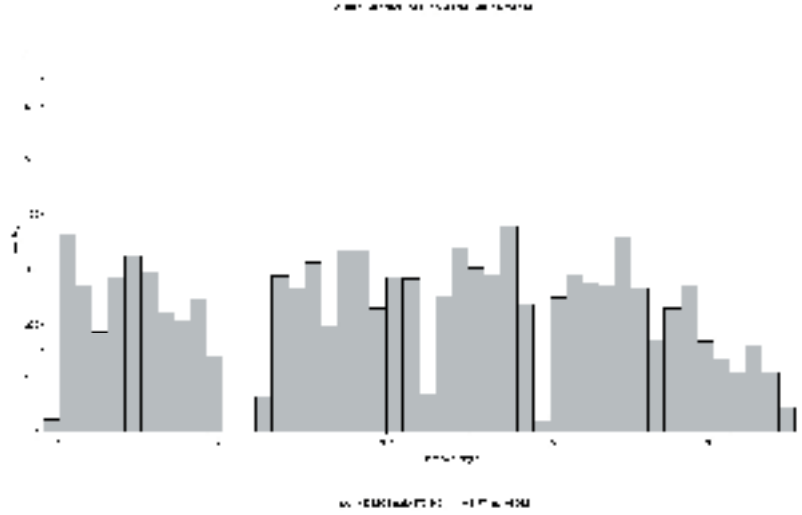
[redacted]	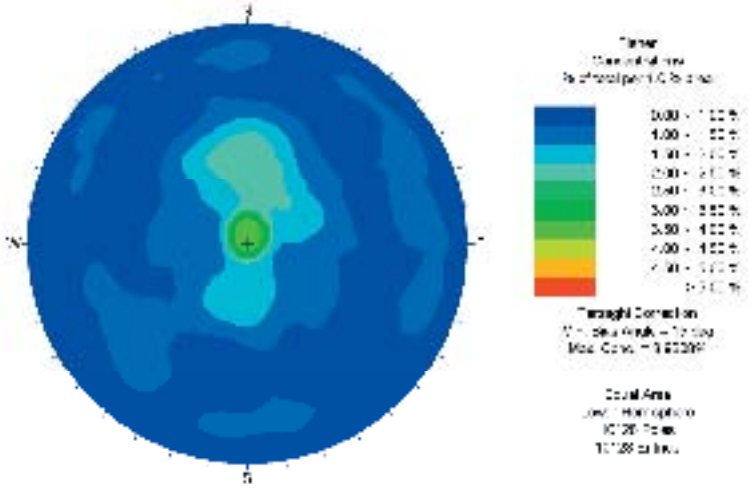
[redacted]	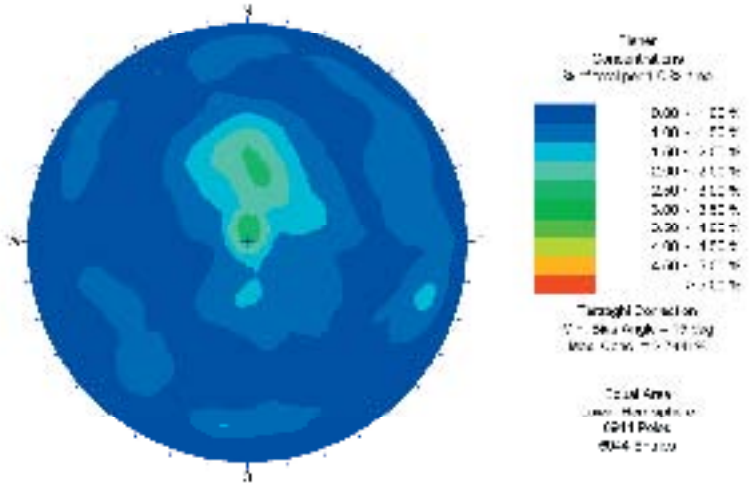

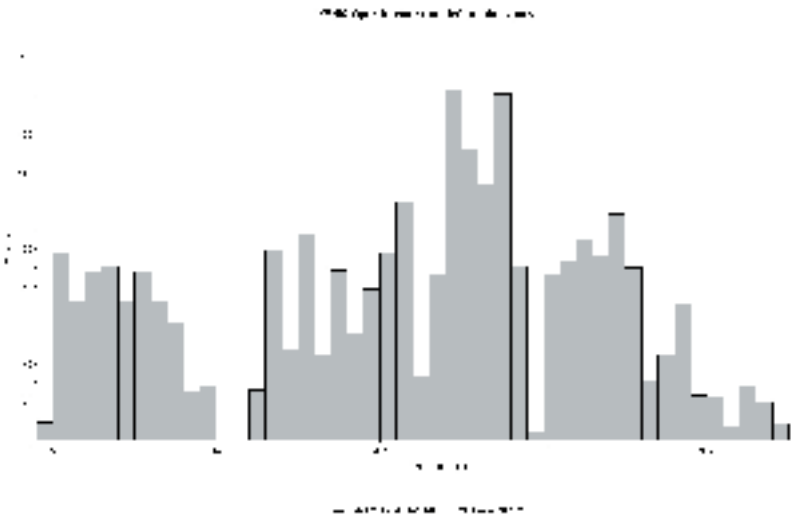

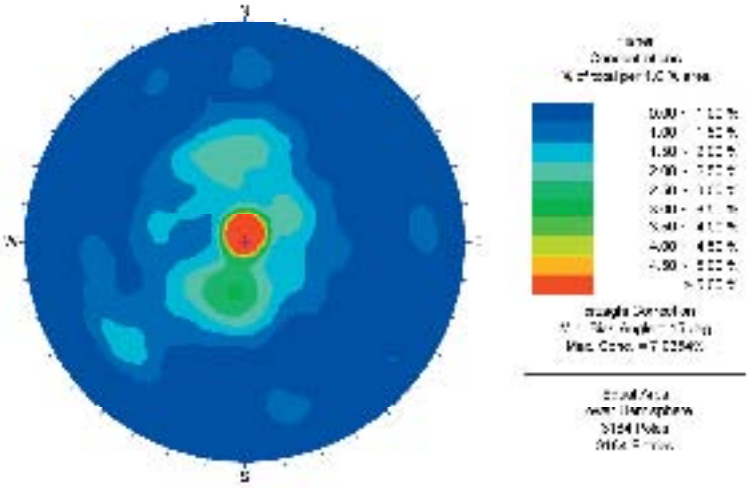

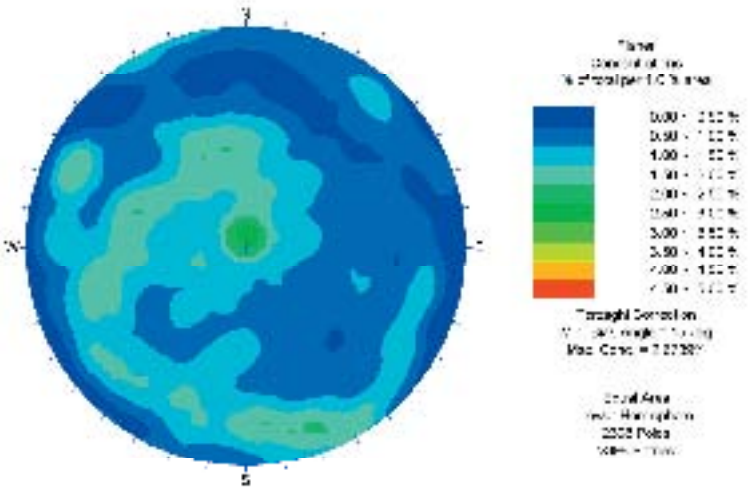

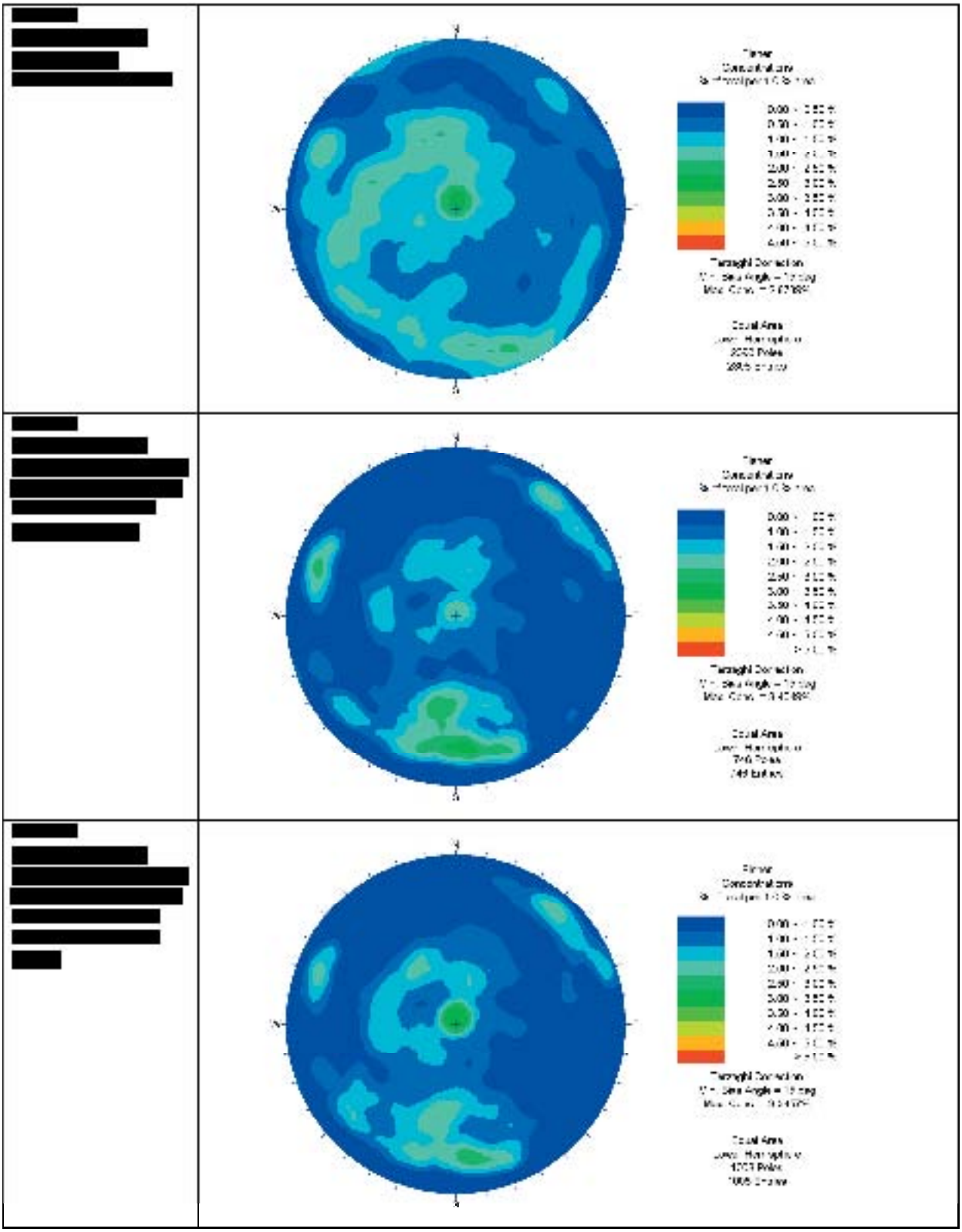

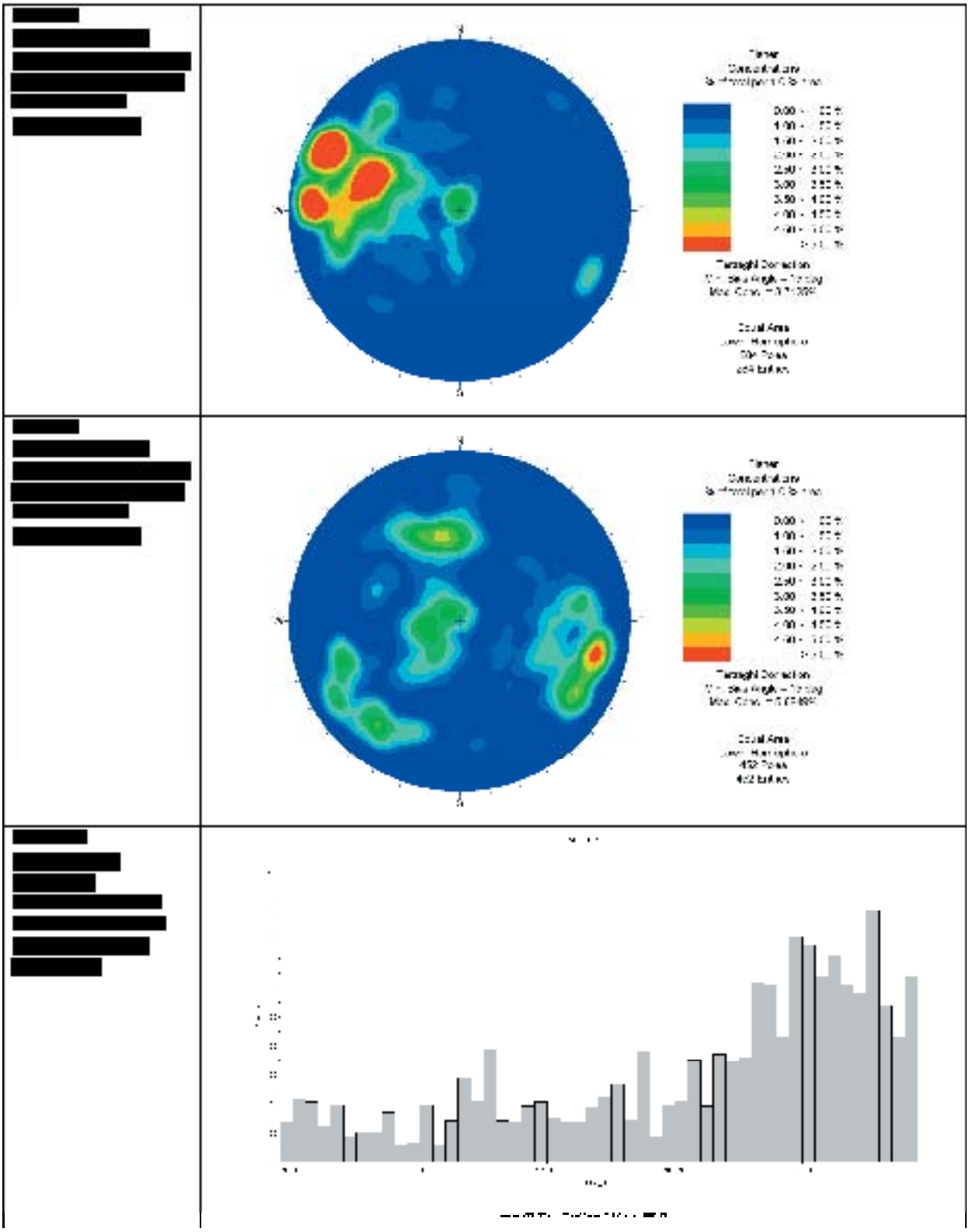

HSH02	
[redacted]	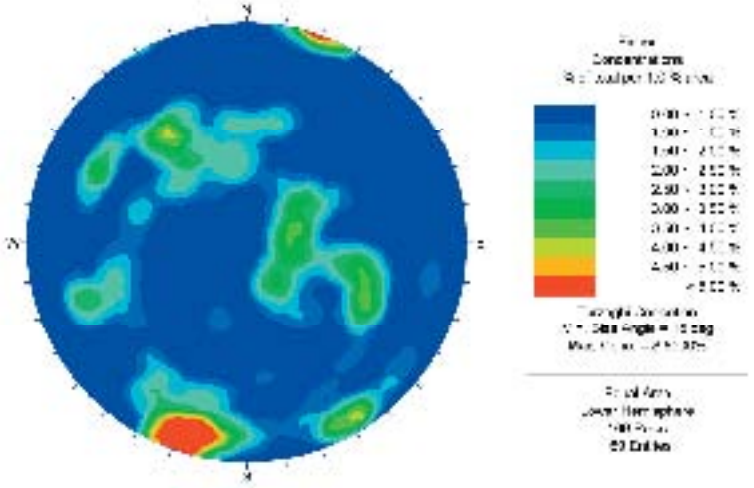
[redacted]	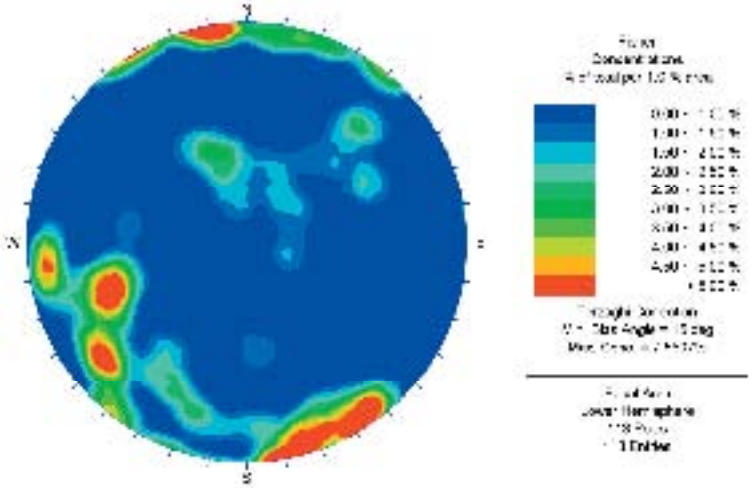
[redacted]	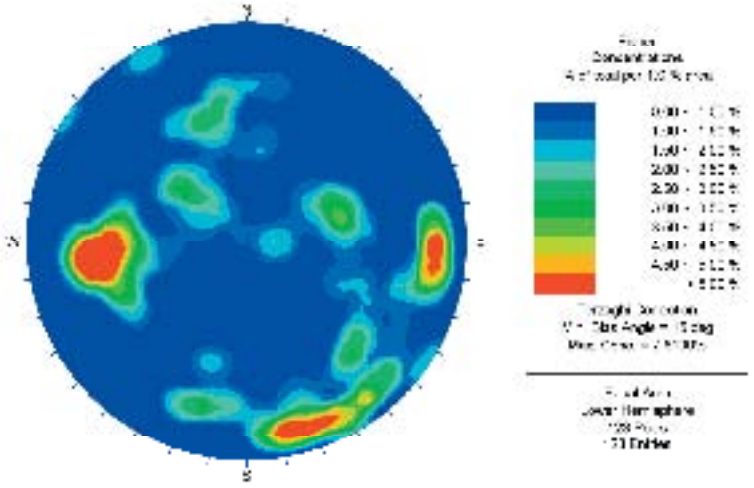

[redacted]	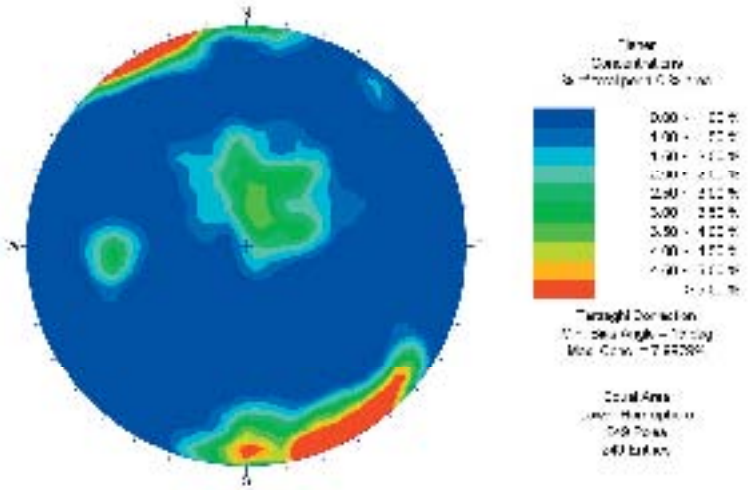
KSH03	
[redacted]	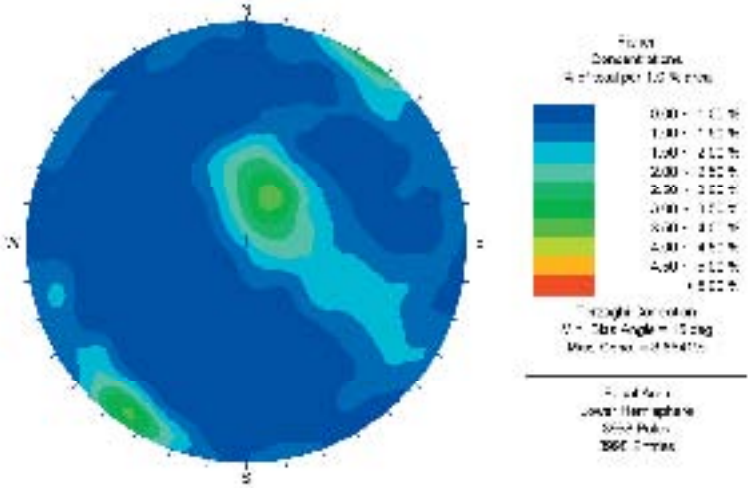
[redacted]	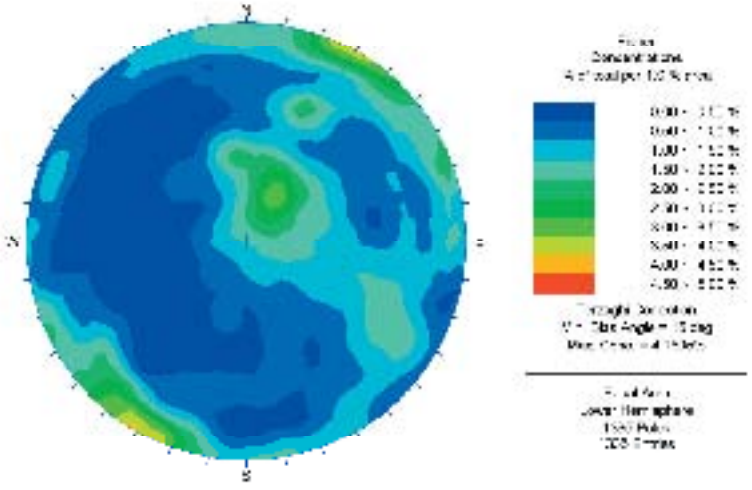

[redacted]	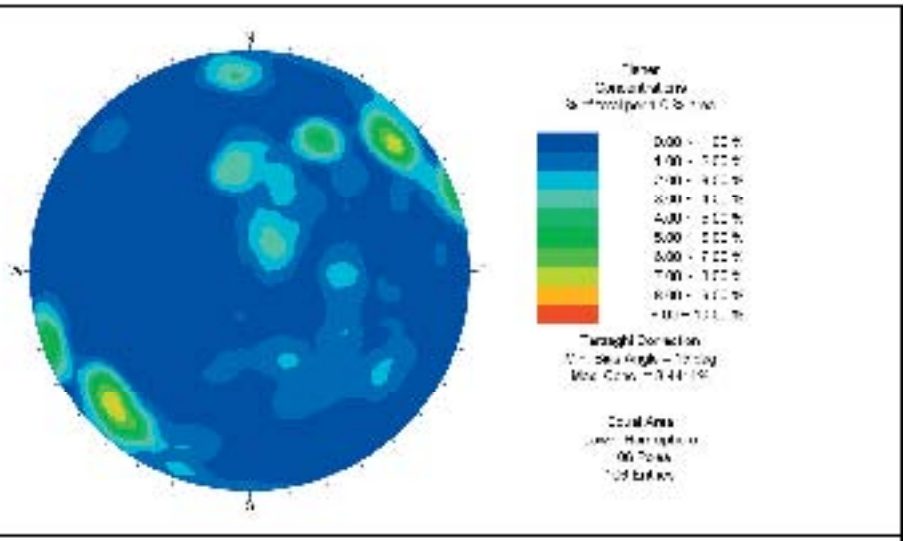
[redacted]	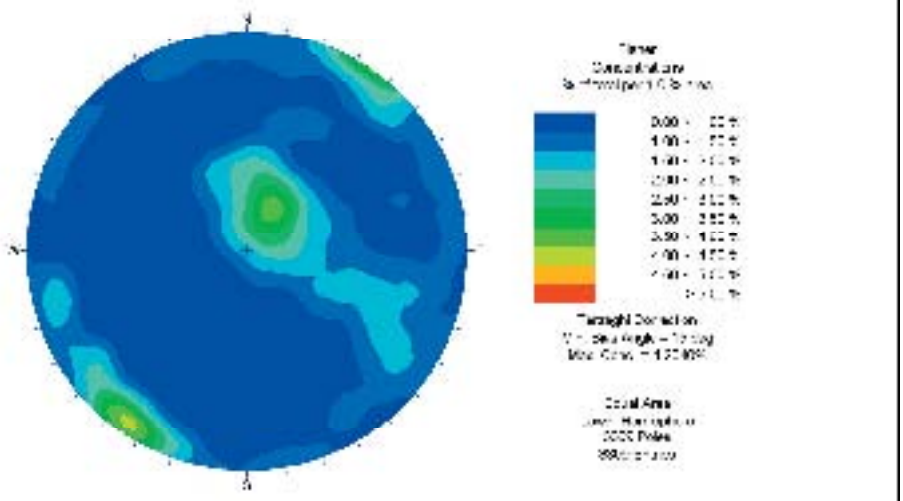
[redacted]	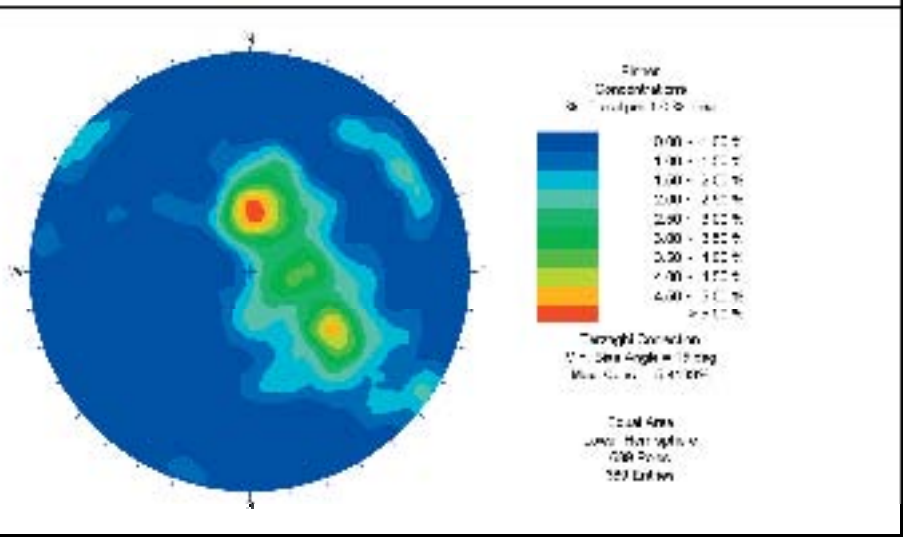

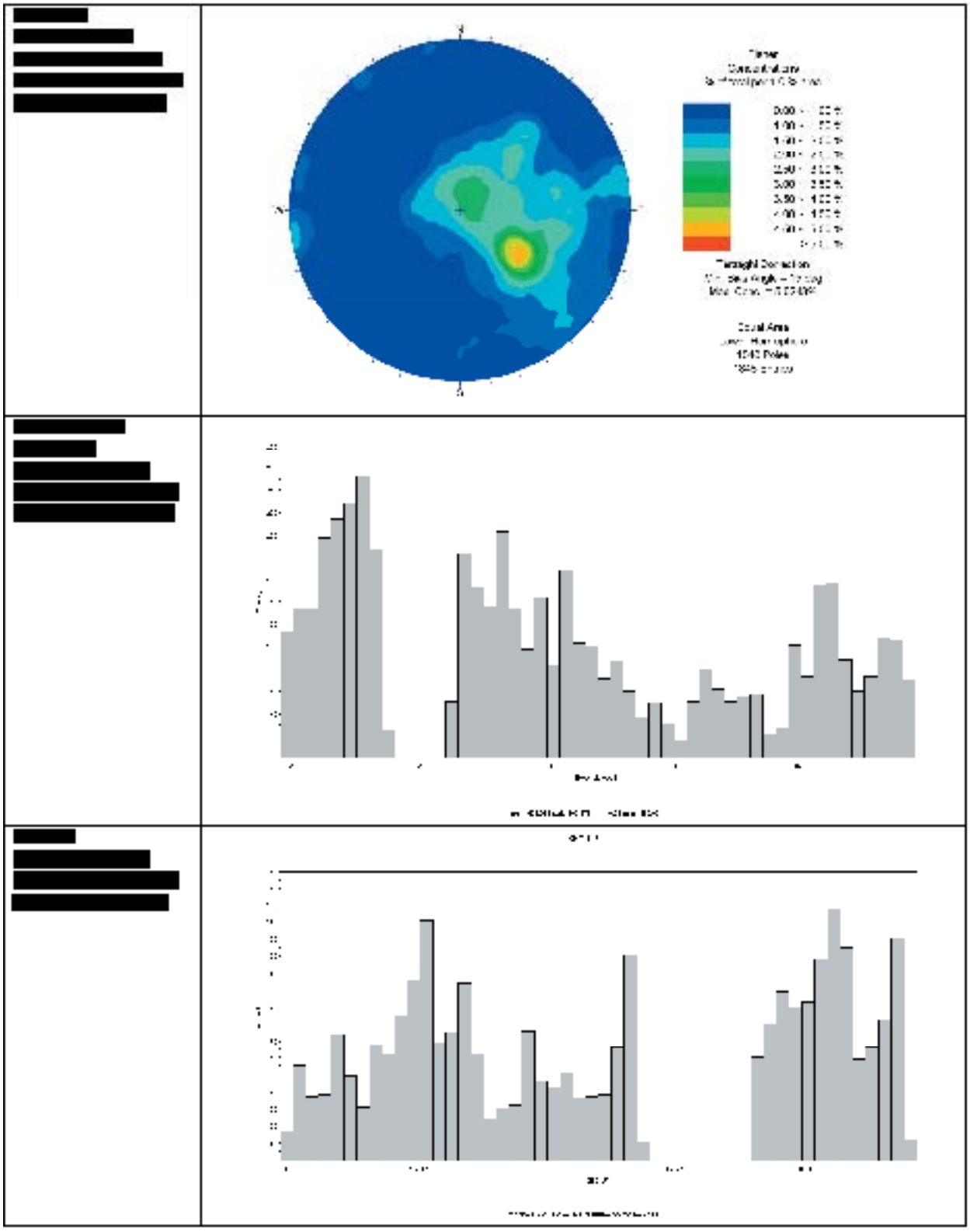

Appendix 3

Rock type occurrence statistics in the rock domains based on the outcrop database from the bedrock mapping of the Simpevarp subarea

The outcrop observations are extracted from the outcrop database that was compiled during the bedrock mapping of the Simpevarp subarea during 2003. The registered rock type nomenclature in the database has been transferred to the nomenclature decided by SKB for the site investigation in Oskarshamn (Table A3-1).

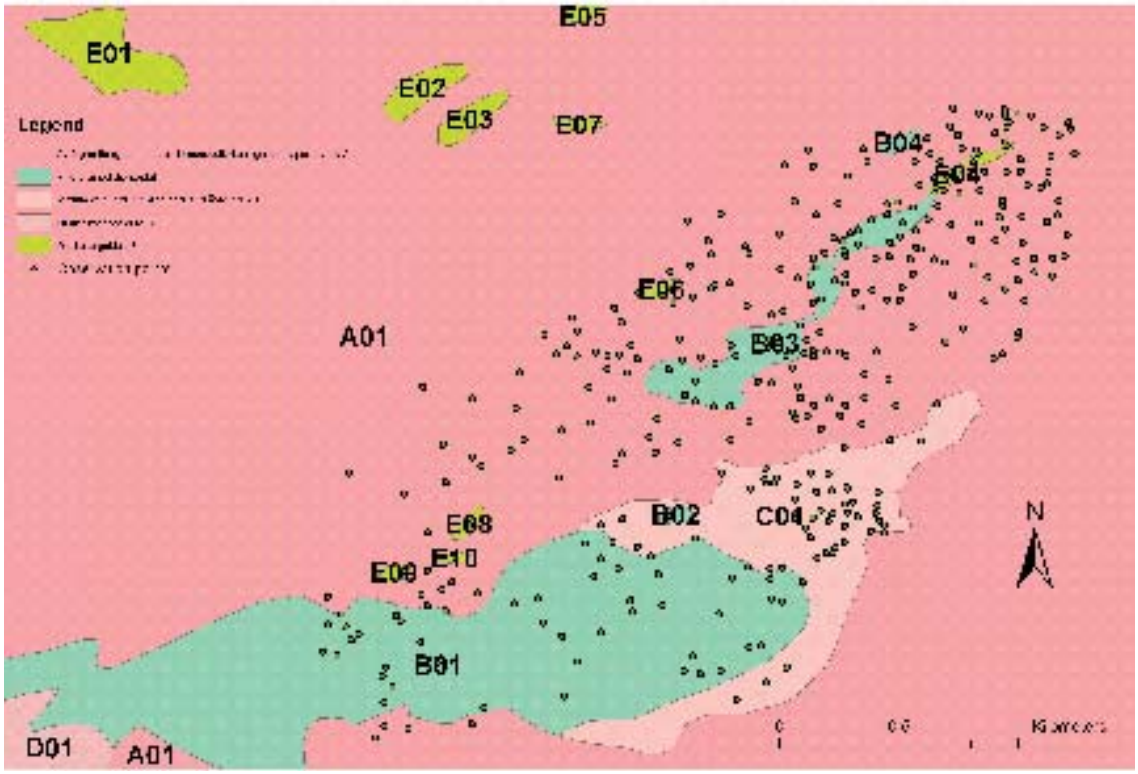

Figure A3-1. *Observation points from the bedrock mapping of the Simpevarp subarea, shown on the top surface of the 3D rock domain model.*

A01 contains 216 observation points

1) Number of observation points where each rock type is dominating.

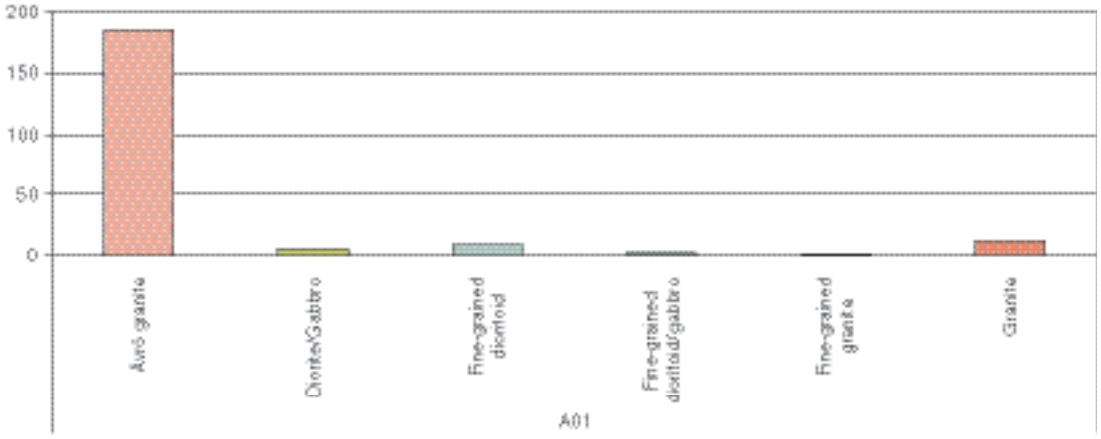

2) Number of observation points with only one rock type present.

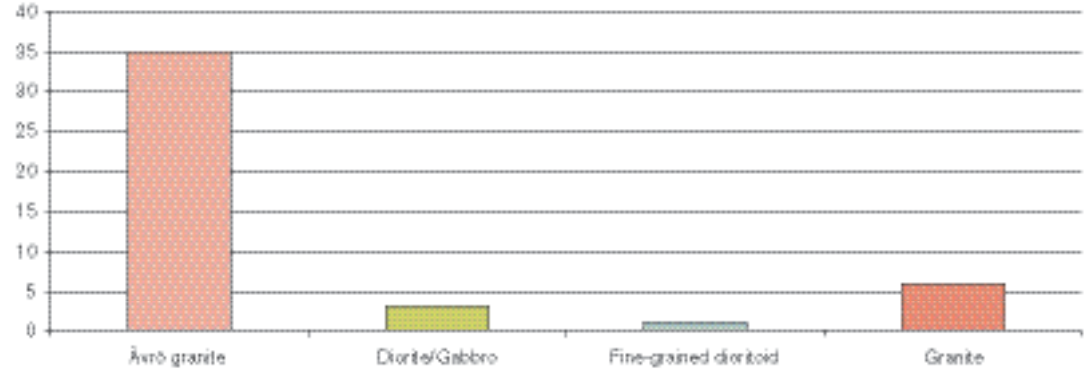

3) Number of occurrences of each rock type, of any order.

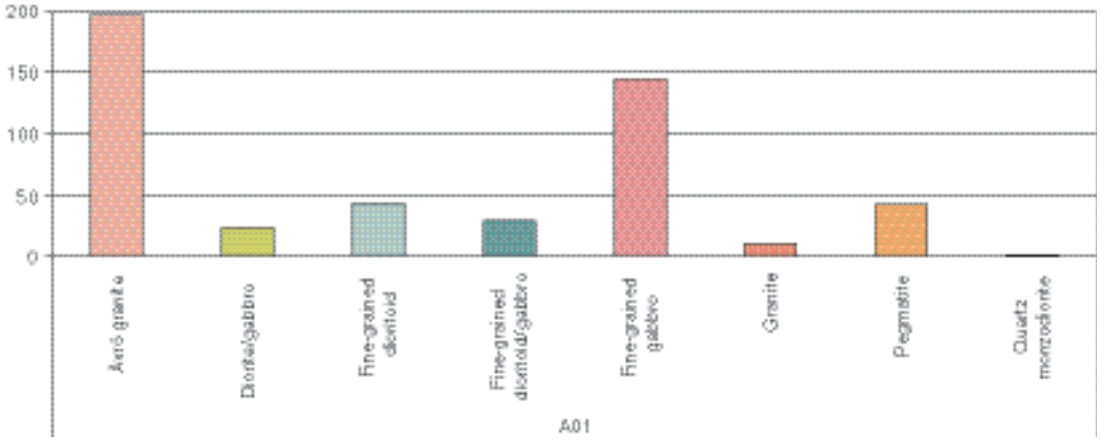

B01 contains 46 observation points

1) Number of observation points where each rock type is dominating.

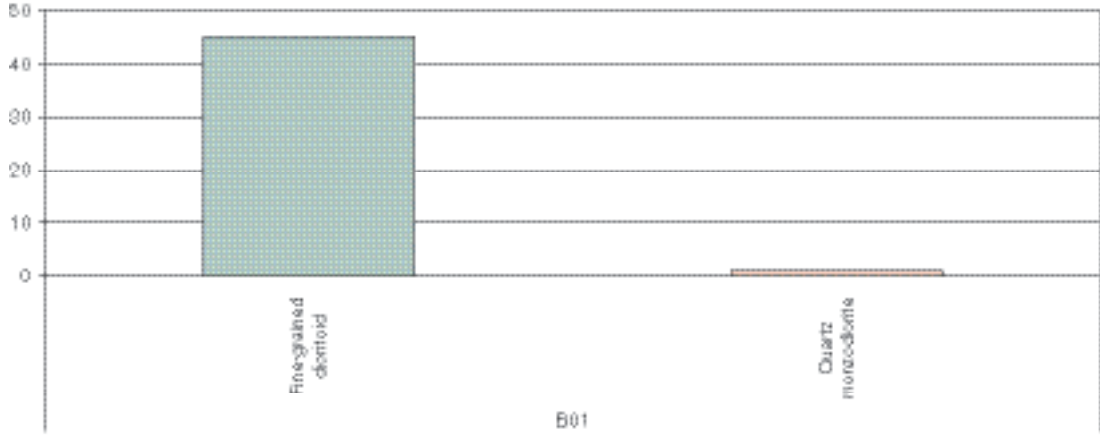

2) In two observation points only fine-grained dioritoid have been observed.

3) Number of occurrences of each rock type, of any order.

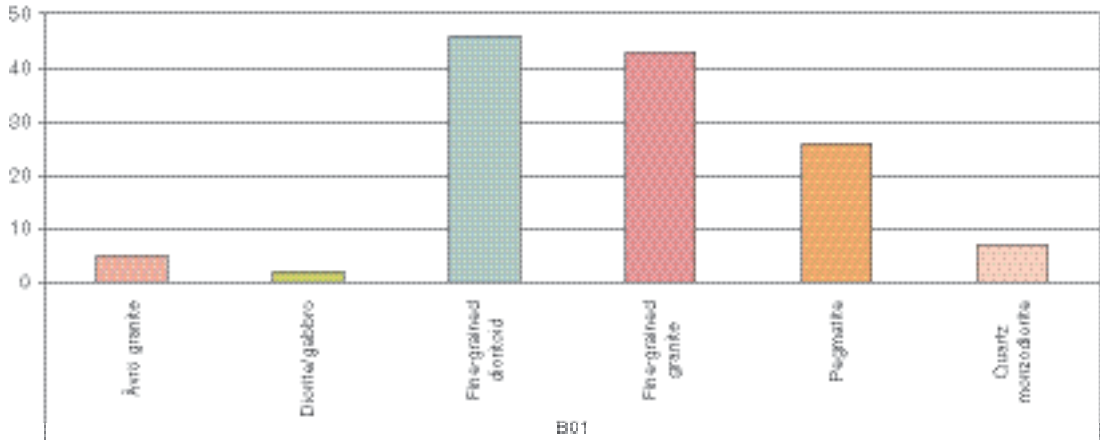

B02 contains only one observation point

The first and second order rock type is fine-grained dioritoid. Pegmatite has been observed as well.

B03 contains 27 observation points

1) Number of observation points where each rock type is dominating.

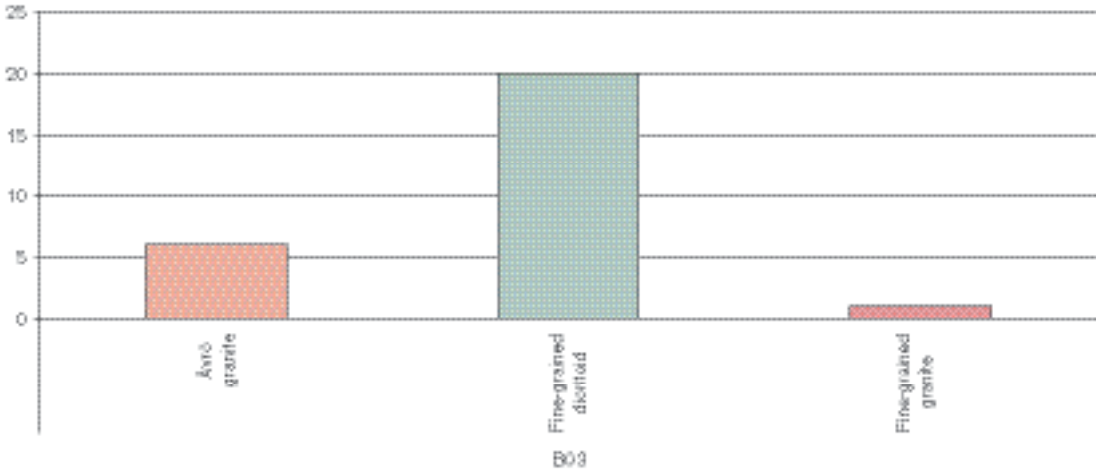

2) In four observation points only fine-grained dioritoid have been observed.

3) Number of occurrences of each rock type, of any order.

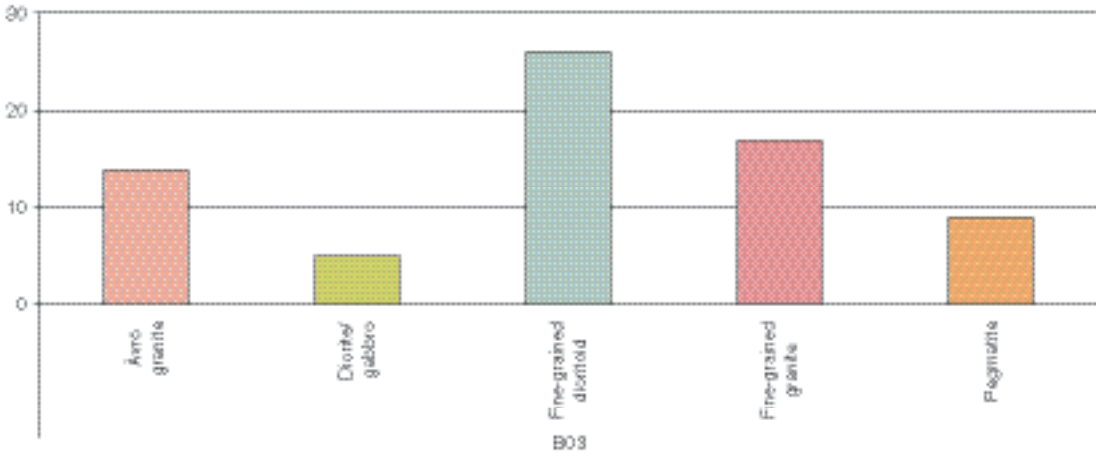

B04 contains no observation points

C01 contains 52 observation points

1) Number of observation points where each rock type is dominating.

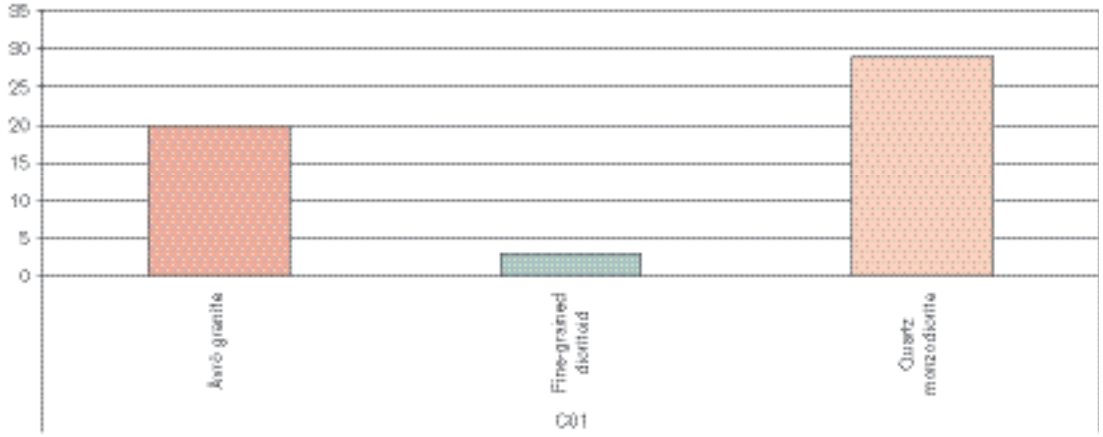

2) Number of observation points with only one rock type present.

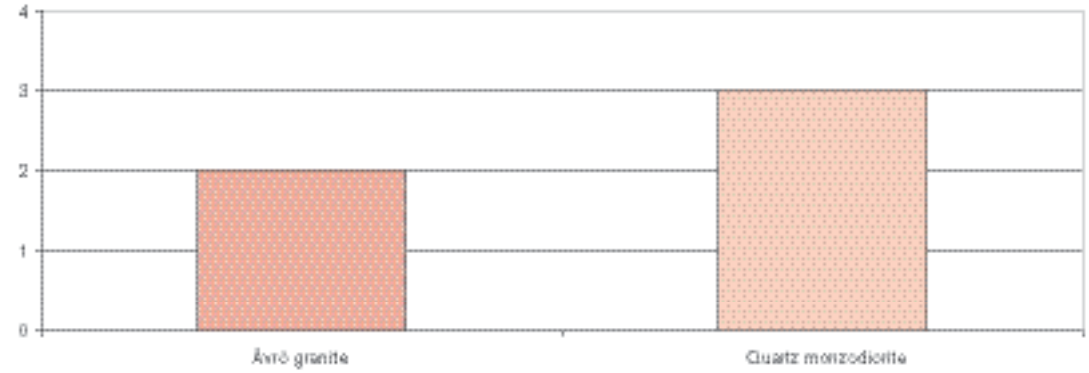

3) Number of occurrences of each rock type, of any order.

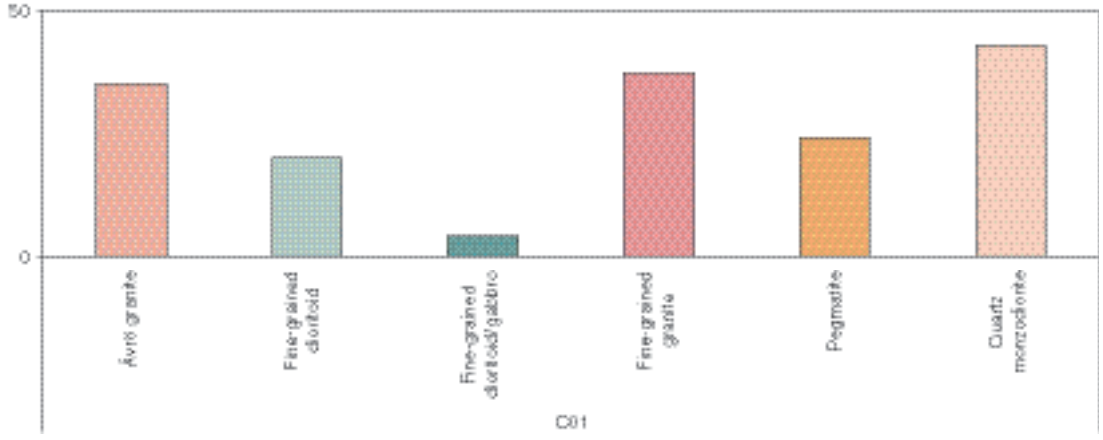

E01 – E03 contains no observation points

E04 contains 8 observation points

1) Number of observation points where each rock type is dominating.

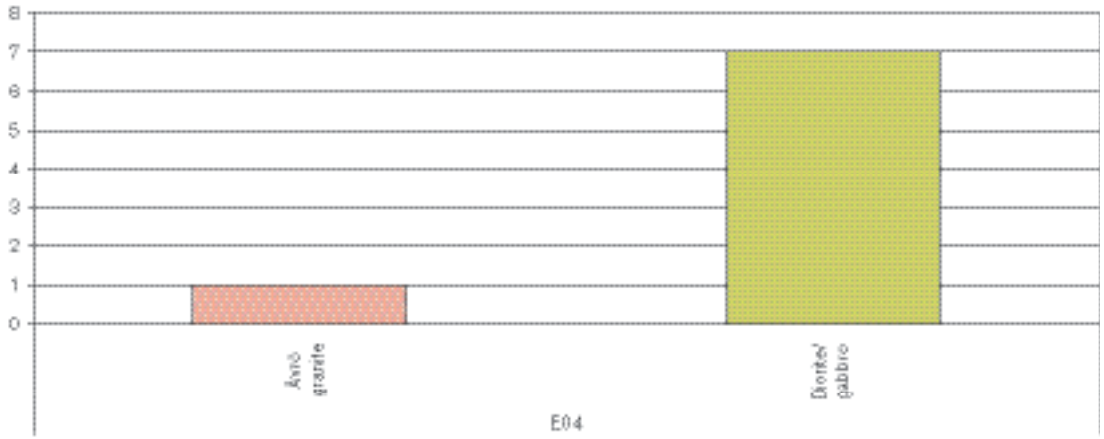

2) On one of the observation points only diorite to gabbro has been observed.

3) Number of occurrences of each rock type, of any order.

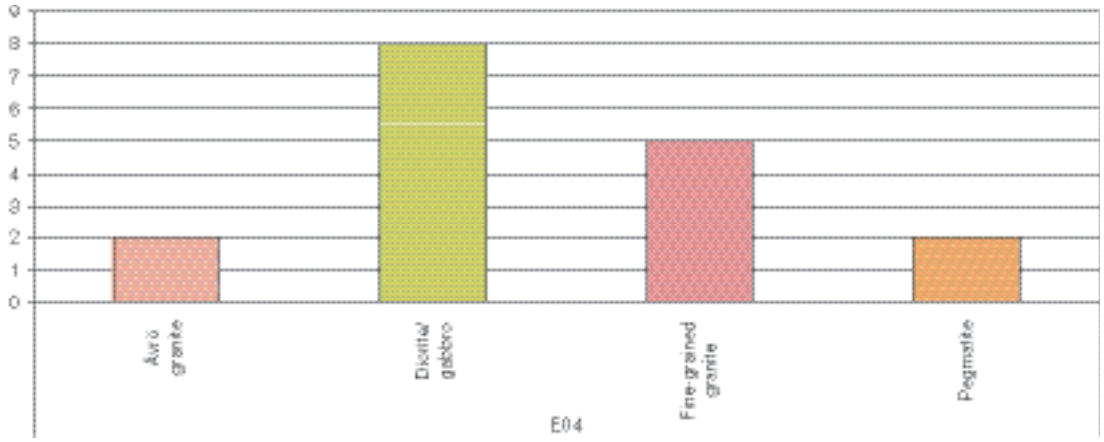

E05 contains no observation points

E06 contains only one observation point

The dominating rock type is diorite/gabbro. Secondary rock type is fine-grained granite. Pegmatite has been observed as well.

E07 and E08 contains no observation points

E08 contains only one observation point

Only diorite to gabbro has been observed on the observation point.

E09 contains only one observation point

The dominating rock type is diorite. Secondary rock type is granite. Pegmatite has been observed as well.

E10 contains only one observation point

Only diorite has been observed on the observation point.

Table A3-1. Translation key from nomenclature in the outcrop database (SGU) to SKB nomenclature. The key is custom made for this analyses and site. It is not for general use.

SGU Code	Comment	SGU Rock type (swedish names)	SKB Code	SKB Rock type
300		Basic rock	505102	Fine-grained diorite/Gabbro
1033		Diorite	501033	Diorite/Gabbro
1020		Gabbroid		
1022		Gabbro		
1036		Monzodiorite		
1038		Quartz diorite		
11146		Monzogranite	501058	Granite
1058		Granite	501058	Granite
1058 to 1098 1058 to 1061		Granite to pegmatitic granite Granite to pegmatite	511058	Fine-grained granite
1058	Remaining obs. of order less than 1	Granite	511058	Fine-grained granite
1058 to 1056 and 1058 to 1046		Granite to granodiorite and granite to quartz monzonite	501044	Ävrö granite
200		Intermediate rock	501030	Fine-grained dioritoid
1058 to 1037		Granite to quartz monzodiorite	501044	Ävrö granite
11146 to 1037		Monzogranite to quartz monzodiorite	501044	Ävrö granite
1046		Quartz monzonite	501044	Ävrö granite
1045		Monzonite		
1037		Quartz monzodiorite	501036	Quartz monzodiorite
1061		Pegmatite	501061	Pegmatite
1098		Pegmatitic granite		

8003 and 8004 = **No SKB code exists. The data is removed, since there are very few observations of these rocktypes.**

Appendix 4

Geological properties of interpreted deformation zones

This appendix presents attributed confidence of occurrence and properties for interpreted deformation zones included in the Simpevarp 1.2 regional scale model.

Table A4-1. Interpreted deformation zones attributed high confidence of occurrence.

Zone ID	Basis for interpretation	Class	Confidence	Comments
ZSMEW002A (Mederhult zone)	Linked lineaments, VLF, seismic refraction. Ground geology.	Regional	High	Position on surface: combination of a short section of XSM013A0 with v0 (Version 0, ref: R-02-35) ZSM0002A0.
ZSMEW004A	Airborne geophysics (magnetic 100 % along the length, low uncertainty), tunnel. v0.	Regional	High	Position on surface and Äspö tunnel. Based on XSM0010A0, B0 & XSM0016A0. Ref: v0.
ZSMEW007A	Airborne geophysics (magnetic 100 % along the length, electrical data, low uncertainty), topography, borehole.	Local Major	High	Ref: ZLEW02 alternative Laxemar model TR-02-19.
ZSMEW009A (EW3)	Topography, ground geology, tunnel, borehole.	Local Major	High	Ref: EW3 Geomod model.
ZSMEW013A	Airborne geophysics (magnetic 100 % along the length, electrical data, low uncertainty), topography, borehole.	Local Major	High	Ref: ZLXNW04 alternative Laxemar model.
ZSMEW028A	Airborne geophysics and BH evidence.	Local Major	High	
ZSMNE005A (Äspö shear zone)	Airborne geophysics (magnetic 100 % along the length, low to medium uncertainty), Ground geology, ground geophysics, Borehole, Äspö data.	Local Major	High	‘Äspö shear zone’. Ref: NEHQ3, EW1b Geomod model. Ref: ZSM0005A0, ZSM0004A0 v0. Ref: ZLXNE01 alternative Laxemar model.
ZSMNE006A (NE1)	Airborne geophysics (magnetic 100 % along the length, low to medium uncertainty), tunnel, boreholes, Äspö data.	Local Major	High	Ref: NE1 Geomod model. Ref: ZSM0006A0 v0. Ref: ZLXNE06 alternative Laxemar model.
ZSMNE010A	Airborne geophysics, topography, field control.	Local Major	High	Ref: ZSM0010A0, v0.
ZSMNE011A	Airborne geophysics, topography, ground geophysics.	Local Major	High	Ref: ZSM0011A0, v0.
ZSMNE012A (NE4)	Airborne geophysics Tunnel, borehole.	Local Major	High	Linked lineaments XSM0012A0, (part of B0), A1, A3 & B1. Ref: NE4, Äspö 96, TR 97-06. Ref: Z15 Ävrö model, R-01-06.
ZSMNE016A	Airborne geophysics, topography, tunnel.	Local Major	High	Only N section of lineament XSM0016A0. Ref: ZSM0004A0/B0 v0.

Table A4-1 (cont). Interpreted deformation zones attributed high confidence of occurrence.

Zone ID	Basis for interpretation	Class	Confidence	Comments
ZSMNE018A	Airborne geophysics borehole.	Local Major	High	Complex zone, single hole interpretation.
ZSMNE024A	Airborne geophysics, tunnel, borehole.	Local Major	High	Modified geometry, cross checked with KSH03, misses KSH01. Ref: Z13 Ävrö model.
ZSMNE040A	Airborne geophysics boreholes.	Local Major	High	Ref: ZSM0003A0 v0. Ref: ZLXNE04 (part ZLXNE03) alternative Laxemar model.
ZSMNS001A	Airborne geophysics, ground geophysics, topography.	Regional (A–D)	High	Ref: ZSM0001A0 /B0 v0 – general alignment agreement.
ZSMNS001B	Airborne geophysics, topography.	Regional (A–D)	High	Ref: ZSM0001A0 /B0 v0 – general alignment agreement.
ZSMNS001C	Airborne geophysics, topography.	Regional (A–D)	High	Ref: ZSM0001A0 /B0 v0 – general alignment agreement.
ZSMNS001D	Airborne geophysics, topography.	Regional (A–D)	High	Ref: ZSM0001A0 /B0 v0 – general alignment agreement.
ZSMNS009A	Airborne geophysics, topography.	Regional	High	Ref: ZSM0009A v0.
ZSMNS017A	Topography, borehole and tunnel evidence.	Local Major	High	Ref: Geomod model, NNW4.
ZSMNW004A	Airborne geophysics, ground geophysics, boreholes, topography.	Local Major	High	Ref: Z14 Ävrö model.
ZSMNW007B	Airborne geophysics, topography.	Local Major	High	Ref: ZSM0007A0 v0. Ref: ZLXNS01 alternative Laxemar model.
ZSMNW012A	Airborne geophysics, topography.	Local Major	High	Ref: ZSM0012A0 v0.
ZSMNW025A	Airborne geophysics, borehole evidence.	Local Major	High	

Table A4-2. Interpreted EW set of possible deformation zones attributed low- to intermediate confidence of occurrence.

Potential Zone	Basis for interpretation	Confidence level	Comments
EW set of possible deformation zones ZSMEW013B, ZSMEW013C ZSMEW014A, ZSMEW014B ZSMEW023A, ZSMEW023B ZSMEW026X, ZSMEW038A ZSMEW038B, ZSMEW039A ZSMEW052A, ZSMEW068A ZSMEW070A, ZSMEW076A ZSMEW114A, ZSMEW120A ZSMEW129A, ZSMEW190A ZSMEW200A, ZSMEW210A ZSMEW230A, ZSMEW240A ZSMEW305A, ZSMEW306A ZSMEW316A, ZSMEW996A ZSMEW997A, ZSMEW998A ZSMEW999A	Airborne geophysics ± topography	Low to intermediate	

Table A4-3. Interpreted NE set of possible deformation zones attributed low- to intermediate confidence of occurrence.

Potential Zone	Basis for interpretation	Confidence level	Comments
NE set of possible deformation zones ZSMNE008A, ZSMNE011X ZSMNE012B, ZSMNE018A ZSMNE019A, ZSMNE019X ZSMNE020A, ZSMNE021A ZSMNE022A, ZSMNE029A ZSMNE031A, ZSMNE032A ZSMNE033A, ZSMNE034A ZSMNE036A, ZSMNE037A ZSMNE041A, ZSMNE043A ZSMNE044A, ZSMNE045A ZSMNE050A, ZSMNE058A ZSMNE062A, ZSMNE063A ZSMNE073A, ZSMNE079A ZSMNE081A, ZSMNE094A ZSMNE095A, ZSMNE096A ZSMNE107A ZSMNE108A ZSMNE132A, ZSMNE133A ZSMNE135A, ZSMNE136A ZSMNE138A, ZSMNE138B ZSMNE185A, ZSMNE218A ZSMNE229A, ZSMNE239A ZSMNE257A, ZSMNE258A ZSMNE259A, ZSMNE267A ZSMNE286A, ZSMNE289A ZSMNE295A, ZSMNE302A ZSMNE307A, ZSMNE308B ZSMNE309A, ZSMNE301A ZSMNE993A, ZSMNE994A ZSMNE995A, ZSMNE996A ZSMNE997A, ZSMNE998A ZSMNE999A	Airborne geophysics topography ±	Low to intermediate	

Table A4-4. nterpreted NS set of possible deformation zones attributed low- to intermediate confidence of occurrence.

Potential Zone	Basis for interpretation	Confidence level	Comments
NS set of possible deformation zones ZSMNS046A, ZSMNS054A ZSMNS057A, ZSMNS059A ZSMNS059B, ZSMNS059C ZSMNS064A, ZSMNS071A ZSMNS084A, ZSMNS085A ZSMNS117A, ZSMNS140A ZSMNS141A, ZSMNS165A ZSMNS182A, ZSMNS182B ZSMNS215A, ZSMNS221A ZSMNS233A, ZSMNS287A ZSMNS291A, ZSMNS301A ZSMNS994A, ZSMNS995A ZSMNS996A, ZSMNS997A ZSMNS998A	Airborne geophysics ± topography	Low to intermediate	

Table A4-5. Interpreted NW set of possible deformation zones deformation attributed low- to intermediate confidence of occurrence.

Potential Zone	Basis for interpretation	Confidence level	Comments
NW set of possible deformation zones ZSMNW006A, ZSMNW006B ZSMNW006C, ZSMNW006D ZSMNW007A, ZSMNW030A ZSMNW035A, ZSMNW042A ZSMNW042B, ZSMNW042C ZSMNW047A, ZSMNW048A ZSMNW051A, ZSMNW052A ZSMNW060A, ZSMNW066A ZSMNW067A, ZSMNW068A ZSMNW075A, ZSMNW083A ZSMNW086A, ZSMNW087A ZSMNW088A, ZSMNW089A ZSMNW106A, ZSMNW113A ZSMNW119A, ZSMNW123A ZSMNW126A, ZSMNW126B ZSMNW131A ZSMNW134A ZSMNW170A, ZSMNW173A ZSMNW178A, ZSMNW184A ZSMNW202A, ZSMNW206A ZSMNW222A, ZSMNW233A ZSMNW234A, ZSMNW234B ZSMNW235A, ZSMNW245A ZSMNW247A, ZSMNW251A ZSMNW254A, ZSMNW261A ZSMNW263A, ZSMNW269A ZSMNW280A, ZSMNW294A ZSMNW296A, ZSMNW312A ZSMNW314A, ZSMNW321A ZSMNW322A, ZSMNW324A ZSMNW325A, ZSMNW993A ZSMNW994A, ZSMNW996A ZSMNW997A, ZSMNW998A	Airborne geophysics ± topography	Low to intermediate	

Table A4-6. Properties of interpreted deformation zone ZSMEW002A.

ZSMEW002A (Mederhult zone)					
Property	**Quantitative estimate**	**Span**	**Confidence level**	**Basis for interpretation**	**Comments**
Position		± 50 m	High	Linked lineaments	Position on surface. Combination of a short section of XSM013A0 with v0 ZSM0002A0
Orientation (strike/dip)	85/55	± 15/ ±15	Medium	Linked lineaments, VLF, seismic refraction	Strike based on model version 0, dip based on Laxemar model
Width	20 m	+50 m	Low	VLF	From model version 0
Length[1]	30 km	± 10 km	Low	Linked lineaments, model version 0	Extension outside local scale model domain based on model version 0
Ductile deformation	Likely, but no evidence				
Brittle deformation	Yes			Ground geology	From model version 0
Alteration					
Fracture orientation					
Fracture frequency					
Fracture filling					

[1] Concerns total length. Extends outside both local scale and local scale model domain.

Table A4-7. Properties of interpreted deformation zone ZSMEW004A.

ZSMEW004A					
Property	**Quantitative estimate**	**Span**	**Confidence level**	**Basis for interpretation**	**Comments**
Position		± 50 m	High	Linked lineaments, tunnel (Äspö TASA ch. 318 m)	Position on surface and Äspö tunnel. Based on XSM0010A0, B0 & XSM0016A0
Orientation (strike/dip)	71/70	± 15/ ±15	High	Linked lineaments, Äspö TASA ch. 318 m	Dip from model version 0, ZSM0004A0. Dip in tunnel =75°
Width	30 m	± 20 m	Medium	v0=50 m	Äspö TASA ch. 318 m =30 m.
Length[1]	c. 11 km	± 5 km	Low	Linked lineaments, model version 0	Based on XSM0010A0, B0 & XSM0016A0
Ductile deformation					
Brittle deformation	Yes			Äspö TASA ch. 318 m	
Alteration					
Water	5 l/min inflow to tunnel		High	Äspö TASA ch. 318 m	
Fracture orientation	Not yet assessed			Äspö TASA ch. 318 m	
Fracture frequency	Not yet assessed			Äspö TASA ch. 318 m	
Fracture filling	Chl, Ca, Cy, Fe, Qz		High	Äspö TASA ch. 318 m	

[1] Concerns total length. Extends outside local scale model domain.

Table A4-8. Properties of interpreted deformation zone ZSMEW007A.

ZSMEW007A					
Property	**Quantitative estimate**	**Span**	**Confidence level**	**Basis for interpretation**	**Comments**
Position		± 50 m	Medium	Linked lineaments	Position on surface
Orientation (strike/dip)	277/52	± 20 / ±	Medium in strike, low in dip	Dip from seismic reflector and KLX02 (340 m)	ZLEW02 alt' Lax' mod'
Width	2 m	1–10 m	Medium		ZLEW02 alt' Lax' mod', based on one observation
Length[1]	4.2 km		Medium	Linked lineaments	does not include EW007B
Ductile deformation					
Brittle deformation	Cataclastic		High	Crush zone and fracture zone in KLX02 (340 m)	Based on one observation
Alteration	C. 50% medium strong oxidation		High	Altered section in KLX02 (340 m)	Based on one observation
Water					
Fracture orientation	Not yet assessed				
Fracture frequency	24.3 fractures per metre		High	Crush zone and fracture zone in KLX02 (340 m)	Based on one observation
Fracture filling	Not yet assessed				

[1] Concerns total length. Extends outside local scale model domain.

Table A4-9. Properties of interpreted deformation zone ZSMEW009A.

ZSMEW009A (EW3)					
Property	**Quantitative estimate**	**Span**	**Confidence level**	**Basis for interpretation**	**Comments**
Position		± 50 m	Medium	Linked lineaments	Position in tunnel, borehole, Geomod
Orientation (strike/dip)	85/76	± 15 / ± 15	High	Tunnel, topo, BH, Mag, Mapping (trench)	EW3 Geomod. Dip from TASA 1,407 m, Trench point X=6367638, Y=1551412, Z=2
Width	12 m	5 to 20 m	High	Äspö TASA 1,407 m	EW3 Geomod
Length	1.8 km		Medium	Linked lineaments	
Ductile deformation					
Brittle deformation	Yes		High	Äspö TASA 1,407 m	
Alteration	1.5–2 m central clay zone		High	Äspö TASA 1,407 m	EW3 Geomod
Water	90 litres/min		High	Äspö TASA 1,407 m	90 litres/min
Fracture orientation	Not yet assessed				
Fracture frequency	10 m^{-1}		High	Borehole KAS06 (66 m)	'mean' value but ignores sections of crushed core
Fracture filling	Chl, Cy, Ca, Fl		High	Borehole KAS06 (66 m)	mapped as mylonitic

[1] Concerns total length. Extends outside local scale model domain.

Table A4-10. Properties of interpreted deformation zone ZSMEW013A.

ZSMEW013A					
Property	**Quantitative estimate**	**Span**	**Confidence level**	**Basis for interpretation**	**Comments**
Position		± 50 m	Medium	Linked lineaments, ZLXNW04,	Position on surface, XSM0013A0, modified to terminate against ZSMEW002A in W, comb' wih XSM0014A0 in E.
Orientation (strike/dip)	270/90	± 15 / ± 15	Medium strike, low dip	Linked lineaments, borehole HLX02	HLX02 penetrates a zone ''related'' to the lineament (Lax' mod').
Width	20 m		Low	Default	
Length	3.2 km		Low	Linked lineaments	XSM0013A0, modified to terminate against ZSMEW002A in W, comb' wih XSM0014A0 in E.
Ductile deformation					
Brittle deformation	Cataclastic		Medium	Topography, HLX02	
Alteration					
Fracture orientation					
Fracture frequency					
Fracture filling					

[1] Concerns total length. Extends outside local scale model domain.

Table A4-11. Properties of interpreted deformation zone ZSMEW028A.

ZSMEW028A					
Property	**Quantitative estimate**	**Span**	**Confidence level**	**Basis for interpretation**	**Comments**
Position		± 50 m	Medium		
Orientation (strike/dip)	095/83				
Width	10 m			HAV09 centred on 87.5 m, width covers 70–105 m	Low resistivity,BH section resistivity < 400
Length	1.1 km			Linked lineaments	
Ductile deformation					
Brittle deformation					
Alteration					
Fracture orientation					
Fracture frequency					
Fracture filling					

[1] Concerns total length. Extends outside local scale model domain.

Table A4-12. Properties of interpreted deformation zone ZSMNE005A.

ZSMNE005A (Äspö shear zone)					
Property	**Quantitative estimate**	**Span**	**Confidence level**	**Basis for interpretation**	**Comments**
Position		+/–50 m	Medium	Linked lineaments, v0	
Orientation (strike/dip)	40/80	Dip 70–90 NW ductile sinistral; 60–90 SE brittle dextral	High	Linked lineaments	Ref: NEHQ3, EW1b Geomod; ZSM0005A0, ZSM0004A0 v0; ZLXNE01 Lax'
Width	40 m	Ductile 10–40 m Brittle 70–200 m	High	v0	
Length	5.1 km		Low	Linked lineaments	
Ductile deformation	Mylonitic		High	Field data, Äspö data	
Brittle deformation	Cataclastic		High	Field data, ground geophysics, Äspö data	
Alteration	Not yet assessed				
Fracture orientation	Not yet assessed				
Fracture frequency	Not yet assessed				
Fracture filling	Not yet assessed				

[1] Concerns total length. Extends outside local scale model domain.

Table A4-13. Properties of interpreted deformation zone ZSMNE006A.

ZSMNE006A (NE1)					
Property	**Quantitative estimate**	**Span**	**Confidence level**	**Basis for interpretation**	**Comments**
Position		+/–50 m	Medium	Linked lineaments	Ref: NE1 Geomod, ZSM0006A0 v0, ZLXNE06 Lax'
Orientation (strike/dip)	224/65	+/–15 / +/–15	Medium	Strike- linked lineaments, dip- Geomod NE1	KA1061 203 m, KA1131B 188 m, KAS07 550 m, KAS08 569 m, KAS09 81 m, KAS11 188 m, KAS14 71 m, KBH02 687 m, KAS02 860 m
Width	28 m		High	Äspö TASA tunnel 1,290 m (northernmost branch)	Complex zone with 3 branches total 60 m
Length	2.0 km	+/–5 km	Low	Linked lineaments	
Ductile deformation					
Brittle deformation	Yes		High	Äspö TASA 1,290 m	
Alteration	1 m wide, central, completely clay altered		High	Äspö TASA l 1,290 m	5–8 m wide partially clay altered
Water	2,000 l/min		High	Äspö TASA 1,290 m	
Fracture orientation	Not yet assessed				
Fracture frequency	Not yet assessed				
Fracture filling	Chl, Cy, Ca, Fl, Fe, Ep, Qz, My		High	Äspö TASA 1,290 m	

[1] Concerns total length. Extends outside local scale model domain.

Table A4-14. Properties of interpreted deformation zone ZSMNE010A.

ZSMNE010A					
Property	**Quantitative estimate**	**Span**	**Confidence level**	**Basis for interpretation**	**Comments**
Position		± 50 m	Medium	Linked lineaments	Ref: v0. Verified by field control- epidote healed fractures
Orientation (strike/dip)	055/90				
Width	20 m (default)				Previously 1 m (default in v0
Length	3.4 km				
Ductile deformation					
Brittle deformation					
Alteration					
Water					
Fracture orientation					
Fracture frequency					
Fracture filling					

[1] Concerns total length. Extends outside local scale model domain.

Table A4-15. Properties of interpreted deformation zone ZSMNE011A.

ZSMNE011A					
Property	**Quantitative estimate**	**Span**	**Confidence level**	**Basis for interpretation**	**Comments**
Position	± 50 m			linked lineaments	Ref: v0. Verified by ground magnetic and VLF measurements
Orientation (strike/dip)	44/90				
Width	10 m				Ref: v0
Length	8.6 km				
Ductile deformation	Yes			Field evidence	Ref: v0
Brittle deformation	Yes			Field evidence	Ref: v0 increased small scale fractoring, mesoscopic brittle and ductile-brittle deformation zones and epidote healed fractures
Alteration					
Water					
Fracture orientation					
Fracture frequency					
Fracture filling	Ep				

[1] Concerns total length. Extends outside local scale model domain.

Table A4-16. Properties of interpreted deformation zone ZSMNE012A.

ZSMNE012A (NE4)					
Property	**Quantitative estimate**	**Span**	**Confidence level**	**Basis for interpretation**	**Comments**
Position		+/–50 m	Medium	Linked lineaments	Linked lineaments XSM0012A0, (part of B0), A1, A3 & B1.
Orientation (strike/dip)	58/50	+/–15 / +/–15	High	Strike from Linked lineaments, Dip from Äspö TASA ch. 827 m, additional points KAV01 413 m, KAV03 190 m, HAV07 98 m, plus 6 points from 3 interpreted reflectors (all Z15 Ävrö model) KAV04A 690–710 m	
Width	41 m		High	Äspö TASA ch. 827 m	NE4
Length	6.7 km	+/–1 km	Low		Linked lineaments XSM0012A0, (part of B0), A1, A3 & B1.
Ductile deformation					
Brittle deformation	Yes		High	Äspö TASA ch. 827 m, KAV01 413 m, Z15 (Ävrö)	
Alteration	Clay		High	KAV01 413 m, Z15 (Ävrö)	
Water	60 l/min		High	Äspö TASA ch. 827 m	
Fracture orientation	Not yet assessed				
Fracture frequency	Not yet assessed				
Fracture filling	Chl, Cy, Ep		High	Äspö TASA ch. 827 m	

[1] Concerns total length. Extends outside local scale model domain.

Table A4-17. Properties of interpreted deformation zone ZSMNE016A.

ZSMNE016A					
Property	**Quantitative estimate**	**Span**	**Confidence level**	**Basis for interpretation**	**Comments**
Position		+/–50 m	Medium	Modified linked lineaments	Only N section of lineament XSM0016A0. Partial coincidence with v0. ZSM0004B0
Orientation (strike/dip)	30/90	+/–15 / +/–15	Medium	Modified linked lineaments. Äspö TASA ch. 359 m	Only N section of lineament XSM0016A0
Width	13 m		High	Äspö TASA ch. 359 m	
Length	1.5 km		Medium	Modified linked lineaments	
Ductile deformation					
Brittle deformation	Yes		High	Äspö TASA ch. 359 m	
Alteration					
Water	0.5 l/min		High	Äspö TASA ch. 359 m	
Fracture orientation					
Fracture frequency					
Fracture filling	Chl, Cy, Ca, Fe		High		

[1] Concerns total length. Extends outside local scale model domain.

Table A4-18. Properties of interpreted deformation zone ZSMNE018A.

ZSMNE018A					
Property	**Quantitative estimate**	**Span**	**Confidence level**	**Basis for interpretation**	**Comments**
Position		± 50 m	Medium		
Orientation (strike/dip)	50/90				
Width	30 m			HSH02 centred on 85 m. Width covers multiple Def zones between 15 to 148 m	Complex zone. Single hole interpretation.
Length	6.5 km			Linked lineaments	
Ductile deformation					
Brittle deformation					
Alteration					
Water					
Fracture orientation					
Fracture frequency					
Fracture filling					
				ZSMNE018A, an interpreted splay of this zone has been identified by ground geophysics Ref: P-03-66)	

[1] Concerns total length. Extends outside local scale model domain.

Table A4-19. Properties of interpreted deformation zone ZSMNE024A.

ZSMNE024A					
Property	**Quantitative estimate**	**Span**	**Confidence level**	**Basis for interpretation**	**Comments**
Position		+/–50 m	Medium	Linked lineaments	
Orientation (strike/dip)	230/73	+/–15 / +/–15	High	Linked lineaments. 6 points from 4 seismic reflectors from Z13 (Ävrö)	Complex zone. Now misses bottom of KSH01. KSH03 (180–280 m reduced RQD, SICADA).
Width	80 m		High	Ävrö Z13 (seismic)	
Length	9.7 km	+10 km	Low	Linked lineaments	
Ductile deformation					
Brittle deformation					
Alteration					
Water					
Fracture orientation					
Fracture frequency					
Fracture filling					

[1] Concerns total length. Extends outside local scale model domain.

Table A4-20. Properties of interpreted deformation zone ZSMNE040A.

ZSMNE040A					
Property	**Quantitative estimate**	**Span**	**Confidence level**	**Basis for interpretation**	**Comments**
Position		+/–50 m	Medium	Linked lineaments	
Orientation (strike/dip)	91/73	+/–15 / +/–15	High	Linked lineaments. Dip based on KLX01 (421 m) & KLX02 (1,040 m)	Linked lineaments, ZSM0003A0 v0, ZLXNE04 and part of ZLXNE03, Laxemar model
Width	15 m	1–30 m	High	KLX01 (421 m) & KLX02 (1,040 m)	ZLXNE03 and ZLXNE04 Laxemar model
Length	3.3 km		Low	Linked lineaments	extended
Ductile deformation					
Brittle deformation	Cataclastic		High	HLX04, KLX01 (421 m) & KLX02 (1,040 m)	ZLXNE03 and ZLXNE04 Laxemar model
Alteration	Oxidation		High	KLX01 (421 m)	ZLXNE04 Laxemar model
Fracture orientation	NNE		High	KLX01 (421 m)	ZLXNE04 Laxemar model
Fracture frequency	14 per m		High	KLX01 (421 m) & KLX02 (1,040 m)	ZLXNE03 and ZLXNE04 Laxemar model
Fracture filling	Ca, Chl, Ep, Fe		High	KLX01 (421 m) & KLX02 (1,040 m)	ZLXNE03 and ZLXNE04 Laxemar model

[1] Concerns total length. Extends outside local model domain.

Table A4-21. Properties of interpreted deformation zone ZSMNS001A–D.

ZSMNS001A–D					
Property	**Quantitative estimate**	**Span**	**Confidence level**	**Basis for interpretation**	**Comments**
Position	± 50	± 50–100			v0. verified by ground geophysics
Orientation (strike/dip)	10/90			Linked lineaments	Steep to vertical dip – VLF
Width	10 m				Ref: v0 ZSMN0001A /B
Length	> 10 km			Linked lineaments	
Ductile deformation	yes			Field evidence	Mesoscopic brittle-ductile shear zones along or close to the marked fracture zone
Brittle deformation	Yes			Field evidence	
Alteration					
Fracture orientation					
Fracture frequency					
Fracture filling	Locally epidote			Field evidence	

[1] Concerns total length. Extends outside local model domain.

Table A4-22. Properties of interpreted deformation zone ZSMNS009A.

ZSMNS009A					
Property	**Quantitative estimate**	**Span**	**Confidence level**	**Basis for interpretation**	**Comments**
Position	± 50–100				v0. Verified by ground magnetic and VLF.
Orientation (strike/dip)	12/90				v0
Width	50 m				v0
Length	10 km				Linked lineaments, XSM0056.
Ductile deformation	Yes			Field evidence	increased small scale fracturing, mesoscopic brittle and brittle-ductile deformation zones and epidote-healed fractures.
Brittle deformation	Yes			Field evidence	
Alteration					
Fracture orientation					
Fracture frequency					
Fracture filling	Ep				

[1] Concerns total length. Extends outside local model domain.

Table A4-23. Properties of interpreted deformation zone ZSMNS017A.

ZSMNS017A					
Property	**Quantitative estimate**	**Span**	**Confidence level**	**Basis for interpretation**	**Comments**
Position		+/–50 m	Medium	Linked lineaments	
Orientation (strike/dip)	174/90	+/–15 / +/–15	High	Äspö TASA ch. 1,876 m, 1,979 m and 3,083 m	One of a number of parallel steep structures present in this area, ref: NNW4 Geomod.
Width	20 m	0.5–10 m	High	Äspö TASA ch. 1,876 m, 1,979 m and 3,083 m	
Length	2.9 km		Low	Linked lineaments	
Ductile deformation					
Brittle deformation	Cataclastic		High	KA2048B 35 m,	
Alteration	Weak to medium		High	Äspö TASA ch. 1,876 m, 1,979 m and 3,083 m	
Water	102 l/min	100–500 l/min	High	TASA 1,876 m	One of a number of parallel steep structures present in this area, ref: NNW4 Geomod.
Fracture orientation					
Fracture frequency	8 fractures per m and crushed core c. 1 m total		High	KA2048B 35 m	
Fracture filling	Clay, Chl, Ca, Ep		High	Äspö TASA ch. 1,876 m, 1,979 m and 3,083 m	

[1] Concerns total length. Extends outside local scale model domain.

Table A4-24. Properties of interpreted deformation zone ZSMNW004A.

ZSMNW004A					
Property	**Quantitative estimate**	**Span**	**Confidence level**	**Basis for interpretation**	**Comments**
Position		+/–50 m	Medium	Linked lineaments	
Orientation (strike/dip)	108/49	+/–15 / +/–15	Medium	Linked lineaments, seismic reflectors from Z14 version 2 (Ävro model)	
Width	50 m	+/–20 m	Medium	Z14 version 2 (Ävro model)	
Length	0.9 km		Low	Linked lineaments	
Ductile deformation					
Brittle deformation					
Alteration					
Fracture orientation					
Fracture frequency					
Fracture filling					

[1] Concerns total length. Extends outside local scale model domain.

Table A4-25. Properties of interpreted deformation zone ZSMNW007B.

ZSMNW007B					
Property	**Quantitative estimate**	**Span**	**Confidence level**	**Basis for interpretation**	**Comments**
Position		+/–50 m	Medium	Linked lineaments	XSM0003A1
Orientation (strike/dip)	165/90	+/–15 / +/–15	Medium	Linked lineaments, ZSM0007A0 v0, ZLXNS01 (Lax')	XSM0003A1
Width	50 m	+/–20 m	Medium	ZSM0007A0 v0 (topo', ground geophys), ZLXNS01 (Lax')	
Length	3.9 km		Low	Linked lineaments	
Ductile deformation					
Brittle deformation	Yes		Low	v0 (topo', ground geophys)	
Alteration					
Fracture orientation					
Fracture frequency					
Fracture filling					

[1] Concerns total length. Extends outside local scale model domain.

Table A4-26. Properties of interpreted deformation zone ZSMNW012A.

ZSMNW012A					
Property	**Quantitative estimate**	**Span**	**Confidence level**	**Basis for interpretation**	**Comments**
Position	± 50–100 m				Verified with ground magnetic and VLF, v0
Orientation (strike/dip)	330/90				XSM0270C1 and XSM0270C4 combined
Width	40 m				v0 ZSM0012A0
Length	2.8 km				XSM0270C1 and XSM0270C4 combined
Ductile deformation					
Brittle deformation					
Alteration					
Fracture orientation					
Fracture frequency					
Fracture filling					

[1] Concerns total length. Extends outside local scale model domain.

Table A4-27. Properties of interpreted deformation zone ZSMNW025A.

ZSMNW025A					
Property	**Quantitative estimate**	**Span**	**Confidence level**	**Basis for interpretation**	**Comments**
Position					
Orientation (strike/dip)	111/88				
Width	5 m			HSH01 centred on 165 m, covering 160–171 m	(HSH01) single hole interpretation DZ2
Length	1.9 km				
Ductile deformation					
Brittle deformation					
Alteration					
Fracture orientation					
Fracture frequency					
Fracture filling					

[1] Concerns total length. Extends outside local scale model domain.

Appendix 5

Accounting of Hydraulic test results

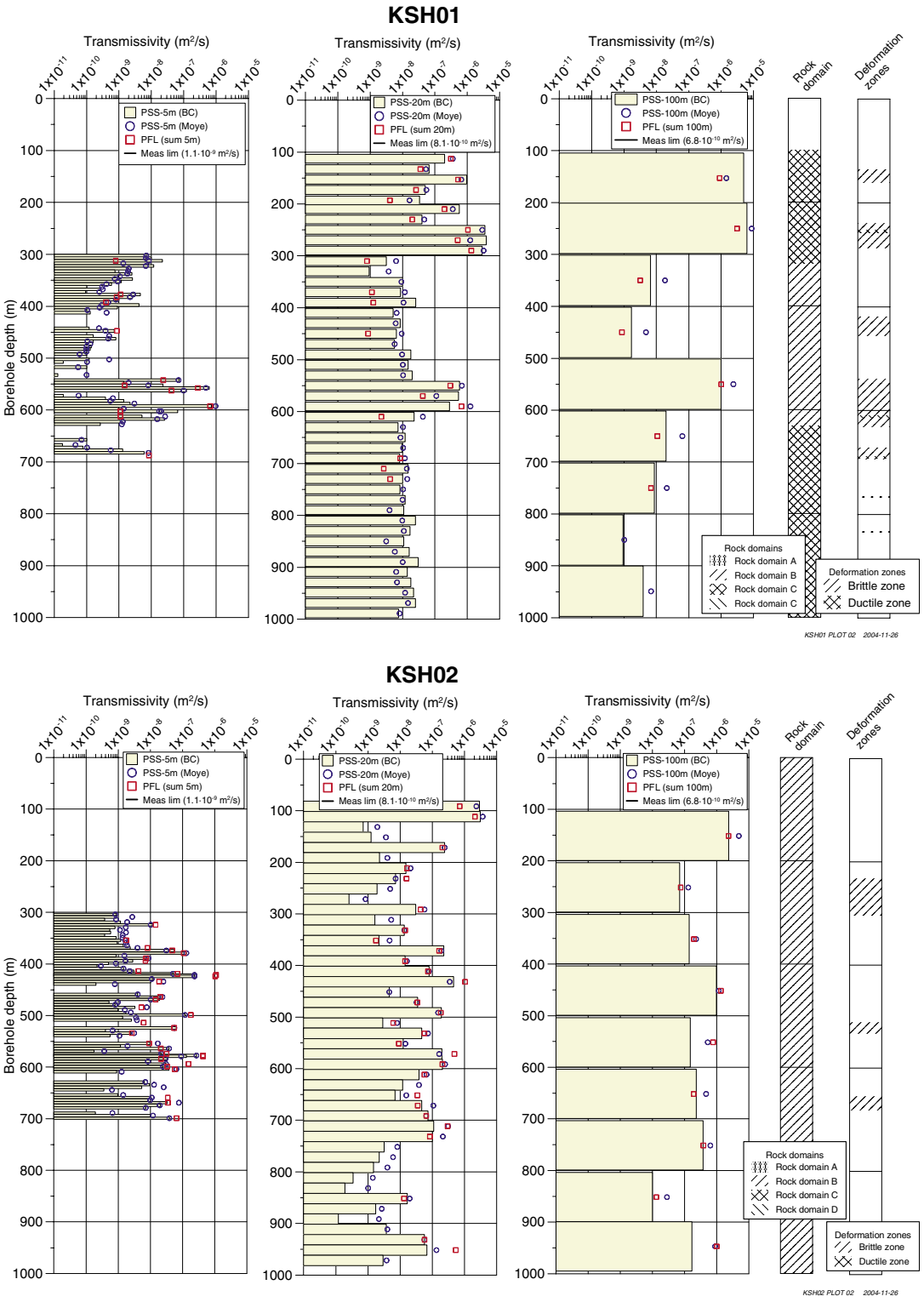

Figure A5-1. *PSS measurements in KSH01A and KSH02 – properties expressed as transmissivities.*

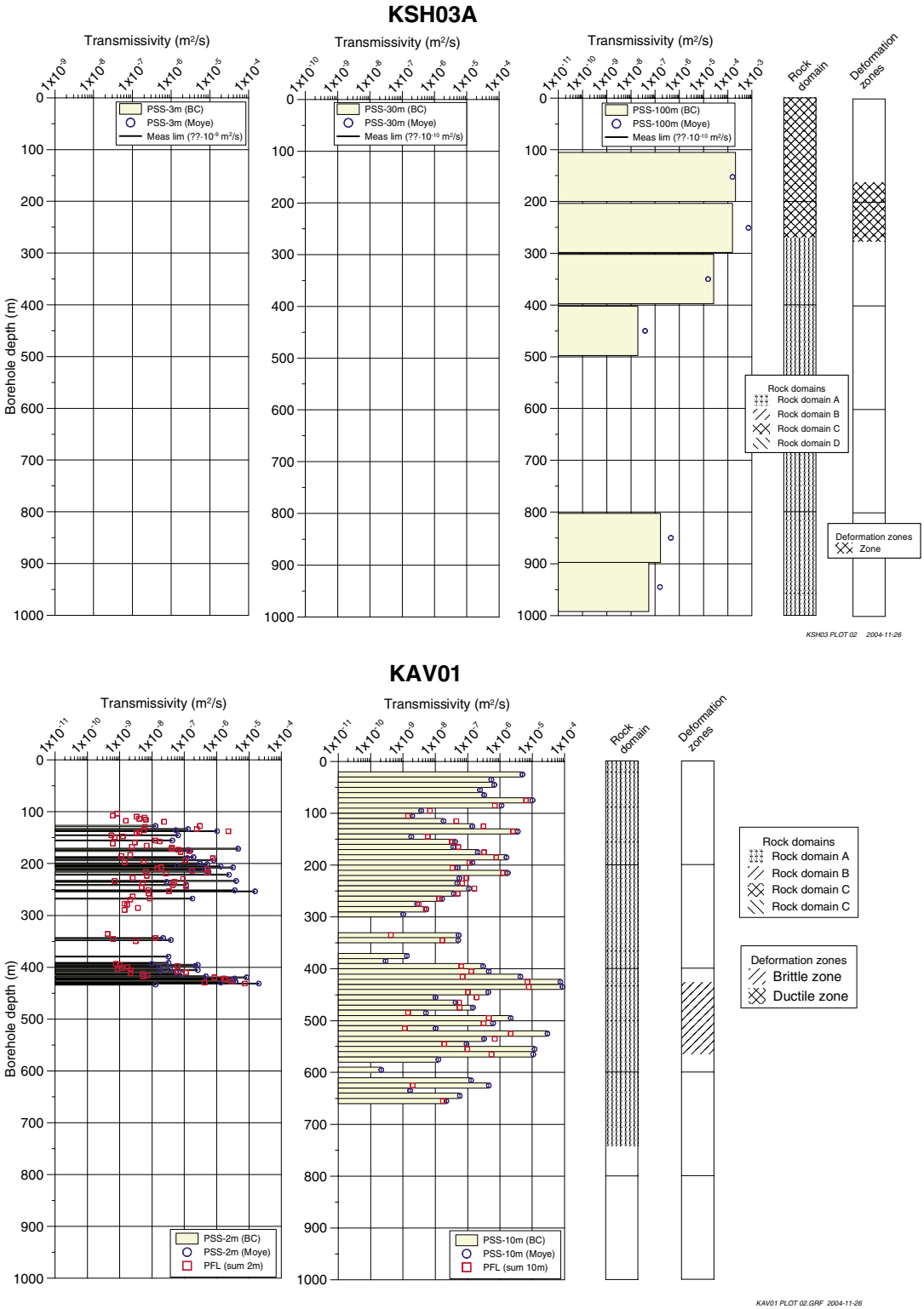

Figure A5-2. *PSS measurements in KSH03A and KAV01 – properties expressed as transmissivities.*

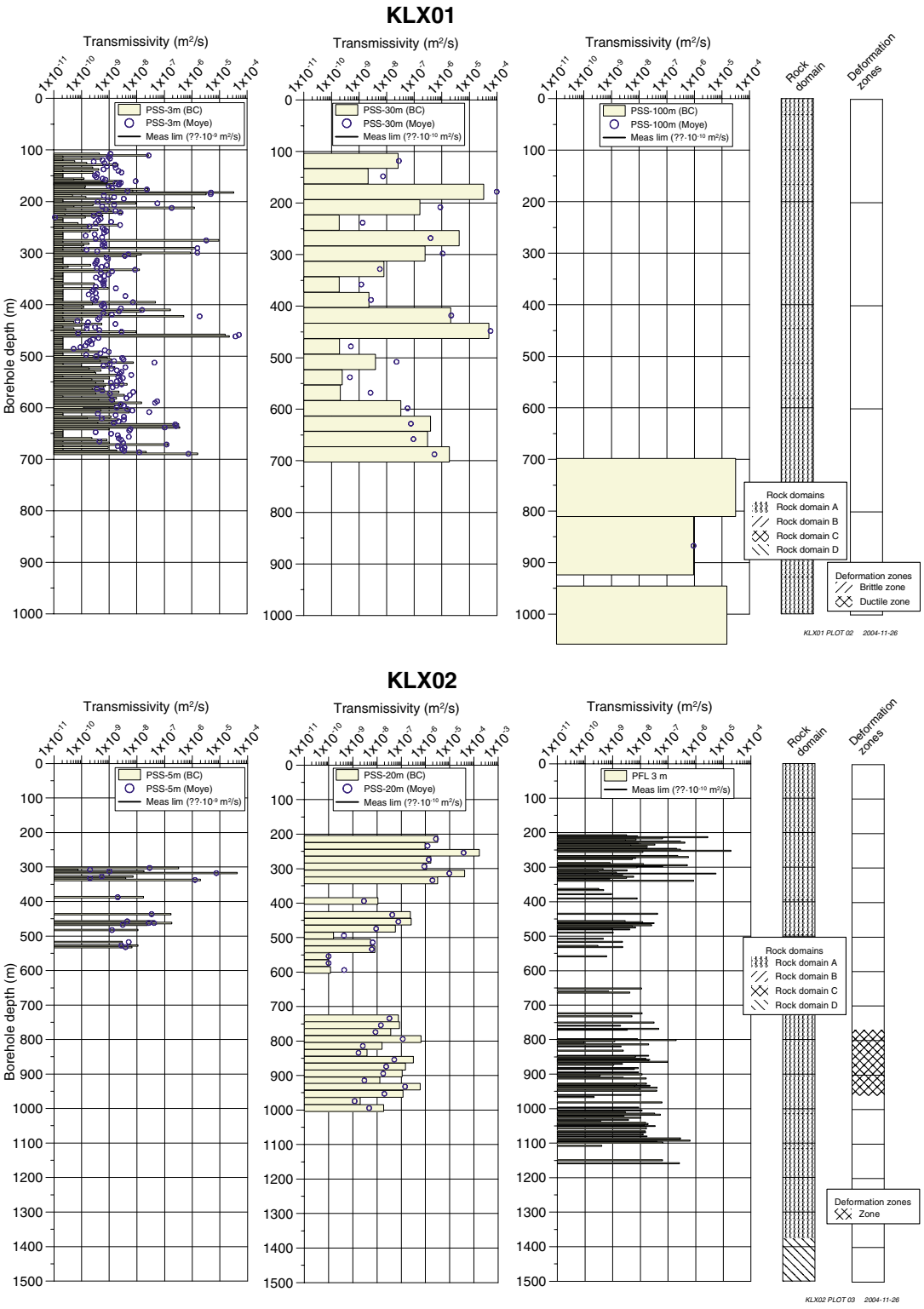

Figure A5-3. *PSS measurements in KLX01 and KLX02 – properties expressed as transmissivities. Transmissivities of borehole KLX02 based on PSS and PFL data.*

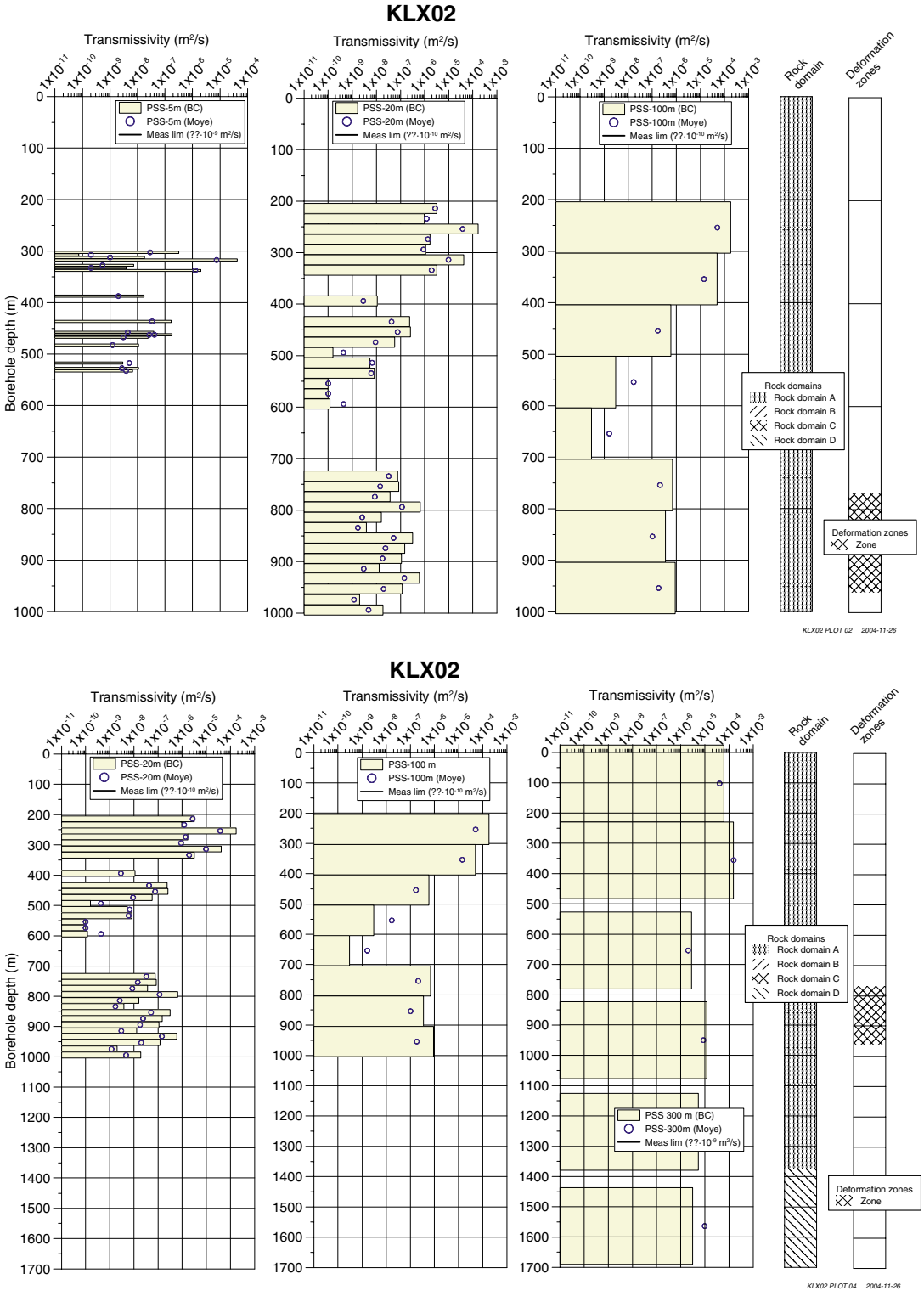

Figure A5-4. *PSS measurements in KLX02 – properties expressed as transmissivities.*

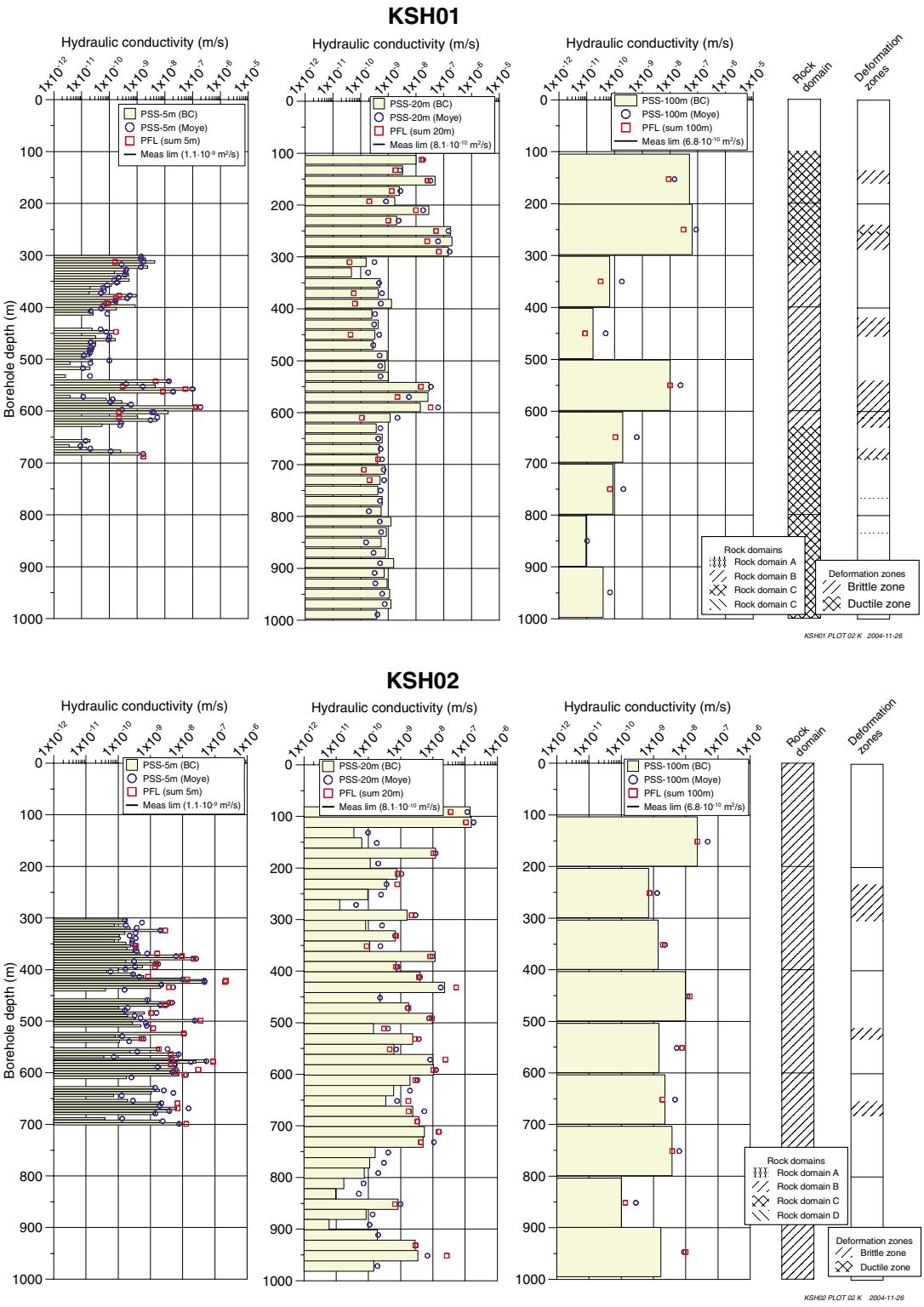

Figure A5-5. *PSS measurements in KSH01A and KSH02 – properties expressed as hydraulic conductivities.*

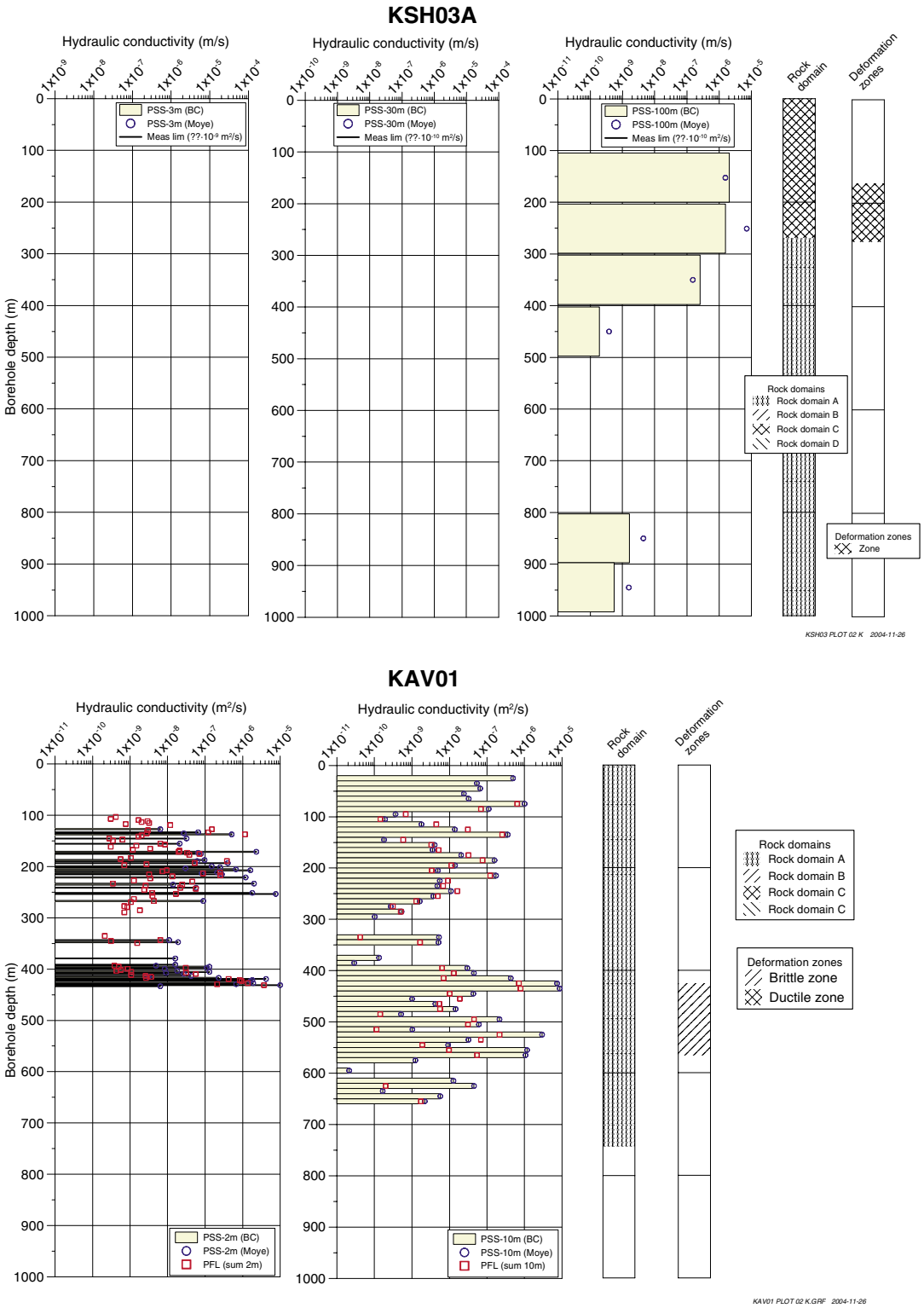

Figure A5-6. *PSS measurements in KSH03A and KAV01 – properties expressed as hydraulic conductivities.*

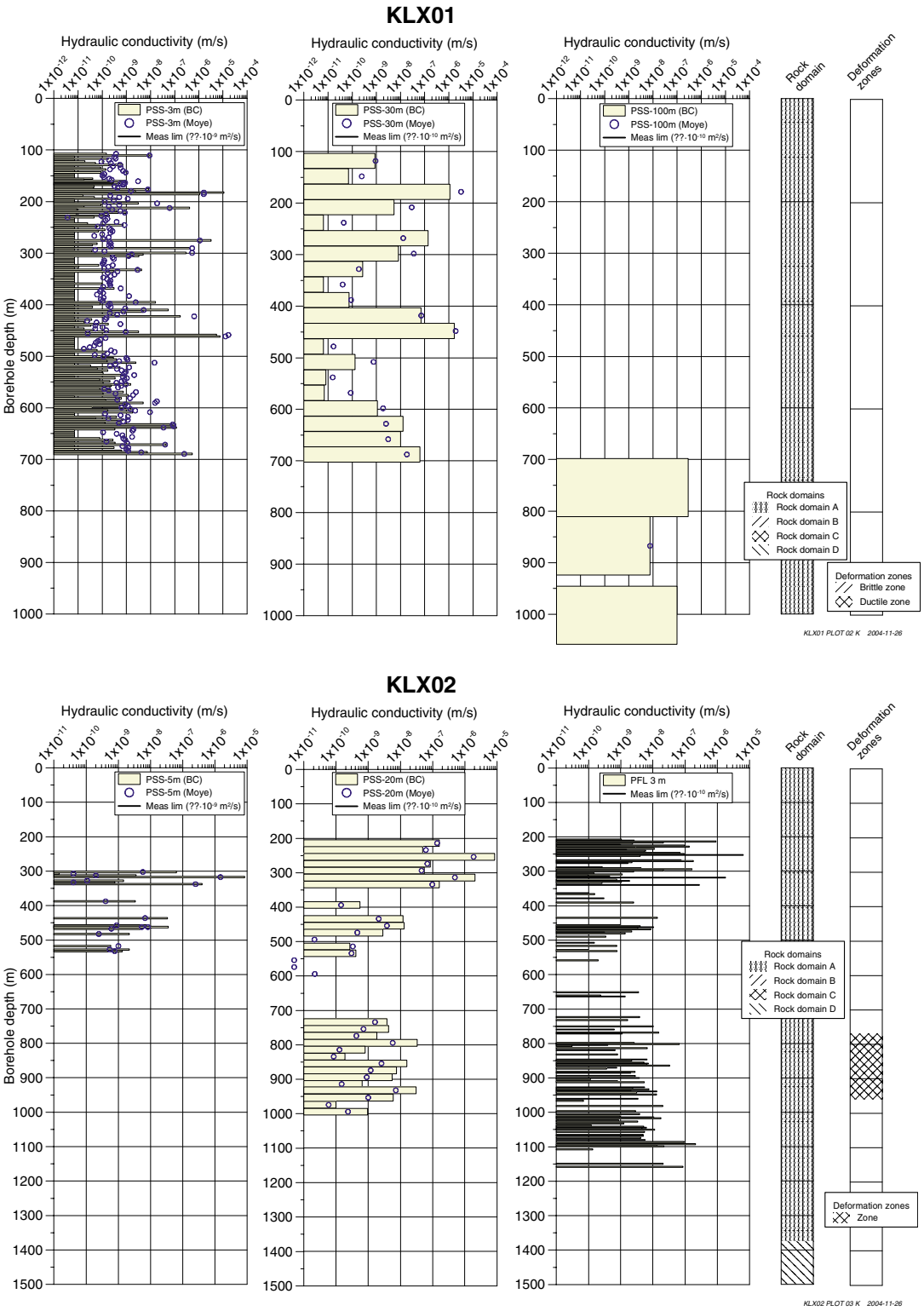

Figure A5-7. *PSS measurements in KLX01 and KLX02 – properties expressed as hydraulic conductivities. Hydraulic conductivities of borehole KLX02 based on PSS and PFL data.*

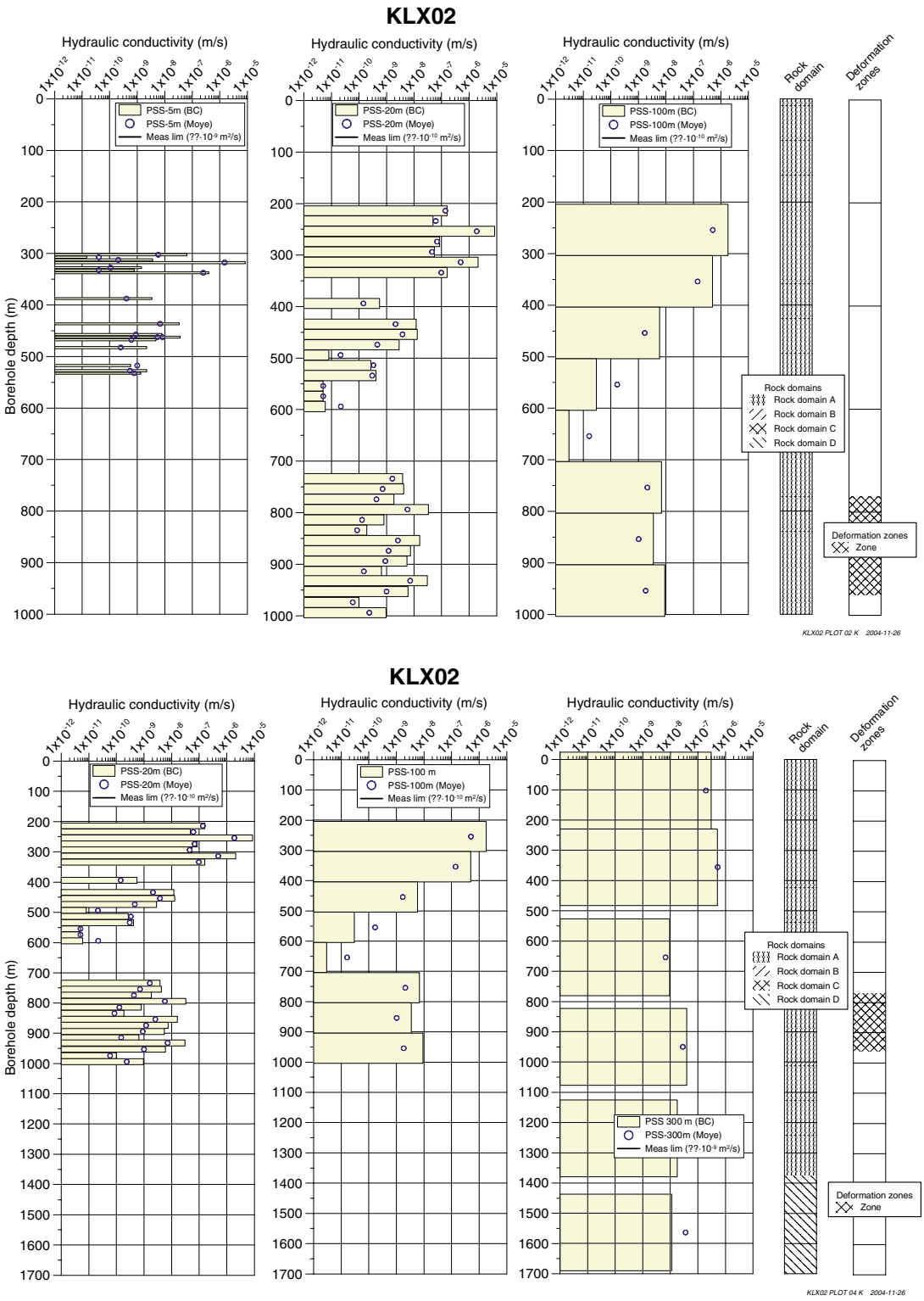

Figure A5-8. *PSS measurements in KLX02 – properties expressed as hydraulic conductivities.*

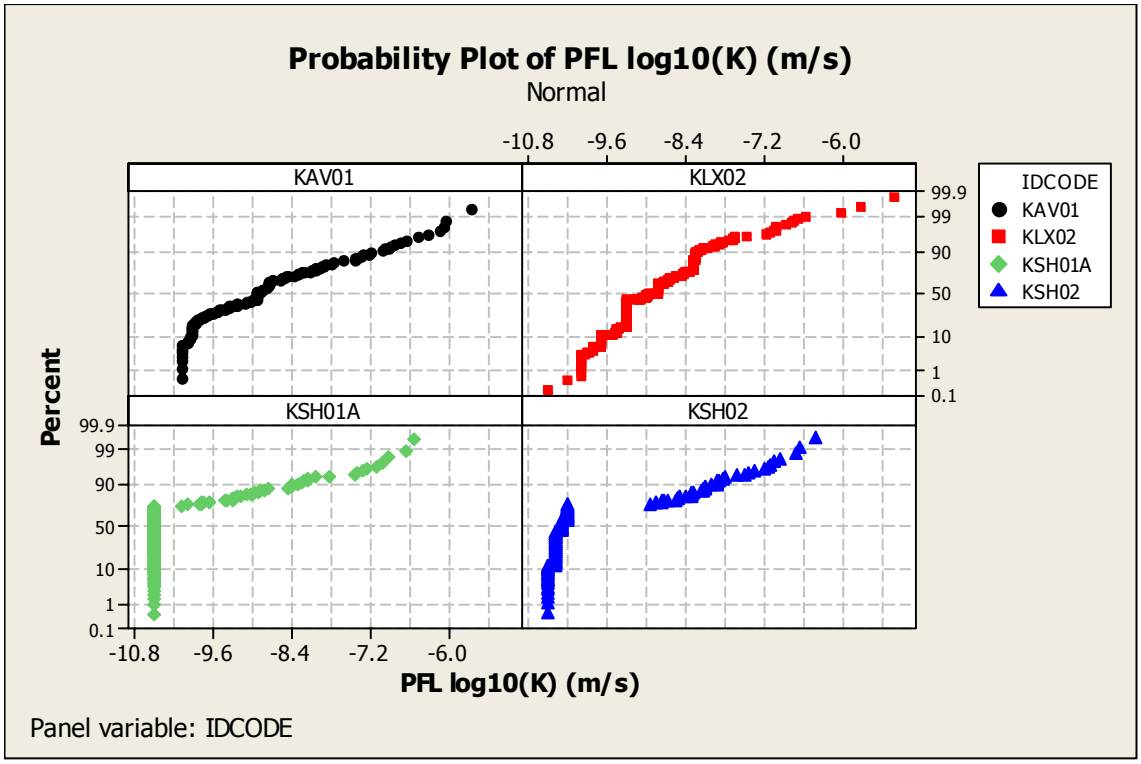

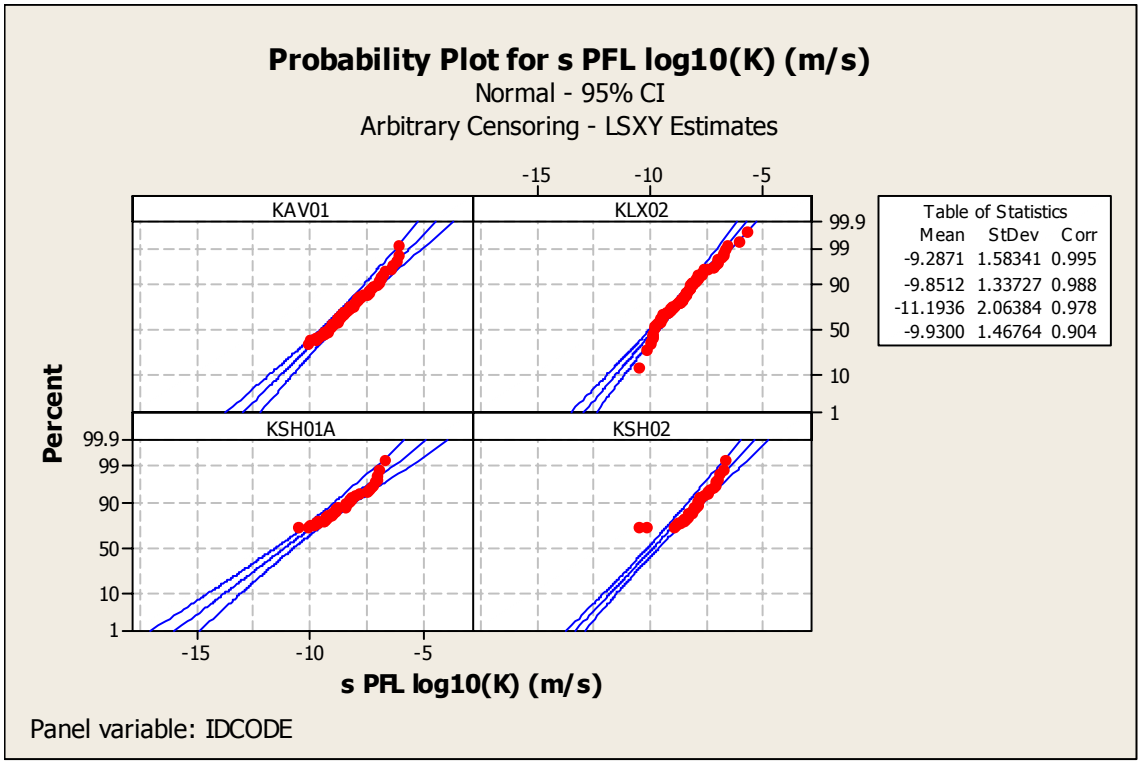

Figure A5-9. *Probability distribution plots of PFL sequential measurements in KSH01A, KSH02, KAV01 and KLX02. Tests scales 5 and 3 m.*

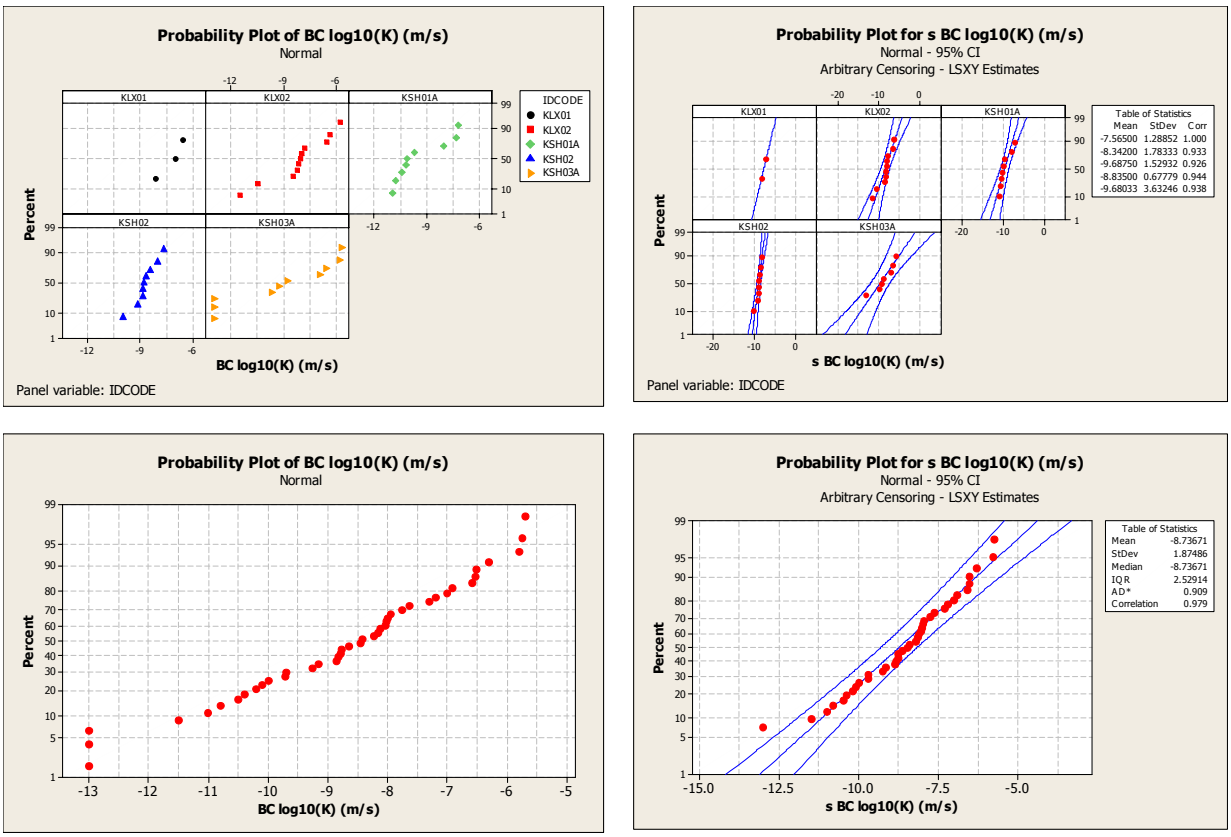

Figure A5-10a. *Probability distribution plots of PSS measurements, test scale 100 m. Boreholes KSH01A, KSH02, KSH03A, KLX01, KLX02.*

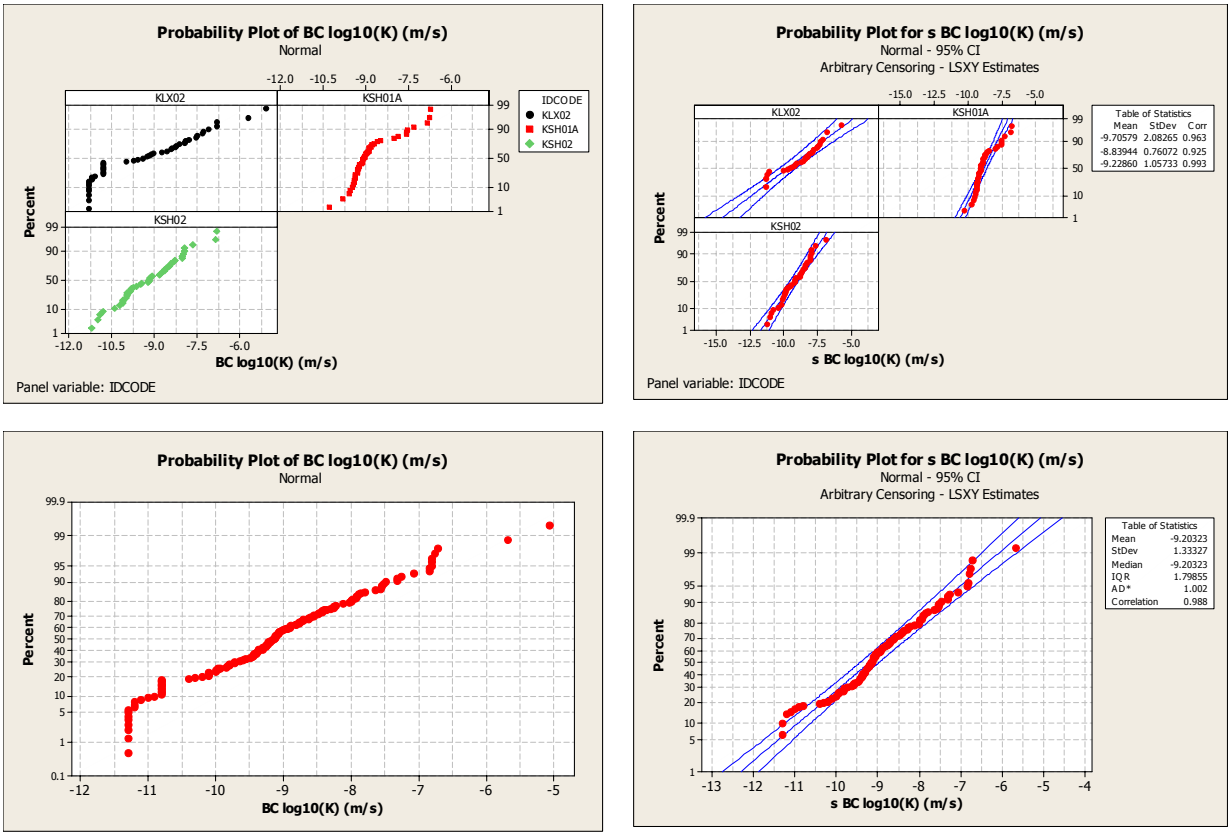

Figure A5-10b. *Probability distribution plots of PSS measurements,, test scale 20 m. Boreholes KSH01A, KSH02, KLX02.*

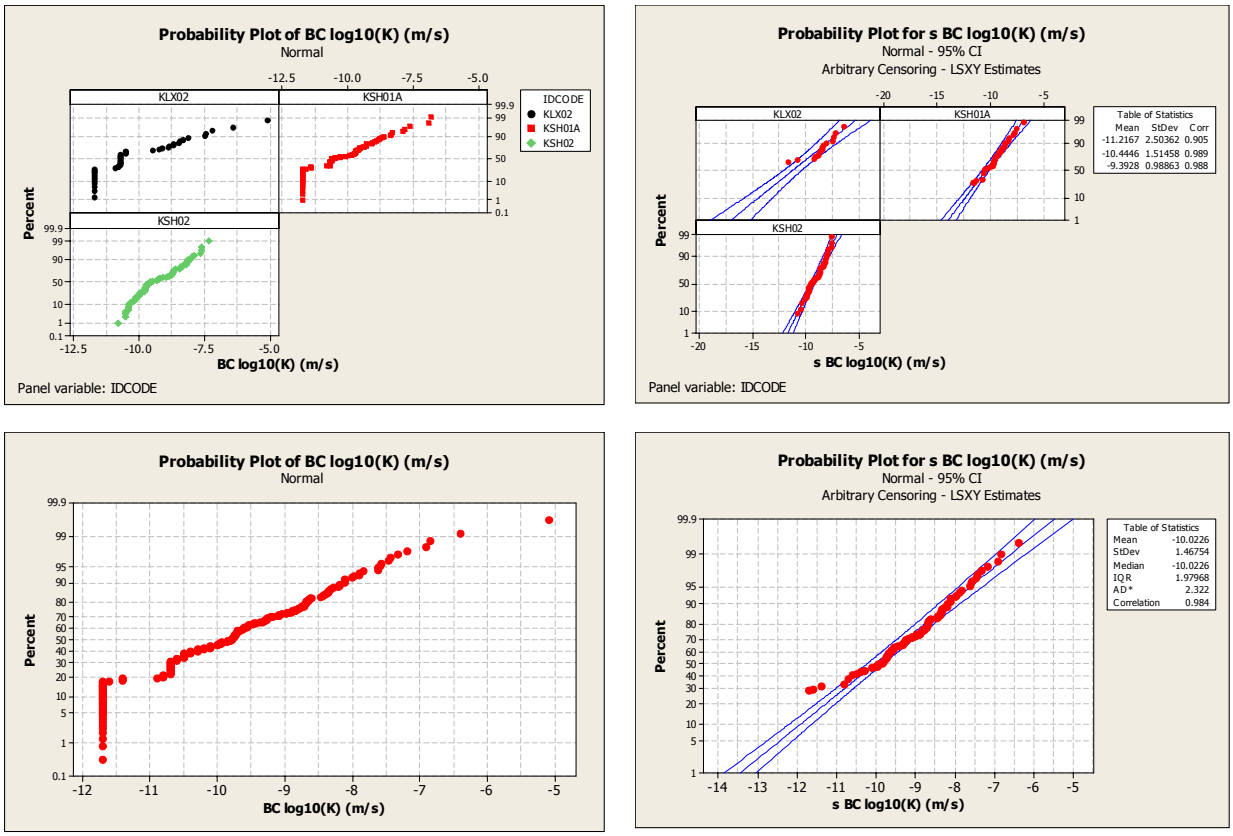

Figure A5-11a. *Probability distribution plots of PSS measurements, test scale 5 m. Boreholes KSH01A, KSH02, KLX02.*

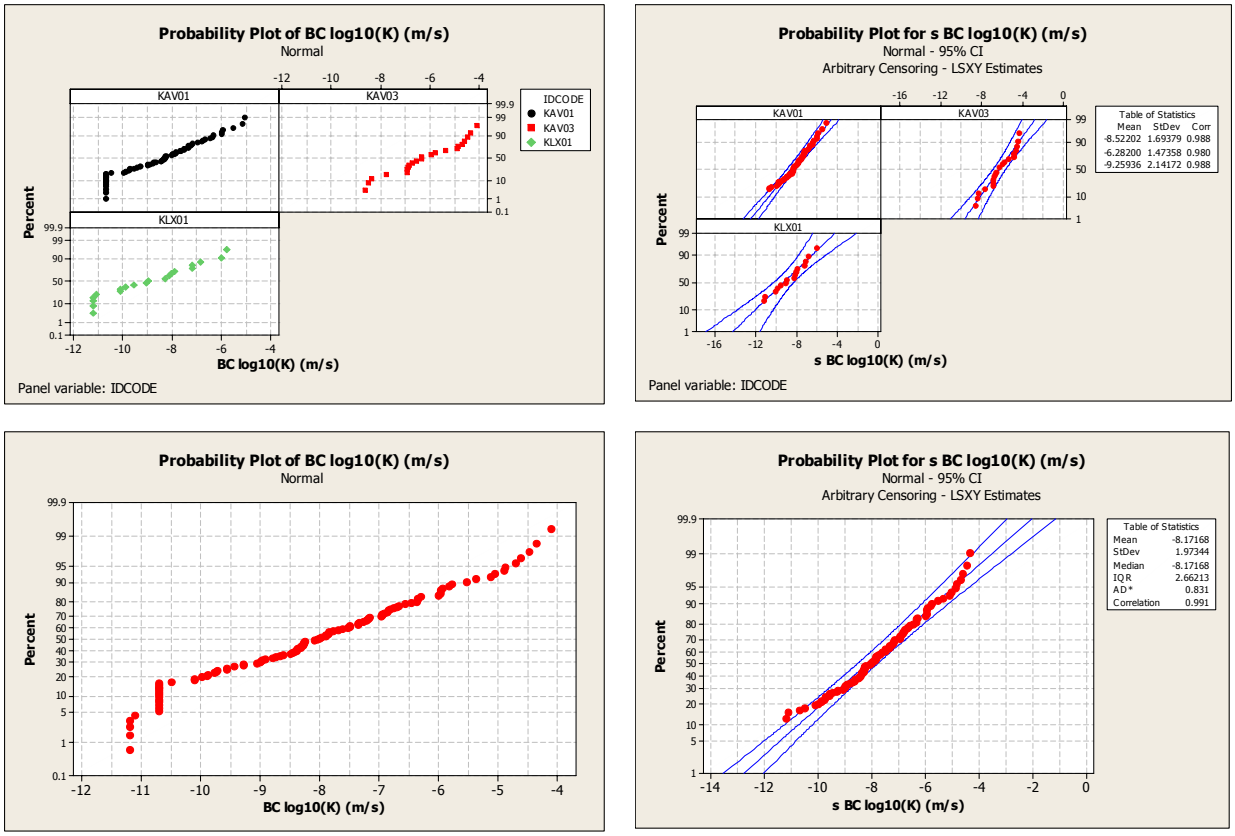

Figure A5-11b. *Probability distribution plots of injection test measurements, test scale 10, 30 m, Boreholes KAV01A, KAV03, KLX01.*

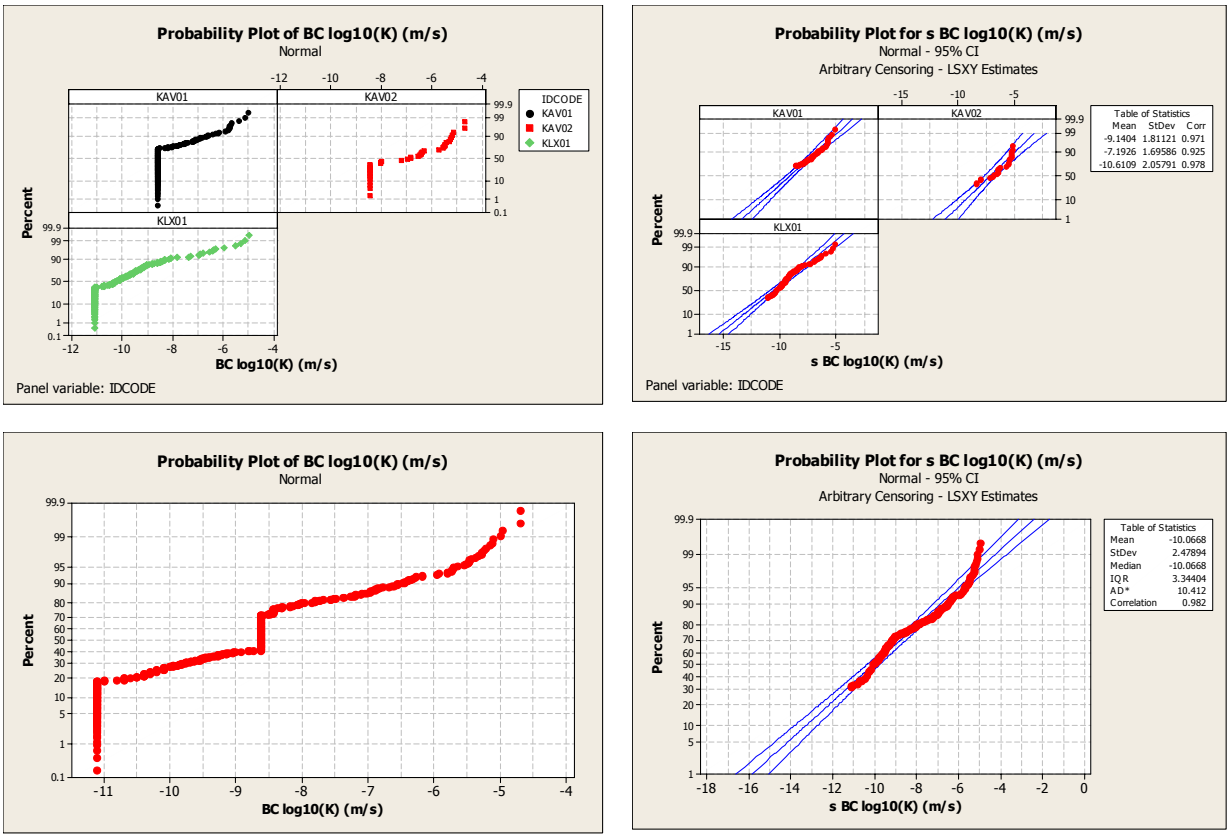

Figure A5-12. *Probability distribution plots of injection test measurements, test scale 2, 3 m. Boreholes KAV01A, KAV03, KLX01.*

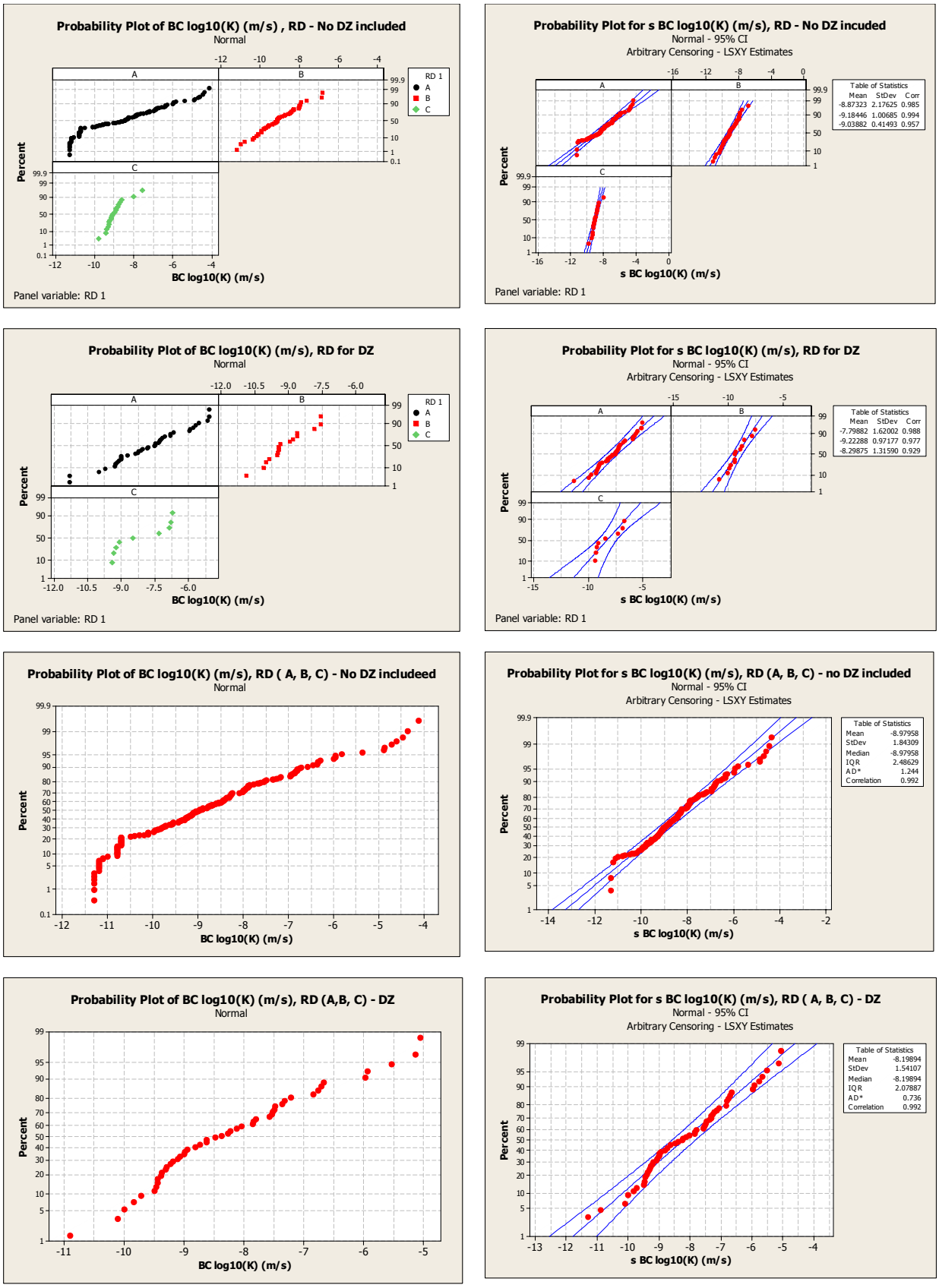

Figure A5-13. *Probability distribution plots injection test measurements, test scale 10, 20, 30 m. Rock domains (RD). Based on data from KSH01A, KSH02, KLX01, KLX02, KA01, KAV03.*

Appendix 6

RSMA01				
Property	**Character**	**Quantitative estimate**	**Confidence**	**Comment**
Dominant rock type (%)	Ävrö granite (501044)	75.8–84.7	High	Quantitative estimate based on occurrence in KSH03A, KAV01, KLX02 and the Äspö tunnel (section 2,265–2,874 m)
Mineralogical composition (%) (dominant minerals)	Quartz	16.4±6.1	High	N=20. Quantitative estimate based on modal analyses of surface samples from the Simpevarp subarea and KSH01A. Mean value ± std
	K-feldspar	18.5±8.0		
	Plagioclase	47.1±7.8		
	Biotite	11.4±5.4		
Grain size	Medium-grained		High	
Age (million years)		1,800	High	
Structure	Isotropic to weakly foliated. Scatttered mesoscopic, ductile shear zones		High	
Texture	Unequigranular to porphyritic		High	
Density (kg/m^3)		2,681±16		N=5. The quantitative estimate is based on surface samples from the Simpevarp subarea. Mean value ± std
Porosity (%)		0.57±0.12		N=5. The quantitative estimate is based on surface samples from the Simpevarp subarea. Mean value ± std
Magnetic susceptibility (SI units)		3.12±0.16		N=5. The quantitative estimate is based on surface samples from the Simpevarp subarea. Average value in logarithmic scale ± std
Electric resistivity in fresh water (ohm m)		4.16±0.18		N=5. The quantitative estimate is based on surface samples from the Simpevarp subarea. Average value in logarithmic scale ± std
Uranium content based on gamma ray spectrometric data (ppm)		4.9±2.2		N=25. The quantitative estimate is based on measurements from the Simpevarp subarea. Mean value ± std
Natural exposure (microR/h)		9.5±1.4		N=25. The quantitative estimate is based on measurements from the Simpevarp subarea. Mean value ± std
Subordinate rock types (%)	Fine- to medium-grained granite (511058)	1.2–21.5	High	Quantitative estimate based on occurrence in KSH03A, KAV01, KLX02 and the Äspö tunnel (section 2,265–2,874 m)
	Pegmatite (501061)	0.7–1.0		
	Fine-grained dioritoid (501030)	9.0–17.0		
	Diorite to gabbro (501033)	0–1.7		
	Fine-grained mafic rock (505102)	3.2–4.9		
	Quartz monzodiorite (501036)	No data		

RSMA01

Property	Character	Quantitative estimate	Confidence	Comment
Degree of inhomogeneity	Medium		High	Based on outcrop database for the Simpevarp subarea and KAV01, KLX02, KSH03
Metamorphism/alteration (%)	Inhomogeneous hydrothermal alteration (secondary red staining)	14–22	High	Quantitative estimate of weak to strong alteration is based on KSH03A, KAV01, KLX02. No data from ther major part of the regional model area
Mineral fabric (type/ orientation)				

RSMA02

Property	Character	Quantitative estimate	Confidence	Comment
Dominant rock type (%)	Ävrö granite (501044)		Medium	
Mineralogical composition (%) (dominant minerals)				No data
Grain size				No data
Age (million years)		1,800	Medium	
Structure				No data
Texture				No data
Density (kg/m^3)				No data
Porosity (%)				No data
Magnetic susceptibility (SI units)				No data
Electric resistivity in fresh water (ohm m)				No data
Uranium content based on gamma ray spectrometric data (ppm)				No data
Natural exposure (microR/h)				No data
Subordinate rock types (%)				No data
Degree of inhomogeneity				No data
Metamorphism/alteration (%)				No data
Mineral fabric (type/ orientation)				No data

RSMB01				
Property	**Character**	**Quantitative estimate**	**Confidence**	**Comment**
Dominant rock type (%)	Fine-grained dioritoid (501030)	90.6–94.2	High	Quantitative estimate based on occurrence in KSH01A and KSH02. High confidence that this rock type is dominanting at the Simpevarp peninsula but lower in the western part of the local model area
Mineralogical composition (%) (dominant minerals)	Quartz	7.4±5.0	High	N=21. Quantitative estimate based on modal analyses of surface samples from the Simpevarp subarea, KSH01A and KSH02. Mean value ± std
	K-feldspar	11.3±6.4		
	Plagioclase	51.4±8.7		
	Biotite	14.7±7.6		
	Amphibole	0–14		
	Pyroxene	0–22		
Grain size	Fine-grained		High	
Age (million years)		1,800	High	
Structure	Isotropic to weakly foliated. Scatttered mesoscopic, ductile shear zones		High	
Texture	Unequigranular		High	
Density (kg/m^3)		2,803±52		N=5. The quantitative estimate is based on surface samples from the Simpevarp subarea. Mean value ± std
Porosity (%)		0.29±0.11		N=5. The quantitative estimate is based on surface samples from the Simpevarp subarea. Mean value ± std
Magnetic susceptibility (SI units)		3.22±0.84		N=5. The quantitative estimate is based on surface samples from the Simpevarp subarea. Average value in logarithmic scale ± std
Electric resistivity in fresh water (ohm m)		4.58±0.41		N=5. The quantitative estimate is based on surface samples from the Simpevarp subarea. Average value in logarithmic scale ± std
Uranium content based on gamma ray spectrometric data (ppm)		3.7±1.8		N=14. The quantitative estimate is based on measurements from the Simpevarp subarea. Mean value ± std
Natural exposure (microR/h)		11.0±3.3		N=14. The quantitative estimate is based on measurements from the Simpevarp subarea. Mean value ± std
Subordinate rock types (%)	Quartz monzodiorite (501036)	0–3.8	High	Quantitative estimate based on occurrence in KSH01A and KSH02
	Fine- to medium-grained granite (511058)	0.9–6.7		
	Pegmatite (501061)	0.8–1.9		
	Fine-grained mafic rock (505102)	0.6–0.8		
Degree of inhomogeneity	Medium		High	Based on outcrop database for the Simpevarp subarea, KSH01and KSH02
Metamorphism/alteration (%)	Inhomogeneous hydrothermal alteration (secondary red staining)	19–24	High	Quantitative estimate of weak to strong alteration is based on KSH01A and KSH02
Mineral fabric (type/ orientation)				

RSMB02				
Property	**Character**	**Quantitative estimate**	**Confidence**	**Comment**
Dominant rock type (%)	Fine-grained dioritoid (501030)		High	
Mineralogical composition (%) (dominant minerals)				No data, cf. RSMB01
Grain size	Fine-grained		High	
Age (million years)		1,800	High	
Structure	Isotropic with scatttered mesoscopic, ductile shear zones		High	
Texture	Unequigranular		High	
Density (kg/m^3)				No data, cf. RSMB01
Porosity (%)				No data, cf. RSMB01
Magnetic susceptibility (SI units)				No data, cf. RSMB01
Electric resistivity in fresh water (ohm m)				No data, cf. RSMB01
Uranium content based on gamma ray spectrometric data (ppm)				No data, cf. RSMB01
Natural exposure (microR/h)				No data, cf. RSMB01
Subordinate rock types (%)	Fine- to medium-grained granite (511058)		High	Based on outcrop database for the Simpevarp subarea
	Pegmatite (501061)			
Degree of inhomogeneity	High		Medium	Based on outcrop database for the Simpevarp subarea
Metamorphism/alteration (%)	Inhomogeneous hydrothermal alteration (secondary red staining)		High	Based on outcrop database for the Simpevarp subarea
Mineral fabric (type/ orientation)				

RSMB03				
Property	**Character**	**Quantitative estimate**	**Confidence**	**Comment**
Dominant rock type (%)	Fine-grained dioritoid (501030)	90.6–94.2	High	Quantitative estimate based on occurrence in KSH01A and KSH02. High confidence that this rock type is dominanting at the Simpevarp peninsula but lower in the western part of the local model area
Mineralogical composition (%) (dominant minerals)	Quartz	7.4±5.0	High	N=21. Quantitative estimate based on modal analyses of surface samples from the Simpevarp subarea, KSH01A and KSH02. Mean value ± std
	K-feldspar	11.3±6.4		
	Plagioclase	51.4±8.7		
	Biotite	14.7±7.6		
	Amphibole	0–14		
	Pyroxene	0–22		
Grain size	Fine-grained		High	
Age (million years)		1,800	High	
Structure	Isotropic to weakly foliated. Scatttered mesoscopic, ductile shear zones		High	
Texture	Unequigranular		High	
Density (kg/m^3)		2,803±52		N=5. The quantitative estimate is based on surface samples from the Simpevarp subarea. Mean value ± std
Porosity (%)		0.29±0.11		N=5. The quantitative estimate is based on surface samples from the Simpevarp subarea. Mean value ± std
Magnetic susceptibility (SI units)		3.22±0.84		N=5. The quantitative estimate is based on surface samples from the Simpevarp subarea. Average value in logarithmic scale ± std
Electric resistivity in fresh water (ohm m)		4.58±0.41		N=5. The quantitative estimate is based on surface samples from the Simpevarp subarea. Average value in logarithmic scale ± std
Uranium content based on gamma ray spectrometric data (ppm)		3.7±1.8		N=14. The quantitative estimate is based on measurements from the Simpevarp subarea. Mean value ± std
Natural exposure (microR/h)		11.0±3.3		N=14. The quantitative estimate is based on measurements from the Simpevarp subarea. Mean value ± std
Subordinate rock types (%)	Fine- to medium-grained granite (511058)		High	Based on outcrop database for the Simpevarp subarea
	Pegmatite (501061)			
	Diorite to gabbro (501033)			
	Ävrö granite (501044)			
Degree of inhomogeneity	Medium		High	Based on outcrop database for the Simpevarp subarea
Metamorphism/alteration (%)	Inhomogeneous hydrothermal alteration (secondary red staining)		High	Based on outcrop database for the Simpevarp subarea
Mineral fabric (type/ orientation)				

RSMB04				
Property	**Character**	**Quantitative estimate**	**Confidence**	**Comment**
Dominant rock type (%)	Fine-grained dioritoid (501030)		Medium	Extension at the surface based on /Kornfält and Wikman, 1987/
Mineralogical composition (%) (dominant minerals)				No data, cf. RSMB01
Grain size				No data, cf. RSMB01
Age (million years)		1,800	High	
Structure				No data, cf. RSMB01
Texture				No data, cf. RSMB01
Density (kg/m^3)				No data, cf. RSMB01
Porosity (%)				No data, cf. RSMB01
Magnetic susceptibility (SI units)				No data, cf. RSMB01
Electric resistivity in fresh water (ohm m)				No data, cf. RSMB01
Uranium content based on gamma ray spectrometric data (ppm)				No data, cf. RSMB01
Natural exposure (microR/h)				No data, cf. RSMB01
Subordinate rock types (%)	Fine- to medium-grained granite (511058)		High	Based on /Kornfält and Wikman, 1987/
	Pegmatite (501061)			
Degree of inhomogeneity	Medium		Medium	
Metamorphism/alteration (%)				No data, cf. RSMB01
Mineral fabric (type/ orientation)				

RSMC01				
Property	**Character**	**Quantitative estimate**	**Confidence**	**Comment**
Dominant rock type (%)	Quartz monzodiorite (501036)	51.5–73.9	High	Mixture of 501036 and 501044. Quantitative estimate based on occurrence in KSH01A and KSH03A
	Ävrö granite (501044)	22.9–34.1		
Mineralogical composition (%) (dominant minerals)				Cf. RSMA01 and RSMD01
Grain size				Cf. RSMA01 and RSMD01
Age (million years)		1,800	High	
Structure				Cf. RSMA01 and RSMD01
Texture				Cf. RSMA01 and RSMD01
Density (kg/m^3)				Cf. RSMA01 and RSMD01
Porosity (%)				Cf. RSMA01 and RSMD01
Magnetic susceptibility (SI units)				Cf. RSMA01 and RSMD01
Electric resistivity in fresh water (ohm m)				Cf. RSMA01 and RSMD01
Uranium content based on gamma ray spectrometric data (ppm)				Cf. RSMA01 and RSMD01
Natural exposure (microR/h)				Cf. RSMA01 and RSMD01
Subordinate rock types (%)	Fine-grained dioritoid (501030)	0–6.5	High	Quantitative estimate based on occurrence in KSH01A and KSH03A
	Fine- to medium-grained granite (511058)	1.8–4.2		
	Granite (501058)	0–2.0		
	Fine-grained mafic rock (505102)	0–1.2		
	Pegmatite (501061)	0.3–1.4		
	Diorite to gabbro (501033)	0–0.2		
Degree of inhomogeneity	High		High	Based on outcrop database for the Simpevarp subarea, KSH01A, B and KSH03A, B
Metamorphism/alteration (%)	Inhomogeneous hydrothermal alteration (secondary red staining)	19–40	High	Based on outcrop database for the Simpevarp subarea, KSH01A, B and KSH03A, B. Quantitative estimate of weak to strong alteration is based on occurrence in KSH01A and KSH03A
Mineral fabric (type/ orientation)				

RSMD01				
Property	**Character**	**Quantitative estimate**	**Confidence**	**Comment**
Dominant rock type (%)	Quartz monzodiorite (501036)			
Mineralogical composition (%) (dominant minerals)	Quartz	10.5±2.5	High	N=7. Quantitative estimate is based on modal analyses of surface samples from the Simpevarp subarea and KSH01A, B
	K-feldspar	12.3±5.4		
	Plagioclase	45.5±3.6		
	Biotite	16.3±5.2		
	Amphibole	6.7±4.5		
	Pyroxene	0–8.2		
Grain size	Medium-grained		High	Based on outcrop database for the Simpevarp subarea
Age (million years)		1,802±4	High	
Structure	Isotropic to weakly foliated. Scatttered mesoscopic, ductile shear zones		High	Based on outcrop database for the Simpevarp subarea
Texture	Equigranular		High	Based on outcrop database for the Simpevarp subarea
Density (kg/m^3)		2,790±33		N=5. The quantitative estimate is based on surface samples from the local model area. Mean value ± std
Porosity (%)		0.51±0.11		N=5. The quantitative estimate is based on surface samples from the local model area. Mean value ± std
Magnetic susceptibility (SI units)		3.54±0.14		N=5. The quantitative estimate is based on surface samples from the local model area. Average value in logarithmic scale ± std
Electric resistivity in fresh water (ohm m)		4.16±0.17		N=5. The quantitative estimate is based on surface samples from the local model area. Average value in logarithmic scale ± std
Uranium content based on gamma ray spectrometric data (ppm)		5.0±2.2		N=14. The quantitative estimate is based on measurements from the local model area. Mean value ± std
Natural exposure (microR/h)		11.3±1.5		N=14. The quantitative estimate is based on measurements from the local model area. Mean value ± std
Subordinate rock types (%)	Fine- to medium-grained granite (511058)		High	Based on outcrop database for the Simpevarp subarea
	Pegmatite (501061)			
	Fine-grained mafic rock (505102)			
	Ävrö granite (501044)			
	Fine-grained dioritoid (501030)			
Degree of inhomogeneity	Medium		High	Based on outcrop database for the Simpevarp subarea
Metamorphism/alteration (%)	Inhomogeneous hydrothermal alteration (secondary red staining)		High	Based on outcrop database for the Simpevarp subarea
Mineral fabric (type/ orientation)				

RSMD02

Property	Character	Quantitative estimate	Confidence	Comment
Dominant rock type (%)	Quartz monzodiorite (501036)		Medium	
Mineralogical composition (%) (dominant minerals)				No data
Grain size				No data
Age (million years)		1,800	High	
Structure				No data
Texture				No data
Density (kg/m^3)				No data
Porosity (%)				No data
Magnetic susceptibility (SI units)				No data
Electric resistivity in fresh water (ohm m)				No data
Uranium content based on gamma ray spectrometric data (ppm)				No data
Natural exposure (microR/h)				No data
Subordinate rock types (%)				No data
Degree of inhomogeneity				No data
Metamorphism/alteration (%)				No data
Mineral fabric (type/orientation)				No data

RSMD03

Property	Character	Quantitative estimate	Confidence	Comment
Dominant rock type (%)	Quartz monzodiorite (501036)		Medium	
Mineralogical composition (%) (dominant minerals)				No data
Grain size				No data
Age (million years)		1,800	High	
Structure				No data
Texture				No data
Density (kg/m^3)				No data
Porosity (%)				No data
Magnetic susceptibility (SI units)				No data
Electric resistivity in fresh water (ohm m)				No data
Uranium content based on gamma ray spectrometric data (ppm)				No data
Natural exposure (microR/h)				No data
Subordinate rock types (%)				No data
Degree of inhomogeneity				No data
Metamorphism/alteration (%)				No data
Mineral fabric (type/orientation)				No data

RSMD04

Property	Character	Quantitative estimate	Confidence	Comment
Dominant rock type (%)	Quartz monzodiorite (501036)		Medium	
Mineralogical composition (%) (dominant minerals)				No data
Grain size				No data
Age (million years)		1,800	High	
Structure				No data
Texture				No data
Density (kg/m^3)				No data
Porosity (%)				No data
Magnetic susceptibility (SI units)				No data
Electric resistivity in fresh water (ohm m)				No data
Uranium content based on gamma ray spectrometric data (ppm)				No data
Natural exposure (microR/h)				No data
Subordinate rock types (%)				No data
Degree of inhomogeneity				No data
Metamorphism/alteration (%)				No data
Mineral fabric (type/orientation)				No data

RSMD05

Property	Character	Quantitative estimate	Confidence	Comment
Dominant rock type (%)	Quartz monzodiorite (501036)		Medium	
Mineralogical composition (%) (dominant minerals)				No data
Grain size				No data
Age (million years)		1,800	High	
Structure				No data
Texture				No data
Density (kg/m^3)				No data
Porosity (%)				No data
Magnetic susceptibility (SI units)				No data
Electric resistivity in fresh water (ohm m)				No data
Uranium content based on gamma ray spectrometric data (ppm)				No data
Natural exposure (microR/h)				No data
Subordinate rock type(s)				No data
Degree of inhomogeneity				No data
Metamorphism/alteration				No data
Mineral fabric (type/orientation)				No data

RSMD06				
Property	**Character**	**Quantitative estimate**	**Confidence**	**Comment**
Dominant rock type (%)	Quartz monzodiorite (501036)		Medium	
Mineralogical composition (%) (dominant minerals)				No data
Grain size				No data
Age (million years)		1,800	High	
Structure				No data
Texture				No data
Density (kg/m^3)				No data
Porosity (%)				No data
Magnetic susceptibility (SI units)				No data
Electric resistivity in fresh water (ohm m)				No data
Uranium content based on gamma ray spectrometric data (ppm)				No data
Natural exposure (microR/h)				No data
Subordinate rock types (%)				No data
Degree of inhomogeneity				No data
Metamorphism/alteration (%)				No data
Mineral fabric (type/orientation)				No data

RSME01

Property	Character	Quantitative estimate	Confidence	Comment
Dominant rock type (%)	Diorite to gabbro (501033)		Medium	
Mineralogical composition (%) (dominant minerals)				No data
Grain size				No data
Age (million years)		1,800	High	
Structure				No data
Texture				No data
Density (kg/m^3)				No data
Porosity (%)				No data
Magnetic susceptibility (SI units)				No data
Electric resistivity in fresh water (ohm m)				No data
Uranium content based on gamma ray spectrometric data (ppm)				No data
Natural exposure (microR/h)				No data
Subordinate rock types (%)	Fine- to medium-grained granite (511058)		Medium	
	Pegmatite (501061)			
	Ävrö granite (501044)			
Degree of inhomogeneity	High		Medium	
Metamorphism/alteration (%)				No data
Mineral fabric (type/ orientation)				No data

RSME02

Property	Character	Quantitative estimate	Confidence	Comment
Dominant rock type (%)	Diorite to gabbro (501033)		High	
Mineralogical composition (%) (dominant minerals)				No data
Grain size				No data
Age (million years)		1,800	High	
Structure				No data
Texture				No data
Density (kg/m^3)				No data
Porosity (%)				No data
Magnetic susceptibility (SI units)				No data
Electric resistivity in fresh water (ohm m)				No data
Uranium content based on gamma ray spectrometric data (ppm)				No data
Natural exposure (microR/h)				No data
Subordinate rock types (%)	Fine- to medium-grained granite (511058)		High	
	Pegmatite (501061)			
Degree of inhomogeneity	High		Low	
Metamorphism/alteration (%)				No data
Mineral fabric (type/ orientation)				No data

RSME03				
Property	**Character**	**Quantitative estimate**	**Confidence**	**Comment**
Dominant rock type (%)	Diorite to gabbro (501033)		High	
Mineralogical composition (%) (dominant minerals)				No data
Grain size				No data
Age (million years)		1,800	High	
Structure				No data
Texture				No data
Density (kg/m^3)				No data
Porosity (%)				No data
Magnetic susceptibility (SI units)				No data
Electric resistivity in fresh water (ohm m)				No data
Uranium content based on gamma ray spectrometric data (ppm)				No data
Natural exposure (microR/h)				No data
Subordinate rock types (%)				No data
Degree of inhomogeneity				No data
Metamorphism/alteration (%)				No data
Mineral fabric (type/ orientation)				No data

RSME04				
Property	**Character**	**Quantitative estimate**	**Confidence**	**Comment**
Dominant rock type (%)	Diorite to gabbro (501033)		High	
Mineralogical composition (%) (dominant minerals)	Quartz	4±0.6	High	N=4. Quantitative estimate based on modal analyses of surface samples from the Simpevarp subarea. Mean value ± std
	Plagioclase	47.4±4.5		
	Biotite	10.8±3.8		
	Amphibole	29.4±5.3		
Grain size	Medium-grained		High	
Age (million years)		1,800	High	
Structure	Isotropic to weakly foliated		High	
Texture	Equigranular		High	
Density (kg/m^3)		2,967±33		N=5. Quantitative estimate based on samples from the local model area. Mean value ± std
Porosity (%)		0.32±0.08		N=5. Quantitative estimate based on samples from the local model area. Mean value ± std
Magnetic susceptibility (SI units)		3.12±0.80		N=5. Quantitative estimate based on samples from the local model area. Average value in logarithmic scale ± std
Electric resistivity in fresh water (ohm m)		4.28±0.16		N=5. Quantitative estimate based on samples from the local model area. Average value in logarithmic scale ± std
Uranium content based on gamma ray spectrometric data (ppm)				No data
Natural exposure (microR/h)				No data
Subordinate rock types (%)	Fine- to medium-grained granite (511058)		High	Based on outcrop database for the Simpevarp subarea
	Pegmatite (501061)			
	Ävrö granite (501044)			
Degree of inhomogeneity	Medium		Medium	Based on outcrop database for the Simpevarp subarea
Metamorphism/alteration (%)				
Mineral fabric (type/ orientation)				

RSME05				
Property	**Character**	**Quantitative estimate**	**Confidence**	**Comment**
Dominant rock type (%)	Diorite to gabbro (501033)		High	
Mineralogical composition (%) (dominant minerals)				No data
Grain size				No data
Age (million years)		1,800	High	
Structure				No data
Texture				No data
Density (kg/m^3)				No data
Porosity (%)				No data
Magnetic susceptibility (SI units)				No data
Electric resistivity in fresh water (ohm m)				No data
Uranium content based on gamma ray spectrometric data (ppm)				No data
Natural exposure (microR/h)				No data
Subordinate rock types (%)				No data
Degree of inhomogeneity				No data
Metamorphism/alteration (%)				No data
Mineral fabric (type/ orientation)				No data

RSME06

Property	Character	Quantitative estimate	Confidence	Comment
Dominant rock type (%)	Diorite to gabbro (501033)		High	
Mineralogical composition (%) (dominant minerals)	Quartz	4±0.6	High	N=4. Quantitative estimate based on modal analyses of surface samples from the Simpevarp subarea. Mean value ± std
	Plagioclase	47.4±4.5		
	Biotite	10.8±3.8		
	Amphibole	29.4±5.3		
Grain size	Medium-grained		High	
Age (million years)		1,800	High	
Structure	Isotropic to weakly foliated			
Texture	Equigranular			
Density (kg/m^3)		2,967±33		N=5. Quantitative estimate based on samples from the local model area. Mean value ± std
Porosity (%)		0.32±0.08		N=5. Quantitative estimate based on samples from the local model area. Mean value ± std
Magnetic susceptibility (SI units)		3.12±0.80		N=5. Quantitative estimate based on samples from the local model area. Average value in logarithmic scale ± std
Electric resistivity in fresh water (ohm m)		4.28±0.16		N=5. Quantitative estimate based on samples from the local model area. Average value in logarithmic scale ± std
Uranium content based on gamma ray spectrometric data (ppm)				No data
Natural exposure (microR/h)				No data
Subordinate rock types (%)	Fine- to medium-grained granite (511058)		High	Based on outcrop database for the Simpevarp subarea
	Pegmatite (501061)			
Degree of inhomogeneity	Medium		Medium	Based on outcrop database for the Simpevarp subarea
Metamorphism/alteration (%)				
Mineral fabric (type/ orientation)				

RSME07				
Property	**Character**	**Quantitative estimate**	**Confidence**	**Comment**
Dominant rock type (%)	Diorite to gabbro (501033)		High	
Mineralogical composition (%) (dominant minerals)				No data
Grain size				No data
Age (million years)		1,800	High	
Structure				No data
Texture				No data
Density (kg/m^3)				No data
Porosity (%)				No data
Magnetic susceptibility (SI units)				No data
Electric resistivity in fresh water (ohm m)				No data
Uranium content based on gamma ray spectrometric data (ppm)				No data
Natural exposure (microR/h)				No data
Subordinate rock types (%)				No data
Degree of inhomogeneity				No data
Metamorphism/alteration (%)				No data
Mineral fabric (type/ orientation)				No data

RSME08				
Property	**Character**	**Quantitative estimate**	**Confidence**	**Comment**
Dominant rock type (%)	Diorite to gabbro (501033)		High	
Mineralogical composition (%) (dominant minerals)	Quartz	4±0.6	High	N=4. Quantitative estimate based on modal analyses of surface samples from the Simpevarp subarea. Mean value ± std
	Plagioclase	47.4±4.5		
	Biotite	10.8±3.8		
	Amphibole	29.4±5.3		
Grain size	Medium-grained		High	
Age (million years)		1,800	High	
Structure	Isotropic to weakly foliated			
Texture	Equigranular			
Density (kg/m^3)		2,967±33		N=5. Quantitative estimate based on samples from the local model area. Mean value ± std
Porosity (%)		0.32±0.08		N=5. Quantitative estimate based on samples from the local model area. Mean value ± std
Magnetic susceptibility (SI units)		3.12±0.80		N=5. Quantitative estimate based on samples from the local model area. Average value in logarithmic scale ± std
Electric resistivity in fresh water (ohm m)		4.28±0.16		N=5. Quantitative estimate based on samples from the local model area. Average value in logarithmic scale ± std
Uranium content based on gamma ray spectrometric data (ppm)				No data
Natural exposure (microR/h)				No data
Subordinate rock types (%)				
Degree of inhomogeneity	Low		High	Based on outcrop database for the Simpevarp subarea
Metamorphism/alteration (%)				
Mineral fabric (type/ orientation)				

RSME09				
Property	**Character**	**Quantitative estimate**	**Confidence**	**Comment**
Dominant rock type (%)	Diorite to gabbro (501033)		High	
Mineralogical composition (%) (dominant minerals)	Quartz	4±0.6	High	N=4. Quantitative estimate based on modal analyses of surface samples from the Simpevarp subarea. Mean value ± std
	Plagioclase	47.4±4.5		
	Biotite	10.8±3.8		
	Amphibole	29.4±5.3		
Grain size	Medium-grained		High	
Age (million years)		1,800	High	
Structure	Isotropic to weakly foliated			
Texture	Equigranular			
Density (kg/m^3)		2,967±33		N=5. Quantitative estimate based on samples from the local model area. Mean value ± std
Porosity (%)		0.32±0.08		N=5. Quantitative estimate based on samples from the local model area. Mean value ± std
Magnetic susceptibility (SI units)		3.12±0.80		N=5. Quantitative estimate based on samples from the local model area. Average value in logarithmic scale ± std
Electric resistivity in fresh water (ohm m)		4.28±0.16		N=5. Quantitative estimate based on samples from the local model area. Average value in logarithmic scale ± std
Uranium content based on gamma ray spectrometric data (ppm)				No data
Natural exposure (microR/h)				No data
Subordinate rock types (%)	Fine- to medium-grained granite (511058)		High	Based on outcrop database for the Simpevarp subarea
	Pegmatite (501061)			
Degree of inhomogeneity	Medium		Medium	Based on outcrop database for the Simpevarp subarea
Metamorphism/alteration (%)				
Mineral fabric (type/ orientation)				

RSME10				
Property	**Character**	**Quantitative estimate**	**Confidence**	**Comment**
Dominant rock type (%)	Diorite to gabbro (501033)		High	
Mineralogical composition (%) (dominant minerals)	Quartz	4±0.6	High	N=4. Quantitative estimate based on modal analyses of surface samples from the Simpevarp subarea. Mean value ± std
	Plagioclase	47.4±4.5		
	Biotite	10.8±3.8		
	Amphibole	29.4±5.3		
Grain size	Medium-grained		High	
Age (million years)		1,800	High	
Structure	Isotropic to weakly foliated			
Texture	Equigranular			
Density (kg/m^3)		2,967±33		N=5. Quantitative estimate based on samples from the local model area. Mean value ± std
Porosity (%)		0.32±0.08		N=5. Quantitative estimate based on samples from the local model area. Mean value ± std
Magnetic susceptibility (SI units)		3.12±0.80		N=5. Quantitative estimate based on samples from the local model area. Average value in logarithmic scale ± std
Electric resistivity in fresh water (ohm m)		4.28±0.16		N=5. Quantitative estimate based on samples from the local model area. Average value in logarithmic scale ± std
Uranium content based on gamma ray spectrometric data (ppm)				No data
Natural exposure (microR/h)				No data
Subordinate rock types (%)				
Degree of inhomogeneity	Low		High	Based on outcrop database for the Simpevarp subarea
Metamorphism/alteration (%)				
Mineral fabric (type/ orientation)				

RSME11

Property	Character	Quantitative estimate	Confidence	Comment
Dominant rock type (%)	Diorite to gabbro (501033)		High	
Mineralogical composition (%) (dominant minerals)				No data
Grain size				No data
Age (million years)		1,800	High	
Structure				No data
Texture				No data
Density (kg/m^3)				No data
Porosity (%)				No data
Magnetic susceptibility (SI units)				No data
Electric resistivity in fresh water (ohm m)				No data
Uranium content based on gamma ray spectrometric data (ppm)				No data
Natural exposure (microR/h)				No data
Subordinate rock types (%)				No data
Degree of inhomogeneity				No data
Metamorphism/alteration (%)				No data
Mineral fabric (type/orientation)				No data

RSME12

Property	Character	Quantitative estimate	Confidence	Comment
Dominant rock type (%)	Diorite to gabbro (501033)		High	
Mineralogical composition (%) (dominant minerals)				No data
Grain size				No data
Age (million years)		1,800	High	
Structure				No data
Texture				No data
Density (kg/m^3)				No data
Porosity (%)				No data
Magnetic susceptibility (SI units)				No data
Electric resistivity in fresh water (ohm m)				No data
Uranium content based on gamma ray spectrometric data (ppm)				No data
Natural exposure (microR/h)				No data
Subordinate rock types (%)				No data
Degree of inhomogeneity				No data
Metamorphism/alteration (%)				No data
Mineral fabric (type/orientation)				No data

RSME13

Property	Character	Quantitative estimate	Confidence	Comment
Dominant rock type (%)	Diorite to gabbro (501033)		High	
Mineralogical composition (%) (dominant minerals)				No data
Grain size				No data
Age (million years)		1,800	High	
Structure				No data
Texture				No data
Density (kg/m^3)				No data
Porosity (%)				No data
Magnetic susceptibility (SI units)				No data
Electric resistivity in fresh water (ohm m)				No data
Uranium content based on gamma ray spectrometric data (ppm)				No data
Natural exposure (microR/h)				No data
Subordinate rock types (%)				No data
Degree of inhomogeneity				No data
Metamorphism/alteration (%)				No data
Mineral fabric (type/orientation)				No data

RSME14

Property	Character	Quantitative estimate	Confidence	Comment
Dominant rock type (%)	Diorite to gabbro (501033)		High	
Mineralogical composition (%) (dominant minerals)				No data
Grain size				No data
Age (million years)		1,800	High	
Structure				No data
Texture				No data
Density (kg/m^3)				No data
Porosity (%)				No data
Magnetic susceptibility (SI units)				No data
Electric resistivity in fresh water (ohm m)				No data
Uranium content based on gamma ray spectrometric data (ppm)				No data
Natural exposure (microR/h)				No data
Subordinate rock types (%)				No data
Degree of inhomogeneity				No data
Metamorphism/alteration (%)				No data
Mineral fabric (type/orientation)				No data

RSME15

Property	Character	Quantitative estimate	Confidence	Comment
Dominant rock type (%)	Diorite to gabbro (501033)		High	
Mineralogical composition (%) (dominant minerals)				No data
Grain size				No data
Age (million years)		1,800	High	
Structure				No data
Texture				No data
Density (kg/m^3)				No data
Porosity (%)				No data
Magnetic susceptibility (SI units)				No data
Electric resistivity in fresh water (ohm m)				No data
Uranium content based on gamma ray spectrometric data (ppm)				No data
Natural exposure (microR/h)				No data
Subordinate rock types (%)				No data
Degree of inhomogeneity				No data
Metamorphism/alteration (%)				No data
Mineral fabric (type/orientation)				No data

RSME16

Property	Character	Quantitative estimate	Confidence	Comment
Dominant rock type (%)	Diorite to gabbro (501033)		High	
Mineralogical composition (%) (dominant minerals)				No data
Grain size				No data
Age (million years)		1,800	High	
Structure				No data
Texture				No data
Density (kg/m^3)				No data
Porosity (%)				No data
Magnetic susceptibility (SI units)				No data
Electric resistivity in fresh water (ohm m)				No data
Uranium content based on gamma ray spectrometric data (ppm)				No data
Natural exposure (microR/h)				No data
Subordinate rock types (%)				No data
Degree of inhomogeneity				No data
Metamorphism/alteration (%)				No data
Mineral fabric (type/orientation)				No data

RSME17

Property	Character	Quantitative estimate	Confidence	Comment
Dominant rock type (%)	Diorite to gabbro (501033)		High	
Mineralogical composition (%) (dominant minerals)				No data
Grain size				No data
Age (million years)		1,800	High	
Structure				No data
Texture				No data
Density (kg/m^3)				No data
Porosity (%)				No data
Magnetic susceptibility (SI units)				No data
Electric resistivity in fresh water (ohm m)				No data
Uranium content based on gamma ray spectrometric data (ppm)				No data
Natural exposure (microR/h)				No data
Subordinate rock types (%)				No data
Degree of inhomogeneity				No data
Metamorphism/alteration (%)				No data
Mineral fabric (type/orientation)				No data

RSME18

Property	Character	Quantitative estimate	Confidence	Comment
Dominant rock type (%)	Diorite to gabbro (501033)		High	
Mineralogical composition (%) (dominant minerals)				No data
Grain size				No data
Age (million years)		1,800	High	
Structure				No data
Texture				No data
Density (kg/m^3)				No data
Porosity (%)				No data
Magnetic susceptibility (SI units)				No data
Electric resistivity in fresh water (ohm m)				No data
Uranium content based on gamma ray spectrometric data (ppm)				No data
Natural exposure (microR/h)				No data
Subordinate rock types (%)				No data
Degree of inhomogeneity				No data
Metamorphism/alteration (%)				No data
Mineral fabric (type/orientation)				No data

RSMF01				
Property	**Character**	**Quantitative estimate**	**Confidence**	**Comment**
Dominant rock type (%)	Fine- to medium-grained granite (511058)		Medium	
Mineralogical composition (%) (dominant minerals)				No data
Grain size				No data
Age (million years)		1,800	High	
Structure				No data
Texture				No data
Density (kg/m^3)				No data
Porosity (%)				No data
Magnetic susceptibility (SI units)				No data
Electric resistivity in fresh water (ohm m)				No data
Uranium content based on gamma ray spectrometric data (ppm)				No data
Natural exposure (microR/h)				No data
Subordinate rock types (%)				No data
Degree of inhomogeneity				No data
Metamorphism/alteration (%)				No data
Mineral fabric (type/ orientation)				No data

RSMF02

Property	Character	Quantitative estimate	Confidence	Comment
Dominant rock type (%)	Fine- to medium-grained granite (511058)		Medium	
Mineralogical composition (%) (dominant minerals)				No data
Grain size				No data
Age (million years)		1,800	High	
Structure				No data
Texture				No data
Density (kg/m^3)				No data
Porosity (%)				No data
Magnetic susceptibility (SI units)				No data
Electric resistivity in fresh water (ohm m)				No data
Uranium content based on gamma ray spectrometric data (ppm)				No data
Natural exposure (microR/h)				No data
Subordinate rock types (%)	Diorite to gabbro (501033)		Medium	
Degree of inhomogeneity				No data
Metamorphism/alteration (%)				No data
Mineral fabric (type/ orientation)				No data

RSMF03				
Property	**Character**	**Quantitative estimate**	**Confidence**	**Comment**
Dominant rock type (%)	Fine- to medium-grained granite (511058)		Medium	
Mineralogical composition (%) (dominant minerals)				No data
Grain size				No data
Age (million years)		1,800	High	
Structure				No data
Texture				No data
Density (kg/m^3)				No data
Porosity (%)				No data
Magnetic susceptibility (SI units)				No data
Electric resistivity in fresh water (ohm m)				No data
Uranium content based on gamma ray spectrometric data (ppm)				No data
Natural exposure (microR/h)				No data
Subordinate rock types (%)				No data
Degree of inhomogeneity				No data
Metamorphism/alteration (%)				No data
Mineral fabric (type/ orientation)				No data

RSMG01				
Property	**Character**	**Quantitative estimate**	**Confidence**	**Comment**
Dominant rock type (%)	Granite (521058)		High	
	Fine-grained granite (531058)			
Mineralogical composition (%) (dominant minerals)	Quartz	31.3±5.6	High	N=10. Quantitative estimate based on modal analyses in /Wikman and Kornfält, 1995/. Mean value ± std
	K-feldspar	36.7±7.1		
	Plagioclase	24.1±6.3		
Grain size	Fine- to medium- and coarse-grained			Based on /Wikman and Kornfält, 1995/
Age (million years)		1,452+11/–9	High	Based on /Åhäll, 2001/
Structure	Isotropic			Based on /Kresten and Chyssler, 1976/ and /Wikman and Kornfält, 1995/
Texture	Equigranular and porphyritic			Based on /Kresten and Chyssler, 1976/ and /Wikman and Kornfält, 1995/
Density (kg/m^3)				
Porosity (%)				
Magnetic susceptibility (SI units)				
Electric resistivity in fresh water (ohm m)				
Uranium content based on gamma ray spectrometric data (ppm)		14.6±8.1		N=7. Based on geochemical analyses /Wikman and Kornfält, 1995/
Natural exposure (microR/h)				
Subordinate rock types (%)				
Degree of inhomogeneity				
Metamorphism/alteration (%)				
Mineral fabric (type/ orientation)				

RSMG02				
Property	**Character**	**Quantitative estimate**	**Confidence**	**Comment**
Dominant rock type (%)	Granite (521058)		High	
Mineralogical composition (%) (dominant minerals)	Quartz	34.6±5.5	High	N=5. Quantitative estimate based on modal analyses in /Wikman and Kornfält, 1995/. Mean value ± std
	K-feldspar	37.4±7.2		
	Plagioclase	21.6±3.8		
Grain size				
Age (million years)		1,441+5/–3	High	Based on /Åhäll, 2001/
Structure	Isotropic			
Texture				
Density (kg/m^3)				
Porosity (%)				
Magnetic susceptibility (SI units)				
Electric resistivity in fresh water (ohm m)				
Uranium content based on gamma ray spectrometric data (ppm)				
Natural exposure (microR/h)				
Subordinate rock type(s)				
Degree of inhomogeneity				
Metamorphism/alteration				
Mineral fabric (type/ orientation)				

Appendix 7

Overall confidence assessment

Table A7-1. Protocol for use of available data and potential biases in the bedrock description.

Question	Geology	Rock Mechanics	Thermal	Hydrogeology	Hydrogeochemistry	Transport
Which data have been used for the current model version (refer to tables in Chapter 2 of the report).	See Table 2-1. Note, also previous models of Äspö, Ävrö and Laxemar have been used as input for the Deformation Zone model. (Also data from the rock caverns on the Simpevarp peninsula).	See Table 2-2. Boremap data from the 5 drill core boreholes (KLX01, KLX02, KSH01A/B, KSH02, KSH03A/B). Laboratory test data from KSH01A and KSH02 (several different mechanical tests). Stress measurements, new and old. *From geological model:* • DFN-model. • Deformation zone model. • Lithological model. • Geological single hole interpretation.	See Table 2-3. Thermal conductivity, heat capacity and density measurements. Data from Äspö and Simpevarp. Modal analyses. Data from previous model version with reclassified rock codes and new modal analyses from boreholes. Thermal expansion measurements. Temperature, gradient and density loggings. Relationship density-thermal conductivity. Lithological model and Boremap core logging from the geological model.	Listed in Table 2-4. SKB P-03-70, P-03-110, P-04-213, R-01-52, IPR-01-06: Difference flow logging in KSH01A, KSH02, KAV01, KLX02. SKB P-03-113, P-04-151, P-xx-xxx. Wireline tests in KSH01A, KSH02, KSH03. SKB P-03-114, P-04-247, P-04-289, P-04-290, P-04-288: Hydraulic tests in HSH01, HSH02, HSH03, KSH01A, KSH02, KSH03, KAV01, KLX02 (transient tests). SKB P-03-56, P-04-212: Hydraulic tests and water sampling in HSH03, HSH02 and KSH03A. SKB reports TR-97-06, TR-02-19, R-98-55, Hydraulic tests in areas Äspö, Ävrö, Hålö, Simpevarp, Mjälen and Laxemar. Previous made evaluations used for DZ propertiy assignment.	Listed in Table 2-5. KSH01A, KSH02, KSH03 – Complete chemical characterization (Class 4 and 5), sampling during drilling, uranine analyses. KSH02; KSH03 – sampling during pump tests, during drilling, uranine analyses. Percussion drilled boreholes HSH02 and HSH03 – Class 3 + isotopes. HSH03 and HSH03 – Class 3 + isotopes. Environmental monitoring boreholes SSM and PSM – Class 3 + isotopes. Precipitation – Class 3 + isotopes. Surface water sampling – Class 3–5 + bio-supplements. Other available data: Äspö site data and data from Laxemar and Ävrö, Nordic site data. SKB P-03-89, SKB P-03-88, SKB P-03-87 where available at the time for the modelling.	See Table 2-6. Laboratory and in situ diffusion parameters from KSH01A and KSH02 (small amount of data available). Selected Äspö data on diffusion and sorption. Data from geological, hydrogeological and hydrogeochemical descriptions.

Question	Geology	Rock Mechanics	Thermal	Hydrogeology	Hydrogeochemistry	Transport
If available data have not been used – what is the reason for their omission (e.g. not relevant, poor quality, lack of time, …).	A) No raw data from CLAB were used (such as fracture statistics). Despite the existing compilation of these data Reasons for non-inclusion are: shallow boreholes, different format for representation, judged to be somewhat poorer quality. Also the raw data from Äspö or Ävrö has not been used, but the modelling has used models developed for Ävrö, Äspö and CLAB, as a starting point and used the new data from the site investigation to assess the information in these models. B) Vibro seismic data (a type of reflection seismic data) were not used due to poor quality. "Traditional" method using explosive source will be used in the future. C) KBH02 (from Hålö to Äspö) has not been fully used. One reason is that the mapping is old. However, the hole has been used as input to Äspö model.	A) Percussion drill hole data have not been used. Reasons: • The empirical approach is built up around drill core interpretation. • The theoretical approach builds directly on the DFN-model for fracture sets, sizes and intensity. • The percussion holes give information only from shallow depths. B) Old drill core raw data. Reasons: • The quality and format of data would be different from current. • The vast amount of data from Äspö could not have been analysed within the time frame. • Characterization based on some Äspö data has already been performed during the development of the methodology. (See R-02-04)	Old modal analyses from surface samples excluded due to different rock classification. New modal analyses in the thermal program from KAV01, KSH01A KSH02 excluded because the results were judged uncertain/less reliable – are being recalculated. The following density loggings were excluded. Reasons: KSH03 poor quality, KLX01 old method and KLX02 no calibration to real density measurements. Temperature loggings have not been fully used for modeling of thermal conductivity. The reason is a combination of lack of time and lack of historical temperature data.	A) Old data from Åspö, Hålö, Ävrö, Mjälen have been only been used for limited comparison due to lack of time. CLAB data not used at all! Some of the available data are most likely relevant. B) PSS data only used to a limited extent for the purpose of testing models. C) TRUE Block Scale Data.	Äspö, Laxemar and Ävrö data: Used for comparison and for conceptual modelling. Nordic site data, used for comparison and for conceptual modelling. Many observations excluded from the detailed modelling due to representativity problems.	Some Äspö data excluded due to methodological differences from established SI methods and/or incomplete supporting geological or hydrochemical information.
(If applicable) What would have been the impact of considering the non-used data?	(Considering all data as "virgin" or "raw" would have been an impossibly huge task). A) Hard to tell, but lineaments on the Simpevarp peninsula are short, i.e. the DZ model is not affected much by the detailed linked lineament interpretation (i.e. the indication is that there are no/few large deformation zones in the Simpevarp peninsula). Could possibly resolve existence/non existence of "stochastic" (i.e. minor) deformation zones – and enhance confidence.	A) The description of spatial variation in fracture intensity and occurrence of fracture zones may have resulted in a more detailed description of the superficial (shallow) rock mass. B) More certain description of the rock mass and the deformation zones in the area around the ÄHRL	Old modal analyses: Larger material for calculation of rock type models (more accurate models). New modal analyses in thermal program: More samples to enable calibration with TPS measurements. Density logging: More data for domain modelling. Adding these data could enhance confidence in the model.	A) The neglect of CLAB data has minor impact since they cover a depth down to about 50m below surface. However, may contribute to the understanding of near-surface conditions? The description of Äspö. Ävrö and Laxemar could have been better. B) The HydroDFN model could have been tested more thoroughly. The integrated hydrogeological and geologic interpretation	The non-representative data have been used for checking the impact on the visualisation and the overall understanding of the site. The results indicate that locally the difference can be ± 50%, at site scale in the order ± 10%.	Small, since it would most likely not have provided new data on additional rock types present within the Simpevarp area.

Question	Geology	Rock Mechanics	Thermal	Hydrogeology	Hydrogeochemistry	Transport
	B) Reflection seismic on the peninsula would potentially have generated important information concerning the geometry of deformation zones and revealed horizontal features, if they exist. The lack of this information in S1.2 will be supplemented in coming model versions. C) KBH02 (from Hålö to Äspö) has not been fully used. Hole covers a volume and direction, which would reduce bias and uncertainty in DFN-model (DZ implications better considered). It could have been possible to define high confidence DZ, with possible location beneath and between CLAB OKG 1, 2 and 3, based on a review of existing archive data.		Temperature loggings: Possibly better understanding of large scale variations in thermal conductivity.	of the model could have benefited of more time (Verification and parameterisation of deformation zones). C) TRUE Data (from Äspö HRL).		
How is data accuracy established (e.g. using QA procedures) for the different data? (Essentially just refer to tables in Chapter 2).	Data from SICADA qualified in accordance with method descriptions. See Table 2-1 and referenced P-reports. Surface data: No systematic revisit of lineament map, unless fully apparent mismatch with observations. Borehole data: No systematic check of SICADA data, or of single-hole geologic interpretation.	Data from SICADA qualified in accordance with method descriptions. In addition the following tests have been made: Boremap data: QA according to methodology document. Used as is, but simple checks – like "double values for same depth" are found and corrected. Shear tests and normal loading tests: Detailed analysis of every single test result. Improvement of test procedure and interpretation suggested. Uniaxial and triaxial tests: QA according to methodology document Tilt tests: Used as is. – P-wave: Used as is. – Stress measurements:	For details about data collection and accuracy refer to the individual reports. In addition to the quality assurance mentioned in reports, the thermal modelling team made their own reasonableness check while working with data. Modal analyses have been compared with TPS measurements to evaluate the validity. Boremap data have been completed with several SICADA deliveries to include both dominating and subordinate rock types and in cases where the data reports were not yet finished, contact with the report producers have been established.	The interpretation of new hydraulic tests presented in the data reports listed above follows standard QA procedures (Method descriptions). Data is also checked when stored in SICADA and when used in the modeling. The hydraulic tests focus mainly on the transmissivity. (Old data (Äspö HRL and Ävrö), are generally of good quality but some tests are of less good quality due to different methodology) (subsequently used in material property assignment to deformation zones).	Surface water data: QA established. Measurement errors in the order of (± 5–10% in analyses), see Chapter 4. GW data: QA established. Measurement errors in the order of (± 5–10%), see Section 9.2.	Site investigation Transport data: QA according to Method Descriptions. QA of data from other disciplines as described in Chapter 2 and references cited there. Accuracy in Äspö data established by evaluating the methods used.

Question	Geology	Rock Mechanics	Thermal	Hydrogeology	Hydrogeochemistry	Transport
		Inherent uncertainty in different measurement techniques applied are discussed and considered (by judgement) in the modelling.				
List data (types) where accuracy is judged low – and answer whether inaccuracy is quantified (with reference to applicable sections of this report or supporting documents).	See Table 2-1 and referenced P-reports. Chapter 5 (and subsections) addresses uncertainty in data. Important examples of inaccuracy are: • Spatial distribution of varieties of Ävrö granite that are "rich" (granite to granodiorite) contra "poor" (quartz monzonite to quartz monzodiorite) in quartz – Section 5.2 • Current evaluation of outcrop data on secondary red-staining (hydrothermal alteration) have poor spatial resolution, which leads to uncertain spatial distribution of secondary red staining – Section 5.3.3. • Lack of confidence in lineament interpretation especially their lengths, continuity and density. Lack of confidence that lineaments can be interpreted as deformation zones, which leads to a low accuracy in the number of possible def zones in the 3D model. • Direction of Deformation Zones in single-hole interpretation not given, but directions of fractures in these zones have high accuracy. • Radar reflectors have low accuracy both in directions and in actually detecting fractures. • Interpretation of open/sealed fractures in boreholes has quite high accuracy as combined BIPs and core mapping have been utilised. But open/sealed interpretation on outcrops is of poor accuracy.	Normal stiffness – Not quantified. Update of methodology report initiated. Shear stiffness – Not quantified. Update of methodology report initiated. Large scatter in results from tilt test – therefore laboratory shear tests are now used. Maximum (horizontal) principal stress from hydraulic (HF or HTPF) measurement methods – Not quantified – although other stress measurements (OC) provide estimates of these stresses. (See Section 6.4)	Modal analyses where the extent of alterations in minerals have not fully been evaluated. These inaccuracies have led to direct measurements of thermal properties being favoured instead of calculation from the mineral content. Temperature loggings from different boreholes show a variation in temperature at canister level. The difference is not large but even small differences influence the design. Possible explanations are water movements in the boreholes, an uncertainty in the temperature logging or inclination measurements in boreholes.	Results from WL-tests or airlift-pumping generally have less accuracy than other hydraulic tests but are still useful if no other tests are available. No quantification of inaccuracy available at present!	Major components, stable isotopes (± 5–10%). The effect of these errors on the interpretation is checked in the section of Explorative analysis.	Not relevant due to the limited amount of site data available.

Question	Geology	Rock Mechanics	Thermal	Hydrogeology	Hydrogeochemistry	Transport
	• Interpretation and combination of borehole and outcrop fracture data which due to different mapping techniques have different resolutions.					
If biased data are being used, can these be corrected for the bias?	Few data from areas covered by the sea and the bedrock information in the regional and local scale model area outside the Simpevarp subarea is only of reconnaissance character: • Location of the sedimentary rock cover in the sea area is uncertain, but it is evident that this boundary must lie east of the deformation zone ZSMNE024A. • There are far more lineaments and, thereby, inferred deformation zones on land and in i) areas covered by airborne geophysical measurements and detailed air photography and ii) in the sea area close to the Simpevarp peninsula and Ävrö, than in the remaining part of the sea area. This reflects the use of one or, in places, two data sets in the off shore area. This bias will remain in future model versions. (Note, topography is judged more important for lineament interpretation in Simpevarp compared to Forsmark due to the thinner cover of Quaternary deposits.) • The reconnaissance character of the surface bedrock information in the regional and western part of the local scale model area will be corrected for in the local scale model area in Laxemar SDM 1.2.	Potential directional bias as essentially sub-vertical boreholes. (Risk for systematic error in laboratory data has been reduced by using different laboratories.) (Potential bias in old data are handled by giving less weight to these old data.) (Spatial coverage of the boreholes is fairly even in the Simpevarp peninsula. i.e. this spatial bias is not judged to be a great problem.) However, laboratory test data for Ävrö granite were not yet available for version 1.2.	Poor representativety of samples measured with TPS in Ävrö granite. Data from Äspö HRL has been included to reduce the bias. Unknown bias resulting from using modal data in the SCA method. Thus SCA data is judged to be more uncertain that direct measurements (when available). SCA data have been compared with TPS data and where it has been possible, a correction of SCA data has been made. Generally, unknown representativety of modal analyses and TPS data due to possible biased sample selection. Sample selection has not been fully probabilistic. Samples were taken in order to characterise the rock type – not to find odd varieties. Bias in data may be reduced (unknown how much) but can be eliminated only for new data (probabilistic sample selection).	The core holes are more or less sub-vertical and may introduce a window effect in the borehole transmissive feature statistics (similar to problem with fracture statistics – see Geology) due to their vertical orientation. Hence, the structural model of the rock between the fracture zones may be biased. (Importance of anisotropy.) This effect can be addressed by incorporating more boreholes with other orientations.	Potential sources of bias include contamination from drilling fluid. Such biased data have been corrected by using back-calculations, but the representativity may be still be questioned.	Not relevant due to the limited amount of site data available.

Question	Geology	Rock Mechanics	Thermal	Hydrogeology	Hydrogeochemistry	Transport
	There is a bias introduced by the data gap between lineaments (lower cutoff > 500 m) and outcrop mapping (window < 30 m). A second bias concerns the fracture data from cored boreholes. All these boreholes, except KSH03, are steep and borehole KLX01 does not have oriented fractures. Both features discussed above introduce a bias in, especially, the orientation of fractures. The emphasis on subhorizontal fractures may be a result of this bias. This problem can partly be tackled with the help of a Terzaghi orientation correction and will be reduced more significantly when data from more inclined boreholes in different orientations together with outcrop observations in direct connection to the drilling site are evaluated in later model versions. Mapping of fractures at the surface will produce a bias towards steeply-dipping fractures. Some correction can be applied with the help of a Terzaghi orientation correction.		Risk for systematic error has been reduced by using different laboratories.			

Table A7-2. Protocol for use of available data and potential biases in the description of the surface system.

Question	Hydrogeochemistry	Hydrology and hydrogeology	Quaternary deposits (Overburden)	Oceanography	Biota
Which data have been used for the current model version (refer to tables in Chapter 2 of the SDM report).	Percussion drilled boreholes HSH02 – Class 3 + isotopes HSH03 – Class 3 + isotopes. Environmental monitoring boreholes SSM and PSM – Class 3 + isotopes. Precipitation – Class 3 + isotopes. Surface water sampling – Class 3–5 + biosupplements. Other available data: Äspö site data and data from Laxemar and Ävrö.	Regional meteorological data (TR-02-03, R-99-70). Local meteorological data, Oct. 2003 to Oct. 2004 (SICADA). Regional discharge data (TR-02-03, R-99-70). Local discharge data – "simple measurements" (SICADA). Topography on land and bathymetry of the Baltic sea; Geometric data on catchment areas, lakes and water courses (SICADA). Groundwater levels (SICADA). Hydraulic properties of Quaternary deposits (P-04-122). Inventory of private wells (P-03-05).	Surface based data on QD in the Simpevarp regional model area interpreted from aerial photos. Detailed map of Quaternary deposits in the Simpevarp detailed model area. Stratigraphical results from the Simpevarp subarea. Total depth of QD in the Simpevarp subarea. Marine geology (map and total depth of QD). Geophysics (areas with clay and/or peat, relative depth of QD). Soil type (soil classification).	Regional oceanographic data (TR-02-03, R-99-70) Local oceanographic data (SKB TR-97-14)	**Terrestrial producer model:** National Forest Inventory /Alling et al. 2004/ /Fridriksson and Öhr, 2003/ /Vogt et al. 1982/ /Andersson, 2004/ /Berggren et al. 2004/ /Lundin et al. 2004/ **Terrestrial consumer model:** Bird inventory P-03-31 Mammal inventory P-04-04, R-02-10 **Aquatic producer model:** P-03-69 **Aquatic consumer model:** P-04-17
If available data have not been used – what is the reason for their omission (e.g. not relevant, poor quality, lack of time, …).	Many observations excluded from modelling due lack of reported analyses at data freeze and due to higher than 10% Ion balance.	Local discharge measurements only summarized, not used for calibration/comparison (poor quality). No attempt was made to infer hydraulic properties from well inventory data (poor quality and data judged not relevant).	Older maps of Quaternary deposits were not used due to poor quality. Stratigraphical data from marine geology has not been used. Some geophysics has not been used. Generic data from national surveys has not been used.		All site specific data have been used. Some regional "no PLU data" have not been used due to poor quality or lack of quantitative information.
(If applicable) What would have been the impact of considering the non-used data?	Better description of spatial processes (more observations).	None	Improved stratigraphical knowledge.		Larger uncertainties would presumably have arisen if these data of poor quality had been used.

Question	Hydrogeochemistry	Hydrology and hydrogeology	Quaternary deposits (Overburden)	Oceanography	Biota
How is data accuracy established (e.g. using QA procedures) for the different data? (Essentially just refer to tables in Chapter 2.)	Surface water data: QA established (± 5–10% in analyses) GW data: QA established (± 5–10%).	Meteorological data measured by following SMHI standard procedures. Catchment areas interpreted from maps and checked in the field. Hydraulic properties in some cases checked by repeated field tests and/or alternative evaluations.	Field classification and sampling according to national standard methods. Calibration between experts. The marine geological interpretations are verified by sampling. Soil classification according to international standard. The map of QD in the regional model area was compared with the QD map in the Simpevarp subarea.	Scientific “status” (TR-97-14)	Data accuracy described by statistical description, and comparison (expert judgement) to generic values, of parameters in each model.
List data (types) where accuracy is judged low – and answer whether accuracy is quantified (with reference to applicable sections of this report or supporting documents).	There are no data where accuracy is really low. Accuracy in major components, stable isotopes is judged to be ± 5–10% The effect of these errors on the interpretation is checked in the section of Explorative analysis.	Data known to have a low accuracy were excluded from the modelling process.	Distribution of till on the seafloor. The geophysical interpretations needs field verifications. The map of QD in the regional model area.		Production of biomass and standing stocks of biomass in lakes and sea. Soil biota property data. Ecosystem process data. Flow of matter.
If biased data are being used, can these be corrected for the bias?	The effect of ion balance errors and drilling water contamination can be back calculated but the representativity may be still put in question.	Meteorology: Precipitation data corrected for measurement errors by standard procedure. Hydrology: Generic information on variations in small areas and influence of topography and land use can be used to infer local discharge estimates from available discharge data in relatively large catchments. Hydrogeology: Potential bias in results of field tests can, to some extent, be checked by comparison with literature data.	There is a bias since the detailed mapping is performed in only a part of the model area. Outside this area uncertainty is much larger.	None	–

Table A7-3. Protocol for assessing uncertainty in the bedrock Geology aspects of the SDM.

Aspect of SDM	Uncertainty	Cause (e.g. data inaccuracy, information density, uncertainty in other discipline model or process understanding)	Has uncertainty been assessed considering information from more than one data source or through a calibration or validation exercise?	Impact on other uncertainties (in all disciplines)	Quantification (provide reference to applicable section of the SDM report)	Potential Alternative representation. (Is there reason for this and has one been developed)	Are there unused data which could be used to reduce uncertainty	What new data would potentially help resolve uncertainty?
Geology – rock domain model	Spatial distribution of Rock Domains, outside the Simpevarp subarea.	Only reconnaissance data available – lack of detailed bedrock map. Surface bedrock information in the regional model area, outside the Simpevarp subarea – discussed in Section 5.2, 5.3.4. Quality of the surface bedrock information.	No, there is only one data source (version 0 bedrock map).	No	Difficult to quantify.	No alternative exists.	No	New bedrock map in the regional model area (deltailed in the local scale model area).
	Offshore lithology (lower quality data in these areas).	No data – bedrock not exposed.	No, there is no data source (except bedrock map version 0).	No	Difficult (impossible) to quantify.	No alternative exists.	No	New bedrock map needed.
	3D geometry of most of the rock domains.	Restriced subsurface information. Pristine igneous bedrock terrain with little structural control (i.e guidance for modelling).	No, very restricted subsurface information.	Spatial distribution of mechanical and thermal properties that depend on rock domains.	Difficult to quantify.	The restricted subsurface information does not allow construction of any alternative models.	No	More subsurface data are needed – cored boreholes, detailed geophysical information (modelling).
	Heterogeneity – Proportion of rock types in domains, veins, patches, dykes, minor bodies, frequency of minor deformation zones. (Statistical anisotropy?)	Restricted information – difficult to estimate both the proportion and spatial distribution. Spatial distribution of subordinate rock types, i.e. inhomogeneities – Section 5.3.3.	Yes, 1) outcrop database for the Simpevarp subarea, 2) cored boreholes, 3) cleaned outcrops.	Spatial distribution of mechanical and thermal and transport properties that depend on rock types.	Section 5.3.3. Proportions given – uncertainty expressed as ranges in the property table. No description of "size" distrubition of heterogeneity.	No – is better expressed as uncertainty range.	No – although the indicator variography made in the thermal analysis should be considered in the next version.	1) Information from new boreholes, 2) detailed investigation of cleaned outcrops what concerns the amount, distribution and character of subordinate rock types.

					(Although indicator variograms from rock types have been assessed in the thermal modelling).			
	Spatial distribution of varieties of rock types – for example the Ävrö granite that are “rich” (granite to granodiorite) contra “poor” (quartz monzonite to quartz monzodiorite).	Restricted data – more or less rapid changes in composition due to mixing and mingling phenomena during formation of the igneous rocks.	Yes, both modal and chemical composition.	Spatial distribution of thermal properties within especially within the Ävrö granite. Impact on mechanical properties possibly low (but lab data not existent in the Ävrö granite yet).	Difficult to quantify but is discussed in in quartz – Section 5.2.	No – is better expressed as uncertainty range.	No	Increased number of modal and chemical analyses both from the surface and cored boreholes.
	3D distribution of secondary alteration, e.g. “red staining” (hydrothermal alteration).	Restricted information – difficult to estimate both the proportion and spatial distribution.	No, only documentation in connection with the Boremap mapping of drillcores.	Thermal and transport properties of altered rock are possibly different compared to surrounding rock. Spatial extent of the red-stained volumes could be in the order of tens of m. However, the alterations usually implies increased thermal conductivity, i.e. ignoring this results in underestimates of the thermal conductivity.	Quantified as proportions. See Section 5.3.3.	No – is better expressed as uncertainty range.	No	
Geology – structural model	Existence of deformation zones (only some interpreted with high confidence) – are all lineaments really deformation zones?	Lack of supporting subsurface data.	Ongoing PLU? Verification HSHs (Lineaments).	Hydrogeology and rock mechanics are directly affected by this uncertainty. The deformation zone model provides the geometrical framework for the hydrogeological modelling.	No	Yes, potentially multiple alternatives could be produced. No, no alternative has actually been.	The underlaying basis for the linked lineament map should ideally have been revisited! Locally perhaps! – review of CLAB, OKG, Ävrö and Äspö data – reinterpretation using local primary data jointly with new data, not over the the entire modelled area.	BH intercepts part of ongoing PLU. Seismic survey results.

	Potentially there are non-included zones (mainly subhorizontal) (e.g. the Nordenskjöld hypothesis. However, there are no indications at present (also applies to ÄHRL).	Non-included zones: the CLAB-OKG 'hole effect'. Subhorizontal zones.	No No	Hydrogeology and rock mechanics are directly affected by this uncertainty. The deformation zone model provides the geometrical framework for the hydrogeological modelling.	No No	Yes – see the Ävrö model. Not included in modelling! Possibly useful for performing alternative models using sub-horizontal deformation zones (L1.2).	Yes, existing archive data (P-03-07, P-03-86).	Ongoing PLU verification! Verification efforts on seismic reflectors! VSP/Drilling/Hydraulic tests.
	Continuity along strike and at depth, dip and termination.	It is intrinsic to the modelling process and questions of scale.	Yes, but more can be done. A few lineaments have been reviewed.	Hydrogeology is possibly affected by this uncertainty, but the impacts are possibly handled within the uncertainty of properties within deformation zones.	No	Not done	Not unused, but needs to be reassessed/reviewed.	Field control of lineaments performed during field bedrock mapping. BH interceptions-ongoing PLU.
	Character and properties – also in the well established (e.g. from Äspö) zones. Strong spatial variation of properties (width, internal structure, fracturing, also hydraulic properties...) as seen in multiple intercepts.	Information density and spread of data. Inherent concentrations of data.	No. Aware of problem but related to flow of new primary data.	Hydrogeology and rock mechanics are directly affected by this uncertainty – and this in turn causes uncertainty in the distribution of e.g. hydraulic properties in the "plane".	No	Not done yet – but there remains potential for alternatives. Impact is partly assessed in hydrogeology.	Review of Äspö data for base case model. (Data in TMS on eg. NE-1, Äspö Shear Zone characteristics plus relevant borehole data.)	Additional boreholes.
Geology – DFN model	Fracture set (orientation) identification.	Subhorizontal outcrops and subvertical boreholes which are also mapped with different resolution.	Yes, implicit in methodology and illustrated in verification example.	Hydrogeology is critically affected by these uncertainties and to some extent also rock mechanics.	See Section 5.5.	Section 5.5. Different conceptual assumptions regarding tools and possible modelling "style". Three different DFN model alternatives are presented and two independent teams are used.	Yes, mainly Äspö (tunnel mapping, 3D) and CLAB data. Scan line data has not been utilised (S1.1/S1.2) (detailed and surveillance)! (L< 0.5 m)	Inclined BHs, Outcrops on drill sites, especially on drill sites where several shorted inclined and vertical cored boreholes are drilled.

Fracture size distribution – interpolation between lineament and mapped outcrop data and for some sets only local information (extrapolation to larger sizes).	Uncertainty in the relevance of lineaments. What do they represent, length, continuity etc. Lack of size data between lineament lower and outcrop higher end!	Uncertainty assessed through possible variability in size fits (upper, lower bounds and best fit).	Hydrogeology (HydroDFN modelling) – Affects intensity of minor stochastic conducting zones.	See Section 5.5.	Three different alternatives, see above and Section 5.5.	No (JH). CLAB II rock cavern mapping!? Connectivity of fractures between CLAB I and CLAB II caverns/tunnels?!	Confirmation of lineaments zones. Alternative lineament interpretations? Aerial photography at low flight altitudes (compl. to long trenches)
Fracture intensity – coupling surface to subsurface, variability with depth. Coupling to DZ-model. Uncertainty in the thickness-size correlation.	Lack of data in superficial bedrock (0–100m). For projection of surface stats to the subsurface. "Stochastic" deformation zones in single hole interpretation are quite wide. Uncertainty in Size Correlation not analysed.	Verification exercises for intensity measures have been performed for conceptual model alternatives 1 and 2.	Hydrogeology is critically affected by these uncertainties and to some extent also rock mechanics.	Yes, see Section 5.5.	Variability by depth has been tested and rejected, see Section 5.5.	Yes, mainly Äspö and CLAB data and LO Ericsson surface observations. Possibly old data (observations on length, width and property relation) from CLAB etc. could be used to observe extent of some of these minor zones.	Inclined BHs, alternative orientations, in different rock domains. Preferably in conjunction with surface area mapping. Use Äspö tunnel mapping data to assess coupling of intensity to lineament proxy! Report exists (check with Roy, GEM).
Assumption of fracture intensity coupled to Rock Domains.	Intensity can be a function of rock type instead of rock domains In that case reasons to revisit rock domain division!	Verification exercises for intensity measures have been performed.	These uncertainties impact hydrogeology and to some extent also rock mechanics modelling (rock mass strength).	See Section 5.5.	Both alternative models presented for each rock domain with varying intensity measures, see Section 5.5.	Yes, mainly Äspö HRL and CLAB data.	
Spatial model.	Is there a correlation to rock domain model? Is there an impact from proximity to deformation zones? Are the sampling windows large sufficient?	Only implicit through coupling to rock domain model and to nearby deformation zones.		See Section 5.5.	The uncertainty is not quantified and is rather listed as a reason for alternative model hypotheses at this stage.	Yes, mainly Äspö and Clab data.	Inclined BHs, in different rock domains.
Spatial distribution (frac stats) in different rock domains.	Coupled to rock domain model but has not been verified.	No		–	–	Yes, mainly Äspö and Clab data.	Inclined BHs, in different rock domains.

Table A7-4. Protocol for assessing uncertainty in the rock mechanics and thermal property aspects of the SDM.

Aspect of SDM	Uncertainty	Cause (e.g. data inaccuracy, information density, uncertainty in other discipline model or process understanding)	Has uncertainty been assessed considering information from more than one data source or through a calibration or validation exercise?	Impact on other uncertainties (in all disciplines)	Quantification (provide reference to applicable section of the SDM report)	Potential Alternative representation. (Is there reason for this and has one been developed)	Are there unused data which could be used to reduce uncertainty	What new data would potentially help resolve uncertainty?
Bedrock in-situ stress state	Rock stress magnitudes and distribution within the model area. (Uncertainty varies in the area, and is lower at Simpevarp peninsula and even less at ÄHRL.)	Data inaccuracy (see Table 12-1) and information density (especially outside ÄHRL, Simpevarp peninsula and Laxemar).	Different measurements have been used and compared, see discussion in Section 6.4. Experiences from excavations at depth in ÄHRL also confirm that extremely high stress magnitudes do not exist in the area, since major stability problems has not been observed.	Low – although note that some Rock Mechanics Parameters are stress dependent (relations are given explicitly in Chapter 6).	Uncertainty in stress magnitude is described as a span of potential values for the mean. See Table 6.3.	No alternative representation has been developed. (Better expressed as an uncertainty interval.)	No	More overcoring measurement data. However, the current understanding of stress is probably sufficient, since the current uncertainty span in stress still suggest rather low overall stress levels.
	Uncertainty in the division of local model area into two stress domains.	Low data coverage over the local model area. Uncertainties in the deformation zone model.	Stress data exists from both two domains. The effect of deformation zones is the cause for the division into different domains.	Possibly impact on (explaining) possible difference in transmissivity anisotropy between ÄHRL and Simpevarp peninsula).	See Table 6.3.	Alternative deformation zone models could be a reason to have alternative stress models. In particular differences in the dip of large zones could be a reason.	No	More measurements in the Laxemar subarea. "Improved confidence in the 3D DZ model, as expected in Laxemar version 1.2."
Bedrock mechanical properties	Extent/occurrence of stochastic (minor) deformation zones, having different mechanical properties, inside the domains between deterministic zones.	Number of drill holes is limited and biased to vertical holes. Uncertainty in the deformation zone model. Uncertainty in the thickness-size correlation.	Both single hole interpretation results and DFN-modelling results have been used.	The understanding should be compatible with the description of hydrogeology.	Not quantified. See Section 6.3.	Not developed. (Should possibly be considered in the DZ model and/or DFN-model.)	Possibly old data (observations on length, width and property relation) from CLAB etc. could be used to observe extent of some of these minor zones (see Table 12-1).	Improved DZ and DFN models also describing the interior of zones.

Effects of pore pressure on rock mass strength properties.	No established approach to assess this effect. Uncertainty in parameter/process understanding.	Pore pressure is part of empirical approach but not part of theoretical approach.	Low	Not quantified, but effect is probably not very large. See Section 6.3.	Not developed.	No	Laboratory testing of fractures with pore pressure. But methodology for this issue is not established. Theoretical approach extended to include impact of pore pressure.
The spread in rock mass mechanical properties from theoretical approach has uncertainties.	The DFN-model does not describe, in this version, the uncertainty or variation in the fracture intensity in the local model area.	Model uncertainties are discussed in SKB R-04-## (update of theoretical approach#).	Low	Uncertainty is estimated using two approaches (see Chapter 6, although uncertainty in intensity contributing to this uncertainty in the theoretical approach is not directly assessed.	No, uncertainty better expressed as range/ distribution.		
Rock mechanical properties for intact rock of rock type Ävrö granite.	Lack of new laboratory tests.	Old data from Äspö has been used, but there are uncertainties in the quality of these data. Furthermore, these data have low coverage, i.e. may give bias.	Minor effect on the rock mass properties.	See Section 6.2.	No reason. (Better expresses as uncertainty.)	No	Already planned additional laboratory test on this rock type.
Mechanical properties – deformation zones. No Division between different types DZ (ductile vs. brittle).	Low data coverage in large deformation zones, since only KSH03 intersects a deterministic deformation zone. Characterisation of DZ does not fully resolve differences in type of deformation (brittle, ductile). For zones only the empirical approach is used. The bedrock material inside zones are not easily sampled for lab. testing.	No	Possibly on the stress model – on the other hand the stress model assumes very low strength of the major zones.	See Section 6.4.	No reason, as long as the site specific data is scarce. Uncertainty is now better expressed as the ranges in Table 6.3.	Possibly data from Äspö HRL tunnel intersection with large deterministic zone.	More geological information on the DZ properties (e.g. from trenches and drill core data from boreholes intersection with large deformation zones).

Bedrock thermal properties	Thermal conductivity – rock type.	Uncertain representativeness for SCA and TPS data. SCA calculations from modal analysis (thermal conductivity of mineral, modal composition, alteration), see Table 12-1. Uncertainty in calculation of thermal conductivity from density loggings.	Uncertainty in SCA data has been evaluated by comparison with TPS data and by sensitivity studies. Validity in using density lto calculate thermal conductivity in rock type Ävrö granite (501044) is demonstrated. Large uncertainties for other rock types. However, no measurements have been made in order to verify the use of density loggings to calculate thermal conductivity.	No	Spatial variability is quantified, see below. Uncertainty in spatial variability is discussed, see Chapter 7.	No, uncertainty captured as distribution.	No	Representative direct measurements of thermal conductivity. More samples with both density and thermal conductivity measurements (501044). Extensive sampling of other rock types to produce variograms of spatial variability. Measurements in density logged boreholes.
	Thermal conductivity – scale transformation	Uncertainties in transformation between different scales e.g. measurement scale to canister scale.	TPS, SCA and density data are used. Density loggings have been used to analyse the spatial variability in Ävrö granite.	No	Spatial variability is quantified. Uncertainty in spatial variability is discussed, see Chapter 7.		No	Measurements In relevant scale.
	Thermal conductivity – rock domains	Uncertainties in large scale variations inside domains with medium or low presence of Ävrö granite (See geology). Problem with representativity of borehole – domain. 3D geometry of most of the rock domains is also uncertain. Uncertainties in the modelling approach.	Different approaches are used to evaluate the variability in thermal conductivity.	No	Spatial variability is quantified. Uncertainty in spatial variability is discussed, see Chapter 7.		No, but range is estimated by considering different approaches, see Chapter 6. Possible to use temperature loggings to evaluate large scale variability in thermal conductivity, see Table 12-1.	Need of more data to evaluate the spatial variability with higher confidence. The representativety problem can be resolved with more boreholes. Also, Improved confidence in Rock Domain model would help.

Thermal properties in DZ	No thermal data from the DZ.	No	No	A range could be set.	No reason.	No	Measurements at a relevant scale.
In situ temperature	Uncertainty in temperature data, possibly due to convection in the boreholes, etc. Shortcircuited flows in the borehole.	Difference between boreholes.	No (the differences are small – but are important for Engineering and layout).	A range is provided (see Chapter 7).	No reason.	No	Uncertainty judged to be of less importance. More temperature logs. Possibly reconsider measurement procedure to mitigate effect of long term thermal convection.
Thermal expansion	Possible data inaccuracy.	Not yet – but comparison between methods and laboratories is done but not reported. Comparison with APSE data could be useful.	No, but effects Rock mechanics evolution due to heating.	A range is provided (see Chapter 7).	Not yet. It could be discussed whether the expansion is linear with T or not.	Data from the APSE experiment at ÄHRL.	Laboratory test method development (is already underway).

Table A7-5. Protocol for assessing uncertainty in the hydrogeology, hydrogeochemistry and transport property aspects of the SDM.

Aspect of SDM	Uncertainty	Cause (e.g. data inaccuracy, information density, uncertainty in other discipline models or process understanding)	Has uncertainty been assessed considering information from more than one data source or through a calibration or validation exercise?	Impact on other uncertainties (in all disciplines)	Quantification (provide reference to applicable section of the SDM report)	Potential Alternative representation. (Is there reason for this and has one been developed)	Are there unused data which could be used to reduce uncertainty	What new data would potentially help resolve uncertainty?
Bedrock hydro-geology	Geometry of deformation zones and their connectivity.	Information density a major cause. More integration with geology can decrease uncertainty.	Modelled a decreased number of DZ and tested in numerical gw-modelling.	Has impact on the flow model and then transport paths and the integrated evaluation together with hydro-geochemistry.	Discussed in Chapter 8.	Yes, and a few cases have been tested.	A few (Äspö data, local coverage), but cannot reduce overall uncertainty much. Conceptual gain?!	New borehole data and reflection seismics (much a integration with geology). Interference data –drilling & cross-hole tests!
	Transmissivity distribution in zones (spatial variability).	Spatial variability: Sparse data in zones (need multiple data points in each zone).	No	Flow field and connectivity within and between deterministic DZ.	None	Yes. Planned for some different cases of T-distribution explored in regional flow modelling for next model version. In principle DZ can be modelled as HydroDFN and effective values as well as correlation models can be estimated and used in continuum models – this has not yet been tested or established.	No! Potentially, existing correlation structure established using Äspö data could be used!	Boremap+BIPS+PFL data for a number of zones and some interference tests within these zones.
	Hydraulic DFN model. Fracture transmissivity distribution.	Uncertainty in DFN-models. Uncertain conceptual models for coupling transmissivity as a function of fracture length. Larger features of the DFN-model usually are made up of many small fractures, and do not represent individual fractures.	Yes. Calibration using inflow measurements from PFL in individual boreholes.	Yes. The heterogeneity of the flow field and its implications for transport paths and expected distribution of ground waters with different composition. Inflow estimates to the open repository.	Yes.	Several Hydro-DFN models with different T-models (T correlated/un-correlated) fractures have been tested.	PSS data can be used more to test the Hydro-DFN models by simulating existing tests performed at various scales. PFL data with the oriented flowing features.	Data to resolve the geometry of fractures using inclined coreholes. Detailed hydraulic tests 0–100m below surface. Interference tests between bore holes may to some extent (generally long distances in a sparsely fractured rock) be used to test model.

		Variable measurement limit for PFL, that is higher than PSS, and affects PFL-anomaly estimates of fracture transmissivity. Also dependent on the lower measurement limit of PSS. Lack of detailed hydraulic tests in Boremaped coreholes 0–100m below surface. uctive features. There are also uncertainties in how to estimate size and intensity models for the cond						Single-hole interference tests (one section for injection and several pressure monitoring sections) is a possibility to tests connectivity but no tools are present available and the usefulness of the methodology is not known.
	Digital elevation model (Point of departure for paleohydro and establishment of groundwater surface)	Lack of unified elevation model (topography and bathymetry) (including well specified shoreline)	Yes (groundwater surface).	Affects distribution of modelled discharge areas.	Yes (Projection to results of modelling in regional scale.)	No reason to test alternatives, uncertainty can be handled by unifying model of topography and bathymetry at key locations.	Yes. Unified DEM available for L1.2.	No need
Palaeohydro-geology	Present day salinity and water type distribution.	Number and spatial distribution of sampling points is limited. One information used is the concentrations of “Water types” which have uncertainties greater than the individual chemical components.	Yes (for the conductive network). In the regional gw-modelling different initial conditions have been applied to reproduce measured values at depth.	Hydrogeochemistry and Transport description! Open repository (initial condition).	Yes (Results presented in Section 8.5.)	No need	No (Although to some extent the implication of the spatial distribution of all salinity data may not have been fully explored in the simulations and analysis). Possibly isotopes can be used more in the testing of models.	New boreholes and new sampling points will improve description of present day salinity distribution (incl. additional matrix data).

		There are also uncertainties of the orogin (conceptual model) of the water types and how they should be introduced as initial and boundary conditions. Matrix water chemistry is not available at present.						
	Regional scale initial and boundary conditions.	Boundary conditions are uncertain since there are no well defined boundaries. One main uncertainty in modelling the paleohydrology is the uncertainty in the initial conditions for the modelling period that also will be more or less unknown and can possibly be assessed by modelling. Other uncertainties are the Littorina water characteristics and time frame.	Yes. Transient simulation of transport (TDS, water types) not accounting for chemical reactions, and comparing with present-day water chemistry.	Transport description! Open repository (initial condition).	Yes (Results presented in Section 8.5.)	Different initial and boundary conditions have been tested.	No. Possibly isotopes can be used more in the testing of models.	New boreholes and new sampling points will improve description of present day salinity distribution (incl. additional matrix data) and distribution of isotopes that may help.
Hydrogeo-chemistry	Spatial variability in 3D at depth.	The information density concerning borehole groundwater chemistry is low. The samples are mixed and represent an average composition.	A validation test has been conducted where representative/non-representative samples have been used as a basis for interpretation.	This may cause uncertainties concerning the salinity interface in e.g. hydrogeological modelling and transport modelling. Causes uncertainties in overall hydrochemical understanding of the site.	Local uncertainty in the order of ± 50% site scale uncertainty in the order of ± 10%, see Section 9.6.	Alternative representation in Section 9.6.	Comparison with hydrogeological description.	More data observations from deep boreholes. Rock matrix samples.

Temporal (seasonal) variability in surface water chemistry, which ultimately impacts the groundwater in the bedrock. Temporal averaging follows from processes being slow.	The sampling may not describe the seasonal variation and samples may be taken at different time intervals from the surface versus the shallow boreholes.	No this has not been done, but a detailed surface hydrogeological modelling may be helpful for this type of exercise.	Can cause uncertainty concerning the interaction between surface and groundwaters and may affect transport modelling. The amount of reactions taking place at the surface may not be properly described.	The effects from seasonal variation have not been quantified but the effects have been identified, see Section 9.3.	Different modelling approaches are applied to the same data set to describe the same processes.	No	Sampling reflecting seasonal variation from selected surface and borehole locations in identified recharge/discharge areas.
Model uncertainties (e.g. equilibrium calculations, migration and mixing).	Inaccurate pH measurements, inaccuracy in the thermodynamic data bases, wrong mineral phase selections, wrong end-members selection, model uncertainties.	For validation different modelling approaches are applied to the same data set.	May cause uncertainties in transport modelling and hydrogeological modelling. Causes uncertainties in overall hydrochemical understanding of the site.	One unit error in the pH measurements may causes one unit error in the equilibrium calculations. The uncertainties of the mixing modelling is ± 10%, see Section 9.2, 9.5 and 9.6	Different modelling approaches are applied to the same data set to describe the same processes thereby confidence is built into the description.	No	No new data needed.
Identification and selection of end-member waters. There is a judgemental aspect of the M3 (principal components) analysis.	Poor understanding of the hydrogeology or modelling requirements.	Integration with hydrogeology to identify and use same end-members.	May cause uncertainties in the chemical process description and in the integration with hydrogeology. Causes uncertainties in overall hydrochemical understanding of the site.	Different end-members have been selected in the regional/local models, no quantification has been conducted, see Section 9.5 and 9.6	Different modelling approaches are applied on the same data set to describe the same processes for confidence building.	No	Data from extreme waters.
Groundwater composition in the rock matrix.	Few measurements.	No	May affect the hydrogeological modelling and transport modelling. The description of the interaction between groundwaters in the highly permeable and low permeable systems will be uncertain.	No	No	No	Samples for rock matrix determination have been collected and the results will be available for Laxemar.

Transport properties	Dffusion parameters for site-specific materials.	Only small amount of site investigation data available.	Identification of data from other sources based on geological comparison.	Related to uncertainties in salt transport and reactive (hydrogeochemical) transport modelling.	None	None	No	Site data on transport parameters – more will be available for L1.2, but most of the data not before CSI.
	Sorption parameters for site-specific materials.	Only small amount of site investigation data available.	Identification of data from other sources based on geological comparison.	Related to uncertainties in salt transport and reactive (hydrogeochemical) transport modelling.	None	None	No	Site data on transport parameters – more will be available for L1.2, but most of the data not before CSI.
	Assignment of parameter values to the "elements" in the geological description (rock units and structures).	All relevant materials and structures are not represented in the site-specific database. Parameterisation to a large extent based on expert judgement.	Use of data from other sources and "extrapolation" of database according to modelling methodology.	Related to uncertainties in salt transport and reactive (hydrogeochemical) transport modelling.	None	Alternatives could follow from alternative geological models. No alternative developed at this stage.	Possibly – potential for further import of Äspö data will be assessed.	Site data on transport and geological parameters.
	Understanding of retention/retardation processes as a basis for selection of parameters in models.	Limited site-specific input to development of process under-standing available.	A study, presently based on Äspö data, of "alternative" processes and process models has been performed.	Coupled to hydro-geochemical description (process modelling).	None	Potential for development of alternative retention models. No alternative developed at this stage.	Possibly – all hydrogeochemical site data not considered in present model version.	Transport data and incorporation on hydrogeochemical data in the analysis.
	Correlation between matrix transport properties and flow paths.	Lack of site-specifc transport data impedes the establishment of quantitative correlations.	An first attempt is made to associate "typical fractures" with hydraulic properties.	Coupled to hydro-geological description (properties of structures in flow models).	None	Quantitative coupling between retardation and flow paths is handled by Safety Assessment.	Possibly – only a limited evaluation of available hydrogeological data performed at this stage.	Site data on transport parameters. Coupled Hydro-Transport evaluation of field data.

Table A7-6. Protocol for assessing uncertainty in the surface system aspects of the SDM.

Aspect of SDM	Uncertainty	Cause (e.g. data inaccuracy, information density, uncertainty in other discipline models or process understanding)	Has uncertainty been assessed considering information from more than one data source or through a calibration or validation exercise?	Impact on other uncertainties (in all disciplines)	Quantification (provide reference to applicable section of the SDM report)	Potential Alternative representation. (Is there reason for this and has one been developed)	Are there unused data which could be used to reduce uncertainty	What new data would potentially help resolve uncertainty?
Surface system – Quaternary deposits	Terrestrial: composition, spatial distribution, depth and thickness of individual strata.	Low information density in the Laxemar subarea.	No	Hydrological and transport modelling (flow of matter). Soil type (jordmån) modelling. Bedrock surface mapping. Hydrogeological modelling of deep rock. Hydrogeochemistry modelling. Ecosystem descriptions and models.	No	No	No	Measurements of composition, spatial distribution, depth and thickness of individual strata. Will partly be provided in version L1.2.
Surface system – Surface hydrology, near-surface hydrogeology	Meteorology – spatial and temporal variability in precipitation and other meteorological parameters.	Only very limited site specific data available.	Temporal variability (spatial, to some extent): Evaluation of data from different SMHI stations in the region (performed in v0; TR-02-03).	Hydrological and hydrogeological models (near surface and deep rock). Oceanographic models. Terrestrial ecosystem models.	No	No	No	Site specific data – measurements started Oct. 2003 at Äspö; a new station was established in W part of model area during fall 2004.
	Water discharge in the surface system – spatial and temporal variability in runoff.	Only results of "simple" (and inaccurate) measurements available; no data from discharge stations in S1.2.	No	Hydrological models (comparison/ calibration). Hydrogeological models (basis for setting BCs). Transport/flow of matter. Ecosystem models.	No	No	No	Site specific data – measurements initiated 2004, but time series will not be available in S1.2 or L1.2.
	Surface water and groundwater levels.	Only very limited and preliminary data.	No	Hydrological models (basic description, comparison/calibration). Hydrogeological models (basis for setting BCs). Transport/flow of matter. Ecosystem models.	No	No	No	Site specific data – monitoring has recently been initiated in some soil tubes and surface waters; additional tubes will be installed.

	Quantification of water balance components (evapotranspiration, distribution of runoff on surface water and groundwater).	Limited site and generic data.	No	Hydrological models (basic description, comparison/calibration). Hydrogeological models (basis for setting BCs). Transport/flow of matter. Ecosystem models.	No	No	No	Site specific input data to different types of mathematical models. Evapotranspiration measurements – direct local measurements of water balance components will be performed.
	Interactions between surface and bedrock systems.	Insufficient data and models/descriptions of hydraulic properties and flow conditions in overburden and uppermost rock.	No	Hydrogeological models (recharge to rock, effects of repository drawdown). Transport/flow of matter (incl. radionuclide transport models). Ecosystem models.	No	No	No	Geologic (e.g. stratigraphy) and hydrogeologic (e.g. hydraulic properties, groundwater levels) data.
Surface system – Chemistry	Temporal and spatial variation in water composition of surface waters.	The sampling may not describe the seasonal variation.	No this has not been done, but a detailed surface hydrogeological modelling may be helpful for this type of exercise.	Can cause uncertainty concerning the transport modelling. The amount of reactions taking place at the surface may not be properly described.	The effect from seasonal variation has not been quantified but the effects have been identified, see Section 9.3.	Different modelling approaches are applied on the same data set to describe the same processes.	No	Sampling reflecting seasonal variation from selected surface locations.
	Uncertainty in model (e.g. equilibrium calculations).	Inaccurate pH measurements, inaccuracy in the thermodynamic data bases and wrong mineral phase selections.	For validation different modelling approaches are applied on the same data set.	May cause uncertainties in transport modelling and hydrogeological modelling. Causes uncertainties in overall hydrochemical understanding of the site.	One unit error in the pH measurements may causes one unit error in the equilibrium calculations. The uncertainties of the mixing modelling is ± 10%.	Different modelling approaches are applied on the same data set to describe the same processes.	No	Accurate in-situ pH measurements from the surface system.
Ecosystems – biotic	Biomass and production (flora and fauna).	Lack of site data.	No	No	No	No	No	Site data of biomass and production.
	Chemical composition of biota.	No site data.	No	No	No	No	No	Site data.

Table A7-7. Interactions judged to be important (green) and to what extent these where actually considered (black).

Bedrock Geology	Spatial distribution of properties based on Rock Domains. DFN geometry is used to infer properties. Is done	Spatial distribution of properties based on Rock Domains. Modal analyses is used as (one) input. Is done	Rock Domains, Deformation zones and DFN-geometry is the geometrical framework. Geometry is considered. Significance of differences between RD assessed, but not resolved. Description of deformation zones not used in the property assignment.	Fracture mineralogy and Chemical composition of Bedrock should be considered. Fracture mineralogy is considered and the chemical composition is used in the modelling of the palaeo effects.	Spatial distribution of properties based on Rock Domains (identified rock types in rock domain model). Porosity measurements on surface and borehole samples. Fracture mineralogy and hydrothermal alteration. Is done, but lack of transport property data in the different RD makes correlation study weak.	No need	No need	Data on geometry (rock surface, fracture zones, etc), mineralogy and geochemistry. Is considered.	No need
Stress orientations in relation to fracture sets could give additional confidence i DZ and DFN model. Reason for division of RD and DZ could be re-assed (less reason to split between domains or reason to split existing domain). Discussed, but not formally. Rock Mechanics modelling group has assessed differences in mech. prop. in different RD, considered in the geological modelling yet.	**Rock Mechanics (in the bedrock)**	No need	Stress orientation expected to affect hydraulic anisotropy field. Hypothesis of anisotropy in T assessed – not yet fully resolved. (Since strong correlation found at ÄHRL – the hypothesis is kept despite unclear evidence in data from Simpevarp subarea.)	No need.	Consider stress impact on “intact” rock samples for laboratory measurements. Part of the data evaluation.	No need	No need	No need	No need

Could affect description of RD – Thermal data could be used as input to mineralogical description. Discussed, but not formally considered in Geological Modelling. The actual impact on the RD model of the thermal data is judged low.	No need (thermal expansion analysis is outside SDM see Table 12-4).	**Thermal (in the bedrock)**	Temp. affects some hydraulic properties. Impact is assessed in the hydrogeological modelling. May later be discarded as an insignificant influence.	No need	No need	No need	No need	No need	No need
Confirmation and indications of structures (i.e. are there hydraulic contacts or not). Control of the hydraulic applicability of the DFN-model. Confirmation of structures in the DZ in KSH03 (as hydraulic anomalies). contacts not yet possible to explore. In previous models (Äspö/Hålö), also based on hydraulic assessments of data from these sites. Control of the hydraulic applicability of the DFN-model.	Water pressure reduces the rock stress to effective stress. Not used in the description (see Table 12-4), but is considered by Repository Engineering.	Thermal convection affects uncertainty in measurement of initial temperature. Is considered when assessing uncertainty in in-situ temperature.	**Hydrogeology in the bedrock**	Mixing is considered main mechanism for distribution and evolution of groundwater composition. Simulation of past salinity and, distribution of end-member waters, evolution, predicted salinity distribution and possibility to compare predicted and measured.	Identification of potential flow paths where description is needed. Correlation between transport and hydrogeo-logical parameters. Flow logs considered in identification of “type structures”.	Input to coupled hydrogeological/ hydrogeochemic almodelling of the surface system. No such modelling has been done.	Integrated models and description. Boundary condition in surface system models. Input of hydraulic properties and BC in rock.	No need	No need

No need	No need	No need	Hypothesis of palaeo-evolution. Density affects flow. Present day salinity and water type distribution are “calibration targets” for simulation. Models consider density effects.	**Hydrogeo-chemistry in the bedrock**	Groundwater composition affects diffusion and sorption parameters. Input to process-based retention modelling. Groundwater composition (identified water types) used to set up laboratory tests and in parametrisation of Retardation model.	Integrated models and description. Boundary condition and water types in surface system models. Some comparisons are made, but no detailed modelling.	No need	No need	No need
No need	No need	No need	Modelling salt migration should be consistent with assessed migration properties. Consistency check as regards porosities and mass transfer parameters used in palaeo-simulations.	Modelling salt migration should be consistent with assessed migration properties. See hydrogeology.	**Bedrock Transport Properties**	No need	No need	No need	No need
No need	No need	No need	Identification of water types and boundary conditions. Input of surface water type considered in the modelling.	Integrated models and description. Identification of water types and boundary conditions. Some data used in simplified coupled/ integrated model.	No need	**Hydrogeo-chemistry (surface and near surface)**	Supporting analyses (evaluation of specific chem. parameters, coupled modelling). Limited by lack of chemical data from the groundwater.	Data on specific processes, e.g. precipitation-dissolution. Limited by lack of chemical data from the groundwater.	Chemical composition of soil and waters. Used in modelling and validation of flow of matter in ecosystem descriptions.

No need	No need	No need	Integrated models and description. Identification of boundary conditions. Simplified description used in deep rock model.	Input to deep rock model (e.g. GW recharge to rock). Hydraulic properties and boundary conditions in coupled models. Some data (e.g. GW levels) used in simplified coupled/ integrated model.	No need	Flow pattern, input to mass balance and mass transport modelling. No coupled modelling of the surface system performed.	**Surface hydrology and near surface hydrogeology**	Hydrogeological properties (comparison/ consistency check). Is done.	Flow rates volumes of surface waters and groundwater. Used in turnover calculations for water and biomass transport modelling.
Post glacial tectonics Mineral composition Only small amount of data available	No need	No need	No need	QD description and soil types provide input to selection of water types and input to coupled modelling. Some data used in simplified coupled model.	No need	Type of QD, solid phases, mineralogy, geochemistry (description, process models). QD/water chemistry correlation studied, but no detailed modelling.	Geological model (QD map and stratigraphic model) used as a basis for numerical model. Is actually done.	**Quaternary Deposits**	Geological model (QD map and stra-tigraphic model) and soil type model used as modelling inputs. Is done.
No need	No need	No need	No need	Modelling of biogeochemical processes. Assignment of boundary conditions to deep rock model. Processes identified, but not quantified.	No need	Modelling of biogeochemical processes. No detailed modelling performed.	Input data to water balance modelling (interception and evapotranspiration) Is done.	Turbation, soil type and accumulation processes. Is considered.	**Biota**